VOLUME 28 / NUMBER 16
AUGUST 23, 1990
ACC. NOS. N90-22530 TO N90-23339

STAR
AN ABSTRACT JOURNAL

Scientific and Technical Aerospace Reports

PRODUCED BY THE
SCIENTIFIC AND TECHNICAL
INFORMATION
DIVISION

NASA

NATIONAL AERONAUTICS AND SPACE ADMINISTRATION

WHAT YOU CAN DO FOR *STAR*

All users of this abstract service are urged to forward reports to be considered for announcement in *STAR*. This will aid NASA in its efforts to provide the fullest possible coverage of all scientific and technical publications that might support aeronautics and space research and development. If you have prepared relevant reports (other than those that you will transmit to NASA, DOD, or DOE through the usual contract- or grant-reporting channels), please send them for consideration to the NASA Scientific and Technical Information Facility, P.O. Box 8757, BWI Airport, MD 21240.

Reprints of journal articles, book chapters, and conference papers are also welcome. These will be considered for announcement in *STAR's* companion journal, *International Aerospace Abstracts*.

You may specify a particular source to be included in a report announcement if you wish; otherwise the report will be placed on public sale at the National Technical Information Service. Copyrighted publications will be announced but not distributed or sold.

PURCHASE OF *STAR*

The semimonthly issues are available to registered users on annual subscription from the NASA Scientific and Technical Information Facility, ATTN: Registration Services, P.O. Box 8757, BWI Airport, MD 21240. *STAR* is publicly available on annual subscription from the Superintendent of Documents, U.S. Government Printing Office, Washington, DC 20402.

PUBLISHED BY:

UNITED STATES GOVERNMENT
NATIONAL AERONAUTICS AND SPACE ADMINISTRATION
SCIENTIFIC AND TECHNICAL INFORMATION DIVISION
Scientific and Technical Aerospace Reports, Volume 28, is prepared by the NASA Scientific and Technical Information Facility operated for the National Aeronautics and Space Administration by RMS Associates.

The Administrator of the National Aeronautics and Space Administration has determined that the publication of this periodical is necessary in the transaction of the public business required by law of this agency. Use of funds for printing this periodical has been approved by the Director of the Office of Management and Budget through March 22, 1991.

US ISSN 0036-8741

Scientific and Technical Aerospace Reports (STAR) is issued twice a month and contains abstracts and indexes of meeting papers, conference proceedings, and unlimited distribution reports that have been added to the NASA Scientific and Technical Information Database during the preceding period. These citations may also be accessed online via NASA/RECON or via AIAA's Aerospace Database (File 108) through Dialog Information Services, Inc.

STAR subject coverage includes all aerospace-related areas that will help NASA achieve its mission. Material is gathered from all over the world and includes significant input from many countries under exchange and access agreements.

Consult the indexes at the back of this volume to help zero in on what you are looking for. These include:

Subject Index
Personal Author Index
Corporate Source Index
Contract Number Index
Report/Accession Number Index

STAR's companion abstract journal *International Aerospace Abstracts* should be used if you are looking for references to periodicals, books, and published meeting papers or conference proceedings.

Questions and comments should be addressed to:

NASA Scientific and Technical Information Facility
User Services
P.O. Box 8757
BWI Airport, MD 21240
301-621-0150

VOLUME 28 NUMBER 16 / AUGUST 23, 1990

TABLE OF CONTENTS

AERONAUTICS

Includes aeronautics (general); aerodynamics; air transportation and safety; aircraft communications and navigation; aircraft design, testing and performance; aircraft instrumentation; aircraft propulsion and power; aircraft stability and control; and research and support facilities (air).

For related information see also *Astronautics.*

01 AERONAUTICS (GENERAL) 2195

02 AERODYNAMICS 2195

Includes aerodynamics of bodies, combinations, wings, rotors, and control surfaces; and internal flow in ducts and turbomachinery.

For related information see also *34 Fluid Mechanics and Heat Transfer.*

03 AIR TRANSPORTATION AND SAFETY 2197

Includes passenger and cargo air transport operations; and aircraft accidents.

For related information see also *16 Space Transportation* and *85 Urban Technology and Transportation.*

04 AIRCRAFT COMMUNICATIONS AND NAVIGATION 2199

Includes digital and voice communication with aircraft; air navigation systems (satellite and ground based); and air traffic control.

For related information see also *17 Space Communications, Spacecraft Communications, Command and Tracking* and *32 Communications and Radar.*

05 AIRCRAFT DESIGN, TESTING AND PERFORMANCE 2199

Includes aircraft simulation technology.

For related information see also *18 Spacecraft Design, Testing and Performance* and *39 Structural Mechanics.* For land transportation vehicles see *85 Urban Technology and Transportation.*

06 AIRCRAFT INSTRUMENTATION 2201

Includes cockpit and cabin display devices; and flight instruments.

For related information see also *19 Spacecraft Instrumentation* and *35 Instrumentation and Photography.*

07 AIRCRAFT PROPULSION AND POWER 2201

Includes prime propulsion systems and systems components, e.g., gas turbine engines and compressors; and onboard auxiliary power plants for aircraft.

For related information see also *20 Spacecraft Propulsion and Power, 28 Propellants and Fuels,* and *44 Energy Production and Conversion.*

08 AIRCRAFT STABILITY AND CONTROL 2202

Includes aircraft handling qualities; piloting; flight controls; and autopilots.

For related information see also *05 Aircraft Design, Testing and Performance.*

09 RESEARCH AND SUPPORT FACILITIES (AIR) 2203

Includes airports, hangars and runways; aircraft repair and overhaul facilities; wind tunnels; shock tubes; and aircraft engine test stands.

For related information see also *14 Ground Support Systems and Facilities (Space).*

ASTRONAUTICS

Includes astronautics (general); astrodynamics; ground support systems and facilities (space); launch vehicles and space vehicles; space transportation; space communications, spacecraft communications, command and tracking; spacecraft design, testing and performance; spacecraft instrumentation; and spacecraft propulsion and power.

For related information see also *Aeronautics.*

12 ASTRONAUTICS (GENERAL) 2203

For extraterrestrial exploration see *91 Lunar and Planetary Exploration.*

13 ASTRODYNAMICS 2204

Includes powered and free-flight trajectories; and orbital and launching dynamics.

14 GROUND SUPPORT SYSTEMS AND FACILITIES (SPACE) 2204

Includes launch complexes, research and production facilities; ground support equipment, e.g., mobile transporters; and simulators.

For related information see also *09 Research and Support Facilities (Air).*

15 LAUNCH VEHICLES AND SPACE VEHICLES 2205

Includes boosters; operating problems of launch/space vehicle systems; and reusable vehicles.

For related information see also *20 Spacecraft Propulsion and Power.*

16 SPACE TRANSPORTATION 2205

Includes passenger and cargo space transportation, e.g., shuttle operations; and space rescue techniques.

For related information see also *03 Air Transportation and Safety* and *18 Spacecraft Design, Testing and Performance.* For space suits see *54 Man/System Technology and Life Support.*

17 SPACE COMMUNICATIONS, SPACECRAFT COMMUNICATIONS, COMMAND AND TRACKING N.A.

Includes telemetry; space communications networks; astronavigation and guidance; and radio blackout.

For related information see also *04 Aircraft Communications and Navigation* and *32 Communications and Radar.*

18 SPACECRAFT DESIGN, TESTING AND PERFORMANCE 2206

Includes satellites; space platforms; space stations; spacecraft systems and components such as thermal and environmental controls; and attitude controls.

For life support systems see *54 Man/System Technology and Life Support.* For related information see also *05 Aircraft Design, Testing and Performance, 39 Structural Mechanics,* and *16 Space Transportation.*

19 SPACECRAFT INSTRUMENTATION 2208

For related information see also *06 Aircraft Instrumentation* and *35 Instrumentation and Photography.*

20 SPACECRAFT PROPULSION AND POWER 2208

Includes main propulsion systems and components, e.g. rocket engines; and spacecraft auxiliary power sources.

For related information see also *07 Aircraft Propulsion and Power, 28 Propellants and Fuels, 44 Energy Production and Conversion,* and *15 Launch Vehicles and Space Vehicles.*

CHEMISTRY AND MATERIALS

Includes chemistry and materials (general); composite materials; inorganic and physical chemistry; metallic materials; nonmetallic materials; propellants and fuels; and materials processing.

23 CHEMISTRY AND MATERIALS (GENERAL) 2210

24 COMPOSITE MATERIALS 2210

Includes physical, chemical, and mechanical properties of laminates and other composite materials.

For ceramic materials see *27 Nonmetallic Materials.*

25 INORGANIC AND PHYSICAL CHEMISTRY 2214

Includes chemical analysis, e.g., chromatography; combustion theory; electrochemistry; and photochemistry.

For related information see also *77 Thermodynamics and Statistical Physics.*

26 METALLIC MATERIALS 2216

Includes physical, chemical, and mechanical properties of metals, e.g., corrosion; and metallurgy.

27 NONMETALLIC MATERIALS 2222

Includes physical, chemical, and mechanical properties of plastics, elastomers, lubricants, polymers, textiles, adhesives, and ceramic materials.

For composite materials see *24 Composite Materials.*

28 PROPELLANTS AND FUELS 2225

Includes rocket propellants, igniters and oxidizers; their storage and handling procedures; and aircraft fuels.

For related information see also *07 Aircraft Propulsion and Power, 20 Spacecraft Propulsion and Power,* and *44 Energy Production and Conversion.*

29 MATERIALS PROCESSING 2226

Includes space-based development of products and processes for commercial application.

For biological materials see *55 Space Biology.*

ENGINEERING

Includes engineering (general); communications and radar; electronics and electrical engineering; fluid mechanics and heat transfer; instrumentation and photography; lasers and masers; mechanical engineering; quality assurance and reliability; and structural mechanics.

For related information see also *Physics.*

31 ENGINEERING (GENERAL) 2226

Includes vacuum technology; control engineering; display engineering; cryogenics; and fire prevention.

32 COMMUNICATIONS AND RADAR 2227

Includes radar; land and global communications; communications theory; and optical communications.

For related information see also *04 Aircraft Communications and Navigation* and *17 Space Communications, Spacecraft Communications, Command and Tracking.* For search and rescue see *03 Air Transportation and Safety,* and *16 Space Transportation.*

33 ELECTRONICS AND ELECTRICAL ENGINEERING 2230

Includes test equipment and maintainability; components, e.g., tunnel diodes and transistors; microminiaturization; and integrated circuitry.

For related information see also *60 Computer Operations and Hardware* and *76 Solid-State Physics.*

34 FLUID MECHANICS AND HEAT TRANSFER 2233

Includes boundary layers; hydrodynamics; fluidics; mass transfer and ablation cooling.

For related information see also *02 Aerodynamics* and *77 Thermodynamics and Statistical Physics.*

35 INSTRUMENTATION AND PHOTOGRAPHY 2238

Includes remote sensors; measuring instruments and gauges; detectors; cameras and photographic supplies; and holography.

For aerial photography see *43 Earth Resources and Remote Sensing.* For related information see also *06 Aircraft Instrumentation* and *19 Spacecraft Instrumentation.*

36 LASERS AND MASERS 2239

Includes parametric amplifiers.

For related information see also *76 Solid-State Physics.*

37 MECHANICAL ENGINEERING 2241

Includes auxiliary systems (nonpower); machine elements and processes; and mechanical equipment.

38 QUALITY ASSURANCE AND RELIABILITY 2244

Includes product sampling procedures and techniques; and quality control.

39 STRUCTURAL MECHANICS 2245

Includes structural element design and weight analysis; fatigue; and thermal stress.

For applications see *05 Aircraft Design, Testing and Performance* and *18 Spacecraft Design, Testing and Performance.*

GEOSCIENCES

Includes geosciences (general); earth resources and remote sensing; energy production and conversion; environment pollution; geophysics; meteorology and climatology; and oceanography.

For related information see also *Space Sciences.*

42 GEOSCIENCES (GENERAL) 2249

43 EARTH RESOURCES AND REMOTE SENSING 2249

Includes remote sensing of earth resources by aircraft and spacecraft; photogrammetry; and aerial photography.

For instrumentation see *35 Instrumentation and Photography.*

44 ENERGY PRODUCTION AND CONVERSION 2250

Includes specific energy conversion systems, e.g., fuel cells; global sources of energy; geophysical conversion; and windpower.

For related information see also *07 Aircraft Propulsion and Power, 20 Spacecraft Propulsion and Power,* and *28 Propellants and Fuels.*

45 ENVIRONMENT POLLUTION 2253

Includes atmospheric, noise, thermal, and water pollution.

46 GEOPHYSICS 2253

Includes aeronomy; upper and lower atmosphere studies; ionospheric and magnetospheric physics; and geomagnetism.

For space radiation see *93 Space Radiation.*

47 METEOROLOGY AND CLIMATOLOGY 2256

Includes weather forecasting and modification.

48 OCEANOGRAPHY 2259

Includes biological, dynamic, and physical oceanography; and marine resources.

For related information see also *43 Earth Resources and Remote Sensing.*

LIFE SCIENCES

Includes life sciences (general); aerospace medicine; behavioral sciences; man/system technology and life support; and space biology.

51 LIFE SCIENCES (GENERAL) 2260

52 AEROSPACE MEDICINE 2260

Includes physiological factors; biological effects of radiation; and effects of weightlessness on man and animals.

53 BEHAVIORAL SCIENCES 2261

Includes psychological factors; individual and group behavior; crew training and evaluation; and psychiatric research.

54 MAN/SYSTEM TECHNOLOGY AND LIFE SUPPORT 2267

Includes human engineering; biotechnology; and space suits and protective clothing.

For related information see also *16 Space Transportation.*

55 SPACE BIOLOGY N.A.

Includes exobiology; planetary biology; and extraterrestrial life.

MATHEMATICAL AND COMPUTER SCIENCES

Includes mathematical and computer sciences (general); computer operations and hardware; computer programming and software; computer systems; cybernetics; numerical analysis; statistics and probability; systems analysis; and theoretical mathematics.

59 MATHEMATICAL AND COMPUTER SCIENCES (GENERAL) 2276

60 COMPUTER OPERATIONS AND HARDWARE 2277

Includes hardware for computer graphics, firmware, and data processing.

For components see *33 Electronics and Electrical Engineering.*

61 COMPUTER PROGRAMMING AND SOFTWARE 2278

Includes computer programs, routines, algorithms, and specific applications, e.g., CAD/CAM.

62 COMPUTER SYSTEMS 2302

Includes computer networks and special application computer systems.

63 CYBERNETICS 2303

Includes feedback and control theory, artificial intelligence, robotics and expert systems.

For related information see also *54 Man/System Technology and Life Support.*

64 NUMERICAL ANALYSIS 2304

Includes iteration, difference equations, and numerical approximation.

65 STATISTICS AND PROBABILITY 2308

Includes data sampling and smoothing; Monte Carlo method; and stochastic processes.

66 SYSTEMS ANALYSIS N.A.

Includes mathematical modeling; network analysis; and operations research.

67 THEORETICAL MATHEMATICS 2309

Includes topology and number theory.

PHYSICS

Includes physics (general); acoustics; atomic and molecular physics; nuclear and high-energy physics; optics; plasma physics; solid-state physics; and thermodynamics and statistical physics.

For related information see also *Engineering.*

70 PHYSICS (GENERAL) 2310

For precision time and time interval (PTTI) see *35 Instrumentation and Photography;* for geophysics, astrophysics or solar physics see *46 Geophysics, 90 Astrophysics,* or *92 Solar Physics.*

71 ACOUSTICS 2312
Includes sound generation, transmission, and attenuation.
For noise pollution see *45 Environment Pollution.*

72 ATOMIC AND MOLECULAR PHYSICS 2314
Includes atomic structure, electron properties, and molecular spectra.

73 NUCLEAR AND HIGH-ENERGY PHYSICS 2316
Includes elementary and nuclear particles; and reactor theory.
For space radiation see *93 Space Radiation.*

74 OPTICS 2317
Includes light phenomena and optical devices.
For lasers see *36 Lasers and Masers.*

75 PLASMA PHYSICS 2319
Includes magnetohydrodynamics and plasma fusion.
For ionospheric plasmas see *46 Geophysics.* For space plasmas see *90 Astrophysics.*

76 SOLID-STATE PHYSICS 2320
Includes superconductivity.
For related information see also *33 Electronics and Electrical Engineering* and *36 Lasers and Masers.*

77 THERMODYNAMICS AND STATISTICAL PHYSICS 2325
Includes quantum mechanics; theoretical physics; and Bose and Fermi statistics.
For related information see also *25 Inorganic and Physical Chemistry* and *34 Fluid Mechanics and Heat Transfer.*

SOCIAL SCIENCES

Includes social sciences (general); administration and management; documentation and information science; economics and cost analysis; law, political science, and space policy; and urban technology and transportation.

80 SOCIAL SCIENCES (GENERAL) N.A.
Includes educational matters.

81 ADMINISTRATION AND MANAGEMENT N.A.
Includes management planning and research.

82 DOCUMENTATION AND INFORMATION SCIENCE 2326
Includes information management; information storage and retrieval technology; technical writing; graphic arts; and micrography.
For computer documentation see *61 Computer Programming and Software.*

83 ECONOMICS AND COST ANALYSIS N.A.
Includes cost effectiveness studies.

84 LAW, POLITICAL SCIENCE AND SPACE POLICY 2328
Includes NASA appropriation hearings; aviation law; space law and policy; international law; international cooperation; and patent policy.

85 URBAN TECHNOLOGY AND TRANSPORTATION N.A.
Includes applications of space technology to urban problems; technology transfer; technology assessment; and surface and mass transportation.
For related information see *03 Air Transportation and Safety, 16 Space Transportation,* and *44 Energy Production and Conversion.*

SPACE SCIENCES

Includes space sciences (general); astronomy; astrophysics; lunar and planetary exploration; solar physics; and space radiation.
For related information see also *Geosciences.*

88 SPACE SCIENCES (GENERAL) 2328

89 ASTRONOMY 2328
Includes radio, gamma-ray, and infrared astronomy; and astrometry.

90 ASTROPHYSICS 2331
Includes cosmology; celestial mechanics; space plasmas; and interstellar and interplanetary gases and dust.
For related information see also *75 Plasma Physics.*

91 LUNAR AND PLANETARY EXPLORATION 2338
Includes planetology; and manned and unmanned flights.
For spacecraft design or space stations see *18 Spacecraft Design, Testing and Performance.*

92 SOLAR PHYSICS 2338
Includes solar activity, solar flares, solar radiation and sunspots.
For related information see *93 Space Radiation.*

93 SPACE RADIATION 2340
Includes cosmic radiation; and inner and outer earth's radiation belts.
For biological effects of radiation see *52 Aerospace Medicine.* For theory see *73 Nuclear and High-Energy Physics.*

GENERAL

Includes aeronautical, astronautical, and space science related histories, biographies, and pertinent reports too broad for categorization; histories or broad overviews of NASA programs.

99 GENERAL 2342

Note: N.A. means that no abstracts were assigned to this category for this issue.

SUBJECT INDEX I-1
PERSONAL AUTHOR INDEX I-53
CORPORATE SOURCE INDEX I-59
CONTRACT NUMBER INDEX I-69
REPORT/ACCESSION NUMBER INDEX .. I-71
APPENDIX—ABOUT STAR A-1

TYPICAL CITATION AND ABSTRACT

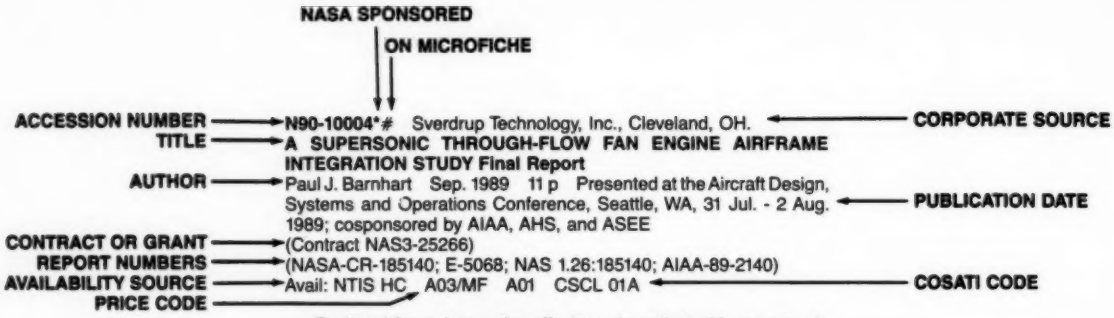
NASA SPONSORED
ON MICROFICHE
ACCESSION NUMBER
N90-10004*# Sverdrup Technology, Inc., Cleveland, OH.
CORPORATE SOURCE
TITLE
A SUPERSONIC THROUGH-FLOW FAN ENGINE AIRFRAME INTEGRATION STUDY Final Report
AUTHOR
Paul J. Barnhart Sep. 1989 11 p Presented at the Aircraft Design, Systems and Operations Conference, Seattle, WA, 31 Jul. - 2 Aug. 1989; cosponsored by AIAA, AHS, and ASEE
PUBLICATION DATE
CONTRACT OR GRANT
(Contract NAS3-25266)
REPORT NUMBERS
(NASA-CR-185140; E-5068; NAS 1.26:185140; AIAA-89-2140)
AVAILABILITY SOURCE
Avail: NTIS HC A03/MF A01 CSCL 01A
COSATI CODE
PRICE CODE

Engine airframe integration effects are investigated for superonsic through-flow fan engines installed on a Mach 3.20 supersonic cruise vehicle. Six different supersonic through-flow fan engine installations covering the effects of engine size, nacelle contour, nacelle placement, and approximate bypass plume effects are presented. The different supersonic through-flow fan installations are compared with a conventional turbine bypass engine configuration on the same basic airframe. The supersonic through-flow fan engine integrations are shown to be comparable to the turbine bypass engine configuration on the basis of installed nacelle wave drag. The supersonic through-flow fan engine airframe integrated vehicles have superior aerodynamic performance on the basis of maximum lift-to-drag ratio than the turbine bypass engine installation over the entire operating Mach number range from 1.10 to 3.20. When approximate bypass plume modeling is included, the supersonic through-flow fan engine configuration shows even larger improvements over the turbine bypass engine configuration. Author

VOLUME 28 NUMBER 16 / AUGUST 23, 1990

Scientific and Technical Aerospace Reports

A Semimonthly Publication of the National Aeronautics and Space Administration

01 AERONAUTICS (GENERAL)

N90-22530# Federal Aviation Administration, Washington, DC. Office of Aviation Policy and Plans.
FAA (FEDERAL AVIATION ADMINISTRATION) AVIATION FORECASTS, FISCAL YEARS 1990-2001
Mar. 1990 250 p
(AD-A219165; FAA-AP0-90-1) Avail: NTIS HC A11/MF A02 CSCL 01/5

The Fiscal Years 1990 to 2001 Federal Aviation Administration (FAA) forecasts of aviation activity at FAA facilities is presented. These include airports with FAA control towers, air route traffic control centers, and flight service stations. Detailed forecasts were made for the four major users of the National Aviation System: air carriers, air taxi-commuters, general aviation and the military. The forecasts were prepared to meet the budget and planning needs of the constituent units of the FAA and to provide information that can be used by state and local authorities, by the aviation industry, and by the general public. The overall outlook for the forecast period is the continued economic growth, rising real fuel prices, and moderate inflation. Based upon these assumptions, aviation activity by fiscal year 2001 is forecast to increase by 29.0 percent at towered airports (commuters, 48.2 percent; air carriers, 33.6 percent; general aviation, 25.4 percent; military, 0.0 percent), 30.1 percent at air route traffic control centers (commuters, 51.9 percent; air carriers, 33.1 percent; general aviation 30.5 percent; military, 0.0 percent), and 5.1 percent in flight services performed. Hours flown by general aviation are forecast to increase 19.2 percent and revenue passenger miles (RPM's) are forecast to increase 67.8 percent, with scheduled international RPM's forecast to increase by 113.2 percent; and regionals/commuters RPM's forecast to increase by 157.1 percent. GRA

02 AERODYNAMICS

Includes aerodynamics of bodies, combinations, wings, rotors, and control surfaces; and internal flow in ducts and turbomachinery.

For related information see also *34 Fluid Mechanics and Heat Transfer.*

N90-22531*# National Aeronautics and Space Administration. Langley Research Center, Hampton, VA.
DYNAMIC GROUND-EFFECT MEASUREMENTS ON THE F-15 STOL AND MANEUVER TECHNOLOGY DEMONSTRATOR (S/MTD) CONFIGURATION
Guy T. Kemmerly Washington Jun. 1990 31 p
(NASA-TP-3000; L-16555; NAS 1.60:3000) Avail: NTIS HC A03/MF A01 CSCL 01A

A moving-model ground-effect testing method was used to study the influence of rate-of-descent on the aerodynamic characteristics for the F-15 STOL and Maneuver Technology Demonstrator (S/MTD) configuration for both the approach and roll-out phases of landing. The approach phase was modeled for three rates of descent, and the results were compared to the predictions from the F-15 S/MTD simulation data base (prediction based on data obtained in a wind tunnel with zero rate of descent). This comparison showed significant differences due both to the rate of descent in the moving-model test and to the presence of the ground boundary layer in the wind tunnel test. Relative to the simulation data base predictions, the moving-model test showed substantially less lift increase in ground effect, less nose-down pitching moment, and less increase in drag. These differences became more prominent at the larger thrust vector angles. Over the small range of rates of descent tested using the moving-model technique, the effect of rate of descent on longitudinal aerodynamics was relatively constant. The results of this investigation indicate no safety-of-flight problems with the lower jets vectored up to 80 deg on approach. The results also indicate that this configuration could employ a nozzle concept using lower reverser vector angles up to 110 deg on approach if a no-flare approach procedure were adopted and if inlet reingestion does not pose a problem. Author

N90-22532*# National Aeronautics and Space Administration. Hugh L. Dryden Flight Research Center, Edwards, CA.
WATER-TUNNEL STUDY RESULTS OF A TF/A-18 AND F/A-18 CANOPY FLOW VISUALIZATION
Steven A. Johnson and David F. Fisher Mar. 1990 29 p
Original contains color illustrations
(NASA-TM-101705; H-1570; NAS 1.15:101705) Avail: NTIS HC A03/MF A01; 13 functional color pages CSCL 01A

A water tunnel study examining the influence of canopy shape on canopy and leading edge extension flow patterns was initiated. The F/A-18 single-place canopy model and the TF/A-18 two place canopy model were the study subjects. Plan view and side view photographs showing the flow patterns created by injected colored dye are presented for 0 deg and 5 deg sideslip angles. Photographs taken at angle of attack and sideslip conditions correspond to test departure points found in flight test. Flight experience has shown that the TF/A-18 airplane departs in regions where the F/A-18 airplane is departure-resistant. The study results provide insight into the differences in flow patterns which may influence the resulting aerodynamics of the TF/A-18 and F/A-18 aircraft. It was found that at 0 deg sideslip, the TF/A-18 model has more downward flow on the sides of the canopy than the F/A-18 model. This could be indicative of flow from the leading edge extension (LEX) vortexes impinging on the sides of the wider TF/A-18 canopy. In addition, the TF/A-18 model has larger areas of asymmetric separated and unsteady flow on the LEXs and fuselage, possibly indicating a lateral and directional destabilizing effect at the conditions studied. Author

N90-22533 Princeton Univ., NJ.
FLOW VISUALIZATION IN SUPERSONIC TURBULENT BOUNDARY LAYERS Ph.D. Thesis
Michael Wayne Smith 1989 174 p
Avail: Univ. Microfilms Order No. DA9003657

Flow visualizations of two different flat-plate, zero pressure gradient, supersonic, turbulent boundary layers are examined. The physics of supersonic shear flows has recently drawn increasing attention with the renewed interest in flight at super and hypersonic speeds. This work was driven by the belief that the study of organized, Reynolds-stress producing turbulence structures will lead to improved techniques for the modelling and control of high-speed boundary layers. Although flow-visualization is often

thought of as a tool for providing qualitative information about complex flow fields, an emphasis is placed on deriving quantitative results from image data whenever possible. Three visualization techniques were applied: selective cut-off schlieren, droplet seeding, and Rayleigh scattering. Two experiments employed selective cut-off schlieren. In the first, high-speed movies (40,000 fps) were made of strong density gradient fronts leaning downstream at between 30 and 60 deg and travelling at about 0.9 U(sub infinity). In the second experiment, the same fronts were detected with hot-wires and imaged in real time, thus allowing the examination of the density gradient fronts and their associated single-point mass-flux signals. Two experiments employed droplet seeding. In both experiments, the boundary layer was seeded by injecting a stream of acetone through a single point in the wall. In the first droplet experiment, the fog was illuminated with copper-vapor laser sheets of various orientations. In the second droplet experiment, high-speed movies were made of the fog under general illumination, thus providing information about the streamwise evolution of the structures seen in the planar stills. Rayleigh scattering from a laser sheet was used to create instantaneous density cross-sections in the M=2.5 boundary layer. The Rayleigh scattering experiment represents the first measurement of the instantaneous 2-D field of an intrinsic fluid property in any boundary layer. Imaged by an intensified UV camera, scattering from the Argon-Flouride laser (193 nm) revealed density structures with sharp interfaces between high and low-density fluid. Dissert. Abstr.

N90-22534 Pennsylvania State Univ., University Park.
REYNOLDS STRESS CLOSURE IN JET FLOWS USING INSTABILITY WAVE MODELING Ph.D. Thesis
Roy Stuart Baty 1989 228 p
Avail: Univ. Microfilms Order No. DA9007827

Large scale coherent structures present in the initial mixing region of turbulent, compressible, free jets of arbitrary cross section are computationally studied. The theory of instability wave modeling is used to close the governing equations of motion, and predict, with a minimum of empiricism, the normalized fluctuating pressure field associated with large scale eddies. The normalized Reynolds stresses and stress forces associated with the large scale coherent structures are also predicted. The computation is performed in the thin shear layer region of jets of rectangular and non-confocal elliptic geometries of aspect ratio 2. An integral component of the instability wave model is the inviscid spatial hydrodynamic stability problem. This eigenvalue problem is governed by the Rayleigh equation: a linear, elliptic, nonseparable, partial differential equation, in which the parameter appears nonlinearly. The Rayleigh problem is defined in annular and disc-like regions of arbitrary shape. The development of an efficient numerical scheme is stressed. To consider jets of arbitrary geometry, conformal transformations are used to map standard computational domains onto realistic jet flow cross sections. Combining conformal transformations with a hybrid finite difference pseudospectral numerical method allows the use of physically realistic jet geometries and mean velocity profiles. Modern, very efficient schemes are applied to determine the conformal mappings. A comparison is made between the pressure distributions associated with the various instability modes in circular, elliptic and rectangular jets. Calculations are presented for the Reynolds stress components for the instability waves. The Reynolds stress gradients are also given and are used to make qualitative predictions on the influence of the instability waves or large scale coherent structures on the development of the mean flow in non-circular jets. Dissert. Abstr.

N90-22535 Connecticut Univ., Storrs.
THE MINIMUM DRAG PROFILE IN LAMINAR FLOW: A NUMERICAL WAY Ph.D. Thesis
Ramakrishnan K. Ganesh 1989 183 p
Avail: Univ. Microfilms Order No. DA9010175

The shape of the body of a given volume which has minimum drag when moving through a viscous fluid at constant speed is examined. Experimental observations in fluid dynamics are either paradoxical or against intuition and look very complicated, yet can in fact be explained in a logical and an orderly manner following the fundamental concepts and principles of fluid dynamics. The concepts and principles involved in a streaming flow past a body in 2-D starting from conservation equations were studied and ways developed to evaluate drag numerically using finite elements in order to use them later as engineering criteria in the evolution process. The gradient optimally criterion for minimum drag profile in laminar flow was derived by Pironneau to be used in his nonlinear gradient algorithm. It establishes a dialog between the optimizer and the engineer in a logical manner until the optimum shape is evolved in an orderly fashion. The present method in 2-D laminar flow with area constraint due to Pironneau and Glowinski uses boundary layer approximation and hence limited to high Reynolds number flows only; besides it is not clear what engineering criterion is being used and how the optimum step size is being decided. It requires an outer and two inner solutions for every iteration which is tedious and cumbersome. A direct numerical simulation is described for the governing elliptic partial differential equations, viz., the Navier-Stokes and the Co-state equations. The latter has the resemblance of the former with no simple mechanical interpretation. The finite element method is ideally suited for elliptic boundary value problems with complex geometry and is used to solve for the flow field and calculate the necessary criteria required in the evolution process with ease. The profile evolution is demonstrated for flows at different Reynolds numbers.
Dissert. Abstr.

N90-22536 Purdue Univ., West Lafayette, IN.
FORCING FUNCTION EFFECTS ON ROTOR ROW UNSTEADY AERODYNAMIC RESPONSE IN A MULTISTAGE COMPRESSOR Ph.D. Thesis
Steven R. Manwaring 1989 282 p
Avail: Univ. Microfilms Order No. DA9008662

The fundamental flow physics of wake and distortion generated periodic rotor blade row unsteady aerodynamics were experimentally investigated. In particular, this was accomplished through a series of experiments performed in an extensively instrumented axial flow research compressor. The effects of aerodynamic forcing functions of different reduced frequency, interblade phase angle, waveform, and amplitude on rotor blade row periodic unsteady aerodynamic response while operating over a range of operating conditions in multistage subresonant and superresonant acoustic resonant environments were investigated. On the rotor blade low camber pressure surface, the unsteady pressure nondimensionalization compressed the magnitude data with mean flow incidence except in the accelerating flow field of the front chord region at negative mean flow incidence. However, for the high camber suction surface, gust interactions with the mean flow field affected the unsteady pressure response over the entire blade surface. The harmonic analysis of blade row unsteady aerodynamic response to complex waveform forcing functions was experimentally demonstrated. Subresonant and superresonant acoustic environments were established, with the magnitude data predictions correlation being very good in the subresonant flow regime and the correlation of these data in the superresonant flow regime only fair. In both acoustic environments, the correlation of the phase data were poor, both in value and trend.
Dissert. Abstr.

N90-22537# Royal Aerospace Establishment, Farnborough (England).
THE AERODYNAMIC CHARACTERISTICS OF POWER-LAW BODIES IN CONTINUUM AND TRANSITIONAL HYPERSONIC FLOW
M. F. Westby and J. D. Regan 3 Aug. 1989 24 p Presented at the International Conference on Hypersonic Aerodynamics, Manchester, England, 4-6 Sep. 1989
(RAE-TM-AERO-2164; BR111667; ETN-90-96442) Copyright
Avail: NTIS HC A03/MF A01

The experimental studies presented were carried out to determine the aerodynamic characteristics of a series of power-law bodies of constant fineness ratio over a Reynolds number range covering both continuum and transitional rarefied flow. The tests

were performed at Mach numbers of 10 in the low density tunnel and 12.8 in the gun tunnel at angles of incidence up to 30 degrees. ESA

N90-22538*# Scientific Research Associates, Inc., Glastonbury, CT.
EXTENSION OF A THREE-DIMENSIONAL VISCOUS WING FLOW ANALYSIS USER'S MANUAL: VISTA 3-D CODE
Bernard C. Weinberg, Shyi-Yaung Chen, Stephen J. Thoren, and Stephen J. Shamroth May 1990 106 p
(Contract NAS1-18140)
(NASA-CR-182024; NAS 1.26:182024; SRA-900049-UM) Avail: NTIS HC A06/MF A01 CSCL 01A

Three-dimensional unsteady viscous effects can significantly influence the performance of fixed and rotary wing aircraft. These effects are important in both flows about helicopter rotors in forward flight and flows about three-dimensional (swept and tapered) supercritical wings. A computational procedure for calculating such flow field was developed. The procedure is based upon an alternating direction technique employing the Linearized Block Implicit method for solving three-dimensional viscous flow problems. In order to demonstrate the viability of this method, two- and three-dimensional problems are computed. These include the flow over a two-dimensional NACA 0012 airfoil under steady and oscillating conditions, and the steady, skewed, three-dimensional flow on a flat plate. Although actual three-dimensional flows over wings were not obtained, the ground work was laid for considering such flows. In this report a description of the computer code is given. Author

N90-22539*# Institute for Computer Applications in Science and Engineering, Hampton, VA.
THE ANALYSIS AND SIMULATION OF COMPRESSIBLE TURBULENCE Final Report
Gordon Erlebacher, M. Y. Hussaini, H. O. Kreiss (California Univ., Los Angeles.), and S. Sarkar Feb. 1990 30 p Submitted for publication
(Contract NAS1-18605)
(NASA-CR-181997; NAS 1.26:181997; ICASE-90-15) Avail: NTIS HC A03/MF A01 CSCL 01A

Compressible turbulent flows at low turbulent Mach numbers are considered. Contrary to the general belief that such flows are almost incompressible, (i.e., the divergence of the velocity field remains small for all times), it is shown that even if the divergence of the initial velocity field is negligibly small, it can grow rapidly on a non-dimensional time scale which is the inverse of the fluctuating Mach number. An asymptotic theory which enables one to obtain a description of the flow in terms of its divergence-free and vorticity-free components has been developed to solve the initial-value problem. As a result, the various types of low Mach number turbulent regimes have been classified with respect to the initial conditions. Formulae are derived that accurately predict the level of compressibility after the initial transients have disappeared. These results are verified by extensive direct numerical simulations of isotropic turbulence. Author

N90-22540*# Institute for Computer Applications in Science and Engineering, Hampton, VA.
SECONDARY FREQUENCIES IN THE WAKE OF A CIRCULAR CYLINDER WITH VORTEX SHEDDING Final Report
Saul S. Abarbanel, Wai Sun Don, David Gottlieb (Brown Univ., Providence, RI.), David H. Rudy, and James C. Townsend Feb. 1990 27 p Submitted for publication
(Contracts NAS1-18107; NAS1-18605)
(NASA-CR-181998; NAS 1.26:181998; ICASE-90-16) Avail: NTIS HC A03/MF A01 CSCL 01A

A detailed numerical study of two-dimensional flow past a circular cylinder at moderately low Reynolds numbers was conducted using three different numerical algorithms for solving the time-dependent compressible Navier-Stokes equations. It was found that if the algorithm and associated boundary conditions were consistent and stable, then the major features of the unsteady wake were well-predicted. However, it was also found that even stable and consistent boundary conditions could introduce additional periodic phenomena reminiscent of the type seen in previous wind-tunnel experiments. However, these additional frequencies were eliminated by formulating the boundary conditions in terms of the characteristic variables. An analysis based on a simplified model provides an explanation for this behavior. Author

N90-22541# Arizona State Univ., Tempe. Dept. of Mechanical and Aerospace Engineering.
MULTI-AXIS, 3-D, SCANNING LDA (LASER DOPPLER ANEMOMETER) SYSTEM FOR UNSTEADY AERODYNAMICS Final Technical Report, 1 Oct. 1986 - 30 Sep. 1988
William S. Saric Dec. 1989 10 p
(Grant AF-AFOSR-0014-87; AF Proj. 2307)
(AD-A218571; AFOSR-90-0247TR) Avail: NTIS HC A02/MF A01 CSCL 20/4

A low noise, two velocity component flow measurement system was developed. It consists of a two color Laser-Doppler anemometer and a two channel hot wire system. GRA

N90-22542# Defence Research Establishment Suffield, Ralston (Alberta).
ESTIMATION OF EXTRA DRAG FORCE ON A CIRCULAR CYLINDER DUE TO THE PRESENCE OF SOLID PARTICLES IN SUBSONIC COMPRESSIBLE FLOW
Stanley B. Mellsen Aug. 1989 69 p
(AD-A218635; DRES-SM-1267; PCN-051-SA) Avail: NTIS HC A04/MF A01 CSCL 19/9

The effect of particles, such as dust in air, on aerodynamic drag of circular cylinders was calculated for compressible flow at critical Mach number and for incompressible flow. The effect of compressibility was found negligible for particles larger than about 10 microns, for which the air can be considered a continuum. Drag coefficient and collection efficiency are provided for a wide range of inertia parameters and Reynolds numbers for both compressible and incompressible flow. GRA

N90-22543# Nielsen Engineering and Research, Inc., Mountain View, CA.
THE EFFECTS OF COMPRESSIBILITY ON A SUPERSONIC MIXING LAYER Annual Report, 1 Dec. 1988 - 30 Nov. 1989
D. Nixon, L. R. Keefe, and G. D. Kuhn 28 Dec. 1989 23 p
(Contract F49620-88-C-0003)
(AD-A219315; AFOSR-90-0191TR) Avail: NTIS HC A03/MF A01 CSCL 20/4

The flow mechanism that cause the decrease in spreading rate of supersonic mixing layers as the convective Mach number increases is identified and means are suggested of enhancing the mixing. Two approaches were taken, one numerical and one analytic. A computer code, TMRC, was used to simulate both time and space developing mixing layers to get some indication of the flow physics. To complement the numerical study a simple analysis was developed which explains the variation of mixing rate with convective Mach number. The analysis seems to indicate that little can be done to enhance mixing as such, although the real problem of simultaneous mixing and combustion may be more amendable to control. GRA

03 AIR TRANSPORTATION AND SAFETY

Includes passenger and cargo air transport operations; and aircraft accidents.

For related information see also *16 Space Transportation* and *85 Urban Technology and Transportation.*

N90-22544 Civil Aviation Authority, London (England).
UK AIRMISSES INVOLVING COMMERCIAL AIR TRANSPORT, JANUARY - APRIL 1989
Dec. 1989 40 p

(ISSN-0951-6301; ETN-90-96445) Copyright Avail: Civil Aviation Authority, Greville House, 37 Gratton Road, Cheltenham, England

Copies of the completed airmiss reports involving commercial air transport aircraft in a four month period are presented. The purpose and the investigation of the airmiss reports are explained. The categorization of airmisses, relating to the degree of risk inherent in each report, is described. The number of incidents, the actual number of commercial air transport aircrafts involved and the airmisses related to flying hours, which took place Jan. to Apr. 1989 are given. ESA

N90-22545# Simula, Inc., Phoenix, AZ.
AIRCRAFT CRASH SURVIVAL DESIGN GUIDE. VOLUME 1: DESIGN CRITERIA AND CHECKLISTS Final Report, Sep. 1986 - Aug. 1989
Richard E. Zimmerman and Norman A. Merritt Dec. 1989 217 p Revised
(Contract DAAJ02-86-C-0028)
(AD-A218434; USAAVSCOM-TR-89-D-22A-Vol-1) Avail: NTIS HC A10/MF A02 CSCL 01/3

This five-volume publication was compiled to assist design engineers in understanding the design considerations associated with the development of crash-resistant U.S. Army aircraft. A collection of available information and data pertinent to aircraft crash resistance is presented, along with suggested design conditions and criteria. The five volumes of the Aircraft Crash Survival Design Guide cover the following topics: Design Criteria and Checklists; Aircraft Design Crash Impact Conditions and Human Tolerance; Aircraft Structural Crash Resistance; Aircraft Seats, Restraints, Litters and Cockpit/Cabin Delethalization; and Aircraft Postcrash Survival. This volume (Volume 1) contains concise criteria drawn from Volumes 2 through 5, supplemented by checklists intended to assist designers in implementing the criteria. GRA

N90-22546# Simula, Inc., Phoenix, AZ.
AIRCRAFT CRASH SURVIVAL DESIGN GUIDE. VOLUME 2: AIRCRAFT DESIGN CRASH IMPACT CONDITIONS AND HUMAN TOLERANCE Final Report, Sep. 1986 - Aug. 1989
J. W. Coltman, C. V. Ingen, N. B. Johnson, and Richard E. Zimmerman Dec. 1989 132 p Revised
(Contract DAAJ02-86-C-0028)
(AD-A218435; USAAVSCOM-TR-89-D-22B-Vol-2) Avail: NTIS HC A07/MF A01 CSCL 01/3

This five-volume publication was compiled to assist design engineers in understanding the design considerations associated with the development of crash-resistant U.S. Army aircraft. A collection of available information and data pertinent to aircraft crash resistance is presented, along with suggested design conditions and criteria. The five volumes of the Aircraft Crash Survival Design guide cover the following topics: Design Criteria and Checklists; Aircraft Design Crash Impact Conditions and Human Tolerance; Aircraft Structural Crash Resistance; Aircraft Seats, Restraints, Litters and Cockpit/Cabin Delethalization; and Aircraft Postcrash Survival. This volume (Volume 2) contains information on the aircraft crash environment, human tolerance to impact, occupant motion during a crash, human anthropometry, and crash test dummies, all of which serves as background for the design information presented in the other volumes. GRA

N90-22547# Simula, Inc., Phoenix, AZ.
AIRCRAFT CRASH SURVIVAL DESIGN GUIDE. VOLUME 3: AIRCRAFT STRUCTURAL CRASH RESISTANCE Final Report, Sep. 1986 - Aug. 1989
Richard E. Zimmerman, James C. Warrick, Alan D. Lane, Norman A. Merritt, and Akif O. Bolukbasi Dec. 1989 265 p Revised
(Contract DAAJ02-86-C-0028)
(AD-A218436; USAAVSCOM-TR-89-D-22C-Vol-3) Avail: NTIS HC A12/MF A02 CSCL 01/3

This five volume publication was compiled to assist design engineers in understanding the design considerations associated with the development of crash resistant U.S. Army aircraft. A collection of available information and data pertinent to aircraft crash resistance is presented, along with suggested design conditions and criteria. The five volumes of the Aircraft Crash Survival Design Guide cover the following topics: Design Criteria and Checklists; Aircraft Design Crash Impact Conditions and Human Tolerance; Aircraft Structural Crash Resistance; Aircraft Seats, Restraints, Litters and Cockpit/Cabin Delethalization; and Aircraft Postcrash Survival. This volume (Volume 3) contains information on the design of aircraft structures and structural elements for improved crash survivability. Current requirements for structural design of U.S. Army aircraft pertaining to crash resistance are discussed. Principles for crash-resistant design are presented in detail for the landing gear and fuselage subject to a range of crash conditions, including impacts that are primarily longitudinal, vertical or lateral in nature and those that involve more complicated dynamic conditions, such as rollover. Analytical methods for evaluating structural crash resistance are described. GRA

N90-22548# Simula, Inc., Phoenix, AZ.
AIRCRAFT CRASH SURVIVAL DESIGN GUIDE. VOLUME 4: AIRCRAFT SEATS, RESTRAINTS, LITTERS, AND COCKPIT/CABIN DELETHALIZATION Final Report, Sep. 1986 - Aug. 1989
S. P. Desjardins, Richard E. Zimmerman, Akif O. Bolukbasi, and Norman A. Merritt Dec. 1989 271 p Revised
(Contract DAAJ02-86-C-0028)
(AD-A218437; USAAVSCOM-TR-89-D-22D-Vol-4) Avail: NTIS HC A12/MF A02 CSCL 01/3

This five-volume publication was compiled to assist design engineers in understanding the design considerations associated with the development of crash-resistant U.S. Army aircraft. A collection of available information and data pertinent to aircraft crash resistance is presented, along with suggested design conditions and criteria. The five volumes of the Aircraft Crash Survival Design Guide cover the following topics: Design Criteria and Checklists; Aircraft Design Crash Impact Conditions and Human Tolerance; Aircraft Structural Crash Resistance; Aircraft Seats, Restraints, Litters and Cockpit/Cabin Delethalization; and Aircraft Postcrash Survival. This Volume (4) contains information on aircraft seats, litters, personnel restraint systems, and hazards on the occupant's immediate environment. Requirements for design of seats, litters, and restraints systems are discussed, as well as design principles for meeting these requirements and testing for verification that the systems perform as desired. Energy-absorbing devices for use in seats are described, as are various types of cushions. Delethalization of cockpit and cabin interiors is discussed, including the use of protective padding and the design of controls for prevention of injury. Finally, computerized methods of analysis for evaluation of seats, restraints, and the occupant's immediate environment are presented. GRA

N90-22549# Simula, Inc., Phoenix, AZ.
AIRCRAFT CRASH SURVIVAL DESIGN GUIDE. VOLUME 5: AIRCRAFT POSTCRASH SURVIVAL Final Report, Sep. 1986 - Aug. 1989
N. B. Johnson, S. H. Robertson, and D. S. Hall Dec. 1989 219 p Revised
(Contract DAAJ02-86-C-0028)
(AD-A218438; USAAVSCOM-TR-89-D-22E-Vol-5) Avail: NTIS HC A10/MF A02 CSCL 01/3

This five-volume publication was compiled to assist design engineers in understanding the design considerations associated with the development of crash-resistant U.S. Army aircraft. A collection of available information and data pertinent to aircraft crash resistance is presented, along with suggested design conditions and criteria. The five volumes of the Aircraft Crash Survival Design Guide cover the following topics: Design Criteria and Checklists; Aircraft Design Crash Impact Conditions and Human Tolerance; Aircraft Structural Crash Resistance; Aircraft Seats, Restraints, Litters and Cockpit/Cabin Delethalization; and Aircraft Postcrash Survival. This volume (Volume 5) contains information on the aircraft postcrash environment and design techniques that can be used to reduce postcrash hazards. Topics include the

postcrash fire environment, crashworthy fuel systems, ignition source control, fire behavior of interior materials, ditching survival, emergency escape, and crash locator beacons. GRA

N90-22550# Oklahoma Univ., Norman. Cooperative Inst. for Mesoscale Meteorological Studies.
TURBULENCE SPECTRAL WIDTHS VIEW ANGLE INDEPENDENCE AS OBSERVED BY DOPPLER RADAR Final Report
J. T. Lee and K. Thomas Oct. 1989 56 p LIMITED REPRODUCIBILITY: Availability: Document partially illegible
(Contract DTFA01-80-Y-10524)
(AD-A219169; DOT/FAA/SA-89/4) Avail: NTIS HC A04/MF A01 CSCL 17/9

As air traffic density increases, effective use of airspace must include consideration of weather. Accurate identification of turbulent volumes is of paramount importance to flight safety. The advent of Doppler radar has made it possible to observe wind motion in connective clouds. Over a number of years, research has lead to the spectral width (standard deviation) of the Doppler velocity measurements as an indicator of turbulence. The hypotheses is addressed which states that turbulence is essentially isotropic in convective systems, and therefore, observations of turbulence are independent of viewing angle. Radar observations were scanned to locate storms amendable to analysis. A number of cases are presented in which a dual-Doppler network provided the essential data. Each case is in a different quadrant with respect to the Norman Doppler. Forty-four horizontal planes were studied from six different storms. The results of four of these storms are presented. Maximum reflectivity of these storms range from 51 to 58 dBZ. Altitudes included range from near surface to 7 km. At these altitudes the maximum spectral width was 12 ms-1. For these cases, involving nearly 30,000 data points, 70 percent of the spectral width observations from CIM and NRO were within 1 ms-1 or less. These results indicate that the use of Doppler radar to detect turbulent regions within thunderstorms has a high probability of success, and the turbulent regions can be detected independent of the direction from which they are viewed. GRA

04 AIRCRAFT COMMUNICATIONS AND NAVIGATION

Includes digital and voice communication with aircraft; air navigation systems (satellite and ground based); and air traffic control.

For related information see also *17 Space Communications, Spacecraft Communications, Command and Tracking* and *Communications and Radar.*

N90-22551 Department of the Navy, Washington, DC.
APPARATUS FOR AND A METHOD OF DETERMINING COMPASS HEADINGS Patent
Daniel G. Jablonski, inventor (to Navy) 14 Nov. 1989 5 p Filed 24 Jun. 1985 Supersedes N86-23584 (24 - 14, p 2234), AD-D012051
(AD-D014436; US-Patent-4,881,080; US-Patent-Appl-SN-748248)
Avail: US Patent and Trademark Office CSCL 17/7

A compass system and method incorporating a global positioning system (GPS), such as the NAVSTAR/GPS multi-satellite system, is configured to acquire accurate compass heading information without being affected by magnetic anomalies and without being dependent on the elapsed time since a previous position fix. The compass system comprises, inter alia, two antenna/preamplifiers located, for example, fore and aft a ship or aircraft separated by a predetermined distance d. A microprocessor/minicomputer portion of the system causes an electronic coaxial switch to switch a GPS receiver between the two antenna/preamplifiers automatically thereby measuring their absolute positions. The microprocessor/minicomputer computers and displays on a display unit a compass heading based on the knowledge of the absolute positions of the antenna/preamplifiers and the distance d there between. GRA

N90-22552# Army Engineer Topographic Labs., Fort Belvoir, VA.
THE DEVELOPMENT OF A REAL-TIME DECIMETER-LEVEL POSITIONING SYSTEM USING GLOBAL POSITIONING SYSTEM (GPS) TECHNOLOGY
Kevin P. Loga 14 Feb. 1990 6 p
(AD-A218695; SEL-R-150) Avail: NTIS HC A02/MF A01 CSCL 17/7

The U.S. Army Corps of Engineers spends in excess of $350 million annually dredging the nation's ports, harbors and waterways. An additional $40 million is spent performing hydrographic surveys supporting the planning, engineering and design phases of this effort. The USAETL has been tasked to develop a real-time decimeter-level positioning system using Global Positioning System (GPS) technology to support the Corps hydrographic surveying and dredging operations. USAETL's research and development efforts involved in the development of this positioning system are discussed. GRA

N90-22553# Army Armor and Engineer Board, Fort Knox, KY.
M1A2 ADJUNCT ANALYSIS (POSNOV VOLUME) Report, Nov. - Dec. 1989
K. S. Collier, David A. Blandford, and William W. Dibble 15 Dec. 1989 68 p
(AD-A218802) Avail: NTIS HC A04/MF A01 CSCL 17/7

The TRADOC Analysis Command (TRAC) completed the M1A2 COEA in March 1989. This report supplements the M1A2 COEA. The Defense Acquisition Board (DAB) authorized full scale development and testing of the preferred M1A2 tank configuration. The DAB stated that additional analytic justification is required to include the Position Navigation unit, the CO2 Laser Rangefinder and the Survivability Enhancements Packages 1 and 2 in the Milestone III production decision. The analysis presented in this report is limited to the Position Navigation (POSNAV) capabilities, its impact on force effectiveness, operational suitability, and training effectiveness, and its cost effectiveness to the force. GRA

N90-22554# Carnegie-Mellon Univ., Pittsburgh, PA. Software Engineering Inst.
INERTIAL NAVIGATION SYSTEM SIMULATOR: BEHAVIORAL SPECIFICATION, REVISION Final Report
Stefan F. Landherr and Mark H. Klein Aug. 1989 39 p
(Contract F19628-85-C-0003)
(AD-A219294; CMU/SEI-89-TR-35-Rev; ESD-TR-89-46-Rev)
Avail: NTIS HC A03/MF A01 CSCL 17/7

The Real-Time Embedded Systems Testbed (REST) Project at the Software Engineering Institute is specifying and developing a representative real-time application. An original set of specifications written by a Navy affiliate is augmented. The purpose of this behavioral specification is to clarify and augment the original. GRA

05 AIRCRAFT DESIGN, TESTING AND PERFORMANCE

Includes aircraft simulation technology.

For related information see also *18 Spacecraft Design, Testing and Performance* and *39 Structural Mechanics.*For land transportation vehicles see *85 Urban Technology and Transportation.*

N90-22555*# National Aeronautics and Space Administration. Langley Research Center, Hampton, VA.
AN EXPERIMENTAL STUDY OF TIP SHAPE EFFECTS ON THE FLUTTER OF AFT-SWEPT, FLAT-PLATE WINGS
Bryan E. Dansberry, Jose A. Rivera, Jr., and Moses G. Farmer Washington Jun. 1990 22 p
(NASA-TM-4180; L-16638; NAS 1.15:4180) Avail: NTIS HC A03/MF A01 CSCL 01C

The effects of tip chord orientation on wing flutter are investigated experimentally using six cantilever-mounted, flat-plate wing models. Experimentally determined flutter characteristics of

the six models are presented covering both the subsonic and transonic Mach number ranges. While all models have a 60 degree leading edge sweep, a 40.97 degree trailing edge sweep, and a root chord of 34.75 inches, they are subdivided into two series characterized by a higher aspect ratio and a lower aspect ratio. Each series is made up of three models with tip chord orientations which are parallel to the free-stream flow, perpendicular to the model mid-chord line, and perpendicular to the free-stream flow. Although planform characteristics within each series of models are held constant, structural characteristics such as mode shapes and natural frequencies are allowed to vary. Author

N90-22556 Georgia Inst. of Tech., Atlanta.
APPLICATION OF A DYNAMIC STALL MODEL TO ROTOR TRIM AND AEROELASTIC RESPONSE Ph.D. Thesis
Mnaouar Chouchane 1989 205 p
Avail: Univ. Microfilms Order No. DA9005475

A unified aerodynamic lift model including stall is used to describe the aerodynamic environment of a rotor blade. The model is successfully used in conjunction with an elastic blade formulation to predict the aerodynamic forces on the helicopter blade and the flap-lag-torsional response before and after stall occurs. The control settings are assumed to be initially unknown and are computed as a part of the solution by an auto-pilot controller. A solution method based on a modified Galerkin's method is used to separate the time and space variables in the differential equations. The numerical solution is obtained by a time marching method for solving systems of first-order differential equations. The structural model consists mainly of flap, lag, and torsion equations. These equations can be reduced to rigid blade equations by using a single mode for each degree of freedom. The fast rate of convergence of the elastic solution shows that the orthogonal polynomials used in this work represented a good choice for the comparison functions. The unified-aerodynamic model is an extension of the model developed by the Office National d'Etudes et de Recherches Aerospaciales and includes plunge, unsteady free stream, and large angles of attack. The model is used to predict both the unsteady nonlinear lift and pitching. Dynamic response was conducted for a variety of thrust coefficients and advance ratios with both rigid and elastic blade assumptions and at several torsional frequencies. The correlation of the results with flight test data from the SA349/2 helicopter has generally resulted in a good prediction of the vehicle control settings.
Dissert. Abstr.

N90-22557*# Lockheed Engineering and Sciences Co., Hampton, VA.
MULTILEVEL DECOMPOSITION APPROACH TO THE PRELIMINARY SIZING OF A TRANSPORT AIRCRAFT WING
Gregory A. Wrenn and Augustine R. Dovi Washington NASA [1990] 31 p
(Contract NAS1-19000)
(NASA-CR-4296; NAS 1.26:4296) Avail: NTIS HC A01/MF A01 CSCL 01C

A multilevel/multidisciplinary optimization scheme for sizing an aircraft wing structure is described. A methodology using nonlinear programming in application to a very large engineering problem is presented. This capability is due to the decomposition approach. Over 1300 design variables are considered for this nonlinear optimization task. In addition, a mathematical link is established coupling the detail of structural sizing to the overall system performance objective, such as fuel consumption. The scheme is implemented as a three level system analyzing aircraft mission performance at the top level, the total aircraft structure as the middle level, and individual stiffened wing skin cover panels at the bottom level. Numerical show effectiveness of the method and its good convergence characteristics. Author

N90-22558*# National Aeronautics and Space Administration. Langley Research Center, Hampton, VA.
DIFFERENTIAL EQUATION BASED METHOD FOR ACCURATE APPROXIMATIONS IN OPTIMIZATION
Jocelyn I. Pritchard (Army Aerostructures Directorate, Hampton, VA.) and Howard M. Adelman Apr. 1990 14 p Presented at the 31st AIAA/ASME/ASCE/AHS/ASC Structures, Structural Dynamics, and Materials Conference, Long Beach, CA, 2-4 Apr. 1990 Previously announced in IAA as A90-29267
(NASA-TM-102639; NAS 1.15:102639; AVSCOM-TM-90-B-006)
Avail: NTIS HC A03/MF A01 CSCL 01C

A method to efficiently and accurately approximate the effect of design changes on structural response is described. The key to this method is to interpret sensitivity equations as differential equations that may be solved explicitly for closed form approximations, hence, the method is denoted the Differential Equation Based (DEB) method. Approximations were developed for vibration frequencies, mode shapes and static displacements. The DEB approximation method was applied to a cantilever beam and results compared with the commonly-used linear Taylor series approximations and exact solutions. The test calculations involved perturbing the height, width, cross-sectional area, tip mass, and bending inertia of the beam. The DEB method proved to be very accurate, and in most cases, was more accurate than the linear Taylor series approximation. The method is applicable to simultaneous perturbation of several design variables. Also, the approximations may be used to calculate other system response quantities. For example, the approximations for displacements are used to approximate bending stresses. Author

N90-22559# Air Force Human Resources Lab., Brooks AFB, TX.
FIELD-OF-VIEW ASSESSMENT OF LOW-LEVEL FLIGHT AND AN AIRDROP IN THE C-130 WEAPON SYSTEM TRAINER (WST) Final Report, Nov. 1988 - Jan. 1989
Kevin W. Dixon, Elizabeth L. Martin, Victoria A. Rojas, and David C. Hubbard (Dayton Univ., OH.) Jan. 1990 27 p
(AD-A218504; AFHRL-TR-89-9) Avail: NTIS HC A03/MF A01 CSCL 01/2

The purpose of this effort was to determine the requirement for the far peripheral windows and associated imagery for low-level navigation and airdrop tasks. Although these windows are available for use by the pilot and copilot, their inclusion was primarily for the navigator position. Currently, the navigator position is not included in the simulator training syllabus. If the imagery currently provided in the peripheral windows could be allocated to the remaining scene, the level of detail in the scene could be considerably enhanced. Previous research has shown that the enhanced scene content resulted in superior pilot performance. A within subjects design was used in which 12 experienced C-130 pilots performed four trials over two different routes under two field-of-view (FOV) conditions. Automated pilot performance measures and eye position data were collected. The pilot performance data showed no strong or consistent effects as a result of the FOV manipulations. However, the eye position data revealed an increased use of the front window and instruments, and a decreased use of the window to the left of the pilot in the limited-FOV condition. The conclusions of the study are that the peripheral windows may not be required for experienced pilots, but that their presence or absence results in different visual behaviors. It is recommended that a full FOV be provided when the training objectives include tasks that require a large amount of peripheral information. GRA

N90-22560# Systems Technology, Inc., Hawthorne, CA.
MINIMUM FLYING QUALITIES. VOLUME 1: PILOTED SIMULATION EVALUATION OF MULTIPLE AXIS FLYING QUALITIES Final Report, Oct. 1985 - Jul. 1989
David G. Mitchell, Bimal L. Aponso, and Roger H. Hoh Jan. 1990 445 p
(Contract F33615-85-C-3610; AF Proj. 2403)
(AD-A218560; STI-TR-1235-1-1; WRDC-TR-89-3125-Vol-1) Avail: NTIS HC A19/MF A01 CSCL 01/2

The project was initiated to explore the modern nature of minimum flying qualities in the presence of modern aircraft and multi-redundant flight control system technology. It had several phases, including: (1) an intensive effort to develop and/or elaborate existing pilot modeling analysis techniques to apply to

situations associated with minimum flying qualities, divided attention pilot operations, and multi-axis control tasks; (2) preliminary analyses and associated fixed base simulations to expand the meager multi-axis data base and to serve as pilot studies for more extensive simulations on the Air Force's Large Amplitude Multimode Aerospace Research Simulator; (3) an extensive simulation program on LAMARS to investigate minimum flying qualities and related situations; and (4) analysis and interpretation of both the early and LAMARS simulation efforts in the context of the pilot modeling advances. The project documentation appears in three volumes. GRA

N90-22561# Systems Technology, Inc., Hawthorne, CA.
MINIMUM FLYING QUALITIES. VOLUME 2: PILOT MODELING FOR FLYING QUALITIES APPLICATIONS Final Report, Oct. 1985 - Jul. 1989
Duane T. McRuer, Warren F. Clement, Peter M. Thompson, and Raymond E. Magdaleno Jan. 1990 132 p
(Contract F33615-85-C-3610; AF Proj. 2403)
(AD-A218561; STI-TR-1235-1-2; WRDC-TR-89-3125-Vol-2) Avail: NTIS HC A07/MF A01 CSCL 17/7

The project was initiated to explore the modern nature of minimum flying qualities in the presence of modern aircraft and multi-redundant flight control system technology. It had several phases, including: (1) an intensive effort to develop and/or elaborate existing pilot modeling analysis techniques to apply to situations associated with minimum flying qualities, divided attention pilot operations, and multi-axis control tasks; (2) preliminary analyses and associated fixed base simulation to expand the meager multi-axis data base and to serve as pilot studies for more extensive simulations on the Air Force's Large Amplitude Multimode Aerospace Research Simulator; (3) an extensive simulation program on LAMARS to investigate minimum flying qualities and related situations; and (4) analysis and interpretation of both early and LAMARS simulation efforts in the context of the pilot modeling advances. The project documentation appears in three volumes. Volume 1 reports on the results of (2) through (4) above. This volume is a stand-alone monograph on pilot modeling, including procedures for estimating pilot workload as measured by pilot ratings. Volume 3 is a stand-alone monograph which presents a detailed implementation of a much expanded version of the human optimal control model on Program CC. GRA

N90-22562# Systems Technology, Inc., Hawthorne, CA.
MINIMUM FLYING QUALITIES. VOLUME 3: PROGRAM CC'S IMPLEMENTATION OF THE HUMAN OPTIMAL CONTROL MODEL Final Report, Oct. 1985 - Jul. 1989
Peter M. Thompson Jan. 1990 88 p
(Contract F33615-85-C-3610; AF Proj. 2403)
(AD-A218562; STI-TR-1235-1-3; WRDC-TR-89-3125-Vol-3) Avail: NTIS HC A05/MF A01 CSCL 12/5

The project was initiated to explore the modern nature of minimum flying qualities in the presence of modern aircraft and multi-redundant flight control system technology. It had several phases, including: (1) an intensive effort to develop and/or elaborate existing pilot modeling analysis techniques to apply to situations associated with minimum flying qualities, divided attention pilot operations, and multi-axis control tasks; (2) preliminary analyses and associated fixed base simulations to expand the meager multi-axis data base and to serve as pilot studies for more extensive simulations on the Air Force's Large Amplitude Multimode Aerospace Research Simulator; (3) an extensive simulation program on LAMARS to investigate minimum flying qualities and related situations; and (4) analysis and interpretation of both the early and LAMARS simulation efforts in the context of the pilot modeling advances. The project documentation appears in three volumes. Volume 1 reports on the results of (2) through (4) above. Volume 2 is a stand-alone monograph on pilot modeling, including procedures for estimating pilot workload as measured by pilot ratings. This volume is a stand-alone monograph which presents a detailed implementation of a much expanded version of the human optimal control model on Program CC. GRA

06 AIRCRAFT INSTRUMENTATION

Includes cockpit and cabin display devices; and flight instruments.

For related information see also *19 Spacecraft Instrumentation* and *35 Instrumentation and Photography.*

N90-22563# Charles River Analytics, Inc., Cambridge, MA.
MODEL-BASED METHOD FOR TERRAIN-FOLLOWING DISPLAY DESIGN Final Report, 15 Jan. - 5 Jun. 1989
Paul G. Gonsalves, Edward W. Kneller, Greg L. Zacharias, Ralph J. St.John, and Bradley D. Purvis 15 Jun. 1989 124 p
(Contract F33615-86-C-0551)
(AD-A219302; AAMRL-TR-89-039) Avail: NTIS HC A06/MF A01 CSCL 17/7

A model-based method for terrain following display design and evaluation is described. The basic approach centers on the use of a pilot/vehicle/display model based on the optimal control model (OCM), which combines general knowledge of human perception and performance, with specific knowledge of terrain following aircraft and avionics capabilities. A real-time terrain following simulation facility was developed, implemented, and exercised to provide an experimental basis for validating model-based display designs, and to serve as a tool for developing and testing displays. Two basic display configurations were studied: a nominal vertical situation display (VSD) along with several enhancements, and a pictorial guidance display (PGD). Model-based analysis of the real-time simulator data demonstrated the ability to closely match performance and frequency response trends across the range of display configurations studied, accounting for both general performance trends and fine-grained pilot dynamic response strategy in the measured data. GRA

07 AIRCRAFT PROPULSION AND POWER

Includes prime propulsion systems and systems components, e.g., gas turbine engines and compressors; and onboard auxilliary power plants for aircraft.

For related information see also *20 Spacecraft Propulsion and Power, 28 Propellants and Fuels,* and *44 Energy Production and Conversion.*

N90-22564*# National Aeronautics and Space Administration. Lewis Research Center, Cleveland, OH.
LARGE-SCALE ADVANCED PROPELLER BLADE PRESSURE DISTRIBUTIONS: PREDICTION AND DATA
M. Nallasamy, O. Yamamoto, S. Warsi (Sverdrup Technology, Inc., Cleveland, OH.), and L. J. Bober 1989 19 p Presented at the 25th Joint Propulsion Conference, Monterey, CA, 10-12 Jul. 1989; cosponsored by AIAA, ASME, SAE, and ASEE Previously announced in IAA as A89-47026 Original contains color illustrations
(NASA-TM-102316; E-4914; NAS 1.15:102316; AIAA-89-2696)
Avail: NTIS HC A03/MF A01; 5 functional color pages CSCL 21E

Two Euler analyses techniques, finite difference and finite volume, were employed to predict the blade surface pressure distributions of a large scale advanced propeller. The predicted pressure distributions were compared with wind tunnel data. Both techniques produced blade pressure distributions that are in fairly good agreement with the data over the range of test Mach numbers of 0.2 to 0.78. However, the numerical simulations fail to predict correctly the measured pressure distributions for the low Mach number, high power case. The data indicate the presence of a leading edge vortex for this case. A discussion of the compressibility effects is also presented. Author

N90-22565 Stevens Inst. of Tech., Hoboken, NJ.
COMPUTATIONAL AND EXPERIMENTAL INVESTIGATIONS OF ROTATING STALL IN COMPRESSOR CASCADES Ph.D. Thesis

Sreenadh S. Jonnavithula 1988 207 p
Avail: Univ. Microfilms Order No. DA9001134

The phenomenon of rotating stall appears in compressors operating under severe loadings at off design points. This causes undesirable loss of performance and the resulting periodic loading on the blades leads to noise, vibration and possibly fatigue failure. Numerical and experimental methods are employed to study this phenomenon. The relatively novel discrete vortex method is employed to numerically predict the occurrence of rotating stall in isolated cascades, and also to establish the stall propagation rates in the post stall regime. This method consists of discretizing the flow field by using a large collection of vortex blobs which are then allowed to convect under their mutual influence. The streamline plots of the stalled cascade obtained aid in the visualization of the phenomenon, showing explicit evidence of strong reverse flows within the stall cell. Detailed parametric studies of the influence of the various flow parameters like the inflow angle and stall cell wavelength, and geometric parameters like the cascade solidity, blade camber and stagger have been performed. It is found that the influence of most of these parameters is quite complex, with strong parameter interaction. Thus, the stall propagation velocity decreased with inflow angle at low stagger angles, but increased with inflow angle for high stagger angles. The effect of camber was found to be primarily in altering the stall inception point and there was little influence on the post stall regime. Increased blade solidity was found to decrease the velocity. An experimental investigation of rotating stall was conducted using the Stevens axial compressor test rig. The occurrence of rotating stall in this research compressor was demonstrated, and some experimental studies were conducted of the effect of the various flow parameters on the propagation velocity. Traverses of the stalled flow field combined with digital data acquisition and ensemble averaging procedures produced detailed information on the variations of axial and tangential velocities throughout the radial extent of the stall cell. Dissert. Abstr.

N90-22566*# National Aeronautics and Space Administration. Lewis Research Center, Cleveland, OH.
A MODELING TECHNIQUE FOR STOVL EJECTOR AND VOLUME DYNAMICS
C. K. Drummond and W. S. Barankiewicz 1990 13 p Presented at the 26th Joint Propulsion Conference, Orlando, FL, 16-18 Jul. 1990; cosponsored by AIAA, SAE, ASME, and ASEE
(NASA-TM-103167; E-5539; NAS 1.15:103167; AIAA-90-2417)
Avail: NTIS HC A03/MF A01 CSCL 21E

New models for thrust augmenting ejector performance prediction and feeder duct dynamic analysis are presented and applied to a proposed Short Take Off and Vertical Landing (STOVL) aircraft configuration. Central to the analysis is the nontraditional treatment of the time-dependent volume integrals in the otherwise conventional control-volume approach. In the case of the thrust augmenting ejector, the analysis required a new relationship for transfer of kinetic energy from the primary flow to the secondary flow. Extraction of the required empirical corrections from current steady-state experimental data is discussed; a possible approach for modeling insight through Computational Fluid Dynamics (CFD) is presented. Author

N90-22567*# General Motors Corp., Indianapolis, IN. Gas Turbine Div.
INVESTIGATION OF ADVANCED COUNTERROTATION BLADE CONFIGURATION CONCEPTS FOR HIGH SPEED TURBOPROP SYSTEMS, TASK 1: DUCTED PROPFAN ANALYSIS Final Report
Edward J. Hall, Robert A. Delaney, and James L. Bettner Apr. 1990 158 p Original contains color illustrations
(Contract NAS3-25270)
(NASA-CR-185217; NAS 1.26:185217; EDR-14622) Avail: NTIS HC A08/MF A01; 11 functional color pages CSCL 21E

The time-dependent three-dimensional Euler equations of gas dynamics were solved numerically to study the steady compressible transonic flow about ducted propfan propulsion systems. Aerodynamic calculations were based on a four-stage Runge-Kutta time-marching finite volume solution technique with added numerical dissipation. An implicit residual smoothing operator was used to aid convergence. Two calculation grids were employed in this study. The first grid utilized an H-type mesh network with a branch cut opening to represent the axisymmetric cowl. The second grid utilized a multiple-block mesh system with a C-type grid about the cowl. The individual blocks were numerically coupled in the Euler solver. Grid systems were generated by a combined algebraic/elliptic algortihm developed specifically for ducted propfans. Numerical calculations were initially performed for unducted propfans to verify the accuracy of the three-dimensional Euler formulation. The Euler analyses were then applied for the calculation of ducted propfan flows, and predicted results were compared with experimental data for two cases. The three-dimensional Euler analyses displayed exceptional accuracy, although certain parameters were observed to be very sensitive to geometric deflections. Both solution schemes were found to be very robust and demonstrated nearly equal efficiency and accuracy, although it was observed that the multi-block C-grid formulation provided somewhat better resolution of the cowl leading edge region. Author

08 AIRCRAFT STABILITY AND CONTROL

Includes aircraft handling qualities; piloting; flight controls; and autopilots.

For related information see also *05 Aircraft Design, Testing and Performance.*

N90-22568 Virginia Univ., Charlottesville.
LIMITING PERFORMANCE BASED STRUCTURAL AND CONTROL OPTIMIZATION FOR LARGE VIBRATING STRUCTURES Ph.D. Thesis
Tae Wook Lim 1989 149 p
Avail: Univ. Microfilms Order No. DA9002838

Systematic design procedures were developed to optimize structural parameters and feedback control gains for large vibrating structures subject to constraints on response variables and control forces. The purpose of these optimal design procedures is to minimize selected peak responses and to suppress effectively structural vibrations generated by external disturbances while satisfying prescribed constraints. The procedures are developed by utilizing the limiting performance method for transient systems, which provides the minimum peak value of certain responses while the other system responses are constrained. In order to meet the design goal, a special limiting performance formulation is developed. This is referred to as the limiting-performance/minimum-settling-time (LP/MST) formulation. It is developed in order to reduce the responses after the peaks within the prescribed limits in minimum time and to incorporate multiple performance indices. The optimization for structural parameters such as sampling and stiffness coefficients or for controller parameters such as feedback gains is achieved indirectly by approximating the LP/MST trajectories as closely as possible. This indirect synthesis method is computationally efficient since the entire system dynamics are solved once to find the optimal trajectory. An indirect synthesis is performed locally by taking the response trajectories of the terminal points where the design portion is attached. The structural or control design parameters are identified by using a least squares solution. Also, as an alternative approach, a time domain modal identification method is employed to find optimal eigenvalues which characterize the optimal displacement trajectories. The optimal structural parameters are located using an efficient iterative algorithm based on these eigenvalues. The optimal feedback gains are identified by assigning the eigenvalues using an eigenvalue assignment method. Numerical examples with realistic design objectives and constraints are provided to illustrate the procedures and to demonstrate the capabilities. Dissert. Abstr.

N90-22569 Texas Univ., Austin.
DETERMINATION OF THE GENERAL OCEAN CIRCULATION USING SATELLITE ALTIMETRY FROM A SIMULTANEOUS SOLUTION FOR THE EARTH'S GRAVITY FIELD Ph.D. Thesis
Robert Steven Nerem 1989 345 p
Avail: Univ. Microfilms Order No. DA8920792

Satellite radar altimeters are used to measure the distance from a satellite to the ocean surface. If an accurate ephemeris for the satellite is known, then the height of the ocean surface can be determined. The height of the ocean surface can be described as the sum of the height of the geoid and the height of the sea surface topography, ignoring tides and other effects. The geoid is the equipotential surface of the Earth's gravity field which approximates the mean sea level. The sea surface topography is the deviation of the ocean surface from the geoid due to ocean currents. If the slope of the sea surface topography relative to the geoid is known, then the geostrophic component of the ocean current velocity may be computed. This investigation has resulted in a simultaneous solution for the sea surface topography and the gravity field of the Earth using satellite altimeter and tracking data. A spherical harmonic model of the sea surface topography complete to degree and order 10 and a spherical harmonic model of the geopotential complete to degree and order 50 were estimated in a simultaneous solution using satellite altimeter data from the Seasat and Geosat missions and laser range and Doppler tracking from 14 different satellites. The orbital parameters of each satellite were also estimated in the solution. Separate models for the sea surface topography were estimated for both Seasat and Geosat. The models compare very well with similar oceanographic models computed using hydrographic data and shipdrift data. Over the oceans, the geoid computed from the gravity field model is accurate to approximately 30 cm. The improvement in the sea surface topography model is due in large part to the nature of the simultaneous solution for the topography, the gravity field, and the satellite orbit. Since these parameters are dynamically and kinematically interrelated, improvements in any one of the parameters produced immediate improvements in the other parameters during the simultaneous solution. Dissert. Abstr.

N90-22570# Aeronautical Research Labs., Melbourne (Australia).
FLUTTER INVESTIGATIONS ON A TRANSAVIA PL12/T-400 AIRCRAFT
A. Goldman, C. D. Rider, and P. Piperias Jul. 1989 41 p
(AD-A219108; ARL-STRUC-TM-515; DODA-AR-005-626) Avail: NTIS HC A03/MF A01 CSCL 01/3

The Transavia T-400 Skyfarmer is the latest version of the twin-boom agricultural aircraft and incorporates several changes from the T-300 aircraft. In a ferrying flight in weather conditions which would not normally be experienced during agricultural work, an incident occurred which is believed to have been a limited amplitude flutter of the rudder and tail boom at a frequency around 3.5 Hz. In subsequent tests, the test pilot found that he could induce a similar oscillation by applying more than 50 percent rudder actuation in a series of quick jabs in alternate directions. The subsequent activity to find a solution to the problem is detailed, as are the tests conducted to verify the effectiveness of the solution. GRA

N90-23032*# Kansas Univ., Lawrence. Dept. of Aerospace Engineering.
APPLICATION OF NUMERICAL OPTIMIZATION TECHNIQUES TO CONTROL SYSTEM DESIGN FOR NONLINEAR DYNAMIC MODELS OF AIRCRAFT
C. Edward Lan and Fuying Ge *In* JPL, Proceedings of the 3rd Annual Conference on Aerospace Computational Control, Volume 1 15 Dec. 1989 p 394-406 (For primary document see N90-22987 16-61)
Avail: NTIS HC A21/MF A03 CSCL 01C

N90-23033*# Toronto Univ., Downsview (Ontario). Inst. for Aerospace Studies.
AN INVERSE KINEMATICS ALGORITHM FOR A HIGHLY REDUNDANT VARIABLE-GEOMETRY-TRUSS MANIPULATOR
Frank Naccarato and Peter Hughes in JPL, Proceedings of the 3rd Annual Conference on Aerospace Computational Control, Volume 1 15 Dec. 1989 p 407-420 Sponsored in part by the Natural Sciences and Engineering Research Council of Canada (For primary document see N90-22987 16-61)
Avail: NTIS HC A21/MF A03 CSCL 01C

09 RESEARCH AND SUPPORT FACILITIES (AIR)

Includes airports, hangars and runways; aircraft repair and overhaul facilities; wind tunnels; shock tubes; and aircraft engine test stands.

For related information see also *14 Ground Support Systems and Facilities (Space).*

N90-22571# Aerospatiale Aquitaine, Saint-Medard en Jalles (France). Div. Systemes Strategiques et Spatiaux.
UNCERTAINTY EVALUATION IN AN AUTOMATED HIGH TEMPERATURE ENVIRONMENTAL SIMULATION OVEN [EVALUATION DES INCERTITUDES D'UNE CHAINE AUTOMATISEE D'ETALONNAGE EN TEMPERATURE]
G. Brigodiot and J. C. Lyon 1989 8 p In FRENCH Presented at the Congres International de Metrologie, Paris, France, 21-23 Nov. 1989
(Rept-892-430-103; ETN-90-96634) Avail: NTIS HC A05/MF A01

A high temperature environmental simulation oven is described. The thermocouples used in measuring the oven temperature are described. The data processing equipment linked to the oven is presented. The accuracy of the heat measuring devices is tested. The results of global uncertainties in the measurements are presented. Comparison between an automated and a manual temperature monitoring system is carried out. The cost aspects of using an automated system are discussed. The automated system is concluded as giving simpler and more flexible analysis of results. ESA

N90-22572# Aerospatiale Aquitaine, Saint-Medard en Jalles (France). Div. Systemes Strategiques et Spatiaux.
SIMOUN: AN OPTIMIZED SUPERSONIC HIGH TEMPERATURE WIND TUNNEL FOR TESTING CONSTRUCTION MATERIALS TO BE USED ON THE SPACEPLANE [SIMOUN - SYSTEME D'INVESTIGATION POUR MATERIAUX OPTIMISES UTILISABLES SUR NAVETTE]
J. P. Serrano 20 Jun. 1989 11 p In FRENCH
(Rept-892-430-111; ETN-90-96642) Avail: NTIS HC A03/MF A01

The SIMOUN supersonic high temperature wind tunnel used to test the parts of the Hermes Spaceplane submitted to the highest temperatures during reentry is described. The nose, leading edge, and mid-fuselage of the Spaceplane are tested in this facility. The wind tunnel is able to accurately reproduce the conditions of temperature, pressure and thermal flow encountered during reentry. The lifecycles of the thermal protection materials chosen are tested over the course of 10 to 30 trials each lasting 1500 seconds. Complete diagrams and photographs of the test facility are presented. ESA

12 ASTRONAUTICS (GENERAL)

For extraterrestrial exploration see *91 Lunar and Planetary Exploration.*

N90-22573# Italspazio, Rome (Italy).
ORBIT ACQUISITION AND CONTROL STRATEGY FOR SMALL

SATELLITES IN INCLINED ECCENTRIC ORBITS
G. Rondinelli and F. Graziani (Rome Univ., Italy) [1990] 7 p
(ETN-90-96551) Avail: NTIS HC A02/MF A01

A set of missions of small satellites in inclined eccentric orbits is analyzed. Small launchers, which require small satellites, can reduce costs and increase flight opportunities. The launch strategy with selected launchers (Scout, Delta 2, Pegasus), the direct orbit achievement and the dog-leg maneuver use, and the ground-track keeping exclusively based on in-plane maneuvers are described in detail. The analysis shows the in orbit mass and the delta-velocity required to fulfill the mission objectives. ESA

N90-22953*# National Aeronautics and Space Administration. Ames Research Center, Moffett Field, CA.
INTERACTIVE ORBITAL PROXIMITY OPERATIONS PLANNING SYSTEM
Arthur J. Grunwald and Stephen R. Ellis *In its* Spatial Displays and Spatial Instruments Jul. 1989 21 p (For primary document see N90-22918 16-54)
Avail: NTIS HC A99/MF A04 CSCL 22A

13 ASTRODYNAMICS

Includes powered and free-flight trajectories; and orbital and launching dynamics.

N90-22574 Colorado Univ., Boulder.
SEMIANALYTIC STUDY OF HIGH-ECCENTRICITY ORBIT STABILITY AND EVOLUTION Ph.D. Thesis
William E. Frazier 1989 170 p
Avail: Univ. Microfilms Order No. DA9009153

Mission planning for high-eccentricity orbits involves two phases: verification of stability, and design of the evolution. Many high-eccentricity orbits are unstable, that is, they suffer eccentric decay. Such missions also require specific changes in the orbital elements over time. Both the stability and evolution to be verified are determined by the initial conditions. This analysis is difficult because the orbit perturbations are highly coupled and nonlinear. Purely analytic solutions often cannot provide sufficient accuracy, yet direct numerical integration usually requires excessive computer time. Semianalytic solutions are considered and one is optimized for application to Geosynchronous Transfer Orbits (GTOs). The tuned semianalytic model, in conjunction with modern computational tools, allows simulation of thousands of initial conditions. Detailed calibration shows that the accuracy of the GTO propagator is superior to the errors inherent in long-term solar activity predictions. Apogee/perigee altitude histories, and Figures of Merit (FOMs) are used to evaluate the orbits. The FOMs summarize the sensitivities of the relevant characteristics of the orbit evolution to combinations of changes in initial conditions. An example of the significance of this technique is analysis supporting an upcoming GTO mission. All initial conditions presently considered are shown to be stable, and ten FOMs are plotted versus 11,000 cases of interest. The planned launch date is shown to offer desirable apogee, perigee, and inclination histories. Launch date slips result in suboptimal orbit evolutions. The results of many variations in the other initial elements are also shown. The GTO-tuned model is also used to study the stability of a wide range of higher-eccentricity and inclination orbits. These are shown for over 1,000 cases to be much less stble than the GTOs. Finally, a simplified semianalytic method is developed to estimate the FOM results found using the more complete model. Dissert. Abstr.

N90-22575# Technische Univ., Delft (Netherlands).
THE ROLE OF ORBIT ERRORS IN PROCESSING OF SATELLITE ALTIMETER DATA Ph.D. Thesis
Ernst J. O. Schrama 1989 181 p Sponsored by Netherlands Organization for Scientific Research
(ETN-90-96699) Avail: NTIS HC A09/MF A01

The processing of distance measurements performed by satellite radar altimetry is discussed. The principles of satellite altimetry are introduced. Observations derived from the altimeter radar consist of distance measurements from the satellite to the closest point at the sea surface in the nadir. A successful application of satellite altimetry is explained. Empirical modeling of radial errors and the properties of this estimation procedure are considered. The armature of gravitational orbit perturbations is worked out for typical altimetric orbits. The effect expected of the gravitational radial orbit error on two observation types frequently employed in the processing of satellite altimer data is discussed. The problem of recovering a radial orbit error from simulated and colinear differences is investigated. Conclusions and recommendations are given. ESA

N90-22576# Naval Postgraduate School, Monterey, CA.
ORBITAL MECHANICS: A LEARNING TOOL ON THE MAIN FRAME M.S. Thesis
Anthony A. Vraa Sep. 1989 98 p
(AD-A218799) Avail: NTIS HC A05/MF A01 CSCL 22/2

An interactive program that enables the student to study the orbital motion of satellites around the earth is presented. The student can investigate the shape of a variety of orbits by varying the initial position and velocity of the satellite, or by supplying select orbital parameters i.e., initial orbital radius, eccentricity, and inclination. Satellite maneuvers can also be studied, like transfer orbits and inclination changes, by command velocity changes at any location in the orbit. Also the effects of the perturbing forces due to the oblateness of the earth, drag for low earth orbits, and gravitational attraction from the sun and moon can be investigated. The orbits are displayed in either the perifocal coordinate system around a model of the earth, or the ground track can be displayed on a map of the world. Orbital data is displayed below the orbital plot. The display is enabled by the use of display integrated software system and plotting language (DISSPLA) subroutines. GRA

14 GROUND SUPPORT SYSTEMS AND FACILITIES (SPACE)

Includes launch complexes, research and production facilities; ground support equipment, e.g., mobile transporters; and simulators.

For related information see also *09 Research and Support Facilities (Air).*

N90-22577# Rome Univ. (Italy). Dipt. di Fisica.
THE SUPER-GRATINGS: HOW TO IMPROVE THE LIMITING RESOLUTION OF GRATING SPECTROMETERS
Vittorio Mazzacurati and G. Ruocco (Aquila Univ., Italy) 7 Sep. 1989 20 p
(Preprint-695; ETN-90-96518) Avail: NTIS HC A03/MF A01

The possibility of practically realizing a super-grating (a single high dispersion element rising from an array of two complanar gratings) is analyzed from a theoretical viewpoint. The most critical parameter (the phase matching between the two elements), is shown to be satisfactorily adjustable using available micropositioning systems. Using two gratings of 40 cm overall dimension as dispersion units the limit resolution in four-passes operation can be estimated to a range close to that usually covered by eterodyne spectrometers. ESA

N90-22578# North Carolina Univ., Raleigh. Dept. of Nuclear Engineering.
CONTROL OF SURFACE MELTING AND ABLATION IN ELECTROMAGNETIC LAUNCHERS VIA THE MAGNETIC VAPOR SHIELDING MECHANISM Final Report, Jul. 1987 - Dec. 1989
John G. Gilligan, M. Bourham, O. Hankins, O. Auciello, and B. Wehring 31 Dec. 1989 43 p
(Contract DAAL03-87-K-0103)
(AD-A219035; ARO-25416.1-EG-SDI) Avail: NTIS HC A03/MF A01 CSCL 20/9

The project has been successful in designing, constructing and operating (over 200 shots) the proof-of-principle experiment

SIRENS to simulate the exposure of material surfaces to high heat fluxes under electromagnetic (EM) and electrothermal (ET) launchers conditions. The vapor shield concept has been experimentally verified and the energy transmission factor through the vapor shield varies from 20 percent to 5 percent as the heat flux increases. Different material surfaces were tested which revealed that the metallic surfaces have strong axial direction. The heat flux is found to be approximately constant along the barrel axis, with an average plasma velocity of 10 to 12 km/s. Multiple exposure of material surfaces showed that about 190 exposures (at 1 kJ input energy) causes an increase of 20 percent in the inner bore diameter. There is initial indications of a reduction in ablation with applied magnetic fields above 5 Tesla, for insulator materials (Lexan). GRA

15 LAUNCH VEHICLES AND SPACE VEHICLES

Includes boosters; operating problems of launch/space vehicle systems; and reusable vehicles.

For related information see also *20 Spacecraft Propulsion and Power.*

N90-22579 Rand Graduate Inst. for Policies Study, Santa Monica, CA.

US ACCESS TO SPACE: LAUNCH VEHICLE CHOICES FOR 1990 TO 2010 Ph.D. Thesis

Scott N. Pace 1989 406 p

Avail: Univ. Microfilms Order No. DA9005500

Combinations of U.S. launch vehicles capable of meeting a range of government space traffic needs between 1990 and 2010 are evaluated. The purpose of this evaluation is to clarify alternatives available to the United States in pursuing potential national goals and to increase understanding of the implications of those alternatives. Wartime requirements for space launches were not included. Four levels of U.S. space traffic demand for 1990 to 2010 were defined. The first level was budget constrained to limit new program starts. The second level was a continuation of current space traffic plans, including the Space Station program. The third level assumed an expansion of civil space efforts such as a return to the Moon. The fourth level assumed expanded military space efforts such as the development of strategic defenses. Differing combination of existing and proposed launch vehicles were defined to fulfill each demand level. The costs and uncertainties (e.g., payload losses) associated with each launch vehicle combination were estimated. The interrelations of payload costs, launch vehicle costs, and system reliabilities are discussed in the appendices. The space transportation planning process, current issues, and political factors affecting analysis are reviewed. Senior space transportation planners and decision-makers were interviewed on differing institutional criteria for evaluating launch vehicle mixes. Evaluation criteria were defined to assess the launch vehicle mixes for each demand level and for the case of uncertain demand. Recommendations on preferred U.S. actions in space transportation are made based both on analyses and interview results. Dissert. Abstr.

N90-22580# Societe Europeenne de Propulsion, Puteaux (France).

SEAL REQUIREMENTS IN ROCKET PROPULSION [EXIGENCES D'ETANCHEITE DANS LE DOMAINE DE LA PROPULSION PAR FUSEE]

M. Choulant and J. C. Sylvestre 1989 19 p In FRENCH Presented at Journee Technique Caoutchouc et Etancheite des Fluides, Paris, France, 7 Dec. 1989

(ETN-90-96611) Avail: NTIS HC A03/MF A01

Research on sealant materials used on the Ariane 4 and 5 launchers is described. Chemical resistance to rocket fuels over the course of periods as long as a month and a half (in the case of delayed launching) is studied. Resistance to combustion products, pressure and relaxation are tested. Thermal stability of the seals is investigated. The types of sealant materials chosen, both elastomeric and plastic, are presented. The quality control policies used in evaluating the seals are described. ESA

N90-22581# Aerospatiale, Les Mureaux (France). Direction Etudes et Essais Systemes.

MULTIVARIATE ANALYSIS OF LAUNCHER GUIDANCE ROBUSTNESS [ANALYSE MULTIVARIABLE DE LA ROBUSTESSE DU PILOTAGE D'UN LANCEUR]

F. Demarquilly 12 Jan. 1989 20 p In FRENCH Presented at the Societe des Mathematiques Appliquees et Industrielles 2nd National Conference l'Automatique pour l'Aeronautique et l'Espace, Paris, France, 13-15 Mar. 1989

(Rept-892-422-105; ETN-90-96629) Avail: NTIS HC A03/MF A01

The role of a launcher guidance system is defined. Integrated methods of studying all the variables involved in guiding a multi-stage launcher are presented. Such a guidance system is used on the Ariane 4 and 5 launchers. The robustness of the guidance system is studied with emphasis placed on stability margins and interstage coupling measurements. The multivariate analysis technique used may also be applied to the analysis of acceptable coupling perturbations and to the analysis of truncated modalities. The technique can be used in dimensional analysis of the launcher guidance chain of command. ESA

N90-22582# Aerospatiale, Les Mureaux (France). Direction Etudes et Essais Systemes.

EQUIPMENT SPECIFICATIONS FOR LAUNCHER GUIDANCE USING MULTIVARIABLE FREQUENCY METHODS [SPECIFICATIONS D'EQUIPEMENTS DE PILOTAGE D'UN LANCEUR PAR METHODES FREQUENTIELLES MULTIVARIABLES]

P. Bonguet 24 Nov. 1988 21 p In FRENCH Presented at the Societe des Mathematiques Appliquees et Industrielles 2nd National Conference l'Automatique pour l'Aeronautique et l'Espace, Paris, France, 13-15 Mar. 1989

(Rept-892-422-106; STS/VDM-TI-683/88; ETN-90-96630) Avail: NTIS HC A03/MF A01

A multivariate frequency quantification method for analyzing stability margin losses due to perturbations in a closed loop system is presented. The method is based on the use of singularity values of transfer matrices to establish guidance equipment specifications. The case of a launcher in-flight, using reorientation jets is used as a test case for the method. The method is shown to be applicable to other guidance and control problems. Its use in qualification tests of launcher motors is described. ESA

16 SPACE TRANSPORTATION

Includes passenger and cargo space transportation, e.g., shuttle operations; and space rescue techniques.

For related information see also *03 Air Transportation and Safety* and *18 Spacecraft Design, Testing and Performance.* For space suits see *54 Man/System Technology and Life Support.*

N90-22583*# National Aeronautics and Space Administration. John F. Kennedy Space Center, Cocoa Beach, FL.

DEBRIS/ICE/TPS ASSESSMENT AND PHOTOGRAPHIC ANALYSIS FOR SHUTTLE MISSION STS-36

Charles G. Stevenson, Gregory N. Katnik, and Scott A. Higginbotham Apr. 1990 228 p Original contains color illustrations

(NASA-TM-102789; NAS 1.15:102789) Avail: NTIS HC A11/MF A02; 110 functional color pages CSCL 22B

A Debris/Ice/TPS (Thermal Protection System) assessment and photographic analysis was conducted for Space Shuttle Mission STS-36. Debris inspections of the flight elements and launch pad are performed before and after launch. Ice/frost conditions on the External Tank are assessed by the use of computer programs, nomographs, and infrared scanner data during cryogenic loading

of the vehicle followed by on-pad visual inspection. High speed photography is analyzed after launch to identify ice/debris sources and evaluate potential vehicle damage and/or in-flight anomalies. The debris/ice/TPS conditions and photographic analysis of Mission STS-36, and their overall effect on the Space Shuttle Program are documented. Author

N90-22584* National Aeronautics and Space Administration. Langley Research Center, Hampton, VA.
EARTH-TO-ORBIT VEHICLE PROVIDING A REUSABLE ORBITAL STAGE Patent
James A. Martin, inventor (to NASA) 5 Dec. 1989 8 p Filed 23 Jul. 1987 Supersedes N87-29582 (25 - 24, p 3278)
(NASA-Case-LAR-13486-1; US-Patent-Appl-SN-076955; US-Patent-Class-244-158R; US-Patent-Class-244-160; US-Patent-Class-244-161; US-Patent-Class-244-172; Int-Patent-Class-B64G-1/14) Avail: US Patent and Trademark Office CSCL 22B

A reusable Earth-to-orbit vehicle is described with an orbital stage sized to fit into a payload bay equipped, Earth-return-capable space vehicle such as the United States Space Shuttle. The orbital stage is equipped with a reusable rocket engine capable of operation from the Earth's surface to Earth orbit. The orbital stage propels itself into Earth orbit with the help of boosters that separate and return to Earth before orbit is reached. After delivering its payload, the orbital stage is placed in the Earth-return-capable space vehicle's payload bay and returned to Earth for reuse.
Official Gazette of the U.S. Patent and Trademark Office

17 SPACE COMM., SPACECRAFT COMM., COMMAND & TRACKING

Includes telemetry; space communications networks; astronavigation and guidance; and radio blackout.

For related information see also *04 Aircraft Communications and Navigation* and *32 Communications and Radar.*

No abstracts in this category.

18 SPACECRAFT DESIGN, TESTING AND PERFORMANCE

Includes satellites; space platforms; space stations; spacecraft systems and components such as thermal and environmental controls; and attitude controls.

For life support systems see *54 Man/System Technology and Life Support.* For related information see also *05 Aircraft Design, Testing and Performance, 39 Structural Mechanics,* and *16 Space Transportation.*

N90-22585 Texas Univ., Austin.
APPROXIMATE OPTIMAL GUIDANCE SCHEMES FOR ATMOSPHERIC ORBITAL MANEUVERING Ph.D. Thesis
Edwin Zachary Crues 1989 200 p
Avail: Univ. Microfilms Order No. DA9005564

A technique for formulating approximate optimal guidance laws for a class of nonlinear dynamical systems is examined for use with gliding aerospace vehicles and applied to the aeroassisted plane change problem. The specified class consists of dynamical systems that separate into primary (zeroth-order) and perturbation portions with respect to a small parameter (epsilon). The Hamilton-Jacobi-Bellman partial differential equation can then be expanded in series form in epsilon. When an integrable solution to the zeroth-order problem (epsilon = O) is obtainable, higher order corrections for perturbation effects can be calculated and added to the zeroth-order control to form a control corrected for the effects of the perturbation dynamics. Unlike certain previous expansion solutions, the dynamics include all the terms associated with a spherical rotating planet. These terms appear in the perturbation portion of the dynamics, allowing for their respective corrections to the control. The expansion is made with respect to a set of small parameters that arise naturally from an analysis of the dynamics. The choices of small parameters are determined from the desired zeroth-order characteristics of the solution. Different small parameters are chosen for the inner atmospheric and outer Keplerian expansion regions. The zeroth-order problem is obtained when the small parameters are set to zero. In the inner atmospheric region, this corresponds to a solution of the problem where the aerodynamic forces dominate the inertial forces (non-aerodynamic forces). In the outer Keplerian region, the zeroth-order solution corresponds to a solution where the aerodynamic forces are neglected, resulting in a Keplerian arc. Higher-order terms in the expansions are determined from the solution of first-order linear partial differential equations requiring only quadrature integration. Dissert. Abstr.

N90-22586# Royal Aerospace Establishment, Farnborough (England).
SATELLITE MOTION IN AXI-SYMMETRIC GRAVITATIONAL FIELD. PART 2: PERTURBATIONS DUE TO AN ARBITRARY J(SUB I)
R. H. Gooding 5 May 1989 103 p
(RAE-TR-89022; RAE-SPACE-675; BR111982; ETN-90-96439) Copyright Avail: NTIS HC A06/MF A01

An untruncated orbital theory is presented. The effects of the general zonal harmonic, J(sub I), are covered, the main results being a trio of formulae for perturbations in the spherical-polar coordinates. The formulae are only first-order in J(sub I), but, in conjunction with the second-order results for J(sub 2), the complete set of formulae may be regarded as constituting a second-order theory, the Earth's J(sub 2) being much larger than J(sub I), for I greater than 2. The mean elements of the theory are defined in such a way that, for each J(sub I), the coordinate-perturbation formulae have their simplest possible form, with no occurrence of zero denominators. The general formulae are used in a rederivation of the results for J(sub 3), and in a derivation of results for J(sub 4). ESA

N90-22587# Italspazio, Rome (Italy).
THE ITALIAN APPROACH TO SMALL SATELLITES FOR LOW COST ACCESS TO SPACE DEVELOPMENTS
G. Rondinelli, G. Barresi, A. Cramarossa, and F. Graziani (Rome Univ., Italy) [1990] 15 p
(ETN-90-96552) Avail: NTIS HC A03/MF A01

Studies directed toward the minimization of costs involved with satellite development and launch are reported. Strategies are described and three possible spacecraft designs are detailed. The rules for the designs are based on the modularity concept in order to take full advantage of each launcher with a common basic bus or bus elements for a mass production. ESA

N90-22588# Italspazio, Rome (Italy).
LOW COST STATION KEEPING MANEUVERS FOR A SMALL-SATELLITES CONSTELLATION IN TUNDRA ORBITS
A. Cramarossa, G. Barresi, G. Rondinelli, and F. Graziani (Rome Univ., Italy) [1990] 11 p
(ETN-90-96553) Avail: NTIS HC A03/MF A01

Effort performed to identify a low cost maneuver strategy is summarized. The strategy provides a great advantage with respect to the total delta-V required for a period of one year. According to a preliminary analysis a small satellite can be conceived to support high inclined orbit missions, being the expected resulting propellant mass for a lifetime of 7 years of about 4 kg. ESA

N90-22589# Laboratoire d'Automatique et d'Analyse des Systemes, Toulouse (France).
ORBITAL MANEUVERS OPTIMIZATION FOR STATION ACQUISITION OF GEOSTATIONARY SATELLITES. DETERMINISTIC AND STOCHASTIC APPROACHES Ph.D. Thesis

Jean-Michel Enjalbert 1989 143 p In FRENCH; ENGLISH summary
(LAAS-89-359; ETN-90-96607) Avail: NTIS HC A07/MF A01

A two level optimization approach is developed and worked out for a class of complex problems in the field of space trajectory optimization. Orbital maneuvers occurring during the station acquisition are considered. It is a control problem where the number of burns and their respective parameters must be determined. The solution requires two level decomposition. An impulsive model (aggregated) is defined and solved by dynamic programming. This solution is used at the second level to initialize the real optimization problem. An iterative dynamic programming algorithm and the simplex are implemented. Multiplicative disturbances on control parameters (thrust of the apogee engine) are included. In order to solve this problem two approaches are developed and compared. The first one is based on stochastic dynamic programming and the second presents a regulator synthesis. For the latest, performances of an LQG (model linearization) are compared to a class of regulator obtained by means of parametric optimization. The TDF1 satellite data is applied. ESA

N90-22590# Aerospatiale Aquitaine, Saint-Medard en Jalles (France). Div. Systemes Strategiques et Spatiaux.
QUALIFICATION TEST RATIONALE FOR MEASURING THE RESISTANCE OF EQUIPMENT TO PYROTECHNIC SHOCK [LOGIQUE D'ESSAI DE QUALIFICATION DES EQUIPEMENTS A L'AGRESSION DE CHOCS PYROTECHNIQUES]
J. J. Domenge 5 Jun. 1989 11 p In FRENCH
(Rept-892-430-117; ETN-90-96648) Avail: NTIS HC A03/MF A01

Spacecraft construction materials are submitted to pyrotechnic shocks during different phases of spaceflight. Difficulties involved in the same shocks during ground-based testing are outlined. Ways of simulating as accurately as possible the conditions of pyrotechnic shock during spaceflight are described. The different types of mechanical and functional damage that can be caused by pyrotechnic shocks are outlined. The rationale for developing qualification criteria for resistance to pyrotechnic shock is explained. ESA

N90-22591 Aerospatiale Aquitaine, Saint-Medard en Jalles (France). Strategic and Space Div.
STUDY AND SIZING OF BONDED JOINTS IN SPACE STRUCTURES
J. P. Maigret, M. Martin, and M. Laborie Feb. 1989 10 p In FRENCH; ENGLISH summary
(Rept-892-430-124; ETN-90-96655) Avail: Aerospatiale, 37 blvd de Montmorency, 75781 Paris, CEDEX 16, France

The industrial and technical context of the strategic and space divisions of Aerospatiale in which bonded structures are studied is presented. The numerous dependances between the variables acting on the quality of bonded joints are summarized. The means developed to increase the reliability of structures and reduce the costs and delays of studies are described. Examples are given to indicate the technical level and field of utilization of these means. LICO software, written to help in rapid analysis of the thermomechanical behavior of bonded joints, is presented. ESA

N90-22592*# National Aeronautics and Space Administration. Langley Research Center, Hampton, VA.
SPACECRAFT ATTITUDE IMPACTS ON COLD-SAT NON-VACUUM JACKETED LH2 SUPPLY TANK THERMAL PERFORMANCE
Hugh Arif 1990 17 p Presented at the 5th Joint Thermophysics and Heat Transfer Conference, Seattle, WA, 18-20 Jun. 1990; cosponsored by the AIAA and ASME
(NASA-TM-103158; E-5525; NAS 1.15:103158; AIAA-90-1672)
Avail: NTIS HC A03/MF A01 CSCL 22B

The Cryogenic On-Orbit Liquid Depot - Storage, Acquisition and Transfer (COLD-SAT) spacecraft will be launched into low earth orbit to perform fluid management experiments on the behavior of subcritical liquid hydrogen (LH2). For determining the optimum on-orbit attitude for the COLD-SAT satellite, a comparative analytical study was performed to determine the thermal impacts of spacecraft attitude on the performance of the COLD-SAT non-vacuum jacketed LH2 supply tank. Tank thermal performance was quantified by total conductive and radiative heat leakage into the pressure vessel due to the absorbed solar, earth albedo and infra-red on-orbit fluxes, and also by the uniformity of the variation of this leakage on the vessel surface area. Geometric and thermal analysis math models were developed for the spacecraft and the tank as part of this analysis, based on their individual thermal/structural designs. Two quasi-inertial spacecraft attitudes were investigated and their effects on the tank performance compared. The results are one of the criteria by which the spacecraft orientation in orbit was selected for the in-house NASA Lewis Research Center design. Author

N90-22593*# National Aeronautics and Space Administration. Marshall Space Flight Center, Huntsville, AL.
SPACE STATION FREEDOM ENVIRONMENTAL CONTROL AND LIFE SUPPORT SYSTEM PHASE 3 SIMPLIFIED INTEGRATED TEST DETAILED REPORT
B. C. Roberts, R. L. Carrasquillo, M. Y. DuBiel, K. Y. Ogle, J. L. Perry, and K. M. Whitley Washington, DC May 1990 99 p
(NASA-TM-4204; NAS 1.15:4204) Avail: NTIS HC A05/MF A01 CSCL 22B

A description of the phase 3 simplified integrated test (SIT) conducted at the Marshall Space Flight Center (MSFC) Core Module Integration Facility (CMIF) in 1989 is presented. This was the first test in the phase 3 series integrated environmental control and life support systems (ECLSS) tests. The basic goal of the SIT was to achieve full integration of the baseline air revitalization (AR) subsystems for Space Station Freedom. Included is a description of the SIT configuration, a performance analysis of each subsystem, results from air and water sampling, and a discussion of lessons learned from the test. Also included is a full description of the preprototype ECLSS hardware used in the test. Author

N90-22594# Howard Univ., Washington, DC. School of Engineering.
DYNAMICS AND CONTROL OF TETHERED ANTENNAS/REFLECTORS IN ORBIT Annual Report, 1 Nov. 1988 - 31 Oct. 1989
Peter M. Bainum Dec. 1989 86 p
(Contract F49620-89-C-0002; AF Proj. 2302)
(AD-A219316) Avail: NTIS HC A05/MF A01 CSCL 09/1

A study is conducted of the dynamics and control of a class of large antenna/reflector systems in orbit which are also partially stabilized using a tether connected subsatellite. The system equations of motion are developed and linearized about the equilibrium position where the reflector's (shell's) symmetry axis nominally follows the local vertical. The shell roll, yaw, tether out-of-plane swing motion and out-of-plane elastic vibrations are decoupled from the shell and tether in-plane pitch motions and in-plane elastic vibrations. The in-plane motion of the system could be asymptotically stable based on Rupp's tether tension control law using only length and length rate information. However, the transient responses can be improved significantly by using an optimal tension feedback control law. When tether flexibility is included, the system dynamics could be further improved by including the state feedback of the tether vibrational modes into the tension control law. GRA

N90-23029*# National Aeronautics and Space Administration. Lyndon B. Johnson Space Center, Houston, TX.
SPACE STATION DYNAMICS, ATTITUDE CONTROL AND MOMENTUM MANAGEMENT Abstract Only
John W. Sunkel, Ramen P. Singh, and Ravi Vengopal (DYNACS Engineering Co., Inc., Clearwater, FL.) *In* JPL, Proceedings of the 3rd Annual Conference on Aerospace Computational Control, Volume 1 15 Dec. 1989 p 370 (For primary document see N90-22987 16-61)
Avail: NTIS HC A21/MF A03 CSCL 22B

N90-23054*# Jet Propulsion Lab., California Inst. of Tech., Pasadena.
MODEL REDUCTION FOR FLEXIBLE SPACECRAFT WITH CLUSTERED NATURAL FREQUENCIES Abstract Only
T. W. C. Williams (National Aeronautics and Space Administration. Langley Research Center, Hampton, VA.) and W. K. Gawronski *In its* Proceedings of the 3rd Annual Conference on Aerospace Computational Control, Volume 2 15 Dec. 1989 p 620 (For primary document see N90-23040 16-61)
Avail: NTIS HC A20/MF A03 CSCL 22B

N90-23059*# Georgia Inst. of Tech., Atlanta. School of Aerospace Engineering.
ROBUST FIXED ORDER DYNAMIC COMPENSATION FOR LARGE SPACE STRUCTURE CONTROL
Anthony J. Calise and Edward V. Byrns, Jr. *In* Jet Propulsion Lab., California Inst. of Tech., Proceedings of the 3rd Annual Conference on Aerospace Computational Control, Volume 2 15 Dec. 1989 p 641-648 (For primary document see N90-23040 16-61)
Avail: NTIS HC A20/MF A03 CSCL 22B

N90-23065*# Hughes Aircraft Co., El Segundo, CA. Guidance and Control Systems Lab.
THE USE OF REAL-TIME, HARDWARE-IN-THE-LOOP SIMULATION IN THE DESIGN AND DEVELOPMENT OF THE NEW HUGHES HS601 SPACECRAFT ATTITUDE CONTROL SYSTEM Abstract Only
Loren I. Slafer *In* Jet Propulsion Lab., California Inst. of Tech., Proceedings of the 3rd Annual Conference on Aerospace Computational Control, Volume 2 15 Dec. 1989 p 713 (For primary document see N90-23040 16-61)
Avail: NTIS HC A20/MF A03 CSCL 22B

N90-23080*# National Aeronautics and Space Administration. Langley Research Center, Hampton, VA.
DYNAMIC ANALYSIS OF FLEXIBLE MECHANICAL SYSTEMS USING LATDYN
Shih-Chin Wu, Che-Wei Chang (Comtek Co., Grafton, VA.), and Jerrold M. Housner *In* Jet Propulsion Lab., California Inst. of Tech., Proceedings of the 3rd Annual Conference on Aerospace Computational Control, Volume 2 15 Dec. 1989 p 844-859 (For primary document see N90-23040 16-61)
Avail: NTIS HC A20/MF A03 CSCL 22B

N90-23086*# Ottawa Univ. (Ontario). Inst. of Electrical Engineering.
MODELING AND CONTROL OF FLEXIBLE SPACE STATIONS (SLEW MANEUVERS)
N. U. Ahmed and S. S. Lim *In* Jet Propulsion Lab., California Inst. of Tech., Proceedings of the 3rd Annual Conference on Aerospace Computational Control, Volume 2 15 Dec. 1989 p 900-914 (For primary document see N90-23040 16-61)
Avail: NTIS HC A20/MF A03 CSCL 22B

19 SPACECRAFT INSTRUMENTATION

For related information see also *06 Aircraft Instrumentation* and *35 Instrumentation and Photography.*

N90-22595*# National Aeronautics and Space Administration. Lewis Research Center, Cleveland, OH.
A CANDIDATE ARCHITECTURE FOR MONITORING AND CONTROL IN CHEMICAL TRANSFER PROPULSION SYSTEMS
Michael P. Binder (Sverdrup Technology, Inc., Cleveland, OH.) and Marc G. Millis 1990 17 p Presented at the 26th Joint Propulsion Conference, Orlando, FL, 16-18 Jul. 1990; cosponsored by AIAA, SAE, ASME, and ASEE
(NASA-TM-103161; E-5529; NAS 1.15:103161; AIAA-90-1882)
Avail: NTIS HC A03/MF A01 CSCL 14B

To support the exploration of space, a reusable space-based rocket engine must be developed. This engine must sustain superior operability and man-rated levels of reliability over several missions with limited maintenance or inspection between flights. To meet these requirements, an expander cycle engine incorporating a highly capable control and health monitoring system is planned. Alternatives for the functional organization and the implementation architecture of the engine's monitoring and control system are discussed. On the basis of this discussion, a decentralized architecture is favored. The trade-offs between several implementation options are outlined and future work is proposed.
Author

20 SPACECRAFT PROPULSION AND POWER

Includes main propulsion systems and components, e.g., rocket engines; and spacecraft auxilliary power sources.

For related information see also *07 Aircraft Propulsion and Power, 28 Propellants and Fuels, 44 Energy Production and Conversion,* and *15 Launch Vehicles and Space Vehicles.*

N90-22596 Johns Hopkins Univ., Laurel, MD. Chemical Propulsion Information Agency.
HCl VAPOR CHARACTERIZATION AND DETECTION. JANNAF SAFETY AND ENVIRONMENTAL PROTECTION SUBCOMMITTEE WORKSHOP
Dorothy L. Becker, ed. Jan. 1989 165 p Workshop held in Los Angeles, CA, 10-12 Jan. 1989
(Contract N00039-89-C-5301)
(AD-A216252; CPIA-Publ-513) Avail: Issuing Activity CSCL 21/2

The instrumentation for remotely sensing HCl vapor in solid rocket exhaust is addressed. Some of the sensing technologies reported upon include passive dosimeter, infrared vapor/aerosol detector, near infrared diode laser detector, and flow analysis detector. Also a field test was conducted to compare the above mentioned sensing technologies. In addition, occupational health and safety baselines when monitoring HCl contamination were defined. For individual titles, see N90-22597 through N90-22601.

N90-22597 Aerospace Corp., El Segundo, CA. Aerophysics Lab.
THE HCl/AEROSOL PROBLEM
L. Robbin Martin *In* JHU, HCl Vapor Characterization and Detection. JANNAF Safety and Environmental Protection Subcommittee Workshop Jan. 1989 p 27-44 (For primary document see N90-22596 16-20)
Avail: Issuing Activity CSCL 21B

Calculations were done on the effect of aerosol formation on the accuracy of gas phase measurements of HCl in the atmosphere. This was done using known thermodynamics and simplified models of the atmospheric conditions. It was predicted that for a pre-existing cloud or fog, most (99 percent) of the HCl will be in the liquid phase over most accessible concentrations. For a natural aerosol of slightly hygroscopic salts, most of the HCl should be in the gas phase from 10 ppb to 10 ppm. At higher HCl concentrations, aerosol condensation will take place at higher relative humidities. When this happens, most of the HCl will go into the aerosol phase, and the gas phase HCl will not increase with further loading.
Author

N90-22598 Aerospace Corp., El Segundo, CA. Aerophysics Lab.
STICKING COEFFICIENT OF HCl ON AEROSOLS
N. Alan Abul-Haj *In* JHU, HCl Vapor Characterization and Detection. JANNAF Safety and Environmental Protection Subcommittee Workshop Jan. 1989 p 45-63 (For primary document see N90-22596 16-20)
Avail: Issuing Activity CSCL 21B

The kinetics of absorption of HCl into aqueous microdroplets was studied. This is done by injecting microdroplets into a carrier gas containing small amounts of HCl and observing the change in pH of the droplets as a function of time. The pH was measured

by including a small concentration of a fluorescent pH indicator in the microdroplets and illuminating them with a tunable dye laser. The resulting fluorescence is imaged into a monochromator and on to a vidicon. This system makes it possible to see changes in the pH of 50 micron diameter droplets on a millisecond time scale. By observing the amount of HCl that enters the microdroplets as a function of HCl partial pressure and carrier gas total pressure, the mass transfer rate can be separated into two parts: a sticking coefficient step and a gas diffusion step. This enables measurement of the true (vacuum) sticking coefficient and calculation of the net rate of mass transfer for other conditions such as different droplet sizes and total pressures. Author

N90-22599 Spectral Sciences, Inc., Burlington, MA.
HCl MONITOR
W. K. Cheng, L. S. Bernstein, F. Bien, R. P. Domingue, and M. D. Smith (Air Force Engineering and Services Center, Tyndall AFB, FL.) *In* JHU, NCl Vapor Characterization and Detection. JANNAF Safety and Environmental Protection Subcommittee Workshop Jan. 1989 p 65-77 (For primary document see N90-22596 16-20)
Avail: Issuing Activity CSCL 21B

At present, the short and long term environmental impacts of massive HCl releases due to Space Shuttle and other solid propellant rocket launches are not well characterized. It is important to measure the atmospheric HCl content in both the vapor and aerosol forms. A combination vapor-aerosol HCl monitor was developed. The instrument consists of four major components: an air sampling, optical measurement unit, a power supply and analog signal output unit, an analog-to-digital (a/d) converter and timing pulse unit, and a personal computer (PC). An air sample is drawn through the aerosol evaporator which vaporizes the aerosols and releases the dissolved HCl into the gas phase. By turning the aerosol heater on and off, one can determine both the total HCl (aerosol and vapor) and the vapor phase HCl. Data acquisition and analysis are controlled by a remotely located PC. A 1000 ft signal cable allows the PC to be located in a bunker or control room and enables real time monitoring of the concentration measurement. The device is based on measuring the infrared absorption of gas phase HCl in the 3.4 micron wavelength region. The measurement approach differs from other infrared devices in that it utilizes a novel infrared light source. In essence, the source consists of HCl in a heated cell which emits the characteristic HCl line spectrum. The primary advantage of using a light source which is spectrally matched to the absorption spectrum is one of species selectivity. This enables quantitative measurement of very small species concentrations in the presence of strongly absorbing species whose absorption line positions are spectrally uncorrelated with the source line emission. The dynamic range of the HCl monitor is 0.1 to 10(exp 3) ppm. Author

N90-22600 Lawrence Livermore National Lab., CA. Environmental Sciences Div.
INFRARED ABSORPTION GAS SENSOR FOR THE DETECTION OF HCl IN LAUNCH VEHICLE EXHAUST CLOUDS
Thomas J. Kulp, Thomas G. McRae, Darrel Garvis, and Randall Kennedy *In* JHU, HCl Vapor Characterization and Detection. JANNAF Safety and Environmental Protection Subcommittee Workshop Jan. 1989 p 79-94 (For primary document see N90-22596 16-20)
Avail: Issuing Activity CSCL 21B

An infrared (IR) absorption sensor was developed for the detection of HCl at concentrations as low as 200 ppb with a 1 Hz data collection rate. The optical components of the sensor consist of a glowbar IR source, a 4 m multipass White cell, a thermoelectrically cooled PbS detector, and a four-channel filter wheel. It is capable of monitoring water vapor and HCl simultaneously, and can thus discriminate between the two species. Data collection from the battery-powered sensor will be performed through a radio link to a central base station. This allows remote operation - a necessary feature in the rugged terrains of many space-vehicle launch sites. Author

N90-22601 Southwest Sciences, Inc., Santa Fe, NM.
MEASUREMENT OF HCl BY NEAR-INFRARED DIODE LASER ABSORPTION
Alan C. Stanton *In* JHU, HCl Vapor Characterization and Detection. JANNAF Safety and Environmental Protection Subcommittee Workshop Jan. 1989 p 95-119 (For primary document see N90-22596 16-20)
Avail: Issuing Activity CSCL 21B

The detection of hydrogen chloride gas was demonstrated by near-infrared absorption using 1200 nm InGaAsP diode lasers. Very high sensitivity is attained using the technique of frequency-modulation spectroscopy combined with a compact, optically stable, multipass absorption cell. In preliminary laboratory experiments, measurement of less than 5 parts per million HCl in air with better than 1-second time response was directly demonstrated. An optimized system would be capable of measuring 0.1 ppm HCl or less. This method is especially attractive because fiber optics may be used to facilitate remote placement of measurement cells operating in an ambient open path. The measurement approach is described in detail, and the results of laboratory experiments to study the sensitivity of the technique are discussed. Author

N90-22602*# Thiokol Corp., Brigham City, UT. Space Operations.
QUALIFICATION OF THE RSRM CASE MEMBRANE CASE-TO-INSULATION BONDLINE INSPECTION USING THE THIOKOL CORPORATION ULTRASONIC RSRM BONDLINE INSPECTION SYSTEM Final Test Report
M. Cook Apr. 1990 43 p Original contains color illustrations
(Contract NAS8-30490)
(NASA-CR-183940; NAS 1.26:183940; TWR-18898) Avail: NTIS HC A03/MF A01; 15 functional color pages CSCL 21H

Qualification testing of Combustion Engineering's AMDATA Intraspect/98 Data Acquisition and Imaging System that applies to the redesigned solid rocket motor (RSRM) case membrane case-to-insulation bondline inspection was performed. Testing was performed at M-67, the Thiokol Corp. RSRM Assembly Facility. The purpose of the inspection was to verify the integrity of the case membrane case-to-insulation bondline. The case membrane scanner was calibrated on the redesigned solid rocket motor case segment calibration standard, which had an intentional 1.0 by 1.0 in. case-to-insulation unbond. The case membrane scanner was then used to scan a 20 by 20 in. membrane area of the case segment. Calibration of the scanner was then rechecked on the calibration standard to ensure that the calibration settings did not change during the case membrane scan. This procedure was successfully performed five times to qualify the unbond detection capability of the case membrane scanner. Author

N90-22603# Aerospatiale, Paris (France). Div. Systemes Strategiques et Spatiaux.
METHODS OF JET CALCULATION [METHODES DE CALCULS DE JETS]
J. C. Astier and F. Corberand 1988 31 p In FRENCH Presented at the 25th AAAF Colloque d'Aerodynamique Appliquee, Talence, France, 12-14 Oct. 1988
(Rept-892-422-102; ETN-90-96627) Avail: NTIS HC A03/MF A01

Formulas for calculating jet flow through rocket engines are presented. The assumptions made in applying the formulas are identified. The flow is assumed to be axisymmetric. No interaction between particles occurs and the volume of these particles is negligable. The effects of altitude on jet flow are investigated. Diagrammatic representations of different jet flow patterns are shown. Various codes used in the analysis of jet flow are presented. The techniques and codes described are used by Aerospatiale in industrial applications. ESA

N90-22604*# National Aeronautics and Space Administration. Lewis Research Center, Cleveland, OH.
THE INTERNATIONAL SPACE UNIVERSITY
Kenneth J. Davidian 1990 11 p Presented at the 26th Joint

Propulsion Conference, Orlando, FL, 16-18 Jul. 1990; cosponsored by AIAA, SAE, ASME, and ASEE
(NASA-TM-103163; E-5531; NAS 1.15:103163; AIAA-90-2389)
Avail: NTIS HC A03/MF A01 CSCL 22A

The International Space University (ISU) was founded on the premise that any major space program in the future would require international cooperation as a necessary first step toward its successful completion. ISU is devoted to being a leading center for educating future authorities in the world space industry. ISU's background, goals, current form, and future plans are described. The results and benefits of the type of education and experience gained from ISU include technical reports describing the design projects undertaken by the students, an exposure to the many different disciplines which are a part of a large space project, an awareness of the existing activities from around the world in the space community, and an international professional network which spans all aspects of space activities and covers the globe.
Author

N90-22605*# National Aeronautics and Space Administration. Lewis Research Center, Cleveland, OH.
COOLING OF ROCKET THRUST CHAMBERS WITH LIQUID OXYGEN
Elizabeth S. Armstrong and Julie A. Schlumberger 1990 11 p Presented at the 26th Joint Propulsion Conference, Orlando, FL, 16-18 Jul. 1990; cosponsored by AIAA, SAE, ASME, and ASEE
(NASA-TM-103146; E-5498; NAS 1.15:103146; AIAA-90-2120)
Avail: NTIS HC A03/MF A01 CSCL 21H

Rocket engines using high pressure liquid oxygen (LOX) and kerosene (RP-1) as the propellants have been considered for future launch vehicle propulsion. Generally, in regeneratively cooled engines, the fuel is used to cool the combustion chamber. However, hydrocarbons such as RP-1 are limited in their cooling capability at high temperatures and pressures. Therefore, LOX is being considered as an alternative coolant. However, there has been concern as to the effect on the integrity of the chamber liner if oxygen leaks into the combustion zone through fatigue cracks that may develop between the cooling passages and the hot-gas side wall. To address this concern, an investigation was previously conducted with simulated fatigue cracks upstream of the thrust chamber throat. When these chambers were tested, an unexpected melting in the throat region developed which was not in line with the simulated fatigue cracks. The current experimental program was conducted in order to determine the cause for the failure in the earlier thrust chambers and to further investigate the effects of cracks in the thrust chamber liner upstream of the throat. The thrust chambers were tested at oxygen-to-fuel mixture ratios from 1.5 to 2.86 at a nominal chamber pressure of 8.6 MPa. As a result of the test series, the reason for the failure occurring in the earlier work was determined to be injector anomalies. The LOX leaking through the simulated fatigue cracks did not affect the integrity of the chambers.
Author

N90-22606*# National Aeronautics and Space Administration. Lewis Research Center, Cleveland, OH.
PROGRAMMATIC STATUS OF NASA'S CSTI HIGH CAPACITY POWER STIRLING SPACE POWER CONVERTER PROGRAM
James E. Dudenhoefer 1990 9 p Proposed for presentation at the 25th Intersociety Energy Conversion Engineering Conference, Reno, NV, 12-17 Aug. 1990; cosponsored by AIChE, SAE, ACS, AIAA, ASME, and IEEE
(NASA-TM-103142; E-5494; NAS 1.15:103142) Avail: NTIS HC A02/MF A01 CSCL 21H

An overview is presented of the NASA Lewis Research Center Free-Piston Stirling Space Power Converter Technology Development Program. This work is being conducted under NASA's Civil Space Technology Initiative (CSTI). The goal of the CSTI High Capacity Power element is to develop the technology base needed to meet the long duration, high capacity power requirements for future NASA space initiatives. Efforts are focused upon increasing system thermal and electric energy conversion efficiency at least fivefold over current SP-100 technology, and on achieving systems that are compatible with space nuclear reactors. The status of test activities with the Space Power Research Engine (SPRE) is discussed. Design deficiencies are gradually being corrected and the power converter is now outputting 11.5 kWe at a temperature ratio of 2 (design output is 12.5 kWe). Detail designs were completed for the 1050 K Component Test Power Converter (CTPC). The success of these and future designs is dependent upon supporting research and technology efforts including heat pipes, gas bearings, superalloy joining technologies and high efficiency alternators. An update of progress in these technologies is provided.
Author

23 CHEMISTRY AND MATERIALS (GENERAL)

N90-22607# Pennsylvania State Univ., University Park. Dept. of Chemistry.
A SECOND-ORDER NONLINEAR OPTICAL POLY(ORGANOPHOSPHAZENE)
Alexa A. Dembek, Chulhee Kim, Harry R. Allcock, Robert L. S. Devine, William H. Steier, and Charles W. Spangler (University of Northern Illinois, De Kalb.) 9 Feb. 1990 19 p Submitted for publication Sponsored in part by AFOSR
(Contract N00014-84-K-0477)
(AD-A218408; TR-53) Avail: NTIS HC A02/MF A01 CSCL 07/6

A mixed substituent polyphosphazenes with the structure (NPOCH2CF3) 64 percent (O)CH2CH2O)3-C6H4-CH=CH-C6H4-NO2) 36 percent(n) has been synthesized and the second-order nonlinear properties have been investigated. A second harmonic coefficient of d(33) = 5.5 pm/V was obtained.
GRA

N90-22608# State Univ. of New York, Buffalo. Dept. of Chemistry.
THE FIRST EXAMPLE OF AN ORGANOGALLIUM COMPOUND CONTAINING A Ga-Te BOND: SYNTHESIS, PROPERTIES, AND MOLECULAR STRUCTURE OF ((Me3CCH2)2GaTePh)2
Michael A. Banks, O. T. Beachley, Jr., Henry J. Gysling, and Henry R. Luss 12 Jun. 1990 22 p Submitted for publication Sponsored in part by Eastman Kodak Co., Rochester, NY
(Contract N00014-87-K-0266)
(AD-A219258; SUNY/AB/TR-24) Avail: NTIS HC A03/MF A01 CSCL 07/3

The first example of an organogallium compound with a Gallium-Tellurium bond ((Me3CCH2)2GaTePh)2, which is stable at room temperature, was synthesized and characterized by elemental analyses, Infrared, Hydrogen Nuclear Magnetic Resonance and (125) Tellurium NMR spectroscopy and an x ray structural study. The dimeric molecule crystallizes in the monoclinic space group P2(1)/c with unit cell dimensions of a = 18.864(7)A, b = 10.041(5), c = 19.869(9), beta = 101.80(3), V = 3684(5)A(3), Z=4, D(ca/cd) = 1.505 (gram 1/cu cm), R = 0.030, R(w) = 0.035. The four membered Ga2Te2 ring has a butterfly arrangement with the phenyl groups in the anti-position relative to the ring. The Ga-Te bond distances are in the range 2.7435(8) to 2.7623(8)A.
GRA

24 COMPOSITE MATERIALS

Includes physical, chemical, and mechanical properties of laminates and other composite materials.
For ceramic materials see *27 Nonmetallic Materials.*

N90-22609*# Boeing Co., Seattle, WA.
BOEING/NASA COMPOSITE COMPONENTS FLIGHT SERVICE EVALUATION Final Progress Report No. 10, Jan. 1987 - Jun. 1989
Randy L. Coggeshall Sep. 1989 43 p
(Contract NAS1-11668)

(NASA-CR-181898; NAS 1.26:181898) Avail: NTIS HC A03/MF A01 CSCL 11D

This tenth and final flight service report covers the flight service experience of 111 graphite-epoxy spoilers on 737 transport aircraft after 15 years of worldwide service. As of June 30, 1989, a total of 2,593,741 spoiler flight hours and 3,499,941 spoiler landings have been accumulated by the fleet. The high time spoiler had 42,007 flight hours. Results of 15 years of residual strength tests conducted on selected spoilers are reported. In addition, the flight service histories of composite elevators and stabilizers developed under NASA contracts NAS1-14952 and NAS1-15025, respectively, are reported. Author

N90-22610 Drexel Univ., Philadelphia, PA.
IMPACT DAMAGE IN GRAPHITE/EPOXY LAMINATES: DAMAGE CHARACTERIZATION, ACOUSTIC EMISSION, AND FINITE ELEMENT SIMULATION, VOLUMES 1 AND 2 Ph.D. Thesis
Shahrokh Ghaffari 1989 383 p
Avail: Univ. Microfilms Order No. DA9005734

Impact damage in graphite/epoxy quasi-isotropic composite laminates is characterized and detected. Particular emphasis is placed on non-visual impact damage. It is well-established that such damage can cause a significant degradation in performance. Therefore, both experimental and analytical investigations were conducted, addressing some of the more critical issues related to the general subject of impact damage in composite laminates. In the experimental phase the impact-damaged zone was fully characterized employing a variety of nondestructive and destructive testing techniques. The effect of the damage on degradation in mechanical performance is discussed. Primary emphasis was given to the acoustic emission technique. During the course of this research it was determined that a significant amount of emission is generated by the grating among existing fracture surfaces. Therefore, emphasis was placed on analyzing and identifying this friction emission. In the analytical phase, two major issues were addressed. First, the state-of-damage during the impact event was predicted using a numerical simulation procedure. A dynamic finite element stress analysis was performed from which the stress distributions across the laminate thickness were calculated for cross-ply and quasi-isotropic laminates. The maximum stress criterion was incorporated into the numerical procedure, based on which failure maps could be constructed. Based on these failure maps the damage initiation and progression during the impact event itself could then be predicted. These predictions were compared for quasi-isotropic laminates with the experimental observations based on nondestructive and destructive examinations. An excellent qualitative agreement between predictions and experiments was established. Second, the initiation and progression of matrix damage in model specimens were investigated employing a numerical simulation procedure. Strain energy release rates were calculated using a finite element stress analysis and employing the crack closure technique. Predictions were compared with experiments and a good agreement was established. Dissert. Abstr.

N90-22611 Wyoming Univ., Laramie.
A STUDY OF WOVEN FABRIC-REINFORCED COMPOSITE MATERIALS USING AN INVARIANT-BASED ORTHOTROPIC PLASTICITY FORMULATION Ph.D. Thesis
Donald Merl Blackketter 1989 333 p
Avail: Univ. Microfilms Order No. DA9003781

The mechanical behavior of woven fabric-reinforced composite materials is investigated. Linear and nonlinear material behavior of a woven fabric reinforced composite was modeled using a three-dimensional finite element computer program. Tension and shear load case were investigated using a minimechanics unit cell and results from the finite element analysis were compared to experimental data. The plain weave finite element cell model was constructed after extensive investigation into the geometry of the minimechanics unit cell, various cross-sections of woven fabric-reinforced composite laminates were examined using an optical microscope. Cross-sectional photographs were studied to insure a representative finite element mesh was developed. The three-dimensional finite element computer program was developed based on an existing computer program known as WYO3D. This computer program was modified in order to conduct a nonlinear finite element analysis for either material nonlinearities and/or nonlinear behavior due to material damage. To perform the analysis a constitutive relation was needed which accurately predicted the nonlinear behavior for a wide range of orthotropic composite materials. An invariant-based flow rule was developed which was able to predict plastic behavior of orthotropic materials without the use of an effective stress-effective strain relation. This orthotropic plasticity formulation represents a major contribution to the analysis of composite materials over previously used theories. The finite element formulation for the invariant-based flow rule was also presented. A finite element formulation was developed and implemented which was able to predict material damage occurring within the composite material. The three-dimensional finite element fabric-reinforced unit cell model, the three-dimensional elastic-plastic finite element program and material damage formulation, and the orthotropic plasticity constitutive relation, provided the basis to predict general mechanical behavior of woven fabric-reinforced composite materials. Analysis techniques presented are generally applicable to the investigation of composite materials. Dissert. Abstr.

N90-22612 Stanford Univ., CA.
AUTOMATED STAR PATTERN RECOGNITION Ph.D. Thesis
Roelof W. H. vanBezooijen 1989 292 p
Avail: Univ. Microfilms Order No. DA8925968

A robust, nominally non-iterative star pattern recognition algorithm, enabling fast autonomous attitude determination was developed and evaluated. The algorithm, intended for use with accurate star trackers capable of tracking multiple stars, has a wide range of applicability. It can be used for automating the acquisition of celestial targets by astronomy telescopes, for updating the attitude of gyro based attitude control systems autonomously, and for automating ground based attitude reconstruction. Integrated with state-of-the-art hardware, the algorithm allows realization of a device capable of determining its attitude without requiring any a-priori attitude knowledge. This device, referred to as an Autonomous Star Tracker (AST), can serve as a key sensor in future autonomous attitude control and navigation systems. It is shown that an AST utilizing a star tracker (STR) like ASTROS 2, an all-sky database of 4,100 guide stars, and 800 Kbytes of memory, can identify the stars within its field of view (FOV) in typically one second with a success rate close to 100 percent. ASTROS 2, being developed for use with the Mariner Mark 2 planetary spacecraft, is a microcomputer (MC68000 class) equipped CCD tracker with a field of view of 11.5 by 11.5 degree and an accuracy of 8 arcsec (1 sigma). Applied to orbiting astronomical facilities, the algorithm allows automation of celestial target acquisition, a function usually performed by a human operator. In addition to being faster and more reliable, automation is a necessity if real time communication is not available, or if a large post-slew pointing error precludes identification by a human operator. The recognition algorithm is evaluated using parameters applicable to the Space Infrared Telescope Facility (SIRTF). Dissert. Abstr.

N90-22613 Virginia Polytechnic Inst. and State Univ., Blacksburg.
LARGE DEFORMATION ANALYSIS OF LAMINATED COMPOSITE STRUCTURES BY A CONTINUUM-BASED SHELL ELEMENT WITH TRANSVERSE DEFORMATION Ph.D. Thesis
Pey Min Wung 1989 149 p
Avail: Univ. Microfilms Order No. DA9008046

A finite element formulation and associated computer program is developed for the transient large deformation analysis of laminated composite plate/shell structures. In order to satisfy the plate/shell surface traction boundary conditions and to have accurate stress description while maintaining the low cost of the analysis, a newly assumed displacement field theory is formulated by adding higher-order terms to the transverse displacement

component of the first-order shear deformation theory. The laminated shell theory is formulated using the Updated Lagrangian description of a general continuum-based theory with assumptions on thickness deformations. The transverse deflection is approximated through the thickness by a quartic polynomial of the thickness coordinate. As a result, both the plate/shell surface tractions and the interlaminar shear stress continuity conditions at interfaces are satisfied simultaneously. Analytical integration through the thickness direction is performed for both the linear analysis and the nonlinear analysis. Resultants of the stress integrations are expressed in terms of the laminate stacking sequence. Finally, a variety of numerical examples are presented to demonstrate the validity and efficiency of the finite element program developed herein. Dissert. Abstr.

N90-22614*# Texas A&M Univ., College Station. Dept. of Aerospace Engineering.
A LIFE PREDICTION MODEL FOR LAMINATED COMPOSITE STRUCTURAL COMPONENTS Final Technical Report, 1 Apr. 1989 - 31 Mar. 1990
David H. Allen May 1990 102 p
(Grant NAG1-979)
(NASA-CR-186587; NAS 1.26:186587) Avail: NTIS HC A06/MF A01 CSCL 11D

A life prediction methodology for laminated continuous fiber composites subjected to fatigue loading conditions was developed. A summary is presented of research completed. A phenomenological damage evolution law was formulated for matrix cracking which is independent of stacking sequence. Mechanistic and physical support was developed for the phenomenological evolution law proposed above. The damage evolution law proposed above was implemented to a finite element computer program. And preliminary predictions were obtained for a structural component undergoing fatigue loading induced damage. Author

N90-22615 Yale Univ., New Haven, CT.
THE ELASTIC-PLASTIC BEHAVIOR OF COMPOSITE MATERIALS Ph.D. Thesis
Chien Hsien Liu 1988 273 p
Avail: Univ. Microfilms Order No. DA9009410

The elastic-plastic behavior of metal-matrix composites reinforced by continuous elastic fibers was investigated by using thin-walled tubular specimens. The unidirectional boron/6061-aluminum composite specimens were incrementally loaded by a computer controlled closed loop MTS servohydraulic system. The specimens were under a combined loading of axial force, torsion, and internal pressure at room temperature. The experimental results show that the initial subsequent yield surfaces have large flat segments associated with a matrix-dominated deformation. Apart from certain changes in size, which may be attributed to the distortions of the underlying matrix yield surfaces, the composite yield surfaces retain their shape during loading. The yield surface moves in a translation along the direction of the applied stress increment. Exceptions from the rule are found at the flat segments of the surface, and at certain vertices. In order to understand and interpret the results of the experimental program, some theoretical studies were undertaken as follows: limit analysis of a thin-walled composite tube; homogenization in elastic-plastic composite materials; axial shear loading of a cylindrical inclusion embedded in a matrix; and on errors in homogenization. Dissert. Abstr.

N90-22616# Office National d'Etudes et de Recherches Aerospatiales, Paris (France). Direction Scientifique de la Resistance des Structures.
ULTRASONIC DETECTION OF CRITICAL DAMAGE IN CARBON-EPOXY COMPOSITE MATERIALS Final Report [DETECTION PAR ULTRASONS DES ENDOMMAGEMENTS CRITIQUES DES MATERIAUX COMPOSITES EN CARBONE-EPOXY]
H. Kaczmarek and G. Baudin Apr. 1989 61 p In FRENCH
(Contract STPA/EG-85/95-004)
(ONERA-RT-5/7256-RY-081-R; ETN-90-96615) Avail: NTIS HC A04/MF A01

Detection of transverse cracking and delamination in carbon-epoxy composite materials using ultrasonic techniques is described. The advantages and disadvantages of the technique are discussed. One of the disadvantages is the difficulty of distinguishing between individual cracks when the transverse crack density is very high. The positioning of the ultrasonic beam is a crucial element in obtaining good detection results. The results indicate that the ultrasonic detection technique can compete with the radiographic techniques most commonly used in such detection work. ESA

N90-22617# Centre d'Essais Aeronautique Toulouse (France). Lab. Essais d'Impacts sur Structures.
BIRD IMPACT TESTS ON KEVLAR 29 AND 49 SANDWICH STRUCTURES UNDER STRAIGHT-ON AND GLANCING IMPACT [ESSAIS D'IMPACTS A L'OISEAU SUR STRUCTURES MONOLITHIQUES ET SANDWICH TYPES 29 ET 49 TIRS NORMAUX ET OBLIQUES. PROCES-VERBAL S34213 PARTIAL NO 6]
M. Letcheto 11 Aug. 1988 28 p In FRENCH Sponsored by Service Technique des Programmes Aeronautiques, Paris, France
(Rept-S3-4273-Partial-6; Rept-NT-10/S/83; ETN-90-96616)
Avail: NTIS HC A03/MF A01

Impact tests of birds on panels of Kevlar 29 and 49 are described. The Kevlar test samples are 475 by 475 mm and 900 by 600 mm in size. They are composed of six layers of Kevlar impregnated with a 145.2 resin. A compressed air canon is used to project a freshly killed bird weighing 1.814 kg. the speed of impact is measured using photoelectric cells. The residual speed after impact is measured using a camera and a background grid. The piercing energy is found to be practically identical for the Kevlar 49 and 29. ESA

N90-22618# METRAVIB, Lyon (France). Dept. Materiaux.
DAMAGE ANALYSIS FOLLOWING SLIGHT DEFORMATIONS OF COMPOSITE MATERIALS [CARACTERISATION DE L'ENDOMMAGEMENT SOUS FAIBLE DEFORMATION DES MATERIAUX COMPOSITES]
C. Chesneau 24 Oct. 1988 44 p In FRENCH Prepared in cooperation with Institut National des Sciences Appliquees, Lyon, France
(Contract DRET-86-34-413-00-470-75-01)
(RDS-1-007-64; ETN-90-96617) Avail: NTIS HC A03/MF A01

Analysis of the results of fatigue test carried out on composite materials is presented. A methodology used in defining damage to composite materials is developed. Macroscopic parameters such as stress, deformation, speed of deformation and temperature are taken into account in the analysis. A series of composite plates are made and their mechanical properties are compared to those developed in the damage simulation model. The result of the actual deformation tests are compared to predictions based on the model. ESA

N90-22619# Centre d'Essais Aeronautique Toulouse (France). Lab. Essais d'Impacts sur Structures.
BIRD IMPACT TESTS ON KEVLAR PLATES. SANDWICH KEVLAR-NIDA SUBMITTED TO STRAIGHT-ON AND GLANCING IMPACT [ESSAIS D'IMPACTS A L'OISEAU SUR STRUCTURES EN KEVLAR PLAQUES PLANES TYPE SANDWICH KEVLAR-NIDA TIRS NORMAUX ET OBLIQUES. PROCES-VERBAL S3-4213 PARTIAL NO. 3]
M. Etcheto 1987 56 p In FRENCH Sponsored by Service Technique des Programmes Aeronautiques, Paris, France
(Rept-S3-4273-Partial-3; Rept-NT-10/S/83; ETN-90-96618)
Avail: NTIS HC A04/MF A01

The minimum energy required for perforation, residual energy, and the type of perforation are studied during the impact tests described. The influence of how the Kevlar plates are fastened to the experimental frames is discussed. A compressed air canon is used to project a freshly killed bird weighing 1.814 kg. The speed

of impact is measured using photoelectric cells. Residual speed after impact is measured using a camera and a background grid. Detailed results of the impact tests are presented. ESA

N90-22620# Centre d'Essais Aeronautique Toulouse (France). Lab. Essais d'Impacts sur Structures.
BIRD IMPACT TESTS ON STRUCTURES MADE OF KEVLAR 49. MONOLITHIC PLATES UNDER STRAIGHT-ON IMPACT [ESSAIS D'IMPACTS D'OISEAUX SUR STRUCTURES EN KEVLAR 49 PLAQUES MONOLITHES TIRS NORMAUX. PROCES-VERBAL S3-4273 PARTIEL NO 1]
M. Etcheto 6 Jul. 1988 48 p In FRENCH Sponsored by Service Technique des Programmes Aeronautiques, Paris, France
(Rept-S3-4273-Partial-1; Rept-NT-10/S/83; ETN-90-96619)
Avail: NTIS HC A03/MF A01

The influence of the distribution of layers in a Kevlar sandwich structure on the impact resistance of the plates is studied. The role played by the bonding resin in determining impact resistance is studied. A compressed air canon is used to project a freshly killed chicken weighing 1.814 kg. The impact speed is measured using photoelectric cells. The residual speed after impact is measured using a camera and a background grid. Better resistance of 8 satin finish compared to 4 satin finish is found. ESA

N90-22621# Aerospatiale Aquitaine, Saint-Medard en Jalles (France). Lab. Materiaux Nouveaux.
POLYMERIZATION OF COMPOSITES [LA POLYMERISATION DES COMPOSITES: UN NOUVEAU PROCEDE]
Daniel Beziers 1989 32 p In FRENCH Presented at the INERN Conference, 10-11 Oct. 1989
(Rept-892-430-102; ETN-90-96633) Avail: NTIS HC A03/MF A01

A polymerization technique for forming composite structures using electron beams is outlined. Its use in the fabrication of thrusters by wrapping techniques is outlined. The electron beam serves to catalyze the hardening of the resin in forming the composite structure. The use of different thermal and radiation techniques to catalyze polymerization are compared. A combination of electron beam and x ray radiation is chosen due to the simplicity of application, the rapid polymerization speed and the high penetration capacity obtained. ESA

N90-22622# Aerospatiale Aquitaine, Saint-Medard en Jalles (France). Dept. des Materiaux Nouveaux.
MACHINING OF NEW MATERIALS AT AEROSPATIALE [L'USINAGE DES MATERIAUX NOUVEAUX A L'AEROSPATIALE]
Michel Gadbin 1989 14 p In FRENCH Presented at the SITEF, Toulouse, France, 19 Oct. 1989
(Rept-892-430-104; ETN-90-96635) Avail: NTIS HC A03/MF A01

The machineability of a new material is identified as a major criterion in determining the utility of such materials. The ease of cutting, planning, and drilling into different types of composite materials are presented in tabular form. Difficulties involved in machining ultrahard ceramic materials are addressed. These include scratching and chipping of the ceramic under finishing, and rapid wear of the machining tools. To work such materials, noncontact machining techniques such as charged fluid jets or sonotrodes in abrasive baths are recommended. ESA

N90-22623# Aerospatiale, Paris (France).
POLYMERIZATION OF COMPOSITE MATERIALS: A TECHNIQUE DEVELOPED BY AEROSPATIALE [POLYMERISATION DES MATERIAUX COMPOSITES: UN NOUVEAU PROCEDE MIS AU POINT PAR AEROSPATIALE]
Georges Teyssier Sep. 1989 4 p In FRENCH
(Rept-892-430-107; ETN-90-96638) Avail: NITS HC A02/MF A01

A polymerization technique for composite materials requiring no elevation in temperature is described. Polymerization is carried out by ionization. An electron beam replaces the ovens used to date. Depending on the thickness of the composite material, either an electron beam or x rays are used to harden the resin. The advantages of the technique are listed. Flexibility and speed of the polymerization process are two of the most practical advantages. Better stability over time of the bonding resins is reported. ESA

N90-22624# Aerospatiale Aquitaine, Saint-Medard en Jalles (France).
THE SURPRISING POSSIBILITIES OF WRAPPING [LE BOBINAGE DES POSSIBILITES ETONNANTES]
J. L. Tisne 22 May 1989 35 p In FRENCH
(Rept-892-430-108; ETN-90-96639) Avail: NTIS HC A03/MF A01

Wrapping, as an aerospace manufacturing technique is discussed. The calculations and constraints involved in wrapping strategies are outlined. The types of fibers and bonding materials used in wrapping techniques are listed. Different types of spools used in wrapping are discussed. These include extractable, soluble and inflatable spools. Different types of wrapping machinery are described. The European and American manufacturers of such machinery are listed. Future developments in wrapping technology are discussed. ESA

N90-22625# Aerospatiale Aquitaine, Saint-Medard en Jalles (France). Div. Systemes Balistiques et Spatiaux.
PRODUCTION OF A VARIETY OF SHAPES USING WRAPPING AND DRAPING TECHNIQUES [CONCEPTION DES STRUCTURES DE FORMES VARIEES REALISEES PAR BOBINAGE ET PAR DRAPAGE]
Jean Lamalle 23 Feb. 1989 43 p In FRENCH
(Rept-892-430-122; AQET-Note-07/89; ETN-90-96653) Avail: NTIS HC A03/MF A01

The production of cylindrical and conical objects by wrapping and draping techniques is outlined. Axisymmetric and nonaxisymmetric structures are treated separately. The dimensional stability of the shapes produced is tested. Comparisons are made between shapes produced by wrapping and by draping. Full mathematical calculations are presented for different wrapping situations. The use of such shapes in forming the nose cone of a rocket engine is investigated. ESA

N90-22626# Aerospatiale Aquitaine, Saint-Medard en Jalles (France). Div. Systemes Strategiques et Spatiaux.
THE POSITION OF CARBON/CARBON COMPOSITES AMONG HIGH TEMPERATURE COMPOSITES [PLACE DES CARBONE/CARBONE DANS LE DOMAINE DES COMPOSITES A HAUTE TEMPERATURE]
A. Hordonneau and J. F. Jamet 1989 17 p In FRENCH
(Rept-892-430-126; ETN-90-96657) Avail: NTIS HC A03/MF A01

The dominant role of carbon/carbon composites in future thermal protection materials is discussed. The thermal resistance characteristics of carbon/carbon composites compared to the ceramic fiber composites presently available makes them the material of choice. The possibility of developing ceramic fiber composites capable of handling higher temperatures is discussed. The ease of ceramic fiber composite production, its dependability and flexibility of use would make it a more attractive material than carbon/carbon composites. The virtually nil dilation coefficient of carbon/carbon composites makes them attractive even for lower temperature applications. ESA

N90-22627# Drexel Univ., Philadelphia, PA.
A COMPREHENSIVE STUDY ON MICROSTRUCTURE MECHANICS RELATIONSHIPS OF CERAMIC MATRIX COMPOSITES Final Report, 1 Apr. 1988 - 30 Jun. 1989
A. S. D. Wang and M. W. Barsoum 20 Dec. 1989 29 p
(Grant AF-AFOSR-0113-88; AF Proj. 2303)
(AD-A219318; AFOSR-90-0192TR) Avail: NTIS HC A03/MF A01 CSCL 11/2

The physical mechanisms of brittle matrix cracks in fiber reinforced ceramic matrix composites are studied. Three major tasks are performed during the research: an in-house fabrication

facility is established; a testing technique is developed; and a theory for matrix crack initiation and a numerical simulation method is formulated. A preliminary correlation between theory and experiment is accomplished. Two individual technical papers are presented: one describes the details of the experimental aspects and the other describes the theoretical and the simulative aspects. GRA

N90-22628*# National Aeronautics and Space Administration. Langley Research Center, Hampton, VA.
PULTRUSION PROCESS DEVELOPMENT FOR LONG SPACE BOOM MODEL
Maywood L. Wilson and Robert Miserentino Jan. 1988 21 p Presented at the 41st Annual Conference of the Society of the Plastics Industry Reinforced Plastics/Composites Inst., Atlanta, GA, 27-31 Jan. 1986 Previously announced in IAA as A87-20083
(NASA-TM-4017; L-16365; NAS 1.15:4017) Avail: NTIS HC A03/MF A01 CSCL 11D

Long flexible-boom models were required to develop ground-vibration test methods for very-low-frequency space structures with applications to the proposed Space Station. Pultruded quasi-isotropic composite beams were selected as an option over extruded aluminum alloy structures because of the lower cost potential, the higher specific strength, the flexural properties, and the dynamic similarity considerations. The reinforcement material that was used was biaxial (0 deg/90 deg) fiberglass roving held in place with knitted polyester yarn such that equal fiber volume in 0 deg and 90 deg orientations provided nearly equal strength in both longitudinal and transverse directions. An isophthalic polyester resin system was used as the matrix. Continuous lengths up to 270 ft were easily pultruded with biaxial fabric. Tracking problems were encountered with similar unidirectional fabrics. Analyses of processing problems were conducted to determine causes for delamination, scaling, and sloughing. Ultrasonic C-scanning and scanning electron microscope examinations were conducted as well as mechanical testing to failure. Test results indicate that pultrusion processes can be used to produce quasi-isotropic composite structures. Author

25 INORGANIC AND PHYSICAL CHEMISTRY

Includes chemical analysis, e.g., chromatography; combustion theory; electrochemistry; and photochemistry.

For related information see also *77 Thermodynamics and Statistical Physics.*.

N90-22629# Westinghouse Savannah River Co., Aiken, SC.
MODELING OF COMBUSTION PROCESSES IN A SOLID FUEL PARTICLE
D. W. Howard 1990 24 p Presented at the IBM 3090 Supercomputing Competition Meeting, White Plains, NY, 1 Mar. 1990 Submitted for publication
(Contract DE-AC09-89SR-18035)
(DE90-009140; WSRC-RP-89-812; CONF-9003132-1) Avail: NTIS HC A03/MF A01

During the production of granules of uranium oxide, granules of ion exchange resin, loaded with uranium ions, are burned to remove the resin matrix and leave a uranium oxide ash. Under some conditions of combustion, the oxide granules are produced in a highly fractured, porous state, while other conditions result in hard, dense, solid granules. ABAQUS, a commercial finite element code, run on an IBM 3090, was used to model the physical processes occurring during combustion: heat transfer with a very nonlinear temperature dependent rate of heat generation, diffusion of reactants and products, and stress/strain resulting from the differential temperatures and from the phase changes during the combustion. The ABAQUS simulation successfully explained the differences in morphology of the granules under different conditions, and lead to control strategies to produce the desired morphology. DOE

N90-22630# EG and G Mound Applied Technologies, Miamisburg, OH.
IGNITION TESTING OF LOW-ENERGY LASER DIODE IGNITED COMPONENTS
David W. Ewick and Thomas M. Beckman 16 Apr. 1990 23 p
(Contract DE-AC04-88DP-43495)
(DE90-009968; MLM-MU-90-64-0003) Avail: NTIS HC A03/MF A01

Laser diode ignition tests were performed on various explosive and pyrotechnic materials, including TiH(x)/KClO(4), BCTK, barium styphnate, and several CP-based blends. Under standard test conditions, the threshold energy levels for laser diode ignition of Ti/KClO(4), TiH(0.65)/KClO(4), and TiH(1.65)/KClO(4) were all between 2.8 and 3.3 mJ. The blending of carbon black with CP significantly lowered the energy required for laser diode ignition. The most sensitive blend tested contained 3.2 wt percent carbon black and had a threshold level of 0.47 mJ for a 10 ms laser diode pulse. Various techniques for reducing the energy required for laser diode ignition of energetic materials were also evaluated. The use of graded index fiber rather than step index fiber lowered the threshold of both Ti/KClO(4) and carbon black-doped CP by approximately 30 percent. A 0.05-mm thick Mylar insulator between the optical fiber and powder reduced the threshold energy by roughly 40 percent. Although powder density was found to have a significant effect on the energy required to ignite Ti/KClO(4), the threshold of carbon black-doped CP was unaffected by density. DOE

N90-22631# Joint Inst. for Nuclear Research, Dubna (USSR).
CONVERGENCE OF HYPERSPHERICAL ADIABATIC EXPANSION FOR HELIUM-LIKE SYSTEMS
A. G. Abrashkevich et al 1988 6 p In RUSSIAN; ENGLISH summary Presented at the International Workshop on Microscopic Methods in Theory of a Few Particle Systems, Kalinin, USSR, Aug. 1988 Submitted for publication
(DE90-620526; JINR-R-4-88-640) Avail: NTIS (US Sales Only) HC A02/MF A01

The convergence of hyperspherical adiabatic expansion was studied numerically. The spectral problems arising after separation of variables are solved by the finite difference and finite element methods. The energies of the ground and some doubly excited states of a hydrogen ion are calculated in the six channel approximation within the 10 (sup -4) a.u. accuracy. Obtained results demonstrate a rapid convergence of the hyperspherical adiabatic expansion. DOE

N90-22632# Aerospatiale, Paris (France).
ON THE VAPOUR PHASE DEPOSITION MECHANISM OF CARBON-BORON-NITROGEN COMPOUNDS BETWEEN 800 AND 1000 C
Frederic Saugnac and Andre Marchand 1989 7 p In FRENCH; ENGLISH summary Submitted for publication
(Rept-892-430-101; ETN-90-96632) Avail: NTIS HC A03/MF A01

Conditions for simultaneous deposition of carbon and boron nitride from a gaseous mixture of ammonia, boron trichloride, and acetylene between 800 and 1000 C are investigated. The deposited compounds are characterized. A reaction model for the process is presented. The three successive steps and corresponding zones activity in the reactor are identified. The acetylene pyrolysis is concluded to be initiated mainly by the active species resulting from the reaction of ammonia and boron trichloride. ESA

N90-22633# Army Construction Engineering Research Lab., Champaign, IL.
CALCIUM CARBONATE SCALE DISSOLUTION IN WATER STABILIZED BY CARBON DIOXIDE TREATMENT Final Report
Prakash M. Temkar, John Harwood, and Richard J. Scholze Jan. 1990 35 p
(AD-A218502; CERL-TR-N-90/01) Avail: NTIS HC A03/MF A01 CSCL 07/4

Calcium carbonate scale in potable water systems (especially hot-water pipes and exchangers) can restrict pipe flow, causing

severe head loss and reducing heat transfer capacity. Chemical and mechanical methods of cleaning the distribution systems are considered unsafe for potable supplies due to the human health hazard. As a result, the only alternative may be complete pipe replacement--which can be very expensive. The U.S. Army Construction Engineering Research Laboratory (USACERL) and Illinois State Water Survey have jointly developed a carbon dioxide treatment system for rehabilitating clogged pipes and controlling scale buildup in nonfouled systems. The treatment method is safe and effective. It is being field-tested successfully at several Army installations. Information is needed on the the characteristics of scale dissolution for optimizing the treatment system because overdoses of carbon dioxide can eventually damage pipes. Therefore, USACERL has explored several models for predicting the effects of carbon dioxide treatment on potable waters. A theoretical model was formulated and used in developing a computer program for assessing a water's propensity to become undersaturated, saturated, or oversaturated with respect to carbon dioxide, and to determine its capacity for calcium carbonate deposition or dissolution. GRA

N90-22634# Columbia Univ., New York, NY. Dept. of Chemistry.
FEMTOSECOND STUDIES OF ELECTRON PHOTODETACHMENT OF SIMPLE IONS IN LIQUID WATER: SOLVATION AND GEMINATE RECOMBINATION DYNAMICS
Frederick H. Long, Hong Lu, and Kenneth B. Eisenthal 1 Oct. 1989 3 p Repr., J. Chem. Phys., Vol. 91, No. 7, 1 Oct. 1989 p 4413-4414
(Grant AF-AFOSR-0014-88; AF Proj. 2303)
(AD-A218520; AFOSR-90-0238TR) Avail: NTIS HC A01/MF A01 CSCL 07/4

Aqueous solutions of simple ions such as OH(-) and Cl(-) have fascinated many scientists. The first femtosecond time-resolve studies of electron photodetachment in aqueous solution are presented. The solvation of the ejected electron in the aqueous media and the subsequent recombination dynamics of the neutral atom with the electron have been measured. Relevant to this are several recent experimental studies of electrons in neat liquids using femtosecond lasers. GRA

N90-22635# Cornell Univ., Ithaca, NY.
NUMERICAL INVESTIGATION OF TURBULENT FLAME SHEETS Annual Technical Report, Dec. 1988 - Dec. 1989
S. B. Pope 1 Jan. 1990 11 p
(Grant AF-AFOSR-0052-88; AF Proj. 2308)
(AD-A218553; AFOSR-90-0190TR) Avail: NTIS HC A03/MF A01 CSCL 21/2

Direct numerical simulations of turbulence are being performed to study fundamental processes of turbulent combustion. In the flame-sheet regime of turbulent premixed combustion an important process is the stretching and bending of the surface by the turbulence. These processes were comprehensively studied for material surfaces, and a similar study for propagating surfaces is nearing completion. A new closure methodology recently proposed by Kraichnan holds much promise for turbulent reacting flows. An analytic solution to the model equations was obtained; and it is found that the results are in remarkable agreement with those from the earlier direct numerical simulations. GRA

N90-22636# Yale Univ., New Haven, CT.
NONLINEAR SPECTROSCOPY OF MULTICOMPONENT DROPLETS AND 2- AND 3-DIMENSIONAL MEASUREMENTS IN FLAMES Annual Technical Report, 1 Jan. - 31 Dec. 1989
Richard K. Chang and Marshall B. Long 15 Jan. 1990 19 p
(Grant AF-AFOSR-0100-88; AF Proj. 2308)
(AD-A218569; AFOSR-90-0262TR) Avail: NTIS HC A03/MF A01 CSCL 20/6

The progress in the area of nonlinear spectroscopy of droplets includes the following: (1) development of a fluorescent imaging technique which is capable of demarcating the liquid phase of the deformed and ejected droplets from the vapor phase of the ejected material; (2) determination that the absorption of the laser induced plasma quenches the stimulated Raman process and sets an upper limit on the incident intensity which can be used to generate stimulated Raman scattering (SRS) within droplets; (3) completion of a statistical study of the SRS from single droplets which are irradiated at a fixed input laser intensity (from a single mode or a multi-mode laser); (4) conclusion that, for single mode laser excitation, SRS is pumped by the stimulated Brillouin radiation, not directly by the laser radiation; and (5) initiation of studies on the phase matching requirement for four wave mixing processes in droplets and on the phase velocity of waves on a morphology-dependent resonance. GRA

N90-22637# Drexel Univ., Philadelphia, PA. Dept. of Mechanical Engineering and Mechanics.
OXIDATION AND IGNITION CHARACTERISTICS OF HYDROCARBON FUELS Final Report, 1 Oct. 1985 - 30 Nov. 1989
Nicholas P. Gernansky 31 Jan. 1990 23 p
(Contract DAAG29-85-K-0253)
(AD-A218666; ARO-22437.17-EG) Avail: NTIS HC A03/MF A01 CSCL 21/4

A research program studying the oxidation and ignition characteristics of hydrocarbon fuels was conducted. The research program entailed mechanistic studies examining the oxidation chemistry of single-component hydrocarbons and ignition studies examining the overall ignition behavior of pure single-component fuels and binary and ternary fuel blends. Three separate and complementary bench scale experiments, which include a static reactor, an atmospheric pressure flow reactor, and a pressurized flow reactor were used to examine the preignition chemistry and ignition behavior of hydrocarbons over a range of temperatures, pressures, and equivalence ratios. Gas chromatography and GC/MS were used for chemical analysis of the stable reaction intermediates and products. GRA

N90-22638# Air Products and Chemicals, Inc., Allentown, PA.
DEVELOPMENT OF HIGH-ACTIVITY PARA- TO ORTHO-HYDROGEN CONVERSION CATALYSTS, VOLUME 2 Final Report, 1 Aug. 1987 - 31 Oct. 1988
James F. White 28 Sep. 1989 102 p
(Contract F33615-87-C-2740; AF Proj. 3048)
(AD-A218700; AFWAL-TR-89-2011-Vol-2) Avail: NTIS HC A06/MF A01 CSCL 21/8

Literature search results for para- to ortho-hydrogen conversion catalysis: Bibliography; 1910 to present by year of publication. GRA

N90-22639# North Carolina Univ., Chapel Hill.
LINEAR AND NONLINEAR ELECTRICAL RESPONSE OF CONDENSED MATTER: IONIC, DIELECTRIC, AND MIXED-CONDUCTION MATERIALS Final Report, 14 Aug. 1984 - 31 Dec. 1989
J. Ross Macdonald Jan. 1990 5 p
(Contract DAAG29-84-K-0132)
(AD-A218771; ARO-21271.27-CH) Avail: NTIS HC A01/MF A01 CSCL 20/3

The problem outlined in the original proposal was broadly concerned with the elucidation of the electrical behavior of a system comprised of a non-metallic solid or liquid material, usually an electrolyte, between two electrodes. It proposed the development of new means of interpreting small signal ac response of such systems (now called Impedance Spectroscopy) and included experimental and theoretical work on mixed (electronic and ionic) conductivity materials. In addition, it proposed a Monte Carlo simulation study of a monolayer of dipoles in an electric field. GRA

N90-22640# North Carolina State Univ., Raleigh. Dept. of Materials Science and Engineering.
HIGH INTENSITY ELECTRO-MAGNETIC AND ULTRASONIC EFFECTS ON INORGANIC MATERIALS BEHAVIOR AND PROCESSING WORKSHOP Final Report, 1 Apr. 1989 - 31 Mar. 1990

Hans Conrad Feb. 1990 298 p Workshop held in Raleigh, NC, 17-18 Jul. 1989
(Contract DAAL03-89-G-0032)
(AD-A218884; ARO-26690.1-MS-CF) Avail: NTIS HC A13/MF A02 CSCL 07/2

The objectives of this workshop were to review the ongoing work on the effects of the various forms of energy, other than thermal and external stresses on the mechanical behavior of materials, and to identify critical technical issues which must be addressed to make a headway to understand the mechanisms involved in these effects and exploit this emerging technology. The program started with the considerations of the fundamental mechanisms relevant to the physical effects to be discussed, followed by the discussion of the mechanisms involved in specific mechanical effects and a full session on materials processing.
GRA

N90-22641# State Univ. of New York, Buffalo. Dept. of Chemistry.
VISCOSITY, DENSITY AND CONDUCTIVITY OF ImCl(HCl) SUB 1.3
Kejiro Sawai and Robert A. Osteryoung 22 Feb. 1990 12 p
(Contract N00014-89-K-0056)
(AD-A218902; SUNYBUF/DC/TR-1) Avail: NTIS HC A03/MF A01 CSCL 07/4

The compound 1-ethyl-3-methylimidazolium hydrogen dichloride, (ImHCl2), was originally synthesized in our laboratory. This material, an ambient temperature molten salt, is currently under investigation by Hughes Aircraft, as a fluid for a thermally regenerative electrochemical fuel cell device. Although we had discovered this material, and utilized it in a number of our studies as a source for the quantitative addition of proton to ambient temperature molten salts consisting of 1-ethyl-3-methylimidazolium chloride (ImCl) and aluminum chloride, we had not carried out any investigations of the physical properties of the material. Here we report on a determination of the density, viscosity and specific conductivity of 1-ethyl-3-methylimidazolium hydrogen dichloride, (ImHCl2) over a limited temperature range.
GRA

N90-22642# Wright State Univ., Dayton, OH. Dept. of Chemistry.
SINGLE-CRYSTAL DIFFRACTION ANALYSIS OF 2-(TRIMETHYLSILYLETHYNYL) 4-NITRO-N,N-DIMETHYLANILINE Interim Report, Jun. 1988 - Jun. 1989
David A. Grossie, Albert V. Fratini (Dayton Univ., OH.), and W. Wade Adams Jul. 1989 49 p
(Contract F49620-88-C-0053; AF Proj. 2303)
(AD-A218955; WRDC-TR-89-4120) Avail: NTIS HC A03/MF A01 CSCL 07/4

Single-crystal x ray diffraction data was collected on 2-(Trimethylsilylethynyl) 4-nitro-N,N dimethylaniline, C13-H18N2O2Si, an intermediate isolated in the synthesis of compounds having potential nonlinear optical (NLO) properties. The title compound is a derivative of 2-Methyl- 4-nitroaniline (NMA), a molecule with known nonlinear optical properties. It crystallizes in a monoclinic crystal lattice with cell constants of a=20.258(6), b=10.444(4), c=7.129(2) A, and B=93.05(2). The observed space group is P2(1)/c, a centric space group. The structure was solved and refined, yielding a R-factor of 0.085. C13H18N2O2Si is planar with little distortion in the internal bond distances and angles.
GRA

N90-22643# Texas A&M Univ., College Station. Dept. of Chemistry.
ELECTROCHEMICAL SYNTHESIS OF ULTRATHIN FILM COMPOSITE MEMBRANES
Chao Liu, Mark W. Espenscheid, Wen-Janq Chen, and Charles R. Martin 5 Mar. 1990 14 p Submitted for publication
(Contract N00014-82-K-0612; ONR Proj. 627-838)
(AD-A219041; TR-46) Avail: NTIS HC A03/MF A01 CSCL 07/6

The development of ultrathin film composite membranes was an important breakthrough in the membranes-separation area. Ultrathin film composite membranes consist of a porous support layer, and a dense, ultrathin active layer. The porous support layer provides mechanical strength yet is highly permeable. The separation process occurs primarily in the ultrathin active layer; because this layer is thin, the overall flux of permeate through the membrane is high. Thus, ultrathin film composite membranes can provide good mechanical strength, high selectivity, and high permeability. This combination of attributes usually cannot be obtained with homogeneous membranes. We have developed a new method for preparing ultrathin film composite membranes. This method involves electrochemically-initiated polymerization at a microporous support-membrane surface and yields an ultrathin polymer film on one face of the support-membrane. Composite membranes with separating layers as thin as 50 nm have been prepared using this new electrosynthetic method. We describe the synthesis and characterization of these new membranes in this correspondence.
GRA

N90-22644# Arizona Univ., Tucson. Dept. of Chemistry.
CONTINUED INVESTIGATIONS OF NEW CONCEPTS FOR IMPROVED SPECTROCHEMICAL ANALYSIS Final Report, 1 May 1986 - 30 Apr. 1989
M. B. Denton 5 Jan. 1990 105 p
(Contract N00014-86-K-0316)
(AD-A219403) Avail: NTIS HC A06/MF A01 CSCL 07/2

A strongly interlocking program designed to yield important new methodology for use in chemical analysis has been conducted. Fundamental investigations designed to gain new insight into areas of plasma spectroscopy through developing improved models of plasma discharges have been made. Studies which are contributing to a revolution in ultraviolet and visible detection have been conducted.
GRA

26 METALLIC MATERIALS

Includes physical, chemical, and mechanical properties of metals, e.g., corrosion; and metallurgy.

N90-22645 California Univ., Davis.
HIGH-TEMPERATURE DEFORMATION OF MECHANICALLY-ALLOYED ALUMINUM IN90211 Ph.D. Thesis
Thomas Rector Bieler 1989 350 p
Avail: Univ. Microfilms Order No. DA9002720

The tensile behavior of mechanically alloyed IN9021, was characterized at strain rates between 3 x 10(exp -9)/sec and 340/sec at temperatures between 425 and 475 C. At strain rates below 0.1/sec, the strain rate sensitivity, m, is low, with corresponding low elongation. At strain rates above 0.1/sec, the strain rate sensitivity increased to 0.26, where superplastic elongations were obtained. The elongations observed were strongly affected by thermal gradients in the deforming specimen, resulting from thermal conduction of adiabatically generated heat. Microscopic observations indicated that the stable submicron (sub)grains formed disc-shaped clusters 0.3 microns thick and 2 to 3 microns in diameter. Oxide and carbide dispersions about 15 nm in diameter and about 45 nm apart were distributed throughout the matrix and in grain boundaries. The data was interpreted on the basis of a threshold stresses analysis. The superplastic stress-strain rate data were linearized on the basis of $n = 2$ and $n = 3$ assumptions for flow behavior, where $n = 1/m$. Extrapolation of zero strain rate provided a temperature dependent threshold stress. The threshold stresses for the $n = 3$ and $n = 2$ analysis had activation energies of 140 and 60 kJ/mol, corresponding with lattice and grain boundary diffusivity, respectively. The true activation energy for the process was between 80 and 130 kJ/mol, depending upon n value assumptions. The $n = 3$ threshold stresses agreed with terminal stresses measured from stress relaxation experiments, and the $n = 2$ threshold stresses corresponded with the low stress limits of superplastic deformation. The threshold stresses were interpreted with respect to theories based upon

local and general climb of dislocations around dispersions. The n = 3 mechanism was determined to be the rate limiting part of the superplastic deformation process of IN9021. Dissert. Abstr.

N90-22646*# National Aeronautics and Space Administration. Lewis Research Center, Cleveland, OH.
FATIGUE CRACK GROWTH IN A UNIDIRECTIONAL SCS-6/Ti-15-3 COMPOSITE
Peter Kantzos, Jack Telesman, and Louis Ghosn (Sverdrup Technology, Inc., Cleveland, OH.) 1989 36 p Presented at the 3rd Symposium on Composite Materials: Fatigue and Fracture, Orlando, FL, 6-9 Nov. 1989; sponsored by American Society for Testing Materials
(NASA-TM-103095; E-5413; NAS 1.15:103095) Avail: NTIS HC A03/MF A01 CSCL 11F

An investigation was conducted to characterize and model the fatigue crack growth (FCG) behavior of a SCS-6/Ti-15-3 metal matrix composite. Part of the study was conducted using a fatigue loading stage mounted inside a scanning electron microscope (SEM). This unique facility allowed high magnification viewing of the composite fatigue processes and measurement of the near crack tip displacements. The unidirectional composite was tested in the (0)8 (i.e., longitudinal) and (90)8 (i.e., transverse) orientations. For comparison purposes unreinforced matrix material produced by the identical process as the reinforced material was also tested. The results of the study reveal that the fatigue crack growth behavior of the composite is a function of specimen geometry, fiber orientation and the interaction of local stress fields with the highly anisotropic composite. In the case of (0)8 oriented single edge notch (SEN) specimens and (90)8 oriented compact tension (CT) specimens, the crack growth was normal to the loading direction. However, for the (0)8 CT specimens the crack grew mostly parallel to the loading and the fiber direction. The unusual fatigue behavior of the (0)8 CT specimens was attributed to the specimen geometry and the associated high tensile bending stresses perpendicular to the fiber direction. These stresses resulted in preferential cracking in the weak interface region perpendicular to the fiber direction. The interface region, and in particular the carbon coating surrounding the fiber proved to be the composites weakest link. In the (0)8 SEN the crack growth was confined to the matrix leaving behind unbroken fibers which bridged the cracked surfaces. As the crack grew longer, more fibers bridged the crack resulting in a progressive decrease in the crack growth rates and eventual crack arrest. The actual near crack tip displacement measurements were used in a proposed formulation for a bridging-corrected effective crack driving force, delta K(sub eff). This parameter was able to account for most of the experienced bridging and correlated the (0)8 SEN fatigue crack growth data reasonably well. Author

N90-22647 United Kingdom Atomic Energy Authority, Harwell (England). Materials Development Div.
THE HIGH TEMPERATURE BEHAVIOR OF GALLIUM AND INDIUM LIQUID METAL ION SOURCES
R. I. Hornsey (Oxford Univ., England) Nov. 1988 44 p
(AERE-R-13321) Copyright Avail: Issuing Activity

Energy distribution diagrams and derived data are presented for gallium and indium liquid metal ion sources operated at elevated temperatures. Results for the gallium source confirm that a secondary peak is formed on the energy distribution diagram at source temperatures above 250 C. Contrary to the findings of other research workers, data presented here show that the indium source displays similar characteristics to that of gallium. Off-axis data are also given, showing that secondary peak formation is not limited to the center of the beam. Characteristics of the two sources are compared and theories for the formation of the secondary peak are examined. It is concluded that present hypotheses do not satisfactorily explain the high temperature behavior of liquid metal ion sources. Author

N90-22648 United Kingdom Atomic Energy Authority, Harwell (England). Materials Development Div.
THE INITIATION OF INTERGRANULAR STRESS CORROSION-CRACKING ON SENSITIZED STAINLESS STEEL IN DILUTE THIOSULPHATE SOLUTIONS
J. Stewart, B. Wells (Oxford Univ., England), and P. M. Scott Oct. 1988 21 p
(AERE-R-13317) Copyright Avail: Issuing Activity

The initiation of intergranular stress corrosion cracking (IGSCC) on sensitized type 304 stainless steel was studied at room temperature using dilute, naturally aerated sodium thiosulphate solutions. Electrochemical techniques are used to detect anodic current transients during slow strain rate experiments at the free corrosion potential. These anodic current transients are caused by the initiation, metastable propagation and repassivation of microstructurally short cracks. The effect of thiosulphate concentration and strain rate on the initiation of cracks was studied. A low strain region (elongation less than 5 percent) was identified in which the crack initiation frequency and electrochemical activity were at a maximum in dilute thiosulphate solutions. The transition to sustained crack propagation was clear and generally occurred at higher strains, where the metastable crack initiation frequency and electrochemical activity were very low. The variation in strain to failure values could be accounted for in the period required to initiate a crack. Crack propagation was shown to be a minor proportion of the total test period. Author

N90-22649 United Kingdom Atomic Energy Authority, Harwell (England). Materials Development Div.
SCANNING LASER PHOTOCURRENT SPECTROSCOPY OF ELECTROCHEMICALLY GROWN BISMUTH SULPHIDE FILMS
Anthony R. Kucernak, Robert Peat, and David E. Williams Oct. 1988 20 p
(AERE-M-3709) Copyright Avail: Issuing Activity

The photoelectrochemical properties of semiconducting bismuth sulfide (Bi2S3) films (in contact with an aqueous electrolyte) grown on bismuth were investigated. Using an optically beam induced contrast (OBIC) technique, it was possible to image these films, and to identify local variations corresponding to grain boundaries and other recombination centers. It was found that the form of these regions varies with the thickness of the film. Both object scanning and beam scanning were investigated for generating images and these two methods are compared. Samples were also investigated by intensity modulated photocurrent spectroscopy (IMPS). This method involves sinusoidal intensity modulation of the incident laser radiation at different frequencies, and the analysis of the resulting photocurrent response. This method was extended by mapping the IMPS response over the specimen surface in order to obtain specific information on local properties. Author

N90-22650 United Kingdom Atomic Energy Authority, Harwell (England). Materials Development Div.
IMPROVED HIGH TEMPERATURE OXIDATION BEHAVIOR OF ALLOYS BY ION IMPLANTATION
M. J. Bennett and A. T. Tuson Aug. 1988 23 p Presented at the International Conference on the Surface Modification of Metals by Ion Beams, Riva Del Garda, Italy, 12-16 Sep. 1988
(AERE-R-13309) Copyright Avail: Issuing Activity

Numerous studies have been undertaken during the last decade examining the potential of ion implantation to improve the high temperature oxidation behavior of a range of metals and alloys. Most of these investigations have focused on improved mechanistic understanding of the roll of specific elements and in particular, the effect of the so called reactive elements such as yttrium and the rare earths. The ion implantation studies have made a unique contribution and these are reviewed. Author

N90-22651*# Virginia Univ., Charlottesville. School of Engineering and Applied Science.
NASA-UVA LIGHT AEROSPACE ALLOY AND STRUCTURES TECHNOLOGY PROGRAM Progress Report, 1 Jan. - 30 Jun. 1990
Richard P. Gangloff, John K. Haviland, Carl T. Herakovich, Walter

D. Pilkey, Marek-Jerzy Pindera, Glenn E. Stoner, Robert E. Swanson (Virginia Polytechnic Inst., Blacksburg.), Earl A. Thornton, Franklin E. Wawner, Jr., and John A. Wert Jun. 1990 400 p
(Grant NAG1-745)
(NASA-CR-182607; NAS 1.26:182607; UVA/528266/MS90/106)
Avail: NTIS HC A17/MF A03 CSCL 11F

The objective of the Light Aerospace Alloy and Structures Technology Program is to conduct interdisciplinary graduate student research on the performance of next generation, light weight aerospace alloys, composites, and associated thermal gradient structures. Individual technical objectives are established for each project. Efforts aim to produce basic understanding of material behavior, monolithic and composite alloys, processing methods, solid and mechanics analyses, measurement advances, and a pool of educated graduate students. Progress is reported for 11 areas of study. For individual titles, see N90-22652 through N90-22663.

N90-22652*# Virginia Univ., Charlottesville.
ENVIRONMENT ENHANCED FATIGUE OF ADVANCED ALUMINUM ALLOYS AND COMPOSITES
Donald C. Slavik and Richard P. Gangloff *In its* NASA-UVA Light Aerospace Alloy and Structures Technology Program Jun. 1990 24 p (For primary document see N90-22651 16-26)
Avail: NTIS HC A17/MF A03 CSCL 11F

The objective is to characterize and understand the environmental fatigue crack propagation behavior of advanced, high stiffness and strength, aluminum alloys and metal matrix composites. Those gases and aqueous electrolytes which are capable of producing atomic hydrogen by reactions on clean crack surfaces are emphasized. Characterizations of the behavior of new materials are sought to provide data for damage tolerant component life prediction. Mechanistic models are sought for crack tip damage processes which are generally applicable to structural aluminum alloys. Such models will enable predictions of cracking behavior outside of the data, metallurgical improvements in material cracking resistance, and insight on hydrogen compatibility. Author

N90-22653*# Virginia Univ., Charlottesville.
ELEVATED TEMPERATURE CRACK GROWTH IN ADVANCED POWDER METALLURGY ALUMINUM ALLOYS
William C. Porr, Jr. and Richard P. Gangloff *In its* NASA-UVA Light Aerospace Alloy and Structures Technology Program Jun. 1990 41 p (For primary document see N90-22651 16-26)
Avail: NTIS HC A17/MF A03 CSCL 11F

Rapidly solidified Al-Fe-V-Si powder metallurgy alloy FVS0812 is among the most promising of the elevated temperature aluminum alloys developed in recent years. The ultra fine grain size and high volume fraction of thermally stable dispersoids enable the alloy to maintain tensile properties at elevated temperatures. In contrast, this alloy displays complex and potentially deleterious damage tolerant and time dependent fracture behavior that varies with temperature. J-Integral fracture mechanics were used to determine fracture toughness (K sub IC) and crack growth resistance (tearing modulus, T) of extruded FVS0812 as a function of temperature. The alloy exhibits high fracture properties at room temperature when tested in the LT orientation, due to extensive delamination of prior ribbon particle boundaries perpendicular to the crack front. Delamination results in a loss of through thickness constraint along the crack front, raising the critical stress intensity necessary for precrack initiation. The fracture toughness and tensile ductility of this alloy decrease with increasing temperature, with minima observed at 200 C. This behavior results from minima in the intrinsic toughness of the material, due to dynamic strain aging, and in the extent of prior particle boundary delaminations. At 200 C FVS0812 fails at K levels that are insufficient to cause through thickness delamination. As temperature increases beyond the minimum, strain aging is reduced and delamination returns. For the TL orientation, K (sub IC) decreased and T increased slightly with increasing temperature from 25 to 316 C. Fracture in the TL orientation is governed by prior particle boundary toughness; increased strain localization at these boundaries may result in lower toughness with increasing temperature. Preliminary results demonstrate a complex effect of loading rate on K (sub IC) and T at 175 C, and indicate that the combined effects of time dependent deformation, environment, and strain aging may play a role. Fractography showed that microvoid coalescence was the microscopic mode of fracture in FVS0812 under all testing conditions. However, the nature of the microvoids varied with test temperature and loading rate, and is complex for the fine grain and dipersoid sizes of FVS0812. Author

N90-22654*# Virginia Univ., Charlottesville.
ELEVATED TEMPERATURE CRACK GROWTH IN ALUMINUM ALLOYS: TENSILE DEFORMATION OF 2618 AND FVS0812 ALUMINUM ALLOYS
Yang Leng and Richard P. Gangloff *In its* NASA-UVA Light Aerospace Alloy and Structures Technology Program Jun. 1990 34 p (For primary document see N90-22651 16-26)
Avail: NTIS HC A17/MF A03 CSCL 11F

Understanding the damage tolerance of aluminum alloys at elevated temperatures is essential for safe applications of advanced materials. The objective of this project is to investigate the time dependent subcritical cracking behavior of powder metallurgy FVS0812 and ingot metallurgy 2618 aluminum alloys at elevated temperatures. The fracture mechanics approach was applied. Sidegrooved compact tension specimens were tested at 175, 250, and 316 C under constant load. Subcritical crack growth occurred in each alloy at applied stress intensity levels (K) of between about 14 and 25 MPa/m, well below K (sub IC). Measured load, crack opening displacement and displacement rate, and crack length and growth rate (da/dt) were analyzed with several continuum fracture parameters including, the C-integral, C (sub t), and K. Elevated temperature growth rate data suggest that K is a controlling parameter during time dependent cracking. For FVS0812, da/dt is highest at 175 C when rates are expressed as a function of K. While crack growth rate is not controlled by C (sub t) at 175 C, da/dt appears to better correlate with C (sub t) at higher temperatures. Creep brittle cracking at intermediate temperatures, and perhaps related to strain aging, is augmented by time dependent transient creep plasticity at higher temperatures. The C (sub t) analysis is, however, complicated by the necessity to measure small differences in the elastic crack growth and creep contributions to the crack opening displacement rate. A microstructural study indicates that 2618 and FVS0812 are likely to be creep brittle materials, consistent with the results obtained from the fracture mechanics study. Time dependent crack growth of 2618 at 175 C is characterized by mixed transgranular and intergranular fracture. Delamination along the ribbon powder particle boundaries occurs in FVS0812 at all temperatures. The fracture mode of FVS0812 changes with temperature. At 175 C, it is characterized as dimpled rupture, and at 316 C as mixed matrix superplastic rupture and matrix-dipersoid debonding. Author

N90-22655*# Virginia Univ., Charlottesville.
DEFORMATION AND FRACTURE OF THIN SHEET ALUMINUM-LITHIUM ALLOYS: THE EFFECT OF CRYOGENIC TEMPERATURES
John A. Wagner and Richard P. Gangloff *In its* NASA-UVA Light Aerospace Alloy and Structures Technology Program Jun. 1990 28 p (For primary document see N90-22651 16-26)
Avail: NTIS HC A17/MF A03 CSCL 11F

The objective is to characterize the fracture behavior and to define the fracture mechanisms for new Al-Li-Cu alloys, with emphasis on the role of indium additions and cryogenic temperatures. Three alloys were investigated in rolled product form: 2090 baseline and 2090 + indium produced by Reynolds Metals, and commercial AA 2090-T81 produced by Alcoa. The experimental 2090 + In alloy exhibited increases in hardness and ultimate strength, but no change in tensile yield strength, compared to the baseline 2090 composition in the unstretched T6 condition. The reason for this behavior is not understood. Based on hardness and preliminary Kahn Tear fracture experiments, a nominally peak-aged condition was employed for detailed fracture studies. Crack initiation and growth fracture toughness were examined as a function of stress state and microstructure using J(delta a) methods applied to precracked compact tension specimens in the

LT orientation. To date, J(delta a) experiments have been limited to 23 C. Alcoa 2090-T81 exhibited the highest toughness regardless of stress state. Fracture was accompanied by extensive delamination associated with high angle grain boundaries normal to the fatigue precrack surface and progressed microscopically by a transgranular shear mechanism. In contrast the two peak-aged Reynolds alloys had lower toughness and fracture was intersubgranular without substantial delamination. The influences of cryogenic temperature, microstructure, boundary precipitate structure, and deformation mode in governing the competing fracture mechanisms will be determined in future experiments. Results contribute to the development of predictive micro-mechanical models for fracture modes in Al-Li alloys, and to fracture resistant materials. Author

N90-22656*# Virginia Univ., Charlottesville.
MEASUREMENTS AND MECHANISMS OF LOCALIZED AQUEOUS CORROSION IN ALUMINUM-LITHIUM ALLOYS
Rudolph G. Buchheit, Jr. and Glenn E. Stoner *In its* NASA-UVA Light Aerospace Alloy and Structures Technology Program Jun. 1990 28 p (For primary document see N90-22651 16-26)
Avail: NTIS HC A17/MF A03 CSCL 11F

Like most heat treatable aluminum alloys, localized corrosion and stress corrosion of Al-Li-Cu alloys is strongly dependent on the nature and distribution of second phase particles. To develop a mechanistic understanding of the role of localized corrosion in the stress corrosion process, bulk samples of T(sub 1) (Al2CuLi) and a range of Al-Cu-Fe impurity phases were prepared for electrochemical experiments. Potentiodynamic polarization and galvanic couple experiments were performed in standard 0.6 M NaCl and in simulated crevice solutions to assess corrosion behavior of these particles with respect to the alpha-Al matrix. A comparison of time to failure versus applied potential using a constant load, smooth bar SCC test technique in Cl(-), Cl(-)/CrO4(2-), and Cl(-)/CO3(2-) environments shows that rapid failures are to be expected when applied potentials are more positive than the breakaway potential (E sub br) of T(sub 1) (crack tip) but less than E(sub br) of alpha-Al (crack walls). It is shown that this criterion is not satisfied in aerated Cl(-) solutions. Accordingly, SCC resistance is good. This criterion is satisfied, however, in an alkaline isolated fissure exposed to a CO2 containing atmosphere. Rapid failure induced by these fissures was recently termed preexposure embrittlement. Anodic polarization shows that the corrosion behavior of T(sub 1) is relatively unaffected in alkaline CO3(2-) environments but the alpha-Al phase is rapidly passivated. X ray diffraction of crevice walls from artificial crevices suggests that passivation of alpha-Al occurs as hydrotalcite-type compound (LiAl2(OH)6)2(+) - CO3(2-) - nH2O. Author

N90-22657*# Virginia Univ., Charlottesville.
THE EFFECTS OF ZINC ADDITION ON THE ENVIRONMENTAL STABILITY OF Al-Li ALLOYS
Raymond J. Kilmer and Glenn E. Stoner *In its* NASA-UVA Light Aerospace Alloy and Structures Technology Program Jun. 1990 21 p (For primary document see N90-22651 16-26)
Avail: NTIS HC A17/MF A03 CSCL 11F

It was found that relatively small addition of Zn can improve the stress corrosion cracking (SCC) resistance of Al-Li alloys. However, the mechanism by which this is accomplished is unclear. The role that Zn plays in altering the behavior of Alloy 8090 is investigated. Early results suggest that Zn additions increase the volume fraction of delta(Al3Li) precipitation and differential scanning calorimetry (DSC) on these alloys confirms this. The four alloys studied each had initial compositions lying in the 8090 window and had varying amounts of Zn added to them. Alloy 8090, like other Al-Li alloys, displays a delta' precipitate free zone (PFZ) upon artificial aging along the grain and subgrain boundaries. However Zn additions greatly decreased or eliminated a delta' PFZ after 100 hours at 160 C. This implies that the subgrain boundary precipitation kinetics are being altered and suppressed. Furthermore, there appears to be a window of Zn concentration above which a delta ' PFZ can reappear with the nucleation and growth of a currently unidentified precipitate on the boundaries. Polarization experiments were performed and the results presented. The experiments were performed in deaerated 3.5 w/o NaCl in both as received (T3) condition and at peak aging of 100 hours at 160 C. The aging profile was determined via Vickers Hardness tests. Author

N90-22658*# Virginia Polytechnic Inst. and State Univ., Blacksburg.
DEFORMATION AND FRACTURE OF ALUMINUM-LITHIUM ALLOYS: THE EFFECT OF DISSOLVED HYDROGEN
F. C. Rivet and R. E. Swanson *In* Virginia Univ., NASA-UVA Light Aerospace Alloy and Structures Technology Program Jun. 1990 42 p (For primary document see N90-22651 16-26)
Avail: NTIS HC A17/MF A03 CSCL 11F

The effects of dissolved hydrogen on the mechanical properties of 2090 and 2219 alloys are studied. The work done during this semi-annual period consists of the hydrogen charging study and some preliminary mechanical tests. Prior to SIMS analysis, several potentiostatic and galvanostatic experiments were performed for various times (going from 10 minutes to several hours) in the cathodic zone, and for the two aqueous solutions: 0.04N of HCl and 0.1N NaOH both combined with a small amount of As2O3. A study of the surface damage was conducted in parallel with the charging experiments. Those tests were performed to choose the best charging conditions without surface damage. Disk rupture tests and tensile tests are part of the study designed to investigate the effect of temperature, surface roughness, strain rate, and environment on the fracture behavior. The importance of the roughness and environment were shown using the disk rupture test as well as the importance of the strain rate under hydrogen environment. The tensile tests, without hydrogen effects, have not shown significant differences between low and room temperature. Author

N90-22659*# Virginia Univ., Charlottesville.
INVESTIGATION OF THE REACTION KINETICS BETWEEN SiC FIBERS AND SELECTIVELY ALLOYED TITANIUM MATRIX COMPOSITES AND DETERMINATION OF THEIR MECHANICAL PROPERTIES
Douglas B. Gundel and Franklin E. Wawner, Jr. *In its* NASA-UVA Light Aerospace Alloy and Structures Technology Program Jun. 1990 26 p (For primary document see N90-22651 16-26)
Avail: NTIS HC A17/MF A03 CSCL 11F

During high temperature exposure, an interfacial reaction occurs between SiC fiber reinforcement and titanium matrices which can be detrimental to the mechanical properties of the composite. The reaction kinetics between SCS-6 fibers and Ti-1100 were determined at 800 to 1000 C and found to be slower than those of other currently used titanium alloys (Ti-15-3, Ti-6-4). The experimentally determined reaction kinetics for Ti-1100 were extrapolated to 700 C and found to accurately predict reaction zone size after 1000 hours of exposure. Predictions of the time to consume the surface layer on the SCS-6 and SCS-9 fibers were made in an effort to estimate the time that the fiber will retain its strength in Ti-1100 during isothermal exposure at high temperatures. Using this approach, the strength of an SCS-6 fiber in Ti-1100 should be retained for over 20,000 hours at isothermal exposures less than 800 C. Strength predictions using the rule of mixtures for a unidirectional Ti-1100/SCS-6 composite are presented for short term exposures up to 700 C. Room temperature tests of an as-fabricated 20 volume percent fiber/Ti-1100 composite yielded a UTS of 226 ksi (1490 MPa) which is close to that predicted by the ROM. Author

N90-22660*# Virginia Univ., Charlottesville.
QUANTITATIVE CHARACTERIZATION OF SPATIAL DISTRIBUTION OF PARTICLES IN MATERIALS: APPLICATION TO MATERIALS PROCESSING
J. B. Parse and John A. Wert *In its* NASA-UVA Light Aerospace Alloy and Structures Technology Program Jun. 1990 15 p (For primary document see N90-22651 16-26)
Avail: NTIS HC A17/MF A03 CSCL 11F

Most engineering materials contain second phase particles or

fibers which serve to reinforce the matrix phase. The effect of reinforcements on material properties is usually analyzed in terms of the average volume fraction and spacing of reinforcements, quantities which are global microstructural characteristics. However, material properties can also depend on local microstructural characteristics; for example, on how uniformly the reinforcing phase is distributed in the material. The analysis method will then be applied to a materials processing problem to discover how processing parameters can be selected to maximize redistribution of the reinforcing phase during processing. Several mathematical analysis methods could be adapted to the problem of characterizing the distribution of particles in materials. A tessellation-based method was selected. In the first phase of the investigation, a software package was written to automate the analysis. Typical results are shown. The analysis technique allows the degree to which particles are clustered together, the size and spacing of particle clusters, and the particle density in clusters to be found. The analysis methods were applied to computer-generated distributions and to a few real particle-containing materials. Methods for analyzing a nonuniform particle distribution in a material can be applied to two broad classes of materials science problems: understanding how the resulting particle distribution affects properties. The analysis method described is applied to a materials processing problem: how to select extrusion conditions to maximize the redistribution of reinforcing particles that are initially nonuniformly distributed. In addition, the tessellation-based method to analyze star distributions in spiral galaxies was adapted, illustrating the diverse types of problems to which the analysis method can be applied. Author

N90-22661*# Virginia Univ., Charlottesville.
INELASTIC RESPONSE OF METAL MATRIX COMPOSITES UNDER BIAXIAL LOADING
F. Mirzadeh, Marek-Jerzy Pindera, and Carl T. Herakovich *In its* NASA-UVA Light Aerospace Alloy and Structures Technology Program Jun. 1990 31 p (For primary document see N90-22651 16-26)
Avail: NTIS HC A17/MF A03 CSCL 11F

Elements of the analytical/experimental program to characterize the response of silicon carbide titanium (SCS-6/Ti-15-3) composite tubes under biaxial loading are outlined. The analytical program comprises prediction of initial yielding and subsequent inelastic response of unidirectional and angle-ply silicon carbide titanium tubes using a combined micromechanics approach and laminate analysis. The micromechanics approach is based on the method of cells model and has the capability of generating the effective thermomechanical response of metal matrix composites in the linear and inelastic region in the presence of temperature and time-dependent properties of the individual constituents and imperfect bonding on the initial yield surfaces and inelastic response of (0) and (+ or - 45)sub s SCS-6/Ti-15-3 laminates loaded by different combinations of stresses. The generated analytical predictions will be compared with the experimental results. The experimental program comprises generation of initial yield surfaces, subsequent stress-strain curves and determination of failure loads of the SCS-6/Ti-15-3 tubes under selected loading conditions. The results of the analytical investigation are employed to define the actual loading paths for the experimental program. A brief overview of the experimental methodology is given. This includes the test capabilities of the Composite Mechanics Laboratory at the University of Virginia, the SCS-6/Ti-15-3 composite tubes secured from McDonnell Douglas Corporation, a text fixture specifically developed for combined axial-torsional loading, and the MTS combined axial-torsion loader that will be employed in the actual testing. Author

N90-22662*# Virginia Univ., Charlottesville.
DESIGN OF CRYOGENIC TANKS FOR LAUNCH VEHICLES **c37**
Charles Copper, Walter D. Pilkey, and John K. Haviland *In its* NASA-UVA Light Aerospace Alloy and Structures Technology Program Jun. 1990 20 p (For primary document see N90-22651 16-26)
Avail: NTIS HC A17/MF A03 CSCL 13I

During the period since January 1990, work was concentrated on the problem of the buckling of the structure of an ALS (advanced launch systems) tank during the boost phase. The primary problem was to analyze a proposed hat stringer made by superplastic forming, and to compare it with an integrally stiffened stringer design. A secondary objective was to determine whether structural rings having the identical section to the stringers will provide adequate support against overall buckling. All of the analytical work was carried out with the TESTBED program on the CONVEX computer, using PATRAN programs to create models. Analyses of skin/stringer combinations have shown that the proposed stringer design is an adequate substitute for the integrally stiffened stringer. Using a highly refined mesh to represent the corrugations in the vertical webs of the hat stringers, effective values were obtained for cross-sectional area, moment of inertia, centroid height, and torsional constant. Not only can these values be used for comparison with experimental values, but they can also be used for beams to replace the stringers and frames in analytical models of complete sections of tank. The same highly refined model was used to represent a section of skin reinforced by a stringer and a ring segment in the configuration of a cross. It was intended that this would provide a baseline buckling analysis representing a basic mode, however, the analysis proved to be beyond the scope of the CONVEX computer. One quarter of this model was analyzed, however, to provide information on buckling between the spot welds. Models of large sections of the tank structure were made, using beam elements to model the stringers and frames. In order to represent the stiffening effects of pressure, stresses and deflections under pressure should first be obtained, and then the buckling analysis should be made on the structure so deflected. So far, uncharacteristic deflections under pressure were obtained from the TESTBED program using two types of structural elements. Similar results were obtained using the ANSYS program on a mainframe computer, although two finite element programs on microcomputers have yielded realistic results. Author

N90-22663*# Virginia Univ., Charlottesville.
EXPERIMENTAL AND COMPUTATIONAL STUDY OF THE VISCOPLASTIC RESPONSE OF HIGH TEMPERATURE STRUCTURES **c39**
Earl A. Thornton, M. F. Coyle, and J. D. Kolenski *In its* NASA-UVA Light Aerospace Alloy and Structures Technology Program Jun. 1990 22 p (For primary document see N90-22651 16-26)
Avail: NTIS HC A17/MF A03 CSCL 20K

The first nine months of experimental and computational studies of the thermal-structural behavior of thin panels subjected to localized heating are described. Initial experimental studies have focused on developing an experimental set-up with well-defined thermal-structure boundary conditions. Preliminary tests with a Heldenfels panel have demonstrated out of plane bending (thermal buckling) due to panel initial imperfections. Initial computational studies have focused on: (1) validation of a thermoviscoplastic code to predict thermal stresses in the unbuckled panel, and (2) investigating in-plane stresses for test panels under transient thermal loading. Plans for future research are described. Author

N90-22664# Texas Univ., Austin.
MODEL CATALYTIC OXIDATION STUDIES USING SUPPORTED MONOMETALLIC AND HETEROBIMETALLIC OXIDES
John G. Ekerdt 20 Apr. 1990 6 p
(Contract DE-FG05-86ER-13604)
(DE90-009984; DOE/ER-13604/8) Avail: NTIS HC A02/MF A01

Current research is focused on molybdenum and tungsten oxide overlayers. The research involves characterization of the organometallic deposition process, characterization of the resulting oxides using spectroscopic and structure sensitive molecular probes, and use of these oxides in catalytic studies. Raman, UV-diffuse reflectance, and photoluminescence spectroscopies are

BEST COPY AVAILABLE
FOR REPRODUCTION

used to characterize the coordination and structure of the supported cations. Thermal oxidation/reduction, photochemical reduction in CO, and IR of adsorbed CO are used to study the adsorptive and reductive characteristics of the cations. simple reactions will be used to probe the catalytic properties. These reactions include methanol oxidation, oxidative dehydrogenation of alkanes, oxidation of olefins, and hydrogenolysis of cyclopropane. We will attempt to determine how cation ensemble size rather than crystallographic orientation influences the selectivity and activity of these oxide catalyzed reactions. DOE

N90-22665# Instituto de Pesquisas Espaciais, Sao Jose dos Campos (Brazil).

CHARACTERIZATION OF MONEL ALLOYS BY X RAY FLUORESCENCE TECHNIQUE

Marcos Antonio Scapin and Vera Lucia RibeiroSalvador Oct. 1989 25 p In PORTUGUESE; ENGLISH summary
(DE90-617175; IPEN-PUB-270) Avail: NTIS (US Sales Only) HC A03/MF A01

Method for the determination of Ni, Cu, Fe, Mn, Si, Al, Ti, Co, Cr and Mo in Monel alloys using thin film for sample preparation and x ray fluorescence techniques is described. Samples in filings form were completely dissolved with inorganic acids and they were made up to a known volume. Then, these samples were deposited in a filter paper, reducing in this form the effect of the matrix. For all elements the first order emission K(sub alpha) lines were selected for measurements and for excitation a rhodium x ray tub was utilized. For the heavier elements the LiF (200) analyzer crystal and scintillation detector were utilized and for lighter elements the PET (002) analyzer crystal and flow proportional counter were used. The calibration curves were adjusted by the least square method and observed deviations were smaller than 5 percent. DOE

N90-22666# Instituto Militar de Engenharia, Rio de Janeiro (Brazil).

HYDROGENATION OF STAINLESS STEELS IMPLANTED WITH NITROGEN M.S. Thesis

Luis Eduardo daSilvaRamos 1989 158 p In PORTUGUESE; ENGLISH summary
(DE90-617397; INIS-BR-1827) Avail: NTIS (US Sales Only) HC A08/MF A01

In the present work the effects of both ion implantation and hydrogenation on the fatigue behavior of an AISI-304 type unstable stainless steel was studied. The material was tested under the following microstructural conditions: annealed; annealed plus hydrogenated; annealed plus ion-implanted; annealed, ion-implanted and hydrogenated. The hydrogen induced phase transformations were also studied during the outgassing of the samples. The ion implanted was observed to retard the kinetics of the hydrogen induced phase transformations. It was also observed that the nitrogen ion implantation followed by both natural (for about 4 months) and artificial (100 C for 6 hours) aging treatments was beneficial to the fatigue life of both non hydrogenated and severely hydrogenated samples. DOE

N90-22667# Zentralinstitut fuer Kernforschung, Rossendorf bei Dresden (German D.R.).

AMORPHIZATION OF METALS BY ION IMPLANTATION AND ION BEAM MIXING

Bernd Rauschenbach and Viton Heera 1988 29 p
(DE90-620571; ZfK-630) Avail: NTIS (US Sales Only) HC A03/MF A01

Amorphous metallic systems can be formed either by high fluence ion implantation of glass forming species or by irradiation of layered metal systems with inert gas ions. Both techniques and experimental examples are presented. Empirical rules are discussed which predict whether a given system can be transformed into an amorphous phase. Influence of temperature, implantation dose and pre-existing crystalline metal composition on amorphization is considered. Examples are given of the implantation induced amorphous structure, recrystallization and formation of quasicrystalline structures. DOE

N90-22668# Naval Postgraduate School, Monterey, CA. Dept. of Mechanical Engineering.

THE LITHIUM CONCENTRATION DEPENDENCE OF CREEP IN BINARY ALUMINUM-LITHIUM ALLOYS M.S. Thesis

David Wayne Taylor Jun. 1989 56 p
(AD-A218706) Avail: NTIS HC A04/MF A01 CSCL 11/6

An investigation was conducted into the concentration dependence of creep of binary aluminum-lithium alloys. Constant true-stress creep and constant extension-rate stress-strain tests were conducted at temperatures ranging from 250 to 500 C. Optical microscopy demonstrated that subgrains formed during deformation and that the predominant physical processes in the creep of aluminum-lithium alloys appears to be dislocation climb, with lithium providing strengthening by its effect on the modulus or the stacking fault energy. GRA

N90-22669# Army Armament Research and Development Command, Watervliet, NY.

FRACTURE TOUGHNESS AND FATIGUE CRACK INITIATION TESTS OF WELDED PRECIPITATION-HARDENING STAINLESS STEEL Final Report

J. H. Underwood, R. A. Farrara, G. P. OHara, J. J. Zalinka, and J. R. Senick Jan. 1990 36 p
(AD-A218745; ARCCB-TR-90004) Avail: NTIS HC A03/MF A01 CSCL 11/6

An analysis of a welded stainless steel box beam that experienced a structural failure during fatigue testing is described. Cracks initiated at notches caused by partial penetration welds and grew to a length of several centimeters in about 100 load cycles. The characterization of fracture toughness and fatigue crack initiation for the precipitation-hardening stainless steels used for the welds and parent plate of the beam is described. Three-point bend specimens were used to measure both fatigue crack initiation life and the J-integral fracture toughness of the parent plate and weld-metal in various conditions. The notch fatigue analysis method of Barsom and Rolfe was used to analyze the crack initiation test results. The crack was lengthened, side notches were added, and Jlc tests were performed using ASTM Method E-813 with a modified load-line displacement unloading-compliance procedure to measure crack growth. GRA

N90-22670# Ballistic Research Labs., Aberdeen Proving Ground, MD.

APPROXIMATE ANALYSIS FOR THE FORMATION OF ADIABATIC SHEAR BANDS

Thomas W. Wright Jan. 1990 38 p
(AD-A218751; BRL-MR-3807) Avail: NTIS HC A03/MF A01 CSCL 11/9

Parametric solutions are given for the formation of adiabatic shear bands in the context of the one-dimensional, nonlinear theory where inertia and elasticity are ignored. When heat condition is also ignored, the exact solution reduces completely to a sequence of quadratures. For a perfectly plastic material with heat conduction, an implicit parametic solution is also constructed. This is similar to the previous one in many ways, but now it involves two quadratures; a single nonautonomous, first-order ODE; and two functions that obey heat equations. This solution appears to be very accurate (compared to the full-finite element solution) until the time of stress collapse. Results indicate that for weak rate hardening of the power-law type, intense localization depends strongly on the initial characteristics. Within the context of rigid/perfect plasticity, a scaling law for the critical strain is given, and a figure of merit is defined that ranks materials according to their tendency to form adiabatic shear bands. GRA

N90-22671# Naval Postgraduate School, Monterey, CA.

A COMPARISON OF CuAlNi AND OTHER HIGH DAMPING ALLOYS FOR THE PURPOSE OF NAVAL SHIP SILENCING APPLICATIONS M.S. Thesis

Kenneth P. Roey Sep. 1989 81 p
(AD-A218801) Avail: NTIS HC A05/MF A01 CSCL 11/6

Five high damping alloys, including titanium nickel, copper aluminum nickel, copper zinc aluminum, copper manganese and

fibers which serve to reinforce the matrix phase. The effect of reinforcements on material properties is usually analyzed in terms of the average volume fraction and spacing of reinforcements, quantities which are global microstructural characteristics. However, material properties can also depend on local microstructural characteristics; for example, on how uniformly the reinforcing phase is distributed in the material. The analysis method will then be applied to a materials processing problem to discover how processing parameters can be selected to maximize redistribution of the reinforcing phase during processing. Several mathematical analysis methods could be adapted to the problem of characterizing the distribution of particles in materials. A tessellation-based method was selected. In the first phase of the investigation, a software package was written to automate the analysis. Typical results are shown. The analysis technique allows the degree to which particles are clustered together, the size and spacing of particle clusters, and the particle density in clusters to be found. The analysis methods were applied to computer-generated distributions and to a few real particle-containing materials. Methods for analyzing a nonuniform particle distribution in a material can be applied to two broad classes of materials science problems: understanding how the resulting particle distribution affects properties. The analysis method described is applied to a materials processing problem: how to select extrusion conditions to maximize the redistribution of reinforcing particles that are initially nonuniformly distributed. In addition, the tessellation-based method to analyze star distributions in spiral galaxies was adapted, illustrating the diverse types of problems to which the analysis method can be applied. Author

N90-22661*# Virginia Univ., Charlottesville.
INELASTIC RESPONSE OF METAL MATRIX COMPOSITES UNDER BIAXIAL LOADING
F. Mirzadeh, Marek-Jerzy Pindera, and Carl T. Herakovich *In its* NASA-UVA Light Aerospace Alloy and Structures Technology Program Jun. 1990 31 p (For primary document see N90-22651 16-26)
Avail: NTIS HC A17/MF A03 CSCL 11F

Elements of the analytical/experimental program to characterize the response of silicon carbide titanium (SCS-6/Ti-15-3) composite tubes under biaxial loading are outlined. The analytical program comprises prediction of initial yielding and subsequent inelastic response of unidirectional and angle-ply silicon carbide titanium tubes using a combined micromechanics approach and laminate analysis. The micromechanics approach is based on the method of cells model and has the capability of generating the effective thermomechanical response of metal matrix composites in the linear and inelastic region in the presence of temperature and time-dependent properties of the individual constituents and imperfect bonding on the initial yield surfaces and inelastic response of (0) and (+ or - 45)sub s SCS-6/Ti-15-3 laminates loaded by different combinations of stresses. The generated analytical predictions will be compared with the experimental results. The experimental program comprises generation of initial yield surfaces, subsequent stress-strain curves and determination of failure loads of the SCS-6/Ti-15-3 tubes under selected loading conditions. The results of the analytical investigation are employed to define the actual loading paths for the experimental program. A brief overview of the experimental methodology is given. This includes the test capabilities of the Composite Mechanics Laboratory at the University of Virginia, the SCS-6/Ti-15-3 composite tubes secured from McDonnell Douglas Corporation, a text fixture specifically developed for combined axial-torsional loading, and the MTS combined axial-torsion loader that will be employed in the actual testing. Author

N90-22662*# Virginia Univ., Charlottesville.
DESIGN OF CRYOGENIC TANKS FOR LAUNCH VEHICLES c37
Charles Copper, Walter D. Pilkey, and John K. Haviland *In its* NASA-UVA Light Aerospace Alloy and Structures Technology Program Jun. 1990 20 p (For primary document see N90-22651 16-26)
Avail: NTIS HC A17/MF A03 CSCL 13I

During the period since January 1990, work was concentrated on the problem of the buckling of the structure of an ALS (advanced launch systems) tank during the boost phase. The primary problem was to analyze a proposed hat stringer made by superplastic forming, and to compare it with an integrally stiffened stringer design. A secondary objective was to determine whether structural rings having the identical section to the stringers will provide adequate support against overall buckling. All of the analytical work was carried out with the TESTBED program on the CONVEX computer, using PATRAN programs to create models. Analyses of skin/stringer combinations have shown that the proposed stringer design is an adequate substitute for the integrally stiffened stringer. Using a highly refined mesh to represent the corrugations in the vertical webs of the hat stringers, effective values were obtained for cross-sectional area, moment of inertia, centroid height, and torsional constant. Not only can these values be used for comparison with experimental values, but they can also be used for beams to replace the stringers and frames in analytical models of complete sections of tank. The same highly refined model was used to represent a section of skin reinforced by a stringer and a ring segment in the configuration of a cross. It was intended that this would provide a baseline buckling analysis representing a basic mode, however, the analysis proved to be beyond the scope of the CONVEX computer. One quarter of this model was analyzed, however, to provide information on buckling between the spot welds. Models of large sections of the tank structure were made, using beam elements to model the stringers and frames. In order to represent the stiffening effects of pressure, stresses and deflections under pressure should first be obtained, and then the buckling analysis should be made on the structure so deflected. So far, uncharacteristic deflections under pressure were obtained from the TESTBED program using two types of structural elements. Similar results were obtained using the ANSYS program on a mainframe computer, although two finite element programs on microcomputers have yielded realistic results. Author

N90-22663*# Virginia Univ., Charlottesville.
EXPERIMENTAL AND COMPUTATIONAL STUDY OF THE VISCOPLASTIC RESPONSE OF HIGH TEMPERATURE STRUCTURES c39
Earl A. Thornton, M. F. Coyle, and J. D. Kolenski *In its* NASA-UVA Light Aerospace Alloy and Structures Technology Program Jun. 1990 22 p (For primary document see N90-22651 16-26)
Avail: NTIS HC A17/MF A03 CSCL 20K

The first nine months of experimental and computational studies of the thermal-structural behavior of thin panels subjected to localized heating are described. Initial experimental studies have focused on developing an experimental set-up with well-defined thermal-structure boundary conditions. Preliminary tests with a Heldenfels panel have demonstrated out of plane bending (thermal buckling) due to panel initial imperfections. Initial computational studies have focused on: (1) validation of a thermoviscoplastic code to predict thermal stresses in the unbuckled panel, and (2) investigating in-plane stresses for test panels under transient thermal loading. Plans for future research are described. Author

N90-22664# Texas Univ., Austin.
MODEL CATALYTIC OXIDATION STUDIES USING SUPPORTED MONOMETALLIC AND HETEROBIMETALLIC OXIDES
John G. Ekerdt 20 Apr. 1990 6 p
(Contract DE-FG05-86ER-13604)
(DE90-009984; DOE/ER-13604/8) Avail: NTIS HC A02/MF A01

Current research is focused on molybdenum and tungsten oxide overlayers. The research involves characterization of the organometallic deposition process, characterization of the resulting oxides using spectroscopic and structure sensitive molecular probes, and use of these oxides in catalytic studies. Raman, UV-diffuse reflectance, and photoluminescence spectroscopies are

BEST COPY AVAILABLE FOR REPRODUCTION

used to characterize the coordination and structure of the supported cations. Thermal oxidation/reduction, photochemical reduction in CO, and IR of adsorbed CO are used to study the adsorptive and reductive characteristics of the cations. simple reactions will be used to probe the catalytic properties. These reactions include methanol oxidation, oxidative dehydrogenation of alkanes, oxidation of olefins, and hydrogenolysis of cyclopropane. We will attempt to determine how cation ensemble size rather than crystallographic orientation influences the selectivity and activity of these oxide catalyzed reactions. DOE

N90-22665# Instituto de Pesquisas Espaciais, Sao Jose dos Campos (Brazil).

CHARACTERIZATION OF MONEL ALLOYS BY X RAY FLUORESCENCE TECHNIQUE

Marcos Antonio Scapin and Vera Lucia RibeiroSalvador Oct. 1989 25 p In PORTUGUESE; ENGLISH summary
(DE90-617175; IPEN-PUB-270) Avail: NTIS (US Sales Only) HC A03/MF A01

Method for the determination of Ni, Cu, Fe, Mn, Si, Al, Ti, Co, Cr and Mo in Monel alloys using thin film for sample preparation and x ray fluorescence techniques is described. Samples in filings form were completely dissolved with inorganic acids and they were made up to a known volume. Then, these samples were deposited in a filter paper, reducing in this form the effect of the matrix. For all elements the first order emission K(sub alpha) lines were selected for measurements and for excitation a rhodium x ray tub was utilized. For the heavier elements the LiF (200) analyzer crystal and scintillation detector were utilized and for lighter elements the PET (002) analyzer crystal and flow proportional counter were used. The calibration curves were adjusted by the least square method and observed deviations were smaller than 5 percent. DOE

N90-22666# Instituto Militar de Engenharia, Rio de Janeiro (Brazil).

HYDROGENATION OF STAINLESS STEELS IMPLANTED WITH NITROGEN M.S. Thesis

Luis Eduardo daSilvaRamos 1989 158 p In PORTUGUESE; ENGLISH summary
(DE90-617397; INIS-BR-1827) Avail: NTIS (US Sales Only) HC A08/MF A01

In the present work the effects of both ion implantation and hydrogenation on the fatigue behavior of an AISI-304 type unstable stainless steel was studied. The material was tested under the following microstructural conditions: annealed; annealed plus hydrogenated; annealed plus ion-implanted; annealed, ion-implanted and hydrogenated. The hydrogen induced phase transformations were also studied during the outgassing of the samples. The ion implanted was observed to retard the kinetics of the hydrogen induced phase transformations. It was also observed that the nitrogen ion implantation followed by both natural (for about 4 months) and artificial (100 C for 6 hours) aging treatments was beneficial to the fatigue life of both non hydrogenated and severely hydrogenated samples. DOE

N90-22667# Zentralinstitut fuer Kernforschung, Rossendorf bei Dresden (German D.R.).

AMORPHIZATION OF METALS BY ION IMPLANTATION AND ION BEAM MIXING

Bernd Rauschenbach and Viton Heera 1988 29 p
(DE90-620571; ZfK-630) Avail: NTIS (US Sales Only) HC A03/MF A01

Amorphous metallic systems can be formed either by high fluence ion implantation of glass forming species or by irradiation of layered metal systems with inert gas ions. Both techniques and experimental examples are presented. Empirical rules are discussed which predict whether a given system can be transformed into an amorphous phase. Influence of temperature, implantation dose and pre-existing crystalline metal composition on amorphization is considered. Examples are given of the implantation induced amorphous structure, recrystallization and formation of quasicrystalline structures. DOE

N90-22668# Naval Postgraduate School, Monterey, CA. Dept. of Mechanical Engineering.

THE LITHIUM CONCENTRATION DEPENDENCE OF CREEP IN BINARY ALUMINUM-LITHIUM ALLOYS M.S. Thesis

David Wayne Taylor Jun. 1989 56 p
(AD-A218706) Avail: NTIS HC A04/MF A01 CSCL 11/6

An investigation was conducted into the concentration dependence of creep of binary aluminum-lithium alloys. Constant true-stress creep and constant extension-rate stress-strain tests were conducted at temperatures ranging from 250 to 500 C. Optical microscopy demonstrated that subgrains formed during deformation and that the predominant physical processes in the creep of aluminum-lithium alloys appears to be dislocation climb, with lithium providing strengthening by its effect on the modulus or the stacking fault energy. GRA

N90-22669# Army Armament Research and Development Command, Watervliet, NY.

FRACTURE TOUGHNESS AND FATIGUE CRACK INITIATION TESTS OF WELDED PRECIPITATION-HARDENING STAINLESS STEEL Final Report

J. H. Underwood, R. A. Farrara, G. P. OHara, J. J. Zalinka, and J. R. Senick Jan. 1990 36 p
(AD-A218745; ARCCB-TR-90004) Avail: NTIS HC A03/MF A01 CSCL 11/6

An analysis of a welded stainless steel box beam that experienced a structural failure during fatigue testing is described. Cracks initiated at notches caused by partial penetration welds and grew to a length of several centimeters in about 100 load cycles. The characterization of fracture toughness and fatigue crack initiation for the precipitation-hardening stainless steels used for the welds and parent plate of the beam is described. Three-point bend specimens were used to measure both fatigue crack initiation life and the J-integral fracture toughness of the parent plate and weld-metal in various conditions. The notch fatigue analysis method of Barsom and Rolfe was used to analyze the crack initiation test results. The crack was lengthened, side notches were added, and Jlc tests were performed using ASTM Method E-813 with a modified load-line displacement unloading-compliance procedure to measure crack growth. GRA

N90-22670# Ballistic Research Labs., Aberdeen Proving Ground, MD.

APPROXIMATE ANALYSIS FOR THE FORMATION OF ADIABATIC SHEAR BANDS

Thomas W. Wright Jan. 1990 38 p
(AD-A218751; BRL-MR-3807) Avail: NTIS HC A03/MF A01 CSCL 11/9

Parametric solutions are given for the formation of adiabatic shear bands in the context of the one-dimensional, nonlinear theory where inertia and elasticity are ignored. When heat condition is also ignored, the exact solution reduces completely to a sequence of quadratures. For a perfectly plastic material with heat conduction, an implicit parametic solution is also constructed. This is similar to the previous one in many ways, but now it involves two quadratures; a single nonautonomous, first-order ODE; and two functions that obey heat equations. This solution appears to be very accurate (compared to the full-finite element solution) until the time of stress collapse. Results indicate that for weak rate hardening of the power-law type, intense localization depends strongly on the initial characteristics. Within the context of rigid/perfect plasticity, a scaling law for the critical strain is given, and a figure of merit is defined that ranks materials according to their tendency to form adiabatic shear bands. GRA

N90-22671# Naval Postgraduate School, Monterey, CA.

A COMPARISON OF CuAlNi AND OTHER HIGH DAMPING ALLOYS FOR THE PURPOSE OF NAVAL SHIP SILENCING APPLICATIONS M.S. Thesis

Kenneth P. Roey Sep. 1989 81 p
(AD-A218801) Avail: NTIS HC A05/MF A01 CSCL 11/6

Five high damping alloys, including titanium nickel, copper aluminum nickel, copper zinc aluminum, copper manganese and

iron chromium molybdenum, were heat treated to produce optimum damping conditions. The strain dependence of specific damping capacity was established using the resonant dwell technique. The results were compared with those of past investigations. For the CuAlNi alloy, six different heat treatment conditions were considered. The CuAlNi specimens were cold worked to determine the effect on damping. An industrial survey was conducted to determine the practicality of shipboard application of these alloys. A comparison of the advantages/disadvantages of each alloy was accomplished and recommendations were made for further study. GRA

N90-22672# Oxford Univ. (England). Dept. of Metallurgy and Science of Materials.
STRUCTURE-PROPERTY RELATIONS IN ALUMINUM-LITHIUM ALLOYS Ph.D. Thesis
David John Nicholls 1989 163 p Sponsored by AFIT, Wright-Patterson AFB, OH
(AD-A219183) Avail: NTIS HC A08/MF A01 CSCL 11/6

The effect is described of microstructure on the behavior of small fatigue cracks in the two Aluminum-Lithium-Copper-Magnesium-Zirconium alloys 8090 and 8091. The slip distribution in these alloys was varied through thermo-mechanical processing. Although slip distribution affected tensile, cyclic and long fatigue crack behavior, it did not affect small fatigue crack behavior due to low levels of closure and reduced slip reversibility near to a free surface. Similarly, underaging and coveraging had no effect on small fatigue crack behavior. Therefore, small fatigue crack growth is concluded to be insensitive to precipitate size and distribution. Due to differences in grain size, small fatigue cracks in 8091 were observed to propagate twice as slowly as in 8090. Small fatigue cracks grew more rapidly than long fatigue cracks under the same nominal Delta(k) and displayed no threshold behavior. This was shown to be due to the combined effects of the low closure levels, high applied stresses and proximity to the surface. Low cycle fatigue behavior was shown to be related to small fatigue crack behavior and similar microstructural effects were observed. Total rather than plastic strain was identified as the critical parameter when comparing small fatigue crack and LCF behavior. GRA

27 NONMETALLIC MATERIALS

Includes physical, chemical, and mechanical properties of plastics, elastomers, lubricants, polymers, textiles, adhesives, and ceramic materials.

For composite materials see *24 Composite Materials.*

N90-22673# Lawrence Livermore National Lab., CA.
MECHANICAL TESTING OF SELECTED ENGINEERING PLASTICS
John J. Scott and Robert L. Brady 22 Jan. 1990 20 p
(Contract W-7405-eng-48)
(DE90-008186; UCID-21761) Avail: NTIS HC A03/MF A01

Tensile stress-strain curves and tensile creep curves were generated for a number of candidate engineering plastics. Creep testing was performed with a sustained stress of 5000 psi. Both unfilled and filled (fiber reinforced) plastics were investigated. Nominal fill levels were 30 and 60 percent of either chopped carbon or glass fibers. DOE

N90-22674# Mound Lab., Miamisburg, OH.
AN ALTERNATE INTERCONNECT METHOD FOR JOINING FLEXIBLE CIRCUITS USING CONDUCTIVE ADHESIVES
Walter R. Schurman 17 Apr. 1990 21 p
(Contract DE-AC04-88DP-43495)
(DE90-008194; MLM-3631) Avail: NTIS HC A03/MF A01

Conductive adhesives were evaluated as a labor saving alternate method for interconnecting flexible circuit layers in slapper detonators. Short term aging, high temperature and high humidity storage, thermal cycle, and thermal shock studies were done. The adhesive interconnections were also studied under the high voltage and high current operating conditions of a slapper detonator. In all tests, interconnections made with conductive adhesive compared favorably with standard diffusion bonded joints, demonstrating the feasibility of joining flexible circuit components without metallic solders, brazes, thermo-compression bonds, diffusion bonds, or welds. DOE

N90-22675 National Physical Lab., Teddington (England). Div. of Materials Applications.
RHEOLOGY OF INJECTION MOULD FILLING WITH DMCS
M. Rides and K. Thomas Oct. 1989 10 p
(NPL-DMA(A)-196; ISSN-0143-7313; ETN-90-96438) Copyright Avail: National Physical Laboratory, Teddington, Middlesex TW11 OLW, England

The rheology of a glass-fiber reinforced unsaturated polyester Dough Molding Compound (DMC) was investigated using capillary and slit-die rheometer geometries, and also on-line on an injection-molding machine. Shear viscosity results obtained using the capillary and slit-die techniques are in very good agreement. On-line viscosity results are in good agreement with capillary die results. The use of the viscosity data in modeling the injection-molding process showed reasonable agreement with measured fill pressures. ESA

N90-22676# Institut National des Sciences Appliquees de Lyon, Villeurbanne (France).
CHARACTERIZATION AND ROLE OF AN ELASTOMERIC INTERPHASE WITHIN POLYEPOXY REINFORCED GLASS, BOTH PARTICULATE AND FIBROUS Ph.D. Thesis [CARACTERISATION ET ROLE D'UNE INTERPHASE ELASTOMERE AU SEIN DE MATERIAUX COMPOSITES POLYEPOXY/RENFORT DE VERRE (PARTICULAIRE OU FIBREUX)]
Nouredine Amdouni 1989 338 p In FRENCH
(ISAL-89-0064; ETN-90-96605) Avail: NTIS HC A15/MF A02

Modification of the interphase as a means of improving the characteristics of composite materials with organic matrices is studied. The need for optimization of the vitreous transition temperature, material thickness and other aspects of the interphase is stressed. A silane treatment provides the best shock resistance to the material. The elasticity of the final product is not affected by the thickness of the interphase. Making use of alterations during the interphase period to provide specific rigidity, fatigue and impact resistance characteristics to composite materials is described. ESA

N90-22677# Aerospatiale, Paris (France).
NONDESTRUCTIVE TESTING (NDT); CERAMIC MATRIX COMPOSITE MATERIALS (CMCM) [CND ET CMC A L'AEROSPATIALE]
F. Albugues Feb. 1989 4 p In FRENCH
(Rept-892-430-123; ETN-90-96654) Avail: NTIS HC A02/MF A01

The difficulties involved in producing high quality ceramic matrix composite materials are described. The use of nondestructive testing techniques to help in the optimization of ceramic matrix composite materials is described. A better understanding of behavior under stress and residual performance possibilities after use are two of the features investigated using nondestructive testing. The use of ultrasonic, radiographic and holographic techniques in nondestructive testing is described. The role of aerospatiale in furthering the evolution of nondestructive testing techniques is discussed. ESA

N90-22678# Northwestern Univ., Evanston, IL. Dept. of Materials Science and Engineering.
CENTER FOR SURFACE RADIATION DAMAGE STUDIES Final Report, 1 Oct. 1986 - 30 Sep. 1989
Laurence D. Marks Oct. 1989 9 p
(Grant AF-AFOSR-0344-86; AF Proj. 3484)
(AD-A218452; AFOSR-90-0221TR) Avail: NTIS HC A02/MF A01 CSCL 06/7

Identifying the surface damage process, two systems were

studied in some depth, TiO2 and NiO. In TiO2 there is a phase transition to TiO which spreads from the surface and is driven by oxygen desorption. The first indications is provided that diffusion was the rate limiting step. In NiO there is no DIET, but knockon damage at higher voltages and two electron beam stimulated reaction, one of which abstracts nickel, and another reduction by carbon contaminants. GRA

N90-22679# Cornell Univ., Ithaca, NY. School of Chemical Engineering.

MODIFIED MALEIC ANHYDRIDE COPOLYMERS AS e-BEAM RESISTS

Sandeep Malhotra, Bernard C. Dems, Yarrow M. N. Namaste, Ferdinand Rodriguez, and S. Kay Obendorf 15 Feb. 1990 15 p Presented at the SPIE Symposium on Microlithography, San Jose, CA, 7-8 Mar. 1990 Sponsored in part by NSF

(Contract N00014-85-K-0474)

(AD-A218470; TR-16) Avail: NTIS HC A03/MF A01 CSCL 07/6

Copolymers of maleic anhydride with styrene, ethylene, and methyl vinyl ether were modified and evaluated for use as negative working resist materials in electron beam lithography. The copolymers used were modified by reaction with an organometallic compound, which resulted in incorporation of tin in the pendant chains of the copolymers. The polymers were blended with a reactive plasticizer, dipentaerythritol pentaacrylate (DPEPA), to enhance sensitivity and to improve resolution. Incorporation of tin into the copolymer resulted in increased sensitivity to the electron beam, improved dimensional stability, and increased oxygen reactive ion resistance. Tin modified polymers blended with DPEPA yielded sensitivities in the range of 0.2 to 1.5 micro(C)/sq cm. GRA

N90-22680# City Coll. of the City Univ. of New York, NY. Dept. of Mechanical Engineering.

MICROCRACKING AND TOUGHNESS OF CERAMIC-FIBER/CERAMIC-MATRIX COMPOSITES UNDER HIGH TEMPERATURE Final Report, 1 Aug. 1987 - 30 Sep. 1989

Feridun Delale and Been Ming Liaw 1 Dec. 1989 90 p

(Grant AF-AFOSR-0288-87; AF Proj. 2302)

(AD-A218516; CUNY-RF-447239; AFOSR-90-0203TR) Avail: NTIS HC A05/MF A01 CSCL 11/2

Microcracking mechanisms and toughness of Nicalon (Silicon carbide)/Silicon carbide composite at elevated temperature are studied analytically and experimentally. First the fiber distribution patterns in the ceramic composite are determined by observing the specimens under optical and scanning electron microscopes. Thus the effect of fibers and fiber interactions on the microcrack propagation are investigated analytically through the single-fiber, the two-fiber, and the ring models. Monolithic SiC specimens are tested under varying temperature to determine the effect of temperature on the toughness of the matrix material. The Nicalon/SiC composite specimens are then tested at various temperatures. The combined effect of temperature and fibers on the toughness of the matrix is expressed by introducing the concept of apparent fracture toughness. The experimental results indicate that for the Nicalon/SiC composite the apparent fracture toughness decreases with local volume fraction of fibers Volume fraction and temperature. GRA

N90-22681# California Univ., San Diego, La Jolla. Dept. of Chemistry.

DEHYDROGENATIVE POLYMERIZATION OF SILANES TO POLYSILANES: A MONOMERIC COPPER(2) SILOXIDE

Hee-Gweon Woo, T. D. Tilley, A. K. McMullen, A. L. Rheingold, and S. J. Geib 1989 3 p Repr., J. Am. Chem. Soc. 1989; 8043; Inorg. Chem. 1989, 28, 3772

(Grant AF-AFOSR-0273-88; AF Proj. 2303)

(AD-A218550; AFOSR-90-0218TR) Avail: NTIS HC A01/MF A01 CSCL 07/3

A possible mechanism was identified for the dehydrogenative polymerization of silanes to polysilanes by zirconium and hafnium catalysts. This mechanism is based on sigma-bond metathesis processes. A new copper siloxide, the first for copper(2), is reported. This compound was designed as a molecular precursor to a copper silicate. GRA

N90-22682# Connecticut Univ., Storrs. Liquid Crystalline Polymer Research Center.

SYNTHESIS AND PROPERTIES OF A THERMOTROPIC COPOLYESTER BASED ON 4,4 PRIME-DIHYDROXY-A,A PRIME-DIMETHYLBENZALAZINE Interim Technical Report

A. Levent Cimecioglu, Hitesh Fruitwala, and R. A. Weiss 26 Feb. 1990 28 p Submitted for publication

(Contract N00014-86-K-0772)

(AD-A218803; TR-38) Avail: NTIS HC A03/MF A01 CSCL 07/3

Thermotropic mesomorphism exhibited by organic compounds has been known and studied extensively for over a century. However, it was not until the mid-1970's that the thermotropic behavior of polymeric liquid crystals (PLCs) was demonstrated. Since then, there has been an ever increasing interest in this field, reflected by an explosion in publications and patents issued, as well as the commercialization of several PLCs. Research on thermotropic PLCs can be divided into two broad categories: main chain PLCs and side chain PLCs. The former field has also branched into several different areas largely as a result of the efforts to reduce the usually very high transition temperatures. One of these involves the incorporation of flexible spacers in the main chain, a subject that was recently reviewed by Ober et al. Roviello and Sirigu, first demonstrated thermotropic behavior in polymers with semi-flexible polyester PLCs based on the mesogen 4,4'-dihydroxy alpha,alpha' dimethylbenzalazine. These nematic polyesters had relatively low transition temperatures and were soluble. Among other things, the authors also established that by using two different aliphatic spacers, the melting transition could be lowered significantly while the clearing temperatures remained more or less unchanged. The biggest effect occurred for a 50/50 mole ratio of the spacers. GRA

N90-22683# Connecticut Univ., Storrs. Liquid Crystalline Polymer Research Center.

PROCESSING OF THERMOTROPIC LIQUID CRYSTALLINE POLYMERS AND THEIR BLENDS Interim Technical Report

Wan-Chung Lee, Anthony T. Dibenedetto, and Jack M. Gromek 23 Feb. 1990 49 p

(Contract N00014-86-K-0772)

(AD-A218804; TR-37) Avail: NTIS HC A03/MF A01 CSCL 07/6

Preliminary studies were conducted on the hot-drawing of aromatic copolyester LCP fibers (KU-9211 and KU-9221 from Bayer A. G.) and blends of one of these with an aliphatic containing LCP (PET/PHB60 from Tennessee Eastman). The properties of the hot drawn fibers were characterized by measuring storage moduli, E, and molecular orientation parameters, (S), as a function of draw ration. A model was developed to correlate both (s) and E with draw ratio by taking account of thermal relaxation during the drawing process. Agreement between experimental data and the model was obtained by use of a single dimensionless parameter, alpha, which depends on the processing conditions. An in-situ LCP composite of KU-9211 and PET/PHB60 was generated by a combination of blending and hot-drawing and then characterized using SEM, TEM and single-fiber mechanical tests. The dispersed phase consists primarily of highly oriented, 0.5 to 2.0 micrometer diameter rigid-rods of aromatic fibers imbedded in a matrix of predominantly aliphatic LCP fibrils with diameters in the range of 20 to 50 nm. Morphological evidence suggests a strong interfacial adhesion between the dispersed and the matrix phases in this specific system. GRA

N90-22684# Army Lab. Command, Watertown, MA. Material Technology Lab.

LOW TEMPERATURE DEGRADATION OF Y-TZP MATERIALS Final Report

Jeffrey J. Swab Jan. 1990 27 p Presented at the 89th

American Ceramic Society Convention, Apr. 1987
(Contract DE-AI05-84OR-21411; DA Proj. 1L1-62105-AH-84)
(AD-A218841; MTL-TR-90-4) Avail: NTIS HC A03/MF A01 CSCL 11/2

Seven yttria-tetragonal zirconia polycrystal materials were examined to determine if they were susceptible to low temperature degradation. Flexure specimens were exposed to approx. 800 Pa of water vapor pressure for 50 hours between 200 C and 400 C. Only one of the tetragonal zirconia polycrystal was unaffected by these low temperature treatments; three underwent catastrophic degradation after all the low temperature treatments, while the final three has property losses to various degrees depending on the treatment temperature. GRA

N90-22685# Virginia Polytechnic Inst. and State Univ., Blacksburg. Dept. of Chemistry.
SYNTHESIS AND CHARACTERIZATION OF AROMATIC POLYESTER AND POLYSILOXANE CONTAINING BLOCK COPOLYMERS: MULTIPHASE TRANSPARENT ATOMIC OXYGEN RESISTANT DAMPING MATERIALS, LIQUID CRYSTAL FILMS, AND TOUGHENING COMPONENTS OF SOL/GEL GLASSES Final Report, 1 May 1986 - 30 Apr. 1989
James E. McGrath 22 Jan. 1990 40 p
(Grant AF-AFOSR-0133-86; AF Proj. 2303)
(AD-A218871; AFOSR-90-0285TR) Avail: NTIS HC A03/MF A01 CSCL 07/6

AFOSR sponsored research on multifunctional polymers which has been conducted in our laboratories over the past three years covers three main areas. Each of the three areas is summarized and described. The synthesis of siloxane modified silicate ceramics produced by sol-gel chemistry followed by ultrastructure processing is examined. Using techniques such as acid free hydrolysis condensation reaction systems, it was possible to incorporate at least 30 percent of siloxane oligomers via cohydrolysis of suitably terminated materials in the presence of TMOS. In different but somewhat related work based upon polyimides, extensive studies were conducted with linear thermoplastic polyimide siloxane copolymers. The polyimide siloxane copolymers prepared to date are based largely upon aliphatic terminated polydimethyl siloxanes which have adequate thermal stability for most purposes. The third area of investigation on multifunctional polymers was the synthesis and characterization of isotropic polyarylene sulfone, anisotropic aromatic polyester liquid crystal copolymers. It was demonstrated that with as little as 10 or 15 weight percent of the liquid crystal segment, organic solvents which would easily dissolve or stress crack the amorphous engineering homopolymers like polysulfones, are no longer able to do so. GRA

N90-22686# Massachusetts Inst. of Tech., Cambridge. Dept. of Mechanical Engineering.
SIMULATION OF INELASTIC DEFORMATION IN GLASSY POLYPROPYLENE AND POLYCARBONATE Interim Technical Report No. 21, 1988-1989
Ali S. Argon, Michelle Hutnik, Peter H. Mott, and Ueli W. Suter (Eidgenoessische Technische Hochschule, Zurich, Switzerland) 1 Dec. 1989 3 p Presented at the ACS Symposium on Computer Simulation, Boston, MA, 23-27 Apr. 1990
(Contract N00014-86-K-0768)
(AD-A218891) Avail: NTIS HC A01/MF A01 CSCL 20/5

A brief summary of research on the simulation of plastic deformation in computer generated glassy polypropylene, and polycarbonate. Determination of the stress-strain response, and elucidation of the molecular segment motions associated with such deformations. Determination of the kinematics and energetics of phenylene ring rotations and carbonate group motions in polycarbonate. GRA

N90-22687# Massachusetts Inst. of Tech., Cambridge.
INVESTIGATION OF ATOMISTIC SIMULATION OF STRUCTURAL AND DYNAMIC DIFFERENCES IN GLASSY AND LIQUID STATES OF ATACTIC POLY(PROPYLENE) Interim Technical Report No. 22, 1988 - 1989
Mark F. Sylvester, Sidney Yip, and Ali S. Argon 1 Dec. 1989 36 p Submitted for publication
(Contract N00014-86-K-0768)
(AD-A218896) Avail: NTIS HC A03/MF A01 CSCL 20/5

Atomistic simulation techniques, in conjunction with experimental and theoretical approaches, have proven themselves to be useful tools for the study of materials. The glass transition is still poorly characterized except in a phenomenological manner. For instance, comprehension of how the structure of a polymer glass differs from that of the liquid is limited to the somewhat vaguely defined concept of free volume. It is not known how the volume associated with atoms might be distributed within the polymer or how changes in the distribution are related to the property changes seen at the glass transition. In addition, what other structural changes occur on passing between the liquid and glass states are not known. These questions involve the local atomic level structure and motion of individual or small groups of atoms. Available experimental and theoretical methods are not well suited to investigate these details. Therefore, simulation is the only way to obtain physical insight into these problems at the present time. Reported here are initial results obtained from a series of such computer simulations carried out on a simple vinyl polymer, atactic poly(propylene). GRA

N90-22688# State Univ. of New York, Brooklyn.
LOW COST PROCESSING ROUTES LEADING TO HIGH-PERFORMANCE CERAMIC TILES Final Report, 15 Sep. 1988 - 14 Dec. 1989
Vladimir Hlavacek, S. Majorowski, and J. A. Puszynski Feb. 1990 28 p
(Contract DAAL03-88-K-0202)
(AD-A219034; ARO-26172.1-MS-A) Avail: NTIS HC A03/MF A01 CSCL 11/2

Production of cheap high-performance ceramic tiles for structural application is an important problem. The search for superior tile exhibits many different facts ranging from establishing routes for manufacturing cheap precursors, through densification to ballistic testing of the material. The main goals of this research were: (1) Synthesis of ultrafine sinterable titanium diboride and titanium boride based composites in a combustion regime; (2) Purification of titanium diboride synthesized by magnesithermal reduction of boric ant titanium oxides; (3) Densification and fabrication of TiB2 based composites by pressureless sintering and hot pressing; and (4) Ballistic testing of fabricated tiles. GRA

N90-22689# Ceramic Process Systems Corp., Milford, MA.
COMPOSITE CERAMIC SUPERCONDUCTING WIRES FOR ELECTRIC MOTOR APPLICATIONS Quarterly Technical Report No. 6, 1 Oct. - 31 Dec . 1989
John W. Halloran 31 Jan. 1990 93 p
(Contract N00014-88-C-0512; DARPA Order 9525)
(AD-A219131; CPS-90-001) Avail: NTIS HC A05/MF A01 CSCL 09/1

The progress on developing YBa2Cu3O7-X (Yttrium Barium Copper Oxide-X) wire for a High Temperature Superconductor motor is described. The wire development activity includes synthesis of Y-123 powder, spinning polymer-containing green fiber, heat treating the fiber to produce metallized superconducting filaments, and characterizing the electrical properties of the filaments. Green fiber is produced in lengths up to 1.5 kilometers. The green clad fiber is converted to silver-clad superconducting wire by a sintering operation. The sintered wire has a Amperes per centimeters squared (77 deg) up to 2800 A/cm in self field, dropping to low values in magnetic fields. Directional solidification efforts are underway to improve the critical current density. The construction of the first prototype HTSC homopolar motor is in progress. The design specifies a 575 ampere-turn HTSC coil. The current collection system was tested in liquid nitrogen. Motor performance was predicted based on actual Jc(B) behavior of wire samples. Motor power and losses were calculated. The efficiency of this initial machine is limited by the magnetic fields obtainable from present HTSC wire coils. GRA

N90-22690# North Dakota State Univ., Fargo.
THEORETICAL STUDIES OF SILICON CHEMISTRY Final Report, 1 Nov. 1986 - 31 Oct. 1989
Mark S. Gordon Feb. 1990 53 p
(Grant AF-AFOSR-0049-87; AF Proj. 2303)
(AD-A219232; AFOSR-90-0309TR) Avail: NTIS HC A04/MF A01 CSCL 07/2

State of the art methods were used in electronic structure theory and dynamics to develop an understanding of a variety of problems in chemistry of silicon and related elements of importance to the Air Force. Problems of interest include: precursors of materials and coatings; mechanisms for polymerization of silicic acid, including an elucidation of the role of hypervalent anionic silicon; interactions of drying agents with silicic acid and related species; and potential mechanisms for chemical vapor deposition of silicon, starting from silane and substituted silanes. Author

28 PROPELLANTS AND FUELS

Includes rocket propellants, igniters, and oxidizers; their storage and handling procedures; and aircraft fuels.

For related information see also *07 Aircraft Propulsion and Power, 20 Spacecraft Propulsion and Power,* and *44 Energy Production and Conversion.*

N90-22691# Aerospatiale Aquitaine, Saint-Medard en Jalles (France). Div. Systemes Strategiques et Spatiaux.
PYROTECHNIC MATERIALS IGNITED USING LASERS. HIGH ENERGY PHOTOPYROTECHNIC CHAINS [COMPOSANTS PYROTECHNIQUES INITIES PAR LASER ET CHAINE FONCTIONNELLE PHOTOPYROTECHNIQUE HAUTE ENERGIE]
J. P. Josse 5 Jun. 1989 23 p In FRENCH Sponsored in part by Direction des Engins
(Rept-892-430-121; AQET/B-3934-TI/88; ETN-90-96652) Avail: NITS HC A03/MF A01

Miniaturization of laser sources has made laser ignition of pyrotechnic materials possible but there is still a need for a sequence or photopyrotechnic chain to ignite the main charge. The architecture of such a chain is presented. The chain involves carrying the laser beam along fiber optics. A YAG laser is used for ignition purposes. The make-up of each of the components of the photopyrotechnic chain is outlined. The advantages of laser ignition over electropyrotechnic methods are presented. One of the advantages is the ability to initiate and sequence up to 20 pyrotechnic functions at one time. Other advantages include the small size and low mass of laser ignition systems. ESA

N90-22692# Ballistic Research Labs., Aberdeen Proving Ground, MD.
A COMPARISON BETWEEN EXPERIMENT AND SIMULATION FOR CONCEPT VIC REGENERATIVE LIQUID PROPELLANT GUNS. PART 1: 30 MM
Terence P. Coffee, Gloria P. Wren, and Walter F. Morrison Dec. 1989 72 p
(AD-A218556; BRL-TR-3072) Avail: NTIS HC A04/MF A01 CSCL 19/1

Regenerative liquid propellant gun (RLPG) technology is sufficiently mature to allow the testing of the first 155-mm liquid propellant gun. In support of the development of this artillery weapon, test fixtures in 30-mm and 105-mm sizes have been built and fired. The analysis and modeling of the 30-mm gun fixture is described. The Concept VIC gun design is described. The basic assumptions in the numerical lumped parameter model are described. Modifications to the model required by the VIC gun are given. There is a brief discussion of the 30-mm test program. The model is first benchmarked against a series of medium charge firings. These are the best characterized set of experiments, with the best reproducibility. The process of choosing input values for the gun code is discussed in detail. The result is excellent agreement with all of the experimental data. The model is then used to predict the performance of some of the short-charge firings. The muzzle velocities are predicted very accurately. The pressure profiles are not. The reasons for the lack of agreement in the pressure profiles are discussed. GRA

N90-22693# Air Force Astronautics Lab., Edwards AFB, CA.
TEMPERATURE MEASUREMENTS THROUGH A SOLID-PROPELLANT COMBUSTION WAVE USING IMBEDDED FINE WIRE THERMOCOUPLES Final Report, Aug. - Dec. 1989
David A. Alspach Jan. 1990 29 p
(AF Proj. 5730)
(AD-A218642; AL-TR-89-085) Avail: NTIS HC A03/MF A01 CSCL 21/2

Temperature profile measurements were measured through the combustion wave of burning solid propellant strands using imbedded fine-wire (75-micron diameter) thermocouples. The techniques necessary to construct, imbed, and measure temperature with this size and type of thermocouple were demonstrated. The experiments were performed at pressures ranging from 100 to 450 psi inside a high-pressure test cell designed for this type of operation. Surface temperature measurements have been estimated from the measured profiles for HMX, AN, and double-base propellants. GRA

N90-22694# Ballistic Research Labs., Aberdeen Proving Ground, MD.
METHODS FOR EVALUATION OF THERMALLY INDUCED REACTIONS IN LIQUID PROPELLANTS Technical Report, Feb. - Oct. 1988
Nathan Klein and Charles S. Leveritt Dec. 1989 35 p
(AD-A218750; BRL-TR-3069) Avail: NTIS HC A03/MF A01 CSCL 19/1

Aqueous mixtures of the nitrate salts of hydroxylamine (HAN) and triethanolamine (TEAN) are homogeneous, ionic solutions that remain liquid over a wide temperature range (less than -60 C). They are sufficiently fluidic that they can be pumped rapidly and are being considered for use in medium to large caliber guns. The physical and chemical properties of the propellants make them difficult or impossible to study to classical propellant evaluation methods. Thermal stability studies that include the effects of impurities and contaminants require special cognizance because of unique reactivity of the propellant mixtures. Reaction initiation by absorption of thermal energy was a major experimental method for determination of propellant stability as well as for the study of ignition and combustion phenomena. A modified high-pressure hydrogenation apparatus (AMINCO bomb) was used for such reaction initiation studies for many years and is now being replaced by an adiabatic calorimeter. The new diagnostic system utilizes a commercially available accelerating rate calorimeter (ARC) that was modified to make it suitable for use with liquid gun propellants. Safe storage temperatures, as determined with the ARC, are independent of the quantity of material being stored thereby eliminating the extrapolation from small laboratory samples that is a common uncertainty in many stability evaluation test methods. GRA

N90-22695# Federal Aviation Administration, Atlantic City, NJ.
TURBINE FUEL ALTERNATIVES (NEAR TERM) Final Report
Augusto M. Ferrara Oct. 1989 49 p
(AD-A219405; DOT/FAA/CT-89/23) Avail: NTIS HC A03/MF A01 CSCL 21/4

This report discusses the results of a study which investigated several alternatives for turbine fuels, which are being considered for use in the near term, with the intent of identifying the necessary certification criteria. The fuels investigated include Jet-A/ethanol blends, Jet-A/methanol blends, JP-4/ethanol blends, and neat ethanol. The tests were conducted using a T-63 turboshaft engine, which was mounted on the Technical Center's dynamometer. The use of dual fuel systems was also considered. A short series of flight tests was conducted with a T-34, Mentor aircraft. These tests were used to identify the operating conditions which might result in elevated fuel temperature. GRA

29 MATERIALS PROCESSING

Includes space-based development of products and processes for commercial applications.
For biological materials see *55 Space Biology.*

N90-22696# Aerospatiale, Paris (France).
MICROGRAVITY, THE SPACE APPLICATION OF THE 21ST CENTURY. CHALLENGES, CONSTRAINTS, AND STRATEGIES [MICROGRAVITE, NOUVEL ESPACE DU 21EME SIECLE. UN PARI, DES CONTRAINTES, UNE STRATEGIE]
Jacques Bouvard 1989 12 p In FRENCH Presented at the Journees le Ciel et l'Espace, Montpellier, France, 20-23 Sep. 1989
(Rept-892-430-105; ETN-90-96636) Avail: NTIS HC A03/MF A01

The use of a microgravity environment for industrial purposes is discussed. The availability of microgravity research and development platforms during the course of the 1990's is shown in diagrammatic form. The constraints inherent in developing microgravity projects are identified. The strategy of Aerospatiale in developing microgravity research and development programs is outlined. This strategy includes helping to develop an orbiting infrastructure, providing support for scientific research, generating interest within the industrial community and helping in the development of material and equipment destined for space applications. ESA

31 ENGINEERING (GENERAL)

Includes vacuum technology; control engineering; display engineering; cryogenics; and fire prevention.

N90-22697 Newcastle-upon-Tyne Univ. (England).
A THEORETICAL AND EXPERIMENTAL INVESTIGATION OF AN ABSORPTION REFRIGERATION SYSTEM FOR APPLICATION WITH SOLAR ENERGY UNITS Ph.D. Thesis
Mahieddine Dalichaouch 1989 257 p
Avail: Univ. Microfilms Order No. BRDX87970

Application of the second law of thermodynamics to refrigeration systems is useful in identifying the thermodynamic losses and in finding out where improvements might be made. Theoretical absorption refrigeration cycles are analyzed using the first law-based equations of energy balances and the second law-based concept of lost work. A thermodynamic efficiency, defined and formulated from the lost work approach, is used to examine a lithium bromide-water absorption cooling cycle with hot water as the heat source and cooling water as the heat sink. The cycle parameters are varied over applicable operating ranges in order to find their effect on the cycle thermodynamic efficiency. To accomplish this objective and to make a parametric analysis for the LiBr-water absorption cycle under steady-state conditions, two computer programs are written. The results indicate the system might be improved by better design. The efficiency variation is compared to variations of coefficient of performance found in literature. A LiBr-water absorption refrigeration system for low hot water temperature applications was proposed and detailed design aspects were considered. Fabrication and testing of a laboratory model of the absorption refrigeration system were described. As new design methodologies of solar energy applications were developed recently, a study of solar thermal systems for absorption refrigeration was presented. This includes the classification, description, and modeling of solar systems. Types of design procedures of solar systems for absorption refrigeration are discussed and a computer program was implemented which prints out the yearly solar fraction of a solar thermal system with daily storage for supplying heat to an absorption cooling cycle.
Dissert. Abstr.

N90-22698*# Massachusetts Inst. of Tech., Cambridge. Space Systems Lab.
H2, FIXED ARCHITECTURE, CONTROL DESIGN FOR LARGE SCALE SYSTEMS Ph.D. Thesis
Mathieu Mercadal Jun. 1990 265 p
(Grant NAG1-126)
(NASA-CR-180471; NAS 1.26:180471; Rept-3-90) Copyright Avail: NTIS HC A12/MF A02 CSCL 13B

The H2, fixed architecture, control problem is a classic linear quadratic Gaussian (LQG) problem whose solution is constrained to be a linear time invariant compensator with a decentralized processing structure. The compensator can be made of p independent subcontrollers, each of which has a fixed order and connects selected sensors to selected actuators. The H2, fixed architecture, control problem allows the design of simplified feedback systems needed to control large scale systems. Its solution becomes more complicated, however, as more constraints are introduced. This work derives the necessary conditions for optimality for the problem and studies their properties. It is found that the filter and control problems couple when the architecture constraints are introduced, and that the different subcontrollers must be coordinated in order to achieve global system performance. The problem requires the simultaneous solution of highly coupled matrix equations. The use of homotopy is investigated as a numerical tool, and its convergence properties studied. It is found that the general constrained problem may have multiple stabilizing solutions, and that these solutions may be local minima or saddle points for the quadratic cost. The nature of the solution is not invariant when the parameters of the system are changed. Bifurcations occur, and a solution may continuously transform into a nonstabilizing compensator. Using a modified homotopy procedure, fixed architecture compensators are derived for models of large flexible structures to help understand the properties of the constrained solutions and compare them to the corresponding unconstrained ones. Author

N90-22699# Sandia National Labs., Albuquerque, NM. Photovoltaic Cell Research Div.
EXPERIMENTAL EVALUATION OF CHEMICAL CLEANING PROCESSES FOR HIGH-LIFETIME SILICON PROCESSING
David L. King, John D. McBrayer, Paul A. Basore, M. Elaine Buck, Jeffrey W. Tingley, James M. Gee, Barry R. Hansen, and Douglas S. Ruby 1990 12 p Presented at the Materials Research Center of Excellence Seminar, El Paso, TX, 5 Mar. 1990 Submitted for publication
(Contract DE-AC04-76DP-00789)
(DE90-009332; SAND-90-0890C; CONF-9003139-1) Avail: NTIS HC A03/MF A01

The first in a series of multi-factor experiments designed to optimize the chemical cleaning procedure for four types of silicon material used in solar cell fabrication was completed. The goal of this first experiment (a 22 factor main effects experiment) was to determine the factors associated with chemical cleaning procedures that are most important in obtaining high excess charge-carrier recombination lifetime following a high temperature furnace oxidation. It was determined that the factors having the strongest influence on charge-carrier lifetime were different for the four different silicon materials considered. In general, the lower the lifetime of the material, the less sensitive the material was to different chemical cleaning steps. The stability of the lifetime was also evaluated with several factors exhibiting a significant effect for high quality silicon. Chemical cleaning procedures were identified that resulted in stable post-oxidation lifetimes greater than 2 ms for high resistivity float zone silicon. DOE

N90-22700# Lawrence Livermore National Lab., CA.
USING OBJECT-ORIENTED ANALYSIS TECHNIQUES TO SUPPORT SYSTEM TESTING
Lin Zucconi Mar. 1990 16 p Presented at the 7th International Conference on Testing Computer Software, San Francisco, CA, 21 Jun. 1990 Submitted for publication
(Contract W-7405-eng-48)
(DE90-009540; UCRL-102052; CONF-9006164-1) Avail: NTIS HC A03/MF A01

Testing of real-time control systems can be greatly facilitated by use of object-oriented and structured analysis modeling techniques. This report describes a project where behavior, process

and information models built for a real-time control system were used to augment and aid traditional system testing. The modeling techniques used were an adaptation of the Ward/Mellor method for real-time systems analysis and design (Ward85) for object-oriented development. The models were used to simulate system behavior by means of hand execution of the behavior or state model and the associated process (data and control flow) and information (data) models. The information model, which uses an extended entity-relationship modeling technique, is used to identify application domain objects and their attributes (instance variables). The behavioral model uses state-transition diagrams to describe the state-dependent behavior of the object. The process model uses a transformation schema to describe the operations performed on or by the object. Together, these models provide a means of analyzing and specifying a system in terms of the static and dynamic properties of the objects which it manipulates. The various models were used to simultaneously capture knowledge about both the objects in the application domain and the system implementation. Models were constructed, verified against the software as-built and validated through informal reviews with the developer. These models were then hand-executed. DOE

N90-22701# Air Force Materials Lab., Wright-Patterson AFB, OH. Electromagnetic Materials and Survivability Div.
COMPUTER CONTROLLED CRYOGENIC TEMPERATURE CONTROLLER Final Report, Sep. 1982 - Jan. 1984
Ronald E. Perrin 10 Jan. 1990 29 p
(AF Proj. 2306)
(AD-A218785; WRDC-TR-89-4140) Avail: NTIS HC A03/MF A01 CSCL 12/6

In laboratories which do materials characterization it is necessary to have a temperature controller which can be computer controlled, is accurate to within .1 to .2 K, can control temperature from 15 to 350 K with a drift of no more than .1, and is relatively unaffected by the presence of a magnetic field on the sample container. The subject controller uses two thermometers to meet these requirements. One is a commercially available calibrated silicon diode manufactured expressly for this type of application. The second thermometer is used for control. Once the sample has reached the setpoint according to the calibrated thermometer the control thermometer's value is sampled and used as the new setpoint. Since the control thermometer should be insensitive to a mag field the sample will remain at the desired temperature when the magnetic field is applied. GRA

N90-22702# Department of Defense, Washington, DC.
THE DEPARTMENT OF DEFENSE CRITICAL TECHNOLOGIES PLAN FOR THE COMMITTEES ON ARMED SERVICES UNITED STATES CONGRESS
Leo Young 15 Mar. 1990 267 p
(AD-A219300) Avail: NTIS HC A12/MF A02 CSCL 05/1

The second Annual Defense Critical Technologies Plan responds to the requirement that the Secretary of Defense submit to the Committees on Armed Services of the Senate and House of Representatives an annual plan for developing the technologies considered by the Secretary of Defense and the Secretary of Energy to be the technologies most critical to ensuring the long term qualitative superiority of the United States weapon systems. Twenty critical technologies are selected. The selection process is described, criteria for selection are set forth, and industrial and international assessments are summarized. The major portion of this report is contained in 20 sections in Appendix A, one section for each critical technology. Each section addresses the questions posed by Congress on funding, plans and milestones, industrial base and manufacturing issues, and the competitiveness of U.S. industry; it also provides an assessment of the positions of the Soviet Union, NATO, Japan and other industrialized countries in niche technologies within each critical technology. GRA

N90-22703*# National Aeronautics and Space Administration. Lewis Research Center, Cleveland, OH.
ELEMENTS OF ACTIVE VIBRATION CONTROL FOR ROTATING MACHINERY
Heinz Ulbrich May 1990 50 p
(NASA-TM-102368; E-5036; NAS 1.15:102368) Avail: NTIS HC A03/MF A01 CSCL 13B

The success or failure of active vibration control is determined by the availability of suitable actuators, modeling of the entire system including all active elements, positioning of the actuators and sensors, and implementation of problem-adapted control concepts. All of these topics are outlined and their special problems are discussed in detail. Special attention is given to efficient modeling of systems, especially for considering the active elements. Finally, design methods for and the application of active vibration control on rotating machinery are demonstrated by several real applications. Author

32 COMMUNICATIONS AND RADAR

Includes radar; land and global communications; communications theory; and optical communications.

For related information see also *04 Aircraft Communications and Navigation* and *17 Space Communications, Spacecraft Communications, Command and Tracking.* For search and rescue see *03 Air Transportation and Safety,* and *16 Space Transportation.*

N90-22704 United Kingdom Atomic Energy Authority, Harwell (England). Materials Physics and Metallurgy Div.
A 2-D ANALYSIS OF PARTICLE VELOCITY AND STRESS OF SH WAVES FROM A STRIP RADIATOR. AN EXPERIMENTAL VERIFICATION OF BOTH AMPLITUDE AND PHASE USING EMA TRANSDUCERS
W. H. B. Cooper, S. Walker, and T. A. Slesenger Feb. 1989 42 p
(AERE-R-12600) Copyright Avail: Issuing Activity

The initial objective of this investigation was to devise a reliable method of measuring the phase delay of SH waves in a homogeneous medium to an accuracy of about 0.01 percent. A two-dimensional strip SH wave radiator was considered. A model representing the special case of propagation along the axis of the sound field was developed in a previous report. This model is extended to consider propagation off axis including propagation along the surface. The calculations include propagation at angles up to pi/2 and hence to SH waves along the surface of a semiinfinite medium. It is shown that the field calculations can be considerably simplified and the physical picture made more realistic by assuming a loss mechanism in the homogeneous medium. Using electromagnetic acoustic (EMA) transducers and a simple theoretical approach to the electromagnetics, together with the 2-D elastic wave model for mild steel, there is excellent agreement with experiment in terms if both amplitude and phase responses. M.G.

N90-22705# Los Alamos National Lab., NM.
HF PROPAGATION THROUGH ACTIVELY MODIFIED IONOSPHERES
Paul E. Argo, T. Joseph Fitzgerald, John H. Wolcott, David J. Simons, Steve Warshaw, and Ralph Carlson (Lawrence Livermore National Lab., CA.) 1990 9 p Presented at the Ionospheric Effects Symposium, Washington, DC, 1-3 May 1990
(Contract W-7405-eng-36)
(DE90-008931; LA-UR-90-906; CONF-9005150-1) Avail: NTIS HC A02/MF A01

A computer modeling capability was developed to predict the effect of localized electron density perturbations created by chemical releases or high power radio frequency heating upon oblique, one-hop hf propagation paths. Three dimensional deterministic descriptions of the depleted or enhanced ionization, including formation, evolution, and drift are included. A homing ray trace code was developed to calculate the path of energy propagation through the modified ionosphere in order to predict multipath effects. Also considered is the effect of random index of refraction variations using a formalism to calculate the mutual coherence functions for spatial and frequency separations based

upon a path integral solution of the parabolic wave equation for a single refracted path through an ionosphere which contains random electron density fluctuations. DOE

N90-22706# Academy of Sciences of the Ukrainian SSR, Kharkov. Fiziko-Tekhnicheskij Inst.
DYNAMICS OF MOTION CHARGED PARTICLES IN A FIELD OF TWO ELECTROMAGNETIC WAVES
1988 17 p In RUSSIAN
(DE90-620690; KFTI-88-6) Avail: NTIS (US Sales Only) HC A03/MF A01

A study was made on dynamics of charged particle motion in external constant magnetic field and in the field of two electromagnetic waves of arbitrary polarization. The general condition of occurrence of local instability of particle motion was obtained. The condition holds true for all particle resonances with the field of: Cherenkov, cyclotron, cyclotron on normal and abnormal Doppler effect, parametric Cherenkov resonance. It is shown that all presently known conditions of local instability occurrence follow from this condition as particular case. DOE

N90-22707# Academy of Sciences of the Ukrainian SSR, Kharkov. Fiziko-Tekhnicheskij Inst.
FORCED SCATTERING OF ELECTROMAGNETIC WAVES ON ELECTRON BEAM IN PERIODICALLY INHOMOGENEOUS PLASMA
1988 20 p In RUSSIAN
(DE90-620705; KFTI-88-5) Avail: NTIS (US Sales Only) HC A03/MF A01

Parametric processes of excitation of short-wave electromagnetic radiation in a periodically inhomogeneous plasma waveguide were investigated. Parametric processes were considered both under conditions of the absence of plasma-beam instability and under the conditions of its development. It is shown that in the first case more complex two-cascade processes (when the beam excites LF+pumping wave on one hand, and scattering on the beam of this wave leads to excitation of HF-radiation, on the other hand) are possible along with a parametric Cherenkov mechanism of HF-radiation excitation. Initial stage of these processes was investigated. Excitation of HF-radiation develops most rapidly under conditions of plasma-beam instability. In this case, the unstable plasma wave is in parametric resonance with back plasma wave which represents a pumping wave. DOE

N90-22708# Royal Aerospace Establishment, Farnborough (England).
EVALUATION OF A PROTOTYPE 6 TONE MODEM
R. C. Bagwell 8 Aug. 1989 16 p
(RAE-TM-FM-28; BR111939; ETN-90-96440) Copyright Avail: NTIS HC A03/MF A01

A prototype 6 tone Multi-Frequency Shift Keying (MFSK) modem intended for tactical data transmissions in the HF band is evaluated. The main testing consisted of extensive trials using the Cobbett Hill HF Channel Simulator. Some limited live ratio trials between Bodo, northern Norway, and Cobbett Hill, southern England, are included. The modem performed satisfactorily during the evaluation period and returned good availability figures, both on the simulator, and during the radio trials. ESA

N90-22709# Rome Univ. (Italy). Dipt. di Fisica.
QUALITATIVE ASPECTS OF SIGNAL PROCESSING THROUGH DYNAMICAL NEURAL NETWORKS
Roberto DAutilia and Francesco Guerra 13 Nov. 1989 16 p Submitted for publication Sponsored in part by the Italian Ministry of Public Education
(Preprint-711; ETN-90-96534) Avail: NTIS HC A03/MF A01

Stochastic dynamical systems based on models of statistical mechanics with a large number of degrees of freedom are introduced. They have great simplicity and modular properties at the level of the elementary constituents, but are able to reproduce properties of high complexity in their global behavior. Input signals can be coded as external fields acting on the model affecting their time behavior. Output signals can be taken as some of the average properties of the dynamical variables. The resulting signal processing shows some extremely interesting qualitative features, as memory phenomena and sensitivity to signal correlations at simultaneous and delayed times. In particular, some elementary effects such as conditioned reflex, rhythm recognition and temporal edge detection are discussed. The models can be considered as a dynamical generalization of the Hopfield model of associative memory, and can be interpreted as models of neural networks, or other similar complex systems. ESA

N90-22710# Selenia S.p.A., Rome (Italy). Radar Dept.
DESIGN OPTIONS FOR SPACE-BASED RADAR SYSTEMS
A. DiVito, G. Galati, and D. Pistoia (Rome Univ., Italy) 1989 7 p Presented at the International Conference on Radar, Paris, France, 1989
(ETN-90-96548) Avail: NTIS HC A02/MF A01

The overall system design for space-based radar and pertaining options, including the optimization of the power-aperture product, the definition of the beamwidths and the use of multiple antenna beams are addressed. A distributed array architecture, made up by many radar modules coherently operating, is recommended in a number of operational situations. ESA

N90-22711# Selenia Industrie Elettroniche Associate S.p.A., Pomezia (Italy).
IMPROVEMENT OF CLUTTER REJECTION BY SCANNING MOTION COMPENSATION IN GROUND-BASED MONOPULSE RADAR
A. DiVito and F. A. Studer 1989 8 p Presented at the International Conference on Radar, Paris, France, 1989
(ETN-90-96550) Avail: NTIS HC A02/MF A01

A technique devised for compensating the effect of antenna scanning motion on MTI (or pulsed Doppler) Improvement Factor based radar equipped with azimuthal monopulse receiver is discussed. Original results are presented for realistic shapes of sum and difference antenna patterns in terms of IF, velocity response, monopulse accuracy. The technique proves to be extremely effective by achieving IF in excess of 40 to 50 dB under most typical operating conditions with a single cancellor MTI. ESA

N90-22712# Rochester Univ., NY. Lab. for Laser Energetics.
TIME-RESOLVED SURFACE STRUCTURAL STUDY BY PICOSECOND REFLECTION HIGH-ENERGY ELECTRON DIFFRACTION Final Report, 1 Aug. 1987 - 31 Jan. 1989
Hani E. Elsayed-Ali 21 Mar. 1989 56 p
(Grant AF-AFOSR-0327-87; AF Proj. 2306)
(AD-A218417; AFOSR-90-0205TR) Avail: NTIS HC A04/MF A01 CSCL 20/5

The objective of this program was to develop an instrument for characterization of nanosecond and picosecond time evolution of surface properties. This instrument was developed based on the technique of picosecond time-resolved reflection high-energy electron diffraction (RHEED). The basic idea of this technique is the utilization of 150 ps laser pulses to generate electron pulses by the photoelectric effect. The photogenerated electrons are accelerated, focused, and collimated using electron optics. Only a very small fraction of the laser pulse energy is needed to generate the fast (10 to 30 kV) well-collimated electron pulses; thus, most of the laser energy is available for sample irradiation. GRA

N90-22713# Office of Naval Research European Office, FPO New York, NY.
THE RACE (RESEARCH AND DEVELOPMENT IN ADVANCED TECHNOLOGIES FOR EUROPE) PROGRAM: A 1989 UPDATE
J. F. Blackburn 15 Dec. 1989 10 p
(AD-A218509; ONREUR-ESNIB-9-13-R) Avail: NTIS HC A02/MF A01 CSCL 25/2

Plans for the program called Research and Development in Advanced Communications Technologies for Europe (RACE) were reported in ESN 39-3:122-123 (1985), a comprehensive description of the work of the definition phases carried out in 1986 was given in ONRL Report No. 8-014-R (August 1988), and the RACE Program

in 1988 was described in ONREUR Report 9-7-C (March 1989). The work in RACE addresses the technical and economic options for the development of an advanced information infrastructure. However, strategic analyses of demand for powerful and cost-effective services determines the orientation of the technical work. GRA

N90-22714# Mission Research Corp., Pacific Grove, CA.
PRELIMINARY RESULTS OF THE PEAK EXPERIMENT. ALTAIR DEEP-SPACE MEASUREMENTS Technical Report, 27 Aug. 1987 - 6 Mar. 1989
Dennis L. Knepp 1 Mar. 1990 43 p
(Contract DNA001-87-C-0169)
(AD-A218622; MRC/MRY-R-014; DNA-TR-89-76) Avail: NTIS HC A03/MF A01 CSCL 17/9

During the DNA PEAK (Propagation Effects Assessment-Kwajalein) experiment in August 1988, the primary use of ALTAIR consisted of the collection of VHF and UHF track data and pulse returns from low-orbiting spherical satellites and other satellites of opportunity. However during the course of the experiment the opportunity occurred to collect a small amount of data while ALTAIR was in its operational deep-space track mode. This brief report summarizes the deep-space track data collected by ALTAIR on the evenings of August 18 and 19. On both evenings the FLTSATCOM 4 satellite was tracked by ALTAIR for a brief period. Simultaneous measurements of the one-way signal from the FLTSATCOM UHF satellite beacon at 244 MHz were also obtained at a receiver site located on Roi-Namur. A comparison of the ALTAIR data collected from the two-way radar propagation path to the FLTSATCOM satellite versus the one-way satellite link data indicates that, during this brief period, ALTAIR experienced about 5 dB of loss in detection sensitivity. If ALTAIR were faced with time-critical deep-space track requirements, mitigation techniques would likely be required to combat the effects of severe equatorial scintillation. GRA

N90-22715# IIT Research Inst., Chicago, IL.
ELF (EXTREMELY LOW FREQUENCY) COMMUNICATIONS SYSTEM ECOLOGICAL MONITORING PROGRAM: SLIME MOLD STUDIES Final Report, 8 Jul. 1972 - 31 Oct. 1988
Eugene Goodman and Ben Greenebaum Jan. 1990 94 p
(Contract N00039-88-C-0065)
(AD-A218623; IITRI-E06620-3) Avail: NTIS HC A05/MF A01 CSCL 20/3

It was previously shown that continuous exposure of the slime mold Physarum polycephalum to extremely low frequency (ELF) electromagnetic fields (EMF) simulating those generated by the Navy's ELF communication system (then Project Sanguine) could depress the rate of respiration, and lengthen the mitotic cell cycle. In a series of experiments beginning in 1981 and ending in 1987, it was determined that whether exposing Physarum to the field environment around the Wisconsin Transmitting Facility (WTF) could induce an altered physiological state. A laboratory component was also included to help verify methodology and to supplement studies performed at the WTF. Initially, the experimental effort was directed to devising methods to maintain axenic Physarum cultures under ambient environmental conditions. This involved using growth chambers that admit the electric field or current density from the surrounding environment; the cultures were returned to the laboratory for analysis. The successful methods placed the organism on an agar bed inside double containment and introduced the samples to be assayed into shaken liquid culture medium upon arrival at the laboratory. Both WTF-generated electromagnetic fields and background strengths were measured with the help of IITRI at study locations near the antenna, at the west ground of the WTF antenna, as well as at control sites. GRA

N90-22716# IIT Research Inst., Chicago, IL.
ELF (EXTREMELY LOW FREQUENCY) COMMUNICATIONS SYSTEMS ECOLOGICAL MONITORING PROGRAM: WETLAND STUDIES Final Report, 1 Nov. 1983 - 31 Oct. 1988
Glenn Guntenspergen, Janet Keough, Forest Stearns, and Douglas Wikum Nov. 1989 259 p
(Contract N00039-88-C-0065)
(AD-A218632; IITRI-E06620-2) Avail: NTIS HC A12/MF A02 CSCL 25/2

The results and conclusions are presented of in situ studies designed to monitor for possible effects on wetland flora from exposure to electromagnetic (EM) fields produced by the U.S. Navy's Extremely Low Frequency (ELF) Communications System. The studies examined for possible effects to herbs, shrubs, and trees growing on peat bogs near the Navy's Wisconsin Transmitting Facility (WTF). Plant characteristics studied included foliar cation content, stomatal resistance, and rate of foliar decomposition. Eleven bogs similar in plant community structure and interstitial water chemistry were used as study sites. Treatment sites were located immediately adjacent to the WTF antenna or its grounds, and experienced EM field intensities at least two orders of magnitude greater than control sites. GRA

N90-22717# Naval Postgraduate School, Monterey, CA.
PERFORMANCE ANALYSIS OF ALOHA NETWORKS WITH POWER CAPTURE AND NEAR/FAR EFFECT M.S. Thesis
Joseph T. McCartin Jun. 1989 68 p
(AD-A218739) Avail: NTIS HC A04/MF A01 CSCL 25/5

An analysis is presented for the throughput characteristics for several classes of Aloha packet networks. Specifically, the throughput for variable packet length Aloha utilizing multiple power levels to induce receiver capture is derived. The results are extended to an analysis of a selective-repeat ARQ Aloha network. Analytical results are presented which indicate a significant increase in throughput for a variable packet network implementing a random two power level capture scheme. Further research into the area of the near/far effect on Aloha networks is included. Improvements in throughput for mobile radio Aloha networks which are subject to the near/far effect are presented. Tactical Command, Control and Communications (C3) systems of the future will rely on Aloha ground mobile data networks. The incorporation of power capture and the near/far effect into future tactical networks will result in improved system analysis, design, and performance. GRA

N90-22718# Teledyne Brown Engineering, Huntsville, AL. Computer Systems Engineering Dept.
EXECUTIVE SUMMARY FOR THE NETWORK ASSESSMENT MODEL
30 Nov. 1989 60 p
(Contract DABT60-85-D-0520)
(AD-A218762; MD89-CDSF-0022) Avail: NTIS HC A04/MF A01 CSCL 25/2

A summary is provied of the Network Assessment Model (NAM). The NAM is a communications performance assessment simulation under development by the U.S. Army Signal Center. The NAM represents the capability to model a specific architecture against a specific scenario. The model simulates each discrete event in the architecture being modeled and records the results, compiles summary statistics, and displays summary graphics representing the performance of the architecture. Current capabilities of NAM version 3.4 (NAM3.4) include: area communications Mobile Subscriber Equipment (MSE) and Echelon Above Corps (EAC-CIP). Combat Net Radio Single Channel Ground and Airborne Radio System (SINCGARS) and Improved High Frequency Radio System (IHFR), Army Data Distribution System (JTIDS and EPLRS), Battlefield Automated Systems (BAS), post simulation analysis, force movement, line-of-sight radio wave loss propagation, network engineering, and threat. Capabilities currently under development: Coding of a Packet Switching overlay for MSE and EAC-CIP is scheduled to be completed by Aug. 90. Two data bases that serve as inputs to the model are also discussed: Communications Data Base (CDB), Operational Facilities (OPFAC) Data Base. Corps; Radio communications; Communications; Tactical; Simulation; NAM; Network assessment model; ATZHC-G-006; Communications data base; OPFAC operational facilities data base; Mobile subscriber equipment. GRA

N90-22719# Aerospace Corp., El Segundo, CA. Electronics Research Lab.
THE EFFECT OF MECHANICAL DEFORMATION ON THE RADIATION PATTERNS OF LARGE SPACE-BASED ARRAYS
Gwendolyn M. Shaw 30 Apr. 1988 65 p
(Contract F04701-85-C-0086)
(AD-A219288; TR-0086A(2925-05)-1; SD-TR-88-49) Avail: NTIS HC A04/MF A01 CSCL 20/14

Large phased arrays for space applications require light-weight deployable structures. As these structures are not completely rigid, they undergo dynamic deformations in orbit that are typically expressed as mechanical modes of surface position. In contrast with conventional antenna tolerance theory, which is based on a random Gaussian representation of manufacturing tolerance, these deformations follow a deterministic function. The effects of these mechanical deformations on the radiation performance of the phased array are analyzed. Closed-form solutions are presented for uniformly illuminated array, and results are shown for various mechanical modes. Tapered-amplitude array excitation is then treated numerically and contrasted with uniformly excited arrays. The array patterns resulting from modal errors and random errors are compared. DOE

N90-22720# Rome Air Development Center, Griffiss AFB, NY.
PERFORMANCE OF ADAPTIVE NULLING ANTENNAS IN A JAMMING ENVIRONMENT Report, Sep. 1988 - Jun. 1989
Lisa M. Sharpe Oct. 1989 21 p
(AF Proj. 4600)
(AD-A219305; RADC-TR-89-211) Avail: NTIS HC A03/MF A01 CSCL 20/14

An analysis is given of the performance of an adaptive nulling array in a jamming environment for various sizes of antenna arrays. Performance of adaptive nulling arrays and arrays with Chebychev tapering are compared. GRA

N90-22721# Rome Air Development Center, Griffiss AFB, NY.
SCATTERING OF A PLANE ELECTROMAGNETIC WAVE FROM A SEMICIRCULAR CRACK IN A PERFECTLY CONDUCTING GROUND PLANE
Mark K. Hinders Apr. 1989 38 p
(AD-A219310; RADC-TR-89-12) Avail: NTIS HC A03/MF A01 CSCL 20/3

The scattering of TM and TE plane electromagnetic waves from a semicylindrical crack in a perfectly conducting ground plane is determined using a dual series eigenfunction expansion technique. Orthogonality properties of the sinusoids are used to reduce the solution to the inversion of a truncated infinite matrix. When the radius of the crack is much smaller than the wavelength, small argument approximations for the spherical radial functions are employed to simplify the results and remove the ka-dependence from the necessary numerical matrix inversion. In this small crack limit, closed form results are developed for both polarizations, and for the TM polarization, results are found to be different by only a constant factor from those for TM scattering from a narrow slit in an infinitely thin conducting screen. TE scattering from a small crack is found to differ significantly from TE scattering from a narrow slit, which indicates that the slit approximation is not valid for real situations that more closely resemble physically an indentation, or crack. GRA

N90-22722# Naval Postgraduate School, Monterey, CA.
OPTICAL EXCISOR MODELING M.S. Thesis
Daniel A. Marinsalta Sep. 1989 93 p
(AD-A219338) Avail: NTIS HC A05/MF A01 CSCL 17/3

This work simulates an acousto-optic signal processing technique that can be used to filter radio-frequency (RF) electronic signals. Of particular interest is the removal or excision of narrowband interference from broadband signals. The program developed simulates the performance of a binary phase shift keying (BPSK) signal with a narrowband interference. The width and depth of notches that model an excisor-detector array are variable. In addition there is a capability to move the notches in order to place a notch over the interference for maximum filtering capability. A summary of several possible excisor techniques is presented. GRA

33 ELECTRONICS AND ELECTRICAL ENGINEERING

Includes test equipment and maintainability; components, e.g., tunnel diodes and transistors; microminiaturization; and integrated circuitry.

For related information see also *60 Computer Operations and Hardware* and *76 Solid-State Physics.*

N90-22723# Edgerton, Germeshausen and Grier, Inc., Idaho Falls, ID.
A MULTIPULSED DYNAMIC DIFFRACTION MOIRE INTERFEROMETER
V. A. Deason and M. B. Ward 1989 8 p Presented at the 3rd International Conference on Laser Interferometry, San Diego, CA, 6-11 Aug. 1989
(Contract DE-AC07-76ID-01570)
(DE90-009765; EGG-M-89049; CONF-8908222-3) Avail: NTIS HC A02/MF A01

A system capable of generating several tens of diffraction moire interferograms at rates on the order of 1 MHz is described. The interferometer consists of a specially modified, segmented ruby rod laser capable of producing a long train of 40-mJ pulses each with a width on the order of 20 to 50 ns. The interferograms are recorded on film using a high speed turbine camera capable of 2,000,000 frames per second for a total record of 80 frames. The interferometer is used in conjunction with any of several devices for impulsively loading a variety of materials so as to study dynamic material deformation, fracture, delamination, or other response to dynamic stress. This apparatus is the latest in a series of dynamic diffraction moire systems built at the Idaho National Engineering Laboratory. Dynamic moire studies of Colorado oil shale are briefly discussed. DOE

N90-22724* National Aeronautics and Space Administration. Lewis Research Center, Cleveland, OH.
MINIATURE TRAVELING WAVE TUBE AND METHOD OF MAKING Patent
Henry G. Kosmahl 26 Dec. 1989 8 p Filed 8 Dec. 1987
Supersedes N88-23936 (26 - 17, p 2335)
(Contract NAS3-24565)
(NASA-Case-LEW-14520-1; US-Patent-Appl-SN-130058; US-Patent-Class-315-3.5; US-Patent-Class-315-3; US-Patent-Class-331-82; Int-Patent-Class-H01J-25/34) Avail: US Patent and Trademark Office CSCL 09A

A miniature traveling wave tube is provided which will have most of the advantages of solid state circuitry but with higher efficiency and without being highly sensitive to temperature and various types of electromagnetic radiation and subatomic particles as are solid state devices. The traveling wave tube is about 2.5 cm in length and includes a slow wave circuit (SWS) comprised of apertured fins with a top cover which is insulated from the fins by strips or rungs of electrically insulating, dielectric material. An extemely small SWS is constructed by employing various grooving and etching methods, and by providing insulating strips or rungs by various deposition and masking techniques.
Official Gazette of the U.S. Patent and Trademark Office

N90-22725 Politecnico di Milano (Italy). Dipt. di Elettronica.
DESIGN FOR TESTABILITY OF STUCK-OPEN AND STACK-ON CMOS COMBINATORIAL CIRCUITS
Giacomo Buonanno and Donatella Sciuto (Brescia Univ., Italy)
Jul. 1989 51 p
(Rept-89-044; ETN-90-96511) Avail: Politecnico di Milano, Dipartimento di Elettronica, Piazza Leonardo da Vinci 32, 20133 Milano, Italy

A design for testability approach for fully CMOS combinational networks is presented. It is based on the addition of two transistors,

a P-MOS and an N-MOS placed in series between the P and the N sections, both controlled by a single input. The definition of the test procedure, which allows the detection of single and multiple stuck-open and stuck-on faults, is given. Simulations of the test procedure on a real circuit are described. ESA

N90-22726 Politecnico di Milano (Italy). Dipt. di Elettronica.
DETECTION OF BRIDGING FAULTS IN DFCMOS COMBINATIONAL GATES
Giacomo Buonanno and Donatella Sciuto Dec. 1989 89 p
(Rept-89-060; ETN-90-96515) Avail: Politecnico di Milano, Dipartimento di Elettronica, Piazza Leonardo da Vinci 32, 20133 Milan, Italy

A method based on the detectability of bridging faults through test sets, developed to locate other kinds of faults, is presented. The detection of bridging faults in CMOS combinational circuits, using a test procedure that detects transistor stuck-at faults in Dynamic Fully CMOS logic, is shown. The detection of most of the possible bridging faults (single and multiple) is achieved, ranking fault coverage to more than 95 percent. ESA

N90-22727# Laboratoire d'Automatique et d'Analyse des Systemes, Toulouse (France).
DEFINITION OF A DESIGN METHODOLOGY AND STUDY OF THE DRIVING AND PROTECTION FUNCTIONS OF A SMART POWER SWITCH Ph.D. Thesis
Abdellatif Elmoznine 1989 150 p In FRENCH; ENGLISH summary
(LAAS-89-330; ETN-90-96606) Avail: NTIS HC A07/MF A01

The design of a smart power switch in MOS technology, in particular the high side switch mode, is studied. Special emphasis is given to the study of unwanted electrical coupling through the substrate between the power and the logic sections of the device. A new concept that leads to a completely latch-up free circuit and based on a floating well is proposed. The driving and protection functions of the power switch are presented. A charge pump circuit is proposed, allowing minimum power dissipation and high speed to be achieved. A circuit for sensing the device's temperature is presented. The short circuit and open circuit protection functions are proposed. The circuit generating, on chip, the voltage supply and a detector of its stability are presented. ESA

N90-22728# Laboratoire d'Automatique et d'Analyse des Systemes, Toulouse (France).
EXCESS NOISE, ANOMALOUS EFFECTS AND RELIABILITY OF HIGH FREQUENCY DEVICES (SCHOTTKY DIODES, MESFET AND HEMT) Ph.D. Thesis
J. Apolinar Reynoso-Hernandez 1989 220 p In FRENCH; ENGLISH summary
(LAAS-89-394; ETN-90-96610) Avail: NTIS HC A10/MF A01

The reliability and some anomalous effects related to the fabrication of high frequency devices (Schottky diodes, MESFET and HEMT) are investigated. Low frequency noise, output impedance frequency dispersion and other electric parameters were measured. Low frequency noise measurements are found to be a powerful tool in detecting electrical inhomogeneities. Devices exhibiting the highest level of low frequency noise presented the earlier failure. The measurements of low frequency noise can be used to determine the best devices exhibiting reliability. A correlation between low frequency noise and output impedance frequency dispersion was established in the MESFET. In the HEMT no correlation was found. Output impedance frequency dispersion in the low frequency range was established as included by the EL2 source in MESFET as well as in HEMT. The output impedance of MESFET and HEMT may exhibit a self-inductance behavior. A unified theory of the Kink effect exhibited by the HEMT and the MESFET is proposed. ESA

N90-22729# Technische Univ., Delft (Netherlands).
DESIGN OF HIGH-PERFORMANCE NEGATIVE-FEEDBACK OSCILLATORS Ph.D. Thesis
Cornelis Alexander M Boon 1989 159 p
(ETN-90-96698) Avail: NTIS HC A08/MF A01

The design of high-performance negative-feedback oscillators is described. These oscillators deliver a signal with an accurate frequency, waveform and amplitude to an inaccurate load. The way in which the feedback stabilizes the transfer of the amplifier in a non-traditional way to that of a memoryless limiter is described. Simple modeling of these oscillators, however, shows that degradation is relatively low. The limiter in the oscillator loop influences the transfer of independent small signals, such as noise present in the oscillator, to amplitude and phase variations in the output signal in a simple way. In negative-feedback oscillators the resonator is a simple LC circuit. In the proposed concept a series LC circuit is terminated by a current controlled negative resistance that has a limiting current-to-voltage characteristic. Expressions are given from which the static frequency error and the frequency stability can be calculated as a function of the gain in the two feedback loops. The larger these two loop gains are, the more the oscillator performance is stabilized by the accurate elements in the feedback paths. ESA

N90-22730# Groningen Rijksuniv. (Netherlands). Dept. of Mathematics.
BIFURCATIONAL ASPECTS OF PARAMETRIC RESONANCE
H. W. Broer and Gert Vegter 1989 65 p
(W-8904; ETN-90-96714) Avail: NTIS HC A04 A01

Generic nonlinear oscillators with parametric forcing are considered near resonance. In particular, the branching off of certain subharmonic periodic solutions from the central equilibrium solution is studied. This can be seen as a case-study in the bifurcation theory of Hamiltonian systems with or without discrete symmetries. Structure preserving normal form or averaging techniques are used. Equivariant singularity theory and theory of flat perturbations are considered. ESA

N90-22731*# National Aeronautics and Space Administration. Lewis Research Center, Cleveland, OH.
FIELD ORIENTED CONTROL OF INDUCTION MOTORS
Linda M. Burrows, Don S. Zinger (Akron Univ., OH.), and Mary Ellen Roth 1990 8 p Proposed for presentation at the 25th Intersociety Energy Conversion Engineering Conference, Reno, NV, 12-17 Aug. 1990; cosponsored by AIChE, SAE, ACS, AIAA, ASME, and IEEE
(NASA-TM-103154; E-5516; NAS 1.15:103154) Avail: NTIS HC A02/MF A01 CSCL 09C

Induction motors have always been known for their simple rugged construction, but until lately were not suitable for variable speed or servo drives due to the inherent complexity of the controls. With the advent of field oriented control (FOC), however, the induction motor has become an attractive option for these types of drive systems. An FOC system which utilizes the pulse population modulation method to synthesize the motor drive frequencies is examined. This system allows for a variable voltage to frequency ratio and enables the user to have independent control of both the speed and torque of an induction motor. A second generation of the control boards were developed and tested with the next point of focus being the minimization of the size and complexity of these controls. Many options were considered with the best approach being the use of a digital signal processor (DSP) due to its inherent ability to quickly evaluate control algorithms. The present test results of the system and the status of the optimization process using a DSP are discussed. Author

N90-22732*# National Aeronautics and Space Administration. Lewis Research Center, Cleveland, OH.
PHOTORESPONSE OF YBa2Cu3O(7-DELTA) GRANULAR AND EPITAXIAL SUPERCONDUCTING THIN FILMS
G. J. Valco, P. Claspy (Case Western Reserve Univ., Cleveland, OH.), J. D. Warner, N. Varaljay, and K. B. Bhasin 1990 12 p Presented at the Technical Symposium on Optical Engineering and Photonics in Aerospace Sensing, Orlando, FL, 16-20 Apr. 1990; sponsored by Society of Photo-Optical Instrumentation Engineers
(Contract NCC3-105)

(NASA-TM-103144; E-5496; NAS 1.15:103144) Avail: NTIS HC A03/MF A01 CSCL 20L

The response is reported of thin films of YBa2Cu3O(7-delta) with either a very grainy or a smooth epitaxial morphology to visible radiation. SrTiO3 substrates were employed for both types of films. The grainy films were formed by sequential multi-layer electron beam evaporation while the epitaxial films were formed by laser ablation. Both films were patterned into H shaped detectors via a negative photolithographic process employing a Br/ethanol etchant. The bridge region of the H was 50 microns wide. The patterned films formed by laser ablation and sequential evaporation had critical temperatures of 74 K and 72 K respectively. The bridge was current biased and illuminated with chopped He-Ne laser radiation and the voltage developed in response to the illumination was measured. A signal was detected only above the critical temperature and the peak of the response coincided with the resistive transition for both types of films although the correspondence was less exact for the grainy film. The details of the responses and their analysis are presented. Author

N90-22733# Massachusetts Inst. of Tech., Cambridge.
REACTIONS OF LASER-GENERATED FREE RADICALS AT SEMICONDUCTOR SURFACES Final Report, 1 Oct. 1985 - 31 Dec. 1989
Jeffrey I. Steinfeld 22 Jan. 1990 7 p
(Contract F49620-86-C-0003)
(AD-A218552; AFOSR-90-0189TR) Avail: NTIS HC A02/MF A01 CSCL 09/1

Reactions of laser generated free radicals at semiconductor surfaces were investigated by photoelectron spectroscopy of adsorbed surface layers and by laser induced fluorescence detection of the gas-phase species. Systems investigated include dissociative chemisorption of XeF2 and CF3 on Si (111), IR multiple photon dissociation of alkylsilanes and characterization of the SiH2 dissociation product and deposition of metallic films from iron carbonyl. From these experiments, quantitative models were developed for the reactivity of fluorocarbon radicals at silicon surfaces, intersystem state coupling in excited SiH2, and formation of metallic films. GRA

N90-22734# Ballistic Research Labs., Aberdeen Proving Ground, MD.
OPTIMIZATION OF A PULSED AIR CORE TRANSFORMER FOR LOW IMPEDANCE INDUCTIVE IGNITION
Alexander E. Zielinski and John A. Bennett (Picatinny Arsenal, Dover, NJ.) Jan. 1990 23 p
(AD-A218748; BRL-MR-3803) Avail: NTIS HC A03/MF A01 CSCL 19/1

A design analysis was conducted to develop an inductive ignition concept for ordnance. Mathematical models were developed to examine the transformer for optimum performance. Results indicate that significant energy transfer to an electric primer can be obtained using a simple pulse transformer. Experimental results using a capacitive pulsed power supply indicate reasonable agreement with the models for short times. Deviations from the theoretical model can be explained by nonlinear materials effects and field diffusion in the surrounding barrel walls. GRA

N90-22735# California Univ., Berkeley. Space Sciences Lab.
CONSTRUCTION OF A 345 GIGAHERTZ RECEIVER BASED ON SUPERCONDUCTING TUNNEL JUNCTIONS Final Report, 1 Oct. 1985 - 31 Dec. 1989
Edmund C. Sutton 12 Feb. 1990 4 p
(Contract DAAG29-85-K-0254)
(AD-A218781; ARO-23136.5-CH) Avail: NTIS HC A01/MF A01 CSCL 09/1

This report describes the construction of a 345 GHz receiver system based on superconducting tunnel junctions. The junctions used are niobium edge junctions, which are mounted in a waveguide mixer mount. Highest sensitivity occurs at 312 GHz with a measured receiver noise temperature of 275 K double sideband. Theoretical calculations and experimental results both indicate the likelihood of good low noise operation out to 1000 GHz using techniques of the sort described. GRA

N90-22736# Rockwell International Corp., Anaheim, CA.
BURNOUT THRESHOLDS AND CROSS SECTION OF POWER MOS TRANSISTORS WITH HEAVY IONS Technical Report, 1 May 1986 - 30 Apr. 1988
A. E. Waskiewicz and J. W. Groninger Feb. 1990 107 p
(Grant DNA-MIPR-88-507)
(AD-A218998) Avail: NTIS HC A06/MF A01 CSCL 09/1

Power MOSFET heavy ion-induced Single Event Burnout tests were performed jointly by representatives of the Aerospace Corporation, NASA Goddard, NWSC Crane and Rockwell International. The results are presented of the burnout threshold and cross section characterizations performed on n-channel power MOSFETs, however a small amount of p-channel data is also included. In addition, data on the effect of temperature, gate bias, total dose and inductive loading on MCSFET Single Event Burnout sensitivity is preferred. At the time of the test effort, radiation hardened devices were being developed by International Rectifier and RCA/GE. The heavy-ion-induced burnout test results on available samples of these devices are also incorporated for comparison to the commercial and JEDEC versions tested. GRA

N90-22737# North Carolina State Univ., Raleigh.
CONTINUED DEVELOPMENT AND CHARACTERIZATION OF DOPED LAYERS, CONTACTS, AND ASSOCIATED ELECTRONIC DEVICES IN SILICON CARBIDE Annual Letter Report, 1 Jul. - 31 Dec. 1989
Robert F. Davis and John W. Palmour 28 Feb. 1990 42 p
Sponsored in part by Westinghouse Electric Corp.
(Contract N00014-88-K-0341)
(AD-A219211) Avail: NTIS HC A03/MF A01 CSCL 09/1

Electronic devices for microwave applications, the science and technology of ohmic and Schottky contacts and equipment fabrication for ultra-high purity thin films were the subjects of concern for the application of growth of the 6H SiC polytype in this reporting period. MESFETs having gate lengths of 2, 4, 13 and 24 microns with maximum transconductances in the range of 1.5 to 22 ms/mm, respectively and with very low subthreshold leakage currents were fabricated. The 2 micron device also had threshold frequency of 510 MHz at OdB gain; the power gain crossed OdB at approx. 380 MHz. IMPATT based on Schottky diodes showed permanent breakdown; those based on p-n junctions appear promising. Ohmic and Schottky contacts are important for devices; thus, a program to examine the interface chemistry and associated electrical properties of high purity contacts deposited under controlled conditions, were initiated. A molecular beam epitaxy system for the deposition of high purity SiC films is also nearing completion. GRA

N90-22738# North Carolina State Univ., Raleigh.
CONTINUED DEVELOPMENT AND CHARACTERIZATION OF DOPED LAYERS, CONTACTS AND ASSOCIATED ELECTRONIC DEVICES IN SILICON CARBIDE Annual Letter Report, 1 Jul. - 31 Dec. 1989
Robert F. Davis and John W. Palmour 28 Feb. 1990 42 p
Sponsored in part by Westinghouse Electric Corp.
(Contract N00014-88-K-0341)
(AD-A219234) Avail: NTIS HC A03/MF A01 CSCL 09/1

Electronic devices for microwave applications, the science and technology of ohmic and Schottky contacts and equipment fabrication for ultra-high purity thin films were the subjects of concern for the application of growth of the 6H SiC polytype in this reporting period. MESFETs having gate lengths of 2, 4, 13 and 24 microns with maximum transconductances in the range of 1.5 to 22 ms/mm, respectively and with very low subthreshold leakage currents were fabricated. The 2 micron OdB at approx. 380 MHz. IMPATT based on Schottky diodes showed permanent breakdown; those based on p-n junctions appear promising. Ohmic and Schottky contacts are important for devices; thus, a program to examine the interface chemistry and associated electrical properties of high purity contacts deposited under controlled

conditions, have been initiated. A molecular beam epitaxy system for the deposition of high purity SiC films is also nearing completion. GRA

N90-22739# Rockwell International Corp., Canoga Park, CA. Rocketdyne Div.
BEAM COMBINING BY PHASE TRANSITION NONLINEAR MEDIA Final Report, 1 Jun. 1987 - 28 Feb. 1990
Glenn Bennett, Kevin Schehrer, and Victor Wang Feb. 1990 108 p
(Contract N00014-87-C-0340)
(AD-A219301; RI/RD90-121) Avail: NTIS HC A06/MF A01 CSCL 09/3

The work carried out to develop a high response nonlinear material suitable for use with high power lasers is described. The objective of this program was to demonstrate the use of a gas or liquid near a phase transition as an efficient phase conjugation material. This enhancement was explored for both static equilibrium conditions near the critical point and for nonequilibrium conditions created by sudden expansion in a nozzle. The achievement of such a high response nonlinear material would make practical the application of nonlinear phase conjugate techniques to the beam combining of multiple lasers with a coherence characteristic of a single laser. GRA

N90-22740# Naval Ocean Systems Center, San Diego, CA.
INDIUM PHOSPHIDE PLANAR GUNN DIODE Final Report, Dec. 1985 - Dec. 1987
M. J. Taylor, D. Rubin, E. R. Schumacher, and A. R. Clawson Sep. 1989 26 p
(AD-A219337; NOSC/TD-1703) Avail: NTIS HC A03/MF A01 CSCL 09/1

An indium phosphide (InP) planar Gunn diode showing oscillations in the 20- to 40-GHz-frequency range was successfully fabricated and tested using epitaxially grown layers. Also demonstrated was the concept of selectively removing portions of one epilayer and refilling the recesses with a second epilayer. The working structure showed low resistance across the n/n+ interface. Processing techniques developed during the InP planar Gunn diode work are now incorporated into current work at NOSC. Also, successes in these experiments resulted in renewed interests in surface-oriented planar Gunn diodes. GRA

N90-22741# Giner, Inc., Waltham, MA.
ADVANCED DOUBLE LAYER CAPACITOR Quarterly Interim Technical Report No. 7, 1 Nov. 1989 - 31 Jan. 1990
Anthony B. LaConti, Philip Lessner, and S. Sarangapani Mar. 1990 13 p
(Contract N00014-88-C-0391; ARPA Order 9526)
(AD-A219419; C87A-25) Avail: NTIS HC A03/MF A01 CSCL 09/1

The overall goal of this project is to develop electrochemical capacitors utilizing a solid ionomer electrolyte. An advantage of these devices over conventional double layer capacitors would be the absence of free liquid electrolyte and thus greater safety and reliability. In the 7th Quarter, we have concentrated our efforts in three areas: (1) preparation of single-cell and multiple-cell stacks, (2) understanding the origin of internal resistance in single-cell and multiple-cell stacks, and (3) measurements of the temperature characteristics of a single cell. GRA

34 FLUID MECHANICS AND HEAT TRANSFER

Includes boundary layers; hydrodynamics; fluidics; mass transfer; and ablation cooling.

For related information see also *02 Aerodynamics* and *77 Thermodynamics and Statistical Physics.*

N90-22742 Michigan Univ., Ann Arbor.
EXPERIMENTAL STUDY OF VORTEX RING INTERACTION WITH A FREE SURFACE Ph.D. Thesis
Jung Tai Kwon 1989 144 p
Avail: Univ. Microfilms Order No. DA9001663

The results of an experimental investigation on the interaction of vortex rings with a free surface are presented. Laminar vortex rings with Reynolds numbers in the range 2 x 10(exp 3) to 10(exp 4) were formed underwater at several incidence angles to the free surface. When the vortex core closest to the surface interacts with it, vortex lines are found to disconnect resulting in open vortex lines beginning and terminating at the surface. This process occurred at all vortex ring Reynolds numbers investigated and incidence angles up to 45 deg. Under certain conditions a second reconnection process is observed resulting in a vortex line topology consisting of two semicircles propagating away from each other on divergent paths. The range of vortex ring Reynolds numbers and incidence angles resulting in double reconnection was determined. The double reconnection process was documented in detail by flow visualization and surface velocity field measurements for a vortex ring Reynolds number of 5 x 10(exp 3) and incidence angle of 20 deg. The surface velocity field measurements were obtained using Laser Speckle Photography combined with automated digital image processing techniques. At zero incidence the vortex ring path turns toward the free surface as a result of the velocity field of the image vortex above the surface. The effect of free surface contamination was further investigated at an incidence angle of 90 deg. The results show the formation of secondary and tertiary rings when the surface is contaminated by surface active agents. Dissert. Abstr.

N90-22743 Michigan Univ., Ann Arbor.
UNSTEADY GROUP BEHAVIOR OF DROPLET CLOUDS IN SWIRLING FLOWS Ph.D. Thesis
Muh-Hsiung Yang 1989 199 p
Avail: Univ. Microfilms Order No. DA9001741

The group behavior of cylindrical droplet clouds in axisymmetric swirling flows (forced, potential and Rankine vortices) is investigated. The vaporization of individual droplets in a stationary cloud was known to be different from the vaporization of an isolated droplet due to the fact that a vaporization layer may occur within a thin sheath at the cloud edge. The effect of axisymmetric swirling flows on the vaporization behavior of droplet clouds will be assessed. The study is carried out in three stages. First, single droplet motion in swirling flows was studied and were found to be characterized by a parameter epsilon (sub v) which is defined by the square of the ratio of a droplet relaxation time to a characteristic flow time. Secondly, the droplet cloud motion in swirling flows was studied considering the interaction between droplets and gas. The unsteady governing equations for both droplet and gas phases were solved for various conditions using numerical methods so that the vaporization of stationary and swirling clouds could be compared with each other. Author

N90-22744 University of Central Florida, Orlando.
ANALYSIS OF VELOCITY AND TEMPERATURE FLUCTUATIONS IN TURBULENT SHEAR FLOWS Ph.D. Thesis
Mahendra L. Joshi 1989 182 p
Avail: Univ. Microfilms Order No. DA9005029

Turbulent velocity and temperature fluctuations in the jet-burner mixing layer were measured. Particular attention was focused on the small scale, high wave number turbulence which strongly affects the optical propagation. Commercial hot wire sensors involving a newly developed temperature measuring scheme were employed.

The velocity and temperature structure functions up to order 18 were measured in the inertial range to establish the power-law relationships, ordered set (delta u) sup n is similar to ordered set epsilon sup n/3 r sup zeta n and ordered set (delta theta) sup n is greater than or similar to ordered set epsilon sup -n/6 ordered set chi sup n/2 r sup zeta n, where zeta n is the exponent due to intermittency. In contrast to Kolmogorov's theory (1941), both viscous dissipation rate epsilon and thermal dissipation rate chi were assumed as random quantities. Measured values of zeta n from velocity structure functions were compared with those predicted by lognormal, beta-model and a new theory based on gamma statistics for the local dissipation rate epsilon sub r. The present data and past measurements agree more closely with the predictions of gamma model rather than those of the lognormal model. Unlike velocity spectra, the measured temperature spectra revealed that at high wave numbers it decreases less rapidly than the k sub 1 sup 5/3 law and has the appearance of a spectral bump just prior to the dissipation ranges. A corresponding bump was also observed in the temperature structure function. Author

N90-22745 Salford Univ. (England).
THREE-DIMENSIONAL SEPARATED FLOW PREDICTION ON FUSIFORM BODY USING EULER AND BOUNDARY LAYER METHODS Ph.D. Thesis
Chung-Ming Kwong 1989 334 p
Avail: Univ. Microfilms Order No. BRD-86846

Three-dimensional transonic/supersonic flow over a three caliber tangent ogive body of revolution at incidence is studied using viscous/inviscid interaction. The proposed viscous/inviscid interaction consists of a three-dimensional turbulent integral boundary layer calculation and a time-marching Euler solver with or without a forced separation model. For the time-marching analysis, the explicit MacCormack scheme is used as the basic algorithm, which has been widely used and in general performs adequately but suffers from spurious oscillations in regions of discontinuities. An improvement of the prediction accuracy is sought by using two approaches. The first approach uses a hybrid scheme which involves operator-switching between the MacCormack scheme and a upwind scheme according to the local flow conditions. In the second approach, a Total Variation Diminishing (TVD) MacCormack scheme is developed. The new scheme consists of the basic MacCormack scheme appended with rational dissipation terms derived from the theory of TVD scheme. Both schemes are shown to be robust, to resolve discontinuities well and to be effective in eliminating the spurious oscillations associated with the original MacCormack scheme. A forced separation model has been proposed to supplement the Euler equations to model separated flow in two and three dimensions. The model has been applied to two-dimensional separated flow over a half circular cylinder at subsonic speed and three-dimensional separated flow over a three caliber tangent ogive cylinder body of revolution over a range of speeds and incidences. It was found that the use of the separation model produced considerable improvements in the prediction of the separated flow fields and surface pressure distribution. Viscous/inviscid interaction techniques have been developed for both attached and separated flows in three dimensions. Dissert. Abstr.

N90-22746*# Rockwell International Science Center, Thousand Oaks, CA.
SUPERSONIC FLOW COMPUTATIONS FOR AN ASTOVL AIRCRAFT CONFIGURATION, PHASE 2, PART 2 Final Report
Sekaripuram V. Ramakrishnan, Sukumar R. Chakravarthy, and Kuo-Yen Szema Washington NASA May 1990 43 p
(Contract NAS1-17492)
(NASA-CR-4284; NAS 1.26:4284) Avail: NTIS HC A03/MF A01 CSCL 20D

A unified space/time marching method was used to solve the Euler and Reynolds-averaged Navier-Stokes equations for supersonic flow past an Advanced Short Take-off and Vertical Landing (ASTOVL) aircraft configuration. Lift and drag values obtained from the computations compare well with wind tunnel measurements. The entire calculation procedure is described starting from the geometry to final postprocessing for lift and drag. The intermediate steps include conversion from IGES to the patch specification needed for the CFD code, grid generation, and solution procedure. The calculations demonstrate the capability of the method used to accurately predict design parameters such as lift and drag for very complex aircraft configurations. Author

N90-22747 United Kingdom Atomic Energy Authority, Harwell (England). Materials Development Div.
TRANSPORT OF GASES THROUGH CONCRETE Annual Progress Report, 1988
A. Atkinson, P. A. Claisse, A. W. Harris, and A. K. Nickerson Jan. 1989 31 p
(Contracts FI1W/0187/00; NASARP-49)
(AERE-G-4977) Copyright Avail: Issuing Activity

Gases will be generated within a radioactive waste repository. The magnitude of the gas pressure caused by the build-up of such gases will depend on the relative rates of gas generation and release from the repository. An increase in the gas pressure has the potential to affect the integrity of the repository structure. The object of this work is to quantify the gas migration rate in several different types of cementitious material as a function of both gas pressure and the degree of water saturation and to establish whether the pressures likely to be achieved in a repository can cause the expected transition to bulk flow migration in water-saturated concrete. Initial experimental work intended to establish the appropriate measurement methods is described along with the main experimental program. M.G.

N90-22748 United Kingdom Atomic Energy Authority, Harwell (England). Materials Development Div.
SOME OBSERVATIONS ON LIQUID FLOW THROUGH FILTERS
M. Roo and M. G. Nicholas Oct. 1988 27 p
(AERE-R-13300) Copyright Avail: Issuing Activity

A series of experiments were conducted to assess the relevance to filtration of the Poiseuille analysis of liquid flow in straight cylindrical pipes. Trials using glass filters through which water, ink and mercury flowed showed that the analysis was qualitatively relevant. As predicted, the flow rates were a simple function of the pressure difference across the filter and were proportional to the density/viscosity ratio of the liquids. However, qualitative predictions made using the Poiseuille analysis were inaccurate because of uncertainty about filter pore dimensions and the lack of flow through narrow pores when the liquid did not wet the filter material. Flow of a suspension was further complicated by the build up on the entry faces of filters of layers of particulates which acted as secondary filters. Author

N90-22749 Wisconsin Univ., Madison.
A NUMERICAL AND ANALYTICAL STUDY OF NORMAL STRESSES AND PRESSURE DIFFERENCES IN NON-NEWTONIAN CREEPING FLOWS Ph.D. Thesis
Minwu Yao 1989 308 p
Avail: Univ. Microfilms Order No. DA9009592

Analytical and numerical studies of some non-Newtonian creeping flows are pursued with particular interests in normal stresses and pressure differences. The study is started with the phenomenon of excess pressure rise across the pressure-hole which was observed in the Couette base flow over a transverse slot. This excess pressure rise phenomenon turns out to be very important in correctly applying the Higashitani and Pritchard (HP) theory. The correct application of HP theory involves a modified hole-pressure relation (MHPR). By studying the MHPR in streamline coordinate formulation, a fortuitous error cancellation phenomenon was found which provides a complete theoretical explanation for the paradox between an apparently flawed derivation and the fortunate success of the HP prediction. This error cancellation is proved to be exact for second-order fluid, and for Tanner's viscoelastic liquids under certain assumptions. For other non-Newtonian models, such as the Maxwell and modified Johnson-Segalman fluids, results also favor the error cancellation postulate. The theory numerical simulations of hole-pressure are

conducted for second-order, Maxwell and Johnson-Segalman fluids. Some important results and conclusions are presented for creeping flows. Two unperturbed shearing flows, i.e., the plane Poiseuille flow and plate-driven tangential annular flow of modified Johnson-Segalman fluid are also studied. By changing integral variable and solving a cubic equation at each location, exact steady solutions were obtained for these two flows. Both monotone and non-monotone stress-strain-rate relations are considered and complete formulation and solution procedures are developed. Then the analytical solution technique and results are applied to the hole-pressure error prediction, convergence study of FEM solutions and reliability verification of the numerical methods used in the hole-pressure simulation. Dissert. Abstr.

N90-22750 Arizona Univ., Tucson.
FLAT PLATE LEADING EDGE RECEPTIVITY TO VARIOUS FREESTREAM DISTURBANCE STRUCTURES Ph.D. Thesis
Roland Adolf Eberhar Heinrich 1989 238 p
Avail: Univ. Microfilms Order No. DA9010479

The receptivity process by which two-dimensional, time-harmonic freestream disturbances generate instability waves in the incompressible Blasius boundary layer is investigated analytically. The importance of the leading edge region and the linear nature of the receptivity process are discussed, and Goldstein's (1983a, 1983b) theoretical framework for the leading edge receptivity problem is reviewed. The approach utilizes asymptotic matching of a region further downstream, which is described by an Orr-Sommerfeld type equation. The linearized unsteady boundary layer equation is solved numerically, using the slip velocity and pressure gradient obtained from the inviscid interaction of the freestream disturbance with the semi-infinite plate. A new method is developed to extract the receptivity coefficient determines the amplitude of the instability wave - a quantity not available from classical stability theory. The freestream disturbances investigated are oblique plane acoustic waves, vortical gusts of various orientations convected downstream with freestream speed U (sub infinity), and a Karman vortex street passing above the plate surface with speed U (sub p). In addition, the case of a semi-infinite plate in a channel of finite width subject to an upstream traveling acoustic wave on the upper plate surface is considered. For oblique acoustic waves, the dominant receptivity mechanism is related to scattering of the waves by the leading edge. In contrast, the vortical gusts the receptivity produced by leading edge scattering is very small. The boundary layer receptivity to a Karman vortex street is found to be a strong function of the speed ratio U (sub p)/U (sub infinity). A pronounced influence of channel walls, which is related to the alternate cut-on of higher modes in the upstream and downstream channel halves, is found. A comparison of the present results with available experiments shows good qualitative and quantitative agreement.
Dissert. Abstr.

N90-22751 Purdue Univ., West Lafayette, IN.
AN INVESTIGATION OF THE THREE-DIMENSIONAL FLOW FIELD IN A CENTRIFUGAL COMPRESSOR Ph.D. Thesis
John Robert Fagan, Jr. 1989 218 p
Avail: Univ. Microfilms Order No. DA9008608

A series of experiments was performed to provide three-dimensional flow field data in centrifugal compressor passages and to describe the characteristic flow phenomena at the point of incipient rotating stall. These experiments entailed the acquisition and analysis of one-dimensional Laser Doppler Velocimeter (LDV) data in the impeller passages of the Purdue Research Centrifugal Compressor at two compressor operating points: the design operating point and the incipient rotating stall operating point. Additionally, the nature of compressor rotating stall was quantified by the acquisition and analysis of unsteady pressure data at the impeller inlet and exit. Finally, predictions at the design operating point from contemporary internal flow models were used for comparison with the LDV data. The LDV data taken at both operating points show the traditional jet-wake structure observed in many centrifugal compressors. The unsteady pressure data show three distinct modes of rotating stall in the compressor depending upon the mass flow rate. One mode is characterized by two stall patterns rotating concurrently with relative rotational speed below 15 percent of the impeller rotational speed. This mode occurs at the highest mass flow rate and is strongest at the impeller inlet. The other two rotating stall modes occur at reduced mass flow rates and are characterized by single rotating stall patterns. The patterns in both modes rotate with relative speeds exceeding 90 percent of the impeller rotational speed, with the patterns strongest at the diffuser inlet. The inviscid flow model did not successfully predict the compressor flow field. The viscous flow model achieved better success. It predicted the major phenomena in the flow field, specifically the wake structure near the end of the passage. However, the viscous model shows poor correlation with the data, predicting that the wake was located in the shroud suction corner different from the LDV results at the design operating point. Dissert. Abstr.

N90-22752 Yale Univ., New Haven, CT.
THE MULTIFRACTAL NATURE OF TURBULENCE Ph.D. Thesis
Charles Vivant Meneveau 1989 242 p
Avail: Univ. Microfilms Order No. DA9011914

The small-scale intermittency in fully developed turbulence is investigated, with special emphasis on its self-similar facets. This is done using a general formulation in terms of multifractals. Measurements are performed and interpreted in light of this formulation. First, the theory of general multiplicative processes and multifractal measures is presented, as well as the reasons for expecting multifractal distributions in fully developed turbulence. The following cascade models are described: Kolmogorov's 1941 theory, log-normality, Mandelbrot's random curdling, beta and alpha models, and binomial and multinomial processes. An attempt is made to rationalize the physical content of each of these models. Measurements of the field of dissipation epsilon along linear cuts are performed in laboratory and atmospheric turbulent flows, using Taylor's hypothesis. Using short data segments, the manifest portion of f(alpha) of epsilon is measured, and shown to have universal features. Also, long data segments obtained in a turbulent boundary layer are used to measure latent portions of f(alpha), confirming the idea (Mandelbrot 1988) that such portions can in principle be obtained from linear cuts. The results are compared with predictions of different cascade models, and the nature of dynamical information that can be inferred from the experimental results is discussed. The same procedure is applied to the field of dissipation chi of passive scalar fluctuations in several flows. The degree of intermittency of chi is found to be consistently higher than the intermittency of epsilon, thus suggesting different inertial-range dynamics for both quantities. Finally, a theory of multivariate multifractal distributions is developed and applied to simultaneous measurements of dissipation of kinetic energy and scalar variance. The results are compared with predictions from joint log-normal and joint binomial models. Dissert. Abstr.

N90-22753# Westinghouse Savannah River Co., Aiken, SC.
PARALLEL CHANNEL FLOW EXCURSIONS
Barry S. Johnson 1990 5 p Presented at the VPI Conference, Blacksburg, VA, 22 Jan. 1990
(Contract DE-AC09-89SR-18035)
(DE90-009129; WSRC-RP-89-1438; CONF-900187-1) Avail: NTIS HC A01/MF A01

Among the many known types of vapor-liquid flow instability is the excursion which may occur in heated parallel channels. Under certain conditions, the pressure drop requirement in a heated channel may increase with decreases in flow rate. This leads to an excursive reduction in flow. For channels heated by electricity or nuclear fission, this can result in overheating and damage to the channel. In the design of any parallel channel device, flow excursion limits should be established. After a review of parallel channel behavior and analysis, a conservative criterion is proposed for avoiding excursions. In support of this criterion, recent experimental work on boiling in downward flow is described.
DOE

N90-22754# Sandia National Labs., Albuquerque, NM. Fluid and Thermal Sciences Dept.

PHASE DOPPLER DROPLET SIZING: SCATTERING ANGLE EFFECTS

D. L. Ceman, T. J. OHern, and D. J. Rader 1990 12 p Presented at the ASME Fluid Measurements and Instrumentation Conference, Toronto, Ontario, 4-7 Jun. 1990

(Contract DE-AC04-76DP-00789)

(DE90-009571; SAND-90-0050C; CONF-9006155-1) Avail: NTIS HC A03/MF A01

The phase Doppler technique is an LDV-based method for the nonintrusive, simultaneous measurement of particle size, velocity, and concentration. It is becoming a standard device for measurement of spray droplets in air as well as cavitation nuclei bubbles in water. The Phase Doppler Particle Analyzer (PDPA) is a commercial phase Doppler instrument. Previous calibrations of the PDPA using well-characterized liquid droplets have revealed nonlinearity of the instrument response for droplet diameters less than 20 microns. For many applications, droplet sizing accuracy in the small diameter range is critical. Light scattering calculations performed by the instrument manufacturer suggest two theoretical approaches to improving the instrument response in this size range: optimizing the collection angle and increasing the collection area. The first approach has been tested experimentally. This paper presents size calibrations of the PDPA with the receiver configured at two angles: 30 degree (the standard configuration) and 70 degree off-forward axis. The calibration was performed with monodisperse oleic acid droplets in the diameter range 3.7 to 32 microns. As in earlier calibration studies, the 30 degree configuration resulted in marked nonlinearity in instrument response below 20 microns. Oscillations were still apparent for the 70 degree configuration, which showed only a modest improvement compared to the response at 30 degree. DOE

N90-22755# Edgerton, Germeshausen and Grier, Inc., Idaho Falls, ID.

HIGH TEMPERATURE CERAMIC-TUBED REFORMER

Joseph J. Williams, Robert A. Rosenberg, and Lane J. McDonough (Stone and Webster Engineering Corp., Boston, MA.) Mar. 1990 37 p Presented at the 1990 AIChE Spring Meeting on Advances in Synthesis Gas Preparation, Orlando, FL, 18-22 Mar. 1990

(Contract DE-FC07-88ID-12797)

(DE90-009617; EGG-M-90040; CONF-900391-5) Avail: NTIS HC A03/MF A01

The overall objective of the HiPHES project is to develop an advanced high-pressure heat exchanger for a convective steam/methane reformer. The HiPHES steam/methane reformer is a convective, shell and tube type, catalytic reactor. The use of ceramic tubes will allow reaction temperature higher than the current state-of-the-art outlet temperatures of about 1600 F using metal tubes. Higher reaction temperatures increase feedstock conversion to synthesis gas and reduce energy requirements compared to currently available radiant-box type reformers using metal tubes. Reforming of natural gas is the principal method used to produce synthesis gas (primarily hydrogen and carbon monoxide, H2 and CO) which is used to produce hydrogen (for refinery upgrading), methanol, as well as several other important materials. The HiPHES reformer development is an extension of Stone and Webster's efforts to develop a metal-tubed convective reformer integrated with a gas turbine cycle. DOE

N90-22756# Institut fuer Theoretische Stroemungsmechanik, Goettingen (Germany, F.R.). Abteilung Instabilitaeten und Abloesung.

NONLINEAR BIFURCATION STUDY OF PLANE POISEUILLE FLOW

Uwe Ehrenstein and Werner Koch Aug. 1989 118 p

(DLR-FB-89-42; ISSN-0171-1342; ETN-90-96453) Avail: NTIS HC A06/MF A01

Nonlinear traveling wave type secondary bifurcation branches are computed for plane Poiseuille flow in the search for a physically more relevant transition criterion. These solutions are approximated by truncated Fourier series in streamwise and spanwise direction together with Chebyshev collocation across the channel. Using the local results near bifurcation points, the global solution is found by Keller's continuation procedure. Several families of nonlinear equilibrium solutions can be distinguished. While searching for bicritical bifurcations, a new family of secondary bifurcation branches was discovered, which reduces the critical mean flow Reynolds number to about 100 and brings the friction factor into the range of the experimentally determined turbulent values. ESA

N90-22757# Institut National des Sciences Appliquees de Lyon, Villeurbanne (France). Lab. de Chimie Physique Appliquee et Environnement.

DESIGN AND CONSTRUCTION OF A PACKED COLUMN SIMULATOR OPERATING UNDER ATMOSPHERIC AND REDUCED PRESSURE Ph.D. Thesis [CONCEPTION ET REALISATION D'UN SIMULATEUR DE COLONNE GARNIE FONCTIONNANT SOUS PRESSION ATMOSPHERIQUE ET SOUS PRESSION REDUITE]

Abdelhamid Messaoudene 1989 249 p In FRENCH; ENGLISH summary

(ISAL-89-60; ETN-90-96612) Avail: NTIS HC A11/MF A02

Distillation under reduced pressure for the separation of constituants is considered. To avoid thermic damage in columns, the most important parameters are pressure loss and resistance time. The development of a simulator, enabling the determination of the hydrodynamic parameters with the mixture air-water under different pressures for any given mixture, is carried out. A bibliographic study and a reference study, performed with a test mixture on a pilot column under reduced pressure, packed with Raschig ring are presented. The simulator and the results obtained are reported. The main hydrodynamic parameters such as pressure drop, hold-ups and flooding rate were taken into account. The packed column was considered as a reactor and the results of the residence time distribution are reported. Theoretical models show that the packed column behaves as an association of continuous stirred-tank reactors in series. A comparison between the actual column results and the simulator results demonstrate the accuracy of the simulation. ESA

N90-22758# Commissariat a l'Energie Atomique, Saclay (France). Inst. de Recherches Fondamentales.

TURBULENCE AND COMPLEX SYSTEMS [TURBULENCE ET SYSTEMES COMPLEXES]

Paul Manneville Jan. 1989 31 p In FRENCH

(Contract IEP-87/822)

(ETN-90-96620) Avail: NTIS HC A03/MF A01

Phase turbulence, transition towards convection turbulence of low Prandtl Figures, and turbulence waves are discussed. Equations for turbulence analysis under a variety of situations are presented. Cellular automata and spatio-temporal intermittence in turbulence analysis are described. Modeling of spatio-temporal intermittence is discussed. Static properties near regions of transition are considered. Experimental evidence for some of the theories discussed is presented. Areas in which more research needs to be carried out are identified. ESA

N90-22759# Centre National de la Recherche Scientifique, Paris (France).

BOUNDARY LAYER TURBULENCE PULSED BY ACOUSTIC WAVES Final Report [COUCHE LIMITE TURBULENTE PULSEE PAR ONDES ACOUSTIQUES; RAPPORT FINAL DE SYNTHESE]

E. Brocher, R. Marmey, V. Pugliesi, J. P. Ardissone, P. Collini, and A. Andrianantoandro 1987 71 p In FRENCH

(Contract DRET-87-105)

(ETN-90-96621) Avail: NTIS HC A04/MF A01

The response of a turbulent bundary layer to an intense acoustic field is studied. The boundary layer is also submitted to a longitudinal pressure gradient. The tests are carried out at different frequencies. The influence of the reflexion coefficient on the response of the turbulent boundary layer is shown to be very important. When this coefficient is low, the amplification is relatively

uniform over the length of the plate. When the coefficient is high, the amplification is strong. A periodicity of response is seen along the length of the plate. ESA

N90-22760# Ecole Nationale Superieure de Mecanique, Nantes (France). Lab. d'Hydrodynamique Navale.
MULTIGRID ACCELERATION OF TRANSONIC FLOW COMPUTATIONS Final Report [UTILISATION D'ALGORITHMES IMPLICITES POUR LE CALCUL DE L'ECOULEMENT VISQUEUX COMPRESSIBLE DANS UNE GRILLE DE PROFILS, RAPPORT FINAL]
G. Capdeville and J. Piquet 25 Mar. 1989 151 p In FRENCH
(Contract DRET-87-34-256-00-470-75-01)
(ENSM-8024; ETN-90-96622) Avail: NTIS HC A08/MF A01

Acceleration techniques to speed the resolution of compressible Navier-Stokes equations are presented. Several implicit methods are tested on different two dimensional configurations. Unless acceleration techniques are used, even on supercomputers the resolution of compressible Navier-Stokes equations require long computing times. The combination of implicit methods with multigrid techniques is shown to lead to efficient steady state computations. Characteristics of separated turbulent flow resulting from shock-boundary layer interaction are studied. The use of implicit methods to describe blade-to-blade flow is discussed. ESA

N90-22761*# National Aeronautics and Space Administration. Lewis Research Center, Cleveland, OH.
ACQUISITION AND CORRELATION OF CRYOGENIC NITROGEN MASS FLOW DATA THROUGH A MULTIPLE ORIFICE JOULE-THOMSON DEVICE
S. Stephen Papell (Analex Corp., Cleveland, OH.), Naseem H. Saiyed, and Ted W. Nyland May 1990 23 p
(NASA-TM-103121; E-5449; NAS 1.15:103121) Avail: NTIS HC A03/MF A01 CSCL 20D

Liquid nitrogen mass flow rate, pressure drop, and temperature drop data were obtained for a series of multiple orifice Joule-Thomson devices, known as Visco Jets, over a wide range of flow resistance. The test rig used to acquire the data was designed to minimize heat transfer so that fluid expansion through the Visco Jets would be isenthalpic. The data include a range of fluid inlet pressures from 30 to 60 psia, fluid inlet temperatures from 118 to 164 R, outlet pressures from 2.8 to 55.8 psia, outlet temperatures from 117 to 162 R and flow rate from 0.04 to 4.0 lbm/hr of nitrogen. A flow rate equation supplied by the manufacturer was found to accurately predict single-phase (noncavitating) liquid nitrogen flow through the Visco Jets. For cavitating flow, the manufacturer's equation was found to be inaccurate. Greatly improved results were achieved with a modified version of the single-phase equation. The modification consists of a multiplication factor to the manufacturer's equation equal to one minus the downstream quality on an isenthalpic expansion of the fluid across the Visco Jet. For a range of flow resistances represented by Visco Jet Lohm ratings between 17,600 and 80,000, 100 percent of the single-phase data and 85 percent of the two-phase data fall within + or - 10 percent of predicted values. Author

N90-22762# Houston Univ., TX. Dept. of Mathematics.
NONSTRICTLY HYPERBOLIC CONSERVATION LAWS Final Report, 15 May 1986 - 14 Nov. 1989
Barbara Lee Keyfitz 14 Nov. 1989 7 p
(Grant AF-AFOSR-0088-86; AF Proj. 2304)
(AD-A218525; AFOSR-90-0233TR) Avail: NTIS HC A02/MF A01 CSCL 20/4

This project has centered on formulating and solving mathematical problems that arise in the study of systems of conservation laws that are not of the classical, strictly hyperbolic type. Potential applications for these results are found in models for three-phases flow in porous media, for compressible two-phase flow, and for flow in elastic and elastoplastic materials (including continuum models for granular flow). Modeling of many different flow processes has led to systems of conservation laws in which the classical assumptions breakdown in a way which leads to distrust of the models. Research in this and allied projects is directed at extending the mathematical theory of conservation laws. The practical goal of this research is to discover which models are well-posed, and, hence, to enable applied scientists to discover which are correct descriptions of various observed instabilities. GRA

N90-22763# Ballistic Research Labs., Aberdeen Proving Ground, MD.
SIDE MOMENT EXERTED BY A SPINNING, CONING, HIGHLY VISCOUS LIQUID PAYLOAD
Charles H. Murphy, James W. Bradley, and William H. Mermagen, Sr. Dec. 1989 87 p
(DA Proj. 1L1-62618-AH-80)
(AD-A218746; BRL-TR-3074) Avail: NTIS HC A05/MF A01 CSCL 16/3

Four liquid payload theories-Stewartson (S), Stewartson-Wedemeyer (SW), Kitchens-Gerber-Sedney (KGS), and Hall-Sedney-Gerber (HSG)—are developed within a single unifying framework. Equations are presented that form the basis of interactive computer programs. These programs apply the SW, KGS, HGS, and HSG theories not only to their original domain, fully filled cylinders, but to partially filled cylinders, cylinders with a central rod and cylinders containing two liquids. Side moment coefficients from the relatively simple KGS calculations are shown to be a good approximation to results from the more exact HSG theory. GRA

N90-22764# Naval Research Lab., Washington, DC. Lab. for Computational Physics and Fluid Dynamics.
PSEUDO-STEADY DIFFUSIONAL GROWTH OR COLLAPSE OF BUBBLES RISING IN TIME DEPENDENT PRESSURE FIELDS Final Report
M. Cerza (David Taylor Research Center, Bethesda, MD.), O. M. Griffin, and M. B. Stewart 13 Mar. 1990 34 p
(AD-A218825; NRL-MR-6584) Avail: NTIS HC A03/MF A01 CSCL 20/4

A pseudo-steady convective model for bubble diffusional growth or collapse while rising in time dependent pressure fields has been developed. The bubble model assumes the neglect of added mass, history, and interfacial momentum terms. Criteria are developed to show when these terms affect the bubble motion.The pressure fields investigated are a simple hydrostatic head, a decompression hydrostatic head, and a hydrostatic head with the oscillation of the reference pressure (atmosphere above the hydrostatic head). GRA

N90-22765# Michigan Univ., Ann Arbor. Dept. of Aerospace Engineering.
HOLOCINEMATOGRAPHY FOR STUDIES OF TURBULENT MULTIPHASE FLOW Final Report, 15 Dec. 1988 - 15 Dec. 1989
G. M. Faeth, G. A. Ruff, and L. P. Bernal 15 Jan. 1990 29 p
(Contract DAAL03-89-G-0004)
(AD-A219130; GDL/GMF-90-02; ARO-26612.1-EG-EQ) Avail: NTIS HC A03/MF A01 CSCL 14/1

The development of a high speed holocinematography system for 3-D time-dependent measurements of the dynamics of dispersed flows is described. An on-line system based on a copper-vapor laser was assembled and used to obtain holocinematogram film strips of a particle-containing flow field. The present system can operate at framing rates up to 6000 holograms per second, yielding film strips up to 70 holograms long with a field of view having a diameter of 35 mm and a length of 120 mm. Extension to an off-axis configuration, for higher resolution also appears to be feasible. Either configuration provides unprecedented capabilities for studying laminar and turbulent single or multiphase flow phenomena that are not accessible using existing methods. GRA

N90-22766# Pennsylvania State Univ., University Park. Applied Research Lab.
FUNDAMENTAL HYDRODYNAMICS RESEARCH Quarterly Technical Progress Report, 1 Oct. - 31 Dec. 1989
S. A. Abdallah, M. L. Billet, H. L. Petrie, P. J. Morris, and S. Deutsch 31 Dec. 1989 27 p
(Contract N00014-87-K-0196)
(AD-A219179) Avail: NTIS HC A03/MF A01 CSCL 20/4

The hydrodynamics research conducted under this program falls into two basic thrust areas: (1) Turbomachinery - To develop an improved understanding of the fluid mechanics and acoustics associated with low speed turbomachines and marine propulsors. To employ this knowledge to the development of improved propulsor and turbomachine design methods; and (2) Drag Reduction - To develop fundamental understanding of the mechanisms that cause drag on bodies and surfaces and to explore novel methods to reduce drag. GRA

N90-23172# Office of Naval Research Liaison Office, Far East, APO San Francisco, CA.
CURRENT JAPANESE SUPERCOMPUTERS FOR COMPUTATIONAL FLUID DYNAMICS APPLICATIONS
Hideo Yoshihara *In its* ONR Far East Scientific Information Bulletin, Volume 13, No. 4 Dec. 1988 p 61-68 (For primary document see N90-23168 16-70)
Avail: NTIS HC A05/MF A01 CSCL 20L

35 INSTRUMENTATION AND PHOTOGRAPHY

Includes remote sensors; measuring instruments and gages; detectors; cameras and photographic supplies; and holography.

For aerial photography see *43 Earth Resources and Remote Sensing*. For related information see also *06 Aircraft Instrumentation*, and *19 Spacecraft Instrumentation*.

N90-22767*# EPITAXX, Inc., Princeton, NJ.
DEVELOPMENT OF A UNIQUE LABORATORY STANDARD INDIUM GALLIUM ARSENIDE DETECTOR FOR THE 500 TO 1700 MICRON SPECTRAL REGION, PHASE 2 Final Report
Vladimir S. Ban and Gregory H. Olsen 31 May 1990 50 p Original contains color illustrations
(Contract NAS5-30312)
(NASA-CR-180482; NAS 1.26:180482) Avail: NTIS HC A03/MF A01; 1 functional color page CSCL 14B

In the course of this work, 5 mm diameter InGaAs pin detectors were produced which met or exceeded all of the goals of the program. The best results achieved were: shunt resistance of over 300 K ohms; rise time of less than 300 ns; contact resistance of less than 20 ohms; quantum efficiency of over 50 percent in the 0.5 to 1.7 micron range; and devices were maintained and operated at 125 C without deterioration for over 100 hours. In order to achieve the goals of this program, several major technological advances were realized, among them: successful design, construction and operation of a hydride VPE reactor capable of growing epitaxial layers on 2 inch diameter InP substrates with a capacity of over 8 wafers per day; wafer processing was upgraded to handle 2 inch wafers; a double layer Si3N4/SiO2 antireflection coating which enhances response over the 0.5 to 1.7 micron range was developed; a method for anisotropic, precisely controlled CH4/H2 plasma etching for enhancement of response at short wavelengths was developed; and electronic and optical testing methods were developed to allow full characterization of detectors with size and spectral response characteristics. On the basis of the work and results achieved in this program, it is concluded that large size, high shunt resistance, high quantum efficiency InGaAs pin detectors are not only feasible but also manufacturable on industrial scale. This device spans a significant portion of visible and near infrared spectral range and it will allow a single detector to be used for the 0.5 to 1.7 micron spectral region, rather than the presently used silicon (for 0.5 to 1.1 microns) and germanium (0.8 to 1.7 microns). Author

N90-22768# Edgerton, Germeshausen and Grier, Inc., Idaho Falls, ID.
A COMPACT PORTABLE DIFFRACTION MOIRE INTERFEROMETER
V. A. Deason and M. B. Ward 1989 6 p Presented at the 3rd International Conference on Laser Interferometry, San Diego, CA, 6-11 Aug. 1989
(Contract DE-AC07-76ID-01570)
(DE90-009780; EGG-M-89050; CONF-8908222-1) Avail: NTIS HC A02/MF A01

This device utilizes single mode polarization maintaining optical fibers to generate the pair of laser beams required by diffraction moire interferometry. Design of the device permits extremely rapid and convenient setup for measurement of in-plane displacement distributions on the surfaces of specimens. The device, applications, and typical data are described. DOE

N90-22769* National Aeronautics and Space Administration. Pasadena Office, CA.
ATMOSPHERIC AUTOROTATING IMAGING DEVICE Patent
James D. Burke, inventor (to NASA) 12 Dec. 1989 7 p Filed 13 Jun. 1988 Supersedes N88-24944 (26 - 18, p 2519) Prepared in cooperation with Jet Propulsion Lab., California Inst. of Tech., Pasadena
(Contract NAS7-918)
(NASA-Case-NPO-17390-1-CU; US-Patent-Appl-SN-205899; US-Patent-Class-244-1R; US-Patent-Class-244-138A; US-Patent-Class-358-109; Int-Patent-Class-B64D-1/00) Avail: US Patent and Trademark Office CSCL 14B

This invention relates to a scanning imaging device for deployment in either terrestrial or extraterrestrial atmospheres. An object of the present invention is to provide an extremely simple device that, upon deployment in an atmospheric environment, automatically rotates without the use of a propulsion system. An image detector appropriately disposed therein scans a panoramic view with each rotation of the device. Data gathered by the image detector may be transmitted to a remote receiver. The present invention may be particularly useful in the exploration of, for example, the Martian surface. The novelty of the present invention resides in the ability of the device to scan an image without the use of any moving parts or the expenditure of fuel energy.
Official Gazette of the U.S. Patent and Trademark Office

N90-22770* National Aeronautics and Space Administration. Langley Research Center, Hampton, VA.
QUANTITATIVE SURFACE TEMPERATURE MEASUREMENT USING TWO-COLOR THERMOGRAPHIC PHOSPHORS AND VIDEO EQUIPMENT Patent
Gregory M. Buck, inventor (to NASA) 5 Dec. 1989 7 p Filed 13 Jun. 1988 Supersedes N88-30105 (26 - 24, p 3376)
(NASA-Case-LAR-13740-1; US-Patent-Appl-SN-205900; US-Patent-Class-358-93; US-Patent-Class-250-459.1; US-Patent-Class-250-461.1; US-Patent-Class-358-113; US-Patent-Class-374-162; Int-Patent-Class-H04N-7/18) Avail: US Patent and Trademark Office CSCL 14B

A thermal imaging system provides quantitative temperature information and is particularly useful in hypersonic wind tunnel applications. An object to be measured is prepared by coating with a two-color, ultraviolet-activated, thermographic phosphor. The colors emitted by the phosphor are detected by a conventional color video camera. A phosphor emitting blue and green light with a ratio that varies depending on temperature is used so that the intensity of light in the blue and green wavelengths detected by the blue and green tubes in the video camera can be compared. Signals representing the intensity of blue and green light at points on the surface of the model in a hypersonic wind tunnel are used to calculate a ratio of blue to green light intensity which provides quantitative temperature information for the surface of the model.
Official Gazette of the U.S. Patent and Trademark Office

N90-22771# Rome Univ. (Italy). Dipt. di Fisica.
REDUCED SIZE HOLOGRAPHY
Daniele Fargion 6 Oct. 1989 11 p Submitted for publication
(Preprint-707; ETN-90-96530) Avail: NTIS HC A03/MF A01

The cancellation of the nonlinear aberration in optical systems for holographic three dimensional reduction is demonstrated. Telescope-like images and more elaborate zoom-like systems are shown to produce undistorted three dimensional demagnified images, within a range of arbitrary magnification values. The role of the reduction-enlargement system in holography may lead to a new holographic display approach where small size diapositive-like holograms are projected by an inverse telescope system to larger real-like images. ESA

N90-22772# Aerospatiale Aquitaine, Saint-Medard en Jalles (France).
LARGE SCALE METROLOGY BY COMPUTER ASSISTED PHOTOGRAMMETRY [METROLOGIE DES GRANDES DIMENSIONS PAR PHOTOGRAMMETRIE ASSISTEE PAR ORDINATEUR]
P. Barbier and D. Loubet Sep. 1989 7 p In FRENCH
(Rept-892-430-116; ETN-90-96647) Avail: NTIS HC A02/MF A01

An industrial application of tank deformation measurement techniques is presented. Pressure tests carried out using monoscopic photogrammetry are described. The technique involves photographing the point at which deformation measurement is required, then carrying out optical analysis of the photograph supplemented by computer-aided image analysis. The technique is used in testing helium tanks destined for use in satellites and launchers. The difficulty of using traditional measuring instruments, or theodolites coupled to computer systems, in measuring deformations of kevlar tanks such as these during pressure tests, necessitates development of photogrammetric of techniques. ESA

N90-22773*# National Aeronautics and Space Administration. Lewis Research Center, Cleveland, OH.
A FIBER-OPTIC CURRENT SENSOR FOR AEROSPACE APPLICATIONS
Richard L. Patterson, A. H. Rose, D. Tang, and G. W. Day (National Inst. of Standards and Technology, Boulder, CO.) 1990 7 p Proposed for presentation at the 25th Intersociety Energy Conversion Engineering Conference, Reno, NV, 12-17 Aug. 1990; cosponsored by AIChE, SAE, ACS, AIAA, ASME, and IEEE
(NASA-TM-103152; E-5513; NAS 1.15:103152) Avail: NTIS HC A02/MF A01 CSCL 14B

A robust, accurate, broad-band, alternating current sensor using fiber optics is being developed for space applications at power frequencies as high as 20 kHz. It can also be used in low and high voltage 60 Hz terrestrial power systems and in 400 Hz aircraft systems. It is intrinsically electromagnetic interference (EMI) immune and has the added benefit of excellent isolation. The sensor uses the Faraday effect in optical fiber and standard polarimetric measurements to sense electrical current. The primary component of the sensor is a specially treated coil of single-mode optical fiber, through which the current carrying conductor passes. Improved precision is accomplished by temperature compensation by means of signals from a novel fiber-optic temperature sensor embedded in the sensing head. The technology contained in the sensor is examined and the results of precision tests conducted at various temperatures within the wide operating range are given. The results of early EMI tests are also given. Author

N90-22774# Pennsylvania State Univ., University Park.
TWO-DIMENSIONAL VELOCIMETRY INSTRUMENTATION Final Report, 1 Dec. 1988 - 30 Nov. 1989
Domenic A. Santavicca 30 Jan. 1990 3 p
(Grant AF-AFOSR-0137-89; AF Proj. 3842)
(AD-A218450; AFOSR-90-0202TR) Avail: NTIS HC A01/MF A01 CSCL 14/2

The acquisition and implementation of instrumentation which will be used to make 2-D velocimetry measurements in a study of premixed turbulent flames is examined. GRA

N90-22775# Rochester Univ., NY. Inst. of Optics.
HIGH PERFORMANCE HOLOGRAPHIC ELEMENTS AND MEDIA Final Technical Report, 1 Aug. 1987 - 31 Jan. 1990
Nicholas George Dec. 1989 18 p
(Contract DAAL03-87-K-0100)
(AD-A218999; ARO-24730.8-PH) Avail: NTIS HC A03/MF A01 CSCL 14/1

Research in the field of holographic optical elements is summarized for the contract period of August 1, 1987 to January 31, 1990. The basic understanding of structure and mechanism of a high performance holographic photopolymer has been extended. Further, novel holographic elements and systems based on these elements have been devised. Discussion of these results is presented. GRA

36 LASERS AND MASERS

Includes parametric amplifiers.
For related information see also *76 Solid-State Physics.*

N90-22776 Stanford Univ., CA.
A FREE ELECTRON LASER MASTER OSCILLATOR POWER AMPLIFIER EXPERIMENT Ph.D. Thesis
Louis C. Vintro 1989 89 p
Avail: Univ. Microfilms Order No. DA8925969

Optimization of gain in a Free Electron Laser Master Oscillator-Power Amplifier system is examined. The parameters explored include the extent of overlap of the electron and light beams in the interaction region and the type of optical mode matching into the amplifier. With these parameters optimized, the behavior of the gain as a function of the amplifier resonance parameter was studied. A time-resolving detection system allowed us to make the measurements at the small signal level. The data acquired shows that a small signal gain of 60 percent per pass in the amplifier was achieved. That result places the amplifier system in the intermediate gain regime. Varying the degree of overlap of electron and optical beams yielded a measure of the physical dimensions of the electron beam. In the longitudinal direction, it was concluded that the electron beam had a square wave distribution. The data from the mode matching experiment is in agreement with the results from the low-gain theory. Yet the measured gain versus resonance parameter curve differs from the symmetric, low gain curve predicted by the Madey theorem: it exhibits an asymmetry in the amplitude of the peak gain with respect to that of the peak loss configuration. This result represents the first evidence of the violation of the Madey theorem in the high gain regime. Computer simulations using the FELEX FEL code at Los Alamos National Laboratory, agree well with the measurements obtained. Dissert. Abstr.

N90-22777 United Kingdom Atomic Energy Authority, Harwell (England). Materials Physics and Metallurgy Div.
APPLICATIONS OF LASER ULTRASOUND
C. B. Scruby Aug. 1988 51 p
(AERE-R-13106) Copyright Avail: Issuing Activity

Laser techniques for generating and receiving ultrasound have potential for a wide range of noncontact ultrasonic measurements, and have received considerable interest over the past decade. After a brief review of the physical principles underlying the generation and reception of ultrasound, the characteristics of lasers used as noncontract ultrasonic probes are reviewed. Laser ultrasonic techniques are only likely to find industrial application where they answer a need that cannot be met by conventional transducers, for instance deployment at elevated temperatures; where access is limited, or where exceptionally high spatial or temporal resolution is needed. In addition to transducer calibration, where laser techniques are already established, some potential industrial applications for laser ultrasound are discussed illustrated

by examples of recent laboratory demonstrations of its potential for nondestructive testing and materials characterization are discussed. Author

N90-22778 Alabama Univ., University.
CONTRIBUTIONS TO THE DEVELOPMENT OF SLM TEA CO2 LASER SOURCES FOR HIGH RESOLUTION MOLECULAR SPECTROSCOPY Ph.D. Thesis
Mohammad Abdur Rob 1989 240 p
Avail: Univ. Microfilms Order No. DA9008418

The emission spectrum of the carbon-dioxide (CO2) laser has an excellent overlap with the ro-vibrational absorption spectrum of a large number of polar molecules. Optical pumping of these molecules by CO2 lasers has produced well over 3000 far-infrared (FIR) laser lines. The molecular transitions for a large number of lines pumped by the narrow-band CW CO2 laser were identified. However, very few lines pumped by the pulsed TEA CO2 laser were assigned. This is due, in part, to the large uncertainty in both the pump and the FIR laser frequencies. Moreover, pumping with a given rotational line in the TEA CO2 laser output spectrum usually produces multiple FIR laser lines. This situation could be improved by the development of a narrow-band TEA CO2 laser, comparable in bandwidth to the width of typical absorption lines, in the FIR laser medium. Spectroscopic techniques making use of narrow-linewidth pulsed pump lasers would greatly facilitate the assignment of the infrared absorption transitions and the FIR laser lines. The narrow-linewidth pulsed laser would also be useful in many other applications. In the present series of experiments, three different techniques were investigated that produce high-power, tunable, single-longitudinal-mode (SLM) operation in a TEA CO2 laser. For the first time, the three SLM TEA CO2 laser configurations which were developed, along with another promising technique which is described in the literature, were analyzed on a common basis; so that their respective performance characteristics can be readily compared. This analysis facilitates the choice of the optimum laser system for a given task. Using a wedged etalon and a pyroelectric detector array combination, it was also shown directly that the intermodal tuning curve for the SLM TEA CO2 laser is a simple staircase function, with the laser output moving discontinuously from one mode to the next in a very regular fashion as the wavelength scan proceeds. To investigate the usefulness of the TEA CO2 laser as a FIR laser pump, a near-optimum dielectric waveguide FIR laser cavity was designed and constructed. Dissert. Abstr.

N90-22779# Lawrence Livermore National Lab., CA.
[LASER PROGRAM OF THE LAWRENCE LIVERMORE NATIONAL LABORATORY] Annual Report, 1987
Eleanor ONeal, ed., Peter W. Murphy, ed., and L. W. Coleman, ed. Jul. 1989 669 p
(Contract W-7405-eng-48)
(DE90-008198; UCRL-50021-87) Avail: NTIS HC A99/MF A04

The following topics are discussed: target design and experiments; target materials development; laboratory x ray lasers; laser science and technology; high average power solid state lasers; and inertial confinement fusion applications studies. DOE

N90-22780# Maryland Univ., College Park. Dept. of Electrical Engineering.
MEASUREMENTS AND SIMULATION OF CONTROLLED BEAMFRONT MOTION IN THE LASER CONTROLLED COLLECTIVE ACCELERATOR
R. L. Yao, W. W. Destler, C. D. Striffler, J. Rodgers, and Z. Segalow 1989 4 p Presented at the 1989 IEEE Particle Accelerator Conference, Chicago, IL, 20-24 Mar. 1989 Sponsored in part by AFOSR, Washington, DC
(Contract DE-AC05-85ER-40216)
(DE90-009992; CONF-890335-277) Avail: NTIS HC A01/MF A01

In the Laser Controlled Collective Accelerator, an intense electron beam is injected at a current above the vacuum space charge limit into an initially evacuated drift tube. A plasma channel, produced by time-sequenced, multiple laser beam ionization of a solid target on the drift tube wall, provides the necessary neutralization to allow for effective beam propagation. By controlling the rate of production of the plasma channel as a function of time down the drift tube, control of the electron beamfront can be achieved. Recent experimental measurements of controlled beamfront motion in this configuration are presented, along with results of ion acceleration experiments conducted using two different accelerating gradients. These results are compared with numerical simulations of the system in which both controlled beamfront motion and ion acceleration is observed consistent with both design expectations and experimental results. DOE

N90-22781# Deutsche Forschungsanstalt fuer Luft- und Raumfahrt, Stuttgart (Germany, F.R.). Inst. fuer Technische Physik.
COMPARISON OF SOLAR PUMPED Nd:YAG AND Nd:Cr:GSGG LASERS AT LIQUID NITROGEN AND ROOM TEMPERATURE
Uwe Brauch, Josef Muckenschnabel, Amnon Yogev, Ruth Benmair, Yoram Noter, Moshe Oron, and Andre Brauch (Soreq Research Establishment, Israel Atomic Energy Commission, Yavneh.) Jun. 1989 48 p Prepared in cooperation with Weizmann Inst. of Science, Rehovoth, Israel
(DLR-FB-89-41; ISSN-0171-1342; ETN-90-96452) Avail: NTIS HC A03/MF A01

The comparison of solar pumped laser oscillators made of Nd:YAG and Nd:Cr:GSGG rods was carried out at 77 and 300 K. The comparison included the powers achieved at various output coupling mirrors and a study of the beam divergence. The study shows that good quality beams, about four times the diffraction limit can be extracted from a rod of 5 mm and 62 mm exposed length. Maximal slope efficiency is 3.4 percent. The powers are 30 percent higher in the GSGG case than in the YAG case. The two cold runs show 3 times higher power than the 300 K runs. The results establish a sound base for the design of a high continuous wave power cold laser. ESA

N90-22782# Rome Univ. (Italy). Dipt. di Fisica.
GRAVITATIONAL RADIATION PRODUCED BY HIGH ENERGY ACCELERATORS AND HIGH POWER LASERS
Giordano DiambriniPalazzi 11 Sep. 1989 12 p Presented at the 14th International Conference on High Energy Accelerators, Tsukuba, Japan, 22-26 Aug. 1989
(Preprint-701; ETN-90-96524) Avail: NTIS HC A03/MF A01

A study of particle accelerators and the possibility of developing very high power lasers and masers to produce sources of detectable Gravitational Waves (GWs) is presented. Peculiar features of the GW, such as the higher frequency than expected from astrophysical sources, are considered. A configuration of the detector, consisting of a two resonant and coupled RF cavities at right angles, is considered. ESA

N90-22783# Aerospatiale, Paris (France).
MEASUREMENT AND VISUALIZATION OF THE SHOCK WAVE CAUSED BY THE IMPACT OF A PULSED YAG LASER IN WATER [MESURE ET VISUALISATION DE L ONDE DE CHOC CREEE PAR UN IMPACT LASER YAG PULSE DANS L EAU]
M. H. Puech 1989 51 p In FRENCH Presented at the 3d International Symposium on the Comportement des Milieux Denses sous Hautes Pressions Dynamiques, La Grande Motte, France, 5-9 Jun. 1989
(Rept-892-430-113; ETN-90-96644) Avail: NTIS HC A04/MF A01

The shock waves caused by a pulsed YAG laser in an aqueous medium are studied with a view to using such lasers in ophthalmology. The shock waves produced by a nanosecond pulsed YAG laser are shown to propagate spherically. The shock pressure was not measured due to the unavailability of a shock receptor of small enough size. Visualization techniques are concluded to be more appropriate for this type of study. Results of tests carried out using a picosecond laser produced by the Biophisic medical company are presented. Jitter of this laser did not permit valid measurement. ESA

N90-22784*# National Aeronautics and Space Administration. Lewis Research Center, Cleveland, OH.
TWO-DIMENSIONAL SURFACE STRAIN MEASUREMENT BASED ON A VARIATION OF YAMAGUCHI'S LASER-SPECKLE STRAIN GAUGE
John P. Barranger 1990 12 p Presented at the Conference on Optical Testing and Metrology 3, San Diego, CA, 8-13 Jul. 1990; sponsored by Society of Photo-Optical Instrumentation Engineers
(NASA-TM-103162; E-5530; NAS 1.15:103162) Avail: NTIS HC A03/MF A01 CSCL 20E

A novel optical method of measuring 2-D surface strain is proposed. Two linear strains along orthogonal axes and the shear strain between those axes is determined by a variation of Yamaguchi's laser-speckle strain gage technique. It offers the advantages of shorter data acquisition times, less stringent alignment requirements, and reduced decorrelation effects when compared to a previously implemented optical strain rosette technique. The method automatically cancels the translational and rotational components of rigid body motion while simplifying the optical system and improving the speed of response. Author

N90-22785# Rochester Univ., NY. Inst. of Optics.
INTERACTION OF ATOMIC HYDROGEN WITH PICO- AND FEMTOSECOND LASER PULSES Ph.D. Thesis
Jonathan S. Parker Dec. 1989 149 p
(Contract DAAL03-86-K-0173)
(AD-A218426; ARO-24626.126-PH-UIR) Avail: NTIS HC A07/MF A01 CSCL 07/5

This thesis presents a theoretical study of the interaction of atomic hydrogen with coherent laser pulses in the 5 femtosecond to 10 picosecond range, in the weak-field limit, and in intense fields. We approach the problem in the weak-field limit by studying the relationship between the Fourier relation of the laser pulse (Delta omega Delta t) and the (Delta E Delta t) relation of the atomic Rydberg wave packet generated by the laser pulse. A derivation of the wave packet based on the WKB approximation is given, permitting the quantity Delta t to be derived for the quantum state, with the conclusion that under certain circumstances a transform-limited laser pulse (satisfying Delta omega Delta t = 1/2) can generate a transform-limited electron (satisfying Delta E Delta t/h = 1/2). A population-trapping effect is found numerically and modeled theoretically. Despite the high field intensities, population representing the excited electron is recaptured from the ionization continuum by bound states during the excitation. Population returns to the atom with just the right phase to strongly inhibit ionization. A theory is presented that models this effect for a variety of laser pulse shapes, with and without the rotating-wave approximation. The numerical integration reveals that a certain amount of above-threshold ionization (ATI) occurs. GRA

N90-22786# Rochester Univ., NY. Inst. of Optics.
DYNAMICS AND INSTABILITIES IN HOMOGENEOUSLY BROADENED LASERS Ph.D. Thesis
Karl William Koch, III Dec. 1989 164 p
(Contract DAAL03-86-K-0173)
(AD-A218427; ARO-24626.127-PH-UIR) Avail: NTIS HC A08/MF A01 CSCL 09/3

This thesis describes theoretical and experimental studies of a homogeneously broadened ring dye laser; particularly the two frequency instability in which a bichromatic field emerges from the laser above the instability threshold. The interaction of a bichromatic field with an isolated atomic resonance is examined. The time averaged inversion and the saturated gain exhibit structure in the form of a series of subharmonic resonances. The stability of a strong bichromatic laser field to the growth of a subharmonic probe field is examined. The gain of the subharmonic bichromatic probe field in the presence of the strong bichromatic laser field is calculated. The strong bichromatic field is stable to the growth of the subharmonic fields when the modulation frequency of the strong field coincides with the Rabi frequency of the lasing transition. The existence of chaos in a strongly driven nonlinear system is experimentally investigated in a multimode ring dye laser. A dye laser is pumped with a modulated pump source. The response of the dye laser to commensurate and incommensurate modulations is reported. For commensurate modulations, the dye laser responds in a periodic fashion and the RF spectrum of the dye is composed of a series of harmonics. For incommensurate modulations, the dye laser responds in a quasiperiodic fashion with a broadband RF spectrum. GRA

N90-23166# Joint Publications Research Service, Arlington, VA.
SHAPING RADIATION PATTERN OF EXCIMER LASER BY MEANS OF CONTROLLABLE INTRACAVITY MIRROR Abstract Only
A. S. Akhmanov, M. A. Borontsov, A. V. Kudryashov, V. Ya. Panchenko, V. K. Popov, A. Yu. Poroykov, and V. I. Shmalgauzen *In its* JPRS Report: Science and Technology. USSR: Physics and Mathematics 3 Mar. 1989 p 10 Transl. into ENGLISH from Kvantovaya Elektronika (Moscow, USSR), v. 15, no. 8(194), Aug. 1988 p 1525-1526 (For primary document see N90-23162 16-70)
Avail: NTIS HC A03/MF A01

N90-23167# Joint Publications Research Service, Arlington, VA.
TUNABLE XeCl-LASER FEATURING HIGH SPECTRAL LUMINANCE Abstract Only
V. Ch. Belash, V. A. Kartazayev, S. Z. Lipinskiy, and V. L. Naumovich *In its* JPRS Report: Science and Technology. USSR: Physics and Mathematics 3 Mar. 1989 p 10 Transl. into ENGLISH from Kvantovaya Elektronika (Moscow, USSR), v. 15, no. 8(194), Aug. 1988 p 1545-1547 Original language document was announced in IAA asA89-18605 (For primary document see N90-23162 16-70)
Avail: NTIS HC A03/MF A01

37 MECHANICAL ENGINEERING

Includes auxiliary systems (nonpower); machine elements and processes; and mechanical equipment.

N90-22787 Pennsylvania State Univ., University Park.
ROBUST CONTROL OF VIBRATION IN FLEXIBLE STRUCTURES Ph.D. Thesis
Chi-Kuan Kao 1989 154 p
Avail: Univ. Microfilms Order No. DA9007877

Robust algorithms are developed for the control of vibration in flexible structures. These algorithms are based on the sliding mode control theory and can be designed to yield a satisfactory performance if the bounds on the parameters' errors are known. The algorithms were developed for both the independent modal space control system and the coupled modal space control system when the bounds on the system parameters' errors are known. An explicit method to construct the desired sliding hyperplanes for coupled modal sliding mode control is formulated. Boundary layers are used around the sliding hyperplanes to eliminate the chattering phenomenon. Three types of steady state solutions for the closed loop system inside the boundary layers are found: the zero solution, the constant nonzero solution and the limit cycle. The amplitude and frequency of the limit cycle were estimated by the describing function approach. Thus, the steady state vibration in the controlled modes and in the residual modes can be evaluated. Numerical examples with a simply supported beam and a flexible tetrahedral truss structure are presented to verify the theoretical analyses. The sliding mode control algorithm was also formulated when states are estimated using an observer. Singular-value approach is used to study the robustness of this control system to observation spillover. For the simply supported beam structure, the natural frequencies are well separated. To have a robust system in this case, the desired sliding manifold and the Luenberger's observer gain matrix can be found by the pole-placement method. However, to have a robust system for the flexible tetrahedral truss structure with closely lumped natural frequencies, it is necessary to use the linear quadratic method for the construction of the

desired sliding manifold and the Kalman filter with fictitious noises for the observer design. Dissert. Abstr.

N90-22788*# Thiokol Corp., Brigham City, UT. Space Operations.

QUALIFICATION OF THE RSRM FIELD JOINT CF CASE-TO-INSULATION BONDLINE INSPECTION USING THE THIOKOL CORPORATION ULTRASONIC RSRM BONDLINE INSPECTION SYSTEM Final Report

M. Cook Mar. 1990 45 p Original contains color illustrations (Contract NAS8-30490)

(NASA-CR-183931; NAS 1.26:183931; TWR-18895) Avail: NTIS HC A03/MF A01; 15 functional color pages CSCL 11A

Qualification testing of Combustion Engineering's AMDATA Intraspect/98 Data Acquisition and Imaging System that applies to the redesigned solid rocket motor field joint capture feature case-to-insulation bondline inspection was performed. Testing was performed at M-111, the Thiokol Corp. Inert Parts Preparation Building. The purpose of the inspection was to verify the integrity of the capture feature area case-to-insulation bondline. The capture feature scanner was calibrated over an intentional 1.0 to 1.0 in. case-to-insulation unbond. The capture feature scanner was then used to scan 60 deg of a capture feature field joint. Calibration of the capture feature scanner was then rechecked over the intentional unbond to ensure that the calibration settings did not change during the case scan. This procedure was successfully performed five times to qualify the unbond detection capability of the capture feature scanner. The capture feature scanner qualified in this test contains many points of mechanical instability that can affect the overall ultrasonic signal response. A new generation scanner, designated the sigma scanner, should be implemented to replace the current configuration scanner. The sigma scanner eliminates the unstable connection points of the current scanner and has additional inspection capabilities. Author

N90-22789 Council for National Academic Awards (England).

THE BEHAVIOUR OF MECHANICALLY FASTENED JOINTS IN COMPOSITE STRUCTURES Ph.D. Thesis

William Stewart Arnold 1989 365 p

Avail: Univ. Microfilms Order No. BRDX87932

Aspects of the behavior of mechanically fastened composite joints are characterized through a combined analytical and experimental investigation. In contrast to previous studies, three dimensional finite element techniques are employed in the analysis of pin loaded and bolted composite laminates, thereby transcending the limitations of classical lamination theory. After a general introduction, a comprehensive review of the relevant published literature is presented. Cross-ply pin loaded laminates are then analyzed using three dimensional finite element methods. Various modeling aspects are discussed while a parametric study is carried out to assess the influence of pin friction, pin elasticity, stacking sequence, plate elasticity, and joint geometry. This study is augmented by a plane stress analysis of pin jointed isotropic and orthotropic carbon fiber reinforced plastic (CFRP) plates subjected to various levels of biaxial loading. The analysis is then extended to encompass bolted joints. Quasi-isotropic and cross-ply laminates are considered under increasing levels of clamp-up. Particular attention is given to the effects of clamping load pressure distribution, stacking sequence, washer diameter, and washer friction. Details of a complementary experimental investigation are presented in which CSM and cross-ply GRP laminates and CFRP laminates of the form (0 sub n/90 sub n)s and (90 sub n/0 sub n)s are tested under pinned and clamped conditions. The influence of washer shape is assessed and where possible the failure process is characterized with the use of microscopic analysis. Joint strengths are predicted using two contrasting methodologies. Limitations of such an approach are established while possible improvements to the analysis are suggested. In a second technique, a semi-empirical method based on an extension to the Whitney and Nuismer Point Stress approach is formulated. The salient points derived from the present investigation are summarized including recommendations of areas which warrant future study. Dissert. Abstr.

N90-22790*# National Aeronautics and Space Administration. Lewis Research Center, Cleveland, OH.

SURFACE PITTING FATIGUE LIFE OF NONINVOLUTE, LOW-CONTACT-RATIO GEARS

Dennis P. Townsend 1990 9 p Presented at the 26th Joint Propulsion Conference, Orlando, FL, 16-18 Jul. 1990; cosponsored by AIAA, SAE, ASME, and ASEE

(DA Proj. 1L1-62209-A4-7A)

(NASA-TM-103116; E-5440; NAS 1.15:103116; AVSCOM-TM-90-C-008; AIAA-90-2153) Avail: NTIS HC A02/MF A01 CSCL 13I

Spur gear endurance tests were conducted to investigate the surface pitting fatigue life of noninvolute gears with low numbers of teeth and low contact ratios for use in advanced applications. The results were compared with those for a standard involute design with a low number of teeth. The gear pitch diameter was 8.89 cm (3.50 in.) with 12 teeth on both gear designs. Test conditions were an oil inlet temperature of 320 K (116 F), an oil outlet temperature of 350 K (170 F), a maximum Hertz stress of 1.49 GPa (216 ksi), and a speed of 10 000 rpm. The following results were obtained: the noninvolute gear had a surface pitting fatigue life approximately 1.6 times that of the standard involute gear of a similar design; and the surface pitting fatigue life of the 3.43-pitch AISI 8620 noninvolute gear was approximately equal to the surface pitting fatigue life of an 8-pitch, 28-tooth AISI 9310 gear at the same load but at a considerably higher maximum Hertz stress. Author

N90-22791# Sandia National Labs., Albuquerque, NM. Measurement Standards Dept.

CHARACTERIZATION AND CALIBRATION OF COORDINATE MEASURING MACHINES

Charles F. Pace 1990 9 p Presented at the Methods and Equipment of Metrology Equipment, Milwaukee, WI, 7-9 May 1990 (Contract DE-AC04-76DP-00789)

(DE90-009320; SAND-90-0906C; CONF-9005157-1) Avail: NTIS HC A02/MF A01

With the increasing use of three axis coordinate measuring machines (CMMs) for product acceptance, part characterization and/or part inspection, there is a corresponding need for acceptable methodologies to calibrate CMMs. Potential error sources in CMMs include scale errors and geometric imperfections as well as possible errors arising from environmental factors such as excessive vibrations or thermally induced structural changes. Although numerous methods for the calibration of CMMs have been reported, two calibration methods are reviewed. The first method is the American Standard for performance testing of CMMs and the second method is a parametric calibration with error compensation of CMMs. Whereas the first method can be used to evaluate the performance of two or more CMMs or for periodically checking a CMM. The second method is more advantageous for the calibration of high accuracy CMMs operating in controlled environments. DOE

N90-22792# Oak Ridge National Lab., TN. Metals and Ceramics Div.

CHARACTERIZATION OF WELDMENTS USING ADVANCED EXPERIMENTAL TECHNIQUES

J. M. Vitek and S. A. David 1990 24 p Presented at the 1st US-Japan Symposium on Advances in Welding Metallurgy, Yokohama, Japan, 12-13 Jun. 1990

(Contract DE-AC05-84OR-21400)

(DE90-009418; CONF-9006162-1) Avail: NTIS HC A03/MF A01

Many advanced experimental techniques that allow for more detailed characterization of materials have been developed over the last decade or two. These experimental techniques are divided into three categories: microstructural characterization, mechanical properties measurement, and simulation. Many of these techniques are ideally suited for the examination of weldments, including the fusion zone and the heat-affected zone. The advanced experimental methods allow for better evaluation of weldment microstructures and properties, given that microstructural and

compositional gradients are present in weldments. Several of these techniques are reviewed and examples of the type of information that can be obtained are given. The application of these techniques can provide new information on weldment phase transformations, phase stability, and weldment properties which should provide a basis for improved welds. DOE

N90-22793# Laboratoire d'Automatique et d'Analyse des Systemes, Toulouse (France).
PLAN EXECUTION CONTROL AND ARCHITECTURE FOR MOBILE ROBOTS Ph.D. Thesis [CONTROLE D'EXECUTION DE PLANS D'ACTIONS ET ARCHITECTURE POUR ROBOTS MOBILES]
Fabrice Noreils 1989 132 p In FRENCH; ENGLISH summary
(LAAS-89-371; ETN-90-96608) Avail: NTIS HC A07/MF A01

Plan execution control by mobile robots is studied. Plan execution control is achieved by a system different from the planner. In order to execute plans or missions given by a human user the following systems are developed: distributed architecture providing a set of elementary functions that the robot can achieve and control system, having both centralized and distributed components, that uses robot functions to execute plans and to control this execution. The control system is able to recognize events that make mission execution impossible, identify their possible cause, and possibly recover from the situation by locally including corrective actions. The presented control structure is to be considered as a kernel around which further extensions were added, without modifying it. A formalism was developed for expressing missions, and a graphic interface was implemented in order to interact with the robot and display mission execution status. A layer was added in the control system and the formalism in order to coordinate the actions of several robots. Petri Nets were used to validate this approach. Several actual real world experimentations are described. ESA

N90-22794# Groningen Rijksuniv. (Netherlands). Dept. of Computing Science.
MODELLING AND COMPUTER CONTROL OF A MECHANICAL SYSTEM M.S. Thesis
P. J. Renken Nov. 1989 46 p
(W-8908; ETN-90-96717) Avail: NTIS HC A03/MF A01

The problem of modeling and computer control of a system is investigated. The system consists of a ball and beam (b and b) and is connected to an electronic device which controls the system in such a way that the ball is steered to a fixed (but arbitrary) position on the beam in a stable way. The motions of the b and b are controlled electronically. The aim of this project was to replace the electronic controller by a PC. A description of the mechanical system is given. A mathematical model of the system is derived, and a linearization of the nonlinear model is discussed. The observer part of the system is calculated. All the constants necessary for control are determined. A pole placement controller is discussed. ESA

N90-22795# Technische Univ., Eindhoven (Netherlands). Dept. of Mathematics and Computing Science.
THE CURVATURE OF CONJUGATE PROFILES IN POINTS OF CONTRACT
D. A. Overdijk Jul. 1989 22 p
(MEMO-COSOR-89-18; ETN-90-96719) Avail: NTIS HC A03/MF A01

The principal curvatures on the conjugate profiles in point of contact are discussed. A survey of the theory of the curvature of surfaces, using elementary algebra, is given. The curvature of two bodies in the points on their curve of contact is discussed. The following formulas are given: for the angle between the corresponding principal directions of the boundary surfaces of the bodies on the curve of contact and for the angle between the direction of the curve of contact and the principal direction of one of the boundary surfaces corresponding to its smaller principal curvature. A point on the curve of contact of two conjugate tooth profiles in a gear pair is considered. The tangent spaces at this point of contact on the conjugate profiles coincide. A new and efficient algorithm for the calculation of the curvature of conjugate profiles in points of contact for the general gear pair is described. ESA

N90-22796*# National Aeronautics and Space Administration. Lewis Research Center, Cleveland, OH.
INFLUENCE OF LINEAR PROFILE MODIFICATION AND LOADING CONDITIONS ON THE DYNAMIC TOOTH LOAD AND STRESS OF HIGH CONTACT RATIO GEARS
Chinwai Lee, Hsiang Hsi Lin (Memphis State Univ., TN.), Fred B. Oswald, and Dennis P. Townsend 1990 13 p Prepared for presentation at the ASME Mechanism Conference, Chicago, IL, 16-19 Sep. 1990 Prepared in cooperation with Army Aviation Systems Command, Cleveland, OH
(NASA-TM-103136; E-5384; NAS 1.15:103136;
AVSCOM-TM-90-C-004) Avail: NTIS HC A03/MF A01
CSCL 13I

A computer simulation for the dynamic response of high-contact-ratio spur gear transmissions is presented. High contact ratio gears have the potential to produce lower dynamic tooth loads and minimum root stress but they can be sensitive to tooth profile errors. The analysis presented examines various profile modifications under realistic loading conditions. The effect of these modifications on the dynamic load (force) between mating gear teeth and the dynamic root stress is presented. Since the contact stress is dependent on the dynamic load, minimizing dynamic loads will also minimize contact stresses. It is shown that the combination of profile modification and the applied load (torque) carried by a gear system has a significant influence on gear dynamics. The ideal modification at one value of applied load will not be the best solution for a different load. High-contact-ratio gears were found to require less modification than standard low-contact-ratio gears. High-contact-ratio gears are more adversely affected by excess modification than by under modification. In addition, the optimal profile modification required to minimize the dynamic load (hence the contact stress) on a gear tooth differs from the optimal modification required to minimize the dynamic root (bending) stress. Computer simulation can help find the design tradeoffs to determine the best profile modification to satisfy the conflicting constraints of minimizing both the load and root stress in gears which must operate over a range of applied loads. Author

N90-22797# Carnegie-Mellon Univ., Pittsburgh, PA. Artificial Intelligence and Psychology Project.
ALVINN: AN AUTONOMOUS LAND VEHICLE IN A NEURAL NETTWORK Technical Report, 15 Sep. 1986 - 14 Sep. 1991
Dean A. Pomerleau Jan. 1989 17 p Presented at the IEEE Conference on Neural Information Processing Systems: Natural and Synthetic, Denver, CO, Nov. 1988 Prepared in cooperation with Pittsburgh Univ., PA
(Contracts N00014-86-K-0678; N00014-87-K-0385;
N00014-87-K-0533; N00039-87-C-0251; DACA76-85-C-0003; NSF EET-87-16324; ARPA Order 5351)
(AD-A218975; AIP-77) Avail: NTIS HC A03/MF A01 CSCL 13/6

ALVINN (Autonomous Land Vehicle In a Neural Network) is an 3 layer back propagation network designed for the task of road following. Currently ALVINN takes images from a camera and a laser range finder as input and produces as output the direction the vehicle should travel in order to follow the road. Training was conducted using simulated road images. Successful tests on the Carnegie Mellon autonomous navigation test vehicle indicate that the network can follow real roads under certain field conditions. The representation developed to perform the task differs greatly when the network is trained under various conditions, suggesting the possibility of a novel adaptive autonomous navigation system capable of tailoring its processing to the conditions at hand. Author

N90-22798# David Taylor Research Center, Bethesda, MD. Dept. of Ship Hydromechanics.
PRESSURE AND SHEAR STRESS MEASUREMENT UNCERTAINTY FOR DARPA SUBOFF EXPERIMENT

Scott Gowing Jan. 1990 30 p
(AD-A219109; DTRC/SHD-1298-06) Avail: NTIS HC A03/MF A01 CSCL 20/11

An uncertainty analysis of the pressure and shear stress measurements in the SUBOFF experiments is presented. Error sources in the measurements are identified, characterized as to the types of error that will result, and then quantified. The propagation of errors in the pressure and friction coefficients is approximated with a Taylor series and the 95 percent confidence intervals for Cp and Cf are presented as a function of the coefficients themselves and thermal drift in the electronics. It is concluded that the true value of the pressure coefficient is within 0.005 to 0.01 of the measured value, and the true friction coefficient is within 0.0002 of its measured value. GRA

N90-22799# Army Materials Technology Lab., Watertown, MA.
ROLE OF SHEAR INSTABILITY IN BALLISTIC PENETRATION Final Report
John F. Mescall and Harry Rogers (Drexel Univ., Philadelphia, PA.) Dec. 1989 32 p Sponsored by Army Lab. Command, Adelphi, MD
(AD-A219186; MTL-TR-89-104) Avail: NTIS HC A03/MF A01 CSCL 20/11

The role of adiabatic shear bands in penetration mechanics is described and an experimental technique is described by means of which conditions for the incipient nucleation and subsequent growth of such localized bands may be determined. There is abundant experimental evidence to indicate that ballistic results are strongly influenced by the mechanical properties of the materials involved. Following a discussion of the role played by adiabatic shear phenomena in ballistic penetration, an experimental procedure is outlined for obtaining quantitative characteristics for specific materials. A computer simulation of the experimental procedure incorporated work hardening and thermal softening effects and is shown to reproduce experiments in which adiabatic shear bands form, as well as several in which they do not occur. From such supplementary simulations, numerical values for important mechanical properties can be extracted for further application. GRA

N90-22800# Ballistic Research Labs., Aberdeen Proving Ground, MD.
LARGE-SCALE SIMULATIONS OF MONOLITHIC AND SEGMENTED PROJECTILES IMPACTING SPACED ARMOR Final Technical Report, period ending Jun. 1988
Daniel R. Scheffler and Thomas M. Sherrick Feb. 1990 65 p
(AD-A219374; BRL-MR-3080) Avail: NTIS HC A04/MF A01 CSCL 19/1

Numerical simulations are presented describing the performance of segmented monolithic kinetic energy penetrators against oblique-spaced rolled homogeneous armor (RHA) plates. The three-dimensional simulations depict the effects of striking velocity; target plate thickness-to-penetrator diameter ratio, (T/D); segment spacing-to-penetrator diameter ratio (S/D); and the number of segments, on penetrator performance. GRA

N90-22662*# Virginia Univ., Charlottesville.
DESIGN OF CRYOGENIC TANKS FOR LAUNCH VEHICLES
Charles Copper, Walter D. Pilkey, and John K. Haviland *In its* NASA-UVA Light Aerospace Alloy and Structures Technology Program Jun. 1990 20 p (For primary document see N90-22651 16-26)
Avail: NTIS HC A17/MF A03 CSCL 13I

N90-23034*# Middle East Technical Univ., Gaziantep (Turkey). Dept. of Mechanical Engineering.
DETERMINATION OF JOINT DRIVES FOR STABLE END-EFFECTOR MOTION IN FLEXIBLE ROBOTIC SYSTEMS
Sitki Kemal Ider *In* JPL, Proceedings of the 3rd Annual Conference on Aerospace Computational Control, Volume 1 15 Dec. 1989 p 421-423 (For primary document see N90-22987 16-61)
Avail: NTIS HC A21/MF A03 CSCL 13I

N90-23035*# State Univ. of New York, Buffalo. Dept. of Mechanical and Aerospace Engineering.
CONTROL OF A FLEXIBLE PLANAR TRUSS USING PROOF MASS ACTUATORS
Constantinos Minas, Ephrahim Garcia, and Daniel J. Inman *In* JPL, Proceedings of the 3rd Annual Conference on Aerospace Computational Control, Volume 1 15 Dec. 1989 p 434-445 (For primary document see N90-22987 16-61)
(Contracts F49620-88-C-00018; F49620-86-C-60111; AF-AFOSR-0119-85; AF-AFOSR-0390-88)
Avail: NTIS HC A21/MF A03 CSCL 13I

N90-23037*# National Aeronautics and Space Administration. Langley Research Center, Hampton, VA.
ON TRAJECTORY GENERATION FOR FLEXIBLE SPACE CRANE: INVERSE DYNAMICS ANALYSIS BY LATDYN
G.-S. Chen, J. M. Housner, S.-C. Wu, and C.-W. Chang (Comtek Co., Yorktown, VA.) *In* JPL, Proceedings of the 3rd Annual Conference on Aerospace Computational Control, Volume 1 15 Dec. 1989 p 447-448 (For primary document see N90-22987 16-61)
Avail: NTIS HC A21/MF A03 CSCL 13I

N90-23061*# Case Western Reserve Univ., Cleveland, OH. Computer Engineering and Science.
DISTRIBUTED NEURAL CONTROL OF A HEXAPOD WALKING VEHICLE
R. D. Beer, L. S. Sterling, R. D. Quinn, H. J. Chiel, and R. Ritzmann *In* Jet Propulsion Lab., California Inst. of Tech., Proceedings of the 3rd Annual Conference on Aerospace Computational Control, Volume 2 15 Dec. 1989 p 664-673 (For primary document see N90-23040 16-61)
Avail: NTIS HC A20/MF A03 CSCL 13I

38 QUALITY ASSURANCE AND RELIABILITY

Includes product sampling procedures and techniques; and quality control.

N90-22801*# National Aeronautics and Space Administration. Lewis Research Center, Cleveland, OH.
RECENT ADVANCES IN NONDESTRUCTIVE EVALUATION MADE POSSIBLE BY NOVEL USES OF VIDEO SYSTEMS
Edward R. Generazio and Don J. Roth 1990 20 p Presented at the MiCon 90: Advances in Video Technology: Materials Science Applications, San Francisco, CA, 23-25 May 1990; sponsored by American Society for Testing and Materials Original contains color illustrations
(NASA-TM-102491; E-5283; NAS 1.15:102491) Avail: NTIS HC A03/MF A01; 4 functional color pages CSCL 14D

Complex materials are being developed for use in future advanced aerospace systems. High temperature materials have been targeted as a major area of materials development. The development of composites consisting of ceramic matrix and ceramic fibers or whiskers is currently being aggressively pursued internationally. These new advanced materials are difficult and costly to produce; however, their low density and high operating temperature range are needed for the next generation of advanced aerospace systems. These materials represent a challenge to the nondestructive evaluation community. Video imaging techniques not only enhance the nondestructive evaluation, but they are also required for proper evaluation of these advanced materials. Specific research examples are given, highlighting the impact that video systems have had on the nondestructive evaluation of ceramics. An image processing technique for computerized determination of grain and pore size distribution functions from microstructural images is discussed. The uses of video and computer systems for displaying, evaluating, and interpreting ultrasonic image data are presented. Author

N90-22802 United Kingdom Atomic Energy Authority, Harwell (England). Nuclear Physics and Instrumentation Div.
APPLICATION OF X RAY ABSORPTION EDGE SPECTROMETRY TO THE NON-DESTRUCTIVE DETERMINATION OF ELEMENT CONCENTRATIONS, COATING THICKNESS AND AREAL DENSITIES
B. L. Taylor, L. C. Russen, and B. Metcalfe Nov. 1988 17 p
(AERE-R-13030) Copyright Avail: Issuing Activity

X ray absorption edge spectrometry is a relatively new technique for measuring the thickness of films and coatings. It can also be used to determine the concentration of the heavier elements in a low atomic number matrix. Although the method has important limitations with regard to the sample types that can be measured, recent developments in equipment have extended the area of applicability and have also made it possible to carry out on line measurements on samples in hostile or inaccessible environments such as vacuum vessels, furnaces, or radioactive areas, where other methods would be difficult if not impossible to apply. Author

N90-22803 United Kingdom Atomic Energy Authority, Harwell (England). Materials Physics and Metallurgy Div.
CRACK DETECTION IN SILICON NITRIDE BY ACOUSTIC MICROSCOPY
C. W. Lawrence, C. B. Scruby, G. A. D. Briggs, and A. Dunhill (Rolls-Royce Ltd., Bristol, England) Dec. 1988 22 p
(AERE-R-13196) Copyright Avail: Issuing Activity

The application of low ductility materials depends upon the successful detection of small defects, which might otherwise cause premature failure. In the case of advanced ceramics such as silicon nitride, it is required to detect surface breaking defects whose depth is a few tens of micrometers, which is beyond the resolution limit of most conventional ultrasonic testing. Although scanning acoustic microscopy has been shown to have sufficient resolution to detect such defects, most demonstrations have been limited to specially prepared laboratory test specimens. The application of acoustic microscopy to the detection of critical defects in a test block and in a finished ball bearing component, both of which were manufactured from the same silicon nitride material is reported. The data demonstrate the importance of choosing a sufficiently high frequency in order to detect shallow surface-openimg cracks. Thus defects that could not be detected or resolved at 250 MHz, were resolvable at 400 MHz. Author

N90-22804# Sandia National Labs., Albuquerque, NM.
INCREASED STUCK-AT FAULT COVERAGE WITH REDUCED I(SUB DDQ) TEST SETS
Ronald R. Fritzemeier, Jerry M. Soden, R. Keith Treece, and Charles F. Hawkins (New Mexico Univ., Albuquerque.) 1990 11 p Presented at the 1990 AT and T Conference on Electronic Testing, Princeton, NJ, 10 May 1990
(Contract DE-AC04-76DP-00789)
(DE90-009509; SAND-90-0608C; CONF-9005158-1) Avail: NTIS HC A03/MF A01

Simplified ATPG and fault simulation algorithms, reduced test set sizes, and increased fault coverage are achieved with I (sub DDQ) testing for stuck-at faults. In addition, I (sub DDQ) testing will detect logically redundant and multiple stuck-at faults, and improve the detection of non-stuck-at fault defects. DOE

N90-22805# Industrial Quality, Inc., Gaithersburg, MD.
REAL-TIME STEREO-MICRORADIOGRAPHY Final Report, Sep. 1987 - Sep. 1989
D. Polansky, R. Placious, E. Criscuolo, E. Gaynor, H. Berger, J. Reed, R. Schirato, R. Polichar, and J. Baltgalvis (Science Applications International Corp., San Diego, CA.) Nov. 1989 89 p
(Contract DAAL04-87-C-0074)
(AD-A218433; IQI-DFR-89-0074; MTL-TR-89-96) Avail: NTIS HC A05/MF A01 CSCL 14/2

A new real-time stereo x ray imaging system is described. Fast X ray source movement (TV field of 1/60 s) is possible in a microfocus x ray source by electromagnetic shifting of the electron beam. The two-view fields are combined in a TV frame for stereo viewing through a polarizing screen. Real-time, stereo x ray images of moving inspection objects can be followed. One can view the stereo x ray images to judge the apparent depth of an x ray indication. One can also measure the depth of selected indications with a developed software system. This report describes the development of this novel stereo x ray inspection system over the two-year period of this SBIR, Phase 2 Project. Plans are being made to offer the stereo, depth measurement system commercially. GRA

N90-22806# Bio-Imaging Research, Inc., Lincolnshire, IL.
ON-LINE X RAY INSPECTION OF MATERIALS AND STRUCTURAL COMPONENTS USING DISCRETE ELEMENT X RAY DETECTORS FOR DIGITAL RADIOGRAPHIC AND COMPUTED TOMOGRAPHIC EVALUATION Final Report, 1 Aug. 1988 - 31 Jan. 1990
Bruce G. Isaacson Feb. 1990 55 p
(Contract DAAL03-88-C-0024)
(AD-A218911; ARO-25952.1-EG-SBI) Avail: NTIS HC A04/MF A01 CSCL 11/4

The effectiveness was studied of industrial computed tomography (CT) and digital radiography (DR) as inspection techniques for the evaluation of materials and structural components manufactured on-line. The results indicate that computed tomography is an appropriate technique if speed and cost are not critical considerations. Digital radiography is the faster technique, but provides less information about the material. Limited view tomography (LVT), which is a simplified form of computed tomography, was compared and found to provide a good compromise between computed tomography and digital radiography when a priori knowledge of material structure is available. For some material configurations, it provides virtually complete computed tomography data in a fraction of the time required for full view computed tomography data collection and reconstruction. It offers the greatest potential for the productive cross-sectional characterization of composite materials. GRA

39 STRUCTURAL MECHANICS

Includes structural element design and weight analysis; fatigue; and thermal stress.

For applications see *05 Aircraft Design, Testing and Performance* and *18 Spacecraft Design, Testing and Performance.*

N90-22807*# National Aeronautics and Space Administration. Langley Research Center, Hampton, VA.
THERMAL/STRUCTURAL ANALYSIS OF THE SHAFT-DISK REGION OF A FAN DRIVE SYSTEM
Peyton B. Gregory and Anne D. Holland Mar. 1990 29 p
Original contains color illustrations
(NASA-TM-101687; NAS 1.15:101687) Avail: NTIS HC A03/MF A01; 8 functional color pages CSCL 20K

In January 1989, a mishap occurred in the National Transonic Facility wind tunnel at NASA-Langley. It is believed that the failure of an insulation retainer holding foam insulation around the exterior of the fan drive shaft resulted in the subsequent damage to other components in the tunnel. The effect was determined of removing the external thermal insulation on the shaft would have on the stresses on the shaft, disk and bolts holding the two together. To accomplish this, a detailed thermal/structural finite element analysis of the shaft-disk interface was performed. The maximum stresses on the three components were determined for several configurations and conditions with and without the external thermal insulation, and then these results were compared to the original analyses to access the effect of removing the external thermal insulation on the proposed future operation of the shaft/disk structures of the fan drive system. Although the stresses were higher without the external insulation, the stresses did meet all stress criteria. In addition, all stresses were within the infinite life

regime of the Modified Goodman diagram. Therefore, it was determined that the structural integrity of the shaft-disk region is not compromised if the external insulation is removed. Author

N90-22808*# National Aeronautics and Space Administration. Lewis Research Center, Cleveland, OH.
FINITE ELEMENT ELASTIC-PLASTIC-CREEP AND CYCLIC LIFE ANALYSIS OF A COWL LIP
Vinod K. Arya (Toledo Univ., OH.), Matthew E. Melis, and Gary R. Halford Apr. 1990 10 p Submitted for publication Original contains color illustrations
(NASA-TM-102342; E-5050; NAS 1.15:102342) Avail: NTIS HC A02/MF A01; 3 functional color pages CSCL 20K

Results are presented of elastic, elastic-plastic, and elastic-plastic-creep analyses of a test-rig component of an actively cooled cowl lip. A cowl lip is part of the leading edge of an engine inlet of proposed hypersonic aircraft and is subject to severe thermal loadings and gradients during flight. Values of stresses calculated by elastic analysis are well above the yield strength of the cowl lip material. Such values are highly unrealistic, and thus elastic stress analyses are inappropriate. The inelastic (elastic-plastic and elastic-plastic-creep) analyses produce more reasonable and acceptable stress and strain distributions in the component. Finally, using the results from these analyses, predictions are made for the cyclic crack initiation life of a cowl lip. A comparison of predicted cyclic lives shows the cyclic life prediction from the elastic-plastic-creep analysis to be the lowest and, hence, most realistic. Author

N90-22809 Rensselaer Polytechnic Inst., Troy, NY.
COMPUTATIONS OF WEIGHT FUNCTIONS IN FRACTURE MECHANICS Ph.D. Thesis
Yansheng Zhou 1989 234 p
Avail: Univ. Microfilms Order No. DA9011321

The variational principle and the resulting displacement based finite element procedure introduced by Sham to determine elastic fields with unbounded strain energy in finite homogeneous bodies were used to compute the weight functions directly for both two- and three-dimensional problems. This procedure determines the weight functions for all three fracture modes and for both traction and displacement boundaries in a unified manner. Two-dimensional weight functions in arbitrary anisotropic solids under mixed boundary conditions are analyzed. Closed-form fundamental fields in all three fracture modes are given for a semi-infinite crack in a monoclinic solid. Numerical examples for Griffith crack and inclined edge crack in fiber-reinforced composite laminates are presented. The use of fundamental fields for assessing the influence of transformation strains on stress intensity factors in piecewise homogeneous anisotropic solids is described. A numerical example of determining the stress intensity factors of a matrix crack in an idealized fiber/matrix configuration due to thermal stress loading is also given. The variational principle for determining the fundamental field in homogeneous bodies is further extended to piecewise homogeneous bodies. Numerical examples for two-dimensional cracks in layered isotropic bodies are presented. Three-dimensional fundamental fields for circular and elliptical cracks in isotropic, finite bodies with mixed boundary conditions are analyzed using the same finite element procedure. A new procedure for determining the Fourier coefficients of the stress intensity factors for arbitrary closed loop planar cracks in a finite body by using ordinary fundamental fields is presented. Author

N90-22810 United Kingdom Atomic Energy Authority, Harwell (England). Material Physics and Metallurgy Div.
CHARACTERIZATION OF PARTICLE IMPACT BY QUANTITATIVE ACOUSTIC EMISSION
D. J. Buttle and C. B. Scruby Sep. 1988 56 p
(AERE-R-13028) Copyright Avail: Issuing Activity

Erosion is often a life limiting factor for many industrial plant components. Acoustic emission (AE) is proposed as a method of monitoring erosion rate from hard particle impact by measuring the signals from impact. In a preliminary study small spherical particles of nominal diameter 53 to 63 microns and 75 to 90 microns of bronze and glass respectively were dropped in vacuum onto steel or aluminum target plates at selected velocities between 2.5 and 7.1 m/s. At these low velocities the collisions are entirely elastic and no erosion occurs. However a quantitative AE signal analysis method was developed which enabled various parameters from the particle impacts to be determined, with the potential for measuring the degree of plasticity of impact in later experiments. AE signals were detected with a calibrated broad bandwidth piezo electric transducer positioned on the opposite face of the target plate at the impact epicenter. The Green's function for the plate, together with the AE transducer and system response obtained by calibration using a capacitance transducer, were deconvolved from AE signals yielding the impact force function of the particle impact. The velocity dependence of the impact time and peak impact force thus determined agreed with that predicted from semiempirical models of elastic particle impact. The absolute magnitude of these two parameters also compared very well with theoretical values. The quantitative acoustic technique developed was capable of sizing the particles, and the results compared favorably with the particle size distribution measured optically, giving the correct mean particle diameter to within 10 percent and the distribution spread to within 26 percent. This fundamental approach provides a framework for later extension to plastic and partially plastic particle impact. Author

N90-22811 Delaware Univ., Newark.
AXISYMMETRIC AND CYLINDRICALLY ORTHOTROPIC ANALYSIS OF FILAMENT WINDING Ph.D. Thesis
Mark Cirino 1989 263 p
Avail: Univ. Microfilms Order No. DA9010403

Analytical models were developed to predict the state of stress in a ring during its fabrication by a winding process. The effect of winding tension and consolidation of the material on the stress state were considered. The winding process was modeled as the sequential addition of concentric layers to a mandrel. Consequently, variation of winding tension and consolidation of the material could be performed on a layer-by-layer basis. Both the concentric layers and mandrel were assumed to be in a state of plane stress. In the elastic model, winding tension was represented by imposing a uniform circumferential stress throughout each layer, and consolidation was represented by subjecting the layer to a uniform temperature change. The winding tension was shown to be a mechanism through which the residual stress state could be controlled. Layer-by-layer consolidation reduced the magnitude of the residual stresses relative to those resulting from post-winding consolidation. The heat transfer model predicted the temperature distribution in the substrate and mandrel due to layer-by-layer consolidation. The resulting temperature distributions were a function of radial position. Accordingly, the thermoelastic model was developed to address the temperature gradients. Also, this model considered the thermal response of the substrate and mandrel during the winding process. The temperature of the mandrel increased during the winding process. The resulting expansion of the mandrel imposes a radial pressure on the substrate such that it maintains a compressive radial stress distribution during the winding process. The viscoelastic model analyzed the state of stress in the ring during a post-winding annealing cycle. Relaxation of the residual state of stress induced during the winding process was predicted. Also, it was shown that an elastic analysis could be utilized to predict the relaxation of the state of stress in a ring subjected to a temperature change. Dissert. Abstr.

N90-22812 Princeton Univ., NJ.
LOCALIZATION OF VIBRATION IN DISORDERED NEARLY CYCLIC STRUCTURES Ph.D. Thesis
Phillip J. Cornwell 1989 214 p
Avail: Univ. Microfilms Order No. DA9008349

An analytical and computational investigation of the effects of disorder on the dynamics of a generic class of cyclic structures such as large space reflectors is presented. When imperfections, typical of those expected in a realistic structure, are introduced, the amplitude of the global modes of vibration may become

confined to a local region of the structure. This phenomenon is called mode localization. A simple SDOF per substructure model is used to illustrate some basic characteristics of mode localization and to demonstrate the phenomenon of wave confinement in finite structures. Mode localization in more realistic structures is investigated using a Rayleigh-Ritz model based on the first five cantilevered beam bending modes and a finite element model using Bernoulli-Euler beam elements. Perturbation methods are developed and applied to predict the qualitative change which occurs in the eigenvectors. Structures found to be most susceptible to mode localization are those consisting of a large number of weakly coupled structures. These structures are characterized by high modal densities. A normalized eigenvalue band that accurately reflects the relative susceptibility of a mode group to localization is defined and is found to serve as a scaling parameter for the behavior of similar modes in different mode groups. Mode localization is found to become progressively more severe with increasing mode number, and if the mode number is large enough, strong localization is unavoidable. Strongly localized modes affect the disturbance propagation associated with impulsive loading of one substructure by confining the energy near the source of excitation. Dissert. Abstr.

N90-22813*# Case Western Reserve Univ., Cleveland, OH. Dept. of Civil Engineering.

DYNAMIC SUBSTRUCTURING BY THE BOUNDARY FLEXIBILITY VECTOR METHOD OF COMPONENT MODE SYNTHESIS Ph.D. Thesis

Ayman Ahmed Abdallah 12 Jan. 1990 139 p
(Grant NAG3-707)
(NASA-CR-182445; NAS 1.26:182445) Avail: NTIS HC A07/MF A01 CSCL 20K

Component mode synthesis (CMS) is a method of dynamic analysis, for structures having a large number of degrees of freedom (DOF). These structures often required lengthy computer CPU time and large computer memory resources, if solved directly by the finite-element method (FEM). In CMS, the structure is divided into independent components in which the DOF are defined by a set of generalized coordinates defined by displacement shapes. The number of the generalized coordinates are much less than the original number of physical DOF, in the component. The displacement shapes are used to transform the component property matrices and any applied external loads, to a reduced system of coordinates. Reduced system property matrices are assembled, and any type of dynamic analysis is carried out in the reduced coordinate system. Any obtained results are back transformed to the original component coordinate systems. In all conventional methods of CMS, the mode shapes used for components are dynamic mode shapes, supplemented by static deflected shapes. Historically, all the dynamic mode shapes used in conventional CMS are the natural modes (eigenvectors) of components. A new method of CMS, namely the boundary flexibility vector method of CMS, is presented. The method provides for the incorporation of a set of static Ritz vectors, referred to as boundary flexibility vectors, as a replacement and/or supplement to conventional eigenvectors, as displacement shapes for components. The generation of these vectors does not require the solution of a costly eigenvalue problem, as in the case of natural modes in conventional CMS, and hence a substantial saving in CPU time can be achieved. The boundary flexibility vectors are generated from flexibility (or stiffness) properties of components. The formulation presented is for both free and fixed-interface components, and for both the free and forced vibration problems. Free and forced vibration numerical examples are presented to verify the accuracy of the method and the saving in CPU time. Compared to conventional methods of CMS, the results indicate that by using the new method, more accurate results can be obtained with a substantial saving in CPU time. Author

N90-22814# Edgerton, Germeshausen and Grier, Inc., Idaho Falls, ID. Materials Technology Group.

COMPARISON BETWEEN DATA GENERATED FROM STANDARD FRACTURE TOUGHNESS SPECIMENS AND FROM NONSTANDARD SPECIMENS MADE OF A SILICON CARBIDE

W. G. Reuter, W. R. Lloyd, and J. R. Knibloe 1990 5 p Presented at the Society for Experimental Mechanics Conference, Albuquerque, NM, 4-6 Jun. 1990
(Contract DE-AC07-76ID-01570)
(DE90-009621; EGG-M-90043; CONF-9006124-3) Avail: NTIS HC A01/MF A01

The ability of methods based upon linear elastic fracture mechanics to predict the structural integrity of a class of monolithic ceramics was investigated experimentally. Three important assumptions related to the hypothesized methodology are identified for verification. The data and discussion presented provide strong support for all three. Obstacles to be overcome in the final design/assessment of a structural ceramic component are also identified. DOE

N90-22815# Aerospatiale Aquitaine, Saint-Medard en Jalles (France). Div. Systemes Strategiques et Spatiaux.

DIMENSIONAL ANALYSIS OF STRUCTURES USING WRAPPING TECHNIQUES [MODE DE DIMENSIONNEMENT DES STRUCTURES REALISEES PAR BOBINAGE]

Jean Lamalle 6 Mar. 1989 27 p In FRENCH
(Rept-892-430-119; AQET-Note-09/89; ETN-90-96650) Avail: NTIS HC A03/MF A01

A technique of forming pieces by longitudinal, circumferential, helicoidal, and planar wrapping is presented. Diagrams of the wrapping apparatus are presented. Detailed formulae for the interpretation of wrapping results are presented. Interpretation of wrapping results for axisymmetric and non axisymmetric pieces is detailed. The need to interpret each wrapping problem in a new way is stressed. Extensions of the wrapping technique to the production of composite filamentous materials are described. ESA

N90-22816# Aerospatiale Aquitaine, Saint-Medard en Jalles (France).

EVALUATION OF JOINTS BONDED WITH ELASTOPLASTIC ADHESIVES

M. Martin 19 Sep. 1989 27 p In FRENCH; ENGLISH summary
(Rept-892-430-120; ETN-90-96651) Avail: NTIS HC A03/MF A01

The mechanical behavior criteria of elastoplastic adhesives and computer-aided methods of analyzing the bonded joints are presented. Several cases of bonded joints are considered. Good correlation between experimental failure test results and theory is observed. The reaction of joints bonded with elastoplastic adhesives to deformations and temperature changes is studied. The mechanical behavior of the joints is integrated into software programs. Stress tests are carried out to validate the joint evaluation methods developed. ESA

N90-22817# University of Southern Illinois, Carbondale. Dept. of Mathematics.

MATERIAL INSTABILITIES IN SOLIDS Final Technical Report, 1 Jun. 1988 - 31 Oct. 1989

Scott J. Spector 31 Oct. 1989 11 p
(Grant AF-AFOSR-0200-88; AF Proj. 2304)
(AD-A218451; AFOSR-90-0232TR) Avail: NTIS HC A03/MF A01 CSCL 07/6

A number of mathematical problems that may help to explain material failures in certain polymers and ductile metals were considered. In particular, useful results were obtained concerning the static instability and surface cracking of a single hole and the formation of crazes in glassy polymers. GRA

N90-22818# Pennsylvania State Univ., State College.

FLAT PLATE VIBRATION ANALYSIS EXPERIMENTAL AND NUMERICAL FILLET STUDY Final Report

R. D. Cook and D. E. Thompson Feb. 1990 60 p
(Contract N00039-88-C-0051)
(AD-A218789; ARL/PSU/TR-90-01) Avail: NTIS HC A04/MF A01 CSCL 20/11

Measurements and predictions of low-order resonant frequencies and mode shapes have been made for three rectangular aluminum plates, each having a different fillet radius at the attached end. Measurements were conducted using a dual-beam laser vibrometer, and predictions were made using the MSC/NASTRAN finite element code. The effects of the fillet radius on the resonant frequencies have been quantified, and a comparison between measured and predicted values is presented. Effects of water loading are also presented. Results show that: (1) resonant frequencies increase as the filet radius increases, (2) the predicted resonant frequencies compare favorably with those measured, and (3) water loading reduces the resonant frequencies determined in air. GRA

N90-22819# Army Armament Research, Development and Engineering Center, Watervliet, NY. Close Combat Armaments Center.
FRACTURE MECHANICS ASSESSMENT OF A CRACKED 16-INCH INNER DIAMETER 1945 VINTAGE-JACKETED PRESSURE VESSEL Final Technical Report
J. A. Kapp, M. D. Witherell, R. R. Fujczak, T. M. Hickey, and J. J. Zalinka Jan. 1990 27 p Sponsored by Army Armament Research, Development, and Engineering Center, Picatinny Arsenal, NJ
(AD-A219135; ARCCB-TR-90003) Avail: NTIS HC A03/MF A01 CSCL 20/11

A fracture mechanics assessment of the structural integrity of a very large 1945 vintage pressure vessel was performed. Many of these old vessels had not been used for several years and have only recently been returned to service. After a relatively short number of pressure cycles, long, but shallow, longitudinal cracks were found in the vessels. The fracture assessment included the development of a stress intensity factor solution for the vessel using finite elements, and the measurement of both the fracture toughness and fatigue crack propagation rates for the two steels from which the line of the vessel was made. A wide range expression was fit to the numerically determined stress intensity factor solution and was used to determine the remaining life of the vessel. Failure of the pressure vessel was assumed to be through fracture of the liner. The results indicate that this vessel has a significant remaining fatigue life. GRA

N90-22820# Naval Postgraduate School, Monterey, CA. Dept. of Aeronautics and Astronautics.
TRANSVERSE VIBRATIONS OF A COMPOSITE CYLINDRICAL TUBE OF CIRCULAR CROSS SECTION M.S. Thesis
Raymond William Etter Sep. 1989 114 p
(AD-A219227) Avail: NTIS HC A06/MF A01 CSCL 22/2

The transverse frequencies of vibration of laminated orthotropic cylindrical shells were studied in order to compare experimental results with results predicted by a modified Euler-Bernoulli beam theory. The structures studied had circular cross sections and were made of graphite/epoxy. Stacking sequences for the test structures were (90, + or - 603,90) and (90, + or -453,90). The structures were tested under clamped-free boundary conditions. Testing was conducted by measuring the Frequency Response Function (FRF) of the structure after exciting it with a modal hammer. Response was measured using an accelerometer. Signal processing was done with a digital signal analyzer and FRFs were analyzed using modal analysis software. The experimental data were used to derive a modal model of the test structure. Analytical predictions were made by one dimensionalizing the two dimensional laminated plate theory equations of motion. Treatment of the test structures as a beam was justified by investigating the equations of motion of classical shell theory and making physically reasonable assumptions. GRA

N90-22821# Naval Postgraduate School, Monterey, CA. Dept. of Mechanical Engineering.
THE MICROSTRUCTURAL BASIS OF DAMPING IN HIGH DAMPING ALLOYS M.S. Thesis
Peter Frederick Rappeline Sep. 1989 54 p
(AD-A219572) Avail: NTIS HC A04/MF A01 CSCL 20/11

The microstructural mechanisms responsible for material damping are analyzed, with emphasis on those mechanisms responsible for the behavior in high damping alloys. A Cu-Al-Ni alloy is metallurgically characterized using transmission electron microscopy and differential scanning calorimetry. The microstructural characterization of the Cu-Mn alloy INCRAMUTE is refined using high resolution transmission electron microscopy and high resolution energy-dispersive x ray spectroscopy. A qualitative theory for the strain dependence of damping capacity is given. GRA

N90-22822*# National Aeronautics and Space Administration. Lewis Research Center, Cleveland, OH.
HIGH TEMPERATURE FATIGUE BEHAVIOR OF A SiC/Ti-24Al-11Nb COMPOSITE
P. A. Bartolotta and P. K. Brindley 1990 15 p Presented at the 10th Symposium on Composite Materials: Testing and Design, San Francisco, CA, 24-25 Apr. 1990; sponsored by American Society for Testing Materials
(NASA-TM-103157; E-5524; NAS 1.15:103157) Avail: NTIS HC A03/MF A01 CSCL 20K

A series of tension-tension strain- and load-controlled tests were conducted on unidirectional SiC/Ti-24Al-11Nb (at percent) composites at 425 and 815 C. Several regimes of damage were identified using Talrega's concept of fatigue life diagrams. Issues of test technique, test control mode, and definition of failure were also addressed. Author

N90-22823*# National Aeronautics and Space Administration. Lewis Research Center, Cleveland, OH.
PROBABILISTIC STRUCTURAL ANALYSIS OF AEROSPACE COMPONENTS USING NESSUS
Michael C. Shiao, Vinod K. Nagpal (Sverdrup Technology, Inc., Cleveland, OH.), and Christos C. Chamis 1988 10 p Presented at the 29th Structures, Structural Dynamics, and Materials Conference, Williamsburg, VA, 18-20 Apr. 1988; cosponsored by AIAA, ASME, ASCE, AHS, and ACS Previously announced in IAA as A88-32310 Original contains color illustrations
(NASA-TM-102324; E-5020; NAS 1.15:102324) Avail: NTIS HC A02/MF A01; 5 functional color pages CSCL 20K

Probabilistic structural analysis of a Space Shuttle main engine turbopump blade is conducted using the computer code NESSUS (numerical evaluation of stochastic structures under stress). The goal of the analysis is to derive probabilistic characteristics of blade response given probabilistic descriptions of uncertainties in blade geometry, material properties, and temperature and pressure distributions. Probability densities are derived for critical blade responses. Risk assessment and failure life analysis is conducted assuming different failure models. Author

N90-22663*# Virginia Univ., Charlottesville.
EXPERIMENTAL AND COMPUTATIONAL STUDY OF THE VISCOPLASTIC RESPONSE OF HIGH TEMPERATURE STRUCTURES
Earl A. Thornton, M. F. Coyle, and J. D. Kolenski *In its* NASA-UVA Light Aerospace Alloy and Structures Technology Program Jun. 1990 22 p (For primary document see N90-22651 16-26)
Avail: NTIS HC A17/MF A03 CSCL 20K

N90-23019*# Illinois Univ., Chicago. Dept. of Mechanical Engineering.
EXPLICIT MODELING OF COMPOSITE PLATES AND BEAMS IN THE DYNAMICS OF MULTIBODY SYSTEMS Abstract Only
F. M. L. Amirouche, Sitki Kemal Ider, and M. Moumene *In* JPL, Proceedings of the 3rd Annual Conference on Aerospace Computational Control, Volume 1 15 Dec. 1989 p 264 (For

primary document see N90-22987 16-61)
Avail: NTIS HC A21/MF A03 CSCL 20K

42 GEOSCIENCES (GENERAL)

N90-22824*# National Aeronautics and Space Administration. Goddard Space Flight Center, Greenbelt, MD.
SEARISE: A MULTIDISCIPLINARY RESEARCH INITIATIVE TO PREDICT RAPID CHANGES IN GLOBAL SEA LEVEL CAUSED BY COLLAPSE OF MARINE ICE SHEETS
Robert A. Bindschadler, ed. 1990 55 p Workshop held in College Park, MD, 23-25 Jan. 1990; sponsored by NASA and NSF
(NASA-CP-3075; Rept-90-077; NAS 1.55:3075) Avail: NTIS HC A04/MF A01 CSCL 08C

The results of a workshop held to discuss the role of the polar ice sheets in global climate change are reported. The participants agreed that the most important aspect of the ice sheets' involvement in climate change is the potential of marine ice sheets to cause a rapid change in global sea level. To address this concern, a research initiative is called for that considers the full complexity of the coupled atmosphere-ocean-cryosphere-lithosphere system. This initiative, called SeaRISE (Sea-level-Response to Ice Sheet Evolution) has the goal of predicting the contribution of marine ice sheets to rapid changes in global sea level in the next decade to few centuries. To attain this goal, a coordinated program of multidisciplinary investigations must be launched with the linked objectives of understanding the current state, internal dynamics, interactions, and history of this environmental system. The key questions needed to satisfy these objectives are presented and discussed along with a plan of action to make the SeaRISE project a reality.
Author

N90-22825# Air Force Geophysics Lab., Hanscom AFB, MA.
TEMPORAL ATTRIBUTES OF THE AMBIENT SEISMO-ACOUSTIC ENVIRONMENT: LA JUNTA, COLORADO Interim Scientific Report
James C. Battis and Christopher J. Center 13 Mar. 1989 46 p Prepared in cooperation with Boston College, MA
(AD-A219369; AFGL-TR-89-0080; ERP-1025) Avail: NTIS HC A03/MF A01 CSCL 08/11

During the period 9 to 29 October 1986, seismic and atmospheric pressure data were recorded at the AFGL operated array at La Junta, Colorado. The purpose of this effort was to develop statistical models of the noise environments at this site for use in defining event detection capabilities of the array. Analysis of these data demonstrates that peak noise amplitudes for 1-second windows could adequately be modeled as Type II Gumbel extreme value distributions, EXII (u,k). Further, it was shown that there is at best only weak correlation between the noise fields in both a broad-and narrow-band sense.
GRA

43 EARTH RESOURCES AND REMOTE SENSING

Includes remote sensing of earth resources by aircraft and spacecraft; photogrammetry; and aerial photography.

For instrumentation see *35 Instrumentation and Photography.*

N90-22826*# Jet Propulsion Lab., California Inst. of Tech., Pasadena.
SPACEBORNE RADAR OBSERVATIONS: A GUIDE FOR MAGELLAN RADAR-IMAGE ANALYSIS
J. P. Ford, R. G. Blom, J. A. Crisp, Charles Elachi, T. G. Farr, R. Stephen Saunders, E. E. Theilig, S. D. Wall, and S. B. Yewell Dec. 1989 132 p Original contains color illustrations
(Contract NAS7-918)
(NASA-CR-184998; JPL-Publ-89-41; NAS 1.26:184998) Avail: NTIS HC A07/MF A01; 25 functional color pages CSCL 17I

Geologic analyses of spaceborne radar images of Earth are reviewed and summarized with respect to detecting, mapping, and interpreting impact craters, volcanic landforms, eolian and subsurface features, and tectonic landforms. Interpretations are illustrated mostly with Seasat synthetic aperture radar and shuttle-imaging-radar images. Analogies are drawn for the potential interpretation of radar images of Venus, with emphasis on the effects of variation in Magellan look angle with Venusian latitude. In each landform category, differences in feature perception and interpretive capability are related to variations in imaging geometry, spatial resolution, and wavelength of the imaging radar systems. Impact craters and other radially symmetrical features may show apparent bilateral symmetry parallel to the illumination vector at low look angles. The styles of eruption and the emplacement of major and minor volcanic constructs can be interpreted from morphological features observed in images. Radar responses that are governed by small-scale surface roughness may serve to distinguish flow types, but do not provide unambiguous information. Imaging of sand dunes is rigorously constrained by specific angular relations between the illumination vector and the orientation and angle of repose of the dune faces, but is independent of radar wavelength. With a single look angle, conditions that enable shallow subsurface imaging to occur do not provide the information necessary to determine whether the radar has recorded surface or subsurface features. The topographic linearity of many tectonic landforms is enhanced on images at regional and local scales, but the detection of structural detail is a strong function of illumination direction. Nontopographic tectonic lineaments may appear in response to contrasts in small-surface roughness or dielectric constant. The breakpoint for rough surfaces will vary by about 25 percent through the Magellan viewing geometries from low to high Venusian latitudes. Examples of anomalies and system artifacts that can affect image interpretation are described.
Author

N90-22827*# National Aeronautics and Space Administration. Ames Research Center, Moffett Field, CA.
A CASE FOR ARCHAEOLOGICAL RECONNAISSANCE OF THE CABO CATOCHE-PORVENIR REGION OF THE NORTHEASTERN YUCATAN PENINSULA
Charles E. Duller Feb. 1990 19 p LIMITED REPRODUCIBILITY: More than 20% of this document may be affected by color photographs Original contains color illustrations
(NASA-TM-102248; A-90002; NAS 1.15:102248) Avail: NTIS HC A03/MF A01; 6 functional color pages CSCL 08B

Satellite remote sensing technology is a tool with which archaeologists can, with relative ease, survey a region that is otherwise inaccessible. The northeast corner of the Yucatan Peninsula is such an area: it is isolated and sparsely inhabited, with dense forest and extensive swamps. From Cabo Catoche inland to Cancun, this remote corner of the ancient Maya world is virtually unexplored. Recent satellite images disclose evidence of past human activity in this unexplored region and offer a compelling argument for an archaeological reconnaissance.
Author

N90-22828# Rome Univ. (Italy). Dipt. di Fisica.
ANALYSIS OF NONLINEAR INTERNAL WAVES OBSERVED BY LANDSAT-TM
V. Artale, D. Levi, S. Marullo, and R. Santoleri (Consiglio Nazionale delle Ricerche, Rome, Italy) 28 Sep. 1989 26 p
(Preprint-704; ETN-90-96527) Avail: NTIS HC A03/MF A01

The compatibility between the theoretical parameters of a nonlinear wave model and the quantitative informations deducible from satellite derived data are tested. The theoretical parameters are obtained by applying an inverse problem to the solution of the Cauchy problem for the Korteweg-de Vries equation. The results are applied to the case of internal wave patterns elaborated from two different satellite sensors at the south of Messina, Italy, (the Thematic Mapper) and at the north of Messina (the synthetic aperture radar).
ESA

N90-22829# Defense Mapping Agency Systems Center, Reston, VA.
GUIDELINES, OPERATIONAL PROCEDURES, AND QUALITY CONTROL FOR THE ESTIMATION OF GEODETIC POINT POSITIONS FROM GPS DATA COLLECTED WITH THE TI4100 RECEIVER
Stephen Malys and Peter A. Jensen 13 Nov. 1989 88 p
(AD-A218460) Avail: NTIS HC A05/MF A01 CSCL 22/3

The TI4100 receiver collects data from the NAVSTAR Global Positioning System of Satellites (GPS). The Defense Mapping Agency (DMA) and a number of other organizations have utilized these receivers to exploit GPS for a variety of geodetic applications. A comprehensive set of operational procedures and guidelines is provided for the estimation of geodetic points positions (absolute positions) from data collected with the TI4100 receiver. The specific algorithms which are addressed were developed into efficient, portable FORTRAN 77 programs which are known as STARPREP and GASP. The name STARPREP is a contraction for GEOSTAR PREProcessor while GASP is an acronym for Geodetic Absolute Sequential Positioning program. These two programs are designed to work in concert to exploit GPS data for geodetic point positioning applications. A few other utility programs are also addressed which perform functions such as data transfer, data screening and data analysis. A set of minimum observation requirements are specified such that a geodetic point positioning survey can be planned and conducted efficiently. The use of GPS data which has been subject to Selective Availability (SA) or Anti-Spoofing (AS) is not addressed. When guidelines and standard operating procedures have been established for such data, an update will be made. GRA

N90-22830# Mississippi Univ., University.
FUNDAMENTAL STUDIES ON HYDROLOGY, HYDRAULICS AND GEOMETRY OF RIVER NETWORKS Final Report, 1 Feb. - 30 Nov. 1989
V. K. Gupta and Ed Waymire (Oregon State Univ., Corvallis.) Jan. 1990 6 p
(Contract DAAL03-89-K-0070)
(AD-A218662; ARO-26220.1-GS) Avail: NTIS HC A02/MF A01 CSCL 08/8

Research was directed toward a mathematical understanding of the empirical main channel length-area relationship for river networks based on the two postulates of the random model. The most significant analytical finding was that, up to a scale factor, the average main channel length L varies as the square root of the network magnitude where mu, as the scale factor, denotes the mean link length. GRA

N90-22831# Army Cold Regions Research and Engineering Lab., Hanover, NH.
ESTIMATING SEA ICE THICKNESS USING TIME-OF-FLIGHT DATA FROM IMPULSE RADAR SOUNDINGS
Austin Kovacs and Rexford M. Morey Dec. 1989 16 p
(Contract N68452-86MP-6003)
(AD-A218736; CRREL-89-22) Avail: NTIS HC A03/MF A01 CSCL 17/9

Two second-year sea ice floes were probed using impulse radar sounding and direct drilling methods. The resulting two-way time of flight of the impulse radar EM wavelet, traveling from the surface to the ice bottom and back to the surface, was compared with snow and ice thickness data obtained from a drill hole. From this comparison, simple relationships are presented that provide an estimate of the thickness of sea ice, from about 1 to 8 m thick, with or without a snow cover. Relations are also presented that show the bulk or apparent dielectric constant of the ice floes vs. ice thickness, again with or without the snow cover. The data revealed that the apparent dielectric constant of the sea ice decreased with increasing ice thickness from a value of about 7 for ice 1 m thick to about 3.5 for ice 6 m thick. GRA

N90-22832# Army Cold Regions Research and Engineering Lab., Hanover, NH.
ACCURACY AND PRECISION OF GOES DATA COLLECTION PLATFORMS FOR TEMPERATURE MEASUREMENTS
Steven F. Daly, Charles H. Clark, and Timothy Pangburn Dec. 1989 18 p
(AD-A218798; CRREL-SR-89-37) Avail: NTIS HC A03/MF A01 CSCL 08/8

This report describes an analysis of the accuracy and precision of data transmitted by 12 Data Collection Platforms (DCPs) over a one-month period. The DCPs were installed on the Monogahela, Ohio and Illinois rivers. A reference resistor with a known and stable resistance was installed at each DCP site. Comparison of the resistance calculated from the transmitted information with the actual resistance of the reference resistor allowed the accuracy and precision of the measurements made by the DCP to be determined. Four brands of DCPs were included in the test; two had 8-bit resolution and two had 12-bit resolution. The results were analyzed with respect to the nominal accuracy provided by the manufacturer and the expected analog-to-digital quantizing error. This error explained most of the imprecision of the 8-bit DCPs but only part of the imprecision of the 12-bit DCPs. A large bias for some of the results was apparently caused by an impedance mismatch. A means of correcting the data based on the reference resistor measurement is proposed. GRA

N90-22833# Naval Ocean Systems Center, San Diego, CA.
SPECIFICATION FOR ENVIRONMENTAL MEASUREMENTS TO ASSESS RADAR SENSORS Final Technical Report, Oct. 1988 - Oct. 1989
Richard A. Paulus Nov. 1989 42 p Sponsored by Naval Sea Systems Command
(AD-A219127; NOSC/TD-1685) Avail: NTIS HC A03/MF A01 CSCL 17/9

The minimum requirements are prescribed for measuring environmental parameters that affect the evaluation of proposed radar systems. These environmental factors must be properly measured to ensure fair appraisals of competing designs and to assess expected long-term performance. The procedures for short-term in-situ measurements pertinent to microwave propagation and sea clutter are addressed. Measurement accuracies are specified and several types of instruments are discussed. Specific manufacturers and retailers are mentioned as sources for various types of instruments and equipment. This listing is not all-inclusive and is not intended to be an endorsement of those companies or products. A glossary of terms used in instrument specification are presented. Appendixes A through F are included as background material for determining refractive structure from surface meteorological measurements. GRA

44 ENERGY PRODUCTION AND CONVERSION

Includes specific energy conversion systems, e.g., fuel cells; global sources of energy; geophysical conversion; and windpower.

For related information see also *07 Aircraft Propulsion and Power, 20 Spacecraft Propulsion and Power,* and *28 Propellants and Fuels.*

N90-22834*# Harris Corp., Melbourne, FL. Government Aerospace Systems Div.
SOLAR CONCENTRATOR ADVANCED DEVELOPMENT PROGRAM Final Report
Don Knasel and Derik Ehresman Oct. 1989 333 p Original contains color illustrations
(Contract NAS3-24670)
(NASA-CR-185173; NAS 1.26:185173) Avail: NTIS HC A15/MF A02; 1 functional color page CSCL 10A

The Solar Concentrator Advanced Development Project has successfully designed, fabricated, and tested a full scale prototypical solar dynamic concentrator for space station applications. A Truss Hexagonal Panel reflector was selected as a viable solar concentrator concept to be used for space station applications. This concentrator utilizes a modular design approach and is flexible in attainable flux profiles and assembly techniques.

The detailed design of the concentrator, which included structural, thermal and optical analysis, identified the feasibility of the design and specific technologies that were required to fabricate it. The needed surface accuracy of the reflectors surface was found to be very tight, within 5 mrad RMS slope error, and results in very close tolerances for fabrication. To meet the design requirements, a modular structure composed of hexagonal panels was used. The panels, made up of graphite epoxy box beams provided the strength, stiffness and dimensional stability needed. All initial project requirements were met or exceeded by hardware demonstration. Initial testing of structural repeatability of a seven panel portion of the concentrator was followed by assembly and testing of the full nineteen panel structure. The testing, which consisted of theodolite and optical measurements over an assembly-disassembly-reassembly cycle, demonstrated that the concentrator maintained the as-built contour and optical characteristics. The facet development effort within the project, which included developing the vapor deposited reflective facet, produced a viable design with demonstrated optical characteristics that are within the project goals. Author

N90-22835*# Case Western Reserve Univ., Cleveland, OH. Center for Electrochemical Sciences.
CATALYSTS FOR ULTRAHIGH CURRENT DENSITY OXYGEN CATHODES FOR SPACE FUEL CELL APPLICATIONS Final Report, 1 Feb. 1989 - 31 Jan. 1990
D. Tryk, E. Yeager, M. Shingler, W. Aldred, and C. Wang 11 Jun. 1990 30 p
(Grant NAG3-694)
(NASA-CR-180650; NAS 1.26:180650) Avail: NTIS HC A03/MF A01 CSCL 10A

The objective of this research was to identify promising electrocatalyst/support systems for the oxygen cathode in alkaline fuel cells operating at relatively high temperatures, O2 pressures and current densities. A number of materials were prepared, including Pb-Ru and Pb-Ir pyrochlores, RuO2 and Pt-doped RuO2, and lithiated NiO. Several of these were prepared using techniques that had not been previously used to prepare them. Particularly interesting is the use of the alkaline solution technique to prepare the Pt-doped Pb-Ru pyrochlore in high area form. Well-crystallized Pb(2)Ru(2)O(7-y) was used to fabricate high performance O2 cathodes with relatively good stability in room temperature KOH. This material was also found to be stable over a useful potential range at approximately 140 C in concentrated KOH. Other pyrochlores were found to be either unstable (amorphous samples) or the fabrication of the gas-fed electrodes could not be fully optimized during this project period. Future work may be directed at this problem. High area platinum supported on conductive metal oxide supports produced mixed results: small improvements in O2 reduction performance for Pb(2)Ru(2)O(7-y) but a large improvement for Li-doped NiO at room temperature. Nearly reversible behavior was observed for the O2/OH couple for Li-doped NiO at approximately 200 C. Author

N90-22836# Midwest Research Inst., Golden, CO.
OCEAN ENERGY PROGRAM SUMMARY
Jan. 1990 15 p
(Contract DE-AC02-83CH-10093)
(DE89-009481; DOE/CH-10093/66) Avail: NTIS HC A03/MF A01

The oceans are the world's largest solar energy collector and storage system. Covering 71 percent of the earth's surface, they collect and store this energy as waves, currents, and thermal and salinity gradients. The purpose of the U.S. Department of Energy's (DOE) Ocean Energy Technology (OET) Program is to develop techniques that harness this ocean energy cost effectively and in a way that does not harm the environment. The program seeks to develop ocean energy technology to a point where industry can accurately assess whether the technology is a viable energy conversion alternative, or supplement, to current power generating systems. In past studies, DOE identified ocean thermal energy conversion (OTEC), which uses the temperature difference between warm surface water and cold deep water, as the most promising of the ocean energy technologies. As a result, the OET Program is concentrating on research that advances the OTEC technology. The program also continues to monitor and study developments in wave energy, ocean current, and salinity gradient concepts; but it is not actively developing these technologies now. DOE

N90-22837# Midwest Research Inst., Golden, CO.
GEOTHERMAL ENERGY PROGRAM SUMMARY
Jan. 1990 20 p
(Contract DE-AC02-83CH-10093)
(DE89-009485; DOE/CH-10093/70) Avail: NTIS HC A03/MF A01

Geothermal Energy Technology and the steps necessary to place it into service are reviewed. Specific topics covered are: four types of geothermal resources; putting the resource to work; power generation; FY 1989 accomplishments; hard rock penetration; conversion technology; and geopressured brine research. DOE

N90-22838# Midwest Research Inst., Golden, CO.
GEOTHERMAL ENERGY PROGRAM SUMMARY
Jan. 1990 70 p
(Contract DE-AC02-83CH-10093)
(DE89-009486; DOE/CH-10093/71) Avail: NTIS HC A04/MF A01

The Geothermal Technology Division (GTD) of the U.S. DOE is charged with the lead federal role in the research and development (R and D) of technologies that will assist industry in economically exploiting the nation's vast geothermal resources. The GTD R and D Program represents a comprehensive, balanced approach to establishing all forms of geothermal energy as significant contributors to the nation's energy supply. It is structured both to maintain momentum in the growth of the existing hydrothermal industry and to develop long-term options offering the greatest promise for practical applications. This volume, Volume 2, contains a detailed compilation of each GTD-funded R and D activity performed by national laboratories or under contract to industrial, academic, and nonprofit research institutions. DOE

N90-22839# Midwest Research Inst., Golden, CO.
PHOTOVOLTAIC ADVANCED RESEARCH AND DEVELOPMENT PROJECT: SOLAR RADIATION RESEARCH Annual Report, 1 Oct. 1988 - 30 Sep. 1989
C. Riordan, R. Hulstrom, T. Cannon, D. Myers, and T. Stoffel Feb. 1990 23 p
(Contract DE-AC02-83CH-10093)
(DE90-000302; SERI/PR-215-3607) Avail: NTIS HC A03/MF A01

The activities and accomplishments of SERI's Photovoltaic Advanced Research and Development Project task on Solar Radiation Research are summarized. The objective is to support the National Photovoltaics Program by helping to develop a fundamental scientific understanding of the relationships between the natural solar radiation environment and the design, performance, and performance measurements of PV devices. The activities that are summarized include: (1) the development of the Atmospheric Optical Calibration System for measuring solar radiation and atmospheric optical conditions during outdoor PV tests; (2) the development of an extended wavelength (290 to 3000 nm) spectroradiometer for measuring outdoor and simulator spectra; (3) data collection and analysis for PV applications at SERI's Solar Radiation Research Laboratory; and (4) collaborative activities, measurement support, and technical information transfer. DOE

N90-22840# Solarex Corp., Rockville, MD. Aerospace Div.
HIGH-EFFICIENCY SILICON SOLAR CELLS FOR A 22-SUN LINE-FOCUS MODULE
J. R. Silver and B. Patel Feb. 1990 21 p Prepared for Sandia National Labs., Albuquerque, NM
(Contract DE-AC04-76DP-00789)
(DE90-010242; SAND-90-7026) Avail: NTIS HC A03/MF A01

The purpose of this program was for Solarex, a commercial

silicon solar cell supplier, to demonstrate the capability of fabricating high efficiency 38.4 sq cm concentrator cells in a production environment. These cells were designed for use in 22-sun line-focus concentrator module that could generate 20 kW for the PVUSA EMT-1 project. The cells were fabricated using p-type, .8 ohm-cm silicon, randomly textured fronts, dual layer anti-reflective coatings, passivated emitters, restricted emitter/metallization contact areas, and silver gridlines with large cross-sectional areas. Prismatic covers were used to eliminate losses from gridline shadowing. Cell efficiencies as high as 20.34 percent were demonstrated on covered cells at 20 suns air mass 1.5 illumination. The process sequence includes a single diffusion step, a thin thermal oxide growth, and two mechanically registered photolithography steps. DOE

N90-22841# Sandia National Labs., Albuquerque, NM.
AN ASSESSMENT OF SECOND-GENERATION STRETCHED-MEMBRANE MIRROR MODULES
D. J. Alpert, R. M. Houser, A. A. Heckes, and W. W. Erdman Feb. 1990 72 p
(Contract DE-AC04-76DP-00789)
(DE90-010243; SAND-90-0183) Avail: NTIS HC A05/MF A01

For more than 10 years, the U.S. Department of Energy's Solar Thermal Program has pioneered the development of heliostats, mirrors that track the sun, for solar central-receiver power plants. The field of heliostats is the single most expensive part of such plants, so their cost must be as low as possible for the technology to be commercially successful. Recent efforts have focused on the development of heliostats that use stretched-membrane reflectors in place of the more familiar glass mirrors. In such heliostats, metal foils are stretched over both sides of a large-diameter metal ring. The reflective surface is a silvered-polymer film glued to the front membrane. A slight vacuum in the space between the two membranes is actively controlled to provide a concave, focused contour to the mirror, and in an emergency this space can be rapidly pressurized to defocus it. Because of their simplicity and lighter weight, stretched-membrane heliostats have the potential to cost significantly less than current glass-mirror designs. The first 50-sq-meter mirror modules, built under contract to Sandia in 1986, demonstrated that membrane heliostats could perform at least as well as heliostats using glass mirrors. Insights gained from Sandia's testing and evaluation of the first-generation units were incorporated into the designs of two improved 50-sq-meter mirror modules. The results of Sandia's evaluation show significant improvement in optical performance over the first-generation designs, especially in windy conditions. DOE

N90-22842# Deutsche Forschungsanstalt fuer Luft- und Raumfahrt, Stuttgart (Germany, F.R.). Abteilung Bauteilgestaltung.
THE PRESSURE LOADED VOLUMETRIC CERAMIC RECEIVER
Walter Pritzkow Sep. 1989 46 p
(DLR-Mitt-89-17; ISSN-0176-7739; ETN-90-96451) Avail: NTIS HC A03/MF A01

The tests carried out with the pressure loaded volumetric ceramic receiver are reported. The system is a solar receiver to convert concentrated solar radiation into process heat. It is designed to heat up air from ambient temperatures to 1000 C and to work at 10 bars gauge pressure. The function of the experiment is described. The main problems were the window and the sealing between the cold metal housing and the hot ceramic structure. The results showed that such a receiver can be used for gas pressure processes with a pressure level of about 3 to 5 bar or a chemical process for energy storage and transportation at a level of about 8 bar. ESA

N90-22843*# National Aeronautics and Space Administration. Lewis Research Center, Cleveland, OH.
LATERAL SPREADING OF Au CONTACTS ON InP
Navid S. Fatemi (Sverdrup Technology, Inc., Cleveland, OH.) and Victor G. Weizer 1990 10 p Presented at the 1990 Spring Meeting of the Materials Research Society, San Francisco, CA, 16-21 Apr. 1990
(Contract NAS3-25266)
(NASA-TM-103133; E-5472; NAS 1.15:103133) Avail: NTIS HC A02/MF A01 CSCL 10A

The contact spreading phenomenon observed when small area Au contacts on InP are annealed at temperatures above about 400 C was investigated. It was found that the rapid lateral expansion of the contact metallization which consumes large quantities of InP during growth is closely related to the third stage in the series of solid state reactions that occur between InP and Au, i.e., to the Au3In-to-Au9In4 transition. Detailed descriptions are presented of both the spreading process and the Au3In-to-Au9In4 transition along with arguments that the two processes are manifestations of the same basic phenomenon. Author

N90-22844# Tunzini Nessi Entreprise Equipement, Rueil-Malmaison (France).
IMPROVEMENT STUDY OF IRON DISILICIDE THERMOELECTRIC MATERIALS Final Technical Report, Sep. 1989 - Jan. 1990
Stanislas Scherrer and Hubert Scherrer 12 Jan. 1990 17 p
(Contract DAJA45-89-M-0234)
(AD-A218946; R/D-6287.PH.09-F) Avail: NTIS HC A03/MF A01 CSCL 11/6

In many applications at high temperature, the semiconducting compound beta-Fe Si2 has been already proposed for power generation. The goal of this part of the study is to obtain pure semiconducting beta-Fe Si2 phase as a material of reference for thermoelectric properties. The melting of elemental Iron and Silicon powders is done at 1250 C and the transition of the metallic (alpha) to semiconducting beta phase is obtained by annealing. This classical preparation of beta-Fe Si2 was time consuming and because of the phase diagram results in the production of inhomogeneous alloys. Mechanical alloying was considered as an alternate method of producing beta-Fe Si2. This method for elaborating the compound from lower temperature must avoid the difficulties of sublimation and evaporation of the components. It also allows the optimization of beta-Fe Si2. The results of the two elaborating methods are compared by x ray diffraction measurements. These results on beta-Fe Si2 obtained by mechanical alloying, were original. This process now appears to be a reliable method to introduce amounts of dopant in the material. GRA

N90-22845# Rockwell International Corp., Canoga Park, CA. Rocketdyne Div.
EXPERIMENTAL STUDIES ON ENERGY STORAGE Final Report, Aug. 1986 - Jul. 1989
Karl O. Christie and William W. Wilson Feb. 1990 69 p
(Contract F04611-86-C-0074; AF Proj. 5730)
(AD-A219032; RI/RD89-225; AL-TR-89-083) Avail: NTIS HC A04/MF A01 CSCL 21/9

The feasibility is demonstrated of synthesizing hypervalent, high oxidation state fluorides of nitrogen, oxygen, and the halogens. Typical target compounds were Nitrogen Pentafluoride, Chlorine Pentafluoride Oxide, Chlorine Hexafluoride Anion, Argon Fluoride Cation, Nitrogen Difluoride Anion, Arsenic Hexafluoride, and combinations of high oxidation state halogen fluoride anions with organic cations. In addition, special experimental techniques, such as low-temperature photolysis and glow-discharge, matrix-isolation spectroscopy and microwave discharge reactions were to be explored for the syntheses of these species. A brief discussion of some of the results is given. In cases where a certain piece of work was completed, the results are summarized as manuscripts which are given in the Appendix and either have been or will be published. GRA

N90-22846# International Fuel Cells Corp., South Windsor, CT.
ENHANCED CERIA SOLID ELECTROLYTE FUEL CELL DEVELOPMENT. REDUCTION OF ELECTRONIC CONDUCTIVITY PERMITS USE OF A SOLID CERIA ELECTROLYTE IN HIGH EFFICIENCY HIGH POWER DENSITY FUEL CELLS AT TEMPERATURES COMPATIBLE WITH METALLIC CELL HARDWARE Quarterly Interim Report No. 5, period ending Sep. 1989
D. L. Maricle Jan. 1990 41 p
(Contract N00014-88-C-0390)
(AD-A219297; FCR-10815) Avail: NTIS HC A03/MF A01 CSCL 10/3

The high operating temperature of zirconia based solid oxide fuel cells has been shown in many studies to have advantages for both space and terrestrial applications. The high heat rejection temperature minimizes radiator size and weight for high atmospheric and space applications. Mobile and stationary terrestrial applications take advantage of a cell temperature high enough to directly reform hydro-carbon fuels, achieving high efficiency and energy density. Government funded solid oxide fuel cell (SOFC) efforts are concentrated on the monolithic and tubular cell designs employing zirconia as the oxide ion conduction membrane. Zirconia requires an operating temperature of 1000 C to achieve adequate electrolyte conductivity. All-ceramic cell structures are used in both cases, leading to fragile, failure prone cells, and manufacturing steps which are difficult to scale up and costly. IFC's molten carbonate fuel cell development demonstrates the reliability of ductile sheet metal parts used for gas flow fields, separator plates, and frames in the 650 C temperature range. Ceria doped with gadolinium has ionic conductivity at 700 C comparable to zirconia at 1000 C. At 700 C a variety of stainless steels offer acceptable strength and oxidation resistance for use as cell hardware. GRA

N90-22847*# National Aeronautics and Space Administration. Lewis Research Center, Cleveland, OH.
NUCLEAR TECHNOLOGY AND THE SPACE EXPLORATION MISSIONS
Henry W. Brandhorst and Ronald J. Sovie 1990 11 p Proposed for presentation at the 25th Intersociety Energy Conversion Engineering Conference, Reno, NV, 12-17 Aug. 1990; cosponsored by AIChE, SAE, ACS, AIAA, ASME, and IEEE
(NASA-TM-103156; E-5518; NAS 1.15:103156) Avail: NTIS HC A03/MF A01 CSCL 10B

The strategy for a major exploration initiative leading to permanent human presence beyond earth orbit is still being developed; however enough is known to begin defining the role of nuclear technologies. Three broad areas are discussed: low power (less than 10 kWe) rover/vehicle power systems; integrated, evolutionary base power systems (25 to 100 kW) and nuclear energy for electric propulsion (2 to 100 MWe); and direct thermal propulsion (1000s MW). A phased, evolutionary approach is described for both the moon and Mars, and the benefits of nuclear technologies relative to solar and their integration are described. Author

45 ENVIRONMENT POLLUTION

Includes atmospheric, noise, thermal, and water pollution.

N90-22848 Kentucky Univ., Lexington.
A STUDY OF MESOSCALE ACID DEPOSITION IN THE LOWER OHIO RIVER VALLEY Ph.D. Thesis
Rick Davis Saylor 1989 565 p
Avail: Univ. Microfilms Order No. DA9001443

Atmospheric processes are inherently difficult to analyze due to the broad spatial and temporal scales that must be considered. The mesoscale is an appropriate spatial scale over which acid deposition phenomena may be studied. Acid deposition in a mesoscale region is investigated. The mesoscale area chosen for analysis is a region in the lower Ohio River valley which is of particular interest due to the high density of major pollutant emission sources located there. There were two major thrusts. First, a detailed statistical analysis of acid deposition data was performed for data obtained from a precipitation chemistry network located within the mesoscale region. The purpose was to characterize precipitation chemistry data over the area. The precipitation chemistry data were analyzed to determine the spatial variation of chemical species over the region, the seasonal trends of the data, and the relationships between various ionic species. Second, a series of numerical simulations were performed using the STEM 2 pollutant transport/transformation/deposition model. The specific acid deposition episode of April 29 to May 2, 1985 was simulated with STEM 2 employing meteorological data obtained from radiosonde flights over the eastern United States. The temperature, pressure, humidity, eddy diffusivity, and wind field data derived from radiosonde observations on April 29 to May 2, 1985 were input into STEM 2 along with pollutant emissions. The STEM 2 simulation of the episode provided predictions of pollutant gas-phase profiles throughout the region as well as estimates of wet and dry deposition to the surface. Predicted sulfate and nitrate wet depositions over the region were compared with actual measured depositions obtained from precipitation chemistry networks within the area. Dissert. Abstr.

N90-22849# Rome Univ. (Italy). Dipt. di Fisica.
ON THE ANTARCTIC OZONE DEPLETION DURING SOLAR CYCLE 21
M. DePetris, M. Gervasi, S. Masi, B. MelchiorriOlivo (Consiglio Nazionale delle Ricerche, Rome, Italy), G. Moreno, M. Storini, and P. Calisse 6 Dec. 1989 18 p Submitted for publication
(Nota-Interna-943; ETN-90-96545) Avail: NTIS HC A03/MF A01

The long term variations of the ozone column density, observed in the Antarctic atmosphere in the period 1964 to 1985, are studied in connection with the trend of the geomagnetic activity. While the current view accounts for the ozone depletion entirely in terms of chemical and dynamical processes occurring in the atmosphere, the present experimental evidences are shown to rely favorably on the contribution of geomagnetic phenomena such as aurorae, induced by solar related disturbances. ESA

46 GEOPHYSICS

Includes aeronomy; upper and lower atmosphere studies; ionospheric and magnetospheric physics; and geomagnetism.

For space radiation see *93 Space Radiation.*

N90-22850*# National Aeronautics and Space Administration. Goddard Space Flight Center, Greenbelt, MD.
SURFACE TOPOGRAPHY OF THE GREENLAND ICE SHEET FROM SATELLITE RADAR ALTIMETRY
Robert A. Bindschadler, H. Jay Zwally, Judith A. Major, and Anita C. Brenner (ST Systems Corp., Greenbelt, MD.) 1989 373 p Original contains color illustrations
(NASA-SP-503; Rept-89B00170; NAS 1.21:503; LC-89-600282)
Avail: NTIS HC A16/MF A02; 3 functional color pages CSCL 08E

Surface elevation maps of the southern half of the Greenland subcontinent are produced from radar altimeter data acquired by the Seasat satellite. A summary of the processing procedure and examples of return waveform data are given. The elevation data are used to generate a regular grid which is then computer contoured to provide an elevation contour map. Ancillary maps show the statistical quality of the elevation data and various characteristics of the surface. The elevation map is used to define ice flow directions and delineate the major drainage basins. Regular maps of the Jakobshavns Glacier drainage basin and the ice divide in the vicinity of Crete Station are presented. Altimeter derived elevations are compared with elevations measured both by satellite geoceivers and optical surveying. Author

N90-22851 Cornell Univ., Ithaca, NY.
PLASMA INSTABILITIES ASSOCIATED WITH THE INJECTION OF ARTIFICIAL ION BEAMS INTO THE IONOSPHERE Ph.D. Thesis
Wayne Anthony Scales 1989 223 p
Avail: Univ. Microfilms Order No. DA8915123

Plasma instabilities that result when a heavy ion beam is injected into the F-region ionosphere are studied using linear theory and one-dimensional electrostatic particle simulations. The background plasma model used consists of a relatively cool, collisionless O+ dominated plasma with concentrations of light ions H+ and He+. The ion beam is taken as homogeneous, and due to its large larmor radius, unmagnetized. The beam density is assumed to be on the order of or less than the O+ density. The frequency range studied is from the lower hybrid frequency down to the O+ gyrofrequency. Important results from the linear theory are as follows. For beam drift velocities, v(sub d), much larger than the H+ thermal velocity, v(sub H), the lower hybrid and ion-ion hybrid instabilities dominate with the lower hybrid instability having the largest growth rate. For drifts on the order of v(sub H), the H+ gyroharmonic instabilities dominate with the harmonics near the lower hybrid frequency having the largest growth rates. The O+ gyroharmonic instability dominates for drifts on the order of the O+ thermal velocity. The simulation results show that for v(sub d)/v(sub H) greater than or = 1, the perpendicular H+ heating is more efficient than the perpendicular O+ or parallel electron heating. At low beam densities, only H+ is heated, but as the density is increased, the waves grow to large enough amplitudes to trap and heat the O+ and electrons. The wave amplitudes begin to decrease for propagation angles larger than (m sub e / m sub o)exp 1/2 which results in comparable O+ and electron heating. In the high beam temperature regime, the beam thermalization is small in comparison to that of the background particles and background particle heating can be a competing saturation mechanism with beam heating. The results of the linear theory and simulations are compared to observations made during ion beam injection experiments performed aboard sounding rockets. Dissert. Abstr.

N90-22852 Maryland Univ., College Park.
A STUDY OF AURORAL ACTIVITY IN THE NIGHTSIDE POLAR CAP Ph.D. Thesis
Qian Wu 1989 204 p
Avail: Univ. Microfilms Order No. DA8924258

Using various ground observations at South Pole, Antarctica and its conjugate point, Frobisher Bay, Canada, the following aspects of nightside polar cap auroral activity were studied: The appearance and disappearance of polar cap auroras associated with substorms and interplanetary magnetic field (IMF) variations; auroral optical emission line intensities; and the seasonal variation of auroral conjugacy. The observations show that the polar cap auroras usually fade away before the expansive phase of a substorm and bright auroral arcs reach high latitude near the recovery phase. Just before the auroras fade away the discrete polar cap auroral arcs, which are usually on the poleward boundary of the diffuse aurora, intensify for 1 to 2 minutes. The observations also indicate that the IMF may have stronger control over polar cap auroral activity than do substorms. A search for energy spectral variation of precipitating electrons using the intensities of 630.0 nm (O) and 427 nm (N2(+)) auroral emission lines reveals no dramatic changes in the energy spectrum; instead, the data show possible atmospheric scattering and geometric effects on the photometric measurements while the bright auroral arc is moving into the polar cap. The conjugate observations show that the stormtime auroral electrojet current, which is associated with the bright auroral arc, in most cases reaches higher (lower) latitudes in the winter (summer) hemisphere. An asymmetric plasma sheet is proposed, which expands deeper into the winter lobe, under a tilted geomagnetic dipole. Accordingly, the winter polar cap would have smaller area and the auroral electrojet would be at higher latitude. Dissert. Abstr.

N90-22853 Illinois Univ. at Urbana-Champaign, Savoy.
A NEW STOCHASTIC MODEL OF TURBULENT DISPERSION IN THE CONVECTIVE PLANETARY BOUNDARY LAYER AND THE RESULTS OF THE ATTERBURY-87 FIELD STUDY Ph.D. Thesis
James Christian Liljegren 1989 315 p
Avail: Univ. Microfilms Order No. DA8924885

The development and validation of a stochastic model for predicting the dispersion of a passive tracer in the convective boundary layer are presented. The methods and procedures employed and the results obtained from the Atterbury-87 field study of the dispersion of fog-oil smoke and hexachloroethane (HC) smoke are also described. The stochastic model represents a substantial improvement over previous modeling approaches. Using the Langevin equation to model the Lagrangian velocities, the dispersion of a large number of passive tracer particles is computationally simulated. The shape of the resulting probability density function closely matches observations. The behavior of the autocorrelation of the modeled Lagrangian velocities also matches the non-exponential form computed from balloon-borne measurements by using the local integral time scale of the turbulence. The model was verified against data gathered from laboratory simulations of the boundary layer carried out in water tanks and wind tunnels as well as from actual field measurements. Comparisons of crosswind-integrated concentration and plume spread computed from the test data with the results of previous field studies of atmospheric dispersion indicated strong agreement. Comparison of concentration data with the predictions of the stochastic model also showed good agreement and confirmed that the centerline of the smoke plume lifted off the ground. Dissert. Abstr.

N90-22854 California Univ., Los Angeles.
QUANTIFYING AND REDUCING UNCERTAINTY IN THE ASSIMILATIVE MAPPING OF IONOSPHERIC ELECTRODYNAMICS Ph.D. Thesis
Delores J. Knipp 1989 191 p
Avail: Univ. Microfilms Order No. DA9003175

The Assimilative Mapping of the Ionospheric Electrodynamics (AMIE) procedure developed by Richmond and Kamide (JGR, p. 5741, 1988) was applied to three periods: 23 to 24 July 1983, 18 to 19 January 1984 and 19 September 1984. The mapping procedure obtains optimal estimates of electrodynamic patterns from basis functions multiplied by an appropriate set of coefficients which are determined from a constrained least squares fit to the data. The impact of several additions to the procedure are shown and some of the geophysics implied by the results are shown. New estimates for auroral conductance are incorporated from satellite particle detectors and a satellite x ray imager. This new information is used to produce global estimates of conductance and to study the effect of uncertainty in those estimates on the estimates of the polar electric field structure. New observations are incorporated relating to the electric field: satellite magnetometer data and the vertical component of the ground magnetometer data. Results demonstrate the ability of the AMIE procedure to define the temporal and spatial development of several important solar-wind-magnetosphere-ionosphere interactions. The mappings of ionospheric response to the Interplanetary Magnetic Field (IMF) east-west component is in excellent agreement with currently accepted theory. Two examples of convection reversals are discussed. Dissert. Abstr.

N90-22855 Illinois Univ. at Urbana-Champaign, Savoy.
EVOLUTION OF ATMOSPHERIC BAROCLINIC WAVES Ph.D. Thesis
Han-Yun Chou 1989 139 p
Avail: Univ. Microfilms Order No. DA9010830

The evolution of atmospheric baroclinic waves is investigated by a six layer forced dissipative quasi-geostrophic beta-plane channel model. In the control run, the model has: a realistic zonal thermal forcing; a surface Ekman layer (a Newtonian cooling and an interior biharmonic friction as the dissipation); and an initial state consisting of a weak but general wave field superimposed

on a jet-like zonal mean flow. The whole evolution of the baroclinic waves can be divided into three periods; namely, the baroclinically growing period in which the synoptic waves grow exponentially, the transition period in which the synoptic waves decay and the planetary waves grow, and the equilibration period in which the planetary waves become dominant. The synoptic waves stop growing exponentially due to the wave-wave interaction as well as the barotropic decay. The planetary waves are forced by the synoptic waves through the nonlinear cascade process. In the sensitivity experiments, it is found that the spectral composition in the equilibrated state is not qualitatively dependent upon the meridional structure in the zonal thermal forcing. But when the latter is absent, the wave field is substantially stronger. A jet zonal mean flow is generated in the center of the domain, although it is initially uniform. As a potential vorticity forcing is applied, it gives rise to a wave field dominated by the (5, 1) wave, which has the same horizontal scale as the most unstable mode according to the linear theory, instead of the long waves in the control run and the other studies. Author

N90-22856# Joint Inst. for Nuclear Research, Dubna (USSR).
SUPERHETERODYNE THREE-WAVE DETECTION OF GRAVITATION WAVES
A. F. Pisarev and S. A. Pisareva 1988 6 p In RUSSIAN; ENGLISH summary Presented at the 3rd School on Research on Automatization in Nuclear Physics and Astrophysics, Nal'chik, USSR, Sep. 1988
(DE90-620465; JINR-18-88-603) Avail: NTIS (US Sales Only) HC A02/MF A01

A superheterodyne method of mutual transformation of wave energies in the non-linear three wave process involving a gravitational wave is considered. A flexible possibility of Transferring the great external gain coefficient from an electromagnetic or acoustic wave to the gravitation one is shown. It can facilitate generation and detection of this wave. DOE

N90-22857# Woods Hole Oceanographic Inst., MA.
CALCULATION OF 3-DIMENSIONAL SYNTHETIC SEISMOGRAMS ON THE CONNECTION MACHINE
J. M. Allen and D. R. Burns Oct. 1989 87 p
(Contracts N00014-87-K-0007; N00014-89-J-1012; F30602-88-C-0031)
(AD-A218472; WHOI-89-48) Avail: NTIS HC A05/MF A01 CSCL 08/3

A 3-D, second order finite difference method was used to create synthetic seismograms for elastic wave propagation in heterogeneous media. These synthetic seismograms are used to model rough seafloor, the shallow crust, or complex structural and stratigraphic settings with strong lateral heterogeneities. The finite difference method is preferred because it allows models of any complexity to be generated and includes all multiple scattering, wave conversion and diffraction effects. The method uses a fully staggered grid as developed by Virieux (1986). Wavefront snapshots and time series output allow the scattering and focussing of different wave modes with direction to be visualized. The extensive calculations required for realistic size models stretches the resources of serial computers like the VAX 8800. On the Connection Machine, a massively parallel computer, the finite difference grid can be directly mapped onto the virtual processors, reducing the nested time and space loops in the serial code to a single time loop. As a result, the computation time is reduced dramatically. GRA

N90-22858# Georgia Tech Research Inst., Atlanta. Electromagnetics Lab.
MEGALIDAR PROOF-OF-CONCEPT DEMONSTRATION Interim Report, Jun. 1988 - Jun. 1989
J. M. Cathcart, A. K. Garrison, G. G. Gimmestad, and D. W. Roberts Oct. 1989 168 p
(Contract F33615-86-C-1051; AF Proj. 2004)
(AD-A218787; WRDC-TR-89-1100) Avail: NTIS HC A08/MF A01 CSCL 09/3

This report describes the MEGALIDAR proof-of-concept demonstration performed on the 100-inch collimator to demonstrate the capability of the MEGALIDAR to measure atmospheric densities to altitudes up to 80 km. The report presents a description of the lidar Nd:YAG laser transmitter, receiver and data acquisition subsystem as well as a description of the steps in adapting the collimator facility to accommodate the lidar system. The results of a series of measurements to altitudes up to 85 km are presented along with the measurement method and analyses procedures. Recommendations, based on experience during the demonstration, for improvement of the collimator facility for lidar are given. GRA

N90-22859# San Calixto Observatory, La Paz (Bolivia).
PROPAGATION AND ATTENUATION OF Lg WAVES IN SOUTH AMERICA Final Report, 1 Aug. 1987 - 31 Jul. 1989
Ramon Roige Cabre, Estela Ramos Minaya, Ivar John Alcocer, and Rene Rodolfo Ayala Sep. 1989 51 p
(Grant AF-AFOSR-0311-87; AF Proj. 7A10)
(AD-A218853; GL-TR-89-0273) Avail: NTIS HC A04/MF A01 CSCL 08/11

Characteristics of Lg waves in La Paz station LPB are analyzed. After realizing that earthquakes with oceanic path and those deep enough do not produce Lg, they were discarded. The remaining 486 earthquakes, occurred from 1974 to 1986, are considered, looking for Lg characteristics, according to origin region. Lg are guided waves SH type, originated in surficial and in subduction intermediate depth earthquakes. Apparent velocity is 3.57 km/s independent of distance, but with some dispersion (beginning often is not clear). Predominant period is 1.1 to 1.3 s. Amplitude in most cases equals P amplitude; it is normalized by dividing Lg/P, with results similar to Bath's normalized wave energy. They are transmitted efficiently through shields, poorly along cordilleran structures; from Peru Lg recording is uneven, meriting a more detailed study; from southern region (Argentina and Chile) waves are weak, but not so much as suggested by a first glance (wave period longer finds lesser recording gain). Recording in several South American stations is considered. Some earthquakes were revised. They confirm previous conclusions and help to identify efficiency of different paths and type of Lg recording, since origin regions and recording stations are at the ends of wave path. Type of recording may unveil hidden cordilleran structure in Andes-plains transition. GRA

N90-22860# Alaska Univ., Fairbanks. Geophysical Inst.
GRAVITY WAVE AND TURBULENCE STUDIES USING A HIGH-RESOLUTION ST RADAR Final Technical Report, 1 Jan. 1987 - 1 Jan. 1990
David C. Fritts 12 Feb. 1990 14 p
(Contract F49620-87-C-0024; AF Proj. 2310)
(AD-A218877; AFOSR-90-0290TR) Avail: NTIS HC A03/MF A01 CSCL 04/1

Research under this contract addressed a number of aspects of gravity wave propagation and effects in the lower and middle atmosphere. Observational studies utilized data sets collected at several radar installations and in situ data obtained during two major rocket campaigns. Theoretical studies examined wave instability and ducting, the relationship between neutral and ion density fluctuations in the presence of chemically active species, and the potential for energy exchange due to resonant wave interactions. Our results showed the motion spectrum in the troposphere, stratosphere, and mesosphere to be highly anisotropic, with an upward flux of horizontal momentum largely opposed to the large-scale mean flow. The motion spectrum was found largely to be consistent with gravity wave theory and saturation. These findings have important implications for the forcing of the mean circulation of the lower and middle atmosphere. Theoretical studies revealed low-frequency motions to favor dynamical instabilities and suggested that resonant wave interactions are not likely to be a major factor for energy transfer in the middle atmosphere due to the rapid vertical transport and dissipation of energy. GRA

N90-22861# California Univ., Berkeley. Dept. of Geology and Geophysics.
REGIONAL STUDIES WITH BROADBAND DATA Final Report, 6 Mar. 1988 - 5 Jun. 1989
Thomas V. McEvilly and Lane R. Johnson 7 Aug. 1989 72 p Prepared in cooperation with California Univ., Berkeley. Lawrence Berkeley Lab.
(Contract F19628-87-K-0032; ARPA Order 5299)
(AD-A219215; GL-TR-89-0224) Avail: NTIS HC A04/MF A01 CSCL 08/11

An experiment was performed in which broadband waveform data were recorded by a seismic network surrounding a series of 8 chemical explosions in a quarry. The experiment is described and all of the waveform data are presented. A velocity model was obtained from the travel time readings and this was used to estimate moment rate tensors for 5 of the events which were single explosions. The results indicate simple source mechanisms for these single explosions, particularly the deeper events. The efficiency with which chemical energy is converted to seismic waves shows a strong dependence upon the depth of the source and this is caused primarily by a decrease in the corner frequency of the source time function as the source depth decreases. When scaled by the size of the explosion, the results for these small chemical explosions are in reasonable agreement with similar results for much larger nuclear explosions. GRA

N90-22862# Massachusetts Inst. of Tech., Cambridge. Earth Resources Lab.
SEISMIC WAVE PROPAGATION, ATTENUATION AND SCATTERING OVER REGIONAL DISTANCES Final Report, 28 Jul. 1988 - 27 Jul. 1989
Nafi Toksoez, Ari Ben-Menahem, Edmond E. Charrette, Anton M. Dainty, and Richard L. Gibson, Jr. 11 Dec. 1989 98 p
(Contract F19628-88-K-0036; AF Proj. 7A10)
(AD-A219358; GL-TR-89-0329) Avail: NTIS HC A05/MF A01 CSCL 08/11

The objective of this project was to conduct basic research on the propagation of seismic energy at regional (100 to 1000 km) distances for purposes of monitoring underground nuclear explosions. The problems studied were the coherency of the seismic S phases, especially Lg, and the implications in terms of the scattering properties of the earth medium; and scattering from anisotropic inclusions. This Final Report consists of preprints of two papers on these subjects. The first concerns the measurement of coherency of the Sn/Lg phases at distances of 200 to 400 km for quarry blasts recorded at the Fennoscandian arrays ARCESS, FINESA, and NORESS, and its interpretation. The measurements indicate wavelength scaling of the spatial coherency, i.e., scaling according to the scale of the wave only, in the frequency band 1 to 10 Hz; the wavelength range is 0.4 to 2 km. This suggests there is no medium scale in this size range. Numerical experiments with randomized time series demonstrate that spatial coherency is mainly controlled by phase (travel time) variations. Preliminary work with finite difference modelling of these regional phases shows that crustal models with random velocity variations have the potential to explain the observations. GRA

N90-22863# Lamont-Doherty Geological Observatory, Palisades, NY.
MEASUREMENTS OF HIGH FREQUENCY SEISMIC WAVES Final Report, 16 Mar. 1987 - 13 Mar. 1989
William H. Menke 4 Dec. 1989 50 p
(Contract F19628-87-K-0011)
(AD-A219370; GL-TR-89-0147) Avail: NTIS HC A03/MF A01 CSCL 08/11

Except for its very onset, the P wave of earthquakes and chemical explosions observed at two narrow-aperture arrays on hard rock sites in the Adirondack Mountains have a nearly random polarization. The amount of energy on the vertical, radial and transverse components is about equal over the frequency range 5 to 30 Hz, for the entire seismogram. The spatial coherence of the seismograms is approximately exp(-cf delta x), where c is in the range 0.4 to 0.7 km 1/km 1/Hz, f is frequency and delta X is the distance between array elements. The spatial coherence is approximately independent of component, epicentral azimuth and range, and whether P or S wave coda is being considered, at least for propagation distances between 5 and 170 km. These results imply a strongly and three-dimensionally heterogeneous crust, with near-receiver scattering in the uppermost crust controlling the coherence properties of the waves. GRA

47 METEOROLOGY AND CLIMATOLOGY

Includes weather forecasting and modification.

N90-22864 Drexel Univ., Philadelphia, PA.
IMPACT OF MARINE BOUNDARY LAYER PARAMETERIZATION ON A NUMERICAL SIMULATION OF CYCLOGENESIS DURING A COLD AIR OUTBREAK EVENT Ph.D. Thesis
Shing Yoh 1989 204 p
Avail: Univ. Microfilms Order No. DA9006143

The Drexel Limited Area Mesoscale Prediction System (LAMPS) is used to study the cyclogenesis during a cold air outbreak event which occurred during the Genesis of Atlantic Lows Experiment (GALE) Intensive Observation Period 2 (IOP 2). A new marine boundary layer parameterization scheme is developed: Businger's similarity profiles is modified to incorporate free convection limit scaling into the surface flux calculations; Deardorff's (1974) unstable boundary layer height equation and Nieuwstadt and Tennekes' (1981) stable boundary layer height equation are used; and the O'Brien K-profile (1970) is modified to incorporate mixed layer scaling for extreme unstable conditions to determine the vertical turbulent mixing. The new parameterization scheme is tested in a one dimensional model using observed oceanic soundings collected during GALE. The sensitivity of the model to different parameterization scheme is studied. Three versions of the LAMPS model with full model physics are used to study the cold air outbreak event. The simplified version uses constant transfer coefficients to determine the oceanic fluxes, a predetermined analytic equation to determine the vertical mixing. The improved version uses the new parameterization scheme discussed above with an air-sea interfacial sublayer formulation proposed by Liu et al. (1979). The strong flux version is the same as the improved version except that the effective roughness length for temperature and moisture are set equal to that of the momentum. Dissert. Abstr.

N90-22865 Pennsylvania State Univ., University Park.
PREDICTABILITY OF WEATHER AND CLIMATE IN A COUPLED OCEAN-ATMOSPHERE MODEL: A DYNAMICAL SYSTEMS APPROACH Ph.D. Thesis
Jon Michael Nese 1989 290 p
Avail: Univ. Microfilms Order No. DA9007904

A dynamical systems approach is used to quantify the instantaneous and time-averaged predictability of a low-order moist general circulation model. Specifically, the effects on predictability of incorporating an active ocean circulation and asynchronously coupling the ocean and atmosphere are evaluated. The predictability of the model attractors is compared using the Lyapunov exponents, the local divergence rates L(x(t)), and several measures of dimension. The predictability of monthly averaged and yearly averaged states is also investigated by using attractor reconstruction techniques. Activating the ocean circulation improves the average predictability of the short time scales by ten percent and decreases the variance of the local divergence rate. Asynchronous coupling more significantly reduces the variability of L(x(t)) and artificially increases the average error doubling time by a factor of four when the update time for the coupling terms exceeds a week. For the attractor of the monthly average states, the largest Lyapunov exponent suggests an error doubling time of approximately three months. However, the predictability enhancement due to the asynchronous coupling methodology is minimal for the yearly averaged states. The dimensions of the attractors of the monthly and yearly averaged

states are not significantly less than the dimensions of the attractors of the instantaneous states. In general, the differences are no larger than the inherent uncertainty estimates of the dimensions of decadal- and century-averaged attractors. A more important contribution is the demonstration that the local divergence rates concisely measure the variations of predictability on attractors and provide a basis for comparing their local predictability characteristics. An algorithm for generating a real-time estimate of local predictability to accompany a forecast is outlined.
Dissert. Abstr.

N90-22866# Instituto de Pesquisas Espaciais, Sao Jose dos Campos (Brazil).
IMPACT OF METEOROLOGY ON THE AGRICULTURAL SECTOR: COMPILATION AND ANALYSIS OF PROJECTS [IMPACTO DA METEOROLOGIA NO SETOR AGRICOLA: COMPILACAO E ANALISE DE CASOS]
Heloneida deCarvalhoKataoka and Antonio Divino Moura Oct. 1989 80 p In PORTUGUESE; ENGLISH summary Presented at the 6th Brazilian Conference on Agrometeorology, Maceio, Brazil, 9-16 Jul. 1989
(INPE-4846-PRE/1475) Avail: NTIS HC A05/MF A01

The results of some projects undertaken in the Brazilian Agricultural Sector, that make explicit use of meteorological information are compiled and reviewed. The aim is to highlight the benefits that may be obtained through the use of such information. Author

N90-22867 Arizona Univ., Tucson.
TROPICAL SQUALL LINES OF THE ARIZONA MONSOON Ph.D. Thesis
Walter Prestont Smith 1989 186 p
Avail: Univ. Microfilms Order No. DA9010487

Squall lines possessing nearly all the characteristics of tropical squall lines occasionally develop during the summer monsoon over southern Arizona and northwestern Mexico. Initial thunderstorm formation is over the mountains along the Continental Divide in the late afternoon. Satellite imagery, cloud-to-ground lightning strike data, and surface observations indicate the squall lines move from east to west or northeast to southwest by discrete propagation faster than all the winds below 20 kPa so that most of the anvil clouds lag behind. The synoptic-scale circulation is anomalous with a strong ridge located over the western United States and a deep trough located over the eastern United States. West to northwest winds are found in the boundary layer over southern Arizona and northwest Mexico while a deep layer of east winds are observed above. As a result, most of the environmental wind shear is confined to the lowest 2.5 km above the ground. The low-level wind shear seems to be required for the westward propagation of thunderstorms and the formation of the squall lines. Extremely dry midtropospheric air develops in the easterly flow through some combination of advection and subsidence and also appears to be an important factor in the development of the squall lines. A two-dimensional, nonhydrostatic, numerical model was able to simulate many of the features observed in these squall lines. Solar heating of the elevated terrain in the model caused the initial thunderstorm to develop over the Continental Divide. Continued development of new thunderstorms to the west of the Divide produced a squall line that travelled westward by translation of cells and discrete propagation, wherein new cells would develop 10 to 25 km ahead of the old ones, at a speed greater than all the winds below 30 kPa. Upward motion produced by westward propagating gravity waves and by the strong low-level convergence found just ahead of the gust front appeared to cause several episodes of discrete propagation. The creation of horizontal potential temperature gradients and the vertical and horizontal advection of preexisting vorticity gradients combined to produce the vorticity field associated with the rear inflow jet that developed beneath the simulated squall line. Dissert. Abstr.

N90-22868*# Wisconsin Univ., Madison. Space Science and Engineering Center.
THE ANALYSIS OF POLAR CLOUDS FROM AVHRR SATELLITE DATA USING PATTERN RECOGNITION TECHNIQUES Final Report
William L. Smith and Elizabeth Ebert May 1990 133 p
(Grant NAG5-1117)
(NASA-CR-183300; NAS 1.26:183300) Avail: NTIS HC A07/MF A01 CSCL 04B

The cloud cover in a set of summertime and wintertime AVHRR data from the Arctic and Antarctic regions was analyzed using a pattern recognition algorithm. The data were collected by the NOAA-7 satellite on 6 to 13 Jan. and 1 to 7 Jul. 1984 between 60 deg and 90 deg north and south latitude in 5 spectral channels, at the Global Area Coverage (GAC) resolution of approximately 4 km. This data embodied a Polar Cloud Pilot Data Set which was analyzed by a number of research groups as part of a polar cloud algorithm intercomparison study. This study was intended to determine whether the additional information contained in the AVHRR channels (beyond the standard visible and infrared bands on geostationary satellites) could be effectively utilized in cloud algorithms to resolve some of the cloud detection problems caused by low visible and thermal contrasts in the polar regions. The analysis described makes use of a pattern recognition algorithm which estimates the surface and cloud classification, cloud fraction, and surface and cloudy visible (channel 1) albedo and infrared (channel 4) brightness temperatures on a 2.5 x 2.5 deg latitude-longitude grid. In each grid box several spectral and textural features were computed from the calibrated pixel values in the multispectral imagery, then used to classify the region into one of eighteen surface and/or cloud types using the maximum likelihood decision rule. A slightly different version of the algorithm was used for each season and hemisphere because of differences in categories and because of the lack of visible imagery during winter. The classification of the scene is used to specify the optimal AVHRR channel for separating clear and cloudy pixels using a hybrid histogram-spatial coherence method. This method estimates values for cloud fraction, clear and cloudy albedos and brightness temperatures in each grid box. The choice of a class-dependent AVHRR channel allows for better separation of clear and cloudy pixels than does a global choice of a visible and/or infrared threshold. The classification also prevents erroneous estimates of large fractional cloudiness in areas of cloudfree snow and sea ice. The hybrid histogram-spatial coherence technique and the advantages of first classifying a scene in the polar regions are detailed. The complete Polar Cloud Pilot Data Set was analyzed and the results are presented and discussed. Author

N90-22869# Oak Ridge National Lab., TN. Carbon Dioxide Information Analysis Center.
GLOBAL AND HEMISPHERIC ANNUAL TEMPERATURE VARIATIONS BETWEEN 1861 AND 1988
P. D. Jones, T. M. L. Wigley, P. B. Wright (East Anglia Univ., Norwich, England), and T. A. Boden, ed. Mar. 1990 82 p
(Contract DE-AC05-84OR-21400)
(DE90-007993; ORNL/CDIAC-31; NDP-022/R1; ESDP-3421)
Avail: NTIS HC A05/MF A01

Two estimates are presented of global and hemispheric annual temperature anomalies, relative to a 1950 to 79 reference period, for 1861 to 1988. In one set of estimates the influence of El Nino/Southern Oscillation (ENSO)-related events are considered. Both estimates are based on corrected land and marine data. These data are available free of charge as a numeric data package (NDP) from the Carbon Dioxide Information Analysis Center. The NDP consists of this document and a magnetic tape or floppy diskette containing machine readable data files. Tabular listings are provided of the annual temperature anomalies, how the data were processed is described, limitations and restrictions of the data are defined, and reprints are provided of pertinent literature.
DOE

N90-22870*# Air Force Inst. of Tech., Wright-Patterson AFB, OH.
A STUDY OF TURBULENCE NEAR THUNDERSTORM TOPS M.S. Thesis
Kim Christine Pantley May 1989 144 p Prepared in cooperation with San Jose State Univ., CA
(Contract NCC2-315)
(NASA-CR-186620; NAS 1.26:186620; AD-A218477; AFIT/CI/CIA-89-072) Avail: NTIS HC A07/MF A01 CSCL 04/2

It has been known for many years that turbulence significant for aviation often occurs near thunderstorm tops. However, that turbulence is not well-predicted because of an incomplete understanding of the processes which generate it and because of inadequate observations. The current study seeks to alleviate these problems via: (1) a comprehensive review of recent theoretical and experimental studies related to turbulence near thunderstorm tops (TNTT), and (2) three case studies designed to examine the feasibility of using data derived from commercial aircraft to study TNTT. The literature review revealed extensive evidence which showed that convection often produces significant barrier effects; several mesoscale phenomena capable of producing turbulence may occur, depending on wind and stability conditions near the thunderstorm tops. These include two- and three-dimensional lee waves, rotors, Kelvin-Helmholtz instabilities, and Karman vortices. Conventional meteorological data were combined with data derived from the aircraft flight tapes to produce quantitative descriptions of the turbulence and its mesoscale environment for the three cases. GRA

N90-22871# Air Force Inst. of Tech., Wright-Patterson AFB, OH.
AN INTERACTIVE METHOD FOR ESTIMATING HAILSTONE SIZE AND CONVECTIVELY-DRIVEN WIND GUSTS FROM FORECAST SOUNDINGS M.S. Thesis
John Philip Pino 1989 9 p Prepared in cooperation with Saint Louis Univ., MO
(AD-A218499; AD-E900914; AFIT/CI/CIA-89-048) Avail: NTIS HC A02/MF A01 CSCL 04/2

Interactive methods for forecasting potential hailstone size and convectively-driven surface wind gust velocities are applied to forecast soundings which better represent atmospheric conditions prior to the onset of convection. The forecast sounding is based upon the 1200 UTC sounding and is developed interactively by the user considering diurnal changes expected to occur in the lower tropospheric levels over the next 6 to 12 hours. Changes to the middle and upper levels are estimated by taking a fraction of the mean geostrophic advection of temperature for consecutive layers and adjusting the 1200 UTC sounding accordingly. Interactive capability allows for final adjustment of any or all of the data. Hailstone size and convectively-driven wind gusts are based upon key thermodynamic parameters (e.g., CCL, LFC, CAPE) derived from the forecast sounding. GRA

N90-22872# Air Force Systems Command, Wright-Patterson AFB, OH. Foreign Technology Div.
CLIMATIC HANDBOOK OF THE USSR, ISSUE 27. KAMCHATSKAYA OBLAST. PART 3: WIND
29 Dec. 1989 184 p Transl. into ENGLISH of Spravochnik po Klimatu SSSR, Leningrad (USSR), no. 27, pt. 3 1967 p 1-228
(AD-A218720; FTD-ID(RS)T-1033-89) Avail: NTIS HC A09/MF A01 CSCL 04/2

The wind conditions for the Kamchatskaya Oblast are covered for the period from 1936 through 1964. For tables 9 and 9a data from the period 1891 to 1964 are used. Prolonged observations of wind velocity are necessary because from year to year considerable variations in the frequency of wind velocities are noted. The frequencies of high velocities are subject to the greatest variations. Included are materials from 58 meteorological stations which are existing now or operated earlier on the territory of Kamchatskaya Oblast. The different characteristics of wind velocity and direction give an idea of the wind conditions in Kamchatskaya Oblast. The material is presented in the form of tables for the individual stations with an explanatory text for them. The text portion contains a brief description of the general regularities of wind conditions, a knowledge of which is necessary for the correct utilization of the materials in the handbook. GRA

N90-22873# Air Force Operational Test and Evaluation Center, Kirtland AFB, NM.
NEXT GENERATION WEATHER RADAR (NEXRAD) INITIAL OPERATIONAL TEST AND EVALUATION. PHASE 2: (IOT AND E(2)) Final Report, 6 Mar. - 6 Aug. 1989
James C. Weyman and Kathleen I. Clancy Dec. 1989 119 p
(AD-A218770; AFOTEC-86-0167) Avail: NTIS HC A06/MF A01 CSCL 04/2

The Next Generation Weather Radar (NEXRAD) initial operational test and evaluation is summarized. NEXRAD is a joint Department of Commerce, Defense, and Transportation effort to develop and procure a Doppler weather radar system to replace the present radar and as a major upgrade to existing capability. The test had four purposes: evaluate the operational effectiveness and suitability of the preproduction NEXRAD; review deficiencies and enhancements documented during previous testing; identify deficiencies and enhancements not previously documented; and identify items to be addressed during follow-on operational test and evaluation. The NEXRAD Program Council will use the test results as an aid to exercising the full scale production option and to identify deficiencies that need to be corrected before NEXRAD becomes fully operational. NEXRAD was an effective aid in providing weather warning, weather advisory, and routine weather services support. However, the usefulness of velocity-based products was severely degraded during periods of widespread convective activity. In addition, reliability, maintainability, and availability problems, such as those associated with power transitions, PUP graphics processors, and the transmitter, severely detracted from mission capability. Software documentation and software support resource deficiencies produce a risk that the government may not be able to assume software support responsibilities at the appropriate time. GRA

N90-22874# Naval Oceanography Command Detachment, Asheville, NC.
US NAVY REGIONAL CLIMATIC STUDY OF SOUTHERN AFRICAN WATERS
Mar. 1989 263 p
(AD-A218792; NAVAIR-50-1C-548) Avail: NTIS HC A12/MF A02 CSCL 04/2

This study is for the region which comprises the waters around southern Africa from 25 deg S to 44 deg S and 6 deg E to 40 deg E. The selected limits allow for a small overlap between this region and that of the study for the Mozambique Channel. Most emphasis in this study was placed on the marine areas, with only a few coastal station summaries included in the text and final section of this publication. GRA

N90-22875# Naval Oceanography Command Detachment, Asheville, NC.
US NAVY REGIONAL CLIMATIC STUDY OF THE MOZAMBIQUE CHANNEL AND ADJACENT WATERS
Jul. 1989 341 p
(AD-A218793; NAVAIR-50-1C-549) Avail: NTIS HC A15/MF A02 CSCL 04/2

This study is centered on the Mozambique Channel between Mozambique in southeast Africa and the island of Madagascar. The study limits extend from 5 deg S to 35 deg S and 31 deg E to 55 deg E, thus allowing a small overlap between this study and the one for the Southern African Waters. Most emphasis was placed on the marine areas, with only a few coastal station summaries included in the text and final section of this publication. GRA

N90-22876# Air Force Global Weather Central, Offutt AFB, NE.
AFGW'S UPPER AIR VALIDATOR SYSTEM
Paul A. Zamiska Feb. 1990 30 p

(AD-A219309; AFGWC/TN-90/001) Avail: NTIS HC A03/MF A01 CSCL 04/2

The Upper Air Validator system is described. Detailed descriptions of internal error checking and data quality assurance functions are the major concern. Problems with the previous Validator and improvements within this Validator are also addressed. Reject and suspect limits for temperature, height, wind speed, and density used by the Validator are included. GRA

48 OCEANOGRAPHY

Includes biological, dynamic, and physical oceanography; and marine resources.

For related information see also *43 Earth Resources and Remote Sensing.*

N90-22877*# Jet Propulsion Lab., California Inst. of Tech., Pasadena.

MONTHLY SURFACE THERMAL FORCING IN THE TROPICAL PACIFIC FROM 1980 TO 1983

W. Timothy Liu, Catherine Gautier, Robert Frouin (Scripps Institution of Oceanography, La Jolla, CA.), and Rebecca Tagett 15 Nov. 1989 17 p Sponsored in part by NOAA, Washington, DC and NSF, Washington, DC Original contains color illustrations

(Contract NAS7-918)

(NASA-CR-183033; JPL-Publ-89-42; NAS 1.26:183033) Avail: NTIS HC A03/MF A01; 8 functional color pages CSCL 08C

Monthly distributions of surface latent heat flux and solar irradiance in the tropical Pacific were computed from observations of the scanning multichannel microwave radiometer on Nimbus-7 and the visible infrared spin scan radiometer on GOES-W. They are the dominant variable components of the surface heat flux, the sum of which gives the approximate thermal forcing on the ocean. Monthly maps of this sum, from January 1980 to September 1983, and within 20 deg N and 20 deg S, 180 deg and 80 deg W, are presented. Author

N90-22878 Reading Univ. (England).

A NUMERICAL STUDY OF BASIC COASTAL UPWELLING PROCESSES Ph.D. Thesis

Zhihong Li 1989 236 p

Avail: Univ. Microfilms Order No. BRDX86893

Two dimensional and three dimensional numerical models with a second order turbulence closure are developed to study coastal upwelling processes. A logarithmic coordinate system is introduced to obtain increased resolution in the regions near the surface and bottom where high velocity shear occurs and in the upwelling zone where its width is confined to the coast. In the experiments performed in the 2-D model, an ocean initially at rest is driven by a spatially uniform alongshore wind-stress. There is a development of an offshore flow in the surface layer and an onshore flow below the surface layer. In the wind-stress direction there is a development of coastal surface jet. The neglect of the alongshore pressure gradient leads to the intensification of the jet, and the concentration of the onshore flow in an over-developed Ekman layer yielding an unrealistic deepening of a bottom mixed layer. When bathymetric variations are introduced, some modifications in the dynamics of upwelling are observed. When an alongshore pressure gradient is added externally into the model, the strength of the coastal jet decreases and a coastal undercurrent exists at greater depth. In addition, the return onshore flow is largely independent of depth and the deepening of the bottom mixed layer disappears. In the experiments performed in the 3-D model a wind-stress with limited domain is used. Coastally trapped waves are generated and propagate along the coastline leading to a development of an alongshore pressure gradient, which has a significant effect on upwelling. The evolution of the alongshore flow, vertical velocity, and the temperature is determined by both remote and local wind due to the propagation of waves. As the integration proceeds, the flow pattern becomes remarkably 3-dimensional. Finally, the influence of bathymetric variations on upwelling processes is examined. Dissert. Abstr.

N90-22879# Naval Ocean Research and Development Activity, Bay Saint Louis, MS.

EVIDENCE FOR SELF-REFRACTION IN A CONVERGENCE ZONE: NPE (NONLINEAR PROGRESSIVE WAVE EQUATION) MODEL RESULTS

B. Edward McDonald and Daniel R. Plante (Berkeley Research Association, Springfield, VA.) Aug. 1989 15 p Sponsored in part by Sandia National Lab.

(AD-A218546; NORDA-223) Avail: NTIS HC A03/MF A01 CSCL 12/1

The nonlinear progressive wave equation (NPE) model was developed by the Naval Ocean Research and Development Activity during 1982 to 1987 to study nonlinear effects in long range oceanic propagation of finite amplitude acoustic waves, including weak shocks. The NPE model was applied to propagation of a generic shock wave (initial condition provided by Sandia Division 1533) in a few illustrative environments. The following consequences of nonlinearity are seen by comparing linear and nonlinear NPE results: (1) a decrease in shock strength versus range (a well-known result of entropy increases at the shock front); (2) an increase in the convergence zone range; and (3) a vertical meandering of the energy path about the corresponding linear ray path. Items (2) and (3) are manifestations of self-refraction. GRA

N90-22880# Naval Postgraduate School, Monterey, CA.

ON THE EFFECTIVENESS OF THE PRODUCTION OF ANTARCTIC BOTTOM WATER IN THE WEDDELL AND ROSS SEAS M.S. Thesis

David B. St.Pierre Sep. 1989 135 p

(AD-A218873) Avail: NTIS HC A07/MF A01 CSCL 08/3

The northward propagation of Antarctic Bottom Water (AABW), from its primary source in the Weddell Sea, was documented since the early part of this century. Despite the striking similarities between the Weddell and the Ross Seas, AABW is mainly produced in the Weddell Sea. The question is posed as to why the Weddell Sea is so effective in the production of AABW as compared to the Ross Sea. Differences are determined by analyzing various physical mechanisms and forcing functions in both basins with respect to the two predominant theories of AABW formation. Foster and Carmack's shelf break process theory and Foldvik and Gammelsrod's theory of ice shelf processes. Results reveal that the strong tidal forcing at the Weddell Sea ice shelf barrier combines with the wind stress field and with the special under-ice-shelf and continental shelf bathymetrics of the Weddell Sea to become the critical elements of the AABW formation process. The shelf theory is found to account for the formation of Weddell Sea Bottom Water (WSBW), the parent constituent of AABW, with a prediction of an Ice Shelf Water outflow rate of approximately 0.7 x 1,000,000 cu m/s (due to tidal action at the barrier allowing ice production by high surface freezing levels and tidal forcing of sea water under the ice shelf) and a production rate of WSBW of 5 x 1,000,000 cu m/s which agrees with observations and current estimates. GRA

N90-22881# Arizona State Univ., Tempe. Dept. of Mechanical and Aerospace Engineering.

STRATIFIED OCEAN MIXING Final Technical Report

Harindra J. S. Fernando 1990 8 p

(Contract N00014-88-K-0250)

(AD-A219233) Avail: NTIS HC A02/MF A01 CSCL 20/4

Some fundamental issues pertinent to the formation of intrusions and fronts and turbulent mixing in stratified fluids are examined, with the hope that the results will be of use in understanding and modeling of oceanic mixing processes. Two different, but somewhat related, investigations were performed, namely; the formation of intrusions due to the collapse of turbulent patches in stratified fluids, and the influence of molecular diffusion during mixing at a density interface. During these studies, several phenomena were discovered, for most of which theoretical explanations were offered; a summary of the findings is given. GRA

N90-22882# Stanford Univ., CA. Environmental Fluid Mechanics Lab.
A STUDY OF THE SURFACE LAYERS AT AN AIR-WATER INTERFACE Final Report
Robert L. Street Feb. 1990 11 p
(Contract N00014-84-K-0242)
(AD-A219378; EFML-90-1) Avail: NTIS HC A03/MF A01 CSCL 08/8

This is the final technical report on a study of the surface layers at an air-water interface. In the work covering the period from 1 January 1984 through 31 December 1989, there were five phases, viz., completion of studies in the air above the interface, numerical simulation of the surface layers, development of instrumentation, studies of the water layer, and the development of flow visualization techniques and wave-generation models. All of the experiments were conducted in the Stanford Wind, Water-Wave Research Facility, which has a 20 meter long test section and can produce windspeeds to about 14 m/s. Studies in the air flow focused on the structure of the pressure and velocity fields, their impact on the transfer of momentum and energy to the water waves, the characteristics of the water waves, and the effect of the waves on turbulence production and the related bursting phenomena. The numerical simulation addressed the heat, mass and momentum exchange at a phase-changing, gas-liquid interface. GRA

51 LIFE SCIENCES (GENERAL)

N90-22883# California Univ., Berkeley. Dept. of Chemistry.
THRESHOLD PHOTODETACHMENT SPECTROSCOPY OF THE I + HI TRANSITION STATE REGION Interim Technical Report, Nov. - Dec. 1989
I. M. Waller, T. N. Kitsopoulos, and D. M. Neumark 1 Jan. 1990 18 p Submitted for publication
(Contract N00014-87-K-0495)
(AD-A218410; TR-3) Avail: NTIS HC A02/MF A01 CSCL 07/4

We have developed a method for probing the transition state region of a neutral bimolecular reaction via photodetachment of a stable negative ion similar in structure to the neutral transition state. In several cases, we have found that the photoelectron spectrum of the hydrogen-bonded anion AHB(-) exhibits resolved vibrational structure which can be assigned to an unstable (AHB) complex located near the transition state for the hydrogen transfer reaction A + HB yields HA + B. The results described previously were obtained with a fixed-frequency negative ion photoelectron spectrometer. Here we report considerably higher resolution results for IHI(-) obtained on a recently constructed threshold photodetachment spectrometer. In this experiment, mass-selected ions are photodetached with a tunable pulsed laser, and only those photoelectrons produced with nearly zero kinetic energy are detected as a function of laser wavelength. The threshold photodetachment spectrum of IHI(-) shows considerably more structure than was observed in the lower resolution photoelectron spectrum. In particular, we observe narrow (30 cm) peaks due to long-lived states of the (IHI) complex which lie well above the I + HI(v=0) asymptote. GRA

N90-22884# Boston Univ., MA. School of Medicine.
HEAT EXHAUSTION IN A RAT MODEL: LITHIUM AS A BIOCHEMICAL PROBE Final Report, 15 Jan. 1988 - 30 Sep. 1989
Steven H. Zeisel 30 Sep. 1989 37 p
(Contract DAMD17-88-C-8055; DA Proj. 3E1-62777-A-879)
(AD-A219361) Avail: NTIS HC A03/MF A01 CSCL 06/10

Our aim was to confirm our hypothesis that chronic lithium treatment predisposes to heat-induced illness using an animal model. We hypothesized that lithium-treated rats would develop heat-induced illness more easily and rapidly than would controls. Rats were treated with lithium (2 mEq/kg body weight/day), or with a matching amount of water, for 20 days. In some experiments rats were offered water ad libitum, in other experiments fluid was restricted from day 14 to 20. During passive heat testing, rats were housed in a small environmental chamber (modified tissue culture incubator) in individual containers. Temperature in the chamber was maintained at 41.5 C with forced hot air, relative humidity at 30 to 50 percent. During active (exercise-induced) heat testing, animals were exercised on a motor-driven treadmill in chambers heated with forced hot air to a temperature of 26 C. Humidity was maintained at 30 percent relative humidity. Lithium treatment did not affect body water distribution, the rate of body temperature rise in either heating model, and the organ damage caused by exposure to heat (as assessed by leakage of enzymes into blood). There was a difference in the tail temperature during cooling after active (exercise-induced) heating - tail temperatures were consistently higher in lithium treated rats. We also observed that lithium treated animals consumed more water when it was offered ad libitum. GRA

52 AEROSPACE MEDICINE

Includes physiological factors; biological effects of radiation; and effects of weightlessness on man and animals.

N90-22885# Naval Submarine Medical Center, Groton, CT.
THE KINETICS OF DARK ADAPTATION IN HYPOXIC SUBJECTS Interim Report
Douglas R. Knight, Kendall Bryant, Curtis W. Ollayos, and S. M. Luria 26 Dec. 1989 12 p
(AD-A218641; NSMRL-1151) Avail: NTIS HC A03/MF A01 CSCL 06/10

A double blind study was made to determine the effect of hypoxia on the rate of dark adaptation. The visual thresholds of 10 subjects were measured as they breathed either 21 or 12 percent O2 for 10 minutes in daylight followed by 50 minutes in the dark. The subjects were exposed to the two gases in counterbalanced order on separate days. Reducing the oxygen level to 12 percent delayed the course of dark adaptation without changing the final scotopic threshold. GRA

N90-22886# Army Research Inst. of Environmental Medicine, Natick, MA. Exercise Physiology Div.
PHYSIOLOGICAL AND PERCEPTUAL RESPONSES TO PROLONGED TREADMILL LOAD CARRIAGE Final Report, May 1988 - Nov. 1989
John F. Patton, John Kaszuba, Robert P. Mello, and Katy L. Reynolds 22 Jan. 1990 46 p
(DA Proj. 3E1-62787-A-879)
(AD-A218910; USARIEM-TP-11-90) Avail: NTIS HC A03/MF A01 CSCL 15/5

The physiological and perceptual responses were determined: prolonged, level treadmill walking at speeds of 3.96, 4.86, and 5.76 kilometers per hour, unloaded and with external loads (load carriage equipment + backpack) of 31.5 and 49.4 kilograms; the ability of subjects to perform high intensity, anaerobic exercise (Wingate test) immediately after load carriage; and the energy cost and perceptual responses of carrying the standard external frame pack to that of the new internal frame system are compared. Fifteen male subjects performed nine load carriage trials with an external frame pack All-Purpose Lightweight Individual Carrying Equipment (ALICE) and two trials with an internal frame pack Integrated Individual Fighting System (IIFS) in random order over a 7 week period. At the end of each trial blood samples were taken for the measurement of lactate and subjects performed either an upper or lower body anaerobic power test. Oxygen Uptake (VO2), Minute Ventilation (VE), heart rate, and differentiated ratings of perceived exertion Ratings of Perceived Exertion (RPE) were determined at the end of the first 10 min and every 20 min thereafter for the duration of the trial. A 10 min rest period was allowed each hour. No changes occurred in VO2 over time in the unloaded condition at any speed. GRA

N90-22887# Johns Hopkins Univ., Laurel, MD. Applied Physics Lab.
A STUDY OF LOW LEVEL LASER RETINAL DAMAGE Final Progress Report, 1 Jan. 1978 - 31 Dec. 1989
B. F. Hochheimer 1 Mar. 1990 29 p Sponsored by Army Medical Research and Development Command
(AD-A218919; JHU/APL/STR-90-01) Avail: NTIS HC A03/MF A01 CSCL 06/10

The general objective of this program is to document changes in the retina due to very low level laser irradiation. We had two primary aims. One was to develop and improve methods that can be used, in vivo, to objectively determine changes that occur in the retina from laser irradiation. The second was to determine the mechanisms that cause these retinal changes. GRA

N90-22888# Tel-Aviv Univ. (Israel). Sackler School of Medicine.
LASER RETINAL EFFECTS: ELECTROPHYSIOLOGICAL DETERMINATION IN VISUAL CORTICAL CELLS OF MONKEYS AND CATS Final Report, 1 Apr. 1987 - 31 Aug. 1988
Uri Yinon 25 Jun. 1989 28 p
(Contract DAMD17-87-C-7095)
(AD-A218937) Avail: NTIS HC A03/MF A01 CSCL 09/3

The effect of laser induced retinal lesions on the visual cortex of mammalian animal model was examined. The effect of threshold energy levels of laser radiation was studied acutely and chronically in cats using the visual evoked response (VER). In addition, electroretinographic (ERG) studies were added to the program to obtain direct physiological evidence on the condition of the retinal area affected by the laser radiation. This study was coordinated with LAIR personnel with regard to the type of laser technology to be used and its availability in the Goldschleger Eye Institute. A Neodymium YAG laser device (Nd:YAG) was used; energy levels applied were 0.1 to 1.0 millijoules (mJ) and 1 to 100 pulses were given to the various cats. The results showed that the ERG is affected; the lased eye was less excitable than the normal eye in most of the cats studied, whatever laser energy has been applied. The findings of the visual evoked response (VER) showed that in most cats the lased eye was inferior to the normal eye. An effect was found even in cases where energy level was as small as 0.1 mJ and whether the animals were exposed to the laser radiation 1 day or 6 weeks prior to the recording session. GRA

N90-22889# City Univ. of New York Research Foundation, NY.
EXPOSURE OF HUMAN CELLS TO ELECTROMAGNETIC FIELDS Final Report, 1 Jan. 1988 - 31 Dec. 1989
Ann S. Henderson 27 Feb. 1990 23 p
(Contract N00014-88-K-0105)
(AD-A219377) Avail: NTIS HC A03/MF A01 CSCL 06/1

This study addressed the following basic question: How does extremely low-level non-ionizing radiation affect human cells, and if there are cellular responses that can be directly related to signal parameters such as frequency, amplitude and time of exposure. The focus of these studies was to identify transcriptional changes in human cultured cells, HL60, which result from exposure of these cells to defined extremely low frequency electromagnetic fields (elf EMFS). Our experiments show a pronounced measurable response observed as transcript increase, with associated changes in protein synthesis. The major findings relative to transcriptional changes are fourfold: (1) transcript changes in human cells correlate with previous findings of transcriptional and translational changes in Drosophila salivary gland cells; (2) the frequency of the signal in the range from 15 to 150 Hz results in a window at 45 Hz, (3) changing the amplitude (with resulting changes in E- and B-fields) in log increments from 0.5 to 500 uV at 60 Hz gives both amplitude and time-dependent windows, and (4) genes not usually expressed in HL-60 are unaffected by exposure to elf EMFs. Changes in the overall protein synthetic pattern have also been observed following exposure of HL60 cells to 60 Hz signals. GRA

N90-22957*# Massachusetts Inst. of Tech., Cambridge. Man Vehicle Lab.
SENSORY CONFLICT IN MOTION SICKNESS: AN OBSERVER THEORY APPROACH
Charles M. Oman *In* NASA, Ames Research Center, Spatial Displays and Spatial Instruments Jul. 1989 15 p (For primary document see N90-22918 16-54)
(Grant NAG9-244)
Avail: NTIS HC A99/MF A04 CSCL 06S

53 BEHAVIORAL SCIENCES

Includes psychological factors; individual and group behavior; crew training and evaluation; and psychiatric research.

N90-22890 Auburn Univ., AL.
RELATIONSHIP BETWEEN FLEXIBILITY OF CLOSURE AND SUCCESS IN PILOT NIGHT VISION SENSOR SYSTEM TRAINING Ph.D. Thesis
William Mitchell Knarr, Jr. 1989 115 p
Avail: Univ. Microfilms Order No. DA8925630

The purpose was two-fold: specifically, to address a small part of evolving aviation technology - the pilot night vision sensor (PNVS) system - and its relationship to flexibility of closure (Cf); and generally, to determine what attributes/experiences are important to training aviators in the AH-64, Attack Helicopter. The subjects included 170 Army aviators entering the AH-64 Qualification Course. The course consisted of three flight training phases which provided the dependent variables for the study: aircraft transition (TRANS), PNVS, and gunnery (GUN). In order to analyze the relationships among the variables, several statistical designs were employed: ANOVA, regression, MANOVA, and LISREL. ANOVA indicated that Cf was a significant contributer (.05 level) to PNVS training, however, the proportion of variance accounted for was very small (.035). Other contributers to PNVS success included aviator's age, total flight time (FT), and instructor pilot (IP) qualifications. Those four variables (including Cf) accounted for almost 25 percent of the variance in PNVS scores. The regression analysis essentially reiterated the significance of the contributors highlighted by the ANOVA, but formatted those variables into a predictive algorithm to support selection and training. MANOVA indicated that flexibility of closure was a significant contributor, at the .05 level, to the AH-64 flight skills of transition, PNVS, and gunnery training. Other contributors, at the .05 level, to AH-64 flight skills included age and instructor pilot qualifications. LISREL capitalized on results of the MANOVA by incorporating its significant sources into causal models. Although achieving only limited success in validating the models, LISREL did highlight several relationships. The most intriguing were the interactions of age with other variables; however, none of the nodels adequately defined those relationships. Dissert. Abstr.

N90-22891# Royal Aerospace Establishment, Farnborough (England).
TRACKING IN UNCERTAIN ENVIRONMENTS
D. J. Salmond 4 Sep. 1989 288 p
(RAE-TM-AW-121; BR112043; ETN-90-96443) Copyright Avail: NTIS HC A13/MF A02

The problem of tracking a target when the origin of the sensor measurements is uncertain is addressed. The full Bayesian solution to this type of problem gives rise to Gaussian mixture distributions. To implement such a tracking filter, the growth of components must be controlled by approximating the mixture distribution. Two algorithms are developed for approximating Gaussian mixture distributions. The performance of the algorithms is assessed by simulation for the problem of tracking a single target in the presence of uniformly distributed false measurements. The tracking example is extended to show how the Bayesian approach may be applied to more complex uncertain tracking problems, including that of fusing data from several independent sources. ESA

N90-22892# University of Northern Arizona, Flagstaff. Dept. of Health, Physical Education, and Recreation.
HUMAN COGNITIVE AND MOTOR PERFORMANCE MEASURES UNDER TYPICAL COOL WHITE FLUORESCENT ILLUMINATION VS RELATIVELY HIGH COOL WHITE ILLUMINANCE/IRRADIANCE LIGHTING Final Technical Report, 1 Dec. 1988 - 30 Dec. 1989
Patrick Roy Hannon 31 Jan. 1990 9 p
(Grant AF-AFOSR-0164-89; AF Proj. 3842)
(AD-A218445; AFOSR-90-0260TR) Avail: NTIS HC A02/MF A01 CSCL 05/8

Possible practice effects and diurnal fluctuations in human motor and cognitive performances under baseline illumination conditions (400 lux) were investigated. Six subjects were tested individually in order to partial out peer social interaction effects. The testing took place over a wide range of testing time epochs. Specifically, subjects were tested from 0800 to 1200 hours, 1400 to 1800 hours and 2000 to 0000 hours in a counter-balanced repeated measures design. GRA

N90-22893# Air Force Human Resources Lab., Williams AFB, AZ.
VISUAL BEHAVIOR IN THE F-15 SIMULATOR FOR AIR-TO-AIR COMBAT Interim Technical Report, Apr. 1988 - Nov. 1989
Kevin W. Dixon, Gretchen M. Krueger, Victoria A. Rojas, and Elizabeth L. Martin Feb. 1990 21 p Prepared in cooperation with Air Force Human Resources Lab., Brooks AFB, TX Submitted for publication
(AD-A218648; AFHRL-TP-89-75) Avail: NTIS HC A03/MF A01 CSCL 01/2

This research effort was conducted to determine visual strategies of F-15 pilots during air-to-air combat through the use of an eye tracking system. This type of work helps simulator designers define field-of-view requirements for simulators. While an increase in field of view size produces a more realistic scenario for the pilots, it results in a decrease in brightness and resolution levels, and increases the cost. Six F-15 pilots flew offensive, defensive, neutral, and mutual support set-ups in the Simulator for Air-to-Air Combat (SAAC) at three different altitudes. Analyses show that the visual strategies and window usage vary greatly among the four set-ups. Before final conclusions are made concerning field-of-view requirements during air-to-air tasks, this experiment should be partially replicated using electronic masking. GRA

N90-22894# Carnegie-Mellon Univ., Pittsburgh, PA. Artificial Intelligence and Psychology Project.
EFFICIENT SPECIALIZATION OF RELATIONAL CONCEPTS Technical Report, 15 Sep. 1986 - 14 Sep. 1991
Kurt VanLehn 10 Mar. 1989 14 p Prepared in cooperation with Pittsburgh Univ., PA
(Contract N00014-86-K-0678)
(AD-A218889; AIP-71) Avail: NTIS HC A03/MF A01 CSCL 12/9

An algorithm is presented for a common induction problem, the specialization of overly general concepts. A concept is too general when it matches a negative example. The particular case addressed assumes that concepts are represented as conjunctions of positive literals, that specialization is performed by conjoining literals to the overly general concept, and that the resulting specializations are to be as general as possible. Although the problem is NP-hard, there exists an algorithm, based on manipulation of bit vectors, that has provided good performance in practice. GRA

N90-22895# Syracuse Univ., NY.
INTELLIGENT SIGNAL PROCESSING TECHNIQUES FOR MULTI-SENSOR SURVEILLANCE SYSTEMS Final Report, Apr. 1988 - Apr. 1989
Harvey Rhody, David Sher, and James Modestino (Rensselaer Polytechnic Inst., Troy, NY.) Dec. 1989 58 p
(Contract F30602-88-D-0027; AF Proj. 4506)
(AD-A218890; RADC-TR-89-292) Avail: NTIS HC A04/MF A01 CSCL 17/9

The purpose of this project is to develop an analytical frame work to represent the modern multi-target, multi-sensor surveillance environment and to investigate the adaptation of intelligent signal processing algorithms to that application. The outcome is to be a road map for the development of the system elements and a plan for integrating them into a functional body. GRA

N90-22896# Carnegie-Mellon Univ., Pittsburgh, PA. Artificial Intelligence and Psychology Project.
A PRELIMINARY ANALYSIS OF THE SOAR ARCHITECTURE AS A BASIS FOR GENERAL INTELLIGENCE Technical Report, 15 Sep. 1986 - 14 Sep. 1991
Paul S. Rosenbloom, John E. Laird, Allen Newell, and Robert McCarl (Michigan Univ., Ann Arbor.) 8 May 1989 49 p Prepared in cooperation with Pittsburgh Univ., PA Submitted for publication
(Contracts N00014-86-K-0678; N00014-86-C-0133)
(AD-A218913; AIP-64) Avail: NTIS HC A03/MF A01 CSCL 05/8

The central scientific problem of artificial intelligence is to understand what constitutes intelligent action and what processing organizations are capable of such action. Human intelligence shows, to first observation, what can only be termed general intelligence. The SOAR project has been attempting to understand the functionality required to support general intelligence. A step is taken towards providing an analysis of the SOAR architecture as a basis for general intelligence. Included are discussions of the basic assumptions underlying the development of SOAR, a description of SOAR cast in terms of the theoretical idea of multiple levels of description, an example of SOAR performing multi-column subtraction, and three analyses of SOAR: its natural tasks, the sources of its power, and its scope and limits. GRA

N90-22897*# Carnegie-Mellon Univ., Pittsburgh, PA. Dept. of Psychology.
TOWARDS THE KNOWLEDGE LEVEL IN SOAR: THE ROLE OF THE ARCHITECTURE IN THE USE OF KNOWLEDGE Technical Report, 15 Sep. 1986 - 14 Sep. 1991
Paul S. Rosenbloom, Allen Newell, and John E. Laird (Michigan Univ., Ann Arbor.) 7 Aug. 1989 77 p Prepared in cooperation with Pittsburgh Univ., PA Submitted for publication
(Contracts NCC2-538; NCC2-517; N00039-86-C-0033; F33615-87-C-1499; N00014-86-K-0678; N00014-88-K-0554; N00014-88-K-0086; ARPA Order 4976)
(NASA-CR-186615; NAS 1.26:186615; AD-A218926; AIP-65)
Avail: NTIS HC A05/MF A01 CSCL 05/9

SOAR has been described as an architecture for a system that is to be capable of general intelligence. One way to specify what this might mean is to define general intelligence as the ability to approximate an ideal knowledge level system across a sufficiently broad set of goals and knowledge. In this chapter, this definition is used as the basis for evaluating the degree to which SOAR achieves general intelligence. A complete evaluation is beyond the scope of this chapter, however, it is focused on how the SOAR architecture supports and constrains the representation, storage, retrieval, use and acquisition of three pervasive forms of knowledge: procedural, episodic, and declarative knowledge. The analysis reveals that SOAR adequately supports procedural knowledge - to some extent it was designed for this - but that there are still significant questions about episodic and declarative knowledge. These questions arise primarily because of consequences of the principle source of constraint in SOAR, the fact that all learning occurs via chunking. New results are also presented on the acquisition of declarative knowledge. GRA

N90-22898# Carnegie-Mellon Univ., Pittsburgh, PA. Dept. of Psychology.
STOCHASTIC INTERACTIVE ACTIVATION AND THE EFFECT OF CONTEXT ON PERCEPTION Technical Report, 15 Sep. 1986 - 14 Sep. 1991

James L. McClelland 14 Jul. 1989 45 p Prepared in cooperation with Pittsburgh Univ., PA
(Contracts N00014-86-K-0678; N00014-86-G-0146; N00014-86-K-0349; NSF BNS-86-09729; NSF BNS-88-12048)
(AD-A218929; AIP-68) Avail: NTIS HC A03/MF A01 CSCL 05/8

Classically, context exerts a biasing effect on perceptual identification responses given without time pressure. Such effects are well described by classical models formulated in terms of signal detection theory or Luce's theory of choice. The classical models do not describe the actual time course of processing, however; they simply produce characterizations of asymptotic response probabilities. Mathematical analysis and computer simulation methods are used to show that interactive activation models exhibit the classical effect of context when they are allowed to run to equilibrium, if there is variability in the input to the network or if there is intrinsic randomness in the processing activity of the network itself. The findings suggest that interactive activation models should not be viewed as alternatives to classical accounts, but as hypotheses about the dynamics of information processing that lead to the asymptotic behavior that the classical models describe. GRA

N90-22899# Carnegie-Mellon Univ., Pittsburgh, PA. Artificial Intelligence and Psychology Project.
COGNITIVE EFFICIENCY CONSIDERATIONS FOR GOOD GRAPHIC DESIGN Technical Report, 15 Sep. 1986 - 14 Sep. 1991
Stephen Casner (Pittsburgh Univ., PA.) and Jill H. Larkin 1989 12 p
(Contracts N00014-86-K-0678; N00014-88-K-0086)
(AD-A218976; AIP-81) Avail: NTIS HC A03/MF A01 CSCL 05/8

Larkin and Simon's (1987) analysis of how graphical representations support task performance is applied to designing graphical displays that streamline information-processing tasks. Theoretically this streamlining is done by designing external data structures that: (1) allow users to substitute less effortful visual operators for more effortful logical operators, and (2) reduce search for needed information. A design program called BOZ is used to produce four alternative displays of airline schedule information to support an airline reservation task. Several procedures that use a set of visual operators to perform the task using the different graphics are postulated. The number of times each operator is executed provides one measure of task difficulty (for a procedure and graphic). A second measure is the difficulty of executing each operator. Seven subjects performed the airline reservation task using each of the four graphics. Response times for the different graphics differ by a factor of two, and this difference is statistically highly significant. Detailed data analyses suggest that these differences arise through substitution of visual operators for logical ones and through the use of visual cues that help reduce search. The analyses provide quantitative estimates of the time saved through operator substitutions. GRA

N90-22900# Carnegie-Mellon Univ., Pittsburgh, PA. Artificial Intelligence and Psychology Project.
DESIGNING GOOD EXPERIMENTS TO TEST BAD HYPOTHESES Technical Report, 15 Sep. 1986 - 14 Sep. 1991
David Klahr, Kevin Dunbar (McGill Univ., Montreal, Quebec), and Anne L. Fay 15 Aug. 1989 41 p Prepared in cooperation with Pittsburgh Univ., PA Submitted for publication
(Contracts N00014-86-K-0349; N00014-86-K-0678)
(AD-A218977; AIP-83) Avail: NTIS HC A03/MF A01 CSCL 05/8

What does it take to design a good experiment. Given an hypothesis to be evaluated (either in isolation or in competition with alternatives) what formal rules, heuristics, and pragmatic constraints combine to yield a potentially informative experiment. How do subjects' expectations about the plausibility of an hypothesis effect the kind of experiments that they design, their ability to accurately observe and encode experimental outcomes and their responses to information that is consistent or inconsistent with the hypothesis. These questions are addressed by creating a simulated discovery context and examining how subjects go about designing experiments to test hypotheses that are always, at the outset, incorrect. Thirty-six adult subjects were trained on the basic functions of a programmable robot. Then they were presented with a new function key (a repeat key) and asked to find out how it worked. The results show that subjects are remarkably adept at designing and interpreting experiments in a novel domain. When subjects are given a plausible hypothesis, they tend to design an experiment that demonstrates the effect that is to be expected. When given inplausible hypothesis, they write programs that are good discriminators. GRA

N90-22901# Carnegie-Mellon Univ., Pittsburgh, PA. Artificial Intelligence and Psychology Project.
WHAT MAKES SOME PROBLEMS HARD: EXPLORATIONS IN THE PROBLEM SPACE OF DIFFICULTY Technical Report, 15 Sep. 1986 - 14 Sep. 1991
Kenneth Kotovsky and Herbert A. Simon 14 Jul. 1989 54 p Prepared in cooperation with Pittsburgh Univ., PA
(Contracts N00014-86-K-0678; N00014-85-K-0696)
(AD-A219002; AIP-97) Avail: NTIS HC A04/MF A01 CSCL 05/8

Two sources are identified, one larger, one smaller, of the great difficulty encountered by subjects solving the Chinese Ring Puzzle. Almost none of the subjects were able to solve the puzzle within two hours unless they were given a demonstration of how to move, and even with that help only half of the subjects obtained solutions. Discovering how to make moves, rather than other features of the problem search space, was the source of its inordinate difficulty. Evidence for this comes from isomorphs that were designed to digitize the moves, which in the original version have analog qualities. These digital isomorphs were solvable by almost all subjects, with average solution times of 10 to 25 minutes, depending on isomorph type. The digitized problems still required considerable effort for their solution. The difficulty of these problems in digital form is particularly surprising, given that the problem search space is linear: there is no branching. Hence, size of search space (exponential explosion) was not the source of difficulty here. The linearity of the search space did not prevent the subjects from making a large number of moves in reaching a solution. The average number of moves ranged from 150 to 450 for different isomorphs. In addition, the subjects' move behavior was often dichotomous, consisting of a very large number of non-progressive, often error-prone moves, followed by a very rapid, often error-free movement to the goal. GRA

N90-22902# Carnegie-Mellon Univ., Pittsburgh, PA. Artificial Intelligence and Psychology Project.
DISCOVERING PROBLEM SOLVING STRATEGIES: WHAT HUMANS DO AND MACHINES DON'T (YET) Technical Report, 15 Sep. 1986 - 14 Sep. 1991
Kurt VanLehn 21 Jul. 1989 18 p Presented at the 6th International Workshop on Machine Learning Prepared in cooperation with Pittsburgh Univ., PA
(Contract N00014-86-K-0678)
(AD-A219008; AIP-74) Avail: NTIS HC A03/MF A01 CSCL 12/9

People can discover new problem solving strategies on their own, without help from a teacher, text or other source. Many machine learning programs exist that discover strategies under similar conditions. Are there a sufficient set of computational models for understanding human strategy discoveries. A detailed analysis is presented of a human problem solving protocol that uncovers 10 cases of strategies being discovered. It is argued that most cases are adequately modeled by existing machine learning techniques, and several are not, which suggests some interesting research problems for machine learning. After a brief discussion of the methods of the analysis and the protocol, the protocol analysis is presented in enough detail to allow evaluation of the accuracy of the empirical claims. A subsequent section that classifies the cases of strategy discovery found in the data are classified according to standard machine learning concepts. The

last section indicates which types of learning exhibited by the subject have not yet been exhibited by machine learning systems. This leads to the view that strategy acquisition by a component human is like scientific theory formation, with the attendant tasks hypothesis generation. Although current machine learning models of strategy acquisition seem pale by comparison, there seems to be nothing stopping us from building machine learning systems with human-level capabilities for strategy discovery. GRA

N90-22903# Carnegie-Mellon Univ., Pittsburgh, PA. Artificial Intelligence and Psychology Project.
RULES AND MAPS IN CONNECTIONIST SYMBOL PROCESSING Technical Report, 15 Sep. 1986 - 14 Sep. 1991
David S. Touretzky Jun. 1989 20 p Presented at the 11th Annual Conference of the Cognitive Science Society, Ann Arbor, MI, Aug. 1989 Prepared in cooperation with Pittsburgh Univ., PA Submitted for publication
(Contract N00014-86-K-0678; NSF EET-87-16324)
(AD-A219028; AIP-79) Avail: NTIS HC A03/MF A01 CSCL 25/4

Two papers to be presented at the Eleventh Annual Conference of the Cognitive Science Society are presented. The first describes a simulation of chunking in a connectionist network. The network applies context sensitive rewrite rules to strings of symbols as they flow through its input buffer. Chunking is implemented as a form of self-supervised learning using back-propagation. Over time, the network improves its efficiency by replacing simple rule sequences with more complex chunks. The second paper describes the first implementation of Lakoff's new theory of cognitive phonology. Lakoff's approach is based on a multilevel representation of utterances to which all rules apply in parallel. Cognitive phonology is free of the rule ordering constraints that make classical generative theories computationally awkward. The connectionist implementation utilizes a novel many maps architecture that may explain certain constraints on phonological rules not adequately accounted for by more abstract models. GRA

N90-22904# Carnegie-Mellon Univ., Pittsburgh, PA. Artificial Intelligence and Psychology Project.
CONNECTIONISM AND COMPOSITIONAL SEMANTICS Technical Report, 15 Sep. 1986 - 14 Sep. 1991
David S. Touretzky May 1989 18 p Prepared in cooperation with Pittsburgh Univ., PA Submitted for publication
(Contract N00014-86-K-0678; NSF EET-87-16324)
(AD-A219029; AIP-78) Avail: NTIS HC A03/MF A01 CSCL 12/9

Quite a few interesting experiments have been done applying neural networks to natural language tasks. Without detracting from the value of these early investigations, it is argued that current neural network architectures are too weak to solve anything but toy language problems. Their downfall is the need for dynamic inference, in which several pieces of information not previously seen together are dynamically combined to derive the meaning of a novel input. A hierarchy of classes of connectionist models is defined, from categorizers and associative memories to pattern transformers are dynamic inferencers. Some well-known connectionist models that deal with natural language are shown to be either categorizers or pattern transformers. The second half examines in detail a particular natural language problem: prepositional phase attachment. Attaching a PP to an NP changes its meaning, thereby influencing other attachments. So PP attachment requires compositional semantics; and compositionality in non-toy domains requires dynamic inference. Mere pattern transformers cannot learn the PP attachment task without an exponential training set. Connectionist-style computation still has many valuable ideas to offer, so this is not an indictment of connectionisms's potential. GRA

N90-22905# Carnegie-Mellon Univ., Pittsburgh, PA. Artificial Intelligence and Psychology Project.
LEARNING EVENTS IN THE ACQUISITION OF THREE SKILLS Technical Report, 15 Sep. 1986 - 14 Sep. 1991
Kurt VanLehn 21 Jul. 1989 11 p Prepared in cooperation with Pittsburgh Univ., PA
(Contract N00014-86-K-0678)
(AD-A219038; AIP-73) Avail: NTIS HC A03/MF A01 CSCL 12/9

Current theories of cognitive skill acquisition, new problem solving rules are constructed by proceduralization, production compounding, chunking, syntactic generalization, and a variety of other mechanisms. All these mechanisms are assumed to run rather quickly, so a rule's acquisition should be a matter of a few seconds at most. Such learning events might be visible in protocol data. A method for locating the initial use of a rule in protocol data is discussed. The method is applied to protocols of subjects learning three tasks: a river crossing puzzle, the Tower of Hanoi, and a topic in college physics. Rules were discovered at the rate of about one every half hour. Most rules required several learning events before they were used consistently, which is not consistent with the one-trial learning predicted by explanation-based learning methods. Some observed patterns of learning events were consistent with a learning mechanism based on syntactic generalization rules. Although most rules seem to have been acquired at impasses (occasions when the subject does not know what to do next) there were clear cases of rules being learned without visible signs of an impasse, which does not support the popular hypothesis that all learning occurs at impasses. GRA

N90-22906# Carnegie-Mellon Univ., Pittsburgh, PA. Artificial Intelligence and Psychology Project.
A CONNECTIONIST IMPLEMENTATION OF COGNITIVE PHONOLOGY Technical Report, 15 Sep. 1986 - 14 Sep. 1991
Deirdre W. Wheeler (Pittsburgh Univ., PA.) and David S. Touretzky 26 May 1989 12 p Presented at the Berkeley Workshop on Cognitive Phonology, 26 May 1989
(Contract N00014-86-K-0678)
(AD-A219095; AIP-75) Avail: NTIS HC A03/MF A01 CSCL 05/8

Initial results of an effort to actually implement Lakoff's theory of cognitive phonology in a connectionist framework are described. For all sorts of reasons, standard generative phonological theories cannot be implemented in connectionist frameworks. Lakoff's theory of cognitive phonology offers solutions to some of these problems in that it offers an alternative way to think about derivations and ordered rules, as well as eliminating the need for right-to-left iterative rule application. Many maps model are described and how Lakoff's cross-level phonological constructions may be implemented is shown. As will become clear, the basic assumption is that all phonological constructions should express correlations between levels and be satisfied in parallel, simultaneously, across the entire input domain. After describing the general properties of the model and how mappings between levels are actually implemented, a number of specific cases are considered. In particular, those apparently involving iterative application of rules are focused on, such as: Slovak shortening, Gidabal shortening, and vowel harmony in Yawelmani. The challenge is obviously to provide alternative accounts of those cases involving intra-level rules in Lakoff's theory. It is believed that the clustering mechanism allows this. Finally, the complex rule interactions in Icelandic is addressed, and it is shown that the theory, though very tightly constrained, can handle this case as well. GRA

N90-22907# Carnegie-Mellon Univ., Pittsburgh, PA. Dept. of Psychology.
COGNITIVE ARCHITECTURES AND RATIONAL ANALYSIS: COMMENT Technical Report, 15 Sep. 1986 - 14 Sep. 1991
Herbert A. Simon 17 Mar. 1989 25 p Submitted for publication
(Contracts N00014-86-K-0678; F33615-81-K-1539; ARPA Order 3597)
(AD-A219199; AIP-58) Avail: NTIS HC A03/MF A01 CSCL 05/8

John Anderson has written a provocative chapter whose thesis may be oversimplified to read: To understand the behavior of an

adaptive organism, don't study the organism; study its environment. To claim that architecture is more notation than substance is to make the same claim for the brain -- the fact that it supports adaptive behavior makes unnecessary any curiosity about how it operates. The exact way in which neurons accomplish their functions is not important -- not only their functional capabilities and the organization of these. Nothing else will show through to behavior. But what does show through is precisely called architecture. And for that reason architecture is by no means all notation; it has real substance in its effects on behavior. In the view of the author, Anderson assigns too little weight to architecture (and by implication to strategies) as determinants of adaptive behavior. GRA

N90-22908# Carnegie-Mellon Univ., Pittsburgh, PA. Dept. of Psychology.
INFORMATION PROCESSING APPROACHES TO COGNITIVE DEVELOPMENT Technical Report, 15 Sep. 1986 - 14 Sep. 1991
David Klahr 4 Aug. 1989 13 p Presented at the Theories of Child Development: Updates and Reformulations Symposium, Kansas City, MO, 27-30 Apr. 1989 Prepared in cooperation with Pittsburgh Univ., PA
(Contract N00014-86-K-0678)
(AD-A219200; AIP-59) Avail: NTIS HC A03/MF A01 CSCL 05/8

The history and current status of information processing approaches to cognitive development is reviewed. Because the approach is so pervasive, it is useful to characterize research in terms of distinctive features, and to organize the features according to whether they are soft-core or hard-core aspects of the information processing approach. Each of these features is illustrated by example, and the hard-core approach is expanded into a detailed analysis of self-modifying production systems and their potential for formulating theories of cognitive development. GRA

N90-22909# Carnegie-Mellon Univ., Pittsburgh, PA. School of Computer Science.
TOWARD A SOAR THEORY OF TAKING INSTRUCTIONS FOR IMMEDIATE REASONING TASKS Technical Report, 15 Sep. 1986 - 14 Sep. 1991
Richard L. Lewis, Allen Newell, and Thad A. Polk Jun. 1989 12 p Submitted for publication Sponsored in part by NSF and Eastman Kodak Co., Rochester, NY Prepared in cooperation with Pittsburgh Univ., PA
(Contract N00014-86-K-0678)
(AD-A219201; AIP-60) Avail: NTIS HC A03/MF A01 CSCL 05/8

SOAR is a theory of the human cognitive architecture. The SOAR theory of taking instructions for immediate reasoning tasks, which involve extracting implicit information from simple situations in a few tens of seconds is presented. This theory is realized in a computer system that comprehends simple English instructions and organizes itself to perform a required task. Comprehending instructions produces a model of future behavior that is interpretively executed to yield task behavior. SOAR thereby acquires task-specific problem spaces that, together with basic reasoning capabilities, model human performance in multiple immediate reasoning tasks. By providing an account of taking instructions, the degrees of freedom available to the theory of immediate reasoning is reduced, and also more support for SOAR as a unified theory of cognition is given. GRA

N90-22910# Delaware Univ., Newark. Dept. of Psychology.
VISUAL SELECTIVE ATTENTION Final Report, 1 Jun. 1986 - 31 Dec. 1989
James E. Hoffman 1 Feb. 1990 7 p
(Contract DAAL03-86-K-0080)
(AD-A219204; ARO-23871.5-LS) Avail: NTIS HC A02/MF A01 CSCL 06/4

Eye movements and attention is studied. Spatial attention can be allocated to different areas of the visual field within a single eye-fixation, showing that there is some degree of independence between the systems controlling attention and the eyes. Previous investigators have explored the degree of independence by requiring subjects to simultaneously attend to different points in the field and move their eyes to the same or different locations. For example, Klein (1979) reasoned that if the two systems are independent, then subjects should be able to move their eyes to one location and attend to another without any mutual interference. Although he reports results consistent with this hypothesis, there are methodological problems with his study that make any conclusions suspect. GRA

N90-22911# Carnegie-Mellon Univ., Pittsburgh, PA. Dept. of Psychology.
LEARNING ARTIFICIAL GRAMMARS WITH COMPETITIVE CHUNKING Technical Report, 15 Sep. 1986 - 14 Sep. 1991
Emile Servan-Schreiber and John R. Anderson 6 Aug. 1989 38 p Submitted for publication Prepared in cooperation with Pittsburgh Univ., PA
(Contract N00014-86-K-0678)
(AD-A219270; AIP-80) Avail: NTIS HC A03/MF A01 CSCL 12/9

When exposed to a regular stimulus field, for instance generated by an artificial grammar, subjects unintentionally learn to respond efficiently to the underlying structure: Miller (1958) reports that subjects memorize letter strings generated by an artificial grammar faster than randomly generated strings. Reber (1967) reports that, following rote memorization of exemplar sentences, subjects efficiently discriminate grammatical from non-grammatical strings. The hypothesis that the learning process is chunking and that grammatical knowledge is implicitly encoded in a hierarchical network of chunks was explored. Grammatical judgments are then based on the degree to which integrated representations of strings can be built using those chunks. Subjects were trained on exemplar sentences while inducing them to form specific chunks. Their grammatical knowledge was then tested with a discrimination task. It was found that subjects were less sensitive to grammatical violations that preserved their chunks than to violations that did not. The theory of competitive chunking (CC) was derived and found that it successfully reproduces, via computer simulations, both Miller's experimental results and our own. GRA

N90-22912# Carnegie-Mellon Univ., Pittsburgh, PA. Learning Research and Development Center.
A TASK-ANALYTIC APPROACH TO THE AUTOMATED DESIGN OF INFORMATION GRAPHICS Technical Report, 15 Sep. 1986 - 14 Sep. 1991
Stephen Casner 1989 53 p Submitted for publication Prepared in cooperation with Pittsburgh Univ., PA
(Contract N00014-86-K-0678)
(AD-A219271; AIP-82) Avail: NTIS HC A04/MF A01 CSCL 14/5

Graphical representations popularly thought to be useful for communicating and processing information yield mixed results when tested with real users. Cognitive research suggests that graphic design methodologies that focus primarily on the information to be presented in a graphic fail to exploit the potentials of graphics for expediting human performance of information processing tasks: (1) allowing users to substitute efficient visual operators in place of more demanding logical operators; and (2) streamlining users' search for needed information. BOZ is a graphic design and presentation tool that constructively applies task-analytic principles of the user tasks. BOZ analyses a procedural description of a user task and derives a provably equivalent visual task by substituting visual operators in place of logical operators. BOZ automatically designs and renders an accompanying graphic, encoding data in the graphic such that performance of each visual operator is supported and visual search is minimized. Graphics produced by BOZ are static 2D images that support interactive manipulations of the graphical objects in a display to allow direct modification of the internally stored information that the graphic

depicts. BOZ is used to design a graphical alternative to a standard tabular display of airline schedule information to support an airline reservation task. GRA

N90-22913# Carnegie-Mellon Univ., Pittsburgh, PA. Dept. of Psychology.
LABORATORY REPLICATION OF SCIENTIFIC DISCOVERY PROCESSES Technical Report, 15 Sep. 1986 - 14 Sep. 1991
Yulin Qin and Herbert A. Simon 30 Apr. 1989 49 p Submitted for publication Prepared in cooperation with Pittsburgh Univ., PA
(Contracts N00014-86-K-0678; F33615-81-K-1539; ARPA Order 3597)
(AD-A219273; AIP-94) Avail: NTIS HC A03/MF A01 CSCL 05/8

Fourteen subjects were tape recorded while they undertook to find a law to summarize numerical data they were given. The source of the data was not identified, nor were the variables labeled semantically. Unknown to the subjects, the data were measurements of the distances of the planets from the Sun and the periods of their revolutions about it (equivalent to the data used by Johannes Kepler to discover his Third Law of planetary motion). Four of the 14 subjects discovered the same law as Kepler did (the period varies as the 3/2 power of the distance), and a fifth came very close to the answer. The subjects' protocols provide a detailed picture of the problem solving search they engaged in, mainly, but not exclusively, in the space of possible functions for fitting the data, and provide explanations as to why some succeeded and the others failed. The search heuristics used by the subjects are similar to those embodied in the BACON program, a computer simulation of certain scientific discovery processes. GRA

N90-22914# Carnegie-Mellon Univ., Pittsburgh, PA. Artificial Intelligence and Psychology Project.
AN INSTRUCTABLE CONNECTIONIST/CONTROL ARCHITECTURE: USING RULE-BASED INSTRUCTIONS TO ACCOMPLISH CONNECTIONIST LEARNING IN A HUMAN TIME SCALE
Walter Schneider and William L. Oliver 1989 54 p Submitted for publication
(Contract N00014-86-K-0678)
(AD-A219274; AIP-95) Avail: NTIS HC A04/MF A01 CSCL 05/8

A hybrid cognitive architecture that combines connectionist and controlled processing is described. The connectionist/control architecture (CAP2) uses instructions to decompose cognitive tasks into subtasks that can be learned in a human time scale. A CAP2 simulation model that uses the same task decomposition used by human subjects learns a logic task ten times faster than a standard connectionist model that does not use task decomposition. Rules for carrying out tasks are stored in a sequential network (Elman, 1988; Jordan, 1986) that controls the flow of information through a modular connectionist network. It is argued that the CAP2 architecture better matches the human cognitive architectures than purely symbolic or purely connectionist architecture. GRA

N90-22915# Carnegie-Mellon Univ., Pittsburgh, PA. Artificial Intelligence and Psychology Project.
HATCHING A THEORY OF INCUBATION EFFECTS
Craig A. Kaplan and Janet Davidson 1989 49 p
(Contract N00014-86-K-0678)
(AD-A219275; AIP-98) Avail: NTIS HC A03/MF A01 CSCL 05/8

Does putting a problem aside to incubate really help, this question is addressed through a review of the literature on incubation that includes discussion of the four stage theory of creative thought (Wallas, 1926), the distinction between conscious and unconscious work, and an in depth look at the cognitive mechanisms that might underlie incubation effects. A critical examination of the experimental studies on incubation reveals a wide range of findings -- some in apparent contradiction. It is argued that this apparent confusion results mostly from a failure to consider the interaction of factors affecting incubation. These factors include the nature of the primary and interpolated tasks, the length and timing of the interruption (incubation period), and individual differences in the knowledge and abilities of subjects. Progress, towards understanding incubation may depend upon developing a unified theory (one that will take into account the interactions of the different factors in a consistent and principled way). One such unified theory is offered as an example, illustrating how a unified approach might account for the existing empirical literature on incubation including several previously puzzling results. GRA

N90-22916# Carnegie-Mellon Univ., Pittsburgh, PA. Artificial Intelligence and Psychology Project.
NON-LIFO (LAST-IN-FIRST-OUT) EXECUTION OF COGNITIVE PROCEDURES
Kurt VanLehn, William Ball, and Bernadette Kowalski 13 Apr. 1989 58 p
(Contracts N00014-86-K-0678; N00014-88-C-0688)
(AD-A219277; AIP-72) Avail: NTIS HC A04/MF A01 CSCL 05/8

Many current theories of human problem solving and skill acquisition assume that people work only on the unsatisfied goal that was created most recently. That is, the architecture obeys a last-in-first-out (LIFO) constraint on the selection of goals. This restriction seems necessary for the proper functioning of automatic learning mechanisms, such as production compilation and chunking. It is argued that this restriction is violated by some subjects on some tasks, and in particular, that 8 subjects from a sample of 26 execute subtraction procedures in a way that violates the LIFO constraint. Although there is a great deal of between- and within-subject strategy variation in the 8 subjects' behavior, it can be simply explained by hypothesizing that: (1) the goal selection is not necessarily LIFO, (2) goal selection knowledge is represented by explicit preferences, and (3) the 8 subjects have preferences that are mostly correct with just a few preferences that are overgeneralized, overspecialized or missing. On the other hand, LIFO-based models seem unable to explain the strategy variations in any simple way. Thus, it seems that part of the flexibility in human problem solving comes from having a choice of which goal to work on next. Fortunately, it is simple to amend automatic learning mechanisms so that they will function correctly in a non-LIFO architecture. GRA

N90-22917# York Univ. (Ontario).
VISUAL SENSITIVITIES AND DISCRIMINATIONS AND THEIR ROLE IN AVIATION Interim Report, 1 Nov. 1988 - 30 Oct. 1989
David Regan 30 Oct. 1989 67 p
(Contract F49620-88-C-0002)
(AD-A219319; AFOSR-90-0235TR) Avail: NTIS HC A04/MF A01 CSCL 06/4

Selective blindness to approaching or receding motion in depth exists and seems to be not uncommon in normally sighted individuals. A perfectly camouflaged bar within a random dot pattern was rendered visible by moving dots within the bar and outside the bar with equal and opposite velocities. Shape discrimination was compared for motion defined and contrast defined dotted rectangles. At high dot speeds and contrasts aspect ratio discrimination equal for the two kinds of rectangle and, at 2 to 3 percent, corresponded to a change of side length of only 24 arc sec. Orientation discrimination and shape discrimination degrade more rapidly at short presentation durations for a motion defined than for a contrast defined target. The findings suggest that helicopter pilots may be at risk of making visual judgement errors in nap of the earth flight where some objects and ground features are seen by motion alone when contrast or speed is low or when inspection duration is brief. A simple portable test was developed for assessing visual ability to see and discriminate motion defined form. The motion defined letter test was used on 25 patients with multiple sclerosis and 50 controls; 34/50 eyes of patients were abnormal even though visual acuity was normal. Nonlinear systems

analysis: A new mathematical approach was developed for testing multi-neuron models in which individuals neurons are modelled as rectifiers. GRA

54 MAN/SYSTEM TECHNOLOGY AND LIFE SUPPORT

Includes human engineering; biotechnology; and space suits and protective clothing.

For related information see also *16 Space Transportation.*

N90-22918*# National Aeronautics and Space Administration. Ames Research Center, Moffett Field, CA.

SPATIAL DISPLAYS AND SPATIAL INSTRUMENTS

Stephen R. Ellis, ed., Mary K. Kaiser, ed., and Arthur J. Grunwald, ed. (Technion - Israel Inst. of Tech., Haifa.) Jul. 1989 623 p Conference held in Pacific Grove, CA, 31 Aug. - 3 Sep. 1987; sponsored by NASA, Ames Research Center, Moffett Field, CA and California Univ., Berkeley

(NASA-CP-10032; A-88090; NAS 1.55:10032) Avail: NTIS HC A99/MF A04 CSCL 05H

The conference proceedings topics are divided into two main areas: (1) issues of spatial and picture perception raised by graphical electronic displays of spatial information; and (2) design questions raised by the practical experience of designers actually defining new spatial instruments for use in new aircraft and spacecraft. Each topic is considered from both a theoretical and an applied direction. Emphasis is placed on discussion of phenomena and determination of design principles. For individual titles, see N90-22919 through N90-22964.

N90-22919*# National Aeronautics and Space Administration. Ames Research Center, Moffett Field, CA.

PICTORIAL COMMUNICATION: PICTURES AND THE SYNTHETIC UNIVERSE

Stephen R. Ellis (California Univ., Berkeley.) *In its* Spatial Displays and Spatial Instruments Jul. 1989 23 p (For primary document see N90-22918 16-54)

Avail: NTIS HC A99/MF A04 CSCL 05H

Principles for the design of dynamic spatial instruments for communicating quantitative information to viewers are considered through a brief review of the history of pictorial communication. Pictorial communication is seen to have two directions: (1) from the picture to the viewer; and (2) from the viewer to the picture. Optimization of the design of interactive instruments using pictorial formats requires an understanding of the manipulative, perceptual, and cognitive limitations of human viewers. Author

N90-22920*# California Univ., Berkeley. School of Optometry.

SPATIAL CONSTRAINTS OF STEREOPSIS IN VIDEO DISPLAYS

Clifton Schor *In* NASA, Ames Research Center, Spatial Displays and Spatial Instruments Jul. 1989 14 p (For primary document see N90-22918 16-54)

Avail: NTIS HC A99/MF A04 CSCL 05H

Recent development in video technology, such as the liquid crystal displays and shutters, have made it feasible to incorporate stereoscopic depth into the 3-D representations on 2-D displays. However, depth has already been vividly portrayed in video displays without stereopsis using the classical artists' depth cues described by Helmholtz (1866) and the dynamic depth cues described in detail by Ittleson (1952). Successful static depth cues include overlap, size, linear perspective, texture gradients, and shading. Effective dynamic cues include looming (Regan and Beverly, 1979) and motion parallax (Rogers and Graham, 1982). Stereoscopic depth is superior to the monocular distance cues under certain circumstances. It is most useful at portraying depth intervals as small as 5 to 10 arc secs. For this reason it is extremely useful in user-video interactions such as telepresence. Objects can be manipulated in 3-D space, for example, while a person who controls the operations views a virtual image of the manipulated object on a remote 2-D video display. Stereopsis also provides structure and form information in camouflaged surfaces such as tree foliage. Motion parallax also reveals form; however, without other monocular cues such as overlap, motion parallax can yield an ambiguous perception. For example, a turning sphere, portrayed as solid by parallax can appear to rotate either leftward or rightward. However, only one direction of rotation is perceived when stereo-depth is included. If the scene is static, then stereopsis is the principal cue for revealing the camouflaged surface structure. Finally, dynamic stereopsis provides information about the direction of motion in depth (Regan and Beverly, 1979). Clearly there are many spatial constraints, including spatial frequency content, retinal eccentricity, exposure duration, target spacing, and disparity gradient, which - when properly adjusted - can greatly enhance stereodepth in video displays. Author

N90-22921*# California Univ., Santa Barbara. Dept. of Psychology.

STEREOSCOPIC DISTANCE PERCEPTION

John M. Foley *In* NASA, Ames Research Center, Spatial Displays and Spatial Instruments Jul. 1989 9 p (For primary document see N90-22918 16-54)

Avail: NTIS HC A99/MF A04 CSCL 05H

Limited cue, open-loop tasks in which a human observer indicates distances or relations among distances are discussed. By open-loop tasks, it is meant tasks in which the observer gets no feedback as to the accuracy of the responses. What happens when cues are added and when the loop is closed are considered. The implications of this research for the effectiveness of visual displays is discussed. Errors in visual distance tasks do not necessarily mean that the percept is in error. The error could arise in transformations that intervene between the percept and the response. It is argued that the percept is in error. It is also argued that there exist post-perceptual transformations that may contribute to the error or be modified by feedback to correct for the error. Author

N90-22922*# Scripps Institution of Oceanography, La Jolla, CA.

PARADOXICAL MONOCULAR STEREOPSIS AND PERSPECTIVE VERGENCE

J. T. Enright *In* NASA, Ames Research Center, Spatial Displays and Spatial Instruments Jul. 1989 9 p (For primary document see N90-22918 16-54)

(Grant NSF BNS-85-19616)

Avail: NTIS HC A99/MF A04 CSCL 05H

The question of how to most effectively convey depth in a picture is a multifaceted problem, both because of potential limitations of the chosen medium (stereopsis, image motion), and because effectiveness can be defined in various ways. Practical applications usually focus on information transfer, i.e., effective techniques for evoking recognition of implied depth relationships, but this issue depends on subjective judgements which are difficult to scale when stimuli are above threshold. Two new approaches to this question are proposed here which are based on alternative criteria for effectiveness. Paradoxical monocular stereopsis is a remarkably compelling impression of depth which is evoked during one-eyed viewing of only certain illustrations; it can be unequivocally recognized because the feeling of depth collapses when one shifts to binocular viewing. An exploration of the stimulus properties which are effective for this phenomenon may contribute useful answers for the more general perceptual problem. Positive vergence is an eye-movement response associated with changes of fixation point within a picture which implies depth; it also arises only during monocular viewing. The response is directionally appropriate (i.e., apparently nearer objects evoke convergence, and vice versa), but the magnitude of the response can be altered consistently by making relatively minor changes in the illustration. The cross-subject agreement in changes of response magnitude would permit systematic exploration to determine which stimulus configurations are most effective in evoking perspective vergence, with quantitative answers based upon this involuntary reflex. It may well be that most effective pictures in this context will embody

features which would increase effectiveness of pictures in a more general sense. Author

N90-22923*# Bristol Univ. (England). Dept. of Psychology.
SEEING BY EXPLORING
Richard L. Gregory *In* NASA, Ames Research Center, Spatial Displays and Spatial Instruments Jul. 1989 9 p (For primary document see N90-22918 16-54)
Avail: NTIS HC A99/MF A04 CSCL 05H

The classical notion of how things are seen is that perception is passive, that the eyes are windows, and in floods reality. Physiological work of the 19th century cast doubt on this view that perception is passive acceptance of reality. Perception is not at the present time a popular topic for philosophers. This must be partly because scientific accounts of perception have now gone a long way away from appearances. They depend on physiological and psycho-physical experiments which require technical investigation and do not fall within traditional concepts of philosophy. Theories of visual perception are examined, both from a physical and psycho-physical standpoint. Author

N90-22924*# Oregon Univ., Eugene. Dept. of Computer Science.
THE PERCEPTION OF THREE-DIMENSIONALITY ACROSS CONTINUOUS SURFACES
Kent A. Stevens *In* NASA, Ames Research Center, Spatial Displays and Spatial Instruments Jul. 1989 8 p (For primary document see N90-22918 16-54)
(Contract N00014-87-K-0321)
Avail: NTIS HC A99/MF A04 CSCL 05H

The apparent three-dimensionality of a viewed surface presumably corresponds to several internal preceptual quantities, such as surface curvature, local surface orientation, and depth. These quantities are mathematically related for points within the silhouette bounds of a smooth, continuous surface. For instance, surface curvature is related to the rate of change of local surface orientation, and surface orientation is related to the local gradient of distance. It is not clear to what extent these 3D quantities are determined directly from image information rather than indirectly from mathematically related forms, by differentiation or by integration within boundary constraints. An open empirical question, for example, is to what extent surface curvature is perceived directly, and to what extent it is quantitative rather than qualitative. In addition to surface orientation and curvature, one derives an impression of depth, i.e., variations in apparent egocentric distance. A static orthographic image is essentially devoid of depth information, and any quantitative depth impression must be inferred from surface orientation and other sources. Such conversion of orientation to depth does appear to occur, and even to prevail over stereoscopic depth information under some circumstances. Author

N90-22925*# National Aeronautics and Space Administration. Ames Research Center, Moffett Field, CA.
PERCEIVING ENVIRONMENTAL PROPERTIES FROM MOTION INFORMATION: MINIMAL CONDITIONS
Dennis R. Proffitt (Virginia Univ., Charlottesville.) and Mary K. Kaiser *In its* Spatial Displays and Spatial Instruments Jul. 1989 14 p (For primary document see N90-22918 16-54)
Avail: NTIS HC A99/MF A04 CSCL 05H

The status of motion as a minimal information source for perceiving the environmental properties of surface segregation, three-dimensional (3-D) form, displacement, and dynamics is discussed. The selection of these particular properties was motivated by a desire to present research on perceiving properties that span the range of dimensional complexity. Author

N90-22926*# National Aeronautics and Space Administration. Ames Research Center, Moffett Field, CA.
VISUAL SLANT UNDERESTIMATION
John A. Perrone and Peter Wenderoth (Sydney Univ., Australia) *In its* Spatial Displays and Spatial Instruments Jul. 1989 9 p (For primary document see N90-22918 16-54)
Avail: NTIS HC A99/MF A04 CSCL 05H

Observers frequently underestimate the in-depth slant of rectangles under reduction conditions. This also occurs for slanted rectangles depicted on a flat display medium. Perrone (1982) provides a model for judged slant based upon properties of the 2-D trapezoidal projection of the rectangle. Two important parameters of this model are the angle of convergence of the sides of the trapezoid and the projected length of the trapezoid. This model was tested using a range of stimulus rectangles and found that the model failed to predict some of the major trends in the data. However, when the projected width of the base of the trapezoid projection was used in the model, instead of the projected length, excellent agreement between the theoretical and obtained slant judgements resulted. The good fit between the experimental data and the new model predictions indicates that perceived slant estimates are highly correlated with specifiable features in the stimulus display. Author

N90-22927*# Forschungsinstitut fuer Anthropotechnik, Wachtberg (Germany, F.R.). Research Inst. for Human Engineering.
THE PHOTO-COLORIMETRIC SPACE AS A MEDIUM FOR THE REPRESENTATION OF SPATIAL DATA
K. Friedrich Kraiss and Heino Widdel *In* NASA, Ames Research Center, Spatial Displays and Spatial Instruments Jul. 1989 13 p (For primary document see N90-22918 16-54)
Avail: NTIS HC A99/MF A04 CSCL 05H

Spatial displays and instruments are usually used in the context of vehicle guidance, but it is hard to find applicable spatial formats in information retrieval and interaction systems. Human interaction with spatial data structures and the applicability of the CIE color space to improve dialogue transparency is discussed. A proposal is made to use the color space to code spatially represented data. The semantic distances of the categories of dialogue structures or, more general, of database structures, are determined empirically. Subsequently the distances are transformed and depicted into the color space. The concept is demonstrated for a car diagnosis system, where the category cooling system could, e.g., be coded in blue, the category ignition system in red. Hereby a correspondence between color and semantic distances is achieved. Subcategories can be coded as luminance differences within the color space. Author

N90-22928*# York Univ., Toronto (Ontario). Human Performance Lab.
SPATIAL VISION WITHIN EGOCENTRIC AND EXOCENTRIC FRAMES OF REFERENCE
Ian P. Howard *In* NASA, Ames Research Center, Spatial Displays and Spatial Instruments Jul. 1989 17 p (For primary document see N90-22918 16-54)
Avail: NTIS HC A99/MF A04 CSCL 05H

The extent to which perceptual judgements within egocentric and exocentric frames of reference are subject to illusory disturbances and long term modifications is discussed. It is argued that well known spatial illusions, such as the oculogyral illusion and induced visual motion have usually been discussed without proper attention being paid to the frame of reference within which they occur, and that this has led to the construction of inadequate theories and inappropriate procedures for testing them. Author

N90-22929*# Stanford Univ., CA.
DISTORTIONS IN MEMORY FOR VISUAL DISPLAYS
Barbara Tversky *In* NASA, Ames Research Center, Spatial Displays and Spatial Instruments Jul. 1989 17 p (For primary document see N90-22918 16-54)
Avail: NTIS HC A99/MF A04 CSCL 05H

Systematic errors in perception and memory present a challenge to theories of perception and memory and to applied psychologists interested in overcoming them as well. A number of systematic errors in memory for maps and graphs are reviewed, and they are accounted for by an analysis of the perceptual processing presumed to occur in comprehension of maps and graphs. Visual stimuli, like verbal stimuli, are organized in

comprehension and memory. For visual stimuli, the organization is a consequence of perceptual processing, which is bottom-up or data-driven in its earlier stages, but top-down and affected by conceptual knowledge later on. Segregation of figure from ground is an early process, and figure recognition later; for both, symmetry is a rapidly detected and ecologically valid cue. Once isolated, figures are organized relative to one another and relative to a frame of reference. Both perceptual (e.g., salience) and conceptual factors (e.g., significance) seem likely to affect selection of a reference frame. Consistent with the analysis, subjects perceived and remembered curves in graphs and rivers in maps as more symmetric than they actually were. Symmetry, useful for detecting and recognizing figures, distorts map and graph figures alike. Top-down processes also seem to operate in that calling attention to the symmetry vs. asymmetry of a slightly asymmetric curve yielded memory errors in the direction of the description. Conceptual frame of reference effects were demonstrated in memory for lines embedded in graphs. In earlier work, the orientation of map figures was distorted in memory toward horizontal or vertical. In recent work, graph lines, but not map lines, were remembered as closer to an imaginary 45 deg line than they had been. Reference frames are determined by both perceptual and conceptual factors, leading to selection of the canonical axes as a reference frame in maps, but selection of the imaginary 45 deg as a reference frame in graphs. Author

N90-22930*# National Aeronautics and Space Administration. Ames Research Center, Moffett Field, CA.
HELMET-MOUNTED PILOT NIGHT VISION SYSTEMS: HUMAN FACTORS ISSUES
Sandra G. Hart and Michael S. Brickner (National Academy of Sciences - National Research Council, Washington, DC.) *In its* Spatial Displays and Spatial Instruments Jul. 1989 21 p (For primary document see N90-22918 16-54)
Avail: NTIS HC A99/MF A04 CSCL 05H

Helmet-mounted displays of infrared imagery (forward-looking infrared (FLIR)) allow helicopter pilots to perform low level missions at night and in low visibility. However, pilots experience high visual and cognitive workload during these missions, and their performance capabilities may be reduced. Human factors problems inherent in existing systems stem from three primary sources: the nature of thermal imagery; the characteristics of specific FLIR systems; and the difficulty of using FLIR system for flying and/or visually acquiring and tracking objects in the environment. The pilot night vision system (PNVS) in the Apache AH-64 provides a monochrome, 30 by 40 deg helmet-mounted display of infrared imagery. Thermal imagery is inferior to television imagery in both resolution and contrast ratio. Gray shades represent temperatures differences rather than brightness variability, and images undergo significant changes over time. The limited field of view, displacement of the sensor from the pilot's eye position, and monocular presentation of a bright FLIR image (while the other eye remains dark-adapted) are all potential sources of disorientation, limitations in depth and distance estimation, sensations of apparent motion, and difficulties in target and obstacle detection. Insufficient information about human perceptual and performance limitations restrains the ability of human factors specialists to provide significantly improved specifications, training programs, or alternative designs. Additional research is required to determine the most critical problem areas and to propose solutions that consider the human as well as the development of technology. Author

N90-22931*# California Univ., Santa Cruz. Dept. of Psychology.
SEPARATE VISUAL REPRESENTATIONS FOR PERCEPTION AND FOR VISUALLY GUIDED BEHAVIOR
Bruce Bridgeman *In* NASA, Ames Research Center, Spatial Displays and Spatial Instruments Jul. 1989 15 p (For primary document see N90-22918 16-54)
Avail: NTIS HC A99/MF A04 CSCL 05H

Converging evidence from several sources indicates that two distinct representations of visual space mediate perception and visually guided behavior, respectively. The two maps of visual space follow different rules; spatial values in either one can be biased without affecting the other. Ordinarily the two maps give equivalent responses because both are veridically in register with the world; special techniques are required to pull them apart. One such technique is saccadic suppression: small target displacements during saccadic eye movements are not preceived, though the displacements can change eye movements or pointing to the target. A second way to separate cognitive and motor-oriented maps is with induced motion: a slowly moving frame will make a fixed target appear to drift in the opposite direction, while motor behavior toward the target is unchanged. The same result occurs with stroboscopic induced motion, where the frame jump abruptly and the target seems to jump in the opposite direction. A third method of separating cognitive and motor maps, requiring no motion of target, background or eye, is the Roelofs effect: a target surrounded by an off-center rectangular frame will appear to be off-center in the direction opposite the frame. Again the effect influences perception, but in half of the subjects it does not influence pointing to the target. This experience also reveals more characteristics of the maps and their interactions with one another, the motor map apparently has little or no memory, and must be fed from the biased cognitive map if an enforced delay occurs between stimulus presentation and motor response. In designing spatial displays, the results mean that what you see isn't necessarily what you get. Displays must be designed with either perception or visually guided behavior in mind. Author

N90-22932*# State Univ. of New York, Albany. Inst. for Vision Research.
THE EFFECTS OF VIEWPOINT ON THE VIRTUAL SPACE OF PICTURES
H. A. Sedgwick *In* NASA, Ames Research Center, Spatial Displays and Spatial Instruments Jul. 1989 24 p (For primary document see N90-22918 16-54)
Avail: NTIS HC A99/MF A04 CSCL 05H

Pictorial displays whose primary purpose is to convey accurate information about the 3-D spatial layout of an environment are discussed. How and how well, pictures can convey such information is discussed. It is suggested that picture perception is not best approached as a unitary, indivisible process. Rather, it is a complex process depending on multiple, partially redundant, interacting sources of visual information for both the real surface of the picture and the virtual space beyond. Each picture must be assessed for the particular information that it makes available. This will determine how accurately the virtual space represented by the picture is seen, as well as how it is distorted when seen from the wrong viewpoint. Author

N90-22933*# Pittsburgh Univ., PA. Dept. of Psychology.
PERCEIVED ORIENTATION, SPATIAL LAYOUT AND THE GEOMETRY OF PICTURES
E. Bruce Goldstein *In* NASA, Ames Research Center, Spatial Displays and Spatial Instruments Jul. 1989 7 p (For primary document see N90-22918 16-54)
Avail: NTIS HC A99/MF A04 CSCL 05H

The purpose is to discuss the role of geometry in determining the perception of spatial layout and perceived orientation in pictures viewed at an angle. This discussion derives from Cutting's (1988) suggestion, based on his analysis of some of the author's data (Goldstein, 1987), that the changes in perceived orientation that occur when pictures are viewed at an angle can be explained in terms of geometrically produced changes in the picture's virtual space. Author

N90-22934*# Cornell Univ., Ithaca, NY. Dept. of Psychology.
ON THE EFFICACY OF CINEMA, OR WHAT THE VISUAL SYSTEM DID NOT EVOLVE TO DO
James E. Cutting *In* NASA, Ames Research Center, Spatial Displays and Spatial Instruments Jul. 1989 8 p (For primary document see N90-22918 16-54)
Avail: NTIS HC A99/MF A04 CSCL 05H

Spatial displays, and a constraint that they do not place on

the use of spatial instruments are discussed. Much of the work done in visual perception by psychologists and by computer scientists has concerned displays that show the motion of rigid objects. Typically, if one assumes that objects are rigid, one can then proceed to understand how the constant shape of the object can be perceived (or computed) as it moves through space. The author maintains that photographs and cinema are visual displays that are also powerful forms of art. Their efficacy, in part, stems from the fact that, although viewpoint is constrained when composing them, it is not nearly so constrained when viewing them. It is obvious, according to the author, that human visual systems did not evolve to watch movies or look at photographs. Thus, what photographs and movies present must be allowed in the rule-governed system under which vision evolved. Machine-vision algorithms, to be applicable to human vision, should show the same types of tolerance. Author

N90-22935*# Vanderbilt Univ., Nashville, TN.
THE PERCEPTION OF GEOMETRICAL STRUCTURE FROM CONGRUENCE
Joseph S. Lappin and Thomas D. Wason (Allotech, Inc., Raleigh, NC.) *In* NASA, Ames Research Center, Spatial Displays and Spatial Instruments Jul. 1989 15 p Sponsored in part by AFOSR, Washington, DC (For primary document see N90-22918 16-54)
(Grant NIH-EY-05926)
Avail: NTIS HC A99/MF A04 CSCL 05H

The principle function of vision is to measure the environment. As demonstrated by the coordination of motor actions with the positions and trajectories of moving objects in cluttered environments and by rapid recognition of solid objects in varying contexts from changing perspectives, vision provides real-time information about the geometrical structure and location of environmental objects and events. The geometric information provided by 2-D spatial displays is examined. It is proposed that the geometry of this information is best understood not within the traditional framework of perspective trigonometry, but in terms of the structure of qualitative relations defined by congruences among intrinsic geometric relations in images of surfaces. The basic concepts of this geometrical theory are outlined. Author

N90-22936*# National Aeronautics and Space Administration. Ames Research Center, Moffett Field, CA.
EXOCENTRIC DIRECTION JUDGEMENTS IN COMPUTER-GENERATED DISPLAYS AND ACTUAL SCENES
Stephen R. Ellis, Stephen Smith, Michael W. McGreevy, and Arthur J. Grunwald *In its* Spatial Displays and Spatial Instruments Jul. 1989 15 p (For primary document see N90-22918 16-54)
Avail: NTIS HC A99/MF A04 CSCL 05H

One of the most remarkable perceptual properties of common experience is that the perceived shapes of known objects are constant despite movements about them which transform their projections on the retina. This perceptual ability is one aspect of shape constancy (Thouless, 1931; Metzger, 1953; Borresen and Lichte, 1962). It requires that the viewer be able to sense and discount his or her relative position and orientation with respect to a viewed object. This discounting of relative position may be derived directly from the ranging information provided from stereopsis, from motion parallax, from vestibularly sensed rotation and translation, or from corollary information associated with voluntary movement. It is argued that: (1) errors in exocentric judgements of the azimuth of a target generated on an electronic perspective display are not viewpoint-independent, but are influenced by the specific geometry of their perspective projection; (2) elimination of binocular conflict by replacing electronic displays with actual scenes eliminates a previously reported equidistance tendency in azimuth error, but the viewpoint dependence remains; (3) the pattern of exocentrically judged azimuth error in real scenes viewed with a viewing direction depressed 22 deg and rotated + or - 22 deg with respect to a reference direction could not be explained by overestimation of the depression angle, i.e., a slant overestimation. Author

N90-22937*# Japan Broadcasting Corp., Tokyo. Science and Technical Research Labs.
HOW TO REINFORCE PERCEPTION OF DEPTH IN SINGLE TWO-DIMENSIONAL PICTURES
S. Nagata *In* NASA, Ames Research Center, Spatial Displays and Spatial Instruments Jul. 1989 18 p (For primary document see N90-22918 16-54)
Avail: NTIS HC A99/MF A04 CSCL 05H

The physical conditions of the display of single 2-D pictures, which produce images realistically, were studied by using the characteristics of the intake of the information for visual depth perception. Depth sensitivity, which is defined as the ratio of viewing distance to depth discrimination threshold, was introduced in order to evaluate the availability of various cues for depth perception: binocular parallax, motion parallax, accommodation, convergence, size, texture, brightness, and air-perspective contrast. The effects of binocular parallax in different conditions, the depth sensitivity of which is greatest at a distance of up to about 10 m, were studied with the new versatile stereoscopic display. From these results, four conditions to reinforce the perception of depth in single pictures were proposed, and these conditions are met by the old viewing devices and the new high-definition and wide television displays. Author

N90-22938*# ILLIANA Aviation Sciences, Las Cruces, NM.
THE EYES PREFER REAL IMAGES
Stanley N. Roscoe *In* NASA, Ames Research Center, Spatial Displays and Spatial Instruments Jul. 1989 9 p (For primary document see N90-22918 16-54)
Avail: NTIS HC A99/MF A04 CSCL 05H

For better or worse, virtual imaging displays are with us in the form of narrow-angle combining-glass presentations, head-up displays (HUD), and head-mounted projections of wide-angle sensor-generated or computer-animated imagery (HMD). All military and civil aviation services and a large number of aerospace companies are involved in one way or another in a frantic competition to develop the best virtual imaging display system. The success or failure of major weapon systems hangs in the balance, and billions of dollars in potential business are at stake. Because of the degree to which national defense is committed to the perfection of virtual imaging displays, a brief consideration of their status, an investigation and analysis of their problems, and a search for realistic alternatives are long overdue. Author

N90-22939*# Marcus (Aaron) and Associates, Berkeley, CA.
SPATIAL ISSUES IN USER INTERFACE DESIGN FROM A GRAPHIC DESIGN PERSPECTIVE
Aaron Marcus *In* NASA, Ames Research Center, Spatial Displays and Spatial Instruments Jul. 1989 7 p (For primary document see N90-22918 16-54)
Avail: NTIS HC A99/MF A04 CSCL 05H

The user interface of a computer system is a visual display that provides information about the status of operations on data within the computer and control options to the user that enable adjustments to these operations. From the very beginning of computer technology the user interface was a spatial display, although its spatial features were not necessarily complex or explicitly recognized by the users. All text and nonverbal signs appeared in a virtual space generally thought of as a single flat plane of symbols. Current technology of high performance workstations permits any element of the display to appear as dynamic, multicolor, 3-D signs in a virtual 3-D space. The complexity of appearance and the user's interaction with the display provide significant challenges to the graphic designer of current and future user interfaces. In particular, spatial depiction provides many opportunities for effective communication of objects, structures, processes, navigation, selection, and manipulation. Issues are presented that are relevant to the graphic designer seeking to optimize the user interface's spatial attributes for effective visual communication. Author

N90-22940*# Illinois Univ., Chicago. Dept. of Biomedical Visualization.
INTERACTIVE DISPLAYS IN MEDICAL ART
Deirdre Alla McConathy and Michael Doyle *In* NASA, Ames Research Center, Spatial Displays and Spatial Instruments Jul. 1989 10 p (For primary document see N90-22918 16-54)
Avail: NTIS HC A99/MF A04 CSCL 05H

Medical illustration is a field of visual communication with a long history. Traditional medical illustrations are static, 2-D, printed images; highly realistic depictions of the gross morphology of anatomical structures. Today medicine requires the visualization of structures and processes that have never before been seen. Complex 3-D spatial relationships require interpretation from 2-D diagnostic imagery. Pictures that move in real time have become clinical and research tools for physicians. Medical illustrators are involved with the development of interactive visual displays for three different, but not discrete, functions: as educational materials, as clinical and research tools, and as data bases of standard imagery used to produce visuals. The production of interactive displays in the medical arts is examined. Author

N90-22941*# Illinois Univ., Urbana. Coll. of Medicine.
THE INTERACTIVE DIGITAL VIDEO INTERFACE
Michael D. Doyle *In* NASA, Ames Research Center, Spatial Displays and Spatial Instruments Jul. 1989 4 p (For primary document see N90-22918 16-54)
Avail: NTIS HC A99/MF A04 CSCL 05H

A frequent complaint in the computer oriented trade journals is that current hardware technology is progressing so quickly that software developers cannot keep up. A example of this phenomenon can be seen in the field of microcomputer graphics. To exploit the advantages of new mechanisms of information storage and retrieval, new approaches must be made towards incorporating existing programs as well as developing entirely new applications. A particular area of need is the correlation of discrete image elements to textural information. The interactive digital video (IDV) interface embodies a new concept in software design which addresses these needs. The IDV interface is a patented device and language independent process for identifying image features on a digital video display and which allows a number of different processes to be keyed to that identification. Its capabilities include the correlation of discrete image elements to relevant text information and the correlation of these image features to other images as well as to program control mechanisms. Sophisticated interrelationships can be set up between images, text, and program control mechanisms. Author

N90-22942*# Kansas Univ., Lawrence. Dept. of Geography.
DISPLAYS, INSTRUMENTS, AND THE MULTI-DIMENSIONAL WORLD OF CARTOGRAPHY
George F. McCleary, Jr. *In* NASA, Ames Research Center, Spatial Displays and Spatial Instruments Jul. 1989 19 p (For primary document see N90-22918 16-54)
Avail: NTIS HC A99/MF A04 CSCL 05H

Cartographers are creators and purveyors of maps. Maps are representations of space, geographical images of the environment. Maps organize spatial information for convenience, particularly for use in performing tasks which involve the environment. There are many different kinds of maps, and there are as many different uses of maps as there are spatial problems to be solved. Maps and the display instrument dichotomy are examined. Also examined are the categories of map use along with the characteristics of maps. Author

N90-22943*# CAE Electronics Ltd., Montreal (Quebec).
MULTI-AXIS CONTROL OF TELEMANIPULATORS
G. M. McKinnon and Ron Kruk *In* NASA, Ames Research Center, Spatial Displays and Spatial Instruments Jul. 1989 11 p (For primary document see N90-22918 16-54)
Avail: NTIS HC A99/MF A04 CSCL 05H

The development of multi-axis hand controllers for use in telemanipulator systems is described. Experience in the control of the SRMS (shuttle remote manipulator system) arm is reviewed together with subsequent tests involving a number of simulators and configurations, including use as a side-arm flight control for helicopters. The factors affecting operator acceptability are reviewed. Author

N90-22944*# Massachusetts Inst. of Tech., Cambridge.
TELEPRESENCE, TIME DELAY, AND ADAPTATION
Richard Held and Nathaniel Durlach (Boston Univ., MA.) *In* NASA, Ames Research Center, Spatial Displays and Spatial Instruments Jul. 1989 16 p (For primary document see N90-22918 16-54)
Avail: NTIS HC A99/MF A04 CSCL 05H

Displays are now being used extensively throughout the society. More and more time is spent watching television, movies, computer screens, etc. Furthermore, in an increasing number of cases, the observer interacts with the display and plays the role of operator as well as observer. To a large extent, the normal behavior in the normal environment can also be thought of in these same terms. Taking liberties with Shakespeare, it might be said, all the world's a display and all the individuals in it are operators in and on the display. Within this general context of interactive display systems, a discussion is began with a conceptual overview of a particular class of such systems, namely, teleoperator systems. The notion is considered of telepresence and the factors that limit telepresence, including decorrelation between the: (1) motor output of the teleoperator as sensed directly via the kinesthetic/tactual system, and (2) the motor output of the teleoperator as sensed indirectly via feedback from the slave robot, i.e., via a visual display of the motor actions of the slave robot. Finally, the deleterious effect of time delay (a particular decorrelation) on sensory-motor adaptation (an important phenomenon related to telepresence) is examined. Author

N90-22945*# National Aeronautics and Space Administration. Ames Research Center, Moffett Field, CA.
ADAPTING TO VARIABLE PRISMATIC DISPLACEMENT
Robert B. Welch and Malcolm M. Cohen *In its* Spatial Displays and Spatial Instruments Jul. 1989 10 p (For primary document see N90-22918 16-54)
Avail: NTIS HC A99/MF A04 CSCL 05H

In each of two studies, subjects were exposed to a continuously changing prismatic displacement with a mean value of 19 prism diopters (variable displacement) and to a fixed 19-diopter displacement (fixed displacement). In Experiment 1, significant adaptation (post-pre shifts in hand-eye coordination) was found for fixed, but not for variable, displacement. Experiment 2 demonstrated that adaptation was obtained for variable displacement, but it was very fragile and is lost if the measures of adaptation are preceded by even a very brief exposure of the hand to normal or near-normal vision. Contrary to the results of some previous studies, an increase in within-S dispersion was not found of target pointing responses as a result of exposure to variable displacement. Author

N90-22946*# California Univ., Berkeley.
VISUAL ENHANCEMENTS IN PICK-AND-PLACE TASKS: HUMAN OPERATORS CONTROLLING A SIMULATED CYLINDRICAL MANIPULATOR
Won S. Kim, Frank Tendick, and Lawrence Stark *In* NASA, Ames Research Center, Spatial Displays and Spatial Instruments Jul. 1989 25 p Previously announced in IAA as A88-23669 (For primary document see N90-22918 16-54)
(Contracts NCC2-86; JPL-956873)
Avail: NTIS HC A99/MF A04 CSCL 05H

A teleoperation simulator was constructed with vector display system, joysticks, and a simulated cylindrical manipulator, in order to quantitatively evaluate various display conditions. The first of two experiments conducted investigated the effects of perspective parameter variations on human operators' pick-and-place performance, using a monoscopic perspective display. The second experiment involved visual enhancements of the monoscopic perspective display, by adding a grid and reference lines, by comparison with visual enhancements of a stereoscopic display; results indicate that stereoscopy generally permits superior

pick-and-place performance, but that monoscopy nevertheless allows equivalent performance when defined with appropriate perspective parameter values and adequate visual enhancements. Author

N90-22947*# Stanford Univ., CA.
DIRECTION OF MOVEMENT EFFECTS UNDER TRANSFORMED VISUAL/MOTOR MAPPINGS
H. A. Cunningham and M. Pavel *In* NASA, Ames Research Center, Spatial Displays and Spatial Instruments Jul. 1989 8 p (For primary document see N90-22918 16-54)
Avail: NTIS HC A99/MF A04 CSCL 05H

Performance in a discrete aiming task was compared under several transformed visual/motor mappings: rotations by 45, 90, 135, and 180 deg and reflections about the horizontal and the vertical midlines. Eight aiming targets were used, corresponding to eight directions of movement: up, down, right, left, up-right, down-left, up-left, and down-right. Direction of movements were characterized in terms of separable visual and motor components, and two kinds of direction of movement effects were considered. First, a direction of movement effect paralleling that seen in rapid aiming under the usual nontransformed mapping. Second, because rotations, but not reflections, are physically realizable 2-D transformations, a visual/motor control system which is sensitive to physical constraints should perform reflections, but not rotations, in a piecemeal fashion. Results supported the hypothesis that a motor factor having to do with complexity of limb movement accounts for differences in movement accuracy between right and left oblique directions. Direction of movement effects were more evident in reflections than in rotations, and were consistent with the hypothesis that the visual/motor-control system seeks a physically realizable 2-D rotation solution to reflections. Results also suggested that reversal of two orthogonal basis dimensions is far less difficult than reversing only one and leaving the other intact. Author

N90-22948*# Jet Propulsion Lab., California Inst. of Tech., Pasadena.
DISPLAYS FOR TELEMANIPULATION
Blake Hannaford, Marcos Salganicoff, and Antal K. Bejczy *In* NASA, Ames Research Center, Spatial Displays and Spatial Instruments Jul. 1989 17 p (For primary document see N90-22918 16-54)
Avail: NTIS HC A99/MF A04 CSCL 05H

Visual displays drive the human operator's highest bandwidth sensory input channel. Thus, no telemanipulation system is adequate which does not make extensive use of visual displays. Although an important use of visual displays is the presentation of a televised image of the work scene, visual displays are examined for presentation of nonvisual information (forces and torques) for simulation and planning, and for management and control of the large numbers of subsystems which make up a modern telemanipulation system. Author

N90-22949*# Texas A&M Univ., College Station. Dept. of Psychology.
PERCEPTION-ACTION RELATIONSHIPS RECONSIDERED IN LIGHT OF SPATIAL DISPLAY INSTRUMENTS
Wayne L. Shebilske *In* NASA, Ames Research Center, Spatial Displays and Spatial Instruments Jul. 1989 8 p (For primary document see N90-22918 16-54)
Avail: NTIS HC A99/MF A04 CSCL 05H

Spatial display instruments convey information about both the identity and the location of objects in order to assist surgeons, astronauts, pilots, blind individuals, and others in identification, remote manipulations, navigation, and obstacle avoidance. Scientists believe that these instruments have not reached their full potential and that progress toward new applications, including the possibility of restoring sight to the blind, will be accelerated by advancing the understanding of perceptual processes. This stimulating challenge to basic researchers was advanced by Paul Bach-Y-Rita (1972) and by the National Academy of Science (1986) report on Electronic Aids for the Blind. Although progress has been made, new applications of spatial display instruments in medicine, space, aviation, and rehabilitation await improved theoretical and empirical foundations. Author

N90-22950*# Texas A&M Univ., College Station. Dept. of Psychology.
A COMMENTARY ON PERCEPTION-ACTION RELATIONSHIPS IN SPATIAL DISPLAY INSTRUMENTS
Wayne L. Shebilske *In* NASA, Ames Research Center, Spatial Displays and Spatial Instruments Jul. 1989 7 p (For primary document see N90-22918 16-54)
Avail: NTIS HC A99/MF A04 CSCL 05H

Transfer of information across disciplines is promoted, while basic and applied researchers are cautioned about the danger of assuming simple relationships between stimulus information, perceptual impressions, and performance including pattern recognition and sensorimotor skills. A theoretical and empirical foundation was developed predicting those relationships. Author

N90-22951*# Boeing Commercial Airplane Co., Seattle, WA.
SPATIAL DISPLAYS AS A MEANS TO INCREASE PILOT SITUATIONAL AWARENESS
Delmar M. Fadden, Rolf Braune, and John Wiedemann *In* NASA, Ames Research Center, Spatial Displays and Spatial Instruments Jul. 1989 12 p (For primary document see N90-22918 16-54)
Avail: NTIS HC A99/MF A04 CSCL 05H

Experiences raise a number of concerns for future spatial-display developers. While the promise of spatial displays is great, the cost of their development will be correspondingly large. The knowledge and skills which must be coordinated to ensure successful results is unprecedent. From the viewpoint of the designer, basic knowledge of how human beings perceive and process complex displays appears fragmented and largely unquantified. Methodologies for display development require prototyping and testing with subject pilots for even small changes. Useful characterizations of the range of differences between individual users is nonexistent or at best poorly understood. The nature, significance, and frequency of interpretation errors associated with complex integrated displays is unexplored and undocumented territory. Graphic displays have intuitive appeal and can achieve face validity much more readily than earlier symbolic displays. The risk of misleading the pilot is correspondingly greater. Thus while some in the research community are developing the tools and techniques necessary for effective spatial-display development, potential users must be educated about the issues so that informed choices can be made. The scope of the task facing all is great. The task is challenging and the potential for meaningful contributions at all levels is high indeed. Author

N90-22952*# Draper (Charles Stark) Lab., Inc., Cambridge, MA.
A COMPUTER GRAPHICS SYSTEM FOR VISUALIZING SPACECRAFT IN ORBIT **c61**
Don E. Eyles *In* NASA, Ames Research Center, Spatial Displays and Spatial Instruments Jul. 1989 10 p (For primary document see N90-22918 16-54)
Avail: NTIS HC A99/MF A04 CSCL 09B

To carry out unanticipated operations with resources already in space is part of the rationale for a permanently manned space station in Earth orbit. The astronauts aboard a space station will require an on-board, spatial display tool to assist the planning and rehearsal of upcoming operations. Such a tool can also help astronauts to monitor and control such operations as they occur, especially in cases where first-hand visibility is not possible. A computer graphics visualization system designed for such an application and currently implemented as part of a ground-based simulation is described. The visualization system presents to the user the spatial information available in the spacecraft's computers by drawing a dynamic picture containing the planet Earth, the Sun, a star field, and up to two spacecraft. The point of view within the picture can be controlled by the user to obtain a number of specific visualization functions. The elements of the display, the methods used to control the display's point of view, and some

of the ways in which the system can be used are described. Author

N90-22953*# National Aeronautics and Space Administration. Ames Research Center, Moffett Field, CA.
INTERACTIVE ORBITAL PROXIMITY OPERATIONS PLANNING SYSTEM c12
Arthur J. Grunwald and Stephen R. Ellis *In its* Spatial Displays and Spatial Instruments Jul. 1989 21 p (For primary document see N90-22918 16-54)
Avail: NTIS HC A99/MF A04 CSCL 22A

An interactive, graphical proximity operations planning system was developed which allows on-site design of efficient, complex, multiburn maneuvers in the dynamic multispacecraft environment about the space station. Maneuvering takes place in, as well as out of, the orbital plane. The difficulty in planning such missions results from the unusual and counterintuitive character of relative orbital motion trajectories and complex operational constraints, which are both time varying and highly dependent on the mission scenario. This difficulty is greatly overcome by visualizing the relative trajectories and the relative constraints in an easily interpretable, graphical format, which provides the operator with immediate feedback on design actions. The display shows a perspective bird's-eye view of the space station and co-orbiting spacecraft on the background of the station's orbital plane. The operator has control over two modes of operation: (1) a viewing system mode, which enables him or her to explore the spatial situation about the space station and thus choose and frame in on areas of interest; and (2) a trajectory design mode, which allows the interactive editing of a series of way-points and maneuvering burns to obtain a trajectory which complies with all operational constraints. Through a graphical interactive process, the operator will continue to modify the trajectory design until all operational constraints are met. The effectiveness of this display format in complex trajectory design is presently being evaluated in an ongoing experimental program. Author

N90-22954*# Sandia National Labs., Albuquerque, NM. Advanced Technology Div.
EXPERIENCES IN TELEOPERATION OF LAND VEHICLES
Douglas E. McGovern *In* NASA, Ames Research Center, Spatial Displays and Spatial Instruments Jul. 1989 11 p (For primary document see N90-22918 16-54)
(Contract DE-AC04-76DP-00789)
Avail: NTIS HC A99/MF A04 CSCL 05H

Teleoperation of land vehicles allows the removal of the operator from the vehicle to a remote location. This can greatly increase operator safety and comfort in applications such as security patrol or military combat. The cost includes system complexity and reduced system performance. All feedback on vehicle performance and on environmental conditions must pass through sensors, a communications channel, and displays. In particular, this requires vision to be transmitted by close-circuit television with a consequent degradation of information content. Vehicular teleoperation, as a result, places severe demands on the operator. Teleoperated land vehicles have been built and tested by many organizations, including Sandia National Laboratories (SNL). The SNL fleet presently includes eight vehicles of varying capability. These vehicles have been operated using different types of controls, displays, and visual systems. Experimentation studying the effects of vision system characteristics on off-road, remote driving was performed for conditions of fixed camera versus steering-coupled camera and of color versus black and white video display. Additionally, much experience was gained through system demonstrations and hardware development trials. The preliminary experimental findings and the results of the accumulated operational experience are discussed. Author

N90-22955*# National Aeronautics and Space Administration. Langley Research Center, Hampton, VA.
DEVELOPMENT OF A STEREO 3-D PICTORIAL PRIMARY FLIGHT DISPLAY
Mark Nataupsky, Timothy L. Turner, Harold Lane, and Lucille Crittenden (Research Triangle Inst., Research Triangle Park, NC.) *In* NASA, Ames Research Center, Spatial Displays and Spatial Instruments Jul. 1989 8 p (For primary document see N90-22918 16-54)
Avail: NTIS HC A99/MF A04 CSCL 05H

Computer-generated displays are becoming increasingly popular in aerospace applications. The use of stereo 3-D technology provides an opportunity to present depth perceptions which otherwise might be lacking. In addition, the third dimension could also be used as an additional dimension along which information can be encoded. Historically, the stereo 3-D displays have been used in entertainment, in experimental facilities, and in the handling of hazardous waste. In the last example, the source of the stereo images generally has been remotely controlled television camera pairs. The development of a stereo 3-D pictorial primary flight display used in a flight simulation environment is described. The applicability of stereo 3-D displays for aerospace crew stations to meet the anticipated needs for 2000 to 2020 time frame is investigated. Although, the actual equipment that could be used in an aerospace vehicle is not currently available, the lab research is necessary to determine where stereo 3-D enhances the display of information and how the displays should be formatted. Author

N90-22956*# National Aeronautics and Space Administration. Ames Research Center, Moffett Field, CA.
SYNTHETIC PERSPECTIVE OPTICAL FLOW: INFLUENCE ON PILOT CONTROL TASKS
C. Thomas Bennett, Walter W. Johnson, John A. Perrone, and Anil V. Phatak (Analytical Mechanics Associates, Inc., Palo Alto, CA.) *In its* Spatial Displays and Spatial Instruments Jul. 1989 9 p (For primary document see N90-22918 16-54)
Avail: NTIS HC A99/MF A04 CSCL 05H

One approach used to better understand the impact of visual flow on control tasks has been to use synthetic perspective flow patterns. Such patterns are the result of apparent motion across a grid or random dot display. Unfortunately, the optical flow so generated is based on a subset of the flow information that exists in the real world. The danger is that the resulting optical motions may not generate the visual flow patterns useful for actual flight control. Researchers conducted a series of studies directed at understanding the characteristics of synthetic perspective flow that support various pilot tasks. In the first of these, they examined the control of altitude over various perspective grid textures (Johnson et al., 1987). Another set of studies was directed at studying the head tracking of targets moving in a 3-D coordinate system. These studies, parametric in nature, utilized both impoverished and complex virtual worlds represented by simple perspective grids at one extreme, and computer-generated terrain at the other. These studies are part of an applied visual research program directed at understanding the design principles required for the development of instruments displaying spatial orientation information. The experiments also highlight the need for modeling the impact of spatial displays on pilot control tasks. Author

N90-22957*# Massachusetts Inst. of Tech., Cambridge. Man Vehicle Lab.
SENSORY CONFLICT IN MOTION SICKNESS: AN OBSERVER THEORY APPROACH c52
Charles M. Oman *In* NASA, Ames Research Center, Spatial Displays and Spatial Instruments Jul. 1989 15 p (For primary document see N90-22918 16-54)
(Grant NAG9-244)
Avail: NTIS HC A99/MF A04 CSCL 06S

Motion sickness is the general term describing a group of common nausea syndromes originally attributed to motion-induced cerebral ischemia, stimulation of abdominal organ afferent, or overstimulation of the vestibular organs of the inner ear. Sea-, car-, and airsicknesses are the most commonly experienced examples. However, the discovery of other variants such as Cinerama-, flight simulator-, spectacle-, and space sickness in which the physical motion of the head and body is normal or absent has led to a succession of sensory conflict theories which offer a more comprehensive etiologic perspective. Implicit in the conflict

theory is the hypothesis that neutral and/or humoral signals originate in regions of the brain subversing spatial orientation, and that these signals somehow traverse to other centers mediating sickness symptoms. Unfortunately, the present understanding of the neurophysiological basis of motion sickness is far from complete. No sensory conflict neuron or process has yet been physiologically identified. To what extent can the existing theory be reconciled with current knowledge of the physiology and pharmacology of nausea and vomiting. The stimuli which causes sickness, synthesizes a contemporary Observer Theory view of the Sensory Conflict hypothesis are reviewed, and a revised model for the dynamic coupling between the putative conflict signals and nausea magnitude estimates is presented. The use of quantitative models for sensory conflict offers a possible new approach to improving the design of visual and motion systems for flight simulators and other virtual environment display systems.
Author

N90-22958*# Max-Planck-Inst. fuer Verhaltensphysiologie, Seewiesen uber Starnberg (Germany, F.R.).
INTERACTIONS OF FORM AND ORIENTATION
Horst Mittelstaedt *In* NASA, Ames Research Center, Spatial Displays and Spatial Instruments Jul. 1989 14 p (For primary document see N90-22918 16-54)
Avail: NTIS HC A99/MF A04 CSCL 05H

It is well known that the orientation of an optical pattern relative to egocentric or extraneous references affects its figural quality, that is, alters its perceived form and concomitantly delays or quickens its identification (Rock 1973). A square presented in the frontal plane to an upright person (S), for instance, changes from a box to a diamond when it is rotated with respect to the S's median plane by 45 deg. This angle, that is, the angle between the orientations of the pattern in which the two apparent figures (Gestalten) attain a summit of purity and distinctness, will be called the figural disparity of the pattern. If, as in this case, the S is upright, the retinal meridian and the subjective vertical (SV) are both in the viewer's median plane. The question arises with respect to which of these orientation references the two figures are identified. The answer may be found when the pattern and the S are oriented in such a way that the projections of the retinal meridian and the SV into the plane of the pattern diverge by the pattern's figural disparity or its periodic multiples: that is, in this case of a square by 45 or 135 deg, respectively. Similarly, which reference determines whether an equilateral triangle is seen as a pyramid or a traffic warning sign may be revealed at a divergence of SV and retinal meridian of 60 or 180 deg, respectively. It is generally found that for head roll tilts (Rho) and figural disparities of up to 90 deg, the figure whose axis coincides with the SV is seen. At head tilts of Rho=180 deg, however, the retinal reference dominates, as a rule independently of the figural disparity.
Author

N90-22959*# National Aeronautics and Space Administration. Ames Research Center, Moffett Field, CA.
OPTICAL, GRAVITATIONAL, AND KINESTHETIC DETERMINANTS OF JUDGED EYE LEVEL
Arnold E. Stoper and Malcolm M. Cohen *In its* Spatial Displays and Spatial Instruments Jul. 1989 18 p (For primary document see N90-22918 16-54)
Avail: NTIS HC A99/MF A04 CSCL 05H

Subjects judged eye level, defined in three distinct ways relative to three distinct reference planes: a gravitational horizontal, giving the gravitationally referenced eye level (GREL); a visible surface, giving the surface-referenced eye level (SREL); and a plane fixed with respect to the head, giving the head-referenced eye level (HREL). The information available for these judgements was varied by having the subjects view an illuminated target that could be placed in a box which: (1) was pitched at various angles, (2) was illuminated or kept in darkness, (3) was moved to different positions along the subject's head-to-foot body axis, and (4) was viewed with the subjects upright or reclining. The results showed: (1) judgements of GREL made in the dark were 2.5 deg lower than in the light, with a significantly greater variability; (2) judged GREL was shifted approximately half of the way toward SREL when these two eye levels did not coincide; (3) judged SREL was shifted about 12 percent of the way toward HREL when these two eye levels did not coincide, (4) judged HREL was shifted about half way toward SREL when these two eye level did not coincide and when the subject was upright (when the subject was reclining, HREL was shifted approx. 90 percent toward SREL); (5) the variability of the judged HREL in the dark was nearly twice as great with the subject reclining than with the subject upright. These results indicate that gravity is an important source of information for judgement of eye level. In the absence of information concerning the direction of gravity, the ability to judge HREL is extremely poor. A visible environment does not seem to afford precise information as to judgements of direction, but it probably does afford significant information as to the stability of these judgements.
Author

N90-22960*# Hamburg Univ. (Germany, F.R.). Neurological Clinic.
VOLUNTARY PRESETTING OF THE VESTIBULAR OCULAR REFLEX PERMITS GAZE STABILIZATION DESPITE PERTURBATION OF FAST HEAD MOVEMENTS
Wolfgang H. Zangemeister *In* NASA, Ames Research Center, Spatial Displays and Spatial Instruments Jul. 1989 11 p (For primary document see N90-22918 16-54)
Avail: NTIS HC A99/MF A04 CSCL 05H

Normal subjects are able to change voluntarily and continuously their head-eye latency together with their compensatory eye movement gain. A continuous spectrum of intent-latency modes of the subject's coordinated gaze through verbal feedback could be demonstrated. It was also demonstrated that the intent to counteract any perturbation of head-eye movement, i.e., the mental set, permitted the subjects to manipulate consciously their vestibular ocular reflex (VOR) gain. From the data, it is inferred that the VOR is always on. It may be, however, variably suppressed by higher cortical control. With appropriate training, head-mounted displays should permit an easy VOR presetting that leads to image stabilization, perhaps together with a decrease of possible misjudgements.
Author

N90-22961*# Jet Propulsion Lab., California Inst. of Tech., Pasadena.
THE MAKING OF THE MECHANICAL UNIVERSE
James Blinn *In* NASA, Ames Research Center, Spatial Displays and Spatial Instruments Jul. 1989 18 p (For primary document see N90-22918 16-54)
Avail: NTIS HC A99/MF A04 CSCL 05H

The Mechanical Universe project required the production of over 550 different animated scenes, totaling about 7 and 1/2 hours of screen time. The project required the use of a wide range of techniques and motivated the development of several different software packages. A documentation is presented of many aspects of the project, encompassing artistic design issues, scientific simulations, software engineering, and video engineering.
Author

N90-22962*# Massachusetts Univ., Amherst. Center for Art and Technology.
SYNESTHETIC ART THROUGH 3-D PROJECTION: THE REQUIREMENTS OF A COMPUTER-BASED SUPERMEDIUM
Robert Mallary *In* NASA, Ames Research Center, Spatial Displays and Spatial Instruments Jul. 1989 13 p (For primary document see N90-22918 16-54)
Avail: NTIS HC A99/MF A04 CSCL 05H

A computer-based form of multimedia art is proposed that uses the computer to fuse aspects of painting, sculpture, dance, music, film, and other media into a one-to-one synthesia of image and sound for spatially synchronous 3-D projection. Called synesthetic art, this conversion of many varied media into an aesthetically unitary experience determines the character and requirements of the system and its software. During the start-up phase, computer stereographic systems are unsuitable for software development. Eventually, a new type of illusory-projective supermedium will be

required to achieve the needed combination of large-format projection and convincing real life presence, and to handle the vast amount of 3-D visual and acoustic information required. The influence of the concept on the author's research and creative work is illustrated through two examples. Author

N90-22963*# SIROCO, Bellevue, WA.
WIDE-ANGLE DISPLAY DEVELOPMENTS BY COMPUTER GRAPHICS **c61**
William A. Fetter *In* NASA, Ames Research Center, Spatial Displays and Spatial Instruments Jul. 1989 5 p (For primary document see N90-22918 16-54)
Avail: NTIS HC A99/MF A04 CSCL 09B

Computer graphics can now expand its new subset, wide-angle projection, to be as significant a generic capability as computer graphics itself. Some prior work in computer graphics is presented which leads to an attractive further subset of wide-angle projection, called hemispheric projection, to be a major communication media. Hemispheric film systems have long been present and such computer graphics systems are in use in simulators. This is the leading edge of capabilities which should ultimately be as ubiquitous as CRTs (cathode-ray tubes). These assertions are not from degrees in science or only from a degree in graphic design, but in a history of computer graphics innovations, laying groundwork by demonstration. The author believes that it is timely to look at several development strategies, since hemispheric projection is now at a point comparable to the early stages of computer graphics, requiring similar patterns of development again. Author

N90-22964*# Princeton Univ., NJ. Dept. of Mechanical and Aerospace Engineering.
VOLUMETRIC VISUALIZATION OF 3D DATA
Gregory Russell and Richard Miles *In* NASA, Ames Research Center, Spatial Displays and Spatial Instruments Jul. 1989 8 p Sponsored in part by Princeton Univ., NJ and ONR, Washington, DC (For primary document see N90-22918 16-54)
Avail: NTIS HC A99/MF A04 CSCL 09B

In recent years, there has been a rapid growth in the ability to obtain detailed data on large complex structures in three dimensions. This development occurred first in the medical field, with CAT (computer aided tomography) scans and now magnetic resonance imaging, and in seismological exploration. With the advances in supercomputing and computational fluid dynamics, and in experimental techniques in fluid dynamics, there is now the ability to produce similar large data fields representing 3D structures and phenomena in these disciplines. These developments have produced a situation in which currently there is access to data which is too complex to be understood using the tools available for data reduction and presentation. Researchers in these areas are becoming limited by their ability to visualize and comprehend the 3D systems they are measuring and simulating. Author

N90-22965*# National Aeronautics and Space Administration. Langley Research Center, Hampton, VA.
DETERMINATION OF DEPTH-VIEWING VOLUMES FOR STEREO THREE-DIMENSIONAL GRAPHIC DISPLAYS
Russell V. Parrish and Steven P. Williams (Army Aviation Systems Command, Saint Louis, MO.) Washington Jun. 1990 21 p (DA Proj. 1L1-61102-AH-45)
(NASA-TP-2999; L-16655; NAS 1.60:2999; AVSCOM-TM-90-B-016) Avail: NTIS HC A03/MF A01 CSCL 05H

Real-world, 3-D, pictorial displays incorporating true depth cues via stereopsis techniques offer a potential means of displaying complex information in a natural way to prevent loss of situational awareness and provide increases in pilot/vehicle performance in advanced flight display concepts. Optimal use of stereopsis requires an understanding of the depth viewing volume available to the display designer. Suggested guidelines are presented for the depth viewing volume from an empirical determination of the effective region of stereopsis cueing (at several viewer-CRT screen distances) for a time multiplexed stereopsis display system. The results provide the display designer with information that will allow more effective placement of depth information to enable the full exploitation of stereopsis cueing. Increasing viewer-CRT screen distances provides increasing amounts of usable depth, but with decreasing fields-of-view. A stereopsis hardware system that permits an increased viewer-screen distance by incorporating larger screen sizes or collimation optics to maintain the field-of-view at required levels would provide a much larger stereo depth-viewing volume. Author

N90-22966*# Bionetics Corp., Cocoa Beach, FL.
THE PHYSIOLOGICAL COST OF WEARING THE PROPELLANT HANDLER'S ENSEMBLE AT THE KENNEDY SPACE CENTER
Brian R. Schonfeld, Donald F. Doerr, and Clare Marie Tomaselli Jan. 1990 47 p Prepared in cooperation with NASA, Kennedy Space Center, Cocoa Beach, FL
(Contract NAS10-10285)
(NASA-TM-102786; NAS 1.15:102786) Avail: NTIS HC A03/MF A01 CSCL 05H

The potential for exposure to toxins used in the propulsion systems of spacecraft dictates the use of a whole body protective suit, the Propellant Handler's Ensemble (PHE) during preflight preparation and launching. The weight, structure, and operating parameters of the PHE may be expected to have a significant impact upon the metabolic, cardiovascular, and thermal responses of the user, especially during ambient temperature extremes and high workload situations. Four male subjects participated in tests in -7, 23, and 43 C (20, 74, and 110 F) environments in two versions of the PHE, the autonomous backpack (BP) and the hoseline (HL) supplied configuration. Measurements included heart rate (HR) rectal temperature, four skin temperatures, oxygen (O2), and carbon dioxide (CO2) in the helmet area, interior suit temperature, and suit pressure. Exercise metabolism was estimated from HR, PHE weight, and treadmill speed and grade. The HR responses between each PHE configuration were not statistically different. As a percentage of HR maximum, the mean values were 79 percent (COLD), 84 percent (LAB), and 90 percent (HOT). Helmet O2 and CO2 levels were correlated with percent HR max (P less than 0.001). Rectal temperatures were similar for each PHE configuration, except in the HOT exposure where the BP version exceeded the HL configuration (P less than 0.05). In nearly every instance the HR was driven to moderately high levels, the supplied respiratory gases were not optimum, and thermal adversity was a primary stressor. Our findings suggest that medical and physical fitness standards, along with operational restrictions, should be imposed upon PHE users to avoid situations that could adversely affect the worker. Author

N90-22967# Southampton Univ. (England). Human Factors Research Unit.
THE APPLICATION OF A NON-LINEAR LEAST SQUARES METHOD TO PREDICTING SEAT TRANSMISSIBILITY
C. Y. Chen and M. J. Griffin Mar. 1989 29 p
(ISVR-TR-173; ETN-90-96446) Avail: NTIS HC A03/MF A01

A standard procedure for measuring seat transmissibility is investigated. The subject-seat system is divided into two subsystems: the human body and the seat. The application of the nonlinear least squares method to both subsystems is described. The predictions and measurements of the apparent mass, M (omega), (of the seated human body) and the dynamic stiffness, S (omega), (of the seat) are in good agreement. Using the Gauss-Newton method, dynamic parameters in both subsystems were obtained and the transmissibility of the seat was determined. The predicted and measured values of seat transmissibility, H (omega), are similar. ESA

N90-22968# Technische Univ., Berlin (Germany, F.R.). Inst. fuer. Luft- und Raumfahrt.
LUNAR BASE 2 (THE SECOND THOUSAND DAYS OF A BASE ON THE MOON)
A. Eckert, A.-J. Henning, A. Monokroussos, R. Schmudlach, and C. Stuurman 1989 61 p Presented at the Summer Semester

Course on Spaceflight Planning, Berlin, Fed. Republic of Germany, 1989
(ILR-Mitt-230(1989); ETN-90-96482) Avail: NTIS HC A04/MF A01

The growth of an initial lunar base is examined. Beginning with a crew of 48 persons, its capacity is expanded to 100 persons after a thousand days. The requirements and effects of this developing lunar outpost are considered. Special attention is payed to further evolution towards a full grown fabrication site for lunar oxygen and other raw materials. The following topics are included: central base configuration, power systems, lunar science, lunar farm, infrastructure and transportation, and operations time schedule. ESA

N90-22969# Naval Submarine Medical Center, Groton, CT.
MOTOR AND COGNITIVE PERFORMANCE DO NOT CHANGE DURING A TEN-WEEK SUBMARINE PATROL Interim Report, Oct. 1988 - Sep. 1989
Christine L. Schlichting, David J. Styer, and Patrick Gray 22 Dec. 1989 11 p
(AD-A218639; NSMRL-1150) Avail: NTIS HC A03/MF A01 CSCL 05/8

Submariners experience many stresses and changes in their normal lifestyles while on patrol. These stresses may affect performance, vitamin levels, mood, and blood chemistry. The effect of vitamin supplementation on performance in submariners before, during, and after a submarine patrol was investigated. While on patrol, half of the subjects were given a vitamin supplement while the other half received a placebo. There were no changes in performance on tests of motor performance, timed mental arithmetic, digit symbol substitution, or choice reaction time that could be attributed to either the vitamin supplement or to the patrol. GRA

N90-22970# Federal Aviation Administration, Washington, DC. Office of Aviation Medicine.
AIRLINER CABIN OZONE: AN UPDATED REVIEW Final Report
C. E. Melton Dec. 1989 19 p
(AD-A219264; SOT/FAA/AM-89/13) Avail: NTIS HC A03/MF A01 CSCL 06/11

The recent literature pertaining to ozone contamination of airliner cabins is reviewed. Measurements in airliner cabins without filters showed that ozone levels were about 50 percent of atmospheric ozone. Filters were about 90 percent effective in destroying ozone. Ozone (0.12 to 0.14 ppmv) caused mild subjective respiratory irritation in exercising men, but 0.20 to 0.30 ppmv did not have adverse effects on patients with chronic heart or lung disease. Ozone (1.0 to 2.0 ppmv) decreased survival time of influenza infected rats and mice and suppressed the capacity of lung macrophages to destroy Listeria. Airway responses to ozone are divided into an early parasympathetically mediated bronchoconstrictive phase and a later histamine-mediated congestive phase. Evidence indicates that intracellular free radicals are responsible for ozone damage and that the damage may be spread to other cells by toxic intermediate products: Antioxidants provide some protection to cells in vitro from ozone but dietary intake of antioxidant vitamins by humans has only a weak effect, if any. This review indicates that earlier findings regarding ozone toxicity do not need to be corrected. Compliance with existing FAA ozone standards appears to provide adequate protection to aircrews and passengers. GRA

N90-22971# Florida Univ., Gainesville.
MULTIMEDIA SYSTEM CONTROL Final Technical Report, Jun. 1988 - May 1989
D. G. Childers, J. C. Principe, and A. A. Arroyo Jan. 1990 25 p
(Contract F30602-88-D-0027)
(AD-A219392; RADC-TR-89-321) Avail: NTIS HC A03/MF A01 CSCL 23/2

The initial objective of this research program was to investigate new ways of interactive communication between the human and the computer. In highly specialized and demanding environments such as computer aided design, computer aided manufacturing, information processing or battle management, an integrated workstation using other than the conventional keyboard, mouse or touch displays may be necessary. Specifically we propose to investigate the use of brain waves (electroencephalogram- EEG) to control cursor movements, such that a desired command could be selected from a given menu. We call this interface, the EEG mouse. The computer user brain waves will have to be transmitted (we propose through radio telemetry) and processed by the workstation. However, the user will control the computer function by selecting functions from a menu by pure thought. No other computer input would have to be activated. With the advances in digital signal processing of the brain waves in real-time would be easily implemented in an I/O subsystem built around one of DSP chips. Our conclusion is that the neural network shows potential to discriminate between YES and NO answers using signal evoked responses. Further tuning of the signal processing is required to increase the reliability of the technique. GRA

N90-23063*# Iowa Univ., Iowa City. Dept. of Mechanical Engineering.
MAN-IN-THE-CONTROL-LOOP SIMULATION OF MANIPULATORS
J. L. Chang, Tsung-Chieh Lin, and K. Harold Yae *In* Jet Propulsion Lab., California Inst. of Tech., Proceedings of the 3rd Annual Conference on Aerospace Computational Control, Volume 2 15 Dec. 1989 p 688-798 (For primary document see N90-23040 16-61)
Avail: NTIS HC A20/MF A03 CSCL 05H

55 SPACE BIOLOGY

Includes exobiology; planetary biology; and extraterrestrial life.

No abstracts in this category.

59 MATHEMATICAL AND COMPUTER SCIENCES (GENERAL)

N90-22972*# Institute for Computer Applications in Science and Engineering, Hampton, VA.
THE PREPROCESSED DOACROSS LOOP Final Report
Joel H. Saltz and Ravi Mirchandaney (Yale Univ., New Haven, CT.) May 1990 15 p
(Contract NAS1-18605)
(NASA-CR-182056; NAS 1.26:182056; ICASE-IR-11) Avail: NTIS HC A03/MF A01 CSCL 12A

Dependencies between loop iterations cannot always be characterized during program compilation. Doacross loops typically make use of a-priori knowledge of inter-iteration dependencies to carry out required synchronizations. A type of doacross loop is proposed that allows the scheduling of iterations of a loop among processors without advance knowledge of inter-iteration dependencies. The method proposed for loop iterations requires that parallelizable preprocessing and postprocessing steps be carried out during program execution. Author

N90-22973*# Institute for Computer Applications in Science and Engineering, Hampton, VA.
A SCHEME FOR SUPPORTING AUTOMATIC DATA MIGRATION ON MULTICOMPUTERS Final Report
Seema Mirchandaney, Joel H. Saltz, Piyush Mehrotra (Purdue Univ., West Lafayette, IN.), and Harry Berryman May 1990 19 p Presented at the 5th Distributed Memory Computing Conference, Charleston, SC, Apr. 1990 Submitted for publication

(Contract NAS1-18605)
(NASA-CR-182038; NAS 1.26:182038; ICASE-90-33) Avail: NTIS HC A03/MF A01 CSCL 12A

A data migration mechanism is proposed that allows an explicit and controlled mapping of data to memory. While read or write copies of each data element can be assigned to any processor's memory, longer term storage of each data element is assigned to a specific location in the memory of a particular processor. Data is presented that suggests that the scheme may be a practical method for efficiently supporting data migration. Author

60 COMPUTER OPERATIONS AND HARDWARE

Includes hardware for computer graphics, firmware, and data processing.

For components see *33 Electronics and Electrical Engineering.*

N90-22974# National Aerospace Lab., Amsterdam (Netherlands).
SUPERCOMPUTER AND TECHNOLOGY [SUPERCOMPUTER EN TECHNOLOGIE]
A. A. C. Klaasse, ed. and H. Schippers, ed. 1988 94 p In DUTCH and ENGLISH Symposium held in Amsterdam, Netherlands, 6 Apr. 1988 Original contains color illustrations
(NLR-PUB-8801; ISBN-90-9002509-X; ETN-90-95409) Avail: NTIS HC A05/MF A01; 1 functional color page

The role of simulations using supercomputers in the present day production processes of the aeronautical and astronautical industry, the development of simulation methods, and the automation policy necessary to provide a large computer capacity for relevant simulations, are described in five contributions. Two contributions explain some special aspects of automation for computer aided engineering. For individual titles, see N90-22975 through N90-22981.

N90-22975# Fokker B.V., Schipol-Oost (Netherlands).
AIRCRAFT TECHNOLOGY MANAGEMENT AND THE RELATED SIGNIFICANCE OF THE SUPERCOMPUTER [VLIEGTUIGTECHNOLOGIEBELEID EN DE BETEKENIS VAN DE SUPERCOMPUTER DAARVOOR]
M. vanderVeen *In* NLR, Supercomputer and Technology 1988 p 3-9 In DUTCH (For primary document see N90-22974 16-60)
Avail: NTIS HC A05/MF A01; 1 functional color page

The development efforts of Fokker in the field of supercomputer applications with a view to aeronautics research and development are presented. The strong connection between design requirements, the narrower and narrower margins imposed upon these requirements, the shorter and shorter times in fulfilling these requirements, and the effect of changes on the design process is outlined. A large computer capacity is indispensable. The changing role of the design specialist in the design process is elucidated, together with the positive and negative effects of an aid such as a supercomputer. ESA

N90-22976# National Aerospace Lab., Amsterdam (Netherlands). Hoofdafdeling Stromingen.
NUMERICAL FLOW SIMULATION AND SUPERCOMPUTERS: MORE THAN A DIGITAL WIND TUNNEL [NUMERIEKE STROMINGSSIMULATIE EN SUPERCOMPUTERS: MEER DAN EEN DIGITALE WINDTUNNEL]
J. W. Slooff and B. Oskam *In its* Supercomputer and Technology 1988 p 11-28 In DUTCH Original contains color illustrations (For primary document see N90-22974 16-60)
Avail: NTIS HC A05/MF A01; 1 functional color page

The fundamentals of numerical flow simulation and the role of supercomputers are outlined. The technique of numerical flow simulation is summarized. The different levels of completeness of mathematical models and the ensuing computer capacity requirements are discussed. The role of numerical flow simulation versus that of wind tunnel tests in the aircraft design processes is examined. Some recent examples of aeronautical applications of numerical flow simulation are given. The importance of numerical flow simulation for the aircraft industry in the fields of competition and risk reduction is explained. ESA

N90-22977# National Aerospace Lab., Amsterdam (Netherlands). Hoofdafdeling Constructies en Materialen.
THE USE OF SUPERCOMPUTERS FOR THE DESIGN AND ANALYSIS OF CONSTRUCTIONS [SUPERCOMPUTERGEBRUIK BIJ ONTWERP EN ANALYSE VAN CONSTRUCTIES]
H. P. vanLeeuwen and H. H. Ottens *In its* Supercomputer and Technology 1988 p 29-40 In DUTCH (For primary document see N90-22974 16-60)
Avail: NTIS HC A05/MF A01; 1 functional color page

The design possibilities offered by the use of supercomputers for strength calculations are discussed. The role of supercomputers in computer aided design, strength calculations, and the maintenance and lifetime surveillance of aircrafts is outlined. Large computer capacity allows the integration of different specialized disciplines by optimizations at different levels. ESA

N90-22978# National Aerospace Lab., Amsterdam (Netherlands). Hoofdafdeling Informatica.
THE AUTOMATION MANAGEMENT TO SUPPORT RESEARCH AND DEVELOPMENT [HET BELEID VOOR AUTOMATISERING TER ONDERSTEUNING VAN ONDERZOEK EN ONTWIKKELING]
W. Loeve *In its* Supercomputer and Technology 1988 p 41-52 In DUTCH (For primary document see N90-22974 16-60)
Avail: NTIS HC A05/MF A01; 1 functional color page

The necessity for the application of digital simulation methods in present and future aircraft production processes is discussed. The role of the digital simulation method in the technical-scientific research as a whole is outlined, and compared with the classical experimental approach. It is shown that simulation methods have to be integrated in an infrastructure of mutually connected methods, such that the user has a single source of information. ESA

N90-22979# National Aerospace Lab., Amsterdam (Netherlands). Rekencentrum en Systeemprogrammering.
ACCESS TO SUPERCOMPUTERS [DE SUPERCOMPUTER: HOE KOM IK ERBIJ]
U. PosthumadeBoer and F. J. vandenBosch *In its* Supercomputer and Technology 1988 p 53-64 In DUTCH (For primary document see N90-22974 16-60)
Avail: NTIS HC A05/MF A01; 1 functional color page

The position of the NEC SX-2 supercomputer in the computer network is treated. Drastic changes in the computer network had to be made, especially with a view to the separation of networks for file transport and for interactive communication. The different solutions for optimal data communication (Hyperchannel, Ethernet TCP/IP and Ethernet XNS) are explained in the light of future ISO-OSI standards for communication functions. The differences between the old and the new application strategies are elucidated. The standardization of the local area network concept allows an infrastructure with emphasis on information sharing rather than on device sharing; the user always has access to information and to processing possibilities. ESA

N90-22980# National Aerospace Lab., Amsterdam (Netherlands). Afdeling Wiskundige Modellen en Methoden.
THE DEVELOPMENT OF A SYSTEM FOR THE NUMERICAL SIMULATION OF EULER FLOWS [DE ONTWIKKELING VAN EEN SYSTEEM VOOR DE NUMERIEKE SIMULATIE VAN EULER-STROMINGEN]
J. W. Boerstoel *In its* Supercomputer and Technology 1988 p 65-83 In DUTCH (For primary document see N90-22974 16-60)
Avail: NTIS HC A05/MF A01; 1 functional color page

The status of the development of a simulation system for the

flow about aircrafts, based on the Euler flow model, is summarized. The most important requirements and boundary conditions for the simulation system are explained. General considerations concerning the design and development of a system for the simulation of Euler flows that fulfills these requirements are given. The present status of the simulation system is described. ESA

N90-22981# Nippon Electric Co. Ltd., Tokyo (Japan).
STRATEGY OF SUPERCOMPUTER DEVELOPMENT
Masato Saito *In* NLR, Supercomputer and Technology 1988 p 85-90 (For primary document see N90-22974 16-60)
Avail: NTIS HC A05/MF A01; 1 functional color page

The development of technology, based on a computers and communications philosophy is presented. Computers and communications research and development during the last nine years are outlined. The worldwide growing demand for supercomputers is explained. Several aspects of user demands have to be taken into account: speed, simulation results output, software development environment, network support, and computer operation environment. The basic philosophy for supercomputer development is to respond actively to the user requirements. ESA

N90-22982*# Institute for Computer Applications in Science and Engineering, Hampton, VA.
COMMUNICATION OVERHEAD ON THE INTEL IPSC-860 HYPERCUBE Final Report
Shahid H. Bokhari (University of Engineering and Technology, Lahore, Pakistan) May 1990 27 p
(Contract NAS1-18605)
(NASA-CR-182055; ICASE-IR-10; NAS 1.26:182055) Avail: NTIS HC A03/MF A01 CSCL 09B

Experiments were conducted on the Intel iPSC-860 hypercube in order to evaluate the overhead of interprocessor communication. It is demonstrated that: (1) contrary to popular belief, the distance between two communicating processors has a significant impact on communication time, (2) edge contention can increase communication time by a factor of more than 7, and (3) node contention has no measurable impact. Author

N90-22983# Colorado Univ., Boulder. Dept. of Electrical and Computer Engineering.
AUTOMATIC COMPILER CONSTRUCTION Final Report, 15 Jun. 1986 - 14 Jun. 1989
Vincent P. Heuring, William M. Waite, and Gerhard Fischer 1 Feb. 1990 7 p
(Contract DAAL03-86-K-0100)
(AD-A218777; Rept-153-6923; ARO-22912.8-EL) Avail: NTIS HC A02/MF A01 CSCL 12/5

The system that we have developed convincingly demonstrates the technology required to: manage complex user requests within the context of a large tool suite; allow users to obtain instruction about how to make complex requests from the system itself; and easily develop processors for problem oriented specification languages. We have used the system routinely in its own development and in a variety of applications from circuit board layout through robot control to database query specification. It is now available for distribution to sites with Sun3 and Sun4 computers. GRA

N90-22984# Carnegie-Mellon Univ., Pittsburgh, PA. Dept. of Psychology.
ENCODING SEQUENTIAL STRUCTURE IN SIMPLE RECURRENT NETWORKS Technical Report, 15 Sep. 1986 - 14 Sep. 1991
David Servan-Schreiber, Axel Cleeremans, and James L. McClelland 14 Jul. 1989 40 p Prepared in cooperation with Pittsburgh Univ., PA Submitted for publication Sponsored in part by an NIMH Individual Fellow Award, the Belgian American Educational Foundation, and the National Fund for Scientific Research (Belgium)
(Contracts N00014-86-K-0678; N00014-86-G-0146; NSF BNS-86-09729)
(AD-A218928; AIP-67) Avail: NTIS HC A03/MF A01 CSCL 12/7

A network architecture introduced by Elman (1988) for predicting successive elements of a sequence is explored. The network uses the pattern of activation over a set of hidden units from time-step t-1, together with element t, to predict element t+1. When the network is trained with strings from a particular finite-state grammar, it can learn to be a perfect finite-state recognizer for the grammar. When the net has a minimal number of hidden units, patterns on the hidden units come to correspond to the nodes of the grammar; however, this correspondence is not necessary for the network to act as a perfect finite-state recognizer. The conditions under which the network can carry information about distant sequential contingencies across intervening elements to distant elements are explored. Such information is maintained with relative ease if it is relevant at each intermediate step; it tends to be lost when intervening elements do not depend on it. At first glance this may suggest that such networks are not relevant to natural language, in which dependencies may span indefinite distances. However, embeddings in natural language are not completely independent of earlier information. The final simulation shows that long distance sequential contingencies can be encoded by the network even if only subtle statistical properties of embedded strings depend on the early information. GRA

N90-22985# George Mason Univ., Fairfax, VA. Center for Computational Statistics.
GRAPHICS EQUIPMENT FOR DATA ANALYSIS Final Report, 1 Dec. 1988 - 30 Nov. 1989
Edward J. Wegman 30 Nov. 1989 3 p
(Grant AF-AFOSR-0206-89; AF Proj. 3842)
(AD-A218983; AFOSR-90-0297TR) Avail: NTIS HC A01/MF A01 CSCL 12/6

This grant is a DURIP instrumentation grant. The focus of the grant was to purchase a high-end graphics workstation for statistical data analysis. Our concept was for the development of a tool that we called data set mapping. This tool will prove beneficial in data sets that are difficult to visualize due to multi-dimensionality. The basic idea is to interface the high end workstation with a high performance minisupercomputer, in our case the Intel iPSC/2 d4/VX, so that processors of the hypercube are tied to graphics windows. The windows are virtual pieces of paper with dynamical graphics in each. This tool is highly interactive. It is assumed that this workstation is on an ethernet with a parallel processor, such that the parallel processor is capable of providing an engine for intense numerical calculations. GRA

N90-23070*# Jet Propulsion Lab., California Inst. of Tech., Pasadena.
JPL CONTROL/STRUCTURE INTERACTION TEST BED REAL-TIME CONTROL COMPUTER ARCHITECTURE
Hugh C. Briggs *In its* Proceedings of the 3rd Annual Conference on Aerospace Computational Control, Volume 2 15 Dec. 1989 p 739-755 (For primary document see N90-23040 16-61)
Avail: NTIS HC A20/MF A03 CSCL 09B

61 COMPUTER PROGRAMMING AND SOFTWARE

Includes computer programs, routines, alogorithms, and specific applications, e.g., CAD/CAM.

N90-22986*# Martin Marietta Corp., Denver, CO. Astronautics Group.
KNOWLEDGE MANAGEMENT: AN ABSTRACTION OF KNOWLEDGE BASE AND DATABASE MANAGEMENT SYSTEMS Final Report
Joel D. Riedesel Washington Jan. 1990 21 p

(Contract NAS8-36433)
(NASA-CR-4273; NAS 1.26:4273) Avail: NTIS HC A03/MF A01 CSCL 09B

Artificial intelligence application requirements demand powerful representation capabilities as well as efficiency for real-time domains. Many tools exist, the most prevalent being expert systems tools such as ART, KEE, OPS5, and CLIPS. Other tools just emerging from the research environment are truth maintenance systems for representing non-monotonic knowledge, constraint systems, object oriented programming, and qualitative reasoning. Unfortunately, as many knowledge engineers have experienced, simply applying a tool to an application requires a large amount of effort to bend the application to fit. Much work goes into supporting work to make the tool integrate effectively. A Knowledge Management Design System (KNOMAD), is described which is a collection of tools built in layers. The layered architecture provides two major benefits; the ability to flexibly apply only those tools that are necessary for an application, and the ability to keep overhead, and thus inefficiency, to a minimum. KNOMAD is designed to manage many knowledge bases in a distributed environment providing maximum flexibility and expressivity to the knowledge engineer while also providing support for efficiency.
Author

N90-22987*# Jet Propulsion Lab., California Inst. of Tech., Pasadena.
PROCEEDINGS OF THE 3RD ANNUAL CONFERENCE ON AEROSPACE COMPUTATIONAL CONTROL, VOLUME 1
Douglas E. Bernard, ed. and Guy K. Man, ed. 15 Dec. 1989 487 p Conference held in Oxnard, CA, Nov. 1989; sponsored in cooperation with NASA, NSF, and DOD
(Contract NAS7-198)
(NASA-CR-186446; JPL-Publ-89-45-Vol-1; NAS 1.26:186446)
Avail: NTIS HC A21/MF A03 CSCL 09B

Conference topics included definition of tool requirements, advanced multibody component representation descriptions, model reduction, parallel computation, real time simulation, control design and analysis software, user interface issues, testing and verification, and applications to spacecraft, robotics, and aircraft. For individual titles, see N90-22988 through N90-23039.

N90-22988*# Jet Propulsion Lab., California Inst. of Tech., Pasadena.
AN ASSESSMENT OF MULTIBODY SIMULATION TOOLS FOR ARTICULATED SPACECRAFT
Guy K. Man and Samuel W. Sirlin *In its* Proceedings of the 3rd Annual Conference on Aerospace Computational Control, Volume 1 15 Dec. 1989 p 12-2 (For primary document see N90-22987 16-61)
Avail: NTIS HC A21/MF A03 CSCL 09B

A survey of multibody simulation codes was conducted in the spring of 1988, to obtain an assessment of the state of the art in multibody simulation codes from the users of the codes. This survey covers the most often used articulated multibody simulation codes in the spacecraft and robotics community. There was no attempt to perform a complete survey of all available multibody codes in all disciplines. Furthermore, this is not an exhaustive evaluation of even robotics and spacecraft multibody simulation codes, as the survey was designed to capture feedback on issues most important to the users of simulation codes. We must keep in mind that the information received was limited and the technical background of the respondents varied greatly. Therefore, only the most often cited observations from the questionnaire are reported here. In this survey, it was found that no one code had both many users (reports) and no limitations. The first section is a report on multibody code applications. Following applications is a discussion of execution time, which is the most troublesome issue for flexible multibody codes. The representation of component flexible bodies, which affects both simulation setup time as well as execution time, is presented next. Following component data preparation, two sections address the accessibility or usability of a code, evaluated by considering its user interface design and examining the overall simulation integrated environment. A summary of user efforts at code verification is reported, before a tabular summary of the questionnaire responses. Finally, some conclusions are drawn.
Author

N90-22989*# Jet Propulsion Lab., California Inst. of Tech., Pasadena.
SPATIAL OPERATOR ALGEBRA FRAMEWORK FOR MULTIBODY SYSTEM DYNAMICS **c64**
G. Rodriguez, Abhinandan Jain, and K. Kreutz *In its* Proceedings of the 3rd Annual Conference on Aerospace Computational Control, Volume 1 15 Dec. 1989 p 26-4 (For primary document see N90-22987 16-61)
Avail: NTIS HC A21/MF A03 CSCL 12A

The Spatial Operator Algebra framework for the dynamics of general multibody systems is described. The use of a spatial operator-based methodology permits the formulation of the dynamical equations of motion of multibody systems in a concise and systematic way. The dynamical equations of progressively more complex grid multibody systems are developed in an evolutionary manner beginning with a serial chain system, followed by a tree topology system and finally, systems with arbitrary closed loops. Operator factorizations and identities are used to develop novel recursive algorithms for the forward dynamics of systems with closed loops. Extensions required to deal with flexible elements are also discussed.
Author

N90-22990*# National Aeronautics and Space Administration. Goddard Space Flight Center, Greenbelt, MD.
AN ORDER (n) ALGORITHM FOR THE DYNAMICS SIMULATION OF ROBOTIC SYSTEMS Abstract Only
H. M. Chun, J. D. Turner, and Harold P. Frisch *In* JPL, Proceedings of the 3rd Annual Conference on Aerospace Computational Control, Volume 1 15 Dec. 1989 p 41 (For primary document see N90-22987 16-61)
Avail: NTIS HC A21/MF A03 CSCL 09B

The formulation of an Order (n) algorithm for DISCOS (Dynamics Interaction Simulation of Controls and Structures), which is an industry-standard software package for simulation and analysis of flexible multibody systems is presented. For systems involving many bodies, the new Order (n) version of DISCOS is much faster than the current version. Results of the experimental validation of the dynamics software are also presented. The experiment is carried out on a seven-joint robot arm at NASA's Goddard Space Flight Center. The algorithm used in the current version of DISCOS requires the inverse of a matrix whose dimension is equal to the number of constraints in the system. Generally, the number of constraints in a system is roughly proportional to the number of bodies in the system, and matrix inversion requires O(p exp 3) operations, where p is the dimension of the matrix. The current version of DISCOS is therefore considered an Order (n exp 3) algorithm. In contrast, the Order (n) algorithm requires inversion of matrices which are small, and the number of matrices to be inverted increases only linearly with the number of bodies. The newly-developed Order (n) DISCOS is currently capable of handling chain and tree topologies as well as multiple closed loops. Continuing development will extend the capability of the software to deal with typical robotics applications such as put-and-place, multi-arm hand-off and surface sliding.
Author

N90-22991*# Deutsche Forschungs- und Versuchsanstalt fuer Luft- und Raumfahrt, Oberpfaffenhofen (Germany, F.R.). Inst. fuer Dynamik der Flugsysteme.
ASPECTS OF EFFICIENT AND RELIABLE MULTIBODY SYSTEM SIMULATION Abstract Only
R. Schwertassek, C. Fuehrer, and W. Rulka (Maschinenfabrik Augsburg-Nuernberg A.G., Munich, Germany, F.R.) *In* JPL, Proceedings of the 3rd Annual Conference on Aerospace Computational Control, Volume 1 15 Dec. 1989 p 42 (For primary document see N90-22987 16-61)
Avail: NTIS HC A21/MF A03 CSCL 09B

Multibody system equations can be generated in various forms. All of these may be interpreted as results of two basic approaches, the augmentation- and the elimination-method. The former method

yields the descriptor form of the system motion, a set of differential-algebraic equations (DAE), and the latter the state space representation, a minimal set of ordinary differential equations (ODE). Both of these methods are surveyed. Particular emphasis is on the discussion of recursive computational schemes, generating the equations of motion with a number of operations, which is proportional to the number N of system bodies (O(N)-formulations). For simulation purposes one would like to create that set of system equations, which can be generated most efficiently and for which the most efficient and reliable solution techniques are available. Numerical solution techniques for ODE have been studied in great detail and they are well-developed. By contrast, DAE have not been investigated for such a long time. In view of new developments in the latter field the generation of all the equations required for an efficient and reliable solution of DAE describing multibody system motion is discussed. These methods, i.e., an O(N)-formulation and new techniques for solving DAE, are implemented in the SIMPACK code. Its capabilities are illustrated by simulation of multibody robot models. Author

N90-22992*# Arizona Univ., Tucson. Computer-Aided Engineering Lab.

SYSTEMATIC GENERATION OF MULTIBODY EQUATIONS OF MOTION SUITABLE FOR RECURSIVE AND PARALLEL MANIPULATION

Parviz E. Nikravesh, Gwanghum Gim, Ara Arabyan, and Udo Rein *In* JPL, Proceedings of the 3rd Annual Conference on Aerospace Computational Control, Volume 1 15 Dec. 1989 p 43-56 (For primary document see N90-22987 16-61)

Avail: NTIS HC A21/MF A03 CSCL 09B

The formulation of a method known as the joint coordinate method for automatic generation of the equations of motion for multibody systems is summarized. For systems containing open or closed kinematic loops, the equations of motion can be reduced systematically to a minimum number of second order differential equations. The application of recursive and nonrecursive algorithms to this formulation, computational considerations and the feasibility of implementing this formulation on multiprocessor computers are discussed. Author

N90-22993*# Iowa Univ., Iowa City. Dept. of Mechanical Engineering.

RECURSIVE LINEARIZATION OF MULTIBODY DYNAMICS EQUATIONS OF MOTION

Tsung-Chieh Lin and K. Harold Yae *In* JPL, Proceedings of the 3rd Annual Conference on Aerospace Computational Control, Volume 1 15 Dec. 1989 p 57-70 (For primary document see N90-22987 16-61)

Avail: NTIS HC A21/MF A03 CSCL 09B

The equations of motion of a multibody system are nonlinear in nature, and thus pose a difficult problem in linear control design. One approach is to have a first-order approximation through the numerical perturbations at a given configuration, and to design a control law based on the linearized model. Here, a linearized model is generated analytically by following the footsteps of the recursive derivation of the equations of motion. The equations of motion are first written in a Newton-Euler form, which is systematic and easy to construct; then, they are transformed into a relative coordinate representation, which is more efficient in computation. A new computational method for linearization is obtained by applying a series of first-order analytical approximations to the recursive kinematic relationships. The method has proved to be computationally more efficient because of its recursive nature. It has also turned out to be more accurate because of the fact that analytical perturbation circumvents numerical differentiation and other associated numerical operations that may accumulate computational error, thus requiring only analytical operations of matrices and vectors. The power of the proposed linearization algorithm is demonstrated, in comparison to a numerical perturbation method, with a two-link manipulator and a seven degrees of freedom robotic manipulator. Its application to control design is also demonstrated. Author

N90-22994*# Jet Propulsion Lab., California Inst. of Tech., Pasadena.

AN INNOVATIONS APPROACH TO DECOUPLING OF MULTIBODY DYNAMICS AND CONTROL Abstract Only

G. Rodriguez *In its* Proceedings of the 3rd Annual Conference on Aerospace Computational Control, Volume 1 15 Dec. 1989 p 71-7 (For primary document see N90-22987 16-61)

Avail: NTIS HC A21/MF A03 CSCL 09B

The problem of hinged multibody dynamics is solved using an extension of the innovations approach of linear filtering and prediction theory to the problem of mechanical system modeling and control. This approach has been used quite effectively to diagonalize the equations for filtering and prediction for linear state space systems. It has similar advantages in the study of dynamics and control of multibody systems. The innovations approach advanced here consists of expressing the equations of motion in terms of two closely related processes: (1) the innovations process e, a sequence of moments, obtained from the applied moments T by means of a spatially recursive Kalman filter that goes from the tip of the manipulator to its base; (2) a residual process, a sequence of velocities, obtained from the joint-angle velocities by means of an outward smoothing operations. The innovations e and the applied moments T are related by means of the relationships e = (I - L)T and T = (I + K)e. The operation (I - L) is a causal lower triangular matrix which is generated by a spatially recursive Kalman filter and the corresponding discrete-step Riccati equation. Hence, the innovations and the applied moments can be obtained from each other by means of a causal operation which is itself casually invertible. Author

N90-22995*# Ohio State Univ., Columbus. Dept. of Electrical Engineering.

EFFICIENT DYNAMIC SIMULATION FOR MULTIPLE CHAIN ROBOTIC MECHANISMS

Kathryn W. Lilly and David E. Orin *In* JPL, Proceedings of the 3rd Annual Conference on Aerospace Computational Control, Volume 1 15 Dec. 1989 p 73-87 (For primary document see N90-22987 16-61)

(Grant NSF EET-87-18434)

Avail: NTIS HC A21/MF A03 CSCL 09B

An efficient O(mN) algorithm for dynamic simulation of simple closed-chain robotic mechanisms is presented, where m is the number of chains, and N is the number of degrees of freedom for each chain. It is based on computation of the operational space inertia matrix (6 x 6) for each chain as seen by the body, load, or object. Also, computation of the chain dynamics, when opened at one end, is required, and the most efficient algorithm is used for this purpose. Parallel implementation of the dynamics for each chain results in an O(N) + O(log sub 2 m+1) algorithm. Author

N90-22996*# Texas Univ. at Dallas, Richardson. School of Engineering and Computer Science.

A NEARLY-LINEAR COMPUTATIONAL-COST SCHEME FOR THE FORWARD DYNAMICS OF AN N-BODY PENDULUM

Jack C. K. Chou *In* JPL, Proceedings of the 3rd Annual Conference on Aerospace Computational Control, Volume 1 15 Dec. 1989 p 88-101 (For primary document see N90-22987 16-61)

Avail: NTIS HC A21/MF A03 CSCL 09B

The dynamic equations of motion of an n-body pendulum with spherical joints are derived to be a mixed system of differential and algebraic equations (DAE's). The DAE's are kept in implicit form to save arithmetic and preserve the sparsity of the system and are solved by the robust implicit integration method. At each solution point, the predicted solution is corrected to its exact solution within given tolerance using Newton's iterative method. For each iteration, a linear system of the form J delta X = E has to be solved. The computational cost for solving this linear system directly by LU factorization is O(n exp 3), and it can be reduced significantly by exploring the structure of J. It is shown that by recognizing the recursive patterns and exploiting the sparsity of the system the multiplicative and additive computational costs for solving J delta X = E are O(n) and O(n exp 2), respectively. The

formulation and solution method for an n-body pendulum is presented. The computational cost is shown to be nearly linearly proportional to the number of bodies. Author

N90-22997*# Illinois Univ., Urbana. Dept. of Aeronautical and Astronautical Engineering.
SLIDING CONTROL OF POINTING AND TRACKING WITH OPERATOR SPLINE ESTIMATION Abstract Only
Thomas A. W. Dwyer, III, Karray Fakhreddine, and Jinho Kim *In* JPL, Proceedings of the 3rd Annual Conference on Aerospace Computational Control, Volume 1 15 Dec. 1989 p 102 (For primary document see N90-22987 16-61)
(Contract NAG1-613; F49620-87-C-01013)
Avail: NTIS HC A21/MF A03 CSCL 09B

It is shown how a variable structure control technique could be implemented to achieve precise pointing and good tracking of a deformable structure subject to fast slewing maneuvers. The correction torque that has to be applied to the structure is based on estimates of upper bounds on the model errors. For a rapid rotation of the deformable structure, the elastic response can be modeled by oscillators driven by angular acceleration, and where stiffness and damping coefficients are also angular velocity and acceleration dependent. By transforming this slew-driven elastic dynamics into bilinear form (be regarding the vector made up of the angular velocity, squared angular velocity and angular acceleration components, which appear in the coefficients as the input to the deformation dynamics), an operator spline can be constructed, that gives a low order estimate of the induced disturbance. Moreover, a worst case error bound between the estimated deformation and the unknown exact deformation is also generated, which can be used where required in the sliding control correction. Author

N90-22998*# California Univ., Santa Barbara. Dept. of Electrical and Computer Engineering.
A SURVEY ON THE STRUCTURED SINGULAR VALUE Abstract Only
Andy Packard and Michael Fan (Maryland Univ., College Park.) *In* JPL, Proceedings of the 3rd Annual Conference on Aerospace Computational Control, Volume 1 15 Dec. 1989 p 103 (For primary document see N90-22987 16-61)
Avail: NTIS HC A21/MF A03 CSCL 09B

The structured singular value, U, is an important linear algebra tool to study a class of matrix perturbation problems. It is useful for analyzing the robustness of stability and performance of uncertain, (nominally) linear systems. Computation of (M) is difficult, and usually, upper and lower bounds are all that can be reliably computed. Upper bounds give conservative estimates of the sizes of allowable perturbations. The maximum singular value of a matrix M is an upper bound for (M). As an upper bound, it can be improved by finding a transformations to the data (i.e. M) which do not change the structured singular value, but do reduce the maximum singular value. Typically, upper bound algorithms involve searches over sets of transformations to yield the tightest bound. Lower bound algorithms are intelligent searches for minimum-norm solutions to multivariable polynomial equations, and are based on various optimality conditions that hold at the global (and, unfortunately, some local) minima. The current methods to compute both of these types of bounds are reviewed. Theoretical justification and extensive numerical experience with the various algorithms are covered. Author

N90-22999*# Northrop Corp., Hawthorne, CA. Flight Control Research.
ALGORITHMS FOR COMPUTING THE MULTIVARIABLE STABILITY MARGIN
Jonathan A. Tekawy, Michael G. Safonov (University of Southern California, Los Angeles.), and Richard Y. Chiang *In* JPL, Proceedings of the 3rd Annual Conference on Aerospace Computational Control, Volume 1 15 Dec. 1989 p 104-118 (For primary document see N90-22987 16-61)
Avail: NTIS HC A21/MF A03 CSCL 09B

Stability margin for multiloop flight control systems has become a critical issue, especially in highly maneuverable aircraft designs where there are inherent strong cross-couplings between the various feedback control loops. To cope with this issue, we have developed computer algorithms based on non-differentiable optimization theory. These algorithms have been developed for computing the Multivariable Stability Margin (MSM). The MSM of a dynamical system is the size of the smallest structured perturbation in component dynamics that will destabilize the system. These algorithms have been coded and appear to be reliable. As illustrated by examples, they provide the basis for evaluating the robustness and performance of flight control systems. Author

N90-23000*# California Inst. of Tech., Pasadena.
ROBUSTNESS ANALYSIS FOR REAL PARAMETRIC UNCERTAINTY Abstract Only
Athanasios Sideris *In* JPL, Proceedings of the 3rd Annual Conference on Aerospace Computational Control, Volume 1 15 Dec. 1989 p 119 (For primary document see N90-22987 16-61)
Avail: NTIS HC A21/MF A03 CSCL 09B

Some key results in the literature in the area of robustness analysis for linear feedback systems with structured model uncertainty are reviewed. Some new results are given. Model uncertainty is described as a combination of real uncertain parameters and norm bounded unmodeled dynamics. Here the focus is on the case of parametric uncertainty. An elementary and unified derivation of the celebrated theorem of Kharitonov and the Edge Theorem is presented. Next, an algorithmic approach for robustness analysis in the cases of multilinear and polynomic parametric uncertainty (i.e., the closed loop characteristic polynomial depends multilinearly and polynomially respectively on the parameters) is given. The latter cases are most important from practical considerations. Some novel modifications in this algorithm which result in a procedure of polynomial time behavior in the number of uncertain parameters is outlined. Finally, it is shown how the more general problem of robustness analysis for combined parametric and dynamic (i.e., unmodeled dynamics) uncertainty can be reduced to the case of polynomic parametric uncertainty, and thus be solved by means of the algorithm.
Author

N90-23001*# Integrated Systems, Inc., Santa Clara, CA.
COMPUTATIONAL ISSUE IN THE ANALYSIS OF ADAPTIVE CONTROL SYSTEMS Abstract Only **c63**
Robert L. Kosut *In* JPL, Proceedings of the 3rd Annual Conference on Aerospace Computational Control, Volume 1 15 Dec. 1989 p 120 (For primary document see N90-22987 16-61)
Avail: NTIS HC A21/MF A03 CSCL 09B

Adaptive systems under slow parameter adaption can be analyzed by the method of averaging. This provides a means to assess stability (and instability) properties of most adaptive systems, either continuous-time or (more importantly for practice) discrete-time, as well as providing an estimate of the region of attraction. Although the method of averaging is conceptually straightforward, even simple examples are well beyond hand calculations. Specific software tools are proposed which can provide the basis for user-friendly environment to perform the necessary computations involved in the averaging analysis.
Author

N90-23002*# California Inst. of Tech., Pasadena.
EXPERIMENTAL EXPERIENCE WITH FLEXIBLE STRUCTURES Abstract Only
Gary J. Balas *In* JPL, Proceedings of the 3rd Annual Conference on Aerospace Computational Control, Volume 1 15 Dec. 1989 p 121 (For primary document see N90-22987 16-61)
Avail: NTIS HC A21/MF A03 CSCL 09B

The focus is on a flexible structure experiment developed at the California Institute of Technology. The main thrust of the experiment is to address the identification and robust control issues associated with large space structures by capturing their characteristics in the laboratory. The design, modeling, identification and control objectives will be discussed. Also, the subject of

uncertainty in structural plant models and the frequency shaping of performance objectives will be expounded upon. Theoretical and experimental results of control laws designed using the identified model and uncertainty descriptions will be presented.
Author

N90-23003*# Cincinnati Univ., OH. Dept. of Aerospace Engineering and Engineering Mechanics.
A DISTURBANCE BASED CONTROL/STRUCTURE DESIGN ALGORITHM
Mark D. McLaren and Gary L. Slater *In* JPL, Proceedings of the 3rd Annual Conference on Aerospace Computational Control, Volume 1 15 Dec. 1989 p 122-139 Sponsored in part by AFOSR, Wright-Patterson AFB, OH and CRAY Research, Inc. (For primary document see N90-22987 16-61)
Avail: NTIS HC A21/MF A03 CSCL 09B

Some authors take a classical approach to the simultaneous structure/control optimization by attempting to simultaneously minimize the weighted sum of the total mass and a quadratic form, subject to all of the structural and control constraints. Here, the optimization will be based on the dynamic response of a structure to an external unknown stochastic disturbance environment. Such a response to excitation approach is common to both the structural and control design phases, and hence represents a more natural control/structure optimization strategy than relying on artificial and vague control penalties. The design objective is to find the structure and controller of minimum mass such that all the prescribed constraints are satisfied. Two alternative solution algorithms are presented which have been applied to this problem. Each algorithm handles the optimization strategy and the imposition of the nonlinear constraints in a different manner. Two controller methodologies, and their effect on the solution algorithm, will be considered. These are full state feedback and direct output feedback, although the problem formulation is not restricted solely to these forms of controller. In fact, although full state feedback is a popular choice among researchers in this field (for reasons that will become apparent), its practical application is severely limited. The controller/structure interaction is inserted by the imposition of appropriate closed-loop constraints, such as closed-loop output response and control effort constraints. Numerical results will be obtained for a representative flexible structure model to illustrate the effectiveness of the solution algorithms. Author

N90-23004*# Memorial Univ. of Newfoundland, Saint Johns. Dept. of Computer Science.
USING DEFLATION IN THE POLE ASSIGNMENT PROBLEM WITH OUTPUT FEEDBACK
George Miminis *In* JPL, Proceedings of the 3rd Annual Conference on Aerospace Computational Control, Volume 1 15 Dec. 1989 p 140-154 (For primary document see N90-22987 16-61)
Avail: NTIS HC A21/MF A03 CSCL 09B

A direct algorithm is suggested for the computation of a linear output feedback for a multi input, multi output system such that the resultant closed-loop matrix has eigenvalues that include a specified set of eigenvalues. The algorithm uses deflation based on unitary similarity transformations. Thus researchers hope the algorithm is numerically stable; however, this has not been proven as yet. Author

N90-23005*# California Inst. of Tech., Pasadena.
COMBINED CONTROL-STRUCTURE OPTIMIZATION **c63**
M. Salama, M. Milman, R. Bruno, R. Scheid, and S. Gibson (California Univ., Los Angeles.) *In* JPL, Proceedings of the 3rd Annual Conference on Aerospace Computational Control, Volume 1 15 Dec. 1989 p 155-169 (For primary document see N90-22987 16-61)
Avail: NTIS HC A21/MF A03 CSCL 09B

An approach for combined control-structure optimization keyed to enhancing early design trade-offs is outlined and illustrated by numerical examples. The approach employs a homotopic strategy and appears to be effective for generating families of designs that can be used in these early trade studies. Analytical results were obtained for classes of structure/control objectives with linear quadratic Gaussian (LQG) and linear quadratic regulator (LQR) costs. For these, researchers demonstrated that global optima can be computed for small values of the homotopy parameter. Conditions for local optima along the homotopy path were also given. Details of two numerical examples employing the LQR control cost were given showing variations of the optimal design variables along the homotopy path. The results of the second example suggest that introducing a second homotopy parameter relating the two parts of the control index in the LQG/LQR formulation might serve to enlarge the family of Pareto optima, but its effect on modifying the optimal structural shapes may be analogous to the original parameter lambda. Author

N90-23006*# Waseda Univ., Tokyo (Japan). Dept. of Electrical Engineering.
PARALLEL PROCESSING OF REAL-TIME DYNAMIC SYSTEMS SIMULATION ON OSCAR (OPTIMALLY SCHEDULED ADVANCED MULTIPROCESSOR) **c62**
Hironori Kasahara, Hiroki Honda, and Seinosuke Narita *In* JPL, Proceedings of the 3rd Annual Conference on Aerospace Computational Control, Volume 1 15 Dec. 1989 p 170-183 (For primary document see N90-22987 16-61)
Avail: NTIS HC A21/MF A03 CSCL 09B

Parallel processing of real-time dynamic systems simulation on a multiprocessor system named OSCAR is presented. In the simulation of dynamic systems, generally, the same calculation are repeated every time step. However, we cannot apply to Do-all or the Do-across techniques for parallel processing of the simulation since there exist data dependencies from the end of an iteration to the beginning of the next iteration and furthermore data-input and data-output are required every sampling time period. Therefore, parallelism inside the calculation required for a single time step, or a large basic block which consists of arithmetic assignment statements, must be used. In the proposed method, near fine grain tasks, each of which consists of one or more floating point operations, are generated to extract the parallelism from the calculation and assigned to processors by using optimal static scheduling at compile time in order to reduce large run time overhead caused by the use of near fine grain tasks. The practicality of the scheme is demonstrated on OSCAR (Optimally SCheduled Advanced multiprocessoR) which has been developed to extract advantageous features of static scheduling algorithms to the maximum extent. Author

N90-23007*# Illinois Univ., Chicago. Dept. of Mathematics, Statistics, and Computer Science.
PARALLEL AND VECTOR COMPUTATION FOR STOCHASTIC OPTIMAL CONTROL APPLICATIONS **c62**
F. B. Hanson *In* JPL, Proceedings of the 3rd Annual Conference on Aerospace Computational Control, Volume 1 15 Dec. 1989 p 184-197 Sponsored in part by the National Center for Supercomputing Applications, Urbana, IL (For primary document see N90-22987 16-61)
(Contracts W-31-109-eng-38; DE-AC05-84ER-21400; NSF DMS-88-06099)
Avail: NTIS HC A21/MF A03 CSCL 09B

A general method for parallel and vector numerical solutions of stochastic dynamic programming problems is described for optimal control of general nonlinear, continuous time, multibody dynamical systems, perturbed by Poisson as well as Gaussian random white noise. Possible applications include lumped flight dynamics models for uncertain environments, such as large scale and background random atmospheric fluctuations. The numerical formulation is highly suitable for a vector multiprocessor or vectorizing supercomputer, and results exhibit high processor efficiency and numerical stability. Advanced computing techniques, data structures, and hardware help alleviate Bellman's curse of dimensionality in dynamic programming computations. Author

N90-23008*# Iowa Univ., Iowa City. The Center for Simulation and Design Optimization.

A ROBOT ARM SIMULATION WITH A SHARED MEMORY MULTIPROCESSOR MACHINE Abstract Only

Sung-Soo Kim and Li-Ping Chuang *In* JPL, Proceedings of the 3rd Annual Conference on Aerospace Computational Control, Volume 1 15 Dec. 1989 p 198 (For primary document see N90-22987 16-61)

Avail: NTIS HC A21/MF A03 CSCL 09B

A parallel processing scheme for a single chain robot arm is presented for high speed computation on a shared memory multiprocessor. A recursive formulation that is derived from a virtual work form of the d'Alembert equations of motion is utilized for robot arm dynamics. A joint drive system that consists of a motor rotor and gears is included in the arm dynamics model, in order to take into account gyroscopic effects due to the spinning of the rotor. The fine grain parallelism of mechanical and control subsystem models is exploited, based on independent computation associated with bodies, joint drive systems, and controllers. Efficiency and effectiveness of the parallel scheme are demonstrated through simulations of a telerobotic manipulator arm. Two different mechanical subsystem models, i.e., with and without gyroscopic effects, are compared, to show the trade-off between efficiency and accuracy. Author

N90-23009*# Jet Propulsion Lab., California Inst. of Tech., Pasadena.

A UNIFYING FRAMEWORK FOR RIGID MULTIBODY DYNAMICS AND SERIAL AND PARALLEL COMPUTATIONAL ISSUES Abstract Only **c62**

Amir Fijany and Abhinandan Jain *In its* Proceedings of the 3rd Annual Conference on Aerospace Computational Control, Volume 1 15 Dec. 1989 p 199 (For primary document see N90-22987 16-61)

Avail: NTIS HC A21/MF A03 CSCL 09B

A unifying framework for various formulations of the dynamics of open-chain rigid multibody systems is discussed. Their suitability for serial and parallel processing is assessed. The framework is based on the derivation of intrinsic, i.e., coordinate-free, equations of the algorithms which provides a suitable abstraction and permits a distinction to be made between the computational redundancy in the intrinsic and extrinsic equations. A set of spatial notation is used which allows the derivation of the various algorithms in a common setting and thus clarifies the relationships among them. The three classes of algorithms viz., O(n), O(n exp 2) and O(n exp 3) or the solution of the dynamics problem are investigated. Researchers begin with the derivation of O(n exp 3) algorithms based on the explicit computation of the mass matrix and it provides insight into the underlying basis of the O(n) algorithms. From a computational perspective, the optimal choice of a coordinate frame for the projection of the intrinsic equations is discussed and the serial computational complexity of the different algorithms is evaluated. The three classes of algorithms are also analyzed for suitability for parallel processing. It is shown that the problem belongs to the class of N C and the time and processor bounds are of O(log2/2(n)) and O(n exp 4), respectively. However, the algorithm that achieves the above bounds is not stable. Researchers show that the fastest stable parallel algorithm achieves a computational complexity of O(n) with O(n exp 4), respectively. However, the algorithm that achieves the above bounds is not stable. Researchers show that the fastest stable parallel algorithm achieves a computational complexity of O(n) with O(n exp 2) processors, and results from the parallelization of the O(n exp 3) serial algorithm. Author

N90-23010*# Jet Propulsion Lab., California Inst. of Tech., Pasadena.

PARALLEL ALGORITHMS AND ARCHITECTURE FOR COMPUTATION OF MANIPULATOR FORWARD DYNAMICS **c62**

Amir Fijany and Antal K. Bejczy *In its* Proceedings of the 3rd Annual Conference on Aerospace Computational Control, Volume 1 15 Dec. 1989 p 200-215 (For primary document see N90-22987 16-61)

Avail: NTIS HC A21/MF A03 CSCL 09B

Parallel computation of manipulator forward dynamics is investigated. Considering three classes of algorithms for the solution of the problem, that is, the O(n), the O(n exp 2), and the O(n exp 3) algorithms, parallelism in the problem is analyzed. It is shown that the problem belongs to the class of NC and that the time and processors bounds are of O(log2/2n) and O(n exp 4), respectively. However, the fastest stable parallel algorithms achieve the computation time of O(n) and can be derived by parallelization of the O(n exp 3) serial algorithms. Parallel computation of the O(n exp 3) algorithms requires the development of parallel algorithms for a set of fundamentally different problems, that is, the Newton-Euler formulation, the computation of the inertia matrix, decomposition of the symmetric, positive definite matrix, and the solution of triangular systems. Parallel algorithms for this set of problems are developed which can be efficiently implemented on a unique architecture, a triangular array of $n(n+2)/2$ processors with a simple nearest-neighbor interconnection. This architecture is particularly suitable for VLSI and WSI implementations. The developed parallel algorithm, compared to the best serial O(n) algorithm, achieves an asymptotic speedup of more than two orders-of-magnitude in the computation the forward dynamics. Author

N90-23011*# Ohio State Univ., Columbus. Dept. of Electrical Engineering.

COMPUTATIONAL DYNAMICS FOR ROBOTICS SYSTEMS USING A NON-STRICT COMPUTATIONAL APPROACH

David E. Orin, Ho-Cheung Wong, and P. Sadayappan *In* JPL, Proceedings of the 3rd Annual Conference on Aerospace Computational Control, Volume 1 15 Dec. 1989 p 216-227 (For primary document see N90-22987 16-61)

(Grant NSF EET-87-18434)

Avail: NTIS HC A21/MF A03 CSCL 09B

A Non-Strict computational approach for real-time robotics control computations is proposed. In contrast to the traditional approach to scheduling such computations, based strictly on task dependence relations, the proposed approach relaxes precedence constraints and scheduling is guided instead by the relative sensitivity of the outputs with respect to the various paths in the task graph. An example of the computation of the Inverse Dynamics of a simple inverted pendulum is used to demonstrate the reduction in effective computational latency through use of the Non-Strict approach. A speedup of 5 has been obtained when the processes of the task graph are scheduled to reduce the latency along the crucial path of the computation. While error is introduced by the relaxation of precedence constraints, the Non-Strict approach has a smaller error than the conventional Strict approach for a wide range of input conditions. Author

N90-23012*# Jet Propulsion Lab., California Inst. of Tech., Pasadena.

COMPUTATIONAL CHAOS IN MASSIVELY PARALLEL NEURAL NETWORKS Abstract Only **c62**

Jacob Barhen and Sandeep Gulati *In its* Proceedings of the 3rd Annual Conference on Aerospace Computational Control, Volume 1 15 Dec. 1989 p 228 (For primary document see N90-22987 16-61)

Avail: NTIS HC A21/MF A03 CSCL 09B

A fundamental issue which directly impacts the scalability of current theoretical neural network models to massively parallel embodiments, in both software as well as hardware, is the inherent and unavoidable concurrent asynchronicity of emerging fine-grained computational ensembles and the possible emergence of chaotic manifestations. Previous analyses attributed dynamical instability to the topology of the interconnection matrix, to parasitic components or to propagation delays. However, researchers have observed the existence of emergent computational chaos in a concurrently asynchronous framework, independent of the network topology. Researcher present a methodology enabling the effective asynchronous operation of large-scale neural networks. Necessary

and sufficient conditions guaranteeing concurrent asynchronous convergence are established in terms of contracting operators. Lyapunov exponents are computed formally to characterize the underlying nonlinear dynamics. Simulation results are presented to illustrate network convergence to the correct results, even in the presence of large delays. Author

N90-23013*# Lockheed Missiles and Space Co., Sunnyvale, CA.
MULTI-FLEXIBLE-BODY DYNAMICS CAPTURING MOTION-INDUCED STIFFNESS Abstract Only **c62**
Arun K. Banerjee, Mark E. Lemak, and John M. Dickens *In* JPL, Proceedings of the 3rd Annual Conference on Aerospace Computational Control, Volume 1 15 Dec. 1989 p 229 (For primary document see N90-22987 16-61)
Avail: NTIS HC A21/MF A03 CSCL 09B

A multi-flexible-body dynamics formulation incorporating a recently developed theory for capturing motion induced stiffness for a arbitrary structure undergoing large rotation and translation accompanied by small vibrations is presented. In essence, the method consists of correcting prematurely linearized dynamical equations for an arbitrary flexible body with generalized active forces due to geometric stiffness corresponding to a system of twelve inertia forces and nine inertia couples distributed over the body. Equations of motion are derived by means of Kane's method. A useful feature of the formulation is its treatment of prescribed motions and interaction forces. Results of simulations of motions of three flexible spacecraft, involving stiffening during spinup motion, dynamic buckling, and a repositioning maneuver, demonstrate the validity and generality of the theory. Author

N90-23014*# Massachusetts Inst. of Tech., Cambridge.
NONLINEAR STRAIN-DISPLACEMENT RELATIONS AND FLEXIBLE MULTIBODY DYNAMICS
Carlos E. Padilla and Andreas H. vonFlotow *In* JPL, Proceedings of the 3rd Annual Conference on Aerospace Computational Control, Volume 1 15 Dec. 1989 p 230-245 Sponsored by NSF, Washington, DC (For primary document see N90-22987 16-61)
Avail: NTIS HC A21/MF A03 CSCL 09B

Dynamics of chains of flexible bodies undergoing large rigid body motions, but small elastic deflections are considered. The role of nonlinear strain-displacement relations in the development of the motion equations correct to first order in elastic deflections is investigated. The general form of these equations linearized only in the small elastic deflections is presented, and the relative significance of various nonlinear terms is studied both analytically and through the use of the numerical simulations. Numerical simulations are performed for a two link chain constrained to move in the plane, subject to hinge torques. Each link is modeled as a thin beam. Slew maneuver simulation results are compared for models with and without properly modeled kinematics of deformation. The goal of this case study is to quantify the importance of the terms in the equations of motion which arise from the inclusion of nonlinear strain-displacement relations. It is concluded that unless the consistently linearized equations in elastic deflections and speeds are available and necessary, the inconsistently (prematurely) linearized equations should be replaced in all cases by ruthlessly linearized equations: equations in which all nonlinear terms involving the elastic deflections and speeds are ignored. Author

N90-23015*# Illinois Univ., Chicago. Dept. of Mechanical Engineering.
NONLINEAR FINITE ELEMENT FORMULATION FOR THE LARGE DISPLACEMENT ANALYSIS IN MULTIBODY SYSTEM DYNAMICS Abstract Only
J. Rismantab-Sany, B. Chang, and A. A. Shabana *In* JPL, Proceedings of the 3rd Annual Conference on Aerospace Computational Control, Volume 1 15 Dec. 1989 p 246 (For primary document see N90-22987 16-61)
Avail: NTIS HC A21/MF A03 CSCL 09B

A total Lagrangian finite element formulation for the deformable bodies in multibody mechanical systems that undergo finite relative rotations is developed. The deformable bodies are discretized using finite element methods. The shape functions that are used to describe the displacement field are required to include the rigid body modes that describe only large translational displacements. This does not impose any limitations on the technique because most commonly used shape functions satisfy this requirement. The configuration of an element is defined using four sets of coordinate systems: Body, Element, Intermediate element, Global. The body coordinate system serves as a unique standard for the assembly of the elements forming the deformable body. The element coordinate system is rigidly attached to the element and therefore it translates and rotates with the element. The intermediate element coordinate system, whose axes are initially parallel to the element axes, has an origin which is rigidly attached to the origin of the body coordinate system and is used to conveniently describe the configuration of the element in undeformed state with respect to the body coordinate system. Author

N90-23016*# Illinois Univ., Chicago. Dept. of Mechanical Engineering.
OPTIMUM CONTROL FORCES FOR MULTIBODY SYSTEMS WITH INTERMITTENT MOTION Abstract Only
Sitki Kemal Ider and F. M. L. Amirouche *In* JPL, Proceedings of the 3rd Annual Conference on Aerospace Computational Control, Volume 1 15 Dec. 1989 p 247 (For primary document see N90-22987 16-61)
Avail: NTIS HC A21/MF A03 CSCL 09B

The objective is to address the continuity of motion when a dynamical system is suddenly subjected to constraint conditions. Motion discontinuity due to the initial constraint violation is avoided by prior control forces that adjust the motion and yield velocity and acceleration consistent at the point of application of the constraint. The optimum control forces are determined for a specified control interval. The method proposed provides an optimum adjustment of the system's motion and assures that the stresses developed at the system components are kept within acceptable limits. The procedures developed will be illustrated making use of inequality constraints applied to obstacle avoidance problems in robotics. Author

N90-23017*# Maryland Univ., College Park. Dept. of Mechanical Engineering.
DEVELOPMENT OF EFFICIENT COMPUTER PROGRAM FOR DYNAMIC SIMULATION OF TELEROBOTIC MANIPULATION
J. Chen and Y. J. Ou *In* JPL, Proceedings of the 3rd Annual Conference on Aerospace Computational Control, Volume 1 15 Dec. 1989 p 248-262 (For primary document see N90-22987 16-61)
(Grant NAG5-1019)
Avail: NTIS HC A21/MF A03 CSCL 09B

Research in robot control has generated interest in computationally efficient forms of dynamic equations for multi-body systems. For a simply connected open-loop linkage, dynamic equations arranged in recursive form were found to be particularly efficient. A general computer program capable of simulating an open-loop manipulator with arbitrary number of links has been developed based on an efficient recursive form of Kane's dynamic equations. Also included in the program is some of the important dynamics of the joint drive system, i.e., the rotational effect of the motor rotors. Further efficiency is achieved by the use of symbolic manipulation program to generate the FORTRAN simulation program tailored for a specific manipulator based on the parameter values given. The formulations and the validation of the program are described, and some results are shown. Author

N90-23018*# Illinois Univ., Chicago. Dept. of Engineering.
THE COUPLING EFFECTS OF KINEMATICS AND FLEXIBILITY ON THE LAGRANGIAN DYNAMIC FORMULATION OF OPEN CHAIN DEFORMABLE LINKS Abstract Only
Koorosh Changizi *In* JPL, Proceedings of the 3rd Annual Conference on Aerospace Computational Control, Volume 1 15

Dec. 1989 p 263 (For primary document see N90-22987 16-61)
Avail: NTIS HC A21/MF A03 CSCL 09B

A nonlinear Lagrangian formulation for the spatial kinematic and dynamic analysis of open chain deformable links consisting of cylindrical joints that connect pairs of flexible links is developed. The special cases of revolute or prismatic joint can also be obtained from the kinematic equations. The kinematic equations are described using a 4x4 matrix method. The configuration of each deformable link in the open loop kinematic chain is identified using a coupled set of relative joint variables, constant geometric parameters, and elastic coordinates. The elastic coordinates define the link deformation with respect to a selected joint coordinate system that is consistent with the kinematic constraints on the boundary of the deformable link. These coordinates can be introduced using approximation techniques such as Rayleigh-Ritz method, finite element technique or any other desired approach. The large relative motion between two neighboring links are defined by a set of joint coordinates which describes the large relative translational and rotational motion between two neighboring joint coordinate systems. The origin of these coordinate systems are rigidly attached to the neighboring links at the joint definition points along the axis of motion. Author

N90-23019*# Illinois Univ., Chicago. Dept. of Mechanical Engineering.
EXPLICIT MODELING OF COMPOSITE PLATES AND BEAMS IN THE DYNAMICS OF MULTIBODY SYSTEMS Abstract Only c39
F. M. L. Amirouche, Sitki Kemal Ider, and M. Moumene *In* JPL, Proceedings of the 3rd Annual Conference on Aerospace Computational Control, Volume 1 15 Dec. 1989 p 264 (For primary document see N90-22987 16-61)
Avail: NTIS HC A21/MF A03 CSCL 20K

The state of the art dynamic response analysis of flexible multibody systems is currently restricted to elastic bodies with homogeneous materials. The requirements for high speed operation has made it necessary to use lightweight multi layered composite bodies in robotic systems and space structure applications. Dynamic modeling and analysis of such systems are particularly important since the effects of body flexibility to the performance are likely to be more pronounced. The eight-noded isoperimetric quadrilateral element with independent rotational and displacement degrees of freedom is extended to laminated composite elements. The element includes an arbitrary number of bonded layers, each of which may have a different thickness. The transverse shear deformation which is a predominant factor in the analysis of laminated composite structures is taken into account in developing the stiffness and mass matrices. The corresponding 3-D mode shapes are then incorporated to the multibody system dynamical equations. Floating body reference frames allow the selection of different boundary conditions, and the dynamical equations contain all the nonlinear interactions between the rigid and elastic motion. Example simulations are presented to illustrate the methods proposed. Author

N90-23020*# Iowa Univ., Iowa City. Center for Simulation and Design Optimization.
EXPERIMENTAL VERIFICATION OF DYNAMIC SIMULATION
K. Harold Yae, Howyoung Hwang, and Su-Tai Chern *In* JPL, Proceedings of the 3rd Annual Conference on Aerospace Computational Control, Volume 1 15 Dec. 1989 p 265-276 (For primary document see N90-22987 16-61)
Avail: NTIS HC A21/MF A03 CSCL 09B

The dynamics model here is a backhoe, which is a four degree of freedom manipulator from the dynamics standpoint. Two types of experiment are chosen that can also be simulated by a multibody dynamics simulation program. In the experiment, recorded were the configuration and force histories; that is, velocity and position, and force output and differential pressure change from the hydraulic cylinder, in the time domain. When the experimental force history is used as driving force in the simulation model, the forward dynamics simulation produces a corresponding configuration history. Then, the experimental configuration history is used in the inverse dynamics analysis to generate a corresponding force history. Therefore, two sets of configuration and force histories--one set from experiment, and the other from the simulation that is driven forward and backward with the experimental data--are compared in the time domain. More comparisons are made in regard to the effects of initial conditions, friction, and viscous damping. Author

N90-23021*# Techno-Sciences, Inc., Greenbelt, MD.
FREQUENCY RESPONSE MODELING AND CONTROL OF FLEXIBLE STRUCTURES: COMPUTATIONAL METHODS
William H. Bennett *In* JPL, Proceedings of the 3rd Annual Conference on Aerospace Computational Control, Volume 1 15 Dec. 1989 p 277-291 (For primary document see N90-22987 16-61)
(Contract F33615-88-C-3215)
Avail: NTIS HC A21/MF A03 CSCL 09B

The dynamics of vibrations in flexible structures can be conventiently modeled in terms of frequency response models. For structural control such models capture the distributed parameter dynamics of the elastic structural response as an irrational transfer function. For most flexible structures arising in aerospace applications the irrational transfer functions which arise are of a special class of pseudo-meromorphic functions which have only a finite number of right half place poles. Computational algorithms are demonstrated for design of multiloop control laws for such models based on optimal Wiener-Hopf control of the frequency responses. The algorithms employ a sampled-data representation of irrational transfer functions which is particularly attractive for numerical computation. One key algorithm for the solution of the optimal control problem is the spectral factorization of an irrational transfer function. The basis for the spectral factorization algorithm is highlighted together with associated computational issues arising in optimal regulator design. Options for implementation of wide band vibration control for flexible structures based on the sampled-data frequency response models is also highlighted. A simple flexible structure control example is considered to demonstrate the combined frequency response modeling and control algorithms. Author

N90-23022*# Maryland Univ., College Park.
EFFICIENT COMPUTER ALGEBRA ALGORITHMS FOR POLYNOMIAL MATRICES IN CONTROL DESIGN Abstract Only
J. S. Baras, D. C. MacEnany, and R. Munach *In* JPL, Proceedings of the 3rd Annual Conference on Aerospace Computational Control, Volume 1 15 Dec. 1989 p 292 (For primary document see N90-22987 16-61)
Avail: NTIS HC A21/MF A03 CSCL 09B

The theory of polynomial matrices plays a key role in the design and analysis of multi-input multi-output control and communications systems using frequency domain methods. Examples include coprime factorizations of transfer functions, cannonical realizations from matrix fraction descriptions, and the transfer function design of feedback compensators. Typically, such problems abstract in a natural way to the need to solve systems of Diophantine equations or systems of linear equations over polynomials. These and other problems involving polynomial matrices can in turn be reduced to polynomial matrix triangularization procedures, a result which is not surprising given the importance of matrix triangularization techniques in numerical linear algebra. Matrices with entries from a field and Gaussian elimination play a fundamental role in understanding the triangularization process. In the case of polynomial matrices, matrices with entries from a ring for which Gaussian elimination is not defined and triangularization is accomplished by what is quite properly called Euclidean elimination. Unfortunately, the numerical stability and sensitivity issues which accompany floating point approaches to Euclidean elimination are not very well understood. New algorithms are presented which circumvent entirely such numerical issues through the use of exact, symbolic methods in computer algebra. The use of such error-free algorithms guarantees

that the results are accurate to within the precision of the model data--the best that can be hoped for. Care must be taken in the design of such algorithms due to the phenomenon of intermediate expressions swell. Author

N90-23023*# Harris Corp., Melbourne, FL.
INTEGRATED CONTROL-SYSTEM DESIGN VIA GENERALIZED LQG (GLQG) THEORY Abstract Only
Dennis S. Bernstein, David C. Hyland, Stephen Richter, and Wassim M. Haddad (Florida Inst. of Tech., Melbourne.) *In* JPL, Proceedings of the 3rd Annual Conference on Aerospace Computational Control, Volume 1 15 Dec. 1989 p 293 (For primary document see N90-22987 16-61)
Avail: NTIS HC A21/MF A03 CSCL 09B

Thirty years of control systems research has produced an enormous body of theoretical results in feedback synthesis. Yet such results see relatively little practical application, and there remains an unsettling gap between classical single-loop techniques (Nyquist, Bode, root locus, pole placement) and modern multivariable approaches (LQG and H infinity theory). Large scale, complex systems, such as high performance aircraft and flexible space structures, now demand efficient, reliable design of multivariable feedback controllers which optimally tradeoff performance against modeling accuracy, bandwidth, sensor noise, actuator power, and control law complexity. A methodology is described which encompasses numerous practical design constraints within a single unified formulation. The approach, which is based upon coupled systems or modified Riccati and Lyapunov equations, encompasses time-domain linear-quadratic-Gaussian theory and frequency-domain H theory, as well as classical objectives such as gain and phase margin via the Nyquist circle criterion. In addition, this approach encompasses the optimal projection approach to reduced-order controller design. The current status of the overall theory will be reviewed including both continuous-time and discrete-time (sampled-data) formulations.
Author

N90-23024*# University of Southern California, Los Angeles. Dept. of Electrical Engineering - Systems.
MODERN CACSD USING THE ROBUST-CONTROL TOOLBOX
Richard Y. Chiang and Michael G. Safonov *In* JPL, Proceedings of the 3rd Annual Conference on Aerospace Computational Control, Volume 1 15 Dec. 1989 p 294-311 (For primary document see N90-22987 16-61)
Avail: NTIS HC A21/MF A03 CSCL 09B

The Robust-Control Toolbox is a collection of 40 M-files which extend the capability of PC/PRO-MATLAB to do modern multivariable robust control system design. Included are robust analysis tools like singular values and structured singular values, robust synthesis tools like continuous/discrete H(exp 2)/H infinity synthesis and Linear Quadratic Gaussian Loop Transfer Recovery methods and a variety of robust model reduction tools such as Hankel approximation, balanced truncation and balanced stochastic truncation, etc. The capabilities of the toolbox are described and illustated with examples to show how easily they can be used in practice. Examples include structured singular value analysis, H infinity loop-shaping and large space structure model reduction.
Author

N90-23025*# Washington Univ., Seattle. Dept. of Aeronautics and Astronautics.
H(2)- AND H(INFINITY)-DESIGN TOOLS FOR LINEAR TIME-INVARIANT SYSTEMS
Uy-Loi Ly *In* JPL, Proceedings of the 3rd Annual Conference on Aerospace Computational Control, Volume 1 15 Dec. 1989 p 312-326 (For primary document see N90-22987 16-61)
Avail: NTIS HC A21/MF A03 CSCL 09B

Recent advances in optimal control have brought design techniques based on optimization of H(2) and H(infinity) norm criteria, closer to be attractive alternatives to single-loop design methods for linear time-variant systems. Significant steps forward in this technology are the deeper understanding of performance and robustness issues of these design procedures and means to perform design trade-offs. However acceptance of the technology is hindered by the lack of convenient design tools to exercise these powerful multivariable techniques, while still allowing single-loop design formulation. Presented is a unique computer tool for designing arbitrary low-order linear time-invarient controllers than encompasses both performance and robustness issues via the familiar H(2) and H(infinity) norm optimization. Application to disturbance rejection design for a commercial transport is demonstrated.
Author

N90-23026*# Cornell Univ., Ithaca, NY. Dept. of Mechanical and Aerospace Engineering.
AN ALGORITHM FOR THE SOLUTION OF DYNAMIC LINEAR PROGRAMS
Mark L. Psiaki *In* JPL, Proceedings of the 3rd Annual Conference on Aerospace Computational Control, Volume 1 15 Dec. 1989 p 327-341 (For primary document see N90-22987 16-61)
(Grant NAG1-1009)
Avail: NTIS HC A21/MF A03 CSCL 09B

The algorithm's objective is to efficiently solve Dynamic Linear Programs (DLP) by taking advantage of their special staircase structure. This algorithm constitutes a stepping stone to an improved algorithm for solving Dynamic Quadratic Programs, which, in turn, would make the nonlinear programming method of Successive Quadratic Programs more practical for solving trajectory optimization problems. The ultimate goal is to being trajectory optimization solution speeds into the realm of real-time control. The algorithm exploits the staircase nature of the large constraint matrix of the equality-constrained DLPs encountered when solving inequality-constrained DLPs by an active set approach. A numerically-stable, staircase QL factorization of the staircase constraint matrix is carried out starting from its last rows and columns. The resulting recursion is like the time-varying Riccati equation from multi-stage LQR theory. The resulting factorization increases the efficiency of all of the typical LP solution operations over that of a dense matrix LP code. At the same time numerical stability is ensured. The algorithm also takes advantage of dynamic programming ideas about the cost-to-go by relaxing active pseudo constraints in a backwards sweeping process. This further decreases the cost per update of the LP rank-1 updating procedure, although it may result in more changes of the active set that if pseudo constraints were relaxed in a non-stagewise fashion. The usual stability of closed-loop Linear/Quadratic optimally-controlled systems, if it carries over to strictly linear cost functions, implies that the saving due to reduced factor update effort may outweigh the cost of an increased number of updates. An aerospace example is presented in which a ground-to-ground rocket's distance is maximized. This example demonstrates the applicability of this class of algorithms to aerospace guidance. It also sheds light on the efficacy of the proposed pseudo constraint relaxation scheme.
Author

N90-23027*# Georgia Inst. of Tech., Atlanta. School of Aerospace Engineering.
A FINITE ELEMENT BASED METHOD FOR SOLUTION OF OPTIMAL CONTROL PROBLEMS **c63**
Robert R. Bless, Dewey H. Hodges, and Anthony J. Calise *In* JPL, Proceedings of the 3rd Annual Conference on Aerospace Computational Control, Volume 1 15 Dec. 1989 p 342-354 (For primary document see N90-22987 16-61)
(Grant NAG1-939)
Avail: NTIS HC A21/MF A03 CSCL 09B

A temporal finite element based on a mixed form of the Hamiltonian weak principle is presented for optimal control problems. The mixed form of this principle contains both states and costates as primary variables that are expanded in terms of elemental values and simple shape functions. Unlike other variational approaches to optimal control problems, however, time derivatives of the states and costates do not appear in the governing variational equation. Instead, the only quantities whose time derivatives appear therein are virtual states and virtual costates. Also noteworthy among characteristics of the finite element formulation is the fact that in the algebraic equations

which contain costates, they appear linearly. Thus, the remaining equations can be solved iteratively without initial guesses for the costates; this reduces the size of the problem by about a factor of two. Numerical results are presented herein for an elementary trajectory optimization problem which show very good agreement with the exact solution along with excellent computational efficiency and self-starting capability. The goal is to evaluate the feasibility of this approach for real-time guidance applications. To this end, a simplified two-stage, four-state model for an advanced launch vehicle application is presented which is suitable for finite element solution. Author

N90-23028*# National Aeronautics and Space Administration. Langley Research Center, Hampton, VA.

A METHODOLOGY FOR FORMULATING A MINIMAL UNCERTAINTY MODEL FOR ROBUST CONTROL SYSTEM DESIGN AND ANALYSIS

Christine M. Belcastro, B.-C. Chang, and Robert Fischl (Drexel Univ., Philadelphia, PA.) *In* JPL, Proceedings of teh 3rd Annual Conference on Aerospace Computational Control, Volume 1 15 Dec. 1989 p 355-369 (For primary document see N90-22987 16-61)

Avail: NTIS HC A21/MF A03 CSCL 09B

In the design and analysis of robust control systems for uncertain plants, the technique of formulating what is termed an M-delta model has become widely accepted and applied in the robust control literature. The M represents the transfer function matrix M(s) of the nominal system, and delta represents an uncertainty matrix acting on M(s). The uncertainty can arise from various sources, such as structured uncertainty from parameter variations or multiple unstructured uncertainties from unmodeled dynamics and other neglected phenomena. In general, delta is a block diagonal matrix, and for real parameter variations the diagonal elements are real. As stated in the literature, this structure can always be formed for any linear interconnection of inputs, outputs, transfer functions, parameter variations, and perturbations. However, very little of the literature addresses methods for obtaining this structure, and none of this literature addresses a general methodology for obtaining a minimal M-delta model for a wide class of uncertainty. Since have a delta matrix of minimum order would improve the efficiency of structured singular value (or multivariable stability margin) computations, a method of obtaining a minimal M-delta model would be useful. A generalized method of obtaining a minimal M-delta structure for systems with real parameter variations is given. Author

N90-23029*# National Aeronautics and Space Administration. Lyndon B. Johnson Space Center, Houston, TX.

SPACE STATION DYNAMICS, ATTITUDE CONTROL AND MOMENTUM MANAGEMENT Abstract Only **c18**

John W. Sunkel, Ramen P. Singh, and Ravi Vengopal (DYNACS Engineering Co., Inc., Clearwater, FL.) *In* JPL, Proceedings of the 3rd Annual Conference on Aerospace Computational Control, Volume 1 15 Dec. 1989 p 370 (For primary document see N90-22987 16-61)

Avail: NTIS HC A21/MF A03 CSCL 22B

The Space Station Attitude Control System software test-bed provides a rigorous environment for the design, development and functional verification of GN and C algorithms and software. The approach taken for the simulation of the vehicle dynamics and environmental models using a computationally efficient algorithm is discussed. The simulation includes capabilities for docking/berthing dynamics, prescribed motion dynamics associated with the Mobile Remote Manipulator System (MRMS) and microgravity disturbances. The vehicle dynamics module interfaces with the test-bed through the central Communicator facility which is in turn driven by the Station Control Simulator (SCS) Executive. The Communicator addresses issues such as the interface between the discrete flight software and the continuous vehicle dynamics, and multi-programming aspects such as the complex flow of control in real-time programs. Combined with the flight software and redundancy management modules, the facility provides a flexible, user-oriented simulation platform. Author

N90-23030*# Sandia National Labs., Albuquerque, NM. Engineering Analysis Dept.

APPROXIMATE MINIMUM-TIME TRAJECTORIES FOR 2-LINK FLEXIBLE MANIPULATORS

G. R. Eisler, D. J. Segalman, and R. D. Robinett *In* JPL, Proceedings of the 3rd Annual Conference on Aerospace Computational Control, Volume 1 15 Dec. 1989 p 371-381 (For primary document see N90-22987 16-61)

Avail: NTIS HC A21/MF A03 CSCL 09B

Powell's nonlinear programming code, VF02AD, was used to generate approximate minimum-time tip trajectories for 2-link semi-rigid and flexible manipulator movements in the horizontal plane. The manipulator is modeled with an efficient finite-element scheme for an n-link, m-joint system with horizontal-plane bending only. Constraints on the trajectory include boundary conditions on position and energy for a rest-to-rest maneuver, straight-line tracking between boundary positions, and motor torque limits. Trajectory comparisons utilize a change in the link stiffness, EI, to transition from the semi-rigid to flexible case. Results show the level of compliance necessary to excite significant modal behavior. Quiescence of the final configuration is examined with the finite-element model. Author

N90-23031*# Middle East Technical Univ., Ankara (Turkey). Dept. of Mechanical Engineering.

MODELING OF CONTROL FORCES FOR KINEMATICAL CONSTRAINTS IN THE DYNAMICS OF MULTIBODY SYSTEMS: A NEW APPROACH

Sitki Kemal Ider *In* JPL, Proceedings of the 3rd Annual Conference on Aerospace Computational Control, Volume 1 15 Dec. 1989 p 382-393 (For primary document see N90-22987 16-61)

Avail: NTIS HC A21/MF A03 CSCL 09B

Conventionally kinematical constraints in multibody systems are treated similar to geometrical constraints and are modeled by constraint reaction forces which are perpendicular to constraint surfaces. However, in reality, one may want to achieve the desired kinematical conditions by control forces having different directions in relation to the constraint surfaces. The conventional equations of motion for multibody systems subject to kinematical constraints are generalized by introducing general direction control forces. Conditions for the selections of the control force directions are also discussed. A redundant robotic system subject to prescribed end-effector motion is analyzed to illustrate the methods proposed. Author

N90-23032*# Kansas Univ., Lawrence. Dept. of Aerospace Engineering.

APPLICATION OF NUMERICAL OPTIMIZATION TECHNIQUES TO CONTROL SYSTEM DESIGN FOR NONLINEAR DYNAMIC MODELS OF AIRCRAFT **c08**

C. Edward Lan and Fuying Ge *In* JPL, Proceedings of the 3rd Annual Conference on Aerospace Computational Control, Volume 1 15 Dec. 1989 p 394-406 (For primary document see N90-22987 16-61)

Avail: NTIS HC A21/MF A03 CSCL 01C

Control system design for general nonlinear flight dynamic models is considered through numerical simulation. The design is accomplished through a numerical optimizer coupled with analysis of flight dynamic equations. The general flight dynamic equations are numerically integrated and dynamic characteristics are then identified from the dynamic response. The design variables are determined iteratively by the optimizer to optimize a prescribed objective function which is related to desired dynamic characteristics. Generality of the method allows nonlinear effects to aerodynamics and dynamic coupling to be considered in the design process. To demonstrate the method, nonlinear simulation models for an F-5A and an F-16 configurations are used to design dampers to satisfy specifications on flying qualities and control systems to prevent departure. The results indicate that the present method is simple in formulation and effective in satisfying the design objectives. Author

N90-23033*# Toronto Univ., Downsview (Ontario). Inst. for Aerospace Studies.

AN INVERSE KINEMATICS ALGORITHM FOR A HIGHLY REDUNDANT VARIABLE-GEOMETRY-TRUSS MANIPULATOR **c08**

Frank Naccarato and Peter Hughes *In* JPL, Proceedings of the 3rd Annual Conference on Aerospace Computational Control, Volume 1 15 Dec. 1989 p 407-420 Sponsored in part by the Natural Sciences and Engineering Research Council of Canada (For primary document see N90-22987 16-61)

Avail: NTIS HC A21/MF A03 CSCL 01C

A new class of robotic arm consists of a periodic sequence of truss substructures, each of which has several variable-length members. Such variable-geometry-truss manipulator (VGTMs) are inherently highly redundant and promise a significant increase in dexterity over conventional anthropomorphic manipulators. This dexterity may be exploited for both obstacle avoidance and controlled deployment in complex workspaces. The inverse kinematics problem for such unorthodox manipulators, however, becomes complex because of the large number of degrees of freedom, and conventional solutions to the inverse kinematics problem become inefficient because of the high degree of redundancy. A solution is presented to this problem based on a spline-like reference curve for the manipulator's shape. Such an approach has a number of advantages: (1) direct, intuitive manipulation of shape; (2) reduced calculation time; and (3) direct control over the effective degree of redundancy of the manipulator. Furthermore, although the algorithm was developed primarily for variable-geometry-truss manipulators, it is general enough for application to a number of manipulator designs. Author

N90-23034*# Middle East Technical Univ., Gaziantep (Turkey). Dept. of Mechanical Engineering.

DETERMINATION OF JOINT DRIVES FOR STABLE END-EFFECTOR MOTION IN FLEXIBLE ROBOTIC SYSTEMS **c37**

Sitki Kemal Ider *In* JPL, Proceedings of the 3rd Annual Conference on Aerospace Computational Control, Volume 1 15 Dec. 1989 p 421-423 (For primary document see N90-22987 16-61)

Avail: NTIS HC A21/MF A03 CSCL 13I

The prescribed tasks in high speed robotic systems are severely deteriorated because of their manipulator dynamic deflections. On the other hand conventional dynamic modeling techniques fail to reveal appropriate control forces in flexible systems. The conventional dynamic equations of motion for systems subject to kinematical constraints are modified by a new concept of control force representation. The directions of the control forces are selected such that they correspond to the joint degrees of freedom. Then the joint control forces and torques that yield unperturbed prescribed motions are solved simultaneously with the system motion. A flexible manipulator is presented to illustrate the methods proposed. Author

N90-23035*# State Univ. of New York, Buffalo. Dept. of Mechanical and Aerospace Engineering.

CONTROL OF A FLEXIBLE PLANAR TRUSS USING PROOF MASS ACTUATORS **c37**

Constantinos Minas, Ephrahim Garcia, and Daniel J. Inman *In* JPL, Proceedings of the 3rd Annual Conference on Aerospace Computational Control, Volume 1 15 Dec. 1989 p 434-445 (For primary document see N90-22987 16-61)

(Contracts F49620-88-C-00018; F49620-86-C-60111; AF-AFOSR-0119-85; AF-AFOSR-0390-88)

Avail: NTIS HC A21/MF A03 CSCL 13I

A flexible structure was modeled and actively controlled by using a single space realizable linear proof mass actuator. The NASA/UVA/UB actuator was attached to a flexible planar truss structure at an optimal location and it was considered as both passive and active device. The placement of the actuator was specified by examining the eigenvalues of the modified model that included the actuator dynamics, and the frequency response functions of the modified system. The electronic stiffness of the actuator was specified, such that the proof mass actuator system was tuned to the fourth structural mode of the truss by using traditional vibration absorber design. The active control law was limited to velocity feedback by integrating of the signals of two accelerometers attached to the structure. The two lower modes of the closed-loop structure were placed further in the LHS of the complex plane. The theoretically predicted passive and active control law was experimentally verified. Author

N90-23036*# Photon Research Associates, Inc., Cambridge, MA.

SIMULATION STUDIES USING MULTIBODY DYNAMICS CODE DART Abstract Only

James E. Keat *In* JPL, Proceedings of the 3rd Annual Conference on Aerospace Computational Control, Volume 1 15 Dec. 1989 p 446 (For primary document see N90-22987 16-61)

Avail: NTIS HC A21/MF A03 CSCL 09B

DART is a multibody dynamics code developed by Photon Research Associates for the Air Force Astronautics Laboratory (AFAL). The code is intended primarily to simulate the dynamics of large space structures, particularly during the deployment phase of their missions. DART integrates nonlinear equations of motion numerically. The number of bodies in the system being simulated is arbitrary. The bodies' interconnection joints can have an arbitrary number of degrees of freedom between 0 and 6. Motions across the joints can be large. Provision for simulating on-board control systems is provided. Conservation of energy and momentum, when applicable, are used to evaluate DART's performance. After a brief description of DART, studies made to test the program prior to its delivery to AFAL are described. The first is a large angle reorientating of a flexible spacecraft consisting of a rigid central hub and four flexible booms. Reorientation was accomplished by a single-cycle sine wave shape torque input. In the second study, an appendage, mounted on a spacecraft, was slewed through a large angle. Four closed-loop control systems provided control of this appendage and of the spacecraft's attitude. The third study simulated the deployment of the rim of a bicycle wheel configuration large space structure. This system contained 18 bodies. An interesting and unexpected feature of the dynamics was a pulsing phenomena experienced by the stays whole playout was used to control the deployment. A short description of the current status of DART is given. Author

N90-23037*# National Aeronautics and Space Administration. Langley Research Center, Hampton, VA.

ON TRAJECTORY GENERATION FOR FLEXIBLE SPACE CRANE: INVERSE DYNAMICS ANALYSIS BY LATDYN **c37**

G.-S. Chen, J. M. Housner, S.-C. Wu, and C.-W. Chang (Comtek Co., Yorktown, VA.) *In* JPL, Proceedings of the 3rd Annual Conference on Aerospace Computational Control, Volume 1 15 Dec. 1989 p 447-448 (For primary document see N90-22987 16-61)

Avail: NTIS HC A21/MF A03 CSCL 13I

For future in-space construction facility, one or more space cranes capable of manipulating and positioning large and massive spacecraft components will be needed. Inverse dynamics was extensively studied as a basis for trajectory generation and control of robot manipulators. The focus here is on trajectory generation in the gross-motion phase of space crane operation. Inverse dynamics of the flexible crane body is much more complex and intricate as compared with rigid robot link. To model and solve the space crane's inverse dynamics problem, LATDYN program which employs a three-dimensional finite element formulation for the multibody truss-type structures will be used. The formulation is oriented toward a joint dominated structure which is suitable for the proposed space crane concept. To track a planned trajectory, procedures will be developed to obtain the actuation profile and dynamics envelope which are pertinent to the design and performance requirements of the space crane concept. Author

N90-23038*# California Univ., Los Angeles.

MINIMUM ATTAINABLE RMS ATTITUDE ERROR USING CO-LOCATED RATE SENSORS

A. V. Balakrishnan *In* JPL, Proceedings of the 3rd Annual

Conference on Aerospace Computational Control, Volume 1 15 Dec. 1989 p 449-459 (For primary document see N90-22987 16-61)
(Contract NAS1-18585)
Avail: NTIS HC A21/MF A03 CSCL 09B

A closed form analytical expression for the minimum attainable attitude error (as well as the error rate) in a flexible beam by feedback control using co-located rate sensors is announced. For simplicity, researchers consider a beam clamped at one end with an offset mass (antenna) at the other end where the controls and sensors are located. Both control moment generators and force actuators are provided. The results apply to any beam-like lattice-type truss, and provide the kind of performance criteria needed under CSI - Controls-Stuctures-Integrated optimization.
Author

N90-23039*# Purdue Univ., West Lafayette, IN. School of Electrical Engineering.
CHARACTERIZATION OF ROBOTICS PARALLEL ALGORITHMS AND MAPPING ONTO A RECONFIGURABLE SIMD MACHINE **c62**
C. S. G. Lee and C. T. Lin *In* JPL, Proceedings of the 3rd Annual Conference on Aerospace Computational Control, Volume 1 15 Dec. 1989 p 460-476 (For primary document see N90-22987 16-61)
Avail: NTIS HC A21/MF A03 CSCL 09B

The kinematics, dynamics, Jacobian, and their corresponding inverse computations are six essential problems in the control of robot manipulators. Efficient parallel algorithms for these computations are discussed and analyzed. Their characteristics are identified and a scheme on the mapping of these algorithms to a reconfigurable parallel architecture is presented. Based on the characteristics including type of parallelism, degree of parallelism, uniformity of the operations, fundamental operations, data dependencies, and communication requirement, it is shown that most of the algorithms for robotic computations possess highly regular properties and some common structures, especially the linear recursive structure. Moreover, they are well-suited to be implemented on a single-instruction-stream multiple-data-stream (SIMD) computer with reconfigurable interconnection network. The model of a reconfigurable dual network SIMD machine with internal direct feedback is introduced. A systematic procedure internal direct feedback is introduced. A systematic procedure to map these computations to the proposed machine is presented. A new scheduling problem for SIMD machines is investigated and a heuristic algorithm, called neighborhood scheduling, that reorders the processing sequence of subtasks to reduce the communication time is described. Mapping results of a benchmark algorithm are illustrated and discussed.
Author

N90-23040*# Jet Propulsion Lab., California Inst. of Tech., Pasadena.
PROCEEDINGS OF THE 3RD ANNUAL CONFERENCE ON AEROSPACE COMPUTATIONAL CONTROL, VOLUME 2
Douglas E. Bernard, ed. and Guy K. Man, ed. 15 Dec. 1989 464 p Conference held in Oxnard, CA, Nov. 1989; sponsored in cooperation by NASA, NSF, and DOD
(Contract NAS7-918)
(NASA-CR-186447; JPL-Publ-89-45-Vol-2; NAS 1.26:186447)
Avail: NTIS HC A20/MF A03 CSCL 09B

This volume of the conference proceedings contain papers and discussions in the following topical areas: Parallel processing; Emerging integrated capabilities; Low order controllers; Real time simulation; Multibody component representation; User environment; and Distributed parameter techniques. For individual titles, see N90-23041 through N90-23089.

N90-23041*# National Aeronautics and Space Administration. Lyndon B. Johnson Space Center, Houston, TX.
CONCURRENT PROCESSING SIMULATION OF THE SPACE STATION **c62**
R. Gluck, A. L. Hale (Supercomputing Solutions, Inc., San Diego, CA.), and John W. Sunkel *In* Jet Propulsion Lab., California Inst. of Tech., Proceedings of the 3rd Annual Conference on Aerospace Computational Control, Volume 2 15 Dec. 1989 p 477-491 (For primary document see N90-23040 16-61)
Avail: NTIS HC A20/MF A03 CSCL 09B

The development of a new capability for the time-domain simulation of multibody dynamic systems and its application to the study of a large angle rotational maneuvers of the Space Station is described. The effort was divided into three sequential tasks, which required significant advancements of the state-of-the art to accomplish. These were: (1) the development of an explicit mathematical model via symbol manipulation of a flexible, multibody dynamic system; (2) the development of a methodology for balancing the computational load of an explicit mathematical model for concurrent processing; and (3) the implementation and successful simulation of the above on a prototype Custom Architectured Parallel Processing System (CAPPS) containing eight processors. The throughput rate achieved by the CAPPS operating at only 70 percent efficiency, was 3.9 times greater than that obtained sequentially by the IBM 3090 supercomputer simulating the same problem. More significantly, analysis of the results leads to the conclusion that the relative cost effectiveness of concurrent vs. sequential digital computation will grow substantially as the computational load is increased. This is a welcomed development in an era when very complex and cumbersome mathematical models of large space vehicles must be used as substitutes for full scale testing which has become impractical.
Author

N90-23042*# Iowa Univ., Iowa City.
A DECOUPLED RECURSIVE APPROACH FOR CONSTRAINED FLEXIBLE MULTIBODY SYSTEM DYNAMICS **c64**
Hao-Jan Lai, Sung-Soo Kim, Edward J. Haug, and Dae-Sung Bae (Kansas Univ., Lawrence.) *In* Jet Propulsion Lab., California Inst. of Tech., Proceedings of the 3rd Annual Conference on Aerospace Computational Control, Volume 2 15 Dec. 1989 p 492-512 (For primary document see N90-23040 16-61)
Avail: NTIS HC A20/MF A03 CSCL 12A

A variational-vector calculus approach is employed to derive a recursive formulation for dynamic analysis of flexible multibody systems. Kinematic relationships for adjacent flexible bodies are derived in a companion paper, using a state vector notation that represents translational and rotational components simultaneously. Cartesian generalized coordinates are assigned for all body and joint reference frames, to explicitly formulate deformation kinematics under small deformation kinematics and an efficient flexible dynamics recursive algorithm is developed. Dynamic analysis of a closed loop robot is performed to illustrate efficiency of the algorithm.
Author

N90-23043*# Ohio State Univ., Columbus. Dept. of Electrical Engineering.
ALGORITHMIC CONSIDERATIONS OF INTEGRATED DESIGN FOR CSI ON A HYPERCUBE ARCHITECTURE
Ue. Oezguener and F. Oezguener *In* Jet Propulsion Lab., California Inst. of Tech., Proceedings of the 3rd Annual Conference on Aerpspace Computational Control, Volume 2 15 Dec. 1989 p 513-524 (For primary document see N90-23040 16-61)
Avail: NTIS HC A20/MF A03 CSCL 12A

An approach is presented to the integrated design problem for actively controlled large, flexible mechanical systems for which Control Structure Interaction (CSI) problems are of concern. The two coupled design problems were identified as the optimal Structural Design problem the optimal Controller Design problem. These two problems can be addressed within a decision making loop that would consider each separately, and then sequentially analyze the effects of one on the other. Embedded in such a loop would be the simulation and coordination tasks as part of the decision tools required in a total (software) package. All of the above are compute-intensive tasks. In any such task, possible decompositions and gains due to the inherent parallelism have to be exploited. The problems under consideration, as applied to large flexible mechanical structures, are particularly suited to be mapped onto multicomputer systems in a hypercube topology.
Author

N90-23044*# Texas Univ., Austin. Dept. of Aerospace Engineering and Engineering Mechanics.
A PARALLEL STRUCTURE TRANSIENT RESPONSE ALGORITHM USING INDEPENDENT SUBSTRUCTURE RESPONSE COMPUTATION
Jeffrey K. Bennighof and Jiann-Yuarn Wu *In* Jet Propulsion Lab., California Inst. of Tech., Proceedings of the 3rd Annual Conference on Aerospace Computational Control, Volume 2 15 Dec. 1989 p 525-536 (For primary document see N90-23040 16-61)
Avail: NTIS HC A20/MF A03 CSCL 12A

An algorithm for parallel computation of transient response for structures is presented in which responses of substructures are computed independently for dozens of time steps at a time, and these substructure responses are then corrected to obtain the response of the overall coupled structure. The correction of the uncoupled substructure responses only requires the responses computed for interfaces at occasional points in time, and is done independently for different substructures in a very efficient procedure. A numerical example is presented to demonstrate the method and show the accuracy of the method. Author

N90-23045*# Jet Propulsion Lab., California Inst. of Tech., Pasadena.
PARALLEL CONJUGATE GRADIENT ALGORITHMS FOR MANIPULATOR DYNAMIC SIMULATION Abstract Only c62
Amir Fijany and Robert E. Scheld *In its* Proceedings of the 3rd Annual Conference on Aerospace Computational Control, Volume 2 15 Dec. 1989 p 537 (For primary document see N90-23040 16-61)
Avail: NTIS HC A20/MF A03 CSCL 12A

Parallel conjugate gradient algorithms for the computation of multibody dynamics are developed for the specialized case of a robot manipulator. For an n-dimensional positive-definite linear system, the Classical Conjugate Gradient (CCG) algorithms are guaranteed to converge in n iterations, each with a computation cost of O(n); this leads to a total computational cost of O(n sq) on a serial processor. A conjugate gradient algorithms is presented that provide greater efficiency using a preconditioner, which reduces the number of iterations required, and by exploiting parallelism, which reduces the cost of each iteration. Two Preconditioned Conjugate Gradient (PCG) algorithms are proposed which respectively use a diagonal and a tridiagonal matrix, composed of the diagonal and tridiagonal elements of the mass matrix, as preconditioners. Parallel algorithms are developed to compute the preconditioners and their inversions in O(log sub 2 n) steps using n processors. A parallel algorithm is also presented which, on the same architecture, achieves the computational time of O(log sub 2 n) for each iteration. Simulation results for a seven degree-of-freedom manipulator are presented. Variants of the proposed algorithms are also developed which can be efficiently implemented on the Robot Mathematics Processor (RMP).
Author

N90-23046*# Boeing Aerospace Co., Seattle, WA.
METHODOLOGY FOR ANALYSIS AND SIMULATION OF LARGE MULTIDISCIPLINARY PROBLEMS c62
William C. Russell, Paul J. Ikeda, and Robert G. Vos *In* Jet Propulsion Lab., California Inst. of Tech., Proceedings of the 3rd Annual Conference on Aerospace Computational Control, Volume 2 15 Dec. 1989 p 538-547 (For primary document see N90-23040 16-61)
Avail: NTIS HC A20/MF A03 CSCL 12A

The Integrated Structural Modeling (ISM) program is being developed for the Air Force Weapons Laboratory and will be available for Air Force work. Its goal is to provide a design, analysis, and simulation tool intended primarily for directed energy weapons (DEW), kinetic energy weapons (KEW), and surveillance applications. The code is designed to run on DEC (VMS and UNIX), IRIS, Alliant, and Cray hosts. Several technical disciplines are included in ISM, namely structures, controls, optics, thermal, and dynamics. Four topics from the broad ISM goal are discussed. The first is project configuration management and includes two major areas: the software and database arrangement and the system model control. The second is interdisciplinary data transfer and refers to exchange of data between various disciplines such as structures and thermal. Third is a discussion of the integration of component models into one system model, i.e., multiple discipline model synthesis. Last is a presentation of work on a distributed processing computing environment. Author

N90-23047*# DYNACS Engineering Co., Inc., Clearwater, FL.
ENHANCED MODELING FEATURES WITHIN TREETOPS
R. J. VanderVoort and Manoj N. Kumar *In* Jet Propulsion Lab., California Inst. of Tech., Proceedings of the 3rd Annual Conference on Aerospace Computational Control, Volume 2 15 Dec. 1989 p 548-562 (For primary document see N90-23040 16-61)
Avail: NTIS HC A20/MF A03 CSCL 12A

The original motivation for TREETOPS was to build a generic multi-body simulation and remove the burden of writing multi-body equations from the engineers. The motivation of the enhancement was twofold: (1) to extend the menu of built-in features (sensors, actuators, constraints, etc.) that did not require user code; and (2) to extend the control system design capabilities by linking with other government funded software (NASTRAN and MATLAB). These enhancements also serve to bridge the gap between structures and control groups. It is common on large space programs for the structures groups to build hi-fidelity models of the structure using NASTRAN and for the controls group to build lower order models because they lack the tools to incorporate the former into their analysis. Now the controls engineers can accept the hi-fidelity NASTRAN models into TREETOPS, add sensors and actuators, perform model reduction and couple the result directly into MATLAB to perform their design. The controller can then be imported directly into TREETOPS for non-linear, time-history simulation. Author

N90-23048*# Air Force Wright Research and Development Center, Wright-Patterson AFB, OH.
IMPLEMENTATION OF GENERALIZED OPTIMALITY CRITERIA IN A MULTIDISCIPLINARY ENVIRONMENT c63
R. A. Canfield and V. B. Venkayya *In* Jet Propulsion Lab., California Inst. of Tech., Proceedings of the 3rd Annual Conference on Aerospace Computational Control, Volume 2 15 Dec. 1989 p 563-576 (For primary document see N90-23040 16-61)
Avail: NTIS HC A20/MF A03 CSCL 12A

A generalized optimality criterion method consisting of a dual problem solver combined with a compound scaling algorithm was implemented in the multidisciplinary design tool, ASTROS. This method enables, for the first time in a production design tool, the determination of a minimum weight design using thousands of independent structural design variables while simultaneously considering constraints on response quantities in several disciplines. Even for moderately large examples, the computational efficiency is improved significantly relative to the conventional approach. Author

N90-23049*# National Aeronautics and Space Administration. Goddard Space Flight Center, Greenbelt, MD.
NEW MULTIVARIABLE CAPABILITIES OF THE INCA PROGRAM
Frank H. Bauer, John P. Downing, and Christopher J. Thorpe (Fairchild Space Co., Germantown, MD.) *In* Jet Propulsion Lab., California Inst. of Tech., Proceedings of the 3rd Annual Conference on Aerospace Computational Control, Volume 2 15 Dec. 1989 p 577-584 (For primary document see N90-23040 16-61)
Avail: NTIS HC A20/MF A03 CSCL 09B

The INteractive Controls Analysis (INCA) program was developed at NASA's Goddard Space Flight Center to provide a user friendly, efficient environment for the design and analysis of control systems, specifically spacecraft control systems. Since its inception, INCA has found extensive use in the design, development, and analysis of control systems for spacecraft, instruments, robotics, and pointing systems. The (INCA) program was initially developed as a comprehensive classical design analysis tool for small and large order control systems. The latest

version of INCA, expected to be released in February of 1990, was expanded to include the capability to perform multivariable controls analysis and design. Author

N90-23050*# Air Force Flight Dynamics Lab., Wright-Patterson AFB, OH.
MULTIDISCIPLINARY EXPERT-AIDED ANALYSIS AND DESIGN (MEAD)
Thomas C. Hummel and James Taylor (General Electric Co., Schenectady, NY.) *In* Jet Propulsion Lab., California Inst. of Tech., Proceedings of the 3rd Annual Conference on Aerospace Computational Control, Volume 2 15 Dec. 1989 p 585-598 (For primary document see N90-23040 16-61)
Avail: NTIS HC A20/MF A03 CSCL 09B

The MEAD Computer Program (MCP) is being developed under the Multidisciplinary Expert-Aided Analysis and Design (MEAD) Project as a CAD environment in which integrated flight, propulsion, and structural control systems can be designed and analyzed. The MCP has several embedded computer-aided control engineering (CACE) packages, a user interface (UI), a supervisor, a data-base manager (DBM), and an expert system (ES). The supervisor monitors and coordinates the operation of the CACE packages, the DBM; the ES, and the UI. The DBM tracks the control design process. Models created or installed by the MCP are tracked by date and version, and results are associated with the specific model version with which they were generated. The ES is used to relieve the control engineer from tedious and cumbersome tasks in the iterative design process. The UI provides the capability for a novice as well as an expert to utilize the MCP easily and effectively. The MCP version 2(MCP-2.0) is fully developed for flight control system design and analysis. Propulsion system modeling, analysis, and simulation is also supported; the same is true for structural models represented in state-space form. The ultimate goal is to cover the integration of flight, propulsion, and structural control engineering, including all discipline-specific functionality and interfaces. The current MCP-2.0 components and functionality are discussed. Author

N90-23051*# Texas Univ., Austin. Dept. of Aerospace Engineering.
OVERVIEW OF COMPUTATIONAL CONTROL RESEARCH AT UT AUSTIN Abstract Only
Wie Bong *In* Jet Propulsion Lab., California Inst. of Tech., Proceedings of the 3rd Annual Conference on Aerospace Computational Control, Volume 2 15 Dec. 1989 p 599 (For primary document see N90-23040 16-61)
Avail: NTIS HC A20/MF A03 CSCL 09B

An overview of current research activities at UT Austin is presented to discuss certain technical issues in the following areas: (1) Computer-Aided Nonlinear Control Design: In this project, the describing function method is employed for the nonlinear control analysis and design of a flexible spacecraft equipped with pulse modulated reaction jets. INCA program has been enhanced to allow the numerical calculation of describing functions as well as the nonlinear limit cycle analysis capability in the frequency domain; (2) Robust Linear Quadratic Gaussian (LQG) Compensator Synthesis: Robust control design techniques and software tools are developed for flexible space structures with parameter uncertainty. In particular, an interactive, robust multivariable control design capability is being developed for INCA program; and (3) LQR-Based Autonomous Control System for the Space Station: In this project, real time implementation of LQR-based autonomous control system is investigated for the space station with time-varying inertias and with significant multibody dynamic interactions. Author

N90-23052*# National Aeronautics and Space Administration. Goddard Space Flight Center, Greenbelt, MD.
ASTEC: CONTROLS ANALYSIS FOR PERSONAL COMPUTERS
John P. Downing, Frank H. Bauer, and Christopher J. Thorpe *In* Jet Propulsion Lab., California Inst. of Tech., Proceedings of the 3rd Annual Conference on Aerospace Computational Control, Volume 2 15 Dec. 1989 p 600-605 (For primary document see N90-23040 16-61)
Avail: NTIS HC A20/MF A03 CSCL 09B

The ASTEC (Analysis and Simulation Tools for Engineering Controls) software is under development at Goddard Space Flight Center (GSFC). The design goal is to provide a wide selection of controls analysis tools at the personal computer level, as well as the capability to upload compute-intensive jobs to a mainframe or supercomputer. The project is a follow-on to the INCA (INteractive Controls Analysis) program that has been developed at GSFC over the past five years. While ASTEC makes use of the algorithms and expertise developed for the INCA program, the user interface was redesigned to take advantage of the capabilities of the personal computer. The design philosophy and the current capabilities of the ASTEC software are described. Author

N90-23053*# Jet Propulsion Lab., California Inst. of Tech., Pasadena.
CONTROL/STRUCTURE INTERACTION DESIGN METHODOLOGY
Hugh C. Briggs and William E. Layman *In its* Proceedings of the 3rd Annual Conference on Aerospace Computational Control, Volume 2 15 Dec. 1989 p 606-619 (For primary document see N90-23040 16-61)
Avail: NTIS HC A20/MF A03 CSCL 09B

The Control Structure Interaction Program is a technology development program for spacecraft that exhibit interactions between the control system and structural dynamics. The program objectives include development and verification of new design concepts (such as active structure) and new tools (such as a combined structure and control optimization algorithm) and their verification in ground and possibly flight test. The new CSI design methodology is centered around interdisciplinary engineers using new tools that closely integrate structures and controls. Verification is an important CSI theme and analysts will be closely integrated to the CSI Test Bed laboratory. Components, concepts, tools and algorithms will be developed and tested in the lab and in future Shuttle-based flight experiments. The design methodology is summarized in block diagrams depicting the evolution of a spacecraft design and descriptions of analytical capabilities used in the process. The multiyear JPL CSI implementation plan is described along with the essentials of several new tools. A distributed network of computation servers and workstations was designed that will provide a state-of-the-art development base for the CSI technologies. Author

N90-23054*# Jet Propulsion Lab., California Inst. of Tech., Pasadena.
MODEL REDUCTION FOR FLEXIBLE SPACECRAFT WITH CLUSTERED NATURAL FREQUENCIES Abstract Only **c18**
T. W. C. Williams (National Aeronautics and Space Administration. Langley Research Center, Hampton, VA.) and W. K. Gawronski *In its* Proceedings of the 3rd Annual Conference on Aerospace Computational Control, Volume 2 15 Dec. 1989 p 620 (For primary document see N90-23040 16-61)
Avail: NTIS HC A20/MF A03 CSCL 22B

Two approaches to the problem of model reduction for flexible spacecraft that have proved very useful are balancing and model truncation. Furthermore, it is well known that a model representation of a lightly damped flexible structure with widely spaced natural frequencies is approximately balanced. Consequently, reduction in either coordinate system gives similar results for this case. It is important to note, however, that flexible space structures typically have clusters of closely spaced frequencies. In such cases, reduction in model coordinates can give large errors, while the error obtained using balancing is generally much smaller. A new reduction procedure which combines the best features of model and balanced reduction is therefore developed. It is more efficient than balanced reduction of the full system, as it only involves balancing those subsystems of close modes that are highly correlated, yet is shown to yield results which are essentially as good. Author

N90-23055*# Texas Univ., Austin. Dept. of Aerospace Engineering and Engineering Mechanics.
SUBSTRUCTURAL CONTROLLER SYNTHESIS
Tzu-Jeng Su and Roy R. Craig, Jr. *In* Jet Propulsion Lab., California Inst. of Tech., Proceedings of the 3rd Annual Conference on Aerospace Computational Control, Volume 2 15 Dec. 1989 p 621-635 (For primary document see N90-23040 16-61)
Avail: NTIS HC A20/MF A03 CSCL 09B

A decentralized design procedure which combines substructural synthesis, model reduction, decentralized controller design, subcontroller synthesis, and controller reduction is proposed for the control design of flexible structures. The structure to be controlled is decomposed into several substructures, which are modeled by component mode synthesis methods. For each substructure, a subcontroller is designed by using the linear quadratic optimal control theory. Then, a controller synthesis scheme called Substructural Controller Synthesis (SCS) is used to assemble the subcontrollers into a system controller, which is to be used to control the whole structure. Author

N90-23056*# Purdue Univ., West Lafayette, IN.
EXTENSIONS OF OUTPUT VARIANCE CONSTRAINED CONTROLLERS TO HARD CONSTRAINTS Abstract Only c64
R. Skelton and G. Zhu *In* Jet Propulsion Lab., California Inst. of Tech., Proceedings of the 3rd Annual Conference on Aerospace Computational Control, Volume 2 15 Dec. 1989 p 636-637 (For primary document see N90-23040 16-61)
Avail: NTIS HC A20/MF A03 CSCL 12A

Covariance Controllers assign specified matrix values to the state covariance. A number of robustness results are directly related to the covariance matrix. The conservatism in known upperbounds on the H infinity, L infinity, and L (sub 2) norms for stability and disturbance robustness of linear uncertain systems using covariance controllers is illustrated with examples. These results are illustrated for continuous and discrete time systems.
Author

N90-23057*# Harris Corp., Melbourne, FL.
MINIMAL COMPLEXITY CONTROL LAW SYNTHESIS Abstract Only
Dennis S. Bernstein, Wassim M. Haddad, and Carl N. Nett (General Electric Co., Schenectady, NY.) *In* Jet Propulsion Lab., California Inst. of Tech., Proceedings of the 3rd Annual Conference on Aerospace Computational Control, Volume 2 15 Dec. 1989 p 638-639 (For primary document see N90-23040 16-61)
Avail: NTIS HC A20/MF A03 CSCL 09B

A paradigm for control law design for modern engineering systems is proposed: Minimize control law complexity subject to the achievement of a specified accuracy in the face of a specified level of uncertainty. Correspondingly, the overall goal is to make progress towards the development of a control law design methodology which supports this paradigm. Researchers achieve this goal by developing a general theory of optimal constrained-structure dynamic output feedback compensation, where here constrained-structure means that the dynamic-structure (e.g., dynamic order, pole locations, zero locations, etc.) of the output feedback compensation is constrained in some way. By applying this theory in an innovative fashion, where here the indicated iteration occurs over the choice of the compensator dynamic-structure, the paradigm stated above can, in principle, be realized. The optimal constrained-structure dynamic output feedback problem is formulated in general terms. An elegant method for reducing optimal constrained-structure dynamic output feedback problems to optimal static output feedback problems is then developed. This reduction procedure makes use of star products, linear fractional transformations, and linear fractional decompositions, and yields as a byproduct a complete characterization of the class of optimal constrained-structure dynamic output feedback problems which can be reduced to optimal static output feedback problems. Issues such as operational/physical constraints, operating-point variations, and processor throughput/memory limitations are considered, and it is shown how anti-windup/bumpless transfer, gain-scheduling, and digital processor implementation can be facilitated by constraining the controller dynamic-structure in an appropriate fashion.
Author

N90-23058*# Sandia National Labs., Albuquerque, NM.
OPTICON: PRO-MATLAB SOFTWARE FOR LARGE ORDER CONTROLLED STRUCTURE DESIGN Abstract Only
Lee D. Peterson *In* Jet Propulsion Lab., California Inst. of Tech., Proceedings of the 3rd Annual Conference on Aerospace Computational Control, Volume 2 15 Dec. 1989 p 640 (For primary document see N90-23040 16-61)
Avail: NTIS HC A20/MF A03 CSCL 09B

A software package for large order controlled structure design is described and demonstrated. The primary program, called OPTICAN, uses both Pro-Matlab M-file routines and selected compiled FORTRAN routines linked into the Pro-Matlab structure. The program accepts structural model information in the form of state-space matrices and performs three basic design functions on the model: (1) open loop analyses; (2) closed loop reduced order controller synthesis; and (3) closed loop stability and performance assessment. The current controller synthesis methods which were implemented in this software are based on the Generalized Linear Quadratic Gaussian theory of Bernstein. In particular, a reduced order Optimal Projection synthesis algorithm based on a homotopy solution method was successfully applied to an experimental truss structure using a 58-state dynamic model. These results are presented and discussed. Current plans to expand the practical size of the design model to several hundred states and the intention to interface Pro-Matlab to a supercomputing environment are discussed. Author

N90-23059*# Georgia Inst. of Tech., Atlanta. School of Aerospace Engineering.
ROBUST FIXED ORDER DYNAMIC COMPENSATION FOR LARGE SPACE STRUCTURE CONTROL c18
Anthony J. Calise and Edward V. Byrns, Jr. *In* Jet Propulsion Lab., California Inst. of Tech., Proceedings of the 3rd Annual Conference on Aerospace Computational Control, Volume 2 15 Dec. 1989 p 641-648 (For primary document see N90-23040 16-61)
Avail: NTIS HC A20/MF A03 CSCL 22B

A simple formulation for designing fixed order dynamic compensators which are robust to both uncertainty at the plant input and structured uncertainty in the plant dynamics is presented. The emphasis is on designing low order compensators for systems of high order. The formulation is done in an output feedback setting which exploits an observer canonical form to represent the compensator dynamics. The formulation also precludes the use of direct feedback of the plant output. The main contribution lies in defining a method for penalizing the states of the plant and of the compensator, and for choosing the distribution on initial conditions so that the loop transfer matrix approximates that of a full state design. To improve robustness to parameter uncertainty, the formulation avoids the introduction of sensitivity states, which has led to complex formulations in earlier studies where only structured uncertainty has been considered. Author

N90-23060*# Arizona State Univ., Tempe. Dept. of Mechanical and Aerospace Engineering.
MULTIVARIABLE FREQUENCY WEIGHTED MODEL ORDER REDUCTION FOR CONTROL SYNTHESIS
David K. Schmidt *In* Jet Propulsion Lab., California Inst. of Tech., Proceedings of the 3rd Annual Conference on Aerospace Computational Control, Volume 2 15 Dec. 1989 p 649-663 (For primary document see N90-23040 16-61)
(AIAA-89-3558) Avail: NTIS HC A20/MF A03 CSCL 09B

Quantitative criteria are presented for model simplification, or order reduction, such that the reduced order model may be used to synthesize and evaluate a control law, and the stability robustness obtained using the reduced order model will be preserved when controlling the full-order system. The error introduced due to model simplification is treated as modeling uncertainty, and some of the results from multivariate robustness

theory are brought to bear on the model simplification problem. A numerical procedure developed previously is shown to lead to results that meet the necessary criteria. The procedure is applied to reduce the model of a flexible aircraft. Also, the importance of the control law itself, in meeting the modeling criteria, is underscored. An example is included that demonstrates that an apparently robust control law actually amplifies modest modeling errors in the critical frequency region, and leads to undesirable results. The cause of this problem is associated with the canceling of lightly damped transmission zeroes in the plant. An attempt is made to expand on some of the earlier results and to further clarify the theoretical basis behind the proposed methodology.
Author

N90-23061*# Case Western Reserve Univ., Cleveland, OH. Computer Engineering and Science.
DISTRIBUTED NEURAL CONTROL OF A HEXAPOD WALKING VEHICLE **c37**
R. D. Beer, L. S. Sterling, R. D. Quinn, H. J. Chiel, and R. Ritzmann *In* Jet Propulsion Lab., California Inst. of Tech., Proceedings of the 3rd Annual Conference on Aerospace Computational Control, Volume 2 15 Dec. 1989 p 664-673 (For primary document see N90-23040 16-61)
Avail: NTIS HC A20/MF A03 CSCL 13I

There has been a long standing interest in the design of controllers for multilegged vehicles. The approach is to apply distributed control to this problem, rather than using parallel computing of a centralized algorithm. Researchers describe a distributed neural network controller for hexapod locomotion which is based on the neural control of locomotion in insects. The model considers the simplified kinematics with two degrees of freedom per leg, but the model includes the static stability constraint. Through simulation, it is demonstrated that this controller can generate a continuous range of statically stable gaits at different speeds by varying a single control parameter. In addition, the controller is extremely robust, and can continue the function even after several of its elements have been disabled. Researchers are building a small hexapod robot whose locomotion will be controlled by this network. Researchers intend to extend their model to the dynamic control of legs with more than two degrees of freedom by using data on the control of multisegmented insect legs. Another immediate application of this neural control approach is also exhibited in biology: the escape reflex. Advanced robots are being equipped with tactile sensing and machine vision so that the sensory inputs to the robot controller are vast and complex. Neural networks are ideal for a lower level safety reflex controller because of their extremely fast response time. The combination of robotics, computer modeling, and neurobiology has been remarkably fruitful, and is likely to lead to deeper insights into the problems of real time sensorimotor control. Author

N90-23062*# Hickman (Robert J.), Newport Beach, CA.
COMBINING HIGH PERFORMANCE SIMULATION, DATA ACQUISITION, AND GRAPHICS DISPLAY COMPUTERS
Robert J. Hickman *In* Jet Propulsion Lab., California Inst. of Tech., Proceedings of the 3rd Annual Conference on Aerospace Computational Control, Volume 2 15 Dec. 1989 p 674-687 (For primary document see N90-23040 16-61)
Avail: NTIS HC A20/MF A03 CSCL 09B

Issues involved in the continuing development of an advanced simulation complex are discussed. This approach provides the capability to perform the majority of tests on advanced systems, non-destructively. The controlled test environments can be replicated to examine the response of the systems under test to alternative treatments of the system control design, or test the function and qualification of specific hardware. Field tests verify that the elements simulated in the laboratories are sufficient. The digital computer is hosted by a Digital Equipment Corp. MicroVAX computer with an Aptec Computer Systems Model 24 I/O computer performing the communication function. An Applied Dynamics International AD100 performs the high speed simulation computing and an Evans and Sutherland PS350 performs on-line graphics display. A Scientific Computer Systems SCS40 acts as a high performance FORTRAN program processor to support the complex, by generating numerous large files from programs coded in FORTRAN that are required for the real time processing. Four programming languages are involved in the process, FORTRAN, ADSIM, ADRIO, and STAPLE. FORTRAN is employed on the MicroVAX host to initialize and terminate the simulation runs on the system. The generation of the data files on the SCS40 also is performed with FORTRAN programs. ADSIM and ADIRO are used to program the processing elements of the AD100 and its IOCP processor. STAPLE is used to program the Aptec DIP and DIA processors.
Author

N90-23063*# Iowa Univ., Iowa City. Dept. of Mechanical Engineering.
MAN-IN-THE-CONTROL-LOOP SIMULATION OF MANIPULATORS **c54**
J. L. Chang, Tsung-Chieh Lin, and K. Harold Yae *In* Jet Propulsion Lab., California Inst. of Tech., Proceedings of the 3rd Annual Conference on Aerospace Computational Control, Volume 2 15 Dec. 1989 p 688-798 (For primary document see N90-23040 16-61)
Avail: NTIS HC A20/MF A03 CSCL 05H

A method to achieve man-in-the-control-loop simulation is presented. Emerging real-time dynamics simulation suggests a potential for creating an interactive design workstation with a human operator in the control loop. The recursive formulation for multibody dynamics simulation is studied to determine requirements for man-in-the-control-loop simulation. High speed computer graphics techniques provides realistic visual cues for the simulator. Backhoe and robot arm simulations are implemented to demonstrate the capability of man-in-the-control-loop simulation. Author

N90-23064*# Michigan Univ., Ann Arbor. Dept. of Aerospace Engineering.
A NEW SECOND-ORDER INTEGRATION ALGORITHM FOR SIMULATING MECHANICAL DYNAMIC SYSTEMS
R. M. Howe *In* Jet Propulsion Lab., California Inst. of Tech., Proceedings of the 3rd Annual Conference on Aerospace Computational Control, Volume 2 15 Dec. 1989 p 700-712 Prepared in cooperation with Applied Dynamics International, Ann Arbor, MI (For primary document see N90-23040 16-61)
Avail: NTIS HC A20/MF A03 CSCL 09B

A new integration algorithm which has the simplicity of Euler integration but exhibits second-order accuracy is described. In fixed-step numerical integration of differential equations for mechanical dynamic systems the method represents displacement and acceleration variables at integer step times and velocity variables at half-integer step times. Asymptotic accuracy of the algorithm is twice that of trapezoidal integration and ten times that of second-order Adams-Bashforth integration. The algorithm is also compatible with real-time inputs when used for a real-time simulation. It can be used to produce simulation outputs at double the integration frame rate, i.e., at both half-integer and integer frame times, even though it requires only one evaluation of state-variable derivatives per integration step. The new algorithm is shown to be especially effective in the simulation of lightly-damped structural modes. Both time-domain and frequency-domain accuracy comparisons with traditional integration methods are presented. Stability of the new algorithm is also examined.
Author

N90-23065*# Hughes Aircraft Co., El Segundo, CA. Guidance and Control Systems Lab.
THE USE OF REAL-TIME, HARDWARE-IN-THE-LOOP SIMULATION IN THE DESIGN AND DEVELOPMENT OF THE NEW HUGHES HS601 SPACECRAFT ATTITUDE CONTROL SYSTEM Abstract Only **c18**
Loren I. Slafer *In* Jet Propulsion Lab., California Inst. of Tech., Proceedings of the 3rd Annual Conference on Aerospace Computational Control, Volume 2 15 Dec. 1989 p 713 (For primary document see N90-23040 16-61)
Avail: NTIS HC A20/MF A03 CSCL 22B

Realtime simulation and hardware-in-the-loop testing is being

used extensively in all phases of the design, development, and testing of the attitude control system (ACS) for the new Hughes HS601 satellite bus. Realtime, hardware-in-the-loop simulation, integrated with traditional analysis and pure simulation activities is shown to provide a highly efficient and productive overall development program. Implementation of high fidelity simulations of the satellite dynamics and control system algorithms, capable of real-time execution (using applied Dynamics International's System 100), provides a tool which is capable of being integrated with the critical flight microprocessor to create a mixed simulation test (MST). The MST creates a highly accurate, detailed simulated on-orbit test environment, capable of open and closed loop ACS testing, in which the ACS design can be validated. The MST is shown to provide a valuable extension of traditional test methods. A description of the MST configuration is presented, including the spacecraft dynamics simulation model, sensor and actuator emulators, and the test support system. Overall system performance parameters are presented. MST applications are discussed; supporting ACS design, developing on-orbit system performance predictions, flight software development and qualification testing (augmenting the traditional software-based testing), mission planning, and a cost-effective subsystem-level acceptance test. The MST is shown to provide an ideal tool in which the ACS designer can fly the spacecraft on the ground. Author

N90-23066*# Oklahoma Univ., Norman. School of Aerospace and Mechanical Engineering.

A REAL TIME, FEM BASED OPTIMAL CONTROL ALGORITHM AND ITS IMPLEMENTATION USING PARALLEL PROCESSING HARDWARE (TRANSISTORS) IN A MICROPROCESSOR ENVIRONMENT Abstract Only

William Neff Patten *In* Jet Propulsion Lab., California Inst. of Tech., Proceedings of the 3rd Annual Conference on Aerospace Computational Control, Volume 2 15 Dec. 1989 p 714 (For primary document see N90-23040 16-61)
Avail: NTIS HC A20/MF A03 CSCL 09B

There is an evident need to discover a means of establishing reliable, implementable controls for systems that are plagued by nonlinear and, or uncertain, model dynamics. The development of a generic controller design tool for tough-to-control systems is reported. The method utilizes a moving grid, time infinite element based solution of the necessary conditions that describe an optimal controller for a system. The technique produces a discrete feedback controller. Real time laboratory experiments are now being conducted to demonstrate the viability of the method. The algorithm that results is being implemented in a microprocessor environment. Critical computational tasks are accomplished using a low cost, on-board, multiprocessor (INMOS T800 Transputers) and parallel processing. Progress to date validates the methodology presented. Applications of the technique to the control of highly flexible robotic appendages are suggested. Author

N90-23067*# Applied Dynamics International, Ann Arbor, MI.

SIX-DEGREE-OF-FREEDOM AIRCRAFT SIMULATION WITH MIXED-DATA STRUCTURE USING THE APPLIED DYNAMICS SIMULATION LANGUAGE, ADSIM

Clare Savaglio *In* Jet Propulsion Lab., California Inst. of Tech., Proceedings of the 3rd Annual Conference on Aerospace Computational Control, Volume 2 15 Dec. 1989 p 715-723 (For primary document see N90-23040 16-61)
Avail: NTIS HC A20/MF A03 CSCL 09B

A realistic simulation of an aircraft in the flight using the AD 100 digital computer is presented. The implementation of three model features is specifically discussed: (1) a large aerodynamic data base (130,00 function values) which is evaluated using function interpolation to obtain the aerodynamic coefficients; (2) an option to trim the aircraft in longitudinal flight; and (3) a flight control system which includes a digital controller. Since the model includes a digital controller the simulation implements not only continuous time equations but also discrete time equations, thus the model has a mixed-data structure. Author

N90-23068*# Applied Dynamics International, Ann Arbor, MI.

SIX-DEGREE-OF-FREEDOM MISSILE SIMULATION USING THE ADI AD 100 DIGITAL COMPUTER AND ADSIM SIMULATION LANGUAGE

Koos Zwaanenburg *In* Jet Propulsion Lab., California Inst. of Tech., Proceedings of the 3rd Annual Conference on Aerospace Computational Control, Volume 2 15 Dec. 1989 p 724-728 (For primary document see N90-23040 16-61)
Avail: NTIS HC A20/MF A03 CSCL 09B

The use of an AD 100 computer and the ADSIM language in the six-degree-of-freedom digital simulation of an air-to-ground missile is illustrated. The missile is launched from a moving platform, typically a helicopter, and is capable of striking a mobile target up to 10 kilometers away. The missile could be any tactical missile. The performance numbers of the AD 100 show that it is possible to implement a high performance missile model in a real-time simulation without the problems associated with an implementation on a general purpose computer using FORTRAN. Author

N90-23069*# National Aeronautics and Space Administration. Langley Research Center, Hampton, VA.

REAL-TIME CLOSED-LOOP SIMULATION AND UPSET EVALUATION OF CONTROL SYSTEMS IN HARSH ELECTROMAGNETIC ENVIRONMENTS

Celeste M. Belcastro *In* Jet Propulsion Lab., California Inst. of Tech., Proceedings of the 3rd Annual Conference on Aerospace Computational Control, Volume 2 15 Dec. 1989 p 729-738 (For primary document see N90-23040 16-61)
Avail: NTIS HC A20/MF A03 CSCL 09B

Digital control systems for applications such as aircraft avionics and multibody systems must maintain adequate control integrity in adverse as well as nominal operating conditions. For example, control systems for advanced aircraft, and especially those with relaxed static stability, will be critical to flight and will, therefore, have very high reliability specifications which must be met regardless of operating conditions. In addition, multibody systems such as robotic manipulators performing critical functions must have control systems capable of robust performance in any operating environment in order to complete the assigned task reliably. Severe operating conditions for electronic control systems can result from electromagnetic disturbances caused by lightning, high energy radio frequency (HERF) transmitters, and nuclear electromagnetic pulses (NEMP). For this reason, techniques must be developed to evaluate the integrity of the control system in adverse operating environments. The most difficult and illusive perturbations to computer-based control systems that can be caused by an electromagnetic environment (EME) are functional error modes that involve no component damage. These error modes are collectively known as upset, can occur simultaneously in all of the channels of a redundant control system, and are software dependent. Upset studies performed to date have not addressed the assessment of fault tolerant systems and do not involve the evaluation of a control system operating in a closed-loop with the plant. A methodology for performing a real-time simulation of the closed-loop dynamics of a fault tolerant control system with a simulated plant operating in an electromagnetically harsh environment is presented. In particular, considerations for performing upset tests on the controller are discussed. Some of these considerations are the generation and coupling of analog signals representative of electromagnetic disturbances to a control system under test, analog data acquisition, and digital data acquisition from fault tolerant systems. In addition, a case study of an upset test methodology for a fault tolerant electromagnetic aircraft engine control system is presented. Author

N90-23070*# Jet Propulsion Lab., California Inst. of Tech., Pasadena.

JPL CONTROL/STRUCTURE INTERACTION TEST BED REAL-TIME CONTROL COMPUTER ARCHITECTURE c60

Hugh C. Briggs *In its* Proceedings of the 3rd Annual Conference on Aerospace Computational Control, Volume 2 15 Dec. 1989 p 739-755 (For primary document see N90-23040 16-61)
Avail: NTIS HC A20/MF A03 CSCL 09B

The Control/Structure Interaction Program is a technology development program for spacecraft that exhibit interactions between the control system and structural dynamics. The program objectives include development and verification of new design concepts - such as active structure - and new tools - such as combined structure and control optimization algorithm - and their verification in ground and possibly flight test. A focus mission spacecraft was designed based upon a space interferometer and is the basis for design of the ground test article. The ground test bed objectives include verification of the spacecraft design concepts, the active structure elements and certain design tools such as the new combined structures and controls optimization tool. In anticipation of CSI technology flight experiments, the test bed control electronics must emulate the computation capacity and control architectures of space qualifiable systems as well as the command and control networks that will be used to connect investigators with the flight experiment hardware. The Test Bed facility electronics were functionally partitioned into three units: a laboratory data acquisition system for structural parameter identification and performance verification; an experiment supervisory computer to oversee the experiment, monitor the environmental parameters and perform data logging; and a multilevel real-time control computing system. The design of the Test Bed electronics is presented along with hardware and software component descriptions. The system should break new ground in experimental control electronics and is of interest to anyone working in the verification of control concepts for large structures. Author

N90-23071*# Hughes Space and Communications Group, Los Angeles, CA.

FASTER SIMULATION PLOTS

Richard A. Fowell *In* Jet Propulsion Lab., California Inst. of Tech., Proceedings of the 3rd Annual Conference on Aerospace Computational Control, Volume 2 15 Dec. 1989 p 756-760 (For primary document see N90-23040 16-61)

Avail: NTIS HC A20/MF A03 CSCL 09B

Most simulation plots are heavily oversampled. Ignoring unnecessary data points dramatically reduces plot time with imperceptible effect on quality. The technique is suited to most plot devices. The departments laser printer's speed was tripled for large simulation plots by data thinning. This reduced printer delays without the expense of a faster laser printer. Surpisingly, it saved computer time as well. All plot data are now thinned, including PostScript and terminal plots. The problem, solution, and conclusions are described. The thinning algorithm is described and performance studies are presented. To obtain FORTRAN 77 or C source listings, mail a SASE to the author. Author

N90-23072*# Jet Propulsion Lab., California Inst. of Tech., Pasadena.

MULTIBODY DYNAMICS: MODELING COMPONENT FLEXIBILITY WITH FIXED, FREE, LOADED, CONSTRAINT, AND RESIDUAL MODES

John T. Spanos and Walter S. Tsuha *In its* Proceedings of the 3rd Annual Conference on Aerospace Computational Control, Volume 2 15 Dec. 1989 p 761-777 (For primary document see N90-23040 16-61)

Avail: NTIS HC A20/MF A03 CSCL 09B

The assumed-modes method in multibody dynamics allows the elastic deformation of each component in the system to be approximated by a sum of products of spatial and temporal functions commonly known as modes and modal coordinates respectively. The choice of component modes used to model articulating and non-articulating flexible multibody systems is examined. Attention is directed toward three classical Component Mode Synthesis (CMS) methods whereby component normal modes are generated by treating the component interface (I/F) as either fixed, free, or loaded with mass and stiffness contributions from the remaining components. The fixed and free I/F normal modes are augmented by static shape functions termed constraint and residual modes respectively. A mode selection procedure is outlined whereby component modes are selected from the Craig-Bampton (fixed I/F plus constraint), MacNeal-Rubin (free I/F plus residual), or Benfield-Hruda (loaded I/F) mode sets in accordance with a modal ordering scheme derived from balance realization theory. The success of the approach is judged by comparing the actuator-to-sensor frequency response of the reduced order system with that of the full order system over the frequency range of interest. A finite element model of the Galileo spacecraft serves as an example in demonstrating the effectiveness of the proposed mode selection method. Author

N90-23073*# Jet Propulsion Lab., California Inst. of Tech., Pasadena.

COMPONENT MODEL REDUCTION VIA THE PROJECTION AND ASSEMBLY METHOD

Douglas E. Bernard *In its* Proceedings of the 3rd Annual Conference on Aerospace Computational Control, Volume 2 15 Dec. 1989 p 778-791 (For primary document see N90-23040 16-61)

Avail: NTIS HC A20/MF A03 CSCL 09B

The problem of acquiring a simple but sufficiently accurate model of a dynamic system is made more difficult when the dynamic system of interest is a multibody system comprised of several components. A low order system model may be created by reducing the order of the component models and making use of various available multibody dynamics programs to assemble them into a system model. The difficulty is in choosing the reduced order component models to meet system level requirements. The projection and assembly method, proposed originally by Eke, solves this difficulty by forming the full order system model, performing model reduction at the the system level using system level requirements, and then projecting the desired modes onto the components for component level model reduction. The projection and assembly method is analyzed to show the conditions under which the desired modes are captured exactly; to the numerical precision of the algorithm. Author

N90-23074*# Iowa Univ., Iowa City. Dept. of Mechanical Engineering.

MODEL REDUCTION IN THE PHYSICAL COORDINATE SYSTEM

K. Harold Yae and K. Y. Joeng *In* Jet Propulsion Lab., California Inst. of Tech., Proceedings of the 3rd Annual Conference on Aerospace Computational Control, Volume 2 15 Dec. 1989 p 792-804 (For primary document see N90-23040 16-61)

Avail: NTIS HC A20/MF A03 CSCL 09B

In the dynamics modeling of a flexible structure, finite element analysis employs reduction techniques, such as Guyan's reduction, to remove some of the insignificant physical coordinates, thus producing a dynamics model that has smaller mass and stiffness matrices. But this reduction is limited in the sense that it removes certain degrees of freedom at a node points themselves in the model. From the standpoint of linear control design, the resultant model is still too large despite the reduction. Thus, some form of the model reduction is frequently used in control design by approximating a large dynamical system with a fewer number of state variables. However, a problem arises from the placement of sensors and actuators in the reduced model, because a model usually undergoes, before being reduced, some form of coordinate transformations that do not preserve the physical meanings of the states. To correct such a problem, a method is developed that expresses a reduced model in terms of a subset of the original states. The proposed method starts with a dynamic model that is originated and reduced in finite element analysis. Then the model is converted to the state space form, and reduced again by the internal balancing method. At this point, being in the balanced coordinate system, the states in the reduced model have no apparent resemblance to those of the original model. Through another coordinate transformation that is developed, however, this reduced model is expressed by a subset of the original states.

Author

N90-23075*# Rockwell International Corp., Seal Beach, CA.
MODAL IDENTITIES FOR MULTIBODY ELASTIC SPACECRAFT: AN AID TO SELECTING MODES FOR SIMULATION
Hari B. Hablani *In* Jet Propulsion Lab., California Inst. of Tech., Proceedings of the 3rd Annual Conference on Aerospace Computational Control, Volume 2 15 Dec. 1989 p 805-817 (For primary document see N90-23040 16-61)
Avail: NTIS HC A20/MF A03 CSCL 09B

The question: Which set of modes furnishes a higher fidelity math model of dynamics of a multibody, deformable spacecraft (hinges-free or hinges-locked vehicle modes) is answered. Two sets of general, discretized, linear equations of motion of a spacecraft with an arbitrary number of deformable appendages, each articulated directly to the core body, are obtained using the above two families of modes. By a comparison of these equations, ten sets of modal identities are constructed which involve modal momenta coefficients and frequencies associated with both classes of modes. The sums of infinite series that appear in the identities are obtained in terms of mass, and first and second moments of inertia of the appendages, core body, and vehicle by using certain basic identities concerning appendage modes. Applying the above identities to a four-body spacecraft, the hinges-locked vehicle modes are found to yield a higher fidelity model than hinges-free modes, because the latter modes have nonconverging modal coefficients; a characteristic proved and illustrated. Author

N90-23076*# SDRC, Inc., San Diego, CA.
ISSUES IN CSI ANALYSIS FOR LARGE SCALE SYSTEMS Abstract Only
Paul Blelloch *In* Jet Propulsion Lab., California Inst. of Tech., Proceedings of the 3rd Annual Conference on Aerospace Computational Control, Volume 2 15 Dec. 1989 p 818 (For primary document see N90-23040 16-61)
Avail: NTIS HC A20/MF A03 CSCL 09B

Future spacecraft such as the International Space Station result in flexible models with hundreds, or perhaps thousands of modes in a frequency range where the potential for control/structure interaction exists. This provides the analyst with a formidable model reduction problem at both the component and the system level. Approaches to normal modes as a structural representation, applicability of alternate structural representations and algorithms for selecting important modal degrees of freedom at both the component and the system level are discussed. Practical implementation of these techniques on a large scale model of the Space Station are presented. Author

N90-23077*# Boeing Aerospace Co., Seattle, WA.
STRUCTURAL MODELING FOR CONTROL DESIGN (ARTICULATED MULTIBODY COMPONENT REPRESENTATION)
E. D. Haugse, R. E. Jones, and W. L. Salus *In* Jet Propulsion Lab., California Inst. of Tech., Proceedings of the 3rd Annual Conference on Aerospace Computational Control, Volume 2 15 Dec. 1989 p 819-830 (For primary document see N90-23040 16-61)
Avail: NTIS HC A20/MF A03 CSCL 09B

High gain, high frequency flexible responses in gimbaled multibody systems are discussed. Their origin and physical significance are described in terms of detailed mass and stiffness modeling at actuator/sensor interfaces. Guyan Reduction, Generalized Dynamic Reduction, inadequate mass modeling detail, as well as system mode truncation, are shown to suppress the high gain high frequency response and thereby lose system flexibility important for stability and performance predictions. Model validation by modal survey testing is shown to risk similar loss of accuracy. Difficulties caused by high frequency responses in component mode simulations, such as DISCOS, and also linearized system mode simulations, are described, and approaches for handling these difficulties are discussed. Author

N90-23078*# Jet Propulsion Lab., California Inst. of Tech., Pasadena.
SIGNIFICANCE OF NORMS AND COMPLETENESS IN VARIATIONAL BASED METHODS
Joel A. Storch *In its* Proceedings of the 3rd Annual Conference on Aerospace Computational Control, Volume 2 15 Dec. 1989 p 831-842 (For primary document see N90-23040 16-61)
Avail: NTIS HC A20/MF A03 CSCL 09B

By means of a simple structural problem, an important requirement often overlooked in practice on the basis functions used in Rayleigh-Ritz-Galerkin type methods is brought into focus. The problem of the static deformation of a uniformly loaded beam is solved variationally by expanding the beam displacement in a Fourier Cosine series. The potential energy functional is rendered stationary subject to the geometric boundary conditions. It is demonstrated that the variational approach does not converge to the true solution. The object is to resolve this paradox, and in so doing, indicate the practical implications of norms and completeness in an appropriate inner product space. Author

N90-23079*# National Aeronautics and Space Administration. Langley Research Center, Hampton, VA.
THE POWER AND EFFICIENCY OF ADVANCED SOFTWARE AND PARALLEL PROCESSING
Ramen P. Singh (DYNACS Engineering Co., Inc., Clearwater, FL.) and Lawrence W. Taylor, Jr. *In* Jet Propulsion Lab., California Inst. of Tech., Proceedings of the 3rd Annual Conference on Aerospace Computational Control, Volume 2 15 Dec. 1989 p 843 (For primary document see N90-23040 16-61)
Avail: NTIS HC A20/MF A03 CSCL 09B

Real-time simulation of flexible and articulating systems is difficult because of the computational burden of the time varying calculations. The mobile servicing system of the NASA Space Station Freedom will handle heavy payloads by local arm manipulations and by translating along the spline of the Station, it is crucial to have real-time simulation available. To enable such a simulation to be of high fidelity and to be able to be hosted on a modest computer, special care must be made in formulating the structural dynamics. Frontal solution algorithms save considerable time in performing these calculations. In addition, it is necessary to take advantage of parallel processing be compatible to take full advantage of both. An approach is offered which will result in high fidelity, real-time simulation for flexible, articulating systems such as the space Station remote servicing system. Author

N90-23080*# National Aeronautics and Space Administration. Langley Research Center, Hampton, VA.
DYNAMIC ANALYSIS OF FLEXIBLE MECHANICAL SYSTEMS USING LATDYN **c18**
Shih-Chin Wu, Che-Wei Chang (Comtek Co., Grafton, VA.), and Jerrold M. Housner *In* Jet Propulsion Lab., California Inst. of Tech., Proceedings of the 3rd Annual Conference on Aerospace Computational Control, Volume 2 15 Dec. 1989 p 844-859 (For primary document see N90-23040 16-61)
Avail: NTIS HC A20/MF A03 CSCL 22B

A 3-D, finite element based simulation tool for flexible multibody systems is presented. Hinge degrees-of-freedom is built into equations of motion to reduce geometric constraints. The approach avoids the difficulty in selecting deformation modes for flexible components by using assumed mode method. The tool is applied to simulate a practical space structure deployment problem. Results of examples demonstrate the capability of the code and approach. Author

N90-23081*# Mechanical Dynamics, Inc., Ann Arbor, MI.
CONTROL DESIGN AND SIMULATION OF SYSTEMS MODELED USING ADAMS
Vikram N. Sohoni *In* Jet Propulsion Lab., California Inst. of Tech., Proceedings of the 3rd Annual Conference on Aerospace Computational Control, Volume 2 15 Dec. 1989 p 860-866 (For primary document see N90-23040 16-61)
Avail: NTIS HC A20/MF A03 CSCL 09B

A technique for control design and simulation using the ADAMS

software and a control design software package is presented. For design of control systems ADAMS generates a minimum realization linear time invariant (LTI), state space representation of multi-body models. This LTI representation can be produced in formats for input to several commercial control design packages. The user can exercise various design strategies in the control design software to arrive at a suitable compensator. The resulting closed loop model can then be simulated using ADAMS. This procedure is illustrated with two examples. Author

N90-23082*# Jet Propulsion Lab., California Inst. of Tech., Pasadena.
MULTIBODY DYNAMICS MODEL BUILDING USING GRAPHICAL INTERFACES
Glenn A. Macala *In its* Proceedings of the 3rd Annual Conference on Aerospace Computational Control, Volume 2 15 Dec. 1989 p 867-878 (For primary document see N90-23040 16-61)
Avail: NTIS HC A20/MF A03 CSCL 09B

In recent years, the extremely laborious task of manually deriving equations of motion for the simulation of multibody spacecraft dynamics has largely been eliminated. Instead, the dynamicist now works with commonly available general purpose dynamics simulation programs which generate the equations of motion either explicitly or implicitly via computer codes. The user interface to these programs has predominantly been via input data files, each with its own required format and peculiarities, causing errors and frustrations during program setup. Recent progress in a more natural method of data input for dynamics programs: the graphical interface, is described. Author

N90-23083*# Buffalo Univ., NY. Dept. of Mechanical and Aerospace Engineering.
CONTROLLING FLEXIBLE STRUCTURES WITH SECOND ORDER ACTUATOR DYNAMICS
Daniel J. Inman, Jeffrey W. Umland, and John Bellos *In* Jet Propulsion Lab., California Inst. of Tech., Proceedings of the 3rd Annual Conference on Aerospace Computational Control, Volume 2 15 Dec. 1989 p 879-890 (For primary document see N90-23040 16-61)
Avail: NTIS HC A20/MF A03 CSCL 09B

The control of flexible structures for those systems with actuators that are modeled by second order dynamics is examined. Two modeling approaches are investigated. First a stability and performance analysis is performed using a low order finite dimensional model of the structure. Secondly, a continuum model of the flexible structure to be controlled, coupled with lumped parameter second order dynamic models of the actuators performing the control is used. This model is appropriate in the modeling of the control of a flexible panel by proof-mass actuators as well as other beam, plate and shell like structural numbers. The model is verified with experimental measurements. Author

N90-23084*# California Univ., Los Angeles. Dept. of Mechanical, Aerospace and Nuclear Engineering.
APPROXIMATION IN LQG CONTROL OF A THERMOELASTIC ROD
J. S. Gibson, I. G. Rosen, and G. Tao (University of Southern California, Los Angeles.) *In* Jet Propulsion Lab., California Inst. of Tech., Proceedings of the 3rd Annual Conference on Aerospace Computational Control, Volume 2 15 Dec. 1989 p 891-898 (For primary document see N90-23040 16-61)
(Grants AF-AFOSR-0373-87; AF-AFOSR-0356-87)
Avail: NTIS HC A20/MF A03 CSCL 09B

Control and estimator gains are computed for linear-quadratic-Gaussian (LQG) optimal control of the axial vibrations of a thermoelastic rod. The computations are based on a modal approximation of the partial differential equations representing the rod, and convergence of the approximations to control and estimator gains is the main issue. Author

N90-23085*# Virginia Univ., Charlottesville. Dept. of Applied Math.
NUMERICAL ALGORITHMS FOR COMPUTATIONS OF FEEDBACK LAWS ARISING IN CONTROL OF FLEXIBLE SYSTEMS Abstract Only
Irena Lasiecka *In* Jet Propulsion Lab., California Inst. of Tech., Proceedings of the 3rd Annual Conference on Aerospace Computational Control, Volume 2 15 Dec. 1989 p 899 (For primary document see N90-23040 16-61)
Avail: NTIS HC A20/MF A03 CSCL 09B

Several continuous models will be examined, which describe flexible structures with boundary or point control/observation. Issues related to the computation of feedback laws are examined (particularly stabilizing feedbacks) with sensors and actuators located either on the boundary or at specific point locations of the structure. One of the main difficulties is due to the great sensitivity of the system (hyperbolic systems with unbounded control actions), with respect to perturbations caused either by uncertainty of the model or by the errors introduced in implementing numerical algorithms. Thus, special care must be taken in the choice of the appropriate numerical schemes which eventually lead to implementable finite dimensional solutions. Finite dimensional algorithms are constructed on a basis of a priority analysis of the properties of the original, continuous (infinite diversional) systems with the following criteria in mind: (1) convergence and stability of the algorithms and (2) robustness (reasonable insensitivity with respect to the unknown parameters of the systems). Examples with mixed finite element methods and spectral methods are provided. Author

N90-23086*# Ottawa Univ. (Ontario). Inst. of Electrical Engineering.
MODELING AND CONTROL OF FLEXIBLE SPACE STATIONS (SLEW MANEUVERS) **c18**
N. U. Ahmed and S. S. Lim *In* Jet Propulsion Lab., California Inst. of Tech., Proceedings of the 3rd Annual Conference on Aerospace Computational Control, Volume 2 15 Dec. 1989 p 900-914 (For primary document see N90-23040 16-61)
Avail: NTIS HC A20/MF A03 CSCL 22B

Large orbiting space structures are expected to experience mechanical vibrations arising from several disturbing forces such as those induced by shuttle takeoff or docking and crew movements. The problem is considered of modeling and control of large space structures subject to these and other disturbing forces. The system consists of a (rigid) massive body, which may play the role of experimental modules located at the center of the space station and flexible configurations, consisting of several beams, forming the space structure. A complete dynamic model of the system was developed using Hamilton's principle. This model consists of radial equations describing the translational motion of the central body, rotational equations describing the attitude motions of the body and several beam equations governing the vibration of the flexible members (platform) including appropriate boundary conditions. In summary, the dynamics of the space structure is governed by a complex system of interconnected partial and ordinary differential equations. Using Lyapunov's approach the asymptotic stability of the space structure is investigated. For asymptotic stability of the rest state (nominal trajectory), feedback controls are suggested. In the investigation, stability of the slewing maneuvers is also considered. Several numerical results are presented for illustration of the impact of coupling and the effectiveness of the stabilizing controls. Some insight is provided into the complexity of modeling, analysis and stabilization of actual space structures. Author

N90-23087*# North Carolina Agricultural and Technical State Univ., Greensboro.
MINI-MAST DYNAMIC ANALYSIS USING THE TRUSS-BEAM MODEL Abstract Only
Elias G. Abu-Saba, William M. McGinley, and Raymond C. Montgomery *In* Jet Propulsion Lab., California Inst. of Tech., Proceedings of the 3rd Annual Conference on Aerospace

Computational Control, Volume 2 15 Dec. 1989 p 915 (For primary document see N90-23040 16-61)
Avail: NTIS HC A20/MF A03 CSCL 09B

The Mini-Mast is a generic space truss designed by Astro Aerospace Corp. A 210 meter truss located in the Structural Dynamics research Lab of NASA Langley is used in comprehensive active vibration control experiments on a realistic large space structure. Some predictions of the natural frequencies and mode shapes were made based on the Finite Element model. The purpose here is to use the Truss-Beam model developed by Elias G. Abu-Saba to predict the natural frequencies of the Mini-Mast and then compare the results with those obtained from the FE model. Imperfections of the joints are modeled, and joint contribution to the flexibility matrix of the structure is noted. The natural frequencies are obtained. An iterative procedure is used to enhance the Truss-Beam model by comparing these results with experimental ones. Author

N90-23088*# National Science Foundation, Washington, DC.
NEURAL NETWORKS IN SUPPORT OF MANNED SPACE
Paul J. Werbos *In* Jet Propulsion Lab., California Inst. of Tech., Proceedings of the 3rd Annual Conference on Aerospace Computational Control, Volume 2 15 Dec. 1989 p 916 (For primary document see N90-23040 16-61)
Avail: NTIS HC A20/MF A03 CSCL 09B

Many lobbyists in Washington have argued that artificial intelligence (AI) is an alternative to manned space activity. In actuality, this is the opposite of the truth, especially as regards artificial neural networks (ANNs), that form of AI which has the greatest hope of mimicking human abilities in learning, ability to interface with sensors and actuators, flexibility and balanced judgement. ANNs and their relation to expert systems (the more traditional form of AI), and the limitations of both technologies are briefly reviewed. A Few highlights of recent work on ANNs, including an NSF-sponsored workshop on ANNs for control applications are given. Current thinking on ANNs for use in certain key areas (the National Aerospace Plane, teleoperation, the control of large structures, fault diagnostics, and docking) which may be crucial to the long term future of man in space is discussed. Author

N90-23089*# National Aeronautics and Space Administration. Goddard Space Flight Center, Greenbelt, MD.
A VERIFICATION LIBRARY FOR MULTIBODY SIMULATION SOFTWARE
Sung-Soo Kim, Edward J. Haug (Iowa Univ., Iowa City.), and Harold P. Frisch *In* Jet Propulsion Lab., California Inst. of Tech., Proceedings of the 3rd Annual Conference on Aerospace Computational Control, Volume 2 15 Dec. 1989 p 917-928 (For primary document see N90-23040 16-61)
Avail: NTIS HC A20/MF A03 CSCL 09B

A multibody dynamics verification library, that maintains and manages test and validation data is proposed, based on RRC Robot arm and CASE backhoe validation and a comparitive study of DADS, DISCOS, and CONTOPS that are existing public domain and commercial multibody dynamic simulation programs. Using simple representative problems, simulation results from each program are cross checked, and the validation results are presented. Functionalities of the verification library are defined, in order to automate validation procedure. Author

N90-23090*# National Aeronautics and Space Administration. Ames Research Center, Moffett Field, CA.
PLOT3D USER'S MANUAL
Pamela P. Walatka, Pieter G. Buning, Larry Pierce, and Patricia A. Elson (Sterling Federal Systems, Inc., Moffett Field, CA.) Mar. 1990 300 p Original contains color illustrations
(Contract NAS2-12961)
(NASA-TM-101067; A-89029; NAS 1.15:101067) Avail: NTIS HC A13/MF A02; 4 functional color pages CSCL 09B

PLOT3D is a computer graphics program designed to visualize the grids and solutions of computational fluid dynamics. Seventy-four functions are available. Versions are available for many systems. PLOT3D can handle multiple grids with a million or more grid points, and can produce varieties of model renderings, such as wireframe or flat shaded. Output from PLOT3D can be used in animation programs. The first part of this manual is a tutorial that takes the reader, keystroke by keystroke, through a PLOT3D session. The second part of the manual contains reference chapters, including the helpfile, data file formats, advice on changing PLOT3D, and sample command files. Author

N90-23091# Instituto de Pesquisas Espaciais, Sao Jose dos Campos (Brazil).
A TOOL FOR AIDING IN THE REUSE OF SOFTWARE [UMA FERRAMENTA PARA AUXILIO NA REUTILIZACAO DE SOFTWARE]
Mario Marcio Ramos Teixeira and Flavio Roberto Dias Velasco Oct. 1989 18 p In PORTUGUESE; ENGLISH summary Presented at the 3rd Brazilian Symposium on Software Engineering, Recife, Brazil, 25-27 Oct.
(INPE-4981-PRE/1545) Avail: NTIS HC A03/MF A01

The applicability of reuse as a way of achieving reduction on software production costs is discussed. The various existing methods of reuse and a hierarchical multiface methodology is proposed, based on Prieto and Diaz-Freeman's method. Aspects and details of the proposed methodology and corresponding tool are also presented with examples. Finally, remaining difficulties and possible solutions are considered. Author

N90-23092 Politecnico di Milano (Italy). Dipt. di Elettronica.
ROBUST MODELLING OF SAMPLED SYSTEMS FOR TIME DELAY ESTIMATION
G. Ferretti, C. Maffezzoni, and R. Scattolini 1989 26 p Sponsored in part by Italian Ministry of Public Education
(Rept-89-047; ETN-90-96512) Avail: Politecnico di Milano, Dipartimento di Elettronica, Piazza Leonardo da Vinci 32, 20133 Milan, Italy

The aim is to show how classical identification algorithms can be used to identify linear plants affected by unknown and/or variable time delays, without overparametrization of the system model. The reformulation of the sampled system model is carried out. This reformulation is based on the removal of overparametrization and parasitics due to the sampling process, reducing the effects of high frequency errors. An identification scheme to deal with time delay systems with different zeros structures is proposed. Simulation results illustrate the performances of the time delay identification algorithm both in an open-loop context and in an adaptive control scheme. ESA

N90-23093 Politecnico di Milano (Italy). Dipt. di Elettronica.
OBJECT-ORIENTED QUERY LANGUAGES: THE NOTION AND THE ISSUES
E. Bertino (Consiglio Nazionale delle Ricerche, Pisa, Italy), M. Negri, G. Pelagatti, and L. Sbattella Oct. 1989 42 p
(Rept-89-054; ETN-90-96514) Avail: Politecnico di Milano, Dipartimento di Elettronica, Piazza Leonardo da Vinci 32, 20133 Milan, Italy

The impact on the design of a query language of the characteristics of an object-oriented data model, such as object-identity, complex object structure, methods and class hierarchies, is addressed Query languages are an important component of any Data Base Management System (DBMS). The object-oriented DBMS provides associative query capabilities. The major differences with respect to traditional query languages are pointed out. ESA

N90-23094 Politecnico di Milano (Italy). Dipt. di Elettronica.
REUSING SOFTWARE COMPONENTS BY SPECIALIZATION
Alberto Coen-Porisini, Flavio DePaoli, Carlo Ghezzi, and Dino Mandrioli 1989 38 p Sponsored in part by ESPRIT
(Rept-89-062; ETN-90-96516) Avail: Politecnico di Milano, Dipartimento di Elettronica, Piazza Leonardo da Vinci 32, 20133 Milan, Italy

A technique and an environment supporting reuse of generalized software components are described. Components are retrieved from a library on the basis of their formal specification and then

possibly transformed. Since a retrieved component may be more general than requested, a specialization phase to make it practically reusable is needed. Specialization is supported by an interactive environment which provides several transformation tools: a symbolic executor/simplifier, an optimizer, and a loop refolder. The conceptual basis of these transformation techniques are described. Examples of their application, and how they cooperate in an environment which is being built for the Ada programming language are discussed. ESA

N90-23095# Groningen Rijksuniv. (Netherlands). Dept. of Computing Science.
PROGRAM INVERSION: MORE THAN FUN
Wei Chen (Washington Univ., Saint Louis, MO.) and Jan Tijmen Udding 27 Apr. 1989 21 p
(CS-8903; ETN-90-96704) Avail: NTIS HC A03/MF A01

Proof rules for inverting a program are presented. An algorithm to compute the preorder and inorder traversals of a binary tree is derived. The inversion of this algorithm is carried out to derive an algorithm to construct a tree from its preorder and inorder traversals. This program is proved correct by using the proof rules for inversion rather than formulating an invariant. Since a proper formulation of a provable invariant of this program appears to be quite awkward, this example shows that program inversion is a useful technique. ESA

N90-23096# Groningen Rijksuniv. (Netherlands). Dept. of Computing Science.
FACTORING HOMOMORPHISMS
Grant Malcolm 1989 17 p
(CS-8908; ETN-90-96705) Avail: NTIS HC A03/MF A01

Data structures for which homomorphisms can always be factored into the composition of a reduction and a map is investigated. A class of data structure presenting such a factoring property is identified. Other interesting algebraic properties of these data structures are discussed. ESA

N90-23097# Groningen Rijksuniv. (Netherlands). Dept. of Computing Science.
ABOUT THE ORDER OF APPEL'S ALGORITHM
Klaas Esselink 14 Jun. 1989 22 p
(Grant Koninklijke/Shell-89012-MSE-4)
(CS-8910; ETN-90-96707) Avail: NTIS HC A03/MF A01

The time complexity of an algorithm for many body simulations is discussed. An order of Appel code, unknown up to now, is investigated. The original Appel code formulation is reviewed. The formulae for the order of the algorithm in one, two and three dimensions are derived. It is not certain if the algorithm behaves when the distribution of particles is less uniform. The modifications applied to Appels code do not affect the order. The order of the algorithm is O(N). ESA

N90-23098# Groningen Rijksuniv. (Netherlands). Dept. of Computing Science.
THE VISIBILITY DIAGRAM: A DATA STRUCTURE FOR VISIBILITY AND MOTION PLANNING PROBLEMS. PART 1: APPLICATION TO THE VISIBILITY POLYGON QUERY PROBLEM
Gert Vegter 1989 23 p
(CS-8913-Pt-1; ETN-90-96708-Pt-1) Avail: NTIS HC A03/MF A01

The visibility diagram is a data structure suitable for representing a set S of segments in the plane which do not intersect except possibly at their boundary points, such that visibility and motion planning queries of a certain type can be answered efficiently. An algorithm to determined the visibility polygon of a query point q with respect to the set S is presented. Such a query can be processed in O(k log(n/k)) time. Preprocessing S takes O(n to the 2nd power) time. The data structure representing S is stored in O(E sub S) space. The visibility diagram is applied to efficiently determine the motion of a rod amidst polygonal obstacles in the plane. ESA

N90-23099# Groningen Rijksuniv. (Netherlands). Dept. of Computing Science.
ON THE PERFORMANCE OF PARALLEL ALGORITHMS
Johan J. Lukkien 9 Aug. 1989 14 p
(CS-8914; ETN-90-96709) Avail: NTIS HC A03/MF A01

A notation to express the performance of a parallel computation is developed. A formalization of the performance measures for a parallel algorithm in which Amdahl's law is a special case is given. The general formulation of Amdahl's law is summarized. The properties of the formalization are derived and examples are presented. The formulae allow arithmetical manipulation and can serve to develop and analyze parallel algorithms. ESA

N90-23100# Groningen Rijksuniv. (Netherlands). Dept. of Computing Science.
CURVATURE-DEPENDENT PARAMETRIZATION OF CURVES AND SURFACES
Menno Kosters Aug. 1989 24 p
(CS-8915; ETN-90-96710) Avail: NTIS HC A03/MF A01

Special parametrizations of curves and surfaces called angle parametrizations are defined. Good approximations to curves and surfaces can be found by uniformly subdividing parameter space and applying the special parametrization. These parametrizations are easily computed numerically. The numerical methods only require explicit expressions for the first and second order derivatives of the original parametrization. The methods presented are applicable to the polynomial and rational curves and surfaces customary in computer-aided design. Concrete examples are presented. The numerical algorithm for surfaces is inherently suited for implementation on a network of processors operating in parallel, and such an implementation is discussed. ESA

N90-23101# Rochester Univ., NY. Inst. of Optics.
QUANTUM-LIMITED IMAGE RECOGNITION
Thomas Arthur Isberg Dec. 1989 209 p
(Contract DAAL03-86-K-0173)
(AD-A218425; ARO-24626.128-PH-UIR) Avail: NTIS HC A10/MF A01 CSCL 20/6

Correlation-based methods for automatic image recognition are implemented using a position-sensitive, photon-counting detection system. It is demonstrated that the information provided by a small number of detected photoevents can be used to accurately estimate the cross correlation between a classical-intensity input scene and a reference (or filter) function stored in computer memory. A theoretical formalism is developed that describes the behavior of the quantum-limited correlation signal for complex filter functions. The theoretical predictions are verified experimentally using a position-sensitive photon-counting detection system. The speed at which the detection system operates makes this an effective technique for implementing correlation based methods for image recognition in real time, even when there is an abundance of input illumination. The estimation of moment invariants for image recognition is also considered. Experiments are performed that demonstrate that the information provided by a few thousand detected photoevents is sufficient to estimate moment invariants that remain unchanged when segmented input images are scaled, change in position, or undergo inplane rotations. The automatic recognition of images from within a cluttered environment is considered. The photon-counting detection system is used to implement a two-stage template matching algorithm to locate objects of interest from within cluttered scenes. Both two-stage matched filtering, and two-stage rotation-invarient filtering is considered. GRA

N90-23102# Office of Naval Research European Office, FPO New York, NY.
PROCEEDINGS OF THE NATO ADVANCED WORKSHOP ON SUPERCOMPUTING
J. F. Blackburn 27 Oct. 1989 23 p Workshop held in Trondheim, Norway, 19-23 Jun. 1989
(AD-A218508; ONREUR-ESNIB-9-12-C) Avail: NTIS HC A03/MF A01 CSCL 12/6

The NATO Advanced Workshop on Supercomputing considered

the following topics: supercomputer architecture, programming for parallel systems, performance measurements, conversion of sequential programs to parallel programs, and applications programming. GRA

N90-23103# Massachusetts Inst. of Tech., Cambridge.
CONCURRENT COMPUTING: NUMERICAL ALGORITHMS AND SOME APPLICATIONS Final Report, 15 May 1982 - 14 Jan. 1989
Virginia C. Klema 23 Jan. 1990 3 p
(Grant AF-AFOSR-0210-82; AF Proj. 2304)
(AD-A218570; AFOSR-90-0214TR) Avail: NTIS HC A01/MF A01 CSCL 12/6

Research on hardware design, operating system support, mathematical software design, and applications programming for concurrent computing systems is presented. Multiple Instruction Multiple Data computing systems constituted the focus of the attention at the hardware and software levels. At every stage hardware that conformed absolutely to the IEEE Standard for Binary Floating Point Arithmetic, P754, IEEE Computer Society was used. GRA

N90-23104# Carnegie-Mellon Univ., Pittsburgh, PA. Artificial Intelligence and Psychology Project.
SENTENCE COMPREHENSION: A PARALLEL DISTRIBUTED PROCESSING APPROACH Technical Report, 15 Sep. 1986 - 14 Sep. 1991
James L. McClelland, Mark St.John, and Roman Taraban 14 Jul. 1989 57 p Prepared in cooperation with Pittsburgh Univ., PA Submitted for publication
(Contracts N00014-86-K-0678; N00014-86-K-0146; N00014-86-K-0349; NSF BNS-86-09729; NSF BNS-88-12048)
(AD-A218886; AIP-70) Avail: NTIS HC A04/MF A01 CSCL 05/7

Basic aspects are reviewed of conventional approaches to sentence comprehension and point out are some of the difficulties faced by models that take these approaches. An alternative approach is described, based on the principles of parallel distributed processing, and shown how it offers different answers to basic questions about the nature of the language processing mechanism. An illustrative simulation model captures the key characteristics of the approach, and illustrates how it can cope with the difficulties faced by conventional models. Alternative ways of conceptualizing basic aspects of language processing within the framework of this approach will consider how it can address several arguments that might be brought to bear against it, and suggest avenues for future development. GRA

N90-23105# David Taylor Research Center, Bethesda, MD. Ship Structures and Protection Dept.
VECTORS AND MATRICES: TWO TURBO PASCAL UNITS FOR FAST PROGRAM DEVELOPMENT
Peter N. Roth Nov. 1989 38 p
(AD-A218917; DTRC/SSPD-90-175-11) Avail: NTIS HC A03/MF A01 CSCL 12/5

Vector and matrix methods in general, and the finite element method in particular, are now common engineering tools. Vectors are used to represent coordinates of points in 3-space, forces displacements, velocities, and so forth. Matrices are typically used to represent finite element stiffness or flexibility, damping, mass, coordinate transformation rules, etc. Any modern college mathematics book may be consulted for vector and matrix theory. A set of vector and matrix arithmetic procedures in Turbo Pascal is documented. Use of the procedures permits fast program development. Pascal, a programming language invented in the early 1970's by Niklaus Wirth, differs from FORTRAN in the way in which parameters are passed to procedures. GRA

N90-23106# Rice Univ., Houston, TX. Dept. of Mathematical Sciences.
LINEAR PROGRAMMING TOOLS FOR INTEGER PROGRAMMING Final Report, 1 Jul. 1987 - 31 Oct. 1989
Robert E. Bixby 31 Oct. 1989 4 p
(Grant AF-AFOSR-0276-87; AF Proj. 2304)
(AD-A219013; AFOSR-90-0313TR) Avail: NTIS HC A01/MF A01 CSCL 12/4

The motivation for this work has been the need for a practical procedure to solve the maximum-weight cut problem (MCP) in undirected graphs. Our primary focus has been on problems arising from considerations in statistical mechanics. These problems are typically posed on grid graphs and some natural variants. There has been significant progress in two areas: solution of the maximum-weight cut problem and development of simplex-based tools for integer programming. Codes developed have been widely used to improve solution time. GRA

N90-23107# Rutgers - The State Univ., New Brunswick, NJ. Dept. of Mathematics.
THE (DURIP) COMPUTER SIMULATIONS OF PLASMAS, NONLINEAR SYSTEMS, AND CONTROL THEORY Final Report, 1 Dec. 1988 - 30 Nov. 1989
Eugene R. Speer 30 Nov. 1989 3 p
(Grant AF-AFOSR-0214-89; AF Proj. 3842)
(AD-A219070; AFOSR-90-0308TR) Avail: NTIS HC A01/MF A01 CSCL 12/7

The Sun 4/60 workstation (SPARCstation) which were purchased according to approved changes in the original proposal were extensively used by faculty, postdoctoral associates and graduate students. An additional station was acquired to be a file server to the other five. Eduardo Sontag was using the equipment in his study of first order controllers. Eugen Speer has investigated interface growth on cellular automation. Zheming Cheng, a postdoctoral associate has done extensive simulations to understand limiting distributions arising from quantum chaos. The SPARCstation is ideally suited for this significant application. The equipment will be used for computerized simulations of nonlinear systems. GRA

N90-23108# Rome Air Development Center, Griffiss AFB, NY.
NATURAL LANGUAGE PROCESSING: A TUTORIAL Report, Jan. - Jul. 1989
Sharon M. Walter Jan. 1990 98 p Revised
(AF Proj. 5581)
(AD-A219096; RADC-TR-90-7) Avail: NTIS HC A05/MF A01 CSCL 05/8

An introduction is presented to Natural Language Processing (NLP) research, the subfield of Artificial Intelligence (AI) attempting to produce computer programs capable of communicating with humans in their own language (English, for instance). Definitions of AI terminology relative to NLP and an overview of Keyword, syntactic, and semantic parsing technologies are included. GRA

N90-23109# Carnegie-Mellon Univ., Pittsburgh, PA. Software Engineering Inst.
COMPARATIVE EVALUATIONS OF FOUR SPECIFICATION METHODS FOR REAL-TIME SYSTEMS Final Report
David P. Wood and William G. Wood Dec. 1989 86 p
(Contract F19628-85-C-0003)
(AD-A219187; CMU/SEI-89-TR-36; ESD-TR-89-47) Avail: NTIS HC A05/MF A01 CSCL 12/5

A number of methods have been proposed in the last decade for the specification of system and software requirements for time-critical systems. The emerging CASE (Computer Aided Software Engineering) technology is based heavily on a subset of these methods; yet little objective attention has been paid to the methods themselves. The objective evaluation of four methods are described (identified as ESML, Harel, Hatley-Pirbhai, and Ward-Mellor), from identification through detailed assessment. The use was avoided of small sample problems as the sole basis of the evaluation. This approach is departed from by involving software developers from various application domains, including extended interviews of those who have applied the methods to large scale projects. The resulting recommendations and conclusions focus on method selection criteria, and on the large-grained impact of using these methods on a given project. Proper context is provided

to assist the practitioner in making appropriate method adoption decisions. GRA

N90-23110# Pennsylvania State Univ., University Park.
FAULT TOLERANT MULTIPROCESSING AND DEVELOPMENT OF TOOLS Final Technical Report, 11 Dec. 1985 - 14 Nov. 1988
T. Feng, C. R. Das, P. T. Hulina, A. R. Hurson, S. Pakzad, M. J. Thazhuthaueetil, C. Wu, D. L. Landis, W. Lin, and J. J. Metzner Dec. 1989 145 p
(Contract F30602-86-C-0005; AF Proj. B413)
(AD-A219216; RADC-TR-89-268) Avail: NTIS HC A07/MF A01 CSCL 12/7

Originally, Pennsylvania State University (PSU) was to develop a conceptual framework for long life, fault tolerant, high performance space based computing system(s) for battle management. However, due to the reduced funding and redirection of the contract, PSU concentrated their research into the development of software tools. PSU has developed a hypercube performance model, an analytical simulation model for the butterfly network, a statistical code simulation, fault diagnosis for fault tolerant multistage networks, and algebraic coding techniques for distributed systems error control. A summary of all the work performed is presented and twenty volumes of reports that were written by Pennsylvania State University are summarized. GRA

N90-23111# Carnegie-Mellon Univ., Pittsburgh, PA. Software Engineering Inst.
THE DURRA APPLICATION DEBUGGER/MONITOR Final Report
Dennis L. Doubleday Sep. 1989 26 p
(Contract F19628-85-C-0003)
(AD-A219290; CMU/SEI-89-TR-32; ESD-TR-89-43) Avail: NTIS HC A03/MF A01 CSCL 12/5

Durra is a language designed to support the construction of distributed applications using concurrent, coarse-grained tasks running on networks of heterogeneous processors. An application written in Durra describes the tasks to be instantiated and executed as concurrent processes, the types of data to be exchanged by the processes, and the intermediate queues required to store the data as they move from producer to consumer processes. The Durra application debugger/monitor, a program that works in conjunction with the Durra runtime software to help the developer locate errors and/or performance bottlenecks in a Durra application, is described. GRA

N90-23112# Carnegie-Mellon Univ., Pittsburgh, PA. Software Engineering Inst.
DARK (DISTRIBUTED Ada REAL-TIME KERNEL) PORTING AND EXTENSION GUIDE KERNEL VERSION 3.0 Final Report
Judy Bamberger, Timothy Coddington, Robert Firth, Daniel Klien, and Dave Stinchcomb Dec. 1989 57 p
(Contract F19628-85-C-0003)
(AD-A219291; CMU/SEI-89-TR-40; ESD-TR-89-51) Avail: NTIS HC A04/MF A01 CSCL 12/5

The modifications are described which were made to the Distributed Ada Real-Time Kernel (DARK) software when porting it from its original execution environment, the 68020-based testbed built at the Software Engineering Institute, to a VAX/VMS system. Information is also present about logical extensions to the Kernel, and the impacts thereof, should the Kernel be used in operational systems. GRA

N90-23113# Carnegie-Mellon Univ., Pittsburgh, PA. Software Engineering Inst.
VERSION DESCRIPTION AND INSTALLATION GUIDE KERNEL VERSION 3.0 Final Report
Judy Bamberger, Timothy Coddington, Robert Firth, Daniel Klein, and Dave Stinchcomb Dec. 1989 53 p
(Contract F19628-85-C-0003)
(AD-A219292; CMU/SEI-89-TR-20; ESD-TR-89-28) Avail: NTIS HC A04/MF A01 CSCL 12/5

A specific version of the Distributed Ada Real-Time Kernel (DARK) software artifact is characterized and documentation is supplied for its installation and use. This document is geared toward: the engineer responsible for installing the Kernal, engineers responsible for porting and maintaining the Kernel, and engineers using the Kernel and needing an awareness of changes from the previous release. GRA

N90-23114# Carnegie-Mellon Univ., Pittsburgh, PA. Software Engineering Inst.
DURRA: A TASK-LEVEL DESCRIPTION LANGUAGE REFERENCE MANUAL, VERSION 2 Final Report
Mario R. Barbacci and Jeannette M. Wing Sep. 1989 54 p
(Contract F19628-85-C-0003)
(AD-A219293; CMU/SEI-89-TR-34; ESD-TR-89-45) Avail: NTIS HC A04/MF A01 CSCL 12/5

Durra is a programming language designed to support the development of large-grained parallel programming applications. These applications are often computation-intensive, or have real-time requirements that require efficient concurrent execution of multiple tasks, devoted to specific pieces of the application. During execution time the application tasks run on possibly separate processors, and communicate with each other by sending messages of different types across various communication links. The application developer is responsible for prescribing a way to manage all of these resources. This prescription is called a task-level application description. It describes the tasks to be executed, the possible assignments of processes to processors, the data paths between the processors, and the intermediate queues required to store the data as they move from source to destination processes. Durra is a task-level description language, a notation in which to write these application descriptions. The syntax and semantics of the language is described and all the language changes introduced as a result of the experiences writing task and application descriptions in Durra are included. GRA

N90-23115# Carnegie-Mellon Univ., Pittsburgh, PA. Software Engineering Inst.
KERNEL ARCHITECTURE MANUAL Final Report
Judy Bamberger, Timothy Coddington, Currie Colket, Robert Firth, and Daniel Klein Dec. 1989 387 p
(Contract F19628-85-C-0003)
(AD-A219295; CMU/SEI-89-TR-19; ESD-TR-89-27) Avail: NTIS HC A17/MF A02 CSCL 12/5

The detailed description of the Kernel is presented. The overall system architecture and the rationale for it are presented as relevant to both the application (i.e., the external view of the Kernel) and the Kernel maintainer (i.e., the internal view of the Kernel). The algorithms and data structures needed to implement the functionality defined in the Kernel Facilities Definition is presented. An in-depth description for the communication protocol used by the Kernel, both the network software and hardware that compose the DARK testbed at the SEI, and a detailed enumeration of all compiler dependencies exploited by Kernel software is also presented. GRA

N90-23116# Naval Ocean Systems Center, San Diego, CA.
RF NETWORK SELECTION IN A RULE-BASED SYSTEM. NOSC PROJECT ZE68: COST METRIC ALGORITHMS FOR INTERNETWORK APPLICATIONS Final Report, for FY 1988 - 89
R. A. Dillard and D. E. Olsen Sep. 1989 51 p
(AD-A219389; NOSC/TR-1318) Avail: NTIS HC A04/MF A01 CSCL 25/2

Algorithms were investigated for dynamically selecting good radio frequency (RF) subnet resources to service transmission requests in a multi-internet environment. The selection algorithms were based on the communications architecture of the 1990 Unified Networking Technology (UNT) Advanced Technology Demonstration. Candidate subnet-selection algorithms were implemented in a rule-based expert system, the C-Language Integrated Production System (CLIPS), and were tested on representative examples of transmission requests. Weighted

fuzzy-logic methods were compared with a weighted-average method. GRA

N90-23117# Harry Diamond Labs., Adelphi, MD.
BASIC GRAPHICS ROUTINE TECHNICAL MANUAL Final Report, Mar. - Aug. 1989
Neal Tesny Feb. 1990 27 p
(AD-A219409; HDL-TM-89-16) Avail: NTIS HC A03/MF A01 CSCL 12/5

A new graphics routine in PC-BASIC for displaying waveforms is described. Linear plots are obtained in automatically scaled and labeled graticules. Specifiable options include window, viewport, and number of tic marks for each axis, and other options. The routine operates on any IBM-compatible PC. DOS is required with a version of the BASIC operating system. Comprehensive samples of output and a program listing are included. GRA

N90-22952*# Draper (Charles Stark) Lab., Inc., Cambridge, MA.
A COMPUTER GRAPHICS SYSTEM FOR VISUALIZING SPACECRAFT IN ORBIT
Don E. Eyles *In* NASA, Ames Research Center, Spatial Displays and Spatial Instruments Jul. 1989 10 p (For primary document see N90-22918 16-54)
Avail: NTIS HC A99/MF A04 CSCL 09B

N90-22963*# SIROCO, Bellevue, WA.
WIDE-ANGLE DISPLAY DEVELOPMENTS BY COMPUTER GRAPHICS
William A. Fetter *In* NASA, Ames Research Center, Spatial Displays and Spatial Instruments Jul. 1989 5 p (For primary document see N90-22918 16-54)
Avail: NTIS HC A99/MF A04 CSCL 09B

62 COMPUTER SYSTEMS

Includes computer networks and special application computer systems.

N90-23118 Politecnico di Milano (Italy). Dipt. di Elettronica.
INTERCONNECTION NETWORKS FOR HIGHLY PARALLEL SUPERCOMPUTING ARCHITECTURES
A. Antola, R. Negrini, M. G. Sami, and R. Stefanelli Sep. 1989 21 p
(Rept-89-053; ETN-90-96513) Avail: Politecnico di Milano, Dipartimento di Elettronica, Piazza Leonardo da Vinci 32, 20133 Milan, Italy

The adoption of Multiple Interconnection Networks (MINs) in supercomputing architectures is discussed. The main properties and characteristics of MINs are reviewed and typical parallel computer architectures adopting MINs are summarized. Two main application classes of MINs are considered: parallel computer systems implemented by connecting powerful processors and large shared memories, and dedicated supercomputing structures directly implementing highly parallel algorithms. For both application classes, the adoption of fault tolerance methods is discussed. Classic approaches to fault tolerance in MINs for parallel computer systems and some recent results in the less known field tolerance in dedicated supercomputing structures are surveyed. ESA

N90-23119# Groningen Rijksuniv. (Netherlands). Dept. of Computing Science.
CONTROLLING REAL-TIME SYSTEMS WITH PARALLEL PROCESSES
Coen Bron 1989 22 p
(CS-8918; ETN-90-96713) Avail: NTIS HC A03/MF A01

An argument as to whether the automatic control of industrial systems can be based on a structure of co-operating sequential processes is presented. This form of control is obtained by means of a tight coupling between the (computer based) controlling processes (tasks), and the (physical) processes being controlled. The real-time aspects of this control are considered. A software package which supports this approach is described. ESA

N90-23120# Massachusetts Inst. of Tech., Cambridge. Lab. for Computer Science.
LOCALITY IN PARALLEL COMPUTATION Ph.D. Thesis
Bruce McDowell Maggs Sep. 1989 163 p
(Contract N00014-87-K-0825)
(AD-A218733; MIT/LCS/TR-469) Copyright Avail: NTIS HC A08/MF A01 CSCL 12/5

This thesis explores strategies for exploiting locality in three major areas of parallel computation: packet routing, graph algorithms, and network emulations. Chapter 1 describes a network-independent approach to the packet-routing problem. Our strategy is to partition the problem into two stages: a path-selection stage and a scheduling stage. Chapter 2 introduces a model for parallel computation, called the distribution random-access machine (DRAM), in which the communication requirements of parallel computer in which memory accesses are evaluated. A DRAM is an abstraction of a parallel computer in which memory accesses are implemented by routing messages through a communication network. Chapter 3 examines the problem of how efficiently a host network can emulate a guest network. The goal is to emulate TG steps of an NG-node guest network on an NH node host network. Chapter 4 presents an algorithm for finding a minimum-cost spanning tree of an N-node graph on an N x N mesh-connected computer. The algorithm has the same O(N) running time as the previous algorithms, but it is much simpler. GRA

N90-23006*# Waseda Univ., Tokyo (Japan). Dept. of Electrical Engineering.
PARALLEL PROCESSING OF REAL-TIME DYNAMIC SYSTEMS SIMULATION ON OSCAR (OPTIMALLY SCHEDULED ADVANCED MULTIPROCESSOR)
Hironori Kasahara, Hiroki Honda, and Seinosuke Narita *In* JPL, Proceedings of the 3rd Annual Conference on Aerospace Computational Control, Volume 1 15 Dec. 1989 p 170-183 (For primary document see N90-22987 16-61)
Avail: NTIS HC A21/MF A03 CSCL 09B

N90-23007*# Illinois Univ., Chicago. Dept. of Mathematics, Statistics, and Computer Science.
PARALLEL AND VECTOR COMPUTATION FOR STOCHASTIC OPTIMAL CONTROL APPLICATIONS
F. B. Hanson *In* JPL, Proceedings of the 3rd Annual Conference on Aerospace Computational Control, Volume 1 15 Dec. 1989 p 184-197 Sponsored in part by the National Center for Supercomputing Applications, Urbana, IL (For primary document see N90-22987 16-61)
(Contracts W-31-109-eng-38; DE-AC05-84ER-21400; NSF DMS-88-06099)
Avail: NTIS HC A21/MF A03 CSCL 09B

N90-23009*# Jet Propulsion Lab., California Inst. of Tech., Pasadena.
A UNIFYING FRAMEWORK FOR RIGID MULTIBODY DYNAMICS AND SERIAL AND PARALLEL COMPUTATIONAL ISSUES Abstract Only
Amir Fijany and Abhinandan Jain *In its* Proceedings of the 3rd Annual Conference on Aerospace Computational Control, Volume 1 15 Dec. 1989 p 199 (For primary document see N90-22987 16-61)
Avail: NTIS HC A21/MF A03 CSCL 09B

N90-23010*# Jet Propulsion Lab., California Inst. of Tech., Pasadena.
PARALLEL ALGORITHMS AND ARCHITECTURE FOR COMPUTATION OF MANIPULATOR FORWARD DYNAMICS
Amir Fijany and Antal K. Bejczy *In its* Proceedings of the 3rd Annual Conference on Aerospace Computational Control, Volume 1 15 Dec. 1989 p 200-215 (For primary document see N90-22987 16-61)
Avail: NTIS HC A21/MF A03 CSCL 09B

N90-23012*# Jet Propulsion Lab., California Inst. of Tech., Pasadena.
COMPUTATIONAL CHAOS IN MASSIVELY PARALLEL NEURAL NETWORKS Abstract Only
Jacob Barhen and Sandeep Gulati *In its* Proceedings of the 3rd Annual Conference on Aerospace Computational Control, Volume 1 15 Dec. 1989 p 228 (For primary document see N90-22987 16-61)
Avail: NTIS HC A21/MF A03 CSCL 09B

N90-23013*# Lockheed Missiles and Space Co., Sunnyvale, CA.
MULTI-FLEXIBLE-BODY DYNAMICS CAPTURING MOTION-INDUCED STIFFNESS Abstract Only
Arun K. Banerjee, Mark E. Lemak, and John M. Dickens *In* JPL, Proceedings of the 3rd Annual Conference on Aerospace Computational Control, Volume 1 15 Dec. 1989 p 229 (For primary document see N90-22987 16-61)
Avail: NTIS HC A21/MF A03 CSCL 09B

N90-23039*# Purdue Univ., West Lafayette, IN. School of Electrical Engineering.
CHARACTERIZATION OF ROBOTICS PARALLEL ALGORITHMS AND MAPPING ONTO A RECONFIGURABLE SIMD MACHINE
C. S. G. Lee and C. T. Lin *In* JPL, Proceedings of the 3rd Annual Conference on Aerospace Computational Control, Volume 1 15 Dec. 1989 p 460-476 (For primary document see N90-22987 16-61)
Avail: NTIS HC A21/MF A03 CSCL 09B

N90-23041*# National Aeronautics and Space Administration. Lyndon B. Johnson Space Center, Houston, TX.
CONCURRENT PROCESSING SIMULATION OF THE SPACE STATION
R. Gluck, A. L. Hale (Supercomputing Solutions, Inc., San Diego, CA.), and John W. Sunkel *In* Jet Propulsion Lab., California Inst. of Tech., Proceedings of the 3rd Annual Conference on Aerospace Computational Control, Volume 2 15 Dec. 1989 p 477-491 (For primary document see N90-23040 16-61)
Avail: NTIS HC A20/MF A03 CSCL 09B

N90-23045*# Jet Propulsion Lab., California Inst. of Tech., Pasadena.
PARALLEL CONJUGATE GRADIENT ALGORITHMS FOR MANIPULATOR DYNAMIC SIMULATION Abstract Only
Amir Fijany and Robert E. Scheld *In its* Proceedings of the 3rd Annual Conference on Aerospace Computational Control, Volume 2 15 Dec. 1989 p 537 (For primary document see N90-23040 16-61)
Avail: NTIS HC A20/MF A03 CSCL 12A

N90-23046*# Boeing Aerospace Co., Seattle, WA.
METHODOLOGY FOR ANALYSIS AND SIMULATION OF LARGE MULTIDISCIPLINARY PROBLEMS
William C. Russell, Paul J. Ikeda, and Robert G. Vos *In* Jet Propulsion Lab., California Inst. of Tech., Proceedings of the 3rd Annual Conference on Aerospace Computational Control, Volume 2 15 Dec. 1989 p 538-547 (For primary document see N90-23040 16-61)
Avail: NTIS HC A20/MF A03 CSCL 12A

63 CYBERNETICS

Includes feedback and control theory, artificial intelligence, robotics and expert systems.

For related information see also *54 Man/System Technology and Life Support.*

N90-23121 Iowa State Univ. of Science and Technology, Ames.
EXPERIMENTAL ADAPTIVE CONTROL OF A HYDRAULIC ROBOT Ph.D. Thesis
S. Ananthakrishnan 1989 269 p
Avail: Univ. Microfilms Order No. DA9003498

An adaptive position controller is investigated to compensate for the effects of both the actuator and linkage dynamics in a four axis hydraulic robot. A simulation study was done, prior to the experimental implementation, in order to compare and contrast different adaptive control algorithms for this system. Implicit and explicit deterministic autoregressive moving average (DARMA) model based adaptive control algorithms were first simulated for hydraulic servo system. Simulation results indicated a satisfactory response. The results of this discrete-time, model-reference adaptive controller (MRAC) were compared with Craig's continuous-time, state-variable-based, adaptive controller. The real-time implementation was then carried out using the DARMA model-based adaptive controllers. A model reference adaptive controller was first used for single testing. Experimental studies were conducted to see the effect of initial parameter estimates, choice of reference model, size of moves, and covariance modification on the position and control response as well as parameter convergence. Dissert. Abstr.

N90-23122 Union for Experimenting Coll. and Univ., Yellow Springs, OH.
APPLICATION OF ARTIFICIAL INTELLIGENCE IN ELECTRONIC CIRCUIT DIAGNOSIS Ph.D. Thesis
Fereydoun Sabour 1989 140 p
Avail: Univ. Microfilms Order No. DA9010768

The field of artificial intelligence (AI) in general and the sub-field of expert system (ES) were examined in particular. Research in automatic fault diagnosis dates back to the 1950s. With increasing complexity of modern electronic systems, the cost of performing any diagnosis can be very high. The historical approach for a human trouble-shooter to detect, isolate, and repair faults is no longer practical in general situation. The skill levels required to maintain and diagnose today's electronic circuits are increasingly demanding. Skilled technicians must undergo long periods of basic classroom education and many years of on the job training before becoming productive. Today's technicians are finding it hard to keep up with technological progress and new product proliferations. On-line expert guidance will be very helpful. The research presented was prompted by need for a system which can preserve, organize, distribute, and present expert knowledge to technicians or engineers. Expert system technology, a subset of modern AI research, was implemented to fulfill these sets of objectives. This research demonstrated that artificially intelligence can model human thinking process. An expert system was built as a part of total contribution to the field. Author

N90-23123# Laboratoire d'Automatique et d'Analyse des Systemes, Toulouse (France).
ABOUT LINEAR SYSTEMS ROBUSTNESS: LINEAR PROGRAMMING APPROACH Ph.D. Thesis
Pedro Luis DiasPeres 1989 130 p In FRENCH; ENGLISH summary Sponsored by Conselho Nacional de Desenvolvimento Cientifico e Tecnologico, Brazil and CEFI/CESELEC, France (LAAS-89-384; ETN-90-96609) Avail: NTIS HC A07/MF A01

Robust control of uncertain dynamic linear systems, continuous or discrete, in state space representation is studied. Robustness is understood as the system capacity to preserve stability under modeling uncertainty. The approach consists of associating to the uncertain system one single quadratic-Lyapunov function for testing stability over the whole uncertain domain. Necessary and sufficient quadratic stabilizability conditions for linear continuous uncertain systems are established. From these conditions, a linear state feedback is obtained. Control decentralization constraints can be taken into account. The extended dynamical formulation enables a synthetic presentation of the obtained results and the formulation of the minimization problem for the feedback gain. Necessary and sufficient quadratic stabilizability conditions for linear discrete uncertain systems are established; the same numerical procedures are used in the discrete and continuous case. Numerical experiments demonstrate the potentialities of the methods. ESA

N90-23124# Technische Univ., Eindhoven (Netherlands). Dept. of Mathematics and Computing Science.
A PRIORI RESULTS IN LINEAR-QUADRATIC OPTIMAL CONTROL THEORY (EXTENDED VERSION)
A. H. W. Geerts Jul. 1989 20 p
(MEMO-COSOR-89-17; ETN-90-96718) Avail: NTIS HC A03/MF A01

The specific nature of Linear-Quadratic optimal Control Problems (LQCPs) yields several a priori statements that are valid for the entire set of these problems. The real symmetric matrix that represents the optimal cost for a particular LQCP necessarily is a rank minimizing solution of the Dissipation Inequality (DI). In the case of a positive definite input weighting matrix, the set of these solutions of the DI is equivalent to the set of real symmetric solutions of the algebraic Riccati equation. The result covers both the regular and the singular case. A characterization of the set of solutions of the DI is provided. An attempt for reducing general (indefinite) LQCPs to non-negative definite LQCP is made. A distributional framework for singular LQCPs is proposed. ESA

N90-23125*# National Aeronautics and Space Administration. Lewis Research Center, Cleveland, OH.
AUTOMATED ELECTRIC POWER MANAGEMENT AND CONTROL FOR SPACE STATION FREEDOM
James L. Dolce, Pamela A. Mellor, and James A. Kish 1990 8 p Proposed for presentation at the 25th Intersociety Energy Conversion Engineering Conference, Reno, NV, 12-17 Aug. 1990; cosponsored by AIChE, SAE, ACS, AIAA, ASME, and IEEE
(NASA-TM-103151; E-5505; NAS 1.15:103151) Avail: NTIS HC A02/MF A01 CSCL 09B

A comprehensive automation design is being developed for Space Station Freedom's electric power system. It strives to increase station productivity by applying expert systems and conventional algorithms to automate power system operation. An integrated approach to the power system command and control problem is defined and used to direct technology development in: diagnosis, security monitoring and analysis, battery management, and cooperative problem-solving for resource allocation. The prototype automated power system is developed using simulations and test-beds. Author

N90-23126# Rome Air Development Center, Griffiss AFB, NY.
ADAPTIVE RESONANCE THEORY 1 In-House Report, Jun. - Aug. 1989
Scott S. Shyne Dec. 1989 28 p
(AF Proj. 4594)
(AD-A219044; RADC-TR-89-358) Avail: NTIS HC A03/MF A01 CSCL 12/9

The function, operation, test and evaluation of a Neural Network that accomplishes unsupervised learning of binary input patterns by classifying them using Adaptive Resonance Theory is described. GRA

N90-23127# Honeywell, Inc., Minneapolis, MN.
ROBUST ADAPTIVE CONTROL: STABILITY AND ASYMPTOTIC PERFORMANCE Report, Oct. - Dec. 1989
James M. Krause, Pramod P. Khargonekar, and Gunter Stein (Massachusetts Inst. of Tech., Cambridge.) Feb. 1990 8 p Submitted for publication
(Contracts F08635-89-C-0027; F08635-89-C-0138; AF Proj. 2304)
(AD-A219259; AFATL-TP-90-02) Avail: NTIS HC A02/MF A01 CSCL 12/2

Systems containing both compact real parametric uncertainty and frequency-weighted bounded operator uncertainty are addressed. It is shown that any parameter adaptive control system is robustly stable provided only that: (1) the unknown parameters lie in a known compact convex set; (2) the control design rule is Lipschitzian; (3) the control design rule would produce a robust controller if given perfect parameter information; and (4) a specified robust parameter estimation algorithm is applied in lieu of perfect parameter information. It is also shown that the asymptotic robust performance level may be arbitrarily close to that of the non-adaptive design which would result from perfect parameter information. GRA

N90-23001*# Integrated Systems, Inc., Santa Clara, CA.
COMPUTATIONAL ISSUE IN THE ANALYSIS OF ADAPTIVE CONTROL SYSTEMS Abstract Only
Robert L. Kosut *In* JPL, Proceedings of the 3rd Annual Conference on Aerospace Computational Control, Volume 1 15 Dec. 1989 p 120 (For primary document see N90-22987 16-61)
Avail: NTIS HC A21/MF A03 CSCL 09B

N90-23005*# California Inst. of Tech., Pasadena.
COMBINED CONTROL-STRUCTURE OPTIMIZATION
M. Salama, M. Milman, R. Bruno, R. Scheid, and S. Gibson (California Univ., Los Angeles.) *In* JPL, Proceedings of the 3rd Annual Conference on Aerospace Computational Control, Volume 1 15 Dec. 1989 p 155-169 (For primary document see N90-22987 16-61)
Avail: NTIS HC A21/MF A03 CSCL 09B

N90-23027*# Georgia Inst. of Tech., Atlanta. School of Aerospace Engineering.
A FINITE ELEMENT BASED METHOD FOR SOLUTION OF OPTIMAL CONTROL PROBLEMS
Robert R. Bless, Dewey H. Hodges, and Anthony J. Calise *In* JPL, Proceedings of the 3rd Annual Conference on Aerospace Computational Control, Volume 1 15 Dec. 1989 p 342-354 (For primary document see N90-22987 16-61)
(Grant NAG1-939)
Avail: NTIS HC A21/MF A03 CSCL 09B

N90-23048*# Air Force Wright Research and Development Center, Wright-Patterson AFB, OH.
IMPLEMENTATION OF GENERALIZED OPTIMALITY CRITERIA IN A MULTIDISCIPLINARY ENVIRONMENT
R. A. Canfield and V. B. Venkayya *In* Jet Propulsion Lab., California Inst. of Tech., Proceedings of the 3rd Annual Conference on Aerospace Computational Control, Volume 2 15 Dec. 1989 p 563-576 (For primary document see N90-23040 16-61)
Avail: NTIS HC A20/MF A03 CSCL 12A

64 NUMERICAL ANALYSIS

Includes iteration, difference equations, and numerical approximation.

N90-23128*# Institute for Computer Applications in Science and Engineering, Hampton, VA.
FOURIER ANALYSIS OF FINITE ELEMENT PRECONDITIONED COLLOCATION SCHEMES Final Report
Michel O. Deville and Ernest H. Mund (Brussels Univ., Belgium) May 1990 25 p Submitted for publication Sponsored in part by Federation Nationale Researche Scientifique, Liege, Belgium
(Contract NAS1-18605)
(NASA-CR-182040; NAS 1.26:182040; ICASE-90-35) Avail: NTIS HC A03/MF A01 CSCL 12A

The spectrum of the iteration operator of some finite element preconditioned Fourier collocation schemes is investigated. The first part of the paper analyses one-dimensional elliptic and hyperbolic model problems and the advection-diffusion equation. Analytical expressions of the eigenvalues are obtained with use of symbolic computation. The second part of the paper considers the set of one-dimensional differential equations resulting from Fourier analysis (in the tranverse direction) of the 2-D Stokes problem. All results agree with previous conclusions on the numerical efficiency of finite element preconditioning schemes. Author

N90-23129# Lawrence Livermore National Lab., CA. Computing and Mathematics Research Div.
INDEX AND CONSISTENCY ANALYSIS FOR DAE (DIFFERENTIAL ALGEBRAIC EQUATION) SYSTEMS FOR STEFAN-MAXWELL DIFFUSION-REACTION PROBLEMS

Alan C. Hindmarsh Mar. 1990 25 p
(Contract W-7405-eng-48)
(DE90-008188; UCRL-ID-103198) Avail: NTIS HC A03/MF A01

The paper by Ilindmarsh and Johnson discusses the formulation and solution of certain reaction diffusion systems involving Stefan-Maxwell diffusion. Supportive analytical results concerning the systems of differential algebraic equations (DAEs) treated in that paper are provided. The systems considered have only one reactant fluid, one product fluid, and one reactant solid; this restricted problem was chosen because the various solvability issues can be settled quite thoroughly. Of particular interest is the index of the DAE systems, the evaluation of consistent initial conditions, and the conservation of the sum of fluid mole fractions. DOE

N90-23130# Joint Inst. for Nuclear Research, Dubna (USSR). Lab. of Computing Techniques and Automation.
ON APPROXIMATION OF NONLINEAR BOUNDARY INTEGRAL EQUATIONS FOR THE COMBINED METHOD
M. Gregus, B. N. Khoromsky, G. E. Mazurkevich, and E. P. Zhidkov 22 Sep. 1989 8 p Presented at the 11th International Conference on Boundary Element Methods in Engineering, Cambridge, MA, 29-31 Aug. 1989
(DE90-009784; JINR-E-11-89-442; CONF-890866-2) Avail: NTIS (US Sales Only) HC A03/MF A01

The nonlinear boundary integral equations that arise in research of nonlinear magnetostatic problems are investigated in combined formulation on an unbounded domain. Approximations of the derived operator equations are studied based on the Galerkin method. The investigated boundary operators are strongly monotone, Lipschitz-continuous, potential and have a symmetrical Gateaux derivative. The error estimates of the Galerkin's approximation in Sobolev spaces of fractional powers are obtained using the above-mentioned properties of the operators, too. The problem was studied on surfaces in two and three-dimensional spaces. Some questions on convergence connected with the discretized systems of equations were also answered. DOE

N90-23131 Politecnico di Milano (Italy). Dipt. di Elettronica.
PERIODIC ARMA MODELS: OPTIMAL PREDICTION AND MINIMUM-PHASE CONDITION
Sergio Bittanti and Giuseppe DeNicolao 1989 8 p Sponsored by CNR and Italian Ministry of Public Education
(Rept-89-006; ETN-90-96509) Avail: Politecnico di Milano, Dipartimento di Elettronica, Piazza Leonardo da Vinci 32, 20133 Milan, Italy

The main objective is to supply the solution of the prediction problem for ARMA models with periodic coefficients (PARMA models). The basic tool is Kalman prediction theory applied to a suitable state-space representation of the given model. The notion of minimum-phase PARMA is introduced. The prediction rule for minimum-phase PARMA's can be given in a simple input/output form which generalizes the time-invariant ARMA predition formula. In the non minimum-phase case, the solution of the prediction problem calls for a suitable notion of canonical representation of the cyclostationary process associated with the original PARMA. ESA

N90-23132 Politecnico di Milano (Italy). Dipt. di Elettronica.
ON A FALLACIOUS CONJECTURE ABOUT THE STABILIZABILITY PROPERTIES OF SOLUTIONS OF THE RICCATI DIFFERENCE EQUATION
Giuseppe DeNicolao 1989 6 p Sponsored by CNR and Italian Ministry of Public Education
(Rept-89-007; ETN-90-96510) Avail: Politecnico di Milano, Dipartimento di Elettronica, Piazza Leonardo da Vinci 32, 20133 Milan, Italy

The monotonicity and stabilizing properties of solutions of the difference Riccati equation were proven to be fallacious by means of suitable counterexamples. A possibly fallacious conjecture was formulated for which no counterexample was found. Such a counterexample is provided together with an interpretation of the counter intuitive behavior of the Riccati equation. ESA

N90-23133# Rome Univ. (Italy). Dipt. di Fisica.
NON-SYMMETRIC DOUBLE WELL AND EUCLIDEAN FUNCTIONAL INTEGRAL
Filippo Cesi, Gian Carlo Rossi, and Massimo Testa (Lecce Univ., Italy) 8 Nov. 1989 20 p Submitted for publication Sponsored in part by the Italian Ministry of Public Education
(Preprint-709; ETN-90-96532) Avail: NTIS HC A03/MF A01

The possibility of discussing in the language of functional integrals the problem of the symmetric double well with a small perturbation, in the semiclassical limit is demonstrated. This problem was previously treated by means of a completely different approach, based on the theory of small random perturbations of dynamical systems. All known results concerning the wave function and the energy splitting of the two lowest lying states are reviewed and an explicit expression for the prefactor of the exponential asymptotic term in the energy splitting is given. ESA

N90-23134# Groningen Rijksuniv. (Netherlands). Dept. of Computing Science.
NATURALNESS OF POLYMORPHISM
Peter J. deBruin 1 Sep. 1989 18 p
(CS-8916; ETN-90-96711) Avail: NTIS HC A03/MF A01

From the type of a polymorphic object, a general uniformity theorem that the object must satisfy is derived. A scheme for arbitrary recursive type-constructors is used. The necessary polymorphic functional languages are specified. Special cases concern natural and dinatural transformations, promotion and induction theorems. The theorem is employed to prove equivalence between different recursion-operators. ESA

N90-23135# Groningen Rijksuniv. (Netherlands). Dept. of Computing Science.
PROCESSES AND FORMALISMS FOR UNBOUNDED CHOICE
Wim H. Hesselink 1989 16 p
(CS-8917; ETN-90-96712) Avail: NTIS HC A03/MF A01

Specification algebras to abstract from semantics while retaining monotonicity of sequential composition are presented. These algebras may have two choice operators: demonic choice and angelic choice. The wish to allow unbounded choice, of both modalities, leads to defining and constructing completions of specifications algebras. A specification algebra is shown not to need a completion. A formalism is developed that allows for any specific combination of unbounded demonic choice, unbounded angelic choice and sequential composition. The formalism is based on transition systems. It is related to the processes of De Bakker and Zucker. The formalism seems to provide a model for the compositional theory of concurrency proposed by Zwiers and De Roever. ESA

N90-23136# Groningen Rijksuniv. (Netherlands). Dept. of Computing Science.
A PROOF OF THE ISOENERGETIC KAM: THEOREM FROM THE ORDINARY ONE
H. W. Broer and G. B. Huitema 1989 11 p
(W-8906; ETN-90-96716) Avail: NTIS HC A03/MF A01

A proof of the isoenergetic KAM-theorem for Hamiltonian systems is given. The ordinary KAM-theorem and a transversality argument are used. The isoenergetic KAM-theorem is related to the persistent tori for a fixed value of the Hamiltonians. A detailed exposition of the results of the integrability of Hamiltonian systems on Canter sets are given. From these results, the isoenergetic KAM-theorem is deduced. ESA

N90-23137*# Institute for Computer Applications in Science and Engineering, Hampton, VA.
HIGH ORDER ESSENTIALLY NON-OSCILLATORY SCHEMES FOR HAMILTON-JACOBI EQUATIONS Final Report
Stanley Osher and Chi-Wang Shu (Brown Univ., Providence, RI.) Feb. 1990 28 p Submitted for publicatcn Sponsored in part by DARPA

(Contracts NAS1-18605; NAG1-270; N00014-86-K-0691; NSF DMS-88-11863; NSF DMS-88-10150)
(NASA-CR-181995; NAS 1.26:181995; ICASE-90-13) Avail: NTIS HC A03/MF A01 CSCL 12A

Hamilton-Jacobi (H-J) equations are frequently encountered in applications, e.g., in control theory and differential games. H-J equations are closely related to hyperbolic conservation laws - in one space dimension the former is simply the integrated version of the latter. Similarity also exists for the multi-dimensional case, and this is helpful in the design of difference approximations. High order essentially non-oscillatory (ENO) schemes for H-J equations are investigated which yield uniform high order accuracy in smooth regions and resolve discontinuities in the derivatives sharply. The ENO scheme construction procedure is adapted from that for hyperbolic conservation laws. The schemes are numerically tested on a variety of one-dimensional and two-dimensional problems, including a problem related to control-optimization. High order accuracy in smooth regions, good resolution of discontinuities in the derivatives, and convergence to viscosity solutions are observed. Author

N90-23138*# Institute for Computer Applications in Science and Engineering, Hampton, VA.
ANALYTIC SEMIGROUPS: APPLICATIONS TO INVERSE PROBLEMS FOR FLEXIBLE STRUCTURES Final Report
H. T. Banks and D. A. Rebnord (Iowa State Univ. of Science and Technology, Ames.) May 1990 18 p Submitted for publication
(Contracts NAS1-18605; NAG1-517; F49620-86-C-0111; NSF DMS-88-18530)
(NASA-CR-182047; NAS 1.26:182047; ICASE-90-36) Avail: NTIS HC A03/MF A01 CSCL 12A

Convergence and stability results for least squares inverse problems involving systems described by analytic semigroups are presented. The practical importance of these results is demonstrated by application to several examples from problems of estimation of material parameters in flexible structures using accelerometer data. Author

N90-23139*# Institute for Computer Applications in Science and Engineering, Hampton, VA.
STABLE BOUNDARY CONDITIONS FOR CARTESIAN GRID CALCULATIONS Final Report
M. J. Berger and R. J. LeVeque (Washington Univ., Seattle.) May 1990 17 p Submitted for publication
(Contracts NAS1-18605; DE-FG02-88ER-25053; NSF ASC-88-58101; NSF DMS-86-57319; AF-AFOSR-0148-86)
(NASA-CR-182048; NAS 1.26:182048; ICASE-90-37) Avail: NTIS HC A03/MF A01 CSCL 12A

The inviscid Euler equations in complicated geometries are solved using a Cartesian grid. This requires solid wall boundary conditions in the irregular grid cells near the boundary. Since these cells may be orders of magnitude smaller than the regular grid cells, stability is a primary concern. An approach to this problem is presented and its use is illustrated. Author

N90-23140# Michigan Univ., Ann Arbor. Dept. of Statistics.
PARAMETRIC MODELS FOR A(SUB n): SPLITTING PROCESSES AND MIXTURES Final Report, 1 Apr. 1987 - 31 Mar. 1989
Bruce M. Hill 24 Aug. 1989 32 p Revised
(Grant AF-AFOSR-0192-87; AF Proj. 2304)
(AD-A218421; AFOSR-90-0212TR) Avail: NTIS HC A03/MF A01 CSCL 12/3

A class of parametric models, called splitting processes, is defined, using de Finetti's concept of adherent mass. Such splitting processes give rise to complex mixtures of distributions. It is proved that the nonparametric Bayesian predictive procedure, A sub n, of Hill (1968), holds exactly for a member of this class called a nested splitting process. It is also shown that the generalization of A sub n, called H sub n, to deal with ties, can hold exactly. A multivariate version of A sub n, based upon the splitting processes, is proposed. Some general considerations concerning ties and adherent masses are discussed, as well as their connection with the Dirichlet process. These include the phenomenon by which in the Dirichlet process, the posterior predictive mass builds up at the observed points, while under A sub n no mass is given to the observed points, and under H sub n some but not necessarily all posterior predictive mass builds up at the observed points. A very general class of splitting processes is then defined, which allows for some of the adherent mass at a point to be replaced by an exact tie. It is proved that both the Dirichlet process of Ferguson and A sub n can arise as different special cases of this general model. GRA

N90-23141# Texas A&M Univ., College Station.
UNDETERMINED COEFFICIENT PROBLEMS FOR QUASI-LINEAR PARABOLIC EQUATIONS Annual Report, 1 Jan. - 31 Dec. 1989
Michael S. Pilant and William Rundell 18 Dec. 1989 124 p
(Contract N00014-89-J-1008)
(AD-A218462) Avail: NTIS HC A06/MF A01 CSCL 12/1

Undetermined coefficient problems in partial differential equations are studied, in particular those problems where the unknown coefficients depend only on the dependent variables. The problems modeled by these equations are related to the determination of unknown physical laws or relationships. The nonlinear terms which are sought to recover in the model problems correspond to material properties that have physical significance. These include temperature dependent specific heats, conductivities, and reaction terms. The main analytical tool is the Fixed Point Projection method, which was developed for use in elliptic and parabolic inverse problems. This method involves projecting the underlying differential operator onto that subset of the domain where the overposed data is given, and reformulating the inverse problem as an equivalent fixed point problem, which is then solved by iteration. Analytical as well as numerical results were obtained, and the FPP method is currently being extended to hyperbolic inverse problems. GRA

N90-23142# Army Natick Research and Development Command, MA.
A COMPUTER PROGRAM TO IMPLEMENT THE CHEN METHOD OF DIMENSIONAL ANALYSIS Final Report, May - Jun. 1989
Philip Cunniff Jan. 1990 29 p
(DA Proj. 1L1-62723-AH-98)
(AD-A218557; NATICK/TR-90/017) Avail: NTIS HC A03/MF A01 CSCL 12/5

A computer program to implement the Chen method of dimensional analysis is presented. The Chen method allows for relatively easy determination of dimensional groups using matrix algebra. The computer program to implement the method provides dimensional groups in simple format and is written in standard FORTRAN 77. Several examples of the use of the program are provided. GRA

N90-23143# North Carolina Univ., Chapel Hill. Dept. of Statistics.
ESTIMATION OF HILBERT SPACE VALUED PARAMETERS BY THE METHOD OF SIEVES
G. Kallianpur and R. S. Selukar Oct. 1989 51 p
(Contract F49620-85-C-0144; AF Proj. 2304)
(AD-A218565; TR-278; AFOSR-90-0273TR) Avail: NTIS HC A04/MF A01 CSCL 12/3

By extending the ideas of Ibragimov and Hasminski in the finite dimensional parameter estimation a large deviation inequality for a sieve estimator estimating a Hilbert space valued parameter is obtained. This sieve estimator corresponds to a sieve which consists of finite-dimensional, compact, convex sets. The inequality suggests a procedure of consistent estimation of Hilbert space valued parameters and naturally provides the convergence rates of the resultant estimators. The usefulness of this approach is demonstrated by applying it to two examples; the first one deals with the estimation of the drift function in a linear stochastic differential equation and the second problem is of the intensity

estimation of a nonstationary Poisson process. A detailed discussion of the convergence rates of the estimators and how they compare with the other estimators proposed in the literature is given in both cases. GRA

N90-23144# North Carolina Univ., Chapel Hill. Dept. of Statistics.

PARAMETER ESTIMATION IN LINEAR FILTERING

G. Kallianpur and R. S. Selukar Oct. 1989 35 p

(Contract F49620-85-C-0144; AF Proj. 2304)

(AD-A218566; TR-279; AFOSR-90-0274TR) Avail: NTIS HC A03/MF A01 CSCL 12/3

Suppose on a probability space (omega, F, P) a partially observable random process (x sub I, Y sub 1) t greater than or = 0; is given where only the second component (y sub 1) is observed. Furthermore assume that (x sub 1, y sub 1) satisfy a certain system of stochastic differential equations driven by independent Wiener processes (W sub 1 (t)) and (W 2 (sub 2)). A large deviation inequality was obtained for the maximum likelihood estimator (m.l.e.) of the unknown parameter theta = (alpha, beta). This inequality enables the proving of the strong consistency, asymptotic normality and covergence of the moments of the m.l.e. The method of proof can be extended to obtain similar results when multi-dimensional instead of 1-D processes are considered and theta is a k-dimensional vector. GRA

N90-23145# Carnegie-Mellon Univ., Pittsburgh, PA. Artificial Intelligence and Psychology Project.

SCIENTIFIC DISCOVERY AS PROBLEM SOLVING Technical Report, 15 Sep. 1986 - 14 Sep. 1991

Herbert A. Simon 19 Feb. 1989 25 p Prepared in cooperation with Pittsburgh Univ., PA Submitted for publication

(Contracts N00014-86-K-0678; F33615-81-K-1539; ARPA Order 3597)

(AD-A218887; AIP-101) Avail: NTIS HC A03/MF A01

The quick and highly incomplete account of the evidence now available about discovery processes confirms both the variety and heterogeneity of the activities that make up the enterprise of science and the consistency with which these activities conform to the pattern of heuristic search. Such phenomena as intuition, insight, and inspiration derive from the capacity for recognition that every expert acquires in the domain of expertise. Author

N90-23146# Arizona State Univ., Tempe. Dept. of Mathematics.

CONTINUATION AND MULTI-GRID METHODS FOR BIFURCATION PROBLEMS Final Report, 30 Sep. 1984 - 30 Nov. 1989

Hans D. Mittelmann 3 Jan. 1990 19 p

(Grant AF-AFOSR-0315-84; AF Proj. 2304)

(AD-A218904; AFOSR-90-0196TR) Avail: NTIS HC A03/MF A01 CSCL 12/1

In the following we give an overview of the work completed under the grant AFOSR-84-0315 entitled Continuation and Multi-grid Methods for Bifurcation Problems since October 1, 1984. The research under that grant concerns the numerical solution of bifurcation and nonlinear eigenvalue problems for parameter-dependent partial differential equations and systems. The scope of the research is rather wide, stressing the development, study and implementation of computational methods for several classes of difficult nonlinear problems, but, also including the derivation of analytic results in cases where these questions had not been settled before. The work under the grant has resulted in 26 papers in refereed journals or refereed proceedings volumes of major conferences; they are listed at the end of this section. GRA

N90-23147# North Carolina State Univ., Raleigh. Dept. of Mathematics.

A COMPUTATIONAL METHOD FOR GENERAL HIGHER INDEX NONLINEAR SINGULAR SYSTEMS OF DIFFERENTIAL EQUATIONS

Stephen L. Campbell 9 Feb. 1990 7 p Repr. from Numerical and Applied Mathematics, v. 12, 1989 p 555-560

(Grants AF-AFOSR-0051-87; NSF DMS-86-13093; AF Proj. 2304)

(AD-A219164; AFOSR-90-0310TR) Avail: NTIS HC A02/MF A01 CSCL 12/2

In the last few years there has been substantial progress on the numerical solution of special classes of nonlinear singular systems of differential equations, F(y',y,t) = O. These systems are also called differential algebraic equations (DAEs). A general numerical procedure for their solution does not currently exist. A general technique developed for the linear time varying singular A(t)y'(t) + B(t)y(t) = f(t) to nonlinear systems is extended. A chemical reactor and robotic arm path control problem are worked to illustrate the technique. GRA

N90-23148# Army Armament Research, Development and Engineering Center, Watervliet, NY. Close Combat Armaments Center.

ADAPTIVE MESH EXPERIMENTS FOR HYPERBOLIC PARTIAL DIFFERENTIAL EQUATIONS Final Report

David C. Arney, Rupak Biswas, and Joseph E. Flaherty Feb. 1990 34 p Presented at the 6th Army Conference on Applied Mathematics and Computing, Boulder, CO, 31 May - 3 Jun. 1988 Submitted for publication Sponsored by Army Armament Research, Development, and Engineering Center, Picatinny Arsenal, NJ

(AD-A219194; ARCCB-TR-90005) Avail: NTIS HC A03/MF A01 CSCL 12/1

Experiments were conducted on mesh moving and local mesh refinement algorithms that are used with a finite difference scheme to solve initial-boundary value problems for vector systems of hyperbolic partial differential equations in one dimension. The mesh moving algorithms move a coarse base mesh by a mesh movement function to follow and isolate spatially distinct phenomena. The local mesh refinement method recursively divides the time step and spatial cells in regions where error indicators are high until a prescribed error tolerance is satisfied. The adaptive mesh algorithms are implemented in a code with an initial mesh generator, a MacCormack finite difference scheme, and an error estimator. Experiments are conducted for several different problems to determine the efficiency of the adaptive methods and their combinations and to gauge their effectiveness in solving one-dimensional problems. GRA

N90-23149# Institut National de Recherche d'Informatique et d'Automatique, Rocquencourt (France).

PROCEEDINGS OF THE 9TH INTERNATIONAL CONFERENCE ON COMPUTING METHODS IN APPLIED SCIENCE AND ENGINEERING

2 Feb. 1990 534 p In ENGLISH and FRENCH Conference held in Paris, France, 29 Jan. - 2 Feb. 1990

(AD-A219307; R/D-6371-MA-02) Avail: NTIS HC A23/MF A03 CSCL 12/1

Partial contents of the conference topics are: Computational Fluid Dynamics; Hypersonic Flow Simulations using DMSC; Recent Progress in Reactive Flow Computations; Two and Three Dimensional Compressible Fluid Flow Computations with Unstructured Grids; Compressible Flow Algorithms on Structured/Unstructured Grids; Implicit Centered Methods for Inviscid and Viscous Hypersonic Flows; Numerical Simulation of Transition to Turbulence in Free-Shear Layers; Far Field Boundary Conditions for Problems in Fluid Dynamics; Supercomputer Architectures; Large Scale Applications of Transputers : Achievement and Perspective; Compiler Optimizations for Superscalar Computers; Parallel Programming Trends : Specifying and Exploiting Parallelism; Numerical Models; Computational Physics and Chemistry; Semiconductor Modelling Via the Boltzmann Equation; Numerical Simulation of Rarefied Gas Flows; Supercomputer Applications; Incompressible Flow Computations Using Various Velocity-Pressure Elements; Data Management for 3-D ADI Algorithm on Hypercube Application to the Design of a Parallel Navier-Stokes Solver; and Numerical Methods. GRA

N90-23150# North Carolina Univ., Chapel Hill. Center for Stochastic Processes.
STOCHASTIC PROCESSES AS FOURIER INTEGRALS AND DILATION OF VECTOR MEASURES
C. Houdre Oct. 1989 7 p
(Contract F49620-85-C-0144)
(AD-A219413; TR-246; AFOSR-90-0275TR) Avail: NTIS HC A02/MF A01 CSCL 12/3

In this note we give an overview of some recent advances in representations of stochastic processes as Fourier integrals. These advances provide a Plancherel and a Hausdorff-Young theory for stochastic processes and random measures which were not previously available. We expect several applications of these methods, two of which are: existence results for linear stochastic differential equations and a framework in which to develop a Fourier theory for the ubiquitous white noise model. GRA

N90-22989*# Jet Propulsion Lab., California Inst. of Tech., Pasadena.
SPATIAL OPERATOR ALGEBRA FRAMEWORK FOR MULTIBODY SYSTEM DYNAMICS
G. Rodriguez, Abhinandan Jain, and K. Kreutz *In its* Proceedings of the 3rd Annual Conference on Aerospace Computational Control, Volume 1 15 Dec. 1989 p 26-4 (For primary document see N90-22987 16-61)
Avail: NTIS HC A21/MF A03 CSCL 12A

N90-23042*# Iowa Univ., Iowa City.
A DECOUPLED RECURSIVE APPROACH FOR CONSTRAINED FLEXIBLE MULTIBODY SYSTEM DYNAMICS
Hao-Jan Lai, Sung-Soo Kim, Edward J. Haug, and Dae-Sung Bae (Kansas Univ., Lawrence.) *In* Jet Propulsion Lab., California Inst. of Tech., Proceedings of the 3rd Annual Conference on Aerospace Computational Control, Volume 2 15 Dec. 1989 p 492-512 (For primary document see N90-23040 16-61)
Avail: NTIS HC A20/MF A03 CSCL 12A

N90-23056*# Purdue Univ., West Lafayette, IN.
EXTENSIONS OF OUTPUT VARIANCE CONSTRAINED CONTROLLERS TO HARD CONSTRAINTS Abstract Only
R. Skelton and G. Zhu *In* Jet Propulsion Lab., California Inst. of Tech., Proceedings of the 3rd Annual Conference on Aerospace Computational Control, Volume 2 15 Dec. 1989 p 636-637 (For primary document see N90-23040 16-61)
Avail: NTIS HC A20/MF A03 CSCL 12A

65 STATISTICS AND PROBABILITY

Includes data sampling and smoothing; Monte Carlo method; and stochastic processes.

N90-23151# Technische Univ., Eindhoven (Netherlands). Dept. of Mathematics and Computer Science.
ON RANDOMNESS OF RANDOM NUMBER GENERATORS
W. E. J. Verhaegh 17 Aug. 1989 9 p
(MEMO-COSOR-89-20; ETN-90-96721) Avail: NTIS HC A02/MF A01

Computer simulations using random number generators are considered. The aim is to warn the users of random number generators that are already implemented in a computer system. These generators can be very bad for simulations. An example of bad generator performance is provided: a queuing network is simulated to determine average waiting time. In the simulation, a long run is split into ten subruns. The obtained results are discussed. ESA

N90-23152# Michigan Univ., Ann Arbor. Dept. of Statistics.
A THEORY OF BAYESIAN DATA ANALYSIS Final Report, 1 Apr. 1987 - 31 Mar. 1989
Bruce M. Hill 10 Oct. 1989 24 p Revised
(Grant AF-AFOSR-0192-87; AF Proj. 2304)
(AD-A218420; AFOSR-90-0213TR) Avail: NTIS HC A02/MF A01 CSCL 12/3

Bayesian data analysis is concerned with the type of data manipulations, transformations, and just plain playing with the data, that any serious scientist engages in during the statistical (or other) analysis of his data. It is largely a post-data procedure, rather than a pre-data procedure, since even when it is desirable to think through such matters quite carefully prior to obtaining the data, in many real world experiments time and other constraints would provide limits on such activities. Compare Hacking or the discussion in Hodges concerning how much is enough. Bayesian data analysis goes beyond the mere data manipulations, however, and attempts to integrate the theory of subjective probability with such data analysis. In this respect it differs from other data-analytic approaches, which appear, more or less, to abandon probability. In this article the author attempts further to elucidate the theory of Bayesian data analysis begun in Hill. GRA

N90-23153# Illinois Univ., Champaign. Model Based Measurement Lab.
ABILITY DISTRIBUTIONS PATTERN PROBABILITIES AND QUASIDENSITIES Final Report
Michael V. Levine Dec. 1989 39 p
(Contracts N00014-83-K-0397; N00014-86-K-0482; RR04204)
(AD-A218471; MEASUREMENT-SERIES-89-2) Avail: NTIS HC A03/MF A01 CSCL 05/9

The quasidensity is a useful surrogate for the ability density in item response theory analyses of multiple choice tests. Like the ability density, it can be used to calculate the probability of sampling an examinee with a specified pattern of responses. Sometimes it is preferable to the density because it is continuous (densities need not be continuous), it is unique (two very different densities can give exactly the same pattern probabilities and all other expected values of random variables that are functions of item responses), it always exists (a discontinuous ability distribution has a quasidensity, but it does not have a density). Some large sample results are proven for quasidensity estimation. It is shown that the maximum likelihood quasidensity estimate (mle) is strongly consistent. The asymptotic distribution of the mle is derived. Some new results on the relation between latent class and latent trait models are also presented. It is shown that every item response model with a smooth density and smooth item response functions is isomorphic to the latent class model obtained with the same item response functions and a discrete ability distribution. An upper bound for the number of points is derived. GRA

N90-23154# Michigan Univ., Ann Arbor. Dept. of Statistics.
BAYESIAN NONPARAMETRIC PREDICTION AND STATISTICAL INFERENCE Final Report, 1 Apr. 1987 - 31 Mar. 1989
Bruce M. Hill 7 Sep. 1989 29 p
(Grants AF-AFOSR-0192-87; NSF DMS-89-01234; AF Proj. 2304)
(AD-A218473; AFOSR-90-0211TR) Avail: NTIS HC A03/MF A01 CSCL 12/3

The problem of Bayesian nonparametric prediction and statistical inference is formulated and discussed. A solution is proposed based upon A sub n and H sub n as in Hill (1968). The meaning of parameters in the subjective Bayesian theory of Bruno de Finetti is discussed in connection both with A sub n and with conventional parametric models. It is argued that the usual sharp distinction between prediction and parametric inference is largely illusory. The finite version of de Finetti's theorem is emphasized for the practice of statistics, with the infinite case used only to obtain approximations and insight. GRA

N90-23155# Washington Univ., Seattle. Applied Physics Lab.
AN EXAMINATION OF THE FULL-WAVE METHOD FOR ROUGH SURFACE SCATTERING Final Report, 1 Apr. 1988 - 30 Sep. 1989
Eric I. Thorsos Jan. 1990 34 p
(Contract N00030-88-C-0054)
(AD-A218664; ARO-26043.2-GS) Avail: NTIS HC A03/MF A01 CSCL 20/14

The goal was to complete a study of Bahar's full-wave approach to rough surface scattering that was begun under ONR support.

The two proposed items of technical work were fully completed. In the ONR-supported work, a study was begun for a simplified scattering problem: Scattering from a one-dimensional (1-D) surface with the Dirichlet (zero field) boundary condition using a Gaussian roughness spectrum. The full-wave method was implemented numerically and used in Monte Carlo calculations of the scattering cross section. Comparisons were then made with exact integral equation results, and with the Kirchholl and perturbation approximations. It was found that the full-wave prediction did not reduce to the lowest order perturbation prediction when the perturbation result was known to be accurate, as shown by exact calculations. This is contrary to conclusions reached by Bahar and is an important finding, showing that the full-wave approach is not as general as previously thought. The full-wave prediction did reduce to the Kirchhoff prediction when the Kirchhoff approximation is known to be accurate, as shown by exact calculations. In fact, the full-wave result was found to agree closely with the Kirchhoff result for all cases studied, whether or not the Kirchhoff result was accurate. GRA

N90-23156# California Univ., San Diego, La Jolla. Dept. of Electrical and Computer Engineering.
STATISTICAL INFERENCE FROM SAMPLED DATA Final Report, 1 Apr. 1984 - 31 Dec. 1989
Elias Masry 28 Feb. 1990 20 p
(Contract N00014-84-K-0042)
(AD-A218731) Avail: NTIS HC A03/MF A01 CSCL 12/3

Research has been concerned with studies in the general area of statistical signal processing. Contributions were made in a wide range of topics many of which were motivated by practical problems in communication systems and digital signal processing. The following is a list of the main topics on which the research was focused: (1) Frequency-Wavenumber Spectral Estimation Using Random Acoustic Arrays; (2) Spread Spectrum Communication Systems; (3) Probability Density and Regression Estimation for Dependent Data; (4) Parametric and Nonparametric Spectral Estimation; (5) Adaptive Linear Estimation Algorithms for Dependent Processes; and (6) Inference for Continuous-Time Processes from Sampled Data. GRA

N90-23157# Pennsylvania Univ., Philadelphia. School of Engineering and Applied Science.
CONTROL OF RANDOMLY SAMPLED ROBOTIC SYSTEMS Interim Technical Report
Hiroaki Kobayashi, Xiaoping Yun, and Richard P. Paul May 1989 33 p
(Contracts DAAL03-89-C-0031; N00014-85-K-0018; DAAG29-84-K-0061; DAAG29-84-9-0027; NSF ECS-84-11879; NSF MCS-82-19196; NSF IRI-84-10413)
(AD-A218948; MS-CIS-89-34; GRASP-LAB-181; ARO-26779.5-EL) Avail: NTIS HC A03/MF A01 CSCL 12/3

This paper studies control problems of sampled data systems which are subject to random sample rate variations and delays. Due to the rapid growth of the use of computers more and more systems are controlled digitally. Complex systems as space telerobotic systems require the integration of a number of sub-systems at different hierarchical levels. While many sub-systems may run on a single processor, some sub-systems require their own processor or processors. The sub-systems are integrated into functioning systems through communications. Communication between processes sharing a single processor are also subject to random delays due to memory management and interrupt latency. Communications between processors involve random delays due to network access and to data collisions. Furthermore, all control processes involve delays due to causal factors in measuring devices and to signal processing. Traditionally, sampling rates are chosen to meet the worst case communication delay. Such a strategy is wasteful as the processors are then idle a great proportion of the time; sample rates are not as high as possible resulting in poor performance or in the over specification of control processors; there is the possibility of missing data no matter how low the sample rate is picked. GRA

N90-23158# Purdue Univ., West Lafayette, IN. Dept. of Statistics.
CHARACTERIZING EXPONENTIAL DISTRIBUTIONS VIA CONDITIONAL INDEPENDENCE
TaChen Liang (Wayne State Univ., Detroit, MI.) Feb. 1990 7 p
(Contract N00014-88-K-0170; NSF DMS-86-06964; NSF DMS-87-02620)
(AD-A219255; TR-90-10) Avail: NTIS HC A02/MF A01 CSCL 12/3

Let Y1,...,Yn be n mutually independent, nonnegative random variables such that for each i=1,...,n,Yi has an absolutely continuous distribution function F(x;0i) = F(0xi), where 0i greater than O, and F(.) has support O,oo). It is shown that given Yi - Yi+1 is greater than O for all i+1,...,n-1, the necessary and sufficient condition for the random variables Y1 - Y2,...,Yn-1-Yn and Yn to be conditionally mutually independent is that for each i+1,...,n,Yi has an exponential distribution. GRA

N90-23159# Purdue Univ., West Lafayette, IN. Dept. of Statistics.
SELECTING MULTINOMIAL POPULATIONS
TaChen Liang and Shanti S. Gupta (Wayne State Univ., Detroit, MI.) Jan. 1990 15 p
(Contract N00014-88-K-0170; NSF DMS-86-06964; NSF DMS-87-02620; NSF DMS-87-17799)
(AD-A219256; TR-90-01C) Avail: NTIS HC A03/MF A01 CSCL 12/2

The problem of selecting fair multinomial populations compared with a standard is studied. The concept of diversity within a population is of considerable importance in statistical theory and applications. The problem of measuring diversity arises in a variety of studies in ecology, sociology, econometrics, genetics and many other sciences. Two selection procedures are investigated: the natural selection procedure of Gupta and Leu (1989) and an empirical Bayes simultaneous selection procedure. It is proved that the natural selection procedure is a Bayes procedure relative to a symmetric Dirichlet prior distribution, and therefore is an admissible selection procedure. For the empirical Bayes simultaneous selection procedure, the associated asymptotic optimality is investigated. It is shown that the proposed empirical Bayes selection procedure is shown to be of order O(exp(-tk+1n k)) for some positive constant t, where k is the number of populations involved in the selection problem. GRA

66 SYSTEMS ANALYSIS

Includes mathematical modeling; network analysis; and operations research.

No abstracts in this category.

67 THEORETICAL MATHEMATICS

Includes topology and number theory.

N90-23160# Army Research Office, Research Triangle Park, NC.
TRANSACTIONS OF THE SEVENTH ARMY CONFERENCE ON APPLIED MATHEMATICS AND COMPUTING Technical Report, Jan. 1989 - Feb. 1990
Feb. 1990 908 p Conference held in West Point, NY, 6-9 Jun. 1989 Sponsored by Army Mathematics Steering Committee
(AD-A219220; ARO-90-1) Avail: NTIS HC A99/MF E06 CSCL 12/1

This conference featured seven invited speakers. These general talks covered several topics of current interest, including: Multi-scale methods and wavelet transforms; High performance computing; Phase transformations; Multivariate splines; and

Stochastic control. The second part of the program consisted of special sessions on topics such as: Stochastic methods for image analysis; Mathematical issues in computer science; Computational methods for multibody dynamics; and Mechanics of large deformations. Partial contents include: Robust Image Models for Image Restoration and Texture Edge Detection; On the Stroh Formalism for Anisotropic Elasticity and its Applications to Composites; Total Absorption in Elastic Media; Quadratic Dynamical Systems Describing Shear Flow of Non-Newtonian Fluids. GRA

N90-23161# Naval Research Lab., Washington, DC. Integrated Warfare Technology Branch.
INCOMPLETE INTEGRALS OF CYLINDRICAL FUNCTIONS Final Report
Allen R. Miller 10 Mar. 1990 15 p
(AD-A219512; NRL-MR-6339) Avail: NTIS HC A03/MF A01
CSCL 12/2

Representations for incomplete Lipschitz-Hankel integrals of cylindrical functions are given in closed form by using Kampe de Feriet hypergeometric functions. In addition, reduction formulas for the Kampe de Feriet functions associated with these integrals are provided for some cases. Incomplete Weber integrals are discussed. GRA

70 PHYSICS (GENERAL)

For precision time and time interval (PTTI) see *35 Instrumentation and Photography;* for geophysics, astrophysics or solar physics see *46 Geophysics, 90 Astrophysics,* or *92 Solar Physics.*

N90-23162# Joint Publications Research Service, Arlington, VA.
JPRS REPORT: SCIENCE AND TECHNOLOGY. USSR: PHYSICS AND MATHEMATICS Abstracts Only
3 Mar. 1989 39 p Transl. into ENGLISH from various Russian articles
(JPRS-UPM-89-001) Avail: NTIS HC A03/MF A01

Topics addressed include: acoustics; crystals, laser glasses; nuclear physics; optics and spectroscopy; plasma physics; superconductivity; game theory; numerical analysis and algorithms; differential equations; and group theory. For individual titles, see N90-23163 through N90-23167.

N90-23163# Joint Publications Research Service, Arlington, VA.
ACOUSTOELECTRONIC INTERACTION OF SURFACE WAVES IN GaAs-InGaAs SUPERLATTICES Abstract Only **c76**
V. A. Vyun, Yu. O. Kanter, S. M. Kikkarin, V. V. Pnev, A. A. Fedorov, and I. B. Yakovkin *In its* JPRS Report: Science and Technology. USSR: Physics and Mathematics 3 Mar. 1989 p 2 Transl. into ENGLISH from Pisma v Zhurnal Tekhnicheskoy Fiziki (Leningrad, USSR), v. 14, no. 20, 26 Oct. 1988 p 1911-1914 (For primary document see N90-23162 16-70)
Avail: NTIS HC A03/MF A01

Although there has been considerable interest in semiconductor superlattices, the interaction of acoustic waves with the charge carriers in them was given no attention. The first experimental data are given on the acoustoelectronic interaction of the superlattice of GaAs during the propagation of surface acoustic waves. The properties of the superlattice are manifested most clearly in the transverse acoustoelectric effect. In an experiment surface acoustic waves were generated in a GaAs backing at a frequency 140 MHz by a high-frequency voltage transducer. All research was at room temperature. Data were obtained on the dependence of the amplitude of the acoustoelectric effect on different current strengths for different intensities of surface acoustic waves. It was found that the redistribution of free charge carriers within the limits of each layer and between layers (40 layers were formed) under the influence of a flowing current and surface acoustic waves leads to a new mechanism of nonlinear acoustoelectronic interaction more intense than the known concentration mechanism. The experiments revealed the essential features of superlattices even at temperature. Author

N90-23164# Joint Publications Research Service, Arlington, VA.
EXCITATION OF HYPERSOUND AT BOUNDARY BETWEEN TYPE-2 SUPERCONDUCTOR AND A CONCENTRATED PARAMAGNETIC COMPOUND Abstract Only **c76**
S. L. Tsarevskiy *In its* JPRS Report: Science and Technology. USSR: Physics and Mathematics 3 Mar. 1989 p 4 Transl. into ENGLISH from Akusticheskiy Zhurnal (Moscow, USSR), v. 34, no. 2, Mar.-Apr. 1988 p 315-320 (For primary document see N90-23162 16-70)
Avail: NTIS HC A03/MF A01

The boundary without acoustic contact between a type-2 superconductor and a paramagnetic rare-earth compound is considered, assuming that the paramagnetic compound with a regular sublattice of paramagnetic ions occupies an entire half-space and the superconductor is a sufficiently thick plate of infinite length but finite width. When a transverse external magnetic field consisting of a constant component and an alternating one is applied, a strongly nonuniform magnetic field with the periodicity of a two-dimensional vortex structure appears in the superconductor near its interface with the paramagnetic. Analysis of strains in such a system, with its Hamiltonian represented as the sum of a quiescent component (energy of phonons and energy of ions in the crystal field) and a perturbation component (Zeeman energy of ions and energy of spin-phonon interactions), indicates that gigahertz Rayleigh surface acoustic waves are excited as a result. Numerical estimates of their amplitude of 10 GHz frequency are shown for a type-2 superconductor on a concentrated LiLnF4 or a van Vleck LitmF4 paramagnetic, in a constant magnetic field of 900 Oe and an alternating one of 1 to 5 Oe. With such materials it is shown to be feasible to generate hypersonic surface acoustic waves of up to 50 GHz frequency and up to 10 W/sg cm intensity, absence of an acoustic contact between the two media being essential at these high frequencies. Author

N90-23165# Joint Publications Research Service, Arlington, VA.
EFFECT ON RELAXATION ON NONLINEAR WAVES IN CRYSTALS Abstract Only **c76**
G. T. Adamashvili *In its* JPRS Report: Science and Technology. USSR: Physics and Mathematics 3 Mar. 1989 p 6 Transl. into ENGLISH from Teoreticheskaya i Matematicheskaya Fizika (Moscow, USSR), v. 75, no. 3, Jun. 1988 p 371-377 (For primary document see N90-23162 16-70)
Avail: NTIS HC A03/MF A01

The effect of transverse relaxation on a soliton of self-induced transparence in anisotropic crystals with nonuniform broadening of the spectral line is analyzed by the methods of inverse scattering-problem and perturbation theory, on which the theory of solitons is based. This mathematical apparatus is applied to propagation of a pulse of a plane extraordinary wave through a uniaxial crystal with low concentration of two-level impurity atoms, their transitions having dipole moments oriented parallel to the optical axis. Interaction of pulse and medium is assumed to be coherent, a necessary condition for self-induced relaxation. Assuming further a slow variation of electric field and impurity polarization parameters, interaction of impurity atoms being ignored, standard procedure yields the Bloch-Maxwell equation for self-induced transparence for an extraordinary wave. Solution of this equation with the aid of the solution to an auxiliary problem, namely Zakharov-Shabat equations, yields a continuous spectrum of scattering data in the latter as a result of transverse relaxation. Its effect is further evident in the modified asymptotic expressions for the complex amplitude and the energy of an extraordinary-wave pulse and for the reflection coefficient of the medium. For a ruby crystal, specifically, integrals in these expressions were evaluated by numerical methods. Author

N90-23166# Joint Publications Research Service, Arlington, VA.
SHAPING RADIATION PATTERN OF EXCIMER LASER BY MEANS OF CONTROLLABLE INTRACAVITY MIRROR Abstract Only **c36**
A. S. Akhmanov, M. A. Borontsov, A. V. Kudryashov, V. Ya. Panchenko, V. K. Popov, A. Yu. Poroykov, and V. I. Shmalgauzen *In its* JPRS Report: Science and Technology. USSR: Physics

and Mathematics 3 Mar. 1989 p 10 Transl. into ENGLISH from Kvantovaya Elektronika (Moscow, USSR), v. 15, no. 8(194), Aug. 1988 p 1525-1526 (For primary document see N90-23162 16-70)
Avail: NTIS HC A03/MF A01

In an experiment with an excimer (XeC) laser its radiation pattern and thus beam structure were shaped by means of an electrically controllable mirror replacing a plain semiopague one in the cavity. The laser was an ELI-91 with a 1:10:1000 HC:Xe:Ne active mixture operating under a pressure of 4 atm and emitting 308 nm radiation in pulses of 80 mJ energy and 30 ps duration without an expanding telescope. The cavity was formed by a plane-parallel quartz plate and an adaptively controllable semipassive bimorphous piezoelectric plate with reflective aluminum coating maximum coverage of its surface by radiation from the discharge being ensured by an expanding telescope made of quartz with magnification. The first resonance frequency of the controllable mirror was 5 kHz. Author

N90-23167# Joint Publications Research Service, Arlington, VA.
TUNABLE XeCl-LASER FEATURING HIGH SPECTRAL LUMINANCE Abstract Only **c36**
V. Ch. Belash, V. A. Kartazayev, S. Z. Lipinskiy, and V. L. Naumovich *In its* JPRS Report: Science and Technology. USSR: Physics and Mathematics 3 Mar. 1989 p 10 Transl. into ENGLISH from Kvantovaya Elektronika (Moscow, USSR), v. 15, no. 8(194), Aug. 1988 p 1545-1547 Original language document was announced in IAA asA89-18605 (For primary document see N90-23162 16-70)
Avail: NTIS HC A03/MF A01

A tunable XeCl-laser was built with the same 1.8:9:1800 HCl:Xe:He active mixture in both master oscillator and amplifier stages, which made it possible to produce a beam with only approximately 0.3 mrad divergence carrying radiation within an only approximately 1 pm wide spectral band in pulses of approximately 0.5 mJ energy and of 5 to 12 ns adjustable duration. The laser operated with a discharge voltage of 23 kV across a 60 pF storage capacitor with a 27 nF peaking capacitor. The cavity was formed by a plane dielectric mirror and a plane-parallel quartz plate. The tuner was formed by a dielectric high-reflectance (99.8 pct) mirror, a holographic granting (3600 lines/mm) mounted for grazing incidents, and a Littrow grating (3600 lines/mm). This laser featuring narrow-band high-energy emission was tunable over the 307.52 to 308.55 nm range, the width of the spectral line increasing as the angle of incidence of the holographic grating was increased. Author

N90-23168# Office of Naval Research Liaison Office, Far East, APO San Francisco, CA.
ONR FAR EAST SCIENTIFIC INFORMATION BULLETIN, VOLUME 13, NO. 4 Quarterly Report, Oct. - Dec. 1988
Sandy Kawano, ed. Dec. 1988 94 p Prepared in cooperation with AFOSR Liaison Office, Far East, APO San Francisco, CA and ARO Liaison Office, Far East, APO San Francisco, CA
(ONRFE-Sci-Info-Bull-13(4)88; ISSN-0271-7077) Avail: NTIS HC A05/MF A01 CSCL 20C

Articles covering recent developments in Far Eastern (particularly Japanese) scientific research are presented. Topics addresed include: high temperature superconducting films, technology transfer; metallic superlattices, Kuroshio current; La2CuO4 superconductors; computational fluid dynamics; supercomputers; and materials processing. For individual titles, see N90-23169 through N90-23172.

N90-23169# Office of Naval Research Liaison Office, Far East, APO San Francisco, CA.
HIGH TEMPERATURE SUPERCONDUCTING THIN FILMS IN JAPAN **c76**
Michael Osofsky, Phillip R. Broussard, and Earl Callen *In its* ONR Far East Scientific Information Bulletin, Volume 13, No. 4 Dec. 1988 p 1-23 (For primary document see N90-23168 16-70)
Avail: NTIS HC A05/MF A01 CSCL 20L

The study of thin films of the new high temperature superconductors can address a wide range of scientific questions and may well lead to many vital technological applications. The fundamentals of high temperature superconducting thin films are reviewed: their structure, how their physical and superconducting properties are characterized, and how they are made. Facilities and programs of several Japanese superconducting thin film groups are described. Author

N90-23170# Office of Naval Research Liaison Office, Far East, APO San Francisco, CA.
RESEARCH AND APPLICATIONS OF METALLIC SUPERLATTICES, HIGH T(SUB c) SUPERCONDUCTORS, X RAY OPTICS, AND COMPACT SYNCHROTRONS **c76**
Charles M. Falco *In its* ONR Far East Scientific Information Bulletin, Volume 13, No. 4 Dec. 1988 p 31-37 (For primary document see N90-23168 16-70)
Avail: NTIS HC A05/MF A01 CSCL 20L

Research on metallic superlattices, high T(sub c) superconductors, and x ray optics are described. The development of compact synchrotrons for generation of soft x rays is also reported. Author

N90-23171# Office of Naval Research Liaison Office, Far East, APO San Francisco, CA.
WHAT IS GOING ON IN THE La2CuO4 SUPERCONDUCTORS **c76**
Earl Callen *In its* ONR Far East Scientific Information Bulletin, Volume 13, No. 4 Dec. 1988 p 43-59 (For primary document see N90-23168 16-70)
Avail: NTIS HC A05/MF A01 CSCL 20L

The ceramic cuprate (La(1-x)Sr(x))2CuO4 is an antiferromagnetic insulator when the Sr concentration is below 1 percent, a spin glass for .01 is less than x is less than .02, and a superconductor at higher Sr levels. Band calculations show a two-dimensional, strongly mixed Cu(d)-O(p) band from planar Cu-O atoms. The bandwidth is wide between 4 and 9 eV depending on the calculation several times the correlation term U in the Hubbard Hamiltonian, but La-Sr 214 behaves like a narrow band, strongly correlated system. Neutron diffraction and Raman scattering evidence support a picture of strong magnon-electron interaction in normal material giving way at higher Sr concentrations to antiferromagnetic fluctuations in Cu spins superexchange coupled through planar O. Fluctuations in the spin system may be the glue coupling electrons into Cooper pairs in the superconductor. Hall data at low Sr concentrations are consistent with a Mott-Hubbard insulating gap model. At higher Sr concentrations the Hubbard gap presumably collapses and the band model prevails; the electronic properties are those of a two-dimensional material of extremely low Fermi energy. Author

N90-23172# Office of Naval Research Liaison Office, Far East, APO San Francisco, CA.
CURRENT JAPANESE SUPERCOMPUTERS FOR COMPUTATIONAL FLUID DYNAMICS APPLICATIONS **c34**
Hideo Yoshihara *In its* ONR Far East Scientific Information Bulletin, Volume 13, No. 4 Dec. 1988 p 61-68 (For primary document see N90-23168 16-70)
Avail: NTIS HC A05/MF A01 CSCL 20L

Current top of the line Japanese supercomputers are described, stressing the vector features significant for highly vectorized computational fluid dynamics (CFD) codes. Covered are the Fujitsu VP400E, Hitachi S820, and NEC SX-24 computers. A benchmarking of these computers, scheduled in the near future, is described using the Navier/Stokes calculation over a delta wing with about one million mesh points. Author

N90-23173# Rome Univ. (Italy). Dipt. di Fisica.
EFFECTIVE ACTION FOR INDUCED GRAVITY ON A 2-DIMENSIONAL MANIFOLD
K. Yoshida 29 Nov. 1989 29 p Submitted for publication
(Preprint-712; ETN-90-96535) Avail: NTIS HC A03/MF A01

The generating functional of the correlation functions of the

stress energy-tensor in conformal field theory is explicitly constructed first on the Euclidean plane and then on an arbitrary Riemann surface. For the first case, anti-holomorphic SL(2C) symmetry as the counterpart of the SL(2R) current algebra of Polyakov's quantized gravity in two dimension is found. For the general real two dimensional manifold, a fundamental change due to the breaking of SL(2C) symmetry and to a loss of locality is expected. ESA

N90-23174# Rome Univ. (Italy). Dipt. di Fisica.
REPLICA SCALING ANALYSIS OF INTERFACES IN RANDOM MEDIA
Yi-Cheng Zhang 1 Dec. 1989 14 p Submitted for publication
(Preprint-713; ETN-90-96536) Avail: NTIS HC A03/MF A01

Interfaces subject to random disorder are analyzed by a replica scaling theory. Long range and short range disorder corresponds to repulsive and attractive interaction among the replicas, respectively. If these interactions are treated properly, a new scaling exponent is given for short range disorder, such as random bonds, while the Imry-Ma-Flory exponent for long range disorder, such as random fields, is reproduced. ESA

N90-23175# Rome Univ. (Italy). Dipt. di Fisica.
RIGOROUS ANALYSIS OF LOW TEMPERATURE STOCHASTIC ISING MODELS: METASTABILITY AND EXPONENTIAL APPROACH TO EQUILIBRIUM
Fabio Martinelli, Enzo Olivieri (Aquila Univ., Italy), and Elisabetta Scoppola 18 Dec. 1989 6 p
(Preprint-720; ETN-90-96540) Avail: NTIS HC A02/MF A01

Rigorous results on the exponential convergence to equilibrium for the Metropolis and Swendsen-Wang (SW) stochastic dynamics for the 2-D Ising ferromagnet in the low temperature case with external magnetic field h in the thermodynamic limit are presented. Various situations in which boundary conditions are homogeneous and parallel or opposite to the external field are considered. In the latter case for the SW dynamics, the tunneling from the metastable phase to the stable one, is analyzed. ESA

N90-23176# North Carolina Univ., Chapel Hill. Dept. of Statistics.
TWO BARRIERS PROBLEM FOR CONTINUOUSLY DIFFERENTIABLE PROCESSES
Igor Rychlik Oct. 1989 35 p Sponsored in part by Swedish Natural Science Research Council
(Contract F49620-85-C-0144; AF Proj. 2304)
(AD-A218564; AFOSR-90-0272TR; TR-277) Avail: NTIS HC A03/MF A01 CSCL 12/3

Durbin has presented a compact formula for the first passage density of a Gaussian process, which is locally like Brownian motion, to a smooth barrier. In previous works, the formula was extended to the case of processes which are smooth functions of a continuously differentiable Gaussian vector process and to more general kinds of first passage time problems, so called marked crossings. Similar results are obtained for the first passage density in presence of a second absorbing barrier and it is used to construct upper and lower bounds for the first passage, rainflow cycle amplitude, zerocrossing wave-length and amplitude densities. Numerical examples illustrate the results. GRA

N90-23177# Scripps Institution of Oceanography, La Jolla, CA.
TRANSDUCTION OF NANOVOLT SIGNALS: LIMITS OF ELECTRIC-FIELD DETECTION Final Report
J. Kalmijn 21 Nov. 1989 5 p Presented at the Biophysics of Electroreception Workshop, La Jolla, CA, 19-21 Nov. 1989
(Contract N00014-90-J-1272)
(AD-A219214) Avail: NTIS HC A01/MF A01 CSCL 20/3

Life scientists discussed the extreme electrical sensitivity of marine sharks, skates, and rays. After reviewing the results of earlier studies on the electric sense at the animal and system levels, the participants discussed the basic process of signal transduction in terms of voltage-sensitive ionic channels. Struck by the small charge displacements needed for excitation, they strongly recommended that sensory biologists, physiologists, and biophysicists join in a concerted effort to initiate new research on the ionic mechanisms of electric field detection. To obtain detailed information on the electroreceptive membrane and its ionic channels, high resolution recording techniques will be mandatory. GRA

71 ACOUSTICS

Includes sound generation, transmission and attenuation. For noise pollution see *45 Environmental Pollution*.

N90-23178 Southampton Univ. (England).
TIME-VARYING FILTER MODELLING AND TIME-FREQUENCY CHARACTERISATION OF NONSTATIONARY SOUND FIELDS DUE TO A MOVING SOURCE Ph.D. Thesis
Jong-Sik Lee 1989 212 p
Avail: Univ. Microfilms Order No. BRDX87355

The problems of modeling, interpretation, and estimation of non-stationary processes are examined with particular reference to acoustic problems. A common assumption in the modeling and analysis of a random process is that the process is stationary. Such an assumption may be a satisfactory approximation in many instances, but there are situations in which the processes are obviously non-stationary. In particular, many physical non-stationary processes exhibit a frequency-modulated structure. An important example of such processes is the sound perceived by an observer due to a moving source emitting a random signal. Two methods are studied for the characterization of such non-stationary processes; time frequency spectral characterization and time-varying filter modeling. Two major candidates for time-frequency (time varying) spectral characterization of non-stationary processes are the Wigner-Ville spectrum and Priestly's evolutionary spectrum. Properties, prediction, and estimation of the two time-frequency spectra and the relationship between them are discussed. The time-frequency spectra of the sound field due to a moving source are predicted and these spectra are used as the basis for estimation of the acoustic directionality pattern of the source. As to the time-varying filter modeling of such non-stationary processes, a technique called the covariance-equivalent method is discussed. The covariance-equivalent technique is used to model the sound field due to a moving source emitting a random signal in single-path/single-sensor cases. The covariance-equivalent method, which was only applicable to single-component processes, is extended to include the sound field in multi-path/multi-sensor cases by using the concept of the complex envelope (complex process). Finally, estimation problems of practical importance, including that of the source acoustic directionality pattern and time-varying delay estimation problems, are formulated and solved in terms of the covariance-equivalent models, and simulation studies are also performed. Dissert. Abstr.

N90-23179 Mississippi Univ., University.
A SCATTERING CENTER BASED NUMERICAL SIMULATION OF SMALL SCALE ATMOSPHERIC TURBULENCE Ph.D. Thesis
Walton Edward McBride, III 1989 227 p
Avail: Univ. Microfilms Order No. DA9005392

A computer simulation of the effect of small scale turbulence on atmospheric sound propagation over a complex impedance boundary is developed. The atmosphere is broken up into spherically symmetric eddies characterized by a Gaussian profile for mu, the change from unity of the index of refraction. Each eddie is assigned a positive or negative sign randomly and is assumed to scatter sound impinging on it. Single scatter is assumed and a closed form of the first Born approximation for scattering is obtained, giving each eddie's contribution to the total fluctuation of the sound pressure at a receiver downrange. Because of its close relationship to the first Born approximation and its widespread use in the literature, the first Rytov approximation is also calculated. The first Rytov approximation was then adopted and a numerical simulation was accomplished with the concept of a realization, or

snapshot of the turbulent medium. Each eddie's scatter contribution was added up for a particular configuration of eddies, giving that realization's total sound pressure fluctuation. The eddies were then given a random change in their Cartesian coordinates up to a predetermined maximum of one meter. The predictions of the standard deviations of the amplitude fluctuations, amplitude probability distributions, and structure functions were then tested against experimental data. Two data runs with a horizontal source-receiver separation of 91 meters were used for comparison, using the same receiver in both cases. Good agreement was found whenever the average intensity of the fluctuations was well above the background noise level. Encouraged by these results, the numerical simulation was compared to data taken in a shadow zone caused by an upward refractive atmosphere. The advantages of the numerical simulation over the analytical approach are discussed, such as the calculation of any desired statistical quantity and also its geometrical flexibility. Dissert. Abstr.

N90-23180# Academy of Sciences of the Ukrainian SSR, Kharkov. Fiziko-Tekhnicheskij Inst.

SOUND WAVES IN WEAKLY IONIZED GAS

1988 7 p In RUSSIAN

(DE90-620704; KFTI-88-4) Avail: NTIS (US Sales Only) HC A02/MF A01

Dispersion properties of low-frequency oscillations in weakly ionized gas are considered. It is shown that the presence of charged component leads to sound wave dispersion. The region of modulation instability was determined for nonlinear wave packets. Possibility of existence of isolated waves is shown. DOE

N90-23181# Southampton Univ. (England). Inst. for Sound and Vibration Research.

NUMERICAL STUDIES OF THE ACTIVE CONTROL OF SOUND TRANSMISSION THROUGH DOUBLE PARTITIONS

P. Vitiello, P. A. Nelson, and M. Petyt Sep. 1989 60 p

(ISVR-TR-183; ETN-90-96447) Avail: NTIS HC A04/MF A01

The possibilities for the active control of sound transmission through double partitions are studied. A finite element analysis is undertaken of a double panel system with an enclosed air-gap. Secondary forces are applied between the two panels. The results are compared applying control strategies which minimize the vibrational energy of the radiating panel and minimize a numerical approximation to the sound power radiated. The former strategy gives far inferior performance to the latter. Attention is given to the accuracy of the numerical technique used for the computation of sound power radiation. The effectiveness of the control as a function of the dynamic properties of the radiating panel is considered. ESA

N90-23182# Max-Planck-Inst. fuer Stroemungsforschung, Goettingen (Germany, F.R.).

EXPERIMENTAL INVESTIGATIONS CONCERNING THE PROPAGATION OF SECOND-SOUND PULSES AT CRITICAL HEAT FLUX

G. Stamm, M. v.Schwerdtner, and W. Fiszdon (Polish Academy of Sciences, Warsaw.) Oct. 1989 26 p Presented at the 3rd Soviet-German Symposium on Cryogenics, Kharkov, USSR, 7-14 Oct. 1989 Sponsored in part by DFG

(MPIS-12/1989; ISSN-0436-1199; ETN-90-96471) Avail: NTIS HC A03/MF A01

The temporal evolution of the vortex line density was measured using a newly developed method and compared with theoretical predictions. Measurements of the temporal evolution of the pulse shape using a specially designed temperature probe at different distances from the heated cylinder show, in the supercritical region, the appearance of a second temperature maximum of the pulse which close to the heater may be larger than the amplitude of the shock front. Temperature measurements were performed to explore the influence of the bath temperature, heat flux, heating time, and the pulse repetition time on the evolution of the heat pulse. The experimental findings and the proposed semi-phenomenological model are compared. ESA

N90-23183# Centre de Recherches Scientifiques et Techniques de l'Industrie des Fabrications Metalliques, Brussels (Belgium). Section Construction Mecanique.

NOISE REDUCTION THEORY ACOUSTIC BARRIER CONSTRUCTION [LA REDUCTION DE BRUIT THEORIE CONSTRUCTION D'ENCEINTES ACOUSTIQUES]

Leo Janssen Nov. 1989 64 p In FRENCH Sponsored by Inst. pour l'Encouragement de la Recherche Scientifique dans l'Industrie et l'Agriculture

(CRIF-MC-87; ETN-90-96575) Avail: NTIS HC A04/MF A01

Research into noise barrier construction is presented. Noise damping, insulation from vibrations and acoustic dispersal are discussed. The noise attenuation measuring instruments, microphones and filters used in the experiments are described. Acoustic reference measurements are identified. Noise levels are measured in industrial work sites. Reverberation and absorption times are measured. Normal testing techniques are described. The use of acoustic absorption cladding and vibration dampers in reducing industrial noise pollution is described. Results of acoustic barrier tests around various types of noise producing machinery are presented. ESA

N90-23184# North Carolina Univ., Chapel Hill. Dept. of Surgery.

AUDITORY SPECTRO-TEMPORAL PATTERN ANALYSIS Final Progress Report, 1 Nov. 1988 - 31 Oct. 1989

Joseph W. Hall 5 Feb. 1990 7 p

(Grant AF-AFOSR-0083-87; AF Proj. 2313)

(AD-A218416; AFOSR-90-0267TR) Avail: NTIS HC A02/MF A01 CSCL 20/1

The major aims of the project were to establish what aspect of the across-frequency modulation pattern is utilized to obtain release from masking in modulated noise; to determine whether comodulation masking release (CMR) occurs for multi-component signals (as contrasted with puretone signals used for previous investigations); to determine whether CMR may apply to comodulation signals (in contrast with comodulated maskers used in previous investigations); to examine the possible relation between CMR and the MLD; and to examine the possible relations between CMR and temporal resolution. GRA

N90-23185# Rice Univ., Houston, TX. Dept. of Mathematical Sciences.

THE EFFECTS OF CAUSTICS IN ACOUSTIC INVERSE SCATTERING EXPERIMENTS Final Technical Report, 1 Nov. 1988 - 31 Oct. 1989

W. W. Symes and Cheryl Bosman Percell 2 Feb. 1990 91 p

(Contract N00014-85-K-0725; AF-AFOSR-0056-89; AF Proj. 2304)

(AD-A218454; TR89-3; AFOSR-90-0263TR) Avail: NTIS HC A05/MF A01 CSCL 20/1

Most inversion techniques described in the literature rely on the validity of ray tracing, which breaks down in the presence of caustics. The linearized acoustic inverse problem with constant reference velocity is analyzed in order to quantify the effects of a caustic in a probing wavefront on the scattered signal. When the sound velocity is perturbed by a localized, unidirectional, high frequency inhomogeneity, the surprising result obtained is that the energy in the scattered field is spread out if the perturbation is located on the caustic. This spreading of energy allows the construction of an oscillatory integral representation of the scattered field, which has the same form, whether or not an incident caustic is present. On the other hand, a sequence of localized high frequency sound velocity perturbations is constructed such that the size of the scattered signal relative to the size of the inhomogeneity becomes arbitrarily large as the support of the perturbation approaches the caustic. In regions where there are no caustics, a general inverse operator is found for smoothly varying reference velocities. This operator is shown to be equivalent to an inverse operator constructed by Beylkin. GRA

N90-23186# Netrologic, Inc., San Diego, CA.
LEARNING ENVIRONMENT FOR NEURAL NETWORKS AND TRANSIENT ACOUSTICS Final Report, 15 Aug. 1989 - 14 Feb. 1990
Dan Greenwood, Fareed Stevenson, Rod Taber, and Steve Deiss 14 Feb. 1990 39 p
(Contract N00014-89-C-0240; ONR Proj. RR-040-209)
(AD-A219000; TR-89-1-ONR) Avail: NTIS HC A03/MF A01 CSCL 20/1

As a result of this Phase 1 research program, a workstation which will enable the user to easily interact with the relevant neural network technologies was developed. The Tutor for Underwater Signature Analysis (TUSA) can predict a user's intentions and will provide assistance in an intelligent manner. Along with its intelligence, the system's other strength is its flexibility. TUSA can adapt or can be modified to suit the user's needs. In Phase 1, a framework was designed which incorporates the fundamental elements of an intelligent tutor and the elements were shown to interact productively. Combining conventional signal processing methods for detection and classification with advanced neural network paradigms will result in a very useful tool. Iterative improvement of TUSA's design through testing with sonar operators will provide a systems which will also be applicable to many scientific and engineering fields. GRA

N90-23187# Naval Ocean Systems Center, San Diego, CA. Transduction Sciences Branch.
CONTRIBUTIONS OF INDIVIDUAL STRUCTURAL MODES TO THE SCATTERED ACOUSTIC FIELD Final Technical Report
G. W. Benthien Nov. 1989 28 p Sponsored by Office of Naval Technology
(AD-A219128; NOSC/TR-1329) Avail: NTIS HC A03/MF A01 CSCL 20/1

The frequency behavior of the scattered acoustic field produced by a plane wave impinging on an elastic body immersed in an infinite fluid medium is dominated in certain frequency ranges by large peaks arising from resonant modes in the elastic structure. Computational models were developed at the Naval Ocean Systems Center for solving these elastic scattering problems. It is shown that the scattered pressure can be represented as a sum of contributions from in vacuo modes of each peak in the overall spectral response of the scattered field. In many cases a small number of modes dominate the response in the vicinity of these peaks. GRA

N90-23188# BBN Systems and Technologies Corp., Canoga Park, CA.
ASSESSMENT SYSTEM FOR AIRCRAFT NOISE (ASAN) CITATION DATABASE. VOLUME 1: USER'S MANUAL Final Report, 25 Feb. 1988 - 15 Feb. 1989
Nicolaas Reddingius Dec. 1989 74 p
(Contract F33615-86-C-0530; AF Proj. 3037)
(AD-A219175; BBN-6832-Vol-1; HSD-TP-89-011-Vol-1) Avail: NTIS HC A04/MF A01 CSCL 20/1

The Assessment System for Aircraft Noise (ASAN) includes a database of several thousand references to the literature on the impact of noise and sonic booms on humans, animals and structures. Bibliographic data, abstracts and critical reviews of key documents can be retrieved. A user's manual for the retrievable module is presented. It describes the types of searches that can be conducted, the options for each and explains all user screens. Installation instructions for the stand-along MS-DOS version are included. GRA

N90-23189# BBN Systems and Technologies Corp., Canoga Park, CA.
ASSESSMENT SYSTEM FOR AIRCRAFT NOISE (ASAN) CITATION DATABASE. VOLUME 2: DATABASE UPDATE MANUAL Final Report, 25 Feb. 1988 - 15 Feb. 1989
Nicolaas Reddingius Dec. 1989 75 p
(Contract F33615-86-C-0530; AF Proj. 3037)
(AD-A219176; BBN-6833-Vol-2; HSD-TP-89-011-Vol-2) Avail: NTIS HC A04/MF A01 CSCL 20/1

The Assessment System for Aircraft Noise (ASAN) includes a database of several thousand references to the literature on the impact of noise and sonic booms on humans, animals and structures. Bibliographic data, abstracts and critical reviews of key documents can be retrieved. The manual for the database maintenance module is presented. It is only intended for use by the critical maintenance organization to prepare new releases of the database. Several programs used to add, delete and update the database are discussed are needed together with Vol. 2 to properly maintain the database. GRA

N90-23190# BBN Systems and Technologies Corp., Canoga Park, CA.
ASSESSMENT SYSTEM FOR AIRCRAFT NOISE (ASAN) CITATION DATABASE. VOLUME 3: NEW CITATION REVIEW PROCEDURES Final Report, 25 Feb. 1988 - 15 Feb. 1989
Nicolaas Reddingius and Andrew B. Kugler Dec. 1989 61 p
(Contract F33615-86-C-0530; AF Proj. 3037)
(AD-A219177; BBN-6953-Vol-3; HSD-TP-89-011-Vol-3) Avail: NTIS HC A04/MF A01 CSCL 20/1

The Assessment System for Aircraft Noise (ASAN) includes a database of several thousand references to the literature on the impact of noise and sonic booms on humans, animals and structures. Bibliographic data, abstracts and critical reviews of key documents can be retrieved. A systematic methodology for the selection and evaluation of new citations to be added to the database consistent with the procedures used in CITASAN is described. GRA

72 ATOMIC AND MOLECULAR PHYSICS

Includes atomic structure, electron properties, and molecular spectra.

N90-23191# Rome Univ. (Italy). Dipt. di Fisica.
THEORETICAL AND COMPUTER SIMULATION STUDY OF THE DENSITY FLUCTUATIONS IN LIQUID WATER
M. A. Ricci, D. Rocca, G. Ruocco, and R. Vallauri (Consiglio Nazionale delle Ricerche, Florence, Italy) 7 Sep. 1989 59 p
(Preprint-697; ETN-90-96520) Avail: NTIS HC A04/MF A01

The hydrogen and oxygen density correlation functions are investigated. In a theoretical study, besides the ordinary sound mode, a high frequency optical-like collective mode is found to propagate through the hydrogen atoms. The dispersion relation of the two modes is discussed. Computer simulation results for the partial intermediate scattering functions are reported and confirm the theoretical predictions. The direct comparison of the theoretical predictions and the computer simulation results with experimental findings suggests an interpretation of the nature of the two modes. The collective character of the propagating modes is pointed out by comparing the self part of the scattering function with the total. ESA

N90-23192# Rome Univ. (Italy). Dipt. di Fisica.
LOW FREQUENCY RAMAN SPECTRA OF LIQUID WATER, A MOLECULAR DYNAMICS SIMULATION
Vittorio Mazzacurati, M. A. Ricci, G. Ruocco, and M. Sampoli (Florence Univ., Italy) 7 Sep. 1989 14 p
(Preprint-698; ETN-90-96521) Avail: NTIS HC A03/MF A01

A molecular dynamics simulation of the very low frequency depolarized Raman spectrum of water is presented and compared with the experimental data. The molecular trajectories of 108 water molecules, interacting via the TIP4P effective potential, were recorded during 200 ps at five thermodynamic states including the supercooled liquid. The Raman spectrum is calculated truncating the polarizability expansion at the first order dipole-induced-dipole term. The agreement of the simulated spectra with the experiments as far as lineshape and intensity is concerned, allows to ascribe the light scattering excess around the incident frequency to collision induced contributions, namely the dipole-induced-dipole spectrum. ESA

N90-23193# Rome Univ. (Italy). Dipt. di Fisica.
IMPROVING FERMION OPERATORS
G. Heatlie, C. T. Sachrajda, G. Martinelli, C. Pittori, and Gian Carlo Rossi (Aquila Univ., Italy) 8 Nov. 1989 5 p Submitted for publication
(Preprint-710; ETN-90-96533) Avail: NTIS HC A01/MF A01

Values of inverse lattice spacing in Monte-Carlo simulations are studied. Values of lattice renormalization constants of the bare currents obtained with different methods are reported. The Monte Carlo results are spread over a numerical interval which is definitively larger than quoted statistical errors, strongly suggesting sizeable effects. ESA

N90-23194# Rome Univ. (Italy). Dipt. di Fisica.
A POSTERIOR STOCHASTIC EQUATION FOR QUANTUM BROWNIAN MOTION
V. P. Belavkin 6 Dec. 1989 29 p Submitted for publication
(Preprint-715; ETN-90-96538) Avail: NTIS HC A03/MF A01

A continuous model for a nondemolition observation of an atom is given. An equation for the corresponding instrument is found and a stochastic dissipative Schroedinger equation for the unnormalized posterior wave function of the atom is derived. The continuously observed isolated atom is shown to relax to the ground state without mixing. A quantum stochastic model for a continuous diffusion measurement of an electron is given. An equation for the moments generating operator of the corresponding observables is derived and posterior equations for wave function and density matrix of the electron is found. Any mixed state of the electron under a complete nondemolition measurement is shown by example to tend exponentially to a pure stochastic state. ESA

N90-23195# Rome Univ. (Italy). Dipt. di Fisica.
THE NUMBER OF NEUTRINO SPECIES, CONFRONTED WITH THE RESULTS AT THE RECENT LEPTON-PHOTON SYMPOSIUM (AUGUST 7-12, 1989)
Giorgio Salvini 29 Aug. 1989 9 p
(Nota-Interna-940; ETN-90-96542) Avail: NTIS HC A02/MF A01

The value of the number of neutron species is deduced from results presented at the symposium. The value was obtained by assuming the mass of the Top quark to be larger than 78 GeV, with 90 percent C.L., in agreement with previous results. A mean value is presented after comparison of experimental results. ESA

N90-23196# Rome Univ. (Italy). Dipt. di Fisica.
THE 16-O PHOTODISINTEGRATION AT LOW ENERGIES
R. Marcovaldi 12 Oct. 1989 24 p
(Nota-Interna-941; ETN-90-96543) Avail: NTIS HC A03/MF A01

A review of the experimental data of the O-16 photodisintegration channels at low energies is presented. Combining both experimental and theoretical considerations, a suggestion is given on how to integrate the data available at low energies, pointing out some relevant quantities to be compared. ESA

N90-23197# Rome Univ. (Italy). Dipt. di Fisica.
RELATIVISTIC CORRECTIONS TO He-3 PHOTODISINTEGRATION SUM RULES
M. DeSanctis, A. Incicchitti, D. Prosperi, P. Belli, R. Bernabei, S. dAngelo, M. P. DePascale, P. Picozza, and M. Scafi 28 Oct. 1989 8 p
(Nota-Interna-942; ETN-90-96544) Avail: NTIS HC A02/MF A01

The role of the relativistic corrections to the electric dipole matrix-elements in the He-3 photodisintegration sum rules is investigated. A phenomenological model for the evaluation of the relativistic corrections and other non-standard effects in He-3 photodisintegration sum rules is presented. ESA

N90-23198# Groningen Rijksuniv. (Netherlands). Kernfysisch Versneller Inst.
AN EFFECTIVE He-3 NUCLEON FORCE FOR THE He-3, t) CHARGE EXCHANGE REACTION
S. Y. vanderWerf 1989 8 p Presented at the 6th Nordic Meeting on Nuclear Physics, Kopervic, Norway, 10-15 Aug. 1989 Submitted for publication Sponsored by Stichting voor Fundamenteel Onderzoek der Materie and Netherlands Organization for Scientific Research
(KVI-813; ETN-90-96701) Avail: NTIS HC A02/MF A01

The feasibility and limitations of a distorted wave born approximation approach to the (He-3, t) reaction formulated as a direct reaction in terms of an effective (He-3)-nucleon force is investigated. While the central V(sub tau) and the tensor component V(sub t tau) can be well determined, the spin-orbit force V(sub LS tau) cannot be used without a spin dependent normalization. Analysis of the analyzing power of the free process (He-3)(n,p)t indicates the need of an imaginary LS tau-component but does not solve the normalization problem. The evidence on energy dependence of the effective force components is discussed. ESA

N90-23199# Groningen Rijksuniv. (Netherlands). Kernfysisch Versneller Inst.
STUDY OF Sn-116 VIA NEUTRON PICKUP AND PROTON STRIPPING REACTIONS
J. M. Schippers, J. M. Schreuder, S. Y. vanderWerf, K. Allaart, N. Blasi, and M. Waroquier (Ghent Univ., Belgium) 1989 19 p Submitted for publication Sponsored by Nederlandse Organisatie voor Wetenschappelijk Onderzoek
(KVI-814; ETN-90-96702) Avail: NTIS HC A03/MF A01

The nucleus Sn-116 was studied via the neutron pickup reactions Sn-117 (d,t) Sn-116 and Sn-117 (He-3,alpha) Sn-116 and via the proton stripping reactions In-115(He-3,d) Sn-116 and In-115(alpha,t) Sn-116. Spectroscopic factors were deduced from the Sn-116(d,t) and the In-115(He-3,d) reactions for final states in Sn-116 below E sub x = 3.8 MeV. By combining the l transfers, observed in these reactions, spin assignments for various states can be given or limits on them can be set. Spectroscopic factors and their fragmentation are compared with those derived from the broken pair model and from a large basis shell model calculation involving both neutron quasi-particle excitations and proton 1p-1h excitations. ESA

N90-23200# City Coll. of the City Univ. of New York, NY.
SUPPORT FOR THE 16TH INTERNATIONAL CONFERENCE ON THE PHYSICS OF ELECTRONIC AND ATOMIC COLLISIONS Final Report, 1 Jun. - 30 Nov. 1989
Michael Lubell Jan. 1990 16 p Conference held in New York, NY, 26 Jul. - 1 Aug. 1989
(Grant AF-AFOSR-0252-89; AF Proj. 2301)
(AD-A218567; AFOSR-90-0216TR) Avail: NTIS HC A03/MF A01 CSCL 20/5

Topics covered included: Photons; Electron-Atom Collisions; Electron-Molecule Collisions; Electron-Ion Collisions; Collisions Involving Exotic Species; Ion-Atom Collisions; Ion-Molecule or Atom-Molecule Collisions; Atom-Atom Collisions; Ion-Ion Collisions; Collisions Involving Rydberg Atoms; Field Assisted Collisions; Collisions Involving Clusters; Collisions Involving Condensed Matter; Experimental Techniques; and Related Topics. Abstracts: Bremstrahlung of Electrons Scattered by Xenon Atoms; The Cs(p(t)) tH2 yields Cs H + H Reactive Collisions: Rotationally Resolved Cross Sections; Experimental and Theoretical Analysis of Collective Effects in Electron Impact Spectra; Resonance in Low Energy Electron. GRA

N90-23201# Clarkson Univ., Potsdam, NY. Div. of Research.
COLLECTIVE PROPERTIES OF NEURAL SYSTEMS AND THEIR RELATION TO OTHER PHYSICAL MODELS Final Report, 1 Dec. 1988 - 30 Nov. 1989
A. S. Fokas 12 Feb. 1990 5 p
(Grant AF-AFOSR-0148-89; AF Proj. 2304)

(AD-A219071; AFOSR-90-0304TR) Avail: NTIS HC A01/MF A01 CSCL 20/5

Solitons in multidimensions were characterized. It is well known that there exist several physically important equations in two dimensions (e.g., KdV, NLS) that support certain stable coherent structures called solitons. The solitons in the last 20 years have played an important role in the understanding of many physical and biological phenomena. Although there exist several equations in 3-D, which share many features with the soliton equations in two dimensions (e.g., KP, DS), these equations could not so far support soliton solutions. Coherent structures were found for such equations; these structures have many novel properties not found in the 1+1 solitons and they are called DROMIONS. The author and V. Zakharov have shown that in addition to Davey-Stewartson equation, many other physical significant nonlinear equations can support Dromions. GRA

73 NUCLEAR AND HIGH-ENERGY PHYSICS

Includes elementary and nuclear particles; and reactor theory.

For space radiation see *93 Space Radiation.*

N90-23202# Committee on Science, Space and Technology (U.S. House).

NUCLEAR POWER IN SPACE

1989 185 p Hearing before the Subcommittee on Energy Research and Development of the Committee on Science, Space, and Technology, 101st Congress, 1st Session, No. 60, 30 Sep. 1989

(GPO-23-835) Avail: Subcommitttee on Energy Research and Development, House of Representatives, Washington, D.C. 20515 HC free

Written and verbal testimony presented before the House Subcommittee on Energy Research and Development is documented. Current research efforts related to space nuclear power are discussed including the SP-100 Space Reactor Program, development of radioisotope thermoelectric generators, and the Advanced Nuclear Systems Program. Funding, research and test facilities, specific space mission requirements, and the comparison of solar and nuclear power systems are addressed. Witnesses included representatives from DOD, NASA, DOE, universities, and private industry. M.G.

N90-23203# Department of Energy, Richland, WA.

NATIONAL EMISSIONS STANDARDS FOR HAZARDOUS AIR POLLUTANTS APPLICATION FOR APPROVAL OF CONSTRUCTION SP-100 GROUND ENGINEERING SYSTEM TEST SITE

Apr. 1990 29 p

(Contract DE-AC06-87RL-10930)

(DE90-007985; DOE/RL-90-15) Avail: NTIS HC A03/MF A01

The following Application for Approval of Construction is being submitted by the U.S. DOE Richland Operations Office, for the SP-100 Ground Engineering System Test Site, which will provide a new source of radioactive emissions to the atmosphere. The U.S. DOE, NASA, and the U.S. DoD have entered into an agreement to jointly develop space nuclear reactor power system. A ground test of a reactor is necessary to demonstrate technology readiness of this major subsystem before proceeding with the flight system development and demonstration. It is proposed that the SP-100 test reactor be tested in the existing decommissioned Plutonium Recycle Test Reactor containment building (309 Building). The reactor will be operated for at least three months and up to 2 yr. Following the test, the 309 Building will be decontaminated for potential use in other programs. It is projected that this new source of emissions will contribute approximately 0.05 mrem/yr dose to the maximally exposed offsite individual. This application is being submitted in response to those projected emissions that would provide the described offsite dose. DOE

N90-23204# Maryland Univ., College Park. Dept. of Electrical Engineering.

INTENSE ELECTRON BEAM PROPAGATION ACROSS A MAGNETIC FIELD

X. Zhang, C. D. Striffler, R. L. Yao, W. W. Destler, and M. P. Reiser 1989 4 p Presented at the 1989 IEEE Particle Accelerator Conference, Chicago, IL, 20-24 Mar. 1989 Sponsored in part by AFOSR, Washington, DC

(Contract DE-AC05-85ER-40216)

(DE90-009993; CONF-890335-276) Avail: NTIS HC A01/MF A01

The propagation of an intense electron-ion beam across an applied magnetic field is considered. In the absence of the applied field, the beam system is in a Bennett equilibrium state that involves electrons with both large axial and thermal velocities and a cold stationary space charge neutralizing ion species. Typical parameters under consideration are V(sub o) approx. 1 MV, I approx. 5 kA, T(sub e) approx. 100 keV, and beam radii approx. 1 cm. It was found that in the intense beam regime, the propagation is limited due to space charge depression caused by the deflection of the electron beam by the transverse field. This critical field is of the order of the peak self-magnetic field of the electron beam which is substantially higher than the single particle cut-off field. DOE

N90-23205# Rome Univ. (Italy). Dipt. di Fisica.

QUARK-ANTIQUARK PAIR PRODUCTION VIA GAMMA W FUSION AT HIGH ENERGY E(+)E(-) COLLIDERS

M. Ciuchini, E. Franco (Istituto Nazionale di Fisica Nucleare, Rome, Italy), and E. Gabrielli 5 Oct. 1989 21 p Submitted for publication

(Preprint-705; ETN-90-96528) Avail: NTIS HC A03/MF A01

A measurement for the total cross section delta(mu) for the positron-electron (e+e-) interaction leading to ve+QdQbar(u), using the Weizsaecker-Williams approximation for the virtual photon is reported. This process is a possible background for the detection of an intermediate Higgs via its decay into QQbar pairs. The comparison with the signal allows us to conclude that actually it is not a problem for the Higgs search at high energy e+e- colliders. ESA

N90-23206# Groningen Rijksuniv. (Netherlands). Kernfysisch Versneller Inst.

INCOMPLETE FUSION REACTORS AT LOW AND INTERMEDIATE ENERGIES

R. H. Siemssen 1989 10 p Presented at the 1989 International Nuclear Physics Conference, Sao Paulo, Brazil, 20-26 Aug. 1989

(KVI-809; ETN-90-96700) Avail: NTIS HC A02/MF A01

A brief review of incomplete fusion reactions is given. The emphasis is placed on a confrontation of low and moderate energy data with those obtained at intermediate energies and with heavier projectiles. Incomplete momentum transfer and the decomposition of fusion-like cross sections are discussed. The vanishing of the fusion-like cross section at high energies is considered. Attention is payed to the question of whether or not there is a qualitative change in reaction mechanism as the energy increases. ESA

N90-23207# Naval Research Lab., Washington, DC.

MEASUREMENT OF PLASMA-NEUTRALIZED SUPER-VACUUM CURRENTS IN A GYROTRON CONFIGURATION Memorandum Report, Feb. 1988 - Sep. 1989

D. A. Kirkpatrick, S. H. Gold, W. M. Manheimer, W. M. Black, A. K. Kinkead, D. L. Hardesty, K. W. Killian, and M. Sucy (JAYCOR, Vienna, VA.) 16 Feb. 1990 20 p

(AD-A218505; NRL-MR-6595) Avail: NTIS HC A03/MF A01 CSCL 20/3

Experimental results are reported on the transport of an electron beam with current in excess of the vacuum space-charge limited value, in a configuration directly applicable to gyrotron oscillators. The vacuum space-charge limit is circumvented by the introduction of a neutralizing background plasma which is produced by an array of four plasma guns placed immediately downstream of the electron gun anode. GRA

N90-23208# Naval Research Lab., Washington, DC. Beam Physics Branch.
FOIL FOCUSING OF ELECTRON BEAMS
R. F. Fernsler, R. F. Hubbard, and S. P. Slinker 14 Mar. 1990 37 p
(ARPA Order 4395)
(AD-A219511; NRL-MR-6620) Avail: NTIS HC A03/MF A01 CSCL 20/7

Thin conducting foils focus charged particle beams through image charges induced on the foils. Such focusing has led to the suggestion that foils be used to transport intense, relativistic electron beams in high energy accelerators. Some of the limitations of foil focusing are examined including sensitivity to the beam parameters, emittance growth from anharmonic focusing, and beam stability in multi-foil transport. The analysis is based on a thin-lens, electrostatic treatment of paraxial beams. GRA

N90-23209# Naval Research Lab., Washington, DC. Beam Physics Branch.
STABILITY REGIMES IN A ROTATING QUADRUPOLE FOCUSING ACCELERATOR Interim Report
C. M. Tang, P. Sprangle, J. Krall, P. Serafim, and F. Mako (FM Technologies, Inc., Alexandria, VA.) 7 Mar. 1990 50 p
(AD-A219513; NRL-MR-6589) Avail: NTIS HC A03/MF A01 CSCL 18/1

A number of high current accelerator designs utilize strong focusing in the form of helical quadrupole and axial guide fields. A linear dispersion relation was obtained for an electron beam propagating in a cylindrical waveguide subject to helical quadrupole and longitudinal magnetic fields, electromagnetic waveguide modes and image fields. The electromagnetic waveguide modes are expressed in terms of right-hand and left-hand circularly polarized waves. It was found that the electron beam centroid, depending on the system parameters, can be: (1) orbit unstable independent of the waveguide modes, (2) three-wave unstable, or (3) fully stable. Analytic expressions for the various stability conditions are obtained in the limit of zero beam current, where the right-hand and left-hand circularly polarized waves decouple. Algebraic expressions for the growth rate in each of the three-wave unstable regimes are presented. The full dispersion relation is solved numerically with results that are in good agreement with both the stability conditions and the growth rate expressions. GRA

74 OPTICS

Includes light phenomena; and optical devices.
For lasers see *36 Lasers and Masers*.

N90-23210# Naval Ocean Systems Center, San Diego, CA. Optical Electronics Branch.
TRANSFER MATRICES FOR MULTIMODE OPTICAL FIBER SYSTEMS Final Report
C. J. Gabriel Dec. 1989 53 p Sponsored by David Taylor Research Center, Bethesda, MD
(AD-A218459; NOSC/TD-1717) Avail: NTIS HC A04/MF A01 CSCL 20/6

A transfer-matrix formalism for expressing the effect of a component on the mode-power distribution is discussed. It is expected this formalism will clarify and extend matrix approaches to the description of this effect presented by others and will result in component loss characterization methods that are independent of the launch conditions chosen to make the characterization. It is shown that a reduced-dimension transfer matrix can be defined in terms of a rectangular matrix transformation from the full-dimension mode space to a reduce-dimension space and its pseudo-inverse. Further, it is shown that the reduced-dimension space need not be a conventional mode-block partition. It is concluded that valid reduce-dimension representation should be attainable directly from vectorization of the near field patterns without first developing the mode distribution. GRA

N90-23211# Carnegie-Mellon Univ., Pittsburgh, PA. Dept. of Chemistry.
INVESTIGATION OF OPTICAL NONLINEARITIES, CONDUCTIVITY AND MAGNETISM IN ORGANOMETALLIC MATERIALS Final Report
Lawrence R. Sita 25 Jan. 1990 3 p
(Contract N00014-88-K-0578)
(AD-A218548) Avail: NTIS HC A01/MF A01 CSCL 07/3

Substantial progress was made in several key areas of the proposed research. With regard to the production of new materials via the organometallic doping of polydiacetylenes with diorganostannylenes, the steric and electronic factors which govern the reactivity of stannylenes towards alkynes are elucidated. New classes of cyclic organostannane compounds were produced which include the first examples of stanna cyclopropenes and 1,2-distanna cyclobut-3-enes. Derivatives of the latter ring system were found to be both air and moisture stable which allows them to be used as important synthetic precursors to new cyclic systems containing tin. Oxidation of a 1,2-distanna cyclobutene with iodine was achieved to produce an air and moisture stable tin-centered cationic species. Future work is being performed to produce monomers for ring-open polymerization via olefin metathesis which contain the 1,2-distannacyclobutene moiety. Upon oxidative doping, new ionic polymers maybe formed. Finally ab initio molecular orbital calculations were performed on the metallacyclopropenes of silicon, germanium, and tin and this information supports the model of reactivity and stability that was formulated for alkynes and stannylenes. GRA

N90-23212# Rochester Univ., NY. Inst. of Optics.
CLASSIFICATION TECHNIQUES FOR QUANTUM-LIMITED AND CLASSICAL-INTENSITY IMAGES Ph.D. Thesis
Miles N. Wernick Dec. 1989 151 p Sponsored in part by Army, and New York State Center for Advanced Optical Technology
(AD-A218693; ARO-24626.129-PH-UIR) Avail: NTIS HC A08/MF A01 CSCL 20/6

Automatic classification of both quantum-limited and classical intensity images is considered. A new discriminant vector for classical intensity images is proposed which can also be applied to general pattern recognition problems. The proposed discriminant vector, based on convex analysis, is shown in all cases to correctly distinguish two image classes. It is the discriminant vector that maximizes the minimum separation of the values obtained by forming the inner products between it and the input images. Experiments are reported in which the discriminant vector is used to successfully distinguish first two classes, then eight classes of images. The classification problem is also considered for the case of quantum-limited input images. Quantum-limited images arise as a matter of course in applications such as night vision, low dose electron microscopy, and radiological imaging. It can also be shown, however, that for reasons of computational efficiency it may be advantageous to use a quantum-limited imaging system as the input to the classifier. The thinner product between a quantum-limited image and a discriminant vector is shown to be a Monte Carlo estimator of the corresponding high light-level inner product. In principle, therefore, any linear classifier can be implemented using the quantum-limited system. New solutions designed for quantum-limited images are derived using statistical decision theory. These solutions are shown experimentally to provide excellent results. GRA

N90-23213# Pennsylvania Univ., Philadelphia. Dept. of Computer and Information Science.
IMAGE SEGMENTATION WITH DETECTION OF HIGHLIGHTS AND INTER-REFLECTIONS USING COLOR Interim Technical Report
Ruzena Bajcsy, Sang W. Lee, and Ales Leonardis Jun. 1989 24 p
(Contracts DAAL03-89-C-0031; F49620-85-K-0018; N00014-88-K-0630; N00014-85-K-0018; NSF MCS-82-19196; NSF IRI-84-10413)

(AD-A218710; MS-CIS-89-39; GRASP-LAB-182; ARO-26779.3-EL-AI) Avail: NTIS HC A03/MF A01 CSCL 20/6

An approach is presented to the construction of a computational model for color image segmentation based on the physical properties of sensors, illumination lights and surface reflectances. Using the established model, color image segmentation are performed and small inter-reflections as well as highlights are detected. GRA

N90-23214# Duke Univ., Durham, NC.
FREQUENCY DOMAIN TECHNIQUES FOR ANALYZING PICOSECOND OPTICAL PULSES Final Report, 10 May 1988 - 1 Oct. 1989
John C. Swartz, Bob D. Guenther, and Frank C. DeLucia 1 Feb. 1990 90 p
(Contract DAAL03-88-C-0014)
(AD-A218856; ARO-25822.3-PH) Avail: NTIS HC A05/MF A01 CSCL 17/5

Using the techniques of Fourier analysis, any periodic time domain function will have a unique frequency domain transform. It is therefore possible to use frequency domain measurements to understand a time domain signal. Fourier analysis implies that picosecond laser pulses would have frequency components which range into the microwave bands. The technique of picosecond demodulation is one way of generating microwaves from laser pulses. Picosecond demodulation uses laser pulses to generate electron bunches at a photocathode. The electron bunches are then accelerated and radiate electromagnetic waves. Based on this technique it is possible to measure the microwave spectrum of a picosecond optical pulse training. This report develops the theory of picosecond demodulation and shows that the frequency spectrum generated is related to the Fidrier transform of the time domain envelope of the laser pulse train. Based on the theoretical development, a prototype device, called a picosecond demodulator, has been built. Using this device, several experiments are reported which (1) verify the theory of picosecond demodulation and (2) demonstrate that frequency domain techniques can be used to characterize picosecond pulses. These results indicate that frequency domain techniques are easy and inexpensive to implement and provide an accurate supplement to time domain measurements using auto-correlators or streak cameras. GRA

N90-23215# Sparta, Inc., Lexington, MA.
AGILE MULTIPLE APERTURE IMAGER RECEIVER DEVELOPMENT Final Report, 15 Aug. 1989 - 14 Feb. 1990
David E. B. Lees and Robert F. Dillon 13 Feb. 1990 44 p
(Contract N00014-89-C-0200)
(AD-A218956; LTR90-001) Avail: NTIS HC A03/MF A01 CSCL 20/6

A variety of unconventional imaging schemes have been investigated in recent years that rely on small, unphased optical apertures (subaperture) to measure properties of an incoming optical wavefront and recover images of distant objects without using precisely figured, large aperture optical elements. Such schemes offer several attractive features. They provide the potential to create very lare effective aperture that are expandable over time and can be launched into space in small pieces. Since the subapertures are identical in construction, they may be mass producible at potentially low cost. A preliminary design for a practical low cost optical receiver is presented. The multiple aperture design has high sensitivity, wide field-of-view, and is lightweight. A combination of spectral, temporal, and spatial background suppression are used to achieve daytime operation at low signal levels. Modular packaging to make the number of receiver subapertures conveniently scalable is also presented. The design is appropriate to a ground-base proof-of-concept experiment for long range active speckle imaging. GRA

N90-23216# Rochester Univ., NY. Inst. of Optics.
HYBRID DIFFRACTIVE-REFRACTIVE TELESCOPE
Thomas W. Stone 1990 11 p Repr. from SPIE, v. 1212, 1990 p 1
(Contract DAAL03-86-K-0173)
(AD-A219241; ARO-24626.137-PH-UIR) Avail: NTIS HC A03/MF A01 CSCL 14/1

Telescopes, microscopes, and similar compound systems often require achromats for objectives, since the longitudinal chromatic aberration from a singlet objective is so large that eyepieces cannot easily correct it. Such achromats can limit large aperture systems because the curvatures required of their components are much stronger than the curvatures of singlets with the same net optical power. The hybrid diffractive-refractive telescope formed by combining a diffractive eyepiece with an unachromatized refractive objective is shown to eliminate the need for such bulky objectives, since a diffractive eyepiece is capable of correcting the large longitudinal chromatic aberrations of singlet refractive objectives. By splitting the holographic eyepiece into two elements, paraxial lateral color may also be corrected. First-order design considerations in these hybrid telescopes are presented, and a practical hybrid telescope layout is developed in which: (1) primary chromatic aberration is eliminated; (2) paraxial lateral color is corrected; and (3) a useful eye relief is obtained. GRA

N90-23217# Rome Air Development Center, Griffiss AFB, NY.
SOME RAY TRACING PROBLEMS RELATED TO CIRCLES AND ELLIPSES Report, May - Jul. 1988
Henning Bach Mar. 1989 47 p
(AF Proj. 2305)
(AD-A219306; RADC-TR-89-31) Avail: NTIS HC A03/MF A01 CSCL 20/6

A classical ray tracing problem, namely the celebrated Alhazen Mirror Problem, is reviewed. An alternative formulation of the law of reflection, leading, in the spherical mirror case, directly to Alhazen's equation is presented. The locus method of ray tracing is introduced and applied to Alhazen's problem. Finally, the technique is applied to some ray tracing problems, which often occur in practice, namely reflection by a circular cylinder and diffraction by a circular edge. Although these problems cannot in general be solved analytically, a technique is devised that may save considerable amounts of computer time in actual applications. GRA

N90-23218# ERG Systems, Inc., Saint James, NY.
FULL SURFACE INTERFEROMETRIC TESTING OF GRAZING INCIDENCE MIRRORS Final Report
John L. Remo Feb. 1990 72 p
(Contract N00014-89-C-0199)
(AD-A219394) Avail: NTIS HC A04/MF A01 CSCL 20/6

This contract demonstrated the proof-of-principle of the Full Surface Interferometric Scanner (FSIS), an instrument which can rapidly and reliably measure both the full surface figure as well as the macroroughness of grazing incidence optics. The FSIS has the potential to fill the need of SDIO to characterize and qualify the necessary off-axis aspherical mirror technology that will be used for weapon pointing, beam control, and beam propagation through several environments and countermeasures. This instrument design is based on the use of normal incidence, sub-aperture interferometry and wavefront shearing interferometry which surmounts many of the problems encountered by other (e.g., long trace profilers) techniques. This new system, the FSIS, for which we have developed a breadboard system which makes novel use of three sequential operations: sub-aperture slope measurement, wavefront integration, and surface profile synthesis. It appears that the FSIS will find application in X ray and UV high resolution lithography, medical imaging, astronomy, physics, microbiology, and industrial (surface) quality control. GRA

N90-23219# George Mason Univ., Fairfax, VA.
ANALYSIS AND EVALUATION OF TECHNICAL DATA ON THE PHOTOCHROMIC AND NON-LINEAR OPTICAL PROPERTIES OF MATERIALS Quarterly Technical Report, No. 5
Robert F. Cozzens 15 Mar. 1990 7 p
(Contract DAAB07-89-F404; ARPA Order 6631)
(AD-A219398) Avail: NTIS HC A02/MF A01 CSCL 20/6

The principle goal of this effort is to provide technical assistance

to DARPA in evaluating data on materials, especially polymers, that may be useful in the development of limiters and switches for the protection of eyes and electro-optic sensors from exposure to damaging levels of laser radiation. A principle task is to assist in the development of a predicative capability in assessing the viability of various approaches and devices and to assess theoretical limitations in the use of organic materials as optical switches and limiters. GRA

75 PLASMA PHYSICS

Includes magnetohydrodynamics and plasma fusion.
For ionospheric plasmas see *46 Geophysics*. For space plasmas see *90 Astrophysics*.

N90-23220# Academy of Sciences of the Ukrainian SSR, Kharkov. Inst. of Radio Astronomy.
GAS DYNAMIC THEORY OF FLIGHT OF FAST ELECTRON FLUX IN PLASMA
V. N. Melnik 1988 25 p In RUSSIAN; ENGLISH summary
(DE90-618767; INIS-SU-157/A) Avail: NTIS (US Sales Only) HC A03/MF A01

The one-dimensional flight of a fast electron flux in plasma is investigated taking into account generation and absorption of plasma waves. The transition from the kinetic description to the gas dynamics is made. The closed set of gas dynamic equations for electrons and plasmons is derived and an automodel solution is obtained in the case of instantaneous injection. This solution represents the beam-plasma formation on natural oscillations in the system electrons+plasmons is considered. DOE

N90-23221# JAYCOR, Torrance, CA. Plasma Technology Div.
THERMAL BARRIER RESEARCH Final Report, Sep. 1985 - Jun. 1986
K. G. Moses Mar. 1990 7 p
(Contract DE-FG03-85ER-51095)
(DE90-009213; J-550-90-601/2454) Avail: NTIS HC A02/MF A01

The thermal barrier region in the TARA device is a complex arrangement combining ion plugging by sloshing ions with an ECRH generated thermal barrier plasma. An axisymmetric, high mirror ratio magnetic field, adjacent to the central cell, provides the confinement of the thermal barrier plasma and sloshing ions. Research being done in this thermal barrier region is discussed. DOE

N90-23222# Texas Univ., Austin. Inst. for Fusion Studies.
RESONANT MHD MODES WITH TOROIDAL COUPLING
J. W. Connor, R. J. Hastie (United Kingdom Atomic Energy Authority, Culham, England), and J. B. Taylor Mar. 1990 15 p
(Contract DE-FG05-80ET-53088)
(DE90-010077; DOE/ET-53088/426; IFSR-426) Avail: NTIS HC A03/MF A01

In a cylindrical plasma, tearing modes can be calculated by asymptotic matching of ideal mhd solutions across a critical layer. This requires a quantity delta' which represents the discontinuity in the ideal solution across the layer. In a torus, poloidal harmonics are coupled and there are many critical surfaces for each toroidal mode number, and correspondingly many discontinuities delta'(sub m). The ideal mhd solutions do not determine the delta'(sub m) but only a relation between them--described by an E-matrix. We discuss the calculation of the E-matrix for a large aspect-ratio tokamak. In a weak-coupling approximation it is tri-diagonal and can be computed from integrals over the uncoupled eigenfunctions or from simple basis-functions comprising triplets of coupled poloidal harmonics. This weak coupling approximation fails if delta'(sub m) is already small for an uncoupled harmonic. An alternative strong-coupling approximation is developed for this case. DOE

N90-23223# Academy of Sciences of the Ukrainian SSR, Kharkov. Fiziko-Tekhnicheskij Inst.
NUMERICAL METHODS FOR THE PROBLEM OF THE FREE-BOUNDARY PLASMA EQUILIBRIUM IN A STELLARATOR (TORSATRON)
1988 12 p In RUSSIAN
(DE90-620580; KFTI-88-10) Avail: NTIS (US Sales Only) HC A03/MF A01

Solution of the neutralized equation of plasma equilibrium in a stellarator was obtained with the use of Green function method. Numerical algorithm, using mobile calculation grid and approximation of magnetic field of the real helical winding with assigned accuracy was developed. Calculation results show that increase of plasma pressure in stellarator leads both to change of the structure of internal magnetic surfaces and sufficient deformation of plasma boundary. DOE

N90-23224# Stuttgart Univ. (Germany, F.R.). Inst. fuer Plasmaforschung.
ANALYTICAL THEORY OF THE BUNEMANN INSTABILITY FOR ELECTRON RUNAWAY
H. J. Kaeppeler Oct. 1988 13 p
(IPF-88-3; ETN-90-96466) Avail: NTIS HC A03/MF A01

Analytical expressions for the growth rate of the Bunemann instability caused by runaway electrons are presented. A simplified dispersion relation including an applied time-variable electric field is derived and an approximate analytical expression for the temporal growth rate is given. The magnetic field is assumed to be zero. ESA

N90-23225# Stuttgart Univ. (Germany, F.R.). Inst. fuer Plasmaforschung.
[ACTIVITIES REPORT OF THE INSTITUTE FOR PLASMA RESEARCH] Annual Report, 1988
1988 30 p
(ETN-90-96467) Avail: NTIS HC A03/MF A01

The 1988 activities of the German Institute for Plasma Research are reported. The main research fields are: Electron Cyclotron Resonance Heating (ECRH), plasma theory focus and technology, laser diagnostics and the Wega stellarator experiment. The activities of the ECRH group were mainly directed to the final construction, operational tests and operation of the 70 GHz microwave system on W VII-AS in Garching. The development of high power 140 GHz transmission lines and quasi-optical components for transmission was continued. The theory group made calculations on ray tracing and transport, plasma simulations and nonlinear waves. The Lidar-Thomson-scattering-system operating at JET will be upgraded for 10 Hz repetition rate. In the far-infrared collective scattering experiment on ASDEX the ohmic phase and the H-mode during neutral beam injection was investigated. In the plasma focus group, a better understanding of the focus-physics was achieved. The studies of the magnetic field configurations in stellarators by means of an electron beam were extended to W VII-AS. The research in the field of plasma technology was continued. ESA

N90-23226# Rome Univ. (Italy). Dipt. di Fisica.
INTERMITTENCY AND MULTIFRACTALITY IN MAGNETIC DYNAMOS
M. Falcioni, G. Paladin, and A. Vulpiani (Istituto Nazionale di Fisica Nucleare, Rome, Italy) 25 Sep. 1989 11 p
(Preprint-702; ETN-90-96525) Avail: NTIS HC A03/MF A01

The convection of magnetic fields in presence of Lagrangian chaos (when nearby fluid elements diverge exponentially in time) is studied. The magnetic field is shown to be of a multifractal nature as a consequence of the spatial fluctuations in the exponential growth of the field. Numerical and theoretical evidence that the magnetic fields can concentrate in small domains of a fluid with weak Lagrangian chaos is given. These properties are also relevant for the study of the case of small but non-zero magnetic diffusivity. ESA

N90-23227# Rome Univ. (Italy). Dipt. di Fisica.
DISPLACEMENT FLOW AND DEUTERON DRAG IN A METAL: A PATH TOWARDS COLD FUSION
Eugenio Tabet (Istituto Superiore di Sanita, Rome, Italy) and Alexander Tenenbaum 27 Sep. 1989 13 p Presented at the Understanding of Cold Fusion Phenomena Workshop, Varenna, Italy, 15-16 Sep. 1989
(Preprint-703; ETN-90-96526) Avail: NTIS HC A03/MF A01

A model recently proposed to account for cold fusion processes on the basis of a lattice collapse in the host metal is developed. A deuteron drag phenomenon, which considerably enhances the neutron yield, is described. Quantitative estimates for the neutron emission are given as a function of thermodynamic parameters of the metal-deuterium system. ESA

N90-23228# Army Military Personnel Center, Alexandria, VA.
TRANSPORT PROPERTIES OF PLASMAS IN MICROWAVE ELECTROTHERMAL THRUSTERS M.S. Thesis
Scott S. Haraburda 1990 132 p
(AD-A219408) Avail: NTIS HC A07/MF A01 CSCL 20/9

The microwave electrothermal thruster is a potential propulsion system for spacecraft applications such as platform station keeping. It is a thruster which allows no contact between the electrodes and the propellant. For this thruster, the electromagnetic energy is transferred to the electrons in the plasma region of the propellant using the TM011 and TM012 modes of a microwave cavity system. The collisional processes by the electrons with the propellant causes transfer of the energy. Work was done to study these processes using several diagnostic techniques - calorimetry, photography, and spectroscopy. Experimental results of these techniques for nitrogen and helium gases are included. These diagnostic techniques are important in understanding plasma phenomena and designing practical plasma rocket thrusters. In addition, a broad theoretical background is included to provide a fundamental description of the plasma phenomena. GRA

76 SOLID-STATE PHYSICS

Includes superconductivity.

For related information, see also *33 Electronics and Electrical Engineering* and *36 Lasers and Masers.*

N90-23229 Tufts Univ., Boston, MA.
SUPERCONDUCTING AND NORMAL COMPOUNDS: SOME HIGH FIELD/HIGH PRESSURE EFFECTS Ph.D. Thesis
Scott Harris Bloom 1989 228 p
Avail: Univ. Microfilms Order No. DA8920013

Experimental results of the effects of high pressure and/or high magnetic fields are presented for three different classes of compounds: magnetic systems based on high temperature superconductors, a heavy fermion system, and a ferromagnetic semiconductor. The experiments involving high temperature superconductors consisted of substituting either Gd for Y or Zn for Cu in the canonical Y-based 1-2-3 compound. For the Gd substituted compound, high pressure had a small positive effect on T(sub N), the magnetic ordering temperature, in both the superconducting and non-superconducting phases. This result is discussed in terms of a modified RKKY-like interaction between the Gd ions. For the Zn-doped compound T(sub c) dropped rapidly upon the addition of small amounts of Zn with T(sub c) going to zero at approximately 10 at. percent Zn. Additionally, T(sub c) decreased upon application of high pressure in contrast to the undoped system which showed T(sub c) increasing with pressure. These results indicate that the d-holes associated with the Cu-O hybridized bonds are becoming localized in the presence of Zn. For the heavy fermion compound U(In(sub 1-x)Sn(sub x))3, large enhancements in the specific heat and magnetic susceptibility, indicative of heavy fermion behavior were observed near x = 0.6. Theoretical fits to Fermi liquid type theories show reasonable agreement with experimental results. For U(Ga(sub 1-x)Ge(sub x))3 no enhancement in the specific heat or magnetic susceptibility was observed. However one unusual property of this compound is that the magnetic susceptibility increased from low to room temperature indicative of a very high spin fluctuation temperature, and therefore, very strong f-electron-conduction electron hybridization. The third compound UFe4P-12 is the first known U-based ferromagnetic semiconductor. This compound displayed a large shift in T(sub c) with the application of high pressure. This result appears consistent with a Bloembergen-Rowlands coupling mechanism between the U-atoms. Dissert. Abstr.

N90-23230 California Univ., Berkeley.
ELECTRONIC THEORY OF SOLIDS, SURFACES, INTERFACES, AND CLUSTERS Ph.D. Thesis
Shengbai Zhang 1989 235 p
Avail: Univ. Microfilms Order No. DA9006579

The electronic and structural properties of several prototype condensed matter systems are studied using ab-initio pseudopotentials and local density functional (LDA) theory. A quasiparticle theory is also developed and used in place of the LDA for computing excited state properties. The goal is to elucidate the relationship between the electronic structure and various physical properties for these systems. Applications are presented for a wide range of systems including covalent bulk semiconductors, surfaces, interfaces, and simple metal clusters. Specific applications include: The bondlengths of AB crystals of different structures including intermetallic compounds are determined using first principles pseudopotential s-orbital radii. The behavior of III-V compounds under pressure is investigated. Several possible structural models for the Si surface with Ge adsorption are examined. The GaAs/110/ surface is studied. It is found that the surface relaxation is unstable for Al/GaAs/110/ interface and the vanished gap states reappear. Mechanisms for the formation of Schottky barriers are also examined. For simple metal heteroclusters, Na(n)Mg, it is found that the Na-Mg bonding is unimportant. Using a quasiparticle theory, which is developed for systems without inversion symmetry, the properties of excited states were determined. The valence band offset and the band structures for ultrathin superlattices of GaAs-AlAs/001/ are obtained using this theory. Dissert. Abstr.

N90-23231 Cleveland State Univ., OH.
THE EFFECT OF ELEVATED GRAVITY ON THE CRYSTALLIZATION OF THE MFI ZEOLITES, ZSM-5, AND SILICALITE Thesis
Wha Jung Kim 1989 212 p
Avail: Univ. Microfilms Order No. DA9005157

The effect of applying an elevated gravitational force on the crystallization of zeolites, in particular, ZSM-5/Silicalite was studied. Experiments were performed to evaluate the influence of gravity on crystal growth rate, size, product yield, and crystal morphology. These results were used to postulate a fundamental synthesis mechanism for zeolite crystals produced under the effects of elevated gravitational field. All the experimental work was carried out at 180 C and different gravities, 1, 10, 30, and 50 G. The molar composition of reaction mixture used for silicalite synthesis was 100SiO2 - 2800H2O - 2.55Na2O - 5TPABr. All the experimental conditions and sources of reactants were kept constant. Three different experimental systems were applied to the above molar composition. The first set of experiments was carried out at one day intervals under gravity conditions, 1, 30, and 50 G. In the second set of experiments, the reaction mixtures were prepared using different silica source, that is, amorphous precipitated silica while the other sources and experimental conditions were kept constant. These experiments were carried out for one day intervals under 1 and 50 G. In final set experiments, the combinations of high and normal gravities were applied and the reactions were carried out under the mixtures of high and normal gravities. Results for all the runs showed the substantial enhancements in crystal size, product yield and a reduction in the reaction time when compared to the normal gravity. Although more extensive experimentation is required to completely understand the role of gravity, the most significant conclusion that can be drawn from this work is that the synthesis of zeolite under an elevated

gravitational field enhances zeolite crystal size and yield.
Dissert. Abstr.

N90-23232 Minnesota Univ., Minneapolis.
THE ONSET OF SUPERCONDUCTIVITY IN TWO-DIMENSIONAL DISORDERED SYSTEMS Ph.D. Thesis
David Brant Haviland 1989 180 p
Avail: Univ. Microfilms Order No. DA9005234

Investigations of ultra-thin films grown by quench-evaporation and studied in-situ show an interesting evolution of normal and superconducting properties as the films are made thinner. The films are categorized into two different classes based on the nature of the evolution of superconductivity in each class: granular and homogeneous. Granular films show rich behavior which is believed to be due to quantum fluctuations of the phase of the superconducting order parameter, such as quasi-resistance of the resistance vs. temperature (R(T)) curves. The onset of quasi-reentrant behavior is correlated with the activation energy of normal state conduction becoming the order of the superconducting gap, where the normal state conduction is modeled by a hopping conduction mechanism in the presence of strong Coulomb interactions. This Josephson coupling of superconducting grains on a local scale gives way to global superconducting coupling as the film is made thicker and less resistive. Homogeneous films begin to conduct at extremely low thickness, and do not exhibit complicated quasi-reentrant behavior in the evolution of superconductivity. The first appearance of superconductivity is a separation of R(T) curves at the lowest temperature attainable. The curves separate between the apparently insulating, and apparently superconducting behavior. In Bi this separatrix occurred at a normal state sheet resistance near h/4e squared, however in Pb and Al the separatrix was above this value. The Al film showed distinct signs of granularity which also cannot be ruled out in the Pb films, because strong suppression of the superconducting transition temperature T(sub c) make it difficult to observe properties associated with granularity. The suppression of T(sub c) is analyzed in light of theories which incorporate the effects of localization, and little agreement is found. However T(sub c) is found to decrease as the inverse film thickness which may be explained by a boundary effect within the context of the Ginzburg-Landau Theory. Dissert. Abstr.

N90-23233 California Univ., Berkeley.
THERMAL PHENOMENA IN HIGH-Tc THIN FILM SUPERCONDUCTORS Ph.D. Thesis
Markus Ivo Flik 1989 123 p
Avail: Univ. Microfilms Order No. DA9006324

Thin films of the recently discovered high-T(sub c) superconductors are the basic elements in highly promising hybrid electronic circuits and detector devices. Two heat transfer problems resulting from the application of high-T(sub c) thin films thermal stability, and thermal conduction in these devices are analyzed. The criterion of intrinsic thermal stability of superconductors, which predicts the maximum operating current for which no Joule heating occurs due to a thermal disturbance is introduced. A parametric study concerning a localized thermal disturbance in a thin-film superconductor shows that the maximum stable current decreases with increasing strength of the thermal disturbance, and that it increases for an augmented heat transfer coefficient and for an increasing ratio of the width of the film to its thickness. Low temperature scanning electron microscopy (LTSEM) is a powerful technique to characterize the local properties of thin film superconductors. The application of the criterion of intrinsic thermal stability to LTSEM determines the maximum bias current for which no voltage is measured along the film for any beam position. The theoretical predictions are in very good agreement with experimental data for superconducting lead films on sapphire substrates. This study shows that at low temperatures, the phonon mean free path in bulk YBa2Cu3O7 is of the order of the thickness of thin film superconductors. In this case, boundary scattering reduces the thermal conductivity with decreasing film thickness. A simple method, which rests solely on geometric arguments, accounts for the size effect on conduction in thin films. The model is also employed to analyze conduction across the film and the influence of anisotropy. Dissert. Abstr.

N90-23234 United Kingdom Atomic Energy Authority, Harwell (England).
A STUDY OF THE RELATION BETWEEN GRAIN BOUNDARY TYPE AND SENSITISATION IN A PARTIALLY-SENSITISED AISI 304 STAINLESS STEEL USING ELECTRON BACK-SCATTERING PATTERNS
S. R. Ortner and V. Randle (Brunel Univ., Uxbridge, England) Oct. 1988 20 p
(AERE-R-13327) Copyright Avail: Issuing Activity

Electron backscattering (ebs) patterns were used to measure the orientations of grains in lightly sensitized 304. The misorientations across grain boundaries were calculated, and correlated with the extent of attack on the boundaries by an electrochemical test designed to reveal sensitization due to Cr depletion. Low-angle boundaries were found to be unsensitized. Twin boundaries were either unsensitized or partly sensitized, probably reflecting the difference between coherent and incoherent twin boundaries. The majority of general, high angle boundaries were found to be completely sensitized, but a significant fraction were unsensitized or only partly sensitized, showing that a variation in susceptibility to sensitization exists even among general, high angle boundaries. High angle boundaries (other than twins) with coincident site lattice misorientations were distinguishable from general high angle boundaries in this respect. The ebs technique is a rapid and useful method of measuring grain boundary misorientations. Author

N90-23235 Saint Andrew's Univ. (Scotland).
OPTICAL PROPERTIES OF NOVEL GaAs-BASED SEMICONDUCTORS Ph.D. Thesis
Ian Thomas Ferguson 1989 326 p
Avail: Univ. Microfilms Order No. BRDX87930

The optical properties of III-V semiconductors and quantum well structures are considered. Detailed optical assessment of the near band-edge luminescence from high quality Al(0.48)In(0.52)As including the use of photoluminescence excitation and the application of hydrostatic pressure is reported. The emission is dominated by a broad luminescence band too large to be accounted for by a simple model of alloy scattering of an excitonic transition. The observation of structure in the free exciton emission from InP was tentatively assigned to polaritons. Scattering of the polariton from neutral donors was proposed as an explanation of the excitation power density dependence of the emission structure. Exciton emission from quantum well heterostructures was also studied. In Ga(0.47)In(0.53)As-InP the exciton was found to be bound to potential fluctuations in the well. The very narrow linewidths observed in the GaAs-Al(x)Ga(1-x)As wells were comparable with the best values reported elsewhere. A detailed study of the growth and luminescence from thin GaAs-Al(x)Ga(1-x)As wells on substrates misorientated towards the (110) direction was undertaken. Dissert. Abstr.

N90-23236 Illinois Univ. at Urbana-Champaign, Savoy.
SINGLE CRYSTAL NMR OF HIGH TEMPERATURE SUPERCONDUCTORS Ph.D. Thesis
Charles Holloway Pennington 1989 145 p
Avail: Univ. Microfilms Order No. DA9010984

Cu NMR studies of the high temperature superconductor YBa2Cu3O(7-delta) (T sub c = 90 K) using a 1 mg single crystal is reported. Three types of measurements were made for both the plane and chain Cu crystallographic sites and with the static magnetic field placed successively along each of the three crystal axes a, b, and c: nuclear magnetic resonance (NMR) lineshapes, spin-lattice relaxation, and transverse relaxation. From these measurements four NMR tensors are deduced: the magnetic shift tensor, the electric field gradient tensor, the spin-lattice relaxation rate tensor, and the transverse relaxation rate tensor. As a preliminary matter, the symmetries of the magnetic shift and electric field gradient tensors were used to assign the two families of

NMR lines to their respective crystallographic sites. From an analysis of the electric field gradient tensors it is shown that both the plane and chain Cu have valences Cu(2+), giving a single hold in the Cu atomic d-shell. The spin-lattice relaxation rate and magnetic shift of the plane and chain Cu were analyzed; included were both analyses in which only normal state data were considered, and in which superconducting state measurements of magnetic shifts were considered as well. These analyses show that the plane Cu atom behaves very nearly as a local moment. The chain Cu is probably also in the local moment limit; however, its NMR properties are largely determined by its interaction with oxygen holes in the chain. Author

N90-23237 Illinois Univ. at Urbana-Champaign, Savoy.
A LOW TEMPERATURE CALORIMETRIC STUDY OF SEVERAL HIGH-T(SUB c) SUPERCONDUCTORS Ph.D. Thesis
Mark Edwin Reeves 1989 199 p
Avail: Univ. Microfilms Order No. DA9010996

Sintered powders of La(1.85)Ba(0.15)CuO(4), La(1.8)Sr(0.2)CuO(4), YBa(2)Cu(3)O(7-x), and GdBa(2)Cu(3)O(7-x) were prepared by solid state reaction. The samples were carefully characterized for impurities by x ray diffraction and Raman spectroscopy. The resistivity and magnetic susceptibility of each sample was measured to characterize its superconducting transition. The specific heat of the samples was measured with an adiabatic, computer-controller calorimeter. The specific heat discontinuity for GdBa(2)Cu(3)O(7-x) was determined, and antiferromagnetic ordering and superconductivity were observed to coexist in this sample. For all the samples, a temperature dependent phonon density of states was inferred from the specific heat measured above 10 K. While the temperature range of the measurements extended from 2 to 180 K, particular attention was paid to the specific heat below 10 K. In this temperature range, the lattice and electronic contributions to the specific heat could be separated. In all the samples measured except for GdBa(2)Cu(3)O(7-x) an unexpected linear contribution to the specific heat was observed. By systematically eliminating the known impurities in a sample of YBa(2)Cu(3)O(7-x) and still observing the linear contribution, an argument is made against attributing this contribution to a parasitic phase. The magnetic field dependence of the specific heat of YBa(2)Cu(3)O(7-x) was determined for fields from O to 3T and in the temperature range 2 to 10 K. The field dependence was compared to a calculation based on Ginzburg-Landau theory. The theory did not predict the experimental results. Author

N90-23238# Lehigh Univ., Bethlehem, PA. Dept. of Physics.
THE EFFECTS OF POINT DEFECTS AND COMPOSITION ON STRUCTURAL PHASE TRANSITION
Jean Toulouse 1990 9 p
(Contract DE-FG02-86ER-45258)
(DE90-010109; DOE/ER-45258/4) Avail: NTIS HC A02/MF A01

Three systems have been studied: KTa(1-x)Nb(x)O3, KZnF(3):Li and KMnF3:Li. The initial goals of the study were to develop the necessary experimental capabilities, to identify the nature of the defects, and to characterize the effect of these defects on the phase transition. These goals were successfully reached. DOE

N90-23239# Joint Inst. for Nuclear Research, Dubna (USSR).
INFLUENCE OF HIGH ENERGY RADIATION ON CRITICAL PARAMETERS OF SUPERCONDUCTING CERAMICS YBa2Cu3O7
A. S. Alexandrov et al 1988 10 p In RUSSIAN; ENGLISH summary
(DE90-620562; JINR-R-14-88-571) Avail: NTIS (US Sales Only)
HC A02/MF A01

Critical parameters T(sub 0) and J(sub 0) of superconducting ceramics YBa2Cu3O7 have been measured after irradiation at 300 K by 0.66, 8.09 GeV protons and by C-12 nuclei with 3.65 GeV/nucleon energy. Maximum irradiation dose was 3x10(exp 8) J/kg (Gy). Strong radiation degradation of T(sub 0) and J(sub 0) was explained by spontaneous recombination of point defects in displacement zones, connected with availability of thermally activating unregulated regions, which lead to electron localization and infringement of Josephson contacts between ceramics grains. Results of T(sub 0)(D) and J(sub 0)(D) measurement are compared with analogous dependencies for reactor spectrum neutrons (E greater than 0.1 MeV) and ions He-4 (E(sub alpha)=6.7 MeV) and ions He-4 (E(sub alpha)=6.7 MeV). The obtained experimental results can further the understanding of the mechanism of higher temperature superconductivity. DOE

N90-23240# Joint Inst. for Nuclear Research, Dubna (USSR).
NEW APPROACH TO THE DYNAMICAL DIFFRACTION THEORY IN THE CASE OF THREE-DIMENSIONAL PERFECT CRYSTAL
V. K. Ignatovich 1988 19 p In RUSSIAN; ENGLISH summary
(DE90-620563; JINR-R-4-88-693) Avail: NTIS (US Sales Only)
HC A03/MF A01

The reflection and transmission amplitudes of a perfect crystal of finite thickness, all possible orders of diffractions being taken into account, are calculated with the help of pure algebraic method. The recursive relations and supposition of the diffraction from crystalline plane parallel to the entrance surface being known are in the basis of the method. For the illustration, the total reflection, one-wave Bragg reflection and two-wave Laue diffraction of neutrons from a tetragonal crystal with one atom in an elementary cell are calculated. The results of calculations coincide with the results of the well known dynamical diffraction theory. The new back reflection effect is predicted. DOE

N90-23241# Joint Inst. for Nuclear Research, Dubna (USSR).
A (mu)SR-INVESTIGATION OF THE MIXED STATE OF THE HIGH-Tc SUPERCONDUCTOR HoBa2Cu3O7-DELTA
V. G. Grebinnik et al 1988 6 p In RUSSIAN; ENGLISH summary
(DE90-620802; JINR-D-14-88-667) Avail: NTIS (US Sales Only)
HC A02/MF A01

The high-T(sub c) superconductor HoBa(sub 2)Cu(sub 3)O(sub 7-delta) has been investigated by the (mu)SR-method (muon spin relaxation) in the magnetic field 0 to 1200 Oe in the temperature interval 10 to 100 K. It was established, that 80 percent of the sample volume is experienced by the diamagnetic shielding effect. The mixed state in the superconductor is formed in the external magnetic field greater than 20 Oe at 30 K. The magnetic penetration depth (lambda) as a function of the temperature was obtained. Its value at 30 K is about 1300 A. DOE

N90-23242* National Aeronautics and Space Administration. Marshall Space Flight Center, Huntsville, AL.
HANGING DROP CRYSTAL GROWTH APPARATUS AND METHOD Patent
Daniel C. Carter, inventor (to NASA) and Robbie Smith, inventor (to NASA) (Tennessee Scientific Glass Co.) 12 Dec. 1989 11 p Filed 23 Mar. 1988 Supersedes N88-25356 (26 - 18, p 2585)
(NASA-Case-MFS-28206-1-SB; US-Patent-Appl-SN-172101; US-Patent-Class-422-245; US-Patent-Class-156-DIG.62; US-Patent-Class-156-DIG.72; US-Patent-Class-156-608; US-Patent-Class-156-600; Int-Patent-Class-C30B-7/02) Avail: US Patent and Trademark Office CSCL 20L

This invention relates generally to hanging drop crystal growth devices and methods, and more particularly to such a device wherein the drop containing protein to be crystallized is exposed to vapor from a flow of control fluid, with this control fluid having a vapor pressure which varies as solvent is drawn from the drop. A hanging drop apparatus is constructed having a cylindrical enclosure, with a wicking element or disc constructed of sintered glass and being mounted in an upper portion thereof. A well or recess is cut into an upper side of the disc. A cover slip or plate having a protein drop disposed thereon is sealably positioned on the disc, with the drop being positioned in the well. A flow of control fluid is generated by a programmable gradient former, with this flow being coupled to the disc. The vapor pressure of the control fluid is initially selected to be considerably lower than that

of the drop, causing solvent in the drop to readily evaporate. As evaporation progresses, the vapor pressure of the control fluid is adjusted to slow the rate of evaporation from the drop, allowing a slow approach to the critical supersaturation point of the protein to be crystallized. The novelty of this invention particularly lies in exposing the drop to a control fluid having a variable pressure. Further novelty lies in the particular apparatuses and methods by which this is accomplished.

Official Gazette of the U.S. Patent and Trademark Office

N90-23243# Rome Univ. (Italy). Dipt. di Fisica.
MIXING OF DIS OPERATORS IN LATTICE QCD
G. Corbo, E. Franco, and Gian Carlo Rossi (Aquila Univ., Italy) 8 Nov. 1989 6 p Submitted for publication
(Preprint-708; ETN-90-96531) Avail: NTIS HC A02/MF A01

The results of the perturbative calculation in lattice quantum chromadynamics are extended to the unquenched case, with Wilson fermions of the mixing and renormalization coefficients of the operators entering into the expression of the lowest moment of the F2 structure function. The rank two finite operator with banishing anomalous dimension, that is constructed for unlike indices, is argued to be identified with the lattice energy momentum tensor. ESA

N90-23244# Rome Univ. (Italy). Dipt. di Fisica.
CRITICAL BEHAVIOR OF THE THERMAL POWER NEAR THE METAL-INSULATOR TRANSITION
C. Castellani, M. Fabrizio, and G. Strinati (Scuola Normale Superiore, Pisa, Italy) 29 Nov. 1989 13 p Submitted for publication
(Preprint-714; ETN-90-96537) Avail: NTIS HC A03/MF A01

The diffusive behavior of the heat-number correlation function for an interacting electronic disordered system is determined at first order in the disorder strength. Singular corrections are found for the coefficient of the thermal power. The resulting scaling behavior in the various universality classes differs from that obtained in the noninteracting case. ESA

N90-23245# Rome Univ. (Italy). Dipt. di Fisica.
LATTICE FIELD THEORY
G. Martinelli 18 Dec. 1989 15 p Submitted for publication
(Preprint-719; ETN-90-96539) Avail: NTIS HC A03/MF A01

Studies of quantum field theories on the lattice are reported. The study of quantum chromodynamics at finite temperature is described. The obtaining of hadron spectrum and meson decay constants is discussed. Results concerning hadronic matrix elements are presented. The progress made on strong interacting Higgs dynamics is reported. ESA

N90-23246# Selenia Industrie Associate S.p.A., Rome (Italy). Direzione Ricerche.
ACTIVATION UNIFORMITY DEPENDENCE OF UNDOPED SEMI-INSULATING GaAs ON POST-IMPLANT ANNEALING CONDITIONS
C. Lanzieri, R. Graffitti, and A. Cetronio 1990 6 p
(ETN-90-96549) Avail: NTIS HC A02/MF A01

An illustration is given as to how by suitable furnace design, the radial thermal gradients generated on a GaAs substrate during the post-implant annealing cycle can be virtually eliminated, and how such a technique can result in appreciable improvement in on-wafer activation uniformity (standard deviation better than + or - 2 percent) with virtually constant activation efficiency in going from seed to tail end wafer of a given ingot. ESA

N90-23247# SRI International Corp., Menlo Park, CA. Physical Electronics Lab.
INVESTIGATION OF SCHOTTKY BARRIERS Final Technical Report, 17 Jul. - 31 Dec. 1989
Mark VanSchilfgaarde Dec. 1989 44 p
(Contract F49620-86-K-0018; AF Proj. 2306)
(AD-A218422; AFOSR-90-0204TR) Avail: NTIS HC A03/MF A01 CSCL 09/1

This final report summarizes the technical progress made under the auspices of AFOSR Contract F49620-86-K-0018. Substantial progress was made in two key areas: electronic structure studies of the Schottky barrier and transport studies. With respect to the electronic structure component, we applied ab initio electronic structure techniques to ideal metal-semiconductor interfaces. In a study of a sequence of metal-semiconductor contacts, we are able to address the problem of Schottky barrier pinning. Another study addresses the early stages of formation of Schottky barriers. With respect to the transport component, we developed some new techniques for treating high-field transport, in particular transport through a Schottky barrier. We also examine scattering from ionized dopants in the interstitial regions. GRA

N90-23248# California Univ., Los Angeles. Dept. of Electrical Engineering.
MEASUREMENT OF LOCALIZED DEEP LEVELS AND WAFER NON-UNIFORMITIES AT 3-5 SEMICONDUCTOR HETEROJUNCTIONS Final Technical Report, Dec. 1986 - Sep. 1988
Stephen R. Forrest Dec. 1989 100 p
(Contract F19628-86-K-0002)
(AD-A218547; RADC-TR-89-270) Avail: NTIS HC A05/MF A01 CSCL 20/12

The results are reported of a two year program in which organic thin films were used to non-destructively study the properties of inorganic semiconductor epitaxial materials. The organic films can be applied to the substrate in vacuum in a non-destructive manner such that many bulk and surface properties of the semiconductor under study can be easily obtained. Once the characterization process is complete, the thin films can be removed without damage to the semiconductor substrate. This allows for the correlation of the fundamental materials properties of the semiconductor to the performance of devices fabricated on the same wafer. GRA

N90-23249# Johns Hopkins Univ., Laurel, MD. Applied Physics Lab.
APPLICATION OF HIGH-TEMPERATURE SUPERCONDUCTING THIN-FILM DEVICES TO ELECTRO-OPTICAL AND ELECTRONIC WARFARE SYSTEMS Technical Memo, Jun. 1988 - Dec. 1989
B. G. Boone Feb. 1990 48 p
(Contract N00039-89-C-5301)
(AD-A218805; JHU/APL-TG-1377) Avail: NTIS HC A03/MF A01 CSCL 17/4

This report gives an assessment of the impact of high-temperature superconductivity on applications in electro-optical and electronic warfare. Prior art in low-temperature superconductivity provides many examples of potential applications. It is essential that the feasibility of developing and using specific high-temperature superconducting devices, such as radiation detectors and passive microwave components, be determined before significant systems investment occurs. Research and development activities at The Johns Hopkins University Applied Physics Laboratory aimed at implementing such thin-film devices are underway. GRA

N90-23250# Carnegie-Mellon Univ., Pittsburgh, PA. Dept. of Electrical and Computer Engineering.
ADVANCED GAS PHASE REACTOR FOR GROWTH OF Ge SUB x Si SUB 1-x Final Report, 1 Dec. 1988 - 30 Nov. 1989
David W. Greve and A. G. Milnes 30 Nov. 1989 6 p
(Grant AF-AFOSR-0144-89; AF Proj. 2917)
(AD-A219012; AFOSR-90-0316TR) Avail: NTIS HC A02/MF A01 CSCL 20/2

A reactor was designed and constructed for the growth of Germanium (x) Silicon (1-x) films by the newly developed technique of Ultrahigh voltage/Chemical vapor deposition epitaxy. Films of varying germanium content were successfully grown and characterized at temperatures as low as 577 C. Work is in progress with respect to optimization of the wafer cleaning procedure and studies of dopant incorporation and device fabrication will be initiated in the near future. GRA

N90-23251# Wright Research Development Center, Wright-Patterson AFB, OH. Electronic Technology Lab.
OPTICAL SPECTROSCOPY OF Ti(3+) DOPED YAlO3 Final Report, Jun. - Aug. 1989
A. L. Potter and Kenneth L. Schepler Aug. 1989 36 p
(AF Proj. 2001)
(AD-A219043; WRDC-TR-89-5052) Avail: NTIS HC A03/MF A01 CSCL 20/2

This project investigated the optical properties of Ti(3+):YAlO3 and its potential as a laser material. A large single crystal sample grown by Heraeus was provided by R. Simms for investigation. Prior Ti(3+);YAlO3 crystals investigated in this lab had been grown by Litton Airtron, but they showed large amounts of scattering and absorption loss in the fluorescence part of the spectrum. Since Heraeus used a different method for growing Ti(3+):YAlO3 (growth under a vacuum), this crystal was studied to see if it might be a better material for lasing. Absorbance, fluorescence, annealing, and lifetime measurements were performed. The crystal of Ti(3+):YAlO3 was grown by Heraeus in West Germany by using the modified Czochralski method under stringent vacuum conditions. It was 0.1 atom percent Ti by melt and had a beige-orange tint. The crystal dimensions were 1.026 cm by 1.509 cm by 3.05 cm. GRA

N90-23252# Stanford Univ., CA. Dept. of Electrical Engineering.
DIRECT IMPLANTATION PROCESS DEVELOPMENT AND CHARACTERIZATION IN ADVANCED Hg(1)-(x)Cd(x) Te EPI LAYERS Final Report, 1 Oct. 1987 - 30 Nov. 1989
Thomas W. Sigmon Nov. 1989 61 p
(Contract DAAL03-87-K-0109)
(AD-A219133; ARO-24988.1-EL) Avail: NTIS HC A04/MF A01 CSCL 20/6

Mercury cadmium telluride (MCT) has been extensively studied over the past thirty years, primarily as an optical detector material for the mid and far infrared. Researchers have also shown interest in other potential uses for the material such as optical communication devices, tunable lasers, and nonlinear optical devices. The properties that make the alloy semiconductor MCT particularly suited for infrared detection include an energy gap that can be adjusted from a value of -0.3 eV for the semimetal HgTe to 1.6 eV for CdTe and a direct energy gap over all values of composition. The direct energy gap gives the material a large absorption coefficient which means that the detector needs to be only several microns thick to absorb all the radiation of interest. It thus lends itself readily to production-line processing utilizing standard photolithographic techniques. Additional favorable properties include a very high electron mobility, a high electron-to-hole mobility ratio, and a fairly low dielectric constant. GRA

N90-23253# Lehigh Univ., Bethlehem, PA. Dept. of Computer Science and Electrical Engineering.
NONRECIPROCAL COMPONENTS IN THE 140 AND 220 GHz BANDS UTILIZING MAGNETOPLASMONS ON SEMICONDUCTING SUBSTRATES Final Report, 1 Jun. 1985 - 30 Sep. 1989
D. M. Bolle, D. R. Decker, Nader Mohsenian, Dong-Hyun Hwang, and Terry J. Delph 9 Jan. 1990 167 p
(Contract DAAG29-85-K-0081)
(AD-A219136; ARO-21125.3-EL) Avail: NTIS HC A08/MF A01 CSCL 20/12

Experimental and theoretical investigations were made of waveguiding structures utilizing surface waves on high quality semiconducting substrates. When exposed to a d.c. biasing magnetic field, these structures display nonreciprocal behavior which can be used to design nonreciprocal devices such as circulators, isolators, and phase shifters in the millimeter and submillimeter wave frequency ranges. Reasonable losses can be achieved for device purposes when operated at cryogenic temperatures. Various experimental techniques were explored to achieve surface plasmon excitation on n-type semiconducting materials in the near-millimeter wave ranges. Although some limited studies have been carried out on this topic in the optical frequency range, very little work is available on experimental derivation of propagation characteristics of surface plasmon on III-V semiconductor compounds. For the purposes, most of the theory was deduced from optics with numerous experiments conducted to obtain a reasonable interpretation for the quasi-optical theory applied to the millimeter wave range. The quasi-optical method employed both the prism coupling and grating coupling techniques to generate surface plasmon on highly doped semiconductor materials in the frequency range of 110 to 160 GHz. GRA

N90-23254# Evans (Charles) and Associates, Redwood City, CA.
SECONDARY ION MASS SPECTROMETRY CHARACTERIZATION OF IMPLANTS INTO GaAs AND GaP FOR WAVEGUIDES AND INTEGRATED OPTICS APPLICATIONS Final Report, 28 Apr. 1986 - 30 Oct. 1989
Robert S. Wilson (Hughes Research Labs., Malibu, CA.) and Charles A. Evans, Jr. 10 Jan. 1990 35 p
(Contract DAAL03-86-C-0010)
(AD-A219203; CEVANS/049/FR-9002; ARO-23324.1-EL-S)
Avail: NTIS HC A03/MF A01 CSCL 20/12

Hydrogen, Helium and most dopant elements were implanted into Gallium Arsenide, Gallium Arsenide Phosphide, Gallium Phosphide, GaSb, InP, InAs, InSb, and LiNbO3 at energies from 10 to 700 keV, and a few elements up to 2.4 MeV, in random and channeling orientations. Included are studies of: characterization of Si implantation into GaAs in random and channeling orientations at energies from 10 keV to 6.0 MeV; a general description of as-implanted and annealed depth profiles of dopant implants (especially Beryllium and Silicon into GaP, GaAs, Indium Phosphide, and Indium Antimonide; illustrations of the effects of heterostructures, including superlattices, on the redistribution of mobile impurities (Hydrogen and Be) during thermal processing; illustrations of implants in other III-V technologies (GaAs/Si and GaAsP); lanthanide rare earth elements in III-V crystals; as-implanted and annealed MeV implants in III-V materials; characterization of proton exchanged Lithium Niobate; and redistribution of implanted H in LiNbO3. GRA

N90-23255# Ecole Nationale Superieure de Physique, Marseilles (France). Laboratoire d'Optique des Surfaces et des Couches Minces.
MICROSTRUCTURE OF THIN FILMS Final Report, 30 Sep. 1988 - 30 Sep. 1989
E. Pelletier and H. A. MacLeod (Arizona Univ., Tucson.) 7 Feb. 1990 104 p
(Grant AF-AFOSR-0319-88; AF Proj. 2301)
(AD-A219262; EOARD-TR-90-03) Avail: NTIS HC A06/MF A01 CSCL 11/3

Much work is devoted to the study of Ion Assisted Deposition (IAD) with different materials: metals, (aluminum, silver) and dielectrics, nitrides, fluorides and oxides. Concerning oxides, a comparison between IAD and ion plating techniques is in progress. For the characterization, two techniques are described which are used for determination of optical losses which are photothermal deflection and measurements of angular scattering distribution. Concerning photothermal deflection, the results of characterization obtained on samples of TiO2 are given; instabilities versus time are observed when the samples are illuminated. The theory and experiments performed on scattering are applied to coatings of special designs produced by Balzers, OCLI, OJAI and Spectra Physics to determine the correlation between interfaces of the multilayers. These results, presented at the OSA 1989 meeting are summarized. This leads indirectly to the measurement of the grain size of the materials in thin film form. A completely different approach is given by growth modeling, but it remains to link the two techniques for a better understanding of the process of growth. GRA

N90-23256# Research Triangle Inst., Research Triangle Park, NC.
PASSIVATION AND GATING OF GaAs AND Si SURFACES USING PSEUDOMORPHIC STRUCTURES Annual Report, 1 Jul. 1988 - 30 Jun. 1989
R. J. Markunas, G. G. Fountain, R. A. Rudder, S. V. Hattangady, and Y. S. Park (Office of Naval Research, Arlington, VA.) 1 Feb. 1990 30 p
(Contract N00014-88-C-0433)
(AD-A219351; RTI-415U-4225) Avail: NTIS HC A03/MF A01 CSCL 07/2

During the first quarter we began work directed at the silicon-gallium arsenide interface formation. This work encompasses the in situ cleaning process and the silicon deposition process. Advances have been made in the GaAs in situ cleaning. The reasons for the advances, recognition of silicon dioxide deposition byproduct residue and additions of a load lock to the system, are described. Work towards improving the pseudomorphic Si deposition is also described. During the second quarter work continued on the gallium arsenide-silicon interface formation. We had noted improvements in the low temperature silicon epitaxial deposition through the incorporation of hydrogen in the deposition environment. Also we noted improvements in the silicon deposition through the use of lower pressure conditions. The results of the use of Metal-insulator Semiconductor results obtained on both p-type and n-type gallium arsenide-silicon with partially optimized processing are described. These silicon deposition conditions for Metal-insulator Semiconductor structure formation are described. During the third and fourth quarters work again continued on the gallium-arsenide-Silicon interface formation. During this period a series of experiments was performed to evaluate the effects of processing conditions on the p-type GaAs MIS structure. GRA

N90-23163# Joint Publications Research Service, Arlington, VA.
ACOUSTOELECTRONIC INTERACTION OF SURFACE WAVES IN GaAs-InGaAs SUPERLATTICES Abstract Only
V. A. Vyun, Yu. O. Kanter, S. M. Kikkarin, V. V. Pnev, A. A. Fedorov, and I. B. Yakovkin *In its* JPRS Report: Science and Technology. USSR: Physics and Mathematics 3 Mar. 1989 p 2 Transl. into ENGLISH from Pisma v Zhurnal Tekhnicheskoy Fiziki (Leningrad, USSR), v. 14, no. 20, 26 Oct. 1988 p 1911-1914 (For primary document see N90-23162 16-70)
Avail: NTIS HC A03/MF A01

N90-23164# Joint Publications Research Service, Arlington, VA.
EXCITATION OF HYPERSOUND AT BOUNDARY BETWEEN TYPE-2 SUPERCONDUCTOR AND A CONCENTRATED PARAMAGNETIC COMPOUND Abstract Only
S. L. Tsarevskiy *In its* JPRS Report: Science and Technology. USSR: Physics and Mathematics 3 Mar. 1989 p 4 Transl. into ENGLISH from Akusticheskiy Zhurnal (Moscow, USSR), v. 34, no. 2, Mar.-Apr. 1988 p 315-320 (For primary document see N90-23162 16-70)
Avail: NTIS HC A03/MF A01

N90-23165# Joint Publications Research Service, Arlington, VA.
EFFECT ON RELAXATION ON NONLINEAR WAVES IN CRYSTALS Abstract Only
G. T. Adamashvili *In its* JPRS Report: Science and Technology. USSR: Physics and Mathematics 3 Mar. 1989 p 6 Transl. into ENGLISH from Teoreticheskaya i Matematicheskaya Fizika (Moscow, USSR), v. 75, no. 3, Jun. 1988 p 371-377 (For primary document see N90-23162 16-70)
Avail: NTIS HC A03/MF A01

N90-23169# Office of Naval Research Liaison Office, Far East, APO San Francisco, CA.
HIGH TEMPERATURE SUPERCONDUCTING THIN FILMS IN JAPAN
Michael Osofsky, Phillip R. Broussard, and Earl Callen *In its* ONR Far East Scientific Information Bulletin, Volume 13, No. 4 Dec. 1988 p 1-23 (For primary document see N90-23168 16-70)
Avail: NTIS HC A05/MF A01 CSCL 20L

N90-23170# Office of Naval Research Liaison Office, Far East, APO San Francisco, CA.
RESEARCH AND APPLICATIONS OF METALLIC SUPERLATTICES, HIGH T(SUB c) SUPERCONDUCTORS, X RAY OPTICS, AND COMPACT SYNCHROTRONS
Charles M. Falco *In its* ONR Far East Scientific Information Bulletin, Volume 13, No. 4 Dec. 1988 p 31-37 (For primary document see N90-23168 16-70)
Avail: NTIS HC A05/MF A01 CSCL 20L

N90-23171# Office of Naval Research Liaison Office, Far East, APO San Francisco, CA.
WHAT IS GOING ON IN THE La2CuO4 SUPERCONDUCTORS
Earl Callen *In its* ONR Far East Scientific Information Bulletin, Volume 13, No. 4 Dec. 1988 p 43-59 (For primary document see N90-23168 16-70)
Avail: NTIS HC A05/MF A01 CSCL 20L

77 THERMODYNAMICS AND STATISTICAL PHYSICS

Includes quantum mechanics; theoretical physics; and Bose and Fermi statistics.

For related information see also *25 Inorganic and Physical Chemistry* and *34 Fluid Mechanics and Heat Transfer.*

N90-23257# Joint Inst. for Nuclear Research, Dubna (USSR).
QUANTUM MECHANICS IN RIEMANNIAN SPACE-TIME
E. A. Tagirov 1988 12 p Submitted for publication
(DE90-620448; JINR-E-2-88-678) Avail: NTIS (US Sales Only) HC A03/MF A01

The asymptotics for c(sup -2) (c being the velocity of light) of the theory of a complex scalar field in the Reimannian space-time and external electromagnetic field is considered. The general-covariant Schroedinger equation with relativistic corrections for a scalar particle in external gravitational and electromagnetic fields is obtained for the case of normal Gaussian systems of reference. Account of the geometric variation of the spatial volume element along the geodesics of the system of reference leads to a Hamiltonian which is (asymptotically) self-adjoint with respect to the standard scalar product. This fact is considered as a ground for the Born interpretation of the wave functions. DOE

N90-23258# Joint Inst. for Nuclear Research, Dubna (USSR).
BACKGROUND CONNECTION: A NECESSARY OBJECT IN GENERAL RELATIVITY
N. A. Chernikov 1988 14 p In RUSSIAN; ENGLISH summary Presented at the 7th Soviet Gravitational Conference on Modern Theoretical and Experimental Problems of Relativity and Gravitation, Erevan, USSR, Oct. 1988
(DE90-620463; JINR-R-2-88-778) Avail: NTIS HC A03/MF A01

It is shown that in Einstein's theory of gravity (ETG), an important geometrical object has been lost while introducing the concept of the energy pseudotensor of the gravitational field. This object found at present is the affine connection, on whose background the gravitational field should be considered. That loss made the ETG contradictory to Einstein's general principle of relativity. To remove the contradiction, it suffices to introduce a primitive affine connection. However, nothing prevents us from considering the background object being not primitive but an arbitrary affine connection without torsion. Under this condition we may rather easily vary both the gravitational field g(sub b) and the affine connection independent of g(sub ab). Owing to restoration of the lost object, the ETG becomes a perfectly geometrical theory in which all physical objects are geometrical ones. DOE

N90-23259# Max-Planck-Inst. fuer Stroemungsforschung, Goettingen (Germany, F.R.).
EXPERIMENTS ON THE BREAKDOWN OF HEAT TRANSFER IN LIQUID HELIUM 2
M. v.Schwerdtner, G. Stamm, and W. Fiszdon (Polish Academy of Sciences, Warsaw.) Oct. 1989 25 p Presented at the 3rd Soviet-German Symposium on Cryogenics, Kharkov, USSR, 7-14 Oct. 1989 Sponsored in part by DFG
(MPIS-13/1989; ISSN-0436-1199; ETN-90-96472) Avail: NTIS HC A03/MF A01

Transient heat transport in counterflowing helium 2 is investigated in a rectangular channel of 2.6 cm by 2.6 cm cross section. Simultaneous measurements of temperature, vortex line density and counterflow velocity are performed, using specially designed high sensitivity probes with a short response time. It is shown that, with increasing input heat flux, the counterflow velocity and hence the internal heat flux reaches a maximum depending on the flow parameters, which leads to a strong increase of temperature in the region close to the heater. As shown by corresponding measurements and supported by theoretical calculations, this is correlated with the presence of a large amount of superfluid vortex lines, that have been produced during the passage of the heat pulse and decay afterwards. The experimental results and a simple phenomenological model are compared. A criterion is found for the occurrence of a supercritical heat transfer, connecting the critical heat flux with all the thermodynamic quantities involved. ESA

N90-23260# Rome Univ. (Italy). Dipt. di Fisica.
QUANTUM NON-DEMOLITION STROBOSCOPIC OBSERVABLES AND MULTIPUMPING BACK-ACTION EVASION SCHEMES
Roberto Onofrio 11 Sep. 1989 14 p
(Preprint-699; ETN-90-96522) Avail: NTIS HC A03/MF A01

A new concept of optimal pumping spectrum is introduced and used to link quantum non demolition stroboscopic measurements and multipumping back-action evasion schemes. Considerations on a new stroboscopic scheme for the detection of small displacements in macroscopic mechanical oscillators are reported. Particular applications are for the current generation of Weber type gravitational wave antennas and for the test of the Copenhagen interpretation of quantum mechanics on macroscopic objects. ESA

N90-23261# Rome Univ. (Italy). Dipt. di Fisica.
ARE QUANTUM MEASUREMENTS ON MACROSCOPIC BODIES FEASIBLE
Roberto Onofrio 11 Sep. 1989 10 p
(Preprint-700; ETN-90-96523) Avail: NTIS HC A02/MF A01

The possibility to test quantum measurement theories is discussed in the more phenomenological framework of the quantum non demolition theory. A way to test the hypothesis of the state vector collapse by means of quantum non demolition measurements on macroscopic oscillators is proposed and its feasibility within the current technology is analyzed. ESA

80 SOCIAL SCIENCES (GENERAL)

Includes educational matters.

No abstracts in this category.

81 ADMINISTRATION AND MANAGEMENT

Includes management planning and research.

No abstracts in this category.

82 DOCUMENTATION AND INFORMATION SCIENCE

Includes information management; information storage and retrieval technology; technical writing; graphic arts; and micrography.

For computer documentation see *61 Computer Programming and Software.*

N90-23262# Instituto de Pesquisas Espaciais, Sao Jose dos Campos (Brazil).
SYNTAX, SEMANTICS, AND PRAGMATISM: AN INTEGRATED FOCUS BASED ON TEXTUAL LINGUISTIC KNOWLEDGE [A SINTAXE, A SEMANTICA E A PRAGMATICA: UM ENFOQUE INTEGRADO BASEADO NO CONHECIMENTO LINGUISTICO TEXTUAL]
Carlos AlbertodeOliveira Oct. 1989 19 p In PORTUGUESE; ENGLISH summary Presented at the 6th Brazilian Symposium on Artificial Intelligence, Rio de Janeiro, Brazil, Nov. 1989
(INPE-4992-PRE/1554) Avail: NTIS HC A03/MF A01

A natural language interface for expert systems that translates Portuguese phrases to a given knowledge representation is discussed. An integrated analysis process is shown in which the role of the users and their world knowledge are focused. Author

N90-23263# Pacific Northwest Lab., Richland, WA.
LOOKING AT LARGE DATA SETS USING BINNED DATA PLOTS
D. B. Carr Apr. 1990 52 p
(Contract DE-AC06-76RL-01830)
(DE90-008206; PNL-7301) Avail: NTIS HC A04/MF A01

The challenge of developing exploratory analysis methods for large data sets is addressed. The goals are to increase awareness of large data sets problems and to contribute simple graphical methods that address some of the problems. The graphical methods focus on 2-D and 3-D data and common task such as finding outliers and tail structure, assessing central structure and comparing central structures. The methods handle large sample size problems through binning, incorporate information from statistical models and adapt image processing algorithms. Examples demonstrate the application of methods to a variety of publicly available large data sets. The most novel application addresses the too many plots to examine problem by using cognostics, computer guiding diagnostics, to prioritize plots. The particular application prioritizes views of computational fluid dynamics solution sets on the fly. That is, as each time step of a solution set is generated on a parallel processor the cognostics algorithms assess virtual plots based on the previous time step. Work in such areas is in its infancy and the examples suggest numerous challenges that remain. DOE

N90-23264# Groningen Rijksuniv. (Netherlands). Dept. of Computing Science.
TOWARDS A CALCULUS OF DATA REFINEMENT
Wei Chen (Washington Univ., Saint Louis, MO.) and Jan Tijmen Udding 31 Mar. 1989 29 p Sponsored in part by Washington Univ., Saint Louis, MO
(CS-8902; ETN-90-96703) Avail: NTIS HC A03/MF A01

A foundation for a calculus of data refinement is provided. The concept of conditional data refinement which enables the incorporation of contextual information in a refinement step is presented. A number of properties and examples showing how

data refinement can be used in practice are given. The proposed concept can be viewed as a generalization of algorithm refinement. It is shown to be equivalent to all currently known characterizations of data refinement. ESA

N90-23265# Groningen Rijksuniv. (Netherlands). Dept. of Computing Science.
AN ALGEBRIC APPROACH TO INFINITE DATA STRUCTURES
Grant Malcolm 1989 17 p
(CS-8909; ETN-90-96706) Avail: NTIS HC A03/MF A01

The notions of homomorphisms and promotability extended to infinite data structures are discussed. Promotability for infinite data structure is proven to be dual to promotability for finite data structures. The extent to which promotability is useful in deriving program transformations for finite data structures is not certain. Homomorphism on finite data structures, together with high projection functions and composition, represent the primitive recursive functions. Primitive recursive functions together with higher order functions are provable in Peano arithmetic: no similar results which characterize those functions which may be expressed as homomorphisms on finite data structures are known. Examples of the homomorphisms and promotability applications on data structures are given. ESA

N90-23266# Technische Univ., Eindhoven (Netherlands). Dept. of Mathematics and Computing Science.
AN APPROXIMATION FOR THE RESPONSE TIME OF AN OPEN CP-DISK SYSTEM
A. Dekkers and J. vanderWal Aug. 1989 27 p Sponsored in part by Foundation for Computer Science, Netherlands and Netherlands Organization for the Advancement of Scientific Research
(MEMO-COSOR-89-19; ETN-90-96720) Avail: NTIS HC A03/MF A01

A computer system consisting of one Central Processing (CP) unit and one disk is described. It is visited by jobs with a special kind of workload, for example database queries. During a visit to the computer system a job is served several times at the CP and several times at the disk. A queuing model representing this system is given. This model is used to estimate the mean and variance of the response time of these jobs. Numerical examples are compared with a simulation of the system to check the correctness of the method. ESA

N90-23267# Naval Ship Research and Development Center, Bethesda, MD. Computation Mathematics-Logistics Dept.
DATA EXCHANGE STRATEGY. PART 1: REVIEW OF DIGITAL DATA EXCHANGE TECHNOLOGY Final Report
Jack Brainin, Lisa Deeds, Ruey Chen, Mary McCarthy, Philip Battey, L. Flitter, Donald Gignac, and Mark Patkus Sep. 1989 108 p
(AD-A218506; DTRC/CMLD-18-89/14) Avail: NTIS HC A06/MF A01 CSCL 15/5

The first phase of a three phase effort directed towards developing a Navy digital data exchange strategy for CALS is documented. The data exchange strategy task was divided into three distinct parts. Part 1 is documented in this report and provides an overview of data exchange. It includes a discussion of data exchange concepts, a summary of current and potential future CALS standards, and a brief overview of selected industry approaches to digital data exchange. It is intended to provide the reader with a single reference source to become familiar with the area of data exchange/data exchange standards and related activities. This document will serve as a reference document to the Navy's Acquisition Guide for Program Managers. GRA

N90-23268# Wright State Univ., Dayton, OH. Dept. of Computer Science and Engineering.
EXPLANATION GENERATION IN EXPERT SYSTEMS (A LITERATURE REVIEW AND IMPLEMENTATION) M.S. Thesis
Vance McMillan Saunders (Air Force Inst. of Tech., Wright-Patterson AFB, OH.) 1989 155 p
(AD-A218741; AFIT/CI/CIA-89-142) Avail: NTIS HC A08/MF A01 CSCL 12/9

Today's technology provides tremendous amounts of information at incredible speeds. In order to make this information useful for more complex, significant problem solving applications, intelligent computer software systems are needed. The expert system (ES) technology of artificial intelligence (AI) is one solution that is emerging to meet this need. However, as this technology continues to develop and expert machines are used more and more, it is crucial that the same explanatory capability be demanded from these mechanical experts as is demanded from human experts. The credibility of human expertise is established by an expert's ability to explain his expertise. The credibility of mechanical expertise must be established in the same way. Additionally, ESs are very complex, sophisticated systems. In order to verify their accuracy and correctness, ESs must be able to explain what they are doing and why. The Explanation Facilities (EFs) of ESs are examined by first conducting an extensive literature review of this topic, and second, by implementing an EF for a frame-based ES shell. The purpose of the literature review is to gain a general understanding of EF research and development while the purpose of the implementation effort is to investigate the specifics of: explaining a frame-based ES, adding an EF to an existing ES, and using Ada as the implementation language for this AI application. GRA

N90-23269# Naval Postgraduate School, Monterey, CA. Dept. of Administrative Sciences.
USE OF OPTICAL STORAGE DEVICES AS SHARED RESOURCES IN LOCAL AREA NETWORKS M.S. Thesis
James C. Hoge Sep. 1989 150 p
(AD-A219198) Avail: NTIS HC A07/MF A01 CSCL 09/5

Since the start of the computer era, information users have been restricted by inadequate and expensive data storage. The development of solid state memory, soft storage media (floppy disk drives), drum memory drives and fixed disk drive mechanisms have improved data storage and retrieval, reducing the cost of information to under $10 per megabyte for large storage devices. The introduction of laser technology and the development of optical data storage now makes tremendous amounts of data available to users. Optical disc drives can be accessed as peripheral devices by most stand alone micro-computers at a cost of less than $.30 per megabyte of information. Although the cost per megabyte is low, the cost per work station can run $1,500 to $2,500 (or more) per year. Optical storage devices and the data bases released in optical format can be: (1) too expensive for addition to individual work stations, or (2) under utilized in a single user environment, or (3) difficult to manage when two or more users share a single work station. Current networking strategies have the potential to reduce data costs even more by allowing data storage devices to be shared by multiple users. The possibility is examined of combining Optical Storage Technology with the data sharing properties of a Local Area Network (LAN) to solve these three problems. GRA

N90-23270# Department of Defense, Washington, DC. Directorate for Information Operations and Reports.
ATLAS/DATA ABSTRACT FOR THE UNITED STATES AND SELECTED AREAS, FISCAL YEAR 1989
1989 168 p
(AD-A219289; DIOR/L03-89; L03) Avail: NTIS HC A08/MF A01 CSCL 05/2

From 1955 to 1982, the Department of Defense (DOD) published the Map Book of Major Military Installations. This book gave DOD managers a convenient reference to locate major military installations in the United States. In the late 1970's, officials in the Office of the Secretary of Defense suggested that the geography information in the Map Book be combined with the financial and personnel data so that a wide range of information about DOD would be available in a single publication. A prototype of this new book, in 1981, resulted in the first Atlas/State Data Abstract, in 1982, and included geographic, financial, and personnel information for the fifty states. The 1984 edition was expanded to include selected U.S. Territories and Possessions, and the 1986 edition added selected foreign countries. GRA

N90-23271# Coast Guard, Alexandria, VA. Information Systems Center.
BTOS DATABASE EVALUATION Final Report
Jon D. Allen 6 Mar. 1990 203 p
(AD-A219304; CGISC-5232-90-01) Avail: NTIS HC A10/MF A02 CSCL 12/5

The results are given of the evaluation from an end-user's point of view. The products evaluated were: ADS, Fasport-dbm, Forms Plus, INFORMIX-SQL, Intelligent Query, Oracle, Paradise, PDS-Adept, PRESTO/REPORTER, PROGRESS, R:BASE 5000, reQuest and reQuest II. Included are: product descriptions, test conditions and environment, results of the performance tests, a subjective evaluation of the major characteristics of each product, and a tabular outline of functional capabilities for each database package. GRA

83 ECONOMICS AND COST ANALYSIS

Includes cost effectiveness studies.

No abstracts in this category.

84 LAW, POLITICAL SCIENCE AND SPACE POLICY

Includes NASA appropriation hearings; aviation law; space law and policy; international law; international cooperation; and patent policy.

N90-23272# Air Force Geophysics Lab., Hanscom AFB, MA.
INTERNATIONAL TREATIES AND ACTIVE EXPERIMENTS IN SPACE Interim Scientific Report
W. J. Burke and R. C. Sagalyn 1 Sep. 1989 26 p
(AD-A219368; GL-TR-89-0251; ERP-1040) Avail: NTIS HC A03/MF A01 CSCL 20/9

Satellite explorations of the near earth environment have vastly increased our understanding of space plasmas and their interactions with systems. A logical next step involves active experiments in which small quantities of matter and energy are injected into space environments. These experiments seek to verify tentative, scientific understanding and to identify ways to control environmental effects on systems. Serious questions may be raised regarding the legitimacy of conducting active experiments in space under United States military auspices. Here we review the treaty obligations regarding space environment modification to which the United States government has committed itself. Experiments involving the detonation of nuclear devices or interference with foreign space assets, especially national technical means to verification, are explicitly forbidden. In planning these experiments great care must be exerted so that they produce no widespread, long-lasting or severe effects on the environment. We also review active experiments programs conducted by U.S. civilian and foreign space agencies. Finally, the treaty restrictions are applied to the case of a hypothetical experiment to establish the feasibility of controlling the flux of energetic particles trapped in the earth's radiation belts. An ability to reduce trapped radiation would increase orbit selection options for future space-based surveillance systems. GRA

85 URBAN TECHNOLOGY AND TRANSPORTATION

Includes applications of space technology to urban problems; technology transfer; technology assessment; and surface and mass transportation.

For related information see also *03 Air Transportation and Safety, 16 Space Transportation,* and *44 Energy Production and Conversion.*

No abstracts in this category.

88 SPACE SCIENCES (GENERAL)

N90-23273*# National Aeronautics and Space Administration. Goddard Space Flight Center, Greenbelt, MD.
THE PIONEER VENUS ORBITER: 11 YEARS OF DATA. A LABORATORY FOR ATMOSPHERES SEMINAR TALK
W. T. Kasprzak Washington May 1990 82 p Original contains color illustrations
(NASA-TM-100761; Rept-90B00109; NAS 1.15:100761) Avail: NTIS HC A05/MF A01; 8 functional color pages CSCL 22A

The Pioneer Venus Orbiter has been in operation since orbit insertion on December 4, 1978. For the past 11 years, it has been acquiring data in the salient features of the planet, its atmosphere, ionosphere, and interaction with the solar wind. A few of the results of this mission are summarized and their contribution to our general understanding of the planet Venus is discussed. Although Earth and Venus are often called twin planets, they are only superficially similar. Possessing no obvious evidence of plate tectonics, lacking water and an intrinsic magnetic field, and having a hot, dense carbon dioxide atmosphere with sulfuric acid clouds makes Venus a unique object of study by the Orbiter's instruments. Author

89 ASTRONOMY

Includes radio, gamma-ray, and infrared astronomy, and astrometry.

N90-23274 Arizona Univ., Tucson.
A SEARCH FOR ADDITIONAL PARAMETERS IN THE INFRARED LUMINOSITY/21 cm LINE-WIDTH RELATION FOR SPIRAL GALAXIES IN CLUSTERS OF GALAXIES Ph.D. Thesis
Mark Edward Cornell 1989 267 p
Avail: Univ. Microfilms Order No. DA8915952

The relationship first pointed out by Tully and Fisher between the luminosity of spiral galaxies and their maximum rotation velocity, as measured by the 21 cm line-width, continues to be one of the best methods available to measure relative distances. At infrared wavelengths, the observation scatter about this relation is typically 0.35 to 0.50 magnitudes, permitting relative distance estimates with an accuracy of about 20 percent. The Malmquist bias in a magnitude-limited sample is 1.38 sigma (exp 2), and while the solution to the general problem is complex, it is clear that reducing the scatter about the Tully-Fisher relation by even a factor of two would make a large difference in our ability to determine the local velocity field from distances and velocities of individual galaxies. In this dissertation the scatter in the Tully-Fisher relation at infrared wavelengths is discussed and ways to reduce that dispersion are sought through the inclusion of additional observable parameters. The data are derived from a CCD survey of 244 spiral galaxies in twenty clusters falling in the redshift range 3,000 to 11,000 km/s. From surface brightness profiles and elliptical aperture photometry, isophotal and total magnitudes at B, R, and I were obtained along with isophotal diameters, mean and nuclear surface brightnesses, and a concentration parameter indicative of the bulge-to-disk ratio.

These quantities were then combined with colors and HI-content measures taken from the literature in a search for correlations with Tully-Fisher residuals. None of the trial second-parameters resulted in substantial decrease in the scatter about the fiducial Tully-Fisher relation. An examination of the properties of the cluster samples shows that many of the clusters exhibit considerable substructure. While it is possible that the implied depth effects are important to the scatter about the magnitude/line-width relation, calculated lower limits to the dispersion in depth turn out to be rather small. Dissert. Abstr.

N90-23275 Colorado Univ., Boulder.
ULTRAVIOLET AND INFRARED STUDIES OF Be STARS Ph.D. Thesis
Karen Beth Shipley Bjorkman 1989 212 p
Avail: Univ. Microfilms Order No. DA8923485

From a comparison of ultraviolet and infrared observations of Be and normal B stars, it was found that the region producing C IV absorption in Be stars is confined in latitude to near the equatorial plane and possibly confined in radial extent close to the star. The C IV-producing region in Be stars appears to be about four times hotter than that in normal B stars of the same spectral type, implying that another mechanism must be active in Be stars in addition to radiatively-driven winds. It was also found that infrared and optical polarization data can be used to deconvolve rotation velocities and inclination angles for Be stars. The statistical correlations which led to these conclusions are based on data obtained with the IUE and IRAS satellites. C IV absorption equivalent widths in Be stars are significantly larger than those in normal B stars. C IV equivalent widths and edge velocities correlate with those of Si IV. C IV excess equivalent widths, defined as log(W(Be)/W(Normal), correlate with 1/T(eff) and with inclination angle, but not with rotation velocity, luminosity class, or 12 micron excesses. Stars with lower T(eff) or larger inclination angle show more excess C IV absorption. C IV edge velocities show similar correlations. The 12 micron excesses correlate with temperature and with rotation velocity, but not with inclination angle, luminosity class, or C IV excess. Hotter stars, or those with higher rotation velocities, tend to have larger 12 micron excesses. Both the C IV excess absorption and 12 micron excess seem to turn on at a rotation velocity of 150 km s(exp -1). Dissert. Abstr.

N90-23276 California Univ., Berkeley.
THE INTERSTELLAR MEDIUM OF A STARBURST GALAXY; MILLIMETER INTERFEROMETRIC OBSERVATIONS OF M82 Ph.D. Thesis
John Eric Carlstrom 1989 173 p
Avail: Univ. Microfilms Order No. DA9006267

The Hat Creek Interferometer was used to obtain multi-frequency high resolution observations of the nuclear region of the starburst galaxy M82. Emission from the J = 1 yields 0 rotational transitions of CO, HCO(+) and HCN and from wavelength 3.3 mm continuum were studied at angular resolutions of 5 to 11 seconds (75 to 165 pc) and velocity resolutions at 3.3 to 4.3 km/s. The observations provide information on the state of the molecular and ionized components of the interstellar medium. The pressure of both components ranges from approximately 10(exp 6)/cu cm K near the edge of the starburst region to greater than or equal to 10(exp 7)/cu cm K in the center. The density of the molecular gas is high greater than or equal to 10(exp 5)/cu cm, and the volume filling factor of the molecular gas is low, less than .001. In contrast, the volume filling factor of the Hill regions is high, greater than or equal to 0.1. The Lyman continuum flux determined from the wavelength 3.3 mm emission measure is greater than 6 x 10(exp 53)/s. This is equivalent to the flux of 3 x 10(exp 5) O8 stars and, even though emitted from only the 500 pc diameter starburst region of M82, is greater than the estimated flux from the entire Milky Way. The observations provide evidence that the starburst is spreading from the core of the nuclear region into dense molecular clouds which surround the central region of bright far-infrared emission. The brightest supernova remnants, observed at radio wavelengths, are found in dense molecular clouds on the periphery of the starburst region. In addition, mechanically tunable Gunn oscillators were developed for use as local oscillators in heterodyne astronomical receivers. They were installed on the three element Hat Creek Interferometer to expand the frequency coverage to 70 to 116 GHz; the entire 3 mm atmospheric window. The double sideband receiver noise temperatures are now between 60 and 150 K across the frequency band. An IF switching technique was developed for quickly measuring and correcting the IF gains. Dissert. Abstr.

N90-23277# Instituto de Pesquisas Espaciais, Sao Jose dos Campos (Brazil).
SPECTRAL PLANE QUASARS, SPECTRAL TURN-OVER, AND FREQUENCY ATLAS M.S. Thesis, 1988 [QUASARES DE ESPECTRO PLANO E O TURN-OVER ESPECTRAL A ALTAS FREQUENCIAS]
Carlos Roberto Rabaca Dec. 1989 102 p
(INPE-5011-TDL/399) Avail: NTIS HC A06/MF A01

A sample of 44 quasars and 5 BL Lac objects were observed at 22 and 43 GHz with the 13.7 m Itapetinga Radio telescope. From the analysis of the obtained spectra, it was possible to determine the approximate turn-over for 46 sources. Assuming that at frequencies higher than the turn-over the spectrum arises from with the optically thin region of a very compact component, it was possible to set up correlations between structural and energetic characteristics of these regions. The results are compatible with a cosmological evolution of the luminosities of compact regions, although there is no evolution in their sizes. Author

N90-23278 Princeton Univ., NJ.
SKEWERING THE UNIVERSE WITH QSO LINES OF SIGHT: LYMAN ALPHA CLOUDS AS PROBES OF LARGE SCALE STRUCTURE Ph.D. Thesis
Arif Babul 1989 138 p
Avail: Univ. Microfilms Order No. DA9008346

The magnitude and the scale of clustering of Quasi-Stellar Objects (QSO) absorption lines provide potentially important clues about their origin and their spatial distribution. Such clues may aid in distinguishing between theories for the formation of large scale structure such as the Cold Dark Matter (CDM) models and explosion scenarios. Formation of low-mass objects is inevitable in the standard CDM cosmogony. Objects that exist in near-mean background density environments are most likely to survive destruction. Models were proposed seeking to identify these isolated low-mass condensates as Ly alpha clouds. However, the accompanying estimates of quantities such as the epoch of formation, or the number density of clouds, are not based on characteristics of isolated density peaks. Isolated peaks result primarily from power in a narrow band at the mass scale of the structures. First, a filter designed to study isolated density fluctuations is introduced. The filter is used to identify Ly alpha cloud candidates in a biased CDM model. If Ly alpha clouds have their origins in primordial density fluctuations, the CDM power spectrum does not have sufficient power on subgalactic scales to account for the observed structures. Further, theories such as the CDM model and the explosion scenario predict different spatial distributions for the Ly alpha clouds. Second, a formalism is developed for testing specific models for the three-dimensional spatial distributions of clouds against line-of-sight observations. The formalism is used to compute the redshift density of lines and the distribution of line intervals along a line-of-sight for the models, for comparison with the observations. Three simple models were considered: clouds arising from density fluctuations with a white noise power spectrum, clouds distributed on shells of constant comoving radii, and clouds restricted to shells expanding in a self-similar fashion. Finally, a summary of preliminary work is presented on the effects of heating of the intergalactic medium on formation of low-mass structures in the CDM model. Dissert. Abstr.

N90-23279 Iowa Univ., Iowa City.
VLA AND VLBI ANGULAR BROADENING MEASUREMENTS: THE DISTRIBUTION OF INTERSTELLAR SCATTERING AT LOW GALACTIC LATITUDES Ph.D. Thesis
Alan Lee Fey 1989 257 p
Avail: Univ. Microfilms Order No. DA9009304

Dual-frquency very large array (VLA) and multifrequency very long base interferometry (VLBI) angular broadening measurements of a number of Galactic plane radio sources in the longitude range l = 20 deg to 90 deg, which includes the Cygnus region of the sky, are reported. The characteristic lambda squared dependence of angular size is used to distinguish between scattered and intrinsic structure. Observations confirm the scattered nature of the extragalactic source 1849+005. This source appears to be one of the most heavily scattered sources known. Angular broadening was also observed for the following sources: 1855+031, 2005+403, 2008+33D, 2021+317, 2023+336, and 2048+313. Five additional sources 1905+079, 1922+155, 1932+204, 1954+282, and 2001+304 show indications of being affected by interstellar scattering. Some of the remaining sources, depending on their observed structure, provide upper limits to scattering. The observed scattering in the Galactic plane decreases rapidly with increasing Galactic longitude, reaching a minimum at l is approximately equal to 60 deg and then becoming prominent again in the Cygnus region. This result indicates that the more intense clumps of interstellar turbulence may be confined to the spiral arms of the Galaxy. Results of a computer simulation designed to investigate the clumped component of interstellar turbulence indicate the need for a complex distribution of turbulent clumps. To account for all the scattering data available, the magnitude of scattering caused by individual clumps must have a Galactocentric radial dependence. Dissert. Abstr.

N90-23280 California Inst. of Tech., Pasadena.
SPECTROSCOPIC OBSERVATIONS OF HIGH REDSHIFT QSOs: GALAXIES AND THE INTERGALACTIC MEDIUM AT EARLY EPOCHS Ph.D. Thesis
Charles Colville Steidel 1990 293 p
Avail: Univ. Microfilms Order No. DA9009391

The properties of intervening gaseous material are investigated making use of high red shift Quasi Stellar Objects (QSOs). Wide-slit spectrophotometry of a sample of very high redshift QSOs is used in combination with high resolution observations of QSO Lyman alpha forests to obtain a new upper limit on the density of generally distributed intergalactic neutral hydrogen (the Gunn-Peterson limit). Implications for the nature of the intergalactic medium are discussed. Observations of a number of high redshift QSOs close to each other on the plane of the sky are presented; based on the occurrence of heavy element absorption systems over a narrow range of redshifts in each of the spectra, evidence for the presence of a huge, elongated supercluster of galaxies at x = 2 is discussed. Results of a survey for heavy element absorption systems at the largest observable redshift are presented. Moderate dispersion spectra of a sample of Lyman limit absorption systems at z is approximately equal to 3 were obtained in order to determine the heavy element abundances and other physical parameters of the gas clouds responsible for the high redshift, heavy-element absorption systems in the spectra of QSOs. The abundances of C, O, and Si are in general between 0.001 and 0.01 of the solar abundances, comparable to the most metal-poor stars in the halo of the Galaxy. The clouds have sizes in the range 1 to 15 kpc and masses in the range 10 (exp 6)-10(exp 9) solar masses. The clouds are discussed within the context of the hypothesis that the heavy element absorption systems are associated with the extended halos of high redshift galaxies. Dissert. Abstr.

N90-23281 Georgia State Univ., Atlanta.
ANDERSON MESA, ARIZONA AS A SITE FOR AN OPTICAL INTERFEROMETRIC ARRAY Ph.D. Thesis
Wean-Shun Tsay 1989 213 p
Avail: Univ. Microfilms Order No. DA9010516

Brief descriptions are presented of an optical interferometric array for high angular resolution astronomy, of modern methods of astronomical facility site testing, and of the physics of seeing. Specific criteria for the CHARA (Center for High Angular Resolution Astronomy) Array, such as terrain, geology, and logistics, were evaluated with special attention given to cloudcover and seeing conditions. A series of modern satellite nighttime cloud cover maps of the southwestern U.S. were analyzed. A simple and inexpensive seeing monitor system was designed and constructed for measuring instantaneous stellar image profiles and was applied to a series of new measurements at the proposed site. An 18-meter micrometerological tower was situated at the Anderson Mesa site to measure the vertical structure of microthermal activity. From measurements of cloud cover, seeing profiles, and microthermal properties, Anderson Mesa near Flagstaff, Arizona, was evaluated as a potential site for an optical interferometric array. Dissert. Abstr.

N90-23282# Astronomische Rechen-Inst., Heidelberg (Germany, F.R.).
FIFTH FUNDAMENTAL CATALOGUE (FK5). PART 1: THE BASIC FUNDAMENTAL STARS
W. Fricke, comp., H. Schwan, comp., T. Lederle, comp., U. Bastian, R. Bien, G. Burkhardt, B. duMont, R. Hering, R. Jaehrling, and H. Jahreiss et al Sep. 1988 107 p Sponsored by Sonderforschungsbereich SFB 132
(Rept-32(1988)-Pt-1; ETN-90-96460) Avail: NTIS HC A06/MF A01

The catalog provides improved mean positions and proper motions for the classical 1535 fundamental stars, already included in catalogs 3 and 4, and mean positions and proper motions for new fundamental stars extending also the fundamental system to the apparent magnitude 9.5. About 300 catalogs providing star positions which were obtained from observations made all over the world are considered. The expressions for general precession, the determination of individual corrections of the positions and proper motions of the fundamental stars, the differences between catalogs 4 and 5, and an explanation of the catalog are included. ESA

N90-23283 Max-Planck-Inst. fuer Physik und Astrophysik, Garching (Germany, F.R.).
HIGH SPATIAL RESOLUTION ISOTOPIC CO AND CS OBSERVATIONS OF M17 SW: THE CLUMPY STRUCTURE OF THE MOLECULAR CLOUD CORE
J. Stutzki and R. Guesten (Max-Planck-Inst. fuer Radioastronomie, Bonn, Germany, F.R.) Sep. 1989 53 p Submitted for publication
(MPE-Preprint-161; ETN-90-96468) Copyright Avail: Max-Planck Institut fuer Physik und Astrophysik, 8046 Garching bei Munich, Fed. Republic of Germany

High angular resolution maps of the M17 SW cloud core in the C(018) and C(S34), for J transitions from 2 to 1, and for line transitions from 3 to 2, were obtained with the 30 m infrared telescope on Pico Valeta (Spain). These maps directly reveal the clumpy structure of the entire cloud core down to linear scales of 0.14 pc (13 arc seconds) and below. Individual clumps have linewidths as small as 0.5 km/s, compared to a linewidth of 3 to 5 km/s observed with lower angular resolution in the same lines. The C(018) 2 to 1 emission line reaches a peak brightness temperature of 24K in the 13 arcsecond beam and probably slightly optically thick in several locations. Spectra in the more abundant CO isotopes obtained toward several selected positions show strong self absorption notches and peak brightness temperatures in between these notches of about 100 K. The main isotope emission comes from only a small fraction of the total material with extreme physical conditions not at all characteristic of the bulk of the cloud. The clump/interclump density contrast is estimated at about at least 23. ESA

N90-23299*# Max-Planck-Inst. fuer Extraterrestrische Physik, Garching (Germany, F.R.).
COMPLEMENTARY INFORMATION FROM mm-WAVE-, INFRARED-, AND GAMMA RAY ASTRONOMY
H. Rothermel, M. Cameron, and A. Eckart *In* NASA, Goddard

Space Flight Center, The Energetic Gamma-Ray Experiment Telescope (EGRET) Science Symposium May 1990 p 51-60 (For primary document see N90-23294 16-90)
Avail: NTIS HC A15/MF A02; 1 functional color page CSCL 03A

N90-23300*# National Aeronautics and Space Administration. Goddard Space Flight Center, Greenbelt, MD.
IMPLICATIONS OF THE IRAS DATA FOR GALACTIC GAMMA RAY ASTRONOMY AND EGRET
Floyd W. Stecker *In its* The Energetic Gamma-Ray Experiment Telescope (EGRET) Science Symposium May 1990 p 61-77 (For primary document see N90-23294 16-90)
Avail: NTIS HC A15/MF A02; 1 functional color page CSCL 03A

N90-23312*# Stanford Univ., CA.
SPECTRAL DETERMINATIONS FOR DISCRETE SOURCES WITH EGRET
E. B. Hughes and P. L. Nolan *In* NASA, Goddard Space Flight Center, The Energetic Gamma-Ray Experiment Telescope (EGRET) Science Symposium May 1990 p 201-213 (For primary document see N90-23294 16-90)
(Contract NAS5-27557)
Avail: NTIS HC A15/MF A02; 1 functional color page CSCL 03A

90 ASTROPHYSICS

Includes cosmology; celestial mechanics; space plasmas; and interstellar and interplanetary gases and dust.
For related information see also *75 Plasma Physics.*

N90-23284 Case Western Reserve Univ., Cleveland, OH.
A GENERAL LOW-HARMONIC COSMIC STRING AND ITS SELF-INTERSECTION AND FRAGMENTATION Ph.D. Thesis
David Burr DeLaney 1989 111 p
Avail: Univ. Microfilms Order No. DA8915642

A short history of cosmic strings is presented, and a discussion of their basic properties, including the standard a', b', decomposition, cusps, kinks, and self-intersection. A proof is given that if the string enjoys a 180 deg rotational symmetry, then it must have cusps. Various examples from the literature of strings with only first and third harmonics are discussed, and the (five-parameter) most general string containing such harmonics is derived from the basic equations and exhibited. It is then explicitly shown to contain all previous examples as subsets. The percentage of the parameter-space corresponding to self-intersecting strings is then found for this and other classes of strings. A report on an attempt to parametrize the most general string containing first through third harmonics is given. Fragmentation of strings is discussed, and a method of treating in closed form the fragments resulting from an intersection of a string is presented, using the greatest-integer function. The fragment velocity is discussed. Criteria for the appearance of self-intersections not seen on the parent string are found, and shown to correspond to certain arrangements of kinks on the fragments which would result from these intersections, for both one-kink and multi-kink cases. Some analytic examples for fragmentation are given, using the Turok string, and found to contain no further intersections on the fragments. The relevance of these results to cosmology is discussed. Dissert. Abstr.

N90-23285 East Anglia Univ., Norwich (England).
DEVELOPMENT AND USE OF A PASSIVE TECHNIQUE FOR MEASURING NITROGEN DIOXIDE IN THE BACKGROUND ATMOSPHERE Ph.D. Thesis
Amanda J. Gair 1989 300 p
Avail: Univ. Microfilms Order No. BRD-87624

A passive sampling technique for the measurement of nitrogen dioxide in urban and rural environments was developed for use at remote locations. Improvements to the technique were achieved by using ion chromatography as the analytical method. Improvements were also obtained by the reduction in contamination of samplers, so that detectable contamination could be reduced below 0.05 NO2 ppbv week. The samplers were evaluated for the possible interference from peroxyacetyl nitrate and the effects of wind speed and turbulence. The accuracy of the samplers was evaluated at remote Scandinavian sites by intercomparison with three other nitrogen dioxide measurement techniques, conventional chemiluminescence, Differential Optical Absorption Spectroscopy, and TGS-ANSA. The samplers were used over a two year period to obtain the seasonal and spatial variation of nitrogen dioxide at ten sites within the U.K. and Scandinavia. The spatial distribution of nitrogen dioxide suggested that concentrations were influenced by the long range transport of pollution and the presence of stable air masses. Comparison of NO2 observations with modeled results indicated an underestimation of the NO2 concentration by the model, especially during the winter. It is suggested that this is due to a low dry deposition velocity for NO2 at concentrations below 1 ppbv, leading to an extended atmospheric lifetime. From the results obtained from the sampler network and free tropospheric measurements of nitrogen dioxide, it was indicated that the potential to photochemically produce ozone existed extensively throughout the background troposphere and it is likely that the spring maximum in tropospheric ozone concentrations is strongly influenced by photochemical activity. Dissert. Abstr.

N90-23286 Texas Univ., Austin.
ANISOTROPIC INFLATION Ph.D. Thesis
Andrew Laurence Berkin 1989 112 p
Avail: Univ. Microfilms Order No. DA9005531

The theory of inflationary cosmology is studied for initially anisotropic cosmological models. New inflation was considered in a Bianchi 1 universe with constant scale factor and the one loop effective potential was derived for a massive, quartically self-interacting, scalar field coupled to gravity. Regularization is accomplished by Hawking's zeta function method, and the effective potential is renormalized. The effects on inflation are discussed for various parameters. The R squared inflation in Bianchi 1 and 9 models are analyzed. The field equations are written as coupled first order differential equations and are solved numerically. Analytical arguments are also given using an R-H (Ricci scalar and Hubble parameter) phase space approach. For the Bianchi 1 case, any amount of initial anisotropy decays quickly relative to the length of the inflationary epoch, and the amount of inflation is enhanced. The same behavior is found in Bianchi 9 universes, with the exception of models near isotropy. In these cases, a wide range of initial parameters causes the universe to recollapse, thus reducing the phase space in which inflation can occur. Next, the b(sub 8) coefficient in the Schwinger-deWitt expansion of the coincident heat kernel for a massive scalar field in an arbitrary curved spacetime was calculated. This expansion is commonly used in the renormalization of the stress energy tensor, and hence is applicable to studying the effects of these fields on the early universe. Other b(sub n) coefficients were derived using recurrence relations, but here a perturbative approach is used. The operator is split into the flat space Laplacian and the perturbation arising from curved space terms. Geometric quantities in the perturbation are expanded using Riemann normal coordinates and terms which contribute to b(sub n) identified by dimensional arguments. Both b(sub 6) and b(sub 8) are found. The former coefficient agrees with previous computations; the latter is derived for the first time. Dissert. Abstr.

N90-23287 Cornell Univ., Ithaca, NY.
THE DYNAMICAL EVOLUTION OF DENSE CLUSTERS OF COMPACT STARS Ph.D. Thesis
Gerald David Quinlan 1989 128 p
Avail: Univ. Microfilms Order No. DA9001206

Clusters of compact stars (neutron stars or black holes) were suggested as an explanation for dark matter in the centers of nearby galaxies, as sources of gravitational radiation, as accretion-models for quasars, and as a possible origin for massive black holes in galactic nuclei. The results of an investigation into

the dynamical evolution of such clusters, starting from initial densities and velocities not far removed from those observed in normal galactic nuclei, are presented. The evolution is first analyzed using an approximate model based on a set of ordinary differential equations for the evolution of the cluster core. This model identifies dissipative binary formation resulting from the emission of gravitational radiation as being the most important physical process modifying the evolution from what would result if only conservative gravitational interactions were included. The binaries decay by gravitational radiation and merge on a time-scale short compared with the cluster evolution time-scale and are not effective in heating the cluster. The model predicts a dramatic rise in the binary formation and merger rates prior to the catastrophic collapse of the cluster core to a massive black hole through the relativistic Zel'dovich-Podurets instability. The compact binary systems that form during the evolution are promising sources of gravitational radiation for detection by large ground-based laser interferometers. The cluster evolution is re-examined by numerically solving the Newtonian Fokker-Planck equation, modified to include dissipation by gravitational radiation and dissipative binary formation. The late stages of the cluster evolution in the Fokker-Planck calculations differ considerably from the predictions of the approximate model, because this model did not allow for the effects of mass segregation. The Fokker-Planck calculations show that successive binary mergers and mass segregation result in a rapid buildup of a massive black hole in the cluster core before the cluster evolves to a relativistic state. Appendix A describes several new methods for including binary formation and stellar mergers in the Fokker-Planck equation. Dissert. Abstr.

N90-23288 Wisconsin Univ., Madison.
COUNTERROTATING CORES IN ELLIPTICAL GALAXIES Ph.D. Thesis
Marc Comas Balcella 1989 147 p
Avail: Univ. Microfilms Order No. DA8923776

The dynamics of the merger between a high- and a low-elliptical galaxy was studied to understand how kinematically peculiar cores in elliptical galaxies might form. Numerical simulations of mergers provide rotation curves, surface density profiles, surface density contour plots and velocity maps of the merger remnants, as well as diagnostics on the dynamics such as phase-space diagrams. This type of merger can create counterrotating cores. The core of the smaller galaxy, of higher density, is not disrupted by the primary tidal field and sinks to the center of the primary as an independent dynamical subsystem. Core counterrotation occurs only when the initial merger orbit is retrograde with respect to the pin of the primary. The remnant has higher effective radius and lower mean central surface density than the primary galaxy, but a smaller core radius. The adsorption of orbital energy and angular momentum by the primary particles greatly modifies the kinematic structure of the larger galaxy. Twisted rotation axes and isophote twists appear over the whole body of the remnant. These diagnostics may be used to determine whether observed peculiar cores might have formed via an elliptical-elliptical merger. Galaxies with counterrotating cores should show a complex velocity field, isophotal irregularities, and, in general, a slow rotation in the main body of the galaxy. The present experiments are the first galaxy-satellite merger experiments involving an active, rotating secondary. They show that part of the orbital angular momentum is absorbed by the secondary, thus the secondary contributes to its own sinking: the sinking rate depends on the orientation of the secondary spin. Long-slit spectroscopic observations of NGC 3656 are reported. Dissert. Abstr.

N90-23289 Illinois Univ. at Urbana-Champaign, Savoy.
RAPID MASS TRANSFER IN BINARY SYSTEMS Ph.D. Thesis
Michael Scott Hjellming 1989 169 p
Avail: Univ. Microfilms Order No. DA9010885

The conditions for rapid mass transfer is investigated in binary stars. Previous theoretical calculations and observations of binary imply the existence of several different timescales for mass transfer: nuclear, thermal, or dynamical. Since the mass transfer rates differ by several orders of magnitude, it is important to know which timescales are relevant to different systems. Dynamical timescale mass transfer is thought to cause substantial decreases in the orbital period through mass and angular momentum losses. Thermal timescale mass transfer is thought to transform the appearance of the binary as mass exchange occurs in a short time. Binaries currently transferring mass are doing so on the longest, nuclear, timescale. The characteristics of binaries which divide the three timescales are estimated by calculating the response of potential mass donors in two idealized limits: an adiabatic response, where the entropy profile does not change with mass loss, and a thermal response. Where thermal relaxation is allowed but nuclear burning is not. A comparison of the changing surface radius, to the Roche lobe radius implies the critical mass ratios for dynamically and thermally unstable mass transfer. These calcualtions are performed here for donors between 0.25 and 20 solar masses which would fill their Roche lobes before helium burning. Dissert. Abstr.

N90-23290 California Inst. of Tech., Pasadena.
STUDIES IN GRAVITATIONAL LENSING AND NUMERICAL HYDRODYNAMICS Ph.D. Thesis
Christopher Sharpe Kochanek 1989 180 p
Avail: Univ. Microfilms Order No. DA9000573

The gravitational lensing cross sections for multiple imaging by elliptical galaxy potentials is examined. Lenses are found to divide into strong and marginal lenses. Three image systems form either allied geometries in which the two brightest images lie on the same side of the lens, or opposed geometries in which the two brightest images lie on opposite sides of the lens. Strong lenses are dominated by the three image opposed geometry at low amplifications. Marginal lenses are dominated by the three image allied geometry. The cross sections for multiple imaging are integrated over the expected distribution of lenses and sources. The sources are taken to be quasars with a standard number-magnitude relation. Approximately one in one thousand quasars will be multiply imaged. Approximately one to ten percent of lens systems will involve more than one lensing galaxy either at the same or at a different redshift. The statistical properties of such two screen gravitational lenses are evaluated. An inversion technique for resolved gravitational lenses is developed and applied to the radio ring image MG1131+0456. The technique works both for intensity and polarization maps. The propagation of a precessing hydrodynamic jet is studied using finite difference techniques in an axisymmetric system. The implications for the precessing jet in SS433 is examined. The tidal disruption of a star on a parabolic orbit past a supermassive black hole is examined using smooth particle hydrodynamics. Dissert. Abstr.

N90-23291 Arizona Univ., Tucson.
MOLECULAR EVOLUTION IN ASTROPHYSICAL ENVIRONMENTS Ph.D. Thesis
William Bruce Latter 1989 225 p
Avail: Univ. Microfilms Order No. DA9010483

Molecular formation and destruction processes are explored in rapidly evolving, non-equilibrium astrophysical environments. First, a semi-classical calculation is made for the rate coefficients of excited atom radiative association to form molecular hydrogen and of the process C(+) + O yields CO(+) + h(nu). The latter process may be important to the formation of CO in the core of Supernova 1987A. It is shown that the excited atom process may have been important to the formation of H2 during the early part of the epoch of recombination in the early Universe. The equations of ionization balance and molecular formation and destruction were integrated through the epoch of recombination. Other processes are examined in detail. These include heating and cooling of the primordial plasma, dampening of fluctuations prior to decoupling, and the possibility of a radiation-driven instability at the onset of recombination. A calculation is presented for the time-dependent chemical evolution in the rapidly expanding outer envelope of SN 1987A. Various cooling rates and hydrogen abundances in the envelope were examined. Near-infrared observations of the proto-planetary nebula CRL 618 are presented and discussed. It is shown by comparison with spectral models that the near-infrared H2 spectrum exhibits emission from thermally excited molecules

at T(sub ex) of approximately 2000 K. A component of fluorescent emission may also be present. The suggestion is explored that large molecules, in particular polycyclic aromatic hydrocarbons (PAHs), are formed in stellar winds. Dissert. Abstr.

N90-23292 Leeds Univ. (England).
THE EFFECT OF A STELLAR WIND ON AN EXPANDING H II REGION Ph.D. Thesis
David Byrom Radcliff 1988 169 p
Avail: Univ. Microfilms Order No. BRD-87853

The evolution of H II regions, and gas affected by the stellar wind surrounding an early type star are reviewed. A thin shell model for the stellar wind is introduced and compared with an earlier model by Dyson and Williams (1980). The model for a plane UV radiation source introduced by Goldsworthy (1968) is expanded to include the effects of a stellar wind. The results for physical stellar winds differ from those for a plane radiation source. Self-similar models for the evolution of the interstellar medium surrounding a UV radiation source (Goldsworthy (1961), and Newman and Axford (1968)), are expanded to include the effects of a stellar wind. Using phase plane analysis the possible forms of the interstellar medium for each type of ionization front are considered by following the motions from the star to the ambient H I gas. A technique by Falle (1975) is then used to produce numerical solutions. Goldsworthy's (1984) analytic model for the evolution of an H II region is expanded to include the effects of a stellar wind. Using dimensional analysis a parameter is introduced that connects the UV photon luminosity of the star to its mechanical luminosity. The effect of the shocked thin shell on the UV photon flux of the star is considered. The evolution is discussed using the three stages of evolution recognized by Goldsworthy. A numerical solution of the problem is given where integration starts at the contact discontinuity and the initial conditions are given by a shock tube model. Finally the form of an H II region that has been overtaken by the stellar wind is discussed. Dissert. Abstr.

N90-23293 Princeton Univ., NJ.
RECONSTRUCTING PRIMORDIAL DENSITY FLUCTUATIONS Ph.D. Thesis
David Hal Weinberg 1989 337 p
Avail: Univ. Microfilms Order No. DA9008361

The hypothesis that large scale structure in the universe developed by gravitational instability from Gaussian primordial density fluctuations is examined. A fast, three-dimensional, numerical implementation of the adhesion approximation is described for large scale structure, and applied to models with scale-free and cold dark matter (CDM) initial conditions. Initially scale-free models develop structures with coherence scale a few times the scale on which rms fluctuations are entering the nonlinear regime. A method is presented for reconstructing primordial density fluctuations. Starting from the galaxy density field, the reconstruction procedure works backward to a model of the smoothed initial conditions by assuming that the observed structure grew from Gaussian initial fluctuations. The model initial conditions are evolved forward numerically and compared to the input data. The technique performs well in tests on numerical simulations, including simulations with sparsely sampled data or biased galaxy formation. Reconstruction analysis can test assumptions about gravitational instability, Gaussian initial conditions, and biased galaxy formation, and it can constrain the properties of primordial density fluctuations and the value of the cosmological density parameter. The reconstruction method is applied to Giovanelli and Haynes' redshift survey of the Perseus-Pisces supercluster and its environs. Reconstructions in which galaxies evenly trace the mass distribution fail, but reconstructions with biased galaxy formation can reproduce the observed structure. Dissert. Abstr.

N90-23294*# National Aeronautics and Space Administration. Goddard Space Flight Center, Greenbelt, MD.
THE ENERGETIC GAMMA-RAY EXPERIMENT TELESCOPE (EGRET) SCIENCE SYMPOSIUM
Carl E. Fichtel, ed., Stanley D. Hunter, ed., Parameswaran Sreekumar, ed., and Floyd W. Stecker, ed. May 1990 327 p Symposium held in Greenbelt, MD, 15-16 Nov. 1989 Original contains color illustrations
(NASA-CP-3071; NAS 1.55:3071) Avail: NTIS HC A15/MF A02; 1 functional color page CSCL 03B

The principle purpose of this symposium is to provide the EGRET (Energetic Gamma-Ray Experiment Telescope) scientists with an opportunity to study and improve their understanding of high energy gamma ray astronomy. The Symposium began with the galactic diffusion radiation both because of its importance in studying galactic cosmic rays, galactic structure, and dynamic balance, and because an understanding of its characteristics is important in the study of galactic sources. The galactic objects to be reviewed included pulsars, bursts, solar flares, and other galactic sources of several types. The symposium papers then proceeded outward from the Milky Way to normal galaxies, active galaxies, and the extragalactic diffuse radiation. For individual titles, see N90-23295 through N90-23323.

N90-23295*# Harvard-Smithsonian Center for Astrophysics, Cambridge, MA.
MOLECULAR CLOUDS AND THE LARGE-SCALE STRUCTURE OF THE GALAXY
Patrick Thaddeus and J. Gregory Stacy *In* NASA, Goddard Space Flight Center, The Energetic Gamma-Ray Experiment Telescope (EGRET) Science Symposium May 1990 p 5-17 (For primary document see N90-23294 16-90)
Avail: NTIS HC A15/MF A02; 1 functional color page CSCL 03B

The application of molecular radio astronomy to the study of the large-scale structure of the Galaxy is reviewed and the distribution and characteristic properties of the Galactic population of Giant Molecular Clouds (GMCs), derived primarily from analysis of the Columbia CO survey, and their relation to tracers of Population 1 and major spiral features are described. The properties of the local molecular interstellar gas are summarized. The CO observing programs currently underway with the Center for Astrophysics 1.2 m radio telescope are described, with an emphasis on projects relevant to future comparison with high-energy gamma-ray observations. Several areas are discussed in which high-energy gamma-ray observations by the EGRET (Energetic Gamma-Ray Experiment Telescope) experiment aboard the Gamma Ray Observatory will directly complement radio studies of the Milky Way, with the prospect of significant progress on fundamental issues related to the structure and content of the Galaxy. Author

N90-23296*# National Aeronautics and Space Administration. Goddard Space Flight Center, Greenbelt, MD.
THE DIFFUSE GALACTIC GAMMA RAY EMISSION **c93**
David L. Bertsch *In its* The Energetic Gamma-Ray Experiment Telescope (EGRET) Science Symposium May 1990 p 19-29 (For primary document see N90-23294 16-90)
Avail: NTIS HC A15/MF A02; 1 functional color page CSCL 03B

The EGRET (Energetic Gamma-Ray Experiment Telescope) detector will provide a much more detailed view of the diffuse galactic gamma ray intensity in terms of higher resolution, greater statistical significance, and broader energy range than earlier missions. These observations will furnish insight into a number of very important questions related to the dynamics and structure of the Galaxy. A diffuse emission model is being developed that incorporates the latest information on matter distribution and source functions. In addition, it is tailored to the EGRET instrument response functions. The analysis code of the model maintains flexibility to accommodate the quality of the data that is anticipated. The discussion here focuses on the issues of the distributions of matter, cosmic rays, and radiation fields, and on the important source functions that enter into the model calculation of diffuse emission. Author

N90-23297*# National Aeronautics and Space Administration. Goddard Space Flight Center, Greenbelt, MD.
A MODEL OF THE DIFFUSE GALACTIC GAMMA RAY EMISSION **c93**
Parameswaran Sreekumar (Universities Space Research Association, Greenbelt, MD.) *In its* The Energetic Gamma-Ray Experiment Telescope (EGRET) Science Symposium May 1990 p 31-41 (For primary document see N90-23294 16-90)
Avail: NTIS HC A15/MF A02; 1 functional color page CSCL 03B

The galaxy was observed to be a source of high energy gamma rays as shown by the two successful satellite experiments, SAS-2 and COS-B. It is generally understood that these diffuse gamma rays result from interactions between energetic cosmic rays and interstellar gas. This work makes use of the most recent data on the distribution of atomic and molecular hydrogen in the galaxy along with new estimates of gamma ray production functions to model the diffuse galactic gamma ray emission. The model allows various spatial distributions for cosmic rays in the Galaxy including non-axisymmetric ones. In the light of the expected data from EGRET (Energetic Gamma-Ray Experiment Telescope), an improved model of cosmic ray-matter-gamma ray interaction will provide new insights into the distribution of cosmic rays and the strength of its coupling to matter. Author

N90-23298*# National Aeronautics and Space Administration. Goddard Space Flight Center, Greenbelt, MD.
GAMMA RAYS FROM GIANT MOLECULAR CLOUDS **c93**
Stanley D. Hunter and Gottfried Kanbach (Max-Planck-Inst. fuer Extraterrestrische Physik, Garching, Germany, F.R.) *In its* The Energetic Gamma-Ray Experiment Telescope (EGRET) Science Symposium May 1990 p 43-50 (For primary document see N90-23294 16-90)
Avail: NTIS HC A15/MF A02; 1 functional color page CSCL 03B

Giant Molecular Clouds (GMCs) are massive, bounded, cool, dense regions containing mostly H2, but also H I, CO, and other molecules. These clouds occupy less than 1 percent of the galactic volume, but are a substantial part of the interstellar mass. They are irradiated by the high energy cosmic rays which are possibly modulated by the matter and magnetic fields within the clouds. The product of cosmic-ray flux and matter density is traced by the emission of high energy gamma-rays. A spherical cloud model is considered and the gamma ray flux from several GMCs within 1 kpc of the sun which should be detectable by the EGRET (Energetic Gamma-Ray Experimental Telescope) instrument on GRO (Gamma Ray Observatory). Author

N90-23299*# Max-Planck-Inst. fuer Extraterrestrische Physik, Garching (Germany, F.R.).
COMPLEMENTARY INFORMATION FROM mm-WAVE-, INFRARED-, AND GAMMA RAY ASTRONOMY **c89**
H. Rothermel, M. Cameron, and A. Eckart *In* NASA, Goddard Space Flight Center, The Energetic Gamma-Ray Experiment Telescope (EGRET) Science Symposium May 1990 p 51-60 (For primary document see N90-23294 16-90)
Avail: NTIS HC A15/MF A02; 1 functional color page CSCL 03A

An overview of the subdivision of wavelength ranges, importance of extinction, observing techniques, and scientific objectives in both IR broadband measurement and spectroscopy is given. Infrared and millimeter wave spectroscopy in the galaxy and IR and millimeter wave observations for Centaurus A are examined and discussed. B.G.

N90-23300*# National Aeronautics and Space Administration. Goddard Space Flight Center, Greenbelt, MD.
IMPLICATIONS OF THE IRAS DATA FOR GALACTIC GAMMA RAY ASTRONOMY AND EGRET **c89**
Floyd W. Stecker *In its* The Energetic Gamma-Ray Experiment Telescope (EGRET) Science Symposium May 1990 p 61-77 (For primary document see N90-23294 16-90)
Avail: NTIS HC A15/MF A02; 1 functional color page CSCL 03A

Using the results of gamma-ray, millimeter wave and far surveys of the galaxy, logically consistent picture of the large scale distribution of galactic gas and cosmic rays was derived, tied to the overall processes of stellar birth and destruction on a galactic scale. Using the results of the IRAS far-infrared survey of te galaxy, the large scale radial distributions of galactic far-infrared emission independently was obtained for both the Northern and Southern Hemisphere sides of the Galaxy. The dominant feature in these distributions was found to be a broad peak coincident with the 5 kpc molecular gas cloud ring. Evidence was found for spiral arm features. Strong correlations are evident between the large scale galactic distributions of far-infrared emission, gamma-ray emission and total CO emission. There is particularly tight correlation between the distribution of warm molecular clouds and far-infrared emission on a galactic scale. The 5 kpc ring was evident in existing galactic gamma-ray data. The extent to which the more detailed spiral arm features are evident in the more resolved EGRET (Energetic Gamma-Ray Experimental Telescope) data will help to determine more precisely the propagation characteristics of cosmic rays. Author

N90-23301*# Princeton Univ., NJ. Dept. of Physics.
RADIO PULSAR TIMING OBSERVATIONS FOR GRO **c93**
J. H. Taylor *In* NASA, Goddard Space Flight Center, The Energetic Gamma-Ray Experiment Telescope (EGRET) Science Symposium May 1990 p 81-87 Sponsored in part by Naval Observatory (For primary document see N90-23294 16-90)
Avail: NTIS HC A15/MF A02; 1 functional color page CSCL 03B

Gamma rays probably provide the best diagnostic tool for probing the enigmatic physics of pulsar magnetospheres. At present, however, only two pulsars - the young, nearby ones in the Crab and Vela X supernova remnants - are reliably detected at gamma-ray energies. With adequate radio observations to provide independent timing information, Gamma Ray Observatory should be able to detect a number of additional pulsars, and the results will be of great benefit in testing magnetospheric theories and models. Timing observations for this purpose were started at a number of radio observatories around the world. The general procedures being used are described. A status report on the work is given. Author

N90-23302*# Columbia Univ., New York, NY. Dept. of Physics.
GAMMA RADIATION FROM RADIO PULSARS **c93**
Malvin Ruderman *In* NASA, Goddard Space Flight Center, The Energetic Gamma-Ray Experiment Telescope (EGRET) Science Symposium May 1990 p 89-99 (For primary document see N90-23294 16-90)
(Grant NSF AST-89-01681)
Avail: NTIS HC A15/MF A02; 1 functional color page CSCL 03B

The probable magnetospheric location and source of the gamma ray emission from some young radiopulsars is discussed. The suggested evolution of this emission as a function of pulsar period gives a diminished gamma-ray luminosity for a more rapidly spinning pre-Crab pulsar. A greatly enhanced one, similar to that of unidentified Cos B sources, is predicted for a slightly slower post-Vela pulsar, followed by a relatively rapid quenching of the gamma-ray luminosity at still longer periods. Possible anomalous exo-magnetospheric pulsed MeV and TeV-PeV radiation from the Crab pulsar is considered. Author

N90-23303*# Max-Planck-Inst. fuer Physik und Astrophysik, Garching (Germany, F.R.). Institut fuer Extraterrestrische Physik.
GAMMA RADIATION FROM THE CRAB AND VELA PULSARS **c93**
Gottfried Kanbach *In* NASA, Goddard Space Flight Center, The Energetic Gamma-Ray Experiment Telescope (EGRET) Science Symposium May 1990 p 101-113 (For primary document see N90-23294 16-90)

Avail: NTIS HC A15/MF A02; 1 functional color page CSCL 03B

The young pulsars in Crab and Vela were observed as very efficient emitters of high energy gamma radiation. While their radiation in the radio, optical, and x ray range was always known to differ considerably, the gamma ray emission on a superficial level appears quite similar: lightcurves with two narrow peaks, separated by 141 deg (Crab) and 153 deg (Vela) and photon energies in excess of 1 GeV with spectra that can be described by a power-law for Crab and a broken power-law for Vela. The detailed observations of these sources with the COS-B instrument, extending over nearly seven years, have revealed significant differences in the characteristics of the pulsars in the gamma-ray domain. Secular changes in the temporal (Crab) and spectral (Vela) properties above 50 MeV were found. These tantalizing signatures of the pulsar emission processes must now be explored in more detail and over a larger spectral range with the GRO (Gamma Ray Observatory) instruments in order to gain a deeper understanding of the physics of young neutron stars. Author

N90-23304*# National Aeronautics and Space Administration. Goddard Space Flight Center, Greenbelt, MD.

GAMMA RAY PULSARS: MODELS AND OBSERVATIONS c93

David J. Thompson *In its* The Energetic Gamma-Ray Experiment Telescope (EGRET) Science Symposium May 1990 p 115-124 (For primary document see N90-23294 16-90)

Avail: NTIS HC A15/MF A02; 1 functional color page CSCL 03B

The two known gamma ray pulsars, the Crab and Vela, were used as guides for the development of models of high-energy radiation from spinning neutron stars. Two general classes of models were developed: those with the gamma radiation originating in the pulsar magnetosphere far from the neutron star surface (outer gap models) and those with the gamma radiation coming from above the polar cap (polar cap models). The goal is to indicate how EGRET can contribute to understanding gamma-ray pulsars, and especially how it can help distinguish between models for emission. Author

N90-23305*# National Aeronautics and Space Administration. Goddard Space Flight Center, Greenbelt, MD.

THE SENSITIVITY OF EGRET TO GAMMA RAY POLARIZATION c93

John R. Mattox (National Academy of Sciences - National Research Council, Greenbelt, MD.) *In its* The Energetic Gamma-Ray Experiment Telescope (EGRET) Science Symposium May 1990 p 125-132 (For primary document see N90-23294 16-90)

Avail: NTIS HC A15/MF A02; 1 functional color page CSCL 03B

A Monte Carlo simulation shows that EGRET (Energetic Gamma-Ray Experimental Telescope) does not even have sufficient sensitivity to detect 100 percent polarized gamma-rays. This is confirmed by analysis of calibration data. A Monte Carlo study shows that the sensitivity of EGRET to polarization peaks around 100 MeV. However, more than 10 (exp 5) gamma-ray events with 100 percent polarization would be required for a 3 sigma significance detection - more than available from calibration, and probably more than will result from a single score source during flight. A drift chamber gamma ray telescope under development (Hunter and Cuddapah 1989) will offer better sensitivity to polarization. The lateral position uncertainty will be improved by an order of magnitude. Also, if pair production occurs in the drift chamber gas (xenon at 2 bar) instead of tantalum foils, the effects of multiple Coulomb scattering will be reduced. Author

N90-23306*# Iowa State Univ. of Science and Technology, Ames.

TeV RADIATION FROM THE CRAB NEBULA AND OTHER MATTERS c93

R. C. Lamb *In* NASA, Goddard Space Flight Center, The Energetic Gamma-Ray Experiment Telescope (EGRET) Science Symposium May 1990 p 135-143 Sponsored in part by DOE (For primary document see N90-23294 16-90)

Avail: NTIS HC A15/MF A02; 1 functional color page CSCL 03B

The detection of the Crab Nebula via the Cherenkov imaging technique places TeV astronomy on a secure observational footing. The motivation for TeV observations, a discussion of the atmospheric Cherenkov technique, the experimental details of the Crab Nebula detection, and its scientific implications are presented. The present dilemma of VHE/UHE astronomy is that the Crab appears to be the only source whose showers match theoretical expectations. The situation will be clarified as improved ground-based detectors come on-line with sensitivities matching those of the GRO (Gamma Ray Observatory) instruments. Author

N90-23307*# National Aeronautics and Space Administration. Goddard Space Flight Center, Greenbelt, MD.

THE ILLUSIVE GEMINGA: WHAT IS IT c93

Donald A. Kniffen *In its* The Energetic Gamma-Ray Experiment Telescope (EGRET) Science Symposium May 1990 p 145-151 (For primary document see N90-23294 16-90)

Avail: NTIS HC A15/MF A02; 1 functional color page CSCL 03B

The first unassociated gamma-ray source was discovered by SAS-2 in 1973 (Kniffen, et al., 1975) and later confirmed by COS-B (Bennett, et al., 1977). Followed the announcement, there were numerous attempts to find a counterpart, and many models were developed to explain the source. Now over fifteen years later this illusive source still remains as one of the major riddles of astrophysics. The question of why an object, which is able to emit such energetic photons is so well concealed at other wavelengths, still remains to be answered. The association with the Einstein source 1E 0630+178 is the most favored (Bignami, Caraveo, and Lamb, 1983), but this cannot be considered proven. The pulsar emission model of Ruderman and Cheng (1988) is appealing in its broad applicability, but awaits observational confirmation. The EGRET (Energetic Gamma-Ray Experimental Telescope) instrument on the Gamma-Ray Observatory provides a major improvement in observational capability to better define the location and spectrum of this source, and hopefully leads to a confident identification. Author

N90-23308*# Max-Planck-Inst. fuer Extraterrestrische Physik, Garching (Germany, F.R.).

COS-B GAMMA RAY SOURCES BEYOND THE PREDICTED DIFFUSE EMISSION c93

H. A. Mayer-Hasselwander and G. Simpson (New Hampshire Univ., Durham.) *In* NASA, Goddard Space Flight Center, The Energetic Gamma-Ray Experiment Telescope (EGRET) Science Symposium May 1990 p 153-159 (For primary document see N90-23294 16-90)

(Grant NSF INT-83-14219)

Avail: NTIS HC A15/MF A02; 1 functional color page CSCL 03B

COS-B data were reanalyzed using for background subtraction the modeled galactic diffuse gamma-ray emission based on HI- and CO-line surveys and the gamma-ray data itself. A methodology was developed for this purpose with the following three features: automatic generation of source catalogs using correlation analysis, simulation of trials to derive significance thresholds for source detection, and bootstrap sampling to drive error boxes and confidence intervals for source parameters. The analysis shows that about half of the 2CG sources are explained by concentrations in the distribution of molecular hydrogen. Indication for a few weak new sources is also obtained. Author

N90-23309*# Leiden Univ. (Netherlands). Lab. for Space Research.

MORE DATA ON (POSSIBLE) GAMMA RAY (POINT) SOURCES c93

W. Hermsen *In* NASA, Goddard Space Flight Center, The Energetic Gamma-Ray Experiment Telescope (EGRET) Science Symposium May 1990 p 161-177 (For primary document see

N90-23294 16-90)
Avail: NTIS HC A15/MF A02; 1 functional color page CSCL 03B

The 2CG catalog of gamma ray sources was compiled before detailed knowledge was available on the fine-scale structure of the diffuse Galactic gamma-ray emission. Two independent analyses to discriminate sources which are either compact objects of due to very local and strong enhancements in the Galactic cosmic-ray distribution from those which are artifacts due to the clumpy gas distribution are about to be completed: a maximum likelihood analysis and a cross correlation analysis. Arguments are given why differences, and therefore confusion, and in resulting source lists can be expected. Detailed analysis of all COS-B gamma-ray data on Geminga (2CG195+04), reveals the existence of a drastic spectral break below 200 MeV. A power-law spectrum with index -1.88 fits the data above about 100 MeV to 3.2 GeV, however, there are also indications for a spectral break above these energies. For energies above about 100 MeV no evidence for a long-term time variability was found. The error region of Geminga was searched for a radio counterpart at wavelengths of 90, 49, 21, 6, and 2 cm using the Westerbork Synthesis Radio Telescope and the Very Large Array. So far, 16 sources were detected in this error region. In the direction of 1E0630+178, the Einstein x ray source proposed to be a Vela-like pulsar and the counterpart of Geminga, no radio source was found at 21, 49, and 90 cm with 3 sigma upper limits on the flux densities ranging from 0.5 mJy at 21 cm to 4.5 mJy at 90 cm. Detailed structures in local molecular cloud complexes are so far only resolved in gamma rays for the closet and most massive complexes, namely those in the Orion-Monoceros and the Ophiuchus regions. For both region, there is circumstantial evidence for gamma ray emission from molecular gas that was photodissociated after the passage of a SN shell. Author

N90-23310*# Northwestern Univ., Evanston, IL. Dept. of Physics and Astronomy.
WHAT CAN GAMMA RAYS TELL US ABOUT BINARY X RAY SOURCES AND SNR'S **c93**
M. P. Ulmer *In* NASA, Goddard Space Flight Center, The Energetic Gamma-Ray Experiment Telescope (EGRET) Science Symposium May 1990 p 179-182 (For primary document see N90-23294 16-90)
Avail: NTIS HC A15/MF A02; 1 functional color page CSCL 03B

Black holes, neutron stars in binary x ray source systems, and supernova remnants (SNRs) are briefly discussed. B.G.

N90-23311*# National Aeronautics and Space Administration. Goddard Space Flight Center, Greenbelt, MD.
GAMMA RAYS FROM PULSAR WIND SHOCK ACCELERATION
Alice K. Harding *In its* The Energetic Gamma-Ray Experiment Telescope (EGRET) Science Symposium May 1990 p 183-199 (For primary document see N90-23294 16-90)
Avail: NTIS HC A15/MF A02; 1 functional color page CSCL 03B

A shock forming in the wind of relativistic electron-positron pairs from a pulsar, as a result of confinement by surrounding material, could convert part of the pulsar spin-down luminosity to high energy particles through first order Fermi acceleration. High energy protons could be produced by this mechanism both in supernova remnants and in binary systems containing pulsars. The pion-decay gamma-rays resulting from interaction of accelerated protons with surrounding target material in such sources might be observable above 70 MeV with EGRET (Energetic Gamma-Ray Experimental Telescope) and above 100 GeV with ground-based detectors. Acceleration of protons and expected gamma-ray fluxes from SN1987A, Cyg X-3 type sources and binary pulsars are discussed. Author

N90-23312*# Stanford Univ., CA.
SPECTRAL DETERMINATIONS FOR DISCRETE SOURCES WITH EGRET **c89**
E. B. Hughes and P. L. Nolan *In* NASA, Goddard Space Flight Center, The Energetic Gamma-Ray Experiment Telescope (EGRET) Science Symposium May 1990 p 201-213 (For primary document see N90-23294 16-90)
(Contract NAS5-27557)
Avail: NTIS HC A15/MF A02; 1 functional color page CSCL 03A

The ability of the EGRET (Energetic Gamma-Ray Experimental Telescope) to determine the spectral parameters of point sources in 14-day exposures, as planned for the initial survey phase of the GRO (Gamma Ray Observatory) mission, is explored by numerical simulation. Results are given for both galactic and extragalactic objects as a function of source strength and for representative levels of diffuse background emission. Author

N90-23313*# National Aeronautics and Space Administration. Marshall Space Flight Center, Huntsville, AL.
GAMMA RAY BURSTS: CURRENT STATUS OF OBSERVATIONS AND THEORY **c93**
Charles A. Meegan *In* NASA, Goddard Space Flight Center, The Energetic Gamma-Ray Experiment Telescope (EGRET) Science Symposium May 1990 p 217-231 (For primary document see N90-23294 16-90)
Avail: NTIS HC A15/MF A02; 1 functional color page CSCL 03B

Gamma-ray bursts display a wide range of temporal and spectral characteristics, but typically last several seconds and emit most of their energy in the low-energy gamma-ray region. The burst sources appear to be isotropically distributed on the sky. Several lines of evidence suggest magnetic neutron stars as sources for bursts. A variety of energy sources and emission mechanisms were proposed. Author

N90-23314*# Grumman Aerospace Corp., Bethpage, NY.
WHAT IS LEARNED FROM HIGH ENERGY BURSTS AND FLARES **c93**
Edward J. Schneid *In* NASA, Goddard Space Flight Center, The Energetic Gamma-Ray Experiment Telescope (EGRET) Science Symposium May 1990 p 233-242 (For primary document see N90-23294 16-90)
Avail: NTIS HC A15/MF A02; 1 functional color page CSCL 03B

The Energetic Gamma Ray Experiment Telescope (EGRET) with its large NaI Total Absorption Shower Counter (TASC) has the scientific capability of performing spectroscopy of high energy cosmic gamma ray bursts and solar flares. EGRET, with a spectroscopy energy range from 0.6 to 140 MeV, provides an opportunity to increase the understanding of the high energy mechanisms of gamma ray bursts and solar flares. A likely interpretation of gamma ray burst sources is that they are rotating, magnetized neutron stars. High magnetic fields can influence the emission of high energy gamma rays, so observational spectroscopic data at high energies can provide information on the upper limits of the magnetic fields in the GRB regions of magnetized neutron stars. Likewise, spectroscopy of high energy gamma rays can provide information useful for deriving the flare proton spectrum which in turn can lead to an understanding of high energy solar flare particle acceleration mechanisms. Author

N90-23315*# National Aeronautics and Space Administration. Goddard Space Flight Center, Greenbelt, MD.
LOCAL NORMAL GALAXIES
Carl E. Fichtel *In its* The Energetic Gamma-Ray Experiment Telescope (EGRET) Science Symposium May 1990 p 245-256 (For primary document see N90-23294 16-90)
Avail: NTIS HC A15/MF A02; 1 functional color page CSCL 03B

In the near future, high energy (E greater than 20 MeV) gamma ray astronomy offers the promise of a new means of examining the closest galaxies. Two and possibly three local galaxies, the Small and Large Magellanic Clouds and M31, should be visible to the high energy gamma ray telescope on the Gamma Ray Observatory, and the first should be seen by GAMMA-1. With the assumptions of adequate cosmic ray production and reasonable

magnetic field strengths, both of which should likely be satisfied, specific predictions of the gamma ray emission can be made separating the concepts of the galactic and universal nature of cosmic rays. A study of the synchrotron radiation from the Large Magellanic Cloud (LMC) suggests that the cosmic ray density is similar to that in the local region of our galaxy, but not uniform. It is hoped the measurements will be able to verify this independent of assumptions about the magnetic fields in the LMC. Author

N90-23316*# National Aeronautics and Space Administration. Goddard Space Flight Center, Greenbelt, MD.
GAMMA RAYS FROM ACTIVE GALACTIC NUCLEI c93
Demosthenes Kazanas *In its* The Energetic Gamma-Ray Experiment Telescope (EGRET) Science Symposium May 1990 p 259-275 (For primary document see N90-23294 16-90)
Avail: NTIS HC A15/MF A02; 1 functional color page CSCL 03B

The general properties of Active Galactic Nuclei (AGN) and quasars are reviewed with emphasis on their continuum spectral emission. Two general classes of models for the continuum are outlined and critically reviewed in view of the impending GRO (Gamma Ray Observatory) launch and observations. The importance of GRO in distinguishing between these models and in general in furthering the understanding of AGN is discussed. The very broad terms the status of the current understanding of AGN are discussed. Author

N90-23317*# National Aeronautics and Space Administration. Goddard Space Flight Center, Greenbelt, MD.
SPECTRAL EVOLUTION OF ACTIVE GALACTIC NUCLEI PENROSE COMPTON SCATTERING PROCESSES AND GAMMA RAY EMISSION FROM SEYFERT GALAXIES c93
Darryl Leiter and Elihu Boldt *In its* The Energetic Gamma-Ray Experiment Telescope (EGRET) Science Symposium May 1990 p 277-287 (For primary document see N90-23294 16-90)
Avail: NTIS HC A15/MF A02; 1 functional color page CSCL 03B

In black hole spectral evolution models for active galactic nuclei (AGN), present epoch Seyfert galaxies evolve from an earlier precursor active galaxy (PAG) stage at redshift z is approximately 7 where they acted as the thermal sources responsible for the residual cosmic x ray background (RCXB). The Seyfert galaxies which emerge in this context emit Penrose Compton Scattering (PCS) gamma ray transients on the order of hours with a kinematic cutoff in the spectrum less than or equal to 3 MeV. The EGRET (Energetic Gamma-Ray Experimental Telescope/ OSSE (Oriented Scintillation Spectrometer Experiment/ COMPTEL (Compton Telescope)/ BATSE (Burst and Transient Source Experiment) instruments on the Gamma Ray Observatory (GRO) are appropriate instruments to carry out further tests of this model by studying: PCS gamma ray transient emission from individual galaxies and, the possibility that present epoch PCS gamma ray emitting Seyfert galaxies contribute observable temporal variability to the excess diffuse gamma ray background component less than or equal to 3 MeV. Author

N90-23318*# Max-Planck-Inst. fuer Physik und Astrophysik, Garching (Germany, F.R.). Institut fuer Extraterrestrische Physik.
THE HIGH ENERGY SOURCE 3C 273 c93
Corinna vonMontigny *In* NASA, Goddard Space Flight Center, The Energetic Gamma-Ray Experiment Telescope (EGRET) Science Symposium May 1990 p 289-301 (For primary document see N90-23294 16-90)
Avail: NTIS HC A15/MF A02; 1 functional color page CSCL 03B

The properties of 3C 273 are reviewed and an attempt is made to find an answer to the question why 3C 273 is the only extragalactic source so far, which was detected at energies greater than or equal to 50 MeV. Author

N90-23319*# Max-Planck-Inst. fuer Extraterrestrische Physik, Garching (Germany, F.R.).
COMPTEL OBSERVATIONS OF ACTIVE GALACTIC NUCLEI
V. Schonfelder *In* NASA, Goddard Space Flight Center, The Energetic Gamma-Ray Experiment Telescope (EGRET) Science Symposium May 1990 p 303-309 (For primary document see N90-23294 16-90)
Avail: NTIS HC A15/MF A02; 1 functional color page CSCL 03B

The number of AGNs (Active Galactic Nuclei) that might be observed by COMPTEL (Compton Telescope) around 1 MeV is of the order of two dozens or less. The estimate is based on the HEAO-1 (High Energy Astronomy Observer) measurements between 2 keV and 100 keV and on the assumption that the power law spectra of AGNs at x ray energies extend to at most 3 MeV before they break off. Author

N90-23320*# Naval Research Lab., Washington, DC.
OSSE OBSERVATIONS OF ACTIVE GALACTIC NUCLEI
W. Neil Johnson *In* NASA, Goddard Space Flight Center, The Energetic Gamma-Ray Experiment Telescope (EGRET) Science Symposium May 1990 p 311-316 (For primary document see N90-23294 16-90)
Avail: NTIS HC A15/MF A02; 1 functional color page CSCL 03B

The Oriented Scintillation Spectrometer Experiment (OSSE) was designed to address a broad range of scientific objectives through gamma ray observations in the 0.05 to 10 MeV energy range. A significant number of these observations shall be directed to the study of Active Galactic Nuclei (AGN). The characteristics of the OSSE instrument and the current observation plans are discussed. Examples of the scientific issues which OSSE expects to address are provided. Author

N90-23321*# California Univ., Los Angeles. Dept. of Physics and Astronomy.
GAMMA RAY COSMOLOGY: THE EXTRA GALACTIC GAMMA SPECTRUM AND METHODS TO DETECT THE UNDERLYING SOURCE
David B. Cline *In* NASA, Goddard Space Flight Center, The Energetic Gamma-Ray Experiment Telescope (EGRET) Science Symposium May 1990 p 319-327 (For primary document see N90-23294 16-90)
Avail: NTIS HC A15/MF A02; 1 functional color page CSCL 03B

The possible sources of extragalactic gamma rays and methods to distinguish the different sources are discussed. The sources considered are early universe decays and annihilation of Particles, active galactic nuclei (AGN) sources, and baryon-antibaryon annihilation in a baryon symmetric cosmology. The energy spectrum and possible angular fluctuations due to these sources are described. Author

N90-23322*# Stanford Univ., CA. High Energy Physics Lab.
DIPOLE ANALYSIS ON EGRET DATA OF EXTRAGALACTIC GAMMA RAY BACKGROUND RADIATION c93
Ying-Chi Lin *In* NASA, Goddard Space Flight Center, The Energetic Gamma-Ray Experiment Telescope (EGRET) Science Symposium May 1990 p 329-332 (For primary document see N90-23294 16-90)
Avail: NTIS HC A15/MF A02; 1 functional color page CSCL 03B

A dipole analysis on the EGRET (Energetic Gamma-Ray Experimental Telescope) data seems to be one of the numerous subjects that can be investigated for the extragalactic gamma ray background radiation. By the end of the first one and half years after launch, the all-sky survey program of GRO (Gamma Ray Observatory) will be completed. The EGRET detector will cover the full sky area fairly well by that time. A set of gamma ray data suitable for dipole moment calculations will be available. Furthermore, there now exist in the literature several dipole anisotropy results calculated for optical and infrared observations on the distribution of galaxies in the full sky. The results of dipole moment analysis from gamma ray observation can be compared with those at other wavebands, and hopefully some deeper

understanding can be gained on the large scale structure of the Universe. Author

N90-23323*# National Aeronautics and Space Administration. Goddard Space Flight Center, Greenbelt, MD.
FEASIBILITY FOR EGRET DETECTION OF ANTIMATTER CONCENTRATIONS IN THE UNIVERSE
R. C. Hartman *In its* The Energetic Gamma-Ray Experiment Telescope (EGRET) Science Symposium May 1990 p 333-342 (For primary document see N90-23294 16-90)
Avail: NTIS HC A15/MF A02; 1 functional color page CSCL 03B

Although the Grand Unified Theories of elementary particle dynamics have to some extent reduced the aesthetic attraction of matter-antimatter symmetry in the Universe, the idea is still not ruled out. Although first introduced by Alfven (1965), most of the theoretical development related to gamma-ray astronomy was carried out by Stecker, who has proposed (Stecker, Morgan, and Bredekamp, 1971) matter-antimatter annihilation extending back to large redshifts as a possible explanation of the apparently extragalactic diffuse gamma radiation. Other candidate explanations were also proposed, such as superposition of extragalactic discrete sources. Clearly, the existence of significant amounts of antimatter in the universe would be of great cosmological importance; its detection, however, is not simple. Since the photon is its own antiparticle, it carries no signature identifying whether it originated in a matter or an antimatter process; even aggregates of photons (spectra) are expected to be identical from matter and antimatter processes. The only likely indicator of the presence of concentrations of antimatter is evidence of its annihilation with normal matter, assuming there is some region of contact or overlap. The EGRET (Energetic Gamma-Ray Experimental Telescope) on the Gamma Ray Observatory, with a substantial increase in sensitivity compared with earlier high energy gamma ray telescopes, may be able to address this issue. The feasibility of using EGRET in such a search for antimatter annihilation in the Universe is considered. Author

N90-23324# Joint Inst. for Nuclear Research, Dubna (USSR).
GRAVITATIONAL COLLAPSE, FRIEDMAN MODELS AND COSMOLOGICAL CONSTANT: DOES THE UNIVERSE OSCILLATE
A. G. Bonch-Osmolovsky 1988 10 p In RUSSIAN; ENGLISH summary Submitted for publication
(DE90-620792; JINR-R-2-88-773) Avail: NTIS HC A02/MF A01

The equivalency of the Tolman-Oppenheimer and Friedman methods is discussed. The solution of Oppenheimer and Synder describes the Friedman flat Universe in a cosmological aspect. On the other hand, the Friedman results contain the description of gravitational collapse in the accompanying reference frame. It should be noted that the collapse and expansion of matter are phenomena connected indissolubly. The analysis of the cosmological consequences Lambda not = to 0 and the classification of homogeneous and isotropic Universe models is made. Using the obtained results, the hypothesis of a cyclic character of the Universe development is expressed. DOE

N90-23325# Arizona Univ., Tucson. Steward Observatory.
OPTICAL PROPERTIES OF COMETARY DUST
David J. Lien 29 Nov. 1989 39 p
(Contract F19628-87-K-0045)
(AD-A218790; GL-TR-89-0328; SR-5) Avail: NTIS HC A03/MF A01 CSCL 03/1

Cometary dust is observed in a variety of ways: scattered light, thermal emission, stellar occultations, dust coma and tail morphology, radar echos, and meteors associated with comets. To interpret these observations with respect to the physical parameters of the dust (size, shape, composition) and the properties of the dust emitting region, the physics of how electromagnetic radiation interacts with small particles must be understood. To understand the interaction of electromagnetic radiation with matter, the measurement and interpretation of optical constants of bulk materials must be understood. Classically, a material can be approximated by a series collection of bound charges with a number of resonant frequencies. The optical constants (index of refraction or dielectric constant) of a material are a measure of the ability of the material to vibrate in response to an incoming electromagnetic wave. The laboratory measurement of optical constants is very difficult, and many published optical constants may be in error. Care must be taken in choosing a set of optical constants which best represent the material being used for modelling cometary dust. Scattering theory is usually synonymous with Mie theory, although Mie theory pertains only to spherical particles. In many cases spheres may be good approximations to the particles in the coma, but an understanding of non-spherical scattering effects is essential to determine the limitations of the spherical approximation. A variety of methods exist which, although computationally intensive, provide insight into shape effects. GRA

91 LUNAR AND PLANETARY EXPLORATION

Includes planetology; and manned and unmanned flights.
For spacecraft design or space stations see *18 Spacecraft Design, Testing and Performance.*

N90-23326 California Univ., Los Angeles.
STUDIES OF IO'S ATMOSPHERE AND PLASMA TORUS Ph.D. Thesis
Miguel Angel Moreno 1989 233 p
Avail: Univ. Microfilms Order No. DA9003177

Jupiter's hot and cold plasma tori and the atmosphere of Io, a jovian moon located in a nearly circular orbit at a distance of 5.9 jovian radii from the center of Jupiter are examined. The hot and cold plasma tori are centered at 5.7 and 5.3 jovian radii from Jupiter. For the hot torus the ion partitioning and energy balance are modeled by assuming that there are independent sources of neutral sulfur and oxygen atoms, that the thermal electrons have a density of 2000/cu cm and a temperature of 5 eV. In the model of energy and mass balance of the cold torus its primary source of plasma is considered a radial diffusion inward from the hot torus. The time scale for this process is assumed to be identical to that required for energetic electrons to supply the energy necessary to power the synchrotron radiation. Charge exchange between thermal ions and an extended neutral cloud of sulfur and oxygen produces fresh ions which are accelerated to corotation by the magnetic field of Jupiter. These fresh accelerated ions are the source of energy which powers the cold torus emissions. The main ion loss mechanism is a two-step process whereby charge exchange between ions and neutral molecules transforms ions into fast neutrals. Since it is generally agreed that the source of neutrals to the hot and cold tori is the atmosphere of Io, then in order to better understand torus processes the behavior of Io's atmosphere needs to be understood. Numerical gasdynamic SO2 models of sublimation and volcanic atmospheres of Io are developed by means of computer simulations. Using a fine computational grid and the computational capabilities of the Cray supercomputers, the relevant atmospheric properties such as pressure, density, temperature, and velocity are found. Day side and night side atmospheres were investigated. It was found that volcanoes form an extended atmosphere on Io. A sublimation H2S atmosphere was also investigated. Dissert. Abstr.

92 SOLAR PHYSICS

Includes solar activity, solar flares, solar radiation and sunspots.
For related information see *93 Space Radiation.*

N90-23327 Denver Univ., CO.
THE LARGE AND SMALL SCALE DENSITY STRUCTURE IN

THE SOLAR CORONA Ph.D. Thesis
Madhulika Guhathakurta 1989 263 p
Avail: Univ. Microfilms Order No. DA9004062

Three-dimensional distribution of the polarization brightness product (pB) were investigated and then electron density distribution was inferred with respect to the heliographic current sheet during the declining phase of the solar cycle 20. This is the first electron density model of the large-scale corona based on its association with the magnetic current sheet. Synoptic pB data from the K coronameter and the White Light Coronograph aboard Skylab were used to locate the current sheet, taken as the center of the band of coronal streamers. Analyses of pB scans as a function of minimum distance from the current sheet between 1.13 to 5.0 solar radii led to the following conclusions: scans of pB are far better organized in terms of the current sheet as the surface of symmetry rather than the equatorial plane, and individual pB scans decreases as a function of minimum angular distance from the current sheet and then a plateau of minimum pB is observed over the polar coronal holes. Following conclusions were drawn on the density distribution: unlike the Munro and Jackson model (1977) it was concluded that for a given solar distance r, the electron density inside the polar coronal hole remains constant with respect to the magnitude latitude and magnetic longitude, the electron density is maximal at the current sheet and not the solar equatorial plane, and the electron density N for the entire corona up to a height of 5 solar radii is expressed. The XUV data and the white-light eclipse data of March 17/18, 1988, was used to study the small-scale density structure in the inner corona. Two coronal regions were sampled, the north and the south pole, and the irregularity factor X was found to be greater than 1.

Dissert. Abstr.

N90-23328 Wyoming Univ., Laramie.
INFRARED CORONAL LINE NOVAE Ph.D. Thesis
Matthew A. Greenhouse 1989 97 p
Avail: Univ. Microfilms Order No. DA9003788

The discovery and analysis of infrared coronal emission lines in Nova Vulpeculae 1984 No. 2, Nova Cygni 1986, and Nova Herculis 1987 is discussed. These new results increase the number of known infrared coronal line novae from one to four, comprise the major body of work done on infrared coronal line emission in novae, and form an important fraction of all near-infrared spectra of these objects. These new observations show that each coronal line nova is characterized by approximately the same (Si VI)/(Si VII) line intensity ratio which reflects a common coronal zone electron temperature of approximately 3.3 x 10(exp 5) K among these objects. Among the most significant results of this study of novae is that each coronal line nova exhibits a remarkably similar near-infrared spectrum. The abundance pattern for Al, Mg, is derived for two of the coronal line novae discussed, and the Ne abundance pattern is derived for QU Vul. These novae are substantially overabundant in these elements. These data double the number of novae for which Al and Mg abundances have been determined. The first speckle interferometry of the coronal line emission region of a nova is presented. A new technique for interpreting the coronal line spectra which relates their infrared spectral evolution to electron temperature and density gradients in the expanding ejecta is presented. The relative role of collisional and photoionization in formation of the coronal species is discussed in detail. This analysis suggests that both collisional and photoionization are important processes for formation of the coronal species. Observational tests which will improve current understanding of the spectral evolution of novae and model constraints which result from these data are also discussed.

Dissert. Abstr.

N90-23329 Yale Univ., New Haven, CT.
EVOLUTIONARY MODELS OF THE ROTATING SUN AND IMPLICATIONS FOR OTHER LOW MASS STARS Ph.D. Thesis
Marc Howard Pinsonneault 1988 152 p
Avail: Univ. Microfilms Order No. DA9009025

A new rotating stellar evolution code was developed and applied to the sun. A hydrostatic fully convective premain sequence model was evolved to the age of the sun. As the model evolves, the code accounts for angular momentum loss via a magnetic wind and angular momentum redistribution by rotationally induced instabilities. Parameters were adjusted to satisfy the usual global properties of the standard solar model, and require that the solar models constructed with this program match the observed solar rotation rate. The resulting models have an oblateness in agreement with observed upper limits. The rotation curves of the models of the present-day sun show two main features: the outer layers exhibit minimal radial differential rotation; and, a rapidly rotating central core is preserved. These basic features persist through a wide range of model parameters. The amount of differential rotation depends primarily on the properties ascribed to the angular momentum redistribution process. The spindown of young cluster stars places a lower limit on the timescale for angular momentum redistribution at the base of the surface convection zone. Transport of angular momentum leads to rotationally induced mixing which reproduces the observed Li depletion in the sun and solar analogues in open clusters. It also produces a depletion of Be in solar models and leads to CNO abundance anomalies in subgiant and giant branch models. The amount of rotationally induced mixing is different for models with different initial angular momenta. Angular momentum loss makes the surface rotation rate of old main sequence stars almost independent of their initial angular momentum. The rotation curves in the models of the present-day sun are in qualitative agreement with the estimates from current oscillation data. Dissert. Abstr.

N90-23330 Stanford Univ., CA.
NUMERICAL SIMULATIONS OF X RAYS AND GAMMA RAYS FROM SOLAR FLARES Ph.D. Thesis
James Michael McTiernan 1989 194 p
Avail: Univ. Microfilms Order No. DA8925919

Radiation of energies from 10 keV to greater than 10 MeV has been observed during solar flares, and is interpreted to be due to bremsstrahlung by relativistic electrons. A complete treatment of this problem requires solution of kinetic equation for relativistic electrons and inclusion of synchrotron energy losses. This equation is solved analytically in some simple limiting cases and numerically for models which have varying densities and magnetic fields using a Fokker-Planck code developed for this purpose. The resulting electron flux distributions are then used to calculate the spectral indices and angular distributions of the radiation and these results are used to compare with Hard X-ray Burst Spectrometer (HXRBS) observations of 30 to 500 keV x rays and Gamma Ray Spectrometer (GRS) observations of 0.3 to 1 MeV and greater than 10 MeV gamma rays. Assuming that electron anisotropy is independent of flare size, the distribution of GRS event fluences are derived from the distribution of HXRBS fluxes. It is also shown that a single population of injected electrons with constant energy spectral index extending from tens of keV to tens of MeV is not consistent with the observed GRS and HXRBS spectral index distributions. The observed variation of the mean spectral index with heliocentric angle is then used to set limits on the average degree of anisotropy of the pitch angle distribution of the injected electrons and the amount of convergence of the magnetic field. The results are compared with stereoscopic observations of individual flares and it is shown that some of this data cannot be reconciled with the above models.

Dissert. Abstr.

N90-23331# Rome Univ. (Italy). Dipt. di Fisica.
NEUTRINO SIGNALS FROM THE POWERFUL SOLAR FLARE ON SEPTEMBER 29, 1989
Daniele Fargion 19 Dec. 1989 20 p
(Preprint-721; ETN-90-96541) Avail: NTIS HC A03/MF A01

A rare energetic solar flare which occurred on 29 Sept. 1989 at 11:20, 11:33, 11:45 UT respectively, and was recorded by radio-X-cosmic rays detectors, is studied. The flare took place in the hidden solar disk and its estimated huge energy has been a source of a secondary neutrino burst by pion-muon chair decays in solar atmosphere. The estimation of the neutrino number events

detectable at the Kamiokande 2 laboratory (Japan) is given. Their prescence (or absence) may infer meaningful bounds on the solar flare energetics. ESA

N90-23332# Louisiana State Univ., Baton Rouge. Dept. of Physics and Astronomy.
SOLAR FLARES AND MAGNETOSPHERIC PARTICLES: INVESTIGATIONS BASED UPON THE ONR-602 AND ONR-604 EXPERIMENTS Final Technical Report
John P. Wefel 14 Feb. 1990 45 p
(Contract N00014-83-K-0365)
(AD-A218844) Avail: NTIS HC A03/MF A01 CSCL 03/2

The study of solar flares, and the interaction of solar flare radiations with the geospace environment, is one of the most fundamental investigations in space science. Involved are basic questions about the mechanism for energy generation in the flare region, the conversion of this energy into high energy charged particles, neutrons, x rays and gamma rays, the interplanetary propagation of the particles to Earth, the access of these particles to the magnetosphere and the changes initiated in our local environment due to the solar flare. In the latter case, the solar particles are superposed upon an existing background of geomagnetically trapped and pseudo-trapped charged particles, which are themselves of fundamental importance in the dynamics of the geospace environment. GRA

N90-23333*# Stanford Univ., CA.
A 154-DAY PERIODICITY IN THE OCCURRENCE RATE OF PROTON FLARES
T. Bai and E. W. Cliver (Air Force Geophysics Lab., Hanscom AFB, MA.) 1989 40 p Submitted for publication
(Contracts NAS8-37334; NGL-05-020-272; N00014-85-K-0111)
(NASA-CR-185826; NAS 1.26:185826; AD-A219333) Avail: NTIS HC A03/MF A01 CSCL 03/2

We have analyzed periodicities in the occurrence rate of proton flares for solar cycles 19 through 21 (1955 to 1986) and have identified two epochs that exhibit a 154-day periodicity. These epochs are a 14-year interval from 1958 January through 1971 December and a 5.5-year interval from 1978 February to 1983 August. The best-determined period is 154.6. We have found that the phase of this periodicity changed between the above-mentioned two epochs by about one half of a period. It appears that the occurrence rate of proton flares is more sensitive to the 154-day periodicity than the occurrence rate of flares selected by other criteria. GRA

93 SPACE RADIATION

Includes cosmic radiation; and inner and outer earth's radiation belts.

For biological effects of radiation see *52 Aerospace Medicine*. For theory see *73 Nuclear and High-Energy Physics*.

N90-23334 California Univ., Berkeley.
SPECTRAL MEASUREMENTS OF THE COSMIC MICROWAVE BACKGROUND Ph.D. Thesis
Alan John Kogut 1989 195 p
Avail: Univ. Microfilms Order No. DA9006397

Three experiments have measured the intensity of the Cosmic Microwave Background (CMB) at wavelengths 4.0, 3.0, and 0.21 cm (frequencies 7.5, 10, and 141 GHz). The measurement at 4.0 cm used a direct-gain total-power radiometer to measure the difference in power between the zenith sky and a large cryogenic reference target. Foreground signals are measured with the same instrument and subtracted from the zenith signal, leaving the CMB as the residual. The reference target consists of a large open-mouth cryostat with a microwave absorber submerged in liquid helium (LHe); thin windows block the radiative heat load and prevent condensation of atmospheric gases within the cryostat. The measurement at 3.0 cm used a superheterodyne Dicke-switched radiometer with a similar reference target to measure the zenith sky temperature. A rotating mirror allowed one of the antenna beams to be redirected to a series of zenith angles, permitting automated atmospheric measurements without moving the radiometer. The measurement at 0.21 cm used Very Large Array (VLA) observations of interstellar ortho-formaldehyde to determine the CMB intensity in molecular clouds toward the giant H II region W51A (G49.5 to 0.4). Solutions of the radiative transfer problem in the context of a large velocity gradient (LVG) model provided estimates of the CMB temperature within the foreground clouds. Collisional excitation from neutral hydrogen molecules (H2) within the clouds limited the precision of the result. These results and other recent measurements have provided a more precise determination of the CMB spectrum. Statistical analysis of long-wavelength ground-based results reveals a significant difference of 0.140 + or - 0.034 K between the ground-based measurements and measurements at higher frequencies using different techniques. The difference can be attributed either to undetected systematic error in either set of measurements or a CMB distortion at wavelengths greater than 1 cm. Dissert. Abstr.

N90-23335 Arizona Univ., Tucson.
LOCAL ATMOSPHERIC ELECTRICITY AND ITS POSSIBLE APPLICATION IN HIGH ENERGY COSMIC RAY AIR SHOWER DETECTION Ph.D. Thesis
Chuxing Chen 1989 104 p
Avail: Univ. Microfilms Order No. DA9003481

Near ground atmospheric electricity was studied experimentally. The main objective was to gain more understanding of this particular aspect of atmospheric phenomena, while testing the possible application to cosmic ray research. The results in atmospheric electricity show that there are certain patterns in ion grouping such as the size and lifetime. The average lifetime of ion group is 0.7 seconds and the average size is about 10 meters at our experimental site. Ultrahigh energy cosmic ray air showers should create sizable slow atmospheric electric pulses according to theoretical calculations. Preliminary studies on air showers with total particle number N equal or greater than 10(exp 5) (10(exp 15) eV) have yielded strong evidence that slow atmospheric current pulses are associated with air showers. The theory and the experiment agree with each other fairly well when averaged over large numbers of events. With the current experimental arrangement, when the air shower exceeds a certain size, the system response saturates. Therefore it is extremely desirable in future research that the counter array be designed for a much higher threshold level, since this prototype experiment indicates that interesting data would be obtained. Another reason for further experimental research being directed toward ultrahigh energy, and higher, is to establish a calibration of the slow atmospheric electric signals generated by cosmic rays as a function of primary cosmic ray energy and core location. This type of slow atmospheric electric signal, if fully understood and calibrated, offers a new and potentially less expensive technique to observe ultrahigh energy cosmic ray events, which hold some fundamental keys to the knowledge of the universe on a large scale. Dissert. Abstr.

N90-23336# Rome Univ. (Italy). Dipt. di Fisica.
THE GROUND-LEVEL COSMIC-RAY EVENT OF SEPTEMBER 29, 1989 AS RECORDED BY THE ROME DETECTORS
M. Alessio, L. Allegri, Daniele Fargion, S. Improta, N. Iucci, M. Parisi, G. Villoresi, and N. L. Zangrilli 13 Dec. 1989 20 p
(Nota-Interna-944; ETN-90-96546) Avail: NTIS HC A03/MF A01

An extraordinary increase in cosmic ray intensity, recorded on 29 Sep. 1989 by the Rome (Italy) detectors (rigidity threshold approx. 6.2 GV) is reported. The time evolution of the event, as recorded at Rome in the nucleonic component and in the total ionizing and muon components, as well as at Campo Imperatore (2300 m a.s.l. near Rome) in the nucleonic component by a special monitor designed for the detection of solar-neutron events, are shown. The one-minute time resolution of the Campo Imperatore data offers the possibility to follow in detail the development of the event for most of the time. The possible contribution of solar

neutrons to the early phase of the Campo Imperatore event has not been clarified so far; further results may be obtained by the analysis of the multiplicity data registered in the event. ESA

N90-23337# Rome Univ. (Italy). Dipt. di. Fisica.
COSMIC RAY NM-64 NEUTRON MONITOR DATA-17
N. Iucci, F. Ro, F. Signoretti, C. Signorini, G. Villoresi, and N. L. Zangrilli 19 Dec. 1989 67 p
(Nota-Interna-945; ETN-90-96547) Avail: NTIS HC A04/MF A01

Pressure corrected data from the Rome (Italy) neutron monitor and barometric pressure data are given in tabular form for the year 1988, together with the graphs of the corrected intensity. Details on the devices employed, operational mode and data handling are given. ESA

N90-23296*# National Aeronautics and Space Administration. Goddard Space Flight Center, Greenbelt, MD.
THE DIFFUSE GALACTIC GAMMA RAY EMISSION
David L. Bertsch *In its* The Energetic Gamma-Ray Experiment Telescope (EGRET) Science Symposium May 1990 p 19-29 (For primary document see N90-23294 16-90)
Avail: NTIS HC A15/MF A02; 1 functional color page CSCL 03B

N90-23297*# National Aeronautics and Space Administration. Goddard Space Flight Center, Greenbelt, MD.
A MODEL OF THE DIFFUSE GALACTIC GAMMA RAY EMISSION
Parameswaran Sreekumar (Universities Space Research Association, Greenbelt, MD.) *In its* The Energetic Gamma-Ray Experiment Telescope (EGRET) Science Symposium May 1990 p 31-41 (For primary document see N90-23294 16-90)
Avail: NTIS HC A15/MF A02; 1 functional color page CSCL 03B

N90-23298*# National Aeronautics and Space Administration. Goddard Space Flight Center, Greenbelt, MD.
GAMMA RAYS FROM GIANT MOLECULAR CLOUDS
Stanley D. Hunter and Gottfried Kanbach (Max-Planck-Inst. fuer Extraterrestrische Physik, Garching, Germany, F.R.) *In its* The Energetic Gamma-Ray Experiment Telescope (EGRET) Science Symposium May 1990 p 43-50 (For primary document see N90-23294 16-90)
Avail: NTIS HC A15/MF A02; 1 functional color page CSCL 03B

N90-23301*# Princeton Univ., NJ. Dept. of Physics.
RADIO PULSAR TIMING OBSERVATIONS FOR GRO
J. H. Taylor *In* NASA, Goddard Space Flight Center, The Energetic Gamma-Ray Experiment Telescope (EGRET) Science Symposium May 1990 p 81-87 Sponsored in part by Naval Observatory (For primary document see N90-23294 16-90)
Avail: NTIS HC A15/MF A02; 1 functional color page CSCL 03B

N90-23302*# Columbia Univ., New York, NY. Dept. of Physics.
GAMMA RADIATION FROM RADIO PULSARS
Malvin Ruderman *In* NASA, Goddard Space Flight Center, The Energetic Gamma-Ray Experiment Telescope (EGRET) Science Symposium May 1990 p 89-99 (For primary document see N90-23294 16-90)
(Grant NSF AST-89-01681)
Avail: NTIS HC A15/MF A02; 1 functional color page CSCL 03B

N90-23303*# Max-Planck-Inst. fuer Physik und Astrophysik, Garching (Germany, F.R.). Institut fuer Extraterrestrische Physik.
GAMMA RADIATION FROM THE CRAB AND VELA PULSARS
Gottfried Kanbach *In* NASA, Goddard Space Flight Center, The Energetic Gamma-Ray Experiment Telescope (EGRET) Science Symposium May 1990 p 101-113 (For primary document see N90-23294 16-90)
Avail: NTIS HC A15/MF A02; 1 functional color page CSCL 03B

N90-23304*# National Aeronautics and Space Administration. Goddard Space Flight Center, Greenbelt, MD.
GAMMA RAY PULSARS: MODELS AND OBSERVATIONS
David J. Thompson *In its* The Energetic Gamma-Ray Experiment Telescope (EGRET) Science Symposium May 1990 p 115-124 (For primary document see N90-23294 16-90)
Avail: NTIS HC A15/MF A02; 1 functional color page CSCL 03B

N90-23305*# National Aeronautics and Space Administration. Goddard Space Flight Center, Greenbelt, MD.
THE SENSITIVITY OF EGRET TO GAMMA RAY POLARIZATION
John R. Mattox (National Academy of Sciences - National Research Council, Greenbelt, MD.) *In its* The Energetic Gamma-Ray Experiment Telescope (EGRET) Science Symposium May 1990 p 125-132 (For primary document see N90-23294 16-90)
Avail: NTIS HC A15/MF A02; 1 functional color page CSCL 03B

N90-23306*# Iowa State Univ. of Science and Technology, Ames.
TeV RADIATION FROM THE CRAB NEBULA AND OTHER MATTERS
R. C. Lamb *In* NASA, Goddard Space Flight Center, The Energetic Gamma-Ray Experiment Telescope (EGRET) Science Symposium May 1990 p 135-143 Sponsored in part by DOE (For primary document see N90-23294 16-90)
Avail: NTIS HC A15/MF A02; 1 functional color page CSCL 03B

N90-23307*# National Aeronautics and Space Administration. Goddard Space Flight Center, Greenbelt, MD.
THE ILLUSIVE GEMINGA: WHAT IS IT
Donald A. Kniffen *In its* The Energetic Gamma-Ray Experiment Telescope (EGRET) Science Symposium May 1990 p 145-151 (For primary document see N90-23294 16-90)
Avail: NTIS HC A15/MF A02; 1 functional color page CSCL 03B

N90-23308*# Max-Planck-Inst. fuer Extraterrestrische Physik, Garching (Germany, F.R.).
COS-B GAMMA RAY SOURCES BEYOND THE PREDICTED DIFFUSE EMISSION
H. A. Mayer-Hasselwander and G. Simpson (New Hampshire Univ., Durham.) *In* NASA, Goddard Space Flight Center, The Energetic Gamma-Ray Experiment Telescope (EGRET) Science Symposium May 1990 p 153-159 (For primary document see N90-23294 16-90)
(Grant NSF INT-83-14219)
Avail: NTIS HC A15/MF A02; 1 functional color page CSCL 03B

N90-23309*# Leiden Univ. (Netherlands). Lab. for Space Research.
MORE DATA ON (POSSIBLE) GAMMA RAY (POINT) SOURCES
W. Hermsen *In* NASA, Goddard Space Flight Center, The Energetic Gamma-Ray Experiment Telescope (EGRET) Science Symposium May 1990 p 161-177 (For primary document see N90-23294 16-90)
Avail: NTIS HC A15/MF A02; 1 functional color page CSCL 03B

N90-23310*# Northwestern Univ., Evanston, IL. Dept. of Physics and Astronomy.
WHAT CAN GAMMA RAYS TELL US ABOUT BINARY X RAY SOURCES AND SNR'S
M. P. Ulmer *In* NASA, Goddard Space Flight Center, The Energetic Gamma-Ray Experiment Telescope (EGRET) Science Symposium May 1990 p 179-182 (For primary document see

N90-23294 16-90)
Avail: NTIS HC A15/MF A02; 1 functional color page CSCL 03B

N90-23313*# National Aeronautics and Space Administration. Marshall Space Flight Center, Huntsville, AL.
GAMMA RAY BURSTS: CURRENT STATUS OF OBSERVATIONS AND THEORY
Charles A. Meegan *In* NASA, Goddard Space Flight Center, The Energetic Gamma-Ray Experiment Telescope (EGRET) Science Symposium May 1990 p 217-231 (For primary document see N90-23294 16-90)
Avail: NTIS HC A15/MF A02; 1 functional color page CSCL 03B

N90-23314*# Grumman Aerospace Corp., Bethpage, NY.
WHAT IS LEARNED FROM HIGH ENERGY BURSTS AND FLARES
Edward J. Schneid *In* NASA, Goddard Space Flight Center, The Energetic Gamma-Ray Experiment Telescope (EGRET) Science Symposium May 1990 p 233-242 (For primary document see N90-23294 16-90)
Avail: NTIS HC A15/MF A02; 1 functional color page CSCL 03B

N90-23316*# National Aeronautics and Space Administration. Goddard Space Flight Center, Greenbelt, MD.
GAMMA RAYS FROM ACTIVE GALACTIC NUCLEI
Demosthenes Kazanas *In its* The Energetic Gamma-Ray Experiment Telescope (EGRET) Science Symposium May 1990 p 259-275 (For primary document see N90-23294 16-90)
Avail: NTIS HC A15/MF A02; 1 functional color page CSCL 03B

N90-23317*# National Aeronautics and Space Administration. Goddard Space Flight Center, Greenbelt, MD.
SPECTRAL EVOLUTION OF ACTIVE GALACTIC NUCLEI PENROSE COMPTON SCATTERING PROCESSES AND GAMMA RAY EMISSION FROM SEYFERT GALAXIES
Darryl Leiter and Elihu Boldt *In its* The Energetic Gamma-Ray Experiment Telescope (EGRET) Science Symposium May 1990 p 277-287 (For primary document see N90-23294 16-90)
Avail: NTIS HC A15/MF A02; 1 functional color page CSCL 03B

N90-23318*# Max-Planck-Inst. fuer Physik und Astrophysik, Garching (Germany, F.R.). Institut fuer Extraterrestrische Physik.
THE HIGH ENERGY SOURCE 3C 273
Corinna vonMontigny *In* NASA, Goddard Space Flight Center, The Energetic Gamma-Ray Experiment Telescope (EGRET) Science Symposium May 1990 p 289-301 (For primary document see N90-23294 16-90)
Avail: NTIS HC A15/MF A02; 1 functional color page CSCL 03B

N90-23322*# Stanford Univ., CA. High Energy Physics Lab.
DIPOLE ANALYSIS ON EGRET DATA OF EXTRAGALACTIC GAMMA RAY BACKGROUND RADIATION
Ying-Chi Lin *In* NASA, Goddard Space Flight Center, The Energetic Gamma-Ray Experiment Telescope (EGRET) Science Symposium May 1990 p 329-332 (For primary document see N90-23294 16-90)
Avail: NTIS HC A15/MF A02; 1 functional color page CSCL 03B

99 GENERAL

N90-23338*# National Aeronautics and Space Administration. Langley Research Center, Hampton, VA.
DESIGN TRENDS FOR ARMY/AIR FORCE AIRPLANES IN THE UNITED STATES
M. Leroy Spearman Washington Jun. 1990 23 p
(NASA-TM-4179; L-16636; NAS 1.15:4179) Avail: NTIS HC A03/MF A01 CSCL 01B

Some design trends in Army/Air Force airplane systems in the U.S. are traced from the pre-World War 2 era to the present time. Various types of aircraft systems are reviewed with a view toward noting design features that were used. Some observations concerning the design trends indicate that some may be driven by advanced technology and some by a need for new mission requirements. In addition, it is noted that some design trends are evolutionary and result in an extension of service life or utility of existing systems. In other cases the design trends may be more revolutionary with the intent of creating a system with a new capability. Some examples are included of designs that did not proceed to production for reasons that sometimes were technical and sometimes were not. Author

N90-23339*# National Aeronautics and Space Administration. Lewis Research Center, Cleveland, OH.
ROMANS TO MARS
D. J. Bents 1990 22 p Presented at the 28th Goddard Memorial Symposium, Washington, DC, 14-16 Mar. 1990; sponsored by the American Astronautical Society
(NASA-TM-103094; E-5416; NAS 1.15:103094) Avail: NTIS HC A03/MF A01 CSCL 05D

The key role played by technology advancement with respect to the anticipated era of discovery and exploration (in space) is illustrated: how bold new initiatives may or may not be enabled. A truly enabling technology not only renders the proposed missions technically feasible, but also makes them viable economically; that is, low enough in cost (relative to the economy supporting them) that urgent national need is not required for justification, low enough in cost that high risk can be programmatically tolerated. A fictional parallel is drawn to the Roman Empire of the second century A.D., shown to have possessed by that time the necessary knowledge, motivation, means, and technical capability of mounting, through the use of innovative mission planning, an initiative similar to Columbus' voyage. They failed to do so because they lacked the advanced technology necessary to make it an acceptable proposition economically. Speculation, based on the historical perspective, is made on the outcome of contemporary plans for future exploration showing how they will be subjected to the same historical forces, within limits imposed by the state of technology development, that shaped the timing of that previous era of discovery and exploration. Author

Typical Subject Index Listing

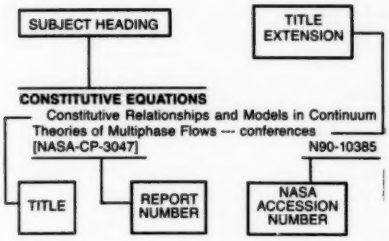

The subject heading is a key to the subject content of the document. Titles, report numbers, and accession numbers of pertinent documents are provided under each subject heading. When the title is insufficiently descriptive of the document content, a title extension has been added, separated from the title by three hyphens. The report number helps to indicate the type of document cited (e.g., NASA report, NASA translation, NASA contractor report). The NASA accession number is the number by which the document abstracts are arranged in this journal and by which the document is sold or requested. The titles, with title extensions if present, are arranged under each subject heading in ascending accession number order. The subject headings have been selected from the latest revision of the *NASA Thesaurus* (NASA SP-7064).

A

ABILITIES
Learning events in the acquisition of three skills
[AD-A219038] N90-22905
Ability distributions pattern probabilities and quasidensities
[AD-A218471] N90-23153

ABLATION
Control of surface melting and ablation in electromagnetic launchers via the magnetic vapor shielding mechanism
[AD-A219035] N90-22578

ABSORPTION COOLING
A theoretical and experimental investigation of an absorption refrigeration system for application with solar energy units N90-22697

ABSORPTION SPECTROSCOPY
Measurement of HCl by near-infrared diode laser absorption N90-22601

ABSORPTIVITY
Measurement of HCl by near-infrared diode laser absorption N90-22601

ABSTRACTS
Atlas/data abstract for the United States and selected areas, fiscal year 1989
[AD-A219289] N90-23270

ACCESS CONTROL
Access to supercomputers N90-22979

ACCURACY
Characterization and calibration of coordinate measuring machines
[DE90-009320] N90-22791

ACETYLENE
On the vapour phase deposition mechanism of carbon-boron-nitrogen compounds between 800 and 1000 C
[REPT-892-430-101] N90-22632

ACID RAIN
A study of mesoscale acid deposition in the lower Ohio River Valley N90-22848

ACOUSTIC ATTENUATION
Evidence for self-refraction in a convergence zone: NPE (Nonlinear progressive wave equation) model results
[AD-A218546] N90-22879
Numerical studies of the active control of sound transmission through double partitions
[ISVR-TR-183] N90-23181

ACOUSTIC EMISSION
Impact damage in graphite/epoxy laminates: Damage characterization, acoustic emission, and finite element simulation, volumes 1 and 2 N90-22610
Characterization of particle impact by quantitative acoustic emission
[AERE-R-13028] N90-22810

ACOUSTIC MEASUREMENT
Applications of laser ultrasound
[AERE-R-13106] N90-22777
Temporal attributes of the ambient seismo-acoustic environment: La Junta, Colorado
[AD-A219369] N90-22825

ACOUSTIC MICROSCOPES
Crack detection in silicon nitride by acoustic microscopy
[AERE-R-13196] N90-22803

ACOUSTIC SCATTERING
The effects of caustics in acoustic inverse scattering experiments
[AD-A218454] N90-23185
Contributions of individual structural modes to the scattered acoustic field
[AD-A219128] N90-23187

ACOUSTIC VELOCITY
The effects of caustics in acoustic inverse scattering experiments
[AD-A218454] N90-23185

ACOUSTICS
JPRS report: Science and technology. USSR: Physics and mathematics
[JPRS-UPM-89-001] N90-23162
Acoustoelectronic interaction of surface waves in GaAs-InGaAs superlattices N90-23163
Learning environment for neural networks and transient acoustics
[AD-A219000] N90-23186

ACOUSTO-OPTICS
Optical excisor modeling
[AD-A219338] N90-22722

ACTIVE CONTROL
Elements of active vibration control for rotating machinery
[NASA-TM-102368] N90-22703
Control of a flexible planar truss using proof mass actuators N90-23035
Distributed neural control of a hexapod walking vehicle N90-23061

ACTIVE GALACTIC NUCLEI
Gamma rays from active galactic nuclei N90-23316
Spectral evolution of active galactic nuclei Penrose Compton scattering processes and gamma ray emission from Seyfert galaxies N90-23317
The high energy source 3C 273 N90-23318
COMPTEL observations of active galactic nuclei N90-23319
OSSE observations of active galactic nuclei N90-23320

ACTUATORS
Elements of active vibration control for rotating machinery
[NASA-TM-102368] N90-22703
Field oriented control of induction motors
[NASA-TM-103154] N90-22731
Control of a flexible planar truss using proof mass actuators N90-23035

ADA (PROGRAMMING LANGUAGE)
DARK (Distributed Ada Real-Time Kernel) porting and extension guide Kernel version 3.0
[AD-A219291] N90-23112
Explanation generation in expert systems (a literature review and implementation)
[AD-A218741] N90-23268

ADAPTATION
Adaptive Resonance Theory 1
[AD-A219044] N90-23126

ADAPTIVE CONTROL
Computational issue in the analysis of adaptive control systems N90-23001
Experimental adaptive control of a hydraulic robot N90-23121
Robust adaptive control: Stability and asymptotic performance
[AD-A219259] N90-23127

ADHESIVE BONDING
Evaluation of joints bonded with elastoplastic adhesives
[REPT-892-430-120] N90-22816

ADHESIVES
An alternate interconnect method for joining flexible circuits using conductive adhesives
[DE90-008194] N90-22674

ADIABATIC CONDITIONS
Methods for evaluation of thermally induced reactions in liquid propellants
[AD-A218750] N90-22694

ADIABATIC EQUATIONS
Convergence of hyperspherical adiabatic expansion for helium-like systems
[DE90-620526] N90-22631
Approximate analysis for the formation of adiabatic shear bands
[AD-A218751] N90-22670

ADVANCED VERY HIGH RESOLUTION RADIOMETER
The analysis of polar clouds from AVHRR satellite data using pattern recognition techniques
[NASA-CR-183300] N90-22868

ADVECTION
An interactive method for estimating hailstone size and convectively-driven wind gusts from forecast soundings
[AD-A218499] N90-22871

AERIAL RUDDERS
Flutter investigations on a Transavia PL12/T-400 aircraft
[AD-A219108] N90-22570

AEROASSIST
Approximate optimal guidance schemes for atmospheric orbital maneuvering N90-22585

AERODYNAMIC CHARACTERISTICS
Dynamic ground-effect measurements on the F-15 STOL and Maneuver Technology Demonstrator (S/MTD) configuration
[NASA-TP-3000] N90-22531
The aerodynamic characteristics of power-law bodies in continuum and transitional hypersonic flow
[RAE-TM-AERO-2164] N90-22537

AERODYNAMIC COEFFICIENTS
Six-degree-of-freedom aircraft simulation with mixed-data structure using the applied dynamics simulation language, ADSIM N90-23067

AERODYNAMIC FORCES
Application of a dynamic stall model to rotor trim and aeroelastic response N90-22556
Approximate optimal guidance schemes for atmospheric orbital maneuvering N90-22585

AERODYNAMIC STALLING
Application of a dynamic stall model to rotor trim and aeroelastic response N90-22556

AERODYNAMICS
Water-tunnel study results of a TF/A-18 and F/A-18 canopy flow visualization
[NASA-TM-101705] N90-22532
Methods of jet calculation
[REPT-892-422-102] N90-22603
Side moment exerted by a spinning, coning, highly viscous liquid payload
[AD-A218746] N90-22763

AEROELASTICITY
Application of a dynamic stall model to rotor trim and aeroelastic response N90-22556

Flutter investigations on a Transavia PL12/T-400 aircraft
[AD-A219108] N90-22570

AERONAUTICAL ENGINEERING
Supercomputer and Technology
[NLR-PUB-8801] N90-22974

AEROSOLS
Estimation of extra drag force on a circular cylinder due to the presence of solid particles in subsonic compressible flow
[AD-A218635] N90-22542
HCl Vapor Characterization and Detection. JANNAF Safety and Environmental Protection Subcommittee Workshop
[AD-A216252] N90-22596
The HCl/aerosol problem N90-22597
Sticking coefficient of HCl on aerosols N90-22598
HCl monitor N90-22599

AEROSPACE VEHICLES
Approximate optimal guidance schemes for atmospheric orbital maneuvering N90-22585

AFRICA
US Navy regional climatic study of southern African waters
[AD-A218792] N90-22874
US Navy regional climatic study of the Mozambique channel and adjacent waters
[AD-A218793] N90-22875

AGRICULTURE
Impact of meteorology on the agricultural sector: Compilation and analysis of projects
[INPE-4846-PRE/1475] N90-22866

AGROMETEOROLOGY
Impact of meteorology on the agricultural sector: Compilation and analysis of projects
[INPE-4846-PRE/1475] N90-22866

AIR DEFENSE
Visual behavior in the F-15 simulator for air-to-air combat
[AD-A218648] N90-22893

AIR FLOW
The effects of compressibility on a supersonic mixing layer
[AD-A219315] N90-22543

AIR MASSES
Development and use of a passive technique for measuring nitrogen dioxide in the background atmosphere N90-23285

AIR POLLUTION
HCl monitor N90-22599
Airliner cabin ozone: An updated review
[AD-A219264] N90-22970
National emissions standards for hazardous air pollutants application for approval of construction SP-100 ground engineering system test site
[DE90-007985] N90-23203

AIR PURIFICATION
Space Station Freedom environmental control and life support system phase 3 simplified integrated test detailed report
[NASA-TM-4204] N90-22593

AIR QUALITY
HCl Vapor Characterization and Detection. JANNAF Safety and Environmental Protection Subcommittee Workshop
[AD-A216252] N90-22596

AIR SAMPLING
Development and use of a passive technique for measuring nitrogen dioxide in the background atmosphere N90-23285

AIR TRAFFIC CONTROL
FAA (Federal Aviation Administration) aviation forecasts, fiscal years 1990-2001
[AD-A219165] N90-22530

AIR TRANSPORTATION
FAA (Federal Aviation Administration) aviation forecasts, fiscal years 1990-2001
[AD-A219165] N90-22530

AIR WATER INTERACTIONS
Impact of marine boundary layer parameterization on a numerical simulation of cyclogenesis during a cold air outbreak event N90-22864
Predictability of weather and climate in a coupled ocean-atmosphere model: A dynamical systems approach N90-22865
A study of the surface layers at an air-water interface
[AD-A219378] N90-22882

AIRBORNE/SPACEBORNE COMPUTERS
A computer graphics system for visualizing spacecraft in orbit N90-22952

AIRCRAFT ACCIDENTS
UK airmisses involving commercial air transport, January - April 1989
[ISSN-0951-6301] N90-22544
Aircraft crash survival design guide. Volume 1: Design criteria and checklists
[AD-A218434] N90-22545
Aircraft crash survival design guide. Volume 2: Aircraft design crash impact conditions and human tolerance
[AD-A218435] N90-22546
Aircraft crash survival design guide. Volume 4: Aircraft seats, restraints, litters, and cockpit/cabin delethalization
[AD-A218437] N90-22548
Aircraft crash survival design guide. Volume 5: Aircraft postcrash survival
[AD-A218438] N90-22549

AIRCRAFT COMPARTMENTS
Airliner cabin ozone: An updated review
[AD-A219264] N90-22970

AIRCRAFT CONFIGURATIONS
Dynamic ground-effect measurements on the F-15 STOL and Maneuver Technology Demonstrator (S/MTD) configuration
[NASA-TP-3000] N90-22531
A modeling technique for STOVL ejector and volume dynamics
[NASA-TM-103167] N90-22566
Supersonic flow computations for an ASTOVL aircraft configuration, phase 2, part 2
[NASA-CR-4284] N90-22746

AIRCRAFT CONSTRUCTION MATERIALS
Boeing/NASA composite components flight service evaluation
[NASA-CR-181898] N90-22609
Bird impact tests on Kevlar 29 and 49 sandwich structures under straight-on and glancing impact
[REPT-S3-4273-PARTIAL-6] N90-22617
Bird impact tests on Kevlar plates. Sandwich Kevlar-nida submitted to straight-on and glancing impact
[REPT-S3-4273-PARTIAL-3] N90-22619
Bird impact tests on structures made of Kevlar 49. Monolithic plates under straight-on impact
[REPT-S3-4273-PARTIAL-1] N90-22620

AIRCRAFT CONTROL
Minimum flying qualities. Volume 1: Piloted simulation evaluation of multiple axis flying qualities
[AD-A218560] N90-22560
Minimum flying qualities. Volume 2: Pilot modeling for flying qualities applications
[AD-A218561] N90-22561
Minimum flying qualities. Volume 3: Program CC's implementation of the human optimal control model
[AD-A218562] N90-22562
Application of numerical optimization techniques to control system design for nonlinear dynamic models of aircraft N90-23032

AIRCRAFT DESIGN
Aircraft crash survival design guide. Volume 1: Design criteria and checklists
[AD-A218434] N90-22545
Aircraft crash survival design guide. Volume 2: Aircraft design crash impact conditions and human tolerance
[AD-A218435] N90-22546
Aircraft technology management and the related significance of the supercomputer N90-22975
The use of supercomputers for the design and analysis of constructions N90-22977
The automation management to support research and development N90-22978
Design trends for Army/Air Force airplanes in the United States
[NASA-TM-4179] N90-23338

AIRCRAFT DETECTION
Temporal attributes of the ambient seismo-acoustic environment: La Junta, Colorado
[AD-A219369] N90-22825

AIRCRAFT FUELS
Turbine fuel alternatives (near term)
[AD-A219405] N90-22695

AIRCRAFT INDUSTRY
FAA (Federal Aviation Administration) aviation forecasts, fiscal years 1990-2001
[AD-A219165] N90-22530
Supercomputer and Technology
[NLR-PUB-8801] N90-22974

AIRCRAFT LANDING
Dynamic ground-effect measurements on the F-15 STOL and Maneuver Technology Demonstrator (S/MTD) configuration
[NASA-TP-3000] N90-22531

AIRCRAFT PILOTS
Field-of-view assessment of low-level flight and an airdrop in the C-130 Weapon System Trainer (WST)
[AD-A218504] N90-22559
Relationship between flexibility of closure and success in pilot night vision sensor system training N90-22890

AIRCRAFT STRUCTURES
Multilevel decomposition approach to the preliminary sizing of a transport aircraft wing
[NASA-CR-4296] N90-22557
NASA-UVA light aerospace alloy and structures technology program
[NASA-CR-182607] N90-22651

AIRDROPS
Field-of-view assessment of low-level flight and an airdrop in the C-130 Weapon System Trainer (WST)
[AD-A218504] N90-22559

AIRFRAME MATERIALS
Aircraft crash survival design guide. Volume 5: Aircraft postcrash survival
[AD-A218438] N90-22549

AIRFRAMES
Aircraft crash survival design guide. Volume 3: Aircraft structural crash resistance
[AD-A218436] N90-22547
Flutter investigations on a Transavia PL12/T-400 aircraft
[AD-A219108] N90-22570

AIRLINE OPERATIONS
FAA (Federal Aviation Administration) aviation forecasts, fiscal years 1990-2001
[AD-A219165] N90-22530

ALGEBRA
Spatial operator algebra framework for multibody system dynamics N90-22989
A survey on the structured singular value N90-22998
Efficient computer algebra algorithms for polynomial matrices in control design N90-23022
A computer program to implement the Chen method of dimensional analysis
[AD-A218557] N90-23142
A computational method for general higher index nonlinear singular systems of differential equations
[AD-A219164] N90-23147
Stability regimes in a rotating quadrupole focusing accelerator
[AD-A219513] N90-23209

ALGORITHMS
Limiting performance based structural and control optimization for large vibrating structures N90-22568
Automated star pattern recognition N90-22612
Detection of bridging faults in DFCMOS combinational gates
[REPT-89-060] N90-22726
Increased stuck-at fault coverage with reduced I(sub DDQ) test sets
[DE90-009509] N90-22804
Guidelines, operational procedures, and quality control for the estimation of geodetic point positions from GPS data collected with the TI4100 receiver
[AD-A218460] N90-22829
The analysis of polar clouds from AVHRR satellite data using pattern recognition techniques
[NASA-CR-183300] N90-22868
Relationship between flexibility of closure and success in pilot night vision sensor system training N90-22890
Tracking in uncertain environments
[RAE-TM-AW-121] N90-22891
Efficient specialization of relational concepts
[AD-A218889] N90-22894
Spatial operator algebra framework for multibody system dynamics N90-22989
An order (n) algorithm for the dynamics simulation of robotic systems N90-22990
Recursive linearization of multibody dynamics equations of motion N90-22993
An innovations approach to decoupling of multibody dynamics and control N90-22994
Efficient dynamic simulation for multiple chain robotic mechanisms N90-22995
Algorithms for computing the multivariable stability margin N90-22999
Robustness analysis for real parametric uncertainty N90-23000
A disturbance based control/structure design algorithm N90-23003
Using deflation in the pole assignment problem with output feedback N90-23004
Parallel processing of real-time dynamic systems simulation on OSCAR (Optimally SCheduled Advanced multiprocessoR) N90-23006
A unifying framework for rigid multibody dynamics and serial and parallel computational issues N90-23009
Parallel algorithms and architecture for computation of manipulator forward dynamics N90-23010
Efficient computer algebra algorithms for polynomial matrices in control design N90-23022
An algorithm for the solution of dynamic linear programs N90-23026
An inverse kinematics algorithm for a highly redundant variable-geometry-truss manipulator N90-23033
Characterization of robotics parallel algorithms and mapping onto a reconfigurable SIMD machine N90-23039
A decoupled recursive approach for constrained flexible multibody system dynamics N90-23042

Algorithmic considerations of integrated design for CSI on a hypercube architecture N90-23043
A parallel structure transient response algorithm using independent substructure response computation N90-23044
Parallel conjugate gradient algorithms for manipulator dynamic simulation N90-23045
Implementation of generalized optimality criteria in a multidisciplinary environment N90-23048
New multivariable capabilities of the INCA program N90-23049
ASTEC: Controls analysis for personal computers N90-23052
Control/structure interaction design methodology N90-23053
OPTICON: Pro-Matlab software for large order controlled structure design N90-23058
Distributed neural control of a hexapod walking vehicle N90-23061
A new second-order integration algorithm for simulating mechanical dynamic systems N90-23064
The use of real-time, hardware-in-the-loop simulation in the design and development of the new Hughes HS601 spacecraft attitude control system N90-23065
A real time, FEM based optimal control algorithm and its implementation using parallel processing hardware (transistors) in a microprocessor environment N90-23066
JPL control/structure interaction test bed real-time control computer architecture N90-23070
Faster simulation plots N90-23071
Component model reduction via the projection and assembly method N90-23073
Issues in CSI analysis for large scale systems N90-23076
The power and efficiency of advanced software and parallel processing N90-23079
Numerical algorithms for computations of feedback laws arising in control of flexible systems N90-23085
Robust modelling of sampled systems for time delay estimation
[REPT-89-047] N90-23092
Program inversion: More than fun
[CS-8903] N90-23095
About the order of Appel's algorithm
[CS-8910] N90-23097
The visibility diagram: A data structure for visibility and motion planning problems. Part 1: Application to the visibility polygon query problem
[CS-8913-PT-1] N90-23098
On the performance of parallel algorithms
[CS-8914] N90-23099
Curvature-dependent parametrization of curves and surfaces
[CS-8915] N90-23100
Concurrent computing: Numerical algorithms and some applications
[AD-A218570] N90-23103
Kernel architecture manual
[AD-A219295] N90-23115
Adaptive mesh experiments for hyperbolic partial differential equations
[AD-A219194] N90-23148
Proceedings of the 9th International Conference on Computing Methods in Applied Science and Engineering
[AD-A219307] N90-23149
Statistical inference from sampled data
[AD-A218731] N90-23156
Looking at large data sets using binned data plots
[DE90-008206] N90-23263
Towards a calculus of data refinement
[CS-8902] N90-23264

ALKALIES
The effects of caustics in acoustic inverse scattering experiments
[AD-A218454] N90-23185

ALLOYS
High Intensity Electro-Magnetic and Ultrasonic Effects on Inorganic Materials Behavior and Processing Workshop
[AD-A218884] N90-22640
Improved high temperature oxidation behavior of alloys by ion implantation
[AERE-R-13309] N90-22650

ALTERNATIVES
US access to space: Launch vehicle choices for 1990 to 2010 N90-22579

ALUMINUM ALLOYS
High-temperature deformation of mechanically-alloyed aluminum IN90211 N90-22645
Environment enhanced fatigue of advanced aluminum alloys and composites N90-22652
Elevated temperature crack growth in advanced powder metallurgy aluminum alloys N90-22653
Elevated temperature crack growth in aluminum alloys: Tensile deformation of 2618 and FVS0812 aluminum alloys N90-22654
Deformation and fracture of thin sheet aluminum-lithium alloys: The effect of cryogenic temperatures N90-22655
Measurements and mechanisms of localized aqueous corrosion in aluminum-lithium alloys N90-22656
The effects of zinc addition on the environmental stability of Al-Li alloys N90-22657
Deformation and fracture of aluminum-lithium alloys: The effect of dissolved hydrogen N90-22658
The lithium concentration dependence of creep in binary aluminum-lithium alloys
[AD-A218706] N90-22668
A comparison of CuAlNi and other high damping alloys for the purpose of naval ship silencing applications
[AD-A218801] N90-22671
Structure-property relations in aluminum-lithium alloys
[AD-A219183] N90-22672

ALUMINUM COATINGS
Shaping radiation pattern of excimer laser by means of controllable intracavity mirror N90-23166

ALUMINUM OXIDES
Optical spectroscopy of Ti(3+) doped YAlO3
[AD-A219043] N90-23251

AMMETERS
A fiber-optic current sensor for aerospace applications
[NASA-TM-103152] N90-22773

AMORPHOUS MATERIALS
Amorphization of metals by ion implantation and ion beam mixing
[DE90-620571] N90-22667

ANALOG TO DIGITAL CONVERTERS
HCI monitor N90-22599

ANALYSIS (MATHEMATICS)
An algebric approach to infinite data structures
[CS-8909] N90-23265

ANDROMEDA GALAXY
Local normal galaxies N90-23315

ANGULAR ACCELERATION
Sliding control of pointing and tracking with operator spline estimation N90-22997

ANGULAR RESOLUTION
Perceived orientation, spatial layout and the geometry of pictures N90-22933

ANGULAR VELOCITY
Sliding control of pointing and tracking with operator spline estimation N90-22997

ANHYDRIDES
Modified maleic anhydride copolymers as e-beam resists
[AD-A218470] N90-22679

ANIONS
Threshold photodetachment spectroscopy of the I + HI transition state region
[AD-A218410] N90-22883

ANISOTROPY
Effect on relaxation on nonlinear waves in crystals N90-23165
Anisotropic inflation N90-23286

ANNEALING
Hydrogenation of stainless steels implanted with nitrogen
[DE90-617397] N90-22666
Low temperature degradation of Y-TZP materials
[AD-A218841] N90-22684
Lateral spreading of Au contacts on InP
[NASA-TM-103133] N90-22843

ANNIHILATION REACTIONS
Gamma ray cosmology: The extra galactic gamma spectrum and methods to detect the underlying source N90-23321
Feasibility for EGRET detection of antimatter concentrations in the universe N90-23323

ANNUAL VARIATIONS
Global and hemispheric annual temperature variations between 1861 and 1988
[DE90-007993] N90-22869

ANTARCTIC REGIONS
SeaRISE: A Multidisciplinary Research Initiative to Predict Rapid Changes in Global Sea Level Caused by Collapse of Marine Ice Sheets
[NASA-CP-3075] N90-22824
A study of auroral activity in the nightside polar cap N90-22852
The analysis of polar clouds from AVHRR satellite data using pattern recognition techniques
[NASA-CR-183300] N90-22868
On the effectiveness of the production of antarctic bottom water in the Weddell and Ross Seas
[AD-A218873] N90-22880

ANTENNA ARRAYS
The effect of mechanical deformation on the radiation patterns of large space-based arrays
[AD-A219288] N90-22719
Performance of adaptive nulling antennas in a jamming environment
[AD-A219305] N90-22720

ANTENNA RADIATION PATTERNS
The effect of mechanical deformation on the radiation patterns of large space-based arrays
[AD-A219288] N90-22719
Spectral measurements of the cosmic microwave background N90-23334

ANTIMATTER
Feasibility for EGRET detection of antimatter concentrations in the universe N90-23323

ANTIPARTICLES
Quark-antiquark pair production via gamma W fusion at high energy e(+)e(-) colliders
[PREPRINT-705] N90-23205

ANTIREFLECTION COATINGS
Development of a unique laboratory standard indium gallium arsenide detector for the 500 to 1700 micron spectral region, phase 2
[NASA-CR-180482] N90-22767

APERTURES
Agile multiple aperture imager receiver development
[AD-A218956] N90-23215

APPLICATIONS PROGRAMS (COMPUTERS)
Extension of a three-dimensional viscous wing flow analysis user's manual: VISTA 3-D code
[NASA-CR-182024] N90-22538
Quantitative characterization of spatial distribution of particles in materials: Application to materials processing N90-22660
An order (n) algorithm for the dynamics simulation of robotic systems N90-22990
Space station dynamics, attitude control and momentum management N90-23029
OPTICON: Pro-Matlab software for large order controlled structure design N90-23058
Combining high performance simulation, data acquisition, and graphics display computers N90-23062
The use of real-time, hardware-in-the-loop simulation in the design and development of the new Hughes HS601 spacecraft attitude control system N90-23065
Control design and simulation of systems modeled using ADAMS N90-23081
The Durra application debugger/monitor
[AD-A219290] N90-23111
Basic graphics routine technical manual
[AD-A219409] N90-23117

APPROXIMATION
Differential equation based method for accurate approximations in optimization
[NASA-TM-102639] N90-22558
Approximation in LQG control of a thermoelastic rod N90-23084
On approximation of nonlinear boundary integral equations for the combined method
[DE90-009784] N90-23130
High order essentially non-oscillatory schemes for Hamilton-Jacobi equations
[NASA-CR-181995] N90-23137
Analytic semigroups: Applications to inverse problems for flexible structures
[NASA-CR-182047] N90-23138
An examination of the full-wave method for rough surface scattering
[AD-A218664] N90-23155

ARCHAEOLOGY
A case for archaeological reconnaissance of the Cabo Catoche-Porvenir region of the northeastern Yucatan Peninsula
[NASA-TM-102248] N90-22827

ARCHITECTURE (COMPUTERS)
A candidate architecture for monitoring and control in chemical transfer propulsion systems
[NASA-TM-103161] N90-22595
H2, fixed architecture, control design for large scale systems
[NASA-CR-180471] N90-22698
Executive summary for the network assessment model
[AD-A218762] N90-22718
Plan execution control and architecture for mobile robots
[LAAS-89-371] N90-22793
A preliminary analysis of the SOAR architecture as a basis for general intelligence
[AD-A218913] N90-22896
Towards the knowledge level in SOAR: The role of the architecture in the use of knowledge
[NASA-CR-186615] N90-22897
Rules and maps in connectionist symbol processing
[AD-A219028] N90-22903
Connectionism and compositional semantics
[AD-A219029] N90-22904

Cognitive architectures and rational analysis: Comment
[AD-A219199] N90-22907
Toward a SOAR theory of taking instructions for immediate reasoning tasks
[AD-A219201] N90-22909
An instructable Connectionist/Control architecture: Using rule-based instructions to accomplish connectionist learning in a human time scale
[AD-A219274] N90-22914
Non-LIFO (Last-In-First-Out) execution of cognitive procedures
[AD-A219277] N90-22916
Encoding sequential structure in simple recurrent networks
[AD-A218928] N90-22984
Parallel algorithms and architecture for computation of manipulator forward dynamics N90-23010
Characterization of robotics parallel algorithms and mapping onto a reconfigurable SIMD machine N90-23039
Algorithmic considerations of integrated design for CSI on a hypercube architecture N90-23043
JPL control/structure interaction test bed real-time control computer architecture N90-23070
Proceedings of the NATO Advanced Workshop on Supercomputing
[AD-A218508] N90-23102
Fault tolerant multiprocessing and development of tools
[AD-A219216] N90-23110
Kernel architecture manual
[AD-A219295] N90-23115
Interconnection networks for highly parallel supercomputing architectures
[REPT-89-053] N90-23118

ARCTIC REGIONS
On the antarctic ozone depletion during solar cycle 21
[NOTA-INTERNA-943] N90-22849
The analysis of polar clouds from AVHRR satellite data using pattern recognition techniques
[NASA-CR-183300] N90-22868

ARIANE LAUNCH VEHICLE
Seal requirements in rocket propulsion
[ETN-90-96611] N90-22580

ARIZONA
Tropical squall lines of the Arizona monsoon N90-22867
Anderson Mesa, Arizona as a site for an optical interferometric array N90-23281

ARMOR
Large-scale simulations of monolithic and segmented projectiles impacting spaced armor
[AD-A219374] N90-22600

ARRAYS
Anderson Mesa, Arizona as a site for an optical interferometric array N90-23281

ARTIFICIAL INTELLIGENCE
The Department of Defense critical technologies plan for the Committees on Armed Services United States Congress
[AD-A219300] N90-22702
Efficient specialization of relational concepts
[AD-A218889] N90-22894
Intelligent signal processing techniques for multi-sensor surveillance systems
[AD-A218890] N90-22895
A preliminary analysis of the SOAR architecture as a basis for general intelligence
[AD-A218913] N90-22896
Towards the knowledge level in SOAR: The role of the architecture in the use of knowledge
[NASA-CR-186615] N90-22897
Stochastic interactive activation and the effect of context on perception
[AD-A218929] N90-22898
Discovering problem solving strategies: What humans do and machines don't (yet)
[AD-A219008] N90-22902
Learning events in the acquisition of three skills
[AD-A219038] N90-22905
A connectionist implementation of cognitive phonology
[AD-A219095] N90-22906
Cognitive architectures and rational analysis: Comment
[AD-A219199] N90-22907
Toward a SOAR theory of taking instructions for immediate reasoning tasks
[AD-A219201] N90-22909
Learning artificial grammars with competitive chunking
[AD-A219270] N90-22911
A task-analytic approach to the automated design of information graphics
[AD-A219271] N90-22912
Laboratory replication of scientific discovery processes
[AD-A219273] N90-22913
An instructable Connectionist/Control architecture: Using rule-based instructions to accomplish connectionist learning in a human time scale
[AD-A219274] N90-22914
Hatching a theory of incubation effects
[AD-A219275] N90-22915
Automatic compiler construction
[AD-A218777] N90-22983
Natural language processing: A tutorial
[AD-A219096] N90-23108
Application of artificial intelligence in electronic circuit diagnosis N90-23122
Adaptive Resonance Theory 1
[AD-A219044] N90-23126
Scientific discovery as problem solving
[AD-A218887] N90-23145
Learning environment for neural networks and transient acoustics
[AD-A219000] N90-23186
Explanation generation in expert systems (a literature review and implementation)
[AD-A218741] N90-23268

ASSEMBLING
Component model reduction via the projection and assembly method N90-23073

ASTRODYNAMICS
Satellite motion in axi-symmetric gravitational field. Part 2: Perturbations due to an arbitrary J(sub l)
[RAE-TR-89022] N90-22586

ASTRONOMICAL CATALOGS
Fifth fundamental catalogue (FK5). Part 1: The basic fundamental stars
[REPT-32(1988)-PT-1] N90-23282

ASTRONOMICAL MODELS
Skewering the universe with QSO lines of sight: Lyman alpha clouds as probes of large scale structure N90-23278
Anisotropic inflation N90-23286
The dynamical evolution of dense clusters of compact stars N90-23287
The effect of a stellar wind on an expanding H II region N90-23292
A model of the diffuse galactic gamma ray emission N90-23297
Gamma rays from giant molecular clouds N90-23298
Gamma radiation from radio pulsars N90-23302
Gravitational collapse, Friedman models and cosmological constant: Does the universe oscillate
[DE90-620792] N90-23324

ASTRONOMICAL OBSERVATORIES
Anderson Mesa, Arizona as a site for an optical interferometric array N90-23281

ASTROPHYSICS
Molecular evolution in astrophysical environments N90-23291
The illusive Geminga: What is it N90-23307

ASYMMETRY
A free electron laser master oscillator power amplifier experiment N90-22776

ASYMPTOTES
Robust adaptive control: Stability and asymptotic performance
[AD-A219259] N90-23127

ASYMPTOTIC METHODS
The analysis and simulation of compressible turbulence
[NASA-CR-181997] N90-22539

ASYMPTOTIC SERIES
Effect on relaxation on nonlinear waves in crystals N90-23165

ATLANTIC OCEAN
US Navy regional climatic study of southern African waters
[AD-A218792] N90-22874

ATMOSPHERIC BOUNDARY LAYER
Impact of marine boundary layer parameterization on a numerical simulation of cyclogenesis during a cold air outbreak event N90-22864

ATMOSPHERIC CIRCULATION
The multifractal nature of turbulence N90-22752
Gravity wave and turbulence studies using a high-resolution ST radar
[AD-A218877] N90-22860

ATMOSPHERIC COMPOSITION
On the antarctic ozone depletion during solar cycle 21
[NOTA-INTERNA-943] N90-22849
Airliner cabin ozone: An updated review
[AD-A219264] N90-22970
Spectral measurements of the cosmic microwave background N90-23334

ATMOSPHERIC DENSITY
MEGALIDAR proof-of-concept demonstration
[AD-A218787] N90-22858

ATMOSPHERIC ELECTRICITY
Local atmospheric electricity and its possible application in high energy cosmic ray air shower detection N90-23335

ATMOSPHERIC MODELS
The HCl/aerosol problem N90-22597
Evolution of atmospheric baroclinic waves N90-22855
Predictability of weather and climate in a coupled ocean-atmosphere model: A dynamical systems approach N90-22865

ATMOSPHERIC PRESSURE
Temporal attributes of the ambient seismo-acoustic environment: La Junta, Colorado
[AD-A219369] N90-22825
Cosmic ray NM-64 neutron monitor data-17
[NOTA-INTERNA-945] N90-23337

ATMOSPHERIC SCATTERING
A study of auroral activity in the nightside polar cap N90-22852

ATMOSPHERIC TEMPERATURE
SeaRISE: A Multidisciplinary Research Initiative to Predict Rapid Changes in Global Sea Level Caused by Collapse of Marine Ice Sheets
[NASA-CP-3075] N90-22824
Accuracy and precision of GOES data collection platforms for temperature measurements
[AD-A218798] N90-22832
Global and hemispheric annual temperature variations between 1861 and 1988
[DE90-007993] N90-22869

ATMOSPHERIC TURBULENCE
The multifractal nature of turbulence N90-22752
Gravity wave and turbulence studies using a high-resolution ST radar
[AD-A218877] N90-22860
A study of turbulence near thunderstorm tops
[NASA-CR-186620] N90-22870
A scattering center based numerical simulation of small scale atmospheric turbulence N90-23179

ATOMIC COLLISIONS
Support for the 16th International Conference on the Physics of Electronic and Atomic Collisions
[AD-A218567] N90-23200

ATOMIC EXCITATIONS
Interaction of atomic hydrogen with pico- and femtosecond laser pulses
[AD-A218426] N90-22785

ATOMIC STRUCTURE
Investigation of atomistic simulation of structural and dynamic differences in glassy and liquid states of atactic poly(propylene)
[AD-A218896] N90-22687
Electronic theory of solids, surfaces, interfaces, and clusters N90-23230
Investigation of Schottky barriers
[AD-A218422] N90-23247

ATTENTION
Visual selective attention
[AD-A219204] N90-22910

ATTITUDE (INCLINATION)
Minimum attainable RMS attitude error using co-located rate sensors N90-23038

ATTITUDE CONTROL
Automated star pattern recognition N90-22612
Space station dynamics, attitude control and momentum management N90-23029
The use of real-time, hardware-in-the-loop simulation in the design and development of the new Hughes HS601 spacecraft attitude control system N90-23065
Modeling and control of flexible space stations (slew maneuvers) N90-23086

ATTRACTION
Replica scaling analysis of interfaces in random media
[PREPRINT-713] N90-23174

AUDITORY PERCEPTION
Auditory spectro-temporal pattern analysis
[AD-A218416] N90-23184

AUDITORY SIGNALS
Auditory spectro-temporal pattern analysis
[AD-A218416] N90-23184

AURORAL ARCS
A study of auroral activity in the nightside polar cap N90-22852

AURORAS
A study of auroral activity in the nightside polar cap N90-22852
Quantifying and reducing uncertainty in the assimilative mapping of ionospheric electrodynamics N90-22854

AUTOMATA THEORY
Encoding sequential structure in simple recurrent networks
[AD-A218928] N90-22984
Collective properties of neural systems and their relation to other physical models
[AD-A219071] N90-23201

AUTOMATIC CONTROL
Automated electric power management and control for Space Station Freedom
[NASA-TM-103151] N90-23125
AUTONOMOUS NAVIGATION
ALVINN: An Autonomous Land Vehicle In a Neural Nettwork
[AD-A218975] N90-22797
AUTONOMY
Automated star pattern recognition N90-22612
AVERAGE
Computational issue in the analysis of adaptive control systems N90-23001
AXIAL LOADS
Inelastic response of metal matrix composites under biaxial loading N90-22661
The behaviour of mechanically fastened joints in composite structures N90-22789
AXISYMMETRIC BODIES
Dimensional analysis of structures using wrapping techniques
[REPT-892-430-119] N90-22815

B

B STARS
Ultraviolet and infrared studies of Be stars N90-23275
BACKGROUND NOISE
Excess noise, anomalous effects and reliability of high frequency devices (Schottky diodes, MESFET and HEMT)
[LAAS-89-394] N90-22728
BACKGROUND RADIATION
COS-B gamma ray sources beyond the predicted diffuse emission N90-23308
COMPTEL observations of active galactic nuclei N90-23319
Dipole analysis on EGRET data of extragalactic gamma ray background radiation N90-23322
Spectral measurements of the cosmic microwave background N90-23334
BARIUM COMPOUNDS
A (mu)SR-investigation of the mixed state of the high-Tc superconductor HoBa2Cu3O7-delta
[DE90-620802] N90-23241
BARIUM OXIDES
Photoresponse of YBa2Cu3O(7-delta) granular and epitaxial superconducting thin films
[NASA-TM-103144] N90-22732
Influence of high energy radiation on critical parameters of superconducting ceramics YBa2Cu3O7
[DE90-620562] N90-23239
BAROCLINIC WAVES
Evolution of atmospheric baroclinic waves N90-22855
BAROMETERS
Cosmic ray NM-64 neutron monitor data-17
[NOTA-INTERNA-945] N90-23337
BAROTROPISM
Evolution of atmospheric baroclinic waves N90-22855
BARRIER LAYERS
Investigation of Schottky barriers
[AD-A218422] N90-23247
BARYONS
Gamma ray cosmology: The extra galactic gamma spectrum and methods to detect the underlying source N90-23321
BASE FLOW
A numerical and analytical study of normal stresses and pressure differences in non-Newtonian creeping flows N90-22749
BAYES THEOREM
Tracking in uncertain environments
[RAE-TM-AW-121] N90-22891
Parametric models for A(sub n): Splitting processes and mixtures
[AD-A218421] N90-23140
A theory of Bayesian data analysis
[AD-A218420] N90-23152
Bayesian nonparametric prediction and statistical inference
[AD-A218473] N90-23154
Selecting multinomial populations
[AD-A219256] N90-23159
BEAM INJECTION
Measurements and simulation of controlled beamfront motion in the Laser Controlled Collective Accelerator
[DE90-009992] N90-22780
Plasma instabilities associated with the injection of artificial ion beams into the ionosphere N90-22851
BEAMS (SUPPORTS)
Pultrusion process development for long space boom model
[NASA-TM-4017] N90-22628
BEDS (GEOLOGY)
Fundamental studies on hydrology, hydraulics and geometry of river networks
[AD-A218662] N90-22830
BENDING
Localization of vibration in disordered nearly cyclic structures N90-22812
BESSEL FUNCTIONS
Incomplete integrals of cylindrical functions
[AD-A219512] N90-23161
BIBLIOGRAPHIES
Development of high-activity para- to ortho-hydrogen conversion catalysts, volume 2
[AD-A218700] N90-22638
BINARY ALLOYS
The lithium concentration dependence of creep in binary aluminum-lithium alloys
[AD-A218706] N90-22668
BINARY STARS
Rapid mass transfer in binary systems N90-23289
What can gamma rays tell us about binary x ray sources and SNR's N90-23310
BINOMIALS
The multifractal nature of turbulence N90-22752
BIOELECTRIC POTENTIAL
Transduction of nanovolt signals: Limits of electric-field detection
[AD-A219214] N90-23177
BIOELECTRICITY
Multimedia system control
[AD-A219392] N90-22971
BIOLOGICAL EFFECTS
A study of low level laser retinal damage
[AD-A218919] N90-22887
Exposure of human cells to electromagnetic fields
[AD-A219377] N90-22889
BIONICS
Collective properties of neural systems and their relation to other physical models
[AD-A219071] N90-23201
BIRD-AIRCRAFT COLLISIONS
Bird impact tests on Kevlar 29 and 49 sandwich structures under straight-on and glancing impact
[REPT-S3-4273-PARTIAL-6] N90-22617
Bird impact tests on Kevlar plates. Sandwich Kevlar-nida submitted to straight-on and glancing impact
[REPT-S3-4273-PARTIAL-3] N90-22619
Bird impact tests on structures made of Kevlar 49. Monolithic plates under straight-on impact
[REPT-S3-4273-PARTIAL-1] N90-22620
BISMUTH SULFIDES
Scanning laser photocurrent spectroscopy of electrochemically grown bismuth sulphide films
[AERE-M-3709] N90-22649
BL LACERTAE OBJECTS
Spectral plane quasars, spectral turn-over, and frequency atlas
[INPE-5011-TDL/399] N90-23277
BLACK HOLES (ASTRONOMY)
The dynamical evolution of dense clusters of compact stars N90-23287
Studies in gravitational lensing and numerical hydrodynamics N90-23290
What can gamma rays tell us about binary x ray sources and SNR's N90-23310
Spectral evolution of active galactic nuclei Penrose Compton scattering processes and gamma ray emission from Seyfert galaxies N90-23317
BLOCK COPOLYMERS
Synthesis and characterization of aromatic polyester and polysiloxane containing block copolymers: Multiphase transparent atomic oxygen resistant damping materials, liquid crystal films, and toughening components of sol/gel glasses
[AD-A218871] N90-22685
BODY TEMPERATURE
Heat exhaustion in a rat model: Lithium as a biochemical probe
[AD-A219361] N90-22884
BOLTED JOINTS
The behaviour of mechanically fastened joints in composite structures N90-22789
BONDING
Study and sizing of bonded joints in space structures
[REPT-892-430-124] N90-22591
Qualification of the RSRM case membrane case-to-insulation bondline inspection using the Thiokol Corporation ultrasonic RSRM bondline inspection system
[NASA-CR-183940] N90-22602
Qualification of the RSRM field joint CF case-to-insulation bondline inspection using the Thiokol Corporation ultrasonic RSRM bondline inspection system
[NASA-CR-183931] N90-22788
BOOSTER ROCKET ENGINES
Earth-to-orbit vehicle providing a reusable orbital stage
[NASA-CASE-LAR-13486-1] N90-22584
BORN APPROXIMATION
A scattering center based numerical simulation of small scale atmospheric turbulence N90-23179
BORON CHLORIDES
On the vapour phase deposition mechanism of carbon-boron-nitrogen compounds between 800 and 1000 C
[REPT-892-430-101] N90-22632
BOUNDARIES
Excitation of hypersound at boundary between Type-2 superconductor and a concentrated paramagnetic compound N90-23164
BOUNDARY INTEGRAL METHOD
On approximation of nonlinear boundary integral equations for the combined method
[DE90-009784] N90-23130
BOUNDARY LAYER EQUATIONS
Extension of a three-dimensional viscous wing flow analysis user's manual: VISTA 3-D code
[NASA-CR-182024] N90-22538
Three-dimensional separated flow prediction on fusiform body using Euler and boundary layer methods N90-22745
BOUNDARY LAYER STABILITY
Boundary layer turbulence pulsed by acoustic waves
[ETN-90-96621] N90-22759
BOUNDARY LAYER TRANSITION
Current Japanese supercomputers for computational fluid dynamics applications N90-23172
BOUNDARY VALUE PROBLEMS
The minimum drag profile in laminar flow: A numerical way N90-22535
Adaptive mesh experiments for hyperbolic partial differential equations
[AD-A219194] N90-23148
BOX BEAMS
Solar Concentrator Advanced Development Program
[NASA-CR-185173] N90-22834
BRAGG ANGLE
New approach to the dynamical diffraction theory in the case of three-dimensional perfect crystal
[DE90-620563] N90-23240
BRAGG CELLS
Optical excisor modeling
[AD-A219338] N90-22722
BRANCHING (MATHEMATICS)
Bifurcational aspects of parametric resonance
[W-8904] N90-22730
Nonlinear bifurcation study of plane Poiseuille flow
[DLR-FB-89-42] N90-22756
Continuation and multi-grid methods for bifurcation problems
[AD-A218904] N90-23146
BRAZIL
Impact of meteorology on the agricultural sector: Compilation and analysis of projects
[INPE-4846-PRE/1475] N90-22866
BREMSSTRAHLUNG
Numerical simulations of x rays and gamma rays from solar flares N90-23330
BRIGHTNESS
The large and small scale density structure in the solar corona N90-23327
BROADBAND
Regional studies with broadband data
[AD-A219215] N90-22861
BROWNIAN MOVEMENTS
A posterior stochastic equation for quantum Brownian motion
[PREPRINT-715] N90-23194
BUBBLES
Pseudo-steady diffusional growth or collapse of bubbles rising in time dependent pressure fields
[AD-A218825] N90-22764
BURNOUT
Burnout thresholds and cross section of power MOS transistors with heavy ions
[AD-A218998] N90-22736

C

CALCIUM CARBONATES
Calcium carbonate scale dissolution in water stabilized by carbon dioxide treatment
[AD-A218502] N90-22633

CALCULUS
A decoupled recursive approach for constrained flexible multibody system dynamics N90-23042
CALIBRATING
Qualification of the RSRM case membrane case-to-insulation bondline inspection using the Thiokol Corporation ultrasonic RSRM bondline inspection system
[NASA-CR-183940] N90-22602
Phase Doppler droplet sizing: Scattering angle effects
[DE90-009571] N90-22754
Qualification of the RSRM field joint CF case-to-insulation bondline inspection using the Thiokol Corporation ultrasonic RSRM bondline inspection system
[NASA-CR-183931] N90-22788
Characterization and calibration of coordinate measuring machines
[DE90-009320] N90-22791
Local atmospheric electricity and its possible application in high energy cosmic ray air shower detection N90-23335
CALORIMETERS
A low temperature calorimetric study of several high-T(sub c) superconductors N90-23237
CANADA
A study of auroral activity in the nightside polar cap N90-22852
CANCELLATION CIRCUITS
Improvement of clutter rejection by scanning motion compensation in ground-based monopulse radar
[ETN-90-96550] N90-22711
CANONICAL FORMS
Robust fixed order dynamic compensation for large space structure control N90-23059
CANOPIES
Water-tunnel study results of a TF/A-18 and F/A-18 canopy flow visualization
[NASA-TM-101705] N90-22532
CANTILEVER BEAMS
Localization of vibration in disordered nearly cyclic structures N90-22812
CAPACITORS
Advanced double layer capacitor
[AD-A219419] N90-22741
CARBON COMPOUNDS
On the vapour phase deposition mechanism of carbon-boron-nitrogen compounds between 800 and 1000 C
[REPT-892-430-101] N90-22632
CARBON DIOXIDE
Calcium carbonate scale dissolution in water stabilized by carbon dioxide treatment
[AD-A218502] N90-22633
CARBON DIOXIDE LASERS
Contributions to the development of SLM TEA CO2 laser sources for high resolution molecular spectroscopy N90-22778
CARBON DIOXIDE REMOVAL
Space Station Freedom environmental control and life support system phase 3 simplified integrated test detailed report
[NASA-TM-4204] N90-22593
CARBON FIBER REINFORCED PLASTICS
The behaviour of mechanically fastened joints in composite structures N90-22789
CARBON MONOXIDE
High spatial resolution isotopic CO and CS observations of M17 SW: The clumpy structure of the molecular cloud core
[MPE-PREPRINT-161] N90-23283
CARBON-CARBON COMPOSITES
The position of carbon/carbon composites among high temperature composites
[REPT-892-430-126] N90-22626
CARRIER LIFETIME
Experimental evaluation of chemical cleaning processes for high-lifetime silicon processing
[DE90-009332] N90-22699
CARTESIAN COORDINATES
Stable boundary conditions for Cartesian grid calculations
[NASA-CR-182048] N90-23139
CATALYSIS
Model catalytic oxidation studies using supported monometallic and heterobimetallic oxides
[DE90-009984] N90-22664
CATALYSTS
Development of high-activity para- to ortho-hydrogen conversion catalysts, volume 2
[AD-A218700] N90-22638
Model catalytic oxidation studies using supported monometallic and heterobimetallic oxides
[DE90 009984] N90-22664
Dehydrogenative polymerization of silanes to polysilanes: A monomeric copper(2) siloxide
[AD-A218550] N90-22681
CATALYTIC ACTIVITY
Model catalytic oxidation studies using supported monometallic and heterobimetallic oxides
[DE90-009984] N90-22664
CAUCHY PROBLEM
Analysis of nonlinear internal waves observed by LANDSAT-TM
[PREPRINT-704] N90-22828
CELESTIAL MECHANICS
Orbital mechanics: A learning tool on the main frame
[AD-A218799] N90-22576
Satellite motion in axi-symmetric gravitational field. Part 2: Perturbations due to an arbitrary J(sub l)
[RAE-TR-89022] N90-22586
CELL CATHODES
Catalysts for ultrahigh current density oxygen cathodes for space fuel cell applications
[NASA-CR-180650] N90-22835
CELLS (BIOLOGY)
Exposure of human cells to electromagnetic fields
[AD-A219377] N90-22889
CEMENTS
Transport of gases through concrete
[AERE-G-4977] N90-22747
CENTRIFUGAL COMPRESSORS
An investigation of the three-dimensional flow field in a centrifugal compressor N90-22751
CERAMIC FIBERS
Fatigue crack growth in a unidirectional SCS-6/Ti-15-3 composite
[NASA-TM-103095] N90-22646
High temperature fatigue behavior of a SiC/Ti-24Al-11Nb composite
[NASA-TM-103157] N90-22822
CERAMIC MATRIX COMPOSITES
The position of carbon/carbon composites among high temperature composites
[REPT-892-430-126] N90-22626
A comprehensive study on microstructure mechanics relationships of ceramic matrix composites
[AD-A219318] N90-22627
Nondestructive Testing (NDT); Ceramic Matrix Composite Materials (CMCM) — Nondestructive testing (ndc); ceramic matrix composite materials (CMMC)
[REPT-892-430-123] N90-22677
Microcracking and toughness of ceramic-fiber/ceramic-matrix composites under high temperature
[AD-A218516] N90-22680
CERAMICS
Machining of new materials at Aerospatiale
[REPT-892-430-104] N90-22622
Microcracking and toughness of ceramic-fiber/ceramic-matrix composites under high temperature
[AD-A218516] N90-22680
Low temperature degradation of Y-TZP materials
[AD-A218841] N90-22684
Low cost processing routes leading to high-performance ceramic tiles
[AD-A219034] N90-22688
Composite ceramic superconducting wires for electric motor applications
[AD-A219131] N90-22689
High temperature ceramic-tubed reformer
[DE90-009617] N90-22755
Recent advances in nondestructive evaluation made possible by novel uses of video systems
[NASA-TM-102491] N90-22801
Crack detection in silicon nitride by acoustic microscopy
[AERE-R-13196] N90-22803
The pressure loaded volumetric ceramic receiver
[DLR-MITT-89-17] N90-22842
What is going on in the La2CuO4 superconductors N90-23171
Influence of high energy radiation on critical parameters of superconducting ceramics YBa2Cu3O7
[DE90-620562] N90-23239
CEREBRAL CORTEX
Laser retinal effects: Electrophysiological determination in visual cortical cells of monkeys and cats
[AD-A218937] N90-22888
CERENKOV RADIATION
TeV radiation from the Crab nebula and other matters N90-23306
CERIUM OXIDES
Enhanced ceria solid electrolyte fuel cell development. Reduction of electronic conductivity permits use of a solid ceria electrolyte in high efficiency high power density fuel cells at temperatures compatible with metallic cell hardware
[AD-A219297] N90-22846
CHANNEL FLOW
Some observations on liquid flow through filters
[AERE-R-13300] N90-22748
Parallel channel flow excursions
[DE90-009129] N90-22753
CHAOS
Computational chaos in massively parallel neural networks N90-23012
Intermittency and multifractality in magnetic dynamos
[PREPRINT-702] N90-23226
CHARACTERIZATION
Impact damage in graphite/epoxy laminates: Damage characterization, acoustic emission, and finite element simulation, volumes 1 and 2 N90-22610
Time-varying filter modelling and time-frequency characterisation of nonstationary sound fields due to a moving source N90-23178
CHARGE EXCHANGE
An effective He-3 nucleon force for the He-3, t) charge exchange reaction
[KVI-813] N90-23198
Studies of Io's atmosphere and plasma torus N90-23326
CHARGED PARTICLES
Dynamics of motion charged particles in a field of two electromagnetic waves
[DE90-620690] N90-22706
Solar flares and magnetospheric particles: Investigations based upon the ONR-602 and ONR-604 experiments
[AD-A218844] N90-23332
CHARPY IMPACT TEST
Characterization of weldments using advanced experimental techniques
[DE90-009418] N90-22792
CHEBYSHEV APPROXIMATION
Performance of adaptive nulling antennas in a jamming environment
[AD-A219305] N90-22720
CHEMICAL ANALYSIS
The first example of an organogallium compound containing a Ga-Te bond: Synthesis, properties, and molecular structure of ((Me3CCH2)2GaTeph)2
[AD-A219258] N90-22608
Continued investigations of new concepts for improved spectrochemical analysis
[AD-A219403] N90-22644
High temperature ceramic-tubed reformer
[DE90-009617] N90-22755
CHEMICAL BONDS
The first example of an organogallium compound containing a Ga-Te bond: Synthesis, properties, and molecular structure of ((Me3CCH2)2GaTeph)2
[AD-A219258] N90-22608
CHEMICAL CLEANING
Experimental evaluation of chemical cleaning processes for high-lifetime silicon processing
[DE90-009332] N90-22699
CHEMICAL COMPOSITION
Application of x ray absorption edge spectrometry to the non-destructive determination of element concentrations, coating thickness and areal densities
[AERE-R-13030] N90-22802
The effects of point defects and composition on structural phase transition
[DE90-010109] N90-23238
CHEMICAL ENERGY
Regional studies with broadband data
[AD-A219215] N90-22861
CHEMICAL EVOLUTION
Molecular evolution in astrophysical environments N90-23291
CHEMICAL EXPLOSIONS
Regional studies with broadband data
[AD-A219215] N90-22861
CHEMICAL PROPERTIES
Methods for evaluation of thermally induced reactions in liquid propellants
[AD-A218750] N90-22694
CHEMICAL PROPULSION
A candidate architecture for monitoring and control in chemical transfer propulsion systems
[NASA-TM-103161] N90-22595
CHEMICAL REACTORS
High temperature ceramic-tubed reformer
[DE90-009617] N90-22755
CHEMISORPTION
Reactions of laser-generated free radicals at semiconductor surfaces
[AD-A218552] N90-22733
CHLORINE FLUORIDES
Experimental studies on energy storage
[AD-A219032] N90-22845

CHROMIUM STEELS
A study of the relation between grain boundary type and sensitisation in a partially-sensitised AISI 304 stainless steel using electron back-scattering patterns
[AERE-R-13327] N90-23234
CINEMATOGRAPHY
Holocinematography for studies of turbulent multiphase flow
[AD-A219130] N90-22765
On the efficacy of cinema, or what the visual system did not evolve to do N90-22934
CIRCUIT DIAGRAMS
An alternate interconnect method for joining flexible circuits using conductive adhesives
[DE90-008194] N90-22674
CIRCUIT PROTECTION
Definition of a design methodology and study of the driving and protection functions of a smart power switch
[LAAS-89-330] N90-22727
CIRCUITS
Application of artificial intelligence in electronic circuit diagnosis N90-23122
CIRCULAR CYLINDERS
Secondary frequencies in the wake of a circular cylinder with vortex shedding
[NASA-CR-181998] N90-22540
Estimation of extra drag force on a circular cylinder due to the presence of solid particles in subsonic compressible flow
[AD-A218635] N90-22542
Transverse vibrations of a composite cylindrical tube of circular cross section
[AD-A219227] N90-22820
Stability regimes in a rotating quadrupole focusing accelerator
[AD-A219513] N90-23209
Some ray tracing problems related to circles and ellipses
[AD-A219306] N90-23217
CITIES
Development and use of a passive technique for measuring nitrogen dioxide in the background atmosphere N90-23285
CLIMATE
Predictability of weather and climate in a coupled ocean-atmosphere model: A dynamical systems approach N90-22865
Global and hemispheric annual temperature variations between 1861 and 1988
[DE90-007993] N90-22869
Climatic handbook of the USSR, issue 27. Kamchatskaya Oblast. Part 3: Wind
[AD-A218720] N90-22872
US Navy regional climatic study of southern African waters
[AD-A218792] N90-22874
US Navy regional climatic study of the Mozambique channel and adjacent waters
[AD-A218793] N90-22875
CLIMATE CHANGE
SeaRISE: A Multidisciplinary Research Initiative to Predict Rapid Changes in Global Sea Level Caused by Collapse of Marine Ice Sheets
[NASA-CP-3075] N90-22824
CLIMATOLOGY
Impact of meteorology on the agricultural sector: Compilation and analysis of projects
[INPE-4846-PRE/1475] N90-22866
Climatic handbook of the USSR, issue 27. Kamchatskaya Oblast. Part 3: Wind
[AD-A218720] N90-22872
Monthly surface thermal forcing in the tropical Pacific from 1980 to 1983
[NASA-CR-183033] N90-22877
CLINICAL MEDICINE
Interactive displays in medical art N90-22940
CLOSED ECOLOGICAL SYSTEMS
Space Station Freedom environmental control and life support system phase 3 simplified integrated test detailed report
[NASA-TM-4204] N90-22593
CLOUD COVER
The analysis of polar clouds from AVHRR satellite data using pattern recognition techniques
[NASA-CR-183300] N90-22868
CLOUDS
Unsteady group behavior of droplet clouds in swirling flows N90-22743
CLUTTER
Improvement of clutter rejection by scanning motion compensation in ground-based monopulse radar
[ETN-90-96550] N90-22711
Specification for environmental measurements to assess radar sensors
[AD-A219127] N90-22833
CMOS
Design for testability of stuck-open and stack-on CMOS combinatorial circuits
[REPT-89-044] N90-22725
Detection of bridging faults in DFCMOS combinational gates
[REPT-89-060] N90-22726
Definition of a design methodology and study of the driving and protection functions of a smart power switch
[LAAS-89-330] N90-22727
COASTS
US Navy regional climatic study of southern African waters
[AD-A218792] N90-22874
US Navy regional climatic study of the Mozambique channel and adjacent waters
[AD-A218793] N90-22875
A numerical study of basic coastal upwelling processes N90-22878
COATINGS
Theoretical studies of silicon chemistry
[AD-A219232] N90-22690
Application of x ray absorption edge spectrometry to the non-destructive determination of element concentrations, coating thickness and areal densities
[AERE-R-13030] N90-22802
Microstructure of thin films
[AD-A219262] N90-23255
CODING
Encoding sequential structure in simple recurrent networks
[AD-A218928] N90-22984
COEFFICIENT OF FRICTION
Pressure and shear stress measurement uncertainty for DARPA SUBOFF experiment
[AD-A219109] N90-22798
COGNITION
Human cognitive and motor performance measures under typical cool white fluorescent illumination vs relatively high cool white illuminance/irradiance lighting
[AD-A218445] N90-22892
Efficient specialization of relational concepts
[AD-A218889] N90-22894
Cognitive efficiency considerations for good graphic design
[AD-A218976] N90-22899
Discovering problem solving strategies: What humans do and machines don't (yet)
[AD-A219008] N90-22902
Rules and maps in connectionist symbol processing
[AD-A219028] N90-22903
Learning events in the acquisition of three skills
[AD-A219038] N90-22905
A connectionist implementation of cognitive phonology
[AD-A219095] N90-22906
Cognitive architectures and rational analysis: Comment
[AD-A219199] N90-22907
Information processing approaches to cognitive development
[AD-A219200] N90-22908
Toward a SOAR theory of taking instructions for immediate reasoning tasks
[AD-A219201] N90-22909
A task-analytic approach to the automated design of information graphics
[AD-A219271] N90-22912
Laboratory replication of scientific discovery processes
[AD-A219273] N90-22913
An instructable Connectionist/Control architecture: Using rule-based instructions to accomplish connectionist learning in a human time scale
[AD-A219274] N90-22914
Hatching a theory of incubation effects
[AD-A219275] N90-22915
Non-LIFO (Last-In-First-Out) execution of cognitive procedures
[AD-A219277] N90-22916
Motor and cognitive performance do not change during a ten-week submarine patrol
[AD-A218639] N90-22969
Application of artificial intelligence in electronic circuit diagnosis N90-23122
COLD PLASMAS
Studies of Io's atmosphere and plasma torus N90-23326
COLD WORKING
A comparison of CuAlNi and other high damping alloys for the purpose of naval ship silencing applications
[AD-A218801] N90-22671
COLLAPSE
Pseudo-steady diffusional growth or collapse of bubbles rising in time dependent pressure fields
[AD-A218825] N90-22764
COLLIMATION
Shaping radiation pattern of excimer laser by means of controllable intracavity mirror N90-23166
COLLIMATORS
MEGALIDAR proof-of-concept demonstration
[AD-A218787] N90-22858
COLLISION AVOIDANCE
UK airmisses involving commercial air transport, January - April 1989
[ISSN-0951-6301] N90-22544
COLLOCATION
Fourier analysis of finite element preconditioned collocation schemes
[NASA-CR-182040] N90-23128
COLOR
Image segmentation with detection of highlights and inter-reflections using color
[AD-A218710] N90-23213
Hybrid diffractive-refractive telescope
[AD-A219241] N90-23216
COLOR CODING
The photo-colorimetric space as a medium for the representation of spatial data N90-22927
COLOR VISION
The photo-colorimetric space as a medium for the representation of spatial data N90-22927
COLORADO
Temporal attributes of the ambient seismo-acoustic environment: La Junta, Colorado
[AD-A219369] N90-22825
COMBUSTIBLE FLOW
Numerical investigation of turbulent flame sheets
[AD-A218553] N90-22635
COMBUSTION
Rapid mass transfer in binary systems N90-23289
COMBUSTION CHAMBERS
Cooling of rocket thrust chambers with liquid oxygen
[NASA-TM-103146] N90-22605
COMBUSTION CHEMISTRY
Oxidation and ignition characteristics of hydrocarbon fuels
[AD-A218666] N90-22637
COMBUSTION PHYSICS
Modeling of combustion processes in a solid fuel particle
[DE90-009140] N90-22629
COMETARY ATMOSPHERES
Optical properties of cometary dust
[AD-A218790] N90-23325
COMETS
Optical properties of cometary dust
[AD-A218790] N90-23325
COMMAND AND CONTROL
Performance analysis of Aloha networks with power capture and near/far effect
[AD-A218739] N90-22717
JPL control/structure interaction test bed real-time control computer architecture N90-23070
COMMUNICATING
Pictorial communication: Pictures and the synthetic universe N90-22919
COMMUNICATION NETWORKS
Performance analysis of Aloha networks with power capture and near/far effect
[AD-A218739] N90-22717
RF network selection in a rule-based system. NOSC project ZE68: Cost metric algorithms for internetwork applications
[AD-A219389] N90-23116
COMPASSES
Apparatus for and a method of determining compass headings
[AD-D014436] N90-22551
COMPENSATORS
Robust fixed order dynamic compensation for large space structure control N90-23059
COMPILERS
Automatic compiler construction
[AD-A218777] N90-22983
COMPLEX SYSTEMS
Spatial operator algebra framework for multibody system dynamics N90-22989
COMPOSITE MATERIALS
Damage analysis following slight deformations of composite materials
[RDS-1-007-64] N90-22618
Polymerization of composites
[REPT-892-430-102] N90-22621
Machining of new materials at Aerospatiale
[REPT-892-430-104] N90-22622
Polymerization of composite materials: A technique developed by Aerospatiale
[REPT-892-430-107] N90-22623
The surprising possibilities of wrapping
[REPT-892-430-108] N90-22624

Low cost processing routes leading to high-performance ceramic tiles
[AD-A219034] N90-22688
Composite ceramic superconducting wires for electric motor applications
[AD-A219131] N90-22689

COMPOSITE STRUCTURES
Boeing/NASA composite components flight service evaluation
[NASA-CR-181898] N90-22609
Large deformation analysis of laminated composite structures by a continuum-based shell element with transverse deformation N90-22613
A life prediction model for laminated composite structural components
[NASA-CR-186587] N90-22614
The elastic-plastic behavior of composite materials N90-22615
Pultrusion process development for long space boom model
[NASA-TM-4017] N90-22628
Environment enhanced fatigue of advanced aluminum alloys and composites N90-22652
Inelastic response of metal matrix composites under biaxial loading N90-22661
The behaviour of mechanically fastened joints in composite structures N90-22789
Explicit modeling of composite plates and beams in the dynamics of multibody systems N90-23019

COMPOSITE WRAPPING
The surprising possibilities of wrapping
[REPT-892-430-108] N90-22624
Production of a variety of shapes using wrapping and draping techniques
[REPT-892-430-122] N90-22625
Dimensional analysis of structures using wrapping techniques
[REPT-892-430-119] N90-22815

COMPRESSIBLE FLOW
The analysis and simulation of compressible turbulence
[NASA-CR-181997] N90-22539
Estimation of extra drag force on a circular cylinder due to the presence of solid particles in subsonic compressible flow
[AD-A218635] N90-22542
The effects of compressibility on a supersonic mixing layer
[AD-A219315] N90-22543
Investigation of advanced counterrotation blade configuration concepts for high speed turboprop systems, task 1: Ducted propfan analysis
[NASA-CR-185217] N90-22567
Nonstrictly hyperbolic conservation laws
[AD-A218525] N90-22762

COMPRESSION LOADS
Axisymmetric and cylindrically orthotropic analysis of filament winding N90-22811

COMPRESSOR BLADES
Forcing function effects on rotor row unsteady aerodynamic response in a multistage compressor N90-22536

COMPTON EFFECT
Spectral evolution of active galactic nuclei Penrose Compton scattering processes and gamma ray emission from Seyfert galaxies N90-23317
OSSE observations of active galactic nuclei N90-23320

COMPUTATION
The preprocessed doacross loop
[NASA-CR-182056] N90-22972
A nearly-linear computational-cost scheme for the forward dynamics of an N-body pendulum N90-22996
Computational issue in the analysis of adaptive control systems N90-23001
Parallel and vector computation for stochastic optimal control applications N90-23007
A unifying framework for rigid multibody dynamics and serial and parallel computational issues N90-23009
Parallel algorithms and architecture for computation of manipulator forward dynamics N90-23010
Computational dynamics for robotics systems using a non-strict computational approach N90-23011
Locality in parallel computation
[AD-A218733] N90-23120
A computational method for general higher index nonlinear singular systems of differential equations
[AD-A219164] N90-23147

COMPUTATIONAL FLUID DYNAMICS
The minimum drag profile in laminar flow: A numerical way N90-22535
Extension of a three-dimensional viscous wing flow analysis user's manual: VISTA 3-D code
[NASA-CR-182024] N90-22538
The analysis and simulation of compressible turbulence
[NASA-CR-181997] N90-22539
Secondary frequencies in the wake of a circular cylinder with vortex shedding
[NASA-CR-181998] N90-22540
A modeling technique for STOVL ejector and volume dynamics
[NASA-TM-103167] N90-22566
Investigation of advanced counterrotation blade configuration concepts for high speed turboprop systems, task 1: Ducted propfan analysis
[NASA-CR-185217] N90-22567
Three-dimensional separated flow prediction on fusiform body using Euler and boundary layer methods N90-22745
Supersonic flow computations for an ASTOVL aircraft configuration, phase 2, part 2
[NASA-CR-4284] N90-22746
Numerical flow simulation and supercomputers: More than a digital wind tunnel N90-22976
PLOT3D user's manual
[NASA-TM-101067] N90-23090
Stable boundary conditions for Cartesian grid calculations
[NASA-CR-182048] N90-23139
Proceedings of the 9th International Conference on Computing Methods in Applied Science and Engineering
[AD-A219307] N90-23149
ONR Far East Scientific Information Bulletin, Volume 13, No. 4
[ONRFE-SCI-INFO-BULL-13(4)88] N90-23168
Current Japanese supercomputers for computational fluid dynamics applications N90-23172

COMPUTATIONAL GRIDS
A study of woven fabric-reinforced composite materials using an invariant-based orthotropic plasticity formulation N90-22611
Multigrid acceleration of transonic flow computations
[ENSM-8024] N90-22760
Calculation of 3-dimensional synthetic seismograms on the connection machine
[AD-A218472] N90-22857
A real time, FEM based optimal control algorithm and its implementation using parallel processing hardware (transistors) in a microprocessor environment N90-23056
PLOT3D user's manual
[NASA-TM-101067] N90-23090
Stable boundary conditions for Cartesian grid calculations
[NASA-CR-182048] N90-23139
Continuation and multi-grid methods for bifurcation problems
[AD-A218904] N90-23146
Adaptive mesh experiments for hyperbolic partial differential equations
[AD-A219194] N90-23148
Proceedings of the 9th International Conference on Computing Methods in Applied Science and Engineering
[AD-A219307] N90-23149
Current Japanese supercomputers for computational fluid dynamics applications N90-23172
Studies of Io's atmosphere and plasma torus N90-23326

COMPUTER AIDED DESIGN
Aircraft technology management and the related significance of the supercomputer N90-22975
Numerical flow simulation and supercomputers: More than a digital wind tunnel N90-22976
The use of supercomputers for the design and analysis of constructions N90-22977
The development of a system for the numerical simulation of Euler flows N90-22980
Strategy of supercomputer development N90-22981
New multivariable capabilities of the INCA program N90-23049
Multidisciplinary Expert-aided Analysis and Design (MEAD) N90-23050
Overview of computational control research at UT Austin N90-23051
Control/structure interaction design methodology N90-23053
Curvature-dependent parametrization of curves and surfaces
[CS-8915] N90-23100
Comparative evaluations of four specification methods for real-time systems
[AD-A219187] N90-23109

COMPUTER AIDED MANUFACTURING
Evaluation of joints bonded with elastoplastic adhesives
[REPT-892-430-120] N90-22816

COMPUTER AIDED TOMOGRAPHY
Large scale metrology by computer assisted photogrammetry
[REPT-892-430-116] N90-22772
On-line x ray inspection of materials and structural components using discrete element x ray detectors for digital radiographic and computed tomographic evaluation
[AD-A218911] N90-22806

COMPUTER DESIGN
Locality in parallel computation
[AD-A218733] N90-23120

COMPUTER GRAPHICS
Spatial Displays and Spatial Instruments
[NASA-CP-10032] N90-22918
Pictorial communication: Pictures and the synthetic universe N90-22919
The photo-colorimetric space as a medium for the representation of spatial data N90-22927
Spatial issues in user interface design from a graphic design perspective N90-22939
Interactive displays in medical art N90-22940
The interactive digital video interface N90-22941
A computer graphics system for visualizing spacecraft in orbit N90-22952
Interactive orbital proximity operations planning system N90-22953
Experiences in teleoperation of land vehicles N90-22954
Development of a stereo 3-D pictorial primary flight display N90-22955
Synthetic perspective optical flow: Influence on pilot control tasks N90-22956
Optical, gravitational, and kinesthetic determinants of judged eye level N90-22959
The making of the mechanical universe N90-22961
Synesthetic art through 3-D projection: The requirements of a computer-based supermedium N90-22962
Wide-angle display developments by computer graphics N90-22963
Volumetric visualization of 3D data N90-22964
Determination of depth-viewing volumes for stereo three-dimensional graphic displays
[NASA-TP-2999] N90-22965
Graphics equipment for data analysis
[AD-A218983] N90-22985
Combining high performance simulation, data acquisition, and graphics display computers N90-23062
Man-in-the-control-loop simulation of manipulators N90-23063
PLOT3D user's manual
[NASA-TM-101067] N90-23090
Basic graphics routine technical manual
[AD-A219409] N90-23117

COMPUTER NETWORKS
Executive summary for the network assessment model
[AD-A218762] N90-22718
Rules and maps in connectionist symbol processing
[AD-A219028] N90-22903
Cognitive architectures and rational analysis: Comment
[AD-A219199] N90-22907
Proceedings of the 3rd Annual Conference on Aerospace Computational Control, volume 2
[NASA-CR-186447] N90-23040
Reusing software components by specialization
[REPT-89-062] N90-23094
Fault tolerant multiprocessing and development of tools
[AD-A219216] N90-23110
The Durra application debugger/monitor
[AD-A219290] N90-23111
Locality in parallel computation
[AD-A218733] N90-23120

COMPUTER PROGRAMMING
Using object-oriented analysis techniques to support system testing
[DE90-009540] N90-22700
Designing good experiments to test bad hypotheses
[AD-A218977] N90-22900
Synesthetic art through 3-D projection: The requirements of a computer-based supermedium N90-22962
A tool for aiding in the reuse of software
[INPE-4981-PRE/1545] N90-23091
Reusing software components by specialization
[REPT-89-062] N90-23094
Proceedings of the NATO Advanced Workshop on Supercomputing
[AD-A218508] N90-23102
Concurrent computing: Numerical algorithms and some applications
[AD-A218570] N90-23103
An algebric approach to infinite data structures
[CS-8909] N90-23265

Explanation generation in expert systems (a literature review and implementation)
[AD-A218741] N90-23268

COMPUTER PROGRAMS

Debris/ice/TPS assessment and photographic analysis for Shuttle Mission STS-36
[NASA-TM-102789] N90-22583

A study of woven fabric-reinforced composite materials using an invariant-based orthotropic plasticity formulation N90-22611

Large deformation analysis of laminated composite structures by a continuum-based shell element with transverse deformation N90-22613

Modeling of combustion processes in a solid fuel particle
[DE90-009140] N90-22629

Calcium carbonate scale dissolution in water stabilized by carbon dioxide treatment
[AD-A218502] N90-22633

A theoretical and experimental investigation of an absorption refrigeration system for application with solar energy units N90-22697

Side moment exerted by a spinning, coning, highly viscous liquid payload
[AD-A218746] N90-22763

Cognitive efficiency considerations for good graphic design
[AD-A218976] N90-22899

The development of a system for the numerical simulation of Euler flows N90-22960

Parallel processing of real-time dynamic systems simulation on OSCAR (Optimally SCheduled Advanced multiprocessoR) N90-23006

Modern CACSD using the Robust-Control Toolbox N90-23024

Simulation studies using multibody dynamics code DART N90-23036

On trajectory generation for flexible space crane: Inverse dynamics analysis by LATDYN N90-23037

Enhanced modeling features within TREETOPS N90-23047

Implementation of generalized optimality criteria in a multidisciplinary environment N90-23048

New multivariable capabilities of the INCA program N90-23049

Multidisciplinary Expert-aided Anaiysis and Design (MEAD) N90-23050

ASTEC: Controls analysis for personal computers N90-23052

Multibody dynamics model building using graphical interfaces N90-23082

PLOT3D user's manual
[NASA-TM-101067] N90-23090

About the order of Appel's algorithm
[CS-8910] N90-23097

Vectors and matrices: Two turbo pascal units for fast program development
[AD-A218917] N90-23105

Natural language processing: A tutorial
[AD-A219096] N90-23108

Comparative evaluations of four specification methods for real-time systems
[AD-A219187] N90-23109

Version description and installation guide Kernel version 3.0
[AD-A219292] N90-23113

Kernel architecture manual
[AD-A219295] N90-23115

A computer program to implement the Chen method of dimensional analysis
[AD-A218557] N90-23142

Current Japanese supercomputers for computational fluid dynamics applications N90-23172

COMPUTER SYSTEMS DESIGN

Six-degree-of-freedom missile simulation using the ADI AD 100 digital computer and ADSIM simulation language N90-23068

Concurrent computing: Numerical algorithms and some applications
[AD-A218570] N90-23103

The Durra application debugger/monitor
[AD-A219290] N90-23111

Interconnection networks for highly parallel supercomputing architectures
[REPT-89-053] N90-23118

Control of randomly sampled robotic systems
[AD-A218948] N90-23157

COMPUTER SYSTEMS PERFORMANCE

Inertial navigation system simulator: Behavioral specification, revision
[AD-A219294] N90-22554

The preprocessed doacross loop
[NASA-CR-182056] N90-22972

Communication overhead on the Intel iPSC-860 hypercube
[NASA-CR-182055] N90-22982

Implementation of generalized optimality criteria in a multidisciplinary environment N90-23048

Comparative evaluations of four specification methods for real-time systems
[AD-A219187] N90-23109

BTOS database evaluation
[AD-A219304] N90-23271

COMPUTER SYSTEMS PROGRAMS

Reusing software components by specialization
[REPT-89-062] N90-23094

Program inversion: More than fun
[CS-8903] N90-23095

COMPUTER TECHNIQUES

Synesthetic art through 3-D projection: The requirements of a computer-based supermedium N90-22962

The automation management to support research and development N90-22978

Aspects of efficient and reliable multibody system simulation N90-22991

Using deflation in the pole assignment problem with output feedback N90-23004

Some ray tracing problems related to circles and ellipses
[AD-A219306] N90-23217

COMPUTER VISION

ALVINN: An Autonomous Land Vehicle In a Neural Nettwork
[AD-A218975] N90-22797

COMPUTERIZED SIMULATION

Minimum flying qualities. Volume 3: Program CC's implementation of the human optimal control model
[AD-A218562] N90-22562

Semianalytic study of high-eccentricity orbit stability and evolution N90-22574

Investigation of atomistic simulation of structural and dynamic differences in glassy and liquid states of atactic poly(propylene)
[AD-A218896] N90-22687

Using object-oriented analysis techniques to support system testing
[DE90-009540] N90-22700

HF propagation through actively modified ionospheres
[DE90-008931] N90-22705

A free electron laser master oscillator power amplifier experiment N90-22776

Influence of linear profile modification and loading conditions on the dynamic tooth load and stress of high contact ratio gears
[NASA-TM-103136] N90-22796

Large-scale simulations of monolithic and segmented projectiles impacting spaced armor
[AD-A219374] N90-22800

Probabilistic structural analysis of aerospace components using NESSUS
[NASA-TM-102324] N90-22823

Stochastic interactive activation and the effect of context on perception
[AD-A218929] N90-22898

Learning artificial grammars with competitive chunking
[AD-A219270] N90-22911

Displays for telemanipulation N90-22948

A computer graphics system for visualizing spacecraft in orbit N90-22952

Volumetric visualization of 3D data N90-22964

Supercomputer and Technology
[NLR-PUB-8801] N90-22974

Numerical flow simulation and supercomputers: More than a digital wind tunnel N90-22976

An assessment of multibody simulation tools for articulated spacecraft N90-22988

An order (n) algorithm for the dynamics simulation of robotic systems N90-22990

Aspects of efficient and reliable multibody system simulation N90-22991

Efficient dynamic simulation for multiple chain robotic mechanisms N90-22995

A robot arm simulation with a shared memory multiprocessor machine N90-23008

Parallel algorithms and architecture for computation of manipulator forward dynamics N90-23010

Computational chaos in massively parallel neural networks N90-23012

Multi-flexible-body dynamics capturing motion-induced stiffness N90-23013

Nonlinear strain-displacement relations and flexible multibody dynamics N90-23014

Development of efficient computer program for dynamic simulation of telerobotic manipulation N90-23017

Explicit modeling of composite plates and beams in the dynamics of multibody systems N90-23019

Experimental verification of dynamic simulation N90-23020

Space station dynamics, attitude control and momentum management N90-23029

Application of numerical optimization techniques to control system design for nonlinear dynamic models of aircraft N90-23032

Simulation studies using multibody dynamics code DART N90-23036

Proceedings of the 3rd Annual Conference on Aerospace Computational Control, volume 2
[NASA-CR-186447] N90-23040

Concurrent processing simulation of the space station N90-23041

Methodology for analysis and simulation of large multidisciplinary problems N90-23046

Enhanced modeling features within TREETOPS N90-23047

ASTEC: Controls analysis for personal computers N90-23052

Combining high performance simulation, data acquisition, and graphics display computers N90-23062

Man-in-the-control-loop simulation of manipulators N90-23063

A new second-order integration algorithm for simulating mechanical dynamic systems N90-23064

The use of real-time, hardware-in-the-loop simulation in the design and development of the new Hughes HS601 spacecraft attitude control system N90-23065

Six-degree-of-freedom missile simulation using the ADI AD 100 digital computer and ADSIM simulation language N90-23068

Real-time closed-loop simulation and upset evaluation of control systems in harsh electromagnetic environments N90-23069

Faster simulation plots N90-23071

Component model reduction via the projection and assembly method N90-23073

Modal identities for multibody elastic spacecraft: An aid to selecting modes for simulation N90-23075

Structural modeling for control design (articulated multibody component representation) N90-23077

The power and efficiency of advanced software and parallel processing N90-23079

Dynamic analysis of flexible mechanical systems using LATDYN N90-23080

Control design and simulation of systems modeled using ADAMS N90-23081

Multibody dynamics model building using graphical interfaces N90-23082

A verification library for multibody simulation software N90-23089

The (DURIP) computer simulations of plasmas, nonlinear systems, and control theory
[AD-A219070] N90-23107

Experimental adaptive control of a hydraulic robot N90-23121

Index and consistency analysis for DAE (Differential Algebraic Equation) systems for Stefan-Maxwell diffusion-reaction problems
[DE90-008188] N90-23129

Scientific discovery as problem solving
[AD-A218887] N90-23145

On randomness of random number generators
[MEMO-COSOR-89-20] N90-23151

A scattering center based numerical simulation of small scale atmospheric turbulence N90-23179

Theoretical and computer simulation study of the density fluctuations in liquid water
[PREPRINT-697] N90-23191

VLA and VLBI angular broadening measurements: The distribution of interstellar scattering at low Galactic latitudes N90-23279

Studies of Io's atmosphere and plasma torus N90-23326

CONCENTRATORS

High-efficiency silicon solar cells for a 22-sun line-focus module
[DE90-010242] N90-22840

CONCRETE STRUCTURES

Transport of gases through concrete
[AERE-G-4977] N90-22747

CONCRETES

Transport of gases through concrete
[AERE-G-4977] N90-22747

CONCURRENT PROCESSING

Concurrent processing simulation of the space station N90-23041

Concurrent computing: Numerical algorithms and some applications
[AD-A218570] N90-23103

The Durra application debugger/monitor
[AD-A219290] N90-23111

CONDENSED MATTER PHYSICS

Linear and nonlinear electrical response of condensed matter: Ionic, dielectric, and mixed-conduction materials
[AD-A218771] N90-22639

Electronic theory of solids, surfaces, interfaces, and clusters N90-23230

CONDUCTIVE HEAT TRANSFER
High-temperature deformation of mechanically-alloyed aluminum IN90211 N90-22645
Thermal phenomena in high-Tc thin film superconductors N90-23233
CONFERENCES
High Intensity Electro-Magnetic and Ultrasonic Effects on Inorganic Materials Behavior and Processing Workshop
[AD-A218884] N90-22640
Spatial Displays and Spatial Instruments
[NASA-CP-10032] N90-22918
Proceedings of the 3rd Annual Conference on Aerospace Computational Control, volume 1
[NASA-CR-186446] N90-22987
Proceedings of the 3rd Annual Conference on Aerospace Computational Control, volume 2
[NASA-CR-186447] N90-23040
Proceedings of the NATO Advanced Workshop on Supercomputing
[AD-A218508] N90-23102
Proceedings of the 9th International Conference on Computing Methods in Applied Science and Engineering
[AD-A219307] N90-23149
Transactions of the Seventh Army Conference on Applied Mathematics and Computing
[AD-A219220] N90-23160
ONR Far East Scientific Information Bulletin, Volume 13, No. 4
[ONRFE-SCI-INFO-BULL-13(4)88] N90-23168
Support for the 16th International Conference on the Physics of Electronic and Atomic Collisions
[AD-A218567] N90-23200
The Energetic Gamma-Ray Experiment Telescope (EGRET) Science Symposium
[NASA-CP-3071] N90-23294
CONGRESSIONAL REPORTS
Nuclear power in space
[GPO-23-835] N90-23202
CONGRUENCES
The perception of geometrical structure from congruence N90-22935
CONICAL BODIES
Side moment exerted by a spinning, coning, highly viscous liquid payload
[AD-A218746] N90-22763
CONJUGATE GRADIENT METHOD
Parallel conjugate gradient algorithms for manipulator dynamic simulation N90-23045
CONSCIOUSNESS
Hatching a theory of incubation effects
[AD-A219275] N90-22915
CONSERVATION LAWS
Nonstrictly hyperbolic conservation laws
[AD-A218525] N90-22762
CONSTRUCTION
Development of a unique laboratory standard indium gallium arsenide detector for the 500 to 1700 micron spectral region, phase 2
[NASA-CR-180482] N90-22767
CONTACT LOADS
Influence of linear profile modification and loading conditions on the dynamic tooth load and stress of high contact ratio gears
[NASA-TM-103136] N90-22796
CONTACT RESISTANCE
Development of a unique laboratory standard indium gallium arsenide detector for the 500 to 1700 micron spectral region, phase 2
[NASA-CR-180482] N90-22767
CONTAMINATION
Development and use of a passive technique for measuring nitrogen dioxide in the background atmosphere N90-23285
CONTEXT
Stochastic interactive activation and the effect of context on perception
[AD-A218929] N90-22898
CONTINENTAL SHELVES
On the effectiveness of the production of antarctic bottom water in the Weddell and Ross Seas
[AD-A218873] N90-22880
CONTINUUMS
The interstellar medium of a starburst galaxy; millimeter interferometric observations of M82 N90-23276
CONTRAROTATING PROPELLERS
Investigation of advanced counterrotation blade configuration concepts for high speed turboprop systems, task 1: Ducted propfan analysis
[NASA-CR-185217] N90-22567
CONTROL SIMULATION
Minimum flying qualities. Volume 2: Pilot modeling for flying qualities applications
[AD-A218561] N90-22561
Space station dynamics, attitude control and momentum management N90-23029
Control design and simulation of systems modeled using ADAMS N90-23081
CONTROL STABILITY
Robust adaptive control: Stability and asymptotic performance
[AD-A219259] N90-23127
CONTROL SYSTEMS DESIGN
A candidate architecture for monitoring and control in chemical transfer propulsion systems
[NASA-TM-103161] N90-22595
H2, fixed architecture, control design for large scale systems
[NASA-CR-180471] N90-22698
Using object-oriented analysis techniques to support system testing
[DE90-009540] N90-22700
Elements of active vibration control for rotating machinery
[NASA-TM-102368] N90-22703
Robust control of vibration in flexible structures N90-22787
Plan execution control and architecture for mobile robots
[LAAS-89-371] N90-22793
Proceedings of the 3rd Annual Conference on Aerospace Computational Control, volume 1
[NASA-CR-186446] N90-22987
Experimental experience with flexible structures N90-23002
A disturbance based control/structure design algorithm N90-23003
Using deflation in the pole assignment problem with output feedback N90-23004
Combined control-structure optimization N90-23005
A robot arm simulation with a shared memory multiprocessor machine N90-23008
Computational dynamics for robotics systems using a non-strict computational approach N90-23011
Efficient computer algebra algorithms for polynomial matrices in control design N90-23022
Integrated control-system design via generalized LQG (GLQG) theory N90-23023
Modern CACSD using the Robust-Control Toolbox N90-23024
H(2)- and H(infinity)-design tools for linear time-invariant systems N90-23025
A methodology for formulating a minimal uncertainty model for robust control system design and analysis N90-23028
Application of numerical optimization techniques to control system design for nonlinear dynamic models of aircraft N90-23032
Control of a flexible planar truss using proof mass actuators N90-23035
Minimum attainable RMS attitude error using co-located rate sensors N90-23038
Proceedings of the 3rd Annual Conference on Aerospace Computational Control, volume 2
[NASA-CR-186447] N90-23040
Algorithmic considerations of integrated design for CSI on a hypercube architecture N90-23043
Enhanced modeling features within TREETOPS N90-23047
New multivariable capabilities of the INCA program N90-23049
Multidisciplinary Expert-aided Analysis and Design (MEAD) N90-23050
Overview of computational control research at UT Austin N90-23051
Substructural controller synthesis N90-23055
OPTICON: Pro-Matlab software for large order controlled structure design N90-23058
Robust fixed order dynamic compensation for large space structure control N90-23059
Multivariable frequency weighted model order reduction for control synthesis
[AIAA-89-3558] N90-23060
Distributed neural control of a hexapod walking vehicle N90-23061
Combining high performance simulation, data acquisition, and graphics display computers N90-23062
A real time, FEM based optimal control algorithm and its implementation using parallel processing hardware (transistors) in a microprocessor environment N90-23066
Six-degree-of-freedom aircraft simulation with mixed-data structure using the applied dynamics simulation language, ADSIM N90-23067
Six-degree-of-freedom missile simulation using the ADI AD 100 digital computer and ADSIM simulation language N90-23068
JPL control/structure interaction test bed real-time control computer architecture N90-23070
Multibody dynamics: Modeling component flexibility with fixed, free, loaded, constraint, and residual modes N90-23072
Component model reduction via the projection and assembly method N90-23073
Model reduction in the physical coordinate system N90-23074
Modal identities for multibody elastic spacecraft: An aid to selecting modes for simulation N90-23075
Issues in CSI analysis for large scale systems N90-23076
Structural modeling for control design (articulated multibody component representation) N90-23077
Significance of norms and completeness in variational based methods N90-23078
Dynamic analysis of flexible mechanical systems using LATDYN N90-23080
Control design and simulation of systems modeled using ADAMS N90-23081
Multibody dynamics model building using graphical interfaces N90-23082
Controlling flexible structures with second order actuator dynamics N90-23083
Numerical algorithms for computations of feedback laws arising in control of flexible systems N90-23085
Modeling and control of flexible space stations (slew maneuvers) N90-23086
Mini-mast dynamic analysis using the truss-beam model N90-23087
Controlling real-time systems with parallel processes
[CS-8918] N90-23119
About linear systems robustness: Linear programming approach
[LAAS-89-384] N90-23123
Control of randomly sampled robotic systems
[AD-A218948] N90-23157
CONTROL THEORY
Dynamics and control of tethered antennas/reflectors in orbit
[AD-A219316] N90-22594
Plan execution control and architecture for mobile robots
[LAAS-89-371] N90-22793
Recursive linearization of multibody dynamics equations of motion N90-22993
Experimental experience with flexible structures N90-23002
Frequency response modeling and control of flexible structures: Computational methods N90-23021
Integrated control-system design via generalized LQG (GLQG) theory N90-23023
Modern CACSD using the Robust-Control Toolbox N90-23024
Control of a flexible planar truss using proof mass actuators N90-23035
Extensions of output variance constrained controllers to hard constraints N90-23056
Minimal complexity control law synthesis N90-23057
Multivariable frequency weighted model order reduction for control synthesis
[AIAA-89-3558] N90-23060
Numerical algorithms for computations of feedback laws arising in control of flexible systems N90-23085
The (DURIP) computer simulations of plasmas, nonlinear systems, and control theory
[AD-A219070] N90-23107
A priori results in linear-quadratic optimal control theory (extended version)
[MEMO-COSOR-89-17] N90-23124
CONTROLLABILITY
Elements of active vibration control for rotating machinery
[NASA-TM-102368] N90-22703
CONTROLLERS
Limiting performance based structural and control optimization for large vibrating structures N90-22568
Field oriented control of induction motors
[NASA-TM-103154] N90-22731
The interactive digital video interface N90-22941
Multi-axis control of telemanipulators N90-22943
Proceedings of the 3rd Annual Conference on Aerospace Computational Control, volume 1
[NASA-CR-186446] N90-22987
A disturbance based control/structure design algorithm N90-23003
A robot arm simulation with a shared memory multiprocessor machine N90-23008
Enhanced modeling features within TREETOPS N90-23047
Substructural controller synthesis N90-23055
Extensions of output variance constrained controllers to hard constraints N90-23056
Minimal complexity control law synthesis N90-23057
Distributed neural control of a hexapod walking vehicle N90-23061
Real-time closed-loop simulation and upset evaluation of control systems in harsh electromagnetic environments N90-23069

CONVECTION
A new stochastic model of turbulent dispersion in the convective planetary boundary layer and the results of the Atterbury-87 field study N90-22853
Quantifying and reducing uncertainty in the assimilative mapping of ionospheric electrodynamics N90-22854
An interactive method for estimating hailstone size and convectively-driven wind gusts from forecast soundings [AD-A218499] N90-22871
CONVECTION CURRENTS
Next generation weather radar (NEXRAD) initial operational test and evaluation. Phase 2: (IOT and E(2)) [AD-A218770] N90-22873
CONVERGENCE
Multilevel decomposition approach to the preliminary sizing of a transport aircraft wing [NASA-CR-4296] N90-22557
Convergence of hyperspherical adiabatic expansion for helium-like systems [DE90-620526] N90-22631
Estimation of Hilbert space valued parameters by the method of sieves [AD-A218565] N90-23143
CONVEXITY
Design of cryogenic tanks for launch vehicles N90-22662
COOLING
Cooling of rocket thrust chambers with liquid oxygen [NASA-TM-103146] N90-22605
COORDINATES
Characterization and calibration of coordinate measuring machines [DE90-009320] N90-22791
COPOLYMERS
Modified maleic anhydride copolymers as e-beam resists [AD-A218470] N90-22679
COPPER ALLOYS
A comparison of CuAlNi and other high damping alloys for the purpose of naval ship silencing applications [AD-A218801] N90-22671
COPPER OXIDES
Photoresponse of YBa2Cu3O(7-delta) granular and epitaxial superconducting thin films [NASA-TM-103144] N90-22732
What is going on in the La2CuO4 superconductors N90-23171
Influence of high energy radiation on critical parameters of superconducting ceramics YBa2Cu3O7 [DE90-620562] N90-23239
CORES
Counterrotating cores in elliptical galaxies N90-23288
CORONAL HOLES
The large and small scale density structure in the solar corona N90-23327
CORONAS
The large and small scale density structure in the solar corona N90-23327
Infrared coronal line novae N90-23328
CORROSION RESISTANCE
Improved high temperature oxidation behavior of alloys by ion implantation [AERE-R-13309] N90-22650
A study of the relation between grain boundary type and sensitisation in a partially-sensitised AISI 304 stainless steel using electron back-scattering patterns [AERE-R-13327] N90-23234
COSINE SERIES
Significance of norms and completeness in variational based methods N90-23078
COSMIC RAYS
A model of the diffuse galactic gamma ray emission N90-23297
Gamma rays from giant molecular clouds N90-23298
More data on (possible) gamma ray (point) sources N90-23309
What is learned from high energy bursts and flares N90-23314
Local normal galaxies N90-23315
Local atmospheric electricity and its possible application in high energy cosmic ray air shower detection N90-23335
The ground-level cosmic-ray event of September 29, 1989 as recorded by the Rome detectors [NOTA-INTERNA-944] N90-23336
Cosmic ray NM-64 neutron monitor data-17 [NOTA-INTERNA-945] N90-23337
COSMOLOGY
Spectral plane quasars, spectral turn-over, and frequency atlas [INPE-5011-TDL/399] N90-23277
Skewering the universe with QSO lines of sight: Lyman alpha clouds as probes of large scale structure N90-23278
A general low-harmonic cosmic string and its self-intersection and fragmentation N90-23284
Anisotropic inflation N90-23286
Reconstructing primordial density fluctuations N90-23293
Complementary information from mm-wave-, infrared-, and gamma ray astronomy N90-23299
Gamma ray cosmology: The extra galactic gamma spectrum and methods to detect the underlying source N90-23321
Dipole analysis on EGRET data of extragalactic gamma ray background radiation N90-23322
Feasibility for EGRET detection of antimatter concentrations in the universe N90-23323
Gravitational collapse, Friedman models and cosmological constant: Does the universe oscillate [DE90-620792] N90-23324
COST ANALYSIS
RF network selection in a rule-based system. NOSC project ZE68: Cost metric algorithms for internetwork applications [AD-A219389] N90-23116
Use of optical storage devices as shared resources in local area networks [AD-A219198] N90-23269
COST EFFECTIVENESS
The RACE (research and development in advanced technologies for Europe) program: A 1989 update [AD-A218509] N90-22713
COST REDUCTION
The Italian approach to small satellites for low cost access to space developments [ETN-90-96552] N90-22587
COUETTE FLOW
A numerical and analytical study of normal stresses and pressure differences in non-Newtonian creeping flows N90-22749
COULOMB COLLISIONS
The sensitivity of EGRET to gamma ray polarization N90-23305
COUNTER ROTATION
Counterrotating cores in elliptical galaxies N90-23288
COUNTERFLOW
Experiments on the breakdown of heat transfer in liquid helium 2 [MPIS-13/1989] N90-23259
COUNTERS
Local atmospheric electricity and its possible application in high energy cosmic ray air shower detection N90-23335
COVALENCE
Electronic theory of solids, surfaces, interfaces, and clusters N90-23230
COVARIANCE
Extensions of output variance constrained controllers to hard constraints N90-23056
CRAB NEBULA
Gamma radiation from radio pulsars N90-23302
Gamma radiation from the Crab and Vela pulsars N90-23303
TeV radiation from the Crab nebula and other matters N90-23306
Spectral determinations for discrete sources with EGRET N90-23312
CRACK ARREST
Fatigue crack growth in a unidirectional SCS-6/Ti-15-3 composite [NASA-TM-103095] N90-22646
CRACK INITIATION
A comprehensive study on microstructure mechanics relationships of ceramic matrix composites [AD-A219318] N90-22627
The initiation of intergranular stress corrosion-cracking on sensitized stainless steel in dilute thiosulphate solutions [AERE-R-13317] N90-22648
Deformation and fracture of thin sheet aluminum-lithium alloys: The effect of cryogenic temperatures N90-22655
Fracture toughness and fatigue crack initiation tests of welded precipitation-hardening stainless steel [AD-A218745] N90-22669
CRACK OPENING DISPLACEMENT
Elevated temperature crack growth in aluminum alloys: Tensile deformation of 2618 and FVS0812 aluminum alloys N90-22654
CRACK PROPAGATION
Fatigue crack growth in a unidirectional SCS-6/Ti-15-3 composite [NASA-TM-103095] N90-22646
The initiation of intergranular stress corrosion-cracking on sensitized stainless steel in dilute thiosulphate solutions [AERE-R-13317] N90-22648
Environment enhanced fatigue of advanced aluminum alloys and composites N90-22652
Elevated temperature crack growth in advanced powder metallurgy aluminum alloys N90-22653
Elevated temperature crack growth in aluminum alloys: Tensile deformation of 2618 and FVS0812 aluminum alloys N90-22654
Deformation and fracture of thin sheet aluminum-lithium alloys: The effect of cryogenic temperatures N90-22655
Structure-property relations in aluminum-lithium alloys [AD-A219183] N90-22672
Fracture mechanics assessment of a cracked 16-inch inner diameter 1945 vintage-jacketed pressure vessel [AD-A219135] N90-22819
CRACK TIPS
Measurements and mechanisms of localized aqueous corrosion in aluminum-lithium alloys N90-22656
CRACKING (FRACTURING)
Cooling of rocket thrust chambers with liquid oxygen [NASA-TM-103146] N90-22605
Low temperature degradation of Y-TZP materials [AD-A218841] N90-22684
CRACKS
Ultrasonic detection of critical damage in carbon-epoxy composite materials [ONERA-RT-5/7256-RY-081-R] N90-22616
Scattering of a plane electromagnetic wave from a semicircular crack in a perfectly conducting ground plane [AD-A219310] N90-22721
Crack detection in silicon nitride by acoustic microscopy [AERE-R-13196] N90-22803
CRANES
On trajectory generation for flexible space crane: Inverse dynamics analysis by LATDYN N90-23037
CRASH LANDING
Aircraft crash survival design guide. Volume 2: Aircraft design crash impact conditions and human tolerance [AD-A218435] N90-22546
CRASHWORTHINESS
Aircraft crash survival design guide. Volume 1: Design criteria and checklists [AD-A218434] N90-22545
Aircraft crash survival design guide. Volume 2: Aircraft design crash impact conditions and human tolerance [AD-A218435] N90-22546
Aircraft crash survival design guide. Volume 3: Aircraft structural crash resistance [AD-A218436] N90-22547
Aircraft crash survival design guide. Volume 4: Aircraft seats, restraints, litters, and cockpit/cabin delethalization [AD-A218437] N90-22548
Aircraft crash survival design guide. Volume 5: Aircraft postcrash survival [AD-A218438] N90-22549
CREEP PROPERTIES
The lithium concentration dependence of creep in binary aluminum-lithium alloys [AD-A218706] N90-22668
A numerical and analytical study of normal stresses and pressure differences in non-Newtonian creeping flows N90-22749
Characterization of weldments using advanced experimental techniques [DE90-009418] N90-22792
CREEP TESTS
Mechanical testing of selected engineering plastics [DE90-008186] N90-22673
CREW SIZE
Lunar base 2 (the second thousand days of a base on the Moon) [ILR-MITT-230(1989)] N90-22968
CRITERIA
Measurements and mechanisms of localized aqueous corrosion in aluminum-lithium alloys N90-22656
CRITICAL MASS
Rapid mass transfer in binary systems N90-23289
CRITICAL TEMPERATURE
Superconducting and normal compounds: Some high field/high pressure effects N90-23229
The onset of superconductivity in two-dimensional disordered systems N90-23232
Influence of high energy radiation on critical parameters of superconducting ceramics YBa2Cu3O7 [DE90-620562] N90-23239
CROPS
Impact of meteorology on the agricultural sector: Compilation and analysis of projects [INPE-4846-PRE/1475] N90-22866
CRYOGENIC FLUID STORAGE
Spacecraft attitude impacts on COLD-SAT non-vacuum jacketed LH2 supply tank thermal performance [NASA-TM-103158] N90-22592

Design of cryogenic tanks for launch vehicles N90-22662
Acquisition and correlation of cryogenic nitrogen mass flow data through a multiple orifice Joule-Thomson device [NASA-TM-103121] N90-22761

CRYOGENIC TEMPERATURE
Deformation and fracture of thin sheet aluminum-lithium alloys: The effect of cryogenic temperatures N90-22655
Computer controlled cryogenic temperature controller [AD-A218785] N90-22701

CRYSTAL DEFECTS
The lithium concentration dependence of creep in binary aluminum-lithium alloys [AD-A218706] N90-22668

CRYSTAL GROWTH
The effect of elevated gravity on the crystallization of the MFI zeolites, ZSM-5, and silicalite N90-23231
Hanging drop crystal growth apparatus and method [NASA-CASE-MFS-28206-1-SB] N90-23242
Advanced gas phase reactor for growth of Ge sub x Si sub 1-x [AD-A219012] N90-23250

CRYSTAL LATTICES
Single-crystal diffraction analysis of 2-(trimethylsilylethynyl) 4-nitro-N,N-dimethylaniline [AD-A218955] N90-22642
Displacement flow and deuteron drag in a metal: A path towards cold fusion [PREPRINT-703] N90-23227
New approach to the dynamical diffraction theory in the case of three-dimensional perfect crystal [DE90-620563] N90-23240
Lattice field theory [PREPRINT-719] N90-23245

CRYSTAL STRUCTURE
The lithium concentration dependence of creep in binary aluminum-lithium alloys [AD-A218706] N90-22668

CRYSTALLIZATION
The effect of elevated gravity on the crystallization of the MFI zeolites, ZSM-5, and silicalite N90-23231

CRYSTALS
JPRS report: Science and technology. USSR: Physics and mathematics [JPRS-UPM-89-001] N90-23162
Effect on relaxation on nonlinear waves in crystals N90-23165
The effect of elevated gravity on the crystallization of the MFI zeolites, ZSM-5, and silicalite N90-23231

CURRENT DENSITY
Catalysts for ultrahigh current density oxygen cathodes for space fuel cell applications [NASA-CR-180650] N90-22835

CURRENT SHEETS
The large and small scale density structure in the solar corona N90-23327

CURVATURE
The curvature of conjugate profiles in points of contract [MEMO-COSOR-89-18] N90-22795

CURVES (GEOMETRY)
Curvature-dependent parametrization of curves and surfaces [CS-8915] N90-23100

CUTTING
Machining of new materials at Aerospatiale [REPT-892-430-104] N90-22622

CYBERNETICS
Multimedia system control [AD-A219392] N90-22971

CYCLES
Periodic ARMA models: Optimal prediction and minimum-phase condition [REPT-89-006] N90-23131

CYCLOGENESIS
Impact of marine boundary layer parameterization on a numerical simulation of cyclogenesis during a cold air outbreak event N90-22864

CYCLOTRON RESONANCE
Activities report of the Institute for Plasma Research [ETN-90-96467] N90-23225

CYCLOTRON RESONANCE DEVICES
Measurement of plasma-neutralized super-vacuum currents in a gyrotron configuration [AD-A218505] N90-23207

CYGNUS CONSTELLATION
Gamma rays from pulsar wind shock acceleration N90-23311
Infrared coronal line novae N90-23328

CYLINDRICAL BODIES
Three-dimensional separated flow prediction on fusiform body using Euler and boundary layer methods N90-22745
Side moment exerted by a spinning, coning, highly viscous liquid payload [AD-A218746] N90-22763

CYLINDRICAL PLASMAS
Resonant MHD modes with toroidal coupling [DE90-010077] N90-23222

CYLINDRICAL SHELLS
Transverse vibrations of a composite cylindrical tube of circular cross section [AD-A219227] N90-22820

CZOCHRALSKI METHOD
Optical spectroscopy of Ti(3+) doped YAlO3 [AD-A219043] N90-23251

D

DAMAGE
Impact damage in graphite/epoxy laminates: Damage characterization, acoustic emission, and finite element simulation, volumes 1 and 2 N90-22610

DAMAGE ASSESSMENT
Damage analysis following slight deformations of composite materials [RDS-1-007-64] N90-22618
Center for surface radiation damage studies [AD-A218452] N90-22678

DAMPING
A comparison of CuAlNi and other high damping alloys for the purpose of naval ship silencing applications [AD-A218801] N90-22671
Sliding control of pointing and tracking with operator spline estimation N90-22997

DARK ADAPTATION
The kinetics of dark adaptation in hypoxic subjects [AD-A218641] N90-22885

DARK MATTER
Skewering the universe with QSO lines of sight: Lyman alpha clouds as probes of large scale structure N90-23278
The dynamical evolution of dense clusters of compact stars N90-23287
Reconstructing primordial density fluctuations N90-23293

DATA ACQUISITION
The ground-level cosmic-ray event of September 29, 1989 as recorded by the Rome detectors [NOTA-INTERNA-944] N90-23336
Cosmic ray NM-64 neutron monitor data-17 [NOTA-INTERNA-945] N90-23337

DATA BASE MANAGEMENT SYSTEMS
Knowledge management: An abstraction of knowledge base and database management systems [NASA-CR-4273] N90-22986
A verification library for multibody simulation software N90-23089
Object-oriented query languages: The notion and the issues [REPT-89-054] N90-23093
Assessment System for Aircraft Noise (ASAN) citation database. Volume 2: Database update manual [AD-A219176] N90-23189
Assessment System for Aircraft Noise (ASAN) citation database. Volume 3: New citation review procedures [AD-A219177] N90-23190
BTOS database evaluation [AD-A219304] N90-23271

DATA BASES
Executive summary for the network assessment model [AD-A218762] N90-22718
Assessment System for Aircraft Noise (ASAN) citation database. Volume 1: User's manual [AD-A219175] N90-23188
Assessment System for Aircraft Noise (ASAN) citation database. Volume 3: New citation review procedures [AD-A219177] N90-23190
Looking at large data sets using binned data plots [DE90-008206] N90-23263
Data exchange strategy. Part 1: Review of digital data exchange technology [AD-A218506] N90-23267
BTOS database evaluation [AD-A219304] N90-23271

DATA COLLECTION PLATFORMS
Accuracy and precision of GOES data collection platforms for temperature measurements [AD-A218798] N90-22832

DATA MANAGEMENT
Program inversion: More than fun [CS-8903] N90-23095

DATA PROCESSING
The role of orbit errors in processing of satellite altimeter data [ETN-90-96699] N90-22575
Tracking in uncertain environments [RAE-TM-AW-121] N90-22891
Towards a calculus of data refinement [CS-8902] N90-23264

DATA SAMPLING
Statistical inference from sampled data [AD-A218731] N90-23156
Control of randomly sampled robotic systems [AD-A218948] N90-23157
Reconstructing primordial density fluctuations N90-23293

DATA SIMULATION
A new stochastic model of turbulent dispersion in the convective planetary boundary layer and the results of the Atterbury-87 field study N90-22853
Robust modelling of sampled systems for time delay estimation [REPT-89-047] N90-23092

DATA STORAGE
Assessment System for Aircraft Noise (ASAN) citation database. Volume 2: Database update manual [AD-A219176] N90-23189
Looking at large data sets using binned data plots [DE90-008206] N90-23263

DATA STRUCTURES
Parallel and vector computation for stochastic optimal control applications N90-23007
Factoring homomorphisms [CS-8908] N90-23096
The visibility diagram: A data structure for visibility and motion planning problems. Part 1: Application to the visibility polygon query problem [CS-8913-PT-1] N90-23098
An algebric approach to infinite data structures [CS-8909] N90-23265

DATA TRANSFER (COMPUTERS)
A scheme for supporting automatic data migration on multicomputers [NASA-CR-182038] N90-22973

DATA TRANSMISSION
Evaluation of a prototype 6 tone modem [RAE-TM-FM-28] N90-22708
Performance analysis of Aloha networks with power capture and near/far effect [AD-A218739] N90-22717

DEBRIS
Debris/ice/TPS assessment and photographic analysis for Shuttle Mission STS-36 [NASA-TM-102789] N90-22583

DECISION MAKING
The RACE (research and development in advanced technologies for Europe) program: A 1989 update [AD-A218509] N90-22713
RF network selection in a rule-based system. NOSC project ZE68: Cost metric algorithms for internetwork applications [AD-A219389] N90-23116

DECOMPOSITION
Multilevel decomposition approach to the preliminary sizing of a transport aircraft wing [NASA-CR-4296] N90-22557

DECOUPLING
An innovations approach to decoupling of multibody dynamics and control N90-22994

DEEP SPACE
Preliminary results of the peak experiment. ALTAIR deep-space measurements [AD-A218622] N90-22714

DEFECTS
Localization of vibration in disordered nearly cyclic structures N90-22812

DEFENSE PROGRAM
The Department of Defense critical technologies plan for the Committees on Armed Services United States Congress [AD-A219300] N90-22702
International treaties and active experiments in space [AD-A219368] N90-23272

DEFLECTION
Nonlinear strain-displacement relations and flexible multibody dynamics N90-23014

DEFORMATION
Large deformation analysis of laminated composite structures by a continuum-based shell element with transverse deformation N90-22613
Damage analysis following slight deformations of composite materials [RDS-1-007-64] N90-22618
High-temperature deformation of mechanically-alloyed aluminum IN90211 N90-22645
Deformation and fracture of thin sheet aluminum-lithium alloys: The effect of cryogenic temperatures N90-22655
Deformation and fracture of aluminum-lithium alloys: The effect of dissolved hydrogen N90-22658

The effect of mechanical deformation on the radiation patterns of large space-based arrays
[AD-A219288] N90-22719
A multipulsed dynamic diffraction moire interferometer
[DE90-009765] N90-22723
Large scale metrology by computer assisted photogrammetry
[REPT-892-430-116] N90-22772
Sliding control of pointing and tracking with operator spline estimation N90-22997
Nonlinear strain-displacement relations and flexible multibody dynamics N90-23014
Nonlinear finite element formulation for the large displacement analysis in multibody system dynamics N90-23015
The coupling effects of kinematics and flexibility on the Lagrangian dynamic formulation of open chain deformable links N90-23018
Explicit modeling of composite plates and beams in the dynamics of multibody systems N90-23019
Modal identities for multibody elastic spacecraft: An aid to selecting modes for simulation N90-23075

DEGREES OF FREEDOM
Dynamic substructuring by the boundary flexibility vector method of component mode synthesis
[NASA-CR-182445] N90-22813
Experimental verification of dynamic simulation N90-23020

DEHYDROGENATION
Dehydrogenative polymerization of silanes to polysilanes: A monomeric copper(2) siloxide
[AD-A218550] N90-22681

DELAMINATING
Elevated temperature crack growth in advanced powder metallurgy aluminum alloys N90-22653

DEMODULATION
Frequency domain techniques for analyzing picosecond optical pulses
[AD-A218656] N90-23214

DENSITOMETERS
Application of x ray absorption edge spectrometry to the non-destructive determination of element concentrations, coating thickness and areal densities
[AERE-R-13030] N90-22802

DENSITY (MASS/VOLUME)
Theoretical and computer simulation study of the density fluctuations in liquid water
[PREPRINT-697] N90-23191

DENSITY DISTRIBUTION
Ability distributions pattern probabilities and quasidensities
[AD-A218471] N90-23153
Reconstructing primordial density fluctuations N90-23293
The large and small scale density structure in the solar corona N90-23327

DENSITY MEASUREMENT
Application of x ray absorption edge spectrometry to the non-destructive determination of element concentrations, coating thickness and areal densities
[AERE-R-13030] N90-22802
MEGALIDAR proof-of-concept demonstration
[AD-A218787] N90-22858

DEPLOYMENT
An inverse kinematics algorithm for a highly redundant variable-geometry-truss manipulator N90-23033

DEPOSITION
A study of mesoscale acid deposition in the lower Ohio River Valley N90-22848

DEPTH
Spatial constraints of stereopsis in video displays N90-22920
Paradoxical monocular stereopsis and perspective vergence N90-22922
The perception of three-dimensionality across continuous surfaces N90-22924
How to reinforce perception of depth in single two-dimensional pictures N90-22937
Determination of depth-viewing volumes for stereo three-dimensional graphic displays
[NASA-TP-2999] N90-22965

DEPTH MEASUREMENT
Real-time stereo-microradiography
[AD-A218433] N90-22805

DESIGN ANALYSIS
Aircraft crash survival design guide. Volume 1: Design criteria and checklists
[AD-A218434] N90-22545
Multilevel decomposition approach to the preliminary sizing of a transport aircraft wing
[NASA-CR-4296] N90-22557
Differential equation based method for accurate approximations in optimization
[NASA-TM-102639] N90-22558
Limiting performance based structural and control optimization for large vibrating structures N90-22568
Design for testability of stuck-open and stack-on CMOS combinatorial circuits
[REPT-89-044] N90-22725
Design of high-performance negative-feedback oscillators
[ETN-90-96698] N90-22729
Supersonic flow computations for an ASTOVL aircraft configuration, phase 2, part 2
[NASA-CR-4284] N90-22746
Lunar base 2 (the second thousand days of a base on the Moon)
[ILR-MITT-230(1989)] N90-22968
Integrated control-system design via generalized LQG (GLQG) theory N90-23023
H(2)- and H(infinity)-design tools for linear time-invariant systems N90-23025
Application of numerical optimization techniques to control system design for nonlinear dynamic models of aircraft N90-23032
Algorithmic considerations of integrated design for CSI on a hypercube architecture N90-23043
Methodology for analysis and simulation of large multidisciplinary problems N90-23046

DESTRUCTIVE TESTS
Impact damage in graphite/epoxy laminates: Damage characterization, acoustic emission, and finite element simulation, volumes 1 and 2 N90-22610

DETONATORS
Ignition testing of low-energy laser diode ignited components
[DE90-009968] N90-22630

DEUTERON IRRADIATION
Displacement flow and deuteron drag in a metal: A path towards cold fusion
[PREPRINT-703] N90-23227

DIAGNOSIS
Application of artificial intelligence in electronic circuit diagnosis N90-23122

DIELECTRICS
Contributions to the development of SLM TEA CO2 laser sources for high resolution molecular spectroscopy N90-22778

DIFFERENTIAL EQUATIONS
Application of a dynamic stall model to rotor trim and aeroelastic response N90-22556
Differential equation based method for accurate approximations in optimization
[NASA-TM-102639] N90-22558
Aspects of efficient and reliable multibody system simulation N90-22991
Systematic generation of multibody equations of motion suitable for recursive and parallel manipulation N90-22992
A nearly-linear computational-cost scheme for the forward dynamics of an N-body pendulum N90-22996
A new second-order integration algorithm for simulating mechanical dynamic systems N90-23064
Index and consistency analysis for DAE (Differential Algebraic Equation) systems for Stefan-Maxwell diffusion-reaction problems
[DE90-008188] N90-23129
Estimation of Hilbert space valued parameters by the method of sieves
[AD-A218565] N90-23143
Parameter estimation in linear filtering
[AD-A218566] N90-23144
A computational method for general higher index nonlinear singular systems of differential equations
[AD-A219164] N90-23147

DIFFRACTION PATTERNS
A multipulsed dynamic diffraction moire interferometer
[DE90-009765] N90-22723
A compact portable diffraction moire interferometer
[DE90-009780] N90-22768

DIFFUSE RADIATION
The diffuse galactic gamma ray emission N90-23296
A model of the diffuse galactic gamma ray emission N90-23297
COS-B gamma ray sources beyond the predicted diffuse emission N90-23308
Feasibility for EGRET detection of antimatter concentrations in the universe N90-23323

DIFFUSION
Pseudo-steady diffusional growth or collapse of bubbles rising in time dependent pressure fields
[AD-A218825] N90-22764
Index and consistency analysis for DAE (Differential Algebraic Equation) systems for Stefan-Maxwell diffusion-reaction problems
[DE90-008188] N90-23129

DIGITAL SIMULATION
Numerical flow simulation and supercomputers: More than a digital wind tunnel N90-22976
The automation management to support research and development N90-22978
The development of a system for the numerical simulation of Euler flows N90-22980

DIGITAL SYSTEMS
On-line x ray inspection of materials and structural components using discrete element x ray detectors for digital radiographic and computed tomographic evaluation
[AD-A218911] N90-22806
Data exchange strategy. Part 1: Review of digital data exchange technology
[AD-A218506] N90-23267

DIMENSIONAL ANALYSIS
Dimensional analysis of structures using wrapping techniques
[REPT-892-430-119] N90-22815
A computer program to implement the Chen method of dimensional analysis
[AD-A218557] N90-23142

DIMENSIONAL MEASUREMENT
Application of x ray absorption edge spectrometry to the non-destructive determination of element concentrations, coating thickness and areal densities
[AERE-R-13030] N90-22802
Dimensional analysis of structures using wrapping techniques
[REPT-892-430-119] N90-22815
Full surface interferometric testing of grazing incidence mirrors
[AD-A219394] N90-23218

DIMENSIONAL STABILITY
Production of a variety of shapes using wrapping and draping techniques
[REPT-892-430-122] N90-22625
Modified maleic anhydride copolymers as e-beam resists
[AD-A218470] N90-22679
Solar Concentrator Advanced Development Program
[NASA-CR-185173] N90-22834

DIOPHANTINE EQUATION
Efficient computer algebra algorithms for polynomial matrices in control design N90-23022

DIPOLE MOMENTS
Dipole analysis on EGRET data of extragalactic gamma ray background radiation N90-23322

DIRICHLET PROBLEM
An examination of the full-wave method for rough surface scattering
[AD-A218664] N90-23155

DISCRIMINANT ANALYSIS (STATISTICS)
Selecting multinomial populations
[AD-A219256] N90-23159

DISILICIDES
Improvement study of iron disilicide thermoelectric materials
[AD-A218946] N90-22844

DISK OPERATING SYSTEM (DOS)
An approximation for the response time of an open CP-disk system
[MEMO-COSOR-89-19] N90-23266

DISPLACEMENT
Limiting performance based structural and control optimization for large vibrating structures N90-22568
Computations of weight functions in fracture mechanics N90-22809
Adapting to variable prismatic displacement N90-22945
Nonlinear finite element formulation for the large displacement analysis in multibody system dynamics N90-23015
Significance of norms and completeness in variational based methods N90-23078

DISPLAY DEVICES
Model-based method for terrain-following display design
[AD-A219302] N90-22563
Cognitive efficiency considerations for good graphic design
[AD-A218976] N90-22899
A task-analytic approach to the automated design of information graphics
[AD-A219271] N90-22912
Spatial Displays and Spatial Instruments
[NASA-CP-10032] N90-22918
Spatial constraints of stereopsis in video displays N90-22920
Perceiving environmental properties from motion information: Minimal conditions N90-22925
The photo-colorimetric space as a medium for the representation of spatial data N90-22927
Distortions in memory for visual displays N90-22929
Separate visual representations for perception and for visually guided behavior N90-22931
The effects of viewpoint on the virtual space of pictures N90-22932
The perception of geometrical structure from congruence N90-22935

Exocentric direction judgements in computer-generated displays and actual scenes N90-22936
How to reinforce perception of depth in single two-dimensional pictures N90-22937
The eyes prefer real images N90-22938
Spatial issues in user interface design from a graphic design perspective N90-22939
Interactive displays in medical art N90-22940
The interactive digital video interface N90-22941
Displays, instruments, and the multi-dimensional world of cartography N90-22942
Visual enhancements in pick-and-place tasks: Human operators controlling a simulated cylindrical manipulator N90-22946
Displays for telemanipulation N90-22948
Perception-action relationships reconsidered in light of spatial display instruments N90-22949
A commentary on perception-action relationships in spatial display instruments N90-22950
Spatial displays as a means to increase pilot situational awareness N90-22951
A computer graphics system for visualizing spacecraft in orbit N90-22952
Experiences in telecperation of land vehicles N90-22954
Development of a stereo 3-D pictorial primary flight display N90-22955
Synthetic perspective optical flow: Influence on pilot control tasks N90-22956
Sensory conflict in motion sickness: An observer theory approach N90-22957
Optical, gravitational, and kinesthetic determinants of judged eye level N90-22959
Voluntary presetting of the vestibular ocular reflex permits gaze stabilization despite perturbation of fast head movements N90-22960

DISSIPATION
Analysis of velocity and temperature fluctuations in turbulent shear flows N90-22744
Evolution of atmospheric baroclinic waves N90-22855

DISSOLVED GASES
Deformation and fracture of aluminum-lithium alloys: The effect of dissolved hydrogen N90-22658

DISSOLVING
Calcium carbonate scale dissolution in water stabilized by carbon dioxide treatment [AD-A218502] N90-22633

DISTANCE
Stereoscopic distance perception N90-22921

DISTILLATION
Design and construction of a packed column simulator operating under atmospheric and reduced pressure [ISAL-89-60] N90-22757

DISTORTION
Distortions in memory for visual displays N90-22929
The effects of viewpoint on the virtual space of pictures N90-22932
Hybrid diffractive-refractive telescope [AD-A219241] N90-23216

DISTRIBUTED PARAMETER SYSTEMS
Proceedings of the 3rd Annual Conference on Aerospace Computational Control, volume 2 [NASA-CR-186447] N90-23040
Distributed neural control of a hexapod walking vehicle N90-23061

DISTRIBUTED PROCESSING
A scheme for supporting automatic data migration on multicomputers [NASA-CR-182038] N90-22973
Methodology for analysis and simulation of large multidisciplinary problems N90-23046
Sentence comprehension: A parallel distributed processing approach [AD-A218886] N90-23104
DARK (Distributed Ada Real-Time Kernel) porting and extension guide Kernel version 3.0 [AD-A219291] N90-23112
Locality in parallel computation [AD-A218733] N90-23120

DOCUMENTS
Atlas/data abstract for the United States and selected areas, fiscal year 1989 [AD-A219289] N90-23270

DOPED CRYSTALS
Continued development and characterization of doped layers, contacts, and associated electronic devices in silicon carbide [AD-A219211] N90-22737
Continued development and characterization of doped layers, contacts and associated electronic devices in silicon carbide [AD-A219234] N90-22738
Optical spectroscopy of Ti(3+) doped YAlO3 [AD-A219043] N90-23251

DOPPLER EFFECT
Phase Doppler droplet sizing: Scattering angle effects [DE90-009571] N90-22754

DOPPLER RADAR
Turbulence spectral widths view angle independence as observed by Doppler radar [AD-A219169] N90-22550
Next generation weather radar (NEXRAD) initial operational test and evaluation. Phase 2: (IOT and E(2)) [AD-A218770] N90-22873

DOUBLE BASE PROPELLANTS
Temperature measurements through a solid-propellant combustion wave using imbedded fine wire thermocouples [AD-A218642] N90-22693

DRAG
Estimation of extra drag force on a circular cylinder due to the presence of solid particles in subsonic compressible flow [AD-A218635] N90-22542

DRAG REDUCTION
Fundamental hydrodynamics research [AD-A219179] N90-22766

DRAWING
Processing of thermotropic liquid crystalline polymers and their blends [AD-A218804] N90-22683

DRILLING
Machining of new materials at Aerospatiale [REPT-892-430-104] N90-22622

DROPS (LIQUIDS)
Flow visualization in supersonic turbulent boundary layers N90-22533
Sticking coefficient of HCl on aerosols N90-22598
Nonlinear spectroscopy of multicomponent droplets and 2- and 3-dimensional measurements in flames [AD-A218569] N90-22636
Unsteady group behavior of droplet clouds in swirling flows N90-22743
Phase Doppler droplet sizing: Scattering angle effects [DE90-009571] N90-22754
Hanging drop crystal growth apparatus and method [NASA-CASE-MFS-28206-1-SB] N90-23242

DUST
Estimation of extra drag force on a circular cylinder due to the presence of solid particles in subsonic compressible flow [AD-A218635] N90-22542
Optical properties of cometary dust [AD-A218790] N90-23325

DYE LASERS
Dynamics and instabilities in homogeneously broadened lasers [AD-A218427] N90-22786

DYNAMIC CHARACTERISTICS
Femtosecond studies of electron photodetachment of simple ions in liquid water: Solvation and geminate recombination dynamics [AD-A218520] N90-22634
Application of numerical optimization techniques to control system design for nonlinear dynamic models of aircraft N90-23032

DYNAMIC CONTROL
Dynamics and control of tethered antennas/reflectors in orbit [AD-A219316] N90-22594
Robust control of vibration in flexible structures N90-22787
An innovations approach to decoupling of multibody dynamics and control N90-22994
Frequency response modeling and control of flexible structures: Computational methods N90-23021
Controlling flexible structures with second order actuator dynamics N90-23083

DYNAMIC LOADS
Influence of linear profile modification and loading conditions on the dynamic tooth load and stress of high contact ratio gears [NASA-TM-103136] N90-22796

DYNAMIC MODELS
Pseudo-steady diffusional growth or collapse of bubbles rising in time dependent pressure fields [AD-A218825] N90-22764
Plan execution control and architecture for mobile robots [LAAS-89-371] N90-22793
Experimental verification of dynamic simulation N90-23020
Approximate minimum-time trajectories for 2-link flexible manipulators N90-23030
Application of numerical optimization techniques to control system design for nonlinear dynamic models of aircraft N90-23032
Modeling and control of flexible space stations (slew maneuvers) N90-23086

DYNAMIC PROGRAMMING
Orbital maneuvers optimization for station acquisition of geostationary satellites. Deterministic and stochastic approaches [LAAS-89-359] N90-22589
Parallel and vector computation for stochastic optimal control applications N90-23007
An algorithm for the solution of dynamic linear programs N90-23026

DYNAMIC RESPONSE
Application of a dynamic stall model to rotor trim and aeroelastic response N90-22556
Influence of linear profile modification and loading conditions on the dynamic tooth load and stress of high contact ratio gears [NASA-TM-103136] N90-22796
Dynamic substructuring by the boundary flexibility vector method of component mode synthesis [NASA-CR-182445] N90-22813
Flat plate vibration analysis experimental and numerical fillet study [AD-A218789] N90-22818
Nonlinear strain-displacement relations and flexible multibody dynamics N90-23014
Explicit modeling of composite plates and beams in the dynamics of multibody systems N90-23019
Frequency response modeling and control of flexible structures: Computational methods N90-23021
Control/structure interaction design methodology N90-23053
Model reduction in the physical coordinate system N90-23074
Structural modeling for control design (articulated multibody component representation) N90-23077
The power and efficiency of advanced software and parallel processing N90-23079
Controlling flexible structures with second order actuator dynamics N90-23083
A verification library for multibody simulation software N90-23089

DYNAMIC STRUCTURAL ANALYSIS
Aircraft crash survival design guide. Volume 3: Aircraft structural crash resistance [AD-A218436] N90-22547
Robust control of vibration in flexible structures N90-22787
Dynamic substructuring by the boundary flexibility vector method of component mode synthesis [NASA-CR-182445] N90-22813
Flat plate vibration analysis experimental and numerical fillet study [AD-A218789] N90-22818
Transverse vibrations of a composite cylindrical tube of circular cross section [AD-A219227] N90-22820
Nonlinear strain-displacement relations and flexible multibody dynamics N90-23014
Explicit modeling of composite plates and beams in the dynamics of multibody systems N90-23019
Frequency response modeling and control of flexible structures: Computational methods N90-23021
Simulation studies using multibody dynamics code DART N90-23036
On trajectory generation for flexible space crane: Inverse dynamics analysis by LATDYN N90-23037
A parallel structure transient response algorithm using independent substructure response computation N90-23044
Control/structure interaction design methodology N90-23053
Model reduction in the physical coordinate system N90-23074
The power and efficiency of advanced software and parallel processing N90-23079
Controlling flexible structures with second order actuator dynamics N90-23083
Mini-mast dynamic analysis using the truss-beam model N90-23087
Analytic semigroups: Applications to inverse problems for flexible structures [NASA-CR-182047] N90-23138

DYNAMICAL SYSTEMS
Approximate optimal guidance schemes for atmospheric orbital maneuvering N90-22585
Qualitative aspects of signal processing through dynamical neural networks [PREPRINT-711] N90-22709
Modelling and computer control of a mechanical system [W-8908] N90-22794
Predictability of weather and climate in a coupled ocean-atmosphere model: A dynamical systems approach N90-22865
Proceedings of the 3rd Annual Conference on Aerospace Computational Control, volume 1 [NASA-CR-186446] N90-22987

Parallel processing of real-time dynamic systems simulation on OSCAR (Optimally SCheduled Advanced multiprocessoR) N90-23006
Parallel and vector computation for stochastic optimal control applications N90-23007
Optimum control forces for multibody systems with intermittent motion N90-23016
Model reduction in the physical coordinate system N90-23074
Non-symmetric double well and Euclidean functional integral [PREPRINT-709] N90-23133

E

E GLASS
Characterization and role of an elastomeric interphase within polyepoxy reinforced glass, both particulate and fibrous [ISAL-89-0064] N90-22676
EARTH GRAVITATION
Determination of the general ocean circulation using satellite altimetry from a simultaneous solution for the Earth's gravity field N90-22569
EARTH MAGNETOSPHERE
Solar flares and magnetospheric particles: Investigations based upon the ONR-602 and ONR-604 experiments [AD-A218844] N90-23332
EARTH OBSERVATIONS (FROM SPACE)
Spaceborne radar observations: A guide for Magellan radar-image analysis [NASA-CR-184998] N90-22826
EARTH ORBITAL ENVIRONMENTS
International treaties and active experiments in space [AD-A219368] N90-23272
Solar flares and magnetospheric particles: Investigations based upon the ONR-602 and ONR-604 experiments [AD-A218844] N90-23332
EARTH ORBITS
Orbital mechanics: A learning tool on the main frame [AD-A218799] N90-22576
EARTHQUAKES
Propagation and attenuation of Lg waves in South America [AD-A218853] N90-22859
ECCENTRIC ORBITS
Orbit acquisition and control strategy for small satellites in inclined eccentric orbits [ETN-90-96551] N90-22573
ECONOMICS
FAA (Federal Aviation Administration) aviation forecasts, fiscal years 1990-2001 [AD-A219165] N90-22530
EDUCATION
The International Space University [NASA-TM-103163] N90-22604
EIGENVALUES
Using deflation in the pole assignment problem with output feedback N90-23004
Fourier analysis of finite element preconditioned collocation schemes [NASA-CR-182040] N90-23128
Continuation and multi-grid methods for bifurcation problems [AD-A218904] N90-23146
EINSTEIN EQUATIONS
Background connection: A necessary object in general relativity [DE90-620463] N90-23258
EKMAN LAYER
A numerical study of basic coastal upwelling processes N90-22878
ELASTIC BODIES
Explicit modeling of composite plates and beams in the dynamics of multibody systems N90-23019
ELASTIC DEFORMATION
Simulation of inelastic deformation in glassy polypropylene and polycarbonate [AD-A218891] N90-22686
Multibody dynamics: Modeling component flexibility with fixed, free, loaded, constraint, and residual modes N90-23072
Transactions of the Seventh Army Conference on Applied Mathematics and Computing [AD-A219220] N90-23160
ELASTIC PROPERTIES
Approximate analysis for the formation of adiabatic shear bands [AD-A218751] N90-22670
Nonstrictly hyperbolic conservation laws [AD-A218525] N90-22762
ELASTIC SCATTERING
Contributions of individual structural modes to the scattered acoustic field [AD-A219128] N90-23187
ELASTIC WAVES
Calculation of 3-dimensional synthetic seismograms on the connection machine [AD-A218472] N90-22857
ELASTOPLASTICITY
Evaluation of joints bonded with elastoplastic adhesives [REPT-892-430-120] N90-22816
ELECTRIC CONTACTS
Continued development and characterization of doped layers, contacts, and associated electronic devices in silicon carbide [AD-A219211] N90-22737
Continued development and characterization of doped layers, contacts and associated electronic devices in silicon carbide [AD-A219234] N90-22738
Lateral spreading of Au contacts on InP [NASA-TM-103133] N90-22843
ELECTRIC CURRENT
A fiber-optic current sensor for aerospace applications [NASA-TM-103152] N90-22773
ELECTRIC FIELD STRENGTH
Analytical theory of the Bunemann instability for electron runaway [IPF-88-3] N90-23224
ELECTRIC FIELDS
Linear and nonlinear electrical response of condensed matter: Ionic, dielectric, and mixed-conduction materials [AD-A218771] N90-22639
Transduction of nanovolt signals: Limits of electric-field detection [AD-A219214] N90-23177
ELECTRIC MOTORS
Composite ceramic superconducting wires for electric motor applications [AD-A219131] N90-22689
ELECTRIC POWER SUPPLIES
Nuclear technology and the space exploration missions [NASA-TM-103156] N90-22847
ELECTRIC PROPULSION
Transport properties of plasmas in microwave electrothermal thrusters [AD-A219408] N90-23228
ELECTRIC PULSES
Local atmospheric electricity and its possible application in high energy cosmic ray air shower detection N90-23335
ELECTRICAL MEASUREMENT
The initiation of intergranular stress corrosion-cracking on sensitized stainless steel in dilute thiosulphate solutions [AERE-R-13317] N90-22648
A fiber-optic current sensor for aerospace applications [NASA-TM-103152] N90-22773
OSSE observations of active galactic nuclei N90-23320
ELECTRICAL RESISTIVITY
Viscosity, density and conductivity of ImCl(HCl) sub 1.3 [AD-A218902] N90-22641
Scattering of a plane electromagnetic wave from a semicircular crack in a perfectly conducting ground plane [AD-A219310] N90-22721
A low temperature calorimetric study of several high-T(sub c) superconductors N90-23237
ELECTRO-OPTICS
Application of high-temperature superconducting thin-film devices to electro-optical and electronic warfare systems [AD-A218805] N90-23249
ELECTROCATALYSTS
Catalysts for ultrahigh current density oxygen cathodes for space fuel cell applications [NASA-CR-180650] N90-22835
ELECTROCHEMICAL CELLS
Advanced double layer capacitor [AD-A219419] N90-22741
ELECTROCHEMISTRY
Electrochemical synthesis of ultrathin film composite membranes [AD-A219041] N90-22643
The initiation of intergranular stress corrosion-cracking on sensitized stainless steel in dilute thiosulphate solutions [AERE-R-13317] N90-22648
ELECTRODE MATERIALS
Catalysts for ultrahigh current density oxygen cathodes for space fuel cell applications [NASA-CR-180650] N90-22835
ELECTRODYNAMICS
Quantifying and reducing uncertainty in the assimilative mapping of ionospheric electrodynamics N90-22854
ELECTROENCEPHALOGRAPHY
Multimedia system control [AD-A219392] N90-22971
ELECTROLYTES
Linear and nonlinear electrical response of condensed matter: Ionic, dielectric, and mixed-conduction materials [AD-A218771] N90-22639
Advanced double layer capacitor [AD-A219419] N90-22741
ELECTROLYTIC CELLS
Enhanced ceria solid electrolyte fuel cell development. Reduction of electronic conductivity permits use of a solid ceria electrolyte in high efficiency high power density fuel cells at temperatures compatible with metallic cell hardware [AD-A219297] N90-22846
ELECTROMAGNETIC ABSORPTION
The 16-O photodisintegration at low energies [NOTA-INTERNA-941] N90-23196
ELECTROMAGNETIC ACCELERATION
Control of surface melting and ablation in electromagnetic launchers via the magnetic vapor shielding mechanism [AD-A219035] N90-22578
ELECTROMAGNETIC FIELDS
Dynamics of motion charged particles in a field of two electromagnetic waves [DE90-620690] N90-22706
ELF (Extremely Low Frequency) communications system ecological monitoring program: Slime mold studies [AD-A218623] N90-22715
ELF (Extremely Low Frequency) communications systems ecological monitoring program: Wetland studies [AD-A218632] N90-22716
Exposure of human cells to electromagnetic fields [AD-A219377] N90-22889
Quantum mechanics in Riemannian space-time [DE90-620448] N90-23257
ELECTROMAGNETIC INTERACTIONS
Interaction of atomic hydrogen with pico- and femtosecond laser pulses [AD-A218426] N90-22785
Optical properties of cometary dust [AD-A218790] N90-23325
ELECTROMAGNETIC PROPULSION
Control of surface melting and ablation in electromagnetic launchers via the magnetic vapor shielding mechanism [AD-A219035] N90-22578
ELECTROMAGNETIC PULSES
Interaction of atomic hydrogen with pico- and femtosecond laser pulses [AD-A218426] N90-22785
Real-time closed-loop simulation and upset evaluation of control systems in harsh electromagnetic environments N90-23069
Frequency domain techniques for analyzing picosecond optical pulses [AD-A218856] N90-23214
ELECTROMAGNETIC RADIATION
High Intensity Electro-Magnetic and Ultrasonic Effects on Inorganic Materials Behavior and Processing Workshop [AD-A218884] N90-22640
ELECTROMAGNETIC SCATTERING
Scattering of a plane electromagnetic wave from a semicircular crack in a perfectly conducting ground plane [AD-A219310] N90-22721
ELECTROMAGNETIC WAVE TRANSMISSION
Superheterodyne three-wave detection of gravitation waves [DE90-620465] N90-22856
ELECTRON AFFINITY
Threshold photodetachment spectroscopy of the I + HI transition state region [AD-A218410] N90-22883
ELECTRON BEAMS
Modified maleic anhydride copolymers as e-beam resists [AD-A218470] N90-22679
Forced scattering of electromagnetic waves on electron beam in periodically inhomogeneous plasma [DE90-620705] N90-22707
Measurements and simulation of controlled beamfront motion in the Laser Controlled Collective Accelerator [DE90-009992] N90-22780
Intense electron beam propagation across a magnetic field [DE90-009993] N90-23204
Foil focusing of electron beams [AD-A219511] N90-23208
Stability regimes in a rotating quadrupole focusing accelerator [AD-A219513] N90-23209

ELECTRON CYCLOTRON HEATING
Activities report of the Institute for Plasma Research [ETN-90-96467] N90-23225
ELECTRON DENSITY (CONCENTRATION)
HF propagation through actively modified ionospheres [DE90-008931] N90-22705
A posterior stochastic equation for quantum Brownian motion [PREPRINT-715] N90-23194
The large and small scale density structure in the solar corona N90-23327
Infrared coronal line novae N90-23328
ELECTRON DIFFRACTION
Time-resolved surface structural study by picosecond reflection high-energy electron diffraction [AD-A218417] N90-22712
ELECTRON DIFFUSION
A posterior stochastic equation for quantum Brownian motion [PREPRINT-715] N90-23194
Critical behavior of the thermal power near the metal-insulator transition [PREPRINT-714] N90-23244
ELECTRON ENERGY
Critical behavior of the thermal power near the metal-insulator transition [PREPRINT-714] N90-23244
ELECTRON IRRADIATION
Polymerization of composites [REPT-892-430-102] N90-22621
Polymerization of composite materials: A technique developed by Aerospatiale [REPT-892-430-107] N90-22623
ELECTRON MOBILITY
Direct implantation process development and characterization in advanced Hg(1)-(x)Cd(x) Te EPI layers [AD-A219133] N90-23252
ELECTRON ORBITALS
Investigation of Schottky barriers [AD-A218422] N90-23247
ELECTRON RUNAWAY (PLASMA PHYSICS)
Analytical theory of the Bunemann instability for electron runaway [IPF-88-3] N90-23224
ELECTRON SCATTERING
A study of the relation between grain boundary type and sensitisation in a partially-sensitised AISI 304 stainless steel using electron back-scattering patterns [AERE-R-13327] N90-23234
Spectral evolution of active galactic nuclei Penrose Compton scattering processes and gamma ray emission from Seyfert galaxies N90-23317
ELECTRON TRANSITIONS
Threshold photodetachment spectroscopy of the I + HI transition state region [AD-A218410] N90-22883
ELECTRON-ION RECOMBINATION
Femtosecond studies of electron photodetachment of simple ions in liquid water: Solvation and geminate recombination dynamics [AD-A218520] N90-22634
ELECTRONIC SPECTRA
Support for the 16th International Conference on the Physics of Electronic and Atomic Collisions [AD-A218567] N90-23200
ELECTRONIC WARFARE
Application of high-temperature superconducting thin-film devices to electro-optical and electronic warfare systems [AD-A218805] N90-23249
ELECTRONS
Gas dynamic theory of flight of fast electron flux in plasma [DE90-618767] N90-23220
ELECTROPHYSIOLOGY
Laser retinal effects: Electrophysiological determination in visual cortical cells of monkeys and cats [AD-A218937] N90-22888
ELECTROTHERMAL ENGINES
Transport properties of plasmas in microwave electrothermal thrusters [AD-A219408] N90-23228
ELEMENTARY EXCITATIONS
Electronic theory of solids, surfaces, interfaces, and clusters N90-23230
ELEVATORS (CONTROL SURFACES)
Boeing/NASA composite components flight service evaluation [NASA-CR-181898] N90-22609
ELLIPSES
Some ray tracing problems related to circles and ellipses [AD-A219306] N90-23217
ELLIPTIC DIFFERENTIAL EQUATIONS
Fourier analysis of finite element preconditioned collocation schemes [NASA-CR-182040] N90-23128
ELLIPTICAL GALAXIES
Counterrotating cores in elliptical galaxies N90-23288
Studies in gravitational lensing and numerical hydrodynamics N90-23290
EMBRITTLEMENT
Measurements and mechanisms of localized aqueous corrosion in aluminum-lithium alloys N90-22656
EMISSION SPECTRA
The diffuse galactic gamma ray emission N90-23296
END EFFECTORS
Modeling of control forces for kinematical constraints in the dynamics of multibody systems: A new approach N90-23031
Determination of joint drives for stable end-effector motion in flexible robotic systems N90-23034
ENERGETIC PARTICLES
The illusive Geminga: What is it N90-23307
ENERGY ABSORPTION
Aircraft crash survival design guide. Volume 4: Aircraft seats, restraints, litters, and cockpit/cabin delethalization [AD-A218437] N90-22548
ENERGY BUDGETS
Superheterodyne three-wave detection of gravitation waves [DE90-620465] N90-22856
ENERGY CONVERSION EFFICIENCY
High-efficiency silicon solar cells for a 22-sun line-focus module [DE90-010242] N90-22840
Enhanced ceria solid electrolyte fuel cell development. Reduction of electronic conductivity permits use of a solid ceria electrolyte in high efficiency high power density fuel cells at temperatures compatible with metallic cell hardware [AD-A219297] N90-22846
ENERGY DISTRIBUTION
The high temperature behavior of gallium and indium liquid metal ion sources [AERE-R-13321] N90-22647
ENERGY GAPS (SOLID STATE)
Direct implantation process development and characterization in advanced Hg(1)-(x)Cd(x) Te EPI layers [AD-A219133] N90-23252
ENERGY SOURCES
The high energy source 3C 273 N90-23318
ENERGY SPECTRA
Spectral determinations for discrete sources with EGRET N90-23312
What is learned from high energy bursts and flares N90-23314
Gamma rays from active galactic nuclei N90-23316
ENERGY STORAGE
Experimental studies on energy storage [AD-A219032] N90-22845
ENERGY TECHNOLOGY
A theoretical and experimental investigation of an absorption refrigeration system for application with solar energy units N90-22697
Ocean energy program summary [DE89-009481] N90-22836
Geothermal energy program summary [DE89-009485] N90-22837
Geothermal energy program summary [DE89-009486] N90-22838
Nuclear power in space [GPO-23-835] N90-23202
ENERGY TRANSFER
Incomplete fusion reactors at low and intermediate energies [KVI-809] N90-23206
ENGINE COOLANTS
Cooling of rocket thrust chambers with liquid oxygen [NASA-TM-103146] N90-22605
ENGINE INLETS
Finite element elastic-plastic-creep and cyclic life analysis of a cowl lip [NASA-TM-102342] N90-22808
ENTROPY
Rapid mass transfer in binary systems N90-23289
ENTROPY (STATISTICS)
Selecting multinomial populations [AD-A219256] N90-23159
ENVIRONMENT EFFECTS
International treaties and active experiments in space [AD-A219368] N90-23272
ENVIRONMENT MODELS
A study of mesoscale acid deposition in the lower Ohio River Valley N90-22848
ENVIRONMENT PROTECTION
HCl Vapor Characterization and Detection. JANNAF Safety and Environmental Protection Subcommittee Workshop [AD-A216252] N90-22596
ENVIRONMENTAL CONTROL
Space Station Freedom environmental control and life support system phase 3 simplified integrated test detailed report [NASA-TM-4204] N90-22593
ENVIRONMENTAL MONITORING
ELF (Extremely Low Frequency) communications systems ecological monitoring program: Wetland studies [AD-A218632] N90-22716
ENVIRONMENTAL SURVEYS
Specification for environmental measurements to assess radar sensors [AD-A219127] N90-22833
Assessment System for Aircraft Noise (ASAN) citation database. Volume 3: New citation review procedures [AD-A219177] N90-23190
EPITAXY
Measurement of localized deep levels and wafer non-uniformities at 3-5 semiconductor heterojunctions [AD-A218547] N90-23248
EPOXY MATRIX COMPOSITES
Characterization and role of an elastomeric interphase within polyepoxy reinforced glass, both particulate and fibrous [ISAL-89-0064] N90-22676
EQUATIONS OF MOTION
Reynolds stress closure in jet flows using instability wave modeling N90-22534
Aspects of efficient and reliable multibody system simulation N90-22991
Systematic generation of multibody equations of motion suitable for recursive and parallel manipulation N90-22992
Recursive linearization of multibody dynamics equations of motion N90-22993
An innovations approach to decoupling of multibody dynamics and control N90-22994
A nearly-linear computational-cost scheme for the forward dynamics of an N-body pendulum N90-22996
A robot arm simulation with a shared memory multiprocessor machine N90-23008
Multi-flexible-body dynamics capturing motion-induced stiffness N90-23013
Nonlinear finite element formulation for the large displacement analysis in multibody system dynamics N90-23015
Determination of joint drives for stable end-effector motion in flexible robotic systems N90-23034
Simulation studies using multibody dynamics code DART N90-23036
Modal identities for multibody elastic spacecraft: An aid to selecting modes for simulation N90-23075
Multibody dynamics model building using graphical interfaces N90-23082
EQUATORIAL REGIONS
Preliminary results of the peak experiment. ALTAIR deep-space measurements [AD-A218622] N90-22714
EQUILIBRIUM EQUATIONS
Rigorous analysis of low temperature stochastic Ising models: Metastability and exponential approach to equilibrium [PREPRINT-720] N90-23175
EROSION
Characterization of particle impact by quantitative acoustic emission [AERE-R-13028] N90-22810
ERROR ANALYSIS
Pressure and shear stress measurement uncertainty for DARPA SUBOFF experiment [AD-A219109] N90-22798
ERROR DETECTION CODES
Detection of bridging faults in DFCMOS combinational gates [REPT-89-060] N90-22726
ERRORS
Increased stuck-at fault coverage with reduced I(sub DDQ) test sets [DE90-009509] N90-22804
ESTIMATES
Quantifying and reducing uncertainty in the assimilative mapping of ionospheric electrodynamics N90-22854
A survey on the structured singular value N90-22998
ESTIMATING
Sliding control of pointing and tracking with operator spline estimation N90-22997
Parameter estimation in linear filtering [AD-A218566] N90-23144
ETHYL ALCOHOL
Turbine fuel alternatives (near term) [AD-A219405] N90-22695

EUCLIDEAN GEOMETRY
Efficient computer algebra algorithms for polynomial matrices in control design N90-23022
Non-symmetric double well and Euclidean functional integral
[PREPRINT-709] N90-23133
Effective action for induced gravity on a 2-dimensional manifold
[PREPRINT-712] N90-23173
EULER EQUATIONS OF MOTION
Investigation of advanced counterrotation blade configuration concepts for high speed turboprop systems, task 1: Ducted propfan analysis
[NASA-CR-185217] N90-22567
The development of a system for the numerical simulation of Euler flows N90-22980
Stable boundary conditions for Cartesian grid calculations
[NASA-CR-182048] N90-23139
EUROPE
The RACE (research and development in advanced technologies for Europe) program: A 1989 update
[AD-A218509] N90-22713
EVOLUTION (DEVELOPMENT)
Spectral plane quasars, spectral turn-over, and frequency atlas
[INPE-5011-TDL/399] N90-23277
EXCIMER LASERS
Shaping radiation pattern of excimer laser by means of controllable intracavity mirror N90-23166
EXCITATION
Forced scattering of electromagnetic waves on electron beam in periodically inhomogeneous plasma
[DE90-620705] N90-22707
Excitation of hypersound at boundary between Type-2 superconductor and a concentrated paramagnetic compound N90-23164
EXHAUST CLOUDS
Infrared absorption gas sensor for the detection of HCl in launch vehicle exhaust clouds N90-22600
EXHAUST EMISSION
A study of mesoscale acid deposition in the lower Ohio River Valley N90-22848
EXPERIMENT DESIGN
Designing good experiments to test bad hypotheses
[AD-A218977] N90-22900
EXPERIMENTATION
International treaties and active experiments in space
[AD-A219368] N90-23272
EXPERT SYSTEMS
Knowledge management: An abstraction of knowledge base and database management systems
[NASA-CR-4273] N90-22986
Multidisciplinary Expert-aided Analysis and Design (MEAD) N90-23050
Neural networks in support of manned space N90-23088
RF network selection in a rule-based system. NOSC project ZE68: Cost metric algorithms for internetwork applications
[AD-A219389] N90-23116
Application of artificial intelligence in electronic circuit diagnosis N90-23122
Automated electric power management and control for Space Station Freedom
[NASA-TM-103151] N90-23125
Syntax, semantics, and pragmatism: An integrated focus based on textual linguistic knowledge
[INPE-4992-PRE/1554] N90-23262
Explanation generation in expert systems (a literature review and implementation)
[AD-A218741] N90-23268
EXPLODING WIRES
Qualification test rationale for measuring the resistance of equipment to pyrotechnic shock
[REPT-892-430-117] N90-22590
EXPLOSIVES
Ignition testing of low-energy laser diode ignited components
[DE90-009968] N90-22630
EXPONENTIAL FUNCTIONS
Characterizing exponential distributions via conditional independence
[AD-A219255] N90-23158
EXPOSURE
The physiological cost of wearing the propellant handler's ensemble at the Kennedy Space Center
[NASA-TM-102786] N90-22966
EXTRATERRESTRIAL MATTER
Skewering the universe with QSO lines of sight: Lyman alpha clouds as probes of large scale structure N90-23278
Reconstructing primordial density fluctuations N90-23293
EXTREMELY LOW FREQUENCIES
ELF (Extremely Low Frequency) communications system ecological monitoring program: Slime mold studies
[AD-A218623] N90-22715
ELF (Extremely Low Frequency) communications systems ecological monitoring program: Wetland studies
[AD-A218632] N90-22716
Exposure of human cells to electromagnetic fields
[AD-A219377] N90-22889
EYE MOVEMENTS
Visual selective attention
[AD-A219204] N90-22910
Voluntary presetting of the vestibular ocular reflex permits gaze stabilization despite perturbation of fast head movements N90-22960
EYE PROTECTION
Analysis and evaluation of technical data on the photochromic and non-linear optical properties of materials
[AD-A219398] N90-23219

F

F REGION
Plasma instabilities associated with the injection of artificial ion beams into the ionosphere N90-22851
F-15 AIRCRAFT
Dynamic ground-effect measurements on the F-15 STOL and Maneuver Technology Demonstrator (S/MTD) configuration
[NASA-TP-3000] N90-22531
Visual behavior in the F-15 simulator for air-to-air combat
[AD-A218648] N90-22893
F-18 AIRCRAFT
Water-tunnel study results of a TF/A-18 and F/A-18 canopy flow visualization
[NASA-TM-101705] N90-22532
FABRICATION
Pultrusion process development for long space boom model
[NASA-TM-4017] N90-22628
Miniature traveling wave tube and method of making
[NASA-CASE-LEW-14520-1] N90-22724
Axisymmetric and cylindrically orthotropic analysis of filament winding N90-22811
Solar Concentrator Advanced Development Program
[NASA-CR-185173] N90-22834
FACTOR ANALYSIS
Explicit modeling of composite plates and beams in the dynamics of multibody systems N90-23019
FACTORIZATION
Spatial operator algebra framework for multibody system dynamics N90-22989
A nearly-linear computational-cost scheme for the forward dynamics of an N-body pendulum N90-22996
Efficient computer algebra algorithms for polynomial matrices in control design N90-23022
An algorithm for the solution of dynamic linear programs N90-23026
Factoring homomorphisms
[CS-8908] N90-23096
FAILURE
Determination of joint drives for stable end-effector motion in flexible robotic systems N90-23034
FAILURE ANALYSIS
Computational and experimental investigations of rotating stall in compressor cascades N90-22565
Damage analysis following slight deformations of composite materials
[RDS-1-007-64] N90-22618
Elevated temperature crack growth in aluminum alloys: Tensile deformation of 2618 and FVS0812 aluminum alloys N90-22654
Measurements and mechanisms of localized aqueous corrosion in aluminum-lithium alloys N90-22656
Thermal/structural analysis of the shaft-disk region of a fan drive system
[NASA-TM-101687] N90-22807
FAILURE MODES
Probabilistic structural analysis of aerospace components using NESSUS
[NASA-TM-102324] N90-22823
FAN BLADES
Thermal/structural analysis of the shaft-disk region of a fan drive system
[NASA-TM-101687] N90-22807
FATIGUE (MATERIALS)
Cooling of rocket thrust chambers with liquid oxygen
[NASA-TM-103146] N90-22605
A life prediction model for laminated composite structural components
[NASA-CR-186587] N90-22614
Fatigue crack growth in a unidirectional SCS-6/Ti-15-3 composite
[NASA-TM-103095] N90-22646
NASA-UVA light aerospace alloy and structures technology program
[NASA-CR-182607] N90-22651
Fracture toughness and fatigue crack initiation tests of welded precipitation-hardening stainless steel
[AD-A218745] N90-22669
Structure-property relations in aluminum-lithium alloys
[AD-A219183] N90-22672
FATIGUE LIFE
Hydrogenation of stainless steels implanted with nitrogen
[DE90-617397] N90-22666
Fracture toughness and fatigue crack initiation tests of welded precipitation-hardening stainless steel
[AD-A218745] N90-22669
Surface pitting fatigue life of noninvolute, low-contact-ratio gears
[NASA-TM-103116] N90-22790
Fracture mechanics assessment of a cracked 16-inch inner diameter 1945 vintage-jacketed pressure vessel
[AD-A219135] N90-22819
High temperature fatigue behavior of a SiC/Ti-24Al-11Nb composite
[NASA-TM-103157] N90-22822
FATIGUE TESTS
Damage analysis following slight deformations of composite materials
[RDS-1-007-64] N90-22618
FAULT TOLERANCE
Detection of bridging faults in DFCMOS combinational gates
[REPT-89-060] N90-22726
Real-time closed-loop simulation and upset evaluation of control systems in harsh electromagnetic environments N90-23069
Fault tolerant multiprocessing and development of tools
[AD-A219216] N90-23110
Interconnection networks for highly parallel supercomputing architectures
[REPT-89-053] N90-23118
FEEDBACK CONTROL
Limiting performance based structural and control optimization for large vibrating structures N90-22568
Equipment specifications for launcher guidance using multivariable frequency methods
[REPT-892-422-106] N90-22582
The elastic-plastic behavior of composite materials N90-22615
Systematic generation of multibody equations of motion suitable for recursive and parallel manipulation N90-22992
Algorithms for computing the multivariable stability margin N90-22999
Robustness analysis for real parametric uncertainty N90-23000
A disturbance based control/structure design algorithm N90-23003
Using deflation in the pole assignment problem with output feedback N90-23004
Efficient computer algebra algorithms for polynomial matrices in control design N90-23022
Integrated control-system design via generalized LQG (GLQG) theory N90-23023
An algorithm for the solution of dynamic linear programs N90-23026
Control of a flexible planar truss using proof mass actuators N90-23035
Simulation studies using multibody dynamics code DART N90-23036
Minimal complexity control law synthesis N90-23057
OPTICON: Pro-Matlab software for large order controlled structure design N90-23058
Robust fixed order dynamic compensation for large space structure control N90-23059
Multivariable frequency weighted model order reduction for control synthesis
[AIAA-89-3558] N90-23060
Man-in-the-control-loop simulation of manipulators N90-23063
The use of real-time, hardware-in-the-loop simulation in the design and development of the new Hughes HS601 spacecraft attitude control system N90-23065
Real-time closed-loop simulation and upset evaluation of control systems in harsh electromagnetic environments N90-23069
Numerical algorithms for computations of feedback laws arising in control of flexible systems N90-23085
About linear systems robustness: Linear programming approach
[LAAS-89-384] N90-23123

FERMIONS
Improving fermion operators
[PREPRINT-710] N90-23193
Mixing of DIS operators in lattice QCD
[PREPRINT-708] N90-23243
FERROMAGNETIC MATERIALS
Superconducting and normal compounds: Some high field/high pressure effects N90-23229
FERROMAGNETISM
Rigorous analysis of low temperature stochastic Ising models: Metastability and exponential approach to equilibrium
[PREPRINT-720] N90-23175
FIBER COMPOSITES
A study of woven fabric-reinforced composite materials using an invariant-based orthotropic plasticity formulation N90-22611
Fatigue crack growth in a unidirectional SCS-6/Ti-15-3 composite
[NASA-TM-103095] N90-22646
Microcracking and toughness of ceramic-fiber/ceramic-matrix composites under high temperature
[AD-A218516] N90-22680
Computations of weight functions in fracture mechanics N90-22809
High temperature fatigue behavior of a SiC/Ti-24Al-11Nb composite
[NASA-TM-103157] N90-22822
FIBER OPTICS
Measurement of HCl by near-infrared diode laser absorption N90-22601
A fiber-optic current sensor for aerospace applications
[NASA-TM-103152] N90-22773
FIBERS
Microcracking and toughness of ceramic-fiber/ceramic-matrix composites under high temperature
[AD-A218516] N90-22680
Composite ceramic superconducting wires for electric motor applications
[AD-A219131] N90-22689
FIELD EFFECT TRANSISTORS
Excess noise, anomalous effects and reliability of high frequency devices (Schottky diodes, MESFET and HEMT)
[LAAS-89-394] N90-22728
Continued development and characterization of doped layers, contacts, and associated electronic devices in silicon carbide
[AD-A219211] N90-22737
Continued development and characterization of doped layers, contacts and associated electronic devices in silicon carbide
[AD-A219234] N90-22738
FIELD OF VIEW
Turbulence spectral widths view angle independence as observed by Doppler radar
[AD-A219169] N90-22550
Helmet-mounted pilot night vision systems: Human factors issues N90-22930
Perceived orientation, spatial layout and the geometry of pictures N90-22933
Wide-angle display developments by computer graphics N90-22963
FIELD STRENGTH
ELF (Extremely Low Frequency) communications system ecological monitoring program: Slime mold studies
[AD-A218623] N90-22715
ELF (Extremely Low Frequency) communications systems ecological monitoring program: Wetland studies
[AD-A218632] N90-22716
FIELD THEORY (PHYSICS)
Replica scaling analysis of interfaces in random media
[PREPRINT-713] N90-23174
FILAMENT WINDING
Production of a variety of shapes using wrapping and draping techniques
[REPT-892-430-122] N90-22625
Axisymmetric and cylindrically orthotropic analysis of filament winding N90-22811
FILE MAINTENANCE (COMPUTERS)
Access to supercomputers N90-22979
Assessment System for Aircraft Noise (ASAN) citation database. Volume 2: Database update manual
[AD-A219176] N90-23189
FILLETS
Flat plate vibration analysis experimental and numerical fillet study
[AD-A218789] N90-22818
FILM THICKNESS
Application of x ray absorption edge spectrometry to the non-destructive determination of element concentrations, coating thickness and areal densities
[AERE-R-13030] N90-22802
The onset of superconductivity in two-dimensional disordered systems N90-23232
FILTERS
Optical excisor modeling
[AD-A219338] N90-22722
FILTRATION
Some observations on liquid flow through filters
[AERE-R-13300] N90-22748
Parameter estimation in linear filtering
[AD-A218566] N90-23144
FINITE DIFFERENCE THEORY
Large-scale advanced propeller blade pressure distributions: Prediction and data
[NASA-TM-102316] N90-22564
Adaptive mesh experiments for hyperbolic partial differential equations
[AD-A219194] N90-23148
Studies in gravitational lensing and numerical hydrodynamics N90-23290
FINITE ELEMENT METHOD
The minimum drag profile in laminar flow: A numerical way N90-22535
Impact damage in graphite/epoxy laminates: Damage characterization, acoustic emission, and finite element simulation, volumes 1 and 2 N90-22610
A study of woven fabric-reinforced composite materials using an invariant-based orthotropic plasticity formulation N90-22611
Large deformation analysis of laminated composite structures by a continuum-based shell element with transverse deformation N90-22613
A life prediction model for laminated composite structural components
[NASA-CR-186587] N90-22614
Design of cryogenic tanks for launch vehicles N90-22662
The behaviour of mechanically fastened joints in composite structures N90-22789
Thermal/structural analysis of the shaft-disk region of a fan drive system
[NASA-TM-101687] N90-22807
Finite element elastic-plastic-creep and cyclic life analysis of a cowl lip
[NASA-TM-102342] N90-22808
Computations of weight functions in fracture mechanics N90-22809
Fracture mechanics assessment of a cracked 16-inch inner diameter 1945 vintage-jacketed pressure vessel
[AD-A219135] N90-22819
Nonlinear finite element formulation for the large displacement analysis in multibody system dynamics N90-23015
The coupling effects of kinematics and flexibility on the Lagrangian dynamic formulation of open chain deformable links N90-23018
A finite element based method for solution of optimal control problems N90-23027
Approximate minimum-time trajectories for 2-link flexible manipulators N90-23030
On trajectory generation for flexible space crane: Inverse dynamics analysis by LATDYN N90-23037
Model reduction in the physical coordinate system N90-23074
Dynamic analysis of flexible mechanical systems using LATDYN N90-23080
Numerical algorithms for computations of feedback laws arising in control of flexible systems N90-23085
Mini-mast dynamic analysis using the truss-beam model N90-23087
Vectors and matrices: Two turbo pascal units for fast program development
[AD-A218917] N90-23105
Fourier analysis of finite element preconditioned collocation schemes
[NASA-CR-182040] N90-23128
Numerical studies of the active control of sound transmission through double partitions
[ISVR-TR-183] N90-23181
FINITE VOLUME METHOD
Large-scale advanced propeller blade pressure distributions: Prediction and data
[NASA-TM-102316] N90-22564
FIRES
Aircraft crash survival design guide. Volume 5: Aircraft postcrash survival
[AD-A218438] N90-22549
FISHES
Transduction of nanovolt signals: Limits of electric-field detection
[AD-A219214] N90-23177
FIXED POINT ARITHMETIC
Undetermined coefficient problems for quasi-linear parabolic equations
[AD-A218462] N90-23141
FLAME PROPAGATION
Numerical investigation of turbulent flame sheets
[AD-A218553] N90-22635
Nonlinear spectroscopy of multicomponent droplets and 2- and 3-dimensional measurements in flames
[AD-A218569] N90-22636
Two-dimensional velocimetry instrumentation
[AD-A218450] N90-22774
FLAME SPECTROSCOPY
Nonlinear spectroscopy of multicomponent droplets and 2- and 3-dimensional measurements in flames
[AD-A218569] N90-22636
FLAT PLATES
Flat plate leading edge receptivity to various freestream disturbance structures N90-22750
Flat plate vibration analysis experimental and numerical fillet study
[AD-A218789] N90-22818
FLAT SURFACES
The multifractal nature of turbulence N90-22752
FLEXIBILITY
Relationship between flexibility of closure and success in pilot night vision sensor system training N90-22890
The coupling effects of kinematics and flexibility on the Lagrangian dynamic formulation of open chain deformable links N90-23018
FLEXIBLE BODIES
Robust control of vibration in flexible structures N90-22787
Spatial operator algebra framework for multibody system dynamics N90-22989
Systematic generation of multibody equations of motion suitable for recursive and parallel manipulation N90-22992
Experimental experience with flexible structures N90-23002
A disturbance based control/structure design algorithm N90-23003
Multi-flexible-body dynamics capturing motion-induced stiffness N90-23013
Nonlinear strain-displacement relations and flexible multibody dynamics N90-23014
Nonlinear finite element formulation for the large displacement analysis in multibody system dynamics N90-23015
Frequency response modeling and control of flexible structures: Computational methods N90-23021
Control of a flexible planar truss using proof mass actuators N90-23035
A decoupled recursive approach for constrained flexible multibody system dynamics N90-23042
Substructural controller synthesis N90-23055
Multibody dynamics: Modeling component flexibility with fixed, free, loaded, constraint, and residual modes N90-23072
Model reduction in the physical coordinate system N90-23074
Structural modeling for control design (articulated multibody component representation) N90-23077
Significance of norms and completeness in variational based methods N90-23078
Controlling flexible structures with second order actuator dynamics N90-23083
Analytic semigroups: Applications to inverse problems for flexible structures
[NASA-CR-182047] N90-23138
FLEXIBLE SPACECRAFT
An assessment of multibody simulation tools for articulated spacecraft N90-22988
Multi-flexible-body dynamics capturing motion-induced stiffness N90-23013
Simulation studies using multibody dynamics code DART N90-23036
Enhanced modeling features within TREETOPS N90-23047
Overview of computational control research at UT Austin N90-23051
Model reduction for flexible spacecraft with clustered natural frequencies N90-23054
Issues in CSI analysis for large scale systems N90-23076
Dynamic analysis of flexible mechanical systems using LATDYN N90-23080
Neural networks in support of manned space N90-23088
FLIGHT CHARACTERISTICS
Minimum flying qualities. Volume 1: Piloted simulation evaluation of multiple axis flying qualities
[AD-A218560] N90-22560
Minimum flying qualities. Volume 2: Pilot modeling for flying qualities applications
[AD-A218561] N90-22561
Minimum flying qualities. Volume 3: Program CC's implementation of the human optimal control model
[AD-A218562] N90-22562

FLIGHT CONTROL
Minimum flying qualities. Volume 1: Piloted simulation evaluation of multiple axis flying qualities
[AD-A218560] N90-22560
Minimum flying qualities. Volume 2: Pilot modeling for flying qualities applications
[AD-A218561] N90-22561
Minimum flying qualities. Volume 3: Program CC's implementation of the human optimal control model
[AD-A218562] N90-22562
Multi-axis control of telemanipulators N90-22943
Synthetic perspective optical flow: Influence on pilot control tasks N90-22956
Algorithms for computing the multivariable stability margin N90-22999
Space station dynamics, attitude control and momentum management N90-23029
Multidisciplinary Expert-aided Analysis and Design (MEAD) N90-23050
Six-degree-of-freedom aircraft simulation with mixed-data structure using the applied dynamics simulation language, ADSIM N90-23067
FLIGHT SAFETY
UK airmisses involving commercial air transport, January - April 1989
[ISSN-0951-6301] N90-22544
FLIGHT SIMULATION
Minimum flying qualities. Volume 1: Piloted simulation evaluation of multiple axis flying qualities
[AD-A218560] N90-22560
Minimum flying qualities. Volume 2: Pilot modeling for flying qualities applications
[AD-A218561] N90-22561
Visual behavior in the F-15 simulator for air-to-air combat
[AD-A218648] N90-22893
Development of a stereo 3-D pictorial primary flight display N90-22955
Six-degree-of-freedom aircraft simulation with mixed-data structure using the applied dynamics simulation language, ADSIM N90-23067
FLIGHT SIMULATORS
Inertial navigation system simulator: Behavioral specification, revision
[AD-A219294] N90-22554
Visual behavior in the F-15 simulator for air-to-air combat
[AD-A218648] N90-22893
FLIGHT TESTS
Application of a dynamic stall model to rotor trim and aeroelastic response N90-22556
Flutter investigations on a Transavia PL12/T-400 aircraft
[AD-A219108] N90-22570
Boeing/NASA composite components flight service evaluation
[NASA-CR-181898] N90-22609
Turbine fuel alternatives (near term)
[AD-A219405] N90-22695
FLIGHT TRAINING
Relationship between flexibility of closure and success in pilot night vision sensor system training N90-22890
FLIR DETECTORS
Helmet-mounted pilot night vision systems: Human factors issues N90-22930
FLOW CHARACTERISTICS
Computational and experimental investigations of rotating stall in compressor cascades N90-22565
Turbulence and complex systems
[ETN-90-96620] N90-22758
FLOW DISTRIBUTION
Water-tunnel study results of a TF/A-18 and F/A-18 canopy flow visualization
[NASA-TM-101705] N90-22532
Flow visualization in supersonic turbulent boundary layers N90-22533
The minimum drag profile in laminar flow: A numerical way N90-22535
Computational and experimental investigations of rotating stall in compressor cascades N90-22565
Investigation of advanced counterrotation blade configuration concepts for high speed turboprop systems, task 1: Ducted propfan analysis
[NASA-CR-185217] N90-22567
An investigation of the three-dimensional flow field in a centrifugal compressor N90-22751
Nonlinear bifurcation study of plane Poiseuille flow
[DLR-FB-89-42] N90-22756
Holocinematography for studies of turbulent multiphase flow
[AD-A219130] N90-22765
A numerical study of basic coastal upwelling processes N90-22878
Numerical flow simulation and supercomputers: More than a digital wind tunnel N90-22976
The development of a system for the numerical simulation of Euler flows N90-22980
FLOW EQUATIONS
Investigation of advanced counterrotation blade configuration concepts for high speed turboprop systems, task 1: Ducted propfan analysis
[NASA-CR-185217] N90-22567
Gas dynamic theory of flight of fast electron flux in plasma
[DE90-618767] N90-23220
FLOW RESISTANCE
Acquisition and correlation of cryogenic nitrogen mass flow data through a multiple orifice Joule-Thomson device
[NASA-TM-103121] N90-22761
FLOW STABILITY
Reynolds stress closure in jet flows using instability wave modeling N90-22534
Parallel channel flow excursions
[DE90-009129] N90-22753
Nonlinear bifurcation study of plane Poiseuille flow
[DLR-FB-89-42] N90-22756
FLOW THEORY
Nonstrictly hyperbolic conservation laws
[AD-A218525] N90-22762
FLOW VELOCITY
Parallel channel flow excursions
[DE90-009129] N90-22753
FLOW VISUALIZATION
Water-tunnel study results of a TF/A-18 and F/A-18 canopy flow visualization
[NASA-TM-101705] N90-22532
Flow visualization in supersonic turbulent boundary layers N90-22533
Experimental study of vortex ring interaction with a free surface N90-22742
A new stochastic model of turbulent dispersion in the convective planetary boundary layer and the results of the Atterbury-87 field study N90-22853
FLUID DYNAMICS
Pseudo-steady diffusional growth or collapse of bubbles rising in time dependent pressure fields
[AD-A218825] N90-22764
FLUID FILTERS
Some observations on liquid flow through filters
[AERE-R-13300] N90-22748
FLUID MANAGEMENT
Spacecraft attitude impacts on COLD-SAT non-vacuum jacketed LH2 supply tank thermal performance
[NASA-TM-103158] N90-22592
Acquisition and correlation of cryogenic nitrogen mass flow data through a multiple orifice Joule-Thomson device
[NASA-TM-103121] N90-22761
FLUID MECHANICS
Fundamental studies on hydrology, hydraulics and geometry of river networks
[AD-A218662] N90-22830
FLUID PRESSURE
Contributions of individual structural modes to the scattered acoustic field
[AD-A219128] N90-23187
FLUORESCENCE
Sticking coefficient of HCl on aerosols N90-22598
Human cognitive and motor performance measures under typical cool white fluorescent illumination vs relatively high cool white illuminance/irradiance lighting
[AD-A218445] N90-22892
FLUOROHYDROCARBONS
Reactions of laser-generated free radicals at semiconductor surfaces
[AD-A218552] N90-22733
FLUTTER
An experimental study of tip shape effects on the flutter of aft-swept, flat-plate wings
[NASA-TM-4180] N90-22555
FLUTTER ANALYSIS
An experimental study of tip shape effects on the flutter of aft-swept, flat-plate wings
[NASA-TM-4180] N90-22555
Flutter investigations on a Transavia PL12/T-400 aircraft
[AD-A219108] N90-22570
FLUX (RATE)
Gas dynamic theory of flight of fast electron flux in plasma
[DE90-618767] N90-23220
FLUX DENSITY
Gamma rays from giant molecular clouds N90-23298
More data on (possible) gamma ray (point) sources N90-23309
FOCUSING
Foil focusing of electron beams
[AD-A219511] N90-23208
Stability regimes in a rotating quadrupole focusing accelerator
[AD-A219513] N90-23209
FOILS (MATERIALS)
Foil focusing of electron beams
[AD-A219511] N90-23208
FORECASTING
FAA (Federal Aviation Administration) aviation forecasts, fiscal years 1990-2001
[AD-A219165] N90-22530
An interactive method for estimating hailstone size and convectively-driven wind gusts from forecast soundings
[AD-A218499] N90-22871
FORESTS
A case for archaeological reconnaissance of the Cabo Catoche-Porvenir region of the northeastern Yucatan Peninsula
[NASA-TM-102248] N90-22827
FORMALISM
Processes and formalisms for unbounded choice
[CS-8917] N90-23135
FORMING TECHNIQUES
Production of a variety of shapes using wrapping and draping techniques
[REPT-892-430-122] N90-22625
Dimensional analysis of structures using wrapping techniques
[REPT-892-430-119] N90-22815
FORMULAS (MATHEMATICS)
Methods of jet calculation
[REPT-892-422-102] N90-22603
FORMULATIONS
A methodology for formulating a minimal uncertainty model for robust control system design and analysis N90-23028
FOURIER ANALYSIS
Fourier analysis of finite element preconditioned collocation schemes
[NASA-CR-182040] N90-23128
Frequency domain techniques for analyzing picosecond optical pulses
[AD-A218856] N90-23214
FOURIER SERIES
Significance of norms and completeness in variational based methods N90-23078
Stochastic processes as Fourier integrals and dilation of vector measures
[AD-A219413] N90-23150
FRACTURE MECHANICS
A comprehensive study on microstructure mechanics relationships of ceramic matrix composites
[AD-A219318] N90-22627
NASA-UVA light aerospace alloy and structures technology program
[NASA-CR-182607] N90-22651
Elevated temperature crack growth in advanced powder metallurgy aluminum alloys N90-22653
Elevated temperature crack growth in aluminum alloys: Tensile deformation of 2618 and FVS0812 aluminum alloys N90-22654
Deformation and fracture of thin sheet aluminum-lithium alloys: The effect of cryogenic temperatures N90-22655
Deformation and fracture of aluminum-lithium alloys: The effect of dissolved hydrogen N90-22658
Quantitative characterization of spatial distribution of particles in materials: Application to materials processing N90-22660
Microcracking and toughness of ceramic-fiber/ceramic-matrix composites under high temperature
[AD-A218516] N90-22680
Computations of weight functions in fracture mechanics N90-22809
Comparison between data generated from standard fracture toughness specimens and from nonstandard specimens made of a silicon carbide
[DE90-009621] N90-22814
Material instabilities in solids
[AD-A218451] N90-22817
Fracture mechanics assessment of a cracked 16-inch inner diameter 1945 vintage-jacketed pressure vessel
[AD-A219135] N90-22819
FRACTURE STRENGTH
Elevated temperature crack growth in advanced powder metallurgy aluminum alloys N90-22653
Fracture toughness and fatigue crack initiation tests of welded precipitation-hardening stainless steel
[AD-A218745] N90-22669
Comparison between data generated from standard fracture toughness specimens and from nonstandard specimens made of a silicon carbide
[DE90-009621] N90-22814
FRACTURING
Deformation and fracture of aluminum-lithium alloys: The effect of dissolved hydrogen N90-22658

FREE BOUNDARIES
Numerical methods for the problem of the free-boundary plasma equilibrium in a stellarator (torsatron)
[DE90-620580] N90-23223
FREE ELECTRON LASERS
A free electron laser master oscillator power amplifier experiment N90-22776
FREE FLOW
Flat plate leading edge receptivity to various freestream disturbance structures N90-22750
FREE JETS
Reynolds stress closure in jet flows using instability wave modeling N90-22534
FREE RADICALS
Reactions of laser-generated free radicals at semiconductor surfaces
[AD-A218552] N90-22733
FREE WING AIRCRAFT
An experimental study of tip shape effects on the flutter of aft-swept, flat-plate wings
[NASA-TM-4180] N90-22555
FREQUENCY SHIFT KEYING
Evaluation of a prototype 6 tone modem
[RAE-TM-FM-28] N90-22708
FREQUENCY STABILITY
Design of high-performance negative-feedback oscillators
[ETN-90-96698] N90-22729
FRONTS (METEOROLOGY)
Tropical squall lines of the Arizona monsoon N90-22867
FROST
Debris/ice/TPS assessment and photographic analysis for Shuttle Mission STS-36
[NASA-TM-102789] N90-22583
FUEL CELLS
Catalysts for ultrahigh current density oxygen cathodes for space fuel cell applications
[NASA-CR-180650] N90-22835
Enhanced ceria solid electrolyte fuel cell development. Reduction of electronic conductivity permits use of a solid ceria electrolyte in high efficiency high power density fuel cells at temperatures compatible with metallic cell hardware
[AD-A219297] N90-22846
FUEL SYSTEMS
Aircraft crash survival design guide. Volume 1: Design criteria and checklists
[AD-A218434] N90-22545
Aircraft crash survival design guide. Volume 5: Aircraft postcrash survival
[AD-A218438] N90-22549
FUEL TESTS
Turbine fuel alternatives (near term)
[AD-A219405] N90-22695
FUNCTIONAL INTEGRATION
Non-symmetric double well and Euclidean functional integral
[PREPRINT-709] N90-23133
FUNGI
ELF (Extremely Low Frequency) communications system ecological monitoring program: Slime mold studies
[AD-A218623] N90-22715
FURNACES
Activation uniformity dependence of undoped semi-insulating GaAs on post-implant annealing conditions
[ETN-90-96549] N90-23246
FUSELAGES
Water-tunnel study results of a TF/A-18 and F/A-18 canopy flow visualization
[NASA-TM-101705] N90-22532
Aircraft crash survival design guide. Volume 3: Aircraft structural crash resistance
[AD-A218436] N90-22547
FUZZY SETS
RF network selection in a rule-based system. NOSC project ZE68: Cost metric algorithms for internetwork applications
[AD-A219389] N90-23116

G

GALACTIC CLUSTERS
A search for additional parameters in the infrared luminosity/21 cm line-width relation for spiral galaxies in clusters of galaxies N90-23274
Spectroscopic observations of high redshift QSOs: Galaxies and the intergalactic medium at early epochs N90-23280
GALACTIC COSMIC RAYS
The Energetic Gamma-Ray Experiment Telescope (EGRET) Science Symposium
[NASA-CP-3071] N90-23294
GALACTIC EVOLUTION
The dynamical evolution of dense clusters of compact stars N90-23287
Reconstructing primordial density fluctuations N90-23293
Gravitational collapse, Friedman models and cosmological constant: Does the universe oscillate
[DE90-620792] N90-23324
GALACTIC NUCLEI
The dynamical evolution of dense clusters of compact stars N90-23287
GALACTIC RADIATION
The Energetic Gamma-Ray Experiment Telescope (EGRET) Science Symposium
[NASA-CP-3071] N90-23294
Spectral evolution of active galactic nuclei Penrose Compton scattering processes and gamma ray emission from Seyfert galaxies N90-23317
GALACTIC ROTATION
A search for additional parameters in the infrared luminosity/21 cm line-width relation for spiral galaxies in clusters of galaxies N90-23274
GALACTIC STRUCTURE
The dynamical evolution of dense clusters of compact stars N90-23287
The Energetic Gamma-Ray Experiment Telescope (EGRET) Science Symposium
[NASA-CP-3071] N90-23294
Molecular clouds and the large-scale structure of the galaxy N90-23295
The diffuse galactic gamma ray emission N90-23296
GALAXIES
Spectroscopic observations of high redshift QSOs: Galaxies and the intergalactic medium at early epochs N90-23280
Reconstructing primordial density fluctuations N90-23293
A model of the diffuse galactic gamma ray emission N90-23297
Complementary information from mm-wave-, infrared-, and gamma ray astronomy N90-23299
Implications of the IRAS data for galactic gamma ray astronomy and EGRET N90-23300
Dipole analysis on EGRET data of extragalactic gamma ray background radiation N90-23322
GALERKIN METHOD
Application of a dynamic stall model to rotor trim and aeroelastic response N90-22556
GALLIUM
The high temperature behavior of gallium and indium liquid metal ion sources
[AERE-R-13321] N90-22647
GALLIUM ANTIMONIDES
Secondary ion mass spectrometry characterization of implants into GaAs and GaP for waveguides and integrated optics applications
[AD-A219203] N90-23254
GALLIUM ARSENIDES
Development of a unique laboratory standard indium gallium arsenide detector for the 500 to 1700 micron spectral region, phase 2
[NASA-CR-180482] N90-22767
Acoustoelectronic interaction of surface waves in GaAs-InGaAs superlattices N90-23163
Optical properties of novel GaAs-based semiconductors N90-23235
Activation uniformity dependence of undoped semi-insulating GaAs on post-implant annealing conditions
[ETN-90-96549] N90-23246
Secondary ion mass spectrometry characterization of implants into GaAs and GaP for waveguides and integrated optics applications
[AD-A219203] N90-23254
Passivation and gating of GaAs and Si surfaces using pseudomorphic structures
[AD-A219351] N90-23256
GALLIUM COMPOUNDS
The first example of an organogallium compound containing a Ga-Te bond: Synthesis, properties, and molecular structure of ((Me3CCH2)2GaTeph)2
[AD-A219258] N90-22608
GALLIUM PHOSPHIDES
Secondary ion mass spectrometry characterization of implants into GaAs and GaP for waveguides and integrated optics applications
[AD-A219203] N90-23254
GAMMA RAY ASTRONOMY
The Energetic Gamma-Ray Experiment Telescope (EGRET) Science Symposium
[NASA-CP-3071] N90-23294
Complementary information from mm-wave-, infrared-, and gamma ray astronomy N90-23299
Implications of the IRAS data for galactic gamma ray astronomy and EGRET N90-23300
Local normal galaxies N90-23315
Feasibility for EGRET detection of antimatter concentrations in the universe N90-23323
GAMMA RAY BURSTS
Gamma ray bursts: Current status of observations and theory N90-23313
What is learned from high energy bursts and flares N90-23314
GAMMA RAY OBSERVATORY
The Energetic Gamma-Ray Experiment Telescope (EGRET) Science Symposium
[NASA-CP-3071] N90-23294
Molecular clouds and the large-scale structure of the galaxy N90-23295
Radio pulsar timing observations for GRO N90-23301
GAMMA RAY SPECTRA
Gamma rays from pulsar wind shock acceleration N90-23311
GAMMA RAY TELESCOPES
The Energetic Gamma-Ray Experiment Telescope (EGRET) Science Symposium
[NASA-CP-3071] N90-23294
Implications of the IRAS data for galactic gamma ray astronomy and EGRET N90-23300
GAMMA RAYS
Molecular clouds and the large-scale structure of the galaxy N90-23295
The diffuse galactic gamma ray emission N90-23296
A model of the diffuse galactic gamma ray emission N90-23297
Gamma rays from giant molecular clouds N90-23298
Complementary information from mm-wave-, infrared-, and gamma ray astronomy N90-23299
Implications of the IRAS data for galactic gamma ray astronomy and EGRET N90-23300
Radio pulsar timing observations for GRO N90-23301
Gamma radiation from radio pulsars N90-23302
Gamma radiation from the Crab and Vela pulsars N90-23303
Gamma ray pulsars: Models and observations N90-23304
The sensitivity of EGRET to gamma ray polarization N90-23305
The illusive Geminga: What is it N90-23307
COS-B gamma ray sources beyond the predicted diffuse emission N90-23308
More data on (possible) gamma ray (point) sources N90-23309
What can gamma rays tell us about binary x ray sources and SNR's N90-23310
Gamma rays from pulsar wind shock acceleration N90-23311
Spectral determinations for discrete sources with EGRET N90-23312
Gamma ray bursts: Current status of observations and theory N90-23313
What is learned from high energy bursts and flares N90-23314
Local normal galaxies N90-23315
Gamma rays from active galactic nuclei N90-23316
Spectral evolution of active galactic nuclei Penrose Compton scattering processes and gamma ray emission from Seyfert galaxies N90-23317
The high energy source 3C 273 N90-23318
COMPTEL observations of active galactic nuclei N90-23319
OSSE observations of active galactic nuclei N90-23320
Gamma ray cosmology: The extra galactic gamma spectrum and methods to detect the underlying source N90-23321
Dipole analysis on EGRET data of extragalactic gamma ray background radiation N90-23322
Feasibility for EGRET detection of antimatter concentrations in the universe N90-23323
Numerical simulations of x rays and gamma rays from solar flares N90-23330
GAS COMPOSITION
Development and use of a passive technique for measuring nitrogen dioxide in the background atmosphere N90-23285
GAS DETECTORS
Infrared absorption gas sensor for the detection of HCl in launch vehicle exhaust clouds N90-22600
GAS DYNAMICS
Gas dynamic theory of flight of fast electron flux in plasma
[DE90-618767] N90-23220
GAS FLOW
Proceedings of the 9th International Conference on Computing Methods in Applied Science and Engineering
[AD-A219307] N90-23149
GAS PRESSURE
Transport of gases through concrete
[AERE-G-4977] N90-22747

GAS TRANSPORT
Transport of gases through concrete
[AERE-G-4977] N90-22747
GASEOUS DIFFUSION
Sticking coefficient of HCl on aerosols N90-22598
GAUSS EQUATION
Two barriers problem for continuously differentiable processes
[AD-A218564] N90-23176
GAUSSIAN ELIMINATION
Efficient computer algebra algorithms for polynomial matrices in control design N90-23022
GEAR TEETH
Surface pitting fatigue life of noninvolute, low-contact-ratio gears
[NASA-TM-103116] N90-22790
The curvature of conjugate profiles in points of contract
[MEMO-COSOR-89-18] N90-22795
Influence of linear profile modification and loading conditions on the dynamic tooth load and stress of high contact ratio gears
[NASA-TM-103136] N90-22796
GEARS
Surface pitting fatigue life of noninvolute, low-contact-ratio gears
[NASA-TM-103116] N90-22790
The curvature of conjugate profiles in points of contract
[MEMO-COSOR-89-18] N90-22795
GEODESY
Guidelines, operational procedures, and quality control for the estimation of geodetic point positions from GPS data collected with the TI4100 receiver
[AD-A218460] N90-22829
GEODETIC COORDINATES
Guidelines, operational procedures, and quality control for the estimation of geodetic point positions from GPS data collected with the TI4100 receiver
[AD-A218460] N90-22829
GEODETIC SURVEYS
Guidelines, operational procedures, and quality control for the estimation of geodetic point positions from GPS data collected with the TI4100 receiver
[AD-A218460] N90-22829
GEOMETRICAL OPTICS
Research and applications of metallic superlattices, high T(sub c) superconductors, x ray optics, and compact synchrotrons N90-23170
GEOMETRICAL THEORY OF DIFFRACTION
Background connection: A necessary object in general relativity
[DE90-620463] N90-23258
GEOPHYSICS
Quantifying and reducing uncertainty in the assimilative mapping of ionospheric electrodynamics N90-22854
GEOPOTENTIAL
Determination of the general ocean circulation using satellite altimetry from a simultaneous solution for the Earth's gravity field N90-22569
Satellite motion in axi-symmetric gravitational field. Part 2: Perturbations due to an arbitrary J(sub l)
[RAE-TR-89022] N90-22586
GEOSTROPHIC WIND
An interactive method for estimating hailstone size and convectively-driven wind gusts from forecast soundings
[AD-A218499] N90-22871
GEOSYNCHRONOUS ORBITS
Semianalytic study of high-eccentricity orbit stability and evolution N90-22574
GEOTHERMAL ENERGY CONVERSION
Geothermal energy program summary
[DE89-009485] N90-22837
Geothermal energy program summary
[DE89-009486] N90-22838
GEOTHERMAL RESOURCES
Geothermal energy program summary
[DE89-009486] N90-22838
GEOTHERMAL TECHNOLOGY
Geothermal energy program summary
[DE89-009485] N90-22837
Geothermal energy program summary
[DE89-009486] N90-22838
GERMANIUM COMPOUNDS
Advanced gas phase reactor for growth of Ge sub x Si sub 1-x
[AD-A219012] N90-23250
GLACIERS
Surface topography of the Greenland Ice Sheet from satellite radar altimetry
[NASA-SP-503] N90-22850
GLASS
Synthesis and characterization of aromatic polyester and polysiloxane containing block copolymers: Multiphase transparent atomic oxygen resistant damping materials, liquid crystal films, and toughening components of sol/gel glasses
[AD-A218871] N90-22685
Simulation of inelastic deformation in glassy polypropylene and polycarbonate
[AD-A218891] N90-22686
Investigation of atomistic simulation of structural and dynamic differences in glassy and liquid states of atactic poly(propylene)
[AD-A218896] N90-22687
Material instabilities in solids
[AD-A218451] N90-22817
GLASS FIBER REINFORCED PLASTICS
Rheology of injection mould filling with DMCs
[NPL-DMA(A)-196] N90-22675
GLOBAL POSITIONING SYSTEM
Apparatus for and a method of determining compass headings
[AD-D014436] N90-22551
The development of a real-time decimeter-level positioning system using Global Positioning System (GPS) technology
[AD-A218695] N90-22552
Guidelines, operational procedures, and quality control for the estimation of geodetic point positions from GPS data collected with the TI4100 receiver
[AD-A218460] N90-22829
GOLD
Lateral spreading of Au contacts on InP
[NASA-TM-103133] N90-22843
GRAIN BOUNDARIES
A study of the relation between grain boundary type and sensitisation in a partially-sensitised AISI 304 stainless steel using electron back-scattering patterns
[AERE-R-13327] N90-23234
GRAIN SIZE
Structure-property relations in aluminum-lithium alloys
[AD-A219183] N90-22672
GRAMMARS
Learning artificial grammars with competitive chunking
[AD-A219270] N90-22911
GRAND UNIFIED THEORY
Feasibility for EGRET detection of antimatter concentrations in the universe N90-23323
GRAPHIC ARTS
Cognitive efficiency considerations for good graphic design
[AD-A218976] N90-22899
A task-analytic approach to the automated design of information graphics
[AD-A219271] N90-22912
Pictorial communication: Pictures and the synthetic universe N90-22919
Synesthetic art through 3-D projection: The requirements of a computer-based supermedium N90-22962
Wide-angle display developments by computer graphics N90-22963
GRAPHITE-EPOXY COMPOSITES
Boeing/NASA composite components flight service evaluation
[NASA-CR-181898] N90-22609
Impact damage in graphite/epoxy laminates: Damage characterization, acoustic emission, and finite element simulation, volumes 1 and 2 N90-22610
Ultrasonic detection of critical damage in carbon-epoxy composite materials
[ONERA-RT-5/7256-RY-081-R] N90-22616
GRAPHS (CHARTS)
Basic graphics routine technical manual
[AD-A219409] N90-23117
GRATINGS (SPECTRA)
The super-gratings: How to improve the limiting resolution of grating spectrometers
[PREPRINT-695] N90-22577
High performance holographic elements and media
[AD-A218999] N90-22775
GRAVITATIONAL COLLAPSE
Gravitational collapse, Friedman models and cosmological constant: Does the universe oscillate
[DE90-620792] N90-23324
GRAVITATIONAL EFFECTS
Optical, gravitational, and kinesthetic determinants of judged eye level N90-22959
The effect of elevated gravity on the crystallization of the MFI zeolites, ZSM-5, and silicalite N90-23231
The dynamical evolution of dense clusters of compact stars N90-23287
GRAVITATIONAL FIELDS
Determination of the general ocean circulation using satellite altimetry from a simultaneous solution for the Earth's gravity field N90-22569
Effective action for induced gravity on a 2-dimensional manifold
[PREPRINT-712] N90-23173
Quantum mechanics in Riemannian space-time
[DE90-620448] N90-23257
GRAVITATIONAL LENSES
Studies in gravitational lensing and numerical hydrodynamics N90-23290
GRAVITATIONAL WAVES
Gravitational radiation produced by high energy accelerators and high power lasers
[PREPRINT-701] N90-22782
Superheterodyne three-wave detection of gravitation waves
[DE90-620465] N90-22856
GRAVITY WAVES
Gravity wave and turbulence studies using a high-resolution ST radar
[AD-A218877] N90-22860
GRAZING INCIDENCE
Full surface interferometric testing of grazing incidence mirrors
[AD-A219394] N90-23218
GREEN'S FUNCTIONS
Numerical methods for the problem of the free-boundary plasma equilibrium in a stellarator (torsatron)
[DE90-620580] N90-23223
GREENHOUSE EFFECT
Global and hemispheric annual temperature variations between 1861 and 1988
[DE90-007993] N90-22869
GREENLAND
Surface topography of the Greenland Ice Sheet from satellite radar altimetry
[NASA-SP-503] N90-22850
GRID GENERATION (MATHEMATICS)
Supersonic flow computations for an ASTOVL aircraft configuration, phase 2, part 2
[NASA-CR-4284] N90-22746
Stable boundary conditions for Cartesian grid calculations
[NASA-CR-182048] N90-23139
GRIFFITH CRACK
Computations of weight functions in fracture mechanics N90-22809
GROUND BASED CONTROL
Improvement of clutter rejection by scanning motion compensation in ground-based monopulse radar
[ETN-90-96550] N90-22711
GROUND EFFECT (AERODYNAMICS)
Dynamic ground-effect measurements on the F-15 STOL and Maneuver Technology Demonstrator (S/MTD) configuration
[NASA-TP-3000] N90-22531
GROUND STATE
Convergence of hyperspherical adiabatic expansion for helium-like systems
[DE90-620526] N90-22631
GROUND TESTS
Dynamic ground-effect measurements on the F-15 STOL and Maneuver Technology Demonstrator (S/MTD) configuration
[NASA-TP-3000] N90-22531
Quantifying and reducing uncertainty in the assimilative mapping of ionospheric electrodynamics N90-22854
National emissions standards for hazardous air pollutants application for approval of construction SP-100 ground engineering system test site
[DE90-007985] N90-23203
GROUP DYNAMICS
Unsteady group behavior of droplet clouds in swirling flows N90-22743
GROUP THEORY
Analytic semigroups: Applications to inverse problems for flexible structures
[NASA-CR-182047] N90-23138
GUN PROPELLANTS
A comparison between experiment and simulation for concept VIC regenerative liquid propellant guns. Part 1: 30 mm
[AD-A218556] N90-22692
Methods for evaluation of thermally induced reactions in liquid propellants
[AD-A218750] N90-22694
GUNN DIODES
Indium phosphide planar Gunn diode
[AD-A219337] N90-22740
GUNS (ORDNANCE)
A comparison between experiment and simulation for concept VIC regenerative liquid propellant guns. Part 1: 30 mm
[AD-A218556] N90-22692
GUSTS
Flat plate leading edge receptivity to various freestream disturbance structures N90-22750

An interactive method for estimating hailstone size and convectively-driven wind gusts from forecast soundings [AD-A218499] N90-22871

H

H II REGIONS
The effect of a stellar wind on an expanding H II region N90-23292
Spectral measurements of the cosmic microwave background N90-23334
HAFNIUM
Dehydrogenative polymerization of silanes to polysilanes: A monomeric copper(2) siloxide [AD-A218550] N90-22681
HAIL
An interactive method for estimating hailstone size and convectively-driven wind gusts from forecast soundings [AD-A218499] N90-22871
HAMILTON-JACOBI EQUATION
High order essentially non-oscillatory schemes for Hamilton-Jacobi equations [NASA-CR-181995] N90-23137
HAMILTONIAN FUNCTIONS
A proof of the isoenergetic KAM: Theorem from the ordinary one [W-8906] N90-23136
Excitation of hypersound at boundary between Type-2 superconductor and a concentrated paramagnetic compound N90-23164
What is going on in the La2CuO4 superconductors N90-23171
HARDENING (MATERIALS)
Approximate analysis for the formation of adiabatic shear bands [AD-A218751] N90-22670
HEAD DOWN TILT
Interactions of form and orientation N90-22958
HEAD MOVEMENT
Voluntary presetting of the vestibular ocular reflex permits gaze stabilization despite perturbation of fast head movements N90-22960
HEAD-UP DISPLAYS
The eyes prefer real images N90-22938
HEAT EXCHANGERS
High temperature ceramic-tubed reformer [DE90-009617] N90-22755
HEAT FLUX
Monthly surface thermal forcing in the tropical Pacific from 1980 to 1983 [NASA-CR-183033] N90-22877
Experimental investigations concerning the propagation of second-sound pulses at critical heat flux [MPIS-12/1989] N90-23182
Experiments on the breakdown of heat transfer in liquid helium 2 [MPIS-13/1989] N90-23259
HEAT STROKE
Heat exhaustion in a rat model: Lithium as a biochemical probe [AD-A219361] N90-22884
HEAT TOLERANCE
Heat exhaustion in a rat model: Lithium as a biochemical probe [AD-A219361] N90-22884
HEAT TRANSFER
Modeling of combustion processes in a solid fuel particle [DE90-009140] N90-22629
Parallel channel flow excursions [DE90-009129] N90-22753
Ocean energy program summary [DE89-009481] N90-22836
Geothermal energy program summary [DE89-009486] N90-22838
HEAT TRANSMISSION
Experiments on the breakdown of heat transfer in liquid helium 2 [MPIS-13/1989] N90-23259
HEAT TREATMENT
A comparison of CuAlNi and other high damping alloys for the purpose of naval ship silencing applications [AD-A218801] N90-22671
HEATING
Experimental and computational study of the viscoplastic response of high temperature structures N90-22663
HEAVY IONS
Burnout thresholds and cross section of power MOS transistors with heavy ions [AD-A218998] N90-22736
Plasma instabilities associated with the injection of artificial ion beams into the ionosphere N90-22851
Solar flares and magnetospheric particles: Investigations based upon the ONR-602 and ONR-604 experiments [AD-A218844] N90-23332
HELICOPTERS
Multi-axis control of telemanipulators N90-22943
HELIOSTATS
An assessment of second-generation stretched-membrane mirror modules [DE90-010243] N90-22841
HELIUM
Rapid mass transfer in binary systems N90-23289
HELIUM ISOTOPES
Relativistic corrections to He-3 photodisintegration sum rules [NOTA-INTERNA-942] N90-23197
An effective He-3 nucleon force for the He-3, t) charge exchange reaction [KVI-813] N90-23198
HELMET MOUNTED DISPLAYS
Helmet-mounted pilot night vision systems: Human factors issues N90-22930
HERMES MANNED SPACEPLANE
SIMOUN: An optimized supersonic high temperature wind tunnel for testing construction materials to be used on the spaceplane [REPT-892-430-111] N90-22572
HETEROJUNCTIONS
Measurement of localized deep levels and wafer non-uniformities at 3-5 semiconductor heterojunctions [AD-A218547] N90-23248
HEURISTIC METHODS
Designing good experiments to test bad hypotheses [AD-A218977] N90-22900
Laboratory replication of scientific discovery processes [AD-A219273] N90-22913
Scientific discovery as problem solving [AD-A218887] N90-23145
HIERARCHIES
A tool for aiding in the reuse of software [INPE-4981-PRE/1545] N90-23091
HIGH ELECTRON MOBILITY TRANSISTORS
Excess noise, anomalous effects and reliability of high frequency devices (Schottky diodes, MESFET and HEMT) [LAAS-89-394] N90-22728
HIGH FREQUENCIES
Excess noise, anomalous effects and reliability of high frequency devices (Schottky diodes, MESFET and HEMT) [LAAS-89-394] N90-22728
HIGH POWER LASERS
Beam combining by phase transition nonlinear media [AD-A219301] N90-22739
Gravitational radiation produced by high energy accelerators and high power lasers [PREPRINT-701] N90-22782
HIGH PRESSURE
Superconducting and normal compounds: Some high field/high pressure effects N90-23229
HIGH RESOLUTION
Contributions to the development of SLM TEA CO2 laser sources for high resolution molecular spectroscopy N90-22778
HIGH SPEED PHOTOGRAPHY
Debris/ice/TPS assessment and photographic analysis for Shuttle Mission STS-36 [NASA-TM-102789] N90-22583
HIGH TEMPERATURE
High-temperature deformation of mechanically-alloyed aluminum IN90211 N90-22645
Elevated temperature crack growth in advanced powder metallurgy aluminum alloys N90-22653
Elevated temperature crack growth in aluminum alloys: Tensile deformation of 2618 and FVS0812 aluminum alloys N90-22654
Experimental and computational study of the viscoplastic response of high temperature structures N90-22663
Microcracking and toughness of ceramic-fiber/ceramic-matrix composites under high temperature [AD-A218516] N90-22680
High temperature ceramic-tubed reformer [DE90-009617] N90-22755
HIGH TEMPERATURE PLASMAS
Studies of Io's atmosphere and plasma torus N90-23326
HIGH TEMPERATURE RESEARCH
The position of carbon/carbon composites among high temperature composites [REPT-892-430-126] N90-22626
HIGH TEMPERATURE SUPERCONDUCTORS
Composite ceramic superconducting wires for electric motor applications [AD-A219131] N90-22689
ONR Far East Scientific Information Bulletin, Volume 13, No. 4 [ONRFE-SCI-INFO-BULL-13(4)88] N90-23168
High temperature superconducting thin films in Japan N90-23169
Research and applications of metallic superlattices, high T(sub c) superconductors, x ray optics, and compact synchrotrons N90-23170
What is going on in the La2CuO4 superconductors N90-23171
Superconducting and normal compounds: Some high field/high pressure effects N90-23229
Thermal phenomena in high-Tc thin film superconductors N90-23233
Single crystal NMR of high temperature superconductors N90-23236
Influence of high energy radiation on critical parameters of superconducting ceramics YBa2Cu3O7 [DE90-620562] N90-23239
A (mu)SR-investigation of the mixed state of the high-Tc superconductor HoBa2Cu3O7-delta [DE90-620802] N90-23241
Application of high-temperature superconducting thin-film devices to electro-optical and electronic warfare systems [AD-A218805] N90-23249
HIGH TEMPERATURE TESTS
Uncertainty evaluation in an automated high temperature environmental simulation oven [REPT-892-430-103] N90-22571
Qualification test rationale for measuring the resistance of equipment to pyrotechnic shock [REPT-892-430-117] N90-22590
HILBERT SPACE
Estimation of Hilbert space valued parameters by the method of sieves [AD-A218565] N90-23143
HINGES
Dynamic analysis of flexible mechanical systems using LATDYN N90-23080
HMX
Temperature measurements through a solid-propellant combustion wave using imbedded fine wire thermocouples [AD-A218642] N90-22693
HOLMIUM
A (mu)SR-investigation of the mixed state of the high-Tc superconductor HoBa2Cu3O7-delta [DE90-620802] N90-23241
HOLOGRAPHIC SUBTRACTION
Reduced size holography [PREPRINT-707] N90-22771
HOLOGRAPHY
Holocinematography for studies of turbulent multiphase flow [AD-A219130] N90-22765
Reduced size holography [PREPRINT-707] N90-22771
High performance holographic elements and media [AD-A218999] N90-22775
Hybrid diffractive-refractive telescope [AD-A219241] N90-23216
HOMOGENEITY
Methods for evaluation of thermally induced reactions in liquid propellants [AD-A218750] N90-22694
HOMOGENEOUS TURBULENCE
Turbulence and complex systems [ETN-90-96620] N90-22758
HOMOMORPHISMS
Factoring homomorphisms [CS-8908] N90-23096
Processes and formalisms for unbounded choice [CS-8917] N90-23135
An algebric approach to infinite data structures [CS-8909] N90-23265
HOMOTOPY THEORY
H2, fixed architecture, control design for large scale systems [NASA-CR-180471] N90-22698
Combined control-structure optimization N90-23005
HUMAN FACTORS ENGINEERING
Helmet-mounted pilot night vision systems: Human factors issues N90-22930
HUMAN REACTIONS
Field-of-view assessment of low-level flight and an airdrop in the C-130 Weapon System Trainer (WST) [AD-A218504] N90-22559
HYDRAULIC EQUIPMENT
Experimental adaptive control of a hydraulic robot N90-23121
HYDROCARBON FUELS
Oxidation and ignition characteristics of hydrocarbon fuels [AD-A218666] N90-22637
HYDROCHLORIC ACID
HCl monitor N90-22599
Infrared absorption gas sensor for the detection of HCl in launch vehicle exhaust clouds N90-22600
Measurement of HCl by near-infrared diode laser absorption N90-22601

HYDROCYANIC ACID
The interstellar medium of a starburst galaxy; millimeter interferometric observations of M82 N90-23276
HYDRODYNAMIC COEFFICIENTS
Design and construction of a packed column simulator operating under atmospheric and reduced pressure [ISAL-89-60] N90-22757
HYDRODYNAMICS
Fundamental hydrodynamics research [AD-A219179] N90-22766
Studies in gravitational lensing and numerical hydrodynamics N90-23290
HYDROGEN
Deformation and fracture of aluminum-lithium alloys: The effect of dissolved hydrogen N90-22658
H2, fixed architecture, control design for large scale systems [NASA-CR-180471] N90-22698
Molecular evolution in astrophysical environments N90-23291
HYDROGEN ATOMS
Interaction of atomic hydrogen with pico- and femtosecond laser pulses [AD-A218426] N90-22785
HYDROGEN CHLORIDES
HCl Vapor Characterization and Detection. JANNAF Safety and Environmental Protection Subcommittee Workshop [AD-A216252] N90-22596
The HCl/aerosol problem N90-22597
Viscosity, density and conductivity of ImCl(HCl) sub 1.3 [AD-A218902] N90-22641
HYDROGEN ENGINES
Development of high-activity para- to ortho-hydrogen conversion catalysts, volume 2 [AD-A218700] N90-22638
HYDROGEN IONS
Convergence of hyperspherical adiabatic expansion for helium-like systems [DE90-620526] N90-22631
HYDROGENATION
Hydrogenation of stainless steels implanted with nitrogen [DE90-617397] N90-22666
Methods for evaluation of thermally induced reactions in liquid propellants [AD-A218750] N90-22694
HYDROGRAPHY
The development of a real-time decimeter-level positioning system using Global Positioning System (GPS) technology [AD-A218695] N90-22552
HYDROLOGY
Fundamental studies on hydrology, hydraulics and geometry of river networks [AD-A218662] N90-22830
HYDROSTATICS
Pseudo-steady diffusional growth or collapse of bubbles rising in time dependent pressure fields [AD-A218825] N90-22764
Evolutionary models of the rotating sun and implications for other low mass stars N90-23329
HYPERBOLIC DIFFERENTIAL EQUATIONS
Fourier analysis of finite element preconditioned collocation schemes [NASA-CR-182040] N90-23128
High order essentially non-oscillatory schemes for Hamilton-Jacobi equations [NASA-CR-181995] N90-23137
Adaptive mesh experiments for hyperbolic partial differential equations [AD-A219194] N90-23148
HYPERCUBE MULTIPROCESSORS
Communication overhead on the Intel iPSC-860 hypercube [NASA-CR-182055] N90-22982
Algorithmic considerations of integrated design for CSI on a hypercube architecture N90-23043
Fault tolerant multiprocessing and development of tools [AD-A219216] N90-23110
HYPERSONIC FLOW
The aerodynamic characteristics of power-law bodies in continuum and transitional hypersonic flow [RAE-TM-AERO-2164] N90-22537
Proceedings of the 9th International Conference on Computing Methods in Applied Science and Engineering [AD-A219307] N90-23149
HYPERSONIC SPEED
Flow visualization in supersonic turbulent boundary layers N90-22533
HYPERSONIC WIND TUNNELS
Quantitative surface temperature measurement using two-color thermographic phosphors and video equipment [NASA-CASE-LAR-13740-1] N90-22770
HYPERSONICS
Excitation of hypersound at boundary between Type-2 superconductor and a concentrated paramagnetic compound N90-23164
HYPERVELOCITY IMPACT
Large-scale simulations of monolithic and segmented projectiles impacting spaced armor [AD-A219374] N90-22800
HYPOTHESES
Designing good experiments to test bad hypotheses [AD-A218977] N90-22900
HYPOXIA
The kinetics of dark adaptation in hypoxic subjects [AD-A218641] N90-22885

I

ICE
Debris/ice/TPS assessment and photographic analysis for Shuttle Mission STS-36 [NASA-TM-102789] N90-22583
ICE ENVIRONMENTS
SeaRISE: A Multidisciplinary Research Initiative to Predict Rapid Changes in Global Sea Level Caused by Collapse of Marine Ice Sheets [NASA-CP-3075] N90-22824
ICE FLOES
Estimating sea ice thickness using time-of-flight data from impulse radar soundings [AD-A218736] N90-22831
ICE FORMATION
On the effectiveness of the production of antarctic bottom water in the Weddell and Ross Seas [AD-A218873] N90-22880
ICE MAPPING
Surface topography of the Greenland Ice Sheet from satellite radar altimetry [NASA-SP-503] N90-22850
IGNITION
Ignition testing of low-energy laser diode ignited components [DE90-009968] N90-22630
Oxidation and ignition characteristics of hydrocarbon fuels [AD-A218666] N90-22637
IGNITION SYSTEMS
Pyrotechnic materials ignited using lasers. High energy photopyrotechnic chains [REPT-892-430-121] N90-22691
Optimization of a pulsed air core transformer for low impedance inductive ignition [AD-A218748] N90-22734
IGNITION TEMPERATURE
Oxidation and ignition characteristics of hydrocarbon fuels [AD-A218666] N90-22637
ILLUMINANCE
Human cognitive and motor performance measures under typical cool white fluorescent illumination vs relatively high cool white illuminance/irradiance lighting [AD-A218445] N90-22892
IMAGE ANALYSIS
Analysis of nonlinear internal waves observed by LANDSAT-TM [PREPRINT-704] N90-22828
Spatial Displays and Spatial Instruments [NASA-CP-10032] N90-22918
Pictorial communication: Pictures and the synthetic universe N90-22919
The perception of three-dimensionality across continuous surfaces N90-22924
The effects of viewpoint on the virtual space of pictures N90-22932
Perceived orientation, spatial layout and the geometry of pictures N90-22933
The eyes prefer real images N90-22938
Spatial issues in user interface design from a graphic design perspective N90-22939
Quantum-limited image recognition [AD-A218425] N90-23101
Classification techniques for quantum-limited and classical-intensity images [AD-A218693] N90-23212
IMAGE PROCESSING
Experimental study of vortex ring interaction with a free surface N90-22742
ALVINN: An Autonomous Land Vehicle In a Neural Nettwork [AD-A218975] N90-22797
The visibility diagram: A data structure for visibility and motion planning problems. Part 1: Application to the visibility polygon query problem [CS-8913-PT-1] N90-23098
Transactions of the Seventh Army Conference on Applied Mathematics and Computing [AD-A219220] N90-23160
Image segmentation with detection of highlights and inter-reflections using color [AD-A218710] N90-23213
Looking at large data sets using binned data plots [DE90-008208] N90-23263
IMAGE RECONSTRUCTION
Reduced size holography [PREPRINT-707] N90-22771
IMAGERY
Atmospheric autorotating imaging device [NASA-CASE-NPO-17390-1-CU] N90-22769
IMAGING TECHNIQUES
Scanning laser photocurrent spectroscopy of electrochemically grown bismuth sulphide films [AERE-M-3709] N90-22649
Quantitative surface temperature measurement using two-color thermographic phosphors and video equipment [NASA-CASE-LAR-13740-1] N90-22770
Reduced size holography [PREPRINT-707] N90-22771
Recent advances in nondestructive evaluation made possible by novel uses of video systems [NASA-TM-102491] N90-22801
Spaceborne radar observations: A guide for Magellan radar-image analysis [NASA-CR-184998] N90-22826
The eyes prefer real images N90-22938
Volumetric visualization of 3D data N90-22964
Studies in gravitational lensing and numerical hydrodynamics N90-23290
TeV radiation from the Crab nebula and other matters N90-23306
IMIDES
Viscosity, density and conductivity of ImCl(HCl) sub 1.3 [AD-A218902] N90-22641
IMPACT DAMAGE
Impact damage in graphite/epoxy laminates: Damage characterization, acoustic emission, and finite element simulation, volumes 1 and 2 N90-22610
Bird impact tests on structures made of Kevlar 49. Monolithic plates under straight-on impact [REPT-S3-4273-PARTIAL-1] N90-22620
Characterization of particle impact by quantitative acoustic emission [AERE-R-13028] N90-22810
IMPACT LOADS
Aircraft crash survival design guide. Volume 2: Aircraft design crash impact conditions and human tolerance [AD-A218435] N90-22546
IMPACT TESTS
Bird impact tests on Kevlar 29 and 49 sandwich structures under straight-on and glancing impact [REPT-S3-4273-PARTIAL-6] N90-22617
Bird impact tests on Kevlar plates. Sandwich Kevlar-nida submitted to straight-on and glancing impact [REPT-S3-4273-PARTIAL-3] N90-22619
Bird impact tests on structures made of Kevlar 49. Monolithic plates under straight-on impact [REPT-S3-4273-PARTIAL-1] N90-22620
IMPACT TOLERANCES
Aircraft crash survival design guide. Volume 2: Aircraft design crash impact conditions and human tolerance [AD-A218435] N90-22546
IMPEDANCE
Linear and nonlinear electrical response of condensed matter: Ionic, dielectric, and mixed-conduction materials [AD-A218771] N90-22639
IMPURITIES
A low temperature calorimetric study of several high-T(sub c) superconductors N90-23237
INCOMPRESSIBLE BOUNDARY LAYER
Flat plate leading edge receptivity to various freestream disturbance structures N90-22750
INCOMPRESSIBLE FLOW
Fundamental hydrodynamics research [AD-A219179] N90-22766
INDIAN OCEAN
US Navy regional climatic study of southern African waters [AD-A218792] N90-22674
INDIUM
The high temperature behavior of gallium and indium liquid metal ion sources [AERE-R-13321] N90-22647

INDIUM ANTIMONIDES
Secondary ion mass spectrometry characterization of implants into GaAs and GaP for waveguides and integrated optics applications
[AD-A219203] N90-23254
INDIUM ARSENIDES
Development of a unique laboratory standard indium gallium arsenide detector for the 500 to 1700 micron spectral region, phase 2
[NASA-CR-180482] N90-22767
Acoustoelectronic interaction of surface waves in GaAs-InGaAs superlattices N90-23163
Secondary ion mass spectrometry characterization of implants into GaAs and GaP for waveguides and integrated optics applications
[AD-A219203] N90-23254
INDIUM PHOSPHIDES
Indium phosphide planar Gunn diode
[AD-A219337] N90-22740
Lateral spreading of Au contacts on InP
[NASA-TM-103133] N90-22843
Secondary ion mass spectrometry characterization of implants into GaAs and GaP for waveguides and integrated optics applications
[AD-A219203] N90-23254
INDUCTION (MATHEMATICS)
Efficient specialization of relational concepts
[AD-A218889] N90-22894
INDUCTION MOTORS
Field oriented control of induction motors
[NASA-TM-103154] N90-22731
INERTIAL CONFINEMENT FUSION
Laser Program of the Lawrence Livermore National Laboratory
[DE90-008198] N90-22779
INERTIAL NAVIGATION
Inertial navigation system simulator: Behavioral specification, revision
[AD-A219294] N90-22554
INFERENCE
Connectionism and compositional semantics
[AD-A219029] N90-22904
Bayesian nonparametric prediction and statistical inference
[AD-A218473] N90-23154
Statistical inference from sampled data
[AD-A218731] N90-23156
INFLATING
Anisotropic inflation N90-23286
INFORMATION PROCESSING (BIOLOGY)
A preliminary analysis of the SOAR architecture as a basis for general intelligence
[AD-A218913] N90-22896
Cognitive efficiency considerations for good graphic design
[AD-A219976] N90-22899
Information processing approaches to cognitive development
[AD-A219200] N90-22908
A task-analytic approach to the automated design of information graphics
[AD-A219271] N90-22912
Laboratory replication of scientific discovery processes
[AD-A219273] N90-22913
An instructable Connectionist/Control architecture: Using rule-based instructions to accomplish connectionist learning in a human time scale
[AD-A219274] N90-22914
How to reinforce perception of depth in single two-dimensional pictures N90-22937
INFORMATION RETRIEVAL
Assessment System for Aircraft Noise (ASAN) citation database. Volume 1: User's manual
[AD-A219175] N90-23188
Assessment System for Aircraft Noise (ASAN) citation database. Volume 2: Database update manual
[AD-A219176] N90-23189
Assessment System for Aircraft Noise (ASAN) citation database. Volume 3: New citation review procedures
[AD-A219177] N90-23190
INFORMATION SYSTEMS
BTOS database evaluation
[AD-A219304] N90-23271
INFRARED ABSORPTION
Infrared absorption gas sensor for the detection of HCl in launch vehicle exhaust clouds N90-22600
INFRARED ASTRONOMY
Ultraviolet and infrared studies of Be stars N90-23275
Complementary information from mm-wave-, infrared-, and gamma ray astronomy N90-23299
Dipole analysis on EGRET data of extragalactic gamma ray background radiation N90-23322
INFRARED ASTRONOMY SATELLITE
Implications of the IRAS data for galactic gamma ray astronomy and EGRET N90-23300
INFRARED DETECTORS
HCl Vapor Characterization and Detection. JANNAF Safety and Environmental Protection Subcommittee Workshop
[AD-A216252] N90-22596
Direct implantation process development and characterization in advanced Hg(1)-(x)Cd(x) Te EPI layers
[AD-A219133] N90-23252
INFRARED RADIATION
A search for additional parameters in the infrared luminosity/21 cm line-width relation for spiral galaxies in clusters of galaxies N90-23274
Infrared coronal line novae N90-23328
INITIATORS (EXPLOSIVES)
Pyrotechnic materials ignited using lasers. High energy photopyrotechnic chains
[REPT-892-430-121] N90-22691
INSPECTION
Debris/ice/TPS assessment and photographic analysis for Shuttle Mission STS-36
[NASA-TM-102789] N90-22583
INSULATION
Qualification of the RSRM case membrane case-to-insulation bondline inspection using the Thiokol Corporation ultrasonic RSRM bondline inspection system
[NASA-CR-183940] N90-22602
Qualification of the RSRM field joint CF case-to-insulation bondline inspection using the Thiokol Corporation ultrasonic RSRM bondline inspection system
[NASA-CR-183931] N90-22788
INTEGERS
A new second-order integration algorithm for simulating mechanical dynamic systems N90-23064
INTEGRAL EQUATIONS
On approximation of nonlinear boundary integral equations for the combined method
[DE90-009784] N90-23130
INTEGRALS
Stochastic processes as Fourier integrals and dilation of vector measures
[AD-A219413] N90-23150
Incomplete integrals of cylindrical functions
[AD-A219512] N90-23161
INTERFEROMETERS
Full surface interferometric testing of grazing incidence mirrors
[AD-A219394] N90-23218
INTERFEROMETRY
Full surface interferometric testing of grazing incidence mirrors
[AD-A219394] N90-23218
The interstellar medium of a starburst galaxy; millimeter interferometric observations of M82 N90-23276
Anderson Mesa, Arizona as a site for an optical interferometric array N90-23281
INTERGALACTIC MEDIA
Skewering the universe with QSO lines of sight: Lyman alpha clouds as probes of large scale structure N90-23278
Spectroscopic observations of high redshift QSOs: Galaxies and the intergalactic medium at early epochs N90-23280
INTERGRANULAR CORROSION
The initiation of intergranular stress corrosion-cracking on sensitized stainless steel in dilute thiosulphate solutions
[AERE-R-13317] N90-22648
INTERMETALLICS
High temperature fatigue behavior of a SiC/Ti-24Al-11Nb composite
[NASA-TM-103157] N90-22822
INTERMITTENCY
The multifractal nature of turbulence N90-22752
INTERNATIONAL COOPERATION
The International Space University
[NASA-TM-103163] N90-22604
INTERNATIONAL RELATIONS
International treaties and active experiments in space
[AD-A219368] N90-23272
INTERORBITAL TRAJECTORIES
Interactive orbital proximity operations planning system N90-22953
INTERPLANETARY MAGNETIC FIELDS
A study of auroral activity in the nightside polar cap N90-22852
INTERPLANETARY SPACE
Solar flares and magnetospheric particles: Investigations based upon the ONR-602 and ONR-604 experiments
[AD-A218844] N90-23332
INTERPROCESSOR COMMUNICATION
A scheme for supporting automatic data migration on multicomputers
[NASA-CR-182038] N90-22975
Communication overhead on the Intel iPSC-860 hypercube
[NASA-CR-182055] N90-22982
Durra: A task-level description language reference manual, version 2
[AD-A219293] N90-23114
Locality in parallel computation
[AD-A218733] N90-23120
Control of randomly sampled robotic systems
[AD-A218948] N90-23157
INTERSTELLAR MATTER
The interstellar medium of a starburst galaxy; millimeter interferometric observations of M82 N90-23276
The effect of a stellar wind on an expanding H II region N90-23292
INVERSE SCATTERING
The effects of caustics in acoustic inverse scattering experiments
[AD-A218454] N90-23185
INVERSIONS
Program inversion: More than fun
[CS-8903] N90-23095
INVISCID FLOW
Stable boundary conditions for Cartesian grid calculations
[NASA-CR-182048] N90-23139
IO
Studies of Io's atmosphere and plasma torus N90-23326
IODINE
Threshold photodetachment spectroscopy of the I + HI transition state region
[AD-A218410] N90-22883
ION BEAMS
The high temperature behavior of gallium and indium liquid metal ion sources
[AERE-R-13321] N90-22647
Amorphization of metals by ion implantation and ion beam mixing
[DE90-620571] N90-22667
Plasma instabilities associated with the injection of artificial ion beams into the ionosphere N90-22851
Intense electron beam propagation across a magnetic field
[DE90-009993] N90-23204
ION IMPLANTATION
Improved high temperature oxidation behavior of alloys by ion implantation
[AERE-R-13309] N90-22650
Hydrogenation of stainless steels implanted with nitrogen
[DE90-617397] N90-22666
Amorphization of metals by ion implantation and ion beam mixing
[DE90-620571] N90-22667
Direct implantation process development and characterization in advanced Hg(1)-(x)Cd(x) Te EPI layers
[AD-A219133] N90-23252
Secondary ion mass spectrometry characterization of implants into GaAs and GaP for waveguides and integrated optics applications
[AD-A219203] N90-23254
ION SOURCES
The high temperature behavior of gallium and indium liquid metal ion sources
[AERE-R-13321] N90-22647
IONIC COLLISIONS
Support for the 16th International Conference on the Physics of Electronic and Atomic Collisions
[AD-A218567] N90-23200
IONIZATION
Molecular evolution in astrophysical environments N90-23291
IONIZED GASES
Sound waves in weakly ionized gas
[DE90-620704] N90-23180
IONOSPHERIC PROPAGATION
HF propagation through actively modified ionospheres
[DE90-008931] N90-22705
IRON COMPOUNDS
Improvement study of iron disilicide thermoelectric materials
[AD-A218946] N90-22844
IRRADIATION
Photovoltaic advanced research and development project: Solar radiation research
[DE90-000302] N90-22839
A study of low level laser retinal damage
[AD-A218919] N90-22887
Influence of high energy radiation on critical parameters of superconducting ceramics YBa2Cu3O7
[DE90-620562] N90-23239
Gamma rays from giant molecular clouds N90-23298

ISING MODEL
Rigorous analysis of low temperature stochastic Ising models: Metastability and exponential approach to equilibrium
[PREPRINT-720] N90-23175
ISOTROPIC TURBULENCE
The analysis and simulation of compressible turbulence
[NASA-CR-181997] N90-22539
Turbulence and complex systems
[ETN-90-96620] N90-22758
ISOTROPY
Anisotropic inflation N90-23286
ITALIAN SPACE PROGRAM
The Italian approach to small satellites for low cost access to space developments
[ETN-90-96552] N90-22587
ITERATION
A nearly-linear computational-cost scheme for the forward dynamics of an N-body pendulum N90-22996
Parallel processing of real-time dynamic systems simulation on OSCAR (Optimally SCheduled Advanced multiprocessoR) N90-23006
Minimal complexity control law synthesis N90-23057
Fourier analysis of finite element preconditioned collocation schemes
[NASA-CR-182040] N90-23128
Undetermined coefficient problems for quasi-linear parabolic equations
[AD-A218462] N90-23141

J

JAMMING
Performance of adaptive nulling antennas in a jamming environment
[AD-A219305] N90-22720
JAPAN
Research and applications of metallic superlattices, high T(sub c) superconductors, x ray optics, and compact synchrotrons N90-23170
Current Japanese supercomputers for computational fluid dynamics applications N90-23172
JET ENGINE FUELS
Turbine fuel alternatives (near term)
[AD-A219405] N90-22695
JET EXHAUST
Methods of jet calculation
[REPT-892-422-102] N90-22603
JET FLOW
Methods of jet calculation
[REPT-892-422-102] N90-22603
JET MIXING FLOW
The effects of compressibility on a supersonic mixing layer
[AD-A219315] N90-22543
JFET
Burnout thresholds and cross section of power MOS transistors with heavy ions
[AD-A218998] N90-22736
JOINTS (JUNCTIONS)
Study and sizing of bonded joints in space structures
[REPT-892-430-124] N90-22591
An alternate interconnect method for joining flexible circuits using conductive adhesives
[DE90-008194] N90-22674
Evaluation of joints bonded with elastoplastic adhesives
[REPT-892-430-120] N90-22816
A nearly-linear computational-cost scheme for the forward dynamics of an N-body pendulum N90-22996
Determination of joint drives for stable end-effector motion in flexible robotic systems N90-23034
JOSEPHSON JUNCTIONS
Construction of a 345 gigahertz receiver based on superconducting tunnel junctions
[AD-A218781] N90-22735
JOULE-THOMSON EFFECT
Acquisition and correlation of cryogenic nitrogen mass flow data through a multiple orifice Joule-Thomson device
[NASA-TM-103121] N90-22761
JUPITER (PLANET)
Studies of Io's atmosphere and plasma torus N90-23326

K

KALMAN FILTERS
An innovations approach to decoupling of multibody dynamics and control N90-22994
On a fallacious conjecture about the stabilizability properties of solutions of the Riccati difference equation
[REPT-89-007] N90-23132
KARMAN VORTEX STREET
Flat plate leading edge receptivity to various freestream disturbance structures N90-22750
KERNEL FUNCTIONS
DARK (Distributed Ada Real-Time Kernel) porting and extension guide Kernel version 3.0
[AD-A219291] N90-23112
Version description and installation guide Kernel version 3.0
[AD-A219292] N90-23113
Kernel architecture manual
[AD-A219295] N90-23115
Anisotropic inflation N90-23286
KEVLAR (TRADEMARK)
Bird impact tests on Kevlar 29 and 49 sandwich structures under straight-on and glancing impact
[REPT-S3-4273-PARTIAL-6] N90-22617
Bird impact tests on Kevlar plates. Sandwich Kevlar-nida submitted to straight-on and glancing impact
[REPT-S3-4273-PARTIAL-3] N90-22619
Bird impact tests on structures made of Kevlar 49. Monolithic plates under straight-on impact
[REPT-S3-4273-PARTIAL-1] N90-22620
KINEMATIC EQUATIONS
Systematic generation of multibody equations of motion suitable for recursive and parallel manipulation N90-22992
The coupling effects of kinematics and flexibility on the Lagrangian dynamic formulation of open chain deformable links N90-23018
KINEMATICS
Systematic generation of multibody equations of motion suitable for recursive and parallel manipulation N90-22992
Recursive linearization of multibody dynamics equations of motion N90-22993
Efficient dynamic simulation for multiple chain robotic mechanisms N90-22995
A nearly-linear computational-cost scheme for the forward dynamics of an N-body pendulum N90-22996
Nonlinear finite element formulation for the large displacement analysis in multibody system dynamics N90-23015
The coupling effects of kinematics and flexibility on the Lagrangian dynamic formulation of open chain deformable links N90-23018
Modeling of control forces for kinematical constraints in the dynamics of multibody systems: A new approach N90-23031
An inverse kinematics algorithm for a highly redundant variable-geometry-truss manipulator N90-23033
Characterization of robotics parallel algorithms and mapping onto a reconfigurable SIMD machine N90-23039
Counterrotating cores in elliptical galaxies N90-23288
Spectral evolution of active galactic nuclei Penrose Compton scattering processes and gamma ray emission from Seyfert galaxies N90-23317
KINETICS
Sticking coefficient of HCl on aerosols N90-22598
The effects of zinc addition on the environmental stability of Al-Li alloys N90-22657
The kinetics of dark adaptation in hypoxic subjects
[AD-A218641] N90-22885
KNOWLEDGE BASES (ARTIFICIAL INTELLIGENCE)
Knowledge management: An abstraction of knowledge base and database management systems
[NASA-CR-4273] N90-22986
KNOWLEDGE REPRESENTATION
Syntax, semantics, and pragmatism: An integrated focus based on textual linguistic knowledge
[INPE-4992-PRE/1554] N90-23262
KORTEWEG-DEVRIES EQUATION
Analysis of nonlinear internal waves observed by LANDSAT-TM
[PREPRINT-704] N90-22828

L

LABORATORY EQUIPMENT
Hanging drop crystal growth apparatus and method
[NASA-CASE-MFS-28206-1-SB] N90-23242
LAGRANGIAN EQUILIBRIUM POINTS
Intermittency and multifractality in magnetic dynamos
[PREPRINT-702] N90-23226
LAMINAR FLOW
The minimum drag profile in laminar flow: A numerical way N90-22535
Some observations on liquid flow through filters
[AERE-R-13300] N90-22748
Nonlinear bifurcation study of plane Poiseuille flow
[DLR-FB-89-42] N90-22756
LAMINATES
Large deformation analysis of laminated composite structures by a continuum-based shell element with transverse deformation N90-22613
A life prediction model for laminated composite structural components
[NASA-CR-186587] N90-22614
Explicit modeling of composite plates and beams in the dynamics of multibody systems N90-23019
LANGUAGE PROGRAMMING
Automatic compiler construction
[AD-A218777] N90-22983
LANTHANUM FLUORIDES
Microstructure of thin films
[AD-A219262] N90-23255
LANTHANUM OXIDES
What is going on in the La2CuO4 superconductors N90-23171
LARGE SPACE STRUCTURES
Pultrusion process development for long space boom model
[NASA-TM-4017] N90-22628
The effect of mechanical deformation on the radiation patterns of large space-based arrays
[AD-A219288] N90-22719
Experimental experience with flexible structures N90-23002
Simulation studies using multibody dynamics code DART N90-23036
On trajectory generation for flexible space crane: Inverse dynamics analysis by LATDYN N90-23037
Robust fixed order dynamic compensation for large space structure control N90-23059
Mini-mast dynamic analysis using the truss-beam model N90-23087
LASER ANEMOMETERS
Multi-axis, 3-D, scanning LDA (Laser Doppler Anemometer) system for unsteady aerodynamics
[AD-A218571] N90-22541
LASER ANNEALING
Direct implantation process development and characterization in advanced Hg(1)-(x)Cd(x) Te EPI layers
[AD-A219133] N90-23252
LASER APPLICATIONS
Ignition testing of low-energy laser diode ignited components
[DE90-009968] N90-22630
Pyrotechnic materials ignited using lasers. High energy photopyrotechnic chains
[REPT-892-430-121] N90-22691
Applications of laser ultrasound
[AERE-R-13106] N90-22777
JPRS report: Science and technology. USSR: Physics and mathematics
[JPRS-UPM-89-001] N90-23162
LASER BEAMS
Beam combining by phase transition nonlinear media
[AD-A219301] N90-22739
Measurements and simulation of controlled beamfront motion in the Laser Controlled Collective Accelerator
[DE90-009992] N90-22780
Comparison of solar pumped Nd:YAG and Nd:Cr:GSGG lasers at liquid nitrogen and room temperature
[DLR-FB-89-41] N90-22781
A study of low level laser retinal damage
[AD-A218919] N90-22887
Laser retinal effects: Electrophysiological determination in visual cortical cells of monkeys and cats
[AD-A218937] N90-22888
LASER CAVITIES
Contributions to the development of SLM TEA CO2 laser sources for high resolution molecular spectroscopy N90-22778
LASER DAMAGE
A study of low level laser retinal damage
[AD-A218919] N90-22887
Laser retinal effects: Electrophysiological determination in visual cortical cells of monkeys and cats
[AD-A218937] N90-22888
LASER DOPPLER VELOCIMETERS
Multi-axis, 3-D, scanning LDA (Laser Doppler Anemometer) system for unsteady aerodynamics
[AD-A218571] N90-22541
An investigation of the three-dimensional flow field in a centrifugal compressor N90-22751
Two-dimensional velocimetry instrumentation
[AD-A218450] N90-22774
LASER MATERIALS
Beam combining by phase transition nonlinear media
[AD-A219301] N90-22739
Comparison of solar pumped Nd:YAG and Nd:Cr:GSGG lasers at liquid nitrogen and room temperature
[DLR-FB-89-41] N90-22781
Optical spectroscopy of Ti(3+) doped YAlO3
[AD-A219043] N90-23251

LASER OUTPUTS
Experimental study of vortex ring interaction with a free surface N90-22742
A free electron laser master oscillator power amplifier experiment N90-22776
Contributions to the development of SLM TEA CO2 laser sources for high resolution molecular spectroscopy N90-22778
Dynamics and instabilities in homogeneously broadened lasers
[AD-A218427] N90-22786
LASER PLASMA INTERACTIONS
Activities report of the Institute for Plasma Research
[ETN-90-96467] N90-23225
LASER PLASMAS
Nonlinear spectroscopy of multicomponent droplets and 2- and 3-dimensional measurements in flames
[AD-A218569] N90-22636
LASER SPECTROSCOPY
Scanning laser photocurrent spectroscopy of electrochemically grown bismuth sulphide films
[AERE-M-3709] N90-22649
Time-resolved surface structural study by picosecond reflection high-energy electron diffraction
[AD-A218417] N90-22712
LASER STABILITY
Dynamics and instabilities in homogeneously broadened lasers
[AD-A218427] N90-22786
LASER TARGETS
Laser Program of the Lawrence Livermore National Laboratory
[DE90-008198] N90-22779
LASERS
Faster simulation plots N90-23071
LATENT HEAT
Monthly surface thermal forcing in the tropical Pacific from 1980 to 1983
[NASA-CR-183033] N90-22877
LATTICE PARAMETERS
Improving fermion operators
[PREPRINT-710] N90-23193
Lattice field theory
[PREPRINT-719] N90-23245
LATTICE VIBRATIONS
Mixing of DIS operators in lattice QCD
[PREPRINT-708] N90-23243
LAUE METHOD
New approach to the dynamical diffraction theory in the case of three-dimensional perfect crystal
[DE90-620563] N90-23240
LAUNCH VEHICLES
US access to space: Launch vehicle choices for 1990 to 2010 N90-22579
Earth-to-orbit vehicle providing a reusable orbital stage
[NASA-CASE-LAR-13486-1] N90-22584
Infrared absorption gas sensor for the detection of HCl in launch vehicle exhaust clouds N90-22600
Design of cryogenic tanks for launch vehicles N90-22662
LAUNCHERS
Control of surface melting and ablation in electromagnetic launchers via the magnetic vapor shielding mechanism
[AD-A219035] N90-22578
Multivariate analysis of launcher guidance robustness
[REPT-892-422-105] N90-22581
Equipment specifications for launcher guidance using multivariable frequency methods
[REPT-892-422-106] N90-22582
LEAD COMPOUNDS
Catalysts for ultrahigh current density oxygen cathodes for space fuel cell applications
[NASA-CR-180650] N90-22835
LEADING EDGES
Large-scale advanced propeller blade pressure distributions: Prediction and data
[NASA-TM-102316] N90-22564
Flat plate leading edge receptivity to various freestream disturbance structures N90-22750
Finite element elastic-plastic-creep and cyclic life analysis of a cowl lip
[NASA-TM-102342] N90-22808
LEARNING
Towards the knowledge level in SOAR: The role of the architecture in the use of knowledge
[NASA-CR-186615] N90-22897
Rules and maps in connectionist symbol processing
[AD-A219028] N90-22903
Cognitive architectures and rational analysis: Comment
[AD-A219199] N90-22907
Learning artificial grammars with competitive chunking
[AD-A219270] N90-22911
Laboratory replication of scientific discovery processes
[AD-A219273] N90-22913
An instructable Connectionist/Control architecture: Using rule-based instructions to accomplish connectionist learning in a human time scale
[AD-A219274] N90-22914
Learning environment for neural networks and transient acoustics
[AD-A219000] N90-23186
LEARNING THEORY
What makes some problems hard: Explorations in the problem space of difficulty
[AD-A219002] N90-22901
Discovering problem solving strategies: What humans do and machines don't (yet)
[AD-A219008] N90-22902
Learning events in the acquisition of three skills
[AD-A219038] N90-22905
Non-LIFO (Last-In-First-Out) execution of cognitive procedures
[AD-A219277] N90-22916
LEAST SQUARES METHOD
Quantifying and reducing uncertainty in the assimilative mapping of ionospheric electrodynamics N90-22854
The application of a non-linear least squares method to predicting seat transmissibility
[ISVR-TR-173] N90-22967
Analytic semigroups: Applications to inverse problems for flexible structures
[NASA-CR-182047] N90-23138
Transfer matrices for multimode optical fiber systems
[AD-A218459] N90-23210
LEGENDRE FUNCTIONS
The 16-O photodisintegration at low energies
[NOTA-INTERNA-941] N90-23196
LENSES
Hybrid diffractive-refractive telescope
[AD-A219241] N90-23216
LIAPUNOV FUNCTIONS
About linear systems robustness: Linear programming approach
[LAAS-89-384] N90-23123
Intermittency and multifractality in magnetic dynamos
[PREPRINT-702] N90-23226
LIFE (DURABILITY)
A life prediction model for laminated composite structural components
[NASA-CR-186587] N90-22614
Finite element elastic-plastic-creep and cyclic life analysis of a cowl lip
[NASA-TM-102342] N90-22808
LIFE SUPPORT SYSTEMS
Space Station Freedom environmental control and life support system phase 3 simplified integrated test detailed report
[NASA-TM-4204] N90-22593
LIFT
Application of a dynamic stall model to rotor trim and aeroelastic response N90-22556
LIGANDS
Theoretical studies of silicon chemistry
[AD-A219232] N90-22690
LIGHT ALLOYS
NASA-UVA light aerospace alloy and structures technology program
[NASA-CR-182607] N90-22651
LIGHT SCATTERING
Phase Doppler droplet sizing: Scattering angle effects
[DE90-009571] N90-22754
Microstructure of thin films
[AD-A219262] N90-23255
Optical properties of cometary dust
[AD-A218790] N90-23325
LIGHTNING
Tropical squall lines of the Arizona monsoon N90-22867
LINE OF SIGHT
Field-of-view assessment of low-level flight and an airdrop in the C-130 Weapon System Trainer (WST)
[AD-A218504] N90-22559
Skewering the universe with QSO lines of sight: Lyman alpha clouds as probes of large scale structure N90-23278
LINE SPECTRA
High spatial resolution isotopic CO and CS observations of M17 SW: The clumpy structure of the molecular cloud core
[MPE-PREPRINT-161] N90-23283
Infrared coronal line novae N90-23328
LINEAR ACCELERATORS
Foil focusing of electron beams
[AD-A219511] N90-23208
LINEAR EQUATIONS
Modal identities for multibody elastic spacecraft: An aid to selecting modes for simulation N90-23075
LINEAR FILTERS
Parameter estimation in linear filtering
[AD-A218566] N90-23144
LINEAR POLARIZATION
The sensitivity of EGRET to gamma ray polarization N90-23305
LINEAR PROGRAMMING
Linear programming tools for integer programming
[AD-A219013] N90-23106
About linear systems robustness: Linear programming approach
[LAAS-89-384] N90-23123
LINEAR QUADRATIC GAUSSIAN CONTROL
H2, fixed architecture, control design for large scale systems
[NASA-CR-180471] N90-22698
Combined control-structure optimization N90-23005
Integrated control-system design via generalized LQG (GLQG) theory N90-23023
Overview of computational control research at UT Austin N90-23051
Substructural controller synthesis N90-23055
Approximation in LQG control of a thermoelastic rod N90-23084
LINEAR QUADRATIC REGULATOR
Combined control-structure optimization N90-23005
An algorithm for the solution of dynamic linear programs N90-23026
A priori results in linear-quadratic optimal control theory (extended version)
[MEMO-COSOR-89-17] N90-23124
LINEAR SYSTEMS
A nearly-linear computational-cost scheme for the forward dynamics of an N-body pendulum N90-22996
A survey on the structured singular value N90-22998
Robustness analysis for real parametric uncertainty N90-23000
H(2)- and H(infinity)-design tools for linear time-invariant systems N90-23025
About linear systems robustness: Linear programming approach
[LAAS-89-384] N90-23123
LINEAR TRANSFORMATIONS
Minimal complexity control law synthesis N90-23057
LINEARIZATION
Recursive linearization of multibody dynamics equations of motion N90-22993
LINGUISTICS
Rules and maps in connectionist symbol processing
[AD-A219028] N90-22903
Sentence comprehension: A parallel distributed processing approach
[AD-A218886] N90-23104
Syntax, semantics, and pragmatism: An integrated focus based on textual linguistic knowledge
[INPE-4992-PRE/1554] N90-23262
LINKAGES
The coupling effects of kinematics and flexibility on the Lagrangian dynamic formulation of open chain deformable links N90-23018
LIOUVILLE EQUATIONS
Convergence of hyperspherical adiabatic expansion for helium-like systems
[DE90-620526] N90-22631
LIQUID CRYSTALS
Synthesis and properties of a thermotropic copolyester based on 4,4 prime-dihydroxy-a,a prime-dimethylbenzalazine
[AD-A218803] N90-22682
Processing of thermotropic liquid crystalline polymers and their blends
[AD-A218804] N90-22683
Synthesis and characterization of aromatic polyester and polysiloxane containing block copolymers: Multiphase transparent atomic oxygen resistant damping materials, liquid crystal films, and toughening components of sol/gel glasses
[AD-A218871] N90-22685
LIQUID FLOW
Some observations on liquid flow through filters
[AERE-R-13300] N90-22748
LIQUID FUELS
A comparison between experiment and simulation for concept VIC regenerative liquid propellant guns. Part 1: 30 mm
[AD-A218556] N90-22692
LIQUID HELIUM 2
Experiments on the breakdown of heat transfer in liquid helium 2
[MPIS-13/1989] N90-23259
LIQUID HYDROGEN
Spacecraft attitude impacts on COLD-SAT non-vacuum jacketed LH2 supply tank thermal performance
[NASA-TM-103158] N90-22592
LIQUID METALS
The high temperature behavior of gallium and indium liquid metal ion sources
[AERE-R-13321] N90-22647

LIQUID NITROGEN
Acquisition and correlation of cryogenic nitrogen mass flow data through a multiple orifice Joule-Thomson device
[NASA-TM-103121] N90-22761
Comparison of solar pumped Nd:YAG and Nd:Cr:GSGG lasers at liquid nitrogen and room temperature
[DLR-FB-89-41] N90-22781
LIQUID OXYGEN
Cooling of rocket thrust chambers with liquid oxygen
[NASA-TM-103146] N90-22605
LIQUID PHASES
The HCl/aerosol problem N90-22597
LIQUID PROPELLANT ROCKET ENGINES
Cooling of rocket thrust chambers with liquid oxygen
[NASA-TM-103146] N90-22605
Development of high-activity para- to ortho-hydrogen conversion catalysts, volume 2
[AD-A218700] N90-22638
LIQUIDS
Femtosecond studies of electron photodetachment of simple ions in liquid water: Solvation and geminate recombination dynamics
[AD-A218520] N90-22634
Side moment exerted by a spinning, coning, highly viscous liquid payload
[AD-A218746] N90-22763
LITHIUM
Heat exhaustion in a rat model: Lithium as a biochemical probe
[AD-A219361] N90-22884
LITHIUM ALLOYS
Deformation and fracture of thin sheet aluminum-lithium alloys: The effect of cryogenic temperatures N90-22655
Measurements and mechanisms of localized aqueous corrosion in aluminum-lithium alloys N90-22656
The effects of zinc addition on the environmental stability of Al-Li alloys N90-22657
Deformation and fracture of aluminum-lithium alloys: The effect of dissolved hydrogen N90-22658
The lithium concentration dependence of creep in binary aluminum-lithium alloys
[AD-A218706] N90-22668
Structure-property relations in aluminum-lithium alloys
[AD-A219183] N90-22672
LITHIUM NIOBATES
Secondary ion mass spectrometry characterization of implants into GaAs and GaP for waveguides and integrated optics applications
[AD-A219203] N90-23254
LITHOGRAPHY
Modified maleic anhydride copolymers as e-beam resists
[AD-A218470] N90-22679
LOAD TESTS
Measurements and mechanisms of localized aqueous corrosion in aluminum-lithium alloys N90-22656
LOADS (FORCES)
Experimental verification of dynamic simulation N90-23020
Modeling of control forces for kinematical constraints in the dynamics of multibody systems: A new approach N90-23031
LOCAL AREA NETWORKS
Access to supercomputers N90-22979
Use of optical storage devices as shared resources in local area networks
[AD-A219198] N90-23269
LOGIC CIRCUITS
An instructable Connectionist/Control architecture: Using rule-based instructions to accomplish connectionist learning in a human time scale
[AD-A219274] N90-22914
LONG DURATION SPACE FLIGHT
The International Space University
[NASA-TM-103163] N90-22604
LOW COST
Low cost station keeping maneuvers for a small-satellites constellation in tundra orbits
[ETN-90-96553] N90-22588
Low cost processing routes leading to high-performance ceramic tiles
[AD-A219034] N90-22688
LOW TEMPERATURE
A low temperature calorimetric study of several high-T(sub c) superconductors N90-23237
LOW TURBULENCE
Turbulence and complex systems
[ETN-90-96620] N90-22758
LUMINANCE
Tunable XeCl-laser featuring high spectral luminance N90-23167
LUMINOSITY
A search for additional parameters in the infrared luminosity/21 cm line-width relation for spiral galaxies in clusters of galaxies N90-23274
Spectral plane quasars, spectral turn-over, and frequency atlas
[INPE-5011-TDL/399] N90-23277
Gamma rays from pulsar wind shock acceleration N90-23311
The high energy source 3C 273 N90-23318
LUNAR BASES
Lunar base 2 (the second thousand days of a base on the Moon)
[ILR-MITT-230(1989)] N90-22968
LYMAN ALPHA RADIATION
Skewering the universe with QSO lines of sight: Lyman alpha clouds as probes of large scale structure N90-23278

M

MACH INERTIA PRINCIPLE
Estimation of extra drag force on a circular cylinder due to the presence of solid particles in subsonic compressible flow
[AD-A218635] N90-22542
MACH NUMBER
The effects of compressibility on a supersonic mixing layer
[AD-A219315] N90-22543
MACHINE LEARNING
Efficient specialization of relational concepts
[AD-A218889] N90-22894
Discovering problem solving strategies: What humans do and machines don't (yet)
[AD-A219008] N90-22902
Learning events in the acquisition of three skills
[AD-A219038] N90-22905
Adaptive Resonance Theory 1
[AD-A219044] N90-23126
MACHINERY
Elements of active vibration control for rotating machinery
[NASA-TM-102368] N90-22703
MACHINING
Machining of new materials at Aerospatiale
[REPT-892-430-104] N90-22622
MACROSCOPIC EQUATIONS
Quantum non-demolition stroboscopic observables and multipumping back-action evasion schemes
[PREPRINT-699] N90-23260
Are quantum measurements on macroscopic bodies feasible
[PREPRINT-700] N90-23261
MAGELLANIC CLOUDS
Local normal galaxies N90-23315
MAGNETIC DIFFUSION
Intermittency and multifractality in magnetic dynamos
[PREPRINT-702] N90-23226
MAGNETIC EFFECTS
High Intensity Electro-Magnetic and Ultrasonic Effects on Inorganic Materials Behavior and Processing Workshop
[AD-A218884] N90-22640
Dynamics of motion charged particles in a field of two electromagnetic waves
[DE90-620690] N90-22706
Superconducting and normal compounds: Some high field/high pressure effects N90-23229
MAGNETIC FIELD RECONNECTION
Experimental study of vortex ring interaction with a free surface N90-22742
MAGNETIC FIELDS
Dynamics of motion charged particles in a field of two electromagnetic waves
[DE90-620690] N90-22706
Intense electron beam propagation across a magnetic field
[DE90-009993] N90-23204
Intermittency and multifractality in magnetic dynamos
[PREPRINT-702] N90-23226
Single crystal NMR of high temperature superconductors N90-23236
A (mu)SR-investigation of the mixed state of the high-Tc superconductor HoBa2Cu3O7-delta
[DE90-620802] N90-23241
Nonreciprocal components in the 140 and 220 GHz bands utilizing magnetoplasmons on semiconducting substrates
[AD-A219136] N90-23253
What is learned from high energy bursts and flares N90-23314
Local normal galaxies N90-23315
MAGNETIC INDUCTION
Optimization of a pulsed air core transformer for low impedance inductive ignition
[AD-A218748] N90-22734
MAGNETIC PERMEABILITY
A low temperature calorimetric study of several high-T(sub c) superconductors N90-23237
MAGNETIC PROPERTIES
Investigation of optical nonlinearities, conductivity and magnetism in organometallic materials
[AD-A218548] N90-23211
MAGNETIC SHIELDING
Control of surface melting and ablation in electromagnetic launchers via the magnetic vapor shielding mechanism
[AD-A219035] N90-22578
MAGNETIC STARS
Gamma ray bursts: Current status of observations and theory N90-23313
MAGNETOHYDRODYNAMIC FLOW
Intermittency and multifractality in magnetic dynamos
[PREPRINT-702] N90-23226
MAGNETOHYDRODYNAMIC STABILITY
Plasma instabilities associated with the injection of artificial ion beams into the ionosphere N90-22851
Resonant MHD modes with toroidal coupling
[DE90-010077] N90-23222
Analytical theory of the Bunemann instability for electron runaway
[IPF-88-3] N90-23224
MAGNIFICATION
Shaping radiation pattern of excimer laser by means of controllable intracavity mirror N90-23166
MAIN SEQUENCE STARS
Evolutionary models of the rotating sun and implications for other low mass stars N90-23329
MALAGASY REPUBLIC
US Navy regional climatic study of the Mozambique channel and adjacent waters
[AD-A218793] N90-22875
MAN MACHINE SYSTEMS
Model-based method for terrain-following display design
[AD-A219302] N90-22563
Telepresence, time delay, and adaptation N90-22944
Visual enhancements in pick-and-place tasks: Human operators controlling a simulated cylindrical manipulator N90-22946
MAN-COMPUTER INTERFACE
Spatial issues in user interface design from a graphic design perspective N90-22939
A computer graphics system for visualizing spacecraft in orbit N90-22952
Interactive orbital proximity operations planning system N90-22953
Experiences in teleoperation of land vehicles N90-22954
Multimedia system control
[AD-A219392] N90-22971
Automatic compiler construction
[AD-A218777] N90-22983
Graphics equipment for data analysis
[AD-A218983] N90-22985
Multibody dynamics model building using graphical interfaces N90-23082
Natural language processing: A tutorial
[AD-A219096] N90-23108
Learning environment for neural networks and transient acoustics
[AD-A219000] N90-23186
MANAGEMENT SYSTEMS
Automated electric power management and control for Space Station Freedom
[NASA-TM-103151] N90-23125
MANDRELS
Axisymmetric and cylindrically orthotropic analysis of filament winding N90-22811
MANEUVERS
Sliding control of pointing and tracking with operator spline estimation N90-22997
MANIPULATORS
Visual enhancements in pick-and-place tasks: Human operators controlling a simulated cylindrical manipulator N90-22946
Displays for telemanipulation N90-22948
Recursive linearization of multibody dynamics equations of motion N90-22993
An innovations approach to decoupling of multibody dynamics and control N90-22994
A robot arm simulation with a shared memory multiprocessor machine N90-23008
Parallel algorithms and architecture for computation of manipulator forward dynamics N90-23010
Development of efficient computer program for dynamic simulation of telerobotic manipulation N90-23017

Experimental verification of dynamic simulation N90-23020
Approximate minimum-time trajectories for 2-link flexible manipulators N90-23030
An inverse kinematics algorithm for a highly redundant variable-geometry-truss manipulator N90-23033
Determination of joint drives for stable end-effector motion in flexible robotic systems N90-23034
Parallel conjugate gradient algorithms for manipulator dynamic simulation N90-23045
Man-in-the-control-loop simulation of manipulators N90-23063
Control of randomly sampled robotic systems [AD-A218948] N90-23157

MANNED SPACE FLIGHT
Neural networks in support of manned space N90-23088

MANUAL CONTROL
Minimum flying qualities. Volume 3: Program CC's implementation of the human optimal control model [AD-A218562] N90-22562
Adapting to variable prismatic displacement N90-22945
Direction of movement effects under transformed visual/motor mappings N90-22947

MANUFACTURING
The surprising possibilities of wrapping [REPT-892-430-108] N90-22624
Rheology of injection mould filling with DMCs [NPL-DMA(A)-196] N90-22675
Increased stuck-at fault coverage with reduced I(sub DDQ) test sets [DE90-009509] N90-22804

MANY BODY PROBLEM
Proceedings of the 3rd Annual Conference on Aerospace Computational Control, volume 1 [NASA-CR-186446] N90-22987
A nearly-linear computational-cost scheme for the forward dynamics of an N-body pendulum N90-22996
Modeling of control forces for kinematical constraints in the dynamics of multibody systems: A new approach N90-23031
About the order of Appel's algorithm [CS-8910] N90-23097

MAPPING
Calculation of 3-dimensional synthetic seismograms on the connection machine [AD-A218472] N90-22857
Displays, instruments, and the multi-dimensional world of cartography N90-22942
Characterization of robotics parallel algorithms and mapping onto a reconfigurable SIMD machine N90-23039

MAPS
Displays, instruments, and the multi-dimensional world of cartography N90-22942
Atlas/data abstract for the United States and selected areas, fiscal year 1989 [AD-A219289] N90-23270

MARINE ENVIRONMENTS
On the effectiveness of the production of antarctic bottom water in the Weddell and Ross Seas [AD-A218873] N90-22550

MARINE METEOROLOGY
Impact of marine boundary layer parameterization on a numerical simulation of cyclogenesis during a cold air outbreak event N90-22864
US Navy regional climatic study of southern African waters [AD-A218792] N90-22874
US Navy regional climatic study of the Mozambique channel and adjacent waters [AD-A218793] N90-22875

MARSHLANDS
A case for archaeological reconnaissance of the Cabo Catoche-Porvenir region of the northeastern Yucatan Peninsula [NASA-TM-102248] N90-22827

MASERS
Gravitational radiation produced by high energy accelerators and high power lasers [PREPRINT-701] N90-22782

MASS FLOW RATE
Acquisition and correlation of cryogenic nitrogen mass flow data through a multiple orifice Joule-Thomson device [NASA-TM-103121] N90-22761

MASS TRANSFER
Sticking coefficient of HCl on aerosols N90-22598
Rapid mass transfer in binary systems N90-23289

MASSIVELY PARALLEL PROCESSORS
Calculation of 3-dimensional synthetic seismograms on the connection machine [AD-A218472] N90-22857
Computational chaos in massively parallel neural networks N90-23012

MATCHED FILTERS
Quantum-limited image recognition [AD-A218425] N90-23101

MATHEMATICAL LOGIC
Increased stuck-at fault coverage with reduced I(sub DDQ) test sets [DE90-009509] N90-22804

MATHEMATICAL MODELS
Reynolds stress closure in jet flows using instability wave modeling N90-22534
Application of a dynamic stall model to rotor trim and aeroelastic response N90-22556
Model-based method for terrain-following display design [AD-A219302] N90-22563
A modeling technique for STOVL ejector and volume dynamics [NASA-TM-103167] N90-22566
A study of woven fabric-reinforced composite materials using an invariant-based orthotropic plasticity formulation N90-22611
A life prediction model for laminated composite structural components [NASA-CR-186587] N90-22614
A comprehensive study on microstructure mechanics relationships of ceramic matrix composites [AD-A219318] N90-22627
Calcium carbonate scale dissolution in water stabilized by carbon dioxide treatment [AD-A218502] N90-22633
Numerical investigation of turbulent flame sheets [AD-A218553] N90-22635
Design of cryogenic tanks for launch vehicles N90-22662
HF propagation through actively modified ionospheres [DE90-008931] N90-22705
Qualitative aspects of signal processing through dynamical neural networks [PREPRINT-711] N90-22709
Optical excisor modeling [AD-A219338] N90-22722
Optimization of a pulsed air core transformer for low impedance inductive ignition [AD-A218748] N90-22734
An investigation of the three-dimensional flow field in a centrifugal compressor N90-22751
Nonstrictly hyperbolic conservation laws [AD-A218525] N90-22762
Modelling and computer control of a mechanical system [W-8908] N90-22794
Axisymmetric and cylindrically orthotropic analysis of filament winding N90-22811
Localization of vibration in disordered nearly cyclic structures N90-22812
Comparison between data generated from standard fracture toughness specimens and from nonstandard specimens made of a silicon carbide [DE90-009621] N90-22814
Fundamental studies on hydrology, hydraulics and geometry of river networks [AD-A218662] N90-22830
A new stochastic model of turbulent dispersion in the convective planetary boundary layer and the results of the Atterbury-87 field study N90-22853
Tropical squall lines of the Arizona monsoon N90-22867
Evidence for self-refraction in a convergence zone: NPE (Nonlinear progressive wave equation) model results [AD-A218546] N90-22879
Stochastic interactive activation and the effect of context on perception [AD-A218929] N90-22898
Sensory conflict in motion sickness: An observer theory approach N90-22957
Experimental experience with flexible structures N90-23002
A finite element based method for solution of optimal control problems N90-23027
A methodology for formulating a minimal uncertainty model for robust control system design and analysis N90-23028
Modeling of control forces for kinematical constraints in the dynamics of multibody systems: A new approach N90-23031
Concurrent processing simulation of the space station N90-23041
Enhanced modeling features within TREETOPS N90-23047
Modal identities for multibody elastic spacecraft: An aid to selecting modes for simulation N90-23075
Factoring homomorphisms [CS-8908] N90-23096
Index and consistency analysis for DAE (Differential Algebraic Equation) systems for Stefan-Maxwell diffusion-reaction problems [DE90-008188] N90-23129
Periodic ARMA models: Optimal prediction and minimum-phase condition [REPT-89-006] N90-23131
On a fallacious conjecture about the stabilizability properties of solutions of the Riccati difference equation [REPT-89-007] N90-23132
Processes and formalisms for unbounded choice [CS-8917] N90-23135
Proceedings of the 9th International Conference on Computing Methods in Applied Science and Engineering [AD-A219307] N90-23149
Selecting multinomial populations [AD-A219256] N90-23159
Time-varying filter modelling and time-frequency characterisation of nonstationary sound fields due to a moving source N90-23178
Looking at large data sets using binned data plots [DE90-008206] N90-23263
Towards a calculus of data refinement [CS-8902] N90-23264
Studies of Io's atmosphere and plasma torus N90-23326

MATHEMATICAL PROGRAMMING
Linear programming tools for integer programming [AD-A219013] N90-23106

MATRICES
On a fallacious conjecture about the stabilizability properties of solutions of the Riccati difference equation [REPT-89-007] N90-23132

MATRICES (MATHEMATICS)
H2, fixed architecture, control design for large scale systems [NASA-CR-180471] N90-22698
Efficient dynamic simulation for multiple chain robotic mechanisms N90-22995
A survey on the structured singular value N90-22998
Parallel algorithms and architecture for computation of manipulator forward dynamics N90-23010
Efficient computer algebra algorithms for polynomial matrices in control design N90-23022
Extensions of output variance constrained controllers to hard constraints N90-23056
Robust adaptive control: Stability and asymptotic performance [AD-A219259] N90-23127
Processes and formalisms for unbounded choice [CS-8917] N90-23135
A proof of the isoenergetic KAM: Theorem from the ordinary one [W-8906] N90-23136
A computer program to implement the Chen method of dimensional analysis [AD-A218557] N90-23142
Transfer matrices for multimode optical fiber systems [AD-A218459] N90-23210

MATRIX MATERIALS
Characterization and role of an elastomeric interphase within polyepoxy reinforced glass, both particulate and fibrous [ISAL-89-0064] N90-22676

MATRIX THEORY
Vectors and matrices: Two turbo pascal units for fast program development [AD-A218917] N90-23105

MAXIMUM LIKELIHOOD ESTIMATES
Parameter estimation in linear filtering [AD-A218566] N90-23144
Ability distributions pattern probabilities and quasidensities [AD-A218471] N90-23153
More data on (possible) gamma ray (point) sources N90-23309

MECHANICAL DEVICES
Modelling and computer control of a mechanical system [W-8908] N90-22794
Spatial operator algebra framework for multibody system dynamics N90-22989

MECHANICAL DRIVES
Determination of joint drives for stable end-effector motion in flexible robotic systems N90-23034

MECHANICAL ENGINEERING
Proceedings of the 3rd Annual Conference on Aerospace Computational Control, volume 1 [NASA-CR-186446] N90-22987

MECHANICAL PROPERTIES
Seal requirements in rocket propulsion [ETN-90-98611] N90-22580
A study of woven fabric-reinforced composite materials using an invariant-based orthotropic plasticity formulation N90-22611

Calcium carbonate scale dissolution in water stabilized by carbon dioxide treatment
[AD-A218502] N90-22633
Deformation and fracture of aluminum-lithium alloys: The effect of dissolved hydrogen N90-22658
Investigation of the reaction kinetics between SiC fibers and selectively alloyed titanium matrix composites and determination of their mechanical properties N90-22659
Approximate analysis for the formation of adiabatic shear bands
[AD-A218751] N90-22670
Characterization and role of an elastomeric interphase within polyepoxy reinforced glass, both particulate and fibrous
[ISAL-89-0064] N90-22676

MELTING
Control of surface melting and ablation in electromagnetic launchers via the magnetic vapor shielding mechanism
[AD-A219035] N90-22578

MEMBRANE STRUCTURES
An assessment of second-generation stretched-membrane mirror modules
[DE90-010243] N90-22841

MEMBRANES
Electrochemical synthesis of ultrathin film composite membranes
[AD-A219041] N90-22643

MEMORY
Distortions in memory for visual displays N90-22929

MEMORY (COMPUTERS)
The use of supercomputers for the design and analysis of constructions N90-22977

MENTAL PERFORMANCE
Human cognitive and motor performance measures under typical cool white fluorescent illumination vs relatively high cool white illuminance/irradiance lighting
[AD-A218445] N90-22892
A preliminary analysis of the SOAR architecture as a basis for general intelligence
[AD-A218913] N90-22896
Cognitive efficiency considerations for good graphic design
[AD-A218976] N90-22899
Cognitive architectures and rational analysis: Comment
[AD-A219199] N90-22907
Information processing approaches to cognitive development
[AD-A219200] N90-22908
Toward a SOAR theory of taking instructions for immediate reasoning tasks
[AD-A219201] N90-22909
Laboratory replication of scientific discovery processes
[AD-A219273] N90-22913
Motor and cognitive performance do not change during a ten-week submarine patrol
[AD-A218639] N90-22969

MERCURY CADMIUM TELLURIDES
Direct implantation process development and characterization in advanced Hg(1)-(x)Cd(x) Te EPI layers
[AD-A219133] N90-23252

MESOMETEOROLOGY
Impact of marine boundary layer parameterization on a numerical simulation of cyclogenesis during a cold air outbreak event N90-22864

MESOSCALE PHENOMENA
A study of mesoscale acid deposition in the lower Ohio River Valley N90-22848
Impact of marine boundary layer parameterization on a numerical simulation of cyclogenesis during a cold air outbreak event N90-22864
A study of turbulence near thunderstorm tops
[NASA-CR-186620] N90-22870

METABOLISM
The physiological cost of wearing the propellant handler's ensemble at the Kennedy Space Center
[NASA-TM-102786] N90-22966

METAL BONDING
Lateral spreading of Au contacts on InP
[NASA-TM-103133] N90-22843

METAL CRYSTALS
Amorphization of metals by ion implantation and ion beam mixing
[DE90-620571] N90-22667

METAL FATIGUE
Environment enhanced fatigue of advanced aluminum alloys and composites N90-22652
Hydrogenation of stainless steels implanted with nitrogen
[DE90-617397] N90-22666

METAL FILMS
Application of x ray absorption edge spectrometry to the non-destructive determination of element concentrations, coating thickness and areal densities
[AERE-R-13030] N90-22802
Microstructure of thin films
[AD-A219262] N90-23255

METAL IONS
The high temperature behavior of gallium and indium liquid metal ion sources
[AERE-R-13321] N90-22647

METAL MATRIX COMPOSITES
The elastic-plastic behavior of composite materials N90-22615
Fatigue crack growth in a unidirectional SCS-6/Ti-15-3 composite
[NASA-TM-103095] N90-22646
NASA-UVA light aerospace alloy and structures technology program
[NASA-CR-182607] N90-22651
Environment enhanced fatigue of advanced aluminum alloys and composites N90-22652
Investigation of the reaction kinetics between SiC fibers and selectively alloyed titanium matrix composites and determination of their mechanical properties N90-22659
Inelastic response of metal matrix composites under biaxial loading N90-22661
High temperature fatigue behavior of a SiC/Ti-24Al-11Nb composite
[NASA-TM-103157] N90-22822

METAL OXIDE SEMICONDUCTORS
Burnout thresholds and cross section of power MOS transistors with heavy ions
[AD-A218998] N90-22736

METAL PLATES
Flat plate vibration analysis experimental and numerical fillet study
[AD-A218789] N90-22818

METAL SHEETS
Deformation and fracture of thin sheet aluminum-lithium alloys: The effect of cryogenic temperatures N90-22655

METAL SURFACES
Characterization of particle impact by quantitative acoustic emission
[AERE-R-13028] N90-22810

METALLIC GLASSES
Amorphization of metals by ion implantation and ion beam mixing
[DE90-620571] N90-22667

METALS
High Intensity Electro-Magnetic and Ultrasonic Effects on Inorganic Materials Behavior and Processing Workshop
[AD-A218884] N90-22640

METASTABLE STATE
Rigorous analysis of low temperature stochastic Ising models: Metastability and exponential approach to equilibrium
[PREPRINT-720] N90-23175

METEOROLOGICAL INSTRUMENTS
Accuracy and precision of GOES data collection platforms for temperature measurements
[AD-A218798] N90-22832
AFGW's upper air validator system
[AD-A219309] N90-22876

METEOROLOGICAL PARAMETERS
Accuracy and precision of GOES data collection platforms for temperature measurements
[AD-A218798] N90-22832
A study of mesoscale acid deposition in the lower Ohio River Valley N90-22848
US Navy regional climatic study of southern African waters
[AD-A218792] N90-22874
US Navy regional climatic study of the Mozambique channel and adjacent waters
[AD-A218793] N90-22875
AFGW's upper air validator system
[AD-A219309] N90-22876
Development and use of a passive technique for measuring nitrogen dioxide in the background atmosphere N90-23285

METEOROLOGICAL RADAR
Gravity wave and turbulence studies using a high-resolution ST radar
[AD-A218877] N90-22860
Next generation weather radar (NEXRAD) initial operational test and evaluation. Phase 2: (IOT and E(2))
[AD-A218770] N90-22873

METEOROLOGY
The HCl/aerosol problem N90-22597
Monthly surface thermal forcing in the tropical Pacific from 1980 to 1983
[NASA-CR-183033] N90-22877

METHYL ALCOHOL
Turbine fuel alternatives (near term)
[AD-A219405] N90-22695

METHYL COMPOUNDS
Single-crystal diffraction analysis of 2-(trimethylsilylethynyl) 4-nitro-N,N-dimethylaniline
[AD-A218955] N90-22642

METROLOGY
Large scale metrology by computer assisted photogrammetry
[REPT-892-430-116] N90-22772

MEXICO
A case for archaeological reconnaissance of the Cabo Catoche-Porvenir region of the northeastern Yucatan Peninsula
[NASA-TM-102248] N90-22827

MICROCOMPUTERS
The interactive digital video interface N90-22941

MICROCRACKS
Microcracking and toughness of ceramic-fiber/ceramic-matrix composites under high temperature
[AD-A218516] N90-22680

MICROGRAVITY APPLICATIONS
Microgravity, the space application of the 21st century. Challenges, constraints, and strategies
[REPT-892-430-105] N90-22696

MICROMECHANICS
Deformation and fracture of thin sheet aluminum-lithium alloys: The effect of cryogenic temperatures N90-22655
Inelastic response of metal matrix composites under biaxial loading N90-22661

MICROPOROSITY
Electrochemical synthesis of ultrathin film composite membranes
[AD-A219041] N90-22643

MICROPROCESSORS
Apparatus for and a method of determining compass headings
[AD-D014436] N90-22551

MICROSTRUCTURE
A comprehensive study on microstructure mechanics relationships of ceramic matrix composites
[AD-A219318] N90-22627
Quantitative characterization of spatial distribution of particles in materials: Application to materials processing N90-22660
Structure-property relations in aluminum-lithium alloys
[AD-A219183] N90-22672
Characterization of weldments using advanced experimental techniques
[DE90-009418] N90-22792
Recent advances in nondestructive evaluation made possible by novel uses of video systems
[NASA-TM-102491] N90-22801
The microstructural basis of damping in high damping alloys
[AD-A219572] N90-22821
High temperature superconducting thin films in Japan N90-23169
A study of the relation between grain boundary type and sensitisation in a partially-sensitised AISI 304 stainless steel using electron back-scattering patterns
[AERE-R-13327] N90-23234
Microstructure of thin films
[AD-A219262] N90-23255

MICROWAVE CIRCUITS
Indium phosphide planar Gunn diode
[AD-A219337] N90-22740

MICROWAVE EQUIPMENT
Construction of a 345 gigahertz receiver based on superconducting tunnel junctions
[AD-A218781] N90-22735
Continued development and characterization of doped layers, contacts and associated electronic devices in silicon carbide
[AD-A219234] N90-22738

MICROWAVE SPECTRA
Frequency domain techniques for analyzing picosecond optical pulses
[AD-A218856] N90-23214

MICROWAVE TUBES
Transport properties of plasmas in microwave electrothermal thrusters
[AD-A219408] N90-23228

MICROWAVES
Spectral measurements of the cosmic microwave background N90-23334

MIDAIR COLLISIONS
UK airmisses involving commercial air transport, January - April 1989
[ISSN-0951-6301] N90-22544

MIDDLE ATMOSPHERE
Gravity wave and turbulence studies using a high-resolution ST radar
[AD-A218677] N90-22860
MIE SCATTERING
Optical properties of cometary dust
[AD-A218790] N90-23325
MILITARY AIRCRAFT
Design trends for Army/Air Force airplanes in the United States
[NASA-TM-4179] N90-23338
MILITARY OPERATIONS
The Department of Defense critical technologies plan for the Committees on Armed Services United States Congress
[AD-A219300] N90-22702
MILITARY TECHNOLOGY
A comparison of CuAlNi and other high damping alloys for the purpose of naval ship silencing applications
[AD-A218801] N90-22671
The Department of Defense critical technologies plan for the Committees on Armed Services United States Congress
[AD-A219300] N90-22702
The RACE (research and development in advanced technologies for Europe) program: A 1989 update
[AD-A218509] N90-22713
Proceedings of the NATO Advanced Workshop on Supercomputing
[AD-A218508] N90-23102
Atlas/data abstract for the United States and selected areas, fiscal year 1989
[AD-A219289] N90-23270
MILKY WAY GALAXY
The interstellar medium of a starburst galaxy; millimeter interferometric observations of M82 N90-23276
Molecular clouds and the large-scale structure of the galaxy N90-23295
MILLIMETER WAVES
The interstellar medium of a starburst galaxy; millimeter interferometric observations of M82 N90-23276
Implications of the IRAS data for galactic gamma ray astronomy and EGRET N90-23300
MILLING (MACHINING)
Machining of new materials at Aerospatiale
[REPT-892-430-104] N90-22622
MIM (SEMICONDUCTORS)
Critical behavior of the thermal power near the metal-insulator transition
[PREPRINT-714] N90-23244
MIMD (COMPUTERS)
Concurrent computing: Numerical algorithms and some applications
[AD-A218570] N90-23103
MINIATURIZATION
Miniature traveling wave tube and method of making
[NASA-CASE-LEW-14520-1] N90-22724
MINIMUM DRAG
The minimum drag profile in laminar flow: A numerical way N90-22535
MIRROR FUSION
Thermal barrier research
[DE90-009213] N90-23221
MIRRORS
An assessment of second-generation stretched-membrane mirror modules
[DE90-010243] N90-22841
Full surface interferometric testing of grazing incidence mirrors
[AD-A219394] N90-23218
MISSILE CONTROL
Six-degree-of-freedom missile simulation using the ADI AD 100 digital computer and ADSIM simulation language N90-23068
MISSILE TRACKING
Preliminary results of the peak experiment. ALTAIR deep-space measurements
[AD-A218622] N90-22714
MISSION PLANNING
Semianalytic study of high-eccentricity orbit stability and evolution N90-22574
MITOSIS
ELF (Extremely Low Frequency) communications system ecological monitoring program: Slime mold studies
[AD-A218623] N90-22715
MIXING LAYERS (FLUIDS)
Reynolds stress closure in jet flows using instability wave modeling N90-22534
The effects of compressibility on a supersonic mixing layer
[AD-A219315] N90-22543
Analysis of velocity and temperature fluctuations in turbulent shear flows N90-22744
MODAL RESPONSE
Transverse vibrations of a composite cylindrical tube of circular cross section
[AD-A219227] N90-22820
MODEL REFERENCE ADAPTIVE CONTROL
Experimental adaptive control of a hydraulic robot N90-23121
MODELS
An experimental study of tip shape effects on the flutter of aft-swept, flat-plate wings
[NASA-TM-4180] N90-22555
Microcracking and toughness of ceramic-fiber/ceramic-matrix composites under high temperature
[AD-A218516] N90-22680
A theoretical and experimental investigation of an absorption refrigeration system for application with solar energy units N90-22697
MODEMS
Evaluation of a prototype 6 tone modem
[RAE-TM-FM-28] N90-22708
MODULARITY
Agile multiple aperture imager receiver development
[AD-A218956] N90-23215
MODULES
The Italian approach to small satellites for low cost access to space developments
[ETN-90-96552] N90-22587
MOIRE INTERFEROMETRY
A multipulsed dynamic diffraction moire interferometer
[DE90-009765] N90-22723
A compact portable diffraction moire interferometer
[DE90-009780] N90-22768
MOLECULAR BEAM EPITAXY
Continued development and characterization of doped layers, contacts, and associated electronic devices in silicon carbide
[AD-A219211] N90-22737
MOLECULAR CLOUDS
High spatial resolution isotopic CO and CS observations of M17 SW: The clumpy structure of the molecular cloud core
[MPE-PREPRINT-161] N90-23283
Molecular clouds and the large-scale structure of the galaxy N90-23295
Gamma rays from giant molecular clouds N90-23298
Implications of the IRAS data for galactic gamma ray astronomy and EGRET N90-23300
More data on (possible) gamma ray (point) sources N90-23309
Spectral measurements of the cosmic microwave background N90-23334
MOLECULAR COLLISIONS
Theoretical and computer simulation study of the density fluctuations in liquid water
[PREPRINT-697] N90-23191
Low frequency Raman spectra of liquid water, a molecular dynamics simulation
[PREPRINT-698] N90-23192
Support for the 16th International Conference on the Physics of Electronic and Atomic Collisions
[AD-A218567] N90-23200
MOLECULAR DIFFUSION
Stratified ocean mixing
[AD-A219233] N90-22881
MOLECULAR GASES
Molecular evolution in astrophysical environments N90-23291
MOLECULAR ORBITALS
Investigation of optical nonlinearities, conductivity and magnetism in organometallic materials
[AD-A218548] N90-23211
MOLECULAR RELAXATION
Investigation of atomistic simulation of structural and dynamic differences in glassy and liquid states of atactic poly(propylene)
[AD-A218896] N90-22687
MOLECULAR ROTATION
Simulation of inelastic deformation in glassy polypropylene and polycarbonate
[AD-A218891] N90-22686
MOLECULAR SPECTRA
Threshold photodetachment spectroscopy of the I + HI transition state region
[AD-A218410] N90-22883
MOLECULAR SPECTROSCOPY
Contributions to the development of SLM TEA CO2 laser sources for high resolution molecular spectroscopy N90-22778
MOLECULAR STRUCTURE
The first example of an organogallium compound containing a Ga-Te bond: Synthesis, properties, and molecular structure of ((Me3CCH2)2GaTeph)2
[AD-A219258] N90-22608
Single-crystal diffraction analysis of 2-(trimethylsilylethynyl) 4-nitro-N,N-dimethylaniline
[AD-A218955] N90-22642
Simulation of inelastic deformation in glassy polypropylene and polycarbonate
[AD-A218891] N90-22686
The microstructural basis of damping in high damping alloys
[AD-A219572] N90-22821
Threshold photodetachment spectroscopy of the I + HI transition state region
[AD-A218410] N90-22883
MOLECULAR TRAJECTORIES
Low frequency Raman spectra of liquid water, a molecular dynamics simulation
[PREPRINT-698] N90-23192
MOLECULES
Molecular evolution in astrophysical environments N90-23291
MOLTEN SALT ELECTROLYTES
Viscosity, density and conductivity of ImCl(HCl) sub 1.3
[AD-A218902] N90-22641
MOLYBDENUM ALLOYS
A comparison of CuAlNi and other high damping alloys for the purpose of naval ship silencing applications
[AD-A218801] N90-22671
MOLYBDENUM OXIDES
Model catalytic oxidation studies using supported monometallic and heterobimetallic oxides
[DE90-009984] N90-22664
MOMENTUM
Space station dynamics, attitude control and momentum management N90-23029
MOMENTUM TRANSFER
Incomplete fusion reactors at low and intermediate energies
[KVI-809] N90-23206
MONEL (TRADEMARK)
Characterization of Monel alloys by x ray fluorescence technique
[DE90-617175] N90-22665
MONITORS
HCl monitor N90-22599
MONOMERS
Investigation of optical nonlinearities, conductivity and magnetism in organometallic materials
[AD-A218548] N90-23211
MONOPROPELLANTS
A comparison between experiment and simulation for concept VIC regenerative liquid propellant guns. Part 1: 30 mm
[AD-A218556] N90-22692
MONOPULSE RADAR
Improvement of clutter rejection by scanning motion compensation in ground-based monopulse radar
[ETN-90-96550] N90-22711
MONSOONS
Tropical squall lines of the Arizona monsoon N90-22867
MONTE CARLO METHOD
Linear and nonlinear electrical response of condensed matter: Ionic, dielectric, and mixed-conduction materials
[AD-A218771] N90-22639
An examination of the full-wave method for rough surface scattering
[AD-A218664] N90-23155
The sensitivity of EGRET to gamma ray polarization N90-23305
MORPHOLOGY
Photoresponse of YBa2Cu3O(7-delta) granular and epitaxial superconducting thin films
[NASA-TM-103144] N90-22732
Spaceborne radar observations: A guide for Magellan radar-image analysis
[NASA-CR-184998] N90-22826
The effect of elevated gravity on the crystallization of the MFI zeolites, ZSM-5, and silicalite N90-23231
MOTION PERCEPTION
Visual sensitivities and discriminations and their role in aviation
[AD-A219319] N90-22917
Perceiving environmental properties from motion information: Minimal conditions N90-22925
On the efficacy of cinema, or what the visual system did not evolve to do N90-22934
MOTION SICKNESS
Sensory conflict in motion sickness: An observer theory approach N90-22957
MOTION SIMULATION
Multibody dynamics model building using graphical interfaces N90-23082
MOTION STABILITY
Dynamics and control of tethered antennas/reflectors in orbit
[AD-A219316] N90-22594

MOZAMBIQUE
US Navy regional climatic study of the Mozambique channel and adjacent waters
[AD-A218793] N90-22875
MULTIPHASE FLOW
Holocinematography for studies of turbulent multiphase flow
[AD-A219130] N90-22765
MULTIPROCESSING (COMPUTERS)
A scheme for supporting automatic data migration on multicomputers
[NASA-CR-182038] N90-22973
Systematic generation of multibody equations of motion suitable for recursive and parallel manipulation N90-22992
Parallel processing of real-time dynamic systems simulation on OSCAR (Optimally SCheduled Advanced multiprocessoR) N90-23006
Parallel and vector computation for stochastic optimal control applications N90-23007
A robot arm simulation with a shared memory multiprocessor machine N90-23008
MULTIPROGRAMMING
Space station dynamics, attitude control and momentum management N90-23029
MULTISENSOR APPLICATIONS
Intelligent signal processing techniques for multi-sensor surveillance systems
[AD-A218890] N90-22895
MULTIVARIATE STATISTICAL ANALYSIS
Multivariate analysis of launcher guidance robustness
[REPT-892-422-105] N90-22581
Equipment specifications for launcher guidance using multivariable frequency methods
[REPT-892-422-106] N90-22582
New multivariable capabilities of the INCA program N90-23049
Transactions of the Seventh Army Conference on Applied Mathematics and Computing
[AD-A219220] N90-23160
MUON SPIN ROTATION
A (mu)SR-investigation of the mixed state of the high-Tc superconductor HoBa2Cu3O7-delta
[DE90-620802] N90-23241

N

N-TYPE SEMICONDUCTORS
Passivation and gating of GaAs and Si surfaces using pseudomorphic structures
[AD-A219351] N90-23256
NAP-OF-THE-EARTH NAVIGATION
Field-of-view assessment of low-level flight and an airdrop in the C-130 Weapon System Trainer (WST)
[AD-A218504] N90-22559
NATURAL LANGUAGE (COMPUTERS)
Connectionism and compositional semantics
[AD-A219029] N90-22904
Natural language processing: A tutorial
[AD-A219096] N90-23108
Syntax, semantics, and pragmatism: An integrated focus based on textual linguistic knowledge
[INPE-4992-PRE/1554] N90-23262
NAVIER-STOKES EQUATION
The minimum drag profile in laminar flow: A numerical way N90-22535
The analysis and simulation of compressible turbulence
[NASA-CR-181997] N90-22539
Secondary frequencies in the wake of a circular cylinder with vortex shedding
[NASA-CR-181998] N90-22540
Multigrid acceleration of transonic flow computations
[ENSM-8024] N90-22760
NAVIGATION AIDS
ALVINN: An Autonomous Land Vehicle In a Neural Nettwork
[AD-A218975] N90-22797
NAVIGATORS
Field-of-view assessment of low-level flight and an airdrop in the C-130 Weapon System Trainer (WST)
[AD-A218504] N90-22559
NEAR FIELDS
Transfer matrices for multimode optical fiber systems
[AD-A218459] N90-23210
NEGATIVE FEEDBACK
Design of high-performance negative-feedback oscillators
[ETN-90-96698] N90-22729
NEGATIVE IONS
Threshold photodetachment spectroscopy of the I + HI transition state region
[AD-A218410] N90-22883
NEODYMIUM LASERS
MEGALIDAR proof-of-concept demonstration
[AD-A218787] N90-22858
NETWORK ANALYSIS
Executive summary for the network assessment model
[AD-A218762] N90-22718
NEURAL NETS
Qualitative aspects of signal processing through dynamical neural networks
[PREPRINT-711] N90-22709
ALVINN: An Autonomous Land Vehicle In a Neural Nettwork
[AD-A218975] N90-22797
Stochastic interactive activation and the effect of context on perception
[AD-A218929] N90-22898
Connectionism and compositional semantics
[AD-A219029] N90-22904
Encoding sequential structure in simple recurrent networks
[AD-A218928] N90-22984
Computational chaos in massively parallel neural networks N90-23012
Distributed neural control of a hexapod walking vehicle N90-23061
Neural networks in support of manned space N90-23088
Sentence comprehension: A parallel distributed processing approach
[AD-A218886] N90-23104
Adaptive Resonance Theory 1
[AD-A219044] N90-23126
Learning environment for neural networks and transient acoustics
[AD-A219000] N90-23186
NEUROPHYSIOLOGY
Sensory conflict in motion sickness: An observer theory approach N90-22957
NEUTRON COUNTERS
The ground-level cosmic-ray event of September 29, 1989 as recorded by the Rome detectors
[NOTA-INTERNA-944] N90-23336
Cosmic ray NM-64 neutron monitor data-17
[NOTA-INTERNA-945] N90-23337
NEUTRON DIFFRACTION
New approach to the dynamical diffraction theory in the case of three-dimensional perfect crystal
[DE90-620563] N90-23240
NEUTRON EMISSION
Displacement flow and deuteron drag in a metal: A path towards cold fusion
[PREPRINT-703] N90-23227
NEUTRON STARS
The dynamical evolution of dense clusters of compact stars N90-23287
Gamma radiation from radio pulsars N90-23302
Gamma radiation from the Crab and Vela pulsars N90-23303
Gamma ray pulsars: Models and observations N90-23304
What can gamma rays tell us about binary x ray sources and SNR's N90-23310
Gamma ray bursts: Current status of observations and theory N90-23313
What is learned from high energy bursts and flares N90-23314
NEUTRONS
The number of neutrino species, confronted with the results at the recent Lepton-Photon Symposium (August 7-12, 1989)
[NOTA-INTERNA-940] N90-23195
Study of Sn-116 via neutron pickup and proton stripping reactions
[KVI-814] N90-23199
NICKEL ALLOYS
A comparison of CuAlNi and other high damping alloys for the purpose of naval ship silencing applications
[AD-A218801] N90-22671
NICKEL OXIDES
Center for surface radiation damage studies
[AD-A218452] N90-22678
NIGHT VISION
Relationship between flexibility of closure and success in pilot night vision sensor system training N90-22890
Helmet-mounted pilot night vision systems: Human factors issues N90-22930
NITROGEN COMPOUNDS
On the vapour phase deposition mechanism of carbon-boron-nitrogen compounds between 800 and 1000 C
[REPT-892-430-101] N90-22632
NITROGEN DIOXIDE
Development and use of a passive technique for measuring nitrogen dioxide in the background atmosphere N90-23285
NITROGEN FLUORIDES
Experimental studies on energy storage
[AD-A219032] N90-22845
NOISE INTENSITY
Noise reduction theory acoustic barrier construction
[CRIF-MC-87] N90-23183
NOISE MEASUREMENT
Noise reduction theory acoustic barrier construction
[CRIF-MC-87] N90-23183
NOISE REDUCTION
Improvement of clutter rejection by scanning motion compensation in ground-based monopulse radar
[ETN-90-96550] N90-22711
Integrated control-system design via generalized LQG (GLQG) theory N90-23023
Noise reduction theory acoustic barrier construction
[CRIF-MC-87] N90-23183
NONDESTRUCTIVE TESTS
Impact damage in graphite/epoxy laminates: Damage characterization, acoustic emission, and finite element simulation, volumes 1 and 2 N90-22610
Nondestructive Testing (NDT); Ceramic Matrix Composite Materials (CMCM) --- Nondestructive testing (ndc); ceramic matrix composite materials (CMMC)
[REPT-892-430-123] N90-22677
Applications of laser ultrasound
[AERE-R-13106] N90-22777
Two-dimensional surface strain measurement based on a variation of Yamaguchi's laser-speckle strain gauge
[NASA-TM-103162] N90-22784
Recent advances in nondestructive evaluation made possible by novel uses of video systems
[NASA-TM-102491] N90-22801
Application of x ray absorption edge spectrometry to the non-destructive determination of element concentrations, coating thickness and areal densities
[AERE-R-13030] N90-22802
Crack detection in silicon nitride by acoustic microscopy
[AERE-R-13196] N90-22803
Real-time stereo-microradiography
[AD-A218433] N90-22805
On-line x ray inspection of materials and structural components using discrete element x ray detectors for digital radiographic and computed tomographic evaluation
[AD-A218911] N90-22806
NONLINEAR EQUATIONS
Nonlinear bifurcation study of plane Poiseuille flow
[DLR-FB-89-42] N90-22756
Evidence for self-refraction in a convergence zone: NPE (Nonlinear progressive wave equation) model results
[AD-A218546] N90-22879
The application of a non-linear least squares method to predicting seat transmissibility
[ISVR-TR-173] N90-22967
On approximation of nonlinear boundary integral equations for the combined method
[DE90-009784] N90-23130
Continuation and multi-grid methods for bifurcation problems
[AD-A218904] N90-23146
Collective properties of neural systems and their relation to other physical models
[AD-A219071] N90-23201
NONLINEAR OPTICS
A second-order nonlinear optical poly(organophosphazene)
[AD-A218408] N90-22607
Single-crystal diffraction analysis of 2-(trimethylsilylethynyl) 4-nitro-N,N-dimethylaniline
[AD-A218955] N90-22642
Analysis and evaluation of technical data on the photochromic and non-linear optical properties of materials
[AD-A219398] N90-23219
NONLINEAR PROGRAMMING
Multilevel decomposition approach to the preliminary sizing of a transport aircraft wing
[NASA-CR-4296] N90-22557
An algorithm for the solution of dynamic linear programs N90-23026
Approximate minimum-time trajectories for 2-link flexible manipulators N90-23030
NONLINEAR SYSTEMS
Approximate optimal guidance schemes for atmospheric orbital maneuvering N90-22585
Bifurcational aspects of parametric resonance
[W-8904] N90-22730
Optimization of a pulsed air core transformer for low impedance inductive ignition
[AD-A218748] N90-22734
The (DURIP) computer simulations of plasmas, nonlinear systems, and control theory
[AD-A219070] N90-23107

A computational method for general higher index nonlinear singular systems of differential equations
[AD-A219164] N90-23147
NONLINEARITY
Semianalytic study of high-eccentricity orbit stability and evolution N90-22574
A study of woven fabric-reinforced composite materials using an invariant-based orthotropic plasticity formulation N90-22611
Nonlinear finite element formulation for the large displacement analysis in multibody system dynamics N90-23015
Application of numerical optimization techniques to control system design for nonlinear dynamic models of aircraft N90-23032
Effect on relaxation on nonlinear waves in crystals N90-23165
Reconstructing primordial density fluctuations N90-23293
NONNEWTONIAN FLOW
A numerical and analytical study of normal stresses and pressure differences in non-Newtonian creeping flows N90-22749
NONPARAMETRIC STATISTICS
Parametric models for A(sub n): Splitting processes and mixtures
[AD-A218421] N90-23140
Bayesian nonparametric prediction and statistical inference
[AD-A218473] N90-23154
Statistical inference from sampled data
[AD-A218731] N90-23156
NONUNIFORM MAGNETIC FIELDS
Excitation of hypersound at boundary between Type-2 superconductor and a concentrated paramagnetic compound N90-23164
NOVAE
Infrared coronal line novae N90-23328
NUCLEAR ELECTRIC POWER GENERATION
Nuclear technology and the space exploration missions
[NASA-TM-103156] N90-22847
NUCLEAR ENERGY
Nuclear power in space
[GPO-23-835] N90-23202
NUCLEAR EXPLOSIONS
Seismic wave propagation, attenuation and scattering over regional distances
[AD-A219358] N90-22862
NUCLEAR FUEL BURNUP
Modeling of combustion processes in a solid fuel particle
[DE90-009140] N90-22629
NUCLEAR FUSION
Displacement flow and deuteron drag in a metal: A path towards cold fusion
[PREPRINT-703] N90-23227
NUCLEAR MAGNETIC RESONANCE
Single crystal NMR of high temperature superconductors N90-23236
NUCLEAR PHYSICS
JPRS report: Science and technology. USSR: Physics and mathematics
[JPRS-UPM-89-001] N90-23162
NUCLEAR PROPULSION
Nuclear technology and the space exploration missions
[NASA-TM-103156] N90-22847
NUCLEAR REACTIONS
Study of Sn-116 via neutron pickup and proton stripping reactions
[KVI-814] N90-23199
Incomplete fusion reactors at low and intermediate energies
[KVI-809] N90-23206
NUCLEATION
The effects of zinc addition on the environmental stability of Al-Li alloys N90-22657
NULL ZONES
Performance of adaptive nulling antennas in a jamming environment
[AD-A219305] N90-22720
NUMERICAL ANALYSIS
A numerical and analytical study of normal stresses and pressure differences in non-Newtonian creeping flows N90-22749
JPRS report: Science and technology. USSR: Physics and mathematics
[JPRS-UPM-89-001] N90-23162
NUMERICAL CONTROL
The elastic-plastic behavior of composite materials N90-22615
Computer controlled cryogenic temperature controller
[AD-A218785] N90-22701
Modelling and computer control of a mechanical system
[W-8908] N90-22794
Application of numerical optimization techniques to control system design for nonlinear dynamic models of aircraft N90-23032
NUMERICAL DIFFERENTIATION
Recursive linearization of multibody dynamics equations of motion N90-22993
NUMERICAL INTEGRATION
Semianalytic study of high-eccentricity orbit stability and evolution N90-22574
A new second-order integration algorithm for simulating mechanical dynamic systems N90-23064
Effective action for induced gravity on a 2-dimensional manifold
[PREPRINT-712] N90-23173

O

OBJECT PROGRAMS
Using object-oriented analysis techniques to support system testing
[DE90-009540] N90-22700
Object-oriented query languages: The notion and the issues
[REPT-89-054] N90-23093
OBSERVABILITY (SYSTEMS)
Elements of active vibration control for rotating machinery
[NASA-TM-102368] N90-22703
OCEAN BOTTOM
On the effectiveness of the production of antarctic bottom water in the Weddell and Ross Seas
[AD-A218873] N90-22880
OCEAN CURRENTS
Determination of the general ocean circulation using satellite altimetry from a simultaneous solution for the Earth's gravity field N90-22569
On the effectiveness of the production of antarctic bottom water in the Weddell and Ross Seas
[AD-A218873] N90-22880
OCEAN DYNAMICS
On the effectiveness of the production of antarctic bottom water in the Weddell and Ross Seas
[AD-A218873] N90-22880
Stratified ocean mixing
[AD-A219233] N90-22881
OCEAN MODELS
Determination of the general ocean circulation using satellite altimetry from a simultaneous solution for the Earth's gravity field N90-22569
Predictability of weather and climate in a coupled ocean-atmosphere model: A dynamical systems approach N90-22865
OCEAN THERMAL ENERGY CONVERSION
Ocean energy program summary
[DE89-009481] N90-22836
OCEANOGRAPHIC PARAMETERS
US Navy regional climatic study of southern African waters
[AD-A218792] N90-22874
US Navy regional climatic study of the Mozambique channel and adjacent waters
[AD-A218793] N90-22875
OCEANOGRAPHY
Determination of the general ocean circulation using satellite altimetry from a simultaneous solution for the Earth's gravity field N90-22569
Monthly surface thermal forcing in the tropical Pacific from 1980 to 1983
[NASA-CR-183033] N90-22877
OCEANS
A numerical study of basic coastal upwelling processes N90-22878
OCULOGRAVIC ILLUSIONS
Spatial vision within egocentric and exocentric frames of reference N90-22928
OGIVES
Three-dimensional separated flow prediction on fusiform body using Euler and boundary layer methods N90-22745
OHIO
A study of mesoscale acid deposition in the lower Ohio River Valley N90-22848
ON-LINE SYSTEMS
On-line x ray inspection of materials and structural components using discrete element x ray detectors for digital radiographic and computed tomographic evaluation
[AD-A218911] N90-22806
Combining high performance simulation, data acquisition, and graphics display computers N90-23062
OPEN CIRCUIT VOLTAGE
Definition of a design methodology and study of the driving and protection functions of a smart power switch
[LAAS-89-330] N90-22727
OPERATING SYSTEMS (COMPUTERS)
Methodology for analysis and simulation of large multidisciplinary problems N90-23046
DARK (Distributed Ada Real-Time Kernel) porting and extension guide Kernel version 3.0
[AD-A219291] N90-23112
BTOS database evaluation
[AD-A219304] N90-23271
OPERATING TEMPERATURE
Turbine fuel alternatives (near term)
[AD-A219405] N90-22695
Enhanced ceria solid electrolyte fuel cell development. Reduction of electronic conductivity permits use of a solid ceria electrolyte in high efficiency high power density fuel cells at temperatures compatible with metallic cell hardware
[AD-A219297] N90-22846
OPERATORS (MATHEMATICS)
Spatial operator algebra framework for multibody system dynamics N90-22989
Naturalness of polymorphism
[CS-8916] N90-23134
A proof of the isoenergetic KAM: Theorem from the ordinary one
[W-8906] N90-23136
The effects of caustics in acoustic inverse scattering experiments
[AD-A218454] N90-23185
Improving fermion operators
[PREPRINT-710] N90-23193
Mixing of DIS operators in lattice QCD
[PREPRINT-708] N90-23243
OPHTHALMOLOGY
Measurement and visualization of the shock wave caused by the impact of a pulsed YAG laser in water
[REPT-892-430-113] N90-22783
OPTICAL EQUIPMENT
High performance holographic elements and media
[AD-A218999] N90-22775
Agile multiple aperture imager receiver development
[AD-A218956] N90-23215
OPTICAL FIBERS
Processing of thermotropic liquid crystalline polymers and their blends
[AD-A218804] N90-22683
Transfer matrices for multimode optical fiber systems
[AD-A218459] N90-23210
OPTICAL MATERIALS
Analysis and evaluation of technical data on the photochromic and non-linear optical properties of materials
[AD-A219398] N90-23219
OPTICAL MEMORY (DATA STORAGE)
Use of optical storage devices as shared resources in local area networks
[AD-A219198] N90-23269
OPTICAL PROPERTIES
A second-order nonlinear optical poly(organophosphazene)
[AD-A218408] N90-22607
Single-crystal diffraction analysis of 2-(trimethylsilylethynyl) 4-nitro-N,N-dimethylaniline
[AD-A218955] N90-22642
Solar Concentrator Advanced Development Program
[NASA-CR-185173] N90-22834
High temperature superconducting thin films in Japan N90-23169
Optical properties of novel GaAs-based semiconductors N90-23235
Optical properties of cometary dust
[AD-A218790] N90-23325
OPTICAL RADAR
MEGALIDAR proof-of-concept demonstration
[AD-A218787] N90-22858
OPTICAL SCANNERS
Multi-axis, 3-D, scanning LDA (Laser Doppler Anemometer) system for unsteady aerodynamics
[AD-A218571] N90-22541
OPTIMAL CONTROL
Minimum flying qualities. Volume 3: Program CC's implementation of the human optimal control model
[AD-A218562] N90-22562
Orbital maneuvers optimization for station acquisition of geostationary satellites. Deterministic and stochastic approaches
[LAAS-89-359] N90-22589
Parallel and vector computation for stochastic optimal control applications N90-23007
Optimum control forces for multibody systems with intermittent motion N90-23016
Frequency response modeling and control of flexible structures: Computational methods N90-23021

H(2)- and H(infinity)-design tools for linear time-invariant systems N90-23025
A finite element based method for solution of optimal control problems N90-23027
Substructural controller synthesis N90-23055
A priori results in linear-quadratic optimal control theory (extended version)
[MEMO-COSOR-89-17] N90-23124

OPTIMIZATION
Multilevel decomposition approach to the preliminary sizing of a transport aircraft wing
[NASA-CR-4296] N90-22557
Differential equation based method for accurate approximations in optimization
[NASA-TM-102639] N90-22558
Limiting performance based structural and control optimization for large vibrating structures N90-22568
A comparison of CuAlNi and other high damping alloys for the purpose of naval ship silencing applications
[AD-A218801] N90-22671
Nondestructive Testing (NDT); Ceramic Matrix Composite Materials (CMCM) — Nondestructive testing (ndc); ceramic matrix composite materials (CMMC)
[REPT-892-430-123] N90-22677
H2, fixed architecture, control design for large scale systems
[NASA-CR-180471] N90-22698
High temperature ceramic-tubed reformer
[DE90-009617] N90-22755
A free electron laser master oscillator power amplifier experiment N90-22776
The use of supercomputers for the design and analysis of constructions N90-22977
A survey on the structured singular value N90-22998
Algorithms for computing the multivariable stability margin N90-22999
Combined control-structure optimization N90-23005
H(2)- and H(infinity)-design tools for linear time-invariant systems N90-23025
Application of numerical optimization techniques to control system design for nonlinear dynamic models of aircraft N90-23032
Implementation of generalized optimality criteria in a multidisciplinary environment N90-23048
Reusing software components by specialization
[REPT-89-062] N90-23094
Periodic ARMA models: Optimal prediction and minimum-phase condition
[REPT-89-006] N90-23131
Towards a calculus of data refinement
[CS-8902] N90-23264

OPTOELECTRONIC DEVICES
A fiber-optic current sensor for aerospace applications
[NASA-TM-103152] N90-22773

ORBIT PERTURBATION
Semianalytic study of high-eccentricity orbit stability and evolution N90-22574

ORBITAL ELEMENTS
Semianalytic study of high-eccentricity orbit stability and evolution N90-22574

ORBITAL MANEUVERS
Orbit acquisition and control strategy for small satellites in inclined eccentric orbits
[ETN-90-96551] N90-22573
Approximate optimal guidance schemes for atmospheric orbital maneuvering N90-22585
Orbital maneuvers optimization for station acquisition of geostationary satellites. Deterministic and stochastic approaches
[LAAS-89-359] N90-22589
A computer graphics system for visualizing spacecraft in orbit N90-22952

ORBITAL MECHANICS
Orbital mechanics: A learning tool on the main frame
[AD-A218799] N90-22576
Low cost station keeping maneuvers for a small-satellites constellation in tundra orbits
[ETN-90-96553] N90-22588
Dynamics and control of tethered antennas/reflectors in orbit
[AD-A219316] N90-22594
Interactive orbital proximity operations planning system N90-22953

ORDER-DISORDER TRANSFORMATIONS
Localization of vibration in disordered nearly cyclic structures N90-22812

ORGANIC CHEMISTRY
Investigation of optical nonlinearities, conductivity and magnetism in organometallic materials
[AD-A218548] N90-23211

ORGANIC MATERIALS
Measurement of localized deep levels and wafer non-uniformities at 3-5 semiconductor heterojunctions
[AD-A218547] N90-23248

ORGANIC PHOSPHORUS COMPOUNDS
A second-order nonlinear optical poly(organophosphazene)
[AD-A218408] N90-22607

ORGANOMETALLIC COMPOUNDS
The first example of an organogallium compound containing a Ga-Te bond: Synthesis, properties, and molecular structure of ((Me3CCH2)2GaTeph)2
[AD-A219258] N90-22608
Investigation of optical nonlinearities, conductivity and magnetism in organometallic materials
[AD-A218548] N90-23211

ORGANOMETALLIC POLYMERS
Modified maleic anhydride copolymers as e-beam resists
[AD-A218470] N90-22679

ORTHO PARA CONVERSION
Development of high-activity para- to ortho-hydrogen conversion catalysts, volume 2
[AD-A218700] N90-22638

ORTHOTROPIC PLATES
The behaviour of mechanically fastened joints in composite structures N90-22789

OSCILLATORS
Design of high-performance negative-feedback oscillators
[ETN-90-96698] N90-22729
Bifurcational aspects of parametric resonance
[W-8904] N90-22730
A free electron laser master oscillator power amplifier experiment N90-22776
Quantum non-demolition stroboscopic observables and multipumping back-action evasion schemes
[PREPRINT-699] N90-23260
Are quantum measurements on macroscopic bodies feasible
[PREPRINT-700] N90-23261

OVENS
Uncertainty evaluation in an automated high temperature environmental simulation oven
[REPT-892-430-103] N90-22571

OXIDATION
Oxidation and ignition characteristics of hydrocarbon fuels
[AD-A218666] N90-22637
Improved high temperature oxidation behavior of alloys by ion implantation
[AERE-R-13309] N90-22650
Model catalytic oxidation studies using supported monometallic and heterobimetallic oxides
[DE90-009984] N90-22664
Experimental evaluation of chemical cleaning processes for high-lifetime silicon processing
[DE90-009332] N90-22699

OXIDIZERS
Airliner cabin ozone: An updated review
[AD-A219264] N90-22970

OXYGEN ATOMS
Synthesis and characterization of aromatic polyester and polysiloxane containing block copolymers: Multiphase transparent atomic oxygen resistant damping materials, liquid crystal films, and toughening components of sol/gel glasses
[AD-A218871] N90-22685

OXYGEN FLUORIDES
Experimental studies on energy storage
[AD-A219032] N90-22845

OXYGEN ISOTOPES
The 16-O photodisintegration at low energies
[NOTA-INTERNA-941] N90-23196

OXYGEN PRODUCTION
Space Station Freedom environmental control and life support system phase 3 simplified integrated test detailed report
[NASA-TM-4204] N90-22593

OXYGEN SUPPLY EQUIPMENT
Lunar base 2 (the second thousand days of a base on the Moon)
[ILR-MITT-230(1989)] N90-22968

OXYGEN-HYDROCARBON ROCKET ENGINES
Cooling of rocket thrust chambers with liquid oxygen
[NASA-TM-103146] N90-22605

OZONE
Airliner cabin ozone: An updated review
[AD-A219264] N90-22970

OZONE DEPLETION
On the antarctic ozone depletion during solar cycle 21
[NOTA-INTERNA-943] N90-22849

P

P WAVES
Measurements of high frequency seismic waves
[AD-A219370] N90-22863

P-TYPE SEMICONDUCTORS
Passivation and gating of GaAs and Si surfaces using pseudomorphic structures
[AD-A219351] N90-23256

PACIFIC OCEAN
Monthly surface thermal forcing in the tropical Pacific from 1980 to 1983
[NASA-CR-183033] N90-22877

PACKETS (COMMUNICATION)
Performance analysis of Aloha networks with power capture and near/far effect
[AD-A218739] N90-22717
Locality in parallel computation
[AD-A218733] N90-23120

PACKINGS (SEALS)
Seal requirements in rocket propulsion
[ETN-90-96611] N90-22580

PAIR PRODUCTION
Quark-antiquark pair production via gamma W fusion at high energy e(+)e(-) colliders
[PREPRINT-705] N90-23205
The sensitivity of EGRET to gamma ray polarization N90-23305

PANELS
Experimental and computational study of the viscoplastic response of high temperature structures N90-22663
Numerical studies of the active control of sound transmission through double partitions
[ISVR-TR-183] N90-23181

PANORAMIC SCANNING
Atmospheric autorotating imaging device
[NASA-CASE-NPO-17390-1-CU] N90-22769

PARABOLIC DIFFERENTIAL EQUATIONS
Undetermined coefficient problems for quasi-linear parabolic equations
[AD-A218462] N90-23141

PARABOLIC REFLECTORS
An assessment of second-generation stretched-membrane mirror modules
[DE90-010243] N90-22841

PARABOLOID MIRRORS
An assessment of second-generation stretched-membrane mirror modules
[DE90-010243] N90-22841

PARALLEL FLOW
An experimental study of tip shape effects on the flutter of aft-swept, flat-plate wings
[NASA-TM-4180] N90-22555
Parallel channel flow excursions
[DE90-009129] N90-22753

PARALLEL PROCESSING (COMPUTERS)
The preprocessed doacross loop
[NASA-CR-182056] N90-22972
A scheme for supporting automatic data migration on multicomputers
[NASA-CR-182038] N90-22973
Communication overhead on the Intel iPSC-860 hypercube
[NASA-CR-182055] N90-22982
Parallel processing of real-time dynamic systems simulation on OSCAR (Optimally SCheduled Advanced multiprocessoR) N90-23006
A robot arm simulation with a shared memory multiprocessor machine N90-23008
A unifying framework for rigid multibody dynamics and serial and parallel computational issues N90-23009
Parallel algorithms and architecture for computation of manipulator forward dynamics N90-23010
Computational chaos in massively parallel neural networks N90-23012
Characterization of robotics parallel algorithms and mapping onto a reconfigurable SIMD machine N90-23039
Proceedings of the 3rd Annual Conference on Aerospace Computational Control, volume 2
[NASA-CR-186447] N90-23040
A parallel structure transient response algorithm using independent substructure response computation N90-23044
Parallel conjugate gradient algorithms for manipulator dynamic simulation N90-23045
A real time, FEM based optimal control algorithm and its implementation using parallel processing hardware (transistors) in a microprocessor environment N90-23066
The power and efficiency of advanced software and parallel processing N90-23079
On the performance of parallel algorithms
[CS-8914] N90-23099
Proceedings of the NATO Advanced Workshop on Supercomputing
[AD-A218508] N90-23102
Sentence comprehension: A parallel distributed processing approach
[AD-A218886] N90-23104

Interconnection networks for highly parallel supercomputing architectures
[REPT-89-053] N90-23118
Controlling real-time systems with parallel processes
[CS-8918] N90-23119
Locality in parallel computation
[AD-A218733] N90-23120
Proceedings of the 9th International Conference on Computing Methods in Applied Science and Engineering
[AD-A219307] N90-23149

PARALLEL PROGRAMMING
On the performance of parallel algorithms
[CS-8914] N90-23099
Durra: A task-level description language reference manual, version 2
[AD-A219293] N90-23114
Controlling real-time systems with parallel processes
[CS-8918] N90-23119

PARAMETER IDENTIFICATION
JPL control/structure interaction test bed real-time control computer architecture N90-23070
Robust adaptive control: Stability and asymptotic performance
[AD-A219259] N90-23127
Estimation of Hilbert space valued parameters by the method of sieves
[AD-A218565] N90-23143
Parameter estimation in linear filtering
[AD-A218566] N90-23144
Spectral determinations for discrete sources with EGRET N90-23312

PARAMETERIZATION
Approximate analysis for the formation of adiabatic shear bands
[AD-A218751] N90-22670
Impact of marine boundary layer parameterization on a numerical simulation of cyclogenesis during a cold air outbreak event N90-22864
Robust modelling of sampled systems for time delay estimation
[REPT-89-047] N90-23092
Curvature-dependent parametrization of curves and surfaces
[CS-8915] N90-23100

PARSING ALGORITHMS
Natural language processing: A tutorial
[AD-A219096] N90-23108

PARTIAL DIFFERENTIAL EQUATIONS
Analytic semigroups: Applications to inverse problems for flexible structures
[NASA-CR-182047] N90-23138
Undetermined coefficient problems for quasi-linear parabolic equations
[AD-A218462] N90-23141
Continuation and multi-grid methods for bifurcation problems
[AD-A218904] N90-23146
Adaptive mesh experiments for hyperbolic partial differential equations
[AD-A219194] N90-23148

PARTICLE ACCELERATORS
Gravitational radiation produced by high energy accelerators and high power lasers
[PREPRINT-701] N90-22782
Stability regimes in a rotating quadrupole focusing accelerator
[AD-A219513] N90-23209

PARTICLE COLLISIONS
The number of neutrino species, confronted with the results at the recent Lepton-Photon Symposium (August 7-12, 1989)
[NOTA-INTERNA-940] N90-23195
Quark-antiquark pair production via gamma W fusion at high energy e(+)e(-) colliders
[PREPRINT-705] N90-23205

PARTICLE DENSITY (CONCENTRATION)
About the order of Appel's algorithm
[CS-8910] N90-23097

PARTICLE ENERGY
Quark-antiquark pair production via gamma W fusion at high energy e(+)e(-) colliders
[PREPRINT-705] N90-23205
Gamma rays from pulsar wind shock acceleration N90-23311

PARTICLE INTERACTIONS
Replica scaling analysis of interfaces in random media
[PREPRINT-713] N90-23174
Support for the 16th International Conference on the Physics of Electronic and Atomic Collisions
[AD-A218567] N90-23200

PARTICLE MOTION
Dynamics of motion charged particles in a field of two electromagnetic waves
[DE90-620690] N90-22706

PARTICLE SIZE DISTRIBUTION
Phase Doppler droplet sizing: Scattering angle effects
[DE90-009571] N90-22754

PASCAL (PROGRAMMING LANGUAGE)
Vectors and matrices: Two turbo pascal units for fast program development
[AD-A218917] N90-23105

PASSIVITY
Passivation and gating of GaAs and Si surfaces using pseudomorphic structures
[AD-A219351] N90-23256

PATTERN RECOGNITION
Automated star pattern recognition N90-22612
The analysis of polar clouds from AVHRR satellite data using pattern recognition techniques
[NASA-CR-183300] N90-22868
Quantum-limited image recognition
[AD-A218425] N90-23101
Adaptive Resonance Theory 1
[AD-A219044] N90-23126
Auditory spectro-temporal pattern analysis
[AD-A218416] N90-23184
Classification techniques for quantum-limited and classical-intensity images
[AD-A218693] N90-23212

PATTERN REGISTRATION
Image segmentation with detection of highlights and inter-reflections using color
[AD-A218710] N90-23213

PECULIAR GALAXIES
Counterrotating cores in elliptical galaxies N90-23288

PENDULUMS
A nearly-linear computational-cost scheme for the forward dynamics of an N-body pendulum N90-22996
Computational dynamics for robotics systems using a non-strict computational approach N90-23011

PENETRATION
Role of shear instability in ballistic penetration
[AD-A219186] N90-22799

PENINSULAS
A case for archaeological reconnaissance of the Cabo Catoche-Porvenir region of the northeastern Yucatan Peninsula
[NASA-TM-102248] N90-22827

PERCEPTION
A connectionist implementation of cognitive phonology
[AD-A219095] N90-22906

PERCEPTUAL ERRORS
Stereoscopic distance perception N90-22921
Paradoxical monocular stereopsis and perspective vergence N90-22922
Distortions in memory for visual displays N90-22929
Exocentric direction judgements in computer-generated displays and actual scenes N90-22936
Adapting to variable prismatic displacement N90-22945
Interactions of form and orientation N90-22958

PERFORMANCE PREDICTION
A modeling technique for STOVL ejector and volume dynamics
[NASA-TM-103167] N90-22566
Environment enhanced fatigue of advanced aluminum alloys and composites N90-22652
Deformation and fracture of thin sheet aluminum-lithium alloys: The effect of cryogenic temperatures N90-22655
Integrated control-system design via generalized LQG (GLQG) theory N90-23023
On the performance of parallel algorithms
[CS-8914] N90-23099

PERFORMANCE TESTS
Characterization and calibration of coordinate measuring machines
[DE90-009320] N90-22791
Next generation weather radar (NEXRAD) initial operational test and evaluation. Phase 2: (IOT and E(2))
[AD-A218770] N90-22873
Proceedings of the 3rd Annual Conference on Aerospace Computational Control, volume 1
[NASA-CR-186446] N90-22987
On randomness of random number generators
[MEMO-COSOR-89-20] N90-23151

PERIODIC VARIATIONS
A 154-day periodicity in the occurrence rate of proton flares
[NASA-CR-185826] N90-23333

PEROVSKITES
The effects of point defects and composition on structural phase transition
[DE90-010109] N90-23238

PERSONAL COMPUTERS
HCI monitor N90-22599
ASTEC: Controls analysis for personal computers N90-23052

PERTURBATION
Recursive linearization of multibody dynamics equations of motion N90-22993
A survey on the structured singular value N90-22998
Algorithms for computing the multivariable stability margin N90-22999
An examination of the full-wave method for rough surface scattering
[AD-A218664] N90-23155
The effects of caustics in acoustic inverse scattering experiments
[AD-A218454] N90-23185

PERTURBATION THEORY
Recursive linearization of multibody dynamics equations of motion N90-22993
Effect on relaxation on nonlinear waves in crystals N90-23165

PH
Sticking coefficient of HCl on aerosols N90-22598

PHASE CONJUGATION
Beam combining by phase transition nonlinear media
[AD-A219301] N90-22739

PHASE DIAGRAMS
Improvement study of iron disilicide thermoelectric materials
[AD-A218946] N90-22844

PHASE MATCHING
The super-gratings: How to improve the limiting resolution of grating spectrometers
[PREPRINT-695] N90-22577
Nonlinear spectroscopy of multicomponent droplets and 2- and 3-dimensional measurements in flames
[AD-A218569] N90-22636

PHASE MODULATION
High performance holographic elements and media
[AD-A218999] N90-22775

PHASE TRANSFORMATIONS
Center for surface radiation damage studies
[AD-A218452] N90-22678
Investigation of atomistic simulation of structural and dynamic differences in glassy and liquid states of atactic poly(propylene)
[AD-A218896] N90-22687
Beam combining by phase transition nonlinear media
[AD-A219301] N90-22739
Characterization of weldments using advanced experimental techniques
[DE90-009418] N90-22792
The effects of point defects and composition on structural phase transition
[DE90-010109] N90-23238

PHASE VELOCITY
Nonlinear spectroscopy of multicomponent droplets and 2- and 3-dimensional measurements in flames
[AD-A218569] N90-22636

PHASED ARRAYS
The effect of mechanical deformation on the radiation patterns of large space-based arrays
[AD-A219288] N90-22719

PHONETICS
A connectionist implementation of cognitive phonology
[AD-A219095] N90-22906

PHOSPHAZENE
A second-order nonlinear optical poly(organophosphazene)
[AD-A218408] N90-22607

PHOSPHORUS POLYMERS
A second-order nonlinear optical poly(organophosphazene)
[AD-A218408] N90-22607

PHOTOCHEMICAL REACTIONS
Interaction of atomic hydrogen with pico- and femtosecond laser pulses
[AD-A218426] N90-22785
Development and use of a passive technique for measuring nitrogen dioxide in the background atmosphere N90-23285

PHOTOCHROMISM
Analysis and evaluation of technical data on the photochromic and non-linear optical properties of materials
[AD-A219398] N90-23219

PHOTODECOMPOSITION
The 16-O photodisintegration at low energies
[NOTA-INTERNA-941] N90-23196
Relativistic corrections to He-3 photodisintegration sum rules
[NOTA-INTERNA-942] N90-23197

PHOTODETACHMENT
Femtosecond studies of electron photodetachment of simple ions in liquid water: Solvation and geminate recombination dynamics
[AD-A218520] N90-22634
Threshold photodetachment spectroscopy of the I + HI transition state region
[AD-A218410] N90-22883

PHOTOELECTROCHEMISTRY
Scanning laser photocurrent spectroscopy of electrochemically grown bismuth sulphide films
[AERE-M-3709] N90-22649
PHOTOGRAMMETRY
Large scale metrology by computer assisted photogrammetry
[REPT-892-430-116] N90-22772
PHOTOGRAPHS
Debris/ice/TPS assessment and photographic analysis for Shuttle Mission STS-36
[NASA-TM-102789] N90-22583
PHOTOIONIZATION
Measurements and simulation of controlled beamfront motion in the Laser Controlled Collective Accelerator
[DE90-009992] N90-22780
Infrared coronal line novae N90-23328
PHOTOLITHOGRAPHY
Photoresponse of YBa2Cu3O(7-delta) granular and epitaxial superconducting thin films
[NASA-TM-103144] N90-22732
PHOTONEUTRONS
The 16-O photodisintegration at low energies
[NOTA-INTERNA-941] N90-23196
PHOTONS
The illusive Geminga: What is it N90-23307
PHOTOOXIDATION
Pyrotechnic materials ignited using lasers. High energy photopyrotechnic chains
[REPT-892-430-121] N90-22691
PHOTOVOLTAIC CELLS
Photovoltaic advanced research and development project: Solar radiation research
[DE90-000302] N90-22839
PHOTOVOLTAIC CONVERSION
Photovoltaic advanced research and development project: Solar radiation research
[DE90-000302] N90-22839
PHYSICAL FITNESS
Physiological and perceptual responses to prolonged treadmill load carriage
[AD-A218910] N90-22886
PHYSIOLOGICAL EFFECTS
Heat exhaustion in a rat model: Lithium as a biochemical probe
[AD-A219361] N90-22884
Assessment System for Aircraft Noise (ASAN) citation database. Volume 1: User's manual
[AD-A219175] N90-23188
Assessment System for Aircraft Noise (ASAN) citation database. Volume 2: Database update manual
[AD-A219176] N90-23189
Assessment System for Aircraft Noise (ASAN) citation database. Volume 3: New citation review procedures
[AD-A219177] N90-23190
PHYSIOLOGICAL RESPONSES
Physiological and perceptual responses to prolonged treadmill load carriage
[AD-A218910] N90-22886
The physiological cost of wearing the propellant handler's ensemble at the Kennedy Space Center
[NASA-TM-102786] N90-22966
PHYSIOLOGICAL TESTS
Physiological and perceptual responses to prolonged treadmill load carriage
[AD-A218910] N90-22886
PHYSIOLOGY
The physiological cost of wearing the propellant handler's ensemble at the Kennedy Space Center
[NASA-TM-102786] N90-22966
PICOSECOND PULSES
Frequency domain techniques for analyzing picosecond optical pulses
[AD-A218856] N90-23214
PIEZOELECTRICITY
Shaping radiation pattern of excimer laser by means of controllable intracavity mirror N90-23166
PILOT ERROR
Spatial displays as a means to increase pilot situational awareness N90-22951
PILOT PERFORMANCE
Field-of-view assessment of low-level flight and an airdrop in the C-130 Weapon System Trainer (WST)
[AD-A218504] N90-22559
Model-based method for terrain-following display design
[AD-A219302] N90-22563
Visual behavior in the F-15 simulator for air-to-air combat
[AD-A218648] N90-22893
Spatial displays as a means to increase pilot situational awareness N90-22951
Synthetic perspective optical flow: Influence on pilot control tasks N90-22956
PILOT TRAINING
Minimum flying qualities. Volume 1: Piloted simulation evaluation of multiple axis flying qualities
[AD-A218560] N90-22560
Visual behavior in the F-15 simulator for air-to-air combat
[AD-A218648] N90-22893
PINS
The behaviour of mechanically fastened joints in composite structures N90-22789
PIONEER PROJECT
The Pioneer Venus Orbiter: 11 years of data. A laboratory for atmospheres seminar talk
[NASA-TM-100761] N90-23273
PIONEER VENUS 1 SPACECRAFT
The Pioneer Venus Orbiter: 11 years of data. A laboratory for atmospheres seminar talk
[NASA-TM-100761] N90-23273
PIPE FLOW
Some observations on liquid flow through filters
[AERE-R-13300] N90-22748
PIPES (TUBES)
The elastic-plastic behavior of composite materials N90-22615
Calcium carbonate scale dissolution in water stabilized by carbon dioxide treatment
[AD-A218502] N90-22633
PITTING
Surface pitting fatigue life of noninvolute, low-contact-ratio gears
[NASA-TM-103116] N90-22790
PLANAR STRUCTURES
Control of a flexible planar truss using proof mass actuators N90-23035
PLANE STRESS
Axisymmetric and cylindrically orthotropic analysis of filament winding N90-22811
PLANE WAVES
Scattering of a plane electromagnetic wave from a semicircular crack in a perfectly conducting ground plane
[AD-A219310] N90-22721
Effect on relaxation on nonlinear waves in crystals N90-23165
PLANETARY BOUNDARY LAYER
A new stochastic model of turbulent dispersion in the convective planetary boundary layer and the results of the Atterbury-87 field study N90-22853
PLANETARY GEOLOGY
The Pioneer Venus Orbiter: 11 years of data. A laboratory for atmospheres seminar talk
[NASA-TM-100761] N90-23273
PLANETARY IONOSPHERES
The Pioneer Venus Orbiter: 11 years of data. A laboratory for atmospheres seminar talk
[NASA-TM-100761] N90-23273
PLANETARY WAVES
Evolution of atmospheric baroclinic waves N90-22855
PLANNING
US access to space: Launch vehicle choices for 1990 to 2010 N90-22579
PLANTS (BOTANY)
ELF (Extremely Low Frequency) communications systems ecological monitoring program: Wetland studies
[AD-A218632] N90-22716
PLASMA DENSITY
Analytical theory of the Bunemann instability for electron runaway
[IPF-88-3] N90-23224
PLASMA DIAGNOSTICS
Thermal barrier research
[DE90-009213] N90-23221
Activities report of the Institute for Plasma Research
[ETN-90-96467] N90-23225
PLASMA ENGINES
Transport properties of plasmas in microwave electrothermal thrusters
[AD-A219408] N90-23228
PLASMA EQUILIBRIUM
Resonant MHD modes with toroidal coupling
[DE90-010077] N90-23222
Numerical methods for the problem of the free-boundary plasma equilibrium in a stellarator (torsatron)
[DE90-620580] N90-23223
PLASMA FOCUS
Activities report of the Institute for Plasma Research
[ETN-90-96467] N90-23225
PLASMA JET WIND TUNNELS
SIMOUN: An optimized supersonic high temperature wind tunnel for testing construction materials to be used on the spaceplane
[REPT-892-430-111] N90-22572
PLASMA PHYSICS
JPRS report: Science and technology. USSR: Physics and mathematics
[JPRS-UPM-89-001] N90-23162
PLASMA PROPULSION
Transport properties of plasmas in microwave electrothermal thrusters
[AD-A219408] N90-23228
PLASMA RADIATION
Nonlinear spectroscopy of multicomponent droplets and 2- and 3-dimensional measurements in flames
[AD-A218569] N90-22636
PLASMA WAVES
Sound waves in weakly ionized gas
[DE90-620704] N90-23180
PLASMA-ELECTROMAGNETIC INTERACTION
Forced scattering of electromagnetic waves on electron beam in periodically inhomogeneous plasma
[DE90-620705] N90-22707
PLASMAGUIDES
Forced scattering of electromagnetic waves on electron beam in periodically inhomogeneous plasma
[DE90-620705] N90-22707
PLASMAS (PHYSICS)
The (DURIP) computer simulations of plasmas, nonlinear systems, and control theory
[AD-A219070] N90-23107
Measurement of plasma-neutralized super-vacuum currents in a gyrotron configuration
[AD-A218505] N90-23207
Gas dynamic theory of flight of fast electron flux in plasma
[DE90-618767] N90-23220
Molecular evolution in astrophysical environments N90-23291
PLASMASPHERE
Solar flares and magnetospheric particles: Investigations based upon the ONR-602 and ONR-604 experiments
[AD-A218844] N90-23332
PLASMONS
Nonreciprocal components in the 140 and 220 GHz bands utilizing magnetoplasmons on semiconducting substrates
[AD-A219136] N90-23253
PLASTIC DEFORMATION
Simulation of inelastic deformation in glassy polypropylene and polycarbonate
[AD-A218891] N90-22686
PLASTIC PROPERTIES
A study of woven fabric-reinforced composite materials using an invariant-based orthotropic plasticity formulation N90-22611
Approximate analysis for the formation of adiabatic shear bands
[AD-A218751] N90-22670
Role of shear instability in ballistic penetration
[AD-A219186] N90-22799
PLASTICS
Mechanical testing of selected engineering plastics
[DE90-008186] N90-22673
PLATES (STRUCTURAL MEMBERS)
Explicit modeling of composite plates and beams in the dynamics of multibody systems N90-23019
PLOTTING
Basic graphics routine technical manual
[AD-A219409] N90-23117
POINT DEFECTS
The effects of point defects and composition on structural phase transition
[DE90-010109] N90-23238
POINT SOURCES
More data on (possible) gamma ray (point) sources N90-23309
Spectral determinations for discrete sources with EGRET N90-23312
POINTING CONTROL SYSTEMS
Sliding control of pointing and tracking with operator spline estimation N90-22997
POLAR CAPS
A study of auroral activity in the nightside polar cap N90-22852
POLAR REGIONS
SeaRISE: A Multidisciplinary Research Initiative to Predict Rapid Changes in Global Sea Level Caused by Collapse of Marine Ice Sheets
[NASA-CP-3075] N90-22824
POLARIZED ELECTROMAGNETIC RADIATION
Scattering of a plane electromagnetic wave from a semicircular crack in a perfectly conducting ground plane
[AD-A219310] N90-22721
Stability regimes in a rotating quadrupole focusing accelerator
[AD-A219513] N90-23209

POLYCARBONATES
Simulation of inelastic deformation in glassy polypropylene and polycarbonate
[AD-A218891] N90-22686
POLYESTER RESINS
Processing of thermotropic liquid crystalline polymers and their blends
[AD-A218804] N90-22683
POLYESTERS
Synthesis and properties of a thermotropic copolyester based on 4,4 prime-dihydroxy-a,a prime-dimethylbenzalazine
[AD-A218803] N90-22682
POLYMER BLENDS
Processing of thermotropic liquid crystalline polymers and their blends
[AD-A218804] N90-22683
POLYMERIC FILMS
Electrochemical synthesis of ultrathin film composite membranes
[AD-A219041] N90-22643
High performance holographic elements and media
[AD-A218999] N90-22775
POLYMERIZATION
Polymerization of composites
[REPT-892-430-102] N90-22621
Polymerization of composite materials: A technique developed by Aerospatiale
[REPT-892-430-107] N90-22623
Dehydrogenative polymerization of silanes to polysilanes: A monomeric copper(2) siloxide
[AD-A218550] N90-22681
Theoretical studies of silicon chemistry
[AD-A219232] N90-22690
POLYMERS
Material instabilities in solids
[AD-A218451] N90-22817
POLYMORPHISM
Naturalness of polymorphism
[CS-8916] N90-23134
POLYNOMIALS
Efficient computer algebra algorithms for polynomial matrices in control design N90-23022
POLYPROPYLENE
Simulation of inelastic deformation in glassy polypropylene and polycarbonate
[AD-A218891] N90-22686
Investigation of atomistic simulation of structural and dynamic differences in glassy and liquid states of atactic poly(propylene)
[AD-A218896] N90-22687
POLYSULFIDES
Synthesis and characterization of aromatic polyester and polysiloxane containing block copolymers: Multiphase transparent atomic oxygen resistant damping materials, liquid crystal films, and toughening components of sol/gel glasses
[AD-A218871] N90-22685
POPULATION THEORY
Selecting multinomial populations
[AD-A219256] N90-23159
POPULATIONS
Selecting multinomial populations
[AD-A219256] N90-23159
POROUS MATERIALS
Electrochemical synthesis of ultrathin film composite membranes
[AD-A219041] N90-22643
PORTABLE EQUIPMENT
A compact portable diffraction moire interferometer
[DE90-009780] N90-22768
POSITION (LOCATION)
Localization of vibration in disordered nearly cyclic structures N90-22812
POSITION ERRORS
The role of orbit errors in processing of satellite altimeter data
[ETN-90-96699] N90-22575
POSITIONING
The development of a real-time decimeter-level positioning system using Global Positioning System (GPS) technology
[AD-A218695] N90-22552
Guidelines, operational procedures, and quality control for the estimation of geodetic point positions from GPS data collected with the Ti4100 receiver
[AD-A218460] N90-22829
Direction of movement effects under transformed visual/motor mappings N90-22947
Perception-action relationships reconsidered in light of spatial display instruments N90-22949
POTABLE WATER
Calcium carbonate scale dissolution in water stabilized by carbon dioxide treatment
[AD-A218502] N90-22633
POWDER (PARTICLES)
A low temperature calorimetric study of several high-T(sub c) superconductors N90-23237
POWDER METALLURGY
Elevated temperature crack growth in advanced powder metallurgy aluminum alloys N90-22653
Elevated temperature crack growth in aluminum alloys: Tensile deformation of 2618 and FVS0812 aluminum alloys N90-22654
POWER AMPLIFIERS
A free electron laser master oscillator power amplifier experiment N90-22776
POWER CONVERTERS
Programmatic status of NASA's CSTI high capacity power Stirling space power converter program
[NASA-TM-103142] N90-22606
PRE-MAIN SEQUENCE STARS
Evolutionary models of the rotating sun and implications for other low mass stars N90-23329
PREAMPLIFIERS
Apparatus for and a method of determining compass headings
[AD-D014436] N90-22551
PRECIPITATION (CHEMISTRY)
A study of mesoscale acid deposition in the lower Ohio River Valley N90-22848
PREDICTION ANALYSIS TECHNIQUES
A life prediction model for laminated composite structural components
[NASA-CR-186587] N90-22614
Inelastic response of metal matrix composites under biaxial loading N90-22661
Impact of marine boundary layer parameterization on a numerical simulation of cyclogenesis during a cold air outbreak event N90-22864
An innovations approach to decoupling of multibody dynamics and control N90-22994
Bayesian nonparametric prediction and statistical inference
[AD-A218473] N90-23154
An examination of the full-wave method for rough surface scattering
[AD-A218664] N90-23155
PREDICTIONS
A numerical and analytical study of normal stresses and pressure differences in non-Newtonian creeping flows N90-22749
An investigation of the three-dimensional flow field in a centrifugal compressor N90-22751
Predictability of weather and climate in a coupled ocean-atmosphere model: A dynamical systems approach N90-22865
Relationship between flexibility of closure and success in pilot night vision sensor system training N90-22890
Periodic ARMA models: Optimal prediction and minimum-phase condition
[REPT-89-006] N90-23131
PREMIXED FLAMES
Numerical investigation of turbulent flame sheets
[AD-A218553] N90-22635
Two-dimensional velocimetry instrumentation
[AD-A218450] N90-22774
PREPROCESSING
The preprocessed doacross loop
[NASA-CR-182056] N90-22972
PRESSURE DISTRIBUTION
Reynolds stress closure in jet flows using instability wave modeling N90-22534
Large-scale advanced propeller blade pressure distributions: Prediction and data
[NASA-TM-102316] N90-22564
Pressure and shear stress measurement uncertainty for DARPA SUBOFF experiment
[AD-A219109] N90-22798
PRESSURE EFFECTS
Design and construction of a packed column simulator operating under atmospheric and reduced pressure
[ISAL-89-60] N90-22757
The pressure loaded volumetric ceramic receiver
[DLR-MITT-89-17] N90-22842
Superconducting and normal compounds: Some high field/high pressure effects N90-23229
PRESSURE MEASUREMENT
Pressure and shear stress measurement uncertainty for DARPA SUBOFF experiment
[AD-A219109] N90-22798
PRESSURE REDUCTION
Pseudo-steady diffusional growth or collapse of bubbles rising in time dependent pressure fields
[AD-A218825] N90-22764
PRINTERS
Faster simulation plots N90-23071
PROBABILITY DISTRIBUTION FUNCTIONS
Ability distributions pattern probabilities and quasidensities
[AD-A218471] N90-23153
PROBABILITY THEORY
Probabilistic structural analysis of aerospace components using NESSUS
[NASA-TM-102364] N90-22823
A theory of Bayesian data analysis
[AD-A218420] N90-23152
Ability distributions pattern probabilities and quasidensities
[AD-A218471] N90-23153
A scattering center based numerical simulation of small scale atmospheric turbulence N90-23179
PROBLEM SOLVING
Nonstrictly hyperbolic conservation laws
[AD-A218525] N90-22762
Towards the knowledge level in SOAR: The role of the architecture in the use of knowledge
[NASA-CR-186615] N90-22897
What makes some problems hard: Explorations in the problem space of difficulty
[AD-A219002] N90-22901
Discovering problem solving strategies: What humans do and machines don't (yet)
[AD-A219008] N90-22902
Laboratory replication of scientific discovery processes
[AD-A219273] N90-22913
Hatching a theory of incubation effects
[AD-A219275] N90-22915
Non-LIFO (Last-In-First-Out) execution of cognitive procedures
[AD-A219277] N90-22916
Using deflation in the pole assignment problem with output feedback N90-23004
Linear programming tools for integer programming
[AD-A219013] N90-23106
Automated electric power management and control for Space Station Freedom
[NASA-TM-103151] N90-23125
Scientific discovery as problem solving
[AD-A218887] N90-23145
Explanation generation in expert systems (a literature review and implementation)
[AD-A218741] N90-23268
PRODUCT DEVELOPMENT
Strategy of supercomputer development N90-22981
PRODUCTIVITY
Impact of meteorology on the agricultural sector: Compilation and analysis of projects
[INPE-4846-PRE/1475] N90-22866
PROFILOMETERS
Full surface interferometric testing of grazing incidence mirrors
[AD-A219394] N90-23218
PROGRAM VERIFICATION (COMPUTERS)
A verification library for multibody simulation software N90-23089
PROGRAMMING LANGUAGES
Six-degree-of-freedom aircraft simulation with mixed-data structure using the applied dynamics simulation language, ADSIM N90-23067
Six-degree-of-freedom missile simulation using the ADI AD 100 digital computer and ADSIM simulation language N90-23068
The Durra application debugger/monitor
[AD-A219290] N90-23111
Durra: A task-level description language reference manual, version 2
[AD-A219293] N90-23114
PROJECT MANAGEMENT
The automation management to support research and development N90-22978
Methodology for analysis and simulation of large multidisciplinary problems N90-23046
PROJECT PLANNING
SeaRISE: A Multidisciplinary Research Initiative to Predict Rapid Changes in Global Sea Level Caused by Collapse of Marine Ice Sheets
[NASA-CP-3075] N90-22824
Lunar base 2 (the second thousand days of a base on the Moon)
[ILR-MITT-230(1989)] N90-22968
PROJECTILE CRATERING
Role of shear instability in ballistic penetration
[AD-A219186] N90-22799
PROJECTILES
Large-scale simulations of monolithic and segmented projectiles impacting spaced armor
[AD-A219374] N90-22800
PROP-FAN TECHNOLOGY
Investigation of advanced counterrotation blade configuration concepts for high speed turboprop systems, task 1: Ducted propfan analysis
[NASA-CR-185217] N90-22567
PROPELLANT TANKS
Large scale metrology by computer assisted photogrammetry
[REPT-892-430-116] N90-22772

PROPELLANTS
The physiological cost of wearing the propellant handler's ensemble at the Kennedy Space Center
[NASA-TM-102786] N90-22966
PROPELLER BLADES
Large-scale advanced propeller blade pressure distributions: Prediction and data
[NASA-TM-102316] N90-22564
PROPELLER FANS
Investigation of advanced counterrotation blade configuration concepts for high speed turboprop systems, task 1: Ducted propfan analysis
[NASA-CR-185217] N90-22567
PROPULSION SYSTEM CONFIGURATIONS
A candidate architecture for monitoring and control in chemical transfer propulsion systems
[NASA-TM-103161] N90-22595
PROPULSION SYSTEM PERFORMANCE
A candidate architecture for monitoring and control in chemical transfer propulsion systems
[NASA-TM-103161] N90-22595
PROTECTIVE CLOTHING
The physiological cost of wearing the propellant handler's ensemble at the Kennedy Space Center
[NASA-TM-102786] N90-22966
PROTEINS
Hanging drop crystal growth apparatus and method
[NASA-CASE-MFS-28206-1-SB] N90-23242
PROTON IRRADIATION
Influence of high energy radiation on critical parameters of superconducting ceramics YBa2Cu3O7
[DE90-620562] N90-23239
PROTONS
Study of Sn-116 via neutron pickup and proton stripping reactions
[KVI-814] N90-23199
PROTOTYPES
Evaluation of a prototype 6 tone modem
[RAE-TM-FM-28] N90-22708
PSYCHOLOGICAL FACTORS
Learning artificial grammars with competitive chunking
[AD-A219270] N90-22911
PSYCHOLOGY
A connectionist implementation of cognitive phonology
[AD-A219095] N90-22906
Hatching a theory of incubation effects
[AD-A219275] N90-22915
PSYCHOMOTOR PERFORMANCE
Human cognitive and motor performance measures under typical cool white fluorescent illumination vs relatively high cool white illuminance/irradiance lighting
[AD-A218445] N90-22892
Visual selective attention
[AD-A219204] N90-22910
Separate visual representations for perception and for visually guided behavior N90-22931
Direction of movement effects under transformed visual/motor mappings N90-22947
Motor and cognitive performance do not change during a ten-week submarine patrol
[AD-A218639] N90-22969
PSYCHOPHYSIOLOGY
Seeing by exploring N90-22923
PULSAR MAGNETOSPHERES
Gamma ray pulsars: Models and observations N90-23304
PULSARS
Radio pulsar timing observations for GRO N90-23301
Gamma radiation from radio pulsars N90-23302
Gamma radiation from the Crab and Vela pulsars N90-23303
Gamma ray pulsars: Models and observations N90-23304
The illusive Geminga: What is it N90-23307
More data on (possible) gamma ray (point) sources N90-23309
Gamma rays from pulsar wind shock acceleration N90-23311
PULSE AMPLITUDE
Experimental investigations concerning the propagation of second-sound pulses at critical heat flux
[MPIS-12/1989] N90-23182
PULSE DURATION
A multipulsed dynamic diffraction moire interferometer
[DE90-009765] N90-22723
PULSE RATE
Experimental investigations concerning the propagation of second-sound pulses at critical heat flux
[MPIS-12/1989] N90-23182
PULSED LASERS
Interaction of atomic hydrogen with pico- and femtosecond laser pulses
[AD-A218426] N90-22785
Frequency domain techniques for analyzing picosecond optical pulses
[AD-A218856] N90-23214
PULTRUSION
Pultrusion process development for long space boom model
[NASA-TM-4017] N90-22628
PURITY
Improvement study of iron disilicide thermoelectric materials
[AD-A218946] N90-22844
PYROTECHNICS
Qualification test rationale for measuring the resistance of equipment to pyrotechnic shock
[REPT-892-430-117] N90-22590
Ignition testing of low-energy laser diode ignited components
[DE90-009968] N90-22630
Pyrotechnic materials ignited using lasers. High energy photopyrotechnic chains
[REPT-892-430-121] N90-22691

Q

QUALITY CONTROL
Guidelines, operational procedures, and quality control for the estimation of geodetic point positions from GPS data collected with the TI4100 receiver
[AD-A218460] N90-22829
Full surface interferometric testing of grazing incidence mirrors
[AD-A219394] N90-23218
QUANTITATIVE ANALYSIS
Characterization of Monel alloys by x ray fluorescence technique
[DE90-617175] N90-22665
QUANTUM CHROMODYNAMICS
Mixing of DIS operators in lattice QCD
[PREPRINT-708] N90-23243
Lattice field theory
[PREPRINT-719] N90-23245
QUANTUM COUNTERS
Quantum non-demolition stroboscopic observables and multipumping back-action evasion schemes
[PREPRINT-699] N90-23260
Are quantum measurements on macroscopic bodies feasible
[PREPRINT-700] N90-23261
QUANTUM EFFICIENCY
Development of a unique laboratory standard indium gallium arsenide detector for the 500 to 1700 micron spectral region, phase 2
[NASA-CR-180482] N90-22767
QUANTUM ELECTRODYNAMICS
Quantum non-demolition stroboscopic observables and multipumping back-action evasion schemes
[PREPRINT-699] N90-23260
QUANTUM MECHANICS
Quantum mechanics in Riemannian space-time
[DE90-620448] N90-23257
QUANTUM OPTICS
Classification techniques for quantum-limited and classical-intensity images
[AD-A218693] N90-23212
QUANTUM WELLS
Optical properties of novel GaAs-based semiconductors N90-23235
QUARK MODELS
The number of neutrino species, confronted with the results at the recent Lepton-Photon Symposium (August 7-12, 1989)
[NOTA-INTERNA-940] N90-23195
QUARKS
Quark-antiquark pair production via gamma W fusion at high energy e(+)e(-) colliders
[PREPRINT-705] N90-23205
QUASARS
Spectral plane quasars, spectral turn-over, and frequency atlas
[INPE-5011-TDL/399] N90-23277
Skewering the universe with QSO lines of sight: Lyman alpha clouds as probes of large scale structure N90-23278
Spectroscopic observations of high redshift QSOs: Galaxies and the intergalactic medium at early epochs N90-23280
The dynamical evolution of dense clusters of compact stars N90-23287
Studies in gravitational lensing and numerical hydrodynamics N90-23290
Gamma rays from active galactic nuclei N90-23316
The high energy source 3C 273 N90-23318
QUERY LANGUAGES
Object-oriented query languages: The notion and the issues
[REPT-89-054] N90-23093
QUEUEING THEORY
An approximation for the response time of an open CP-disk system
[MEMO-COSOR-89-19] N90-23266

R

RADAR DETECTION
Intelligent signal processing techniques for multi-sensor surveillance systems
[AD-A218890] N90-22895
RADAR EQUIPMENT
Design options for space-based radar systems
[ETN-90-96548] N90-22710
RADAR IMAGERY
Spaceborne radar observations: A guide for Magellan radar-image analysis
[NASA-CR-184998] N90-22626
RADAR RECEIVERS
Specification for environmental measurements to assess radar sensors
[AD-A219127] N90-22833
RADAR TRACKING
Determination of the general ocean circulation using satellite altimetry from a simultaneous solution for the Earth's gravity field N90-22569
Intelligent signal processing techniques for multi-sensor surveillance systems
[AD-A218890] N90-22895
RADIAL FLOW
Activation uniformity dependence of undoped semi-insulating GaAs on post-implant annealing conditions
[ETN-90-96549] N90-23246
RADIATION
Shaping radiation pattern of excimer laser by means of controllable intracavity mirror N90-23166
RADIATION ABSORPTION
The pressure loaded volumetric ceramic receiver
[DLR-MITT-89-17] N90-22842
RADIATION DAMAGE
Center for surface radiation damage studies
[AD-A218452] N90-22678
A study of low level laser retinal damage
[AD-A218919] N90-22887
RADIATION DISTRIBUTION
The diffuse galactic gamma ray emission N90-23296
RADIATION EFFECTS
High Intensity Electro-Magnetic and Ultrasonic Effects on Inorganic Materials Behavior and Processing Workshop
[AD-A218884] N90-22640
Laser retinal effects: Electrophysiological determination in visual cortical cells of monkeys and cats
[AD-A218937] N90-22888
Exposure of human cells to electromagnetic fields
[AD-A219377] N90-22889
Influence of high energy radiation on critical parameters of superconducting ceramics YBa2Cu3O7
[DE90-620562] N90-23239
RADIATION HARDENING
Burnout thresholds and cross section of power MOS transistors with heavy ions
[AD-A218998] N90-22736
RADIATION SOURCES
COS-B gamma ray sources beyond the predicted diffuse emission N90-23308
RADIATIVE TRANSFER
Spectral measurements of the cosmic microwave background N90-23334
RADIO ASTRONOMY
Molecular clouds and the large-scale structure of the galaxy N90-23295
RADIO EQUIPMENT
Executive summary for the network assessment model
[AD-A218762] N90-22718
RADIO FREQUENCIES
HF propagation through actively modified ionospheres
[DE90-008931] N90-22705
RADIO OBSERVATION
Radio pulsar timing observations for GRO N90-23301
RADIO RECEIVERS
Construction of a 345 gigahertz receiver based on superconducting tunnel junctions
[AD-A218781] N90-22735
RADIO SIGNALS
Optical excisor modeling
[AD-A219338] N90-22722

RADIO TELEMETRY
Multimedia system control
[AD-A219392] N90-22971
RADIO TRANSMISSION
Preliminary results of the peak experiment. ALTAIR deep-space measurements
[AD-A218622] N90-22714
RADIOACTIVE MATERIALS
National emissions standards for hazardous air pollutants application for approval of construction SP-100 ground engineering system test site
[DE90-007985] N90-23203
RADIOACTIVE WASTES
Transport of gases through concrete
[AERE-G-4977] N90-22747
RADIOGRAPHY
Real-time stereo-microradiography
[AD-A218433] N90-22805
RAMAN SPECTRA
Nonlinear spectroscopy of multicomponent droplets and 2- and 3-dimensional measurements in flames
[AD-A218569] N90-22636
Low frequency Raman spectra of liquid water, a molecular dynamics simulation
[PREPRINT-696] N90-23192
RANDOM ACCESS
Locality in parallel computation
[AD-A218733] N90-23120
RANDOM NOISE
Parallel and vector computation for stochastic optimal control applications N90-23007
RANDOM NUMBERS
On randomness of random number generators
[MEMO-COSOR-89-20] N90-23151
RANDOM PROCESSES
On randomness of random number generators
[MEMO-COSOR-89-20] N90-23151
Control of randomly sampled robotic systems
[AD-A218948] N90-23157
RANDOM SIGNALS
Time-varying filter modelling and time-frequency characterisation of nonstationary sound fields due to a moving source N90-23178
RARE EARTH ELEMENTS
Excitation of hypersound at boundary between Type-2 superconductor and a concentrated paramagnetic compound N90-23164
RAREFIED GASES
The aerodynamic characteristics of power-law bodies in continuum and transitional hypersonic flow
[RAE-TM-AERO-2164] N90-22537
RATS
Heat exhaustion in a rat model: Lithium as a biochemical probe
[AD-A219361] N90-22884
RAY TRACING
The effects of caustics in acoustic inverse scattering experiments
[AD-A218454] N90-23185
Some ray tracing problems related to circles and ellipses
[AD-A219306] N90-23217
RAYLEIGH-RITZ METHOD
The coupling effects of kinematics and flexibility on the Lagrangian dynamic formulation of open chain deformable links N90-23018
REACTION KINETICS
Modeling of combustion processes in a solid fuel particle
[DE90-009140] N90-22629
Investigation of the reaction kinetics between SiC fibers and selectively alloyed titanium matrix composites and determination of their mechanical properties N90-22659
An effective He-3 nucleon force for the He-3, t) charge exchange reaction
[KVI-813] N90-23198
Incomplete fusion reactors at low and intermediate energies
[KVI-809] N90-23206
REACTIVITY
Investigation of optical nonlinearities, conductivity and magnetism in organometallic materials
[AD-A218548] N90-23211
REACTOR SAFETY
National emissions standards for hazardous air pollutants application for approval of construction SP-100 ground engineering system test site
[DE90-007985] N90-23203
REACTOR TECHNOLOGY
Incomplete fusion reactors at low and intermediate energies
[KVI-809] N90-23206
REAL TIME OPERATION
The development of a real-time decimeter-level positioning system using Global Positioning System (GPS) technology
[AD-A218695] N90-22552
Inertial navigation system simulator: Behavioral specification, revision
[AD-A219294] N90-22554
Model-based method for terrain-following display design
[AD-A219302] N90-22563
Automated star pattern recognition N90-22612
Using object-oriented analysis techniques to support system testing
[DE90-009540] N90-22700
Real-time stereo-microradiography
[AD-A218433] N90-22805
The perception of geometrical structure from congruence N90-22935
Interactive displays in medical art N90-22940
Parallel processing of real-time dynamic systems simulation on OSCAR (Optimally SCheduled Advanced multiprocessoR) N90-23006
Computational dynamics for robotics systems using a non-strict computational approach N90-23011
An algorithm for the solution of dynamic linear programs N90-23026
A finite element based method for solution of optimal control problems N90-23027
Space station dynamics, attitude control and momentum management N90-23029
Proceedings of the 3rd Annual Conference on Aerospace Computational Control, volume 2
[NASA-CR-186447] N90-23040
A real time, FEM based optimal control algorithm and its implementation using parallel processing hardware (transistors) in a microprocessor environment N90-23066
Six-degree-of-freedom aircraft simulation with mixed-data structure using the applied dynamics simulation language, ADSIM N90-23067
Real-time closed-loop simulation and upset evaluation of control systems in harsh electromagnetic environments N90-23069
JPL control/structure interaction test bed real-time control computer architecture N90-23070
Comparative evaluations of four specification methods for real-time systems
[AD-A219187] N90-23109
DARK (Distributed Ada Real-Time Kernel) porting and extension guide Kernel version 3.0
[AD-A219291] N90-23112
Version description and installation guide Kernel version 3.0
[AD-A219292] N90-23113
Durra: A task-level description language reference manual, version 2
[AD-A219293] N90-23114
Controlling real-time systems with parallel processes
[CS-8918] N90-23119
Experimental adaptive control of a hydraulic robot N90-23121
RECEIVERS
Agile multiple aperture imager receiver development
[AD-A218956] N90-23215
RECEPTORS (PHYSIOLOGY)
Transduction of nanovolt signals: Limits of electric-field detection
[AD-A219214] N90-23177
RECOMBINATION REACTIONS
Experimental evaluation of chemical cleaning processes for high-lifetime silicon processing
[DE90-009332] N90-22699
RECTANGULAR PLATES
Flat plate vibration analysis experimental and numerical fillet study
[AD-A218789] N90-22818
RECURSIVE FUNCTIONS
A decoupled recursive approach for constrained flexible multibody system dynamics N90-23042
Naturalness of polymorphism
[CS-8916] N90-23134
RED SHIFT
Spectroscopic observations of high redshift QSOs: Galaxies and the intergalactic medium at early epochs N90-23280
REDUCED GRAVITY
Microgravity, the space application of the 21st century. Challenges, constraints, and strategies
[REPT-892-430-105] N90-22696
REDUNDANCY
An inverse kinematics algorithm for a highly redundant variable-geometry-truss manipulator N90-23033
REENTRY SHIELDING
SIMOUN: An optimized supersonic high temperature wind tunnel for testing construction materials to be used on the spaceplane
[REPT-892-430-111] N90-22572
REENTRY VEHICLES
Earth-to-orbit vehicle providing a reusable orbital stage
[NASA-CASE-LAR-13486-1] N90-22584
REFLECTANCE
Image segmentation with detection of highlights and inter-reflections using color
[AD-A218710] N90-23213
REFLECTION
Some ray tracing problems related to circles and ellipses
[AD-A219306] N90-23217
REFLECTOR ANTENNAS
Dynamics and control of tethered antennas/reflectors in orbit
[AD-A219316] N90-22594
REFLECTORS
Solar Concentrator Advanced Development Program
[NASA-CR-185173] N90-22834
REFRACTED WAVES
Evidence for self-refraction in a convergence zone: NPE (Nonlinear progressive wave equation) model results
[AD-A218546] N90-22879
REFRACTING TELESCOPES
Hybrid diffractive-refractive telescope
[AD-A219241] N90-23216
REFRACTION
Specification for environmental measurements to assess radar sensors
[AD-A219127] N90-22833
REFRACTIVITY
A scattering center based numerical simulation of small scale atmospheric turbulence N90-23179
REFRACTORY MATERIALS
Approximate analysis for the formation of adiabatic shear bands
[AD-A218751] N90-22670
Recent advances in nondestructive evaluation made possible by novel uses of video systems
[NASA-TM-102491] N90-22801
REFRIGERATING
A theoretical and experimental investigation of an absorption refrigeration system for application with solar energy units N90-22697
REGENERATION (ENGINEERING)
A comparison between experiment and simulation for concept VIC regenerative liquid propellant guns. Part 1: 30 mm
[AD-A218556] N90-22692
REGENERATIVE FUEL CELLS
Viscosity, density and conductivity of ImCl(HCl) sub 1.3
[AD-A218902] N90-22641
REGRESSION ANALYSIS
Relationship between flexibility of closure and success in pilot night vision sensor system training N90-22890
REINFORCED PLASTICS
Mechanical testing of selected engineering plastics
[DE90-008186] N90-22673
RELATIVISTIC EFFECTS
Relativistic corrections to He-3 photodisintegration sum rules
[NOTA-INTERNA-942] N90-23197
RELATIVITY
Background connection: A necessary object in general relativity
[DE90-620463] N90-23258
RELIABILITY ANALYSIS
Study and sizing of bonded joints in space structures
[REPT-892-430-124] N90-22591
A numerical and analytical study of normal stresses and pressure differences in non-Newtonian creeping flows N90-22749
RELIABILITY ENGINEERING
Excess noise, anomalous effects and reliability of high frequency devices (Schottky diodes, MESFET and HEMT)
[LAAS-89-394] N90-22728
RELIC RADIATION
Gamma ray cosmology: The extra galactic gamma spectrum and methods to detect the underlying source N90-23321
REMOTE MANIPULATOR SYSTEM
Multi-axis control of telemanipulators N90-22943
Space station dynamics, attitude control and momentum management N90-23029
REMOTE SENSING
HCl Vapor Characterization and Detection. JANNAF Safety and Environmental Protection Subcommittee Workshop
[AD-A216252] N90-22596

Measurement of HCl by near-infrared diode laser absorption N90-22601

REMOTE SENSORS
MEGALIDAR proof-of-concept demonstration [AD-A218787] N90-22858

REPLICAS
Replica scaling analysis of interfaces in random media [PREPRINT-713] N90-23174

REQUIREMENTS
Visual behavior in the F-15 simulator for air-to-air combat [AD-A218648] N90-22893

RESEARCH AND DEVELOPMENT
Microgravity, the space application of the 21st century. Challenges, constraints, and strategies [REPT-892-430-105] N90-22696
The automation management to support research and development N90-22978
JPRS report: Science and technology. USSR: Physics and mathematics [JPRS-UPM-89-001] N90-23162
Research and applications of metallic superlattices, high T(sub c) superconductors, x ray optics, and compact synchrotrons N90-23170

RESEARCH MANAGEMENT
Aircraft technology management and the related significance of the supercomputer N90-22975

RESIDUAL STRENGTH
Boeing/NASA composite components flight service evaluation [NASA-CR-181898] N90-22609

RESIDUAL STRESS
Axisymmetric and cylindrically orthotropic analysis of filament winding N90-22811

RESIN MATRIX COMPOSITES
Pultrusion process development for long space boom model [NASA-TM-4017] N90-22628

RESONANCE
Bifurcational aspects of parametric resonance [W-8904] N90-22730

RESONANT FREQUENCIES
Differential equation based method for accurate approximations in optimization [NASA-TM-102639] N90-22558
Model reduction for flexible spacecraft with clustered natural frequencies N90-23054
Multibody dynamics: Modeling component flexibility with fixed, free, loaded, constraint, and residual modes N90-23072
Structural modeling for control design (articulated multibody component representation) N90-23077
Mini-mast dynamic analysis using the truss-beam model N90-23087
Shaping radiation pattern of excimer laser by means of controllable intracavity mirror N90-23166
Numerical studies of the active control of sound transmission through double partitions [ISVR-TR-183] N90-23181

RESONANT VIBRATION
Forcing function effects on rotor row unsteady aerodynamic response in a multistage compressor N90-22536

RESOURCE ALLOCATION
Automated electric power management and control for Space Station Freedom [NASA-TM-103151] N90-23125

RESPIRATORY RATE
ELF (Extremely Low Frequency) communications system ecological monitoring program: Slime mold studies [AD-A218623] N90-22715

RESPONSE BIAS
An approximation for the response time of an open CP-disk system [MEMO-COSOR-89-19] N90-23266

RESPONSE TIME (COMPUTERS)
Multigrid acceleration of transonic flow computations [ENSM-8024] N90-22760
Cognitive efficiency considerations for good graphic design [AD-A218976] N90-22899

RETINA
A study of low level laser retinal damage [AD-A218919] N90-22887
Laser retinal effects: Electrophysiological determination in visual cortical cells of monkeys and cats [AD-A218937] N90-22888

RETINAL IMAGES
Paradoxical monocular stereopsis and perspective vergence N90-22922
Exocentric direction judgements in computer-generated displays and actual scenes N90-22936
Interactions of form and orientation N90-22958

REUSABLE ROCKET ENGINES
Earth-to-orbit vehicle providing a reusable orbital stage [NASA-CASE-LAR-13486-1] N90-22584

REUSE
A tool for aiding in the reuse of software [INPE-4981-PRE/1545] N90-23091

REYNOLDS STRESS
Reynolds stress closure in jet flows using instability wave modeling N90-22534

RHEOLOGY
Rheology of injection mould filling with DMCs [NPL-DMA(A)-196] N90-22675

RIBONUCLEIC ACIDS
Exposure of human cells to electromagnetic fields [AD-A219377] N90-22889

RICCATI EQUATION
On a fallacious conjecture about the stabilizability properties of solutions of the Riccati difference equation [REPT-89-007] N90-23132

RIEMANN MANIFOLD
Effective action for induced gravity on a 2-dimensional manifold [PREPRINT-712] N90-23173
Quantum mechanics in Riemannian space-time [DE90-620448] N90-23257

RIGID STRUCTURES
Nonlinear strain-displacement relations and flexible multibody dynamics N90-23014

RING LASERS
Dynamics and instabilities in homogeneously broadened lasers [AD-A218427] N90-22786

RIVERS
Fundamental studies on hydrology, hydraulics and geometry of river networks [AD-A218662] N90-22830
Accuracy and precision of GOES data collection platforms for temperature measurements [AD-A218798] N90-22832
A study of mesoscale acid deposition in the lower Ohio River Valley N90-22848

ROBOT ARMS
An order (n) algorithm for the dynamics simulation of robotic systems N90-22990
Recursive linearization of multibody dynamics equations of motion N90-22993
A robot arm simulation with a shared memory multiprocessor machine N90-23008
An inverse kinematics algorithm for a highly redundant variable-geometry-truss manipulator N90-23033
On trajectory generation for flexible space crane: Inverse dynamics analysis by LATDYN N90-23037
Parallel conjugate gradient algorithms for manipulator dynamic simulation N90-23045
Man-in-the-control-loop simulation of manipulators N90-23063

ROBOT DYNAMICS
Determination of joint drives for stable end-effector motion in flexible robotic systems N90-23034

ROBOTICS
An assessment of multibody simulation tools for articulated spacecraft N90-22988
Spatial operator algebra framework for multibody system dynamics N90-22989
An order (n) algorithm for the dynamics simulation of robotic systems N90-22990
Systematic generation of multibody equations of motion suitable for recursive and parallel manipulation N90-22992
An innovations approach to decoupling of multibody dynamics and control N90-22994
Efficient dynamic simulation for multiple chain robotic mechanisms N90-22995
A robot arm simulation with a shared memory multiprocessor machine N90-23008
Computational dynamics for robotics systems using a non-strict computational approach N90-23011
Optimum control forces for multibody systems with intermittent motion N90-23016
Development of efficient computer program for dynamic simulation of telerobotic manipulation N90-23017
Explicit modeling of composite plates and beams in the dynamics of multibody systems N90-23019
Modeling of control forces for kinematical constraints in the dynamics of multibody systems: A new approach N90-23031
Characterization of robotics parallel algorithms and mapping onto a reconfigurable SIMD machine N90-23039
Control of randomly sampled robotic systems [AD-A218948] N90-23157

ROBOTS
Plan execution control and architecture for mobile robots [LAAS-89-371] N90-22793
Telepresence, time delay, and adaptation N90-22944
An order (n) algorithm for the dynamics simulation of robotic systems N90-22990
Aspects of efficient and reliable multibody system simulation N90-22991
An innovations approach to decoupling of multibody dynamics and control N90-22994
Efficient dynamic simulation for multiple chain robotic mechanisms N90-22995
Computational dynamics for robotics systems using a non-strict computational approach N90-23011
Development of efficient computer program for dynamic simulation of telerobotic manipulation N90-23017
Experimental adaptive control of a hydraulic robot N90-23121

ROBUSTNESS (MATHEMATICS)
Multivariate analysis of launcher guidance robustness [REPT-892-422-105] N90-22581
A survey on the structured singular value N90-22998
Algorithms for computing the multivariable stability margin N90-22999
Robustness analysis for real parametric uncertainty N90-23000
Modern CACSD using the Robust-Control Toolbox N90-23024
A methodology for formulating a minimal uncertainty model for robust control system design and analysis N90-23028
Multivariable frequency weighted model order reduction for control synthesis [AIAA-89-3558] N90-23060
Robust adaptive control: Stability and asymptotic performance [AD-A219259] N90-23127

ROCK MECHANICS
Geothermal energy program summary [DE89-009486] N90-22838

ROCKET ENGINE CASES
Qualification of the RSRM case membrane case-to-insulation bondline inspection using the Thiokol Corporation ultrasonic RSRM bondline inspection system [NASA-CR-183940] N90-22602
Qualification of the RSRM field joint CF case-to-insulation bondline inspection using the Thiokol Corporation ultrasonic RSRM bondline inspection system [NASA-CR-183931] N90-22788

ROCKET EXHAUST
HCl Vapor Characterization and Detection. JANNAF Safety and Environmental Protection Subcommittee Workshop [AD-A216252] N90-22596

ROCKET LININGS
Cooling of rocket thrust chambers with liquid oxygen [NASA-TM-103146] N90-22605

ROCKET PROPELLANTS
Experimental studies on energy storage [AD-A219032] N90-22845

ROOM TEMPERATURE
Comparison of solar pumped Nd:YAG and Nd:Cr:GSGG lasers at liquid nitrogen and room temperature [DLR-FB-89-41] N90-22781

ROOT-MEAN-SQUARE ERRORS
Minimum attainable RMS attitude error using co-located rate sensors N90-23038

ROSS ICE SHELF
On the effectiveness of the production of antarctic bottom water in the Weddell and Ross Seas [AD-A218873] N90-22880

ROTARY STABILITY
Stability regimes in a rotating quadrupole focusing accelerator [AD-A219513] N90-23209

ROTATING STALLS
Computational and experimental investigations of rotating stall in compressor cascades N90-22565
An investigation of the three-dimensional flow field in a centrifugal compressor N90-22751

ROTATION
Atmospheric autorotating imaging device [NASA-CASE-NPO-17390-1-CU] N90-22769
Direction of movement effects under transformed visual/motor mappings N90-22947
Multi-flexible-body dynamics capturing motion-induced stiffness N90-23013
Counterrotating cores in elliptical galaxies N90-23288

ROTOR AERODYNAMICS
Forcing function effects on rotor row unsteady aerodynamic response in a multistage compressor N90-22536

ROTOR BLADES (TURBOMACHINERY)
Forcing function effects on rotor row unsteady aerodynamic response in a multistage compressor N90-22536

ROTOR DYNAMICS
Elements of active vibration control for rotating machinery
[NASA-TM-102368] N90-22703
ROTORS
Application of a dynamic stall model to rotor trim and aeroelastic response N90-22556
Computational and experimental investigations of rotating stall in compressor cascades N90-22565
RUN TIME (COMPUTERS)
The preprocessed doacross loop
[NASA-CR-182056] N90-22972
Faster simulation plots N90-23071
The Durra application debugger/monitor
[AD-A219290] N90-23111
RURAL AREAS
Development and use of a passive technique for measuring nitrogen dioxide in the background atmosphere N90-23285
RUTHENIUM COMPOUNDS
Catalysts for ultrahigh current density oxygen cathodes for space fuel cell applications
[NASA-CR-180650] N90-22835

S

SACCADIC EYE MOVEMENTS
Separate visual representations for perception and for visually guided behavior N90-22931
SAFETY
HCl Vapor Characterization and Detection. JANNAF Safety and Environmental Protection Subcommittee Workshop
[AD-A216252] N90-22596
SAMPLING
Development and use of a passive technique for measuring nitrogen dioxide in the background atmosphere N90-23285
COS-B gamma ray sources beyond the predicted diffuse emission N90-23308
SATELLITE ALTIMETRY
Determination of the general ocean circulation using satellite altimetry from a simultaneous solution for the Earth's gravity field N90-22569
The role of orbit errors in processing of satellite altimeter data
[ETN-90-96699] N90-22575
Surface topography of the Greenland Ice Sheet from satellite radar altimetry
[NASA-SP-503] N90-22850
SATELLITE ANTENNAS
The effect of mechanical deformation on the radiation patterns of large space-based arrays
[AD-A219288] N90-22719
SATELLITE CONFIGURATIONS
The Italian approach to small satellites for low cost access to space developments
[ETN-90-96552] N90-22587
Low cost station keeping maneuvers for a small-satellites constellation in tundra orbits
[ETN-90-96553] N90-22588
SATELLITE CONTROL
Orbit acquisition and control strategy for small satellites in inclined eccentric orbits
[ETN-90-96551] N90-22573
SATELLITE DRAG
Orbital mechanics: A learning tool on the main frame
[AD-A218799] N90-22576
SATELLITE IMAGERY
A case for archaeological reconnaissance of the Cabo Catoche-Porvenir region of the northeastern Yucatan Peninsula
[NASA-TM-102248] N90-22827
Tropical squall lines of the Arizona monsoon N90-22867
The analysis of polar clouds from AVHRR satellite data using pattern recognition techniques
[NASA-CR-183300] N90-22868
SATELLITE OBSERVATION
A case for archaeological reconnaissance of the Cabo Catoche-Porvenir region of the northeastern Yucatan Peninsula
[NASA-TM-102248] N90-22827
Anderson Mesa, Arizona as a site for an optical interferometric array N90-23281
SATELLITE ORBITS
Orbit acquisition and control strategy for small satellites in inclined eccentric orbits
[ETN-90-96551] N90-22573
The role of orbit errors in processing of satellite altimeter data
[ETN-90-96699] N90-22575
Satellite motion in axi-symmetric gravitational field. Part 2: Perturbations due to an arbitrary J(sub l)
[RAE-TR-89022] N90-22586
Low cost station keeping maneuvers for a small-satellites constellation in tundra orbits
[ETN-90-96553] N90-22588
SATELLITE ORIENTATION
Spacecraft attitude impacts on COLD-SAT non-vacuum jacketed LH2 supply tank thermal performance
[NASA-TM-103158] N90-22592
SATELLITE ROTATION
Concurrent processing simulation of the space station N90-23041
SATELLITE TEMPERATURE
Spacecraft attitude impacts on COLD-SAT non-vacuum jacketed LH2 supply tank thermal performance
[NASA-TM-103158] N90-22592
SATELLITE-BORNE INSTRUMENTS
Complementary information from mm-wave-, infrared-, and gamma ray astronomy N90-23299
SCALARS
The multifractal nature of turbulence N90-22752
SCALE (CORROSION)
Improved high temperature oxidation behavior of alloys by ion implantation
[AERE-R-13309] N90-22650
SCANNERS
Qualification of the RSRM case membrane case-to-insulation bondline inspection using the Thiokol Corporation ultrasonic RSRM bondline inspection system
[NASA-CR-183940] N90-22602
Atmospheric autorotating imaging device
[NASA-CASE-NPO-17390-1-CU] N90-22769
Qualification of the RSRM field joint CF case-to-insulation bondline inspection using the Thiokol Corporation ultrasonic RSRM bondline inspection system
[NASA-CR-183931] N90-22788
Volumetric visualization of 3D data N90-22964
SCATTERING
An examination of the full-wave method for rough surface scattering
[AD-A218664] N90-23155
A scattering center based numerical simulation of small scale atmospheric turbulence N90-23179
Optical properties of novel GaAs-based semiconductors N90-23235
VLA and VLBI angular broadening measurements: The distribution of interstellar scattering at low Galactic latitudes N90-23279
SCENE ANALYSIS
Exocentric direction judgements in computer-generated displays and actual scenes N90-22936
SCHEDULING
Parallel processing of real-time dynamic systems simulation on OSCAR (Optimally SCheduled Advanced multiprocessoR) N90-23006
SCHOTTKY DIODES
Excess noise, anomalous effects and reliability of high frequency devices (Schottky diodes, MESFET and HEMT)
[LAAS-89-394] N90-22728
Continued development and characterization of doped layers, contacts, and associated electronic devices in silicon carbide
[AD-A219211] N90-22737
Investigation of Schottky barriers
[AD-A218422] N90-23247
SCHROEDINGER EQUATION
A posterior stochastic equation for quantum Brownian motion
[PREPRINT-715] N90-23194
SCIENTIFIC SATELLITES
Spacecraft attitude impacts on COLD-SAT non-vacuum jacketed LH2 supply tank thermal performance
[NASA-TM-103158] N90-22592
SCINTILLATION
Preliminary results of the peak experiment. ALTAIR deep-space measurements
[AD-A218622] N90-22714
SEA ICE
SeaRISE: A Multidisciplinary Research Initiative to Predict Rapid Changes in Global Sea Level Caused by Collapse of Marine Ice Sheets
[NASA-CP-3075] N90-22824
SEA LEVEL
SeaRISE: A Multidisciplinary Research Initiative to Predict Rapid Changes in Global Sea Level Caused by Collapse of Marine Ice Sheets
[NASA-CP-3075] N90-22824
SEA SURFACE TEMPERATURE
Monthly surface thermal forcing in the tropical Pacific from 1980 to 1983
[NASA-CR-183033] N90-22877
SEALERS
Seal requirements in rocket propulsion
[ETN-90-96611] N90-22580
SEALING
Seal requirements in rocket propulsion
[ETN-90-96611] N90-22580
SEATS
The application of a non-linear least squares method to predicting seat transmissibility
[ISVR-TR-173] N90-22967
SEISMIC ENERGY
Regional studies with broadband data
[AD-A219215] N90-22861
SEISMIC WAVES
Propagation and attenuation of Lg waves in South America
[AD-A218853] N90-22859
Regional studies with broadband data
[AD-A219215] N90-22861
Seismic wave propagation, attenuation and scattering over regional distances
[AD-A219358] N90-22862
Measurements of high frequency seismic waves
[AD-A219370] N90-22863
SEISMOGRAMS
Calculation of 3-dimensional synthetic seismograms on the connection machine
[AD-A218472] N90-22857
SEISMOLOGY
Temporal attributes of the ambient seismo-acoustic environment: La Junta, Colorado
[AD-A219369] N90-22825
Seismic wave propagation, attenuation and scattering over regional distances
[AD-A219358] N90-22862
Measurements of high frequency seismic waves
[AD-A219370] N90-22863
SEMANTICS
Connectionism and compositional semantics
[AD-A219029] N90-22904
Durra: A task-level description language reference manual, version 2
[AD-A219293] N90-23114
Syntax, semantics, and pragmatism: An integrated focus based on textual linguistic knowledge
[INPE-4992-PRE/1554] N90-23262
SEMICONDUCTING FILMS
Scanning laser photocurrent spectroscopy of electrochemically grown bismuth sulphide films
[AERE-M-3709] N90-22649
SEMICONDUCTOR DEVICES
Lateral spreading of Au contacts on InP
[NASA-TM-103133] N90-22843
Electronic theory of solids, surfaces, interfaces, and clusters N90-23230
SEMICONDUCTOR JUNCTIONS
Direct implantation process development and characterization in advanced Hg(1)-(x)Cd(x) Te EPI layers
[AD-A219133] N90-23252
SEMICONDUCTOR LASERS
Measurement of HCl by near-infrared diode laser absorption N90-22601
Ignition testing of low-energy laser diode ignited components
[DE90-009968] N90-22630
SEMICONDUCTORS (MATERIALS)
Reactions of laser-generated free radicals at semiconductor surfaces
[AD-A218552] N90-22733
Improvement study of iron disilicide thermoelectric materials
[AD-A218946] N90-22844
Acoustoelectronic interaction of surface waves in GaAs-InGaAs superlattices N90-23163
Superconducting and normal compounds: Some high field/high pressure effects N90-23229
Optical properties of novel GaAs-based semiconductors N90-23235
Investigation of Schottky barriers
[AD-A218422] N90-23247
Measurement of localized deep levels and wafer non-uniformities at 3-5 semiconductor heterojunctions
[AD-A218547] N90-23248
Nonreciprocal components in the 140 and 220 GHz bands utilizing magnetoplasmons on semiconducting substrates
[AD-A219136] N90-23253
SENSITIZING
A study of the relation between grain boundary type and sensitisation in a partially-sensitised AISI 304 stainless steel using electron back-scattering patterns
[AERE-R-13327] N90-23234
SENSORIMOTOR PERFORMANCE
Telepresence, time delay, and adaptation N90-22944
A commentary on perception-action relationships in spatial display instruments N90-22950

SENSORY DISCRIMINATION
Auditory spectro-temporal pattern analysis
[AD-A218416] N90-23184
SENSORY FEEDBACK
Paradoxical monocular stereopsis and perspective vergence N90-22922
Seeing by exploring N90-22923
Adapting to variable prismatic displacement N90-22945
Sensory conflict in motion sickness: An observer theory approach N90-22957
Voluntary presetting of the vestibular ocular reflex permits gaze stabilization despite perturbation of fast head movements N90-22960
SENSORY PERCEPTION
Stochastic interactive activation and the effect of context on perception
[AD-A218929] N90-22898
Transduction of nanovolt signals: Limits of electric-field detection
[AD-A219214] N90-23177
SEPARATED FLOW
Three-dimensional separated flow prediction on fusiform body using Euler and boundary layer methods N90-22745
SEPARATORS
Electrochemical synthesis of ultrathin film composite membranes
[AD-A219041] N90-22643
SEQUENCING
Encoding sequential structure in simple recurrent networks
[AD-A218928] N90-22984
SERIES EXPANSION
Effect on relaxation on nonlinear waves in crystals N90-23165
SERVICE LIFE
Boeing/NASA composite components flight service evaluation
[NASA-CR-181898] N90-22609
SERVOCONTROL
Equipment specifications for launcher guidance using multivariable frequency methods
[REPT-892-422-106] N90-22582
SERVOMECHANISMS
Experimental adaptive control of a hydraulic robot N90-23121
SEYFERT GALAXIES
Spectral evolution of active galactic nuclei Penrose Compton scattering processes and gamma ray emission from Seyfert galaxies N90-23317
The high energy source 3C 273 N90-23318
SH WAVES
A 2-D analysis of particle velocity and stress of SH waves from a strip radiator. An experimental verification of both amplitude and phase using EMA transducers
[AERE-R-12600] N90-22704
Propagation and attenuation of Lg waves in South America
[AD-A218853] N90-22859
SHAFTS (MACHINE ELEMENTS)
Thermal/structural analysis of the shaft-disk region of a fan drive system
[NASA-TM-101687] N90-22807
SHAPES
The minimum drag profile in laminar flow: A numerical way N90-22535
An experimental study of tip shape effects on the flutter of aft-swept, flat-plate wings
[NASA-TM-4180] N90-22555
Exocentric direction judgements in computer-generated displays and actual scenes N90-22936
SHEAR FLOW
Flow visualization in supersonic turbulent boundary layers N90-22533
Analysis of velocity and temperature fluctuations in turbulent shear flows N90-22744
Transactions of the Seventh Army Conference on Applied Mathematics and Computing
[AD-A219220] N90-23160
SHEAR PROPERTIES
Approximate analysis for the formation of adiabatic shear bands
[AD-A218751] N90-22670
Role of shear instability in ballistic penetration
[AD-A219186] N90-22799
SHEAR STRAIN
Two-dimensional surface strain measurement based on a variation of Yamaguchi's laser-speckle strain gauge
[NASA-TM-103162] N90-22784
SHEAR STRESS
Large deformation analysis of laminated composite structures by a continuum-based shell element with transverse deformation N90-22613
Pressure and shear stress measurement uncertainty for DARPA SUBOFF experiment
[AD-A219109] N90-22798
A numerical study of basic coastal upwelling processes N90-22878
SHELL THEORY
Large deformation analysis of laminated composite structures by a continuum-based shell element with transverse deformation N90-22613
Transverse vibrations of a composite cylindrical tube of circular cross section
[AD-A219227] N90-22820
SHOCK WAVE ATTENUATION
Measurement and visualization of the shock wave caused by the impact of a pulsed YAG laser in water
[REPT-892-430-113] N90-22783
SHOCK WAVE PROPAGATION
Measurement and visualization of the shock wave caused by the impact of a pulsed YAG laser in water
[REPT-892-430-113] N90-22783
Evidence for self-refraction in a convergence zone: NPE (Nonlinear progressive wave equation) model results
[AD-A218546] N90-22879
SHOCK WAVES
Gamma rays from pulsar wind shock acceleration N90-23311
SHORT TAKEOFF AIRCRAFT
Dynamic ground-effect measurements on the F-15 STOL and Maneuver Technology Demonstrator (S/MTD) configuration
[NASA-TP-3000] N90-22531
SHORT WAVE RADIATION
Forced scattering of electromagnetic waves on electron beam in periodically inhomogeneous plasma
[DE90-620705] N90-22707
SHUTTLE IMAGING RADAR
Spaceborne radar observations: A guide for Magellan radar-image analysis
[NASA-CR-184998] N90-22826
SIGNAL DETECTION
Preliminary results of the peak experiment. ALTAIR deep-space measurements
[AD-A218622] N90-22714
Transduction of nanovolt signals: Limits of electric-field detection
[AD-A219214] N90-23177
Neutrino signals from the powerful solar flare on September 29, 1989
[PREPRINT-721] N90-23331
SIGNAL ENCODING
Executive summary for the network assessment model
[AD-A218762] N90-22718
SIGNAL MEASUREMENT
Preliminary results of the peak experiment. ALTAIR deep-space measurements
[AD-A218622] N90-22714
SIGNAL PROCESSING
Infrared absorption gas sensor for the detection of HCl in launch vehicle exhaust clouds N90-22600
Qualitative aspects of signal processing through dynamical neural networks
[PREPRINT-711] N90-22709
Optical excisor modeling
[AD-A219338] N90-22722
Field oriented control of induction motors
[NASA-TM-103154] N90-22731
Quantitative surface temperature measurement using two-color thermographic phosphors and video equipment
[NASA-CASE-LAR-13740-1] N90-22770
Intelligent signal processing techniques for multi-sensor surveillance systems
[AD-A218890] N90-22895
Multimedia system control
[AD-A219392] N90-22971
Statistical inference from sampled data
[AD-A218731] N90-23156
Learning environment for neural networks and transient acoustics
[AD-A219000] N90-23186
SIGNATURE ANALYSIS
Gamma radiation from the Crab and Vela pulsars N90-23303
SILANES
Characterization and role of an elastomeric interphase within polyepoxy reinforced glass, both particulate and fibrous
[ISAL-89-0064] N90-22676
Dehydrogenative polymerization of silanes to polysilanes: A monomeric copper(2) siloxide
[AD-A218550] N90-22681
SILICATES
The effect of elevated gravity on the crystallization of the MFI zeolites, ZSM-5, and silicalite N90-23231
SILICON
Theoretical studies of silicon chemistry
[AD-A219232] N90-22690
Experimental evaluation of chemical cleaning processes for high-lifetime silicon processing
[DE90-009332] N90-22699
Reactions of laser-generated free radicals at semiconductor surfaces
[AD-A218552] N90-22733
Continued development and characterization of doped layers, contacts, and associated electronic devices in silicon carbide
[AD-A219211] N90-22737
Passivation and gating of GaAs and Si surfaces using pseudomorphic structures
[AD-A219351] N90-23256
SILICON CARBIDES
Investigation of the reaction kinetics between SiC fibers and selectively alloyed titanium matrix composites and determination of their mechanical properties N90-22659
Inelastic response of metal matrix composites under biaxial loading N90-22661
Continued development and characterization of doped layers, contacts, and associated electronic devices in silicon carbide
[AD-A219211] N90-22737
Continued development and characterization of doped layers, contacts and associated electronic devices in silicon carbide
[AD-A219234] N90-22738
Comparison between data generated from standard fracture toughness specimens and from nonstandard specimens made of a silicon carbide
[DE90-009621] N90-22814
High temperature fatigue behavior of a SiC/Ti-24Al-11Nb composite
[NASA-TM-103157] N90-22822
SILICON FILMS
Advanced gas phase reactor for growth of Ge sub x Si sub 1-x
[AD-A219012] N90-23250
SILICON NITRIDES
Crack detection in silicon nitride by acoustic microscopy
[AERE-R-13196] N90-22803
SILOXANES
Synthesis and characterization of aromatic polyester and polysiloxane containing block copolymers: Multiphase transparent atomic oxygen resistant damping materials, liquid crystal films, and toughening components of sol/gel glasses
[AD-A218871] N90-22685
SIMD (COMPUTERS)
Characterization of robotics parallel algorithms and mapping onto a reconfigurable SIMD machine N90-23039
SIMPLEX METHOD
Linear programming tools for integer programming
[AD-A219013] N90-23106
SIMPLIFICATION
Two-dimensional surface strain measurement based on a variation of Yamaguchi's laser-speckle strain gauge
[NASA-TM-103162] N90-22784
Multivariable frequency weighted model order reduction for control synthesis
[AIAA-89-3558] N90-23060
SIMULATION
Increased stuck-at fault coverage with reduced I(sub DDQ) test sets
[DE90-009509] N90-22804
Low frequency Raman spectra of liquid water, a molecular dynamics simulation
[PREPRINT-698] N90-23192
COS-B gamma ray sources beyond the predicted diffuse emission N90-23308
SIMULATORS
Design and construction of a packed column simulator operating under atmospheric and reduced pressure
[ISAL-89-60] N90-22757
SINGLE CRYSTALS
Single-crystal diffraction analysis of 2-(trimethylsilylethynyl) 4-nitro-N,N-dimethylaniline
[AD-A218955] N90-22642
Single crystal NMR of high temperature superconductors N90-23236
Optical spectroscopy of Ti(3+) doped YAlO3
[AD-A219043] N90-23251
SINGLE EVENT UPSETS
Burnout thresholds and cross section of power MOS transistors with heavy ions
[AD-A218998] N90-22736
Real-time closed-loop simulation and upset evaluation of control systems in harsh electromagnetic environments N90-23069

SINTERING
A low temperature calorimetric study of several high-T(sub c) superconductors N90-23237
SIS (SUPERCONDUCTORS)
Construction of a 345 gigahertz receiver based on superconducting tunnel junctions
[AD-A218781] N90-22735
SITE SELECTION
Anderson Mesa, Arizona as a site for an optical interferometric array N90-23281
SITTING POSITION
The application of a non-linear least squares method to predicting seat transmissibility
[ISVR-TR-173] N90-22967
SIZE (DIMENSIONS)
An interactive method for estimating hailstone size and convectively-driven wind gusts from forecast soundings
[AD-A218499] N90-22871
SIZE DETERMINATION
Dimensional analysis of structures using wrapping techniques
[REPT-892-430-119] N90-22815
SLENDER BODIES
The aerodynamic characteristics of power-law bodies in continuum and transitional hypersonic flow
[RAE-TM-AERO-2164] N90-22537
SLEWING
Sliding control of pointing and tracking with operator spline estimation N90-22997
Modeling and control of flexible space stations (slew maneuvers) N90-23086
SLIDING
Sliding control of pointing and tracking with operator spline estimation N90-22997
SLOPES
Visual slant underestimation N90-22926
SLOTS
A numerical and analytical study of normal stresses and pressure differences in non-Newtonian creeping flows N90-22749
SMOOTHING
An innovations approach to decoupling of multibody dynamics and control N90-22984
SOBOLEV SPACE
On approximation of nonlinear boundary integral equations for the combined method
[DE90-009784] N90-23130
SODIUM SULFATES
The initiation of intergranular stress corrosion-cracking on sensitized stainless steel in dilute thiosulphate solutions
[AERE-R-13317] N90-22648
SOFTWARE ENGINEERING
The interactive digital video interface N90-22941
The making of the mechanical universe N90-22961
Object-oriented query languages: The notion and the issues
[REPT-89-054] N90-23093
Comparative evaluations of four specification methods for real-time systems
[AD-A219187] N90-23109
Version description and installation guide Kernel version 3.0
[AD-A219292] N90-23113
SOFTWARE TOOLS
Orbital mechanics: A learning tool on the main frame
[AD-A218799] N90-22576
A task-analytic approach to the automated design of information graphics
[AD-A219271] N90-22912
The making of the mechanical universe N90-22961
An assessment of multibody simulation tools for articulated spacecraft N90-22988
Computational issue in the analysis of adaptive control systems N90-23001
Overview of computational control research at UT Austin N90-23051
ASTEC: Controls analysis for personal computers N90-23052
A tool for aiding in the reuse of software
[INPE-4981-PRE/1545] N90-23091
Reusing software components by specialization
[REPT-89-062] N90-23094
Fault tolerant multiprocessing and development of tools
[AD-A219216] N90-23110
SOL-GEL PROCESSES
Synthesis and characterization of aromatic polyester and polysiloxane containing block copolymers: Multiphase transparent atomic oxygen resistant damping materials, liquid crystal films, and toughening components of sol/gel glasses
[AD-A218871] N90-22685
SOLAR ACTIVITY
A 154-day periodicity in the occurrence rate of proton flares
[NASA-CR-185826] N90-23333
SOLAR ACTIVITY EFFECTS
On the antarctic ozone depletion during solar cycle 21
[NOTA-INTERNA-943] N90-22849
The Pioneer Venus Orbiter: 11 years of data. A laboratory for atmospheres seminar talk
[NASA-TM-100761] N90-23273
SOLAR CELLS
High-efficiency silicon solar cells for a 22-sun line-focus module
[DE90-010242] N90-22840
SOLAR COLLECTORS
Solar Concentrator Advanced Development Program
[NASA-CR-185173] N90-22834
High-efficiency silicon solar cells for a 22-sun line-focus module
[DE90-010242] N90-22840
SOLAR COOLING
A theoretical and experimental investigation of an absorption refrigeration system for application with solar energy units N90-22697
SOLAR CORONA
The large and small scale density structure in the solar corona N90-23327
SOLAR COSMIC RAYS
Neutrino signals from the powerful solar flare on September 29, 1989
[PREPRINT-721] N90-23331
SOLAR CYCLES
On the antarctic ozone depletion during solar cycle 21
[NOTA-INTERNA-943] N90-22849
The large and small scale density structure in the solar corona N90-23327
A 154-day periodicity in the occurrence rate of proton flares
[NASA-CR-185826] N90-23333
SOLAR ENERGY CONVERSION
A theoretical and experimental investigation of an absorption refrigeration system for application with solar energy units N90-22697
Photovoltaic advanced research and development project: Solar radiation research
[DE90-000302] N90-22839
The pressure loaded volumetric ceramic receiver
[DLR-MITT-89-17] N90-22842
SOLAR FLARES
What is learned from high energy bursts and flares N90-23314
Numerical simulations of x rays and gamma rays from solar flares N90-23330
Neutrino signals from the powerful solar flare on September 29, 1989
[PREPRINT-721] N90-23331
Solar flares and magnetospheric particles: Investigations based upon the ONR-602 and ONR-604 experiments
[AD-A218844] N90-23332
A 154-day periodicity in the occurrence rate of proton flares
[NASA-CR-185826] N90-23333
SOLAR NEUTRINOS
Neutrino signals from the powerful solar flare on September 29, 1989
[PREPRINT-721] N90-23331
SOLAR NEUTRONS
The ground-level cosmic-ray event of September 29, 1989 as recorded by the Rome detectors
[NOTA-INTERNA-944] N90-23336
SOLAR PROTONS
A 154-day periodicity in the occurrence rate of proton flares
[NASA-CR-185826] N90-23333
SOLAR RADIATION
Photovoltaic advanced research and development project: Solar radiation research
[DE90-000302] N90-22839
Numerical simulations of x rays and gamma rays from solar flares N90-23330
SOLAR RADIO BURSTS
Neutrino signals from the powerful solar flare on September 29, 1989
[PREPRINT-721] N90-23331
SOLAR ROTATION
Evolutionary models of the rotating sun and implications for other low mass stars N90-23329
SOLAR SEA POWER PLANTS
Ocean energy program summary
[DE89-009481] N90-22836
SOLAR TERRESTRIAL INTERACTIONS
Orbital mechanics: A learning tool on the main frame
[AD-A218799] N90-22576
SOLAR X-RAYS
Numerical simulations of x rays and gamma rays from solar flares N90-23330
SOLAR-PUMPED LASERS
Comparison of solar pumped Nd:YAG and Nd:Cr:GSGG lasers at liquid nitrogen and room temperature
[DLR-FB-89-41] N90-22781
SOLID ELECTROLYTES
Advanced double layer capacitor
[AD-A219419] N90-22741
Enhanced ceria solid electrolyte fuel cell development. Reduction of electronic conductivity permits use of a solid ceria electrolyte in high efficiency high power density fuel cells at temperatures compatible with metallic cell hardware
[AD-A219297] N90-22846
SOLID MECHANICS
NASA-UVA light aerospace alloy and structures technology program
[NASA-CR-182607] N90-22651
SOLID PROPELLANT COMBUSTION
Temperature measurements through a solid-propellant combustion wave using imbedded fine wire thermocouples
[AD-A218642] N90-22693
SOLID PROPELLANTS
HCl monitor N90-22599
SOLID ROCKET PROPELLANTS
HCl Vapor Characterization and Detection. JANNAF Safety and Environmental Protection Subcommittee Workshop
[AD-A216252] N90-22596
SOLID STATE LASERS
Laser Program of the Lawrence Livermore National Laboratory
[DE90-008198] N90-22779
SOLIDS
Computations of weight functions in fracture mechanics N90-22809
Electronic theory of solids, surfaces, interfaces, and clusters N90-23230
SOLITARY WAVES
Analysis of nonlinear internal waves observed by LANDSAT-TM
[PREPRINT-704] N90-22828
Effect on relaxation on nonlinear waves in crystals N90-23165
SONIC BOOMS
Assessment System for Aircraft Noise (ASAN) citation database. Volume 1: User's manual
[AD-A219175] N90-23188
Assessment System for Aircraft Noise (ASAN) citation database. Volume 2: Database update manual
[AD-A219176] N90-23189
Assessment System for Aircraft Noise (ASAN) citation database. Volume 3: New citation review procedures
[AD-A219177] N90-23190
SOUND FIELDS
Time-varying filter modelling and time-frequency characterisation of nonstationary sound fields due to a moving source N90-23178
Contributions of individual structural modes to the scattered acoustic field
[AD-A219128] N90-23187
SOUND PROPAGATION
A scattering center based numerical simulation of small scale atmospheric turbulence N90-23179
SOUND TRANSMISSION
Numerical studies of the active control of sound transmission through double partitions
[ISVR-TR-183] N90-23181
Noise reduction theory acoustic barrier construction
[CRIF-MC-87] N90-23183
SOUND WAVES
Boundary layer turbulence pulsed by acoustic waves
[ETN-90-96621] N90-22759
Sound waves in weakly ionized gas
[DE90-620704] N90-23180
SOUNDING
Estimating sea ice thickness using time-of-flight data from impulse radar soundings
[AD-A218736] N90-22831
SPACE BASED RADAR
Design options for space-based radar systems
[ETN-90-96548] N90-22710
Spaceborne radar observations: A guide for Magellan radar-image analysis
[NASA-CR-184998] N90-22826
SPACE CHARGE
Intense electron beam propagation across a magnetic field
[DE90-009993] N90-23204
Measurement of plasma-neutralized super-vacuum currents in a gyrotron configuration
[AD-A218505] N90-23207
SPACE COMMERCIALIZATION
Microgravity, the space application of the 21st century. Challenges, constraints, and strategies
[REPT-892-430-105] N90-22696

SPACE EXPLORATION
Romans to Mars
[NASA-TM-103094] N90-23339
SPACE LAW
International treaties and active experiments in space
[AD-A219368] N90-23272
SPACE MISSIONS
Nuclear technology and the space exploration missions
[NASA-TM-103156] N90-22847
Romans to Mars
[NASA-TM-103094] N90-23339
SPACE PERCEPTION
Visual sensitivities and discriminations and their role in aviation
[AD-A219319] N90-22917
Spatial constraints of stereopsis in video displays N90-22920
Stereoscopic distance perception N90-22921
Seeing by exploring N90-22923
The perception of three-dimensionality across continuous surfaces N90-22924
Perceiving environmental properties from motion information: Minimal conditions N90-22925
Spatial vision within egocentric and exocentric frames of reference N90-22928
Separate visual representations for perception and for visually guided behavior N90-22931
How to reinforce perception of depth in single two-dimensional pictures N90-22937
Spatial issues in user interface design from a graphic design perspective N90-22939
Determination of depth-viewing volumes for stereo three-dimensional graphic displays
[NASA-TP-2999] N90-22965
SPACE PLASMAS
International treaties and active experiments in space
[AD-A219368] N90-23272
Solar flares and magnetospheric particles: Investigations based upon the ONR-602 and ONR-604 experiments
[AD-A218844] N90-23332
SPACE POWER REACTORS
Nuclear technology and the space exploration missions
[NASA-TM-103156] N90-22847
Nuclear power in space
[GPO-23-835] N90-23202
National emissions standards for hazardous air pollutants application for approval of construction SP-100 ground engineering system test site
[DE90-007985] N90-23203
SPACE PROGRAMS
The International Space University
[NASA-TM-103163] N90-22604
SPACE SHUTTLES
Debris/ice/TPS assessment and photographic analysis for Shuttle Mission STS-36
[NASA-TM-102789] N90-22583
HCl monitor N90-22599
SPACE STATION POWER SUPPLIES
Automated electric power management and control for Space Station Freedom
[NASA-TM-103151] N90-23125
SPACE STATIONS
Space Station Freedom environmental control and life support system phase 3 simplified integrated test detailed report
[NASA-TM-4204] N90-22593
Space station dynamics, attitude control and momentum management N90-23029
Concurrent processing simulation of the space station N90-23041
Overview of computational control research at UT Austin N90-23051
SPACE TRANSPORTATION
US access to space: Launch vehicle choices for 1990 to 2010 N90-22579
SPACE TRANSPORTATION SYSTEM FLIGHTS
Debris/ice/TPS assessment and photographic analysis for Shuttle Mission STS-36
[NASA-TM-102789] N90-22583
SPACE-TIME FUNCTIONS
Quantum mechanics in Riemannian space-time
[DE90-620448] N90-23257
Anisotropic inflation N90-23286
SPACEBORNE EXPERIMENTS
Spacecraft attitude impacts on COLD-SAT non-vacuum jacketed LH2 supply tank thermal performance
[NASA-TM-103158] N90-22592
SPACECRAFT CONFIGURATIONS
Modeling and control of flexible space stations (slew maneuvers) N90-23086
SPACECRAFT CONSTRUCTION MATERIALS
Qualification test rationale for measuring the resistance of equipment to pyrotechnic shock
[REPT-892-430-117] N90-22590
Production of a variety of shapes using wrapping and draping techniques
[REPT-892-430-122] N90-22625
Evaluation of joints bonded with elastoplastic adhesives
[REPT-892-430-120] N90-22816
SPACECRAFT CONTROL
Approximate optimal guidance schemes for atmospheric orbital maneuvering N90-22585
Proceedings of the 3rd Annual Conference on Aerospace Computational Control, volume 1
[NASA-CR-186446] N90-22987
New multivariable capabilities of the INCA program N90-23049
The use of real-time, hardware-in-the-loop simulation in the design and development of the new Hughes HS601 spacecraft attitude control system N90-23065
Multibody dynamics: Modeling component flexibility with fixed, free, loaded, constraint, and residual modes N90-23072
Issues in CSI analysis for large scale systems N90-23076
SPACECRAFT DESIGN
Proceedings of the 3rd Annual Conference on Aerospace Computational Control, volume 1
[NASA-CR-186446] N90-22987
Concurrent processing simulation of the space station N90-23041
Implementation of generalized optimality criteria in a multidisciplinary environment N90-23048
Control/structure interaction design methodology N90-23053
SPACECRAFT GUIDANCE
Multivariate analysis of launcher guidance robustness
[REPT-892-422-105] N90-22581
SPACECRAFT LAUNCHING
Orbit acquisition and control strategy for small satellites in inclined eccentric orbits
[ETN-90-96551] N90-22573
US access to space: Launch vehicle choices for 1990 to 2010 N90-22579
SPACECRAFT MANEUVERS
Low cost station keeping maneuvers for a small-satellites constellation in tundra orbits
[ETN-90-96553] N90-22588
Interactive orbital proximity operations planning system N90-22953
Concurrent processing simulation of the space station N90-23041
Modeling and control of flexible space stations (slew maneuvers) N90-23086
SPACECRAFT POWER SUPPLIES
Programmatic status of NASA's CSTI high capacity power Stirling space power converter program
[NASA-TM-103142] N90-22606
Nuclear power in space
[GPO-23-835] N90-23202
SPACECRAFT PROPULSION
Transport properties of plasmas in microwave electrothermal thrusters
[AD-A219408] N90-23228
SPACECRAFT STRUCTURES
Study and sizing of bonded joints in space structures
[REPT-892-430-124] N90-22591
Pultrusion process development for long space boom model
[NASA-TM-4017] N90-22628
Explicit modeling of composite plates and beams in the dynamics of multibody systems N90-23019
Dynamic analysis of flexible mechanical systems using LATDYN N90-23080
SPATIAL DISTRIBUTION
Quantitative characterization of spatial distribution of particles in materials: Application to materials processing N90-22660
Skewering the universe with QSO lines of sight: Lyman alpha clouds as probes of large scale structure N90-23278
Development and use of a passive technique for measuring nitrogen dioxide in the background atmosphere N90-23285
SPATIAL RESOLUTION
Spaceborne radar observations: A guide for Magellan radar-image analysis
[NASA-CR-184998] N90-22826
Spatial Displays and Spatial Instruments
[NASA-CP-10032] N90-22918
Spatial constraints of stereopsis in video displays N90-22920
Visual slant underestimation N90-22926
The photo-colorimetric space as a medium for the representation of spatial data N90-22927
Spatial vision within egocentric and exocentric frames of reference N90-22928
On the efficacy of cinema, or what the visual system did not evolve to do N90-22934
The perception of geometrical structure from congruence N90-22935
Interactive displays in medical art N90-22940
Perception-action relationships reconsidered in light of spatial display instruments N90-22949
A commentary on perception-action relationships in spatial display instruments N90-22950
Spatial displays as a means to increase pilot situational awareness N90-22951
Interactions of form and orientation N90-22958
Optical, gravitational, and kinesthetic determinants of judged eye level N90-22959
Wide-angle display developments by computer graphics N90-22963
High spatial resolution isotopic CO and CS observations of M17 SW: The clumpy structure of the molecular cloud core
[MPE-PREPRINT-161] N90-23283
SPECIFICATIONS
Equipment specifications for launcher guidance using multivariable frequency methods
[REPT-892-422-106] N90-22582
SPECKLE PATTERNS
Two-dimensional surface strain measurement based on a variation of Yamaguchi's laser-speckle strain gauge
[NASA-TM-103162] N90-22784
SPECTRA
Turbulence spectral widths view angle independence as observed by Doppler radar
[AD-A219169] N90-22550
SPECTRAL LINE WIDTH
Tunable XeCl-laser featuring high spectral luminance N90-23167
A search for additional parameters in the infrared luminosity/21 cm line-width relation for spiral galaxies in clusters of galaxies N90-23274
SPECTRAL METHODS
Fourier analysis of finite element preconditioned collocation schemes
[NASA-CR-182040] N90-23128
SPECTRAL RESOLUTION
The super-gratings: How to improve the limiting resolution of grating spectrometers
[PREPRINT-695] N90-22577
SPECTROMETERS
The super-gratings: How to improve the limiting resolution of grating spectrometers
[PREPRINT-695] N90-22577
SPECTROSCOPIC ANALYSIS
Continued investigations of new concepts for improved spectrochemical analysis
[AD-A219403] N90-22644
Characterization of Monel alloys by x ray fluorescence technique
[DE90-617175] N90-22665
SPECTROSCOPIC TELESCOPES
Hybrid diffractive-refractive telescope
[AD-A219241] N90-23216
SPECTROSCOPY
Linear and nonlinear electrical response of condensed matter: Ionic, dielectric, and mixed-conduction materials
[AD-A218771] N90-22639
Continued investigations of new concepts for improved spectrochemical analysis
[AD-A219403] N90-22644
Spectroscopic observations of high redshift QSOs: Galaxies and the intergalactic medium at early epochs N90-23280
SPECTRUM ANALYSIS
Spectral plane quasars, spectral turn-over, and frequency atlas
[INPE-5011-TDL/399] N90-23277
Spectral determinations for discrete sources with EGRET N90-23312
Gamma ray bursts: Current status of observations and theory N90-23313
COMPTEL observations of active galactic nuclei N90-23319
Spectral measurements of the cosmic microwave background N90-23334
SPECULAR REFLECTION
Agile multiple aperture imager receiver development
[AD-A218956] N90-23215
SPEECH RECOGNITION
A connectionist implementation of cognitive phonology
[AD-A219095] N90-22906
Adaptive Resonance Theory 1
[AD-A219044] N90-23126
SPIN DYNAMICS
Side moment exerted by a spinning, coning, highly viscous liquid payload
[AD-A218746] N90-22763
SPIN-LATTICE RELAXATION
Single crystal NMR of high temperature superconductors N90-23236

A (mu)SR-investigation of the mixed state of the high-Tc superconductor HoBa2Cu3O7-delta
[DE90-620802] N90-23241
SPIN-ORBIT INTERACTIONS
An effective He-3 nucleon force for the He-3, t) charge exchange reaction
[KVI-813] N90-23198
SPIRAL GALAXIES
A search for additional parameters in the infrared luminosity/21 cm line-width relation for spiral galaxies in clusters of galaxies N90-23274
VLA and VLBI angular broadening measurements: The distribution of interstellar scattering at low Galactic latitudes N90-23279
SPIRAL WRAPPING
Polymerization of composites
[REPT-892-430-102] N90-22621
The surprising possibilities of wrapping
[REPT-892-430-106] N90-22624
SPLINE FUNCTIONS
Sliding control of pointing and tracking with operator spline estimation N90-22997
Transactions of the Seventh Army Conference on Applied Mathematics and Computing
[AD-A219220] N90-23160
SPOILERS
Boeing/NASA composite components flight service evaluation
[NASA-CR-181898] N90-22609
SQUALLS
Tropical squall lines of the Arizona monsoon N90-22667
STABILITY
Semianalytic study of high-eccentricity orbit stability and evolution N90-22574
Measurement of HCl by near-infrared diode laser absorption N90-22601
The effects of zinc addition on the environmental stability of Al-Li alloys N90-22657
Side moment exerted by a spinning, coning, highly viscous liquid payload
[AD-A218746] N90-22763
Algorithms for computing the multivariable stability margin N90-22999
Determination of joint drives for stable end-effector motion in flexible robotic systems N90-23034
On a fallacious conjecture about the stabilizability properties of solutions of the Riccati difference equation
[REPT-89-007] N90-23132
Thermal phenomena in high-Tc thin film superconductors N90-23233
STACKING FAULT ENERGY
The lithium concentration dependence of creep in binary aluminum-lithium alloys
[AD-A218706] N90-22668
STAGE SEPARATION
Qualification test rationale for measuring the resistance of equipment to pyrotechnic shock
[REPT-892-430-117] N90-22590
STAINLESS STEELS
The initiation of intergranular stress corrosion-cracking on sensitized stainless steel in dilute thiosulphate solutions
[AERE-R-13317] N90-22648
Hydrogenation of stainless steels implanted with nitrogen
[DE90-617397] N90-22666
Fracture toughness and fatigue crack initiation tests of welded precipitation-hardening stainless steel
[AD-A218745] N90-22669
A study of the relation between grain boundary type and sensitisation in a partially-sensitised AISI 304 stainless steel using electron back-scattering patterns
[AERE-R-13327] N90-23234
STANDARD DEVIATION
Turbulence spectral widths view angle independence as observed by Doppler radar
[AD-A219169] N90-22550
STANDARDS
Comparison between data generated from standard fracture toughness specimens and from nonstandard specimens made of a silicon carbide
[DE90-009621] N90-22814
Data exchange strategy. Part 1: Review of digital data exchange technology
[AD-A218506] N90-23267
STAR CLUSTERS
The dynamical evolution of dense clusters of compact stars N90-23287
Evolutionary models of the rotating sun and implications for other low mass stars N90-23329
STAR DISTRIBUTION
Fifth fundamental catalogue (FK5). Part 1: The basic fundamental stars
[REPT-32(1988)-PT-1] N90-23282
STAR TRACKERS
Automated star pattern recognition N90-22612
STARBURST GALAXIES
The interstellar medium of a starburst galaxy; millimeter interferometric observations of M82 N90-23276
STATE ESTIMATION
Robust modelling of sampled systems for time delay estimation
[REPT-89-047] N90-23092
STATIC DEFORMATION
Significance of norms and completeness in variational based methods N90-23078
STATIC STABILITY
Material instabilities in solids
[AD-A218451] N90-22817
STATISTICAL ANALYSIS
A study of mesoscale acid deposition in the lower Ohio River Valley N90-22848
Graphics equipment for data analysis
[AD-A218983] N90-22985
Two barriers problem for continuously differentiable processes
[AD-A218564] N90-23176
Looking at large data sets using binned data plots
[DE90-008206] N90-23263
The diffuse galactic gamma ray emission N90-23296
STATISTICAL DECISION THEORY
Classification techniques for quantum-limited and classical-intensity images
[AD-A218693] N90-23212
STATISTICAL DISTRIBUTIONS
Characterizing exponential distributions via conditional independence
[AD-A219255] N90-23158
Gamma rays from active galactic nuclei N90-23316
STATISTICAL MECHANICS
Replica scaling analysis of interfaces in random media
[PREPRINT-713] N90-23174
STELLAR EVOLUTION
Evolutionary models of the rotating sun and implications for other low mass stars N90-23329
STELLAR LUMINOSITY
Ultraviolet and infrared studies of Be stars N90-23275
Gamma radiation from radio pulsars N90-23302
STELLAR MAGNITUDE
Fifth fundamental catalogue (FK5). Part 1: The basic fundamental stars
[REPT-32(1988)-PT-1] N90-23282
STELLAR MASS
Evolutionary models of the rotating sun and implications for other low mass stars N90-23329
STELLAR MODELS
Gamma ray pulsars: Models and observations N90-23304
The illusive Geminga: What is it N90-23307
STELLAR ORBITS
Fifth fundamental catalogue (FK5). Part 1: The basic fundamental stars
[REPT-32(1988)-PT-1] N90-23282
STELLAR ROTATION
Ultraviolet and infrared studies of Be stars N90-23275
What is learned from high energy bursts and flares N90-23314
Evolutionary models of the rotating sun and implications for other low mass stars N90-23329
STELLAR TEMPERATURE
Ultraviolet and infrared studies of Be stars N90-23275
STELLAR WINDS
The effect of a stellar wind on an expanding H II region N90-23292
STELLARATORS
Numerical methods for the problem of the free-boundary plasma equilibrium in a stellarator (torsatron)
[DE90-620580] N90-23223
Activities report of the Institute for Plasma Research
[ETN-90-96467] N90-23225
STEREOPHOTOGRAPHY
Real-time stereo-microradiography
[AD-A218433] N90-22805
STEREOSCOPIC VISION
Spatial constraints of stereopsis in video displays N90-22920
Stereoscopic distance perception N90-22921
Paradoxical monocular stereopsis and perspective vergence N90-22922
The perception of three-dimensionality across continuous surfaces N90-22924
Perceiving environmental properties from motion information: Minimal conditions N90-22925
How to reinforce perception of depth in single two-dimensional pictures N90-22937
Visual enhancements in pick-and-place tasks: Human operators controlling a simulated cylindrical manipulator N90-22946
Development of a stereo 3-D pictorial primary flight display N90-22955
Determination of depth-viewing volumes for stereo three-dimensional graphic displays
[NASA-TP-2999] N90-22965
STIFFNESS
Multi-flexible-body dynamics capturing motion-induced stiffness N90-23013
STIRLING ENGINES
Programmatic status of NASA's CSTI high capacity power Stirling space power converter program
[NASA-TM-103142] N90-22606
STOCHASTIC PROCESSES
A new stochastic model of turbulent dispersion in the convective planetary boundary layer and the results of the Atterbury-87 field study N90-22853
Stochastic interactive activation and the effect of context on perception
[AD-A218929] N90-22898
Parallel and vector computation for stochastic optimal control applications N90-23007
Modern CACSD using the Robust-Control Toolbox N90-23024
Periodic ARMA models: Optimal prediction and minimum-phase condition
[REPT-89-006] N90-23131
Stochastic processes as Fourier integrals and dilation of vector measures
[AD-A219413] N90-23150
Transactions of the Seventh Army Conference on Applied Mathematics and Computing
[AD-A219220] N90-23160
Rigorous analysis of low temperature stochastic Ising models: Metastability and exponential approach to equilibrium
[PREPRINT-720] N90-23175
A posterior stochastic equation for quantum Brownian motion
[PREPRINT-715] N90-23194
STORAGE TANKS
Spacecraft attitude impacts on COLD-SAT non-vacuum jacketed LH2 supply tank thermal performance
[NASA-TM-103158] N90-22592
Design of cryogenic tanks for launch vehicles N90-22662
STRAIN DISTRIBUTION
Finite element elastic-plastic-creep and cyclic life analysis of a cowl lip
[NASA-TM-102342] N90-22808
STRAIN GAGES
Two-dimensional surface strain measurement based on a variation of Yamaguchi's laser-speckle strain gauge
[NASA-TM-103162] N90-22784
STRAIN MEASUREMENT
Two-dimensional surface strain measurement based on a variation of Yamaguchi's laser-speckle strain gauge
[NASA-TM-103162] N90-22784
STRAPS
Aircraft crash survival design guide. Volume 4: Aircraft seats, restraints, litters, and cockpit/cabin delethalization
[AD-A218437] N90-22548
STRATEGY
Microgravity, the space application of the 21st century. Challenges, constraints, and strategies
[REPT-892-430-105] N90-22696
Data exchange strategy. Part 1: Review of digital data exchange technology
[AD-A218506] N90-23267
STRATIFICATION
Stratified ocean mixing
[AD-A219233] N90-22881
STRATOSPHERE
Gravity wave and turbulence studies using a high-resolution ST radar
[AD-A218877] N90-22860
STRESS (PHYSIOLOGY)
ELF (Extremely Low Frequency) communications system ecological monitoring program: Slime mold studies
[AD-A218623] N90-22715
STRESS (PSYCHOLOGY)
Motor and cognitive performance do not change during a ten-week submarine patrol
[AD-A218639] N90-22969
STRESS ANALYSIS
Impact damage in graphite/epoxy laminates: Damage characterization, acoustic emission, and finite element simulation, volumes 1 and 2 N90-22610
High temperature ceramic-tubed reformer
[DE90-009617] N90-22755
The behaviour of mechanically fastened joints in composite structures N90-22789

Comparison between data generated from standard fracture toughness specimens and from nonstandard specimens made of a silicon carbide
[DE90-009621] N90-22814

STRESS CONCENTRATION
Fracture mechanics assessment of a cracked 16-inch inner diameter 1945 vintage-jacketed pressure vessel
[AD-A219135] N90-22819

STRESS CORROSION
Measurements and mechanisms of localized aqueous corrosion in aluminum-lithium alloys N90-22656

STRESS CORROSION CRACKING
The initiation of intergranular stress corrosion-cracking on sensitized stainless steel in dilute thiosulphate solutions
[AERE-R-13317] N90-22648
The effects of zinc addition on the environmental stability of Al-Li alloys N90-22657

STRESS DISTRIBUTION
Finite element elastic-plastic-creep and cyclic life analysis of a cowl lip
[NASA-TM-102342] N90-22808
Axisymmetric and cylindrically orthotropic analysis of filament winding N90-22811

STRESS INTENSITY FACTORS
Elevated temperature crack growth in aluminum alloys: Tensile deformation of 2618 and FVS0812 aluminum alloys N90-22654

STRESS MEASUREMENT
A 2-D analysis of particle velocity and stress of SH waves from a strip radiator. An experimental verification of both amplitude and phase using EMA transducers
[AERE-R-12600] N90-22704

STRESS-STRAIN DIAGRAMS
Mechanical testing of selected engineering plastics
[DE90-008186] N90-22673

STRESS-STRAIN RELATIONSHIPS
High-temperature deformation of mechanically-alloyed aluminum IN90211 N90-22645
Inelastic response of metal matrix composites under biaxial loading N90-22661
The lithium concentration dependence of creep in binary aluminum-lithium alloys
[AD-A218706] N90-22668
The microstructural basis of damping in high damping alloys
[AD-A219572] N90-22821

STRESSES
Influence of linear profile modification and loading conditions on the dynamic tooth load and stress of high contact ratio gears
[NASA-TM-103136] N90-22796

STRING THEORY
A general low-harmonic cosmic string and its self-intersection and fragmentation N90-23284

STRUCTURAL ANALYSIS
Large deformation analysis of laminated composite structures by a continuum-based shell element with transverse deformation N90-22613
Probabilistic structural analysis of aerospace components using NESSUS
[NASA-TM-102324] N90-22823
Solar Concentrator Advanced Development Program
[NASA-CR-185173] N90-22834
Spatial operator algebra framework for multibody system dynamics N90-22989
A unifying framework for rigid multibody dynamics and serial and parallel computational issues N90-23009
A decoupled recursive approach for constrained flexible multibody system dynamics N90-23042
Model reduction for flexible spacecraft with clustered natural frequencies N90-23054
OPTICON: Pro-Matlab software for large order controlled structure design N90-23058

STRUCTURAL DESIGN
An experimental study of tip shape effects on the flutter of aft-swept, flat-plate wings
[NASA-TM-4180] N90-22555
Differential equation based method for accurate approximations in optimization
[NASA-TM-102639] N90-22558
Limiting performance based structural and control optimization for large vibrating structures N90-22568
Design of cryogenic tanks for launch vehicles N90-22662
A disturbance based control/structure design algorithm N90-23003
Combined control-structure optimization N90-23005
Implementation of generalized optimality criteria in a multidisciplinary environment N90-23048

STRUCTURAL ENGINEERING
Aircraft crash survival design guide. Volume 3: Aircraft structural crash resistance
[AD-A218436] N90-22547
NASA-UVA light aerospace alloy and structures technology program
[NASA-CR-182607] N90-22651

STRUCTURAL RELIABILITY
Boeing/NASA composite components flight service evaluation
[NASA-CR-181898] N90-22609

STRUCTURAL STABILITY
OPTICON: Pro-Matlab software for large order controlled structure design N90-23058
Multivariable frequency weighted model order reduction for control synthesis
[AIAA-89-3558] N90-23060
Structural modeling for control design (articulated multibody component representation) N90-23077

STRUCTURAL VIBRATION
Limiting performance based structural and control optimization for large vibrating structures N90-22568
Robust control of vibration in flexible structures N90-22787
Dynamic substructuring by the boundary flexibility vector method of component mode synthesis
[NASA-CR-182445] N90-22813
Flat plate vibration analysis experimental and numerical fillet study
[AD-A218789] N90-22818
Contributions of individual structural modes to the scattered acoustic field
[AD-A219128] N90-23187

STUDENTS
The International Space University
[NASA-TM-103163] N90-22604

SUBMILLIMETER WAVES
Construction of a 345 gigahertz receiver based on superconducting tunnel junctions
[AD-A218781] N90-22735

SUBSONIC FLOW
Estimation of extra drag force on a circular cylinder due to the presence of solid particles in subsonic compressible flow
[AD-A218635] N90-22542

SUBSTRATES
Development of a unique laboratory standard indium gallium arsenide detector for the 500 to 1700 micron spectral region, phase 2
[NASA-CR-180482] N90-22767
Optical properties of novel GaAs-based semiconductors N90-23235
Nonreciprocal components in the 140 and 220 GHz bands utilizing magnetoplasmons on semiconducting substrates
[AD-A219136] N90-23253

SUBSTRUCTURES
Substructural controller synthesis N90-23055

SULFUR COMPOUNDS
High spatial resolution isotopic CO and CS observations of M17 SW: The clumpy structure of the molecular cloud core
[MPE-PREPRINT-161] N90-23283

SUM RULES
Relativistic corrections to He-3 photodisintegration sum rules
[NOTA-INTERNA-942] N90-23197

SUN
Evolutionary models of the rotating sun and implications for other low mass stars N90-23329

SUPERCOMPUTERS
Supercomputer and Technology
[NLR-PUB-8801] N90-22974
Aircraft technology management and the related significance of the supercomputer N90-22975
Numerical flow simulation and supercomputers: More than a digital wind tunnel N90-22976
The use of supercomputers for the design and analysis of constructions N90-22977
Access to supercomputers N90-22979
Strategy of supercomputer development N90-22981
Parallel and vector computation for stochastic optimal control applications N90-23007
Proceedings of the NATO Advanced Workshop on Supercomputing
[AD-A218508] N90-23102
Interconnection networks for highly parallel supercomputing architectures
[REPT-89-053] N90-23118
ONR Far East Scientific Information Bulletin, Volume 13, No. 4
[ONRFE-SCI-INFO-BULL-13(4)88] N90-23168
Current Japanese supercomputers for computational fluid dynamics applications N90-23172

SUPERCONDUCTING FILMS
Photoresponse of YBa2Cu3O(7-delta) granular and epitaxial superconducting thin films
[NASA-TM-103144] N90-22732
ONR Far East Scientific Information Bulletin, Volume 13, No. 4
[ONRFE-SCI-INFO-BULL-13(4)88] N90-23168
High temperature superconducting thin films in Japan N90-23169
The onset of superconductivity in two-dimensional disordered systems N90-23232
Thermal phenomena in high-Tc thin film superconductors N90-23233

SUPERCONDUCTIVITY
Photoresponse of YBa2Cu3O(7-delta) granular and epitaxial superconducting thin films
[NASA-TM-103144] N90-22732
The onset of superconductivity in two-dimensional disordered systems N90-23232
A low temperature calorimetric study of several high-T(sub c) superconductors N90-23237

SUPERCONDUCTORS
Construction of a 345 gigahertz receiver based on superconducting tunnel junctions
[AD-A218781] N90-22735
Excitation of hypersound at boundary between Type-2 superconductor and a concentrated paramagnetic compound N90-23164
A low temperature calorimetric study of several high-T(sub c) superconductors N90-23237
Influence of high energy radiation on critical parameters of superconducting ceramics YBa2Cu3O7
[DE90-620562] N90-23239

SUPERLATTICES
Acoustoelectronic interaction of surface waves in GaAs-InGaAs superlattices N90-23163
ONR Far East Scientific Information Bulletin, Volume 13, No. 4
[ONRFE-SCI-INFO-BULL-13(4)88] N90-23168
Research and applications of metallic superlattices, high T(sub c) superconductors, x ray optics, and compact synchrotrons N90-23170
Electronic theory of solids, surfaces, interfaces, and clusters N90-23230

SUPERNOVA REMNANTS
Radio pulsar timing observations for GRO N90-23301
What can gamma rays tell us about binary x ray sources and SNR's N90-23310
Gamma rays from pulsar wind shock acceleration N90-23311

SUPERPLASTICITY
High-temperature deformation of mechanically-alloyed aluminum IN90211 N90-22645
Elevated temperature crack growth in aluminum alloys: Tensile deformation of 2618 and FVS0812 aluminum alloys N90-22654
Design of cryogenic tanks for launch vehicles N90-22662

SUPERSONIC BOUNDARY LAYERS
Flow visualization in supersonic turbulent boundary layers N90-22533

SUPERSONIC FLOW
The effects of compressibility on a supersonic mixing layer
[AD-A219315] N90-22543
Supersonic flow computations for an ASTOVL aircraft configuration, phase 2, part 2
[NASA-CR-4284] N90-22746

SUPERSONIC WIND TUNNELS
SIMOUN: An optimized supersonic high temperature wind tunnel for testing construction materials to be used on the spaceplane
[REPT-892-430-111] N90-22572

SUPPORT SYSTEMS
Using object-oriented analysis techniques to support system testing
[DE90-009540] N90-22700

SURFACE CRACKS
Material instabilities in solids
[AD-A218451] N90-22817

SURFACE DEFECTS
Crack detection in silicon nitride by acoustic microscopy
[AERE-R-13196] N90-22803

SURFACE DISTORTION
Curvature-dependent parametrization of curves and surfaces
[CS-8915] N90-23100

SURFACE FINISHING
Machining of new materials at Aerospatiale
[REPT-892-430-104] N90-22622

SURFACE LAYERS
A numerical study of basic coastal upwelling processes N90-22878
A study of the surface layers at an air-water interface
[AD-A219378] N90-22882
Microstructure of thin films
[AD-A219262] N90-23255

SURFACE NAVIGATION
M1A2 adjunct analysis (POSNOV volume)
[AD-A218802] N90-22553
SURFACE NOISE INTERACTIONS
Boundary layer turbulence pulsed by acoustic waves
[ETN-90-96621] N90-22759
SURFACE PROPERTIES
Scanning laser photocurrent spectroscopy of electrochemically grown bismuth sulphide films
[AERE-M-3709] N90-22649
Time-resolved surface structural study by picosecond reflection high-energy electron diffraction
[AD-A218417] N90-22712
SURFACE REACTIONS
Improved high temperature oxidation behavior of alloys by ion implantation
[AERE-R-13309] N90-22650
Time-resolved surface structural study by picosecond reflection high-energy electron diffraction
[AD-A218417] N90-22712
Reactions of laser-generated free radicals at semiconductor surfaces
[AD-A218552] N90-22733
Quantitative surface temperature measurement using two-color thermographic phosphors and video equipment
[NASA-CASE-LAR-13740-1] N90-22770
SURFACE ROUGHNESS
An examination of the full-wave method for rough surface scattering
[AD-A218664] N90-23155
Full surface interferometric testing of grazing incidence mirrors
[AD-A219394] N90-23218
SURFACE WAVES
Acoustoelectronic interaction of surface waves in GaAs-InGaAs superlattices N90-23163
Nonreciprocal components in the 140 and 220 GHz bands utilizing magnetoplasmons on semiconducting substrates
[AD-A219136] N90-23253
SURFACES
The curvature of conjugate profiles in points of contract
[MEMO-COSOR-89-18] N90-22795
SURVEILLANCE
Intelligent signal processing techniques for multi-sensor surveillance systems
[AD-A218890] N90-22895
SURVIVAL
Aircraft crash survival design guide. Volume 1: Design criteria and checklists
[AD-A218434] N90-22545
Aircraft crash survival design guide. Volume 4: Aircraft seats, restraints, litters, and cockpit/cabin delethalization
[AD-A218437] N90-22548
Aircraft crash survival design guide. Volume 5: Aircraft postcrash survival
[AD-A218438] N90-22549
SUSPENDING (HANGING)
Hanging drop crystal growth apparatus and method
[NASA-CASE-MFS-28206-1-SB] N90-23242
SWEPTBACK WINGS
An experimental study of tip shape effects on the flutter of aft-swept, flat-plate wings
[NASA-TM-4180] N90-22555
SWIRLING
Unsteady group behavior of droplet clouds in swirling flows N90-22743
SWITCHES
Definition of a design methodology and study of the driving and protection functions of a smart power switch
[LAAS-89-330] N90-22727
SWITCHING CIRCUITS
Definition of a design methodology and study of the driving and protection functions of a smart power switch
[LAAS-89-330] N90-22727
SYMBOLIC PROGRAMMING
Rules and maps in connectionist symbol processing
[AD-A219028] N90-22903
SYMMETRY
Spaceborne radar observations: A guide for Magellan radar-image analysis
[NASA-CR-184998] N90-22826
Non-symmetric double well and Euclidean functional integral
[PREPRINT-709] N90-23133
Feasibility for EGRET detection of antimatter concentrations in the universe N90-23323
SYNCHRONISM
Preliminary results of the peak experiment. ALTAIR deep-space measurements
[AD-A218622] N90-22714
SYNCHRONOUS SATELLITES
Orbital maneuvers optimization for station acquisition of geostationary satellites. Deterministic and stochastic approaches
[LAAS-89-359] N90-22589
SYNCHROTRONS
Research and applications of metallic superlattices, high T(sub c) superconductors, x ray optics, and compact synchrotrons N90-23170
SYNTAX
Durra: A task-level description language reference manual, version 2
[AD-A219293] N90-23114
Syntax, semantics, and pragmatism: An integrated focus based on textual linguistic knowledge
[INPE-4992-PRE/1554] N90-23262
SYNTHESIS (CHEMISTRY)
The first example of an organogallium compound containing a Ga-Te bond: Synthesis, properties, and molecular structure of ((Me3CCH2)2GaTeph)2
[AD-A219258] N90-22608
Synthesis and properties of a thermotropic copolyester based on 4,4 prime-dihydroxy-a,a prime-dimethylbenzalazine
[AD-A218803] N90-22682
Synthesis and characterization of aromatic polyester and polysiloxane containing block copolymers: Multiphase transparent atomic oxygen resistant damping materials, liquid crystal films, and toughening components of sol/gel glasses
[AD-A218871] N90-22685
Experimental studies on energy storage
[AD-A219032] N90-22845
SYNTHETIC APERTURE RADAR
Spaceborne radar observations: A guide for Magellan radar-image analysis
[NASA-CR-184998] N90-22826
SYNTHETIC FIBERS
Synthesis and properties of a thermotropic copolyester based on 4,4 prime-dihydroxy-a,a prime-dimethylbenzalazine
[AD-A218803] N90-22682
Processing of thermotropic liquid crystalline polymers and their blends
[AD-A218804] N90-22683
SYSTEMS ANALYSIS
Performance analysis of Aloha networks with power capture and near/far effect
[AD-A218739] N90-22717
SYSTEMS ENGINEERING
Design options for space-based radar systems
[ETN-90-96548] N90-22710
Component model reduction via the projection and assembly method N90-23073
SYSTEMS INTEGRATION
Minimum attainable RMS attitude error using co-located rate sensors N90-23038
SYSTEMS SIMULATION
Parallel processing of real-time dynamic systems simulation on OSCAR (Optimally SCheduled Advanced multiprocessoR) N90-23006
SYSTEMS STABILITY
A priori results in linear-quadratic optimal control theory (extended version)
[MEMO-COSOR-89-17] N90-23124

T

TANDEM MIRRORS
Thermal barrier research
[DE90-009213] N90-23221
TANKS (COMBAT VEHICLES)
M1A2 adjunct analysis (POSNOV volume)
[AD-A218802] N90-22553
TANTALUM OXIDES
Microstructure of thin films
[AD-A219262] N90-23255
TARGET ACQUISITION
Tracking in uncertain environments
[RAE-TM-AW-121] N90-22891
TARGET RECOGNITION
Intelligent signal processing techniques for multi-sensor surveillance systems
[AD-A218890] N90-22895
TASK COMPLEXITY
Cognitive efficiency considerations for good graphic design
[AD-A218976] N90-22899
What makes some problems hard: Explorations in the problem space of difficulty
[AD-A219002] N90-22901
TEA LASERS
Contributions to the development of SLM TEA CO2 laser sources for high resolution molecular spectroscopy N90-22778
TEARING MODES (PLASMAS)
Resonant MHD modes with toroidal coupling
[DE90-010077] N90-23222
TECHNOLOGIES
JPRS report: Science and technology. USSR: Physics and mathematics
[JPRS-UPM-89-001] N90-23162
TECHNOLOGY ASSESSMENT
US access to space: Launch vehicle choices for 1990 to 2010 N90-22579
The Department of Defense critical technologies plan for the Committees on Armed Services United States Congress
[AD-A219300] N90-22702
An assessment of second-generation stretched-membrane mirror modules
[DE90-010243] N90-22841
Application of high-temperature superconducting thin-film devices to electro-optical and electronic warfare systems
[AD-A218805] N90-23249
Quantum non-demolition stroboscopic observables and multipumping back-action evasion schemes
[PREPRINT-699] N90-23260
Are quantum measurements on macroscopic bodies feasible
[PREPRINT-700] N90-23261
Romans to Mars
[NASA-TM-103094] N90-23339
TECHNOLOGY TRANSFER
ONR Far East Scientific Information Bulletin, Volume 13, No. 4
[ONRFE-SCI-INFO-BULL-13(4)88] N90-23168
TECHNOLOGY UTILIZATION
Impact of meteorology on the agricultural sector: Compilation and analysis of projects
[INPE-4846-PRE/1475] N90-22866
Application of high-temperature superconducting thin-film devices to electro-optical and electronic warfare systems
[AD-A218805] N90-23249
TELECOMMUNICATION
The RACE (research and development in advanced technologies for Europe) program: A 1989 update
[AD-A218509] N90-22713
TELEMETRY
Preliminary results of the peak experiment. ALTAIR deep-space measurements
[AD-A218622] N90-22714
TELEOPERATORS
Multi-axis control of telemanipulators N90-22943
Telepresence, time delay, and adaptation N90-22944
Visual enhancements in pick-and-place tasks: Human operators controlling a simulated cylindrical manipulator N90-22946
Displays for telemanipulation N90-22948
Experiences in teleoperation of land vehicles N90-22954
Development of efficient computer program for dynamic simulation of telerobotic manipulation N90-23017
TELEVISION SYSTEMS
Experiences in teleoperation of land vehicles N90-22954
TELLURIUM
The first example of an organogallium compound containing a Ga-Te bond: Synthesis, properties, and molecular structure of ((Me3CCH2)2GaTeph)2
[AD-A219258] N90-22608
TEMPERATURE CONTROL
Computer controlled cryogenic temperature controller
[AD-A218785] N90-22701
TEMPERATURE DEPENDENCE
High-temperature deformation of mechanically-alloyed aluminum IN90211 N90-22645
A (mu)SR-investigation of the mixed state of the high-Tc superconductor HoBa2Cu3O7-delta
[DE90-620802] N90-23241
TEMPERATURE EFFECTS
Deformation and fracture of thin sheet aluminum-lithium alloys: The effect of cryogenic temperatures N90-22655
Low temperature degradation of Y-TZP materials
[AD-A218841] N90-22684
Methods for evaluation of thermally induced reactions in liquid propellants
[AD-A218750] N90-22694
High-efficiency silicon solar cells for a 22-sun line-focus module
[DE90-010242] N90-22840
TEMPERATURE GRADIENTS
Ocean energy program summary
[DE89-009481] N90-22836
Activation uniformity dependence of undoped semi-insulating GaAs on post-impiant annealing conditions
[ETN-90-96549] N90-23246

TEMPERATURE MEASUREMENT
Uncertainty evaluation in an automated high temperature environmental simulation oven
[REPT-892-430-103] N90-22571
Temperature measurements through a solid-propellant combustion wave using imbedded fine wire thermocouples
[AD-A218642] N90-22693
Analysis of velocity and temperature fluctuations in turbulent shear flows N90-22744
Quantitative surface temperature measurement using two-color thermographic phosphors and video equipment
[NASA-CASE-LAR-13740-1] N90-22770
Accuracy and precision of GOES data collection platforms for temperature measurements
[AD-A218798] N90-22832
TEMPERATURE PROFILES
Temperature measurements through a solid-propellant combustion wave using imbedded fine wire thermocouples
[AD-A218642] N90-22693
TEMPORAL RESOLUTION
Time-resolved surface structural study by picosecond reflection high-energy electron diffraction
[AD-A218417] N90-22712
TENSILE DEFORMATION
Elevated temperature crack growth in aluminum alloys: Tensile deformation of 2618 and FVS0812 aluminum alloys N90-22654
TENSILE PROPERTIES
Elevated temperature crack growth in advanced powder metallurgy aluminum alloys N90-22653
TENSILE STRESS
Mechanical testing of selected engineering plastics
[DE90-008186] N90-22673
TENSILE TESTS
Deformation and fracture of aluminum-lithium alloys: The effect of dissolved hydrogen N90-22658
TENSORS
Effective action for induced gravity on a 2-dimensional manifold
[PREPRINT-712] N90-23173
TERMINAL BALLISTICS
Role of shear instability in ballistic penetration
[AD-A219186] N90-22799
Large-scale simulations of monolithic and segmented projectiles impacting spaced armor
[AD-A219374] N90-22800
TERRAIN FOLLOWING AIRCRAFT
Model-based method for terrain-following display design
[AD-A219302] N90-22563
TEST FACILITIES
Design and construction of a packed column simulator operating under atmospheric and reduced pressure
[ISAL-89-60] N90-22757
National emissions standards for hazardous air pollutants application for approval of construction SP-100 ground engineering system test site
[DE90-007985] N90-23203
TEST FIRING
A comparison between experiment and simulation for concept VIC regenerative liquid propellant guns. Part 1: 30 mm
[AD-A218556] N90-22692
TEST PATTERN GENERATORS
Design for testability of stuck-open and stack-on CMOS combinatorial circuits
[REPT-89-044] N90-22725
TETHERING
Dynamics and control of tethered antennas/reflectors in orbit
[AD-A219316] N90-22594
THEMATIC MAPPERS (LANDSAT)
Analysis of nonlinear internal waves observed by LANDSAT-TM
[PREPRINT-704] N90-22828
THEMATIC MAPPING
A case for archaeological reconnaissance of the Cabo Catoche-Porvenir region of the northeastern Yucatan Peninsula
[NASA-TM-102248] N90-22827
THEOREM PROVING
A proof of the isoenergetic KAM: Theorem from the ordinary one
[W-8906] N90-23136
THERMAL ANALYSIS
Spacecraft attitude impacts on COLD-SAT non-vacuum jacketed LH2 supply tank thermal performance
[NASA-TM-103158] N90-22592
Solar Concentrator Advanced Development Program
[NASA-CR-185173] N90-22834
THERMAL BARRIERS (PLASMA CONTROL)
Thermal barrier research
[DE90-009213] N90-23221
THERMAL BUCKLING
Experimental and computational study of the viscoplastic response of high temperature structures N90-22663
THERMAL CONDUCTIVITY
Approximate analysis for the formation of adiabatic shear bands
[AD-A218751] N90-22670
Thermal phenomena in high-Tc thin film superconductors N90-23233
THERMAL DEGRADATION
Low temperature degradation of Y-TZP materials
[AD-A218841] N90-22684
THERMAL FATIGUE
High temperature fatigue behavior of a SiC/Ti-24Al-11Nb composite
[NASA-TM-103157] N90-22822
THERMAL INSULATION
Control of surface melting and ablation in electromagnetic launchers via the magnetic vapor shielding mechanism
[AD-A219035] N90-22578
Thermal/structural analysis of the shaft-disk region of a fan drive system
[NASA-TM-101687] N90-22807
THERMAL PROTECTION
SIMOUN: An optimized supersonic high temperature wind tunnel for testing construction materials to be used on the spaceplane
[REPT-892-430-111] N90-22572
Debris/ice/TPS assessment and photographic analysis for Shuttle Mission STS-36
[NASA-TM-102789] N90-22583
The position of carbon/carbon composites among high temperature composites
[REPT-892-430-126] N90-22626
THERMAL SIMULATION
Uncertainty evaluation in an automated high temperature environmental simulation oven
[REPT-892-430-103] N90-22571
THERMAL STABILITY
Seal requirements in rocket propulsion
[ETN-90-96611] N90-22580
Elevated temperature crack growth in advanced powder metallurgy aluminum alloys N90-22653
Methods for evaluation of thermally induced reactions in liquid propellants
[AD-A218750] N90-22694
Thermal phenomena in high-Tc thin film superconductors N90-23233
THERMAL STRESSES
Computations of weight functions in fracture mechanics N90-22809
Activation uniformity dependence of undoped semi-insulating GaAs on post-implant annealing conditions
[ETN-90-96549] N90-23246
THERMOCOUPLES
Temperature measurements through a solid-propellant combustion wave using imbedded fine wire thermocouples
[AD-A218642] N90-22693
THERMODYNAMIC EFFICIENCY
A theoretical and experimental investigation of an absorption refrigeration system for application with solar energy units N90-22697
THERMODYNAMIC PROPERTIES
Displacement flow and deuteron drag in a metal: A path towards cold fusion
[PREPRINT-703] N90-23227
Critical behavior of the thermal power near the metal-insulator transition
[PREPRINT-714] N90-23244
THERMODYNAMICS
The HCl/aerosol problem N90-22597
Inelastic response of metal matrix composites under biaxial loading N90-22661
High temperature ceramic-tubed reformer
[DE90-009617] N90-22755
Geothermal energy program summary
[DE89-009485] N90-22837
THERMOELASTICITY
Axisymmetric and cylindrically orthotropic analysis of filament winding N90-22811
Approximation in LQG control of a thermoelastic rod N90-23084
THERMOELECTRIC MATERIALS
Improvement study of iron disilicide thermoelectric materials
[AD-A218946] N90-22644
THERMOELECTRIC POWER GENERATION
Improvement study of iron disilicide thermoelectric materials
[AD-A218946] N90-22844
THERMOMECHANICAL TREATMENT
Study and sizing of bonded joints in space structures
[REPT-892-430-124] N90-22591
THERMOMETERS
Computer controlled cryogenic temperature controller
[AD-A218785] N90-22701
THICK FILMS
Scanning laser photocurrent spectroscopy of electrochemically grown bismuth sulphide films
[AERE-M-3709] N90-22649
THICKNESS
Estimating sea ice thickness using time-of-flight data from impulse radar soundings
[AD-A218736] N90-22831
THIN FILMS
Electrochemical synthesis of ultrathin film composite membranes
[AD-A219041] N90-22643
Scanning laser photocurrent spectroscopy of electrochemically grown bismuth sulphide films
[AERE-M-3709] N90-22649
Photoresponse of YBa2Cu3O(7-delta) granular and epitaxial superconducting thin films
[NASA-TM-103144] N90-22732
Continued development and characterization of doped layers, contacts and associated electronic devices in silicon carbide
[AD-A219234] N90-22738
High temperature superconducting thin films in Japan N90-23169
Thermal phenomena in high-Tc thin film superconductors N90-23233
Measurement of localized deep levels and wafer non-uniformities at 3-5 semiconductor heterojunctions
[AD-A218547] N90-23248
Application of high-temperature superconducting thin-film devices to electro-optical and electronic warfare systems
[AD-A218805] N90-23249
Microstructure of thin films
[AD-A219262] N90-23255
THIN WALLS
The elastic-plastic behavior of composite materials N90-22615
THREE DIMENSIONAL BODIES
Volumetric visualization of 3D data N90-22964
THREE DIMENSIONAL BOUNDARY LAYER
Three-dimensional separated flow prediction on fusiform body using Euler and boundary layer methods N90-22745
THREE DIMENSIONAL FLOW
Extension of a three-dimensional viscous wing flow analysis user's manual: VISTA 3-D code
[NASA-CR-182024] N90-22538
Investigation of advanced counterrotation blade configuration concepts for high speed turboprop systems, task 1: Ducted propfan analysis
[NASA-CR-185217] N90-22567
Three-dimensional separated flow prediction on fusiform body using Euler and boundary layer methods N90-22745
An investigation of the three-dimensional flow field in a centrifugal compressor N90-22751
THREE DIMENSIONAL MODELS
A numerical study of basic coastal upwelling processes N90-22878
THRESHOLDS
Ignition testing of low-energy laser diode ignited components
[DE90-009968] N90-22630
THRUST
A modeling technique for STOVL ejector and volume dynamics
[NASA-TM-103167] N90-22566
Fundamental hydrodynamics research
[AD-A219179] N90-22766
THRUST CHAMBERS
Cooling of rocket thrust chambers with liquid oxygen
[NASA-TM-103146] N90-22605
THUNDERSTORMS
Turbulence spectral widths view angle independence as observed by Doppler radar
[AD-A219169] N90-22550
Tropical squall lines of the Arizona monsoon N90-22867
A study of turbulence near thunderstorm tops
[NASA-CR-186620] N90-22870
TILES
Low cost processing routes leading to high-performance ceramic tiles
[AD-A219034] N90-22688
TIME
Time-varying filter modelling and time-frequency characterisation of nonstationary sound fields due to a moving source N90-23178
TIME DEPENDENCE
Molecular evolution in astrophysical environments N90-23291

TIME DISCRIMINATION
Visual sensitivities and discriminations and their role in aviation
[AD-A219319] N90-22917
TIME LAG
Telepresence, time delay, and adaptation N90-22944
Robust modelling of sampled systems for time delay estimation
[REPT-89-047] N90-23092
TIME MARCHING
Application of a dynamic stall model to rotor trim and aeroelastic response N90-22556
Three-dimensional separated flow prediction on fusiform body using Euler and boundary layer methods N90-22745
A parallel structure transient response algorithm using independent substructure response computation N90-23044
TIME MEASUREMENT
Frequency domain techniques for analyzing picosecond optical pulses
[AD-A218656] N90-23214
Radio pulsar timing observations for GRO N90-23301
TIME OF FLIGHT SPECTROMETERS
Estimating sea ice thickness using time-of-flight data from impulse radar soundings
[AD-A218736] N90-22831
TIME OPTIMAL CONTROL
A real time, FEM based optimal control algorithm and its implementation using parallel processing hardware (transistors) in a microprocessor environment N90-23066
TIME SHARING
Use of optical storage devices as shared resources in local area networks
[AD-A219198] N90-23269
TIN COMPOUNDS
Investigation of optical nonlinearities, conductivity and magnetism in organometallic materials
[AD-A218548] N90-23211
TIN ISOTOPES
Study of Sn-116 via neutron pickup and proton stripping reactions
[KVI-814] N90-23199
TITANIUM
Investigation of the reaction kinetics between SiC fibers and selectively alloyed titanium matrix composites and determination of their mechanical properties N90-22659
Inelastic response of metal matrix composites under biaxial loading N90-22661
TITANIUM BORIDES
Low cost processing routes leading to high-performance ceramic tiles
[AD-A219034] N90-22688
TITANIUM COMPOUNDS
Optical spectroscopy of Ti(3+) doped YAlO3
[AD-A219043] N90-23251
TITANIUM OXIDES
Center for surface radiation damage studies
[AD-A218452] N90-22678
TOKAMAK DEVICES
Resonant MHD modes with toroidal coupling
[DE90-010077] N90-23222
TOLERANCES (MECHANICS)
Solar Concentrator Advanced Development Program
[NASA-CR-185173] N90-22834
TOLERANCES (PHYSIOLOGY)
Aircraft crash survival design guide. Volume 2: Aircraft design crash impact conditions and human tolerance
[AD-A218435] N90-22546
TOPOGRAPHY
Determination of the general ocean circulation using satellite altimetry from a simultaneous solution for the Earth's gravity field N90-22569
Surface topography of the Greenland Ice Sheet from satellite radar altimetry
[NASA-SP-503] N90-22850
TOPOLOGY
Experimental study of vortex ring interaction with a free surface N90-22742
Computational chaos in massively parallel neural networks N90-23012
TOROIDAL PLASMAS
Resonant MHD modes with toroidal coupling
[DE90-010077] N90-23222
TORUSES
Studies of Io's atmosphere and plasma torus N90-23326
TOUGHNESS
Microcracking and toughness of ceramic-fiber/ceramic-matrix composites under high temperature
[AD-A218516] N90-22680
TOXICITY
Airliner cabin ozone: An updated review
[AD-A219264] N90-22970
TRACKING (POSITION)
Preliminary results of the peak experiment. ALTAIR deep-space measurements
[AD-A218622] N90-22714
Visual behavior in the F-15 simulator for air-to-air combat
[AD-A218648] N90-22893
Sliding control of pointing and tracking with operator spline estimation N90-22997
TRACKING FILTERS
Tracking in uncertain environments
[RAE-TM-AW-121] N90-22891
TRAINING DEVICES
Field-of-view assessment of low-level flight and an airdrop in the C-130 Weapon System Trainer (WST)
[AD-A218504] N90-22559
TRAJECTORIES
Approximate minimum-time trajectories for 2-link flexible manipulators N90-23030
On trajectory generation for flexible space crane: Inverse dynamics analysis by LATDYN N90-23037
TRAJECTORY CONTROL
On trajectory generation for flexible space crane: Inverse dynamics analysis by LATDYN N90-23037
TRAJECTORY OPTIMIZATION
An algorithm for the solution of dynamic linear programs N90-23026
A finite element based method for solution of optimal control problems N90-23027
TRANSFER FUNCTIONS
Frequency response modeling and control of flexible structures: Computational methods N90-23021
Efficient computer algebra algorithms for polynomial matrices in control design N90-23022
A methodology for formulating a minimal uncertainty model for robust control system design and analysis N90-23026
Transfer matrices for multimode optical fiber systems
[AD-A218459] N90-23210
TRANSFER ORBITS
Semianalytic study of high-eccentricity orbit stability and evolution N90-22574
TRANSFORMATIONS (MATHEMATICS)
Naturalness of polymorphism
[CS-8916] N90-23134
Processes and formalisms for unbounded choice
[CS-8917] N90-23135
TRANSFORMERS
Optimization of a pulsed air core transformer for low impedance inductive ignition
[AD-A218748] N90-22734
TRANSIENT RESPONSE
A parallel structure transient response algorithm using independent substructure response computation N90-23044
TRANSISTOR CIRCUITS
Design for testability of stuck-open and stack-on CMOS combinatorial circuits
[REPT-89-044] N90-22725
Detection of bridging faults in DFCMOS combinational gates
[REPT-89-060] N90-22726
TRANSITION PROBABILITIES
Critical behavior of the thermal power near the metal-insulator transition
[PREPRINT-714] N90-23244
TRANSITION TEMPERATURE
The onset of superconductivity in two-dimensional disordered systems N90-23232
Influence of high energy radiation on critical parameters of superconducting ceramics YBa2Cu3O7
[DE90-620562] N90-23239
TRANSLATIONAL MOTION
The coupling effects of kinematics and flexibility on the Lagrangian dynamic formulation of open chain deformable links N90-23018
TRANSMISSIONS (MACHINE ELEMENTS)
Influence of linear profile modification and loading conditions on the dynamic tooth load and stress of high contact ratio gears
[NASA-TM-103136] N90-22796
TRANSONIC FLOW
Investigation of advanced counterrotation blade configuration concepts for high speed turboprop systems, task 1: Ducted propfan analysis
[NASA-CR-185217] N90-22567
Multigrid acceleration of transonic flow computations
[ENSM-8024] N90-22760
TRANSPARENCE
Synthesis and characterization of aromatic polyester and polysiloxane containing block copolymers: Multiphase transparent atomic oxygen resistant damping materials, liquid crystal films, and toughening components of sol/gel glasses
[AD-A218871] N90-22685
TRANSPORT AIRCRAFT
UK airmisses involving commercial air transport, January - April 1989
[ISSN-0951-6301] N90-22544
Multilevel decomposition approach to the preliminary sizing of a transport aircraft wing
[NASA-CR-4296] N90-22557
TRANSVERSE OSCILLATION
Transverse vibrations of a composite cylindrical tube of circular cross section
[AD-A219227] N90-22820
TRAVELING WAVE TUBES
Miniature traveling wave tube and method of making
[NASA-CASE-LEW-14520-1] N90-22724
TREADMILLS
Physiological and perceptual responses to prolonged treadmill load carriage
[AD-A218910] N90-22886
TREES (MATHEMATICS)
Program inversion: More than fun
[CS-8803] N90-23095
TROPICAL REGIONS
Monthly surface thermal forcing in the tropical Pacific from 1980 to 1983
[NASA-CR-183033] N90-22877
VLA and VLBI angular broadening measurements: The distribution of interstellar scattering at low Galactic latitudes N90-23279
TRUSSES
Solar Concentrator Advanced Development Program
[NASA-CR-185173] N90-22834
An inverse kinematics algorithm for a highly redundant variable-geometry-truss manipulator N90-23033
Control of a flexible planar truss using proof mass actuators N90-23035
Minimum attainable RMS attitude error using co-located rate sensors N90-23038
Mini-mast dynamic analysis using the truss-beam model N90-23087
TUNABLE LASERS
Tunable XeCl-laser featuring high spectral luminance N90-23167
TUNGSTEN OXIDES
Model catalytic oxidation studies using supported monometallic and heterobimetallic oxides
[DE90-009984] N90-22664
TURBINE BLADES
Probabilistic structural analysis of aerospace components using NESSUS
[NASA-TM-102324] N90-22823
TURBOCOMPRESSORS
Forcing function effects on rotor row unsteady aerodynamic response in a multistage compressor N90-22536
Computational and experimental investigations of rotating stall in compressor cascades N90-22565
TURBOMACHINERY
Fundamental hydrodynamics research
[AD-A219179] N90-22766
TURBULENCE
Turbulence spectral widths view angle independence as observed by Doppler radar
[AD-A219169] N90-22550
The multifractal nature of turbulence N90-22752
A new stochastic model of turbulent dispersion in the convective planetary boundary layer and the results of the Atterbury-87 field study N90-22853
A numerical study of basic coastal upwelling processes N90-22878
VLA and VLBI angular broadening measurements: The distribution of interstellar scattering at low Galactic latitudes N90-23279
TURBULENCE EFFECTS
Numerical investigation of turbulent flame sheets
[AD-A218553] N90-22635
TURBULENCE MODELS
The analysis and simulation of compressible turbulence
[NASA-CR-181997] N90-22539
TURBULENT BOUNDARY LAYER
Flow visualization in supersonic turbulent boundary layers N90-22533
Three-dimensional separated flow prediction on fusiform body using Euler and boundary layer methods N90-22745
Boundary layer turbulence pulsed by acoustic waves
[ETN-90-96621] N90-22759

TURBULENT FLOW
The analysis and simulation of compressible turbulence
[NASA-CR-181997] N90-22539
Analysis of velocity and temperature fluctuations in turbulent shear flows N90-22744
Nonlinear bifurcation study of plane Poiseuille flow
[DLR-FB-89-42] N90-22756
Holocinematography for studies of turbulent multiphase flow
[AD-A219130] N90-22765
Stratified ocean mixing
[AD-A219233] N90-22881
TURBULENT JETS
Reynolds stress closure in jet flows using instability wave modeling N90-22534
TURBULENT MIXING
Stratified ocean mixing
[AD-A219233] N90-22881
TVD SCHEMES
Three-dimensional separated flow prediction on fusiform body using Euler and boundary layer methods N90-22745
TWO DIMENSIONAL FLOW
The analysis and simulation of compressible turbulence
[NASA-CR-181997] N90-22539
Secondary frequencies in the wake of a circular cylinder with vortex shedding
[NASA-CR-181998] N90-22540
TWO DIMENSIONAL MODELS
A 2-D analysis of particle velocity and stress of SH waves from a strip radiator. An experimental verification of both amplitude and phase using EMA transducers
[AERE-R-12600] N90-22704
Tropical squall lines of the Arizona monsoon N90-22867
A numerical study of basic coastal upwelling processes N90-22878
TWO PHASE FLOW
Parallel channel flow excursions
[DE90-009129] N90-22753
Nonstrictly hyperbolic conservation laws
[AD-A218525] N90-22762

U

ULTRASONIC FLAW DETECTION
Ultrasonic detection of critical damage in carbon-epoxy composite materials
[ONERA-RT-5/7256-RY-081-R] N90-22616
Nondestructive Testing (NDT); Ceramic Matrix Composite Materials (CMCM) — Nondestructive testing (ndc); ceramic matrix composite materials (CMMC)
[REPT-892-430-123] N90-22677
Applications of laser ultrasound
[AERE-R-13106] N90-22777
ULTRASONIC RADIATION
High Intensity Electro-Magnetic and Ultrasonic Effects on Inorganic Materials Behavior and Processing Workshop
[AD-A218884] N90-22640
Superheterodyne three-wave detection of gravitation waves
[DE90-620465] N90-22856
ULTRASONIC SPECTROSCOPY
Ultrasonic detection of critical damage in carbon-epoxy composite materials
[ONERA-RT-5/7256-RY-081-R] N90-22616
ULTRASONIC TESTS
Qualification of the RSRM case membrane case-to-insulation bondline inspection using the Thiokol Corporation ultrasonic RSRM bondline inspection system
[NASA-CR-183940] N90-22602
A 2-D analysis of particle velocity and stress of SH waves from a strip radiator. An experimental verification of both amplitude and phase using EMA transducers
[AERE-R-12600] N90-22704
Applications of laser ultrasound
[AERE-R-13106] N90-22777
Qualification of the RSRM field joint CF case-to-insulation bondline inspection using the Thiokol Corporation ultrasonic RSRM bondline inspection system
[NASA-CR-183931] N90-22788
Recent advances in nondestructive evaluation made possible by novel uses of video systems
[NASA-TM-102491] N90-22801
Crack detection in silicon nitride by acoustic microscopy
[AERE-R-13196] N90-22803
ULTRAVIOLET ASTRONOMY
Ultraviolet and infrared studies of Be stars N90-23275
ULTRAVIOLET SPECTROSCOPY
Continued investigations of new concepts for improved spectrochemical analysis
[AD-A219403] N90-22644
UNDERGROUND EXPLOSIONS
Seismic wave propagation, attenuation and scattering over regional distances
[AD-A219358] N90-22862
UNITED STATES
The Department of Defense critical technologies plan for the Committees on Armed Services United States Congress
[AD-A219300] N90-22702
UNIVERSE
Skewering the universe with QSO lines of sight: Lyman alpha clouds as probes of large scale structure N90-23278
A general low-harmonic cosmic string and its self-intersection and fragmentation N90-23284
Anisotropic inflation N90-23286
Reconstructing primordial density fluctuations N90-23293
Gamma ray cosmology: The extra galactic gamma spectrum and methods to detect the underlying source N90-23321
Dipole analysis on EGRET data of extragalactic gamma ray background radiation N90-23322
Feasibility for EGRET detection of antimatter concentrations in the universe N90-23323
Gravitational collapse, Friedman models and cosmological constant: Does the universe oscillate
[DE90-620792] N90-23324
UNSTEADY AERODYNAMICS
Forcing function effects on rotor row unsteady aerodynamic response in a multistage compressor N90-22536
Multi-axis, 3-D, scanning LDA (Laser Doppler Anemometer) system for unsteady aerodynamics
[AD-A218571] N90-22541
UNSTEADY FLOW
Extension of a three-dimensional viscous wing flow analysis user's manual: VISTA 3-D code
[NASA-CR-182024] N90-22538
Secondary frequencies in the wake of a circular cylinder with vortex shedding
[NASA-CR-181998] N90-22540
Multi-axis, 3-D, scanning LDA (Laser Doppler Anemometer) system for unsteady aerodynamics
[AD-A218571] N90-22541
UPPER ATMOSPHERE
AFGW's upper air validator system
[AD-A219309] N90-22876
UPWELLING WATER
A numerical study of basic coastal upwelling processes N90-22878
URANIUM
Modeling of combustion processes in a solid fuel particle
[DE90-009140] N90-22629
USER MANUALS (COMPUTER PROGRAMS)
Extension of a three-dimensional viscous wing flow analysis user's manual: VISTA 3-D code
[NASA-CR-182024] N90-22538
PLOT3D user's manual
[NASA-TM-101067] N90-23090
Basic graphics routine technical manual
[AD-A219409] N90-23117

V

V/STOL AIRCRAFT
A modeling technique for STOVL ejector and volume dynamics
[NASA-TM-103167] N90-22566
Supersonic flow computations for an ASTOVL aircraft configuration, phase 2, part 2
[NASA-CR-4284] N90-22746
VACUUM
Measurement of plasma-neutralized super-vacuum currents in a gyrotron configuration
[AD-A218505] N90-23207
VACUUM SPECTROSCOPY
Optical spectroscopy of Ti(3+) doped YAlO3
[AD-A219043] N90-23251
VALLEYS
A study of mesoscale acid deposition in the lower Ohio River Valley N90-22848
VAPOR DEPOSITION
On the vapour phase deposition mechanism of carbon-boron-nitrogen compounds between 800 and 1000 C
[REPT-892-430-101] N90-22632
Theoretical studies of silicon chemistry
[AD-A219232] N90-22690
Indium phosphide planar Gunn diode
[AD-A219337] N90-22740
Advanced gas phase reactor for growth of Ge sub x Si sub 1-x
[AD-A219012] N90-23250
VAPOR PHASE EPITAXY
Indium phosphide planar Gunn diode
[AD-A219337] N90-22740
Advanced gas phase reactor for growth of Ge sub x Si sub 1-x
[AD-A219012] N90-23250
VAPOR PHASES
HCl Vapor Characterization and Detection. JANNAF Safety and Environmental Protection Subcommittee Workshop
[AD-A216252] N90-22596
The HCl/aerosol problem N90-22597
HCl monitor N90-22599
On the vapour phase deposition mechanism of carbon-boron-nitrogen compounds between 800 and 1000 C
[REPT-892-430-101] N90-22632
Unsteady group behavior of droplet clouds in swirling flows N90-22743
VAPORIZING
Unsteady group behavior of droplet clouds in swirling flows N90-22743
VAPORS
Control of surface melting and ablation in electromagnetic launchers via the magnetic vapor shielding mechanism
[AD-A219035] N90-22578
VARIATIONAL PRINCIPLES
Computations of weight functions in fracture mechanics N90-22809
A decoupled recursive approach for constrained flexible multibody system dynamics N90-23042
VARIATIONS
Time-varying filter modelling and time-frequency characterisation of nonstationary sound fields due to a moving source N90-23178
VECTOR ANALYSIS
Vectors and matrices: Two turbo pascal units for fast program development
[AD-A218917] N90-23105
VELOCITY DISTRIBUTION
Experimental study of vortex ring interaction with a free surface N90-22742
VELOCITY MEASUREMENT
Analysis of velocity and temperature fluctuations in turbulent shear flows N90-22744
Two-dimensional velocimetry instrumentation
[AD-A218450] N90-22774
VENUS (PLANET)
The Pioneer Venus Orbiter: 11 years of data. A laboratory for atmospheres seminar talk
[NASA-TM-100761] N90-23273
VENUS ATMOSPHERE
The Pioneer Venus Orbiter: 11 years of data. A laboratory for atmospheres seminar talk
[NASA-TM-100761] N90-23273
VENUS SURFACE
The Pioneer Venus Orbiter: 11 years of data. A laboratory for atmospheres seminar talk
[NASA-TM-100761] N90-23273
VERY LARGE ARRAY (VLA)
VLA and VLBI angular broadening measurements: The distribution of interstellar scattering at low Galactic latitudes N90-23279
Spectral measurements of the cosmic microwave background N90-23334
VERY LARGE SCALE INTEGRATION
Fault tolerant multiprocessing and development of tools
[AD-A219216] N90-23110
VERY LONG BASE INTERFEROMETRY
VLA and VLBI angular broadening measurements: The distribution of interstellar scattering at low Galactic latitudes N90-23279
VESTIBULAR NYSTAGMUS
Voluntary presetting of the vestibular ocular reflex permits gaze stabilization despite perturbation of fast head movements N90-22960
VIBRATION
Computational and experimental investigations of rotating stall in compressor cascades N90-22565
Localization of vibration in disordered nearly cyclic structures N90-22812
Control of a flexible planar truss using proof mass actuators N90-23035
VIBRATION DAMPING
Dynamics and control of tethered antennas/reflectors in orbit
[AD-A219316] N90-22594

Elements of active vibration control for rotating machinery
[NASA-TM-102368] N90-22703
The microstructural basis of damping in high damping alloys
[AD-A219572] N90-22821
The application of a non-linear least squares method to predicting seat transmissibility
[ISVR-TR-173] N90-22967
Frequency response modeling and control of flexible structures: Computational methods N90-23021
Model reduction for flexible spacecraft with clustered natural frequencies N90-23054
Controlling flexible structures with second order actuator dynamics N90-23083
Approximation in LQG control of a thermoelastic rod N90-23084
Modeling and control of flexible space stations (slew maneuvers) N90-23086
Numerical studies of the active control of sound transmission through double partitions
[ISVR-TR-183] N90-23181

VIBRATION ISOLATORS
Noise reduction theory acoustic barrier construction
[CRIF-MC-87] N90-23183

VIBRATION MODE
An experimental study of tip shape effects on the flutter of aft-swept, flat-plate wings
[NASA-TM-4180] N90-22555
Flat plate vibration analysis experimental and numerical fillet study
[AD-A218789] N90-22818

VIBRATION TESTS
Flutter investigations on a Transavia PL12/T-400 aircraft
[AD-A219108] N90-22570

VIBRATIONAL SPECTRA
Transverse vibrations of a composite cylindrical tube of circular cross section
[AD-A219227] N90-22820
Contributions of individual structural modes to the scattered acoustic field
[AD-A219128] N90-23187

VIDEO DATA
Spatial constraints of stereopsis in video displays N90-22920
The interactive digital video interface N90-22941

VIDEO DISKS
Use of optical storage devices as shared resources in local area networks
[AD-A219198] N90-23269

VINYL POLYMERS
Investigation of atomistic simulation of structural and dynamic differences in glassy and liquid states of atactic poly(propylene)
[AD-A218896] N90-22687

VIRTUAL PROPERTIES
The effects of viewpoint on the virtual space of pictures N90-22932
The eyes prefer real images N90-22938

VISCOELASTICITY
A numerical and analytical study of normal stresses and pressure differences in non-Newtonian creeping flows N90-22749
Axisymmetric and cylindrically orthotropic analysis of filament winding N90-22811

VISCOPLASTICITY
NASA-UVA light aerospace alloy and structures technology program
[NASA-CR-182607] N90-22651
Experimental and computational study of the viscoplastic response of high temperature structures N90-22663

VISCOSITY
Viscosity, density and conductivity of ImCl(HCl) sub 1.3
[AD-A218902] N90-22641
Rheology of injection mould filling with DMCs
[NPL-DMA(A)-196] N90-22675

VISCOUS FLOW
Extension of a three-dimensional viscous wing flow analysis user's manual: VISTA 3-D code
[NASA-CR-182024] N90-22538

VISCOUS FLUIDS
The minimum drag profile in laminar flow: A numerical way N90-22535

VISIBILITY
The visibility diagram: A data structure for visibility and motion planning problems. Part 1: Application to the visibility polygon query problem
[CS-8913-PT-1] N90-23098

VISION
Field-of-view assessment of low-level flight and an airdrop in the C-130 Weapon System Trainer (WST)
[AD-A218504] N90-22559
The kinetics of dark adaptation in hypoxic subjects
[AD-A218841] N90-22885
Laser retinal effects: Electrophysiological determination in visual cortical cells of monkeys and cats
[AD-A218937] N90-22888
Visual behavior in the F-15 simulator for air-to-air combat
[AD-A218648] N90-22893

VISUAL ACUITY
Visual sensitivities and discriminations and their role in aviation
[AD-A219319] N90-22917

VISUAL CONTROL
Synthetic perspective optical flow: Influence on pilot control tasks N90-22956

VISUAL DISCRIMINATION
Visual sensitivities and discriminations and their role in aviation
[AD-A219319] N90-22917
Seeing by exploring N90-22923

VISUAL FIELDS
Spatial vision within egocentric and exocentric frames of reference N90-22928

VISUAL PERCEPTION
Cognitive efficiency considerations for good graphic design
[AD-A218976] N90-22899
Visual selective attention
[AD-A219204] N90-22910
A task-analytic approach to the automated design of information graphics
[AD-A219271] N90-22912
Spatial Displays and Spatial Instruments
[NASA-CP-10032] N90-22918
Pictorial communication: Pictures and the synthetic universe N90-22919
Visual slant underestimation N90-22926
The photo-colorimetric space as a medium for the representation of spatial data N90-22927
Distortions in memory for visual displays N90-22929
The effects of viewpoint on the virtual space of pictures N90-22932
Perceived orientation, spatial layout and the geometry of pictures N90-22933
On the efficacy of cinema, or what the visual system did not evolve to do N90-22934
The perception of geometrical structure from congruence N90-22935
Exocentric direction judgements in computer-generated displays and actual scenes N90-22936
How to reinforce perception of depth in single two-dimensional pictures N90-22937
The eyes prefer real images N90-22938
Displays, instruments, and the multi-dimensional world of cartography N90-22942
Adapting to variable prismatic displacement N90-22945
Direction of movement effects under transformed visual/motor mappings N90-22947
Displays for telemanipulation N90-22948
Perception-action relationships reconsidered in light of spatial display instruments N90-22949
A commentary on perception-action relationships in spatial display instruments N90-22950
Spatial displays as a means to increase pilot situational awareness N90-22951
Interactive orbital proximity operations planning system N90-22953
Experiences in teleoperation of land vehicles N90-22954
Development of a stereo 3-D pictorial primary flight display N90-22955
Interactions of form and orientation N90-22958
Optical, gravitational, and kinesthetic determinants of judged eye level N90-22959
Voluntary presetting of the vestibular ocular reflex permits gaze stabilization despite perturbation of fast head movements N90-22960
Synesthetic art through 3-D projection: The requirements of a computer-based supermedium N90-22962
Wide-angle display developments by computer graphics N90-22963
Volumetric visualization of 3D data N90-22964

VISUAL SIGNALS
Determination of depth-viewing volumes for stereo three-dimensional graphic displays
[NASA-TP-2999] N90-22965

VISUAL STIMULI
Paradoxical monocular stereopsis and perspective vergence N90-22922
Visual slant underestimation N90-22926
Distortions in memory for visual displays N90-22929
Perception-action relationships reconsidered in light of spatial display instruments N90-22949
A commentary on perception-action relationships in spatial display instruments N90-22950
Sensory conflict in motion sickness: An observer theory approach N90-22957
The making of the mechanical universe N90-22961

VISUAL TASKS
Stereoscopic distance perception N90-22921
Visual slant underestimation N90-22926
Visual enhancements in pick-and-place tasks: Human operators controlling a simulated cylindrical manipulator N90-22946
Synthetic perspective optical flow: Influence on pilot control tasks N90-22956
The making of the mechanical universe N90-22961

VITAMINS
Motor and cognitive performance do not change during a ten-week submarine patrol
[AD-A218639] N90-22969

VOICE COMMUNICATION
Rules and maps in connectionist symbol processing
[AD-A219028] N90-22903

VORTEX RINGS
Experimental study of vortex ring interaction with a free surface N90-22742

VORTEX SHEDDING
Secondary frequencies in the wake of a circular cylinder with vortex shedding
[NASA-CR-181998] N90-22540

VORTICES
Large-scale advanced propeller blade pressure distributions: Prediction and data
[NASA-TM-102316] N90-22564
Experimental study of vortex ring interaction with a free surface N90-22742
A scattering center based numerical simulation of small scale atmospheric turbulence N90-23179

W

WAFERS
Measurement of localized deep levels and wafer non-uniformities at 3-5 semiconductor heterojunctions
[AD-A218547] N90-23248

WAKES
Secondary frequencies in the wake of a circular cylinder with vortex shedding
[NASA-CR-181998] N90-22540

WALKING
Physiological and perceptual responses to prolonged treadmill load carriage
[AD-A218910] N90-22886

WALLS
Transport of gases through concrete
[AERE-G-4977] N90-22747

WARFARE
Visual behavior in the F-15 simulator for air-to-air combat
[AD-A218648] N90-22893

WASTE DISPOSAL
Transport of gases through concrete
[AERE-G-4977] N90-22747

WATER
Theoretical and computer simulation study of the density fluctuations in liquid water
[PREPRINT-697] N90-23191
Low frequency Raman spectra of liquid water, a molecular dynamics simulation
[PREPRINT-698] N90-23192

WATER TEMPERATURE
Accuracy and precision of GOES data collection platforms for temperature measurements
[AD-A218798] N90-22832

WATER WAVES
A study of the surface layers at an air-water interface
[AD-A219378] N90-22882

WAVE ATTENUATION
Propagation and attenuation of Lg waves in South America
[AD-A218853] N90-22859
Seismic wave propagation, attenuation and scattering over regional distances
[AD-A219358] N90-22862

WAVE DISPERSION
Sound waves in weakly ionized gas
[DE90-620704] N90-23180

WAVE EQUATIONS
Evidence for self-refraction in a convergence zone: NPE (Nonlinear progressive wave equation) model results
[AD-A218546] N90-22879
Approximation in LQG control of a thermoelastic rod N90-23084

WAVE EXCITATION
Convergence of hyperspherical adiabatic expansion for helium-like systems
[DE90-620526] N90-22631

WAVE FUNCTIONS
Non-symmetric double well and Euclidean functional integral
[PREPRINT-709] N90-23133

WAVE GENERATION
A study of the surface layers at an air-water interface [AD-A219378] N90-22882
WAVE PACKETS
Sound waves in weakly ionized gas [DE90-620704] N90-23180
WAVE PROPAGATION
A 2-D analysis of particle velocity and stress of SH waves from a strip radiator. An experimental verification of both amplitude and phase using EMA transducers [AERE-R-12600] N90-22704
Specification for environmental measurements to assess radar sensors [AD-A219127] N90-22833
Propagation and attenuation of Lg waves in South America [AD-A218853] N90-22859
Seismic wave propagation, attenuation and scattering over regional distances [AD-A219358] N90-22862
Experimental investigations concerning the propagation of second-sound pulses at critical heat flux [MPIS-12/1989] N90-23182
New approach to the dynamical diffraction theory in the case of three-dimensional perfect crystal [DE90-620563] N90-23240
WAVE SCATTERING
Forced scattering of electromagnetic waves on electron beam in periodically inhomogeneous plasma [DE90-620705] N90-22707
Calculation of 3-dimensional synthetic seismograms on the connection machine [AD-A218472] N90-22857
Seismic wave propagation, attenuation and scattering over regional distances [AD-A219358] N90-22862
WAVEFORMS
Regional studies with broadband data [AD-A219215] N90-22861
WAVEGUIDES
Stability regimes in a rotating quadrupole focusing accelerator [AD-A219513] N90-23209
WEAPON SYSTEMS
Field-of-view assessment of low-level flight and an airdrop in the C-130 Weapon System Trainer (WST) [AD-A218504] N90-22559
The Department of Defense critical technologies plan for the Committees on Armed Services United States Congress [AD-A219300] N90-22702
WEAR TESTS
Characterization of particle impact by quantitative acoustic emission [AERE-R-13028] N90-22810
WEATHER
AFGW's upper air validator system [AD-A219309] N90-22876
WEATHER FORECASTING
Impact of marine boundary layer parameterization on a numerical simulation of cyclogenesis during a cold air outbreak event N90-22864
Predictability of weather and climate in a coupled ocean-atmosphere model: A dynamical systems approach N90-22865
Next generation weather radar (NEXRAD) initial operational test and evaluation. Phase 2: (IOT and E(2)) [AD-A218770] N90-22873
WELD TESTS
Fracture toughness and fatigue crack initiation tests of welded precipitation-hardening stainless steel [AD-A218745] N90-22669
WELDED JOINTS
Characterization of weldments using advanced experimental techniques [DE90-009418] N90-22792
WETLANDS
ELF (Extremely Low Frequency) communications systems ecological monitoring program: Wetland studies [AD-A218632] N90-22716
WHITE NOISE
Parallel and vector computation for stochastic optimal control applications N90-23007
WIND (METEOROLOGY)
Climatic handbook of the USSR, issue 27. Kamchatskaya Oblast. Part 3: Wind [AD-A218720] N90-22872
WIND EFFECTS
A study of the surface layers at an air-water interface [AD-A219378] N90-22882
WIND SHEAR
Tropical squall lines of the Arizona monsoon N90-22867
A numerical study of basic coastal upwelling processes N90-22878
WIND TUNNEL TESTS
The aerodynamic characteristics of power-law bodies in continuum and transitional hypersonic flow [RAE-TM-AERO-2164] N90-22537
WIND TUNNELS
Thermal/structural analysis of the shaft-disk region of a fan drive system [NASA-TM-101667] N90-22807
WIND VELOCITY
Turbulence spectral widths view angle independence as observed by Doppler radar [AD-A219169] N90-22550
WING OSCILLATIONS
An experimental study of tip shape effects on the flutter of aft-swept, flat-plate wings [NASA-TM-4180] N90-22555
WINGS
Extension of a three-dimensional viscous wing flow analysis user's manual: VISTA 3-D code [NASA-CR-182024] N90-22538
Multilevel decomposition approach to the preliminary sizing of a transport aircraft wing [NASA-CR-4296] N90-22557
WIRE
Composite ceramic superconducting wires for electric motor applications [AD-A219131] N90-22689
WORDS (LANGUAGE)
Sentence comprehension: A parallel distributed processing approach [AD-A218886] N90-23104
WORK CAPACITY
Physiological and perceptual responses to prolonged treadmill load carriage [AD-A218910] N90-22886
WORKLOADS (PSYCHOPHYSIOLOGY)
Minimum flying qualities. Volume 2: Pilot modeling for flying qualities applications [AD-A218561] N90-22561
Helmet-mounted pilot night vision systems: Human factors issues N90-22930
The physiological cost of wearing the propellant handler's ensemble at the Kennedy Space Center [NASA-TM-102786] N90-22966
WORKSTATIONS
Multimedia system control [AD-A219392] N90-22971
Graphics equipment for data analysis [AD-A218983] N90-22985
Learning environment for neural networks and transient acoustics [AD-A219000] N90-23186

X

X RAY ABSORPTION
Application of x ray absorption edge spectrometry to the non-destructive determination of element concentrations, coating thickness and areal densities [AERE-R-13030] N90-22802
X RAY DIFFRACTION
Single-crystal diffraction analysis of 2-(trimethylsilylethynyl) 4-nitro-N,N-dimethylaniline [AD-A218955] N90-22642
X RAY FLUORESCENCE
Characterization of Monel alloys by x ray fluorescence technique [DE90-617175] N90-22665
X RAY IMAGERY
Real-time stereo-microradiography [AD-A218433] N90-22805
X RAY INSPECTION
Application of x ray absorption edge spectrometry to the non-destructive determination of element concentrations, coating thickness and areal densities [AERE-R-13030] N90-22802
Real-time stereo-microradiography [AD-A218433] N90-22805
On-line x ray inspection of materials and structural components using discrete element x ray detectors for digital radiographic and computed tomographic evaluation [AD-A218911] N90-22806
X RAY IRRADIATION
Polymerization of composites [REPT-892-430-102] N90-22621
Polymerization of composite materials: A technique developed by Aerospatiale [REPT-892-430-107] N90-22623
X RAY SCATTERING
Gamma ray pulsars: Models and observations N90-23304
X RAY SOURCES
More data on (possible) gamma ray (point) sources N90-23309
What can gamma rays tell us about binary x ray sources and SNR's N90-23310
X RAY SPECTROSCOPY
Characterization of Monel alloys by x ray fluorescence technique [DE90-617175] N90-22665
Application of x ray absorption edge spectrometry to the non-destructive determination of element concentrations, coating thickness and areal densities [AERE-R-13030] N90-22802
X RAYS
Research and applications of metallic superlattices, high T(sub c) superconductors, x ray optics, and compact synchrotrons N90-23170
Gamma radiation from the Crab and Vela pulsars N90-23303
The high energy source 3C 273 N90-23318
COMPTEL observations of active galactic nuclei N90-23319
OSSE observations of active galactic nuclei N90-23320
XENON CHLORIDE LASERS
Tunable XeCl-laser featuring high spectral luminance N90-23167

Y

YAG LASERS
Comparison of solar pumped Nd:YAG and Nd:Cr:GSGG lasers at liquid nitrogen and room temperature [DLR-FB-89-41] N90-22781
Measurement and visualization of the shock wave caused by the impact of a pulsed YAG laser in water [REPT-892-430-113] N90-22783
MEGALIDAR proof-of-concept demonstration [AD-A218787] N90-22858
YTTERBIUM COMPOUNDS
Photoresponse of YBa2Cu3O(7-delta) granular and epitaxial superconducting thin films [NASA-TM-103144] N90-22732
YTTRIUM COMPOUNDS
Low temperature degradation of Y-TZP materials [AD-A218841] N90-22684
YTTRIUM OXIDES
Influence of high energy radiation on critical parameters of superconducting ceramics YBa2Cu3O7 [DE90-620562] N90-23239

Z

ZEEMAN EFFECT
Excitation of hypersound at boundary between Type-2 superconductor and a concentrated paramagnetic compound N90-23164
ZEOLITES
The effect of elevated gravity on the crystallization of the MFI zeolites, ZSM-5, and silicalite N90-23231
ZINC
The effects of zinc addition on the environmental stability of Al-Li alloys N90-22657
ZIRCONIUM
Dehydrogenative polymerization of silanes to polysilanes: A monomeric copper(2) siloxide [AD-A218550] N90-22681
ZIRCONIUM OXIDES
Low temperature degradation of Y-TZP materials [AD-A218841] N90-22684
ZONAL FLOW (METEOROLOGY)
Evolution of atmospheric baroclinic waves N90-22855

Typical Personal Author Index Listing

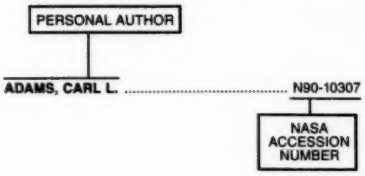

Listings in this index are arranged alphabetically by personal author. The NASA accession number denotes the number by which the citation is identified.

A

ABARBANEL, SAUL S. N90-22540
ABDALLAH, AYMAN AHMED N90-22813
ABDALLAH, S. A. N90-22766
ABRASHKEVICH, A. G. N90-22631
ABU-SABA, ELIAS G. N90-23087
ABUL-HAJ, N. ALAN N90-22598
ADAMASHVILI, G. T. N90-23165
ADAMS, W. WADE N90-22642
ADELMAN, HOWARD M. N90-22558
AHMED, N. U. N90-23086
AKHMANOV, A. S. N90-23166
ALBERTODEOLIVEIRA, CARLOS N90-23262
ALBUGUES, F. N90-22677
ALCOCER, IVAR JOHN N90-22859
ALDRED, W. N90-22835
ALESSIO, M. N90-23336
ALEXANDROV, A. S. N90-23239
ALLAART, K. N90-23199
ALLCOCK, HARRY R. N90-22607
ALLEGRI, L. N90-23336
ALLEN, DAVID H. N90-22614
ALLEN, J. M. N90-22857
ALLEN, JON D. N90-23271
ALPERT, D. J. N90-22841
ALSPACH, DAVID A. N90-22693
AMDOUNI, NOUREDINE N90-22676
AMIROUCHE, F. M. L. N90-23016
N90-23019
ANANTHAKRISHNAN, S. N90-23121
ANDERSON, JOHN R. N90-22911
ANDRIANANTOANDRO, A. N90-22759
ANTOLA, A. N90-23118
APONSO, BIMAL L. N90-22560
ARABYAN, ARA N90-22992
ARDISSONE, J. P. N90-22759
ARGO, PAUL E. N90-22705
ARGON, ALI S. N90-22686
N90-22687
ARIF, HUGH N90-22592
ARMSTRONG, ELIZABETH S. N90-22605
ARNEY, DAVID C. N90-23148
ARNOLD, WILLIAM STEWART N90-22789
ARROYO, A. A. N90-22971
ARTALE, V. N90-22828
ARYA, VINOD K. N90-22808
ASTIER, J. C. N90-22603
ATKINSON, A. N90-22747
AUCIELLO, O. N90-22578
AYALA, RENE RODOLFO N90-22859

B

BABUL, ARIF N90-23278
BACH, HENNING N90-23217
BAE, DAE-SUNG N90-23042
BAGWELL, R. C. N90-22708
BAI, T. N90-23333
BAINUM, PETER M. N90-22594
BAJCSY, RUZENA N90-23213
BALAKRISHNAN, A. V. N90-23038
BALAS, GARY J. N90-23002
BALCELLA, MARC COMAS N90-23288
BALL, WILLIAM N90-22916
BALTGALVIS, J. N90-22805
BAMBERGER, JUDY N90-23112
N90-23113
N90-23115
BAN, VLADIMIR S. N90-22767
BANERJEE, ARUN K. N90-23013
BANKS, H. T. N90-23138
BANKS, MICHAEL A. N90-22608
BARANKIEWICZ, W. S. N90-22566
BARAS, J. S. N90-23022
BARBACCI, MARIO R. N90-23114
BARBIER, P. N90-22772
BARHEN, JACOB N90-23012
BARRANGER, JOHN P. N90-22784
BARRESI, G. N90-22587
N90-22588
BARSOUM, M. W. N90-22627
BARTOLOTTA, P. A. N90-22822
BASORE, PAUL A. N90-22699
BASTIAN, U. N90-23282
BATTEY, PHILIP N90-23267
BATTIS, JAMES C. N90-22825
BATY, ROY STUART N90-22534
BAUDIN, G. N90-22616
BAUER, FRANK H. N90-23049
N90-23052
BEACHLEY, O. T., JR. N90-22608
BECKER, DOROTHY L. N90-22596
BECKMAN, THOMAS M. N90-22630
BEER, R. D. N90-23061
BEJCZY, ANTAL K. N90-22948
N90-23010
BELASH, V. CH. N90-23167
BELAVKIN, V. P. N90-23194
BELCASTRO, CELESTE M. N90-23069
BELCASTRO, CHRISTINE M. N90-23028
BELLI, P. N90-23197
BELLOS, JOHN N90-23083
BEN-MENAHEM, ARI N90-22862
BENMAIR, RUTH N90-22781
BENNETT, C. THOMAS N90-22956
BENNETT, GLENN N90-22739
BENNETT, JOHN A. N90-22734
BENNETT, M. J. N90-22650
BENNETT, WILLIAM H. N90-23021
BENNIGHOF, JEFFREY K. N90-23044
BENTHIEN, G. W. N90-23187
BENTS, D. J. N90-23339
BERGER, H. N90-22805
BERGER, M. J. N90-23139
BERKIN, ANDREW LAURENCE N90-23286
BERNABEI, R. N90-23197
BERNAL, L. P. N90-22765
BERNARD, DOUGLAS E. N90-22987
N90-23040
N90-23073
BERNSTEIN, DENNIS S. N90-23023
N90-23057
BERNSTEIN, L. S. N90-22599
BERRYMAN, HARRY N90-22973
BERTINO, E. N90-23093
BERTSCH, DAVID L. N90-23296
BETTNER, JAMES L. N90-22567
BEZIERS, DANIEL N90-22621
BHASIN, K. B. N90-22732
BIELER, THOMAS RECTOR N90-22645
BIEN, F. N90-22599
BIEN, R. N90-23282
BILLET, M. L. N90-22766
BINDER, MICHAEL P. N90-22595
BINDSCHADLER, ROBERT A. N90-22824
N90-22850
BISWAS, RUPAK N90-23148
BITTANTI, SERGIO N90-23131
BIXBY, ROBERT E. N90-23106
BJORKMAN, KAREN BETH SHIPLEY N90-23275
BLACK, W. M. N90-23207
BLACKBURN, J. F. N90-22713
N90-23102
BLACKKETTER, DONALD MERL N90-22611
BLANDFORD, DAVID A. N90-22553
BLASI, N. N90-23199
BLELLOCH, PAUL N90-23076
BLESS, ROBERT R. N90-23027
BLINN, JAMES N90-22961
BLOM, R. G. N90-22826
BLOOM, SCOTT HARRIS N90-23229
BOBER, L. J. N90-22564
BODEN, T. A. N90-22869
BOERSTOEL, J. W. N90-22980
BOKHARI, SHAHID H. N90-22982
BOLDT, ELIHU N90-23317
BOLLE, D. M. N90-23253
BOLUKBASI, AKIF O. N90-22547
N90-22548
BONCH-OSMOLOVSKY, A. G. N90-23324
BONG, WIE N90-23051
BONGUET, P. N90-22582
BOON, CORNELIS ALEXANDER MARIA N90-22729
BOONE, B. G. N90-23249
BORONTSOV, M. A. N90-23166
BOURHAM, M. N90-22578
BOUVARD, JACQUES N90-22696
BRADLEY, JAMES W. N90-22763
BRADY, ROBERT L. N90-22673
BRAININ, JACK N90-23267
BRANDHORST, HENRY W. N90-22847
BRAUCH, ANDRE N90-22781
BRAUCH, UWE N90-22781
BRAUNE, ROLF N90-22951
BRENNER, ANITA C. N90-22850
BRICKNER, MICHAEL S. N90-22930
BRIDGEMAN, BRUCE N90-22931
BRIGGS, G. A. D. N90-22803
BRIGGS, HUGH C. N90-23053
N90-23070
BRIGODIOT, G. N90-22571
BRINDLEY, P. K. N90-22822
BROCHER, E. N90-22759
BROER, H. W. N90-22730
N90-23136
BRON, COEN N90-23119
BROUSSARD, PHILLIP R. N90-23169
BRUNO, R. N90-23005
BRYANT, KENDALL N90-22885
BUCHHEIT, RUDOLPH G., JR. N90-22656
BUCK, GREGORY M. N90-22770
BUCK, M. ELAINE N90-22699
BUNING, PIETER G. N90-23090
BUONANNO, GIACOMO N90-22725
N90-22726
BURKE, JAMES D. N90-22769
BURKE, W. J. N90-23272
BURKHARDT, G. N90-23282
BURNS, D. R. N90-22857
BURROWS, LINDA M. N90-22731
BUTTLE, D. J. N90-22810
BYRNS, EDWARD V., JR. N90-23059

C

CABRE, RAMON ROIGE N90-22859
CALISE, ANTHONY J. N90-23027
N90-23059
CALISSE, P. N90-22849
CALLEN, EARL N90-23169
N90-23171
CAMERON, M. N90-23299
CAMPBELL, STEPHEN L. N90-23147
CANFIELD, R. A. N90-23048
CANNON, T. N90-22839
CAPDEVILLE, G. N90-22760
CARLSON, RALPH N90-22705
CARLSTROM, JOHN ERIC N90-23276
CARR, D. B. N90-23263
CARRASQUILLO, R. L. N90-22593
CARTER, DANIEL C. N90-23242
CASNER, STEPHEN N90-22899
N90-22912
CASTELLANI, C. N90-23244
CATHCART, J. M. N90-22858
CEMAN, D. L. N90-22754

CENTER, CHRISTOPHER J. N90-22825
CERZA, M. N90-22764
CESI, FILIPPO N90-23133
CETRONIO, A. N90-23246
CHAKRAVARTHY, SUKUMAR R. N90-22746
CHAMIS, CHRISTOS C. N90-22823
CHANG, B. N90-23015
CHANG, B.-C. N90-23028
CHANG, C.-W. N90-23037
CHANG, CHE-WEI N90-23080
CHANG, J. L. N90-23063
CHANG, RICHARD K. N90-22636
CHANGIZI, KOOROSH N90-23018
CHARRETTE, EDMOND E. N90-22862
CHEN, C. Y. N90-22967
CHEN, CHIUXING N90-23335
CHEN, G.-S. N90-23037
CHEN, J. N90-23017
CHEN, RUEY N90-23267
CHEN, SHYI-YAUNG N90-22538
CHEN, WEI N90-23095
N90-23264
CHEN, WEN-JANQ N90-22643
CHENG, W. K. N90-22599
CHERN, SU-TAI N90-23020
CHERNIKOV, N. A. N90-23258
CHESNEAU, C. N90-22618
CHIANG, RICHARD Y. N90-22999
N90-23024
CHIEL, H. J. N90-23061
CHILDERS, D. G. N90-22971
CHOU, HAN-YUN N90-22855
CHOU, JACK C. K. N90-22996
CHOUCHANE, MNAOUAR N90-22556
CHOULANT, M. N90-22580
CHRISTIE, KARL O. N90-22845
CHUANG, LI-PING N90-23008
CHUN, H. M. N90-22990
CIMECIOGLU, A. LEVENT N90-22682
CIRINO, MARK N90-22811
CIUCHINI, M. N90-23205
CLAISSE, P. A. N90-22747
CLANCY, KATHLEEN I. N90-22873
CLARK, CHARLES H. N90-22832
CLASPY, P. N90-22732
CLAWSON, A. R. N90-22740
CLEEREMANS, AXEL N90-22984
CLEMENT, WARREN F. N90-22561
CLINE, DAVID B. N90-23321
CLIVER, E. W. N90-23333
CODDINGTON, TIMOTHY N90-23112
N90-23113
N90-23115
COEN-PORISINI, ALBERTO N90-23094
COFFEE, TERENCE P. N90-22692
COGGESHALL, RANDY L. N90-22609
COHEN, MALCOLM M. N90-22945
N90-22959
COLEMAN, L. W. N90-22779
COLKET, CURRIE N90-23115
COLLIER, K. S. N90-22553
COLLINI, P. N90-22759
COLTMAN, J. W. N90-22546
CONNOR, J. W. N90-23222
CONRAD, HANS N90-22640
COOK, M. N90-22602
N90-22788
COOK, R. D. N90-22818
COOPER, W. H. B. N90-22704
COPPER, CHARLES N90-22662
CORBERAND, F. N90-22603
CORBO, G. N90-23243
CORNELL, MARK EDWARD N90-23274
CORNWELL, PHILLIP J. N90-22812
COYLE, M. F. N90-22663
COZZENS, ROBERT F. N90-23219
CRAIG, ROY R., JR. N90-23055
CRAMAROSSA, A. N90-22587
N90-22588
CRISCUOLO, E. N90-22805
CRISP, J. A. N90-22826
CRITTENDEN, LUCILLE N90-22955
CRUES, EDWIN ZACHARY N90-22585
CUNNIFF, PHILIP N90-23142
CUNNINGHAM, H. A. N90-22947
CUTTING, JAMES E. N90-22934

D

DAINTY, ANTON M. N90-22862
DALICHAOUCH, MAHIEDDINE N90-22697
DALY, STEVEN F. N90-22832
DANGELO, S. N90-23197
DANSBERRY, BRYAN E. N90-22555
DAS, C. R. N90-23110
DASILVARAMOS, LUIS EDUARDO N90-22666
DAUTILIA, ROBERTO N90-22709
DAVID, S. A. N90-22792
DAVIDIAN, KENNETH J. N90-22604
DAVIDSON, JANET N90-22915
DAVIS, ROBERT F. N90-22737
N90-22738
DAY, G. W. N90-22773
DEASON, V. A. N90-22723
N90-22768
DEBRUIN, PETER J. N90-23134
DECARVALHOKATAOKA, HELONEIDA N90-22866
DECKER, D. R. N90-23253
DEEDS, LISA N90-23267
DEISS, STEVE N90-23186
DEKKERS, A. N90-23266
DELALE, FERIDUN N90-22680
DELANEY, DAVID BURR N90-23284
DELANEY, ROBERT A. N90-22567
DELPH, TERRY J. N90-23253
DELUCIA, FRANK C. N90-23214
DEMARQUILLY, F. N90-22581
DEMBEK, ALEXA A. N90-22607
DEMS, BERNARD C. N90-22679
DENICOLAO, GIUSEPPE N90-23131
N90-23132
DENTON, M. B. N90-22644
DEPAOLI, FLAVIO N90-23094
DEPASCALE, M. P. N90-23197
DEPETRIS, M. N90-22849
DESANCTIS, M. N90-23197
DESJARDINS, S. P. N90-22548
DESTLER, W. W. N90-22780
N90-23204
DEUTSCH, S. N90-22766
DEVILLE, MICHEL O. N90-23128
DEVINE, ROBERT L. S. N90-22607
DIAMBRINIPALAZZI, GIORDANO N90-22782
DIASPERES, PEDRO LUIS N90-23123
DIBBLE, WILLIAM W. N90-22553
DIBENEDETTO, ANTHONY T. N90-22683
DICKENS, JOHN M. N90-23013
DILLARD, R. A. N90-23116
DILLON, ROBERT F. N90-23215
DIVITO, A. N90-22710
N90-22711
DIXON, KEVIN W. N90-22559
N90-22893
DOERR, DONALD F. N90-22966
DOLCE, JAMES L. N90-23125
DOMENGE, J. J. N90-22590
DOMINGUE, R. P. N90-22599
DON, WAI SUN N90-22540
DOUBLEDAY, DENNIS L. N90-23111
DOVI, AUGUSTINE R. N90-22557
DOWNING, JOHN P. N90-23049
N90-23052
DOYLE, MICHAEL N90-22940
DOYLE, MICHAEL D. N90-22941
DRUMMOND, C. K. N90-22566
DUBIEL, M. Y. N90-22593
DUDENHOEFER, JAMES E. N90-22606
DULLER, CHARLES E. N90-22627
DUMONT, B. N90-23282
DUNBAR, KEVIN N90-22900
DUNHILL, A. N90-22803
DURLACH, NATHANIEL N90-22944
DWYER, THOMAS A. W., III N90-22997

E

EBERT, ELIZABETH N90-22868
ECKART, A. N90-23299
ECKERT, A. N90-22968
EHRENSTEIN, UWE N90-22756
EHRESMAN, DERIK N90-22834
EISENTHAL, KENNETH B. N90-22634
EISLER, G. R. N90-23030
EKERDT, JOHN G. N90-22664
ELACHI, CHARLES N90-22826
ELLIS, STEPHEN R. N90-22918
N90-22919
N90-22936
N90-22953
ELMOZNINE, ABDELLATIF N90-22727
ELSAYED-ALI, HANI E. N90-22712
ELSON, PATRICIA A. N90-23090
ENJALBERT, JEAN-MICHEL N90-22589
ENRIGHT, J. T. N90-22922
ERDMAN, W. W. N90-22841
ERLEBACHER, GORDON N90-22539
ESPENSCHEID, MARK W. N90-22643
ESSELINK, KLAAS N90-23097
ETCHETO, M. N90-22619
N90-22620
ETTER, RAYMOND WILLIAM N90-22820
EVANS, CHARLES A., JR. N90-23254
EWICK, DAVID W. N90-22630
EYLES, DON E. N90-22952

F

FABRIZIO, M. N90-23244
FADDEN, DELMAR M. N90-22951
FAETH, G. M. N90-22765
FAGAN, JOHN ROBERT, JR. N90-22751
FAKHREDDINE, KARRAY N90-22997
FALCIONI, M. N90-23226
FALCO, CHARLES M. N90-23170
FAN, MICHAEL N90-22998
FARGION, DANIELE N90-22771
N90-23331
N90-23336
FARMER, MOSES G. N90-22555
FARR, T. G. N90-22826
FARRARA, R. A. N90-22669
FATEMI, NAVID S. N90-22843
FAY, ANNE L. N90-22900
FEDOROV, A. A. N90-23163
FENG, T. N90-23110
FERGUSON, IAN THOMAS N90-23235
FERNANDO, HARINDRA J. S. N90-22881
FERNSLER, R. F. N90-23208
FERRARA, AUGUSTO M. N90-22695
FERRETTI, G. N90-23092
FETTER, WILLIAM A. N90-22963
FEY, ALAN LEE N90-23279
FICHTEL, CARL E. N90-23294
N90-23315
FIJANY, AMIR N90-23009
N90-23010
N90-23045
FIRTH, ROBERT N90-23112
N90-23113
N90-23115
FISCHER, GERHARD N90-22983
FISCHL, ROBERT N90-23028
FISHER, DAVID F. N90-22532
FISZDON, W. N90-23182
N90-23259
FITZGERALD, T. JOSEPH N90-22705
FLAHERTY, JOSEPH E. N90-23148
FLIK, MARKUS IVO N90-23233
FLITTER, L. N90-23267
FOKAS, A. S. N90-23201
FOLEY, JOHN M. N90-22921
FORD, J. P. N90-22826
FORREST, STEPHEN R. N90-23248
FOUNTAIN, G. G. N90-23256
FOWELL, RICHARD A. N90-23071
FRANCO, E. N90-23205
N90-23243
FRATINI, ALBERT V. N90-22642
FRAZIER, WILLIAM E. N90-22574
FRICKE, W. N90-23262
FRISCH, HAROLD P. N90-22990
N90-23089
FRITTS, DAVID C. N90-22860
FRITZEMEIER, RONALD R. N90-22804
FROUIN, ROBERT N90-22877
FRUITWALA, HITESH N90-22682
FUEHRER, C. N90-22991
FUJCZAK, R. R. N90-22819

G

GABRIEL, C. J. N90-23210
GABRIELLI, E. N90-23205
GADBIN, MICHEL N90-22622
GAIR, AMANDA J. N90-23285
GALATI, G. N90-22710
GANESH, RAMAKRISHNAN K. N90-22535
GANGLOFF, RICHARD P. N90-22651
N90-22652
N90-22653
N90-22654
N90-22655
GARCIA, EPHRAHIM N90-23035
GARRISON, A. K. N90-22858
GARVIS, DARREL N90-22600
GAUTIER, CATHERINE N90-22877
GAWRONSKI, W. K. N90-23054
GAYNOR, E. N90-22805
GE, FUYING N90-23032
GEE, JAMES M. N90-22699
GEERTS, A. H. W. N90-23124
GEIB, S. J. N90-22681
GENERAZIO, EDWARD R. N90-22801
GEORGE, NICHOLAS N90-22775

GERNANSKY, NICHOLAS P. N90-22637
GERVASI, M. N90-22849
GHAFFARI, SHAHROKH N90-22610
GHEZZI, CARLO N90-23094
GHOSN, LOUIS N90-22646
GIBSON, J. S. N90-23084
GIBSON, RICHARD L., JR. N90-22862
GIBSON, S. N90-23005
GIGNAC, DONALD N90-23267
GILLIGAN, JOHN G. N90-22578
GIM, GWANGHUM N90-22992
GIMMESTAD, G. G. N90-22858
GLUCK, R. N90-23041
GOLD, S. H. N90-23207
GOLDMAN, A. N90-22570
GOLDSTEIN, E. BRUCE N90-22933
GONSALVES, PAUL G. N90-22563
GOODING, R. H. N90-22586
GOODMAN, EUGENE N90-22715
GORDON, MARK S. N90-22690
GOTTLIEB, DAVID N90-22540
GOWING, SCOTT N90-22798
GRAFFITTI, R. N90-23246
GRAY, PATRICK N90-22969
GRAZIANI, F. N90-22573
N90-22587
N90-22588
GREBINNIK, V. G. N90-23241
GREENEBAUM, BEN N90-22715
GREENHOUSE, MATTHEW A. N90-23328
GREENWOOD, DAN N90-23186
GREGORY, PEYTON B. N90-22807
GREGORY, RICHARD L. N90-22923
GREGUS, M. N90-23130
GREVE, DAVID W. N90-23250
GRIFFIN, M. J. N90-22967
GRIFFIN, O. M. N90-22764
GROMEK, JACK M. N90-22683
GRONINGER, J. W. N90-22736
GROSSIE, DAVID A. N90-22642
GRUNWALD, ARTHUR J. N90-22918
N90-22936
N90-22953
GUENTHER, BOB D. N90-23214
GUERRA, FRANCESCO N90-22709
GUESTEN, R. N90-23283
GUHATHAKURTA, MADHULIKA N90-23327
GULATI, SANDEEP N90-23012
GUNDEL, DOUGLAS B. N90-22659
GUNTENSPERGEN, GLENN N90-22716
GUPTA, SHANTI S. N90-23159
GUPTA, V. K. N90-22830
GYSLING, HENRY J. N90-22608

H

HABLANI, HARI B. N90-23075
HADDAD, WASSIM M. N90-23023
N90-23057
HALE, A. L. N90-23041
HALFORD, GARY R. N90-22808
HALL, D. S. N90-22549
HALL, EDWARD J. N90-22567
HALL, JOSEPH W. N90-23184
HALLORAN, JOHN W. N90-22689
HANKINS, O. N90-22578
HANNAFORD, BLAKE N90-22948
HANNON, PATRICK ROY N90-22892
HANSEN, BARRY R. N90-22699
HANSON, F. B. N90-23007
HARABURDA, SCOTT S. N90-23228
HARDESTY, D. L. N90-23207
HARDING, ALICE K. N90-23311
HARRIS, A. W. N90-22747
HART, SANDRA G. N90-22930
HARTMAN, R. C. N90-23323
HARWOOD, JOHN N90-22633
HASTIE, R. J. N90-23222
HATTANGADY, S. V. N90-23256
HAUG, EDWARD J. N90-23042
N90-23089
HAUGSE, E. D. N90-23077
HAVILAND, DAVID BRANT N90-23232
HAVILAND, JOHN K. N90-22651
N90-22662
HAWKINS, CHARLES F. N90-22804
HEATLIE, G. N90-23193
HECKES, A. A. N90-22841
HEERA, VITON N90-22667
HEINRICH, ROLAND ADOLF EBERHARD N90-22750
HELD, RICHARD N90-22944
HENDERSON, ANN S. N90-22889
HENNING, A.-J. N90-22968
HERAKOVICH, CARL T. N90-22651
N90-22661
HERING, R. N90-23282
HERMSEN, W. N90-23309
HESSELINK, WIM H. N90-23135
HEURING, VINCENT P. N90-22983
HICKEY, T. M. N90-22819
HICKMAN, ROBERT J. N90-23062
HIGGINBOTHAM, SCOTT A. N90-22583
HILL, BRUCE M. N90-23140
N90-23152
N90-23154
HINDERS, MARK K. N90-22721
HINDMARSH, ALAN C. N90-23129
HJELLMING, MICHAEL SCOTT N90-23289
HLAVACEK, VLADIMIR N90-22688
HOCHHEIMER, B. F. N90-22887
HODGES, DEWEY H. N90-23027
HOFFMAN, JAMES E. N90-22910
HOGE, JAMES C. N90-23269
HOH, ROGER H. N90-22560
HOLLAND, ANNE D. N90-22807
HONDA, HIROKI N90-23006
HORDONNEAU, A. N90-22626
HORNSEY, R. I. N90-22647
HOUDRE, C. N90-23150
HOUSER, R. M. N90-22841
HOUSNER, J. M. N90-23037
HOUSNER, JERROLD M. N90-23080
HOWARD, D. W. N90-22629
HOWARD, IAN P. N90-22928
HOWE, R. M. N90-23064
HUBBARD, DAVID C. N90-22559
HUBBARD, R. F. N90-23208
HUGHES, E. B. N90-23312
HUGHES, PETER N90-23033
HUITEMA, G. B. N90-23136
HULINA, P. T. N90-23110
HULSTROM, R. N90-22839
HUMMEL, THOMAS C. N90-23050
HUNTER, STANLEY D. N90-23294
N90-23298
HURSON, A. R. N90-23110
HUSSAINI, M. Y. N90-22539
HUTNIK, MICHELLE N90-22686
HWANG, DONG-HYUN N90-23253
HWANG, HOWYOUNG N90-23020
HYLAND, DAVID C. N90-23023

I

IDER, SITKI KEMAL N90-23016
N90-23019
N90-23031
N90-23034
IGNATOVICH, V. K. N90-23240
IKEDA, PAUL J. N90-23046
IMPROTA, S. N90-23336
INCICCHITTI, A. N90-23197
INGEN, C. V. N90-22546
INMAN, DANIEL J. N90-23035
N90-23083
ISAACSON, BRUCE G. N90-22806
ISBERG, THOMAS ARTHUR N90-23101
IUCCI, N. N90-23336
N90-23337

J

JABLONSKI, DANIEL G. N90-22551
JAEHRLING, R. N90-23282
JAHREISS, H. N90-23282
JAIN, ABHINANDAN N90-22989
N90-23009
JAMET, J. F. N90-22626
JANSSEN, LEO N90-23183
JENSEN, PETER A. N90-22829
JOENG, K. Y. N90-23074
JOHNSON, BARRY S. N90-22753
JOHNSON, LANE R. N90-22861
JOHNSON, N. B. N90-22546
N90-22549
JOHNSON, STEVEN A. N90-22532
JOHNSON, W. NEIL N90-23320
JOHNSON, WALTER W. N90-22956
JONES, P. D. N90-22869
JONES, R. E. N90-23077
JONNAVITHULA, SREENADH S. N90-22565
JOSHI, MAHENDRA L. N90-22744
JOSSE, J. P. N90-22691

K

KACZMAREK, H. N90-22616
KAEPPELER, H. J. N90-23224
KAISER, MARY K. N90-22918
N90-22925
KALLIANPUR, G. N90-23143
N90-23144
KALMIJN, J. N90-23177
KANBACH, GOTTFRIED N90-23298
N90-23303
KANTER, YU. O. N90-23163
KANTZOS, PETER N90-22648
KAO, CHI-KUAN N90-22787
KAPLAN, CRAIG A. N90-22915
KAPP, J. A. N90-22819
KARTAZAYEV, V. A. N90-23167
KASAHARA, HIRONORI N90-23006
KASPRZAK, W. T. N90-23273
KASZUBA, JOHN N90-22886
KATNIK, GREGORY N. N90-22583
KAWANO, SANDY N90-23168
KAZANAS, DEMOSTHENES N90-23316
KEAT, JAMES E. N90-23036
KEEFE, L. R. N90-22543
KEMMERLY, GUY T. N90-22531
KENNEDY, RANDALL N90-22800
KEOUGH, JANET N90-22716
KEYFITZ, BARBARA LEE N90-22762
KHARGONEKAR, PRAMOD P. N90-23127
KHOROMSKY, B. N. N90-23130
KIKKARIN, S. M. N90-23163
KILLIAN, K. W. N90-23207
KILMER, RAYMOND J. N90-22657
KIM, CHULHEE N90-22607
KIM, JINHO N90-22997
KIM, SUNG-SOO N90-23008
N90-23042
N90-23089
KIM, WHA JUNG N90-23231
KIM, WON S. N90-22948
KING, DAVID L. N90-22699
KINKEAD, A. K. N90-23207
KIRKPATRICK, D. A. N90-23207
KISH, JAMES A. N90-23125
KITSOPOULOS, T. N. N90-22883
KLAASSE, A. A. C. N90-22974
KLAHR, DAVID N90-22900
N90-22908
KLEIN, DANIEL N90-23113
N90-23115
KLEIN, MARK H. N90-22554
KLEIN, NATHAN N90-22694
KLEMA, VIRGINIA C. N90-23103
KLIEN, DANIEL N90-23112
KNARR, WILLIAM MITCHELL, JR. N90-22890
KNASEL, DON N90-22834
KNELLER, EDWARD W. N90-22563
KNEPP, DENNIS L. N90-22714
KNIBLOE, J. R. N90-22814
KNIFFEN, DONALD A. N90-23307
KNIGHT, DOUGLAS R. N90-22885
KNIPP, DELORES J. N90-22854
KOBAYASHI, HIROAKI N90-23157
KOCH, KARL WILLIAM, III N90-22786
KOCH, WERNER N90-22756
KOCHANEK, CHRISTOPHER SHARPE N90-23290
KOGUT, ALAN JOHN N90-23334
KOLENSKI, J. D. N90-22663
KOSMAHL, HENRY G. N90-22724
KOSTERS, MENNO N90-23100
KOSUT, ROBERT L. N90-23001
KOTOVSKY, KENNETH N90-22901
KOVACS, ALEXANDER N90-22831
KOWALSKI, BERNADETTE N90-22916
KRAISS, K. FRIEDRICH N90-22927
KRALL, J. N90-23209
KRAUSE, JAMES M. N90-23127
KREISS, H. O. N90-22539
KREUTZ, K. N90-22989
KRUEGER, GRETCHEN M. N90-22893
KRUK, RON N90-22943
KUCERNAK, ANTHONY R. N90-22649
KUDRYASHOV, A. V. N90-23166
KUGLER, ANDREW B. N90-23190
KUHN, G. D. N90-22543
KULP, THOMAS J. N90-22600
KUMAR, MANOJ N. N90-23047
KWON, JUNG TAI N90-22742
KWONG, CHUNG-MING N90-22745

L

LABORIE, M. N90-22591
LACONTI, ANTHONY B. N90-22741
LAI, HAO-JAN N90-23042
LAIRD, JOHN E. N90-22896
N90-22897
LAMALLE, JEAN N90-22625
N90-22815
LAMB, R. C. N90-23306

LAN, C. EDWARD N90-23032
LANDHERR, STEFAN F. N90-22554
LANDIS, D. L. N90-23110
LANE, ALAN D. N90-22547
LANE, HAROLD N90-22955
LANZIERI, C. N90-23246
LAPPIN, JOSEPH S. N90-22935
LARKIN, JILL H. N90-22899
LASIECKA, IRENA N90-23085
LATTER, WILLIAM BRUCE N90-23291
LAWRENCE, C. W. N90-22803
LAYMAN, WILLIAM E. N90-23053
LEDERLE, T. N90-23282
LEE, C. S. G. N90-23039
LEE, CHINWAI N90-22796
LEE, J. T. N90-22550
LEE, JONG-SIK N90-23178
LEE, SANG W. N90-23213
LEE, WAN-CHUNG N90-22683
LEES, DAVID E. B. N90-23215
LEITER, DARRYL N90-23317
LEMAK, MARK E. N90-23013
LENG, YANG N90-22654
LEONARDIS, ALES N90-23213
LESSNER, PHILIP N90-22741
LETCHETO, M. N90-22617
LEVEQUE, R. J. N90-23139
LEVERITT, CHARLES S. N90-22694
LEVI, D. N90-22828
LEVINE, MICHAEL V. N90-23153
LEWIS, RICHARD L. N90-22909
LI, ZHIHONG N90-22878
LIANG, TACHEN N90-23158
N90-23159
LIAW, BEEN MING N90-22680
LIEN, DAVID J. N90-23325
LILJEGREN, JAMES CHRISTIAN N90-22853
LILLY, KATHRYN W. N90-22995
LIM, S. S. N90-23086
LIM, TAE WOOK N90-22568
LIN, C. T. N90-23039
LIN, HSIANG HSI N90-22796
LIN, TSUNG-CHIEH N90-22993
N90-23063
LIN, W. N90-23110
LIN, YING-CHI N90-23322
LIPINSKIY, S. Z. N90-23167
LIU, CHAO N90-22643
LIU, CHIEN HSIEN N90-22615
LIU, W. TIMOTHY N90-22877
LLOYD, W. R. N90-22814
LOEVE, W. N90-22978
LOGA, KEVIN P. N90-22552
LONG, FREDERICK H. N90-22634
LONG, MARSHALL B. N90-22636
LOUBET, D. N90-22772
LU, HONG N90-22634
LUBELL, MICHAEL N90-23200
LUKKIEN, JOHAN J. N90-23099
LURIA, S. M. N90-22885
LUSS, HENRY R. N90-22608
LY, UY-LOI N90-23025
LYON, J. C. N90-22571

M

MACALA, GLENN A. N90-23082
MACDONALD, J. ROSS N90-22639
MACENANY, D. C. N90-23022
MACLEOD, H. A. N90-23255
MAFFEZZONI, C. N90-23092
MAGDALENO, RAYMOND E. N90-22561
MAGGS, BRUCE MCDOWELL N90-23120
MAIGRET, J. P. N90-22591
MAJOR, JUDITH A. N90-22850
MAJOROWSKI, S. N90-22688
MAKO, F. N90-23209
MALCOLM, GRANT N90-23096
N90-23265
MALHOTRA, SANDEEP N90-22679
MALLARY, ROBERT N90-22962
MALYS, STEPHEN N90-22829
MAN, GUY K. N90-22987
N90-22988
N90-23040
MANDRIOLI, DINO N90-23094
MANHEIMER, W. M. N90-23207
MANNEVILLE, PAUL N90-22758
MANWARING, STEVEN R. N90-22536
MARCHAND, ANDRE N90-22632
MARCOVALDI, R. N90-23196
MARCUS, AARON N90-22939
MARICLE, D. L. N90-22846
MARINSALTA, DANIEL A. N90-22722
MARKS, LAURENCE D. N90-22678
MARKUNAS, R. J. N90-23256
MARMEY, R. N90-22759
MARTIN, CHARLES R. N90-22643
MARTIN, ELIZABETH L. N90-22559
N90-22893
MARTIN, JAMES A. N90-22584
MARTIN, L. ROBBIN N90-22597
MARTIN, M. N90-22591
N90-22816
MARTINELLI, FABIO N90-23175
MARTINELLI, G. N90-23193
N90-23245
MARULLO, S. N90-22828
MASI, S. N90-22849
MASRY, ELIAS N90-23156
MATTOX, JOHN R. N90-23305
MAYER-HASSELWANDER, H. A. N90-23308
MAZURKEVICH, G. E. N90-23130
MAZZACURATI, VITTORIO N90-22577
N90-23192
MCBRAYER, JOHN D. N90-22699
MCBRIDE, WALTON EDWARD, III N90-23179
MCCARL, ROBERT N90-22896
MCCARTHY, MARY N90-23267
MCCARTIN, JOSEPH T. N90-22717
MCCLEARY, GEORGE F., JR. N90-22942
MCCLELLAND, JAMES L. N90-22898
N90-22984
N90-23104
MCCONATHY, DEIRDRE ALLA N90-22940
MCDONALD, B. EDWARD N90-22879
MCDONOUGH, LANE J. N90-22755
MCEVILLY, THOMAS V. N90-22861
MCGINLEY, WILLIAM M. N90-23087
MCGOVERN, DOUGLAS E. N90-22954
MCGRATH, JAMES E. N90-22685
MCGREEVY, MICHAEL W. N90-22936
MCKINNON, G. M. N90-22943
MCLAREN, MARK D. N90-23003
MCMULLEN, A. K. N90-22681
MCRAE, THOMAS G. N90-22600
MCRUER, DUANE T. N90-22561
MCTIERNAN, JAMES MICHAEL N90-23330
MEEGAN, CHARLES A. N90-23313
MEHROTRA, PIYUSH N90-22973
MELCHIORRIOLIVO, B. N90-22849
MELIS, MATTHEW E. N90-22808
MELLO, ROBERT P. N90-22886
MELLOR, PAMELA A. N90-23125
MELLSEN, STANLEY B. N90-22542
MELNIK, V. N. N90-23220
MELTON, C. E. N90-22970
MENEVEAU, CHARLES VIVANT N90-22752
MENKE, WILLIAM H. N90-22863
MERCADAL, MATHIEU N90-22698
MERMAGEN, WILLIAM H., SR. N90-22763
MERRITT, NORMAN A. N90-22545
N90-22547
N90-22548
MESCALL, JOHN F. N90-22799
MESSAOUDENE, ABDELHAMID N90-22757
METCALFE, B. N90-22802
METZNER, J. J. N90-23110
MILES, RICHARD N90-22964
MILLER, ALLEN R. N90-23161
MILLIS, MARC G. N90-22595
MILMAN, M. N90-23005
MILNES, A. G. N90-23250
MIMINIS, GEORGE N90-23004
MINAS, CONSTANTINOS N90-23035
MINAYA, ESTELA RAMOS N90-22859
MIRCHANDANEY, RAVI N90-22972
MIRCHANDANEY, SEEMA N90-22973
MIRZADEH, F. N90-22661
MISERENTINO, ROBERT N90-22628
MITCHELL, DAVID G. N90-22560
MITTELMANN, HANS D. N90-23146
MITTELSTAEDT, HORST N90-22958
MODESTINO, JAMES N90-22895
MOHSENIAN, NADER N90-23253
MONOKROUSSOS, A. N90-22968
MONTGOMERY, RAYMOND C. N90-23087
MORENO, G. N90-22849
MORENO, MIGUEL ANGEL N90-23326
MOREY, REXFORD M. N90-22631
MORRIS, P. J. N90-22766
MORRISON, WALTER F. N90-22692
MOSES, K. G. N90-23221
MOTT, PETER H. N90-22686
MOUMENE, M. N90-23019
MOURA, ANTONIO DIVINO N90-22866
MUCKENSCHNABEL, JOSEF N90-22781
MUNACH, R. N90-23022
MUND, ERNEST H. N90-23128
MURPHY, CHARLES H. N90-22763
MURPHY, PETER W. N90-22779
MYERS, D. N90-22839

N

NACCARATO, FRANK N90-23033
NAGATA, S. N90-22937
NAGPAL, VINOD K. N90-22823
NALLASAMY, M. N90-22564
NAMASTE, YARROW M. N. N90-22679
NARITA, SEINOSUKE N90-23006
NATAUPSKY, MARK N90-22955
NAUMOVICH, V. L. N90-23167
NEGRI, M. N90-23093
NEGRINI, R. N90-23118
NELSON, P. A. N90-23181
NEREM, ROBERT STEVEN N90-22569
NESE, JON MICHAEL N90-22865
NETT, CARL N. N90-23057
NEUMARK, D. M. N90-22883
NEWELL, ALLEN N90-22896
N90-22897
N90-22909
NICHOLAS, M. G. N90-22748
NICHOLLS, DAVID JOHN N90-22672
NICKERSON, A. K. N90-22747
NIKRAVESH, PARVIZ E. N90-22992
NIXON, D. N90-22543
NOLAN, P. L. N90-23312
NOREILS, FABRICE N90-22793
NOTER, YORAM N90-22781
NYLAND, TED W. N90-22761

O

OBENDORF, S. KAY N90-22679
OEZGUENER, F. N90-23043
OEZGUENER, UE. N90-23043
OGLE, K. Y. N90-22593
OHARA, G. P. N90-22669
OHERN, T. J. N90-22754
OLIVER, WILLIAM L. N90-22914
OLIVIERI, ENZO N90-23175
OLLAYOS, CURTIS W. N90-22885
OLSEN, D. E. N90-23116
OLSEN, GREGORY H. N90-22767
OMAN, CHARLES M. N90-22957
ONEAL, ELEANOR N90-22779
ONOFRIO, ROBERTO N90-23260
N90-23261
ORIN, DAVID E. N90-22995
N90-23011
ORON, MOSHE N90-22781
ORTNER, S. R. N90-23234
OSHER, STANLEY N90-23137
OSKAM, B. N90-22976
OSOFSKY, MICHAEL N90-23169
OSTERYOUNG, ROBERT A. N90-22641
OSWALD, FRED B. N90-22796
OTTENS, H. H. N90-22977
OU, Y. J. N90-23017
OVERDIJK, D. A. N90-22795

P

PACE, CHARLES F. N90-22791
PACE, SCOTT N. N90-22579
PACKARD, ANDY N90-22998
PADILLA, CARLOS E. N90-23014
PAKZAD, S. N90-23110
PALADIN, G. N90-23226
PALMOUR, JOHN W. N90-22737
N90-22738
PANCHENKO, V. YA. N90-23166
PANGBURN, TIMOTHY N90-22832
PANTLEY, KIM CHRISTINE N90-22870
PAPELL, S. STEPHEN N90-22761
PARISI, M. N90-23336
PARK, Y. S. N90-23256
PARKER, JONATHAN S. N90-22785
PARRISH, RUSSELL V. N90-22965
PARSE, J. B. N90-22660
PATEL, B. N90-22840
PATKUS, MARK N90-23267
PATTEN, WILLIAM NEFF N90-23066
PATTERSON, RICHARD L. N90-22773
PATTON, JOHN F. N90-22886
PAUL, RICHARD P. N90-23157
PAULUS, RICHARD A. N90-22833
PAVEL, M. N90-22947
PEAT, ROBERT N90-22649
PELAGATTI, G. N90-23093
PELLETIER, E. N90-23255
PENNINGTON, CHARLES HOLLOWAY N90-23236
PERCELL, CHERYL BOSMAN N90-23185

PERRIN, RONALD E. N90-22701
PERRONE, JOHN A. N90-22926
N90-22956
PERRY, J. L. N90-22593
PETERSON, LEE D. N90-23058
PETRIE, H. L. N90-22766
PETYT, M. N90-23181
PHATAK, ANIL V. N90-22956
PICOZZA, P. N90-23197
PIERCE, LARRY N90-23090
PILANT, MICHAEL S. N90-23141
PILKEY, WALTER D. N90-22651
N90-22662
PINDERA, MAREK-JERZY N90-22651
N90-22661
PINO, JOHN PHILIP N90-22871
PINSONNEAULT, MARC HOWARD N90-23329
PIPERIAS, P. N90-22570
PIQUET, J. N90-22760
PISAREV, A. F. N90-22856
PISAREVA, S. A. N90-22856
PISTOIA, D. N90-22710
PITTORI, C. N90-23193
PLACIOUS, R. N90-22805
PLANTE, DANIEL R. N90-22879
PNEV, V. V. N90-23163
POLANSKY, D. N90-22805
POLICHAR, R. N90-22805
POLK, THAD A. N90-22909
POMERLEAU, DEAN A. N90-22797
POPE, S. B. N90-22635
POPOV, V. K. N90-23166
POROYKOV, A. YU. N90-23166
PORR, WILLIAM C., JR. N90-22653
POSTHUMADEBOER, U. N90-22979
POTTER, A. L. N90-23251
PRINCIPE, J. C. N90-22971
PRITCHARD, JOCELYN I. N90-22558
PRITZKOW, WALTER N90-22842
PROFFITT, DENNIS R. N90-22925
PROSPERI, D. N90-23197
PSIAKI, MARK L. N90-23026
PUECH, M. H. N90-22783
PUGLIESI, V. N90-22759
PURVIS, BRADLEY D. N90-22563
PUSZYNSKI, J. A. N90-22688

Q

QIN, YULIN N90-22913
QUINLAN, GERALD DAVID N90-23287
QUINN, R. D. N90-23061

R

RABACA, CARLOS ROBERTO N90-23277
RADCLIFF, DAVID BYROM N90-23292
RADER, D. J. N90-22754
RAMAKRISHNAN, SEKARIPURAM V. N90-22746
RANDLE, V. N90-23234
RAPPELINE, PETER FREDERICK N90-22821
RAUSCHENBACH, BERND N90-22667
RE, F. N90-23337
REBNORD, D. A. N90-23138
REDDINGIUS, NICOLAAS N90-23188
N90-23189
N90-23190
REED, J. N90-22805
REEVES, MARK EDWIN N90-23237
REGAN, DAVID N90-22917
REGAN, J. D. N90-22537
REIN, UDO N90-22992
REISER, M. P. N90-23204
REMO, JOHN L. N90-23218
RENKEN, P. J. N90-22794
REUTER, W. G. N90-22814
REYNOLDS, KATY L. N90-22886
REYNOSO-HERNANDEZ, J. APOLINAR N90-22728
RHEINGOLD, A. L. N90-22681
RHODY, HARVEY N90-22895
RIBEIROSALVADOR, VERA LUCIA N90-22665
RICCI, M. A. N90-23191
N90-23192
RICHTER, STEPHEN N90-23023
RIDER, C. D. N90-22570
RIDES, M. N90-22675
RIEDESEL, JOEL D. N90-22986
RIORDAN, C. N90-22839
RISMANTAB-SANY, J. N90-23015
RITZMANN, R. N90-23061
RIVERA, JOSE A., JR. N90-22555
RIVET, F. C. N90-22658
ROB, MOHAMMAD ABDUR N90-22778
ROBERTS, B. C. N90-22593
ROBERTS, D. W. N90-22858
ROBERTSON, S. H. N90-22549
ROBINETT, R. D. N90-23030
ROCCA, D. N90-23191
RODGERS, J. N90-22780
RODRIGUEZ, FERDINAND N90-22679
RODRIGUEZ, G. N90-22989
N90-22994
ROEY, KENNETH P. N90-22671
ROGERS, HARRY N90-22799
ROJAS, VICTORIA A. N90-22559
N90-22893
RONDINELLI, G. N90-22573
N90-22587
N90-22588
ROO, M. N90-22748
ROSCOE, STANLEY N. N90-22938
ROSE, A. H. N90-22773
ROSEN, I. G. N90-23084
ROSENBERG, ROBERT A. N90-22755
ROSENBLOOM, PAUL S. N90-22896
N90-22897
ROSSI, GIAN CARLO N90-23133
N90-23193
N90-23243
ROTH, DON J. N90-22801
ROTH, MARY ELLEN N90-22731
ROTH, PETER N. N90-23105
ROTHERMEL, H. N90-23299
RUBIN, D. N90-22740
RUBY, DOUGLAS S. N90-22699
RUDDER, R. A. N90-23256
RUDERMAN, MALVIN N90-23302
RUDY, DAVID H. N90-22540
RUFF, G. A. N90-22765
RULKA, W. N90-22991
RUNDELL, WILLIAM N90-23141
RUOCCO, G. N90-22577
N90-23191
N90-23192
RUSSELL, GREGORY N90-22964
RUSSELL, WILLIAM C. N90-23046
RUSSEN, L. C. N90-22802
RYCHLIK, IGOR N90-23176

S

SABOUR, FEREYDOUN N90-23122
SACHRAJDA, C. T. N90-23193
SADAYAPPAN, P. N90-23011
SAFONOV, MICHAEL G. N90-22999
N90-23024
SAGALYN, R. C. N90-23272
SAITO, MASATO N90-22981
SAIYED, NASEEM H. N90-22761
SALAMA, M. N90-23005
SALGANICOFF, MARCOS N90-22948
SALMOND, D. J. N90-22891
SALTZ, JOEL H. N90-22972
N90-22973
SALUS, W. L. N90-23077
SALVINI, GIORGIO N90-23195
SAMI, M. G. N90-23118
SAMPOLI, M. N90-23192
SANTAVICCA, DOMENIC A. N90-22774
SANTOLERI, R. N90-22828
SARANGAPANI, S. N90-22741
SARIC, WILLIAM S. N90-22541
SARKAR, S. N90-22539
SAUGNAC, FREDERIC N90-22632
SAUNDERS, R. STEPHEN N90-22826
SAUNDERS, VANCE MCMILLAN N90-23268
SAVAGLIO, CLARE N90-23067
SAWAI, KEJIRO N90-22641
SAYLOR, RICK DAVIS N90-22848
SBATTELLA, L. N90-23093
SCAFI, M. N90-23197
SCALES, WAYNE ANTHONY N90-22851
SCAPIN, MARCOS ANTONIO N90-22665
SCATTOLINI, R. N90-23092
SCHEFFLER, DANIEL R. N90-22800
SCHEHRER, KEVIN N90-22739
SCHEID, R. N90-23005
SCHELD, ROBERT E. N90-23045
SCHEPLER, KENNETH L. N90-23251
SCHERRER, HUBERT N90-22844
SCHERRER, STANISLAS N90-22844
SCHIPPERS, H. N90-22974
SCHIPPERS, J. M. N90-23199
SCHIRATO, R. N90-22805
SCHLICHTING, CHRISTINE L. N90-22969
SCHLUMBERGER, JULIE A. N90-22605
SCHMIDT, DAVID K. N90-23060
SCHMUDLACH, R. N90-22968
SCHNEID, EDWARD J. N90-23314
SCHNEIDER, WALTER N90-22914
SCHOLZE, RICHARD J. N90-22633
SCHONFELD, BRIAN R. N90-22966
SCHONFELDER, V. N90-23319
SCHOR, CLIFTON N90-22920
SCHRAMA, ERNST J. O. N90-22575
SCHREUDER, J. M. N90-23199
SCHUMACHER, E. R. N90-22740
SCHURMAN, WALTER R. N90-22674
SCHWAN, H. N90-23282
SCHWERTASSEK, R. N90-22991
SCIUTO, DONATELLA N90-22725
N90-22726
SCOPPOLA, ELISABETTA N90-23175
SCOTT, JOHN J. N90-22673
SCOTT, P. M. N90-22648
SCRUBY, C. B. N90-22777
N90-22803
N90-22810
SEDGWICK, H. A. N90-22932
SEGALMAN, D. J. N90-23030
SEGALOW, Z. N90-22780
SELUKAR, R. S. N90-23143
N90-23144
SENICK, J. R. N90-22669
SERAFIM, P. N90-23209
SERRANO, J. P. N90-22572
SERVAN-SCHREIBER, DAVID N90-22984
SERVAN-SCHREIBER, EMILE N90-22911
SHABANA, A. A. N90-23015
SHAMROTH, STEPHEN J. N90-22538
SHARPE, LISA M. N90-22720
SHAW, GWENDOLYN M. N90-22719
SHEBILSKE, WAYNE L. N90-22949
N90-22950
SHER, DAVID N90-22895
SHERRICK, THOMAS M. N90-22800
SHIAO, MICHAEL C. N90-22823
SHINGLER, M. N90-22835
SHMALGAUZEN, V. I. N90-23166
SHU, CHI-WANG N90-23137
SHYNE, SCOTT S. N90-23126
SIDERIS, ATHANASIOS N90-23000
SIEMSSEN, R. H. N90-23206
SIGMON, THOMAS W. N90-23252
SIGNORETTI, F. N90-23337
SIGNORINI, C. N90-23337
SILVER, J. R. N90-22840
SIMON, HERBERT A. N90-22901
N90-22907
N90-22913
N90-23145
SIMONS, DAVID J. N90-22705
SIMPSON, G. N90-23308
SINGH, RAMEN P. N90-23029
N90-23079
SIRLIN, SAMUEL W. N90-22988
SITA, LAWRENCE R. N90-23211
SKELTON, R. N90-23056
SLAFER, LOREN I. N90-23065
SLATER, GARY L. N90-23003
SLAVIK, DONALD C. N90-22652
SLESENGER, T. A. N90-22704
SLINKER, S. P. N90-23208
SLOOFF, J. W. N90-22976
SMITH, M. D. N90-22599
SMITH, MICHAEL WAYNE N90-22533
SMITH, ROBBIE N90-23242
SMITH, STEPHEN N90-22936
SMITH, WALTER PRESTONT N90-22867
SMITH, WILLIAM L. N90-22868
SODEN, JERRY M. N90-22804
SOHONI, VIKRAM N. N90-23081
SOVIE, RONALD J. N90-22847
SPANGLER, CHARLES W. N90-22607
SPANOS, JOHN T. N90-23072
SPEARMAN, M. LEROY N90-23338
SPECTOR, SCOTT J. N90-22817
SPEER, EUGENE R. N90-23107
SPRANGLE, P. N90-23209
SREEKUMAR, PARAMESWARAN N90-23294
N90-23297
ST.JOHN, MARK N90-23104
ST.JOHN, RALPH J. N90-22563
ST.PIERRE, DAVID B. N90-22880
STACY, J. GREGORY N90-23295
STAMM, G. N90-23182
N90-23259
STANTON, ALAN C. N90-22601
STARK, LAWRENCE N90-22946
STEARNS, FOREST N90-22716
STECKER, FLOYD W. N90-23294
N90-23300
STEFANELLI, R. N90-23118
STEIDEL, CHARLES COLVILLE N90-23280
STEIER, WILLIAM H. N90-22607

STEIN, GUNTER N90-23127
STEINFELD, JEFFREY I. N90-22733
STERLING, L. S. N90-23061
STEVENS, KENT A. N90-22924
STEVENSON, CHARLES G. N90-22583
STEVENSON, FAREED N90-23186
STEWART, J. N90-22648
STEWART, M. B. N90-22764
STINCHCOMB, DAVE N90-23112
N90-23113
STOFFEL, T. N90-22839
STONE, THOMAS W. N90-23216
STONER, GLENN E. N90-22651
N90-22656
N90-22657
STOPER, ARNOLD E. N90-22959
STORCH, JOEL A. N90-23078
STORINI, M. N90-22849
STREET, ROBERT L. N90-22882
STRIFFLER, C. D. N90-22780
N90-23204
STRINATI, G. N90-23244
STUDER, F. A. N90-22711
STUTZKI, J. N90-23283
STUURMAN, C. N90-22968
STYER, DAVID J. N90-22969
SU, TZU-JENG N90-23055
SUCY, M. N90-23207
SUNKEL, JOHN W. N90-23029
N90-23041
SUTER, UELI W. N90-22686
SUTTON, EDMUND C. N90-22735
SWAB, JEFFREY J. N90-22684
SWANSON, R. E. N90-22658
SWANSON, ROBERT E. N90-22651
SWARTZ, JOHN C. N90-23214
SYLVESTER, MARK F. N90-22687
SYLVESTRE, J. C. N90-22580
SYMES, W. W. N90-23185
SZEMA, KUO-YEN N90-22746

T

TABER, ROD N90-23186
TABET, EUGENIO N90-23227
TAGETT, REBECCA N90-22877
TAGIROV, E. A. N90-23257
TANG, C. M. N90-23209
TANG, D. N90-22773
TAO, G. N90-23084
TARABAN, ROMAN N90-23104
TAYLOR, B. L. N90-22802
TAYLOR, DAVID WAYNE N90-22668
TAYLOR, J. B. N90-23222
TAYLOR, J. H. N90-23301
TAYLOR, JAMES N90-23050
TAYLOR, LAWRENCE W., JR. N90-23079
TAYLOR, M. J. N90-22740
TEIXEIRA, MARIO MARCIO RAMOS N90-23091
TEKAWY, JONATHAN A. N90-22999
TELESMAN, JACK N90-22646
TEMKAR, PRAKASH M. N90-22633
TENDICK, FRANK N90-22946
TENENBAUM, ALEXANDER N90-23227
TESNY, NEAL N90-23117
TESTA, MASSIMO N90-23133
TEYSSIER, GEORGES N90-22623
THADDEUS, PATRICK N90-23295
THAZHUTHAUEETIL, M. J. N90-23110
THEILIG, E. E. N90-22826
THOMAS, K. N90-22550
N90-22675
THOMPSON, D. E. N90-22818
THOMPSON, DAVID J. N90-23304
THOMPSON, PETER M. N90-22561
N90-22562
THOREN, STEPHEN J. N90-22538
THORNTON, EARL A. N90-22651
N90-22663
THORPE, CHRISTOPHER J. N90-23049
N90-23052
THORSOS, ERIC I. N90-23155
TILLEY, T. D. N90-22681
TINGLEY, JEFFREY W. N90-22699
TISNE, J. L. N90-22624
TOKSOEZ, NAFI N90-22862
TOMASELLI, CLARE MARIE N90-22966
TOULOUSE, JEAN N90-23238
TOURETZKY, DAVID S. N90-22903
N90-22904
N90-22906
TOWNSEND, DENNIS P. N90-22790
N90-22796
TOWNSEND, JAMES C. N90-22540
TREECE, R. KEITH N90-22804
TRYK, D. N90-22835
TSAREVSKIY, S. L. N90-23164
TSAY, WEAN-SHUN N90-23281
TSUHA, WALTER S. N90-23072
TURNER, J. D. N90-22990
TURNER, TIMOTHY L. N90-22955
TUSON, A. T. N90-22650
TVERSKY, BARBARA N90-22929

U

UDDING, JAN TIJMEN N90-23095
N90-23264
ULBRICH, HEINZ N90-22703
ULMER, M. P. N90-23310
UMLAND, JEFFREY W. N90-23083
UNDERWOOD, J. H. N90-22669

V

V.SCHWERDTNER, M. N90-23182
N90-23259
VALCO, G. J. N90-22732
VALLAURI, R. N90-23191
VANBEZOOIJEN, ROELOF W. H. N90-22612
VANDENBOSCH, F. J. N90-22979
VANDERVEEN, M. N90-22975
VANDERVOORT, R. J. N90-23047
VANDERWAL, J. N90-23266
VANDERWERF, S. Y. N90-23198
N90-23199
VANLEEUWEN, H. P. N90-22977
VANLEHN, KURT N90-22894
N90-22902
N90-22905
N90-22916
VANSCHILFGAARDE, MARK N90-23247
VARALJAY, N. N90-22732
VEGTER, GERT N90-22730
N90-23098
VELASCO, FLAVIO ROBERTO DIAS N90-23091
VENGOPAL, RAVI N90-23029
VENKAYYA, V. B. N90-23048
VERHAEGH, W. E. J. N90-23151
VILLORESI, G. N90-23336
N90-23337
VINTRO, LOUIS C. N90-22776
VITCK, J. M. N90-22792
VITIELLO, P. N90-23181
VONFLOTOW, ANDREAS H. N90-23014
VONMONTIGNY, CORINNA N90-23318
VOS, ROBERT G. N90-23046
VRAA, ANTHONY A. N90-22576
VULPIANI, A. N90-23226
VYUN, V. A. N90-23163

W

WAGNER, JOHN A. N90-22655
WAITE, WILLIAM M. N90-22983
WALATKA, PAMELA P. N90-23090
WALKER, S. N90-22704
WALL, S. D. N90-22826
WALLER, I. M. N90-22883
WALTER, SHARON M. N90-23108
WANG, A. S. D. N90-22627
WANG, C. N90-22835
WANG, VICTOR N90-22739
WARD, M. B. N90-22723
N90-22768
WARNER, J. D. N90-22732
WAROQUIER, M. N90-23199
WARRICK, JAMES C. N90-22547
WARSHAW, STEVE N90-22705
WARSI, S. N90-22564
WASKIEWICZ, A. E. N90-22736
WASON, THOMAS D. N90-22935
WAWNER, FRANKLIN E., JR. N90-22651
N90-22659
WAYMIRE, ED N90-22830
WEFEL, JOHN P. N90-23332
WEGMAN, EDWARD J. N90-22985
WEHRING, B. N90-22578
WEINBERG, BERNARD C. N90-22538
WEINBERG, DAVID HAL N90-23293
WEISS, R. A. N90-22682
WEIZER, VICTOR G. N90-22843
WELCH, ROBERT B. N90-22945
WELLS, B. N90-22648
WENDEROTH, PETER N90-22926
WERBOS, PAUL J. N90-23088
WERNICK, MILES N. N90-23212
WERT, JOHN A. N90-22651
N90-22660
WESTBY, M. F. N90-22537
WEYMAN, JAMES C. N90-22873
WHEELER, DEIRDRE W. N90-22906
WHITE, JAMES F. N90-22638
WHITLEY, K. M. N90-22593
WIDDEL, HEINO N90-22927
WIEDEMANN, JOHN N90-22951
WIGLEY, T. M. L. N90-22869
WIKUM, DOUGLAS N90-22716
WILLIAMS, DAVID E. N90-22649
WILLIAMS, JOSEPH J. N90-22755
WILLIAMS, STEVEN P. N90-22965
WILLIAMS, T. W. C. N90-23054
WILSON, MAYWOOD L. N90-22628
WILSON, ROBERT S. N90-23254
WILSON, WILLIAM W. N90-22845
WING, JEANNETTE M. N90-23114
WITHERELL, M. D. N90-22819
WOLCOTT, JOHN H. N90-22705
WONG, HO-CHEUNG N90-23011
WOO, HEE-GWEON N90-22681
WOOD, DAVID P. N90-23109
WOOD, WILLIAM G. N90-23109
WREN, GLORIA P. N90-22692
WRENN, GREGORY A. N90-22557
WRIGHT, P. B. N90-22869
WRIGHT, THOMAS W. N90-22670
WU, C. N90-23110
WU, JIANN-YUARN N90-23044
WU, QIAN N90-22852
WU, S.-C. N90-23037
WU, SHIH-CHIN N90-23080
WUNG, PEY MIN N90-22613

Y

YAE, K. HAROLD N90-22993
N90-23020
N90-23063
N90-23074
YAKOVKIN, I. B. N90-23163
YAMAMOTO, O. N90-22564
YANG, MUH-HSIUNG N90-22743
YAO, MINWU N90-22749
YAO, R. L. N90-22780
N90-23204
YEAGER, E. N90-22835
YEWELL, S. B. N90-22826
YINON, URI N90-22888
YIP, SIDNEY N90-22687
YOGEV, AMNON N90-22781
YOH, SHING N90-22864
YOSHIDA, K. N90-23173
YOSHIHARA, HIDEO N90-23172
YOUNG, LEO N90-22702
YUN, XIAOPING N90-23157

Z

ZACHARIAS, GREG L. N90-22563
ZALINKA, J. J. N90-22669
N90-22819
ZAMISKA, PAUL A. N90-22876
ZANGEMEISTER, WOLFGANG H. N90-22960
ZANGRILLI, N. L. N90-23336
N90-23337
ZEISEL, STEVEN H. N90-22684
ZHANG, SHENGBAI N90-23230
ZHANG, X. N90-23204
ZHANG, YI-CHENG N90-23174
ZHIDKOV, E. P. N90-23130
ZHOU, YANSHENG N90-22809
ZHU, G. N90-23056
ZIELINSKI, ALEXANDER E. N90-22734
ZIMMERMAN, RICHARD E. N90-22545
N90-22546
N90-22547
N90-22548
ZINGER, DON S. N90-22731
ZUCCONI, LIN N90-22700
ZWAANENBURG, KOOS N90-23068
ZWALLY, H. JAY N90-22850

Typical Corporate Source Index Listing

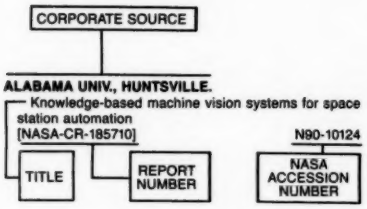

Listings in this index are arranged alphabetically by corporate source. The title of the document provides the user with a brief description of the subject matter. The report number helps to indicate the type of document cited (e.g., NASA report, translation, NASA contractor report). The NASA accession number denotes the number by which the citation is identified. The titles are arranged under each corporate source in ascending accession number order.

A

ACADEMY OF SCIENCES OF THE UKRAINIAN SSR, KHARKOV.
Dynamics of motion charged particles in a field of two electromagnetic waves
[DE90-620690] N90-22706
Forced scattering of electromagnetic waves on electron beam in periodically inhomogeneous plasma
[DE90-620705] N90-22707
Sound waves in weakly ionized gas
[DE90-620704] N90-23180
Gas dynamic theory of flight of fast electron flux in plasma
[DE90-618767] N90-23220
Numerical methods for the problem of the free-boundary plasma equilibrium in a stellarator (torsatron)
[DE90-620580] N90-23223

AERONAUTICAL RESEARCH LABS., MELBOURNE (AUSTRALIA).
Flutter investigations on a Transavia PL12/T-400 aircraft
[AD-A219108] N90-22570

AEROSPACE CORP., EL SEGUNDO, CA.
The HCl/aerosol problem N90-22597
Sticking coefficient of HCl on aerosols N90-22598
The effect of mechanical deformation on the radiation patterns of large space-based arrays
[AD-A219288] N90-22719

AEROSPATIALE, LES MUREAUX (FRANCE).
Multivariate analysis of launcher guidance robustness
[REPT-892-422-105] N90-22581
Equipment specifications for launcher guidance using multivariable frequency methods
[REPT-892-422-106] N90-22582

AEROSPATIALE, PARIS (FRANCE).
Methods of jet calculation
[REPT-892-422-102] N90-22603
Polymerization of composite materials: A technique developed by Aerospatiale
[REPT-892-430-107] N90-22623
On the vapour phase deposition mechanism of carbon-boron-nitrogen compounds between 800 and 1000 C
[REPT-892-430-101] N90-22632
Nondestructive Testing (NDT); Ceramic Matrix Composite Materials (CMCM)
[REPT-892-430-123] N90-22677
Microgravity, the space application of the 21st century. Challenges, constraints, and strategies
[REPT-892-430-105] N90-22696
Measurement and visualization of the shock wave caused by the impact of a pulsed YAG laser in water
[REPT-892-430-113] N90-22783

AEROSPATIALE AQUITAINE, SAINT-MEDARD EN JALLES (FRANCE).
Uncertainty evaluation in an automated high temperature environmental simulation oven
[REPT-892-430-103] N90-22571
SIMOUN: An optimized supersonic high temperature wind tunnel for testing construction materials to be used on the spaceplane
[REPT-892-430-111] N90-22572
Qualification test rationale for measuring the resistance of equipment to pyrotechnic shock
[REPT-892-430-117] N90-22590
Study and sizing of bonded joints in space structures
[REPT-892-430-124] N90-22591
Polymerization of composites
[REPT-892-430-102] N90-22621
Machining of new materials at Aerospatiale
[REPT-892-430-104] N90-22622
The surprising possibilities of wrapping
[REPT-892-430-108] N90-22624
Production of a variety of shapes using wrapping and draping techniques
[REPT-892-430-122] N90-22625
The position of carbon/carbon composites among high temperature composites
[REPT-892-430-126] N90-22626
Pyrotechnic materials ignited using lasers. High energy photopyrotechnic chains
[REPT-892-430-121] N90-22691
Large scale metrology by computer assisted photogrammetry
[REPT-892-430-116] N90-22772
Dimensional analysis of structures using wrapping techniques
[REPT-892-430-119] N90-22815
Evaluation of joints bonded with elastoplastic adhesives
[REPT-892-430-120] N90-22816

AIR FORCE ASTRONAUTICS LAB., EDWARDS AFB, CA.
Temperature measurements through a solid-propellant combustion wave using imbedded fine wire thermocouples
[AD-A218642] N90-22693

AIR FORCE FLIGHT DYNAMICS LAB., WRIGHT-PATTERSON AFB, OH.
Multidisciplinary Expert-aided Analysis and Design (MEAD) N90-23050

AIR FORCE GEOPHYSICS LAB., HANSCOM AFB, MA.
Temporal attributes of the ambient seismo-acoustic environment: La Junta, Colorado
[AD-A219369] N90-22825
International treaties and active experiments in space
[AD-A219368] N90-23272

AIR FORCE GLOBAL WEATHER CENTRAL, OFFUTT AFB, NE.
AFGW's upper air validator system
[AD-A219309] N90-22876

AIR FORCE HUMAN RESOURCES LAB., BROOKS AFB, TX.
Field-of-view assessment of low-level flight and an airdrop in the C-130 Weapon System Trainer (WST)
[AD-A218504] N90-22559
Visual behavior in the F-15 simulator for air-to-air combat
[AD-A218648] N90-22893

AIR FORCE HUMAN RESOURCES LAB., WILLIAMS AFB, AZ.
Visual behavior in the F-15 simulator for air-to-air combat
[AD-A218648] N90-22893

AIR FORCE INST. OF TECH., WRIGHT-PATTERSON AFB, OH.
A study of turbulence near thunderstorm tops
[NASA-CR-186620] N90-22870
An interactive method for estimating hailstone size and convectively-driven wind gusts from forecast soundings
[AD-A218499] N90-22871

AIR FORCE MATERIALS LAB., WRIGHT-PATTERSON AFB, OH.
Computer controlled cryogenic temperature controller
[AD-A218785] N90-22701

AIR FORCE OFFICE OF SCIENTIFIC RESEARCH LIAISON OFFICE, FAR EAST, APO SAN FRANCISCO, CA.
ONR Far East Scientific Information Bulletin, Volume 13, No. 4
[ONRFE-SCI-INFO-BULL-13(4)88] N90-23168

AIR FORCE OPERATIONAL TEST AND EVALUATION CENTER, KIRTLAND AFB, NM.
Next generation weather radar (NEXRAD) initial operational test and evaluation. Phase 2: (IOT and E(2))
[AD-A218770] N90-22873

AIR FORCE SYSTEMS COMMAND, WRIGHT-PATTERSON AFB, OH.
Climatic handbook of the USSR, issue 27. Kamchatskaya Oblast. Part 3: Wind
[AD-A218720] N90-22872

AIR FORCE WRIGHT RESEARCH AND DEVELOPMENT CENTER, WRIGHT-PATTERSON AFB, OH.
Implementation of generalized optimality criteria in a multidisciplinary environment N90-23048

AIR PRODUCTS AND CHEMICALS, INC., ALLENTOWN, PA.
Development of high-activity para- to ortho-hydrogen conversion catalysts, volume 2
[AD-A218700] N90-22638

ALABAMA UNIV., UNIVERSITY.
Contributions to the development of SLM TEA CO2 laser sources for high resolution molecular spectroscopy N90-22778

ALASKA UNIV., FAIRBANKS.
Gravity wave and turbulence studies using a high-resolution ST radar
[AD-A218877] N90-22860

APPLIED DYNAMICS INTERNATIONAL, ANN ARBOR, MI.
A new second-order integration algorithm for simulating mechanical dynamic systems N90-23064
Six-degree-of-freedom aircraft simulation with mixed-data structure using the applied dynamics simulation language, ADSIM N90-23067
Six-degree-of-freedom missile simulation using the ADI AD 100 digital computer and ADSIM simulation language N90-23068

ARIZONA STATE UNIV., TEMPE.
Multi-axis, 3-D, scanning LDA (Laser Doppler Anemometer) system for unsteady aerodynamics
[AD-A218571] N90-22541
Stratified ocean mixing
[AD-A219233] N90-22881
Multivariable frequency weighted model order reduction for control synthesis
[AIAA-89-3558] N90-23060
Continuation and multi-grid methods for bifurcation problems
[AD-A218904] N90-23146

ARIZONA UNIV., TUCSON.
Continued investigations of new concepts for improved spectrochemical analysis
[AD-A219403] N90-22644
Flat plate leading edge receptivity to various freestream disturbance structures N90-22750
Tropical squall lines of the Arizona monsoon N90-22867
Systematic generation of multibody equations of motion suitable for recursive and parallel manipulation N90-22992
A search for additional parameters in the infrared luminosity/21 cm line-width relation for spiral galaxies in clusters of galaxies N90-23274
Molecular evolution in astrophysical environments N90-23291
Optical properties of cometary dust
[AD-A218790] N90-23325
Local atmospheric electricity and its possible application in high energy cosmic ray air shower detection N90-23335

ARMY ARMAMENT RESEARCH, DEVELOPMENT AND ENGINEERING CENTER, WATERVLIET, NY.
Fracture mechanics assessment of a cracked 16-inch inner diameter 1945 vintage-jacketed pressure vessel
[AD-A219135] N90-22819

Adaptive mesh experiments for hyperbolic partial differential equations
[AD-A219194] N90-23148

ARMY ARMAMENT RESEARCH AND DEVELOPMENT COMMAND, WATERVLIET, NY.
Fracture toughness and fatigue crack initiation tests of welded precipitation-hardening stainless steel
[AD-A218745] N90-22669

ARMY ARMOR AND ENGINEER BOARD, FORT KNOX, KY.
M1A2 adjunct analysis (POSNOV volume)
[AD-A218802] N90-22553

ARMY AVIATION SYSTEMS COMMAND, CLEVELAND, OH.
Surface pitting fatigue life of noninvolute, low-contact-ratio gears
[NASA-TM-103116] N90-22790
Influence of linear profile modification and loading conditions on the dynamic tooth load and stress of high contact ratio gears
[NASA-TM-103136] N90-22796

ARMY COLD REGIONS RESEARCH AND ENGINEERING LAB., HANOVER, NH.
Estimating sea ice thickness using time-of-flight data from impulse radar soundings
[AD-A218736] N90-22831
Accuracy and precision of GOES data collection platforms for temperature measurements
[AD-A218798] N90-22832

ARMY CONSTRUCTION ENGINEERING RESEARCH LAB., CHAMPAIGN, IL.
Calcium carbonate scale dissolution in water stabilized by carbon dioxide treatment
[AD-A218502] N90-22633

ARMY ENGINEER TOPOGRAPHIC LABS., FORT BELVOIR, VA.
The development of a real-time decimeter-level positioning system using Global Positioning System (GPS) technology
[AD-A218695] N90-22552

ARMY LAB. COMMAND, WATERTOWN, MA.
Low temperature degradation of Y-TZP materials
[AD-A218841] N90-22684

ARMY MATERIALS TECHNOLOGY LAB., WATERTOWN, MA.
Role of shear instability in ballistic penetration
[AD-A219186] N90-22799

ARMY MILITARY PERSONNEL CENTER, ALEXANDRIA, VA.
Transport properties of plasmas in microwave electrothermal thrusters
[AD-A219408] N90-23228

ARMY NATICK RESEARCH AND DEVELOPMENT COMMAND, MA.
A computer program to implement the Chen method of dimensional analysis
[AD-A218557] N90-23142

ARMY RESEARCH INST. OF ENVIRONMENTAL MEDICINE, NATICK, MA.
Physiological and perceptual responses to prolonged treadmill load carriage
[AD-A218910] N90-22886

ARMY RESEARCH OFFICE, RESEARCH TRIANGLE PARK, NC.
Transactions of the Seventh Army Conference on Applied Mathematics and Computing
[AD-A219220] N90-23160

ARMY RESEARCH OFFICE, FAR EAST LIAISON OFFICE, APO SAN FRANCISCO, CA.
ONR Far East Scientific Information Bulletin, Volume 13, No. 4
[ONRFE-SCI-INFO-BULL-13(4)88] N90-23168

ASTRONOMISCHE RECHEN-INST., HEIDELBERG (GERMANY, F.R.).
Fifth fundamental catalogue (FK5). Part 1: The basic fundamental stars
[REPT-32(1988)-PT-1] N90-23282

AUBURN UNIV., AL.
Relationship between flexibility of closure and success in pilot night vision sensor system training N90-22890

B

BALLISTIC RESEARCH LABS., ABERDEEN PROVING GROUND, MD.
Approximate analysis for the formation of adiabatic shear bands
[AD-A218751] N90-22670
A comparison between experiment and simulation for concept VIC regenerative liquid propellant guns. Part 1: 30 mm
[AD-A218556] N90-22692
Methods for evaluation of thermally induced reactions in liquid propellants
[AD-A218750] N90-22694
Optimization of a pulsed air core transformer for low impedance inductive ignition
[AD-A218748] N90-22734
Side moment exerted by a spinning, coning, highly viscous liquid payload
[AD-A218746] N90-22763
Large-scale simulations of monolithic and segmented projectiles impacting spaced armor
[AD-A219374] N90-22800

BBN SYSTEMS AND TECHNOLOGIES CORP., CANOGA PARK, CA.
Assessment System for Aircraft Noise (ASAN) citation database. Volume 1: User's manual
[AD-A219175] N90-23188
Assessment System for Aircraft Noise (ASAN) citation database. Volume 2: Database update manual
[AD-A219176] N90-23189
Assessment System for Aircraft Noise (ASAN) citation database. Volume 3: New citation review procedures
[AD-A219177] N90-23190

BIO-IMAGING RESEARCH, INC., LINCOLNSHIRE, IL.
On-line x ray inspection of materials and structural components using discrete element x ray detectors for digital radiographic and computed tomographic evaluation
[AD-A218911] N90-22806

BIONETICS CORP., COCOA BEACH, FL.
The physiological cost of wearing the propellant handler's ensemble at the Kennedy Space Center
[NASA-TM-102786] N90-22966

BOEING AEROSPACE CO., SEATTLE, WA.
Methodology for analysis and simulation of large multidisciplinary problems N90-23046
Structural modeling for control design (articulated multibody component representation) N90-23077

BOEING CO., SEATTLE, WA.
Boeing/NASA composite components flight service evaluation
[NASA-CR-181898] N90-22609

BOEING COMMERCIAL AIRPLANE CO., SEATTLE, WA.
Spatial displays as a means to increase pilot situational awareness N90-22951

BOSTON UNIV., MA.
Temporal attributes of the ambient seismo-acoustic environment: La Junta, Colorado
[AD-A219369] N90-22825
Heat exhaustion in a rat model: Lithium as a biochemical probe
[AD-A219361] N90-22884

BRISTOL UNIV. (ENGLAND).
Seeing by exploring N90-22923

BUFFALO UNIV., NY.
Controlling flexible structures with second order actuator dynamics N90-23083

C

CAE ELECTRONICS LTD., MONTREAL (QUEBEC).
Multi-axis control of telemanipulators N90-22943

CALIFORNIA INST. OF TECH., PASADENA.
Robustness analysis for real parametric uncertainty N90-23000
Experimental experience with flexible structures N90-23002
Combined control-structure optimization N90-23005
Spectroscopic observations of high redshift QSOs: Galaxies and the intergalactic medium at early epochs N90-23280
Studies in gravitational lensing and numerical hydrodynamics N90-23290

CALIFORNIA UNIV., BERKELEY.
Construction of a 345 gigahertz receiver based on superconducting tunnel junctions
[AD-A218781] N90-22735
Regional studies with broadband data
[AD-A219215] N90-22861
Threshold photodetachment spectroscopy of the I + HI transition state region
[AD-A218410] N90-22883
Spatial constraints of stereopsis in video displays N90-22920
Visual enhancements in pick-and-place tasks: Human operators controlling a simulated cylindrical manipulator N90-22946
Electronic theory of solids, surfaces, interfaces, and clusters N90-23230
Thermal phenomena in high-Tc thin film superconductors N90-23233
The interstellar medium of a starburst galaxy; millimeter interferometric observations of M82 N90-23276
Spectral measurements of the cosmic microwave background N90-23334

CALIFORNIA UNIV., BERKELEY. LAWRENCE BERKELEY LAB.
Regional studies with broadband data
[AD-A219215] N90-22861

CALIFORNIA UNIV., DAVIS.
High-temperature deformation of mechanically-alloyed aluminum IN90211 N90-22645

CALIFORNIA UNIV., LOS ANGELES.
Quantifying and reducing uncertainty in the assimilative mapping of ionospheric electrodynamics N90-22854
Minimum attainable RMS attitude error using co-located rate sensors N90-23038
Approximation in LQG control of a thermoelastic rod N90-23084
Measurement of localized deep levels and wafer non-uniformities at 3-5 semiconductor heterojunctions
[AD-A218547] N90-23248
Gamma ray cosmology: The extra galactic gamma spectrum and methods to detect the underlying source N90-23321
Studies of Io's atmosphere and plasma torus N90-23326

CALIFORNIA UNIV., SAN DIEGO, LA JOLLA.
Dehydrogenative polymerization of silanes to polysilanes: A monomeric copper(2) siloxide
[AD-A218550] N90-22681
Statistical inference from sampled data
[AD-A218731] N90-23156

CALIFORNIA UNIV., SANTA BARBARA.
Stereoscopic distance perception N90-22921
A survey on the structured singular value N90-22998

CALIFORNIA UNIV., SANTA CRUZ.
Separate visual representations for perception and for visually guided behavior N90-22931

CARNEGIE-MELLON UNIV., PITTSBURGH, PA.
Inertial navigation system simulator: Behavioral specification, revision
[AD-A219294] N90-22554
ALVINN: An Autonomous Land Vehicle In a Neural Nettwork
[AD-A218975] N90-22797
Efficient specialization of relational concepts
[AD-A218889] N90-22894
A preliminary analysis of the SOAR architecture as a basis for general intelligence
[AD-A218913] N90-22896
Towards the knowledge level in SOAR: The role of the architecture in the use of knowledge
[NASA-CR-186615] N90-22897
Stochastic interactive activation and the effect of context on perception
[AD-A218929] N90-22898
Cognitive efficiency considerations for good graphic design
[AD-A218976] N90-22899
Designing good experiments to test bad hypotheses
[AD-A218977] N90-22900
What makes some problems hard: Explorations in the problem space of difficulty
[AD-A219002] N90-22901
Discovering problem solving strategies: What humans do and machines don't (yet)
[AD-A219008] N90-22902
Rules and maps in connectionist symbol processing
[AD-A219028] N90-22903
Connectionism and compositional semantics
[AD-A219029] N90-22904
Learning events in the acquisition of three skills
[AD-A219038] N90-22905
A connectionist implementation of cognitive phonology
[AD-A219095] N90-22906
Cognitive architectures and rational analysis: Comment
[AD-A219199] N90-22907
Information processing approaches to cognitive development
[AD-A219200] N90-22908
Toward a SOAR theory of taking instructions for immediate reasoning tasks
[AD-A219201] N90-22909
Learning artificial grammars with competitive chunking
[AD-A219270] N90-22911
A task-analytic approach to the automated design of information graphics
[AD-A219271] N90-22912
Laboratory replication of scientific discovery processes
[AD-A219273] N90-22913
An instructable Connectionist/Control architecture: Using rule-based instructions to accomplish connectionist learning in a human time scale
[AD-A219274] N90-22914
Hatching a theory of incubation effects
[AD-A219275] N90-22915
Non-LIFO (Last-In-First-Out) execution of cognitive procedures
[AD-A219277] N90-22916

Encoding sequential structure in simple recurrent networks
[AD-A218928] N90-22984
Sentence comprehension: A parallel distributed processing approach
[AD-A218886] N90-23104
Comparative evaluations of four specification methods for real-time systems
[AD-A219187] N90-23109
The Durra application debugger/monitor
[AD-A219290] N90-23111
DARK (Distributed Ada Real-Time Kernel) porting and extension guide Kernel version 3.0
[AD-A219291] N90-23112
Version description and installation guide Kernel version 3.0
[AD-A219292] N90-23113
Durra: A task-level description language reference manual, version 2
[AD-A219293] N90-23114
Kernel architecture manual
[AD-A219295] N90-23115
Scientific discovery as problem solving
[AD-A218687] N90-23145
Investigation of optical nonlinearities, conductivity and magnetism in organometallic materials
[AD-A218548] N90-23211
Advanced gas phase reactor for growth of Ge sub x Si sub 1-x
[AD-A219012] N90-23250

CASE WESTERN RESERVE UNIV., CLEVELAND, OH.
Dynamic substructuring by the boundary flexibility vector method of component mode synthesis
[NASA-CR-182445] N90-22813
Catalysts for ultrahigh current density oxygen cathodes for space fuel cell applications
[NASA-CR-180650] N90-22835
Distributed neural control of a hexapod walking vehicle N90-23061
A general low-harmonic cosmic string and its self-intersection and fragmentation N90-23284

CENTRE D'ESSAIS AERONAUTIQUE TOULOUSE (FRANCE).
Bird impact tests on Kevlar 29 and 49 sandwich structures under straight-on and glancing impact
[REPT-S3-4273-PARTIAL-6] N90-22617
Bird impact tests on Kevlar plates. Sandwich Kevlar-nida submitted to straight-on and glancing impact
[REPT-S3-4273-PARTIAL-3] N90-22619
Bird impact tests on structures made of Kevlar 49. Monolithic plates under straight-on impact
[REPT-S3-4273-PARTIAL-1] N90-22620

CENTRE DE RECHERCHES SCIENTIFIQUES ET TECHNIQUES DE L'INDUSTRIE DES FABRICATIONS METALLIQUES, BRUSSELS (BELGIUM).
Noise reduction theory acoustic barrier construction
[CRIF-MC-87] N90-23183

CENTRE NATIONAL DE LA RECHERCHE SCIENTIFIQUE, PARIS (FRANCE).
Boundary layer turbulence pulsed by acoustic waves
[ETN-90-96621] N90-22759

CERAMIC PROCESS SYSTEMS CORP., MILFORD, MA.
Composite ceramic superconducting wires for electric motor applications
[AD-A219131] N90-22689

CHARLES RIVER ANALYTICS, INC., CAMBRIDGE, MA.
Model-based method for terrain-following display design
[AD-A219302] N90-22563

CINCINNATI UNIV., OH.
A disturbance based control/structure design algorithm N90-23003

CITY COLL. OF THE CITY UNIV. OF NEW YORK, NY.
Microcracking and toughness of ceramic-fiber/ceramic-matrix composites under high temperature
[AD-A218516] N90-22680
Support for the 16th International Conference on the Physics of Electronic and Atomic Collisions
[AD-A218567] N90-23200

CITY UNIV. OF NEW YORK RESEARCH FOUNDATION, NY.
Exposure of human cells to electromagnetic fields
[AD-A219377] N90-22889

CIVIL AVIATION AUTHORITY, LONDON (ENGLAND).
UK airmisses involving commercial air transport, January - April 1989
[ISSN-0951-6301] N90-22544

CLARKSON UNIV., POTSDAM, NY.
Collective properties of neural systems and their relation to other physical models
[AD-A219071] N90-23201

CLEVELAND STATE UNIV., OH.
The effect of elevated gravity on the crystallization of the MFI zeolites, ZSM-5, and silicalite N90-23231

COAST GUARD, ALEXANDRIA, VA.
BTOS database evaluation
[AD-A219304] N90-23271

COLORADO UNIV., BOULDER.
Semianalytic study of high-eccentricity orbit stability and evolution N90-22574
Automatic compiler construction
[AD-A218777] N90-22983
Ultraviolet and infrared studies of Be stars N90-23275

COLUMBIA UNIV., NEW YORK, NY.
Femtosecond studies of electron photodetachment of simple ions in liquid water: Solvation and geminate recombination dynamics
[AD-A218520] N90-22634
Gamma radiation from radio pulsars N90-23302

COMMISSARIAT A L'ENERGIE ATOMIQUE, SACLAY (FRANCE).
Turbulence and complex systems
[ETN-90-96620] N90-22758

COMMITTEE ON SCIENCE, SPACE AND TECHNOLOGY (U.S. HOUSE).
Nuclear power in space
[GPO-23-835] N90-23202

CONNECTICUT UNIV., STORRS.
The minimum drag profile in laminar flow: A numerical way N90-22535
Synthesis and properties of a thermotropic copolyester based on 4,4 prime-dihydroxy-a,a prime-dimethylbenzalazine
[AD-A218803] N90-22682
Processing of thermotropic liquid crystalline polymers and their blends
[AD-A218804] N90-22683

CORNELL UNIV., ITHACA, NY.
Numerical investigation of turbulent flame sheets
[AD-A218553] N90-22635
Modified maleic anhydride copolymers as e-beam resists
[AD-A218470] N90-22679
Plasma instabilities associated with the injection of artificial ion beams into the ionosphere N90-22851
On the efficacy of cinema, or what the visual system did not evolve to do N90-22934
An algorithm for the solution of dynamic linear programs N90-23026
The dynamical evolution of dense clusters of compact stars N90-23287

COUNCIL FOR NATIONAL ACADEMIC AWARDS (ENGLAND).
The behaviour of mechanically fastened joints in composite structures N90-22789

D

DAVID TAYLOR RESEARCH CENTER, BETHESDA, MD.
Pressure and shear stress measurement uncertainty for DARPA SUBOFF experiment
[AD-A219109] N90-22798
Vectors and matrices: Two turbo pascal units for fast program development
[AD-A218917] N90-23105

DEFENCE RESEARCH ESTABLISHMENT SUFFIELD, RALSTON (ALBERTA).
Estimation of extra drag force on a circular cylinder due to the presence of solid particles in subsonic compressible flow
[AD-A218635] N90-22542

DEFENSE MAPPING AGENCY SYSTEMS CENTER, RESTON, VA.
Guidelines, operational procedures, and quality control for the estimation of geodetic point positions from GPS data collected with the TI4100 receiver
[AD-A218460] N90-22829

DELAWARE UNIV., NEWARK.
Axisymmetric and cylindrically orthotropic analysis of filament winding N90-22811
Visual selective attention
[AD-A219204] N90-22910

DENVER UNIV., CO.
The large and small scale density structure in the solar corona N90-23327

DEPARTMENT OF DEFENSE, WASHINGTON, DC.
The Department of Defense critical technologies plan for the Committees on Armed Services United States Congress
[AD-A219300] N90-22702
Atlas/data abstract for the United States and selected areas, fiscal year 1989
[AD-A219289] N90-23270

DEPARTMENT OF ENERGY, RICHLAND, WA.
National emissions standards for hazardous air pollutants application for approval of construction SP-100 ground engineering system test site
[DE90-007985] N90-23203

DEPARTMENT OF THE NAVY, WASHINGTON, DC.
Apparatus for and a method of determining compass headings
[AD-D014436] N90-22551

DEUTSCHE FORSCHUNGS- UND VERSUCHSANSTALT FUER LUFT- UND RAUMFAHRT, OBERPFAFFENHOFEN (GERMANY, F.R.).
Aspects of efficient and reliable multibody system simulation N90-22991

DEUTSCHE FORSCHUNGSANSTALT FUER LUFT- UND RAUMFAHRT, STUTTGART (GERMANY, F.R.).
Comparison of solar pumped Nd:YAG and Nd:Cr:GSGG lasers at liquid nitrogen and room temperature
[DLR-FB-89-41] N90-22781
The pressure loaded volumetric ceramic receiver
[DLR-MITT-89-17] N90-22842

DRAPER (CHARLES STARK) LAB., INC., CAMBRIDGE, MA.
A computer graphics system for visualizing spacecraft in orbit N90-22952

DREXEL UNIV., PHILADELPHIA, PA.
Impact damage in graphite/epoxy laminates: Damage characterization, acoustic emission, and finite element simulation, volumes 1 and 2 N90-22610
A comprehensive study on microstructure mechanics relationships of ceramic matrix composites
[AD-A219318] N90-22627
Oxidation and ignition characteristics of hydrocarbon fuels
[AD-A218666] N90-22637
Impact of marine boundary layer parameterization on a numerical simulation of cyclogenesis during a cold air outbreak event N90-22864

DUKE UNIV., DURHAM, NC.
Frequency domain techniques for analyzing picosecond optical pulses
[AD-A218856] N90-23214

DYNACS ENGINEERING CO., INC., CLEARWATER, FL.
Enhanced modeling features within TREETOPS N90-23047

E

EAST ANGLIA UNIV., NORWICH (ENGLAND).
Development and use of a passive technique for measuring nitrogen dioxide in the background atmosphere N90-23285

ECOLE NATIONALE SUPERIEURE DE MECANIQUE, NANTES (FRANCE).
Multigrid acceleration of transonic flow computations
[ENSM-8024] N90-22760

ECOLE NATIONALE SUPERIEURE DE PHYSIQUE, MARSEILLES (FRANCE).
Microstructure of thin films
[AD-A219262] N90-23255

EDGERTON, GERMESHAUSEN AND GRIER, INC., IDAHO FALLS, ID.
A multipulsed dynamic diffraction moire interferometer
[DE90-009765] N90-22723
High temperature ceramic-tubed reformer
[DE90-009617] N90-22755
A compact portable diffraction moire interferometer
[DE90-009780] N90-22768
Comparison between data generated from standard fracture toughness specimens and from nonstandard specimens made of a silicon carbide
[DE90-009621] N90-22814

EG AND G MOUND APPLIED TECHNOLOGIES, MIAMISBURG, OH.
Ignition testing of low-energy laser diode ignited components
[DE90-009968] N90-22630

EPITAXX, INC., PRINCETON, NJ.
Development of a unique laboratory standard indium gallium arsenide detector for the 500 to 1700 micron spectral region, phase 2
[NASA-CR-180482] N90-22767

ERG SYSTEMS, INC., SAINT JAMES, NY.
Full surface interferometric testing of grazing incidence mirrors
[AD-A219394] N90-23218

EVANS (CHARLES) AND ASSOCIATES, REDWOOD CITY, CA.
Secondary ion mass spectrometry characterization of implants into GaAs and GaP for waveguides and integrated optics applications
[AD-A219203] N90-23254

F

FEDERAL AVIATION ADMINISTRATION, ATLANTIC CITY, NJ.
Turbine fuel alternatives (near term)
[AD-A219405] N90-22695

FEDERAL AVIATION ADMINISTRATION, WASHINGTON, DC.
FAA (Federal Aviation Administration) aviation forecasts, fiscal years 1990-2001
[AD-A219165] N90-22530
Airliner cabin ozone: An updated review
[AD-A219264] N90-22970
FLORIDA UNIV., GAINESVILLE.
Multimedia system control
[AD-A219392] N90-22971
FOKKER B.V., SCHIPOL-OOST (NETHERLANDS).
Aircraft technology management and the related significance of the supercomputer N90-22975
FORSCHUNGSINSTITUT FUER ANTHROPOTECHNIK, WACHTBERG (GERMANY, F.R.).
The photo-colorimetric space as a medium for the representation of spatial data N90-22927

G

GENERAL MOTORS CORP., INDIANAPOLIS, IN.
Investigation of advanced counterrotation blade configuration concepts for high speed turboprop systems, task 1: Ducted propfan analysis
[NASA-CR-185217] N90-22567
GEORGE MASON UNIV., FAIRFAX, VA.
Graphics equipment for data analysis
[AD-A218983] N90-22985
Analysis and evaluation of technical data on the photochromic and non-linear optical properties of materials
[AD-A219398] N90-23219
GEORGIA INST. OF TECH., ATLANTA.
Application of a dynamic stall model to rotor trim and aeroelastic response N90-22556
A finite element based method for solution of optimal control problems N90-23027
Robust fixed order dynamic compensation for large space structure control N90-23059
GEORGIA STATE UNIV., ATLANTA.
Anderson Mesa, Arizona as a site for an optical interferometric array N90-23281
GEORGIA TECH RESEARCH INST., ATLANTA.
MEGALIDAR proof-of-concept demonstration
[AD-A218787] N90-22858
GINER, INC., WALTHAM, MA.
Advanced double layer capacitor
[AD-A219419] N90-22741
GRONINGEN RIJKSUNIV. (NETHERLANDS).
Bifurcational aspects of parametric resonance
[W-8904] N90-22730
Modelling and computer control of a mechanical system
[W-8908] N90-22794
Program inversion: More than fun
[CS-8903] N90-23095
Factoring homomorphisms
[CS-8908] N90-23096
About the order of Appel's algorithm
[CS-8910] N90-23097
The visibility diagram: A data structure for visibility and motion planning problems. Part 1: Application to the visibility polygon query problem
[CS-8913-PT-1] N90-23098
On the performance of parallel algorithms
[CS-8914] N90-23099
Curvature-dependent parametrization of curves and surfaces
[CS-8915] N90-23100
Controlling real-time systems with parallel processes
[CS-8916] N90-23119
Naturalness of polymorphism
[CS-8916] N90-23134
Processes and formalisms for unbounded choice
[CS-8917] N90-23135
A proof of the isoenergetic KAM: Theorem from the ordinary one
[W-8906] N90-23136
An effective He-3 nucleon force for the He-3, t) charge exchange reaction
[KVI-813] N90-23198
Study of Sn-116 via neutron pickup and proton stripping reactions
[KVI-814] N90-23199
Incomplete fusion reactors at low and intermediate energies
[KVI-809] N90-23206
Towards a calculus of data refinement
[CS-8902] N90-23264
An algebric approach to infinite data structures
[CS-8909] N90-23265
GRUMMAN AEROSPACE CORP., BETHPAGE, NY.
What is learned from high energy bursts and flares N90-23314

H

HAMBURG UNIV. (GERMANY, F.R.).
Voluntary presetting of the vestibular ocular reflex permits gaze stabilization despite perturbation of fast head movements N90-22960
HARRIS CORP., MELBOURNE, FL.
Solar Concentrator Advanced Development Program
[NASA-CR-185173] N90-22834
Integrated control-system design via generalized LQG (GLQG) theory N90-23023
Minimal complexity control law synthesis N90-23057
HARRY DIAMOND LABS., ADELPHI, MD.
Basic graphics routine technical manual
[AD-A219409] N90-23117
HARVARD-SMITHSONIAN CENTER FOR ASTROPHYSICS, CAMBRIDGE, MA.
Molecular clouds and the large-scale structure of the galaxy N90-23295
HICKMAN (ROBERT J.), NEWPORT BEACH, CA.
Combining high performance simulation, data acquisition, and graphics display computers N90-23062
HONEYWELL, INC., MINNEAPOLIS, MN.
Robust adaptive control: Stability and asymptotic performance
[AD-A219259] N90-23127
HOUSTON UNIV., TX.
Nonstrictly hyperbolic conservation laws
[AD-A218525] N90-22762
HOWARD UNIV., WASHINGTON, DC.
Dynamics and control of tethered antennas/reflectors in orbit
[AD-A219316] N90-22594
HUGHES AIRCRAFT CO., EL SEGUNDO, CA.
The use of real-time, hardware-in-the-loop simulation in the design and development of the new Hughes HS601 spacecraft attitude control system N90-23065
HUGHES SPACE AND COMMUNICATIONS GROUP, LOS ANGELES, CA.
Faster simulation plots N90-23071

I

IIT RESEARCH INST., CHICAGO, IL.
ELF (Extremely Low Frequency) communications system ecological monitoring program: Slime mold studies
[AD-A218623] N90-22715
ELF (Extremely Low Frequency) communications systems ecological monitoring program: Wetland studies
[AD-A218632] N90-22716
ILLIANA AVIATION SCIENCES, LAS CRUCES, NM.
The eyes prefer real images N90-22938
ILLINOIS UNIV., CHAMPAIGN.
Ability distributions pattern probabilities and quasidensities
[AD-A218471] N90-23153
ILLINOIS UNIV., CHICAGO.
Interactive displays in medical art N90-22940
Parallel and vector computation for stochastic optimal control applications N90-23007
Nonlinear finite element formulation for the large displacement analysis in multibody system dynamics N90-23015
Optimum control forces for multibody systems with intermittent motion N90-23016
The coupling effects of kinematics and flexibility on the Lagrangian dynamic formulation of open chain deformable links N90-23018
Explicit modeling of composite plates and beams in the dynamics of multibody systems N90-23019
ILLINOIS UNIV., URBANA.
The interactive digital video interface N90-22941
Sliding control of pointing and tracking with operator spline estimation N90-22997
ILLINOIS UNIV. AT URBANA-CHAMPAIGN, SAVOY.
A new stochastic model of turbulent dispersion in the convective planetary boundary layer and the results of the Atterbury-87 field study N90-22853
Evolution of atmospheric baroclinic waves N90-22855
Single crystal NMR of high temperature superconductors N90-23236
A low temperature calorimetric study of several high-T(sub c) superconductors N90-23237
Rapid mass transfer in binary systems N90-23289
INDUSTRIAL QUALITY, INC., GAITHERSBURG, MD.
Real-time stereo-microradiography
[AD-A218433] N90-22805
INSTITUT FUER THEORETISCHE STROEMUNGSMECHANIK, GOETTINGEN (GERMANY, F.R.).
Nonlinear bifurcation study of plane Poiseuille flow
[DLR-FB-89-42] N90-22756
INSTITUT NATIONAL DE RECHERCHE D'INFORMATIQUE ET D'AUTOMATIQUE, ROCQUENCOURT (FRANCE).
Proceedings of the 9th International Conference on Computing Methods in Applied Science and Engineering
[AD-A219307] N90-23149
INSTITUT NATIONAL DES SCIENCES APPLIQUEES DE LYON, VILLEURBANNE (FRANCE).
Characterization and role of an elastomeric interphase within polyepoxy reinforced glass, both particulate and fibrous
[ISAL-89-0064] N90-22676
Design and construction of a packed column simulator operating under atmospheric and reduced pressure
[ISAL-89-60] N90-22757
INSTITUT NATIONAL DES SCIENCES APPLIQUEES, LYON (FRANCE).
Damage analysis following slight deformations of composite materials
[RDS-1-007-64] N90-22618
INSTITUTE FOR COMPUTER APPLICATIONS IN SCIENCE AND ENGINEERING, HAMPTON, VA.
The analysis and simulation of compressible turbulence
[NASA-CR-181997] N90-22539
Secondary frequencies in the wake of a circular cylinder with vortex shedding
[NASA-CR-181998] N90-22540
The preprocessed doacross loop
[NASA-CR-182056] N90-22972
A scheme for supporting automatic data migration on multicomputers
[NASA-CR-182038] N90-22973
Communication overhead on the Intel iPSC-860 hypercube
[NASA-CR-182055] N90-22982
Fourier analysis of finite element preconditioned collocation schemes
[NASA-CR-182040] N90-23128
High order essentially non-oscillatory schemes for Hamilton-Jacobi equations
[NASA-CR-181995] N90-23137
Analytic semigroups: Applications to inverse problems for flexible structures
[NASA-CR-182047] N90-23138
Stable boundary conditions for Cartesian grid calculations
[NASA-CR-182048] N90-23139
INSTITUTO DE PESQUISAS ESPACIAIS, SAO JOSE DOS CAMPOS (BRAZIL).
Characterization of Monel alloys by x ray fluorescence technique
[DE90-617175] N90-22665
Impact of meteorology on the agricultural sector: Compilation and analysis of projects
[INPE-4846-PRE/1475] N90-22866
A tool for aiding in the reuse of software
[INPE-4981-PRE/1545] N90-23091
Syntax, semantics, and pragmatism: An integrated focus based on textual linguistic knowledge
[INPE-4992-PRE/1554] N90-23262
Spectral plane quasars, spectral turn-over, and frequency atlas
[INPE-5011-TDL/399] N90-23277
INSTITUTO MILITAR DE ENGENHARIA, RIO DE JANEIRO (BRAZIL).
Hydrogenation of stainless steels implanted with nitrogen
[DE90-617397] N90-22668
INTEGRATED SYSTEMS, INC., SANTA CLARA, CA.
Computational issue in the analysis of adaptive control systems N90-23001
INTERNATIONAL FUEL CELLS CORP., SOUTH WINDSOR, CT.
Enhanced ceria solid electrolyte fuel cell development. Reduction of electronic conductivity permits use of a solid ceria electrolyte in high efficiency high power density fuel cells at temperatures compatible with metallic cell hardware
[AD-A219297] N90-22846
IOWA STATE UNIV. OF SCIENCE AND TECHNOLOGY, AMES.
Experimental adaptive control of a hydraulic robot N90-23121
TeV radiation from the Crab nebula and other matters N90-23306
IOWA UNIV., IOWA CITY.
Recursive linearization of multibody dynamics equations of motion N90-22993
A robot arm simulation with a shared memory multiprocessor machine N90-23008
Experimental verification of dynamic simulation N90-23020
A decoupled recursive approach for constrained flexible multibody system dynamics N90-23042

Man-in-the-control-loop simulation of manipulators N90-23063
Model reduction in the physical coordinate system N90-23074
VLA and VLBI angular broadening measurements: The distribution of interstellar scattering at low Galactic latitudes N90-23279

ITALSPAZIO, ROME (ITALY).
Orbit acquisition and control strategy for small satellites in inclined eccentric orbits
[ETN-90-96551] N90-22573
The Italian approach to small satellites for low cost access to space developments
[ETN-90-96552] N90-22587
Low cost station keeping maneuvers for a small-satellites constellation in tundra orbits
[ETN-90-96553] N90-22588

J

JAPAN BROADCASTING CORP., TOKYO.
How to reinforce perception of depth in single two-dimensional pictures N90-22937

JAYCOR, TORRANCE, CA.
Thermal barrier research
[DE90-009213] N90-23221

JET PROPULSION LAB., CALIFORNIA INST. OF TECH., PASADENA.
Atmospheric autorotating imaging device
[NASA-CASE-NPO-17390-1-CU] N90-22769
Spaceborne radar observations: A guide for Magellan radar-image analysis
[NASA-CR-184998] N90-22826
Monthly surface thermal forcing in the tropical Pacific from 1980 to 1983
[NASA-CR-183033] N90-22877
Displays for telemanipulation N90-22948
The making of the mechanical universe N90-22961
Proceedings of the 3rd Annual Conference on Aerospace Computational Control, volume 1
[NASA-CR-186446] N90-22987
An assessment of multibody simulation tools for articulated spacecraft N90-22988
Spatial operator algebra framework for multibody system dynamics N90-22989
An innovations approach to decoupling of multibody dynamics and control N90-22994
A unifying framework for rigid multibody dynamics and serial and parallel computational issues N90-23009
Parallel algorithms and architecture for computation of manipulator forward dynamics N90-23010
Computational chaos in massively parallel neural networks N90-23012
Proceedings of the 3rd Annual Conference on Aerospace Computational Control, volume 2
[NASA-CR-186447] N90-23040
Parallel conjugate gradient algorithms for manipulator dynamic simulation N90-23045
Control/structure interaction design methodology N90-23053
Model reduction for flexible spacecraft with clustered natural frequencies N90-23054
JPL control/structure interaction test bed real-time control computer architecture N90-23070
Multibody dynamics: Modeling component flexibility with fixed, free, loaded, constraint, and residual modes N90-23072
Component model reduction via the projection and assembly method N90-23073
Significance of norms and completeness in variational based methods N90-23078
Multibody dynamics model building using graphical interfaces N90-23082

JOHNS HOPKINS UNIV., LAUREL, MD.
HCl Vapor Characterization and Detection. JANNAF Safety and Environmental Protection Subcommittee Workshop
[AD-A216252] N90-22596
A study of low level laser retinal damage
[AD-A219919] N90-22887
Application of high-temperature superconducting thin-film devices to electro-optical and electronic warfare systems
[AD-A218805] N90-23249

JOINT INST. FOR NUCLEAR RESEARCH, DUBNA (USSR).
Convergence of hyperspherical adiabatic expansion for helium-like systems
[DE90-620526] N90-22631
Superheterodyne three-wave detection of gravitation waves
[DE90-620465] N90-22856
On approximation of nonlinear boundary integral equations for the combined method
[DE90-009784] N90-23130
Influence of high energy radiation on critical parameters of superconducting ceramics YBa2Cu3O7
[DE90-620562] N90-23239
New approach to the dynamical diffraction theory in the case of three-dimensional perfect crystal
[DE90-620563] N90-23240
A (mu)SR-investigation of the mixed state of the high-Tc superconductor HoBa2Cu3O7-delta
[DE90-620602] N90-23241
Quantum mechanics in Riemannian space-time
[DE90-620448] N90-23257
Background connection: A necessary object in general relativity
[DE90-620463] N90-23258
Gravitational collapse, Friedman models and cosmological constant: Does the universe oscillate
[DE90-620792] N90-23324

JOINT PUBLICATIONS RESEARCH SERVICE, ARLINGTON, VA.
JPRS report: Science and technology. USSR: Physics and mathematics
[JPRS-UPM-89-001] N90-23162
Acoustoelectronic interaction of surface waves in GaAs-InGaAs superlattices N90-23163
Excitation of hypersound at boundary between Type-2 superconductor and a concentrated paramagnetic compound N90-23164
Effect on relaxation on nonlinear waves in crystals N90-23165
Shaping radiation pattern of excimer laser by means of controllable intracavity mirror N90-23166
Tunable XeCl-laser featuring high spectral luminance N90-23167

K

KANSAS UNIV., LAWRENCE.
Displays, instruments, and the multi-dimensional world of cartography N90-22942
Application of numerical optimization techniques to control system design for nonlinear dynamic models of aircraft N90-23032

KENTUCKY UNIV., LEXINGTON.
A study of mesoscale acid deposition in the lower Ohio River Valley N90-22848

L

LABORATOIRE D'AUTOMATIQUE ET D'ANALYSE DES SYSTEMES, TOULOUSE (FRANCE).
Orbital maneuvers optimization for station acquisition of geostationary satellites. Deterministic and stochastic approaches
[LAAS-89-359] N90-22589
Definition of a design methodology and study of the driving and protection functions of a smart power switch
[LAAS-89-330] N90-22727
Excess noise, anomalous effects and reliability of high frequency devices (Schottky diodes, MESFET and HEMT)
[LAAS-89-394] N90-22728
Plan execution control and architecture for mobile robots
[LAAS-89-371] N90-22793
About linear systems robustness: Linear programming approach
[LAAS-89-384] N90-23123

LAMONT-DOHERTY GEOLOGICAL OBSERVATORY, PALISADES, NY.
Measurements of high frequency seismic waves
[AD-A219370] N90-22863

LAWRENCE LIVERMORE NATIONAL LAB., CA.
Infrared absorption gas sensor for the detection of HCl in launch vehicle exhaust clouds N90-22600
Mechanical testing of selected engineering plastics
[DE90-008186] N90-22673
Using object-oriented analysis techniques to support system testing
[DE90-009540] N90-22700
Laser Program of the Lawrence Livermore National Laboratory
[DE90-008198] N90-22779
Index and consistency analysis for DAE (Differential Algebraic Equation) systems for Stefan-Maxwell diffusion-reaction problems
[DE90-008188] N90-23129

LEEDS UNIV. (ENGLAND).
The effect of a stellar wind on an expanding H II region N90-23292

LEHIGH UNIV., BETHLEHEM, PA.
The effects of point defects and composition on structural phase transition
[DE90-010109] N90-23238
Nonreciprocal components in the 140 and 220 GHz bands utilizing magnetoplasmons on semiconducting substrates
[AD-A219136] N90-23253

LEIDEN UNIV. (NETHERLANDS).
More data on (possible) gamma ray (point) sources N90-23309

LOCKHEED ENGINEERING AND SCIENCES CO., HAMPTON, VA.
Multilevel decomposition approach to the preliminary sizing of a transport aircraft wing
[NASA-CR-4296] N90-22557

LOCKHEED MISSILES AND SPACE CO., SUNNYVALE, CA.
Multi-flexible-body dynamics capturing motion-induced stiffness N90-23013

LOS ALAMOS NATIONAL LAB., NM.
HF propagation through actively modified ionospheres
[DE90-008931] N90-22705

LOUISIANA STATE UNIV., BATON ROUGE.
Solar flares and magnetospheric particles: Investigations based upon the ONR-602 and ONR-604 experiments
[AD-A218844] N90-23332

M

MARCUS (AARON) AND ASSOCIATES, BERKELEY, CA.
Spatial issues in user interface design from a graphic design perspective N90-22939

MARTIN MARIETTA CORP., DENVER, CO.
Knowledge management: An abstraction of knowledge base and database management systems
[NASA-CR-4273] N90-22986

MARYLAND UNIV., COLLEGE PARK.
Measurements and simulation of controlled beamfront motion in the Laser Controlled Collective Accelerator
[DE90-009992] N90-22780
A study of auroral activity in the nightside polar cap N90-22852
Development of efficient computer program for dynamic simulation of telerobotic manipulation N90-23017
Efficient computer algebra algorithms for polynomial matrices in control design N90-23022
Intense electron beam propagation across a magnetic field
[DE90-009993] N90-23204

MASSACHUSETTS INST. OF TECH., CAMBRIDGE.
Simulation of inelastic deformation in glassy polypropylene and polycarbonate
[AD-A218891] N90-22686
Investigation of atomistic simulation of structural and dynamic differences in glassy and liquid states of atactic poly(propylene)
[AD-A218896] N90-22687
H2, fixed architecture, control design for large scale systems
[NASA-CR-180471] N90-22698
Reactions of laser-generated free radicals at semiconductor surfaces
[AD-A218552] N90-22733
Seismic wave propagation, attenuation and scattering over regional distances
[AD-A219358] N90-22862
Telepresence, time delay, and adaptation N90-22944
Sensory conflict in motion sickness: An observer theory approach N90-22957
Nonlinear strain-displacement relations and flexible multibody dynamics N90-23014
Concurrent computing: Numerical algorithms and some applications
[AD-A218570] N90-23103
Locality in parallel computation
[AD-A218733] N90-23120

MASSACHUSETTS UNIV., AMHERST.
Synesthetic art through 3-D projection: The requirements of a computer-based supermedium N90-22962

MAX-PLANCK-INST. FUER EXTRATERRESTRISCHE PHYSIK, GARCHING (GERMANY, F.R.).
Complementary information from mm-wave-, infrared-, and gamma ray astronomy N90-23299
COS-B gamma ray sources beyond the predicted diffuse emission N90-23308
COMPTEL observations of active galactic nuclei N90-23319

MAX-PLANCK-INST. FUER PHYSIK UND ASTROPHYSIK, GARCHING (GERMANY, F.R.).
High spatial resolution isotopic CO and CS observations of M17 SW: The clumpy structure of the molecular cloud core
[MPE-PREPRINT-161] N90-23283
Gamma radiation from the Crab and Vela pulsars N90-23303
The high energy source 3C 273 N90-23318

MAX-PLANCK-INST. FUER STROEMUNGSFORSCHUNG, GOETTINGEN (GERMANY, F.R.).
Experimental investigations concerning the propagation of second-sound pulses at critical heat flux
[MPIS-12/1989] N90-23182
Experiments on the breakdown of heat transfer in liquid helium 2
[MPIS-13/1989] N90-23259

MAX-PLANCK-INST. FUER VERHALTENSPHYSIOLOGIE, SEEWIESEN UBER STARNBERG (GERMANY, F.R.).
Interactions of form and orientation N90-22958

MECHANICAL DYNAMICS, INC., ANN ARBOR, MI.
Control design and simulation of systems modeled using ADAMS N90-23081

MEMORIAL UNIV. OF NEWFOUNDLAND, SAINT JOHNS.
Using deflation in the pole assignment problem with output feedback N90-23004

METRAVIB, LYON (FRANCE).
Damage analysis following slight deformations of composite materials
[RDS-1-007-64] N90-22618

MICHIGAN UNIV., ANN ARBOR.
Experimental study of vortex ring interaction with a free surface N90-22742
Unsteady group behavior of droplet clouds in swirling flows N90-22743
Holocinematography for studies of turbulent multiphase flow
[AD-A219130] N90-22765
A new second-order integration algorithm for simulating mechanical dynamic systems N90-23064
Parametric models for A(sub n): Splitting processes and mixtures
[AD-A218421] N90-23140
A theory of Bayesian data analysis
[AD-A218420] N90-23152
Bayesian nonparametric prediction and statistical inference
[AD-A218473] N90-23154

MIDDLE EAST TECHNICAL UNIV., ANKARA (TURKEY).
Modeling of control forces for kinematical constraints in the dynamics of multibody systems: A new approach N90-23031

MIDDLE EAST TECHNICAL UNIV., GAZIANTEP (TURKEY).
Determination of joint drives for stable end-effector motion in flexible robotic systems N90-23034

MIDWEST RESEARCH INST., GOLDEN, CO.
Ocean energy program summary
[DE89-009481] N90-22836
Geothermal energy program summary
[DE89-009485] N90-22837
Geothermal energy program summary
[DE89-009486] N90-22838
Photovoltaic advanced research and development project: Solar radiation research
[DE90-000302] N90-22839

MINNESOTA UNIV., MINNEAPOLIS.
The onset of superconductivity in two-dimensional disordered systems N90-23232

MISSION RESEARCH CORP., PACIFIC GROVE, CA.
Preliminary results of the peak experiment. ALTAIR deep-space measurements
[AD-A218622] N90-22714

MISSISSIPPI UNIV., UNIVERSITY.
Fundamental studies on hydrology, hydraulics and geometry of river networks
[AD-A218662] N90-22830
A scattering center based numerical simulation of small scale atmospheric turbulence N90-23179

MOUND LAB., MIAMISBURG, OH.
An alternate interconnect method for joining flexible circuits using conductive adhesives
[DE90-008194] N90-22674

N

NATIONAL AERONAUTICS AND SPACE ADMINISTRATION. AMES RESEARCH CENTER, MOFFETT FIELD, CA.
A case for archaeological reconnaissance of the Cabo Catoche-Porvenir region of the northeastern Yucatan Peninsula
[NASA-TM-102248] N90-22827
Spatial Displays and Spatial Instruments
[NASA-CP-10032] N90-22918
Pictorial communication: Pictures and the synthetic universe N90-22919
Perceiving environmental properties from motion information: Minimal conditions N90-22925
Visual slant underestimation N90-22926
Helmet-mounted pilot night vision systems: Human factors issues N90-22930
Exocentric direction judgements in computer-generated displays and actual scenes N90-22936
Adapting to variable prismatic displacement N90-22945
Interactive orbital proximity operations planning system N90-22953
Synthetic perspective optical flow: Influence on pilot control tasks N90-22956
Optical, gravitational, and kinesthetic determinants of judged eye level N90-22959
PLOT3D user's manual
[NASA-TM-101067] N90-23090

NATIONAL AERONAUTICS AND SPACE ADMINISTRATION. GODDARD SPACE FLIGHT CENTER, GREENBELT, MD.
SeaRISE: A Multidisciplinary Research Initiative to Predict Rapid Changes in Global Sea Level Caused by Collapse of Marine Ice Sheets
[NASA-CP-3075] N90-22624
Surface topography of the Greenland Ice Sheet from satellite radar altimetry
[NASA-SP-503] N90-22850
An order (n) algorithm for the dynamics simulation of robotic systems N90-22990
New multivariable capabilities of the INCA program N90-23049
ASTEC: Controls analysis for personal computers N90-23052
A verification library for multibody simulation software N90-23089
The Pioneer Venus Orbiter: 11 years of data. A laboratory for atmospheres seminar talk
[NASA-TM-100761] N90-23273
The Energetic Gamma-Ray Experiment Telescope (EGRET) Science Symposium
[NASA-CP-3071] N90-23294
The diffuse galactic gamma ray emission N90-23296
A model of the diffuse galactic gamma ray emission N90-23297
Gamma rays from giant molecular clouds N90-23298
Implications of the IRAS data for galactic gamma ray astronomy and EGRET N90-23300
Gamma ray pulsars: Models and observations N90-23304
The sensitivity of EGRET to gamma ray polarization N90-23305
The illusive Geminga: What is it N90-23307
Gamma rays from pulsar wind shock acceleration N90-23311
Local normal galaxies N90-23315
Gamma rays from active galactic nuclei N90-23316
Spectral evolution of active galactic nuclei Penrose Compton scattering processes and gamma ray emission from Seyfert galaxies N90-23317
Feasibility for EGRET detection of antimatter concentrations in the universe N90-23323

NATIONAL AERONAUTICS AND SPACE ADMINISTRATION. HUGH L. DRYDEN FLIGHT RESEARCH CENTER, EDWARDS, CA.
Water-tunnel study results of a TF/A-18 and F/A-18 canopy flow visualization
[NASA-TM-101705] N90-22532

NATIONAL AERONAUTICS AND SPACE ADMINISTRATION. JOHN F. KENNEDY SPACE CENTER, COCOA BEACH, FL.
Debris/ice/TPS assessment and photographic analysis for Shuttle Mission STS-36
[NASA-TM-102789] N90-22583
The physiological cost of wearing the propellant handler's ensemble at the Kennedy Space Center
[NASA-TM-102786] N90-22966

NATIONAL AERONAUTICS AND SPACE ADMINISTRATION. LYNDON B. JOHNSON SPACE CENTER, HOUSTON, TX.
Space station dynamics, attitude control and momentum management N90-23029
Concurrent processing simulation of the space station N90-23041

NATIONAL AERONAUTICS AND SPACE ADMINISTRATION. LANGLEY RESEARCH CENTER, HAMPTON, VA.
Dynamic ground-effect measurements on the F-15 STOL and Maneuver Technology Demonstrator (S/MTD) configuration
[NASA-TP-3000] N90-22531
An experimental study of tip shape effects on the flutter of aft-swept, flat-plate wings
[NASA-TM-4160] N90-22555
Differential equation based method for accurate approximations in optimization
[NASA-TM-102639] N90-22558
Earth-to-orbit vehicle providing a reusable orbital stage
[NASA-CASE-LAR-13486-1] N90-22584
Spacecraft attitude impacts on COLD-SAT non-vacuum jacketed LH2 supply tank thermal performance
[NASA-TM-103158] N90-22592
Pultrusion process development for long space boom model
[NASA-TM-4017] N90-22628
Quantitative surface temperature measurement using two-color thermographic phosphors and video equipment
[NASA-CASE-LAR-13740-1] N90-22770
Thermal/structural analysis of the shaft-disk region of a fan drive system
[NASA-TM-101687] N90-22807
Development of a stereo 3-D pictorial primary flight display N90-22955
Determination of depth-viewing volumes for stereo three-dimensional graphic displays
[NASA-TP-2999] N90-22965
A methodology for formulating a minimal uncertainty model for robust control system design and analysis N90-23028
On trajectory generation for flexible space crane: Inverse dynamics analysis by LATDYN N90-23037
Real-time closed-loop simulation and upset evaluation of control systems in harsh electromagnetic environments N90-23069
The power and efficiency of advanced software and parallel processing N90-23079
Dynamic analysis of flexible mechanical systems using LATDYN N90-23080
Design trends for Army/Air Force airplanes in the United States
[NASA-TM-4179] N90-23338

NATIONAL AERONAUTICS AND SPACE ADMINISTRATION. LEWIS RESEARCH CENTER, CLEVELAND, OH.
Large-scale advanced propeller blade pressure distributions: Prediction and data
[NASA-TM-102316] N90-22564
A modeling technique for STOVL ejector and volume dynamics
[NASA-TM-103167] N90-22566
A candidate architecture for monitoring and control in chemical transfer propulsion systems
[NASA-TM-103161] N90-22595
The International Space University
[NASA-TM-103163] N90-22604
Cooling of rocket thrust chambers with liquid oxygen
[NASA-TM-103146] N90-22605
Programmatic status of NASA's CSTI high capacity power Stirling space power converter program
[NASA-TM-103142] N90-22606
Fatigue crack growth in a unidirectional SCS-6/Ti-15-3 composite
[NASA-TM-103095] N90-22648
Elements of active vibration control for rotating machinery
[NASA-TM-102368] N90-22703
Miniature traveling wave tube and method of making
[NASA-CASE-LEW-14520-1] N90-22724
Field oriented control of induction motors
[NASA-TM-103154] N90-22731
Photoresponse of YBa2Cu3O(7-delta) granular and epitaxial superconducting thin films
[NASA-TM-103144] N90-22732
Acquisition and correlation of cryogenic nitrogen mass flow data through a multiple orifice Joule-Thomson device
[NASA-TM-103121] N90-22761
A fiber-optic current sensor for aerospace applications
[NASA-TM-103152] N90-22773
Two-dimensional surface strain measurement based on a variation of Yamaguchi's laser-speckle strain gauge
[NASA-TM-103162] N90-22784
Surface pitting fatigue life of noninvolute, low-contact-ratio gears
[NASA-TM-103116] N90-22790
Influence of linear profile modification and loading conditions on the dynamic tooth load and stress of high contact ratio gears
[NASA-TM-103136] N90-22796
Recent advances in nondestructive evaluation made possible by novel uses of video systems
[NASA-TM-102491] N90-22801
Finite element elastic-plastic-creep and cyclic life analysis of a cowl lip
[NASA-TM-102342] N90-22808
High temperature fatigue behavior of a SiC/Ti-24Al-11Nb composite
[NASA-TM-103157] N90-22822
Probabilistic structural analysis of aerospace components using NESSUS
[NASA-TM-102324] N90-22823
Lateral spreading of Au contacts on InP
[NASA-TM-103133] N90-22843
Nuclear technology and the space exploration missions
[NASA-TM-103156] N90-22847

Automated electric power management and control for Space Station Freedom
[NASA-TM-103151] N90-23125
Romans to Mars
[NASA-TM-103094] N90-23339

NATIONAL AERONAUTICS AND SPACE ADMINISTRATION. MARSHALL SPACE FLIGHT CENTER, HUNTSVILLE, AL.

Space Station Freedom environmental control and life support system phase 3 simplified integrated test detailed report
[NASA-TM-4204] N90-22593
Hanging drop crystal growth apparatus and method
[NASA-CASE-MFS-28206-1-SB] N90-23242
Gamma ray bursts: Current status of observations and theory N90-23313

NATIONAL AERONAUTICS AND SPACE ADMINISTRATION. PASADENA OFFICE, CA.

Atmospheric autorotating imaging device
[NASA-CASE-NPO-17390-1-CU] N90-22769

NATIONAL AEROSPACE LAB., AMSTERDAM (NETHERLANDS).

Supercomputer and Technology
[NLR-PUB-8801] N90-22974
Numerical flow simulation and supercomputers: More than a digital wind tunnel N90-22976
The use of supercomputers for the design and analysis of constructions N90-22977
The automation management to support research and development N90-22978
Access to supercomputers N90-22979
The development of a system for the numerical simulation of Euler flows N90-22980

NATIONAL PHYSICAL LAB., TEDDINGTON (ENGLAND).

Rheology of injection mould filling with DMCs
[NPL-DMA(A)-196] N90-22675

NATIONAL SCIENCE FOUNDATION, WASHINGTON, DC.

Neural networks in support of manned space N90-23088

NAVAL OCEAN RESEARCH AND DEVELOPMENT ACTIVITY, BAY SAINT LOUIS, MS.

Evidence for self-refraction in a convergence zone: NPE (Nonlinear progressive wave equation) model results
[AD-A218546] N90-22879

NAVAL OCEAN SYSTEMS CENTER, SAN DIEGO, CA.

Indium phosphide planar Gunn diode
[AD-A219337] N90-22740
Specification for environmental measurements to assess radar sensors
[AD-A219127] N90-22833
RF network selection in a rule-based system. NOSC project ZE68: Cost metric algorithms for internetwork applications
[AD-A219389] N90-23116
Contributions of individual structural modes to the scattered acoustic field
[AD-A219128] N90-23187
Transfer matrices for multimode optical fiber systems
[AD-A218459] N90-23210

NAVAL OCEANOGRAPHY COMMAND DETACHMENT, ASHEVILLE, NC.

US Navy regional climatic study of southern African waters
[AD-A218792] N90-22874
US Navy regional climatic study of the Mozambique channel and adjacent waters
[AD-A218793] N90-22875

NAVAL POSTGRADUATE SCHOOL, MONTEREY, CA.

Orbital mechanics: A learning tool on the main frame
[AD-A218799] N90-22576
The lithium concentration dependence of creep in binary aluminum-lithium alloys
[AD-A218706] N90-22668
A comparison of CuAlNi and other high damping alloys for the purpose of naval ship silencing applications
[AD-A218801] N90-22671
Performance analysis of Aloha networks with power capture and near/far effect
[AD-A218739] N90-22717
Optical excisor modeling
[AD-A219338] N90-22722
Transverse vibrations of a composite cylindrical tube of circular cross section
[AD-A219227] N90-22820
The microstructural basis of damping in high damping alloys
[AD-A219572] N90-22821
On the effectiveness of the production of antarctic bottom water in the Weddell and Ross Seas
[AD-A218873] N90-22880
Use of optical storage devices as shared resources in local area networks
[AD-A219198] N90-23269

NAVAL RESEARCH LAB., WASHINGTON, DC.

Pseudo-steady diffusional growth or collapse of bubbles rising in time dependent pressure fields
[AD-A218825] N90-22764
Incomplete integrals of cylindrical functions
[AD-A219512] N90-23161
Measurement of plasma-neutralized super-vacuum currents in a gyrotron configuration
[AD-A218505] N90-23207
Foil focusing of electron beams
[AD-A219511] N90-23208
Stability regimes in a rotating quadrupole focusing accelerator
[AD-A219513] N90-23209
OSSE observations of active galactic nuclei N90-23320

NAVAL SHIP RESEARCH AND DEVELOPMENT CENTER, BETHESDA, MD.

Data exchange strategy. Part 1: Review of digital data exchange technology
[AD-A218506] N90-23267

NAVAL SUBMARINE MEDICAL CENTER, GROTON, CT.

The kinetics of dark adaptation in hypoxic subjects
[AD-A218641] N90-22885
Motor and cognitive performance do not change during a ten-week submarine patrol
[AD-A218639] N90-22969

NETROLOGIC, INC., SAN DIEGO, CA.

Learning environment for neural networks and transient acoustics
[AD-A219000] N90-23186

NEWCASTLE-UPON-TYNE UNIV. (ENGLAND).

A theoretical and experimental investigation of an absorption refrigeration system for application with solar energy units N90-22697

NIELSEN ENGINEERING AND RESEARCH, INC., MOUNTAIN VIEW, CA.

The effects of compressibility on a supersonic mixing layer
[AD-A219315] N90-22543

NIPPON ELECTRIC CO. LTD., TOKYO (JAPAN).

Strategy of supercomputer development N90-22981

NORTH CAROLINA AGRICULTURAL AND TECHNICAL STATE UNIV., GREENSBORO.

Mini-mast dynamic analysis using the truss-beam model N90-23087

NORTH CAROLINA STATE UNIV., RALEIGH.

High Intensity Electro-Magnetic and Ultrasonic Effects on Inorganic Materials Behavior and Processing Workshop
[AD-A218884] N90-22640
Continued development and characterization of doped layers, contacts, and associated electronic devices in silicon carbide
[AD-A219211] N90-22737
Continued development and characterization of doped layers, contacts and associated electronic devices in silicon carbide
[AD-A219234] N90-22738
A computational method for general higher index nonlinear singular systems of differential equations
[AD-A219164] N90-23147

NORTH CAROLINA UNIV., CHAPEL HILL.

Linear and nonlinear electrical response of condensed matter: Ionic, dielectric, and mixed-conduction materials
[AD-A218771] N90-22639
Estimation of Hilbert space valued parameters by the method of sieves
[AD-A218565] N90-23143
Parameter estimation in linear filtering
[AD-A218566] N90-23144
Stochastic processes as Fourier integrals and dilation of vector measures
[AD-A219413] N90-23150
Two barriers problem for continuously differentiable processes
[AD-A218564] N90-23176
Auditory spectro-temporal pattern analysis
[AD-A218416] N90-23184

NORTH CAROLINA UNIV., RALEIGH.

Control of surface melting and ablation in electromagnetic launchers via the magnetic vapor shielding mechanism
[AD-A219035] N90-22578

NORTH DAKOTA STATE UNIV., FARGO.

Theoretical studies of silicon chemistry
[AD-A219232] N90-22690

NORTHROP CORP., HAWTHORNE, CA.

Algorithms for computing the multivariable stability margin N90-22999

NORTHWESTERN UNIV., EVANSTON, IL.

Center for surface radiation damage studies
[AD-A218452] N90-22678
What can gamma rays tell us about binary x ray sources and SNR's N90-23310

O

OAK RIDGE NATIONAL LAB., TN.

Characterization of weldments using advanced experimental techniques
[DE90-009418] N90-22792
Global and hemispheric annual temperature variations between 1861 and 1988
[DE90-007993] N90-22869

OFFICE NATIONAL D'ETUDES ET DE RECHERCHES AEROSPATIALES, PARIS (FRANCE).

Ultrasonic detection of critical damage in carbon-epoxy composite materials
[ONERA-RT-5/7256-RY-081-R] N90-22616

OFFICE OF NAVAL RESEARCH EUROPEAN OFFICE, FPO NEW YORK, NY.

The RACE (research and development in advanced technologies for Europe) program: A 1989 update
[AD-A218509] N90-22713
Proceedings of the NATO Advanced Workshop on Supercomputing
[AD-A218508] N90-23102

OFFICE OF NAVAL RESEARCH LIAISON OFFICE, FAR EAST, APO SAN FRANCISCO, CA.

ONR Far East Scientific Information Bulletin, Volume 13, No. 4
[ONRFE-SCI-INFO-BULL-13(4)88] N90-23168
High temperature superconducting thin films in Japan N90-23169
Research and applications of metallic superlattices, high T(sub c) superconductors, x ray optics, and compact synchrotrons N90-23170
What is going on in the La2CuO4 superconductors N90-23171
Current Japanese supercomputers for computational fluid dynamics applications N90-23172

OHIO STATE UNIV., COLUMBUS.

Efficient dynamic simulation for multiple chain robotic mechanisms N90-22995
Computational dynamics for robotics systems using a non-strict computational approach N90-23011
Algorithmic considerations of integrated design for CSI on a hypercube architecture N90-23043

OKLAHOMA UNIV., NORMAN.

Turbulence spectral widths view angle independence as observed by Doppler radar
[AD-A219169] N90-22550
A real time, FEM based optimal control algorithm and its implementation using parallel processing hardware (transistors) in a microprocessor environment N90-23066

OREGON UNIV., EUGENE.

The perception of three-dimensionality across continuous surfaces N90-22924

OTTAWA UNIV. (ONTARIO).

Modeling and control of flexible space stations (slew maneuvers) N90-23086

OXFORD UNIV. (ENGLAND).

Structure-property relations in aluminum-lithium alloys
[AD-A219183] N90-22672

P

PACIFIC NORTHWEST LAB., RICHLAND, WA.

Looking at large data sets using binned data plots
[DE90-008206] N90-23263

PENNSYLVANIA STATE UNIV., STATE COLLEGE.

Flat plate vibration analysis experimental and numerical fillet study
[AD-A218789] N90-22818

PENNSYLVANIA STATE UNIV., UNIVERSITY PARK.

Reynolds stress closure in jet flows using instability wave modeling N90-22534
A second-order nonlinear optical poly(organophosphazene)
[AD-A218408] N90-22607
Fundamental hydrodynamics research
[AD-A219179] N90-22766
Two-dimensional velocimetry instrumentation
[AD-A218450] N90-22774
Robust control of vibration in flexible structures N90-22787
Predictability of weather and climate in a coupled ocean-atmosphere model: A dynamical systems approach N90-22865
Fault tolerant multiprocessing and development of tools
[AD-A219216] N90-23110

PENNSYLVANIA UNIV., PHILADELPHIA.

Control of randomly sampled robotic systems
[AD-A218948] N90-23157
Image segmentation with detection of highlights and inter-reflections using color
[AD-A218710] N90-23213

PHOTON RESEARCH ASSOCIATES, INC., CAMBRIDGE, MA.
Simulation studies using multibody dynamics code DART N90-23036
PITTSBURGH UNIV., PA.
ALVINN: An Autonomous Land Vehicle In a Neural Network
[AD-A218975] N90-22797
Efficient specialization of relational concepts
[AD-A218889] N90-22894
A preliminary analysis of the SOAR architecture as a basis for general intelligence
[AD-A218913] N90-22896
Towards the knowledge level in SOAR: The role of the architecture in the use of knowledge
[NASA-CR-186615] N90-22897
Stochastic interactive activation and the effect of context on perception
[AD-A218929] N90-22898
Designing good experiments to test bad hypotheses
[AD-A218977] N90-22900
What makes some problems hard: Explorations in the problem space of difficulty
[AD-A219002] N90-22901
Discovering problem solving strategies: What humans do and machines don't (yet)
[AD-A219008] N90-22902
Rules and maps in connectionist symbol processing
[AD-A219028] N90-22903
Connectionism and compositional semantics
[AD-A219029] N90-22904
Learning events in the acquisition of three skills
[AD-A219038] N90-22905
Information processing approaches to cognitive development
[AD-A219200] N90-22908
Toward a SOAR theory of taking instructions for immediate reasoning tasks
[AD-A219201] N90-22909
Learning artificial grammars with competitive chunking
[AD-A219270] N90-22911
A task-analytic approach to the automated design of information graphics
[AD-A219271] N90-22912
Laboratory replication of scientific discovery processes
[AD-A219273] N90-22913
Perceived orientation, spatial layout and the geometry of pictures N90-22933
Encoding sequential structure in simple recurrent networks
[AD-A218928] N90-22984
Sentence comprehension: A parallel distributed processing approach
[AD-A218886] N90-23104
Scientific discovery as problem solving
[AD-A218887] N90-23145
POLITECNICO DI MILANO (ITALY).
Design for testability of stuck-open and stack-on CMOS combinatoral circuits
[REPT-89-044] N90-22725
Detection of bridging faults in DFCMOS combinational gates
[REPT-89-060] N90-22726
Robust modelling of sampled systems for time delay estimation
[REPT-89-047] N90-23092
Object-oriented query languages: The notion and the issues
[REPT-89-054] N90-23093
Reusing software components by specialization
[REPT-89-062] N90-23094
Interconnection networks for highly parallel supercomputing architectures
[REPT-89-053] N90-23118
Periodic ARMA models: Optimal prediction and minimum-phase condition
[REPT-89-006] N90-23131
On a fallacious conjecture about the stabilizability properties of solutions of the Riccati difference equation
[REPT-89-007] N90-23132
PRINCETON UNIV., NJ.
Flow visualization in supersonic turbulent boundary layers N90-22533
Localization of vibration in disordered nearly cyclic structures N90-22812
Volumetric visualization of 3D data N90-22964
Skewering the universe with QSO lines of sight: Lyman alpha clouds as probes of large scale structure N90-23278
Reconstructing primordial density fluctuations N90-23293
Radio pulsar timing observations for GRO N90-23301
PURDUE UNIV., WEST LAFAYETTE, IN.
Forcing function effects on rotor row unsteady aerodynamic response in a multistage compressor N90-22536
An investigation of the three-dimensional flow field in a centrifugal compressor N90-22751
Characterization of robotics parallel algorithms and mapping onto a reconfigurable SIMD machine N90-23039
Extensions of output variance constrained controllers to hard constraints N90-23056
Characterizing exponential distributions via conditional independence
[AD-A219255] N90-23158
Selecting multinomial populations
[AD-A219256] N90-23159

R

RAND GRADUATE INST. FOR POLICIES STUDY, SANTA MONICA, CA.
US access to space: Launch vehicle choices for 1990 to 2010 N90-22579
READING UNIV. (ENGLAND).
A numerical study of basic coastal upwelling processes N90-22878
RENSSELAER POLYTECHNIC INST., TROY, NY.
Computations of weight functions in fracture mechanics N90-22809
RESEARCH TRIANGLE INST., RESEARCH TRIANGLE PARK, NC.
Passivation and gating of GaAs and Si surfaces using pseudomorphic structures
[AD-A219351] N90-23256
RICE UNIV., HOUSTON, TX.
Linear programming tools for integer programming
[AD-A219013] N90-23106
The effects of caustics in acoustic inverse scattering experiments
[AD-A218454] N90-23185
ROCHESTER UNIV., NY.
Time-resolved surface structural study by picosecond reflection high-energy electron diffraction
[AD-A218417] N90-22712
High performance holographic elements and media
[AD-A218999] N90-22775
Interaction of atomic hydrogen with pico- and femtosecond laser pulses
[AD-A218426] N90-22785
Dynamics and instabilities in homogeneously broadened lasers
[AD-A218427] N90-22786
Quantum-limited image recognition
[AD-A218425] N90-23101
Classification techniques for quantum-limited and classical-intensity images
[AD-A218693] N90-23212
Hybrid diffractive-refractive telescope
[AD-A219241] N90-23216
ROCKWELL INTERNATIONAL CORP., ANAHEIM, CA.
Burnout thresholds and cross section of power MOS transistors with heavy ions
[AD-A218998] N90-22736
ROCKWELL INTERNATIONAL CORP., CANOGA PARK, CA.
Beam combining by phase transition nonlinear media
[AD-A219301] N90-22739
Experimental studies on energy storage
[AD-A219032] N90-22845
ROCKWELL INTERNATIONAL CORP., SEAL BEACH, CA.
Modal identities for multibody elastic spacecraft: An aid to selecting modes for simulation N90-23075
ROCKWELL INTERNATIONAL SCIENCE CENTER, THOUSAND OAKS, CA.
Supersonic flow computations for an ASTOVL aircraft configuration, phase 2, part 2
[NASA-CR-4284] N90-22746
ROME AIR DEVELOPMENT CENTER, GRIFFISS AFB, NY.
Performance of adaptive nulling antennas in a jamming environment
[AD-A219305] N90-22720
Scattering of a plane electromagnetic wave from a semicircular crack in a perfectly conducting ground plane
[AD-A219310] N90-22721
Natural language processing: A tutorial
[AD-A219096] N90-23108
Adaptive Resonance Theory 1
[AD-A219044] N90-23126
Some ray tracing problems related to circles and ellipses
[AD-A219306] N90-23217
ROME UNIV. (ITALY).
The super-gratings: How to improve the limiting resolution of grating spectrometers
[PREPRINT-695] N90-22577
Qualitative aspects of signal processing through dynamical neural networks
[PREPRINT-711] N90-22709
Reduced size holography
[PREPRINT-707] N90-22771
Gravitational radiation produced by high energy accelerators and high power lasers
[PREPRINT-701] N90-22782
Analysis of nonlinear internal waves observed by LANDSAT-TM
[PREPRINT-704] N90-22828
On the antarctic ozone depletion during solar cycle 21
[NOTA-INTERNA-943] N90-22849
Non-symmetric double well and Euclidean functional integral
[PREPRINT-709] N90-23133
Effective action for induced gravity on a 2-dimensional manifold
[PREPRINT-712] N90-23173
Replica scaling analysis of interfaces in random media
[PREPRINT-713] N90-23174
Rigorous analysis of low temperature stochastic Ising models: Metastability and exponential approach to equilibrium
[PREPRINT-720] N90-23175
Theoretical and computer simulation study of the density fluctuations in liquid water
[PREPRINT-697] N90-23191
Low frequency Raman spectra of liquid water, a molecular dynamics simulation
[PREPRINT-698] N90-23192
Improving fermion operators
[PREPRINT-710] N90-23193
A posterior stochastic equation for quantum Brownian motion
[PREPRINT-715] N90-23194
The number of neutrino species, confronted with the results at the recent Lepton-Photon Symposium (August 7-12, 1989)
[NOTA-INTERNA-940] N90-23195
The 16-O photodisintegration at low energies
[NOTA-INTERNA-941] N90-23196
Relativistic corrections to He-3 photodisintegration sum rules
[NOTA-INTERNA-942] N90-23197
Quark-antiquark pair production via gamma W fusion at high energy e(+)e(-) colliders
[PREPRINT-705] N90-23205
Intermittency and multifractality in magnetic dynamos
[PREPRINT-702] N90-23226
Displacement flow and deuteron drag in a metal: A path towards cold fusion
[PREPRINT-703] N90-23227
Mixing of DIS operators in lattice QCD
[PREPRINT-708] N90-23243
Critical behavior of the thermal power near the metal-insulator transition
[PREPRINT-714] N90-23244
Lattice field theory
[PREPRINT-719] N90-23245
Quantum non-demolition stroboscopic observables and multipumping back-action evasion schemes
[PREPRINT-699] N90-23260
Are quantum measurements on macroscopic bodies feasible
[PREPRINT-700] N90-23261
Neutrino signals from the powerful solar flare on September 29, 1989
[PREPRINT-721] N90-23331
The ground-level cosmic-ray event of September 29, 1989 as recorded by the Rome detectors
[NOTA-INTERNA-944] N90-23336
Cosmic ray NM-64 neutron monitor data-17
[NOTA-INTERNA-945] N90-23337
ROYAL AEROSPACE ESTABLISHMENT, FARNBOROUGH (ENGLAND).
The aerodynamic characteristics of power-law bodies in continuum and transitional hypersonic flow
[RAE-TM-AERO-2164] N90-22537
Satellite motion in axi-symmetric gravitational field. Part 2: Perturbations due to an arbitrary J(sub l)
[RAE-TR-89022] N90-22586
Evaluation of a prototype 6 tone modem
[RAE-TM-FM-28] N90-22708
Tracking in uncertain environments
[RAE-TM-AW-121] N90-22891
RUTGERS - THE STATE UNIV., NEW BRUNSWICK, NJ.
The (DURIP) computer simulations of plasmas, nonlinear systems, and control theory
[AD-A219070] N90-23107

S

SAINT ANDREW'S UNIV. (SCOTLAND).
Optical properties of novel GaAs-based semiconductors N90-23235
SAINT LOUIS UNIV., MO.
An interactive method for estimating hailstone size and convectively-driven wind gusts from forecast soundings
[AD-A218499] N90-22871
SALFORD UNIV. (ENGLAND).
Three-dimensional separated flow prediction on fusiform body using Euler and boundary layer methods N90-22745
SAN CALIXTO OBSERVATORY, LA PAZ (BOLIVIA).
Propagation and attenuation of Lg waves in South America
[AD-A218853] N90-22859
SAN JOSE STATE UNIV., CA.
A study of turbulence near thunderstorm tops
[NASA-CR-186620] N90-22870
SANDIA NATIONAL LABS., ALBUQUERQUE, NM.
Experimental evaluation of chemical cleaning processes for high-lifetime silicon processing
[DE90-009332] N90-22699
Phase Doppler droplet sizing: Scattering angle effects
[DE90-009571] N90-22754
Characterization and calibration of coordinate measuring machines
[DE90-009320] N90-22791
Increased stuck-at fault coverage with reduced I(sub DDQ) test sets
[DE90-009509] N90-22804
High-efficiency silicon solar cells for a 22-sun line-focus module
[DE90-010242] N90-22840
An assessment of second-generation stretched-membrane mirror modules
[DE90-010243] N90-22841
Experiences in teleoperation of land vehicles N90-22954
Approximate minimum-time trajectories for 2-link flexible manipulators N90-23030
OPTICON: Pro-Matlab software for large order controlled structure design N90-23058
SCIENTIFIC RESEARCH ASSOCIATES, INC., GLASTONBURY, CT.
Extension of a three-dimensional viscous wing flow analysis user's manual: VISTA 3-D code
[NASA-CR-182024] N90-22538
SCRIPPS INSTITUTION OF OCEANOGRAPHY, LA JOLLA, CA.
Paradoxical monocular stereopsis and perspective vergence N90-22922
Transduction of nanovolt signals: Limits of electric-field detection
[AD-A219214] N90-23177
SDRC, INC., SAN DIEGO, CA.
Issues in CSI analysis for large scale systems N90-23076
SELENIA INDUSTRIE ASSOCIATE S.P.A., ROME (ITALY).
Activation uniformity dependence of undoped semi-insulating GaAs on post-implant annealing conditions
[ETN-90-96549] N90-23246
SELENIA INDUSTRIE ELETTRONICHE ASSOCIATE S.P.A., POMEZIA (ITALY).
Improvement of clutter rejection by scanning motion compensation in ground-based monopulse radar
[ETN-90-96550] N90-22711
SELENIA S.P.A., ROME (ITALY).
Design options for space-based radar systems
[ETN-90-96548] N90-22710
SIMULA, INC., PHOENIX, AZ.
Aircraft crash survival design guide. Volume 1: Design criteria and checklists
[AD-A218434] N90-22545
Aircraft crash survival design guide. Volume 2: Aircraft design crash impact conditions and human tolerance
[AD-A218435] N90-22546
Aircraft crash survival design guide. Volume 3: Aircraft structural crash resistance
[AD-A218436] N90-22547
Aircraft crash survival design guide. Volume 4: Aircraft seats, restraints, litters, and cockpit/cabin delethalization
[AD-A218437] N90-22548
Aircraft crash survival design guide. Volume 5: Aircraft postcrash survival
[AD-A218438] N90-22549
SIROCO, BELLEVUE, WA.
Wide-angle display developments by computer graphics N90-22963
SOCIETE EUROPEENNE DE PROPULSION, PUTEAUX (FRANCE).
Seal requirements in rocket propulsion
[ETN-90-96611] N90-22580
SOLAREX CORP., ROCKVILLE, MD.
High-efficiency silicon solar cells for a 22-sun line-focus module
[DE90-010242] N90-22840
SOUTHAMPTON UNIV. (ENGLAND).
The application of a non-linear least squares method to predicting seat transmissibility
[ISVR-TR-173] N90-22967
Time-varying filter modelling and time-frequency characterisation of nonstationary sound fields due to a moving source N90-23178
Numerical studies of the active control of sound transmission through double partitions
[ISVR-TR-183] N90-23181
SOUTHWEST SCIENCES, INC., SANTA FE, NM.
Measurement of HCl by near-infrared diode laser absorption N90-22601
SPARTA, INC., LEXINGTON, MA.
Agile multiple aperture imager receiver development
[AD-A218956] N90-23215
SPECTRAL SCIENCES, INC., BURLINGTON, MA.
HCl monitor N90-22599
SRI INTERNATIONAL CORP., MENLO PARK, CA.
Investigation of Schottky barriers
[AD-A218422] N90-23247
STANFORD UNIV., CA.
Automated star pattern recognition N90-22612
A free electron laser master oscillator power amplifier experiment N90-22776
A study of the surface layers at an air-water interface
[AD-A219378] N90-22882
Distortions in memory for visual displays N90-22929
Direction of movement effects under transformed visual/motor mappings N90-22947
Direct implantation process development and characterization in advanced Hg(1)-(x)Cd(x) Te EPI layers
[AD-A219133] N90-23252
Spectral determinations for discrete sources with EGRET N90-23312
Dipole analysis on EGRET data of extragalactic gamma ray background radiation N90-23322
Numerical simulations of x rays and gamma rays from solar flares N90-23330
A 154-day periodicity in the occurrence rate of proton flares
[NASA-CR-185826] N90-23333
STATE UNIV. OF NEW YORK, ALBANY.
The effects of viewpoint on the virtual space of pictures N90-22932
STATE UNIV. OF NEW YORK, BROOKLYN.
Low cost processing routes leading to high-performance ceramic tiles
[AD-A219034] N90-22688
STATE UNIV. OF NEW YORK, BUFFALO.
The first example of an organogallium compound containing a Ga-Te bond: Synthesis, properties, and molecular structure of ((Me3CCH2)2GaTeph)2
[AD-A219258] N90-22608
Viscosity, density and conductivity of ImCl(HCl) sub 1.3
[AD-A218902] N90-22641
Control of a flexible planar truss using proof mass actuators N90-23035
STEVENS INST. OF TECH., HOBOKEN, NJ.
Computational and experimental investigations of rotating stall in compressor cascades N90-22565
STUTTGART UNIV. (GERMANY, F.R.).
Analytical theory of the Bunemann instability for electron runaway
[IPF-88-3] N90-23224
Activities report of the Institute for Plasma Research
[ETN-90-96467] N90-23225
SYRACUSE UNIV., NY.
Intelligent signal processing techniques for multi-sensor surveillance systems
[AD-A218890] N90-22895
SYSTEMS TECHNOLOGY, INC., HAWTHORNE, CA.
Minimum flying qualities. Volume 1: Piloted simulation evaluation of multiple axis flying qualities
[AD-A218560] N90-22560
Minimum flying qualities. Volume 2: Pilot modeling for flying qualities applications
[AD-A218561] N90-22561
Minimum flying qualities. Volume 3: Program CC's implementation of the human optimal control model
[AD-A218562] N90-22562

T

TECHNISCHE UNIV., BERLIN (GERMANY, F.R.).
Lunar base 2 (the second thousand days of a base on the Moon)
[ILR-MITT-230(1989)] N90-22968
TECHNISCHE UNIV., DELFT (NETHERLANDS).
The role of orbit errors in processing of satellite altimeter data
[ETN-90-96699] N90-22575
Design of high-performance negative-feedback oscillators
[ETN-90-96698] N90-22729
TECHNISCHE UNIV., EINDHOVEN (NETHERLANDS).
The curvature of conjugate profiles in points of contract
[MEMO-COSOR-89-18] N90-22795
A priori results in linear-quadratic optimal control theory (extended version)
[MEMO-COSOR-89-17] N90-23124
On randomness of random number generators
[MEMO-COSOR-89-20] N90-23151
An approximation for the response time of an open CP-disk system
[MEMO-COSOR-89-19] N90-23266
TECHNO-SCIENCES, INC., GREENBELT, MD.
Frequency response modeling and control of flexible structures: Computational methods N90-23021
TEL-AVIV UNIV. (ISRAEL).
Laser retinal effects: Electrophysiological determination in visual cortical cells of monkeys and cats
[AD-A218937] N90-22888
TELEDYNE BROWN ENGINEERING, HUNTSVILLE, AL.
Executive summary for the network assessment model
[AD-A218762] N90-22718
TEXAS A&M UNIV., COLLEGE STATION.
A life prediction model for laminated composite structural components
[NASA-CR-186587] N90-22614
Electrochemical synthesis of ultrathin film composite membranes
[AD-A219041] N90-22643
Perception-action relationships reconsidered in light of spatial display instruments N90-22949
A commentary on perception-action relationships in spatial display instruments N90-22950
Undetermined coefficient problems for quasi-linear parabolic equations
[AD-A218462] N90-23141
TEXAS UNIV., AUSTIN.
Determination of the general ocean circulation using satellite altimetry from a simultaneous solution for the Earth's gravity field N90-22589
Approximate optimal guidance schemes for atmospheric orbital maneuvering N90-22585
Model catalytic oxidation studies using supported monometallic and heterobimetallic oxides
[DE90-009984] N90-22664
A parallel structure transient response algorithm using independent substructure response computation N90-23044
Overview of computational control research at UT Austin N90-23051
Substructural controller synthesis N90-23055
Resonant MHD modes with toroidal coupling
[DE90-010077] N90-23222
Anisotropic inflation N90-23286
TEXAS UNIV. AT DALLAS, RICHARDSON.
A nearly-linear computational-cost scheme for the forward dynamics of an N-body pendulum N90-22996
THIOKOL CORP., BRIGHAM CITY, UT.
Qualification of the RSRM case membrane case-to-insulation bondline inspection using the Thiokol Corporation ultrasonic RSRM bondline inspection system
[NASA-CR-183940] N90-22602
Qualification of the RSRM field joint CF case-to-insulation bondline inspection using the Thiokol Corporation ultrasonic RSRM bondline inspection system
[NASA-CR-183931] N90-22788
TORONTO UNIV., DOWNSVIEW (ONTARIO).
An inverse kinematics algorithm for a highly redundant variable-geometry-truss manipulator N90-23033
TUFTS UNIV., BOSTON, MA.
Superconducting and normal compounds: Some high field/high pressure effects N90-23229
TUNZINI NESSI ENTREPRISE EQUIPEMENT, RUEIL-MALMAISON (FRANCE).
Improvement study of iron disilicide thermoelectric materials
[AD-A218946] N90-22844

U

UNION FOR EXPERIMENTING COLL. AND UNIV., YELLOW SPRINGS, OH.
Application of artificial intelligence in electronic circuit diagnosis N90-23122
UNITED KINGDOM ATOMIC ENERGY AUTHORITY, HARWELL (ENGLAND).
The high temperature behavior of gallium and indium liquid metal ion sources
[AERE-R-13321] N90-22647
The initiation of intergranular stress corrosion-cracking on sensitized stainless steel in dilute thiosulphate solutions
[AERE-R-13317] N90-22648
Scanning laser photocurrent spectroscopy of electrochemically grown bismuth sulphide films
[AERE-M-3709] N90-22649
Improved high temperature oxidation behavior of alloys by ion implantation
[AERE-R-13309] N90-22650
A 2-D analysis of particle velocity and stress of SH waves from a strip radiator. An experimental verification of both amplitude and phase using EMA transducers
[AERE-R-12600] N90-22704
Transport of gases through concrete
[AERE-G-4977] N90-22747
Some observations on liquid flow through filters
[AERE-R-13300] N90-22748
Applications of laser ultrasound
[AERE-R-13106] N90-22777
Application of x ray absorption edge spectrometry to the non-destructive determination of element concentrations, coating thickness and areal densities
[AERE-R-13030] N90-22802
Crack detection in silicon nitride by acoustic microscopy
[AERE-R-13196] N90-22803
Characterization of particle impact by quantitative acoustic emission
[AERE-R-13028] N90-22810
A study of the relation between grain boundary type and sensitisation in a partially-sensitised AISI 304 stainless steel using electron back-scattering patterns
[AERE-R-13327] N90-23234
UNIVERSITY OF CENTRAL FLORIDA, ORLANDO.
Analysis of velocity and temperature fluctuations in turbulent shear flows N90-22744
UNIVERSITY OF NORTHERN ARIZONA, FLAGSTAFF.
Human cognitive and motor performance measures under typical cool white fluorescent illumination vs relatively high cool white illuminance/irradiance lighting
[AD-A218445] N90-22892
UNIVERSITY OF SOUTHERN CALIFORNIA, LOS ANGELES.
Modern CACSD using the Robust-Control Toolbox N90-23024
UNIVERSITY OF SOUTHERN ILLINOIS, CARBONDALE.
Material instabilities in solids
[AD-A218451] N90-22817

V

VANDERBILT UNIV., NASHVILLE, TN.
The perception of geometrical structure from congruence N90-22935
VIRGINIA POLYTECHNIC INST. AND STATE UNIV., BLACKSBURG.
Large deformation analysis of laminated composite structures by a continuum-based shell element with transverse deformation N90-22613
Deformation and fracture of aluminum-lithium alloys: The effect of dissolved hydrogen N90-22658
Synthesis and characterization of aromatic polyester and polysiloxane containing block copolymers: Multiphase transparent atomic oxygen resistant damping materials, liquid crystal films, and toughening components of sol/gel glasses
[AD-A218871] N90-22685
VIRGINIA UNIV., CHARLOTTESVILLE.
Limiting performance based structural and control optimization for large vibrating structures N90-22568
NASA-UVA light aerospace alloy and structures technology program
[NASA-CR-182607] N90-22651
Environment enhanced fatigue of advanced aluminum alloys and composites N90-22652
Elevated temperature crack growth in advanced powder metallurgy aluminum alloys N90-22653
Elevated temperature crack growth in aluminum alloys: Tensile deformation of 2618 and FVS0812 aluminum alloys N90-22654
Deformation and fracture of thin sheet aluminum-lithium alloys: The effect of cryogenic temperatures N90-22655
Measurements and mechanisms of localized aqueous corrosion in aluminum-lithium alloys N90-22656
The effects of zinc addition on the environmental stability of Al-Li alloys N90-22657
Investigation of the reaction kinetics between SiC fibers and selectively alloyed titanium matrix composites and determination of their mechanical properties N90-22659
Quantitative characterization of spatial distribution of particles in materials: Application to materials processing N90-22660
Inelastic response of metal matrix composites under biaxial loading N90-22661
Design of cryogenic tanks for launch vehicles N90-22662
Experimental and computational study of the viscoplastic response of high temperature structures N90-22663
Numerical algorithms for computations of feedback laws arising in control of flexible systems N90-23085

W

WASEDA UNIV., TOKYO (JAPAN).
Parallel processing of real-time dynamic systems simulation on OSCAR (Optimally SCheduled Advanced multiprocessoR) N90-23006
WASHINGTON UNIV., SEATTLE.
H(2)- and H(infinity)-design tools for linear time-invariant systems N90-23025
An examination of the full-wave method for rough surface scattering
[AD-A218664] N90-23155
WEIZMANN INST. OF SCIENCE, REHOVOTH (ISRAEL).
Comparison of solar pumped Nd:YAG and Nd:Cr:GSGG lasers at liquid nitrogen and room temperature
[DLR-FB-89-41] N90-22781
WESTINGHOUSE SAVANNAH RIVER CO., AIKEN, SC.
Modeling of combustion processes in a solid fuel particle
[DE90-009140] N90-22629
Parallel channel flow excursions
[DE90-009129] N90-22753
WISCONSIN UNIV., MADISON.
A numerical and analytical study of normal stresses and pressure differences in non-Newtonian creeping flows N90-22749
The analysis of polar clouds from AVHRR satellite data using pattern recognition techniques
[NASA-CR-183300] N90-22868
Counterrotating cores in elliptical galaxies N90-23288
WOODS HOLE OCEANOGRAPHIC INST., MA.
Calculation of 3-dimensional synthetic seismograms on the connection machine
[AD-A218472] N90-22857
WRIGHT RESEARCH DEVELOPMENT CENTER, WRIGHT-PATTERSON AFB, OH.
Optical spectroscopy of Ti(3+) doped YAlO3
[AD-A219043] N90-23251
WRIGHT STATE UNIV., DAYTON, OH.
Single-crystal diffraction analysis of 2-(trimethylsilylethynyl) 4-nitro-N,N-dimethylaniline
[AD-A218955] N90-22642
Explanation generation in expert systems (a literature review and implementation)
[AD-A218741] N90-23268
WYOMING UNIV., LARAMIE.
A study of woven fabric-reinforced composite materials using an invariant-based orthotropic plasticity formulation N90-22611
Infrared coronal line novae N90-23328

Y

YALE UNIV., NEW HAVEN, CT.
The elastic-plastic behavior of composite materials N90-22615
Nonlinear spectroscopy of multicomponent droplets and 2- and 3-dimensional measurements in flames
[AD-A218569] N90-22638
The multifractal nature of turbulence N90-22752
Evolutionary models of the rotating sun and implications for other low mass stars N90-23329
YORK UNIV. (ONTARIO).
Visual sensitivities and discriminations and their role in aviation
[AD-A219319] N90-22917
YORK UNIV., TORONTO (ONTARIO).
Spatial vision within egocentric and exocentric frames of reference N90-22928

Z

ZENTRALINSTITUT FUER KERNFORSCHUNG, ROSSENDORF BEI DRESDEN (GERMAN D.R.).
Amorphization of metals by ion implantation and ion beam mixing
[DE90-620571] N90-22667

Typical Contract Number Index Listing

Listings in this index are arranged alphanumerically by contract number. Under each contract number the NASA accession numbers denoting documents that have been produced as a result of research done under that contract are arranged in ascending order. The NASA accession number denotes the number by which the citation is identified.

AF PROJ. B413 ..... N90-23110
AF PROJ. 7A10 ..... N90-22859
N90-22862
AF PROJ. 2001 ..... N90-23251
AF PROJ. 2004 ..... N90-22858
AF PROJ. 2301 ..... N90-23200
N90-23255
AF PROJ. 2302 ..... N90-22594
N90-22680
AF PROJ. 2303 ..... N90-22627
N90-22634
N90-22642
N90-22681
N90-22685
N90-22690
AF PROJ. 2304 ..... N90-22762
N90-22817
N90-23103
N90-23106
N90-23127
N90-23140
N90-23143
N90-23144
N90-23146
N90-23147
N90-23152
N90-23154
N90-23176
N90-23185
N90-23201
AF PROJ. 2305 ..... N90-23217
AF PROJ. 2306 ..... N90-22701
N90-22712
N90-23247
AF PROJ. 2307 ..... N90-22541
AF PROJ. 2308 ..... N90-22635
N90-22636
AF PROJ. 2310 ..... N90-22860
AF PROJ. 2313 ..... N90-23184
AF PROJ. 2403 ..... N90-22560
N90-22561
N90-22562
AF PROJ. 2917 ..... N90-23250
AF PROJ. 3037 ..... N90-23188
N90-23189
N90-23190
AF PROJ. 3048 ..... N90-22638
AF PROJ. 3484 ..... N90-22678
AF PROJ. 3842 ..... N90-22774
N90-22892
N90-22985
N90-23107
AF PROJ. 4506 ..... N90-22895
AF PROJ. 4594 ..... N90-23126
AF PROJ. 4600 ..... N90-22720
AF PROJ. 5581 ..... N90-23108
AF PROJ. 5730 ..... N90-22693
N90-22845
AF-AFOSR-0014-87 ..... N90-22541
AF-AFOSR-0014-88 ..... N90-22634
AF-AFOSR-0049-87 ..... N90-22690
AF-AFOSR-0051-87 ..... N90-23147
AF-AFOSR-0052-88 ..... N90-22635
AF-AFOSR-0056-89 ..... N90-23185
AF-AFOSR-0083-87 ..... N90-23184
AF-AFOSR-0088-86 ..... N90-22762
AF-AFOSR-0100-88 ..... N90-22636
AF-AFOSR-0113-88 ..... N90-22627
AF-AFOSR-0119-85 ..... N90-23035
AF-AFOSR-0133-86 ..... N90-22685
AF-AFOSR-0137-89 ..... N90-22774
AF-AFOSR-0144-89 ..... N90-23250
AF-AFOSR-0148-86 ..... N90-23139
AF-AFOSR-0148-89 ..... N90-23201
AF-AFOSR-0164-89 ..... N90-22892
AF-AFOSR-0192-87 ..... N90-23140
N90-23152
N90-23154
AF-AFOSR-0200-88 ..... N90-22817
AF-AFOSR-0206-89 ..... N90-22985
AF-AFOSR-0210-82 ..... N90-23103
AF-AFOSR-0214-89 ..... N90-23107
AF-AFOSR-0252-89 ..... N90-23200
AF-AFOSR-0273-88 ..... N90-22681
AF-AFOSR-0276-87 ..... N90-23106
AF-AFOSR-0288-87 ..... N90-22680
AF-AFOSR-0311-87 ..... N90-22859
AF-AFOSR-0315-84 ..... N90-23146
AF-AFOSR-0319-88 ..... N90-23255
AF-AFOSR-0327-87 ..... N90-22712
AF-AFOSR-0344-86 ..... N90-22678
AF-AFOSR-0356-87 ..... N90-23084
AF-AFOSR-0373-87 ..... N90-23084
AF-AFOSR-0390-88 ..... N90-23035
ARPA ORDER 3597 ..... N90-22907
N90-22913
N90-23145
ARPA ORDER 4395 ..... N90-23208
ARPA ORDER 4976 ..... N90-22897
ARPA ORDER 5299 ..... N90-22861
ARPA ORDER 5351 ..... N90-22797
ARPA ORDER 6631 ..... N90-23219
ARPA ORDER 9526 ..... N90-22741
DA PROJ. 1L1-61102-AH-45 ..... N90-22965
DA PROJ. 1L1-62105-AH-84 ..... N90-22684
DA PROJ. 1L1-62209-A4-7A N90-22790
DA PROJ. 1L1-62618-AH-80 ..... N90-22763
DA PROJ. 1L1-62723-AH-98 ..... N90-23142
DA PROJ. 3E1-62777-A-879 ..... N90-22884
DA PROJ. 3E1-62787-A-879 ..... N90-22886
DAAB07-89-F404 ..... N90-23219
DAAG29-84-K-0061 ..... N90-23157
DAAG29-84-K-0132 ..... N90-22639
DAAG29-84-9-0027 ..... N90-23157
DAAG29-85-K-0081 ..... N90-23253
DAAG29-85-K-0253 ..... N90-22637
DAAG29-85-K-0254 ..... N90-22735
DAAJ02-86-C-0028 ..... N90-22545
N90-22546
N90-22547
N90-22548
N90-22549
DAAL03-86-C-0010 ..... N90-23254
DAAL03-86-K-0080 ..... N90-22910
DAAL03-86-K-0100 ..... N90-22983
DAAL03-86-K-0173 ..... N90-22785
N90-22786
N90-23101
N90-23216
DAAL03-87-K-0100 ..... N90-22775
DAAL03-87-K-0103 ..... N90-22578
DAAL03-87-K-0109 ..... N90-23252
DAAL03-88-C-0014 ..... N90-23214
DAAL03-88-C-0024 ..... N90-22806
DAAL03-88-K-0202 ..... N90-22688
DAAL03-89-C-0031 ..... N90-23157
N90-23213
DAAL03-89-G-0004 ..... N90-22765
DAAL03-89-G-0032 ..... N90-22640
DAAL03-89-K-0070 ..... N90-22830
DAAL04-87-C-0074 ..... N90-22805
DABT60-85-D-0520 ..... N90-22718
DACA76-85-C-0003 ..... N90-22797
DAJA45-89-M-0234 ..... N90-22844
DAMD17-87-C-7095 ..... N90-22888
DAMD17-88-C-8055 ..... N90-22884
DARPA ORDER 9525 ..... N90-22689
DE-AC02-83CH-10093 ..... N90-22836
N90-22837
N90-22838
N90-22839
DE-AC04-76DP-00789 ..... N90-22699
N90-22754
N90-22791
N90-22804
N90-22840
N90-22841
N90-22954
DE-AC04-88DP-43495 ..... N90-22630
N90-22674
DE-AC05-84ER-21400 ..... N90-23007
DE-AC05-84OR-21400 ..... N90-22792
N90-22869
DE-AC05-85ER-40216 ..... N90-22780
N90-23204
DE-AC06-76RL-01830 ..... N90-23263
DE-AC06-87RL-10930 ..... N90-23203
DE-AC07-76ID-01570 ..... N90-22723
N90-22768
N90-22814
DE-AC09-89SR-18035 ..... N90-22629
N90-22753
DE-AI05-84OR-21411 ..... N90-22684
DE-FC07-88ID-12797 ..... N90-22755
DE-FG02-86ER-45258 ..... N90-23238
DE-FG02-88ER-25053 ..... N90-23139
DE-FG03-85ER-51095 ..... N90-23221
DE-FG05-80ET-53088 ..... N90-23222
DE-FG05-86ER-13604 ..... N90-22664
DNA-MIPR-88-507 ..... N90-22736
DNA001-87-C-0169 ..... N90-22714
DRET-86-34-413-00-470-75-01 ..... N90-22618
DRET-87-34-256-00-470-75-01 ..... N90-22760
DRET-87-105 ..... N90-22759
DTFA01-80-Y-10524 ..... N90-22550
FI1W/0187/00 ..... N90-22747
F04611-86-C-0074 ..... N90-22845
F04701-85-C-0086 ..... N90-22719
F08635-89-C-0027 ..... N90-23127
F08635-89-C-0138 ..... N90-23127
F19628-85-C-0003 ..... N90-22554
N90-23109
N90-23111
N90-23112
N90-23113
N90-23114
N90-23115
F19628-86-K-0002 ..... N90-23248
F19628-87-K-0011 ..... N90-22863
F19628-87-K-0032 ..... N90-22861
F19628-87-K-0045 ..... N90-23325
F19628-88-K-0036 ..... N90-22862
F30602-86-C-0005 ..... N90-23110
F30602-88-C-0031 ..... N90-22857
F30602-88-D-0027 ..... N90-22895
N90-22971
F33615-81-K-1539 ..... N90-22907
N90-22913
N90-23145
F33615-85-C-3610 ..... N90-22560
N90-22561
N90-22562
F33615-86-C-0530 ..... N90-23188
N90-23189
N90-23190
F33615-86-C-0551 ..... N90-22563
F33615-86-C-1051 ..... N90-22858
F33615-87-C-1499 ..... N90-22897
F33615-87-C-2740 ..... N90-22638
F33615-88-C-3215 ..... N90-23021
F49620-85-C-0144 ..... N90-23143
N90-23144
N90-23150
N90-23176
F49620-85-K-0018 ..... N90-23213
F49620-86-C-0003 ..... N90-22733
F49620-86-C-0111 ..... N90-23138

F49620-86-C-60111 ..... N90-23035
F49620-86-K-0018 ..... N90-23247
F49620-87-C-0024 ..... N90-22860
F49620-87-C-01013 ..... N90-22997
F49620-88-C-0002 ..... N90-22917
F49620-88-C-0003 ..... N90-22543
F49620-88-C-0053 ..... N90-22642
F49620-88-C-00018 ..... N90-23035
F49620-89-C-0002 ..... N90-22594
IEP-87/822 ..... N90-22758
JPL-956873 ..... N90-22946
KONINKLIJKE/SHELL-89012-MSE-4 ..... N90-23097
NAG1-126 ..... N90-22698
NAG1-270 ..... N90-23137
NAG1-517 ..... N90-23138
NAG1-613 ..... N90-22997
NAG1-745 ..... N90-22651
NAG1-939 ..... N90-23027
NAG1-979 ..... N90-22614
NAG1-1009 ..... N90-23026
NAG3-694 ..... N90-22835
NAG3-707 ..... N90-22813
NAG5-1019 ..... N90-23017
NAG5-1117 ..... N90-22868
NAG9-244 ..... N90-22957
NASARP-49 ..... N90-22747
NAS1-11668 ..... N90-22609
NAS1-17492 ..... N90-22746
NAS1-18107 ..... N90-22540
NAS1-18140 ..... N90-22538
NAS1-18585 ..... N90-23038
NAS1-18605 ..... N90-22539
N90-22540
N90-22972
N90-22973
N90-22982
N90-23128
N90-23137
N90-23138
N90-23139
NAS1-19000 ..... N90-22557
NAS2-12961 ..... N90-23090
NAS3-24565 ..... N90-22724
NAS3-24670 ..... N90-22834
NAS3-25266 ..... N90-22843
NAS3-25270 ..... N90-22567
NAS5-27557 ..... N90-23312
NAS5-30312 ..... N90-22767
NAS7-198 ..... N90-22987
NAS7-918 ..... N90-22769
N90-22826
N90-22877
N90-23040
NAS8-30490 ..... N90-22602
N90-22788
NAS8-36433 ..... N90-22986
NAS8-37334 ..... N90-23333
NAS10-10285 ..... N90-22966
NCC2-86 ..... N90-22948
NCC2-315 ..... N90-22870
NCC2-517 ..... N90-22897
NCC2-538 ..... N90-22897
NCC3-105 ..... N90-22732
NGL-05-020-272 ..... N90-23333
NIH-EY-05926 ..... N90-22935
NSF ASC-88-58101 ..... N90-23139
NSF AST-89-01681 ..... N90-23302
NSF BNS-85-19616 ..... N90-22922
NSF BNS-86-09729 ..... N90-22898
N90-22984
N90-23104
NSF BNS-88-12048 ..... N90-22898
N90-23104
NSF DMS-86-06964 ..... N90-23158
N90-23159
NSF DMS-86-13093 ..... N90-23147
NSF DMS-86-57319 ..... N90-23139
NSF DMS-87-02620 ..... N90-23158
N90-23159
NSF DMS-87-17799 ..... N90-23159
NSF DMS-88-06099 ..... N90-23007
NSF DMS-88-10150 ..... N90-23137
NSF DMS-88-11863 ..... N90-23137
NSF DMS-88-18530 ..... N90-23138
NSF DMS-89-01234 ..... N90-23154
NSF ECS-84-11879 ..... N90-23157
NSF EET-87-16324 ..... N90-22797
N90-22903
N90-22904
NSF EET-87-18434 ..... N90-22995
N90-23011
NSF INT-83-14219 ..... N90-23308
NSF IRI-84-10413 ..... N90-23157
N90-23213
NSF MCS-82-19196 ..... N90-23157
N90-23213
N00014-82-K-0612 ..... N90-22643
N00014-83-K-0365 ..... N90-23332
N00014-83-K-0397 ..... N90-23153
N00014-84-K-0042 ..... N90-23156
N00014-84-K-0242 ..... N90-22882
N00014-84-K-0477 ..... N90-22607
N00014-85-K-0018 ..... N90-23157
N90-23213
N00014-85-K-0111 ..... N90-23333
N00014-85-K-0474 ..... N90-22579
N00014-85-K-0696 ..... N90-22901
N00014-85-K-0725 ..... N90-23185
N00014-86-C-0133 ..... N90-22896
N00014-86-G-0146 ..... N90-22898
N90-22984
N00014-86-K-0146 ..... N90-23104
N00014-86-K-0316 ..... N90-22644
N00014-86-K-0349 ..... N90-22898
N90-22900
N90-23104
N00014-86-K-0482 ..... N90-23153
N00014-86-K-0678 ..... N90-22797
N90-22894
N90-22896
N90-22897
N90-22898
N90-22899
N90-22900
N90-22901
N90-22902
N90-22903
N90-22904
N90-22905
N90-22906
N90-22907
N90-22908
N90-22909
N90-22911
N90-22912
N90-22913
N90-22914
N90-22915
N90-22916
N90-22984
N90-23104
N90-23145
N00014-86-K-0691 ..... N90-23137
N00014-86-K-0768 ..... N90-22686
N90-22687
N00014-86-K-0772 ..... N90-22682
N90-22683
N90-22739
N00014-87-C-0340 ..... N90-22857
N00014-87-K-0007 ..... N90-22766
N00014-87-K-0196 ..... N90-22608
N00014-87-K-0266 ..... N90-22924
N00014-87-K-0321 ..... N90-22797
N00014-87-K-0365 ..... N90-22883
N00014-87-K-0495 ..... N90-22797
N00014-87-K-0533 ..... N90-23120
N00014-87-K-0825 ..... N90-22846
N00014-88-C-0390 ..... N90-22741
N00014-88-C-0391 ..... N90-23256
N00014-88-C-0433 ..... N90-22689
N00014-88-C-0512 ..... N90-22916
N00014-88-C-0688 ..... N90-22897
N00014-88-K-0086 ..... N90-22899
N90-22889
N00014-88-K-0105 ..... N90-23158
N00014-88-K-0170 ..... N90-23159
N90-22881
N00014-88-K-0250 ..... N90-22737
N00014-88-K-0341 ..... N90-22738
N90-22897
N00014-88-K-0554 ..... N90-23211
N00014-88-K-0578 ..... N90-23213
N00014-88-K-0630 ..... N90-23218
N00014-89-C-0199 ..... N90-23215
N00014-89-C-0200 ..... N90-23186
N00014-89-C-0240 ..... N90-23141
N00014-89-J-1008 ..... N90-22857
N00014-89-J-1012 ..... N90-22641
N00014-89-K-0056 ..... N90-23177
N00014-90-J-1272 ..... N90-23155
N00030-88-C-0054 ..... N90-22897
N00039-86-C-0033 ..... N90-22797
N00039-87-C-0251 ..... N90-22818
N00039-88-C-0051 ..... N90-22715
N00039-88-C-0065 ..... N90-22716
N90-22596
N00039-89-C-5301 ..... N90-23249
N68452-86MP-6003 ..... N90-22831
ONR PROJ. RR-040-209 ..... N90-23186
ONR PROJ. 627-838 ..... N90-22643
RR04204 ..... N90-23153
STPA/EG-85/95-004 ..... N90-22616
W-31-109-ENG-38 ..... N90-23007
W-7405-ENG-36 ..... N90-22705
W-7405-ENG-48 ..... N90-22673
N90-22700
N90-22779
N90-23129
161-40-21 ..... N90-22850
161-80-15-40 ..... N90-22877
488-51-03 ..... N90-23125
501-14-11 ..... N90-23339
505-47-11 ..... N90-22918
505-60-01-02 ..... N90-22746
505-61-71-02 ..... N90-22531
505-62-4D N90-22567
505-62-71 ..... N90-22566
505-63-1B N90-22703
505-63-01-07 ..... N90-22557
505-63-21-01 ..... N90-22538
505-63-21-09 ..... N90-22555
505-63-51 ..... N90-22790
N90-22796
505-63-51-10 ..... N90-22558
505-66-11-02 ..... N90-22965
505-69-41-01 ..... N90-23338
505-90-21-01 ..... N90-22539
N90-22540
N90-22972
N90-22973
N90-22982
N90-23128
N90-23137
N90-23138
N90-23139
506-41-11 ..... N90-22843
506-42-11 ..... N90-22604
506-42-21 ..... N90-22595
506-43-41-02 ..... N90-22807
506-46-31-01 ..... N90-22987
N90-23040
506-48-21 ..... N90-22592
506-53-43 ..... N90-22628
510-01-0A N90-22822
510-01-1A N90-22801
510-01-01 ..... N90-22646
533-02-01 ..... N90-22532
535-03-01 ..... N90-22564
553-13-00 ..... N90-22808
N90-22823
582-01-11 ..... N90-22784
590-01-21 ..... N90-22605
590-13-11 ..... N90-22606
N90-22847
590-13-41 ..... N90-22773
591-21-00 ..... N90-22761
844-20-00-30-02 ..... N90-22826
946-02-20 ..... N90-22731

Typical Report Number Index Listing

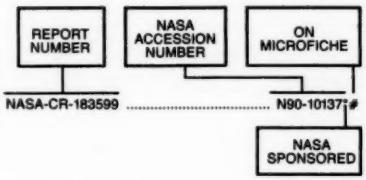

Listings in this index are arranged alphanumerically by report number. The NASA accession number denotes the number by which the citation is identified. An asterisk (*) indicates that the item is a NASA report. A pound sign (#) indicates that the item is available on microfiche.

A-88090 ..... N90-22918* #
A-89029 ..... N90-23090* #
A-90002 ..... N90-22827* #

AAMRL-TR-89-039 ..... N90-22563 #

AD-A216252 ..... N90-22596
AD-A218408 ..... N90-22607 #
AD-A218410 ..... N90-22883 #
AD-A218416 ..... N90-23184 #
AD-A218417 ..... N90-22712 #
AD-A218420 ..... N90-23152 #
AD-A218421 ..... N90-23140 #
AD-A218422 ..... N90-23247 #
AD-A218425 ..... N90-23101 #
AD-A218426 ..... N90-22785 #
AD-A218427 ..... N90-22786 #
AD-A218433 ..... N90-22805 #
AD-A218434 ..... N90-22545 #
AD-A218435 ..... N90-22546 #
AD-A218436 ..... N90-22547 #
AD-A218437 ..... N90-22548 #
AD-A218438 ..... N90-22549 #
AD-A218445 ..... N90-22892 #
AD-A218450 ..... N90-22774 #
AD-A218451 ..... N90-22817 #
AD-A218452 ..... N90-22678 #
AD-A218454 ..... N90-23185 #
AD-A218459 ..... N90-23210 #
AD-A218460 ..... N90-22829 #
AD-A218462 ..... N90-23141 #
AD-A218470 ..... N90-22679 #
AD-A218471 ..... N90-23153 #
AD-A218472 ..... N90-22857 #
AD-A218473 ..... N90-23154 #
AD-A218477 ..... N90-22870* #
AD-A218499 ..... N90-22871 #
AD-A218502 ..... N90-22633 #
AD-A218504 ..... N90-22559 #
AD-A218505 ..... N90-23207 #
AD-A218506 ..... N90-23267 #
AD-A218508 ..... N90-23102 #
AD-A218509 ..... N90-22713 #
AD-A218516 ..... N90-22680 #
AD-A218520 ..... N90-22634 #
AD-A218525 ..... N90-22762 #
AD-A218546 ..... N90-22879 #
AD-A218547 ..... N90-23248 #
AD-A218548 ..... N90-23211 #
AD-A218550 ..... N90-22681 #
AD-A218552 ..... N90-22733 #
AD-A218553 ..... N90-22635 #
AD-A218556 ..... N90-22692 #
AD-A218557 ..... N90-23142 #
AD-A218560 ..... N90-22560 #
AD-A218561 ..... N90-22561 #
AD-A218562 ..... N90-22562 #
AD-A218564 ..... N90-23176 #
AD-A218565 ..... N90-23143 #
AD-A218566 ..... N90-23144 #
AD-A218567 ..... N90-23200 #
AD-A218569 ..... N90-22636 #
AD-A218570 ..... N90-23103 #
AD-A218571 ..... N90-22541 #
AD-A218622 ..... N90-22714 #
AD-A218623 ..... N90-22715 #
AD-A218632 ..... N90-22716 #
AD-A218635 ..... N90-22542 #
AD-A218639 ..... N90-22969 #
AD-A218641 ..... N90-22885 #
AD-A218642 ..... N90-22693 #
AD-A218648 ..... N90-22893 #
AD-A218662 ..... N90-22830 #
AD-A218664 ..... N90-23155 #
AD-A218666 ..... N90-22637 #
AD-A218693 ..... N90-23212 #
AD-A218695 ..... N90-22552 #
AD-A218700 ..... N90-22638 #
AD-A218706 ..... N90-22668 #
AD-A218710 ..... N90-23213 #
AD-A218720 ..... N90-22872 #
AD-A218731 ..... N90-23156 #
AD-A218733 ..... N90-23120 #
AD-A218736 ..... N90-22831 #
AD-A218739 ..... N90-22717 #
AD-A218741 ..... N90-23268 #
AD-A218745 ..... N90-22669 #
AD-A218746 ..... N90-22763 #
AD-A218748 ..... N90-22734 #
AD-A218750 ..... N90-22694 #
AD-A218751 ..... N90-22670 #
AD-A218762 ..... N90-22718 #
AD-A218770 ..... N90-22873 #
AD-A218771 ..... N90-22639 #
AD-A218777 ..... N90-22983 #
AD-A218781 ..... N90-22735 #
AD-A218785 ..... N90-22701 #
AD-A218787 ..... N90-22858 #
AD-A218789 ..... N90-22818 #
AD-A218790 ..... N90-23325 #
AD-A218792 ..... N90-22874 #
AD-A218793 ..... N90-22875 #
AD-A218798 ..... N90-22832 #
AD-A218799 ..... N90-22576 #
AD-A218801 ..... N90-22671 #
AD-A218802 ..... N90-22553 #
AD-A218803 ..... N90-22682 #
AD-A218804 ..... N90-22683 #
AD-A218805 ..... N90-23249 #
AD-A218825 ..... N90-22764 #
AD-A218841 ..... N90-22684 #
AD-A218844 ..... N90-23332 #
AD-A218853 ..... N90-22859 #
AD-A218856 ..... N90-23214 #
AD-A218871 ..... N90-22685 #
AD-A218873 ..... N90-22880 #
AD-A218877 ..... N90-22860 #
AD-A218884 ..... N90-22640 #
AD-A218886 ..... N90-23104 #
AD-A218887 ..... N90-23145 #
AD-A218889 ..... N90-22894 #
AD-A218890 ..... N90-22895 #
AD-A218891 ..... N90-22686 #
AD-A218896 ..... N90-22687 #
AD-A218902 ..... N90-22641 #
AD-A218904 ..... N90-23146 #
AD-A218910 ..... N90-22886 #
AD-A218911 ..... N90-22806 #
AD-A218913 ..... N90-22896 #
AD-A218917 ..... N90-23105 #
AD-A218919 ..... N90-22887 #
AD-A218926 ..... N90-22897* #
AD-A218928 ..... N90-22984 #
AD-A218929 ..... N90-22898 #
AD-A218937 ..... N90-22888 #
AD-A218946 ..... N90-22844 #
AD-A218948 ..... N90-23157 #
AD-A218955 ..... N90-22642 #
AD-A218956 ..... N90-23215 #
AD-A218975 ..... N90-22797 #
AD-A218976 ..... N90-22899 #
AD-A218977 ..... N90-22900 #
AD-A218983 ..... N90-22985 #
AD-A218998 ..... N90-22736 #
AD-A218999 ..... N90-22775 #
AD-A219000 ..... N90-23186 #
AD-A219002 ..... N90-22901 #
AD-A219008 ..... N90-22902 #
AD-A219012 ..... N90-23250 #
AD-A219013 ..... N90-23106 #
AD-A219028 ..... N90-22903 #
AD-A219029 ..... N90-22904 #
AD-A219032 ..... N90-22845 #
AD-A219034 ..... N90-22688 #
AD-A219035 ..... N90-22578 #
AD-A219038 ..... N90-22905 #
AD-A219041 ..... N90-22643 #
AD-A219043 ..... N90-23251 #
AD-A219044 ..... N90-23126 #
AD-A219070 ..... N90-23107 #
AD-A219071 ..... N90-23201 #
AD-A219095 ..... N90-22906 #
AD-A219096 ..... N90-23108 #
AD-A219108 ..... N90-22570 #
AD-A219109 ..... N90-22798 #
AD-A219127 ..... N90-22833 #
AD-A219128 ..... N90-23187 #
AD-A219130 ..... N90-22765 #
AD-A219131 ..... N90-22689 #
AD-A219133 ..... N90-23252 #
AD-A219135 ..... N90-22819 #
AD-A219136 ..... N90-23253 #
AD-A219164 ..... N90-23147 #
AD-A219165 ..... N90-22530 #
AD-A219169 ..... N90-22550 #
AD-A219175 ..... N90-23188 #
AD-A219176 ..... N90-23189 #
AD-A219177 ..... N90-23190 #
AD-A219179 ..... N90-22766 #
AD-A219183 ..... N90-22672 #
AD-A219186 ..... N90-22799 #
AD-A219187 ..... N90-23109 #
AD-A219194 ..... N90-23148 #
AD-A219198 ..... N90-23269 #
AD-A219199 ..... N90-22907 #
AD-A219200 ..... N90-22908 #
AD-A219201 ..... N90-22909 #
AD-A219203 ..... N90-23254 #
AD-A219204 ..... N90-22910 #
AD-A219211 ..... N90-22737 #
AD-A219214 ..... N90-23177 #
AD-A219215 ..... N90-22861 #
AD-A219216 ..... N90-23110 #
AD-A219220 ..... N90-23160 #
AD-A219227 ..... N90-22820 #
AD-A219232 ..... N90-22690 #
AD-A219233 ..... N90-22881 #
AD-A219234 ..... N90-22738 #
AD-A219241 ..... N90-23216 #
AD-A219255 ..... N90-23158 #
AD-A219256 ..... N90-23159 #
AD-A219258 ..... N90-22608 #
AD-A219259 ..... N90-23127 #
AD-A219262 ..... N90-23255 #
AD-A219264 ..... N90-22970 #
AD-A219270 ..... N90-22911 #
AD-A219271 ..... N90-22912 #
AD-A219273 ..... N90-22913 #
AD-A219274 ..... N90-22914 #
AD-A219275 ..... N90-22915 #
AD-A219277 ..... N90-22916 #
AD-A219288 ..... N90-22719 #
AD-A219289 ..... N90-23270 #
AD-A219290 ..... N90-23111 #
AD-A219291 ..... N90-23112 #
AD-A219292 ..... N90-23113 #
AD-A219293 ..... N90-23114 #
AD-A219294 ..... N90-22554 #
AD-A219295 ..... N90-23115 #
AD-A219297 ..... N90-22846 #
AD-A219300 ..... N90-22702 #
AD-A219301 ..... N90-22739 #
AD-A219302 ..... N90-22563 #
AD-A219304 ..... N90-23271 #
AD-A219305 ..... N90-22720 #
AD-A219306 ..... N90-23217 #
AD-A219307 ..... N90-23149 #

AD-A219309 ..... N90-22876 #
AD-A219310 ..... N90-22721 #
AD-A219315 ..... N90-22543 #
AD-A219316 ..... N90-22594 #
AD-A219318 ..... N90-22627 #
AD-A219319 ..... N90-22917 #
AD-A219333 ..... N90-23333* #
AD-A219337 ..... N90-22740 #
AD-A219338 ..... N90-22722 #
AD-A219351 ..... N90-23256 #
AD-A219358 ..... N90-22862 #
AD-A219361 ..... N90-22884 #
AD-A219368 ..... N90-23272 #
AD-A219369 ..... N90-22825 #
AD-A219370 ..... N90-22863 #
AD-A219374 ..... N90-22800 #
AD-A219377 ..... N90-22889 #
AD-A219378 ..... N90-22882 #
AD-A219389 ..... N90-23116 #
AD-A219392 ..... N90-22971 #
AD-A219394 ..... N90-23218 #
AD-A219398 ..... N90-23219 #
AD-A219403 ..... N90-22644 #
AD-A219405 ..... N90-22695 #
AD-A219408 ..... N90-23228 #
AD-A219409 ..... N90-23117 #
AD-A219413 ..... N90-23150 #
AD-A219419 ..... N90-22741 #
AD-A219511 ..... N90-23208 #
AD-A219512 ..... N90-23161 #
AD-A219513 ..... N90-23209 #
AD-A219572 ..... N90-22821 #

AD-D014436 ..... N90-22551

AD-E900914 ..... N90-22871 #

AERE-G-4977 ..... * N90-22747

AERE-M-3709 ..... N90-22649

AERE-R-12600 ..... N90-22704
AERE-R-13028 ..... N90-22810
AERE-R-13030 ..... N90-22802
AERE-R-13106 ..... N90-22777
AERE-R-13196 ..... N90-22803
AERE-R-13300 ..... N90-22748
AERE-R-13309 ..... N90-22650
AERE-R-13317 ..... N90-22648
AERE-R-13321 ..... N90-22647
AERE-R-13327 ..... N90-23234

AFATL-TP-90-02 ..... N90-23127 #

AFGL-TR-89-0080 ..... N90-22825 #

AFGWC/TN-90/001 ..... N90-22876 #

AFHRL-TP-89-75 ..... N90-22893 #

AFHRL-TR-89-9 ..... N90-22559 #

AFIT/CI/CIA-89-048 ..... N90-22871 #
AFIT/CI/CIA-89-072 ..... N90-22870* #
AFIT/CI/CIA-89-142 ..... N90-23268 #

AFOSR-90-0189TR ..... N90-22733 #
AFOSR-90-0190TR ..... N90-22635 #
AFOSR-90-0191TR ..... N90-22543 #
AFOSR-90-0192TR ..... N90-22627 #
AFOSR-90-0196TR ..... N90-23146 #
AFOSR-90-0202TR ..... N90-22774 #
AFOSR-90-0203TR ..... N90-22680 #
AFOSR-90-0204TR ..... N90-23247 #
AFOSR-90-0205TR ..... N90-22712 #
AFOSR-90-0211TR ..... N90-23154 #
AFOSR-90-0212TR ..... N90-23140 #
AFOSR-90-0213TR ..... N90-23152 #
AFOSR-90-0214TR ..... N90-23103 #
AFOSR-90-0216TR ..... N90-23200 #
AFOSR-90-0218TR ..... N90-22681 #
AFOSR-90-0221TR ..... N90-22678 #
AFOSR-90-0232TR ..... N90-22817 #
AFOSR-90-0233TR ..... N90-22762 #
AFOSR-90-0235TR ..... N90-22917 #
AFOSR-90-0238TR ..... N90-22634 #
AFOSR-90-0247TR ..... N90-22541 #
AFOSR-90-0260TR ..... N90-22892 #
AFOSR-90-0262TR ..... N90-22636 #
AFOSR-90-0263TR ..... N90-23185 #
AFOSR-90-0267TR ..... N90-23184 #
AFOSR-90-0272TR ..... N90-23176 #
AFOSR-90-0273TR ..... N90-23143 #
AFOSR-90-0274TR ..... N90-23144 #
AFOSR-90-0275TR ..... N90-23150 #
AFOSR-90-0285TR ..... N90-22685 #
AFOSR-90-0290TR ..... N90-22860 #
AFOSR-90-0297TR ..... N90-22985 #
AFOSR-90-0304TR ..... N90-23201 #
AFOSR-90-0308TR ..... N90-23107 #
AFOSR-90-0309TR ..... N90-22690 #
AFOSR-90-0310TR ..... N90-23147 #
AFOSR-90-0313TR ..... N90-23106 #
AFOSR-90-0316TR ..... N90-23250 #

AFOTEC-86-0167 ..... N90-22873 #

AFWAL-TR-89-2011-VOL-2 ..... N90-22638 #

AIAA-89-2696 ..... N90-22564* #
AIAA-89-3558 ..... N90-23060* #
AIAA-90-1672 ..... N90-22592* #
AIAA-90-1882 ..... N90-22595* #
AIAA-90-2120 ..... N90-22605* #
AIAA-90-2153 ..... N90-22790* #
AIAA-90-2389 ..... N90-22604* #
AIAA-90-2417 ..... N90-22566* #

AIP-58 ..... N90-22907 #
AIP-59 ..... N90-22908 #
AIP-60 ..... N90-22909 #
AIP-64 ..... N90-22896 #
AIP-65 ..... N90-22897* #
AIP-67 ..... N90-22984 #
AIP-68 ..... N90-22898 #
AIP-70 ..... N90-23104 #
AIP-71 ..... N90-22894 #
AIP-72 ..... N90-22916 #
AIP-73 ..... N90-22905 #
AIP-74 ..... N90-22902 #
AIP-75 ..... N90-22906 #
AIP-77 ..... N90-22797 #
AIP-78 ..... N90-22904 #
AIP-79 ..... N90-22903 #
AIP-80 ..... N90-22911 #
AIP-81 ..... N90-22899 #
AIP-82 ..... N90-22912 #
AIP-83 ..... N90-22900 #
AIP-94 ..... N90-22913 #
AIP-95 ..... N90-22914 #
AIP-97 ..... N90-22901 #
AIP-98 ..... N90-22915 #
AIP-101 ..... N90-23145 #

AL-TR-89-083 ..... N90-22845 #
AL-TR-89-085 ..... N90-22693 #

AQET-NOTE-07/89 ..... N90-22625 #
AQET-NOTE-09/89 ..... N90-22815 #

AQET/B-3934-TI/88 ..... N90-22691 #

ARCCB-TR-90003 ..... N90-22819 #
ARCCB-TR-90004 ..... N90-22669 #
ARCCB-TR-90005 ..... N90-23148 #

ARL-STRUC-TM-515 ..... N90-22570 #

ARL/PSU/TR-90-01 ..... N90-22818 #

ARO-90-1 ..... N90-23160 #
ARO-21125.3-EL ..... N90-23253 #
ARO-21271.27-CH ..... N90-22639 #
ARO-22437.17-EG ..... N90-22637 #
ARO-22912.8-EL ..... N90-22983 #
ARO-23136.5-CH ..... N90-22735 #
ARO-23324.1-EL-S ..... N90-23254 #
ARO-23871.5-LS ..... N90-22910 #
ARO-24626.126-PH-UIR ..... N90-22785 #
ARO-24626.127-PH-UIR ..... N90-22786 #
ARO-24626.128-PH-UIR ..... N90-23101 #
ARO-24626.129-PH-UIR ..... N90-23212 #
ARO-24626.137-PH-UIR ..... N90-23216 #
ARO-24730.8-PH ..... N90-22775 #
ARO-24988.1-EL ..... N90-23252 #
ARO-25416.1-EG-SDI ..... N90-22578 #
ARO-25822.3-PH ..... N90-23214 #
ARO-25952.1-EG-SBI ..... N90-22806 #
ARO-26043.2-GS ..... N90-23155 #
ARO-26172.1-MS-A ..... N90-22688 #
ARO-26220.1-GS ..... N90-22830 #
ARO-26612.1-EG-EQ ..... N90-22765 #
ARO-26690.1-MS-CF ..... N90-22640 #
ARO-26779.3-EL-AI ..... N90-23213 #
ARO-26779.5-EL ..... N90-23157 #

AVSCOM-TM-90-B-006 ..... N90-22558* #
AVSCOM-TM-90-B-016 ..... N90-22965* #
AVSCOM-TM-90-C-004 ..... N90-22796* #
AVSCOM-TM-90-C-008 ..... N90-22790* #

BBN-6832-VOL-1 ..... N90-23188 #
BBN-6833-VOL-2 ..... N90-23189 #
BBN-6953-VOL-3 ..... N90-23190 #

BRL-MR-3080 ..... N90-22800 #
BRL-MR-3803 ..... N90-22734 #
BRL-MR-3807 ..... N90-22670 #

BRL-TR-3069 ..... N90-22694 #
BRL-TR-3072 ..... N90-22692 #
BRL-TR-3074 ..... N90-22763 #

BR111667 ..... N90-22537 #
BR111939 ..... N90-22708 #
BR111982 ..... N90-22586 #
BR112043 ..... N90-22891 #

CERL-TR-N-90/01 ..... N90-22633 #

CEVANS/049/FR-9002 ..... N90-23254 #

CGISC-5232-90-01 ..... N90-23271 #

CMU/SEI-89-TR-19 ..... N90-23115 #
CMU/SEI-89-TR-20 ..... N90-23113 #
CMU/SEI-89-TR-32 ..... N90-23111 #
CMU/SEI-89-TR-34 ..... N90-23114 #
CMU/SEI-89-TR-35-REV ..... N90-22554 #
CMU/SEI-89-TR-36 ..... N90-23109 #
CMU/SEI-89-TR-40 ..... N90-23112 #

CONF-890335-276 ..... N90-23204 #
CONF-890335-277 ..... N90-22780 #
CONF-890866-2 ..... N90-23130 #
CONF-900187-1 ..... N90-22753 #
CONF-900391-5 ..... N90-22755 #
CONF-8908222-1 ..... N90-22768 #
CONF-8908222-3 ..... N90-22723 #
CONF-9003132-1 ..... N90-22629 #
CONF-9003139-1 ..... N90-22699 #
CONF-9005150-1 ..... N90-22705 #
CONF-9005157-1 ..... N90-22791 #
CONF-9005158-1 ..... N90-22804 #
CONF-9006124-3 ..... N90-22814 #
CONF-9006155-1 ..... N90-22754 #
CONF-9006162-1 ..... N90-22792 #
CONF-9006164-1 ..... N90-22700 #

CPIA-PUBL-513 ..... N90-22596

CPS-90-001 ..... N90-22689 #

CRIF-MC-87 ..... N90-23183 #

CRREL-SR-89-37 ..... N90-22832 #

CRREL-89-22 ..... N90-22831 #

CS-8902 ..... N90-23264 #
CS-8903 ..... N90-23095 #
CS-8908 ..... N90-23096 #
CS-8909 ..... N90-23265 #
CS-8910 ..... N90-23097 #
CS-8913-PT-1 ..... N90-23098 #
CS-8914 ..... N90-23099 #
CS-8915 ..... N90-23100 #
CS-8916 ..... N90-23134 #
CS-8917 ..... N90-23135 #
CS-8918 ..... N90-23119 #

CUNY-RF-447239 ..... N90-22680 #

C87A-25 ..... N90-22741 #

DE89-009481 ..... N90-22836 #
DE89-009485 ..... N90-22837 #
DE89-009486 ..... N90-22838 #
DE90-000302 ..... N90-22839 #
DE90-007985 ..... N90-23203 #
DE90-007993 ..... N90-22869 #
DE90-008186 ..... N90-22673 #
DE90-008188 ..... N90-23129 #
DE90-008194 ..... N90-22674 #
DE90-008198 ..... N90-22779 #
DE90-008206 ..... N90-23263 #
DE90-008931 ..... N90-22705 #
DE90-009129 ..... N90-22753 #
DE90-009140 ..... N90-22629 #
DE90-009213 ..... N90-23221 #
DE90-009320 ..... N90-22791 #
DE90-009332 ..... N90-22699 #
DE90-009418 ..... N90-22792 #
DE90-009509 ..... N90-22804 #
DE90-009540 ..... N90-22700 #
DE90-009571 ..... N90-22754 #
DE90-009617 ..... N90-22755 #
DE90-009621 ..... N90-22814 #

DE90-009765 ..... N90-22723 #
DE90-009780 ..... N90-22768 #
DE90-009784 ..... N90-23130 #
DE90-009968 ..... N90-22630 #
DE90-009984 ..... N90-22664 #
DE90-009992 ..... N90-22780 #
DE90-009993 ..... N90-23204 #
DE90-010077 ..... N90-23222 #
DE90-010109 ..... N90-23238 #
DE90-010242 ..... N90-22840 #
DE90-010243 ..... N90-22841 #
DE90-617175 ..... N90-22665 #
DE90-617397 ..... N90-22666 #
DE90-618767 ..... N90-23220 #
DE90-620448 ..... N90-23257 #
DE90-620463 ..... N90-23258 #
DE90-620465 ..... N90-22856 #
DE90-620526 ..... N90-22631 #
DE90-620562 ..... N90-23239 #
DE90-620563 ..... N90-23240 #
DE90-620571 ..... N90-22667 #
DE90-620580 ..... N90-23223 #
DE90-620690 ..... N90-22706 #
DE90-620704 ..... N90-23180 #
DE90-620705 ..... N90-22707 #
DE90-620792 ..... N90-23324 #
DE90-620802 ..... N90-23241 #

DIOR/L03-89 ..... N90-23270 #

DLR-FB-89-41 ..... N90-22781 #
DLR-FB-89-42 ..... N90-22756 #

DLR-MITT-89-17 ..... N90-22842 #

DNA-TR-89-76 ..... N90-22714 #

DODA-AR-005-626 ..... N90-22570 #

DOE/CH-10093/66 ..... N90-22836 #
DOE/CH-10093/70 ..... N90-22837 #
DOE/CH-10093/71 ..... N90-22838 #

DOE/ER-13604/8 ..... N90-22664 #
DOE/ER-45258/4 ..... N90-23238 #

DOE/ET-53088/426 ..... N90-23222 #

DOE/RL-90-15 ..... N90-23203 #

DOT/FAA/CT-89/23 ..... N90-22695 #

DOT/FAA/SA-89/4 ..... N90-22550 #

DRES-SM-1267 ..... N90-22542 #

DTRC/CMLD-18-89/14 ..... N90-23267 #

DTRC/SHD-1298-06 ..... N90-22798 #

DTRC/SSPD-90-175-11 ..... N90-23105 #

E-4914 ..... N90-22564* #
E-5020 ..... N90-22823* #
E-5036 ..... N90-22703* #
E-5050 ..... N90-22808* #
E-5283 ..... N90-22801* #
E-5384 ..... N90-22796* #
E-5413 ..... N90-22646* #
E-5416 ..... N90-23339* #
E-5440 ..... N90-22790* #
E-5449 ..... N90-22761* #
E-5472 ..... N90-22843* #
E-5494 ..... N90-22608* #
E-5496 ..... N90-22732* #
E-5498 ..... N90-22605* #
E-5505 ..... N90-23125* #
E-5513 ..... N90-22773* #
E-5516 ..... N90-22731* #
E-5518 ..... N90-22847* #
E-5524 ..... N90-22822* #
E-5525 ..... N90-22592* #
E-5529 ..... N90-22595* #
E-5530 ..... N90-22784* #
E-5531 ..... N90-22604* #
E-5539 ..... N90-22566* #

EDR-14622 ..... N90-22567* #

EFML-90-1 ..... N90-22882 #

EGG-M-89049 ..... N90-22723 #
EGG-M-89050 ..... N90-22768 #
EGG-M-90040 ..... N90-22755 #
EGG-M-90043 ..... N90-22814 #

ENSM-8024 ..... N90-22760 #

EOARD-TR-90-03 ..... N90-23255 #

ERP-1025 ..... N90-22825 #
ERP-1040 ..... N90-23272 #

ESD-TR-89-27 ..... N90-23115 #
ESD-TR-89-28 ..... N90-23113 #
ESD-TR-89-43 ..... N90-23111 #
ESD-TR-89-45 ..... N90-23114 #
ESD-TR-89-46-REV ..... N90-22554 #
ESD-TR-89-47 ..... N90-23109 #
ESD-TR-89-51 ..... N90-23112 #

ESDP-3421 ..... N90-22869 #

ETN-90-95409 ..... N90-22974 #
ETN-90-96438 ..... N90-22675
ETN-90-96439 ..... N90-22586 #
ETN-90-96440 ..... N90-22708 #
ETN-90-96442 ..... N90-22537 #
ETN-90-96443 ..... N90-22891 #
ETN-90-96445 ..... N90-22544
ETN-90-96446 ..... N90-22967 #
ETN-90-96447 ..... N90-23181 #
ETN-90-96451 ..... N90-22842 #
ETN-90-96452 ..... N90-22781 #
ETN-90-96453 ..... N90-22756 #
ETN-90-96460 ..... N90-23282 #
ETN-90-96466 ..... N90-23224 #
ETN-90-96467 ..... N90-23225 #
ETN-90-96468 ..... N90-23283
ETN-90-96471 ..... N90-23182 #
ETN-90-96472 ..... N90-23259 #
ETN-90-96482 ..... N90-22968 #
ETN-90-96509 ..... N90-23131
ETN-90-96510 ..... N90-23132
ETN-90-96511 ..... N90-22725
ETN-90-96512 ..... N90-23092
ETN-90-96513 ..... N90-23118
ETN-90-96514 ..... N90-23093
ETN-90-96515 ..... N90-22726
ETN-90-96516 ..... N90-23094
ETN-90-96518 ..... N90-22577 #
ETN-90-96520 ..... N90-23191 #
ETN-90-96521 ..... N90-23192 #
ETN-90-96522 ..... N90-23260 #
ETN-90-96523 ..... N90-23261 #
ETN-90-96524 ..... N90-22782 #
ETN-90-96525 ..... N90-23226 #
ETN-90-96526 ..... N90-23227 #
ETN-90-96527 ..... N90-22828 #
ETN-90-96528 ..... N90-23205 #
ETN-90-96530 ..... N90-22771 #
ETN-90-96531 ..... N90-23243 #
ETN-90-96532 ..... N90-23133 #
ETN-90-96533 ..... N90-23193 #
ETN-90-96534 ..... N90-22709 #
ETN-90-96535 ..... N90-23173 #
ETN-90-96536 ..... N90-23174 #
ETN-90-96537 ..... N90-23244 #
ETN-90-96538 ..... N90-23194 #
ETN-90-96539 ..... N90-23245 #
ETN-90-96540 ..... N90-23175 #
ETN-90-96541 ..... N90-23331 #
ETN-90-96542 ..... N90-23195 #
ETN-90-96543 ..... N90-23196 #
ETN-90-96544 ..... N90-23197 #
ETN-90-96545 ..... N90-22849 #
ETN-90-96546 ..... N90-23336 #
ETN-90-96547 ..... N90-23337 #
ETN-90-96548 ..... N90-22710 #
ETN-90-96549 ..... N90-23246 #
ETN-90-96550 ..... N90-22711 #
ETN-90-96551 ..... N90-22573 #
ETN-90-96552 ..... N90-22587 #
ETN-90-96553 ..... N90-22588 #
ETN-90-96575 ..... N90-23183 #
ETN-90-96605 ..... N90-22676 #
ETN-90-96606 ..... N90-22727 #
ETN-90-96607 ..... N90-22589 #
ETN-90-96608 ..... N90-22793 #
ETN-90-96609 ..... N90-23123 #
ETN-90-96610 ..... N90-22728 #
ETN-90-96611 ..... N90-22580 #
ETN-90-96612 ..... N90-22757 #
ETN-90-96615 ..... N90-22616 #
ETN-90-96616 ..... N90-22617 #
ETN-90-96617 ..... N90-22618 #
ETN-90-96618 ..... N90-22619 #
ETN-90-96619 ..... N90-22620 #
ETN-90-96620 ..... N90-22758 #
ETN-90-96621 ..... N90-22759 #
ETN-90-96622 ..... N90-22760 #
ETN-90-96627 ..... N90-22603 #

ETN-90-96629 ..... N90-22581 #
ETN-90-96630 ..... N90-22582 #
ETN-90-96632 ..... N90-22632 #
ETN-90-96633 ..... N90-22621 #
ETN-90-96634 ..... N90-22571 #
ETN-90-96635 ..... N90-22622 #
ETN-90-96636 ..... N90-22696 #
ETN-90-96638 ..... N90-22623 #
ETN-90-96639 ..... N90-22624 #
ETN-90-96642 ..... N90-22572 #
ETN-90-96644 ..... N90-22783 #
ETN-90-96647 ..... N90-22772 #
ETN-90-96648 ..... N90-22590 #
ETN-90-96650 ..... N90-22815 #
ETN-90-96651 ..... N90-22816 #
ETN-90-96652 ..... N90-22691 #
ETN-90-96653 ..... N90-22625 #
ETN-90-96654 ..... N90-22677 #
ETN-90-96655 ..... N90-22591
ETN-90-96657 ..... N90-22626 #
ETN-90-96698 ..... N90-22729 #
ETN-90-96699 ..... N90-22575 #
ETN-90-96700 ..... N90-23206 #
ETN-90-96701 ..... N90-23198 #
ETN-90-96702 ..... N90-23199 #
ETN-90-96703 ..... N90-23264 #
ETN-90-96704 ..... N90-23095 #
ETN-90-96705 ..... N90-23096 #
ETN-90-96706 ..... N90-23265 #
ETN-90-96707 ..... N90-23097 #
ETN-90-96708-PT-1 ..... N90-23098 #
ETN-90-96709 ..... N90-23099 #
ETN-90-96710 ..... N90-23100 #
ETN-90-96711 ..... N90-23134 #
ETN-90-96712 ..... N90-23135 #
ETN-90-96713 ..... N90-23119 #
ETN-90-96714 ..... N90-22730 #
ETN-90-96716 ..... N90-23136 #
ETN-90-96717 ..... N90-22794 #
ETN-90-96718 ..... N90-23124 #
ETN-90-96719 ..... N90-22795 #
ETN-90-96720 ..... N90-23266 #
ETN-90-96721 ..... N90-23151 #

FAA-AP0-90-1 ..... N90-22530 #

FCR-10815 ..... N90-22846 #

FTD-ID(RS)T-1033-89 ..... N90-22872 #

GDL/GMF-90-02 ..... N90-22765 #

GL-TR-89-0147 ..... N90-22863 #
GL-TR-89-0224 ..... N90-22861 #
GL-TR-89-0251 ..... N90-23272 #
GL-TR-89-0273 ..... N90-22859 #
GL-TR-89-0328 ..... N90-23325 #
GL-TR-89-0329 ..... N90-22862 #

GPO-23-835 ..... N90-23202 #

GRASP-LAB-181 ..... N90-23157 #
GRASP-LAB-182 ..... N90-23213 #

H-1570 ..... N90-22532* #

HDL-TM-89-16 ..... N90-23117 #

HSD-TP-89-011-VOL-1 ..... N90-23188 #
HSD-TP-89-011-VOL-2 ..... N90-23189 #
HSD-TP-89-011-VOL-3 ..... N90-23190 #

ICASE-IR-10 ..... N90-22982* #
ICASE-IR-11 ..... N90-22972* #

ICASE-90-13 ..... N90-23137* #
ICASE-90-15 ..... N90-22539* #
ICASE-90-16 ..... N90-22540* #
ICASE-90-33 ..... N90-22973* #
ICASE-90-35 ..... N90-23128* #
ICASE-90-36 ..... N90-23138* #
ICASE-90-37 ..... N90-23139* #

IFSR-426 ..... N90-23222 #

IITRI-E06620-2 ..... N90-22716 #
IITRI-E06620-3 ..... N90-22715 #

ILR-MITT-230(1989) ..... N90-22968 #

INIS-BR-1827 ..... N90-22666 #

INIS-SU-157/A ..... N90-23220 #

INPE-4846-PRE/1475 ..... N90-22866 #
INPE-4981-PRE/1545 ..... N90-23091 #

INPE-4992-PRE/1554 ..... N90-23262 #
INPE-5011-TDL/399 ..... N90-23277 #

INT-PATENT-CLASS-B64D-1/00 ..... N90-22769*
INT-PATENT-CLASS-B64G-1/14 ..... N90-22584*

INT-PATENT-CLASS-C30B-7/02 ..... N90-23242*

INT-PATENT-CLASS-H01J-25/34 ..... N90-22724*
INT-PATENT-CLASS-H04N-7/18 ..... N90-22770*

IPEN-PUB-270 ..... N90-22665 #

IPF-88-3 ..... N90-23224 #

IQI-DFR-89-0074 ..... N90-22805 #

ISAL-89-60 ..... N90-22757 #
ISAL-89-0064 ..... N90-22676 #

ISBN-90-9002509-X ..... N90-22974 #

ISSN-0143-7313 ..... N90-22675
ISSN-0171-1342 ..... N90-22756 #
ISSN-0171-1342 ..... N90-22781 #
ISSN-0176-7739 ..... N90-22842 #
ISSN-0271-7077 ..... N90-23166 #
ISSN-0436-1199 ..... N90-23182 #
ISSN-0436-1199 ..... N90-23259 #
ISSN-0951-6301 ..... N90-22544

ISVR-TR-173 ..... N90-22967 #
ISVR-TR-183 ..... N90-23181 #

J-550-90-601/2454 ..... N90-23221 #

JHU/APL-TG-1377 ..... N90-23249 #

JHU/APL/STR-90-01 ..... N90-22887 #

JINR-D-14-88-667 ..... N90-23241 #

JINR-E-2-88-678 ..... N90-23257 #
JINR-E-11-89-442 ..... N90-23130 #

JINR-R-2-88-773 ..... N90-23324 #
JINR-R-2-88-778 ..... N90-23258 #
JINR-R-4-88-640 ..... N90-22631 #
JINR-R-4-88-693 ..... N90-23240 #
JINR-R-14-88-571 ..... N90-23239 #

JINR-18-88-603 ..... N90-22856 #

JPL-PUBL-89-41 ..... N90-22826* #
JPL-PUBL-89-42 ..... N90-22877* #
JPL-PUBL-89-45-VOL-1 ..... N90-22987* #
JPL-PUBL-89-45-VOL-2 ..... N90-23040* #

JPRS-UPM-89-001 ..... N90-23162 #

KFTI-88-4 ..... N90-23160 #
KFTI-88-5 ..... N90-22707 #
KFTI-88-6 ..... N90-22706 #
KFTI-88-10 ..... N90-23223 #

KVI-809 ..... N90-23206 #
KVI-813 ..... N90-23198 #
KVI-814 ..... N90-23199 #

L-16365 ..... N90-22628* #
L-16555 ..... N90-22531* #
L-16636 ..... N90-23338* #
L-16638 ..... N90-22555* #
L-16655 ..... N90-22965* #

LA-UR-90-906 ..... N90-22705 #

LAAS-89-330 ..... N90-22727 #
LAAS-89-359 ..... N90-22589 #
LAAS-89-371 ..... N90-22793 #
LAAS-89-384 ..... N90-23123 #
LAAS-89-394 ..... N90-22728 #

LC-89-600282 ..... N90-22850* #

LTR90-001 ..... N90-23215 #

L03 ..... N90-23270 #

MD89-CDSF-0022 ..... N90-22718 #

MEASUREMENT-SERIES-89-2 ..... N90-23153 #

MEMO-COSOR-89-17 ..... N90-23124 #
MEMO-COSOR-89-18 ..... N90-22795 #
MEMO-COSOR-89-19 ..... N90-23266 #

MEMO-COSOR-89-20 ..... N90-23151 #

MIT/LCS/TR-469 ..... N90-23120 #

MLM-MU-90-64-0003 ..... N90-22630 #

MLM-3631 ..... N90-22674 #

MPE-PREPRINT-161 ..... N90-23283

MPIS-12/1989 ..... N90-23182 #
MPIS-13/1989 ..... N90-23259 #

MRC/MRY-R-014 ..... N90-22714 #

MS-CIS-89-34 ..... N90-23157 #
MS-CIS-89-39 ..... N90-23213 #

MTL-TR-89-96 ..... N90-22805 #
MTL-TR-89-104 ..... N90-22799 #
MTL-TR-90-4 ..... N90-22684 #

NAS 1.15:4017 ..... N90-22628* #
NAS 1.15:4179 ..... N90-23338* #
NAS 1.15:4180 ..... N90-22555* #
NAS 1.15:4204 ..... N90-22593* #
NAS 1.15:100761 ..... N90-23273* #
NAS 1.15:101067 ..... N90-23090* #
NAS 1.15:101687 ..... N90-22807* #
NAS 1.15:101705 ..... N90-22532* #
NAS 1.15:102248 ..... N90-22827* #
NAS 1.15:102316 ..... N90-22564* #
NAS 1.15:102324 ..... N90-22823* #
NAS 1.15:102342 ..... N90-22808* #
NAS 1.15:102368 ..... N90-22703* #
NAS 1.15:102491 ..... N90-22801* #
NAS 1.15:102639 ..... N90-22558* #
NAS 1.15:102786 ..... N90-22966* #
NAS 1.15:102789 ..... N90-22583* #
NAS 1.15:103094 ..... N90-23339* #
NAS 1.15:103095 ..... N90-22646* #
NAS 1.15:103116 ..... N90-22790* #
NAS 1.15:103121 ..... N90-22761* #
NAS 1.15:103133 ..... N90-22843* #
NAS 1.15:103136 ..... N90-22796* #
NAS 1.15:103142 ..... N90-22606* #
NAS 1.15:103144 ..... N90-22732* #
NAS 1.15:103146 ..... N90-22605* #
NAS 1.15:103151 ..... N90-23125* #
NAS 1.15:103152 ..... N90-22773* #
NAS 1.15:103154 ..... N90-22731* #
NAS 1.15:103156 ..... N90-22847* #
NAS 1.15:103157 ..... N90-22822* #
NAS 1.15:103158 ..... N90-22592* #
NAS 1.15:103161 ..... N90-22595* #
NAS 1.15:103162 ..... N90-22784* #
NAS 1.15:103163 ..... N90-22604* #
NAS 1.15:103167 ..... N90-22566* #
NAS 1.21:503 ..... N90-22850* #
NAS 1.26:4273 ..... N90-22986* #
NAS 1.26:4284 ..... N90-22746* #
NAS 1.26:4296 ..... N90-22557* #
NAS 1.26:180471 ..... N90-22698* #
NAS 1.26:180482 ..... N90-22767* #
NAS 1.26:180650 ..... N90-22835* #
NAS 1.26:181898 ..... N90-22609* #
NAS 1.26:181995 ..... N90-23137* #
NAS 1.26:181997 ..... N90-22539* #
NAS 1.26:181998 ..... N90-22540* #
NAS 1.26:182024 ..... N90-22538* #
NAS 1.26:182038 ..... N90-22973* #
NAS 1.26:182040 ..... N90-23128* #
NAS 1.26:182047 ..... N90-23138* #
NAS 1.26:182048 ..... N90-23139* #
NAS 1.26:182055 ..... N90-22982* #
NAS 1.26:182056 ..... N90-22972* #
NAS 1.26:182445 ..... N90-22813* #
NAS 1.26:182607 ..... N90-22651* #
NAS 1.26:183033 ..... N90-22877* #
NAS 1.26:183300 ..... N90-22868* #
NAS 1.26:183931 ..... N90-22788* #
NAS 1.26:183940 ..... N90-22602* #
NAS 1.26:184998 ..... N90-22826* #
NAS 1.26:185173 ..... N90-22834* #
NAS 1.26:185217 ..... N90-22567* #
NAS 1.26:185826 ..... N90-23333* #
NAS 1.26:186446 ..... N90-22987* #
NAS 1.26:186447 ..... N90-23040* #
NAS 1.26:186587 ..... N90-22614* #
NAS 1.26:186615 ..... N90-22897* #
NAS 1.26:186620 ..... N90-22870* #
NAS 1.55:3071 ..... N90-23294* #
NAS 1.55:3075 ..... N90-22624* #
NAS 1.55:10032 ..... N90-22918* #
NAS 1.60:2999 ..... N90-22965* #
NAS 1.60:3000 ..... N90-22531* #

NASA-CASE-LAR-13486-1 ..... N90-22584*
NASA-CASE-LAR-13740-1 ..... N90-22770*

NASA-CASE-LEW-14520-1 ..... N90-22724*

NASA-CASE-MFS-28206-1-SB N90-23242*

NASA-CASE-NPO-17390-1-CU N90-22769*

NASA-CP-3071 ..... N90-23294* #
NASA-CP-3075 ..... N90-22824* #
NASA-CP-10032 ..... N90-22918* #

NASA-CR-4273 ..... N90-22986* #
NASA-CR-4284 ..... N90-22746* #
NASA-CR-4296 ..... N90-22557* #
NASA-CR-180471 ..... N90-22698* #
NASA-CR-180482 ..... N90-22767* #
NASA-CR-180650 ..... N90-22835* #
NASA-CR-181898 ..... N90-22609* #
NASA-CR-181995 ..... N90-23137* #
NASA-CR-181997 ..... N90-22539* #
NASA-CR-181998 ..... N90-22540* #
NASA-CR-182024 ..... N90-22538* #
NASA-CR-182038 ..... N90-22973* #
NASA-CR-182040 ..... N90-23128* #
NASA-CR-182047 ..... N90-23138* #
NASA-CR-182048 ..... N90-23139* #
NASA-CR-182055 ..... N90-22982* #
NASA-CR-182056 ..... N90-22972* #
NASA-CR-182445 ..... N90-22813* #
NASA-CR-182607 ..... N90-22651* #
NASA-CR-183033 ..... N90-22877* #
NASA-CR-183300 ..... N90-22868* #
NASA-CR-183931 ..... N90-22788* #
NASA-CR-183940 ..... N90-22602* #
NASA-CR-184998 ..... N90-22826* #
NASA-CR-185173 ..... N90-22834* #
NASA-CR-185217 ..... N90-22567* #
NASA-CR-185826 ..... N90-23333* #
NASA-CR-186446 ..... N90-22987* #
NASA-CR-186447 ..... N90-23040* #
NASA-CR-186587 ..... N90-22614* #
NASA-CR-186615 ..... N90-22897* #
NASA-CR-186620 ..... N90-22870* #

NASA-SP-503 ..... N90-22850* #

NASA-TM-4017 ..... N90-22628* #
NASA-TM-4179 ..... N90-23338* #
NASA-TM-4180 ..... N90-22555* #
NASA-TM-4204 ..... N90-22593* #
NASA-TM-100761 ..... N90-23273* #
NASA-TM-101067 ..... N90-23090* #
NASA-TM-101687 ..... N90-22807* #
NASA-TM-101705 ..... N90-22532* #
NASA-TM-102248 ..... N90-22827* #
NASA-TM-102316 ..... N90-22564* #
NASA-TM-102324 ..... N90-22823* #
NASA-TM-102342 ..... N90-22808* #
NASA-TM-102368 ..... N90-22703* #
NASA-TM-102491 ..... N90-22801* #
NASA-TM-102639 ..... N90-22558* #
NASA-TM-102786 ..... N90-22966* #
NASA-TM-102789 ..... N90-22583* #
NASA-TM-103094 ..... N90-23339* #
NASA-TM-103095 ..... N90-22646* #
NASA-TM-103116 ..... N90-22790* #
NASA-TM-103121 ..... N90-22761* #
NASA-TM-103133 ..... N90-22843* #
NASA-TM-103136 ..... N90-22796* #
NASA-TM-103142 ..... N90-22606* #
NASA-TM-103144 ..... N90-22732* #
NASA-TM-103146 ..... N90-22605* #
NASA-TM-103151 ..... N90-23125* #
NASA-TM-103152 ..... N90-22773* #
NASA-TM-103154 ..... N90-22731* #
NASA-TM-103156 ..... N90-22847* #
NASA-TM-103157 ..... N90-22822* #
NASA-TM-103158 ..... N90-22592* #
NASA-TM-103161 ..... N90-22595* #
NASA-TM-103162 ..... N90-22784* #
NASA-TM-103163 ..... N90-22604* #
NASA-TM-103167 ..... N90-22566* #

NASA-TP-2999 ..... N90-22965* #
NASA-TP-3000 ..... N90-22531* #

NATICK/TR-90/017 ..... N90-23142 #

NAVAIR-50-1C-548 ..... N90-22874 #
NAVAIR-50-1C-549 ..... N90-22875 #

NDP-022/R1 ..... N90-22869 #

NLR-PUB-8801 ..... N90-22974 #

NORDA-223 ..... N90-22879 #

NOSC/TD-1685 ..... N90-22833 #
NOSC/TD-1703 ..... N90-22740 #
NOSC/TD-1717 ..... N90-23210 #

NOSC/TR-1318 ..... N90-23116 #
NOSC/TR-1329 ..... N90-23187 #

NOTA-INTERNA-940 ..... N90-23195 #
NOTA-INTERNA-941 ..... N90-23196 #
NOTA-INTERNA-942 ..... N90-23197 #
NOTA-INTERNA-943 ..... N90-22849 #
NOTA-INTERNA-944 ..... N90-23336 #
NOTA-INTERNA-945 ..... N90-23337 #

NPL-DMA(A)-196 ..... N90-22675

NRL-MR-6339 ..... N90-23161 #
NRL-MR-6584 ..... N90-22764 #
NRL-MR-6589 ..... N90-23209 #
NRL-MR-6595 ..... N90-23207 #
NRL-MR-6620 ..... N90-23208 #

NSMRL-1150 ..... N90-22969 #
NSMRL-1151 ..... N90-22885 #

ONERA-RT-5/7256-RY-081-R ..... N90-22616 #

ONREUR-ESNIB-9-12-C ..... N90-23102 #
ONREUR-ESNIB-9-13-R ..... N90-22713 #

ONRFE-SCI-INFO-BULL-13(4)88 ..... N90-23168 #

ORNL/CDIAC-31 ..... N90-22869 #

PCN-051-SA ..... N90-22542 #

PNL-7301 ..... N90-23263 #

PREPRINT-695 ..... N90-22577 #
PREPRINT-697 ..... N90-23191 #
PREPRINT-698 ..... N90-23192 #
PREPRINT-699 ..... N90-23260 #
PREPRINT-700 ..... N90-23261 #
PREPRINT-701 ..... N90-22782 #
PREPRINT-702 ..... N90-23226 #
PREPRINT-703 ..... N90-23227 #
PREPRINT-704 ..... N90-22828 #
PREPRINT-705 ..... N90-23205 #
PREPRINT-707 ..... N90-22771 #
PREPRINT-708 ..... N90-23243 #
PREPRINT-709 ..... N90-23133 #
PREPRINT-710 ..... N90-23193 #
PREPRINT-711 ..... N90-22709 #
PREPRINT-712 ..... N90-23173 #
PREPRINT-713 ..... N90-23174 #
PREPRINT-714 ..... N90-23244 #
PREPRINT-715 ..... N90-23194 #
PREPRINT-719 ..... N90-23245 #
PREPRINT-720 ..... N90-23175 #
PREPRINT-721 ..... N90-23331 #

R/D-6287.PH.09-F ..... N90-22844 #
R/D-6371-MA-02 ..... N90-23149 #

RADC-TR-89-12 ..... N90-22721 #
RADC-TR-89-31 ..... N90-23217 #
RADC-TR-89-211 ..... N90-22720 #
RADC-TR-89-268 ..... N90-23110 #
RADC-TR-89-270 ..... N90-23248 #
RADC-TR-89-292 ..... N90-22895 #
RADC-TR-89-321 ..... N90-22971 #
RADC-TR-89-358 ..... N90-23126 #
RADC-TR-90-7 ..... N90-23108 #

RAE-SPACE-675 ..... N90-22586 #

RAE-TM-AERO-2164 ..... N90-22537 #

RAE-TM-AW-121 ..... N90-22891 #

RAE-TM-FM-28 ..... N90-22708 #

RAE-TR-89022 ..... N90-22586 #

RDS-1-007-64 ..... N90-22618 #

REPT-NT-10/S/83 ..... N90-22617 #
REPT-NT-10/S/83 ..... N90-22619 #
REPT-NT-10/S/83 ..... N90-22620 #

REPT-S3-4273-PARTIAL-1 ..... N90-22620 #
REPT-S3-4273-PARTIAL-3 ..... N90-22619 #
REPT-S3-4273-PARTIAL-6 ..... N90-22617 #

REPT-3-90 ..... N90-22698* #
REPT-32(1988)-PT-1 ..... N90-23262 #
REPT-89-006 ..... N90-23131
REPT-89-007 ..... N90-23132
REPT-89-044 ..... N90-22725
REPT-89-047 ..... N90-23092
REPT-89-053 ..... N90-23118
REPT-89-054 ..... N90-23093
REPT-89-060 ..... N90-22726
REPT-89-062 ..... N90-23094
REPT-89B00170 ..... N90-22850* #
REPT-90-077 ..... N90-22824* #
REPT-90B00109 ..... N90-23273* #
REPT-153-6923 ..... N90-22983 #
REPT-892-422-102 ..... N90-22603 #
REPT-892-422-105 ..... N90-22581 #
REPT-892-422-106 ..... N90-22582 #
REPT-892-430-101 ..... N90-22632 #
REPT-892-430-102 ..... N90-22621 #
REPT-892-430-103 ..... N90-22571 #
REPT-892-430-104 ..... N90-22622 #
REPT-892-430-105 ..... N90-22696 #
REPT-892-430-107 ..... N90-22623 #
REPT-892-430-108 ..... N90-22624 #
REPT-892-430-111 ..... N90-22572 #
REPT-892-430-113 ..... N90-22783 #
REPT-892-430-116 ..... N90-22772 #
REPT-892-430-117 ..... N90-22590 #
REPT-892-430-119 ..... N90-22815 #
REPT-892-430-120 ..... N90-22816 #
REPT-892-430-121 ..... N90-22691 #
REPT-892-430-122 ..... N90-22625 #
REPT-892-430-123 ..... N90-22677 #
REPT-892-430-124 ..... N90-22591
REPT-892-430-126 ..... N90-22626 #

RI/RD89-225 ..... N90-22845 #
RI/RD90-121 ..... N90-22739 #

RTI-415U-4225 ..... N90-23256 #

SAND-90-0050C ..... N90-22754 #
SAND-90-0183 ..... N90-22841 #
SAND-90-0608C ..... N90-22804 #
SAND-90-0890C ..... N90-22699 #
SAND-90-0906C ..... N90-22791 #
SAND-90-7026 ..... N90-22840 #

SD-TR-88-49 ..... N90-22719 #

SEL-R-150 ..... N90-22552 #

SERI/PR-215-3607 ..... N90-22839 #

SOT/FAA/AM-89/13 ..... N90-22970 #

SR-5 ..... N90-23325 #

SRA-900049-UM ..... N90-22538* #

STI-TR-1235-1-1 ..... N90-22560 #
STI-TR-1235-1-2 ..... N90-22561 #
STI-TR-1235-1-3 ..... N90-22562 #

STS/VDM-TI-683/88 ..... N90-22582 #

SUNY/AB/TR-24 ..... N90-22608 #

SUNYBUF/DC/TR-1 ..... N90-22641 #

TR-3 ..... N90-22883 #
TR-16 ..... N90-22679 #
TR-37 ..... N90-22683 #
TR-38 ..... N90-22682 #
TR-46 ..... N90-22643 #
TR-53 ..... N90-22607 #
TR-89-1-ONR ..... N90-23186 #
TR-90-01C ..... N90-23159 #
TR-90-10 ..... N90-23158 #
TR-246 ..... N90-23150 #
TR-277 ..... N90-23176 #
TR-278 ..... N90-23143 #
TR-279 ..... N90-23144 #
TR-0086A(2925-05)-1 ..... N90-22719 #

TR89-3 ..... N90-23185 #

TWR-18895 ..... N90-22788* #
TWR-18898 ..... N90-22602* #

UCID-21761 ..... N90-22673 #

UCRL-ID-103198 ..... N90-23129 #

UCRL-50021-87 ..... N90-22779 #
UCRL-102052 ..... N90-22700 #

US-PATENT-APPL-SN-076955 ..... N90-22584*
US-PATENT-APPL-SN-130058 ..... N90-22724*
US-PATENT-APPL-SN-172101 ..... N90-23242*
US-PATENT-APPL-SN-205899 ..... N90-22769*
US-PATENT-APPL-SN-205900 ..... N90-22770*
US-PATENT-APPL-SN-748248 ..... N90-22551

US-PATENT-CLASS-156-DIG.62 ..... N90-23242*
US-PATENT-CLASS-156-DIG.72 ..... N90-23242*
US-PATENT-CLASS-156-600 ..... N90-23242*
US-PATENT-CLASS-156-608 ..... N90-23242*
US-PATENT-CLASS-244-1R N90-22769*
US-PATENT-CLASS-244-138A N90-22769*
US-PATENT-CLASS-244-158R N90-22584*
US-PATENT-CLASS-244-160 ..... N90-22584*
US-PATENT-CLASS-244-161 ..... N90-22584*
US-PATENT-CLASS-244-172 ..... N90-22584*
US-PATENT-CLASS-250-459.1 ..... N90-22770*
US-PATENT-CLASS-250-461.1 ..... N90-22770*
US-PATENT-CLASS-315-3 ..... N90-22724*
US-PATENT-CLASS-315-3.5 ..... N90-22724*
US-PATENT-CLASS-331-82 ..... N90-22724*
US-PATENT-CLASS-358-93 ..... N90-22770*
US-PATENT-CLASS-358-109 ..... N90-22769*
US-PATENT-CLASS-358-113 ..... N90-22770*
US-PATENT-CLASS-374-162 ..... N90-22770*
US-PATENT-CLASS-422-245 ..... N90-23242*

US-PATENT-4,881,080 ..... N90-22551

USAAVSCOM-TR-89-D-22A-VOL-1 ..... N90-22545 #
USAAVSCOM-TR-89-D-22B-VOL-2 ..... N90-22546 #
USAAVSCOM-TR-89-D-22C-VOL-3 ..... N90-22547 #
USAAVSCOM-TR-89-D-22D-VOL-4 ..... N90-22548 #
USAAVSCOM-TR-89-D-22E-VOL-5 ..... N90-22549 #

USARIEM-TP-11-90 ..... N90-22886 #

UVA/528266/MS90/106 ..... N90-22651* #

W-8904 ..... N90-22730 #
W-8906 ..... N90-23136 #
W-8908 ..... N90-22794 #

WHOI-89-48 ..... N90-22857 #

WRDC-TR-89-1100 ..... N90-22858 #
WRDC-TR-89-3125-VOL-1 ..... N90-22560 #
WRDC-TR-89-3125-VOL-2 ..... N90-22561 #
WRDC-TR-89-3125-VOL-3 ..... N90-22562 #
WRDC-TR-89-4120 ..... N90-22642 #
WRDC-TR-89-4140 ..... N90-22701 #
WRDC-TR-89-5052 ..... N90-23251 #

WSRC-RP-89-812 ..... N90-22629 #
WSRC-RP-89-1438 ..... N90-22753 #

ZFK-630 ..... N90-22667 #

Appendix—About STAR

Scientific and Technical Aerospace Reports (STAR) is a major component of a comprehensive National Aeronautics and Space Administration information system covering aeronautics, space, and supporting disciplines. *STAR* is issued on the 8th and 23rd of each month and announces current publications of the following types:

- NASA, NASA contractor, and NASA grantee reports
- Reports issued by other U.S. Government agencies, domestic and foreign institutions, universities, and private firms
- Translations in report form
- NASA-owned patents and patent applications
- Other U.S. Government agency and foreign patents and patent applications
- Domestic and foreign dissertations and theses

Journal, book, and conference literature, cover-to-cover journal translations, and certain foreign dissertations are announced in a companion journal, *International Aerospace Abstracts (IAA),* available on subscription from the American Institute of Aeronautics and Astronautics, Technical Information Service, 555 West 57th Street, 12th Floor, New York, NY 10019.

SUBJECT SCOPE

The subject scope of *STAR* and *IAA* includes all aspects of aeronautics and space research and development, supporting basic and applied research, and applications. Aerospace aspects of earth resources, energy development, conservation, oceanography, environmental protection, urban transportation, and other topics of high national priority are also covered.

OTHER NASA PUBLICATIONS

Other NASA publications and information services are described in the publication, *The NASA Scientific and Technical Information System ... and How to Use It,* available without charge from the NASA Scientific and Technical Information Facility, P.O. Box 8757, BWI Airport, MD 21240.

HOW TO USE *STAR* SUBJECT CATEGORIES

STAR is categorized by 10 major subject divisions broken down further into 76 specific subject categories and one general division/category. The major subject divisions are listed on page ii in the Table of Contents, together with a note for each that defines its scope and provides any cross-references. For example:

AERONAUTICS

Includes aeronautics (general); aerodynamics; air transportation and safety; aircraft communications and navigation; aircraft design, testing and performance; aircraft instrumentation; aircraft propulsion and power; aircraft stability and control; and research and support facilities (air).

For related information see also *Astronautics.*

Each major division is further divided into as many as nine specific categories, which are identified by category numbers.

Abstracts in *STAR* are grouped by subject category, the categories appearing in sequential order. Category breaks in the abstract section are identified by the category number and title, and a scope note. Cross-references to other categories are provided as appropriate. For example:

02 AERODYNAMICS

Includes aerodynamics of bodies, combinations, wings, rotors, and control surfaces; and internal flow in ducts and turbomachinery.

For related information see also *34 Fluid Mechanics and Heat Transfer.*

CROSS-REFERENCES

Individual *STAR* abstracts are not ordinarily cross-referenced, except for certain conference reports or book translations that have had separate abstracts written for their component papers or chapters. Citations and abstracts of the components follow immediately after those of the parent document. When the subject content of a component differs sufficiently from the general content of the parent, a cross-reference citation also is printed at the end of the category to which it normally would have been assigned if it were independent.

DOCUMENTS ON MICROFICHE

Documents on microfiche[1] are designated by a pound sign (#) following the accession number. The pound sign is used without regard to the source or quality of the microfiche.

LIMITED REPRODUCIBILITY

A Note of Limited Reproducibility appears in the citation, if one or a combination of the following factors affect the reproducibility of more than 20% of the document. These factors include: faint or broken type, color photographs, black and white photographs, foldouts, dot matrix print, charts/graphs with script notation, non-Roman alphabet, or some other factor that limits the reproducibility of that document. This notation also appears on the microfiche header, with the specific causing factor checked off on a list visible in the second frame.

COLOR COPIES

An increasing number of NASA scientific and technical reports are being produced with color graphs, charts, illustrations, and photographs. A message indicating that a document has color pages follows the Sales and Pricing (SAP) information in the *STAR* citation.

Registered users of the NASA Scientific and Technical Information System will receive ordered documents with color at no *additional* cost, as long as stock copies of that document are available. Otherwise, an additional fee of $2.00 per color page, over and above the standard document price will be charged. The NASA STI Facility staff will work with registered users over the telephone to inform and meet each individual's ordering needs.

AVAILABILITIES

One or more sources from which a document announced in *STAR* is available to the public is given in each citation. The most commonly indicated sources and their acronyms or abbreviations are listed below. If the publication is available from a source other than those listed, the publisher and his address will be displayed on the availability line or in combination with the corporate source line.

Avail: NTIS. Sold by the National Technical Information Service. Prices for hard copy (HC) and microfiche (MF) are indicated by a price code following the letters HC or MF in the *STAR* citation. Current values for the price codes are given in the tables on page A-7.

(1) A microfiche is a transparent sheet of film, 105 by 148 mm in size, containing as many as 60 to 98 pages of information reduced to micro images (not to exceed 26:1 reduction).

Initially distributed microfiche under the NTIS SRIM (Selected Research in Microfiche) is available at greatly reduced unit prices. For this service and for information concerning subscription to NASA printed reports, consult the NTIS Subscription Section, Springfield, VA 22161.

NOTE ON ORDERING DOCUMENTS: When ordering NASA publications (those followed by the * symbol), use the N accession number. NASA patent applications (only the specifications are offered) should be ordered by the US-Patent-Appl-SN number. Non-NASA publications (no asterisk) should be ordered by the AD, PB, or other *report number* shown on the last line of the citation, not by the N accession number. It is also advisable to cite the title and other bibliographic identification.

Avail: SOD (or GPO). Sold by the Superintendent of Documents, U.S. Government Printing Office, in hard copy. The current price and order number are given following the availability line. (NTIS will fill microfiche requests, as indicated above, for those documents identified by a # symbol.)

Avail: BLL (formerly NLL): British Library Lending Division, Boston Spa, Wetherby, Yorkshire, England. Photocopies available from this organization at the price shown. (If none is given, address inquiry to the BLL.)

Avail: DOE Depository Libraries. Organizations in U.S. cities and abroad that maintain collections of Department of Energy reports, usually in microfiche form, are listed in *Energy Research Abstracts*. Services available from the DOE and its depositories are described in a booklet, *DOE Technical Information Center - Its Functions and Services* (TID-4660), which may be obtained without charge from the DOE Technical Information Center.

Avail: ESDU. Pricing information on specific data, computer programs, and details on Engineering Sciences Data Unit (ESDU) topic categories can be obtained from ESDU International Ltd. Requesters in North America should use the Virginia address while all other requesters should use the London address, both of which are on page A-6.

Avail: Fachinformationszentrum, Karlsruhe. Sold by the Fachinformationszentrum Energie, Physik, Mathematik GMBH, Eggenstein Leopoldshafen, Federal Republic of Germany, at the price shown in deutschmarks (DM).

Avail: HMSO. Publications of Her Majesty's Stationery Office are sold in the U.S. by Pendragon House, Inc. (PHI), Redwood City, CA. The U.S. price (including a service and mailing charge) is given, or a conversion table may be obtained from PHI.

Avail: NASA Public Document Rooms. Documents so indicated may be examined at or purchased from the National Aeronautics and Space Administration, Public Documents Room (Room 126), 600 Independence Ave., S.W., Washington, DC 20546, or public document rooms located at NASA installations, and the NASA Pasadena Office at the Jet Propulsion Laboratory.

Avail: Univ. Microfilms. Documents so indicated are dissertations selected from *Dissertation Abstracts* and are sold by University Microfilms as xerographic copy (HC) and microfilm. All requests should cite the author and the Order Number as they appear in the citation.

Avail: US Patent and Trademark Office. Sold by Commissioner of Patents and Trademarks, U.S. Patent and Trademark Office, at the standard price of

$1.50 each, postage free. (See discussion of NASA patents and patent applications below.)

Avail: (US Sales Only). These foreign documents are available to users within the United States from the National Technical Information Service (NTIS). They are available to users outside the United States through the International Nuclear Information Service (INIS) representative in their country, or by applying directly to the issuing organization.

Avail: USGS. Originals of many reports from the U.S. Geological Survey, which may contain color illustrations, or otherwise may not have the quality of illustrations preserved in the microfiche or facsimile reproduction, may be examined by the public at the libraries of the USGS field offices whose addresses are listed in this Introduction. The libraries may be queried concerning the availability of specific documents and the possible utilization of local copying services, such as color reproduction.

Avail: Issuing Activity, or Corporate Author, or no indication of availability. Inquiries as to the availability of these documents should be addressed to the organization shown in the citation as the corporate author of the document.

NASA PATENTS AND PATENT APPLICATIONS

Patents and patent applications owned by NASA are announced in *STAR* under appropriate subject categories and are referenced in the *STAR* indexes. In the Report/Accession Number Index, patents are indexed by the NASA Case Number (which appears in lieu of the report number in other indexes), the U.S. Patent Number, the U.S. Patent Application Serial Number, and the U.S. Patent Class. Patent applications for which patents have not yet been issued are indexed by the NASA Case Number and the U.S. Patent Application Serial Number.

NASA *patent application specifications* are sold in paper copy and microfiche by the National Technical Information Service (NTIS). The US-Patent-Appl-SN- number should be used in ordering either paper copy or microfiche from NTIS. Printed copies of *patents* (which are not microfiched) are available for purchase from:

Commissioner of Patents and Trademarks
U.S. Patent and Trademark Office
Washington, DC 20231

When ordering patents, the U.S. Patent Number should be used, and payment must be remitted in advance, by money order or check payable to the Commissioner of Patents and Trademarks. Prepaid purchase coupons for ordering are also available from the Patent and Trademark Office. The patents and patent applications announced in *STAR* are owned by NASA and are available for royalty-free licensing. Requests for licensing terms and further information should be addressed to:

Associate General Counsel for Intellectual Property/Code GP
National Aeronautics and Space Administration
Washington, DC 20546

ELIGIBILITY AND REGISTRATION FOR NASA INFORMATION PRODUCTS AND SERVICES

A variety of services is available to organizations of the following types that have registered with NASA to receive specific services or products:

1. NASA offices and installations, contractors, subcontractors, grantees, and consultants;
2. Other U.S. Government agencies and their contractors;
3. Libraries in the United States that have arrangements with NASA to maintain collections of NASA documents for public reference;
4. Other organizations in the United States having a need for NASA documents in work related to aeronautics and space research;
5. Organizations abroad that have established reciprocal document exchange arrangements with NASA.

Only the central service points or central points of document acquisition and control within qualified organizations are eligible to register for NASA products and services. Domestic organizations that may be eligible to receive various classes of NASA publications and services should address their requests for registration or for further information to:

NASA Scientific and Technical Information Facility
ATTN: Registration Services
P.O. Box 8757
BWI Airport, MD 21240
301-621-0153

Organizations abroad should direct requests to Manager, International STI Activities, NTT, NASA Headquarters, Washington, DC 20546.

AVAILABILITY OF *STAR* ABSTRACTS ON MICROFICHE

Microfiche of the abstract sections of this issue and other issues of *STAR* are available on annual subscription from NTIS as PB90-911300, Attn: Subscriptions, 5285 Port Royal Road, Springfield, VA 22161. Annual subscription rates are $75.50 North America; $151.00 foreign. Abstract sections for previous years retroactive to 1964 are available at the current rates. Microfiche for individual *STAR* issue abstract sections are not available.

PUBLIC COLLECTIONS OF NASA DOCUMENTS

DOMESTIC: NASA and NASA-sponsored documents and a large number of aerospace publications are available to the public for reference purposes at the library maintained by the American Institute of Aeronautics and Astronautics, Technical Information Service, 555 West 57th Street, 12th Floor, New York, NY 10019

EUROPEAN: An extensive collection of NASA and NASA-sponsored publications is maintained by the British Library Lending Division, Boston Spa, Wetherby, Yorkshire, England, for public access. The British Library Lending Division also has available many of the non-NASA publications cited in *STAR*. European requesters may purchase facsimile copy or microfiche of NASA and NASA-sponsored documents, those identified by both the symbols # and * from ESA - Information Retrieval Service, European Space Agency, 8-10 rue Mario-Nikis, 75738 Paris CEDEX 15, France.

FEDERAL DEPOSITORY LIBRARY PROGRAM

In order to provide the general public with greater access to U.S. Government publications, Congress established the Federal Depository Library Program under the Government Printing Office (GPO), with 51 regional depositories responsible for permanent retention of material, inter-library loan, and reference services. At least one copy of nearly every NASA and NASA-sponsored publication, either in printed or microfiche format, is received and retained by the 51 regional depositories. A list of the regional GPO libraries, arranged alphabetically by state, appears on the inside back cover. These libraries are *not* sales outlets. A local library can contact a Regional Depository to help locate specific reports, or direct contact may be made by an individual.

ADDRESSES OF ORGANIZATIONS

American Institute of Aeronautics and Astronautics
Technical Information Service
555 West 57th Street, 12th Floor
New York, New York 10019

British Library Lending Division,
Boston Spa, Wetherby, Yorkshire,
England

Commissioner of Patents and Trademarks
U.S. Patent and Trademark Office
Washington, DC 20231

Department of Energy
Technical Information Center
P.O. Box 62
Oak Ridge, Tennessee 37830

European Space Agency-Information Retrieval Service
ESRIN
Via Galileo Galilei
00044 Frascati (Rome) Italy

Engineering Sciences Data Unit International
P.O. Box 1633
Manassas, Virginia 22110

Engineering Sciences Data Unit International, Ltd.
251-259 Regent Street
London, W1R 7AD, England

Fachinformationszentrum Energie, Physik, Mathematik
GMBH
7514 Eggenstein Leopoldshafen
Federal Republic of Germany

Her Majesty's Stationery Office
P.O. Box 569, S.E. 1
London, England

NASA Scientific and Technical Information Facility
P.O. Box 8757
BWI Airport, Maryland 21240

National Aeronautics and Space Administration
Scientific and Technical Information Division (NTT)
Washington, DC 20546

National Technical Information Service
5285 Port Royal Road
Springfield, Virginia 22161

Pendragon House, Inc.
899 Broadway Avenue
Redwood City, California 94063

Superintendent of Documents
U.S. Government Printing Office
Washington, DC 20402

University Microfilms
A Xerox Company
300 North Zeeb Road
Ann Arbor, Michigan 48106

University Microfilms, Ltd.
Tylers Green
London, England

U.S. Geological Survey Library National Center
MS 950
12201 Sunrise Valley Drive
Reston, Virginia 22092

U.S. Geological Survey Library
2255 North Gemini Drive
Flagstaff, Arizona 86001

U.S. Geological Survey
345 Middlefield Road
Menlo Park, California 94025

U.S. Geological Survey Library
Box 25046
Denver Federal Center, MS914
Denver, Colorado 80225

NTIS PRICE SCHEDULES

(Effective January 1, 1990)

Schedule A
STANDARD PRICE DOCUMENTS AND MICROFICHE

PRICE CODE	NORTH AMERICAN PRICE	FOREIGN PRICE
A01	$ 8.00	$ 16.00
A02	11.00	22.00
A03	15.00	30.00
A04-A05	17.00	34.00
A06-A09	23.00	46.00
A10-A13	31.00	62.00
A14-A17	39.00	78.00
A18-A21	45.00	90.00
A22-A25	53.00	106.00
A99	*	*
N01	60.00	120.00
N02	59.00	118.00
N03	20.00	40.00

Schedule E
EXCEPTION PRICE DOCUMENTS AND MICROFICHE

PRICE CODE	NORTH AMERICAN PRICE	FOREIGN PRICE
E01	$10.00	$ 20.00
E02	12.00	24.00
E03	14.00	28.00
E04	16.50	33.00
E05	18.50	37.00
E06	21.50	43.00
E07	24.00	48.00
E08	27.00	54.00
E09	29.50	59.00
E10	32.50	65.00
E11	35.00	70.00
E12	38.50	77.00
E13	41.00	82.00
E14	45.00	90.00
E15	48.50	97.00
E16	53.00	106.00
E17	57.50	115.00
E18	62.00	124.00
E19	69.00	138.00
E20	80.00	160.00
E99	*	*

* Contact NTIS for price quote.

IMPORTANT NOTICE

NTIS Shipping and Handling Charges

U.S., Canada, Mexico — ADD $3.00 per TOTAL ORDER

All Other Countries — ADD $4.00 per TOTAL ORDER

Exceptions — Does NOT apply to:

ORDERS REQUESTING NTIS RUSH HANDLING

ORDERS FOR SUBSCRIPTION OR STANDING ORDER PRODUCTS *ONLY*

NOTE: Each additional delivery address on an order requires a separate shipping and handling charge.

FEDERAL REGIONAL DEPOSITORY LIBRARIES

ALABAMA

AUBURN UNIV. AT MONTGOMERY LIBRARY
Documents Department
Montgomery, AL 36193
(205) 279-9110 ext.253

UNIV. OF ALABAMA LIBRARY
Reference Department/Documents
Box S
Tuscaloosa, AL 35486
(205) 348-6046

ARIZONA

DEPT. OF LIBRARY, ARCHIVES, AND PUBLIC RECORDS
Third Floor State Capitol
1700 West Washington
Phoenix, AZ 85007
(602) 255-4121

ARKANSAS

ARKANSAS STATE LIBRARY
Documents Service Section
One Capitol Mall
Little Rock, AR 72201
(501) 371-2090

CALIFORNIA

CALIFORNIA STATE LIBRARY
Govt. Publications Section
914 Capitol Mall
Sacramento, CA 95814
(916) 322-4572

COLORADO

UNIV. OF COLORADO
Norlin Library
Government Publications Division
Campus Box 184
Boulder, CO 80309
(303) 492-8834

DENVER PUBLIC LIBRARY
Govt. Pub. Department
1357 Broadway
Denver, CO 80203
(303) 571-2346

CONNECTICUT

CONNECTICUT STATE LIBRARY
231 Capitol Avenue
Hartford, CT 06106
(203) 566-4971

FLORIDA

UNIV. OF FLORIDA LIBRARIES
Documents Department
Library West
Gainesville, FL 32611
(904) 392-0367

GEORGIA

UNIV. OF GEORGIA LIBRARIES
Government Documents Dept.
Athens, GA 30602
(404) 542-8949

HAWAII

UNIV. OF HAWAII
Hamilton Library
Government Documents Collection
2550 The Mall
Honolulu, HI 96822
(808) 948-8230

IDAHO

UNIV. OF IDAHO LIBRARY
Documents Section
Moscow, ID 83843
(208) 885-6344

ILLINOIS

ILLINOIS STATE LIBRARY
Federal Documents
Centennial Building
Springfield, IL 62756
(217) 782-5012

INDIANA

INDIANA STATE LIBRARY
Serials Section
140 North Senate Avenue
Indianapolis, IN 46204
(317) 232-3686

IOWA

UNIV. OF IOWA LIBRARIES
Government Publications Dept.
Iowa City, IA 52242
(319) 335-5926

KANSAS

UNIVERSITY OF KANSAS
Spencer Research Library
Government Documents
Lawrence, KS 66045
(913) 864-4662

KENTUCKY

UNIV. OF KENTUCKY LIBRARIES
Government Publications/Maps Dept.
Lexington, KY 40506
(606) 257-8400

LOUISIANA

LOUISIANA STATE UNIVERSITY
Middleton Library
Government Documents Dept.
Baton Rouge, LA 70803
(504) 388-2570

LOUISIANA TECHNICAL UNIV.
Prescott Memorial Library
Government Documents Dept.
Ruston, LA 71272
(318) 257-4962

MAINE

UNIVERSITY OF MAINE
Raymond H. Fogler Library
Govt. Documents & Microforms Dept.
Orono, ME 04469
(207) 581-1680

MARYLAND

UNIVERSITY OF MARYLAND
McKeldin Library
Documents/Maps Room
College Park, MD 20742
(301) 454-3034

MASSACHUSETTS

BOSTON PUBLIC LIBRARY
Government Documents Dept.
666 Boylston Street
Boston, MA 02117
(617) 536-5400 ext.226

MICHIGAN

DETROIT PUBLIC LIBRARY
5201 Woodward Avenue
Detroit, MI 48202
(313) 833-1409

LIBRARY OF MICHIGAN
Government Documents
P.O. Box 30007
735 E. Michigan Avenue
Lansing, MI 48909
(517) 373-1593

MINNESOTA

UNIVERSITY OF MINNESOTA
Wilson Library
Government Publications
309 Nineteenth Avenue South
Minneapolis, MN 55455
(612) 373-7813

MISSISSIPPI

UNIV. OF MISSISSIPPI LIB.
Government Documents Dept.
106 Old Gym Bldg.
University, MS 38677
(601) 232-5857

MISSOURI

University of Missouri at Columbia Library
Government Documents
Columbia, MO 65201
(314) 882-6733

MONTANA

UNIV. OF MONTANA
Mansfield Library
Documents Division
Missoula, MT 59812
(406) 243-6700

NEBRASKA

UNIVERSITY OF NEBRASKA - LINCOLN
Love Memorial Library
Documents Department
Lincoln, NE 68588
(402) 472-2562

NEVADA

UNIV. OF NEVADA-RENO LIB.
Govt. Pub. Department
Reno, NV 89557
(702) 784-6579

NEW JERSEY

NEWARK PUBLIC LIBRARY
U.S. Documents Division
5 Washington Street
P.O. Box 630
Newark, NJ 07101
(201) 733-7812

NEW MEXICO

UNIVERSITY OF NEW MEXICO
General Library
Government Publications/Maps Dept.
Albuquerque, NM 87131
(505) 277-5441

NEW MEXICO STATE LIBRARY
325 Don Gaspar Avenue
Santa Fe, NM 87501
(505) 827-3826

NEW YORK

NEW YORK STATE LIBRARY
Documents Sect. Cultural Educ. Ctr.
Empire State Plaza
Albany, NY 12230
(518) 474-5563

NORTH CAROLINA

UNIVERSITY OF NORTH CAROLINA AT CHAPEL HILL
Davis Library 080A
BA/SS Department Documents
Chapel Hill, NC 27514
(919) 962-1151

NORTH DAKOTA

NORTH DAKOTA STATE UNIVERSITY LIBRARY
Government Documents Dept.
Fargo, ND 58105
(701) 237-8352
In cooperation with Univ. of North Dakota, Chester Fritz Library
Grand Forks

OHIO

STATE LIBRARY OF OHIO
Documents Section
65 South Front Street
Columbus, OH 43266
(614) 644-7051

OKLAHOMA

OKLAHOMA DEPT. OF LIBRARIES
Government Documents
200 NE 18th Street
Oklahoma City, OK 73105
(405) 521-2502, ext. 252

OKLAHOMA STATE UNIV. LIB.
Documents Department
Stillwater, OK 74078
(405) 624-0489

OREGON

PORTLAND STATE UNIV.
Millar Library
934 SW Harrison - P.O. Box 1151
Portland, OR 97207
(503) 229-3673

PENNSYLVANIA

STATE LIBRARY OF PENN.
Government Publications Section
Box 1601
Walnut St. & Commonwealth Ave.
Harrisburg, PA 17105
(717) 787-3752

SOUTH CAROLINA

CLEMSON UNIV. COOPER LIB.
Documents Department
Clemson, SC 29634
(803) 656-5174
In cooperation with Univ. of South Carolina, Thomas Cooper Library, Columbia

TEXAS

TEXAS STATE LIBRARY
Public Services Department
P.O. Box 12927 - 1201 Brazos
Austin, TX 78711
(512) 463-5455

TEXAS TECH. UNIV. LIBRARY
Documents Department
Lubbock, TX 79409
(806) 742-2268

UTAH

UTAH STATE UNIVERSITY
Merrill Library & Learning Resources Center, UMC-30
Documents Department
Logan, UT 84322
(801) 750-2682

VIRGINIA

UNIVERSITY OF VIRGINIA
Alderman Library
Government Documents
Charlottesville, VA 22903
(804) 924-3133

WASHINGTON

WASHINGTON STATE LIBRARY
Document Section
Olympia, WA 98504
(206) 753-4027

WEST VIRGINIA

WEST VIRGINIA UNIV. LIB.
Government Documents Section
P.O. Box 6069
Morgantown, WV 26506
(304) 293-3640

WISCONSIN

ST. HIST SOC. OF WISCONSIN LIB.
Government Pub. Section
816 State Street
Madison, WI 53706
(608) 262-2781
In cooperation with Univ. of Wisconsin-Madison, Memorial Library

MILWAUKEE PUBLIC LIBRARY
Documents Division
814 West Wisconsin Avenue
Milwaukee, WI 53233
(414) 278-3065

WYOMING

WYOMING STATE LIBRARY
Supreme Court & Library Bldg.
Cheyenne, WY 82002
(307) 777-5919

National Aeronautics and
Space Administration
Code NTT
Washington, D.C.
20546
Official Business
Penalty for Private Use, $300

SPECIAL FOURTH-CLASS RATE
POSTAGE & FEES PAID
NASA
PERMIT No. G27

POSTMASTER: If Undeliverable (Section 158
Postal Manual) Do Not Return